EUROPEAN WATER RESOURCES ASSOCIATION

EWRA 2025

XIII WORLD CONGRESS

of the European Water Resources Association - EWRA2025

New challenges in understanding and managing water-related risks in a changing environment

24 - 28 June 2025, Palermo, Italy

Proceedings

Editors

Leonardo Valerio Noto
Francesco Alongi
Dario Treppiedi
Harris Vangelis
Dimitris Tigkas



2025

EUROPEAN WATER RESOURCES ASSOCIATION

13th World Congress of EWRA
on Water Resources and Environment
[EWRA 2025]

New challenges in understanding and managing water-related risks in a changing environment

24 - 28 June 2025, Palermo, Italy

PROCEEDINGS

Editors

Leonardo Valerio Noto
Francesco Alongi
Dario Treppiedi
Harris Vangelis
Dimitris Tigkas

2025

© 2025. European Water Resources Association (EWRA)
ISBN: 978-618-84419-2-7

New challenges in understanding and managing water-related risks in a changing environment
Proceedings of the 13th World Congress of EWRA on Water Resources and Environment
[EWRA 2025]
24 - 28 June 2025, Palermo, Italy

Editors:
Leonardo Valerio Noto, Francesco Alongi, Dario Treppiedi, Harris Vangelis, Dimitris Tigkas

Disclaimer:
Although this book of proceedings has been compiled with utmost care, the Editors cannot be held responsible for any misprints and/or omissions. The opinions expressed by the authors are not necessarily endorsed by the Association.

EWRA Editorial Office:
Iroon Polytechniou 9, 157 80, Athens, Greece
e-mail: puboffice@ewra.net

Cite this publication as:
Noto L.V., Alongi F., Treppiedi D., Vangelis H., Tigkas D. (eds.) 2025. New challenges in understanding and managing water-related risks in a changing environment. Proceedings of the 13th World Congress of EWRA on Water Resources and Environment, 24 - 28 June 2025, Palermo, Italy.

Organising Bodies

University of Palermo

Department of Engineering | UNIPA

Consorzio Interuniversitario per l'Idrologia

Patronages

Sponsors

Gold Sponsors

Silver Sponsors

Bronze Sponsors

Organising and Scientific Committee

Leonardo Valerio **Noto** (chair)	University of Palermo	Italy
Giuseppe **Ciraolo** (vice-chair)	University of Palermo	Italy
Antonio **Francipane** (vice-chair)	University of Palermo	Italy
Francesco **Alongi**	University of Palermo	Italy
Dario **Treppiedi**	University of Palermo	Italy
Mauro **De Marchis**	University of Palermo	Italy
Federica **Bruno**	University of Enna “Kore”	Italy
Harris **Vangelis**	National Technical University of Athens	Greece
Dimitris **Tigkas**	National Technical University of Athens	Greece

Scientific Committee

Yeşim **Ahi**	Ankara University	Turkey
Stefano **Alvisi**	University of Ferrara	Italy
Elisa **Arnone**	University of Udine	Italy
Luigi **Berardi**	University of "G. d'Annunzio" Chieti-Pescara	Italy
Brunella **Bonaccorso**	University of Messina	Italy
Antonino **Cancelliere**	University of Catania	Italy
Enrica **Caporali**	University of Firenze	Italy
Pierluigi **Claps**	Polytechnic University of Turin	Italy
Enrico **Creaco**	University of Pavia	Italy
Christophe **Cudenecc**	Institut Agro, UMR SAS	France
João Pedroso **de Lima**	University of Coimbra	Portugal
Roberto **Deidda**	University of Cagliari	Italy
Nicholas **Dercas**	Agricultural University of Athens	Greece
Maria **do Céu Almeida**	Laboratório Nacional de Engenharia Civil (LNEC)	Portugal
Svenja **Fischer**	Wageningen University and Research	Netherlands
Gabriele **Freni**	University of Enna "Kore"	Italy
Luis **Garrote**	University of Madrid	Spain
Margaret **Gitau**	Purdue University	USA
Salvatore **Grimaldi**	University of Tuscia	Italy
Vito **Iacobellis**	Polytechnic University of Bari	Italy
Ana **Iglesias**	University of Madrid	Spain
Erkan **Istanbulluoglu**	University of Washington	USA
Janos **Josza**	University of Budapest	Hungary
George P. **Karatzas**	Technical University of Crete	Greece
Joong Hoon "Jay" **Kim**	Korea University	South Korea
Andreas **Langousis**	University of Patras	Greece
Daniele Biagio **Laucelli**	Polytechnic University of Bari	Italy
Maria Carmen **Llasat**	University of Barcelona	Spain
Rodrigo **Maia**	University of Porto	Portugal
Salvatore **Manfreda**	University of Napoli Federico II	Italy
Marco **Marani**	University of Padova	Italy
Mario Rosario **Mazzola**	University of Palermo	Italy
Silvia **Meniconi**	Università of Perugia	Italy

Paola **Mercogliano**	Centro euro-Mediterraneo sui Cambiamenti Climatici	Italy
Bruno **Merz**	GFZ – Potsdam	Germany
Fernando **Nardi**	University of Rome Tor Vergata	Italy
Gülay Onuşluel **Gül**	Dokuz Eylul University	Turkey
Simon Michael **Papalexiou**	University of Calgary	Canada
Maria Cristina **Rulli**	Polytechnic University of Milan	Italy
Dragan **Savic**	Exeter	UK
Mike **Spiliotis**	Democritus University of Thrace	Greece
Cecilia **Tortajada**	University of Glasgow	UK
Vassilios **Tsihrintzis**	National Technical University of Athens	Greece
Gabriele **Villarini**	Princeton University	USA
Francesco **Viola**	University of Cagliari	Italy
Elena **Volpi**	University of Roma Tre	Italy

Support Staff

Francesco **Alongi** (Coordinator)	University of Palermo	Italy
Caterina **Alonzo**	University of Palermo	Italy
Giorgio **Gullotti**	University of Palermo	Italy
Calogero **Mattina**	University of Palermo	Italy
Lorenzo **Gianni**	University of Palermo	Italy
Marco **Avanti**	University of Palermo	Italy
Diego **Ciriminna**	University of Palermo	Italy
Giorgia **Patti**	University of Palermo	Italy
Matteo **Ippolito**	University of Palermo	Italy
Piero **Scala**	University of Palermo	Italy
Francesco **Castaldo**	University of Palermo	Italy
Niloufar **Beikahmadi**	University of Palermo	Italy
Caterina **Miranti**	University of Palermo	Italy

Editors' Preface

The European Water Resources Association (EWRA) is an international non-profit scientific association founded in 1992 to promote cooperation and exchange in the field of water resources. Among its key initiatives, the biennial EWRA World Congress serves as a significant platform for scientists, engineers, and decision-makers to engage in constructive dialogue on critical water-related challenges.

This volume contains the Proceedings of the *13th World Congress of EWRA on Water Resources and Environment*, held in Palermo, Italy, from 24 to 28 June 2025, under the theme: *"New Challenges in Understanding and Managing Water-Related Risks in a Changing Environment."* The Congress was hosted by the *University of Palermo – Department of Engineering*, in collaboration with the *Consorzio Interuniversitario per l'Idrologia*, and supported by a range of academic and professional institutions.

The 2025 Congress convened during a time of increasing concern over the multifaceted risks posed by global change. Topics such as extreme hydrological events, climate-induced variability, emerging pollutants, water-energy-food interdependencies, and ethical and governance considerations were addressed with urgency and scientific depth. The Congress provided a dynamic forum for interdisciplinary knowledge-sharing and solution-building.

The event featured several keynote lectures by internationally recognized scholars, who explored critical issues such as the driving processes of flood changes, the challenges in designing infiltration systems for aquifer recharge, and the analysis of Mediterranean cyclones and their associated risks. The programme also included special sessions, poster presentations, and a technical field trip, showcasing practical applications of sustainable water and land management.

The papers included in this volume underwent a peer-review process and represent a wide array of topics, both theoretical and applied. The Proceedings are organised into sixteen thematic areas that reflect the breadth and complexity of today's water-related issues:

I. Hydrological Processes in a Changing Environment
II. Extreme Weather Events: Floods, Droughts, Geomorphic, and Coastal Risk Management
III. Data and Models for Environmental, Social, and Governance (ESG) Risk Assessment
IV. Geo-information and Water Resources
V. Climate and Land Use Changes
VI. Environmental Vulnerability and Risk
VII. Water-Energy-Food-Ecosystem Nexus
VIII. Water Pollution and Eco-systems Conservancy
IX. Sustainable and Adaptive Water Resources Management
X. Remote Sensing, Artificial Intelligence, and New Technologies in Water Sciences
XI. Water Distribution and Water Treatment
XII. Groundwater Hydrology and Contamination
XIII. Non-Conventional Water Resources, Wastewater Reuse, and Desalinization
XIV. Social, Political, Institutional, Legislative Aspects, and Ethics
XV. Ecohydrological Approaches for Enhancing Water Resource Sustainability
XVI. Water Resources in Natural Ecosystems: Monitoring, Modelling, and Conserving Biodiversity

Following the Congress, selected contributions will be invited to submit extended and enhanced versions of their work for peer-reviewed publication in EWRA-affiliated journals, including *Water Resources Management, Environmental Processes, European Water*, and *Water Utility Journal*.

The editors wish to extend their sincere thanks to:

- The *University of Palermo* for hosting the event and providing a vibrant academic environment,
- All *authors and participants*, for enriching the Congress with their contributions and insights,
- The *Scientific and Organising Committees*, for their dedicated work in structuring the programme and overseeing the review process,
- The *sponsors and supporting institutions*, for their essential role in making this Congress a success.

We hope this volume serves not only as a record of academic excellence but also as a source of inspiration for continued progress toward sustainable, inclusive, and resilient water resources management.

The Editors

Leonardo Valerio Noto
Francesco Alongi
Dario Treppiedi
Harris Vangelis
Dimitris Tigkas

Table of Contents

Keynote Speakers

Driving processes of flood changes and their extreme values **3**
Günter Blöschl

Challenges in the design of infiltration basins for Managed Aquifer Recharge **5**
Aldo Fiori

Are we ready for the storms ahead? Record-shattering rainfall and flood events in a rapidly changing climate **7**
Hayley J. Fowler

Medicane induced floods. Lessons learned by the analysis and modelling of storms Ianos and Daniel **9**
Athanasios Loukas

I. Hydrological Processes in a Changing Environment

Hydrological invariance, Buenos Aires, Argentina **13**
M.P. Torrero, S.V. Viñes, P.A. Lee

Adaptation of the Yang formulas to an intermittent and an ephemeral stream **15**
L. Avgeris, V. Hrissanthou, K. Kaffas

Hydrological pathways: The impact of stable water isotopes on moisture source contribution in Brahmaputra river basin **17**
M. Nanda, A.M. Nair

A comparative assessment on the future drought characteristics of South Korea using AR6 climate change scenario **19**
M.H. Lee, S.W. Hwang

An integrated approach to baseflow estimation: a comparison of empirical methods and physically based models in the Tanagro basin **21**
M.F. Palmiero, M. Bancheri, A. Longobardi, S.B.M. Hassan

Over 150 years of streamflow behaviour inferred from freshwater pearl mussel shell $\delta^{18}O$ in northern Sweden **23**
G. Türk, C.J. Gey, B.R. Schöne, L. Pfister, H. Laudon, F. Thielen

Study on the impacts of water surface expansion on runoff in the Ob River basin **25**
G. Gan, J. Wu

Adaptive hydrologic modeling approaches for optimizing water infrastructure design and management under nonstationarity 27
K. Hunu, S. Conrad

Introducing integrated event calibration: A novel framework for rainfall-runoff modelling in urban hydrology..... 29
M.N. Assaf, S. Manenti, L. Tamellini, S. Todeschini

Mega flood events: The bivariate flow-volume frequency analysis 31
V. Tsakiris, H. Vangelis, G. Tsakiris

Analysis of evapotranspiration trends in India..... 33
V.K. Gunturu, V. Jothiprakash, B. Sivakumar

Fault-controlled groundwater flow in karst aquifers of the Italian Prealps: implications for geomorphic hazards in a changing environment..... 35
V. Francani, P. Gattinoni, L. Longoni, M. Papini

Precise determination of water surface evaporation for refining hydrological balance 37
A. Beran, A. Vizina, P. Pavlík, V. Moravec, R. Kožín

Performance assessment of two high-resolution precipitation datasets over a large basin in Southern Italy for water resources modelling..... 39
R. Padulano, A. Avino, G. Del Giudice, M. Borga, S. Manfreda

How climate change affects Hargreaves model accuracy over time..... 41
V. Rattayová, M. Garaj, M. Onderka

Assessing streamflow uncertainty in mountainous watersheds: a comparative study of two monthly rainfall-runoff models..... 43
L. Vasiliades, I. Mastraftsis

Modelling future irrigation requirements for durum wheat cultivation in southern Sardinia 45
D. Svanidze, R. Ludwig, M. Dettori, G. Urracci

Application of the UTHBAL monthly hydrological model in fuzzy environment..... 47
S. Stavris, M. Spiliotis, A. Loukas

An explorative analysis for discharge data long time series reconstruction in the Campania region 49
G. Nicoletti, A. Longobardi

Surface runoff concentration time sensitivity to several parameters involved in Log Erosion Barriers (LEBs) implementation 51
A. Stoikopoulou, G. Papaioannou

Uncertainty assessment of rainfall-runoff simulation of the Reno Italy river basin under climate change scenarios..... 53
M. Niazkar, O. Cenobio-Cruz, G. Mozzi , J. Pal, G. Di Baldassarre

Application of reanalysis data in hydrological studies: A case study in Georgia..... 55
A. Nobile, F. Zanello, F. Lubrano, M. Nicolini, E. Arnone

Using ERA5-Land reanalysis for assessing spatio-temporal trends of standardized drought indices in Sicily..... 57
T.M. Aschale, N. Palazzolo, G. Buonacera, A. Cancelliere, D.J. Peres

Seawater-freshwater interface dynamics and characterization in River Neretva estuary 59
I. Aljinović, V. Srzić, J. Čarija

Dynamical and descriptive assessment of daily rainfall in Savitri river basin, India 61
E. S. Namitha, V. Jothiprakash, B. Sivakumar

Future low flow in Bavaria: Drought characteristics under climate change and land use scenarios - a large ensemble study 63
A. Sasse, A. Böhnisch, R. Ludwig

Deep learning-assisted estimation of Manning coefficient maps using high-resolution UAV imagery for hydrodynamic modeling 65
V. Bellos, G. Kopsiaftis, M. Skamantzari, J. Tzortzis, I. Rallis, A. Doulamis

Coupling an Ecohydrological and a Biogeochemical Model: A Case Study on Enhanced Weathering in Southern Italy 67
L. Gianni, F.D. Pacia, S. Manfreda, L.V. Noto

II. Extreme Weather Events: Floods, Droughts, Geomorphic, and Coastal Risk Management

Improving hyperlocal 3-hourly urban rainfall forecasting using CNN-LSTM based downscaling 71
P. Tripathy, S. Ghosh

Medium-range forecast of flash drought using the Copernicus soil moisture global dataset 73
C. Cammalleri, S. Maffei, A. Ceppi, G. Fioravanti, A. Toreti

Analysis of upper dam failure and cascade impacts in pumped-storage hydropower systems: a case study of Brava - Sfikia scheme, Aliakmon River, Greece 75
P. Dimas, A. Lykou, A. Zarkadoulas, G.K. Sakki, A. Efstratiadis, C. Makropoulos

Knowledge-based vs. data-driven seasonal precipitation forecasts in the Mediterranean region 77
A. Senatore, L. Furnari, G. Nikravesh, F. Cortale, C. Lorenz, A. Naghibi, L.A. Cuartas, H. Kunstmann, C. Bertacchi Uvo, G. Mendicino

Estimation of flood damage costs due to climate change and storm surge in Busan, South Korea 79
S. Shin, K. Jung, J. Kim, D. Park

Identifying optimal probability distributions for SPI and SPEI drought indices in South Korea 81
H.J. Kim, E.S. Chung

Nature-based Solutions in catchment scale flood mitigation: mechanisms and limitations 83
P. Herath, R. Prinsley, B. Croke, J. Vaze, C. Pollino

Hydrological extremes: The New Zealand experience 85
J. Renwick

On the use of TCEV distribution in at-site flood frequency analysis: insights from eastern Australia 87
V. Totaro, G. Kuczera, V. Iacobellis

Non-stationary flood frequency analysis – the role of physical covariates and flood generating mechanisms 89
M.N. Khaliq

Is ERA5 dataset adequate for drought characterisation? The case of river basin areas of Peloponnese, Greece 91
P. Golfinopoulou, I.M. Kourtis, D. Tigkas, H. Vangelis

Effects of the flood event of August 2023 on the design discharge values in Slovenia 93
N. Bezak, M. Šraj

Flood forecasting in the Kosi basin (India): A comparative study of singular and hybrid NARX models utilising satellite rainfall products 95
A.K. Singh, V. Singh, T. Roshni

Stochastic rainfall simulation at sub-daily scales preserving IDF curves 97
F. Cappelli, E. Volpi, A. Langousis, R. Deidda, A. Perdios, S. Grimaldi

Urban flood management considering a Bayesian approach to analyse extreme rainfall events 99
C. Iliadis, P. Galiatsatou, J.P. De La Fuente Cusicanqui, L. Vasiliades, V. Glenis, C. G. Kilsby

Multi-objective algorithms to improve urban flood resilience. 101
C. Iliadis, J. Mckenna, V. Glenis

Unravelling the paradox of a flash flood event in northern Greece 103
S.P. Stefanidis, N.D. Proutsos, P.S. Stefanidis, D. Tigkas, I. Tsevreni

The PRIME Index: Prioritization of cultivated Regions IMpacted by drought in agriculturE..... 105
L. Cappellato, B. Moccia, E. Ridolfi, D.D. Chiarelli, F. Russo, F. Napolitano, M. C. Rulli

Evaluation of Survivability from Droughts Index (SDI) with EO-based indicators..... 107
M.C. Gunacti, C.P. Cetinkaya

Assessment of drought by precipitation variability in Mediterranean coastal countries using entropy-based analysis..... 109
F. Barbaros, D. De Ketelaere, F. Vargun, M.C. Gunacti, C.P. Cetinkaya

Advancing the detection of multi-sector drought impacts via feature extraction and multi-task learning 111
M. Merlo, M. Giuliani, A. Castelletti

Using lagged ERA5-Land soil moisture data and Artificial Neural Networks for identifying landslide triggering conditions..... 113
N. Palazzolo, D.J. Peres, G. Buonacera, A. Cancelliere

Comparative assessment of drought characteristics obtained using gridded and station datasets from India Meteorological Department (IMD) in a semi-arid basin of India 115
A. Gupta, M.K. Jain, R.P. Pandey, D.M. Hannah

Parameter sensitivity in network-based clustering: Implications for regional frequency analysis of extreme rainfall..... 117
M. Billios, L. Vasiliades

Assessing critical soil moisture to demarcate terrain stability 119
J. Thomas, L.V. Noto, R.L. Bras, E. Arnone

Red flags on the map: Exceptional rainfall and temperature events in Portugal (1980/1981 – 2023/2024) 121
L.A. Espinosa, M.M. Portela

Spatiotemporal drought patterns and their impact on water resources: A case study of Thessaly, Greece 123
A. Psilovikos, V. Leivadiotis, T. Papathanasiou, S. Sakellariou, N. Alpanakis, M. Spiliotopoulos, G. Tziatzios, I. Faraslis, N. Dalezios

A combined methodology to address the frequency of extreme discharge and precipitation: Muriaé river basin case study (Brazil)..... 125
C.L.F. Silva, M.M. Portela, J.P. Matos

A non-stationary GEV-based bias correction method..... 127
M. Onderka, J. Pecho, M. Garaj, V. Rattayová

Comparing modelling approaches to estimate the impact of check dams as a Nature-Based Solution against flooding 129
C. Ouzounis, G.Sylaios, V. Bellos

A multi-source methodological framework for drought monitoring: Integration of remote sensing and meteorological indicators 131
C. Chatzichristaki , A. Moumtzidou, K. Karystinakis, I. Gialampoukidis , S. Vrochidis, I. Kompatsiaris, M. Bügelmayer-Blaschek, T. Tötzer, D. Havlik

Development and implementation of a regional flood regression model in Pieria, Greece..... 133
S. Bouzos, A. Bournas, E. Baltas

HAMR system: seasonal discharge prediction..... 135
A. Vizina, P. Pavlík, M. Hanel, I. Georgievová, A. Beran

Meteorological drought assessment using gridded data: Case study of Croatia 137
J.F. Santos, L. Tadic,M.M. Portela, T. Brlekovic , L. Espinosa

Cynefin categories meet ensemble forecasting: A novel framework for forecast analysis 139
Z. Bovermann, J. Dietrich

An integrated strategy for improving drinking water supply system resilience to regional drought..... 141
F.Zanello, P.Martinis, V. Baù, D. Russo

Evaluation of agro-hydrological sub-seasonal forecasting within two extremely wet and dry seasons in Northern Germany 2017/2018 143
E. Fallah-Mehdipour, J. Dietrich

Flood damage assessment: A methodological approach using AI-based flood mapping 145
J. Saavedra Navarro, R. Zhuang, C. Albertini, C. Samela, S. Chaturvedi, S. Riccardi, P. Macciacchera, L. Luzietti, G. Murchio, S. Manfreda

Investigation of uncertainties in flood risk assessment under climate change in urban cities in South Korea 147
J.Y. Song, Y.H. Song, E.S. Chung

Addressing the effects of storm Daniel floods on land reclamation works in Thessaly, Greece: aftermath and restoration management..... 149
D. Tigkas, D. Papalexis, N. Proutsos, G. Sofou, H. Vangelis, K. Stournaras, G. Tsakiris

Improvement of early warning systems for flood risk with a distributed hydrological model and an analog-based precipitation forecast..... 151
M.C. Llasat, R. Marcos Matamoros, C. Guzzon, J. Arzaibar, A. Cabañas, D. Carril Rojas, A. Díaz Guilera, L. Garrote, M. Llasat-Botija, D. Marinelli, L. Mediero, O. Varela

An erosive Sicilian beach: a multidisciplinary approach to study the coastal dynamic effects..... 153
G. Manno, F. Capodici, P. Scala, G. Ciraolo

Reliable estimates of the probability of record-breaking weather extremes through the Metastatistical approach 155
M. Marani, S. Andria, M.F. Caruso, P. Devò

Estimates of point rainfall extremes from satellite precipitation products: application and testing in Northeastern Italy..... 157
C.A. Sanchez Pena, F. Marra, M. Marani

Extreme precipitation in Italy: detection of changes and trends in satellite data 159
M. Darienzo, M. Marani, F. Marra

Using agent-based modeling to address climate change in coastal areas: The case of Vouliagmeni, Greece 161
C.N. Roukounis, V.A. Tsihrintzis

Assessment methodology of flash flood susceptibility for the river basins of Sardinia (Italy) 163
J. Napolitano, D. Caracciolo, A. Cera, S. Frongia, G. La Gumina, S. Liberatore, A. Carletti

Climate change impact on compounding streamflow flood and drought characteristics in Europe 165
R.A. Odongo,T. Koenen, P. Reija Zamora, S.J. Sutanto

The characteristics of flash droughts across Thessaly, Central Greece, from 1990 to 2024 167
V. Leivadiotis, A. Psilovikos

Using complex networks in Reconnaissance Drought Index (RDI) non-stationary estimation 169
H. Vangelis, K. Spiliotis, K. Voudouris, M. Spiliotis

Unravelling the role of temperature for convective storms in Sicily 171
G. Patti, D. Treppiedi, A. Francipane, L.V. Noto

Where floodwater meets mobility: A GIS approach to bridge risk and rerouting in the Flood@Road project..... 173
L. Pavesi, F. Nardi, M. Amaddii , C.B. Amirehsan, A. Carboni, F. Castelli, P. Claps, F.P. Deflorio, M. Ferraro, P. Mazzoglio, F. Vagnon, C. Arrighi

An observational quality-controlled hourly precipitation database for Italy 175
D. Treppiedi, E. Arnone, M. Darienzo, A. Ezeaba, A. Francipane, U. Khan, M. Marani, F. Marra, L.V. Noto, R. Paranunzio, C.A. Sanchez Pena

Image-based surface velocity mapping in rivers: study case and calibration by ADCP data 177
P. Peykani, D. Termini

III. Data and Models for Environmental, Social, and Governance (ESG) Risk Assessment

Bayesian analysis in assessing water quality: lessons learned from case studies..... 181
Z. Srđević, M. Ilić-Paunić, B. Srđević

An engineering model based on the renovation times of impacted building for estimating indirect damage to residential properties 183
S. Molica, G. Brigandì, G.T. Aronica

Estimating sediment concentration, fluxes and trends in selected tributaries of the Illinois River 185
E. Getahun

Identification of critical source areas related to diffuse pollution in an agricultural watershed – using SWAT model..... 187
F.N. Dogan, G. Capar

Machine learning-enhanced flood risk assessment model for local government-level decision support..... 189
H.Park, H.W. Jee, S.B. Seo

A spatially explicit risk assessment of future climate change on ecosystem services provided by surface irrigation in the Veneto region, Italy..... 191
A. Santini, S. Balbi, Y. Casali, M. Masiero

Impact of climate change on water supply systems vulnerability to drought events: a methodological framework to assess uncertainty 193
E. Romano, F. Ercolani, E. Volpi, N. Guyennon, S. Passaretti, C. Mineo, E. Boscariol, A. Trotta, A.B. Petrangeli

Forests and wetlands as Nature-Based Solutions to address resource costs in water management: a case study in the Brenta river area 195
M. Masiero, L.F. Eusse-Villa, S. Iacopino, G. Amato, G. Laghetto, G. Cristofani, P. Gatto

Risk-based design of hydraulic infrastructures for flood risk mitigation using Cost-Benefit Analysis 197
G.T. Aronica, G.M.Sechi, M.L.V. Martina, G. Brigandì, C. Arena, A. Candela, M. Arosio, M. D'Ayala, J. Napolitano, I. Scolaro

Data-driven high-resolution rainfall reconstruction of 85-year Atlas: A two-tier approach integrating occurrence probability and magnitude 199
N. Beikahmadi, A. Francipane, D. Treppiedi, L.V. Noto

Geostatistical methods for temperature estimation: A high-resolution Atlas of daily temperatures in Sicily 201
C. Mattina, D. Treppiedi, A. Francipane, L.V. Noto

Retrospective analysis of the accuracy of SEAS5 ECMWF seasonal forecasts and their bias correction: An application to Sicily 203
F. Castaldo, A. Francipane, D. Treppiedi, L.V. Noto

The theoretically derived probability distribution of water level in detention dams 205
A. Avino, F.D. Pacia, S. Manfreda

A Digital Twin for the management of the urban drainage system and flooding events in the city of Palermo 207
M. Avanti, A. Francipane, L.V. Noto

Comparative analysis of data-driven techniques for spring yield prediction 209
G. Gullotti, C. Arena, M. Cannarozzo, L.V. Noto

A novel Data Cube framework for environmental and climate change monitoring in coastal areas 211
I. Kavouras, G. Kopsiaftis, I. Rallis, N. Bakalos, A. Doulamis, N. Doulamis, D. Kalogeras

IV. Geo-information and Water Resources

Assessment of potentially vulnerable glacial lakes of the Eastern Himalayan region 215
A.K. Shukla, I. Ahmad, S.K. Jain

DATASET: GrounDwater sAlinizaTion and pollution AsseSsmEnt Tool: a holistic approach for coastal areas 217
G. Busico, D. Potrykus, M. Mastrocicco

Dam break assessment and flood hazards mapping of Minimata Bango dam 219
G. Sahu, I. Ahmad

Assessment of snow water equivalent reanalyses and improving snow process simulations in rainfall-runoff model across Northern Italy 221
G. Sarigil, M. Neri, F. Avanzi, E. Toth

AQUADMC: Smart solutions for a sustainable aquaculture value chain 223
V. Santarsiero, D. Iasillo, G. Ceriola, L. Martino, C. Rossignoli, L. Longobardi, A. Aiello

High resolution agricultural water demands on refined crop-specific spatializations 225
N. Galli, H. Nanesha, A. Tolazzi, D.D. Chiarelli, M.C. Rulli

Estimation of soil runoff in a fire affected mountain landscape..... 227
F. Diana, G. Busico, M. Mastrocicco. S. Castaldi

Assessment of potential evapotranspiration formulas at catchment scale for rainfall-runoff modelling around the globe..... 229
G. Selleri, M. Neri, E. Toth

AMAPGeo: Smart water infrastructure for water management 231
T. Borruso

Assessment of flood vulnerable areas in the river basin district of Thrace 233
C.S. Pantoulas, I.M. Kourtis, H. Vangelis, I. Nalbantis, V.A. Tsihrintzis

Evaluation of the effectiveness of satellite data in hydrological modeling using SWAT model..... 235
S.N. Yeşilyurt, G. Onuşluel Gül

GEOframe: A first attempt of regionalization on Sicilian basins..... 237
D. Ciriminna, G. Formetta, A. Francipane, L.V. Noto

IHACRES model regionalization for water resource management in Sicily 239
C. Alonzo, F. Alongi, A. Francipane, L.V. Noto

V. Climate and Land Use Changes

An integrated method for the characterization of climate change scenarios 243
J. Kim, M.H. Lee, J.H. Ahn, S.B. Seo

Water storage strategies to adapt to climate change: the case of Val d'Orcia, Central Italy..... 245
L. Villani, G. Castelli, E. Forzini, I. Bouizrou, L. Piemontese, G. Bertoli, M. Lompi, A. Giuliano, T. Pacetti, E. Caporali, E. Bresci

The impact of hydraulic-hydrological model calibration on SuDS assessments: preliminary analyses..... 247
R. D'Ambrosio, A. Longobardi

Land use and solar power: Maximizing photovoltaic potential in Singapore 249
S. Maroufpoor, X.S. Qin

Monitoring soil sealing in the Mediterranean: The ESA Ulysses project for sustainable land management..... 251
D. Iasillo, V. De Pasquale, P. Di Lauro, V. Santarsiero, W. De Simone, L. Congedo , M. Munafò

Evaluation of heat stress in a Mediterranean watershed under the influence of climate change 253
H. Boyacioglu, M.C. Gunacti, F. Barbaros

From IDF curves to urban drainage systems parameters in the context of climate change: an application on Vilnius, Lithuania 255
L.A. Gomez-Mogollon, L. Napolitano, G. Rianna, R. Padulano, K. Virsilaite

Climate and land-uses changes contribute to water scarcity in a rural basin..... 257
A. Yfanti, I. Kourtis, M.P. Papadopoulou

Using uncertain rainfall projections in hydrological models: An approach to collate practical insights for decision-making under climate change..... 259
F.M. Mourot, D.J. Irvine, T.A. Remenyi, L.B. Hutley, R.S. Crosbie, C.R. Moore

Evaporation fraction presented in a climatic energy balance diagram illustrates climate change and its consequences 261
L. Báder

Flood frequency analysis of two Mediterranean river basins by using convection-permitting model projections and a rainfall-runoff model 263
M. Lompi, J. El Jeitany, O. Boulariah, F. Viola, M. Borga, R. Deidda, E. Caporali

Hydrologic and hydraulic modeling of an urban area using SWMM: climate change and land use impacts 265
A.V. Tsihrintzis, I.M. Kourtis, E. Baltas

A long-term analysis for changes in temperature regime over Sicily 267
D. Treppiedi, C. Mattina, N. Scinta, A. Francipane, L.V. Noto

A semi-analytical approach for drainage network sizing and verification 269
D. Martino, D. Pirone, A. D'Aniello, L. Cimorelli, D. Pianese

VI. Environmental Vulnerability and Risk

Impact of light-absorbing impurities in snow on snowmelt runoff and hydrological processes in the Ili basin, Central Asia 273
B. Wu, J. Abuduwaili

Risk assessment of land-based marine debris in an estuarine ecosystem with high river discharge in South Korea 275
C.K. Kim, K.S. Kim, H.J. Hong, K.Y. Bang

Water management in disasters: an analysis of recent earthquakes and risks in Turkey 277
E. Tuncbilek, G. Capar

Investigating heavy metal contamination in soil-water systems: a case study of Hindon tributary, India 279
P. Dwivedi, B.K. Yadav

Assessment of sediment production in transboundary Douro River Basin 281
M. Ferreira, J. Mendes, R. Maia

On the correlation between earthern leeves' vulnerability to seepage and flood events probability of occurrence 283
B. Bonaccorsi, S. Barbetta, L. Ciabatta, M. Dionigi, G.T. Aronica

GIS-based flood vulnerability mapping using fuzzy AHP: An integrated indicator approach 285
E. Efraimidou, M. Spiliotis

Investigation of the habitats' state in Natura 2000 site coded "GR1410001" in Lake Tavropou area 287
A. Psilovikos, T. Papathanasiou, I. Vergos

Understanding the relationship between ecosystem services and pressures of islands: Fuzzy-cognitive modelling approach 289
M. Ilić Paunić, R.M.Pacheco, A. Moustakas, Z. Srđević, B. Srđević

Flood exposure of environmental assets in Tuscany, Italy 291
G. Bertoli, C. Arrighi, E. Caporali

Challenges in determining the displacement of anti-personnel landmines by flooding 293
G. Keve, B. Abonyi, S. Krikovszky, D. Csátaljay, Z. Kovács, I. Ember, J. Padányi

Effectiveness of emergency postfire rehabilitation treatments in Mediterranean forests: A nature-based solution for erosion control 295
N. Proutsos, A. Bourletsikas, S. Stefanidis, A. Solomou, P. Michopoulos

Drought vulnerability parameters: a literature review 297
A. Theodoroulis, H. Vangelis, V.A. Tsihrintzis

Vulnerability assessment of wastewater treatment plants using a territorial multi-hazard multi-scale approach 299
M. Castiglione, S.F. Corsino, M. Capodici, M. Torregrossa

Assessing the Individual Flood Risk index to identify areas with lower risk sustainability 301
D. Biondi, G. Capparelli, D. Spina, F. Cruscomagno

VII. Water-Energy-Food-Ecosystem Nexus

Setting greenhouse gas mitigation targets in the water sector through cost-effective approaches 305
H. Han, D. Ahn, B. Hwang

Metals concentration in selected fish species available in Polish food markets 307
P. Biedka, I.A. Tałałaj

How farm management can improve the ability of soil to retain water: Adaptation to less water for agriculture in Europe 309
A. Iglesias, A. Sordo-Ward, D. Santillán, L. Garrote

The uncertainty of agricultural production: A case study from Pianura Padana 311
D.D. Chiarelli, E. Volpi, A. Fiori, M.C. Rulli

Integrating a pumped-storage hydropower plant with photovoltaics: impacts on energy production and on the water resource system 313
D. Micocci, C. Bragalli, E. Toth, M. Zappa

Empowering smart renewable cities through hydropower technology in urban drinking water supply system 315
Á. Alcaide Royo, C. Sánchez Briones, A. Pérez Lleó, A. Gamón, R. Ponz Carcelén, H. Royo, M. Pedro Monzonís, C. de Diego, G. Dasí, T. Oltra Benavent

Assessing the water footprint of livestock feed: insights from a global analysis 317
C. Govoni, D.D. Chiarelli, M.C. Rulli

Users perspectives on water access management and technologies in irrigation distribution systems 319
G. Ferrarese, D. Troiani, S. Malavasi

Navigating climate change: The water-food nexus and its role in durum wheat production in Mediterranean regions 321
M. Grosse-Heilmann, E. Cristiano, G. Pusceddu, M. Marrocu, F. Viola, R. Deidda

Water-Energy-Food-Ecosystem Nexus factors driving global agrivoltaic potential. 323
N.Galli, M. Curioni, F. Capone, G. Manzolini, M.C. Rulli

Enhancing irrigated agroecosystem resilience through a Nexus approach with numerical modelling and multidimensional indicators 325
V.R. Coletta, U. Fratino, N. Lamaddalena, S. Mohammedi, I. Portoghese, A. Pagano

Mapping a Water-oriented Energy Food Ecosystems (WEFE) Nexus in the Nestos / Mesta river basin 327
C. Papadopoulos, D. Latinopoulos, M. Karasani, I. Kagalou, , C. Stylios, M. Spiliotis

A socio-hydrological analysis of the Water – Energy – Food - Ecosystems Nexus in a meso-scale watershed in Northern Italy 329
E. Lucca, G. Castelli, J. Sušnik, J. Wenninger, L. Villani, L. Piemontese, E. Bresci

Analysis of water scarcity through the lens of Water – Energy – Food – Ecosystem (WEFE) Nexus approach at basin scale: A study from Mahi basin, India 331
G.E. Nagashree, A. Sharma

Assessing water scarcity hotspots with refined water demand data for Italy 333
F. Capone, N. Galli, C. Govoni, H. Nanesha, D.D. Chiarelli, M.C. Rulli

Towards a climate resilient region through systemic solutions and innovations: the Bavarian case study in the ARSINOE project 335
A. Böhnisch, I. Beck, M. Zilker, G. Braun, R. Ludwig

Replacing staple crops with pulses to meet sustainable diet targets while ensuring water savings 337
L. Ricciardi, P. D'Odorico, D.D. Chiarelli, M.C. Rulli

Assessing flood impact on agriculture: A high-resolution hydrodynamic approach for crop damage evaluation 339
T. Lucaora, A. Annis, F. Nardi, M.C. Rulli, D.D. Chiarelli

VIII. Water Pollution and Eco-systems Conservancy

Impacts of intensified water pumping on the aquifer and wetlands in a region of the Southern Mediterranean 343
A. Hani, S. Hani, N. Bougherira, S. Lallahem, H. Chaffai, L. Djabri

Persistent organic pollutants as indicators of contamination status in surface waters of western Tianshan Mountains, Kyrgyzstan 345
B. Shen, J. Wu

Evaluating effectiveness of technical interventions on lake health: A case from Bengaluru, India 347
P. Jamwal

Bacteriostatic activity of ion-exchange samples of the Armenian clinoptilolite as new effective sorbent for aqueous systems purification 349
L. Harutyunyan, A. Manukyan, K. Nazaretyan, H. Sargsyan, N. Dolaberidze, M. Nijaradze, N. Mirdzveli, V. Tsitsishvili

Exploring microbial contamination in the Vjosa river: A year-long study 351
K. Peli, B. Parllaku, M. Lika, A. Lugaj, S. Amalfitano, E. Hamzaraj

Assessing the health of the Erzeni River: a multidimensional approach to water quality 353
E. Hamzaraj, V. Gjeci,B. Parllaku, P. Lazo, A. Paparisto, E. Keçi, S. Duka, L. Vallja

Analysis of transport of selected heavy metals to the Baltic Sea along the continuum of the largest Polish rivers - Vistula River case study 355
D. Matuszewska, E. Kiedrzyńska, M. Kiedrzyński

A GIS-grid nonpoint pollution and self-purification model for hydropower reservoirs 357
J.R. Ribas, M.E.A. Fariña, J.C.R. Severo, L.S. Santos , J.V.F. Guedes

'Prove to me it's my molecule of nitrogen': Nitrate-sensing technologies and water quality engagement with Australian farmers 359
A.M. Davis, L. Buono, T. Webster

Storage of drinking water in underground concrete tanks: The case of Tajoura, Libya 361
B. Brika, N. Elaziby, M. Orhuma

Numerical study of the formation of water pollution zones from various industrial emissions..... 363
A. Issakhov, A. Sabyrkulova, A. Abylkassymova

Numerical investigation of air and air-water jets in two-layer stratified flow 365
E. Budak Cotel

Bacterial communities of water and sediment of an artificial reservoir in Mexico: their metabolic inference and biotechnological potential 367
J. Cordovillo-Armijo, M.J. Aguilar-Méndez, N.G. Rojas-Avelizapa, A.M. Rivas-Castillo

Circular economy and biodiversity in the treatment of wastewater using an industrial waste - LIFE RENATURWAT..... 369
M. Añó, P. Almenar, J. Macián-Cervera

Impacts of long-term poultry manure applications on subsurface drain water quality under continuous corn production systems..... 371
S. Lenka, N. Hoover, M. Soupir, D. Anderson, R. Kanwar

Investigation of microplastics in five natural Greek lakes..... 373
G. Kehayias, P. Kanellopoulou, A. Kechagias, A.E. Giannakas, C.E. Salmas

Distribution, sources and risk assessment of polycyclic aromatic hydrocarbons (PAHs) in waters of Amu Darya Basin, Uzbekistan 375
M. Jin, J. Wu, S. Zhan, S. Shakhimardan

Use of machine learning tools in predicting contaminant removal in full-scale coal mine water treatment schemes 377
A. Almpanis, V.G. Ioannidou

Roles of riverine wetlands in diffusive greenhouse gas emissions: Comparative insights from before and after wetland destruction 379
W. Zhang, H. Li

Are combined sewer overflows from wastewater treatment plants a critical source of microplastics discharge into water bodies? 381
G. Beringheli, S.F. Corsino, M. Capodici, M. Torregrossa

IX. Sustainable and Adaptive Water Resources Management

Questioning efficiency targets at river basin scale: A practical assessment in southern Spain 385
A. Expósito, C. Gutiérrez-Martín, F. Delgado, J. Berbel

Recovery of metals from livestock bio-sludge with acetic acid extraction followed by biosorption of baker's yeast 387
J.J. Su, K.W. Yen, W.C. Chen

Rainwater harvesting system as a solution for increasing the water self-sufficiency of road infrastructure facilities 389
A. Stec, D. Słyś

Impact of LID area segments and design storms on optimal LID combinations 391
J.H. Lee, S.T. Chae, I. Park, E.S. Chung

Modelling scenarios for sustainable water supply and demand in Annaba city, Algeria 393
S. Hani, I.E. Bouznad, N. Guezgouz, A. Hani, S. Lallahem

RICHWATER nutrients calculation tool for water and fertilizers sustainable and adaptive management 395
A.M. Lorenzo-López, R. Casielles, Á. García

Comparative models of sustainable urban drainage systems in a watershed in central Mexico 397
L. Lizárraga-Mendiola, O.S. Areu-Rangel, G.A. Vázquez-Rodríguez, J.R. Pérez-Hernández, C.M. López-León

River velocity distribution and discharge estimation using entropy theory: an application at river site in Central Apennines (Italy) 399
E. Boscariol, S. Passaretti, M. Lapomarda, E. Volpi, C. Mineo, A. Trotta

Supervised approaches for a sustainable water resources management: Forecasting and "similarity" procedure 401
S. Passaretti, N. Guyennon, C. Mineo, E. Boscariol, A.B. Petrangeli, A. Varriale, E. Romano

Estimation of the current and future potential sediment transport capacity of the Ebro River 403
L. Garrote, D. Santillán, F. Martin-Carrasco, A. Iglesias

Sustainable adaptation of urban areas: the case of a Hamburg neighbourhood 405
A. Bornancin, N. Manojlovic, A. Marzadri, G. Formetta

Development of resilient and adaptable drainage system through the integration of multiple SuDS techniques 407
R.N. Nyawo, T.T. Tanyimboh

Enhancing water availability in Mediterranean basins through improved reservoir management 409
P. Bianucci, A. Sordo-Ward, L. Garrote

Traditional Water Management Systems (TWMS) for climate change adaptation: Case study of Jaipur, India 411
K. Bimrah, I. Saizen

Floating Photo Voltaic on reservoirs: a sustainable solution with challenges 413
F. Viola, M. Lo Iacono, F. Lo Iacono

Retrospective analysis of water availability in Sardinian reservoirs 415
F. Viola, P. Corongiu, C. Jakomin, R. Deidda

Adapting reservoir operating rules in a changing climate for a sustainable management of drinking water sources 417
M. Neri, E. Toth

Degradation testing of PET bottles as floating covers in reservoirs 419
V. Benjaoran, L. Raksaksri, J. Settakhumpoo

A decision support tool for rainfed rice cultivation: Integrating rainfall patterns and ENSO predictions 421
T. Supriyasilp, K. Pongput, N. Nongharnpitak, A. Sapet, J. Khiripet

Enhancing streamflow prediction using hydroclimatic variables and machine learning: A case study of the N'fis basin, Morocco 423
M. Naim, B. Bonaccorso

Modeling and projecting hydropower production across the Upper Colorado River Basin 425
F. Marconi, G. Villarini, T. Kim, H. Kim, E. Ridolfi, F. Russo, C. Veatch, W. Veatch, F. Napolitano

Investigation of a river basin water potential use under climate change and demand management scenarios 427
C.P. Cetinkaya, E. Mammadli

Guiding SmAR placement: The role of irrigation water demand 429
H. Nanesha, M. Lompi, M.S. Goodarzi, N. Galli, E. Caporali, M.C. Rulli, D.D. Chiarelli

Multi-site stochastic precipitation scenarios for water management 431
A. De Vera, R. Terra

Assessment of urban stormwater quality by informing a hydrologic-hydraulic model with microscopic traffic simulations. 433
G. Formetta, A. Marzadri, M. Guerrieri

Towards digital twin for sustainable irrigation water management in Mediterranean agriculture 435
A. Borgo, M. Debolini, G. Rianna, S. Mereu

Integrating multimodal seasonal forecasts with SWAT to predict seasonal water availability in the Imera Meridionale river basin, Sicily 437
S. Lemma Tekle, B. Bonaccorso, P. Block

Hydrologic conditions quantification for sustainable water resources management of ungauged river basin 439
B. Matić, B. Karleuša

Water scarcity and future management scenarios assessment in Naxos island, Cyclades, Greece 441
S. Mike, M. Ntoi, A. Lyra, G. Tziatzios, N. Mylopoulos, A. Loukas, L. Vasiliades, P. Sidiropoulos

Improved methodology for closing water balances and modeling water levels in a reservoir-lake system: Application to Lake Velence, Hungary 443
M. Chappon, K. Bene, A. Kálmán

A self-assessment tool for climate adaptation in urban water management: the water sensitive cities index..... 445
T. Pilevneli, G. Ozerol, G. Capar

The "Cistern City Concept" for climate change coping (the 3 for 3 Cs): an integrated solution related to water resources management in cities 447
F. Megdiche-Kharrat, F. Belcadhi

Generating synthetic wind speed time series: An analysis of Negra et al., Weibull, Haar and Daubechies Wavelets approaches..... 449
S. Skroufouta, E. Baltas

Application of nanobubbles on growth and quality of lettuce (*Lactuca Sativa L.*) under variable salinity water range in hydroponic systems..... 451
K. Zoukidis, A. Gertsis, C. Kissoudis, E. Mouratidou, V. Hantzara, R. Kosheleva, A. Apostolidis, G. Strouthopoulos, A. Giannakoula

Balancing water scarcity and stakeholder interests: A study on water management challenges and solutions in the Lake Velence area 453
A. Kálmán, M. Chappon, K. Bene

Application of nanobubbles irrigation technology, in combination with biostimulants, in leafy vegetables production using hydroponic grow bags 455
K. Zoukidis, M.T. Chatziathanasiou, A. Gertsis, C. Vasilikiotis, A. Apostolidis, A. Varoutoglou, E.P. Favvas

Evaluation of irrigation with nanobubble-enriched water in combination with Biostimulants on lettuce production (*Lactuca sativa L.*)..... 457
K. Zoukidis, M.T. Chatziathanasiou, A. Gertsis, C. Vasilikiotis, A. Apostolidis, A. Varoutoglou, E.P. Favvas

Formulation of an optimization framework for pumped storage with floating photovoltaics integration: Towards smart hydropower 459
P. Dhawan, M. Righetti, A. Puchkova, M. Herrera

X. Remote Sensing, Artificial Intelligence, and New Technologies in Water Sciences

How digital revolution is reshaping water resources management? Insights from Spain 463
A. Expósito, E. Díez-Cebollero

Remote sensing and direct monitoring of plant salinity stress in a coastal back-barrier environment in Volturno Licola Falciano natural reserve 465
E. Giuditta, L. Alessandrino, N. Colombani, M. Mastrocicco

Validation of ET interpolation for the new Landsat Provisional Actual Evapotranspiration (ETa) product in semi-arid climate 467
J.M. Carricondo-Antón, A. Garcia-Prats, M.A. Jiménez Bello, J. Manzano Juarez, V. Jiménez, Ll. Simón, F. Montoya, M.Pulido-Velazquez

Mapping irrigated farms using actual evapotranspiration and machine learning for woody crops 469
M.A. Jiménez Bello, J.M. Carricondo-Antón, A. Garcia-Prats, E. López-Pérez, J. Huertas-Bastidas

Modernizing the Hydroclimatic Atlas: Building for transparency, robustness and sustainability 471
G. Rondeau-Genesse, L. Arnal, L.P. Caron, E. Mailhot, J. Pelletier-Dumont, R. Turcotte, R. Arsenault, J.L. Martel

Regional frequency analysis for design flood estimation using EANN and GAM models with sensitivity analysis in South Korea 473
J. Kim, K. Jung, S. Shin, D. Park

Lab-on-a-chip system for real-time monitoring of emerging contaminants in water and sewage systems 475
R. La Cognata, S. Piazza, G. Freni

Integrating weather forecast into a physics-based model for short-term soil moisture and temperature prediction 477
M. Hájková, M. Kuráž

Enhancing rainfall monitoring in urban areas by integrating crowdsourced personal weather stations into official networks 479
B. Moccia, P. Mazzoglio, E. Ridolfi, F. Russo, P. Claps, F. Napolitano

From coarse to fine: Relative humidity downscaling using AI model 481
S.K. Jha, V. Gupta

Comparison of machine learning methods for the prediction of Water Quality Index 483
Ç. Coskun Dilcan, H.T. Gültaş, Y. Ahi, D.D. Köksal

Integrating machine learning models to assess treated wastewater quality and agricultural reuse potential 485
H.T. Gültaş, Y. Ahi, Ç. Coşkun Dilcan, D.D. Köksal

Human-AI teaming for water quality documentation analysis with large language models 487
S. Conrad, J. Rodriguez, G. Vizarreta Luna

3D visualization of hydrodynamic models for virtual reality to predict and interpret the level of flood risk for the general public 489
K. Micko, M. Dobransky

Preliminary results on water quality modelling and mapping in a small river using UAV multispectral imagery **491**
K. Vatitsi, K. Bellos, D. Latinopoulos, C.S. Akratos, I. Kagalou, V. Tsioukas , G. Mallinis

Seamless retrieval of coastal water quality from Landsat-9 and Sentinel-2 imagery based on an AI-enhanced physical model **493**
M. Niroumand-Jadidi, L. Mentaschi, S. Silvestri

Neural networks for hydrological modelling in Santa Lucía basin, Uruguay **495**
F. Vilaseca, A. Castro, C. Chreties, A. Gorgoglione

A comprehensive comparative study on potential evapotranspiration in mainland Portugal based on reanalysis data **497**
J.P. Pegas, M.M. Portela, J.F. Santos

Effects of urban green areas on heat islands with large impact on urban water demand **499**
M.B. Akduman, A. Gül

An innovative initiative in water education based on digitalization through extended reality learning environments: WATERLINE **501**
G. Onuşluel Gül, O.C. Doğanlar, A. Gül, E. Zammit, A. Rizzo, D. Scerri, M. Š ťastná, D. Prochazka, P. Oppeltová, M. Ćirić, V. Milošević, M. Gocić, A. Chen, M.B. Johns, J.H. Körber, W. Ravyse

Enhancing the performance of a flood early warning system with the incorporation of SMOS satellite-soil-moisture data **503**
S. Narbondo, C. Chreties

Bridging global teleconnections and local data for subseasonal-to-seasonal forecasting of Lake Como inflows **505**
G. Palcic, G. Ascenso, M. Giuliani, A. Castelletti

Comparison of two innovative devices for water treatment in production of nanobubbles under regular and saline water **507**
K. Zoukidis, A. Gertsis, N. Kasviki, R. Kosheleva, I. Avdana, A. Giannakoula

Laboratory analyses for beach litter detection via remote sensing **509**
L. Corbari, M. Minacapilli, G. Ciraolo, Fulvio Capodici

Evaluating the capability of multispectral satellite images in identifying small agricultural reservoirs (SmARs) **511**
M.S. Goodarzi, M. Lompi, G. Bertoli, N. Mannucci, T. Pacetti, E. Caporali, D.D. Chiarelli

Towards estimating water use efficiency of irrigated orchards from remote sensing: an application to a citrus orchard in Sicily **513**
D. De Caro, O. Merlin, V. Rivalland, V. Simonneaux, G. Boulet, M. Ippolito, F. Capodici, C. Cammalleri, G. Ciraolo

Tracking water resources in Sicilian reservoirs: A Google Earth Engine application using Sentinel-1 SAR and machine learning **515**
C. Martins Jr, G. Ciraolo, F. Capodici, M. de Marchis

Optimizing image-based surface velocity measurements: sensitivity to graphical enhancement and processing parameters **517**
S.F. Dal Sasso, F. Alongi, R. Ljubičić, D. Pumo, L.V. Noto

Physics-informed neural networks for flood modelling: A conceptual framework **519**
M. Herrera, V. Glenis, X. Xie, B.M. Brentan

XI. Water Distribution and Water Treatment

Decision support tools for early warning and optimized surveillance of drinking water quality from source to tap 523
M. Rodriguez, C. Ortiz-Lopez, A Carabin, A. Ardila, G. Pelletier, C. Bouchard, C. Dorea

Anomaly detection in water distribution networks based on the analysis of differential pressure values 525
F. Mazzoni, V. Marsili, S. Alvisi

Kinetic and isotherm evaluation of simazine adsorption using natural Chilean zeolites: Basis for process optimization 527
S. Sanzana, A. Fenti, P.Iovino, A. Panico

Supporting regulation and planning in real water distribution systems by water loss performance indicators 529
S. Ripani, S. Piazza, L. Berardi, D.B. Laucelli, G. Freni, O.Giustolisi

Prospects for PFAS removal from wastewater using nitrogen-containing mesoporous silica 531
O. Dudarko, P. Agback, T. Agback, G. Seisenbaeva

A new perspective on head loss estimation in water systems: Refining the Hazen-Williams equation 533
N. Samarinas, C. Arapakis, C. Evangelides, A. Loukas

Residential water consumption data: integrating parametric and non-parametric approaches to select suitable probability models 535
A. Cozzolino, R. Padulano, G. Del Giudice

Resilience and performance indices for water supply systems: The case study of Valle Umbra 537
M. Ferrante, G. Piccirillo, F. Provvisiero, F. Rossi, S. Schiaroli

LIFE SAFE_T_WATER: Validation of a new natural organic polymer for drinking water treatment 539
M. Añó, P. Almenar, J.F. Cabeza

Combining SCADA and smart meter data to improve anomaly detection at the DMA-level 541
C. Cincotta, L. Pedroni, M. Lombardi, G. Nicoli, L.C. Zingali, C. Bragalli

Liquid and solid phase effects of elevated bioreactor dissolved oxygen 543
G. Posadas, K. Davis, S. Miller

Water meter management in water distribution systems: An experimental analysis 545
A.N. Rizvanoglu, F.B. Guneysu, I.E. Karadirek

Short-term water demand forecast using machine learning models in northern Italy across different time resolutions 547
M. Niazkar, A. Menapace, F. Peretti, M. Righetti

Surplus volumes in the Hornád river basin in eastern Slovakia 549
P. Nagy, M. Zeleňáková, R. Fijko, P Purcz

An innovative management strategy for WDN under water scarcity conditions 551
L. Bozzelli, D.B. Laucelli, D. Laforgia

Emerging contaminants occurrence and treatment with Natural Based Solutions: A pilot setup 553
M. Perdikaki, E. Chrysanthopoulos, K. Markantonis, P. Kofakis, E. Efstathiou, S. Samios, I. Dafnos, G. Fragkogiannis, A. Kallioras

Deep learning approaches for water distribution networks: A comparative study on pressure estimation 555
G. Restuccia, F. Giuliano, A. Pagano, D. Croce, D. Garlisi, I. Tinnirello

A novel methodological approach to handle high-turbidity events of drinking water treatment plant..... 557
F. De Marines, A. Cosenza, M. Capodici, M Torregrossa, G. Viviani, S.F. Corsino

Water loss estimation and pipe deformation in water distribution network: Laboratory and numerical experiments..... 559
M. De Marchis, F. Bruno, D. Saccone, G. Freni, E. Napoli

Lab experiments on an innovative smart pipe for potable water supply..... 561
F. Bruno, G. Freni, C. Giaconia, M. De Marchis

Investigating transient flow phenomena and measurement accuracy in revenue water meters..... 563
F. Traina, A. Vella, F. Lo Valvo, S. Sapienza, C. Giaconia, M. De Marchis

Distributed vibration monitoring system for AI leakage detection 565
F. Lo Valvo, A. Vella, S. Sapienza, F. Di Puma, K. Ladjeri, G. C. Giaconia

Impulsive force acquisition system for drop test stress analysis on composite materials 567
S. Sapienza, A. Vella, F. Lo Valvo, R. Miranda, M. Luciano, V. Fiore, A. Valenza, C.G. Giaconia

Synchronous data aggregation system for flow and pressure measurements in water distribution networks..... 569
A. Vella, S. Sapienza, F. Lo Valvo, F. Traina, M. De Marchis, G.C. Giaconia

XII. Groundwater Hydrology and Contamination

Managed aquifer recharge as an effective climate change adaptation strategy: a case study in Friuli Venezia Giulia region, Italy..... 573
M. Sufyan, G. Martelli, P. Teatini, D. Goi

Groundwater index development for mapping suitable borehole sites: A case study of the Dakhla aquifer, southwestern Morocco 575
Y. Ez-zaouy, L. Bouchaou, A. Saad, A. Afquir, G. Busico, M. Mastrocicco, M. Bordbar, F. Raibi, S.M. El Kanti, M. Hssaisoune, Y. Ait Brahim

Multi-dimensional assessment of groundwater sustainability in South Korea using groundwater sustainability management indicators..... 577
Y. Hyun, A. Jeong

Modelling scenarios of contaminant transport in an equivalent porous medium..... 579
A. Campobasso

Hydrological modelling of a fractured volcanic aquifer: Interactions between anthropogenic usage and the natural system 581
M. Silipigni, C. Di Salvo, E. Preziosi, I. Borzì, B. Bonaccorso

Assessment of groundwater nitrate pollution in agricultural catchments at the southwestern Thessaly plain, Greece 583
V. Sapountzis, G. Tziatzios, A. Lyra, P. Sidiropoulos, A. Loukas

Integrated modelling of diffuse and point-source pollutants fate and transport in surface water and groundwater using SWAT+gwflow..... 585
L. Estrada, R.T. Bailey, V. Acuña

Determination of baseline values in evaporitic aquifers: A case study from southern Sicily (Montallegro-Siculiana area) 587
E. Rotigliano, F. Lo Medico, P. Rizzo, C. Cappadonia, F. Celico

Assessment of the NPI index in Algerian bottled water 589
N. Bougherira, D. Nechem, H. Bouguerra, L. Djabri, H. Chaffai, A. Hani, S. Ouled Meriem

Control of seawater intrusion in semi-arid Mediterranean islands through brackish groundwater desalination and artificial recharge 591
V. Christelis, G. Kopsiaftis, K. Mazi, A.D. Koussis

Simulation and optimization of the Agia aquifer in Crete 593
G.P. Karatzas, N.A Diangelakis

XIII. Non-Conventional Water Resources, Wastewater Reuse, and Desalinization

Use of nanofiltration and reverse osmosis filtration for treatment the rainwater runoff from expressway 597
I.A. Tałałaj, P. Biedka

Development of a proxy for optimally treated wastewater chemical composition focused on fertigation purposes 599
A. Osorio, A. Panico, G. Busico, M. Mastrocicco

Assessing environmental impacts in rice production with treated domestic wastewater: a life cycle perspective 601
Y. Ahi, H.T. Gültaş, Ç. Coşkun Dilcan, U. Çebi, M.A. Gürbüz, S. Özer, G. Yıldız Töre, Ü. Geçgel

Evaluation of efficiency of MOFs/MOFCs to serve as adsorbent material to remove heavy metals from the effluent of constructed wetlands 605
D. Matziri, M P. Christodoulou, A. Gropali, E. Hadjikyprianou, I. Stavrakakis, P.K. Simeou, N. Remmas, K.N. Pantelis, P. Melidis, A. Tasiopoulos, S. Ntougias

XIV. Social, Political, Institutional, Legislative Aspects, and Ethics

The inviolability of water? On the trail of state violations of the norm 609
E. Pohnerová

Cascading effects of carbon neutrality: multi-tiered transition risks in floating solar, offshore wind, and hydropower 611
H.W. Jee, S.B. Seo

Assessing young people's emotions and perceptions on climate crisis after experiencing a major flood hazard in a Mediterranean region 613
I. Tsevreni, D. Tigkas, A.M. Kali, H. Vangelis, N. Proutsos

Trust deficit and rumours as drivers of community opposition to rural water management reforms in Ghana 615
E.O. Denchie, K. Lo

Establishing shared governance and R&I strategies: WATERLINE 617
S. Duman, M. Šťastná, M. Menšíková, P. Oppeltová, O. Ulrich, D. Procházka, J. Zloch, G. Onuşluel Gül, S.N. Yeşilyurt, H. Boyacıoğlu, F. Barbaros, M.C. Günaçtı, A. Chen, M. Gocic, A. Gül, R. Hassan, P. Leskinen, M. Mistretta, E. Zammit

Model-assisted cost-benefit analysis for regional water supply systems: understanding the tools 619
C. Arena, M. Cannarozzo, G. Gullotti

Local river basin water retention developments: Requirement for governance instruments 621
R. Ernsteins, T. Bringulis, K. Konkovs, A. Skute

XV. Ecohydrological Approaches for Enhancing Water Resource Sustainability

An ecohydrological waterfront management approach associated with civilian science 625
T. Shim, H.W. Jee, S.B. Seo

Estimation of wetland water balance using the WetMAT lumped model in different hydrological contexts 627
C. Panciera, I. Portoghese, A. Pagano, R. Giordano

Key steps in the E-Flow definition under the climate change impact at the river basin scale 629
G. Ćosić-Flajsig, B. Karleuša, Ivan Vučković, G.Volf

A simulation-based study on the effect of bed topography on wetland performance 631
A. Bottacin-Busolin, G. Santovito, A. Marion

Framing the Nature Based Solutions (NBS) in Lake Karla (Thessaly, Greece): What's the status after the Storm Daniel disaster? 633
I. Kagalou, I. Vergos, D. Latinopoulos

A novel framework to assess the hydrological connectivity of lake wetlands in plain river networks with dense hydraulic facilities 635
S. Yang, R. Wan, G. Yang, B. Li

XVI. Water Resources in Natural Ecosystems: Monitoring, Modelling, and Conserving Biodiversity

Comparing hydrologic models for improved discharge simulations in regional earth system models for the Euro-Mediterranean region 639
M. Hamitouche, G. Fosser, A. Anav

Spatio-temporal changes of littoral macrophytes along hydrological conditions in Yliki, a Greek lake 641
E. Mavromati, V. Giourieva, D. Papadimos, A. Apostolakis, V. Tsiaoussi

Assessment of minimum ecological water requirements in Lake Pamvotida – Greece, using an adaptation of the IFIM method 643
D. Papademos, V. Chrysopolitou, H. Hadjicharalambous, E. Karadimou,D. Bousbouras, I. Leonardos, I. Kagkalou, K. Chiotelli

Application of a 2D-hydrodynamic model to assess the impact of spring water discharge into Lake Pamvotida in Ioannina, Greece 645
K. Zachopoulos, D. Papademos

Risk assessment of Ramsar areas: A multi-criteria and social choice approach to information base expansion and reduction 647
B. Srđević, M. Ilić-Paunić, Z. Srđević, S. Ždero

Developing a new criterion to evaluate monthly streamflow modelling in frequency domain 649
S. Piran, U. Panu

Use of a lake coupled hydrodynamic/ecological numerical model to help integrating Nature-based Solutions into environmental urban planning 651
C. Dresti, A. Fenocchi, C. Cammalleri, G. di Chiano, G. Becciu

Changes in water related ecosystem services following wildfires: The case of the Dadia-Lefkimi-Soufli Forest National Park 653
S. Stefanidis, I. Chrysafis, I. Kokkoris, I.M. Mitsopoulos, G. Mallinis

Calliope Earth Observation Platform: the water quality monitoring service 655
G. Ceriola, A. Zilli, M. Lippi, M. Rossi

Climate change and its impact on water quality of the Zarafshan river basin..... 657
S. Shoergashova, B. Karimov, T. Liu

Impacts and effects of climate variations on the Lake Fetzara ecosystem (NE Algeria)..... 659
L. Djabri, Z. Bouhali, F. Halimi, S. Saidi, B. Hamza, S.E. Tachi, B. Nabil

Assessing water availability in the High Plain of Friuli Venezia Giulia, Italy, by integrating hydrological and hydrogeological modelling 661
E. Arnone, L. Polese, M.Brandalise,G. Paiero, P. Teatini, G. Martelli

Investigation on the lasting effects of an extend drought on the trophic status of Lake Pusiano (Northern Italy) through numerical models..... 663
N. Pella, D. Copetti, L. Valsecchi, P. Dezuanni, C. Dresti, F. Buzzi, A. Fenocchi

ALIAS: a smart classifier for monitoring *Ailanthus altissima* expansion in hydrologically sensitive areas 665
F. Alongi, D. De Caro, E. Badalamenti, F. Capodici, R. Silveira Bueno, D. Pumo, T. La Mantia, G. Ciraolo, L.V. Noto

How to monitor river turbidity using camera systems: Best practice guidelines..... 667
D. Miglino, S. Jomaa, K. C. Saddi, A.C. Moe, M. Rode, S. Manfreda

Recovery and characterization of structural extracellular biopolymers from aerobic granular sludge treating citrus industrial wastewater..... 669
M. Castiglione, R. Campo, M. Capodici, S.F. Corsino, A. Cosenza, F. De Marines, D. Di Trapani, G. Di Bella, M. Torregrossa

Keynote Speakers

Driving processes of flood changes and their extreme values

Günter Blöschl
TU Wien, Ausrtria
University of Bologna, Italy

Understanding the changing dynamics of river flood hazards requires a comprehensive analysis of the multiple factors influencing them. This seminar explores three key drivers: land-use changes, hydraulic interventions, and climate change. While land-use alterations such as deforestation, urbanisation, and agricultural soil compaction significantly affect small catchments, especially through reduced infiltration, their influence diminishes at larger scales where soil saturation dominates runoff processes. Hydraulic structures – including levees, dams, and river training – tend to affect floods of moderate magnitude and have largely localized impacts, though their long-term effects must be assessed within roader human-environment interactions.

Climate change emerges as a complex driver, influencing small catchments via intense convective storms and larger basins through a nuanced interplay of soil moisture, snowmelt, and seasonal precipitation extremes. This seminar highlights recent advances in understanding these factors and underscores the importance of avoiding oversimplified narratives. Integrating these insights into flood risk management is essential for both safety and effective public communication.



Prof. Günter Blöschl is Head of the Institute of Hydraulic Engineering and Water Resources Management at the Vienna University of Technology. He is currently teaching courses on Engineering Hydrology, Risk Assessment, Modelling and Simulation, Water Resources Management and Planning, and Climate Change. His main research interests are in hydrology and water resources management and in particular understanding and predicting floods.

An ERC Advanced Grant on 'Deciphering River Flood Change' was awarded to him. Using this grant, he demonstrated the role of climate change in increasing flood risk at the European scale which he published in Science (2017) and in Nature (2019 and 2020). He has recently led the HORA project, where flood risk was mapped for 30,000 km of Austrian streams. As the director of the Vienna Doctoral Programme on Water Resource Systems, funded by the Austrian Science Fund, Blöschl is coordinating interdisciplinary water research.

He is also directing the Hydrology Open Air Laboratory (HOAL) where detailed field observations are performed to understand water and matter fluxes in the landscape. Throughout his career, Günter Blöschl has been a strong advocate of bridging the gap between understanding fundamental processes and the practice of water resources management. He has published about 300 peer-reviewed papers and several books. Prof. Blöschl received the Horton Medal from the American Geophysical Union (AGU), the Wegener Medal from the European Geosciences Union (EGU), and the International Hydrology Prize from IAHS/WMO/UNESCO. He is a member of the Austrian Academy of Sciences (ÖAW), the German National Academy of Science and Engineering (acatech) and the US National Academy of Engineering (NAE). He recently received two honorary doctorates.

Challenges in the design of infiltration basins for Managed Aquifer Recharge

Aldo Fiori
University of Roma Tre, Italy

Managed Aquifer Recharge (MAR) plays a crucial role in increasing groundwater storage capacity and enhancing water security. Spreading methods like infiltration basins are simple and widely employed measures for MAR. The effectiveness of an infiltration basin is shaped by various natural factors, such as climatic conditions and soil properties.

Additionally, engineered variables have a significant impact on its performance and the potential risk of groundwater contamination. This contamination risk arises from the interaction between the system's hydraulic properties and the characteristics of the soil and solutes. The design of infiltration basins often focuses on addressing the issue of reduced infiltration rates over time, which is caused by clogging at the basin's bottom.

However, less emphasis is placed on the threat of groundwater contamination from the infiltrating water. Ultimately, designing infiltration basins requires balancing the complex interaction of natural and engineering factors to optimize MAR efficiency and minimize contamination risks. Some of the challenges associated with these processes are discussed, together with a novel risk-oriented analytical framework.



Aldo Fiori obtained a M.S. and a Ph.D. in Civil and Hydraulic Engineering from the University of Rome "La Sapienza" in 1990 and 1995, respectively.

He also did a postdoctoral research at Tel Aviv University in 1995. Principal research interests are the theory of flow and solute transport in heterogeneous porous media, subsurface stochastic hydrology, streamflow generation processes and hillslope hydrology, statistical hydrology, flood modeling, design and verification of hydraulic structures.

He has been involved in various editorial and scientific roles, such as the president of the International Committee on Ground Water of the International Association of Hydrological Sciences (IAHS), Co-Editor of Hydrological Sciences Journal, Associate Editor of several journals, such as Water Resources Research and Journal of Hydrology.

He is the recipient of the 2023 International Hydrology Prize – Dooge Medal. Aldo Fiori has been a member or a coordinator of various academic and administrative committees.

Are we ready for the storms ahead? Record-shattering rainfall and flood events in a rapidly changing climate

Hayley J. Fowler
Newcastle University, England

The intensification of extreme precipitation in a warming climate has been shown in observations and climate models to follow approximately theoretical Clausius-Clapeyron scaling. However, larger changes have been indicated in events of short-duration which frequently trigger flash floods or landslides, causing loss of life. At the same time heatwaves and associated droughts and water shortages are increasing in frequency. Together these provide cascading impacts on water quality, agricultural production and increase other societal risks. Continental-scale convection-permitting climate models (CPCMs) and new observational datasets provide the state-of-the-art in understanding future changes to extreme weather (rainfall, wind, hail, lightning) and their compounding effects with global warming. But global climate models underestimate the rate of change of warming in the real world, and the observed increase in extreme weather events, due to their poor representation of dynamical circulation changes and feedbacks from the land, ocean and cryosphere. It will be argued that a shift in focus is needed from our reliance on climate models towards embedding different lines of evidence in a transdisciplinary storylines approach. Ultimately we must work together across disciplines to address these rapid changes and co-create actionable information hat can be quickly embedded into policy and practice, using this approach to improve both early warning systems and projections of extreme weather events for climate adaptation.



Hayley J. Fowler is Professor of Climate Change Impacts in the School of Engineering at Newcastle University. Her research focuses on improved physical understanding of changing precipitation extremes and providing better projections for climate adaptation; winning the EGU's Sergey Soloviev Medal in 2024.

She is a Fellow of the American Geophysical Union (2018) and was a Royal Society Wolfson Research Fellow (2014-19) for her work on understanding climate change impacts on hydrological risks, from extreme rainfall and flooding to droughts She was a Contributing Author to Chapter 8: Water Cycle and Chapter 11: Extremes for the IPCC 6th Assessment Report WGI. From 2021-2023, she was President of the British Hydrological Society.

She advises the UK government on climate risks and resilience through her roles on the Strategic Advisory Board for the Rural and Environment Science and Analytical Services Division in Scotland and on the Department for Energy Security and Net Zero's Science Expert Group.

Medicane induced floods. Lessons learned by the analysis and modelling of storms Ianos and Daniel

Athanasios Loukas
Aristotle University of Thessaloniki, Greece

Mediterranean tropical-like cyclones (TLC), often referred to as Medicanes, are meteorological phenomena observed over the Mediterranean Sea. The formation of tropical, subtropical cyclones and tropical-like cyclones is infrequent, due to the dry nature of the Mediterranean region. They are predominantly formed over the western and central Mediterranean Sea and moved eastwards, while the area east of Crete is almost devoid of them. Medicanes can occur year-round, peaking between September and January, with an estimated frequency of about one event per year. Climate change is expected to increase their intensity and frequency. Medicanes pose serious threats, including heavy rainfall, flooding, strong winds, lightning, tornadoes, high waves, and storm surges. Between 2016 and 2023, five strong Medicanes affected the Ionian Sea, notably Ianos (September 2020) and Daniel (September 2023), which caused four fatalities and extensive damage in the Ionian Islands and Central Greece. Flooding covered 400 km² and 1,410 km² in Thessaly during Ianos and Daniel, respectively. Statistical analyses were conducted to characterize these events, and hydrological-hydraulic modeling was applied for flood mapping. Key questions and challenges in modelling these floods have been identified to improve understanding and forecasting of such extreme events.



Athanasios Loukas is a Professor of Engineering Hydrology – Management and Development of Water Resources, Head of Transportation and Hydraulic Engineering Department, Director of "Hydraulic Works and Environmental Management" Lab, Director of Master Program "Water Resources" of the School of Rural and Surveying Engineering, Aristotle University of Thessaloniki (2018-today). Previously, he was affiliated with University of Thessaly in which he served as a Professor, Head of the Department of Civil Engineering (2008-2012) and Dean of Faculty of Engineering (2015-2018), Laboratory Director and Director of an international Master Program (2010-2018). His research and activity focus on hydrology, hydrological hazards and risks (droughts and floods), climate change impacts, and water resources management, fields in which he has more than 400 scientific referred international journal publications, conference proceedings publications, books and technical reports. He coordinated and participated in numerous national and international research programs. Besides his research activity, he develops a strong outreach activity, and acts as mentor of a high number of post-graduate and Ph.D. students. He received, during his academic studies and carrier, numerous fellowships, prices and awards such as the Fulbright Research Scholarship in 2013. He is listed in the top world-wide 2% of the most influential scientists (according to his publications and the citations to his publications for his carrier period until 2022) of Stanford University (2023). His is a visiting professor in U.S.A. and European Universities. He is, currently, Editor-in-Chief of European Water, Section Editor-in-Chief "Water Resources Management Policy and Governance" of Water and Editorial Board Member of Water Resources Management and Scientific Review Engineering and Environmental Sciences. He is regular reviewer of national and European research proposals as well as evaluator and responsible of research projects certification. He is affiliated with national and international scientific organizations such as EWRA and EGU.

I. Hydrological Processes in a Changing Environment

Hydrological invariance, Buenos Aires, Argentina

M.P. Torrero[1,2], S.V. Viñes[1], P.A. Lee[1]
[1] Faculty of Engineering and Agricultural Sciences, Pontifical Catholic University of Argentina, Buenos Aires, Argentina
[2] National Defense University
* e-mail: mptorrero@gmail.com; susanavines@yahoo.com.ar; paule1994@gmail.com

Introduction

The alteration of land use as a consequence of urban growth has hydrological implications, which, if mismanaged, can harm the population. The consequences include higher volumes of runoff and increased flow velocity, which can lead to flooding and result in loss of life and property. In response to these issues, the study of hydrological cycles becomes crucial to mitigate the events that affect the population, particularly by controlling peak flows. Planning is essential in the pursuit of hydric invariance (hydrological-hydraulic), understood as the prevention of exceeding the volumes of runoff discharged into the natural environment after urbanization, through the analysis of ways to mitigate the disruption of the original functioning of watersheds (Cuerda Romero et al, 2021).

Storms have always been managed through the systems of traditional urban drainage, ending up insufficient and costly. Thus, alternatives arise that complement or replace traditional systems, such as Sustainable Urban Drainage Systems (SUDS), also called Best Management Practices or Low Impact Development (Escobar Ruíz, 2021; Fernández Rodríguez et al., 2020; Uvini and Upaka, 2017). This study will analyze detention basins and artificial lagoons, which are SUDS alternatives in the area. The former would be located within the property, and the latter, outside, upstream from it. The effectiveness of these alternatives will be investigated through hydrological modeling (at this stage) of the watershed to evaluate their impacts (Abellán, 2021a, b, and c) of a future urban development project on a property located in the Merlo district. The property is crossed by an unnamed stream, a tributary of the Arroyo El Pantanoso, which belongs to the Matanza-Riachuelo River basin.

Materials and methods

The survey of the cross-sectional profiles used for the hydraulic study was carried out by a consultancy responsible for conducting the hydrological and hydraulic study of the watershed in which the property is located. As for the topographic sheets for the delineation of the watershed, they were obtained from the National Geographic Institute (IGN) website in the Geodesy section, Digital Elevation Model, at a 1:50,000 scale. These sheets are: 3560-18-1b, 3560-18-1d, 3560-18-2a, and 3560-18-2c. Additionally, to visualize the type of vegetation cover and land use, satellite images from Google Maps or Google Earth Pro were used. The HEC-HMS program was used for the hydrological modeling of the watershed.

The used method, 'Outflow Curve,' was employed to design the reservoirs by relating storage and discharge. It was assumed that the water surface was level, and the mentioned relationship should be provided by the user. Regarding the storage and discharge method, the 'Elevation-Storage-Discharge' method was chosen, where the user must select a curve representing the reservoir's storage as a function of height and another discharge curve as a function of the reservoir's storage.

Results and concluding remarks

Four scenarios were developed and evaluated for the study of the area.

Scenario 1: Prior to the urban development project. All considerations for this scenario were developed previously.

Scenario 2: With the urban development project but without SUDS elements. Like Scenario 1, all considerations for this scenario were developed previously.

Scenario 3: With the urban development project and detention basins. Three detention basins were

considered, which will have a transient water volume instead of permanent water volume. Each will have a 50 cm diameter and 10 m long reinforced concrete circular outlet pipe, discharging into one of the trenches located on the sides of the interior streets of the property, which will eventually flow into the stream. Since they are located within the property, plots at higher contour levels will need to be arranged to receive runoff from their sub-watershed.

Scenario 4: With the urban development project and retention pond. An artificial lagoon was considered, upstream and outside the property, to be used as a storage area, for mitigation and peak flow control.

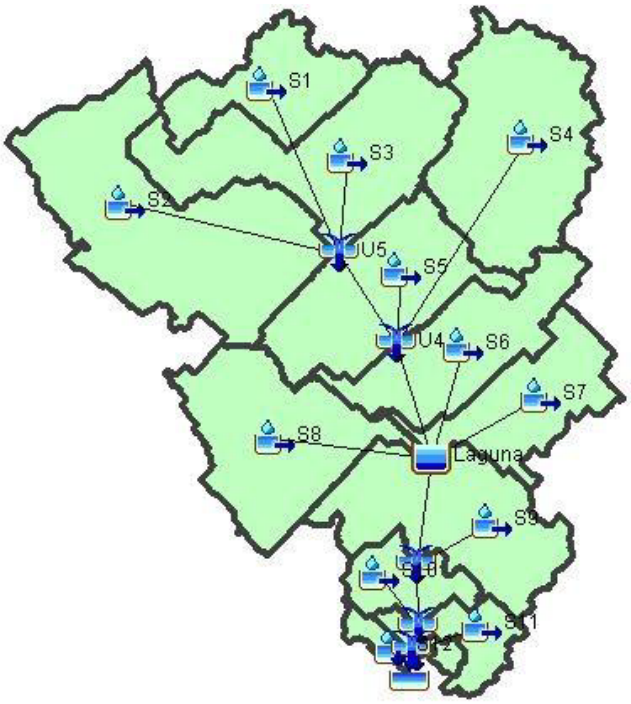


Figure 1. Basin and sub-basins of the simulation model for scenario 4.

SUDS are a good complement or alternative to the traditional system, improving the efficiency in controlling and directing surface runoff generated by storms. For the studied area, both the detention basins and the retention pond reduced the peak flow by storing and then controlling the discharge. The first reduced the flow from 35.5 m^3/s to 33.6 m^3/s, resulting in a reduction of 1.9 m^3/s. The second reduced it from 35.5 m^3/s to 12.2 m^3/s, decreasing the discharge flow by 23.3 m^3/s. The optimal solution for this case is the retention pond due to the massive reduction in flow in the watershed. However, the detention basins alone are sufficient to achieve hydrological-hydraulic invariance, reaching the pre-development flow rates.

References

Cuerda Romero JM, Seoane R, Arzuaga I M, Viñes S (2021) Invarianza hidrológica e hidráulica en cuencas periurbanas del Gran Buenos Aires (Argentina). Revista de Investigaciones Científicas de la Universidad de Morón. Año 5 / N°9. p. 88. https://repositorio.unimoron.edu.ar/handle/10.34073/309

Escobar Ruíz G (2021). Sistemas de drenaje urbano sostenibles SUDS. Tesis de Máster universitario en hidrología y recursos hídricos. Universidad de Alcalá.

Fernández Rodríguez H, Trapote Jaume A, Fernández Mejuto M (2020 Sistemas urbanos de drenaje sostenible. Tipos y objetivos. En: López Ortiz, Mª Inmaculada; Melgarejo Moreno, Joaquín (eds.). Riesgo de inundación en España: análisis y soluciones para la generación de territorios resilientes. Alacant: Universitat d'Alacant. ISBN 978-84-1302-091-4, pp. 773-786

Uvini S, Upaka R (2017) Sustainable urban drainage systems (SUDS) – what it is and where do we stand today? Engineering and Applied Science Research (EASR). Khon Kaen University, Thailand. 235-241 https://doi.org/10.14456/easr.2017.36.

Adaptation of the Yang formulas to an intermittent and an ephemeral stream

L. Avgeris[1*], V. Hrissanthou[1], K. Kaffas[2]
[1] Department of Civil Engineering, Democritus University of Thrace, Xanthi, Greece;
[2] Department of Science, University "Roma Tre", Rome, Italy
* e-mail: lavgeris@civil.duth.gr

Introduction

Intermittent Rivers and Ephemeral Streams (I.R.E.S.) are characterized by periodic flow triggered by rainfall or snowmelt, occurring only during specific times of the year or under particular conditions. These systems often remain dry for extended periods but can experience intermittent flow during wet seasons or in response to precipitation events. The timing and duration of flow are highly dependent on local climatic conditions, land-use patterns, and hydrological factors (Sefton et al. 2019).

This study aims to recalibrate the arithmetic coefficients in Yang's total sediment transport rate formulas using field data from an intermittent stream, the Kimmeria torrent (41° 08' 50.8" N, 24° 56' 17.5" E), and an ephemeral stream (41° 08' 13.4" N, 25° 00' 42.7" E). The accuracy of these methods was evaluated by comparing calculated sediment concentrations with observed measurements. Previous research has explored the application of Yang's 1973 and 1979 sediment transport formulas to various watercourse types, through multiple regression. Regression analysis has been widely employed in the literature to either develop sediment transport equations based on hydraulic or hydrometeorological parameters, or to adapt established models to environments with characteristics differing from those for which they were initially designed (Avgeris et al., 2020).

Materials and methods

A comprehensive analysis of sediment transport was conducted using data from the Kimmeria torrent and an ephemeral stream. Total sediment concentration was estimated, and the measured values were compared with those calculated using Yang's sediment transport formulas, as expressed in Equation (1):

$$m_F=0.001C_F h V_m \quad (1)$$

where m_F is total sediment load transport per unit width [kg s^{-1} m^{-1}]; C_F denotes the total sediment concentration (in ppm by weight); h is the flow depth [m]; and V_m is the mean flow velocity [m s^{-1}].

To estimate C_F, Yang (1973) proposed a formula for estimating total sediment transport in rivers and streams, as detailed in Equation (2).

$$\log C_F=5.435-0.286\log(V_s d_{50}/\nu)-0.457\log(V_0^*/V_s)+(1.799-0.409\log(V_s d_{50}/\nu)-0.314\log(V_0^*/V_s))\log(V_m I/V_s-V_{m,cr} I/V_s) \quad (2)$$

where V_s is the terminal fall velocity of sediment particles [m s^{-1}]; d_{50} is the median particle diameter [m]; v is the kinematic viscosity of water [m^2 s^{-1}]; I is the energy slope; $V_{m,cr}$ is the critical mean flow velocity [m s^{-1}]; and V_0^* is the shear velocity [m s^{-1}]. The term $V_m I$ is characterized as unit stream power.

In 1979, Yang demonstrated that the critical unit stream power term could be omitted with minimal loss of accuracy when measured sediment concentration exceeds 20 ppm, leading to the development of an alternative formula, shown in Equation (3).

$$\log C_F=5.165-0.153\log(V_s d_{50}/\nu)-0.297\log(V_0^*/V_s)+(1.780-0.360\log(V_s d_{50}/\nu)-0.480\log(V_0^*/V_s))\log(V_m I/V_s) \quad (3)$$

For Kimmeria torrent, 22 datasets collected between June 2004 and December 2014 were analyzed, enabling a comparison of observed values with those predicted by Yang's formulas (Avgeris et al., 2020). In the ephemeral stream, 15 field measurements were conducted between April 2017 and April 2018, with 10 deemed suitable for analysis due to sufficient sediment trapping. Despite variations in hydrological

conditions, the same analytical approach was applied, emphasizing the comparison between computed and measured sediment concentrations using Yang's models (Avgeris et al., 2024).

To enhance the accuracy of Yang's formulas for these watercourses, the coefficients were recalibrated using nonlinear regression. The updated equations for the Kimmeria torrent dataset are:

$$\log C_F=0.892+1.065\log(V_s d_{50}/\nu)+3.004\log(V_0^*/V_s)-(0.436-0.297\log(V_s d_{50}/\nu)-1.287\log(V_0^*/V_s))\log(V_m I/V_s-V_{m,cr} I/V_s) \quad (4)$$

$$\log C_F=0.179+1.551\log(V_s d_{50}/\nu)+3.830\log(V_0^*/V_s)-(1.042-0.693\log(V_s d_{50}/\nu)-2.096\log(V_0^*/V_s))\log(V_m I/V_s) \quad (5)$$

Similarly, the ephemeral stream dataset yielded further recalibrations, represented by Eqs. (6) and (7):

$$\log C_F=-4.661+2.014\log(V_s d_{50}/\nu)+0.494\log(V_0^*/V_s)-(4.681-1.599\log(V_s d_{50}/\nu)-1.729\log(V_0^*/V_s))\log(V_m I/V_s-V_{m,cr} I/V_s) \quad (6)$$

$$\log C_F=-14.377+5.853\log(V_s d_{50}/\nu)+3.030\log(V_0^*/V_s)-(23.101-8.495\log(V_s d_{50}/\nu)-7.437\log(V_0^*/V_s))\log(V_m I/V_s) \quad (7)$$

Results and concluding remarks

The evaluation of calculated versus measured sediment concentrations used statistical criteria including Mean Relative Error (MRE), Nash-Sutcliffe Efficiency (NSE), linear correlation coefficient (r), coefficient of determination (R^2), and the discrepancy ratio, which reflects the proportion of calculated values within one-fourth to four times the measured values. Results are summarized in Table 1.

Table 1. Statistical criteria of Yang's original and calibrated formulas for the intermittent and the ephemeral stream

	INTERMITTENT				**EPHEMERAL**			
	Yang 1973		**Yang 1979**		**Yang 1973**		**Yang 1979**	
	Original	**Calibrated**	**Original**	**Calibrated**	**Original**	**Calibrated**	**Original**	**Calibrated**
M.R.E. (%)	-8.326	1.164	-11.080	1.129	1351.115	461.362	1425.909	439.779
N.S.E.	-2.265	0.084	-1.752	0.062	-39.468	0.373	-47.557	0.437
r	-0.409	0.126	-0.439	0.042	-0.370	0.611	-0.344	0.661
R^2	0.167	0.016	0.193	0.002	0.137	0.371	0.118	0.437
Discrepancy Ratio	1.000	1.000	1.000	1.000	0.200	0.700	0.100	0.700

The results indicate that the original formulas for the intermittent stream already demonstrated good applicability, as reflected by a consistent discrepancy ratio of 1. Although calibration improved metrics like MRE and NSE, it failed to significantly enhance other metrics such r and R^2. In contrast, for the ephemeral stream, calibration led to substantial reductions in MRE and notable gains in NSE, r, R^2, and the discrepancy ratio, improving predictive accuracy considerably. Calibration significantly improved ephemeral stream models but had limited impact on the intermittent stream, indicating the need for further refinement. A more comprehensive dataset could improve model accuracy through regression analysis.

References

Avgeris L, Kaffas K, Hrissanthou V (2020) Comparison between Calculation and Measurement of Total Sediment Load: Application to Nestos River. Environmental Sciences Proceedings, 2(1), 19. https://doi.org/10.3390/environsciproc2020002019

Avgeris L, Kaffas K, Hrissanthou V (2022) Comparison between Calculation and Measurement of Total Sediment Load: Application to Streams of NE Greece. Geosciences, 12(2). https://doi.org/10.3390/geosciences12020091

Avgeris L, Kaffas K, Hrissanthou V (2024) Measurement and Calculation of Sediment Transport on an Ephemeral Stream. Hydrology, 11(7), 96. https://doi.org/10.3390/hydrology11070096

Sefton CEM, Parry S, England J, Angell G (2019) Visualising and quantifying the variability of hydrological state in intermittent rivers. Fundamental and Applied Limnology, 193(1), 21–38. https://doi.org/10.1127/fal/2019/1149

Yang CT (1973) Incipient Motion and Sediment Transport. Journal of the Hydraulics Division, 99, HY10, 1679–1704. https://doi.org/10.1061/JYCEAJ.0003766

Yang CT (1979) Unit stream power equations for total load. Journal of Hydrology, 40(1–2), 123–138. https://doi.org/10.1016/0022-1694(79)90092-1

Hydrological pathways: The impact of stable water isotopes on moisture source contribution in Brahmaputra river basin

M. Nanda, A.M. Nair*
Earth System Science and Engineering Division, Department of Civil Engineering, Indian Institute of Technology Guwahati, Guwahati–781039, India
** e-mail: nair.archana@iitg.ac.in*

Introduction

The river basins in high mountainous regions are particularly snow and glacier-fed. These regions are among the most vulnerable areas to climate change due to intricate hydrological processes (Dimri et al., 2013). The Tibetan plateau region and the Himalayas are shaping the weather pattern for the Brahmaputra river basin. The spatial and temporal distribution of precipitation in this region is being controlled by the principal moisture sources: Indian summer monsoons (ISM) and western disturbances (WD) (Bookhagen and Burbank, 2010). Each moisture source carries a distinct fingerprint in stable water isotopic composition, depending upon the pathways it covers and the intensity of rain (Jeelani et al., 2018). Despite the importance, limited data availability has made it challenging to understand the impact of these moisture regimes on the hydrological system of the Brahmaputra river. Therefore, there is a necessity to quantify the relative contribution of moisture sources to the river system for management, planning and better assessment of water resources. However, stable water isotopes emerged as a powerful tool to unravel these intricacies. This study uses isotopic data from Brahmaputra river basin at Guwahati for precipitation (rain) of ISM and at Tawang (Mago Basin) for precipitation (snow) of WD. The objective of the present study is to estimate the contributions of ISM and WD to the Brahmaputra river system. This will provide a comprehensive perspective on dynamic hydrological processes and their implications under changing climatic conditions.

Materials and methods

Water samples were collected from the Brahmaputra river basin from April 2023 to April 2024 including river water, rain water and snow (Figure 1). Sampling has been done under water and kept away from sunlight to avoid further fractionation due to evaporation. The stable isotope analysis was performed for all samples by following the analytical procedure of off axis integrated cavity output spectroscopy in a laser based isotope analyser. The result expressed in δ-notation (‰) for oxygen and hydrogen isotope relative to Vienna Standard Mean Ocean water (VSNOW), as follows: $\delta = (R_{sample}/R_{VSMOW} - 1) \times 1000$
Deuterium excess (d-excess) was calculated from the expression: $\delta D - 8 \times \delta^{18}O$, established by Dansgaard (1964) to trace moisture sources.
To estimate the contributions from WD and ISM to the Brahmaputra river system, a two component hydrograph separation technique was used. However, d-excess was used as key tracer because the isotopic composition of d-excess in precipitation is highly variable for both the moisture sources. The WD end member values are considered as snow and rain precitation during October to May and ISM values considered from June to September.
The two-component hydrograph separation equation by Engel et al., 2016 expressed as: $Q_R = Q_{WD} + Q_{ISM}$
Where Q_{WD} and Q_{ISM} are the contribution from western disturbances and Indian summer monsoon to the Brahmaputra river discharge (Q_R).

$$\delta_R = \delta_{WD} \times f_{WD} + \delta_{ISM} \times f_{ISM} \quad (1)$$

$$f_{WD} + f_{ISM} = 1 \quad (2)$$

where δ_{WD}, δ_{ISM} and δ_R are d-excess value for western disturbances, Indian summer monsoon and river water respectively. f_{WD} and f_{ISM} are the fractional contribution of western disturbances and Indian summer monsoon to the total river discharge.

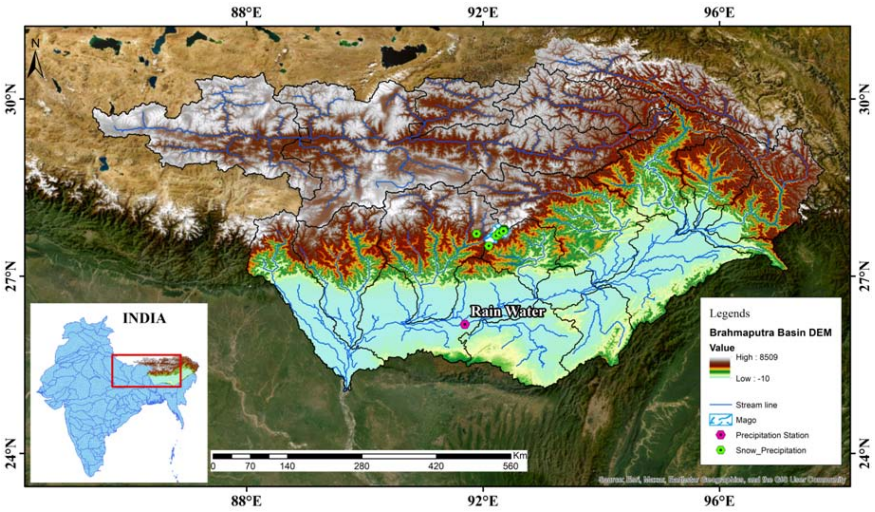


Figure 1. Study area map showing spatial extent of Brahmaputra river basin and sampling locations.

Results and concluding remarks

This study highlights the significant influence of WD and ISM in shaping the hydrology of Brahmaputra river basin. Western disturbances contribute dominantly during post monsoon period, while Indian summer monsoon contributes more significantly during summer months.

Table 1. Estimated contribution of western disturbances and Indian summer monsoon to Brahmaputra river water

Month	WD%	ISM%	Month	WD%	ISM%
January	62	38	July	56	44
February	58	42	August	53	47
March	63	37	September	78	22
April	57	43	October	74	26
May	65	35	November	70	30
June	48	52	December	70	30

The isotopic signature of WD period observes depleted $\delta^{18}O$ and higher d-excess, while ISM exhibits enriched $\delta^{18}O$ and lower d-excess. This variation is due to seasonal change in temperature, snow/glacier melting and moisture circulation. The result from mixing calculation shows that Western Disturbances contribute dominantly (63%) compared to Indian summer monsoon (37%) to the regional hydrology of Brahmaputra river system.

Acknowledgments: The authors greatly acknowledge the Department of Science and Technology (DST), Government of India (Project No – DST/CCP/MRDP/185/2019). The help from National Institute of Mountaineering and Allied Sports (NIMAS, Dirang) during sampling is duly acknowledged.

References

Bookhagen B, Burbank DW (2010) Toward a complete Himalayan hydrological budget: Spatiotemporal distribution of snowmelt and rainfall and their impact on river discharge. Journal of Geophysical Research 115: 1-25. https://doi.org/10.1029/2009JF001426

Dansgaard W (1964) Stable isotopes in precipitation. Tellus 16(4): 436-468. https://doi.org/10.3402/tellusa.v16i4.8993

Dimri AP, Yasunari T, Wiltshire A, Kumar P, Mathison C, Ridley J, Jacob D (2013) Application of regional climate models to the Indian winter monsoon over the western Himalayas. Science of the Total Environment 468: S36-S47. https://doi.org/10.1016/j.scitotenv.2013.01.040

Engel M, Penna D, Bertoldi G, Dell'Agnese A, Soulsby C, Comiti F (2016) Identifying run-off contributions during melt-induced run-off events in a glacierized alpine catchment. Hydrological Processes 30: 343–364. https://doi.org/10.1002/hyp.10577

Jeelani G, Shah RA, Fryar AE, Deshpande RD, Mukherjee A, Perrin J (2018) Hydrological processes in glacierized high-altitude basins of the western Himalayas. Hydrogeology Journal 26: 615–628. https://doi.org/10.1007/s10040-017-1666-1

A comparative assessment on the future drought characteristics of South Korea using AR6 climate change scenario

M.H. Lee*, S.W. Hwang
Division for Integrated Water Management/Korea Environment Institute/Sejong, South Korea
** e-mail: mhlee@kei.re.kr*

Introduction

Global water demand continues to rise due to socio-economic development and changing consumption patterns (United Nations, 2023). Climate change exacerbates this challenge, increasing the frequency and intensity of droughts, and heightening the risk of water scarcity. The Sixth Assessment Report (AR6) by the Intergovernmental Panel on Climate Change (IPCC) warns that, with a global temperature rise of 1.5°C, more than 350 million people in urban areas worldwide may suffer from drought and water shortages (IPCC, 2022). To ensure the stability of water supply in line with the increasingly severe climate and socio-economic changes, it is essential to understand and predict the characteristics of future droughts at the regional level. While various AR6-based climate change scenarios have been developed and research on drought projections is actively underway, uncertainties in future projections remain due to factors such as greenhouse gas emission scenarios, climate modeling, and the selection of drought indices (Lee et al, 2019). Research interpreting a wide range of possible outcomes is still limited. Therefore, this study aims to identify the uncertainties in climate change scenarios based on data from the Korea Meteorological Administration (KMA) and analyze the changes in the frequency and severity of future droughts accordingly.

Materials and methods

This study utilizes climate change scenarios generated by the Korea Meteorological Administration (KMA). These scenarios are derived from RCM models, including CCLM, GRIMs, HadGEM3-RA, RegCM4, and WRF, all with a 1 km × 1 km resolution, based on the UKESM1 GCM model. These scenarios reflect various emission pathways under the IPCC's AR6 framework, including SSP5-8.5, SSP3-7.0, SSP2-4.5, and SSP1-2.6. Precipitation and temperature data are produced for these scenarios. To conduct a more comprehensive and detailed study, the spatial domain is set at Korea's standard watershed units, which consist of 850 hydrologically delineated regions based on river basins, commonly used for water resource management and policy planning. The temporal scope covers the past (1981–2020), near future (2021–2060), and distant future (2061–2100), with a daily timescale applied for analysis. For drought assessment, the study applies drought indices commonly used in existing research, including the Standardized Precipitation Index (SPI) and Standardized Precipitation Evapotranspiration Index (SPEI). Key drought characteristics, such as mean drought intensity, drought occurrence frequency, and drought duration, are compared and analyzed to systematically evaluate the impact of changes in temperature and precipitation on future drought characteristics.

Results and concluding remarks

The results of comparing future drought change characteristics by climate change scenario show that droughts based solely on precipitation, as represented by the SPI, are expected to mitigate in most scenarios. Average annual precipitation is projected to increase by approximately 5.7% to 23.8% in the near future period (2021–2060) compared to the past period (1981–2020), and by 1.5% to 52.3% in the distant future period (2061–2100). Therefore, the results observed in the SPI, which is directly influenced by precipitation, can be attributed to the anticipated increase in precipitation as a climate factor. Except for the CCLM_SSP5-8.5 scenario, the occurrence frequency and duration of droughts, classified as severe

droughts with an index value below -2.0, are expected to decrease significantly in all climate change scenarios of SPI.

On the other hand, the results for the drought index that considers temperature, SPEI show differing projections for future droughts. Temperature projections across all climate change scenarios indicate an increase ranging from 0.9°C to 6.3°C, with variations depending on the specific scenario and future period. As average temperatures are projected to rise, the increase in average annual potential evapotranspiration has been clearly observed. Furthermore, this increase becomes more pronounced in the distant future and under higher greenhouse gas emission scenarios. Since changes in potential evapotranspiration exceed those in precipitation in future periods, drought conditions are projected to be more severe when assessed using the SPEI. Notably, the CCLM scenario suggests that under all SSP pathways, the frequency and duration of droughts are expected to increase, along with a likely intensification of average drought intensity. Due to the nature of the SPEI, which accounts for the effect of rising temperatures on potential evapotranspiration, increased evapotranspiration leads to more severe drought conditions, particularly under the SSP5-8.5 scenario and in the distant future. Consequently, the frequency and duration of droughts are expected to intensify.

In conclusion, considering both temperature and precipitation, future drought issues may be more severe than in the past. The results of comparing the five climate change scenarios under the SSP3-7.0 Shared Socioeconomic Pathway (SSP) by region show that, according to the Standardized Precipitation Index (SPI), the frequency and duration of droughts are expected to decrease in most areas of South Korea, except in certain regions of Jeollabuk-do and Gyeongsangbuk-do. Under the CCLM scenario, the average drought intensity is projected to intensify in Gyeonggi-do, Chungcheong-do, and Jeollabuk-do, while in most other regions under the remaining scenarios, the average drought intensity is expected to decrease. In contrast, the analysis using the Standardized Precipitation Evapotranspiration Index (SPEI) indicates that the frequency and duration of future droughts are expected to intensify across the majority of South Korea. Notably, significant increases are anticipated in Seoul, the Gyeonggi area, Chungcheongnam-do, and Jeollabuk-do.

This study identifies regions likely to face significant drought impacts by analyzing drought severity across various scenarios and drought indices. These findings are expected to serve as essential data for effectively responding to climate change. Based on these results, a comprehensive methodology for drought risk assessment and region-specific adaptation strategies will be developed.

Acknowledgments: This work was supported by Korea Environment Industry & Technology Institute (KEITI) through Water Management Program for Drought Project, funded by Korea Ministry of Environment (MOE) (RS-2023-00230286).

References

IPCC (2022). *Climate Change 2022: Impacts, Adaptation, and Vulnerability. Contribution of Working Group II to the Sixth Assessment Report of the Intergovernmental Panel on Climate Change.* Full Report 3056, Cambridge University Press, Cambridge, UK and New York, NY, USA

Lee, M.H., Im, E.S., Bae, D.H. (2019). A comparative assessment of climate change impacts on drought over Korea based on multiple climate projections and multiple drought indices. *Climate Dynamics* 53: 389-404. http://doi.org/10.1007/s00382-018-4588-2

United Nations (2023). The United Nations World Water Development Report 2023. Partnerships and cooperation for water, UNESCO, Paris

An integrated approach to baseflow estimation: a comparison of empirical methods and physically based models in the Tanagro basin

M.F. Palmiero[1*], M. Bancheri[2], A. Longobardi[1], S.B.M. Hassan[3]
[1] Department of Civil Engineering, University of Salerno, Italy Department of Civil Engineering, University of Salerno, Italy
[2] Institute for Mediterranean Agricultural and Forestry Systems (ISAFOM), National Research Council (CNR), Naples, Italy
[3] School of Agricultural Forestry Food and Environmental Sciences (SAFE), University of Basilicata, Potenza, Italy
* e-mail: mpalmiero@unisa.it

Introduction

Baseflow, the slow streamflow component associated with groundwater discharge, is critical for sustainable water management, hydrological modelling, and assessment of climate change and human impacts (Longobardi et al., 2016). Determining baseflow is challenging because of conceptual and modelling uncertainties in separating discharge components. Mass balance methods using site-specific chemical and physical properties are often used. An alternative approach could be the use of empirical filter methods, which, however, require validation for which purpose, the application of physically based models has been considered to be an efficient methodology. The objective of this study is to analyse the correspondence in terms of baseflow between the results obtained from a physically based hydrological model and those obtained from empirical separation methods, with the aim of achieving mutual validation and calibration.

Materials and methods

The Tanagro river basin (about 660 km² catchment area) in the Campania region was selected for this case study. The physically based hydrological model used is FLOWS-HAGES (Coppola et.al 2019). It is a dynamic, physically based model designed to simulate the movement of water and solutes within the soil-plant-atmosphere system. The meteorological data used for the simulation come from the SIMN historical monitoring network (precipitation, temperature). Reference evapotranspiration was estimated using the Hargreaves formula. Durum wheat was chosen as the crop for the analysis, covering the whole catchment. In addition, a hydro-geomorphological soil characterisation was carried out using the soil map of Campania region (1:250000). Selected empirical methods for determining baseflow were the Lyne and Hollick's filter, the weighted moving average method (EWMA) and the UKIHfilter.

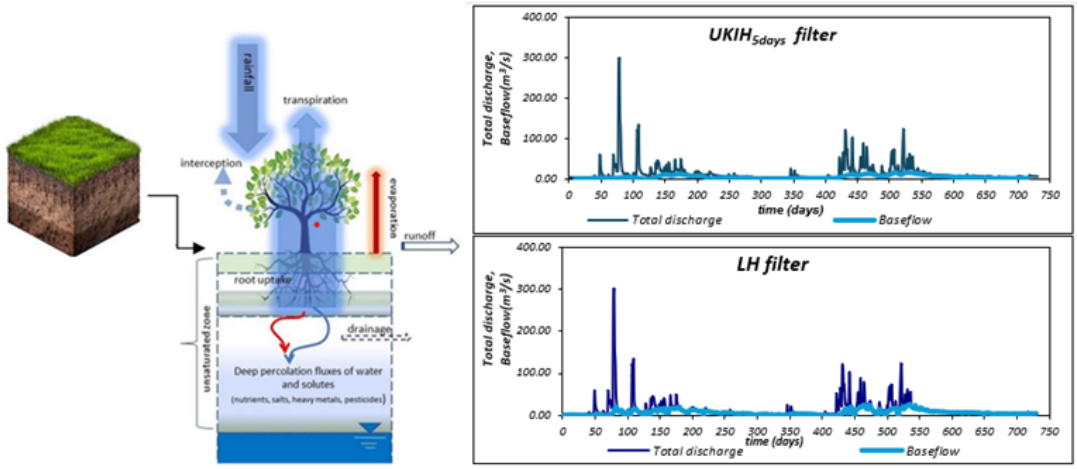


Figure 1. FLOWS-HAGES model scheme (left side); empirical methods for baseflow determination (right side).

Lyne and Hollick's (Nathan and McMahon 1990) recursive digital filter works as a low-pass filter. The application does not require measurement of chemical-physical parameters. The filter was applied recursively to attenuate distortions, with the parameter set to 0.92 as recommended in the literature. The UKIH method, involves identification and interpolation of turning points in streamflow data. The data are divided into five-day segments, in each of which a minimum value is identified. A revised approach suggests that the number of days should depend on the drainage area of basin (Pigott et al., 2005). The exponential weighted moving average (EWMA) approach assumes that the rate of baseflow increase is influenced by the proportion of surface flow (Tularam and Ilahee 2008). The filter parameter α was set equal to 0.013.

Results and concluding remarks

The period of analysis is from October 1968 to October 1970. According to the soil map, the catchment consists of 20 soil types, four of which were excluded from the analysis because their shallow depth makes them unsuitable for durum wheat cultivation, as the length of the root system would exceed the thickness of the soil. A specific analysis is planned for these soils, considering alternative crops. The groundwater recharge component for each soil type was assessed by model simulation. The groundwater recharge index was calculated for each soil as the ratio of groundwater recharge to the difference between rainfall and interception, and then the total recharge index for the catchment was determined as the weighted average of the individual components, depending on the area covered by each soil. The baseflow calculated by empirical methods is summarised in the baseflow index (BFI), which is the ratio of baseflow volume to streamflow volume. The results are presented in the following table (Table 1). To quantify the variation between the results, a relative percentage error index was calculated. The data analysis shows a good correlation between the physical hydrological model and the UKIH filter, with a relative error of less than 10%. In contrast, the error is higher for the other two methods. In particular, the Lyne and Hollick filter is affected by the wide spectral bandwidth of the streamflow, which includes a significant low frequency component, making perfect separation difficult due to overlapping frequencies, especially in the presence of high data variability. Finally, the EWMA (Exponential Weighted Moving Average) method shows variable performance depending on the hydrological regime of the basin and often overestimates the baseflow component due to its specific formulation.

Table 1. Estimation of groundwater recharge index and baseflow index with relative errors for each method.

GWr_Index	BFI_UKIH 5 days	BFI_UKIH N days	BFI_LH	BFI_EWMA	Error UKIH 5 days	Error UKIH N days	Error LH	Error EWMA
41.01%	43.00%	37.00%	50.00%	62.00%	4.8%	9.8%	21.9%	51.2%

In conclusion, the analysis highlights the potential of an integrated approach, as demonstrated by the high correlation with the UKIH filter and the minimal error observed, which provides a comprehensive understanding of the processes. However, site specific considerations are required for the Lyne and Hollick filter and the EWMA as their performance is influenced by the hydrological regime of the basin.

References

Coppola A, Randazzo L, Basile A, Fenu C (2018). FLOWS-HAGES (FLOw of Water and Solutes in Heterogeneous AGri-Environmental Systems): A MatLab Code for the Transport of Water and Solutes in Unsaturated Soils with Vegetation in Heterogenous System *D.S.U. o*. B. Tech. Rep. Soil and Contaminant Hydrology Laboratory, Italy.

Longobardi A, Villani P, Guida D, Cuomo A. Hydro-geo-chemical streamflow analysis as a support for digital hydrograph filtering in a small, rainfall dominated, sandstone watershed (2016). Journal of Hydrology 539:177-187.

Lyne V, Hollick M, Stochastic Time-Variable Rainfall-Runoff Modelling (1979). Institute of Engineers Australia National Conference: 89-93.

Nathan R.J, McMahon T.A (1990) Evaluation of automated techniques for base flow and recession analyses. Water Resources Research 26 (7): 1465-1473.

Piggott A.R, Moin S, Southam C (2005). A revised approach to the UKIH method for the calculation of baseflow. Hydrological Sciences Journal 50 (5): 920.

Tularam G.A, Ilahee M. (2008). Exponential Smoothing Method of Base Flow Separation and Its Impact on Continuous Loss Estimates. American Journal of Environmental Sciences, 4(2), 136-144.

Over 150 years of streamflow behaviour inferred from freshwater pearl mussel shell $\delta^{18}O$ in northern Sweden

G. Türk[1,2*], C.J. Gey[3], B.R. Schöne[3], L. Pfister[1,2], H. Laudon[4], F. Thielen[5]
[1] *CATchment and ecohydrology research group, Environmental sensing and modelling research unit (ENVISION), Luxembourg Institute of Science and Technology, Belvaux, Luxembourg*
[2] *University of Luxembourg, Faculty of Science, Technology and Medicine, Esch-sur-Alzette, Luxembourg*
[3] *Institute of Geosciences, University of Mainz, Germany*
[4] *Department of Forest Ecology and Management, Swedish University of Agricultural Sciences, Umeå, Sweden*
[5] *natur&ëmwelt Fondation Hëllef fir d'Natur, Marnach, Luxembourg*
** e-mail: guilhem.turk@list.lu*

Introduction

In boreal regions of the northern hemisphere, climate change is disrupting the freeze-thaw cycle. This does not only affect spring snowmelt floods and the related redistribution of the annual available streamflow but also exacerbate drought conditions. Therefore, analysing the dynamics of historical seasonal water budgets is essential to assess drought vulnerability. Stable isotopes of oxygen (O) and hydrogen (H) in streams and precipitation are cardinal tools in this respect. However, their potential for assessing the spatial and temporal variability in water sources and flow paths is stymied due to the limited availability of long-term records of $\delta^{18}O$ and $\delta^{2}H$ signatures. Here, we use two innovative approaches for reconstructing pre-instrumental $\delta^{18}O$ series and assessing seasonal stream water contributions from precipitation in northern Sweden.

First, we use $\delta^{18}O$ archived in shells of freshwater bivalves as a proxy for stream water $\delta^{18}O$ prior to instrumental records. Some species such as *Margaritifera margaritifera* can live for up to 200 years, and proof-of-concept work has shown that shell $\delta^{18}O$ values closely mirror stream water $\delta^{18}O$ signatures (Pfister et al., 2019). Second, we rely on existing numerical models to reconstruct precipitation $\delta^{18}O$, based on machine learning (Piso.AI, Nelson et al., 2021), and based on empirical relationships with atmospheric circulation patterns (Türk et al., 2025). Reconstructed $\delta^{18}O$ in streams and precipitation allow us to assess the seasonal origin of stream water during main the main growing period of bivalves (i.e., June to August). We used this dual approach to test our hypothesis that climate change has already led to altered seasonal contributions of precipitation and meltwater to streamflow and baseflow in boreal river basins.

Materials and methods

A total of 20 shells from freshwater pearl mussels (*M. margaritifera*) were collected in a small headwater stream (tributary of the Vindel River) in northern Sweden. Distinct annual growth lines enabled precise dating of each shell portion to the nearest calendar year allowing (summer) $\delta^{18}O$ chronologies to be retrieved (Fig. 1). Three specimens were selected for isotope analysis, yielding 1,654 $\delta^{18}O_{shell}$ values covering the time interval of 1836 – 2023. To derive stream water oxygen isotope ($\delta^{18}O_{SW}$) data from $\delta^{18}O_{shell}$, we used the methods described in Gey et al. (2024). Furthermore, previously published shell-based $\delta^{18}O_{SW}$ reconstructions (Schöne et al., 2020) from specimens collected in three neighboring catchments were incorporated, expanding the dataset to over 2,700 precisely dated isotope samples from four catchments in northern Sweden.

Taking the reconstructed shell-based $\delta^{18}O_{SW}$ and model-based precipitation $\delta^{18}O_{P}$ data starting in year 1881, we calculated the seasonal origin index (SOI) (Allen et al., 2019), i.e., the winter to summer precipitation in streamflow ratio with values ranging from -1.0 (winter) to +1.0 (summer). We used a12-year monthly *in-situ* $\delta^{18}O_{SW}$ record in the experimental Krycklan catchment as a reference and calculated the baseflow with the one-parameter Lyne-Hollick digital filter for hydrograph separation following Ladson et al. (2013).

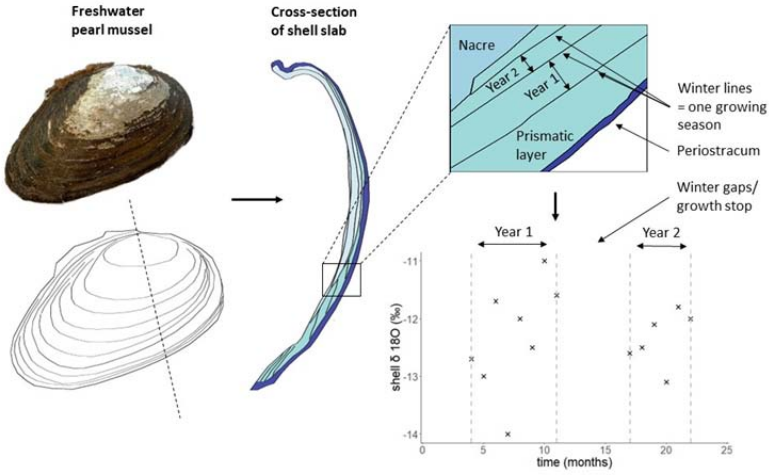


Figure 1. Scheme of stream water isotope reconstruction using shells of freshwater bivalves.

Results and concluding remarks

Our results suggest that the relative contribution of winter vs summer precipitation to streamflow during the main growing season varied with catchment size, with the largest catchment dominated by winter precipitation (SOI between -0.50 and 0.00), while smaller catchments showed a mix of winter and summer signatures (SOI between 0.00 and 0.50), except for one fed by an upstream lake (SOI between -0.50 and 0.10). This could be an indication of larger groundwater contributions in the larger catchment, while summer precipitation has greater contributions in the small headwater catchments. In the reference Krycklan catchment, the SOI was significantly and negatively correlated to the BFI in summer (Pearson's r = -0.52, p = 0.001) and positively to the specific discharge (r = 0.32, p = 0.06). This suggests that freshwater pearl mussel $\delta^{18}O$ is a useful proxy for summer baseflow contributions in northern Sweden. Our novel approach provides unprecedented insights into nearly two centuries (SOI chronologies starting in 1836) of catchment-scale hydrological changes in subarctic rivers basins.

Acknowledgments: This study was funded through the German Research Foundation (DFG, grant SCHO793/25) to B.R.S. and the Fonds National de la Recherche of Luxembourg (FNR, grant C20/SR/14757154) to L.P. within the framework of the joint D-LUX – CORE 2020 project MUSES.

References

Allen, S. T., von Freyberg, J., Weiler, M., Goldsmith, G. R., & Kirchner, J. W. (2019). The seasonal origins of streamwater in Switzerland. Geophysical Research Letters, 46, 10425–10434.

Gey, C.J., Pfister, L., Türk, G., Thielen, F., Leonard, L., Schmitt, K.E., Schöne, B.R., (2024). Biologically driven isotope fractionation in ultrastructurally different shell portions of freshwater pearl mussels (Margaritifera margaritifera): Implications for streamwater $\delta^{18}O$ reconstructions. Limnol. Oceanogr. Lett. 9, 827–836.

Ladson, A.R., Brown, R., Neal, B., Nathan, R., (2013). A Standard Approach to Baseflow Separation Using The Lyne and Hollick Filter. Australas. J. Water Resour. 17, 25–34.

Nelson, D. B., Basler, D., & Kahmen, A. (2021). Precipitation isotope time series predictions from machine learning applied in Europe. Proceedings of the National Academy of Sciences of the United States of America, 118 (26).

Pfister, L., Thielen, F., Deloule, E., Valle, N., Lentzen, E., Grave, C., Beisel, J. N., & McDonnell, J. J. (2018). Freshwater pearl mussels as a stream water stable isotope recorder. Ecohydrology, 11, 1–10.

Schöne, B.R., Meret, A.E., Baier, S.M., Fiebig, J., Esper, J., McDonnell, J., Pfister, L., (2020). Freshwater pearl mussels from northern Sweden serve as long-term, high-resolution streamwater isotope recorders. Hydrol. Earth Syst. Sci. 24, 673–696.

Türk, G., Gey, C. J., Schöne, B. R., and Pfister, L. (2025). Effects of synoptic atmospheric variability on sub-daily precipitation $\delta^{18}O$-air temperature functions in reconstructions of pre-instrumental $\delta^{18}O$ chronicles across Europe, EGUsphere [preprint].

Study on the impacts of water surface expansion on runoff in the Ob River basin

G. Gan, J. Wu*
Nanjing Institute of Geography and Limnology, Chinese Academy of Sciences, Nanjing 211135, China
** e-mail: gjgan@niglas.ac.cn, w.jinglu@niglas.ac.cn*

Introduction

As the climate continues to warm, the water cycle in Arctic regions has been intensively altered. Glaciers are accelerating to melt, and seasonal snow melts earlier in the Arctic regions. The seasonal water surface has been surging in the last 30 years in some Arctic regions, e.g., the Ob River basin (Huang et al., 2021), due to the increasing precipitation and earlier snowmelt. The Ob River basin, with a total river length of 5410 km and a drainage area of 2.973 million km^2, has witnessed a lasting increasing trend in streamflow since the 1900s (Xu et al., 2020). However, few studies have studied the links between the expansion of water bodies and the increasing runoff. However, it is widely known that water bodies have a storage effect on runoff, which can, directly and indirectly, replenish rivers. In this study, we analyze the impacts of water surface expansion on the runoff in the Ob River basin.

Materials and methods

The Ob River is the third largest river in the Russian Federation and a famous river in the world, belonging to the Arctic Ocean water system. The upstream originates from the Altay Mountains, flows north-westward after the source, crosses the western Siberian plain, and flows into the Ob Bay in the Kara Sea in the Arctic Ocean. We acquired monthly streamflow data at 14 stations in the Ob River basin from the GRDC website.

To obtain the change sequence of the water body area in the study area from 1990 to 2020, this study selected the Landsat 5, 7, and 8 series data. This study conducted a relevant analysis based on Google Earth Engine (GEE) to process massive remote sensing data. Water surface classification was conducted at a resolution of 30m, and all remote sensing images within the study area were classified according to certain classification rules. Then, each pixel's Water Inundation Frequency (WIF) was calculated. WIF is defined as the ratio of the number of remote sensing images with water coverage to all remote sensing images, with WIF ranging from 0 to 100%. The classification rules need formulas for NDVI, NDWI, and MNDWI, shown as follows:

$$NDVI= [b(NIR)-b(RED)]/[(b(NIR)+b(RED)] \quad (1)$$

$$NDWI=[b(GREEN)-b(NIR)]/(b(NIR)+b(GREEN)] \quad (2)$$

$$MNDWI=[b(GREEN)-b(MIR)]/[(b(MIR)+b(GREEN)] \quad (3)$$

In the formula, b (RED) represents the red-light band, b (GREEN) represents the green-light band, b (NIR) represents the near-infrared band, and b (MIR) represents the mid-infrared band. Based on NDWI and MNDWI index methods, this study adopts the comprehensive discrimination rule, as shown in Equation 4.

$$(NDWI>-0.1) \text{ AND } (MNNWI>0.1) \text{ AND } (EVI<0.1) \text{ AND } (MNDWI>EVI \text{ OR } MNDWI>NDVI) \quad (4)$$

Results and concluding remarks

The water surface in the Ob River basin has generally been increasing since 1990, as shown in Fig.1, especially the seasonal water surface (WIF < 75%). Analysis shows that compared to permanent water bodies, the interannual variation of seasonal water body area within each sub-basin was highly correlated with the interannual variation of runoff.

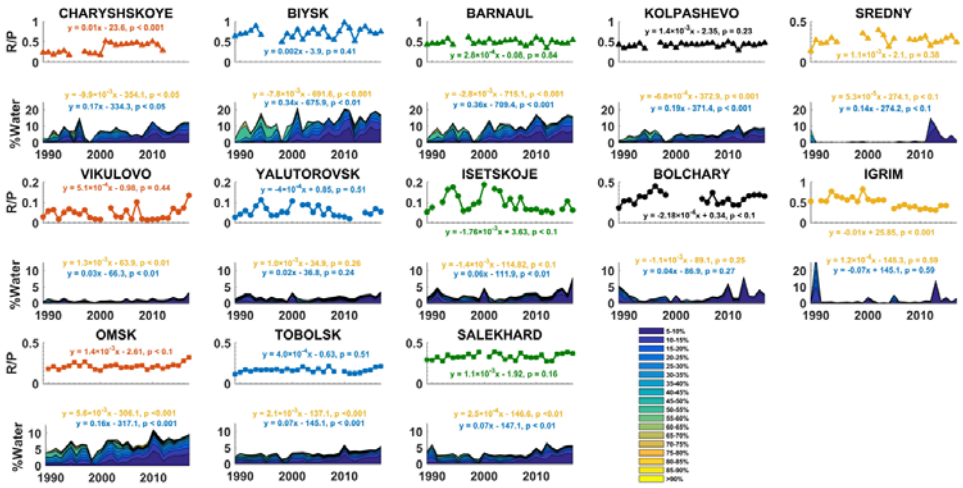


Figure 1. Annual runoff and WIF for watersheds in the Ob River basin.

The change in water surface area is an important aspect of the change in the underlying surface (Fig. 2). For permanent water bodies (with a submergence frequency greater than 75%), the correlation coefficient between water surface area and runoff coefficient R/P is less than 0.3. In comparison, for nodular water bodies with a submergence frequency between 10-75%, the correlation coefficient between water surface area and runoff coefficient is as high as 0.84. Research has shown that the spatiotemporal differences in runoff coefficients of each sub-basin are related to seasonal changes in the water body area, and this relationship is also controlled by the geographical conditions of the basin, especially the hydrothermal conditions.

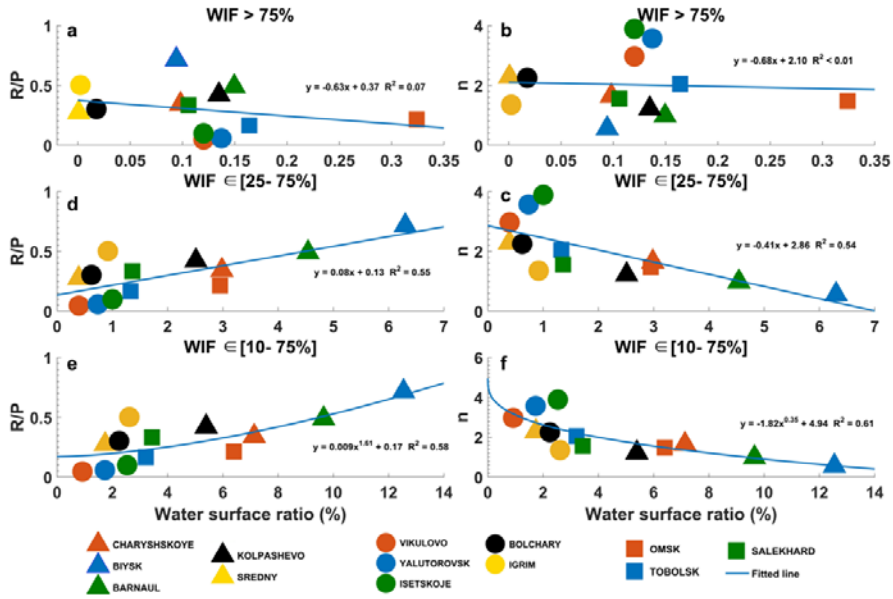


Figure 2. Correlation between Runoff coefficient (or the parameter n in the Budyko equation) with water surface ratio in different watersheds in the Ob River basin.

Acknowledgments: Our research is jointly funded by the Third Xingjiang Scientific Expedition and Research Program (Grant No. 2022xjkk070201), and the National Natural Science Foundation of China (U2003202, 42071054).

References

Huang, W.J., Duan, W.L., Nover, D., Sahu, N. and Chen, Y.N., 2021. An integrated assessment of surface water dynamics in the Irtysh River Basin during 1990-2019 and exploratory factor analyses. J Hydrol, 593.

Xu M, Kang S, Wang X, Wu H, Hu D, Yang D. Climate and hydrological changes in the Ob River Basin during 1936–2017. Hydrological Processes. 2020; 34: 1821–1836. https://doi.org/10.1002/hyp.13695

Adaptive hydrologic modeling approaches for optimizing water infrastructure design and management under nonstationarity

K. Hunu[1*], S. Conrad[2*]
[1] AtkinsRealis, 1616 E. Millbrook Rd, Suite 160, Raleigh, NC 27609
[2] Department of systems engineering, Colorado State University, 6029 Campus Delivery, Fort Collins, CO 80523
* e-mail: steve.conrad@colostate.edu; kenneth.hunu@atkinsrealis.com

Introduction

Traditional hydrologic design, which assumes static climate conditions, fails to consider the fluctuating nature of weather patterns and the need for multiple-objective consideration, like flood control, recreation, and energy production. Hunu et al. (2024) proposed an adaptive management framework that provides a practical approach for accounting for a changing climate and multiple objectives. The proposed adaptive management framework consists of: (1) a hydrologic modeling approach that accounts for climate nonstationarity and multiple objectives, and (2) a strategy to handle uncertainties, such as climate predictions, urbanization effects, and evolving basin objectives. It suggests biennial updates for baseline conditions to maintain both adaptability and practicality.

This paper describes the adaptive hydrologic modeling approach. A case study of the Buckhorn Creek Basin in North Carolina illustrates the application and outcomes. This basin serves various purposes including recreation, energy production, and water supply. The study demonstrates the necessity for innovative hydrologic modeling approaches in water infrastructure design and management due to climate change and varied stakeholder goals

Material and methods

The method for developing the modeling approach involved three main stages:

1. Collection of data including terrain data, land cover data, soils data, historical rainfall data, hydrologic and hydraulic infrastructure data, and observed data such as peak flow rates and water surface elevations for model calibration and verification.
2. Future rainfall data development from projections from General Circulation Models (GCMs)
3. Model development using the public domain United States Army Corps of Engineers (USACE) HEC-RAS model (USACE, 2022). HEC-RAS was chosen because it is both a hydrologic and hydraulic analysis, has considerably faster runtimes compared to the other available options, and has desirable features such as two dimensional (2D) flexible meshing ability, rain-on-grid modeling ability, ability to model hydraulic structures in 2D, ability to model infiltration and flow extractions such as pumping, and the ability to directly create and export results as GIS files.

Due to the nonstationarity of climate, future precipitation projections are needed for designing water infrastructure as climate conditions may be different at the end of the design life of the infrastructure than they are at present. Precipitation projections are usually derived from GCMs. There are multiple GCMs available, most of which provide projections that may be biased and, therefore, need to be downscaled to provide more accurate estimates. For this project, the Bias Corrected Constructed Analogs (BCCA) V2 Daily Climate Projections (Bracken, 2016) was used. The GCM projections were downscaled to improve their accuracy.

The process used for developing the hydrologic model involved delineation of the contributing drainage area for the basin, building of the 2D computational mesh, application of inflow and outflow boundary conditions, and validation of the model. The computational mesh was configured to model all the key features within the Buckhorn Creek basin including the Shearon Harris Lake, Sharon Harris Dam, Buckhorn Dam, and the impoundment behind Buckhorn Dam. The validated model was used to simulate several scenarios developed based on the traditional approach and the adaptive management framework and the

results compared to ascertain the advantages of the new adaptive management framework. The scenarios represent expected changes in climate and basin stakeholder priorities.

Results and concluding remarks

The results in Table 1 demonstrate how the adaptive hydrologic modeling approach can be applied in water infrastructure design within multi-use basins to account for a changing climate and stakeholder priorities. It also shows the need for the application of the new adaptive approach in our changing environment.

The traditional approach fails to account for all basin needs for most of the scenarios because of predicted changes in basin needs, which the traditional approach is inadequate to handle. However, using the new approach makes it possible to meet the basin requirements even under uncertain and nonstationary conditions such as changing climate, basin uses, and land use.

The combination of the hydrologic modeling method and the adaptive management framework results in more accurate data for decision making since the climate projections being used for the design and management of the water infrastructure are reviewed and updated bi-annually. It also provides an opportunity to tailor the design and management of water infrastructure to changes to basin use requirements, and land uses.

Table 1. Comparison of results from the hydrologic model for traditional and new approach

Basin Use	Wet / Dry Conditions	Traditional Approach		New Approach	
		Scenario 1 (Year 2020)	Scenario 2 (Year 2022)	Scenario 1 (Year 2020)	Scenario 2 (Year 2022)
Water Supply	Wet Conditions	Pass	Fail	Pass	Pass
	Dry Conditions	Pass	Fail	Pass	Pass
Power Generation	Wet Conditions	Pass	Pass	Pass	Pass
	Dry Conditions	Pass	Fail	Pass	Pass
Recreation	Wet Conditions	Fail	Fail	Pass	Pass
	Dry Conditions	Fail	Fail	Pass	Pass
Environmental Flows	Wet Conditions	Pass	Pass	Pass	Pass
	Dry Conditions	Pass	Fail	Pass	Pass

References

Bracken, C. (2016). Downscaled CMIP3 and CMIP5 Climate Projections-Addendum Release of Downscaled CMIP5 Climate Projections (LOCA) and Comparison with Preceding Information. Technical Service Center, Bureau of Reclamation, US Department of the Interior: Denver, CO, USA.

Hunu, K., Conrad, S., DePue, M., Grigg, N., Bradley, T., & Sharvelle, S. (2024). Optimization of Water Infrastructure Design and Management in Multi-Use River Basins Under a Changing Climate.

USACE (2022). Hydrologic Engineering Center's River Analysis System (HEC-RAS), Version 6.0.

Introducing integrated event calibration: A novel framework for rainfall-runoff modelling in urban hydrology

M.N. Assaf[1*], S. Manenti[1,2], L. Tamellini[3], S. Todeschini[1,2]
[1] *Department of Civil Engineering and Architecture (DICAr), University of Pavia, Pavia, Italy*
[2] *Interdepartmental Centre for Water Research (CRA), University of Pavia, Pavia, Italy*
[3] *CNR-IMATI, National Research Council - Institute for Applied Mathematics and Information Technologies, Pavia, Italy*
** e-mail: mohammed.assaf@unipv.it*

Introduction

Urban expansion and land sealing have significantly impacted the hydrological cycle, resulting in highly changes to the rainfall-runoff process and intense degradation of water quality. Rainfall-runoff modelling is of fundamental importance for accurate analysis and planning of the drainage system, for the design of interventions and flood mitigation strategies. However, the inflow-outflow transformation is a complex hydrological phenomenon, which involves several variables related to rainfall patterns, basin characteristics, type of soil and physiography. The precision of the rainfall-runoff model depends on parameter determination. In event-based modelling, the commonly used calibration method is event-by-event approach, which generates a unique set of parameters for each event (Hossain et al., 2019). Mathematical methods, such as averaging or weighted averaging, are then applied to synthesize these groups set of parameters into a single calibration set (Barco et al., 2008). However, this approach faces several challenges. Primarily, generating multiple sets of calibrated parameters for specific events introduces variability and potential inconsistencies in the modelling process. Also, the synthesis process may produce generalized parameters that fail to capture event-specific nuances.

This work introduces a new approach that integrates event calibration by calibrating all events collectively rather than individually. The consideration of all events provides a holistic view of stormwater dynamics, eliminates the need for post-calibration synthesis, and improves model generalizability and applicability. This research compares the traditional event-by-event approach with the new integrated event calibration approach in an experimental urban catchment in Pavia, Italy.

Materials and methods

The selected study case is Cascina Scala, located in Pavia, Northern Italy. It's an urban catchment used for residential purposes, with a total area of 13 hectares, consisting of 61.5% impervious surfaces and 38.5% pervious surfaces. The catchment is divided into 42 sub-catchments, each equipped with its own single pipe drain system. Fifty-seven events were used for the calibration and validation process. The first stage involves the development of the Hydrology Module and the Hydraulics Module for the case study using the EPA Storm Water Management Model (SWMM) (Rossman, 2010). These modules are key parts of the SWMM, designed to simulate the hydrological processes and water movement through the system. The hydrograph is the output of these modules, displaying the way wet-weather flow or runoff changes over time in response to precipitation events. Mat-SWMM plays the role of the interface linking MATLAB and SWMM to enable simple data exchange and analysis (Riaño-Briceño et al. 2016). Ten model parameters are fine-tuned through an optimization process employing a Genetic Algorithm (GA), where the GA and SWMM integration is enabled by Mat-SWMM. These parameters are iteratively adjusted by the GA to optimise the performance of the model, with the objective of either maximising or minimising an objective function reflecting the hydrograph prediction's accuracy. Two calibration approaches were compared: the traditional event-by-event approach and the new integrated event calibration approach.

Results and concluding remarks

Figure 1 presents the hydrographs for event 61 from the calibration set and event 57 from the validation

set, obtained with the event-by-event approach (dark-grey dotted line) and the integrated event calibration approach (grey solid line). Results indicate that the new approach provides a better agreement with the measured data in both the validation and calibration steps.

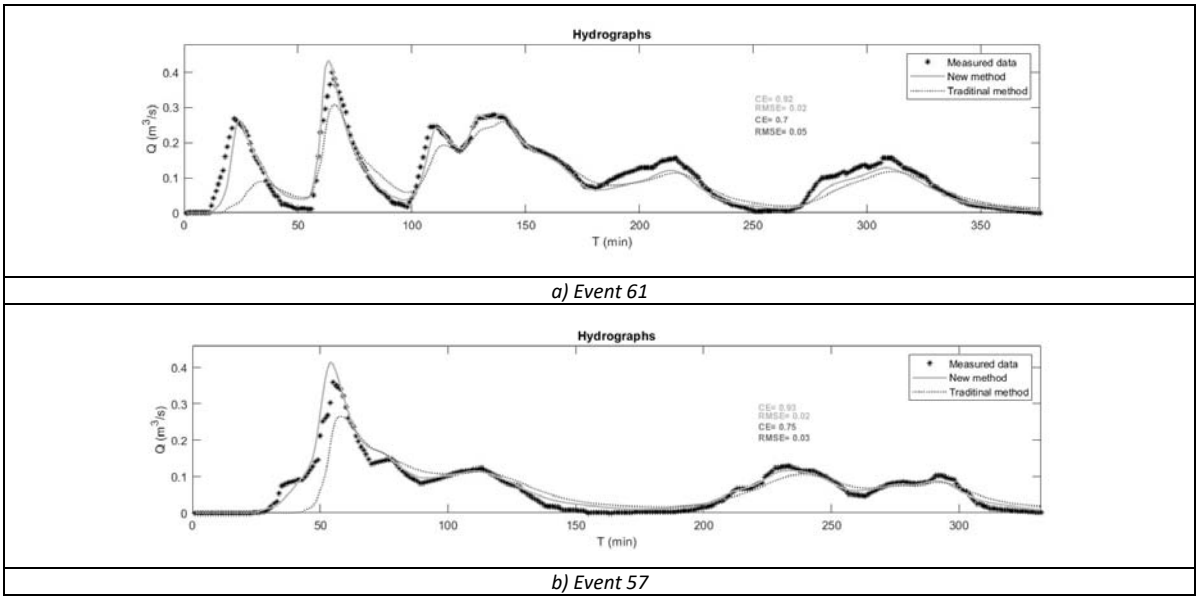


Figure 1. Comparison of the hydrographs from event by event approach and integrated event calibration approach

Table 1 presents a comparison of total volume, peak flow rate, and time to peak for the two approaches. The results indicate that the new approach exhibits a better estimation of total volume and peak flow rate, especially in the validation phase. A better estimation in the validation phase is shown also for time to peak.

Table 1. Goodness-of-fit indices for total volume, peak flow rate, and time to peak for the two approaches.

		Traditional		New methods	
		CE	RMSE	CE	RMSE
Total volume (m^3)	Calibration	0.91	299	0.93	265.5
	Validation	0.88	270.4	0.9	248.9
Peak flow rate (m^3/s)	Calibration	0.78	0.13	0.78	0.13
	Validation	0.4	0.2	0.81	0.11
Time to Peak (min)	Calibration	0.98	11.5	0.97	16.04
	Validation	0.93	55.6	0.99	6.41

Acknowledgments: Mohammed N. Assaf, Sauro Manenti, Lorenzo Tamellini and Sara Todeschini have been supported by the PRIN 2022 PNRR project "Uncertainty Quantification of coupled models for water flow and contaminant transport" (No. P2022LXLYY), financed by the European Union - Next Generation EU.

References

Barco J, Wong KM, Stenstrom MK (2008) Automatic calibration of the US EPA SWMM model for a large urban catchment. Journal of Hydraulic Engineering 134(4): 466–474. https://doi.org/10.1061/(ASCE)0733-9429(2008)134:4(466

Hossain S, Hewa GA, Wella-Hewage S (2019) A comparison of continuous and event-based rainfall–runoff (RR) modelling using EPA-SWMM. Water 11(3): 611. https://doi.org/10.3390/w11030611

Riaño-Briceño G, Barreiro-Gomez J, Ramirez-Jaime A, Quijano N, Ocampo-Martínez C (2016) MatSWMM–an open-source toolbox for designing real-time control of urban drainage systems. Environmental Modelling & Software 83: 143–154. https://doi.org/10.1016/j.envsoft.2016.05.009

Rossman LA (2010) Storm Water Management Model User's Manual; Version 5.0. U.S. Environmental Protection Agency, Cincinnati, OH, USA.

Mega flood events: The bivariate flow-volume frequency analysis

V. Tsakiris[1], H. Vangelis[2], G. Tsakiris[2*]
[1] SEEMAN Environmental, Anixi, Athens 14569, Greece
[2] Laboratory of Reclamation Works and Water Resources Management, School of Rural, Surveying and Geoinformatics Engineering, National Technical University of Athens, Athens, Greece
* e-mail: gtsakir@hotmail.gr

Introduction

Conventionally the design of works for flood protection of cities is based on unilateral frequency analysis of annual maxima of peak flows using suitable probability distributions. The engineering term of the "Return Period" has been established as the key variable for communicating the capacity of the works to withstand certain flood flows.

However, in mega flood events, as those experienced during the last few years in Europe (Bertola et al., 2023) and areas around the Mediterranean basin, it was observed that the extended catastrophes occurred due to the high flood volumes rather than the peak flows. It should be emphasized that extreme phenomena like the DANIEL in Thessaly-Greece and Libya and DANA in Valencia and Sicily with hundreds of dead people (11500 lost lives in Libya), thousands of drowned animals and catastrophes of billions of euros underscore the necessity of some changes in the way we design the flood protection measures and we act during such mega flood events.

This short presentation aims at pointing out some aspects which have not been discussed adequately after these catastrophic events.

Materials and methods

The traditional engineering approach uses univariate probability analysis which concentrates on the peak intensity of the phenomenon. This simplistic approach, however, cannot be applied to the affected systems in which the flood volume may be more critical than the peak flow.

The last catastrophic events worldwide show that these events should be statistically studied as bivariate phenomena including both peak flows and flood volumes. For this purpose, if both variates follow the same probability distribution, the analysis can be performed using a bivariate probability distribution (Gumbel and Mustafi, 1967). That is if both the flow and the volume of flood follow the Extreme Value distribution Type I, known as Gumbel distribution, the probability distribution for the simultaneous frequency analysis of both variates is the bivariate Gumbel distribution (Yue, 2000).

However, if the two variates follow different (marginal) probability distributions the above approach cannot be applied. In this case the method of bivariate copulas may be applied.

Results and concluding remarks

There are three important points which should be stressed out when evaluating the recent mega flood events.

Point 1: More room for the high flood volumes (bivariate analysis flow vs volume)

In case the method of bivariate copulas should be applied, using Archimedean bivariate copulas is proposed. Figure 1 was derived for the estimation of the return period based on pairwise frequency analysis of both flow and volume, utilising data from Ashuapmushuan river (Canada) to estimate the parameters of the bivariate Gumbel-Hougaard Archimedean copulas. Based on this case study, it was shown that the results concerning the "OR" return period are practically identical irrespective of the method for parameter estimation of the selected copula (e.g. maximum likelihood method or Kendall τ) which is shown in Figure 1 (Tsakiris et al., 2015).

As can be seen from Figure 1, for low values of return periods the peak flows pay the major role.

However, for more important events such those in which the return period exceeds the level of 100 years, the role of the flood volume plays a significant role. Therefore, the customary analysis of frequency of flood flows is not sufficient and the frequency of both peak flows and flood volumes is the most appropriate way to capture the significance of the mega events.

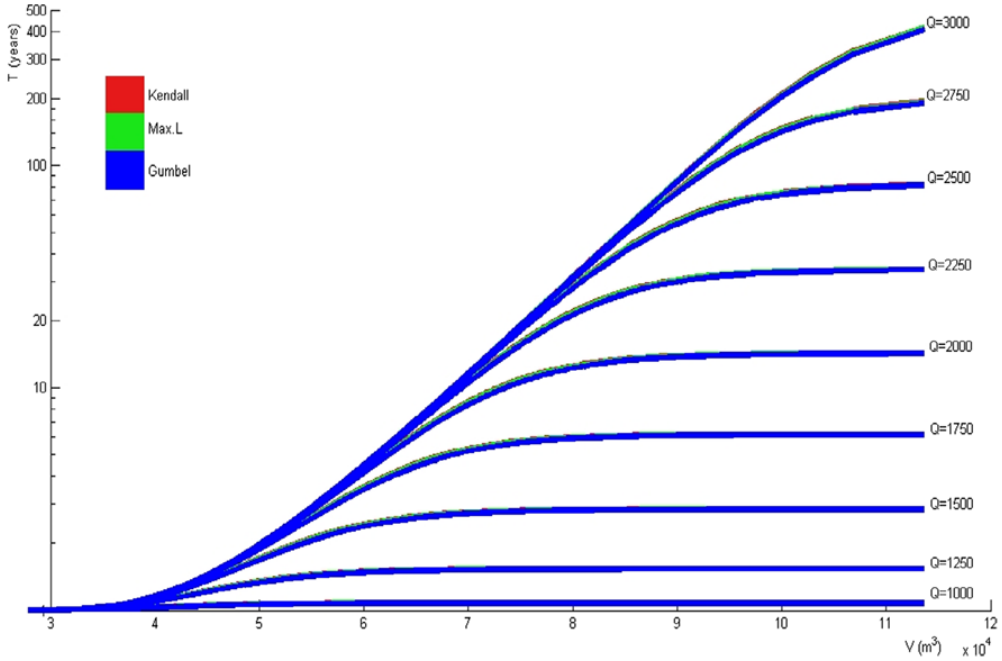


Figure 1. Estimation of the "OR" return period (flow and volume) derived by Gumbel-Hougaard Archimedean copula (data from Ashuapmushuan river- Canada).

Point 2: Roads without drainage facilities

A high percentage of roads in the cities do not have the appropriate drainage infrastructure so they are working as linear conveyance conduits with low Manning coefficient transporting flood waters and moving cars and other materials as floating objects quickly at lower levels.

Point 3: Management of flood flows for fluvial floods coming out of the built-up areas

This may be achieved by various structures such as check dams, relief outlets etc., after a rational selection of the locations of structures which impede or accelerate the flood flow in parts of the hydrographic network targeting into avoiding the coincidence of high flows. This may be achieved by a systematic simulation of flows in the entire system of streams of the basin.

In conclusion, the recent mega flood events in the Mediterranean point out that some drastic decisions for changes in the design of flood protection from of these events should be taken. Among the most important of them is that the design should be based on the frequency analysis of the flood volumes and the peak flows in a pairwise dependence. Also, the flows coming outside the built-up basins should be managed to avoid coincidence of high flows. Finally, all the roads should be equipped with flood protection infrastructure.

References

Bertola M, Blöschl G, Bohac M et al. (2023) Megafloods in Europe can be anticipated from observations in hydrologically similar catchments. Nature Geoscience 16(11): 982–988. https://doi.org/10.1038/s41561-023-01300-5

Gumbel E J, Mustafi C K (1967) Some Analytical Properties of Bivariate Extremal Distributions. Journal of the American Statistical Association, 62(318): 569–588. https://doi.org/10.1080/01621459.1967.10482930

Tsakiris G, Kordalis N, Tsakiris V (2015) Flood Double frequency analysis: 2D-Archimedean Copulas vs Bivariate Probability Distributions. Environmental Processes 2: 705–716. https://doi.org/10.1007/s40710-015-0078-2

Yue S (2000) The Gumbel Mixed Model Applied to Storm Frequency Analysis. Water Resources Management 14(5): 377–389. https://doi.org/10.1023/A:1011124423923

Analysis of evapotranspiration trends in India

V.K. Gunturu, V. Jothiprakash*, B. Sivakumar
Department of Civil Engineering , Indian Institute of Techology Bombay, Bombay, India
** e-mail: vprakash@iitb.ac.in*

Introduction

Evapotranspiration (ET) refers to the combined process of evaporation from land surface and transpiration from plants. It is the second largest component of the hydrological cycle over land, following precipitation. ET primarily depends on the water-availability and show considerable differences across geographical regions as well as temporal scales. These variations necessitate studies employing trend, homogeneity, and various statistical methods for the effective management of water-resources.

Since ET is difficult to measure, several global studies have used modelled ET data to study these trends and found increasing trends of ET. During the same period, decreasing trends were observed over India. Recent studies on ET over India show both increasing and decreasing trends (Goroshi et al., 2017). Studying these trends is crucial for India, given its predominantly agrarian economy. Therefore, in this study, trends of ET over longer temporal period (1980 – 2020) using daily, monthly, and annual data were analysed. Furthermore, a novel data which indicates agriculture activity as well as increasing temperatures is also considered. This novel data is derived from maximum value in a month, called as daily maximum of monthly data.

Materials and methods

To study the trends of ET over India, data from the Global Land Evaporation Amsterdam Model (GLEAM), developed by Miralles et al. (2011) were used. The GLEAM product employs the Priestley-Taylor method for estimating ET and offers a higher temporal resolution (1-day) as compared to other ET data. With 0.25° of spatial resolution, a total of 4,597 grids of ET data over India were extracted. In this study, daily, monthly, annual, and daily maximum of monthly data from 1980 to 2020 were analysed using two trend tests: Mann-Kendall test (MK) and Sen's Slope estimator (SS).

To evaluate the trends in GLEAM data, both the MK test and SS estimator were employed. A significance level of 5% (α = 0.05) was adopted for hypothesis testing. For better interpretation of the results from both the tests, the trends were categorized into significant increasing trend (SIT), significant decreasing trend (SDT), insignificant increasing trend (IIT), and insignificant decreasing trend (IDT) based on the sign of the test statistics (z-statistic for MK test and the magnitude of trend for SS estimator) and significance level. The categorization is summarized in Table 1.

Table 1 Categorization of trend based on the sign and significance level

	MK		SS	
	Z-value	**Significance level (α)**	**sign (SS estimator)**	**Significance level (α)**
Significant Increasing Trend (SIT)	>0	<0.05	>0	<0.05
Significant Decreasing Trend (SDT)	<0	<0.05	<0	<0.05
Insignificant Increasing Trend (IIT)	>0	>0.05	>0	>0.05
Insignificant Decreasing Trend (IDT)	<0	>0.05	<0	>0.05

Results and concluding remarks

The type of trend identified by both MK test and SS estimator for each grid are consistent (Table 2). It can be observed that increasing trends (both SIT and IIT) accounts for more than 90% of the study area for daily, monthly, and annual data. However, for the daily maximum of monthly data, only 79.96% (53.40% + 26.56%) of study area show increasing trend. In case of decreasing trend for the daily maximum of monthly data, the percentage of decreasing trends are highest (5.45% + 13.81%). Similarly, the decreasing trends in

daily, monthly, and annual data are lower. The spatial variations of these trends are shown in Figure 1.

Table 2. Comparison of ET_a trends among the time series (numbers indicate percentages).

Time series	MK				SS			
	SIT	SDT	IIT	IDT	SIT	SDT	IIT	IDT
Daily	91.64	2.28	3.27	2.02	91.64	2.28	3.27	2.02
Monthly	69.25	0.06	26.30	3.59	69.25	0.06	26.30	3.59
Annual	70.93	0.73	22.83	4.71	70.93	0.73	22.83	4.71
Daily Maximum of Monthly	53.40	5.45	26.56	13.81	53.40	5.45	26.56	13.81

The spatial variations are consistent for both the MK (Figure 1a-d) and SS (Figure 1e-h) test. A large portion of the study area as well as temporal scales shows increasing trend, these trends could be attributed to the increased irrigation activity through canal irrigation. Furthermore, the present study shows increasing trends, as compared to the previous studies (Goroshi et al., 2017). The rest of the study area shows decreasing trends, these are observed in North (cold arid), East (humid), and South-East (sub-humid) of the study area. The decreasing ET trends in these regions will increase in air temperature, thus causing more evaporation, leading to heatwaves and drought conditions, which will lower agricultural productivity. The results of the present study will be useful for long-term water-management strategies.

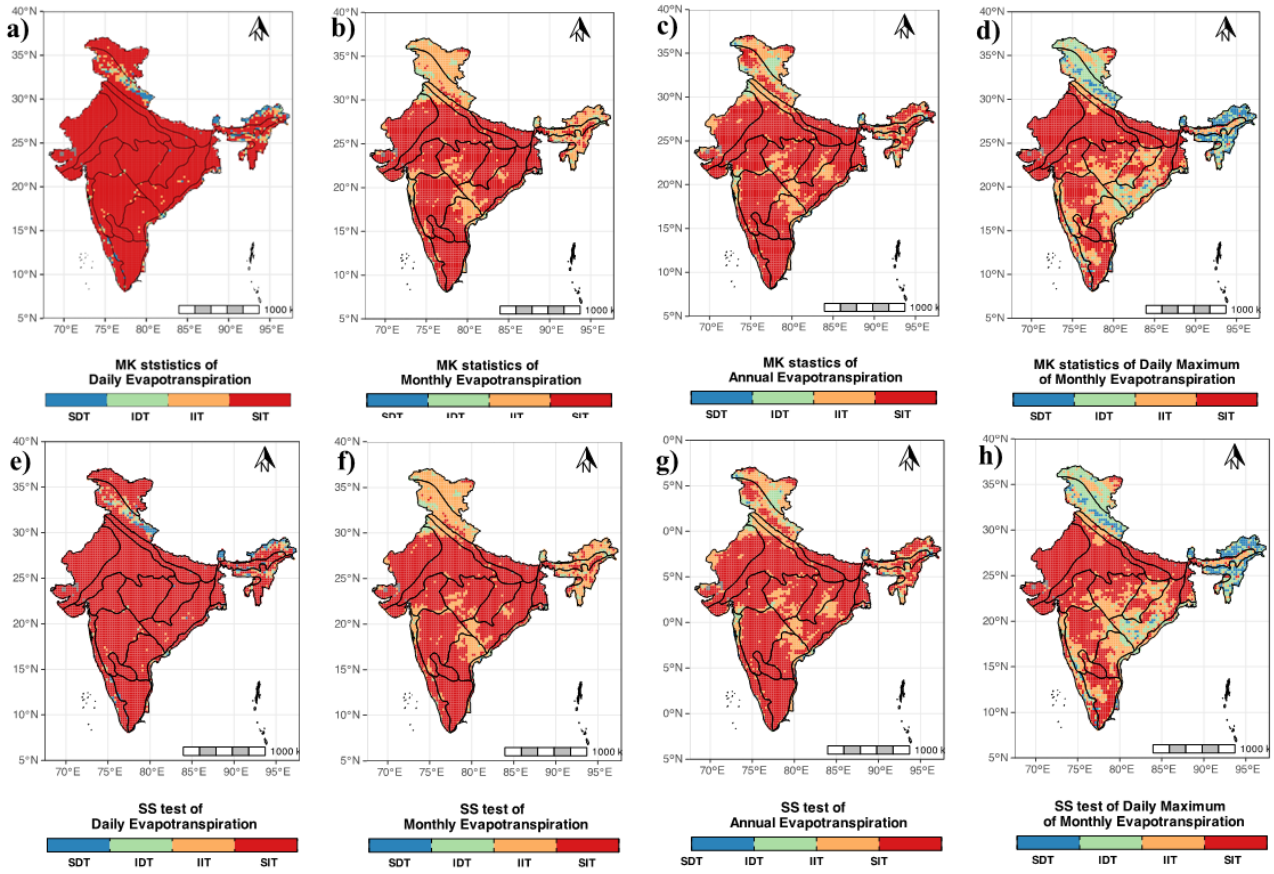


Figure 1. MK and SS tests over India, where maps a to d show for MK test and e to h show for SS tests.

References

Goroshi S, Pradhan R, Singh R.P, Singh K.K, Parihar J.S (2017) Trend analysis of evapotranspiration over India: Observed from long-term satellite measurements. Journal of Earth System Science 126 (8): 113.

Miralles D.G, Holmes T.R.H, De Jeu R.A.M, Gash J.H, Meesters A.G.C.A, Dolman A.J (2011) Global land-surface evaporation estimated from satellite-based observations. Hydrology and Earth System Sciences 15 (2): 453–469

Fault-controlled groundwater flow in karst aquifers of the Italian Prealps: implications for geomorphic hazards in a changing environment

V. Francani[1], P. Gattinoni[2*], L. Longoni[2], M. Papini[2]
[1] Tethys srl, Milan, Italy
[2] Dept. of Civil and Environmental Engineering, Politecnico di Milano, Milan, Italy
* e-mail: paola.gattinoni@polimi.it

Introduction

Landslides, among the most significant natural hazards in mountain regions, are frequently triggered by groundwater (Gattinoni 2009), especially where fault zone-related permeability structures exert primary control on fluid flow (Scheingross et al. 2013; Faulkner et al. 2010, and reference therein). Within karst aquifers and normal tectonic systems, fault breccias often occur within the fault core, and the contrasting permeabilities of breccias and fault gouge governs fluid flow, often triggering slope instabilities. This is particularly critical in fault-controlled karst systems with large catchment basins, where the tectonic setting (i.e., systems of close, deep and subvertical faults) causes underground and surface water flow to converge towards highly restricted flow sections, leading to landslides as consequence of extreme climatic events.

This paper provides field data and modelling results that document the significant influence of fault-induced permeability changes on landslide susceptibility within karstified carbonate aquifers of the Italian Prealps, to guide the ongoing monitoring efforts towards the most appropriate system (Agliardi et al. 2009).

Materials and methods

The study area is located at the Southern border of the Alps, within the Southalpine basement (Fig. 1), characterized by high-grade metamorphic rocks, overlain by sedimentary sequences including Triassic limestones and siliciclastic deposits. To assess the hydrogeological susceptibility to landslides, and its possible correlation to both karst and fault zones, the groundwater flow was reconstructed using a multi-scale modelling approach, from catchment to slope scale, which allowed to compare flow rates and pressure to the landslide distribution. The study concerns with the following three steps, involving both field surveys and data analysis: fault zone analysis and fracture data collection; analysis of slope instability through data collection, aerial photographs, and field surveys; assessment of the hydrogeological characteristics, i.e. interconnectivity, hydraulic conductivity and main flow direction.

Afterwards, the hydrogeological structure was analysed using a 3D numerical flow model to simulate the groundwater flow path at the catchment scale accounting for the influence of faults, fractures and karst zones. To investigate local effects on rock stability, this flow model was coupled to a discrete one at the slope scale. At this aim, data from onsite geostructural surveys were used for characterising joint sets, whereas the boundary conditions were assigned based on the hydraulic head simulated by the catchment scale model. The flow model at the slope scale was also coupled to a mechanical one to assess the local slope stability conditions. Finally, the correlation between the distribution of slope instabilities and the structural and hydrogeological features of fault zones was discussed to identify the tectonic features most likely to affect slope stability.

Results and concluding remarks

The study area is crossed by several joint sets (Fig. 1). The most relevant one for karsts evolution and slope stability belongs to a subvertical faults system (Lecco Faults), having strike parallel to the Lake and involving a significant decrease in mechanical strength of widespread rock slopes. The morphological setting is significantly affected by tectonic features, as demonstrated by valleys (having the same trend as tectonic lines) and frequent rockfalls occurring along steep slopes parallel to the faults.

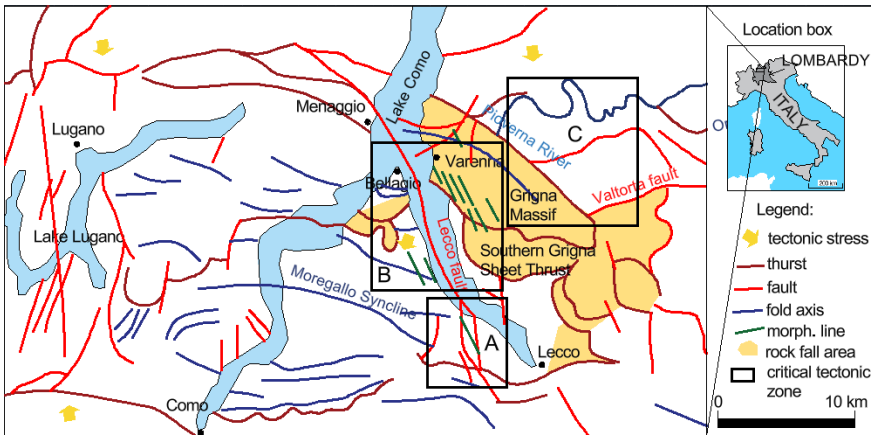


Figure 1. Tectonic framework of the study area and zonation of its hydrogeological susceptibility to landslides.

The groundwater flow is ruled by karsts features mainly developed along fracture zones. The recharge arises from rainfall, and it is concentrated in karstified uplands, where large dissymmetric sinkholes favour infiltration. Groundwater flows primarily along tectonic alignments, characterized by a high fracturing degree and almost parallel to steep rock slopes, supplying both rivers and springs. Based on modelling results, the most critical conditions for slope stability occur wherever the hydraulic conductivity of joints decreases along the flow path, leading to a significant increase in local water pressure. Water pressure, estimated about 50-60 kPa, corresponding to a specific discharge on the order of 10^{-4} m/s, can trigger rock instabilities similar to past events, involving blocks with size from few dm^3 to 5-6 m^3. These instabilities are particularly likely to occur at the convergence of surface water and groundwater flowing along karst/fault joints. Actually, the water infiltrated into the epikarst flows towards the valley heads, locally generating waterfalls and bringing about erosion, thus affecting the stability of both the rocky ridges (due to groundwater flowing within the highly weathered rock mass) and debris fans accumulated along the valleys (due to surface water channelling). Notably, faults with flower structure are characterised by lots of tensile cracks, affecting the infiltration rate and therefore increasing the groundwater recharge from the epikarst towards the heads of the valleys. The huge groundwater supply arising from these structures is a key factor in slope instability, as exemplified by the Fiumelatte event in 2023, occurred during exceptional rainfall. This hydrogeological setting resulted to be the most vulnerable also based on geophysical surveys, carried out on different Alpine and Apennine areas. These flow modelling results were compared to the landslide map, to highlight landslide susceptibility related to groundwater conditions, identifying three main situations which enhance hydrogeological susceptibility to landslide. Figure 1 shows the resulting zonation:

- zone A: the combined effects of overthrusting, fault reactivation, and karstification in flower faults;
- zone B: the overlapping of fault networks associated with subsequent stresses brought about a hydrogeological setting conveying water towards rocky ridges and debris fans along the lake;
- zone C: the uplift along the Orobic Anticline with the related deformation and fracturing of the crystalline basement, favours the recharge from the epikasrt to the deep aquifer and then to springs.

The study area exhibits a peculiar hydrogeological setting, strongly controlled by its tectonic structure and evidently decisive in governing the geomorphological processes. The comparison between modelling results and field data surveys validated this correlation, enabling a more comprehensive assessment of hydrogeological hazards of the Lombard Prealps under climate change scenarios.

References

Agliardi F, Crosta GB, Frattini P (2009) Integrating rockfall risk assessment and countermeasure design by 3D modelling techniques, Nat Hazard Earth Syst Sci, 9: 1059-1073.

Faulkner DR, Jackson CAL, Lunn RJ, Schlische RW, Shipton ZK, Wibberley CAJ (2010) A review of recent developments concerning the structure, mechanics and fluid flow properties of fault zones, Journal of Structural Geology, 32: 1557-1575.

Gattinoni P (2009) Parametrical landslide modeling for the hydrogeological susceptibility assessment: from the Crati Valley to the Cavallerizzo landslide (Southern Italy). Natural Hazard, 50: 161-178.

Scheingross JS, Minchew BM, Mackey BH, Simons M, Lamb MP, Hensley S (2013) Fault-zone controls on the spatial distribution of slow-moving landslides. GSA Bulletin; March/April 2013; v. 125; no. 3/4; p. 473–489

Precise determination of water surface evaporation for refining hydrological balance

A. Beran*, A. Vizina, P. Pavlík, V. Moravec, R. Kožín
T.G. Masaryk Water Research Institute, Prague, Czech Republic
** e-mail: adam.beran@vuv.cz*

Introduction

Due to climate change, the average air temperature is increasing (IPCC, 2021), leading to more intense water evaporation from surface areas (Kohn et al., 2018). Accurate measurement of evaporation is crucial for understanding the hydrological balance and effective water resource management. Traditional calculation methods based on meteorological data may show inaccuracies; therefore, direct monitoring using floating evaporimeters is a significant advantage. Studies conducted at water reservoirs in the Czech Republic demonstrate a difference between modeled and actually measured evaporation, confirming the necessity of direct measurement.

Materials and methods

Evaporation measurement was carried out using floating evaporimeters equipped with meteorological sensors. The evaporimeters operate at water reservoirs from April to November, recording evaporation, precipitation, air and water temperature, wind speed, relative humidity, and solar radiation. Data are collected at ten-minute intervals and transmitted to a server. Water surface evaporation is verified by modeling using empirical formulas.

Two locations were included in the study, both in the Czech Republic – Vavřinec pond in Central Bohemia and Karhov reservoir in the south of the Czech Republic. The T. G. Masaryk Water Research Institute has been conducting research at these sites for the past six years.

Empirical equations dependent on air temperature, derived from long-term evaporation and meteorological monitoring in the Czech Republic, were used for evaporation calculations (Ansorge and Beran, 2019).



Figure 1. Floating evaporimeter placed at Vavřinecký pond

Results and concluding remarks

The results showed that the modeled evaporation differed from the actual measured values depending on the chosen formula and measurement conditions. The most significant deviations were recorded during extreme meteorological events, highlighting the limitations of model-based approaches.

Similar measurements were conducted at Vavřinec pond between 2020 and 2024 (Beran et al., 2023). The results showed that during summer months, evaporation exceeded precipitation by more than 100 mm, impacting the hydrological balance of the watercourse. The floating evaporimeter enabled a detailed analysis of water temperature changes, wind speed, and other factors influencing evaporation.

Accurate measurement of evaporation is crucial for assessing the hydrological balance in the context of climate change. Floating evaporimeters provide more detailed and precise data compared to model-based calculations. Studies at different water reservoirs within the Czech Republic demonstrates that evaporation could significantly affect water availability in catchments (Table 1 – in some months evaporation exceeds precipitation), which is particularly important during drought periods. The measurement results confirm the necessity of continuing direct monitoring and improving modeling approaches for better evaporation prediction under changing climatic conditions.

Table 2. Measured evaporation and precipitation in 2024 at Karhov Reservoir

	Evaporation [mm]	**Precipitation [mm]**
April	61.1	34.8
May	77.5	160.9
June	107.0	99.3
July	118.3	165.0
August	120.7	56.8
September	70.8	220.9
October	24.6	120.0
November	14.2	25.5

Acknowledgments: This research was supported by projects SS02030040 “Prediction, Evaluation and Research for Understanding National sensitivity and impacts of drought and climate change for Czechia (PERUN)” and SS02030027 “Water systems and water management in the Czech Republic under climate change conditions (Water Centre)” funded by the Technology Agency of the Czech Republic.

References

Ansorge, L. and Beran, A. (2019) Performance of simple temperature-based evaporation methods compared with a time series of pan evaporation measures frm a standart 20 m2 tank. Journal of Water and Land Development. No. 41 (IV-VI) p. 1-11. DOI: 102478/jwld-2019.0021.

Beran, A, David, V, and Tyl, R (2023) Direct monitoring of water vapor from the free water level of the Vavřinecký pond and its influence on the hydrological balance. *Water Management Technical and Economical Information Journal*, 2023, vol. 65, No. 5, p. 4–8. ISSN 0322-8916.

IPCC (Intergovernmental Panel on Climate Change) (2021) Climate Change 2021: The Physical Science Basis. Contribution of working group I to the sixth assessment report of the Intergovernmental Panel on Climate Change. Cambridge University Press. DOI: 10.1017/9781009157896.

Kohn, I., Schume, H. and Jost, G. (2018) Why has catchment evaporation increased in the past 40 years? A data-based study in Austrie. Hydrology and Earth System Sciences, 22(10), 5143-5158. DOI: 10.5194/hess-22-5143-2018.

Performance assessment of two high-resolution precipitation datasets over a large basin in Southern Italy for water resources modelling

R. Padulano[1*], A. Avino[1], G. Del Giudice[1], M. Borga[2], S. Manfreda[1]
[1] Department of Civil, Architectural and Environmental Engineering, Università degli Studi di Napoli Federico II, Naples, Italy.
[2] Department of Land Environment Agriculture and Forestry, University of Padova, Padova, Italy.
* e-mail: roberta.padulano@unina.it

Introduction

Climate change is expected to have a deep influence over the Mediterranean area, on one hand exacerbating flood risks, on the other hand reducing ordinary rainfall events and, consequently, impacting water resources (Ali et al., 2021). In Southern Italy, impacts of climate change are not clearly understood yet, as research studies reveal heterogeneous seasonal trends. Notably, positive trends are more prevalent in autumn (Cammalleri et al., 2024), while negative trends dominate in winter and, more broadly, on an annual scale (Chiaravalloti et al., 2023). This underscores the complexity of the issue, highlighting the need for further investigation.

Many climate projections are available for precipitation over Italy under various climate scenarios (e.g., Jacob et al., 2020). However, these future projections often exhibit significant biases, which can only be corrected if current precipitation conditions are accurately assessed across the entire region. Unfortunately, the accuracy of such assessments is hindered by inadequate precipitation monitoring systems, characterized by sparse rain gauges and short or incomplete records. Gridded climate products can provide a useful alternative to point-scale data, provided that they show a good performance in reproducing observed patterns.

This contribution aims at investigating the performance of two high-resolution gridded products – VHR-REA_IT and SPHERA – considered as possible candidates to represent current climate for the bias correction of high-resolution climate projections. The assessment particularly focuses on the probabilistic features of ordinary rainfall events. In perspective, this will allow to project future ordinary rainfall regime at high spatial and temporal resolutions, shedding light on the expected availability of surface water resources.

Materials and methods

For this contribution the gridded datasets are compared with point-scale rainfall recordings over the Volturno Basin, the largest catchment in Southern Italy, with an area of 5630 km^2. Below is the key information of the materials used:

- VHR-REA_IT (Very High-Resolution PROjections for Italy; Raffa et al., 2021) consists of a dynamical downscaling of the ERA5 reanalysis, originally available at ≃31 km horizontal resolution, to ≃2.2 km horizontal and hourly temporal resolution (i.e., convection permitting scale). Dynamical downscaling is conducted through the COSMO Regional Climate Model. This dataset is freely available and covers 41 years (1981-2022).
- SPHERA (High rEsolution ReAnalysis over Italy; Giordani et al., 2023) is a high-resolution convection-permitting reanalysis centred over Italy. It is based on the non-hydrostatic limited-area model COSMO by dynamically downscaling the global reanalysis ERA5 with a nudging data assimilation scheme. It covers 26years (1995 -2020) with an hourly temporal resolution and a grid spacing of ≃2.2 km, consistent with VHR-REA_IT.
- Rainfall observations are provided by a network of 57 rain gauges which provide daily observations over the period 1994-2021 (27 years), with average completeness level of about 70% and elevation ranging between 100 and 1000 m a.s.l. (Avino et al., 2024).

Rainfall information from each rain gauge is compared the closest point of each gridded product. Performance of the gridded datasets with respect to observations is evaluated using multiple goodness-of-fit metrics, including RMSE, MAE, PBIAS and the Kling-Gupta Efficiency index.

Results and concluding remarks

Figure 1 compares the overall probabilistic features of the observational dataset with those exhibited by the gridded products. The results are presented in terms of L-moments ratio diagram, which captures the overall behaviour of the 57 samples (each point in the diagram represents a rain gauge, or its closest grid point). Focusing on the observational dataset (blue crosses), the probabilistic features of the rain gauges appear quite homogeneous, as all samples fall within a narrow range of coordinates. They are well represented by the Pearson Type III distribution or, more simply, by a Gamma distribution (both shown by the same curve in the diagram). Comparing observed data with the gridded products, both VHR-REA_IT and SPHERA suggest similar distributions, but they are not able to reproduce the same variability, particularly for VHR-REA_IT. This can be explained noting that VHR-REA_IT is a mere downscaling of a reanalysis: as such, it does not include any data assimilation process.

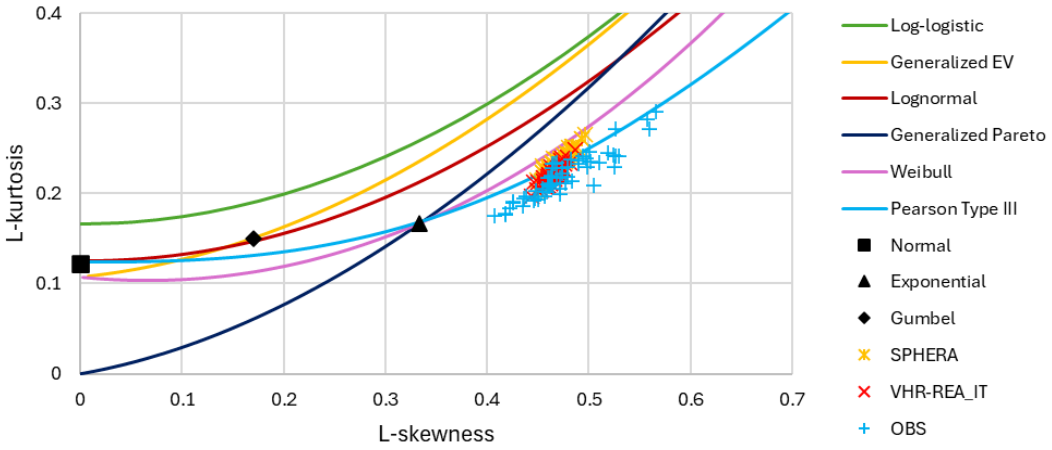


Figure 1. L-moments ratio diagram for the OBS, VHR-REA_IT and SPHERA samples.

Although Figure 1 offers a partial view of the agreement between daily observed and modelled data, SPHERA seems to provide a more accurate probabilistic representation of reality compared to VHR-REA_IT. However, a persistent bias remains, which should be carefully assessed to avoid its propagation through the bias correction of climate projections.

References

Ali, E., W. Cramer, J. Carnicer, E. Georgopoulou, N.J.M. Hilmi, G. Le Cozannet, and P. Lionello, 2022: Cross-Chapter Paper 4: Mediterranean Region. In: Climate Change 2022: Impacts, Adaptation and Vulnerability. Contribution of Working Group II to the Sixth Assessment Report of the Intergovernmental Panel on Climate Change [H.-O. Pörtner, D.C. Roberts, M. Tignor, E.S. Poloczanska, K. Mintenbeck, A. Alegría, M. Craig, S. Langsdorf, S. Löschke, V. Möller, A. Okem, B. Rama (eds.)]. Cambridge University Press, Cambridge, UK and New York, NY, USA, pp. 2233-2272, doi:10.1017/9781009325844.021.

Avino, A., L. Cimorelli, P. Furcolo, V. Noto, A. Pelosi, D. Pianese, P. Villani, S. Manfreda (2024). Are rainfall extremes intensifying in Southern Italy?, Journal of Hydrology. https://doi.org/10.1016/j.jhydrol.2024.130684

Cammalleri, C., Sarwar, A. N., Avino, A., Nikravesh, G., Bonaccorso, B., Mendicino, G., ... & Manfreda, S. (2024). Testing trends in gridded rainfall datasets at relevant hydrological scales: A comparative study with regional ground observations in Southern Italy. Journal of Hydrology: Regional Studies, 55, 101950. https://doi.org/10.1016/j.ejrh.2024.101950

Chiaravalloti, F., Caloiero, T., & Coscarelli, R. (2022). The long-term ERA5 data series for trend analysis of rainfall in Italy. Hydrology, 9(2), 18. https://doi.org/10.3390/hydrology9020018

Giordani, A., Cerenzia, I. M. L., Paccagnella, T., & Di Sabatino, S. (2023). SPHERA, a new convection-permitting regional reanalysis over Italy: Improving the description of heavy rainfall. Quarterly Journal of the Royal Meteorological Society, 149(752), 781-808. https://doi.org/10.1002/qj.4428

Jacob, D., Teichmann, C., Sobolowski, S., Katragkou, E., Anders, I., Belda, M., ... & Wulfmeyer, V. (2020). Regional climate downscaling over Europe: perspectives from the EURO-CORDEX community. Regional environmental change, 20, 1-20. https://doi.org/10.1007/s10113-020-01606-9

Raffa, M., Reder, A., Marras, G. F., Mancini, M., Scipione, G., Santini, M., & Mercogliano, P. (2021). VHR-REA_IT dataset: very high resolution dynamical downscaling of ERA5 reanalysis over Italy by COSMO-CLM. Data, 6(8), 88

How climate change affects Hargreaves model accuracy over time

V. Rattayová*, M. Garaj, M. Onderka
Climatological Service Department, Slovak Hydrometeorological institute, Jesséniova 17, Bratislava, Slovakia
** e-mail: viera.rattayova@shmu.sk*

Introduction

The Hargreaves model is one of the most commonly used alternatives to the FAO56 Penman-Monteith (P-M) model for calculating reference and crop evapotranspiration, particularly in regions where the extensive climatological data required for the P-M model are unavailable (Allen, 1998). The Hargreaves model is available in several modified and regionally calibrated versions (Maestre-Valero et al., 2013), including adaptations that incorporate altitude into the model structure (Ravazzani et al., 2012). Previous research has shown that the Hargreaves coefficients are influenced by climatological conditions, station altitude, and seasonal variation, for instance Guntilucci et al. (2021). Our research primarily focused on the regional calibration of the Hargreaves model; however, the results indicate that regional calibration alone is insufficient to maintain model accuracy over time. The findings reveal that model parameters are not stable over time, and in recent decades, optimal parameter values have exhibited a decreasing trend.

Materials and methods

The general Hargreaves model for reference evapotranspiration (ET0) is given as:

$$ET_0 = A * \left(\frac{T_{max}+T_{min}}{2} + B\right) * (T_{max} - T_{min})^C * R_a * D \quad (1)$$

where Ra is the extraterrestrial radiation [MJ m^{-2} d^{-1}]; T_{max} is the maximum air temperature [°C]; T_{min} is the minimum air temperature [°C]; T_{mean} is the mean air temperature calculated from the maximum and minimum daily temperature [°C] and coefficients A=0.0023, B=17.8, C=0.5, and D=0.408.

To improve the model's (Eg. 1) accuracy for Central Europe, we employed the lmfit Model class fitting method (Newville et al., 2014) for regional calibration. Since model accuracy varied across different altitudes, we introduced an altitude parameter to the equation to ensure similar accuracy across meteorological stations at various elevations. Our newly proposed modification of the Hargreaves model for the Central European region, incorporating altitude, is:

$$ET_{0,MODIF.2} = 0.0029 * \left(\frac{T_{max}+T_{min}}{2} + 21.27\right) * (T_{max} - T_{min})^{0.39} * R_a * 0.408 * (0.00014 * z + 0.97) \quad (2)$$

This modification was validated using data from 60 climatological stations in Slovakia, chosen to represent diverse morphological and climatic conditions. The daily meteorological data were sourced from the Slovak Hydrometeorological Institute (SHMI) database.

To evaluate model performance over time, we analysed trends in the B coefficient. Model accuracy was assessed using the Weighted Absolute Percentage Error (WAPE) and Pearson correlation Coefficient (R).

Results and concluding remarks

We observed a significant change in the trend of the "B" and "C" parameter values. After the year 2000, both parameters exhibited a strong decreasing trend. Specifically, the "B" parameter showed an R value of approximately 0.97 (Fig.1), a p-value of 0.0007, and a decline of -1 [-] per 10 years. These findings are crucial for future research, as they highlight the need for regular validation of the Hargreaves equations.

We conducted separate calibrations for the periods 1981–2000 and 2001–2020. The optimal B coefficient decreased from 20.2 to 19.7, indicating a shift in model behaviour over time. Using the general-purpose B value of 21.27 for the 2001–2020 period reduced model accuracy, with WAPE decreasing from 17.4% (using the general B value, Eg.2) to 16.9% (with the recalibrated B). Figure 2 presents a heatmap of

the mean station WAPE [%] for 1981–2020, using various B and C coefficient values for specific years.

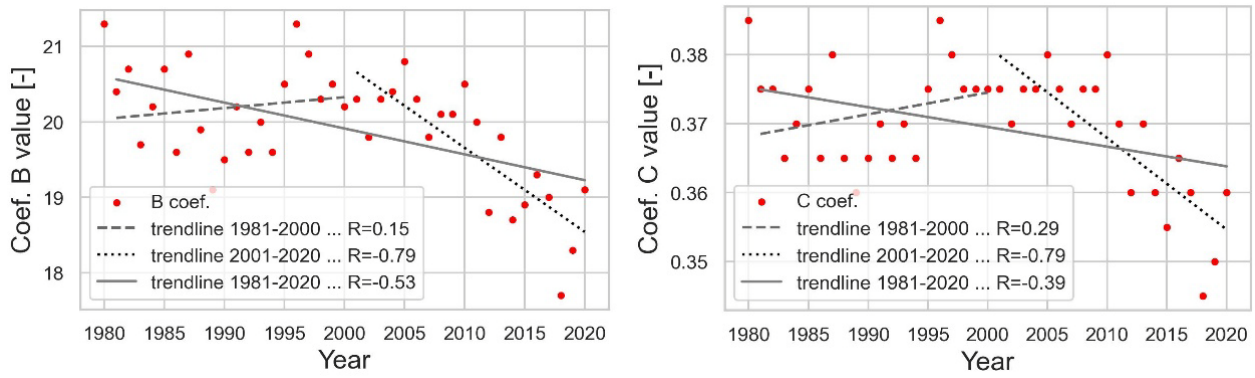


Figure 1. Temporal stability of Hargreaves model parameters B and C.

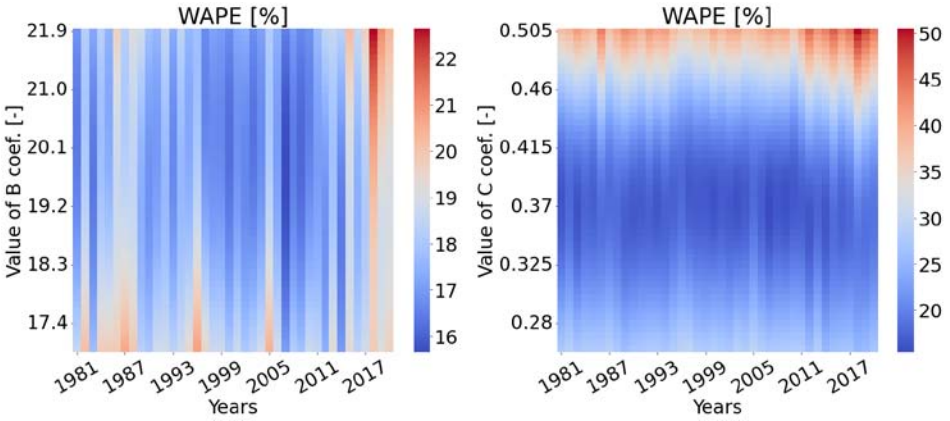


Figure 2. Heat map of the WAPE (%) estimated for Hargreaves model parameters B (left panel) and C (right panel) in the period 1981-2020.

Although selecting the best-fitting coefficient values for all stations ensures reasonable long-term accuracy, using a general coefficient value can lead to substantial errors for specific years. Our results bring a new finding indicating that model coefficients values vary over time. Therefore, for short-term applications, we recommend model validation against reference datasets to maintain accuracy.

Acknowledgments: This work was supported by the Interreg Central Europe project ("Clim4Cast", No. CE0100059) and by the Slovak Research and Development Agency under Contract No. APVV 23-0332.

References

Allen, R. G., Pereira, L. S., Raes, D., Smith, M., & W, a B. (1998). Crop evapotranspiration - Guidelines for computing crop water requirements - FAO Irrigation and drainage paper 56. Irrigation and Drainage. https://doi.org/10.1016/j.eja.2010.12.001

Gentilucci, M., Bufalini, M., Materazzi, M., Barbieri, M., Aringoli, D., Farabollini, P., & Pambianchi, G. (2021). Calculation of potential evapotranspiration and calibration of the hargreaves equation using geostatistical methods over the last 10 years in central Italy. Geosciences (Switzerland), 11(8). https://doi.org/10.3390/geosciences11080348

Maestre-Valero, J. F., Martínez-Álvarez, V., & González-Real, M. M. (2013). Regionalization of the Hargreaves coefficient to estimate long-term reference evapotranspiration series in SE Spain. Spanish Journal of Agricultural Research, 11(4). https://doi.org/10.5424/sjar/2013114-3869

Newville, M., Ingargiola, A., Stensitzki, T., & Allen, D. B. (2014). LMFIT: Non-Linear Least-Square Minimization and Curve-Fitting for Python. Zenodo.

Ravazzani, G., Corbari, C., Morella, S., Gianoli, P., & Mancini, M. (2012). Modified Hargreaves-Samani Equation for the Assessment of Reference Evapotranspiration in Alpine River Basins. Journal of Irrigation and Drainage Engineering, 138(7), 592–599. https://doi.org/10.1061/(asce)ir.1943-4774.0000453

Assessing streamflow uncertainty in mountainous watersheds: a comparative study of two monthly rainfall-runoff models

L. Vasiliades*, I. Mastraftsis
Laboratory of Hydrology and Aquatic Systems Analysis, Department of Civil Engineering, School of Engineering, University of Thessaly, 38334 Volos, Greece
** e-mail: lvassil@gmail.com*

Introduction

Hydrological models play a vital role in estimating runoff and analysing water balance dynamics. Parameter calibration is typically employed to align simulated outputs with observed data; however, inherent uncertainties remain due to both random variability and knowledge gaps. Errors in input datasets, inaccuracies in calibration data, and limitations in model parameters or structural formulation contribute to these uncertainties. As a result, assessing uncertainty is essential for reliable hydrological and water resource management studies. This study investigates uncertainty in streamflow estimation by applying two monthly water balance models (WBMs) in four mountainous watersheds located in Thessaly region at Pindus mountain range, Greece. The models examined are the 6-parameter R-UTHBAL (Vasiliades and Mastraftsis 2023) and the 2-parameter GR2M (Mouelhi et al. 2006). Three primary sources of uncertainty (input data, model structure, and model parameters) are assessed using the "hydroPSO" R-package, which employs a global Particle Swarm Optimization (PSO) algorithm (Zambrano-Bigiarini and Rojas 2013). The integration of these models with hydroPSO facilitates sensitivity, optimization, and uncertainty analyses, offering visual tools to aid in result interpretation and model performance evaluation.

Materials and methods

This study examines four forested watersheds: two within the Pinios River basin (Pamisos and Portaikos watersheds) and two in the Acheloos River basin (Mesochora and Sykia watersheds). Hydrometeorological and streamflow data are used for the period 1960-1993. Precipitation and mean temperature were spatially averaged using standard hydrological techniques, while potential evapotranspiration was estimated using the Thornthwaite method based on monthly temperature. Figure 1 presents the flowchart of the methodology.

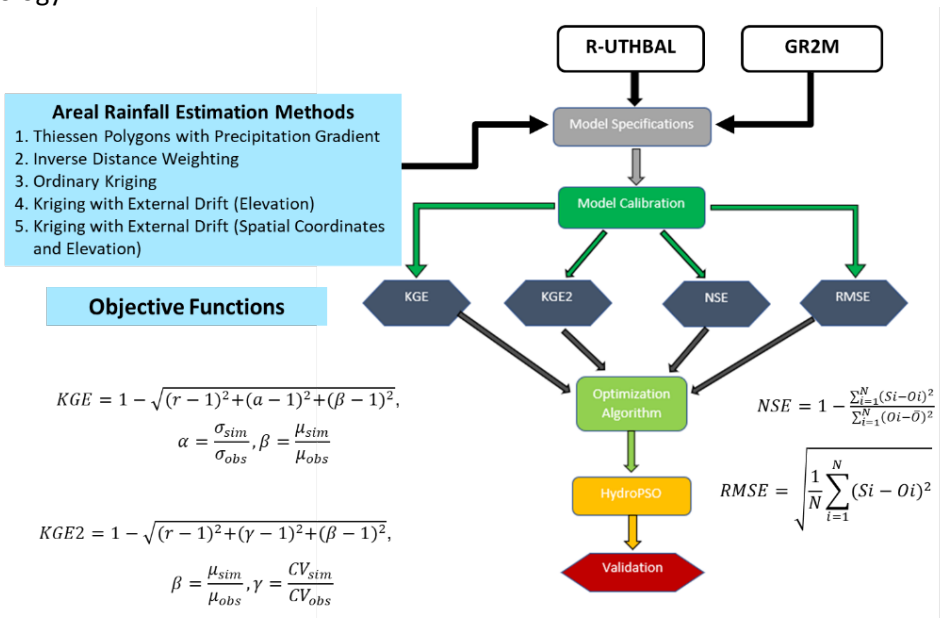


Figure 1. Flowchart methodology.

R-UTHBAL and GR2M models, adapted in the R programming environment, require monthly inputs of precipitation, mean temperature, and potential evapotranspiration. To assess key parameters and the necessary mathematical framework, the Latin-Hypercube One-factor-At-a-Time (LH-OAT) sensitivity analysis (van Griensven et al. 2006) was first applied. Model robustness and predictive consistency were then evaluated using the temporal split-sample test. Uncertainty in streamflow estimation was analyzed using multiple objective functions, including Root Mean Square Error (RMSE), Nash-Sutcliffe Efficiency (NSE), and two variations of the Kling-Gupta Efficiency (KGE). The hydroPSO package was employed to quantify uncertainty stemming from input data, model parameters, and structural limitations. HydroPSO integrates calibration and optimization routines through flexible ASCII files and R wrapper functions, enabling seamless interaction with hydrological models. By iterating until a predefined convergence threshold or iteration limit is reached, hydroPSO refines model performance while offering enhanced visualization tools for interpreting results.

Results and concluding remarks

The sensitivity analysis indicated that all model parameters contribute significantly to the mathematical structure and should be retained. To evaluate uncertainty in model parameters, simulations exceeding a predefined threshold (KGE2>0.3) were considered acceptable. Weighted quantiles of parameter distributions were then computed to quantify uncertainty in each calibrated parameter. Figure 2 illustrates the flow duration curves for the Portaikos watershed, comparing observed streamflows (black line) with the most accurate simulated values (blue line). Additionally, the 2.5% and 97.5% weighted quantiles of model outputs during the validation period are presented, providing a confidence interval for streamflow variability. The results emphasize the necessity of incorporating uncertainty analysis in hydrological modeling to enhance reliability in streamflow predictions, particularly in complex, mountainous terrains where water availability is crucial for resource management.

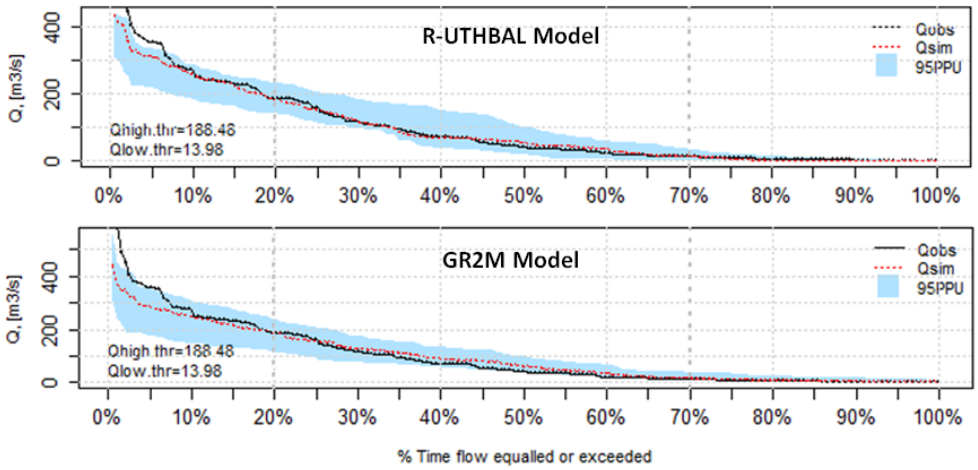


Figure 2. Flow duration curves for Pamisos watershed.

References

Mouelhi S, Michel C, Perrin C, Andréassian V (2006) Stepwise development of a two-parameter monthly water balance model. Journal of Hydrology 318:200–214. https://doi.org/10.1016/j.jhydrol.2005.06.014

van Griensven A, Meixner T, Grunwald S, et al (2006) A global sensitivity analysis tool for the parameters of multi-variable catchment models. Journal of Hydrology 324:10–23. https://doi.org/10.1016/j.jhydrol.2005.09.008

Vasiliades L, Mastraftsis I (2023) A monthly water balance model for assessing streamflow uncertainty in hydrologic studies. Environmental Sciences Proceedings 25(1):39. https://doi.org/10.3390/ECWS-7-14192

Zambrano-Bigiarini M, Rojas R (2013) A model-independent Particle Swarm Optimisation software for model calibration. Environmental Modelling & Software 43:5–25. https://doi.org/10.1016/j.envsoft.2013.01.004

Modelling future irrigation requirements for durum wheat cultivation in southern Sardinia

D. Svanidze[1*], R. Ludwig[1], M. Dettori[2], G. Urracci[2]
[1] Department of Geography, Ludwig-Maximilians-University, Munich, Germany
[2] Agricultural Research Agency of Sardinia (AGRIS Sardegna), Cagliary, Italy
* e-mail: d.svanidze@lmu.de

Introduction

Climate change is expected to exacerbate warming and drying trends in the Mediterranean region, negatively impacting agriculture and crop productivity (Lionello and Scarascia 2018). Durum wheat, the region's most widely grown crop, may face significant challenges as a result (Dettori et al. 2022). This study investigates the potential of low input irrigation to mitigate these effects.

Based on a field experiment in Sardinia, Italy, applying the agro-hydrological model SWAP (Soil-Water-Atmosphere-Plant), soil water content patterns and additional irrigation needs are simulated using projected climate data, for durum wheat cultivation under different irrigation treatments.

Materials and methods

The field experiment was conducted at the experimental farm San Michele of the Agricultural Research Agency of Sardinia (AGRIS Sardegna), located in the south of Sardinia in the Campidano Plain. The experiment includes two sites, Ussana and Benatzu, situated approximately 1 km apart, representing typical durum wheat growing areas for Sardinia and the Mediterranean region, however differing largely in soil texture and soil variability (Dettori et al. 2022). The experimental plots are located at each site on a 1.3 ha field, containing 12 plots of durum wheat cultivation under different irrigation treatments.

Climate data, soil properties and crop characteristics from the field experiment are used to parameterize the SWAP model (Kroes et al. 2017). The modelled soil water content curves for both sites show overall good performance for multiple soil depths after calibration.

To assess the effects of a changing climate, this study uses climate projection data from the ClimEx project (Climate Change and Hydrological Extremes) (Leduc et al. 2019) to run the calibrated SWAP model. From the CRCM5-LE (Canadian Regional Climate Model version 5 – Large Ensemble) European domain one pixel (12 km) is extracted, containing both study site locations. Five randomly selected members of the 50 CRCM5-LE members are used as the climatic driver for the model to account for climatic variability and the assessment of extreme events (Leduc et al. 2019). For the evaluation of the study results under future climate projections, global warming levels (GWLs) are considered.

Results and concluding remarks

The results indicate that while future temperatures steadily increase, precipitation decreases during the summer months, while within the cropping season, December to mid-July, precipitation changes show no uniform trend with higher GWLs. In the Mediterranean region, winter precipitation is predominantly caused by synoptic processes and large-scale ocean to land transport. Large scale circulation changes are poorly understood, with climate models showing opposing trends on projected drying, both in large scale ensembles and regional simulations. More reliable model projections of winter precipitation require further improvement in representing circulation changes (Brogli et al. 2019). Future precipitation development during the winter half-year remains uncertain, often with no clear trends, with high interannual and intermonthly variability, and highly depends on the used climate projection (Marras et al. 2021).

Soil water content in the upper soil layers (5 – 15 cm) at both study sites exhibits a wide range of values, with no distinct trend under different GWLs. However, during the summer months, the soil water content

mainly shows a negative trend.

Soil water content in deeper soil layers (25 – 55 cm) tends to rise in the first months of the year at both sites, and then decreases in Ussana, but remains high in Benatzu, however showing high uncertainty of future developments due to wide value ranges, as can be seen in Figure 1a and 1b. The difference in soil moisture distribution between the two study sites can be explained by their different soil types, with sandy-clay loam in Ussana and mostly clay loam in Benatzu, as in the study's region, the magnitude of variations in soil water content is highly controlled by the soil texture (Piras et al. 2014). Thus, the variability of soil water content between years and months within a single growing period is expected to increase in the future, with more pronounced dry and wet periods, leading to more extreme growing conditions for durum wheat.

Irrigation demand at the study sites exhibits only minor long-term average changes with higher GWLs, but with an increasing and more robust value range, as can be seen in Figure 1c. This indicates higher variability between consecutive dry and wet cropping seasons.

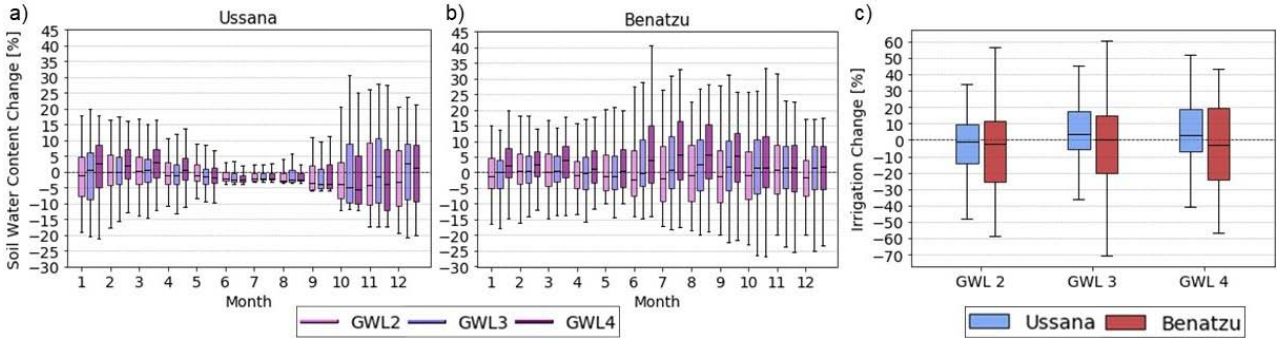


Figure 1. a, b) Average long-term soil water content percent change between reference period and GWL 2, 3, and 4 for bottom soil layer (depth 25 – 55 cm) in Ussana (sandy-clay loam) (a) and Benatzu (mostly clay loam) (b); c) Percentage change in water demand for irrigation during one cropping season between reference period and GWL 2, 3, and 4 for Ussana and Benatzu.

To save yields and minimize the risk of crop failures during dry periods, or generally enhance yields, a precise and adapted irrigation management is required. In this way, the consequences of climate change related to altered precipitation patterns can be minimized, although other potential risks remain.

Acknowledgments: This project has received funding from the European Union's Horizon H2020 innovation action programme under grant agreement 101036683 (ARSINOE).

References

Brogli R, Sorland SL, Kröner N, Schär C (2019) Causes of future Mediterranean precipitation decline depends on the season. Environmental Research Letters 14, 114017: 1-11. https://doi.org/10.1088/1748-9326/ab4438

Dettori M, Cesaraccio C, Duce P, Mereu V (2022) Perfomance Prediction of Durum Wheat Genotypes in Response to Drought and Heat in Climate Change Conditions. Genes 13(3): 1-25. https://doi.org/10.3390/genes13030488

Kroes JG, Van Dam JC, Bartholomeus RP, Groenendijk P, Heinen M, Hendriks RFA, Mulder HM, Supit I, Van Walsum PEV (2017) SWAP version 4 – Theory description and user manual. Wageningen Environmental Research, Wageningen

Leduc M, Mailhot A, Frigon A, Martel J-L, Ludwig R, Brietzke GB, Giguère M, Brissette F, Turcotte R, Braun M, Scinocca J (2019) The ClimEx Project: A 50-Member Ensemble of Climate Change Projections at 12-km Resolution over Europe and Northeastern North America with the Canadian Regional Climate Model (CRCM5). Journal of Applied Meteorology and Climatology 58(4): 663-693. https://doi.org/10.1175/JAMC-D-18-0021.1

Lionello P, Scarascia L (2018) The relation between climate change in the Mediterranean region and global warming. Regional Environmental Change 18: 1481-1493. https://doi.org/10.1007/s10113-018-1290-1

Marras PA, Lima DCA, Soares PMM, Cardoso RM, Medas D, Dore E, De Giudici G (2021) Future precipitation in a Mediterranean island and streamflow changes for a small basin using EURO-CORDEX regional climate simulations and the SWAT model. Journal of Hydrology 603: 1-15. https://doi.org/10.1016/j.jhydrol.2021.127025

Piras M, Mascaro G, Deidda R, Vivoni ER (2014) Quantification of hydrological impacts of climate change in a Mediterranean basin in Sardinia, Italy, through high-resolution simulations. Hydrology and Earth System Sciences 18: 5201-5217. https://doi.org/10.5194/hess-18-5201-2014

Application of the UTHBAL monthly hydrological model in fuzzy environment

S. Stavris[1], M. Spiliotis[1*], A. Loukas[2]
[1] Department of Civil Engineers, Democritus University of Thrace, Xanthi, Greece
[2] School of Rural and Surveying Engineering, Aristotle University of Thessaloniki
* e-mail: mspiliot@civil.duth.gr

Introduction

Although the water balance problem of transforming precipitation into runoff of watersheds, individual distributed land surfaces or hydrological units has been subject to investigation and engineering for more than a century, it is still a popular scientific issue for research. The reason is rather simple, and it is relevant on one hand with its importance, as the resolution of this problem leads to an effective water resources exploitation and on the other hand with the complexity of solving such a problem, where the deterministic models are not functionable. The main objective of this research is to calibrate existing conceptual water balance models in fuzzy environment by creating corresponding algorithms.

The model to which refers this paper is UTHBAL (Loukas et al. 2007) a conceptual monthly rainfall-runoff model, which has been widely used to simulate surface-, inter- and baseflows (Vasiliadis and Mastraftsis 2023). The method which is described herein is the calibration of this model with fuzzy systemic parameters using the Zadeh's extension principle fuzzification of fuzzy sets (Klir and Yuan 1995) and an objective function, which was proposed by Spiliotis and associates (Spiliotis et al. 2021).

Materials and methods

The study area is the mountainous watershed of Portaikos river, a tributary of Pinios river in the region of Thessaly, Greece named Pyli with total area of about 132 km^2. Thessaly is in central mainland Greece located. The study watershed belongs to Trikala prefecture, it has intense relief with average elevation of about 944 m and its climate can be classified as typical continental in the Mediterranean climate zone characterized by cold winters with frequent snowfalls, and warm summers.

In the present study, the conceptual monthly model, UTHBAL, was developed in MATLAB. The model has six parameters to be calibrated, i.e. the coefficient of real evapotranspiration, the coefficient of soil infiltration, the soil moisture storage, the coefficients of inter- and baseflow and the snowmelt coefficient. The surface, intermediate and base runoff components are derived by determination of the parameters' values, which are calculated by applying the model water balance equation (Loukas et al. 2007). This procedure results in an optimization problem and its resolution was realized with the least squares method.

The calibration of the model in fuzzy environment is achieved by fuzzification of its parameters converting them into fuzzy symmetric triangular numbers, so that their fuzzy boundaries result from the corresponding semi-widths as distances from their central values. By applying the algorithm via new optimization for each time step, extreme and central fuzzy runoff values are obtained, due to the monotonicity assumption. In this way, the left Q_c^- and right-hand Q_c^+ runoff values of the *0*-cut are calculated, as well as the fuzzy central value $\overline{Q_c}$ for every period. This new optimization takes place for the six systemic parameters, plus the corresponding widths of the fuzzy quantities. Therefore, simulation incorporates the uncertainty of the parameters. Fuzziness is integrated into the model based on the extension principle (Spiliotis et al. 2021; Klir and Yuan 1995). Hence, some additional terms, such as the magnitude of the produced fuzzy band and the inclusion of the observed values within this fuzzy band are taken under consideration in the fuzzified objective function *f* (Spiliotis et al. 2021):

$$f = w_1\left[\sum_{j=1}^{M} a_{Rj}\left(Q_{o,j} - Q_{c,j}^{+}\right)^2 + \sum_{j=1}^{M} a_{Lj}\left(Q_{c,j}^{-} - Q_{o,j}\right)^2\right] + \frac{1}{M}\left[\sum_{j=1}^{M}\left(Q_{o,j} - \overline{Q_{c,j}}\right)^2\right] + \frac{1}{M}\left[\sum_{j=1}^{M}\left(Q_{c,j}^{+} - Q_{c,j}^{-}\right)^2\right] \quad (1)$$

where w_1 weight coefficient of the first disturbance term of this objective function, j = 1, 2, ..., M periods, M total periods (in this case months), $Q_{o,j}$ observed outflow value in j^{th} month, a_{Rj}, a_{Lj} dummy variables, in order to express the inclusion or not of the observed values within the created fuzzy band. Thus, when $Q^{+}_{c,j} \geq Q_{o,j}$ a_{Rj} = 0, otherwise a_{Rj} = 1. Similarly, if $Q^{-}_{c,j} \leq Q_{o,j}$, then a_{Lj} = 0, otherwise a_{Lj} = 1.

The first term of this objective function f expresses the divergence of the resulted fuzzy width aiming to include all observed and fuzzy outflow values. The second term is the distance between the central fuzzy and the observed outflow values, while the third one gives the magnitude of the created fuzzy band.

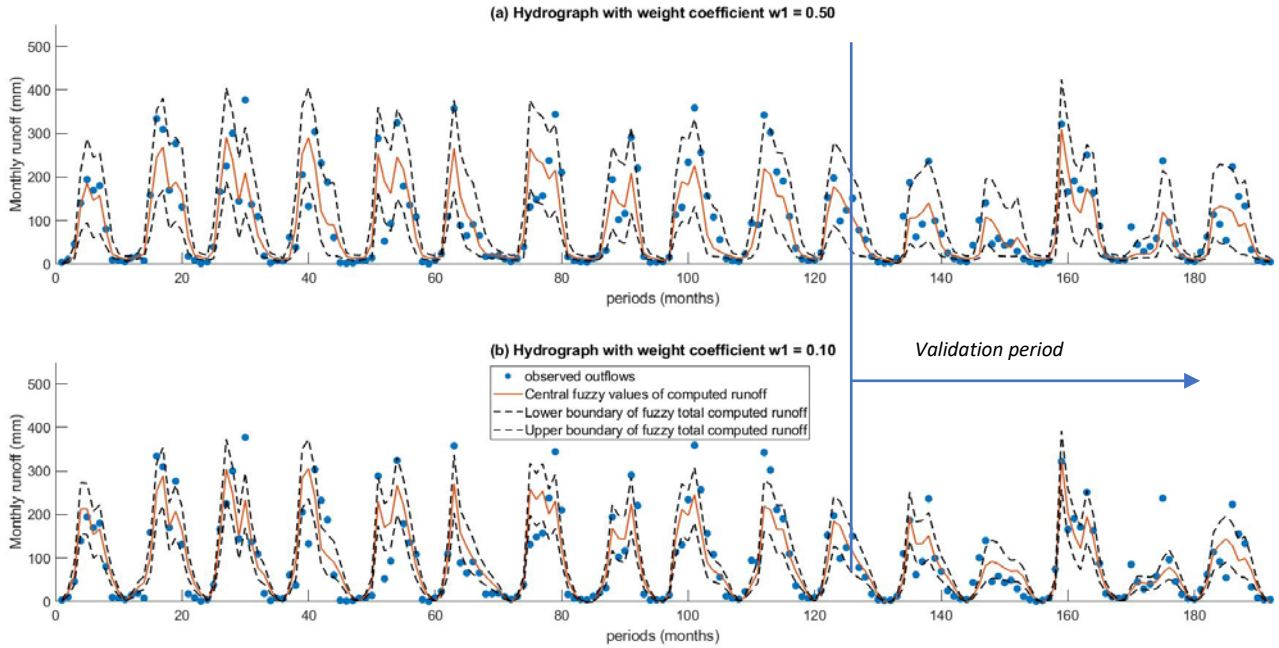


Figure 1. Comparison between observed and centre / boundary fuzzy flows of UTHBAL for Pyli watershed (calibration period Oct1977 - Sep1988 and validation period Oct1988 - Sep1993). a) w_1 = 0.50 and b) w_1 = 0.10

Results and concluding remarks

Two optimization exercises were performed: one for w_1=0.50 (Fig. 1a) and another for w_1=0.10 (Fig. 1b). It is evident that the problem is ill-constructed, as the value of the weight coefficient w_1 leads to either a functional fuzzy band with some points outside or, for larger values of w_1 to a wider fuzzy band that includes most of the observed points (similar to fuzzy regression models). The choice with more emphasis on the inclusion constraint seems to perform better during the validation procedure.

Nevertheless, the results of this research are encouraging and lead to the conclusion that a more targeted optimization in the resulting real Euclidean intervals of the model parameters will provide an even better calibration of simulated to the observed runoff.

References

Klir G, Yuan B (1995) Fuzzy sets and fuzzy logic: theory and applications. Prentice Hall P T R Upper Saddle River, New Jersey 07458

Loukas A, Mylopoulos N, Vasiliades L (2007) Modeling System for the Evaluation of Water Resources Management Strategies in Thessaly, Greece. Water Resource Management (2007) 21:1673–1702. DOI 10.1007/s11269-006-9120-5

Spiliotis M, Sordo-Ward A, Garrotte L (2021) Estimation of Fuzzy Parameters in the Linear Muskingum Model with the Aid of Particle Swarm Optimization. Sustainability 2021, 13, 7152. https://doi.org/10.3390/ su13137152

Vasiliades L, Mastraftsis I (2023) A Monthly Water Balance Model for Assessing Streamflow Uncertainty in Hydrologic Studies. Environ. Sci. Proc. 2023, 25, 39. https://doi.org/10.3390/ECWS-7-14192

An explorative analysis for discharge data long time series reconstruction in the Campania region

G. Nicoletti*, A. Longobardi
Department of Civil Engineering, University of Salerno, Fisciano, Italy
** e-mail: ginicoletti@unisa.it*

Introduction

The lack of monitoring stations and the consequent limited availability of hydrological data are an internationally acknowledged issue (Ma et al., 2021). This is also evident in Italy, where monitoring networks are affected by spatial and temporal discontinuities. A representative case is the Campania region which, in the 2000s, was subject to a structural change of its hydro-climate monitoring network. New sensors were installed, while the existing ones (historical network) were upgraded with new technology. However, only a few stations retained their original location and characteristics, thereby causing a discontinuity in the databases. In the case of raingauge stations, the problem of time series continuity has typically been addressed through a geostatistical interpolation (Longobardi et al. 2021). For the discharge data, an approach based on hydrological watershed modelling can be considered. Unfortunately, while the historical network, despite the limited number of stations, allowed for discharge data recording, the lack of rating curves for the period 2000-on going, strongly impact the possibility for discharge long time series reconstruction. While hydrological models can be calibrated with historical discharge data, they cannot be validated for the period 2000-on going indeed. Considering these difficulties, there is a necessity to adopt methodologies that integrate hydraulic and hydrological modelling, which could additionally benefit from data provided by non-conventional ground-based sensors and by remote sensors.

In this context, the analysis of historical hydro-climate time series becomes of fundamental relevance in order to characterize the catchment hydrological response including the relevant stationarity in the climate and hydrological regimes. In the same way, data revealing the rating curves models and their temporal changes are furthermore essential. This study presents an overview of the results obtained from an application to four major rivers in the Campania region featured by long-term consistency in their monitoring stations location: the Calore Irpino, the Sele, the Tanagro and the Volturno river basins.

Materials and methods

Precipitation, temperature, water levels and discharge records between 1950 and 1994 were collected at the daily scale for the cases study (Figure 1a). Being the analysed river basins characterized by a gauge station that has remained unchanged over time, in order to evaluate the possibility of extending the hydrological modelling results to the period without measured discharge data, an explorative analysis was conducted to assess the homogeneity and stationarity of the observed streamflow and precipitation series. The non-parametric statistical tests CUSUM and Pettitt were applied to identify the presence of time series non homogneity. Similarly, the rating curves measured at the annual scale were plotted on a Q-H diagram to examine the temporal variability of the stage-discharge relationship. Confidence boundaries were reconstructed to quantify the mentioned variability. The stage-discharge relationship for each year was furthermore fitted with a two-parameter model (Venetis 1970):

$$Q=a(H)^b \quad (1)$$

where "Q" represents the discharge, "H" is the hydrometric level relative to a given datum, "a" and "b" the model parameters assessed in the perspective of the best fit between observed and modelled values.

Results and concluding remarks

The stationarity analysis conducted on the four river basins revealed overall a homogeneity condition for discharge data over the considered time window, except for the Tanagro river basin. For the latter, there was a significant change point in early 1980, however this was related to a variation in the pluviometric regime, detected by statistical testing in the same period. Regarding the rating curves, the Calore Irpino and Tanagro hydrometric stations reported a tight envelope for the yearly relationships, which suggests a rather temporal stability in the stage-discharge relationship. In contrast, the envelopes of curves for the hydrometric stations of the Sele and Volturno rivers showed a large variability (Figure 1c). This is confirmed by the time series analysis of parameters a and b for which confidence boundaries are provided (Table 1). The parameter values obtained are consistent with the literature (Hrafnkelsson et al., 2022). In particular, parameter a is proportional to the geometric characteristics of the relative catchment, such as the area and width of the section.

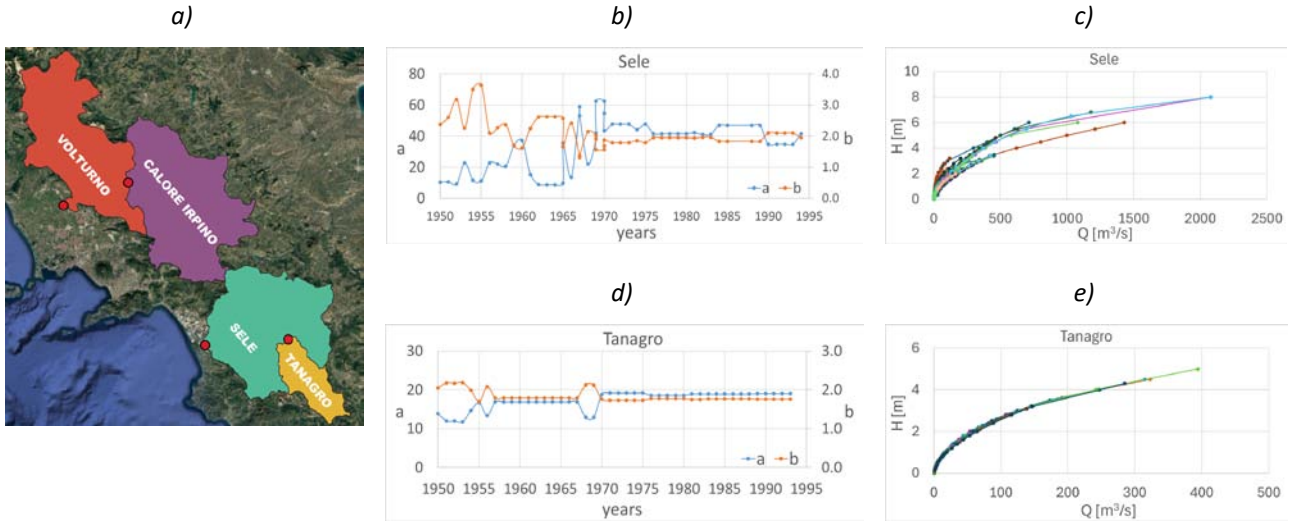


Figure 1. Study area (panel a); variation of the "a" and "b" coefficients of the rating curves for the Sele River (panel b) and the Tanagro River (panel d); rating curve for the Sele (panel c) and the Tanagro (panel e) rivers.

Table 3. Basin area, mean discharge, mean parameters a and b with their 95% confidence intervals.

	Area [km^2]	μ(Q) [m^3/s]	μ (a)	Upper μ (a)	Lower μ (a)	μ (b)	Upper μ (b)	Lower μ (b)
Calore	2991	33.25	41.48	43.66	38.30	1.71	1.83	1.59
Sele	3216	55.61	34.09	38.77	29.82	2.06	2.21	1.95
Tanagro	660	9.72	17.26	17.94	16.58	1.83	1.89	1.76
Volturno	5586	80.45	52.62	63.86	46.48	1.78	1.80	1.68

In conclusion, the overall homogeneity observed in the analysed time series, for what concerns both the catchment scale and the cross section where discharge data were observed, at least for two of the studied catchments suggests the potentiality for a hydrological modelling analysis that could be extended to the reconstruction of the discharge database for the years after 2000.

References

Hrafnkelsson B., Sigurdarson H., Rögnvaldsson S., Jansson A. Ö., Vias R. D., Gardarsson, S. M. (2022). Generalization of the power-law rating curve using hydrodynamic theory and Bayesian hierarchical modeling. Environmetrics, 33(2). https://doi.org/10.1002/env.2711

Longobardi A., Boulariah O., Villani P. (2021). Assessment of centennial (1918–2019) drought features in the Campania region by historical in situ measurements (southern Italy). Natural Hazards and Earth System Sciences, 21(7), 2181-2196. https://doi.org/10.5194/nhess-21-2181-2021

Ma K., Feng D., Lawson K., Tsai W.P., Liang C., Huang X., et al. (2021). Transferring hydrologic data across continents–leveraging data-rich regions to improve hydrologic prediction in data-sparse regions. Water Resources Research, 57(5). https://doi.org/10.1029/2020WR028600

Venetis C. (1970). A note on the estimation of the parameters in logarithmic stage-discharge relationships with estimates of their error, International Association of Scientific Hydrology. Bulletin, 15(2), 105–111. https://doi.org/10.1080/02626667009493957

Surface runoff concentration time sensitivity to several parameters involved in Log Erosion Barriers (LEBs) implementation

A. Stoikopoulou*, G. Papaioannou
Department of Forestry and Management of the Environment and Natural Resources (FMENR), Democritus University of Thrace (DUTH), 68200 Orestiada, Greece
** e-mail: astoikop@fmenr.duth.gr*

Introduction

Wildfires significantly threaten life, property, and the natural environment and can induce direct and indirect effects, including flash floods and erosion. Several erosion and flood protection treatments are implemented in the post-fire period to mitigate impacts and facilitate ecosystem recovery. A typical treatment implemented to slow surface runoff and trap sediments is the Log Erosion Barriers (LEBs). Several researchers have investigated the effectiveness of LEBs through field experiments (Wohlgemuth P.M, et al. 2001.; Kastridis and Kamperidou 2015). After an extensive literature review, we found limited investigation of LEBs performance through experiments (e.g. Martínez-Murillo and López-Vicente 2018). Based on our knowledge, no study has been found to conduct surface runoff concentration time sensitivity to a wide range of conditions and various parameter configurations concerning LEBs positioning and construction. Therefore, this work aims to conduct a sensitivity analysis of parameters associated with the positioning and construction of LEBs through hydraulic-hydrodynamic modeling to evaluate their efficiency in relation to runoff concentration time.

Materials and methods

The methodological framework, utilizing the 2D hydraulic-hydrodynamic model HEC-RAS, encompasses the execution of sensitivity analyses on specific parameters related to the positioning and construction of LEBs. The study focuses on several key parameters that influence concentration time, including the distance between the LEBs based on contour positioning (8 m and 20 m), their size (0.2 m and 0.3 m), the surface slope (20%, 30%, and 40%), rainfall intensity (50 mm/hr), and the roughness coefficient representing vegetation cover in the post-fire era (empty cover due to very high burn severity with a value of 0.011 and low regrowth cover with a value of 0.2). These parameters were combined to generate all possible scenarios. Rainfall was implemented only to the upper 10 m of the experimental terrain for all scenarios, and different scenarios were simulated using a rain-on-grid modeling approach. All modeling configurations and model parameters were applied as constants except the parameters examined for the sensitivity analysis. The HEC-RAS model was employed to simulate the rainfall-runoff process for each scenario. GIS tools were used to generate the spatially distributed rainfall raster data and the high-resolution experimental DEM surfaces of varying slopes. The experimental surfaces were designed with a width of 5 meters and a length of 130 meters so that a sufficient number of LEBs would be placed. The simulation results provide concentration times at the lower boundary of the terrain, which will be compared to identify the parameter that most significantly influences the concentration time.

Results and concluding remarks

The visualization of the results is presented in Figure 1 as Box and Whisker plots according to the concentration-time as a function of (a) Slope(%), (b) Diameter of LEBs, (c) Manning's n values, (d) Distance between LEBs for all combined modeling configurations. Specifically, it is observed in Figure 1a that an increase in the surface's slope results in a decreased concentration time and a decrease in the variability of the outcomes. Notably, the comparison of the median value of concentration time for slopes with 30% and 40% is very small. Moreover, experiments using 20% slope exhibit a higher median value of concentration

time, indicating that a much longer duration is required for the flow to arrive at the downstream boundary. Experiments using LEBs with 0.3 m diameter provided a significant increase in concentration time compared to the 0.2 m diameter LEBs because the area behind the LEB increased, resulting in a bigger water storage area and a delay in the water travel time. The comparison of the experiments concerning Manning's n roughness coefficient (Figure 1c) showed that low regeneration of vegetation (value of 0.2) that can hypothetically reflect the first year or years after a wildfire with high burn severity (value of 0.011) results in an important slowdown of the flow, thereby increasing the concentration time. In addition, the same comparison concerning Manning's n roughness coefficient (Figure 1c) showed that the variability of the results between the two examined scenarios is similar. The experiments comparing the distance between the LEBs (Figure 1d) exhibit an opposite behavior to that of the diameter, with the concentration time decreasing as the parameter decreases. Specifically, positioning the LEBs using a contour interval of 8 m increases the concentration time significantly compared to the 20 m. The results of this study indicate that the diameter of the LEBs and the distance of their positioning have the most pronounced impact on the time required for the water to reach the downstream boundary, followed by the Manning's n roughness value and the slope. Further sensitivity analysis concerning supplementary factors and enrichment of the current ones should be implemented to strengthen the preliminary outcomes of this study. We expect that Manning's n roughness value for overland flow in a condition of more considerable vegetation regeneration or smaller burnt severity can play important role in the concentration time. Finally, this study contributes to an improved understanding of how Log Erosion Barriers implementation can affect the surface runoff travel time, which can also affect the watershed concentration time and the peak flow.

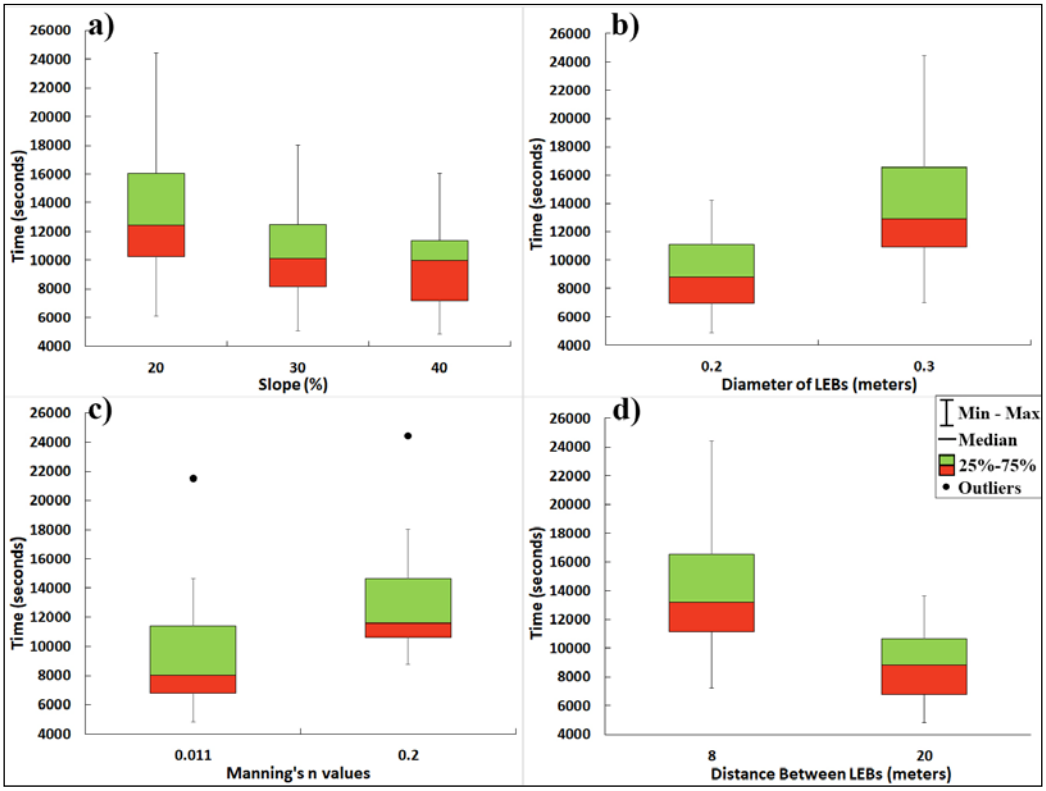


Figure 1. Concentration time as a function of (a) Slope(%), (b) Diameter of LEBs, (c) Manning's n values, (d) Distance between LEBs

Reference

Kastridis A, Kamperidou V (2015) Evaluation of the Post-Fire Erosion and Flood Control Works in the Area of Cassandra (Chalkidiki, North Greece). Journal of Forestry Research 26(1): 209–217, doi:10.1007/s11676-014-0005-9.

Martínez-Murillo, J.F, López-Vicente M, (2018) Effect of Salvage Logging and Check Dams on Simulated Hydrological Connectivity in a Burned Area. Land Degradation and Development, 29(3): 701–712, doi:10.1002/ldr.2735.

Wohlgemuth P.M, Hubbert K.R, Robichaud, P.R (2001) The Effects of Log Erosion Barriers on Post-Fire Hydrologic Response and Sediment Yield in Small Forested Watersheds, Southern California. Hydrological Process 15: 3053–3066, doi:10.1002/hyp.391.

Uncertainty assessment of rainfall-runoff simulation of the Reno Italy river basin under climate change scenarios

M. Niazkar[1, 2*], O. Cenobio-Cruz[3], G. Mozzi[1,2] , J. Pal[1, 2], G. Di Baldassarre[3]
[1] Risk Assessment and Adaptation Strategy division, Euro-Mediterranean Center of Climate Change, Venice, Italy
[2] Ca' Foscari University of Venice, Venice, Italy
[3] Department of Earth Sciences, Centre of Natural Hazards and Disaster Science, Uppsala University, Uppsala, Sweden
* e-mail: majid.niazkar@cmcc.it

Introduction

Uncertainty assessment is crucial for rainfall-runoff simulations in a typical watershed. Generally, three major sources of uncertainty are input forcing, model structure, and model parameterization. The uncertainty of hydrological modelling may become more evident when it estimates unseen conditions. For instance, when studying climate change impacts, using climate projections as input for hydrological modelling brings about an inevitable uncertainty in streamflow predictions. This study aims to investigate the uncertainty of future streamflow using a semi-distributed hydrological model in the Reno basin, Italy.

Materials and methods

The upper Reno River Basin in northern Italy was selected as the case study and divided into three sub-basins: (i) 1316 is Pracchia, (ii) 2580 is Vergato, and (iii) 4240 is Casalecchio (Figure 1). The catchment area is 1055 km^2, and its outlet streamflow is measured at the gauge station of Casalecchio di Reno (latitude: 44.47°, longitude: 11.28°).

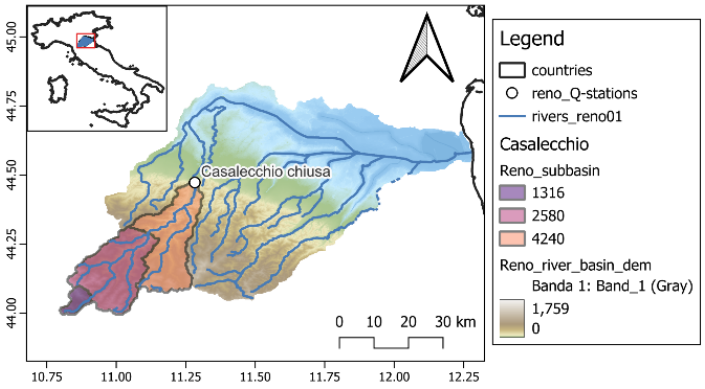


Figure 1. Study area and location of the streamflow gauge station Casalecchio.

For calibrating the hydrological model, high-resolution gridded meteorological data, called the ERG5 dataset (Antolini et al., 2016), was utilized. The 5-km gridded data of daily precipitation and temperature, developed by ARPAe-SIMC, was aggregated and averaged for each sub-basin.

A process-based and semi-distributed Hydrological Predictions for the Environment (HYPE, Lindström et al., 2010) model, which was developed by the Swedish Meteorological and Hydrological Institute (SMHI), was used. The precipitation and temperature of three sub-basins were input data of the HYPE model, while the streamflow measured at the Casalecchio station was considered as output data. The calibration period was between 2001 and 2018, while the data from 2019 to 2022 was used for validation.

The HYPE model achieved high values of the Kling-Gupta Efficiency (KGE) metric for calibration (KGE =0.835) and for validation (KGE= 0.813). Afterwards, the calibrated model simulated 6 future projections for IPCC RCP4.5 and RCP8.5 climate scenarios. Among these projections, 5 of them have coarse resolutions, whereas the CMCC-CM global model (VHR-REA_IT) has a fine resolution, i.e., 2.2 km. So, they were downscaled to a fine resolution, and all projections were aggregated to each sub-basin (Figure 2).

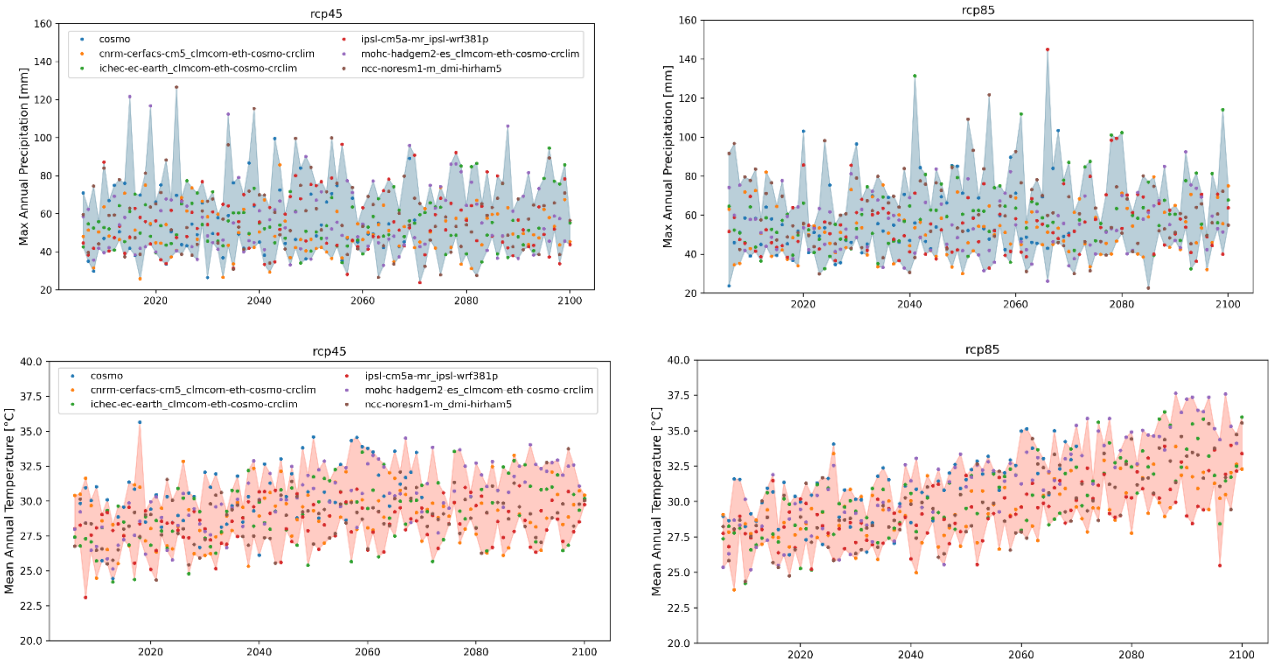


Figure 2. Future projections of maximum annual precipitation and mean annual temperature.

Results and concluding remarks

The maximum annual discharge at the outlet of the basin was obtained from 2006 to 2100 for different future projections (Figure 3). As shown, for both RCP scenarios, all climate models indicate a decrease in the maximum annual discharge in mid-century. Finally, the obtained results revealed that studying the model uncertainty can provide a better understanding of water balance in a typical watershed, particularly when forecasting runoff under climate change scenarios.

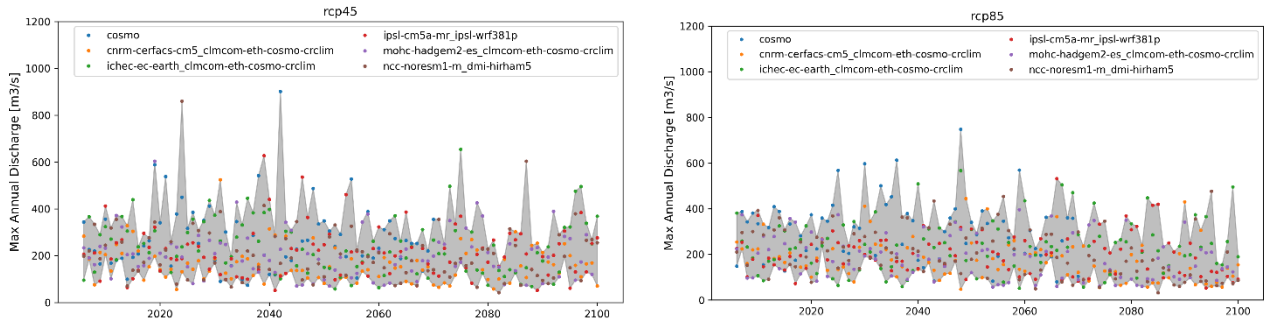


Figure 3. Future projections of maximum annual discharge simulated by the HYPE model.

Acknowledgments: This research work was carried out as part of the TRANSCEND project with funding received from the European Union Horizon Europe Research and Innovation Programme under Grant Agreement No. 10108411.

References

Antolini, G., Auteri, L., Pavan, V., Tomei, F., Tomozeiu, R. and Marletto, V. (2016) A daily high-resolution gridded climatic data set for Emilia-Romagna, Italy, during 1961–2010. Int. J. Climatol., 36: 1970-1986. https://doi.org/10.1002/joc.4473

Lindström, G., Pers, C., Rosberg, J., Strömqvist, J., and Berit, A. (2010) Development and testing of the HYPE (Hydrological Predictions for the Environment) water quality model for different spatial scales, Hydrol. Res., 4, 295–319, https://doi.org/10.2166/nh.2010.007

Application of reanalysis data in hydrological studies: A case study in Georgia

A. Nobile[1], F. Zanello[2], F. Lubrano[2], M. Nicolini[1], E. Arnone[1]
[1] University of Udine, Polytechnic Department of Engineering and Architecture, Udine, Italy
[2] Idrostudi S.r.l.,Trieste, ITALY
* e-mail: nobile@idrostudi.it

Introduction

Reanalysis data have proven to be a valuable support for hydrologic modeling and calculation of standardized climate indices, useful tools for characterizing local climate regimes and improving water resource management in areas with limited availability of observational data. Previous investigations, e.g. Arnone et al. (2018), Tarek et al. (2020), and Ahmed et al. (2024) reported several case studies on the use of reanalysis data, produced by the ECMWF, in hydrological applications. It has been demonstrated that the application of various bias correction techniques enhances the quality of reanalysis data, as highlighted by studies from Smitha et al. (2018), Francipane et al. (2023), and Teutschbein and Seibert (2012).

This study examines the use of ERA5 reanalysis dataset, with its spatial resolution of approximately 31 km, in hydrological applications, emphasizing the critical role of bias correction (BS) techniques to improve data applicability and understand their limitations through a case study in Georgia, where observational climate data is scarce. Specifically, this work aims to compare five different bias correction techniques to identify the most effective method for improving raw reanalysis.

Materials and Methods

The work assesses the effectiveness of five bias correction techniques applied to daily and monthly reanalysis time series of precipitation data. The techniques evaluated include Linear Scaling (LS), Empirical Quantile Mapping (QM-EMP), Quantile Mapping Spline Bias Correction (QM-SBC), Mean Bias Subtraction (MBS), and Simple Linear Regression (SLR). Each technique is examined through two different bias correction approaches: classical and sliding window (Smitha et al., 2018), as can be seen from the flowchart represented in Figure 1.

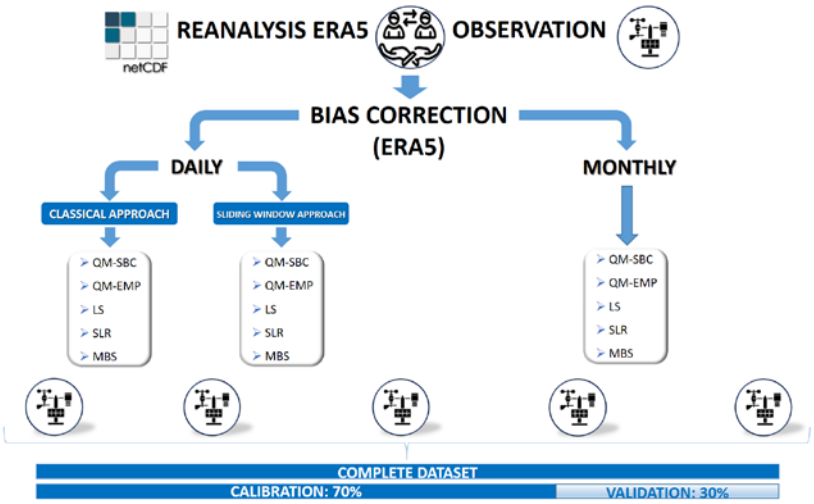


Figure 1. Diagram of the applied methodology that performs: 5 bias correction methods, two approaches (classical and sliding window), two temporal scale, 3 datasets, for a total of 150 analyses.

Classical approach uses monthly statistics to derive correction factors for reanalysis precipitation data, while sliding window approach involves a fixed size moving window to calculate daily correction factors,

providing a more accurate adjustment to daily variations and improving the representation of short-term variability in the corrected data.

The extraction of ERA5 reanalysis data for the entire nation of Georgia was performed automatically by using an in-house developed algorithm. Moreover, the algorithm, developed using the open-source programming language *Python*, employ observed data collected by five meteorological stations across diverse climatic zones of Georgia to test and compare the five BS methodologies at daily and monthly scales. As a preliminary application, one gauge is used to correct a single ERA5 cell. The techniques were evaluated carrying out two experiments, i.e. using (i) the complete datasets and (ii) the series that were split into a calibration (70% of the data) and validation (30% of the data) subset; metrics such as Root Mean Square Error (RMSE) and Nash-Sutcliffe Efficiency (NSE) were used to assess the performance.

Results and Concluding Remarks

Results demonstrate that the LS method has emerged as the most effective among the 5 analysed techniques for BS in daily-scale reanalysis data when all data are available, with NSE values ranging from 0.18 to 1.00 (Table 1). The introduction of the Sliding Window approach has further enhanced the performance of all techniques, adapting the correction to local variations and improving accuracy for daily precipitation events, as denoted by the increased NSE values (Table 1). In the experiment (ii), techniques based on distributions such as QM-EMP, QM-SBC, and SLR proved to be more robust, showing higher values of NSE (up to 0.76), compared to the simple LS method (0.72) (Table 1).

Table 4. RMSE/NSE before and after bias correction, at a selected station for the configurations described in Figure 1.

Methods	Complete Series			Calibration / Validation	
	Classical Approach		SW Approach	Classical Approach	SW Approach
	Daily RMSE/NSE	Monthly RMSE/NSE	Daily RMSE/NSE	Monthly RMSE/NSE	Daily RMSE/NSE
QM-EMP	5.90 / 0.44	34.97 / 0.66	5.03 / 0.60	31.92 / 0.76	5.46 / 0.56
QM-SBC	5.99 / 0.43	35.83 / 0.64	5.00 / 0.60	31.98 / 0.76	5.44 / 0.57
SLR	5.43 / 0.53	0.00 / 1.00	4.22 / 0.71	35.07 / 0.71	4.55 / 0.70
LS	5.16 / 0.57	0.00 / 1.00	4.72 / 0.64	34.45 / 0.72	5.71 / 0.52
MBS	5.79 / 0.46	0.18 / 1.00	5.36 / 0.54	34.84 / 0.71	5.62 / 0.54
ORIGINAL	5.96 / 0.43	54.28 / 0.18	5.96 / 0.43	54.70 / 0.28	6.20 / 0.44

These results underline the importance of selecting the appropriate bias correction technique based on the quality and availability of data, as well as the specific objectives of the analysis. Additional studies are needed for a further optimization of bias correction approaches.

References

Ahmed, A., Muthoni, F., Hansen, J., & Kilavi, M. (2024). Climate Information Services for Sub-Saharan Africa: Challenges and Opportunities. Climate Services, 25, 100278. doi: 10.1016/j.cliser.2024.100278.

Arnone, E., Cucchi, M., Dal Gesso, S., & Petitta, M. (2018). A multi-hazard Extreme Climate Index across Europe. EPiC Series in Engineering, 3, 95–102.

Francipane, A., Arnone, E., & Noto, L. V. (2023). Combining a data-driven approach with seasonal forecast data to predict reservoir water volume in the Mediterranean area. Hydrological Sciences Journal. https://doi.org/10.1080/02626667.2023.2189521.

Smitha, P. S., Narasimhan, B., Sudheer, K. P., & Annamalai, H. (2018). An improved bias correction method of daily rainfall data using a sliding window technique for climate change impact assessment. Journal of Hydrology, 556, 100-118.

Tarek, M., Martel, J. L., Boucher, M. A., & Brissette, F. (2020). ERA5 Reanalysis as a Potential Reference Dataset for Hydrological Modeling Over North America. Journal of Hydrometeorology, 21(3), 645-666. doi:10.1175/JHM-D-19-0242.1.

Teutschbein, C., & Seibert, J. (2010). Regional Climate Models for Hydrological Impact Studies at the Catchment Scale: A Review of Recent Modeling Strategies. Geography Compass, 4(7), 834–860. https://doi.org/10.1111/j.1749-8198.2010.00357.x

Using ERA5-Land reanalysis for assessing spatio-temporal trends of standardized drought indices in Sicily

T.M. Aschale*, N. Palazzolo, G. Buonacera, A. Cancelliere, D.J. Peres
Department of Civil Engineering and Architecture, University of Catania, Catania, Italy
** e-mail: tagele.aschale@unict.it*

Introduction

Drought is among the most critical hydroclimatic hazards, due to its significant impact on water resources, agriculture, and ecosystems, particularly in semi-arid Mediterranean regions such as Sicily (Tramblay et al, 2020; Baronetti et al., 2022). Understanding drought characteristics is essential for effective water resource management and adaptation strategies. While previous studies have assessed drought patterns in Sicily (Peres et al., 2023), comprehensive analyses on possible drought trends remain limited. Recent advances in reanalysis datasets, such as ERA5-Land, provide the spatiotemporal trends of drought occurrences in Sicily over the period 1950–2023 using standardized drought indices computed based on ERA5-Land reanalysis precipitation and potential evapotranspiration datasets.

Materials and methods

To assess drought trends, we computed SPI and SPEI at multiple timescales (3, 6, 12, and 24 months) using monthly precipitation and potential evapotranspiration data from ERA5-Land, available on the Copernicus website (https://cds.climate.copernicus.eu/datasets/reanalysis-era5-land). Then the Modified Mann-Kendall (MMK) test was applied to detect statistical significance of trends, while Sen's slope estimator was used to quantify their magnitude (Figure 1). Spatial interpolation techniques were employed to analyze regional drought variations across Sicily.

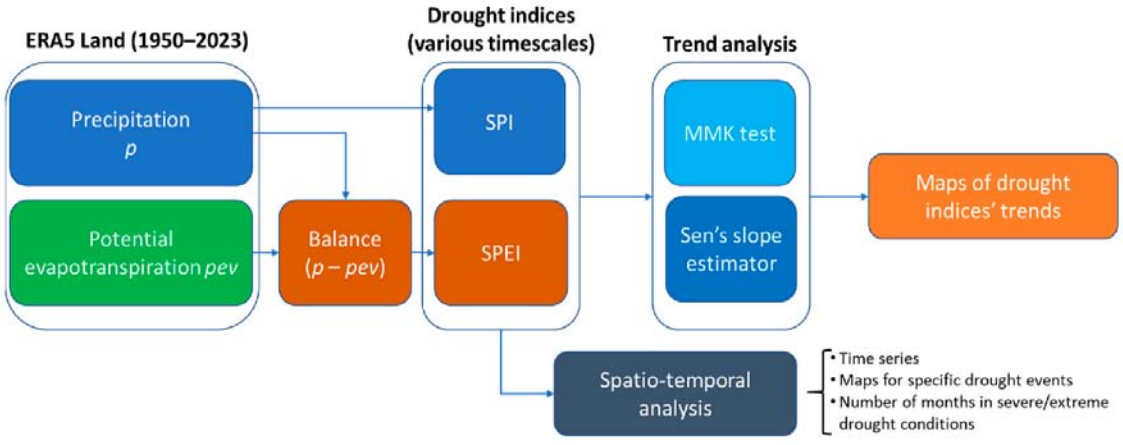


Figure 1. Diagram illustrating the steps of drought spatiotemporal and trend analysis (Aschale et al., 2024)

Results and concluding remarks

The results of the MMK test indicate a significant increase of drought conditions (decreasing SPEI), particularly in western and southern coastal areas Sicily (Figure 2). Western Sicily exhibited the most pronounced negative trends, while for the eastern coastal areas a decrease of drought conditions is indicated, as computed from the SPI (increasing trend of precipitation).

Our findings suggest a change in drought patterns over the past seven decades, with an increasing trend in drought conditions possibly reflecting changing climate conditions deriving mainly from increasing potential evapotranspiration, particularly in the western part of Sicily. The results provide some important

insights for policymakers and water resource managers in Sicily, emphasizing the need for adaptive strategies to mitigate future drought impacts (Peres et al., 2023). Future research will explore the integration of longer datasets and the use of climate projection models to further enhance the reliability of our analysis.

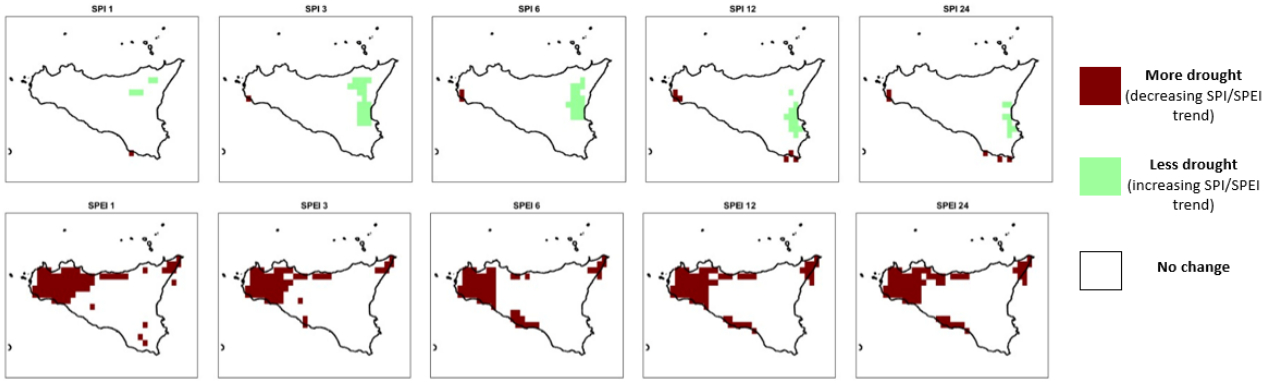


Figure 2. Areas with significant trends of drought indices over Sicily from 1950 to 2023 and related direction, based on the Modified Mann–Kendall test.

Acknowledgments: The authors acknowledge the funding support from the PRIN 2022 Integrated Monitoring & Modelling for the Sustainability of Irrigated Crops (I-MOSAIC) project, funded by the Ministry of University and Research (project code 202249HJLX, CUP E53D23010560006) and PRIN 2022 PNRR INFORES - INnovative FOrecast-informed REServoir operations for sustainable use of water resources and climate change adaptation (project cods P2022WMH7K, CUP E53D23022030001). The research was also supported by ESTREMI— Analysis and sustainable management of hydrological extremes in a changing climate – funded within the Piano di incentivi per la ricerca di Ateneo (Pia.ce.ri.) of University of Catania.

References

Aschale, T. M., Cancelliere, A., Palazzolo, N., Buonacera, G., & Peres, D. J. (2024). Analysis of the Spatiotemporal Trends of Standardized Drought Indices in Sicily Using ERA5-Land Reanalysis Data (1950–2023). Water, 16(18), 2593. https://doi.org/10.3390/w16182593

Baronetti, A.; Dubreuil, V.; Provenzale, A.; Fratianni, S. Future Droughts in Northern Italy: High-Resolution Projections Using EURO-CORDEX and MED-CORDEX Ensembles. Clim. Chang. 2022, 172, 22. https://doi.org/10.1007/s10584-022-03370-7.

Peres, D. J., Bonaccorso, B., Palazzolo, N., Cancelliere, A., Mendicino, G., & Senatore, A. (2023). A dynamic approach for assessing climate change impacts on drought: An analysis in southern Italy. Hydrological Sciences Journal, 68, 1213-1228.

Tramblay, Y.; Koutroulis, A.; Samaniego, L.; Vicente-Serrano, S.M.; Volaire, F.; Boone, A.; Le Page, M.; Llasat, M.C.; Albergel, C.; Burak, S.; et al. Challenges for Drought Assessment in the Mediterranean Region under Future Climate Scenarios. Earth-Sci. Rev. 2020, 210, 103348. https://doi.org/10.1016/j.earscirev.2020.103348.

Seawater-freshwater interface dynamics and characterization in River Neretva estuary

I. Aljinović*, V. Srzić, J. Čarija
Faculty of Civil Engineering, Architecture and Geodesy, University of Split, Matice hrvatske 15, 21000 Split
** e-mail: iva.matic@gradst.hr*

Introduction

Seawater intrusion (SWI) in estuaries is a complex process mainly driven by the interplay of freshwater discharge, marine system parameters, climatological settings, land use, melioration system operation, land subsidence, and many others. Unless the interplay leading towards SWI occurrence, the main factors controlling the SWI dynamics can be found in sea level rise, tidal oscillations, and natural river discharge. SWI adverse effects include water quality degradation, and consequently, threats to water supply and agricultural production.

The River Neretva delta, located in southeastern Croatia, is a 4500 ha low-lying agricultural area with a melioration infrastructure implemented during the 1960s and 1970s. Due to the fact that the average groundwater level is maintained below the pedological layer and below the mean sea level, this coastal system is subjected to active seawater intrusion (Badaruddin et al. 2017). The primary seawater intrusion pathways during the dry season mainly occur through the Diga embankment from the Adriatic Sea and through the River Neretva riverbed (Lovrinović et al. 2021). Principal forces defining salt wedge parameters along the River Neretva are freshwater discharge upstream and the Adriatic Sea mean level (Krvavica et al. 2020).

This paper examines the dynamics of the seawater-freshwater interface (SFI) in the River Neretva and defines the intensity of the driving forces contributing to the SFI shape, ranging from typical salt wedge to complete stratification diminishing conditions. From a practical point of view, simple statistical functions have been applied to wide range of salinity profile shapes to enable salinity profile characterization.

Materials and methods

To investigate water column vertical stratification of temperature (T), electrical conductivity (EC), and salinity (S), water column profiling has been conducted multiple times annually from 2019 to 2023 by using SEBA KLL-Q-2 multiparameter probe. Profiling has been primarily performed during the dry season at two locations along the River Neretva: Komin and Opuzen, located 9 and 12 km upstream from the river mouth, respectively.

Supplementary to these periodic observations, continuous monitoring of T and EC has been conducted at two fixed depths in Metković, 21 km upstream from the river mouth. Probes are positioned at -0.37 m and -5.40 m (HVRS71) to assess surface (fresh water) and bottom (saline water) layer conditions. The surface layer probe is a MANTA 2 +40 with the capacity to measure T and EC. The bottom layer probe is a TruBlue CTD 585, capable of monitoring water level (WL), T and EC.

A tide gauge station has been installed at the coast to observe the Adriatic Sea level (SWL). The station is equipped with the instrument/shaft encoder THALIMEDES OTT for continuous observations. Contrary to SWL observations, River Neretva discharge has been determined from the surface water elevation observed by the THALIMEDES OTT, riverbed profile geometry and velocity observations performed by three horizontal ADCPs installed at Metković most profile fields.

Profiling results have been used for the identification of driving forces shaping the depth and transition zone width of the SFI. Joint analysis of profiling results and time series gives insight into the intensity of driving forces shaping SFI. Coherence has been applied to identify the influence of the change of freshwater discharge and sea level to the change in EC by correlation and to define time lags between specified variables.

To ensure the capacity to assess the salinity profiles in the River Neretva, a statistical function-based approach has been applied. Statistical parameters have been determined based on the non-parametric goodness of fit test between developed statistically based curves and salinity profiles observed on Komin and Opuzen profiles.

Results and concluding remarks

Water column profiling results indicate the presence of a highly stratified salinity in both profiles for nearly all profiling dates. SFI has been located at a depth between -1.9 and -6.25 m for the Opuzen profile and between -1.95 and -6.5 m for the Komin profile. EC values observed at the Komin profile have been consistently higher than values observed at the Opuzen profile. Profiling results indicate that an increase in freshwater discharge lowers the position of SFI and vice versa, unless the increase in mean SWL raises the position of SFI. The salt wedge exhibits a very narrow transition zone, with an average value of 0.5 m, mainly controlled by tidal oscillations.

Coherence model results indicate the SFI dynamics are influenced by the change in freshwater discharge and change in SWL. Time lags obtained from the coherence model provide EC changes at the Metković profile occur with a delay of 1-hour relative to SWL change. The occurrence of intermittent changes in river discharge controlled by the upstream hydropower plant leads to diminishing of the stratification in river water column salinity hereby, which is additionally supported by the Metković T time series.

The primary parameters governing SWI and defining SFI of the River Neretva can be identified and evaluated by examining changes in salinity:

- Increased values of the River Neretva discharge result in the stratification diminishing conditions and the complete displacement of the saltwater wedge from the riverbed. The influence of discharge plays a dominant role in controlling seawater intrusion hereby.
- River Neretva discharge values below 250 m^3/s emphasise the dominance of the mean sea level over the position of SFI. Variations in the mean sea level induce the most significant changes in the elevation of the SFI for low discharge values.
- Tidal oscillations demonstrate minor alterations in the SFI dynamics compared to mean sea level and river discharge.

Although the distribution parameters do not rely on the SWI physics, a demonstration of wide range fit capacity has been performed with statistical parameter values corresponding to different salinity profile conditions. This particularly allows to assess the salinity profile based on the general on-site conditions like the increase of the mean sea level, change in river discharge and tidal influence.

Acknowledgments: This research is funded by the contribution from the EU co-financing, the Interreg Italy-Croatia CBC Programme 2021–2027 call as a part of project Subsurface WAter monitoring and Management to prevent drought risk in coastal systems (SWAMrisk) (ITHR0200479) and Interreg Croatia-Bosnia and Herzegovina-Montenegro IPA CBC Programme 2021-2027 call as a part of project Monitoring interaction between the ground and surface Water to improve the sustainable agricultural resilience to climate changes impact in coastal systems (MoWaCLIM) (HR-BA-ME00405).

References

Badaruddin S, Werner A, D, Morgan L, K, (2017) Characteristics of active seawater intrusion. Journal of Hydrology. https://doi.org/10.1016/j.jhydrol.2017.04.031

Badaruddin S, Werner A, D, Morgan L, K, (2015) Water table salinization due to seawater intrusion. Water Resources. https://doi:10.1002/2015WR017098

Krvavica N, Ružić I, (2020) Assessment of sea-level rise impacts on salt-wedge intrusion in idealized and Neretva River Estuary. Estuarine, Coastal and Shelf Science. https://doi.org/10.1016/j.ecss.2020.106638

Lovrinović I, Srzić V, Aljinović I, (2024) Characterization of seawater intrusion dynamics under the influence of hydro-meteorological conditions, tidal oscillations and melioration system operative regimes to groundwater in Neretva valley coastal aquifer system, Journal of Hydrology: Regional Studies. https://doi.org/10.1016/j.ejrh.2023.101363

Lovrinović I, Bergamasco A, Srzić V, Cavallina C, Holjević D, Donnici S, Erceg J, Zaggia L, Tosi L, (2021) Groundwater Monitoring Systems to Understand Sea Water Intrusion Dynamics in the Mediterranean: The Neretva Valley and the Southern Venice Coastal Aquifers Case Studies. Water. https://doi.org/10.3390/w13040561

Dynamical and descriptive assessment of daily rainfall in Savitri river basin, India

E. S. Namitha*, V. Jothiprakash, B. Sivakumar
Indian Institute of Technology Bombay, India
** e-mail:* namithaelza@gmail.com

Introduction

In India, rainfall has a significant impact on agriculture, water resources, and disaster relief, as well as the hydrological cycle's formation. An accurate estimate of rainfall variability is required for understanding long-term climate patterns, enhancing the planning of water resources, and reducing the effects of catastrophic weather events like floods and droughts. Both dynamical (identifying complexity) and descriptive (trend, stationarity, homogeneity, noise, etc.) assessments can be used to understand the temporal variation (Salas et al. 1995; Machiwal and Jha 2012; Sivakumar 2017; Sreelash et al. 2018). The objective of this study is to examine rainfall time series from observed sites and gridded points throughout the Savitri River basin, one of India's west-flowing river basins. The analysis here uses the daily observed rainfall from eight stations and the gridded rainfall from sixteen sites in and around the basin during the monsoon season (July-September).

Materials and methods

Phase space reconstruction is typically the first step in estimating a time series' dimensionality and, subsequently, complexity. The False Nearest Neighbour (FNN) approach is then used to determine the time series' complexity using this reconstructed phase space (Packard et al. 1980; Kennel et al. 1992). In this study, the hydro-meteorological series is subjected to trend, stationarity, homogeneity, and noise tests in order to perform the descriptive analysis. Numerous techniques have been created over time to investigate descriptive qualities; however, the likelihood of rejecting the correct null hypothesis will increase if more tests are used to examine the same criteria (Machiwal and Jha 2008). As a result, this study uses two widely recognized tests for each analysis. The Mann-Kendall (MK) and Sen's slope test, two popular trend identification methods, are applied here. The popular Augmented Dickey-Fuller (ADF) and Kwiatkowski-Philips-Schmidt-Shin (KPSS) tests are used to verify stationarity, the Pettitt and Standard Normal Homogeneity (SNH) test is used to determine homogeneity, and the Box-Pierce and Ljung-Box tests are used to evaluate the noise in the series.

Results and concluding remarks

In this study, phase space reconstruction required for FNN analysis is carried out using embedding dimension values (m) ranging from 1 to 15 and a delay time of 1, which is equivalent to the sampling time. The optimum embedding dimension (m_{opt}) which indicates the number of influencing variables is identified as the dimension of the phase space corresponding to the minimum percentage of false nearest neighbours (%FNN) value. For the daily rainfall series in the basin, the FNN dimension values fall between 5 and 7 (Table 1). As can be seen from the minimal %FNN values, the FNN analysis also appears to suggest that rainfall contains some noise.

A significance level of 5% is used for the descriptive tests. Rainfall in the basin is decreasing ($Z < 0$) in all regions except for the eastern side of the basin. This will affect the Kharif crop production. Therefore, an adequate amount of irrigation water needs to be provided in those regions. The daily rainfall series is determined to be stationary at all rain gauges and gridded points by the ADF and KPSS tests. According to both homogeneity tests, the daily rainfall at the majority of the basin's locations is nonhomogeneous (p value <0.05). The Box-Pierce and Ljung-Box tests show that all the daily rainfall series have p-values less

than 0.05. This suggests that the series contains white noise.

Table 5. Results of dynamical and descriptive tests for the observed and gridded rainfall in the Savitri River basin

Rainfall Stations	FNN analysis		Trend		stationarity		homogeneity		Noise	
			MK	Sen's	ADF	KPSS	Pettitt	SNHT test	Box-Pierce	Ljung-Box
	%FNN	m_{opt}	Z	slope	p value	p value	p value	p value	p value	p value
Bhave	15.34	5	1.289	0.000	<0.0001	0.675	0.065	0.013	<0.0001	<0.0001
Kotheri	14.33	5	6.788	0.003	<0.0001	0.140	<0.0001	0.009	<0.0001	<0.0001
Ambiwali	14.70	5	-0.777	0.000	<0.0001	0.895	0.015	0.018	<0.0001	<0.0001
Birwadi	15.09	5	0.904	0.000	<0.0001	0.352	0.014	0.034	<0.0001	<0.0001
Raigad	16.76	5	-3.211	-0.002	<0.0001	0.152	<0.0001	<0.0001	<0.0001	<0.0001
Kangule	16.01	5	-1.796	0.000	<0.0001	0.665	0.003	0.023	<0.0001	<0.0001
Varandoli	15.18	6	-1.200	0.000	<0.0001	0.672	0.008	0.006	<0.0001	<0.0001
Waki	14.30	6	0.273	0.000	<0.0001	0.477	0.030	0.005	<0.0001	<0.0001
gp1	17.03	5	1.163	0.000	0.001	0.076	0.003	0.006	<0.0001	<0.0001
gp2	15.01	5	-1.871	0.000	0.001	0.315	0.030	0.005	<0.0001	<0.0001
gp3	11.40	5	1.888	0.001	0.001	0.128	0.003	<0.0001	<0.0001	<0.0001
gp4	15.85	6	0.009	0.000	0.001	0.486	0.003	0.054	<0.0001	<0.0001
gp5	16.56	5	1.041	0.000	0.001	0.567	0.013	0.028	<0.0001	<0.0001
gp6	14.65	5	-0.225	0.000	0.001	0.779	0.045	0.011	<0.0001	<0.0001
gp7	10.67	5	-0.556	0.000	0.001	0.752	0.020	0.007	<0.0001	<0.0001
gp8	15.82	6	-2.044	0.000	0.001	0.497	0.011	0.063	<0.0001	<0.0001
gp9	16.49	5	-0.044	0.000	0.001	0.840	0.129	0.021	<0.0001	<0.0001
gp10	15.47	6	-0.160	0.000	0.001	0.707	0.029	0.019	<0.0001	<0.0001
gp11	12.00	6	2.904	0.001	0.001	0.086	<0.0001	0.001	<0.0001	<0.0001
gp12	14.09	5	2.074	0.000	0.001	0.125	<0.0001	0.011	<0.0001	<0.0001
gp13	16.60	6	0.031	0.000	0.001	0.850	0.076	0.009	<0.0001	<0.0001
gp14	15.90	5	-0.634	0.000	0.001	0.255	<0.0001	0.018	<0.0001	<0.0001
gp15	16.36	6	5.098	0.001	0.001	0.010	<0.0001	0.001	<0.0001	<0.0001
gp16	18.33	7	4.093	0.000	0.001	0.000	<0.0001	0.001	<0.0001	<0.0001

In general, the rainfall series can be interpreted as having a medium degree of complexity, meaning that the rainfall from the Savitri basin can be adequately modeled with a simpler model. Traditional time-series forecasting techniques might not be able to produce precise forecasts because of the data's white noise characteristics. Incorporating extra meteorological or climatic factors (such as pressure, humidity, and ocean indices) could increase the basin's rainfall prediction. The planning for water storage becomes more predictable since the series is stationary whereas the short-term drought prediction becomes challenging because of the random changes in the series.

References

Kennel MB, Brown R, Abarbanel HDI (1992) Determining embedding dimension for phase-space reconstruction using a geometrical construction. Physical Review A 45(6): 3403-3411.

Machiwal D, Jha MK (2008) Comparative evaluation of statistical tests for time series analysis: application to hydrological time series. Hydrological Sciences Journal 53(2): 353-366.

Machiwal D, Jha MK (2012) Hydrologic Time Series analysis: theory and practice. Springer, Dordrecht

Packard NB, Crutchfield JP, Farmer JD, Shaw RS (1980) Geometry from a time series. Physical Review Letters 45(9): 712–716.

Salas JD, Delleur JW, Yevjevich V, Lane WL (1995) Applied modelling of hydrologic time series. Water Resources Publications, Littleton.

Sivakumar B (2017) Chaos in hydrology: bridging determinism and stochasticity. Springer, Dordrecht.

Sreelash K, Sharma RK, Gayathri JA, Upendra B, Maya K, Padmalal D (2018) Impact of rainfall variability on river hydrology: A case study of southern Western Ghats, India. Journal Geological Society of India 92: 548-554.

Future low flow in Bavaria: Drought characteristics under climate change and land use scenarios - a large ensemble study

A. Sasse*, A. Böhnisch, R. Ludwig
Department für Geogrpahie, Ludwig-Maximilians Universität, München, Germany
** e-mail: a.sasse@iggf.geo.uni-muenchen.de*

Introduction

In the past two decades, central Europe has been hit by major summer heat waves and droughts, with heavy impacts on ecology, economy and civil society. While climate change is a primary driver of these challenges, land use management presents a significant opportunity for increasing landscape water retention.

The implementation of climate protection measures through targeted land use changes could enhance the natural water storage capacity of landscapes, potentially buffering the impacts of droughts. To explore these interactions, we developed land use change scenarios representing different societal pathways: one prioritizing climate protection and sustainability, and another focusing on adaptation while maintaining current development patterns. To address these challenges comprehensively, setting up a hydrological model based on a large ensemble climate simulation provides the required data to evaluate the water availability under rare and extreme future heat and drought conditions. This study focuses on Bavaria (Germany) as a heterogeneous study area, aiming to provide robust estimates of future low-flow conditions while considering both climate change and land use change scenarios.

Materials and methods

The core methodology is mainly based on the Water balance Simulation Model (WaSiM), used to create a hydrological large ensemble with 50 realizations for the period 1990-2099 (Willkofer et al. 2020). Based on the modeling results, we define the scope of low-flow conditions using a variable threshold approach for event definition (Beyene et al. 2014). An undershoot of this threshold for at least seven days is considered a hydrological drought event (Brunner et al. 2021).

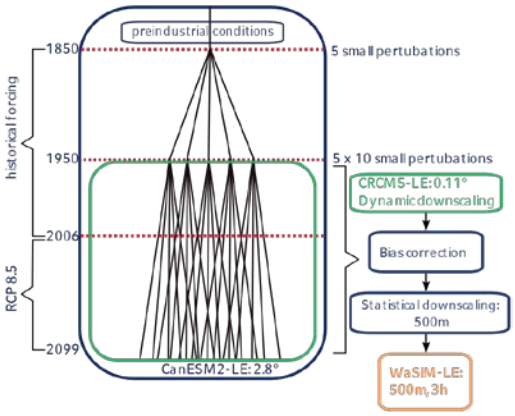


Figure 1. Modelling framework of the study

The use of climate simulation data (Leduc et al. 2019) allows for an analysis of how the event characteristics and spatial occurrence will change in the future due to climate change (von Trentini et al. 2019). By using an ensemble approach and therefore accounting for natural variability of the climate system, the results become more robust, particularly with respect to the definition of extreme events. This strengthens the confidence in the observed change signals and reduces one uncertainty aspect within the modelling chain. Another major factor is the bias correction of the climate simulation data, the results of which have a significant influence on the runoff values.

The land use change scenarios developed through expert consultation were integrated into the modeling framework to assess how different societal approaches to climate change might influence hydrological responses, particularly during low-flow conditions.

Results and concluding remarks

The comprehensive modeling approach of this study reveals detailed insights across a heterogeneous study area in central Europe, highlighting common features as well as unique characteristics of the different watersheds (Poschlod et al. 2020). Our analyses particularly identify distinct regional patterns in the response to climate change across Bavaria's landscape. Northern Bavaria shows particular vulnerability to climate change impacts, with model results indicating a significant increase in both severity and frequency of low flow events, especially during the summer half-year. This heightened sensitivity is attributed to the region's lower elevations and absence of snow-based water storage systems, making it more susceptible to the combined effects of increased summer evapotranspiration and reduced precipitation.

In contrast, the Alpine region in Southern Bavaria exhibits a more nuanced response pattern. Winter low flow conditions show a slight amelioration, primarily due to increased winter precipitation at higher elevations. However, the projected temperature rise indicates a significant shift in seasonal hydrological patterns. While early summer flows benefit from snowmelt processes, providing a natural buffer against low flow conditions, this mitigating effect is expected to diminish as rising temperatures reduce snow storage capacity in future decades.

Beyond these climate change impacts, the heterogeneous distribution of potential land use changes across Bavaria suggests that their effects on low flow conditions has to be expected to vary significantly between regions. The ongoing analysis of the land use change scenarios will provide detailed insights into these regional differences and their implications for water resource management strategies. This highlights the importance of considering both climate change trajectories and societal responses in future water resource planning. Overall, the evaluations provide important evidence for the basic definition of low-flow events and a robust estimate of how their intensity, frequency, and seasonality changes in the future as a result of climate change.

Acknowledgments: This research was conducted within the ClimEx II project. CRCM5 was developed by the ESCER Centre of Université du Québec à Montréal (UQAM; https://escer.uqam.ca/, last access: 7 July 2020) in collaboration with Environment and Climate Change Canada. We acknowledge Environment and Climate Change Canada's Canadian Centre for Climate Modelling and Analysis for executing and making available the CanESM2 Large Ensemble simulations used in this study, and the Canadian Sea Ice and Snow Evolution Network for proposing the simulations. Computations with CRCM5 for the ClimEx II project were made on the SuperMUC supercomputer at the Leibniz Supercomputing Centre (LRZ) of the Bavarian Academy of Sciences and Humanities. The operation of this supercomputer is funded via the Gauss Centre for Supercomputing (GCS) by the German Federal Ministry of Education and Research and the Bavarian State Ministry of Education, Science and the Arts.

References

Beyene S, Van Loon AF, Van Lanen HAJ, Torfs PJJF (2014) Investigation of variable threshold level approaches for hydrological drought identification. Hydrol Earth Syst Sci Discuss 11:12765-12797. http://doi.org/10.5194/hessd-11-12765-2014

Brunner MI, Swain DL, Gilleland E, Wood AW (2021) Increasing importance of temperature as a contributor to the spatial extent of streamflow drought. Environ Res Lett 16:024038. http://doi.org/10.1088/1748-9326/abd2f0

Leduc M, Mailhot A, Frigon A, Martel J-L, Ludwig R, Brietzke GB, Giguére M, Brissette F, Turcotte R, Braun M, Scinocca J (2019) ClimEx project: a 50-member ensemble of climate change projections at 12-km resolution over Europe and northeastern North America with the Canadian Regional Climate Model (CRCM5). Journal of Applied Meteorology and Climatology 58:663-693. http://doi.org/10.1175/JAMC-D-18-0021.1

Poschlod B, Willkofer F, Ludwig R (2020) Impact of Climate Change on the Hydrological Regimes in Bavaria. Water 12:1599. https://doi.org/10.3390/w12061599

von Trentini F, Leduc M, Ludwig R (2019) Assessing natural variability in RCM signals: comparison of a multi model EURO-CORDEX ensemble with a 50-member single model large ensemble. Climate Dynamics. doi: 10.1007/s00382-019-04755-8

Willkofer F, Wood R, von Trentini F, Weismüller J, Poschlod B, Ludwig R (2020) A Holistic Modelling Approach for the Estimation of Return Levels of Peak Flows in Bavaria. Water 12(9):2349. http://doi.org/10.3390/w12092349

Deep learning-assisted estimation of Manning coefficient maps using high-resolution UAV imagery for hydrodynamic modeling

V. Bellos[1*], G. Kopsiaftis[2], M. Skamantzari[3], J. Tzortzis[3], I. Rallis[3], A. Doulamis[3]
[1] Laboratory of Ecological Engineering and Technology, Department of Environmental Engineering, DUTH, Greece
[2] Laboratory of Reclamation Works and Water Resources Management, School of Rural, Surveying and Geoinformatics Engineering, NTUA, Greece
[3] Laboratory of Photogrammetry, School of Rural, Surveying and Geoinformatics Engineering, NTUA, Greece
* e-mail: vbellos@env.duth.gr

Introduction

Accurately defining the Manning coefficient is crucial for flood flow simulations, as it directly affects the estimation of bottom shear stresses and overall flow resistance. Traditionally, the Manning equation has been widely used due to its simplicity and empirical reliability. However, its assumption of a constant friction factor, regardless of water depth or velocity, introduces uncertainties, especially in dynamic flood conditions where energy losses from turbulence can vary significantly. Papanikolaou et al. (2011) attempted to calibrate friction coefficients using historical flood data or field measurements. Christelis et al. (2016) implemented an optimization framework to determine the Manning friction coefficient, yielding optimal values that are higher than those typically found in the literature. This increase is attributed to the incorporation of turbulence energy losses. Bellos et al. (2018) proposed a three-parameter friction model to replace the Manning equation, while Bellos et al. (2020) applied a multi-step methodological approach that includes the classification of friction elements in each cell of the flow domain.

Building on the work of Bellos et al. (2020), this work develops an automated, deep-learning-assisted framework for generating Manning coefficient maps using high-resolution UAV imagery. This enhances the precision and efficiency of friction parameter estimation in hydrodynamic modeling.

Materials and methods

A substantial number of high-resolution digital images were used to create the Manning coefficient maps. For the present study, we identified a focal region located at the Galati Port in Romania, the largest port on the Danube River. The specific area was selected due to its distinct geomorphological features that increase the risk of severe flooding events. For the survey in the study area, we used the DJI M3 RTK UAV to acquire RGB photos that cover the entire area, emphasizing the Danube bank. Figure 1 shows indicative aspects of the Galati Port area.

To develop a robust framework for estimating surface roughness in the study area, a manual annotation process was employed to create masks identifying key land cover categories. Specifically, four distinct surface types were delineated: (i) soil areas, (ii) cement-covered areas, (iii) tree-covered areas, and (iv) areas with low vegetation. This manual annotation ensures high-quality labeled data, essential for training segmentation algorithms to accurately distinguish between different frictional surfaces. The annotated images serve as training data for various segmentation algorithms, enabling the automated classification of surface roughness features. A standard machine learning pipeline is followed, which involves dividing the dataset into training, validation, and test sets. To enhance model accuracy and generalization, a hyperparameter fine-tuning process is adopted. This iterative refinement process ensures that the algorithms efficiently learn the distinguishing features of different surface types.

Results and concluding remarks

The preliminary results indicate promising performance, with the models demonstrating strong learning capabilities from the early epochs of training. The evolution of key metrics, such as the F1 score and loss function, further validates the effectiveness of the segmentation process. Beyond numerical metrics, the

qualitative assessment of model performance confirms the effectiveness of the trained algorithms. The inference results on test images show that the segmentation outputs align well with the manually annotated ground truth.



Figure 1. Indicative views of the study area, showcasing distinct regions with varying friction characteristics. These images highlight the spatial heterogeneity of surface roughness, which plays a crucial role in flood flow dynamics and Manning coefficient estimation.

The proposed technique has the potential to use as input high-resolution landscape images and to derive as output friction coefficient maps, which can be used by hydrodynamic simulators. This is a significant progress compared to the current rough approach, in which land use maps are associated with friction coefficients using bibliographic values.

Acknowledgments: This work was supported by DesirMED project (Grant Agreement No. 101112972).

References

Bellos, V., Nalbantis, I., & Tsakiris, G. (2020). A new strategy for the estimation of friction parameters in hydrodynamic modelling: Implementation to an ephemeral river. In River Flow 2020 (pp. 1246-1253). CRC Press.

Bellos, V., Nalbantis, I., & Tsakiris, G. (2018). Friction modeling of flood flow simulations. Journal of Hydraulic Engineering, 144(12), 04018073.

Christelis, V., Bellos, V., & Tsakiris, G. (2016, July). Employing surrogate modelling for the calibration of a 2D flood simulation model. In Sustainable Hydraulics in the Era of Global Change, Proceedings of 4th IAHR Congress, Liege, Belgium (pp. 27-29).

Papanicolaou, A. N., Elhakeem, M., & Wardman, B. (2011). Calibration and verification of a 2D hydrodynamic model for simulating flow around emergent bendway weir structures. Journal of Hydraulic Engineering, 137(1), 75-89.

Coupling an Ecohydrological and a Biogeochemical Model: A Case Study on Enhanced Weathering in Southern Italy

L. Gianni[1,3], F.D. Pacia[2,3], S. Manfreda[2*], L.V. Noto[1]
[1] Università di Palermo, Palermo, Italy
[2] Università degli Studi di Napoli Federico I, Napoli,Italy
[3] Istituto Superiore degli Studi di Pavia IUSS, Pavia, Italy
* e-mail: lorenzo.gianni@iusspavia.it

Introduction

Enhanced Weathering (EW) is a land-based negative emission strategy relying on the application of ground silicate rocks (e.g. basalt, dunite) on agricultural soils. During mineral dissolution, protons are consumed, and major cations are released, supporting CO_2 sequestration in the form of aqueous and solid (bi)carbonates (Bertagni et al., 2025). Additionally, amending soil with silicate rock dust can have positive effects on ocean acidification and soil fertility (Hartmann et al., 2013). Releasing nutrients, buffering highly acidic soils, stabilizing organic matter (Buss et al., 2024), increasing soil water retention and reducing tropospheric ozone can lead to a boost in plant yield, a reduction in fertilizers need and a further carbon dioxide removal (CDR) (Beerling et al., 2025).

In this study, we explore the capacity of EW to remove CO_2 in agro-ecosystems within Southern Italy. Our approach combines a physically based ecohydrological model, the Distributed model for Runoff, Evapotranspiration, and Antecedent soil Moisture (DREAM model), that quantifies water balance and fluxes at high spatial resolution, with the Soil Model for Enhanced Weathering (SMEW), that focuses on silicate dissolution and associated biogeochemical processes. The overarching objective is to evaluate how hydroclimatic, topographic, and soil characteristics influence the rate of mineral weathering, carbon cycling, and potential carbon sequestration.

Materials and methods

Our work centres on the Volturno river basin in Southern Italy. The DREAM model (Manfreda et al., 2018) employs a raster-based discretization to capture the spatial heterogeneity of the study area (e.g., digital elevation models, land use maps, soil texture, vegetation). The soil is treated as a limited-capacity bucket. Two mass-balance equations describe vertical water fluxes and total runoff over each time step. In essence, the model updates soil water content based on infiltration, evapotranspiration, percolation, and lateral flow, and calculates total runoff, including saturation-excess overland flow.

The SMEW model (Bertagni et al., 2025) employs a spatially lumped approach that captures the temporal dynamics of average quantities withing the upper soil layer. Key features include dynamic soil biogeochemistry, which tracks changes in organic and inorganic carbon pools and major ions, factoring in adsorption–desorption processes on soil colloids; vegetation dynamics, which simulates plant growth, transpiration, nutrient uptake, and respiration; and weathering kinetics, which uses a semi-empirical formulation to estimate mineral weathering rates based on soil moisture, pH, and mineral saturation indices.

Hydrological outputs from the DREAM model (soil moisture, percolation, runoff) are coupled with soil parameters—cation exchange capacity, depth, pH, soil organic carbon (SOC), bulk density, root depth, and soil type (SoilGrids, Poggio et al., 2021) – and used as input for the SMEW model. A spatial mask is applied to isolate cultivated areas in the Volturno basin. We run the SMEW model with 5 kg/m² of pure forsterite at a particle size of 100 µm. The simulation spans one year, using a spatial resolution of 500 meters and an hourly temporal resolution.

Results and concluding remarks

Figure 1 illustrates significant spatial variability in effective carbon dioxide removal, with weathering rates primarily controlled by temperature and soil moisture gradients and effective CDR by water leaching. Effective CDR in the subset area resulted at ~183 kg CO_2 ha^{-1} yr^{-1}. These findings emphasize the importance of site-specific factors when designing large-scale EW interventions for climate mitigation.

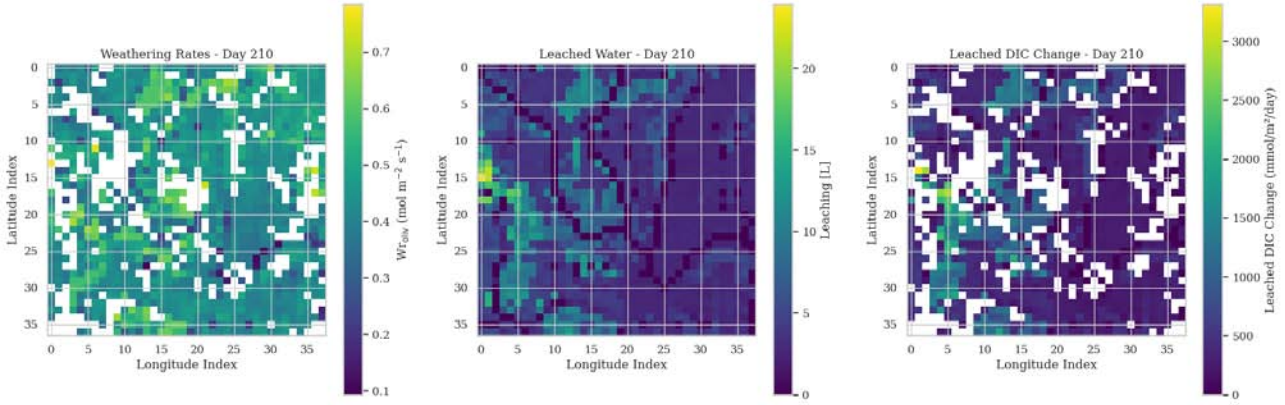


Figure 1. Weathering rates, leached water, and change in leached dissolved inorganic carbon (DIC) due to forsterite application (effective CDR) across the simulation area on day 210. White pixels indicate areas outside the cultivated zone.

Future work will refine model resolution, integrate detailed soil and vegetation datasets, and incorporate regional rock characteristics to enhance EW feasibility assessments. Additionally, incorporating local rock characteristics (e.g., basalt mineralogy) will enable more accurate assessments of region-specific EW potential. These advancements will provide policymakers with actionable insights for scaling EW as an effective nature-based climate solution.

Acknowledgments: this research received funding from European Union NextGenerationEU – National Recovery and Resilience Plan (PNRR), Mission 4, Component 2, PRIN 2022 PNRR P20225K9YW – CUP B53D23033470001.

References

Beerling, D. J., Kantzas, E. P., Lomas, M. R., Taylor, L. L., Zhang, S., Kanzaki, Y., ... & Val Martin, M. (2025). Transforming US agriculture for carbon removal with enhanced weathering. Nature, 1-10.

Bertagni, M. B., Calabrese, S., Cipolla, G., Noto, L. V., & Porporato, A. (2025). Advancing enhanced weathering modeling in soils: Critical comparison with experimental data. Journal of Advances in Modeling Earth Systems, 17(1), e2024MS004224.

Buss, W., Hasemer, H., Ferguson, S., & Borevitz, J. (2024). Stabilisation of soil organic matter with rock dust partially counteracted by plants. Global Change Biology, 30(1), e17052.

Hartmann, J., West, A. J., Renforth, P., Köhler, P., De La Rocha, C. L., Wolf-Gladrow, D. A., ... & Scheffran, J. (2013). Enhanced chemical weathering as a geoengineering strategy to reduce atmospheric carbon dioxide, supply nutrients, and mitigate ocean acidification. Reviews of Geophysics, 51(2), 113-149.

Manfreda, S., L. Mita, S. F. Dal Sasso, C. Samela, L. Mancusi, Exploiting the Use of Physical Information for the Calibration of a Lumped Hydrological Model, Hydrological Processes, 32(10), 1420-1433, (doi: 10.1002/hyp.11501) 2018

Poggio, L., de Sousa, L. M., Batjes, N. H., Heuvelink, G. B. M., Kempen, B., Ribeiro, E., & Rossiter, D. (2021). SoilGrids 2.0: Producing soil information for the globe with quantified spatial uncertainty. SOIL, 7, 217–240.

II. Extreme Weather Events: Floods, Droughts, Geomorphic, and Coastal Risk Management

Improving hyperlocal 3-hourly urban rainfall forecasting using CNN-LSTM based downscaling

P. Tripathy[1], S. Ghosh[1,2*]
[1] Center for Climate Studies, Indian Institute of Technology Bombay, Mumbai 400076, India
[2] Department of Civil Engineering, Indian Institute of Technology Bombay, Mumbai 400076, India
* e-mail: subimal@iitb.ac.in

Introduction

The intensifying frequency and severity of extreme weather events, such as heavy rainfall and flooding, underscore the critical need for advanced early warning systems. The increasing rainfall intensity at sub-daily timescale, exacerbated by climate change, significantly increase the frequency and magnitude of flash floods (Westra et al., 2014), particularly in urban coastal cities like Mumbai. Mumbai's vulnerability arises from rapid urbanization, its coastal location, and variable topography, which contribute to significant spatial variability in rainfall (Ramesh & Iqbal, 2020). Forecasting such events at hyperlocal scale is crucial for regional disaster management but remains a challenge for numerical weather prediction (NWP) models (Hess & Boers, 2022). Deep Learning (DL) models such as Convolutional Neural Network (CNN), Long Short Term Memory (LSTM) etc have been effectively used in rainfall forecasting (Aderyani et al., 2022; Badrinath et al., 2023). Wu et al. (2020) demonstrated that CNN-LSTM outperformed other models in improving Tropical Rainfall Measurement Mission (TRMM) precipitation data but underestimated high-intensity precipitation peaks. To address this issue, the DL models can be optimized with a loss function that includes weights to account for heavy rainfall events, and shows substantially improved performance in their prediction (Chen et al., 2023; Hess & Boers, 2022). Despite Mumbai's high flood susceptibility, station level hourly rainfall forecasting has not been addressed adequately. This study aims to enhance the 3 hourly forecasts at hyperlocal scale for the city.

Materials and Methods

For this study, we utilized Global Forecast System (GFS) variables provided by the National Centers for Environmental Prediction (NCEP). The GFS data has a temporal resolution of 6 hours, with forecasts available at 00:00, 06:00, 12:00, and 18:00 Coordinated Universal Time (UTC). We selected the daily 00:00 UTC GFS data with a 3-hour interval between forecasts, covering a prediction period from 0 to 24 hours. The GFS data has a spatial resolution of 0.25° × 0.25°. We have taken data spanning from 18.5°N-19.25°N and 72.5°E-73.25°E from 2015 to 2023. To identify the key predictors for this study area, we employed a Correlation Matrix. The selected GFS predictors are shown in Figure 1.

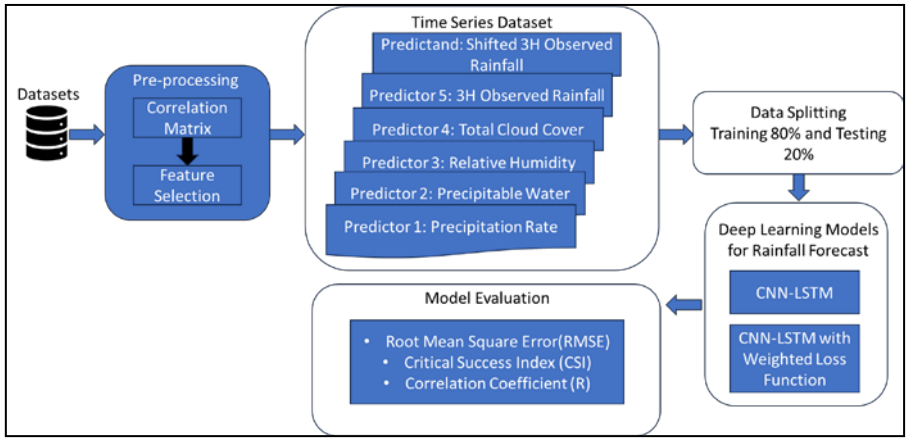


Figure 1. Methodological Flowchart for hyperlocal 3 hourly rainfall forecast using DL models.

We also incorporated past 3-hour observed rainfall data as a predictor, with the observed rainfall data being used as the predictand. This data was obtained from the Municipal Corporation of Greater Mumbai (MCGM) and spans from 2015 to 2023. The dataset was divided into 80% for training and 20% for testing. We developed a hybrid model combining CNN- LSTM model for forecasting 3-hour rainfall. CNNs effectively learn dominant spatial dynamic features, while LSTMs excel in capturing long dependencies in sequential data. We have also applied a weighted Mean Square Error (WMSE) to minimize the impact of light rainfall during training and enhance forecasts for extreme events (≥95th percentile), assigning a weight of 1.5 for extreme events and 1 otherwise.

Results and concluding remarks

The results presented in Table 1 demonstrate that the GFS data exhibits the highest RMSE, along with the lowest R and CSI values at the 95th percentile for all stations. Using CNN-LSTM model has significantly reduced the RMSE by 3.54%-12.38%, increased the R and CSI values by 70.37%-113.04% and 160% -183.3% respectively.

Table 1: Performance of GFS, CNN-LSTM and Weighted CNN-LSTM for stations.

	CSI (95th percentile)			**RMSE (mm)**			**R**		
Stations	GFS	CNN-LSTM	Weighted CNN-LSTM	GFS	CNN-LSTM	Weighted CNN-LSTM	GFS	CNN-LSTM	Weighted CNN-LSTM
Kandivali	0.05	0.13 (160%)	**0.23 (360%)**	7.94	7.18 (9.57%)	**7.15 (9.95%)**	0.23	0.49 (113.04%)	**0.52 (126.09%)**
Andheri	0.08	0.21 (162.5%)	**0.24 (200%)**	5.93	5.72 (3.54%)	**5.7 (3.88%)**	0.29	0.5 (72.41%)	**0.52 (79.31%)**
Chembur	0.06	0.17 (183.3%)	**0.22 (266.67%)**	7.33	6.64 (9.41%)	**6.54 (10.78%)**	0.27	0.46 (70.37%)	**0.5 (85.19%)**
F North	0.06	0.18 (200%)	**0.21 (250%)**	7.06	6.26 (11.33%)	**6.23 (11.76%)**	0.25	0.49 (96%)	**0.5 (100%)**
Colaba	0.08	0.21 (162.5%)	**0.22 (175%)**	6.3	5.52 (12.38%)	**5.49 (12.86%)**	0.26	0.48 (84.62%)	**0.5 (92.31%)**

Using WMSE has further reduced the RMSE values by 3.88%-12.86%, increased the R and CSI values by 79.31%-126.09% and 175%-360% respectively. Weighted CNN-LSTM have lowest RMSE, highest CSI, and highest R values compared to both the GFS and CNN-LSTM models. These findings emphasize that training with a weighted loss function allows the CNN-LSTM model to capture the heavy-tailed target distribution better, leading to improved categorical skill scores for extreme rainfall forecasts in Mumbai which is crucial for enhancing early warning systems and mitigating flood risks.

References

Aderyani, F. R., Jamshid Mousavi, S., & Jafari, F. (2022). Short-term rainfall forecasting using machine learning-based approaches of PSO-SVR, LSTM and CNN. Journal of Hydrology, 614, 128463. https://doi.org/10.1016/j.jhydrol.2022.128463

Badrinath, A., Monache, L. D., Hayatbini, N., Chapman, W., Cannon, F., & Ralph, M. (2023). Improving Precipitation Forecasts with Convolutional Neural Networks. https://doi.org/10.1175/WAF-D-22-0002.1

Chen, Y., Huang, G., Wang, Y., Tao, W., Tian, Q., Yang, K., Zheng, J., & He, H. (2023). Improving the heavy rainfall forecasting using a weighted deep learning model. Frontiers in Environmental Science, 11, 1116672. https://doi.org/10.3389/fenvs.2023.1116672

Hess, P., & Boers, N. (2020). Deep Learning for Improving Numerical Weather Prediction of Heavy Rainfall. Journal of Advances in Modeling Earth Systems, 14(3), e2021MS002765. https://doi.org/10.1029/2021MS002765

Ramesh, V., & Iqbal, S. S. (2022). Urban flood susceptibility zonation mapping using evidential belief function, frequency ratio and fuzzy gamma operator models in GIS: A case study of Greater Mumbai, Maharashtra, India. Geocarto International, 37(2), 581–606. https://doi.org/10.1080/10106049.2020.1730448

Westra, S., Fowler, H. J., Evans, J. P., Alexander, L. V., Berg, P., Johnson, F., Kendon, E. J., Lenderink, G., & Roberts, N. M. (2014). Future changes to the intensity and frequency of short-duration extreme rainfall. Reviews of Geophysics, 52(3), 522–555. https://doi.org/10.1002/2014RG000464

Wu, H., Yang, Q., Liu, J., & Wang, G. (2020). A spatiotemporal deep fusion model for merging satellite and gauge precipitation in China. Journal of Hydrology, 584, 124664. https://doi.org/10.1016/j.jhydrol.2020.124664

Medium-range forecast of flash drought using the Copernicus soil moisture global dataset

C. Cammalleri[1*], S. Maffei[1], A. Ceppi[1], G. Fioravanti[2], A. Toreti[2]
[1] Politecnico di Milano, Dipartimento di Ingegneria Civile e Ambientale (DICA), Milan, Italy;
[2] European Commission, Joint Research Centre (JRC), Isrpa, Italy.
* e-mail: carmelo.cammalleri@polimi.it

Introduction

Droughts are generally considered slow-evolving phenomena, developing over long periods of time with starting and ending dates difficult to determine (Wilhite and Vanyarkho, 2000). However, a particular sub-group of drought events, known as flash drought, are characterized by a fast initial development phase, reaching peak conditions in less than a month (Svoboda et al., 2002). Flash drought events are particularly challenging for drought early warning systems, and they pose a serious treat for agricultural and natural environments. Modelling of flash drought is commonly based on the analysis of quantities related to vegetation water stress, such as soil moisture and actual evapotranspiration.

In this study, an indicator designed to quantify the initial development rate of droughts (for both slow and flash events) is applied at global scale using the soil moisture medium-range forecasts generated within the Copernicus Emergency management Service (CEMS, https://emergency.copernicus.eu). This dataset is compared against estimations based on a reanalysis product, with the goal of quantifying the predictability of the initial development speed of upcoming events and the possibility to provide an early warning on flash droughts.

Materials and methods

The datasets used in this study are based on the simulations of the LISFLOOD model generated within the CEMS operational framework (https://ewds.climate.copernicus.eu/datasets/cems-glofas-historical?tab=overview). Data are produced quasi-globally at a spatial resolution of 0.1 degree daily.

The main variable used here to characterise agricultural drought is the soil wetness anomaly (SWA). SWA maps at global scale are obtained every dekad (roughly 10-day, 3 times a month) starting from a 30-day mowing average and via a standardization of SWI based on the climatology in the period 1991-2020.

Two main datasets are used in this study: SWA data obtained from LISFLOOD simulations forced with ERA5 reanalysis inputs (monitoring from hereafter), and SWA forecasts generated daily using an ensemble (15 members) medium-range seasonal forecast (forecast for hereafter). The analysis is performed on the common study period 2004-2023.

The indicator used to quantify the development speed of the drought in the initial stage is the Initial Development Rate computed on a 3 dekad period (IDR_3). This index measures the cumulative deficit in SWA under a threshold value defying the start of dry conditions (SWA = -0.25 in this study). The index can be expressed as:

$$\mathrm{IDR}_3 = \frac{1}{(\mathrm{T}_3 - \mathrm{T}_0 + 1)} \sum_{t=\mathrm{T}_0}^{\mathrm{T}_3} \begin{matrix} (q - \mathrm{SWA}_t) & \mathrm{SWA}_t \le -0.25 \\ 0 & \mathrm{SWA}_t > -0.25 \end{matrix} \quad (1)$$

where T_0 is the first timestep (t) where SWA is lower than the threshold and T_3 is the third timestep after the start of the dry period.

In order to apply the index using forecast data, the dekad where the event start (T_0) is obtained in near real time using the monitoring data, and then the velocity of the event is quantified using the forecast data in the next 2 dekads (roughly 20-day). The ensemble mean is used to provide a best guess estimation of the index, while the ensemble is used to generate two quantities: the most likely speed class and the

probability to obtain that class. Classification of the IDR_3 is based on previous studies. A schematic description of this approach is reported in Fig. 1.

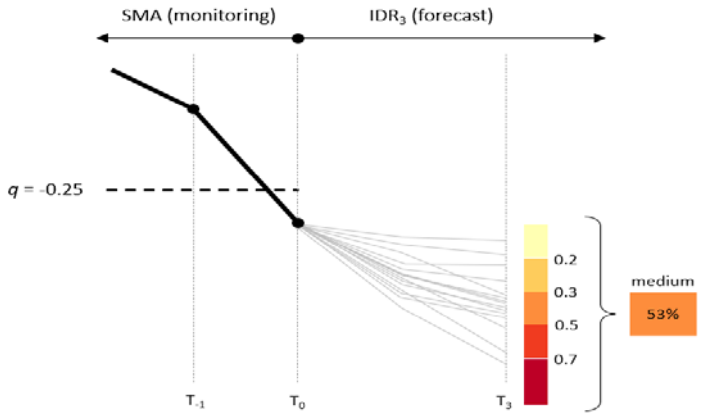


Figure 1. Scheme of the application of the index using medium-range forecasts.

Results and concluding remarks

The IDR3 index is applied on both the forecast and the monitoring data, with the latter representing a reference ideal outcome in case of a perfect forecast. The bar plots in Fig. 2 report the frequency distribution of the observed values of IDR3 in the two cases, showing a good resemblance of the forecast and the monitoring, with only a slight tendency of the forecasts to underestimate the initial speed.

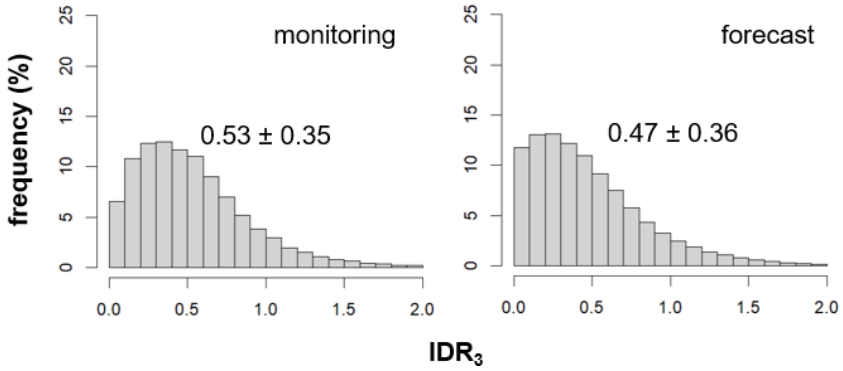


Figure 2. Bar plots of simulated IDR_3 values for the period 2004-2023 using monitoring (left) and forecast (right) data.

This consideration is also supported by a statistical analysis, returning a high Pearson correlation coefficient (0.90) and a small negative bias (-0.05). Overall, the obtained results suggest that the index is suitable for an operation implantation for the forecasting of upcoming flash droughts.

Acknowledgments: This research has been supported by the Horizon Europe project SEED-FD (Strengthening Extreme Events Detection for Flood and Drought) HORIZON-CL4-2023-SPACE-01-32 (https://www.seed-fd.eu/).

References

Svoboda, M, LeComte D, Hayes D, Heim R, Gleason K, Angel J, Rippey B, Tinker R, Palecki M, Stooksbury D, Miskus D, Stephens S (2002). The drought monitor. Bull. Am. Meteorol. Soc. 83(8): 1181-1190. doi:10.1175/1520-0477-83.8.1181.

Wilhite DA, Vanyarkho O (2000). Drought: Pervasive Impacts of a Creeping Phenomenon. In: Drought: A Global Assessment, Vol. 1, ed. D.A. Wilhite, chap. 18, pp. 245-255.

Analysis of upper dam failure and cascade impacts in pumped-storage hydropower systems: a case study of Brava - Sfikia scheme, Aliakmon River, Greece

P. Dimas*, A. Lykou, A. Zarkadoulas, G.K. Sakki, A. Efstratiadis, C. Makropoulos
Dept. of Water Resources and Environmental Engineering, School of Civil Engineering, NTUA, Athens, Greece
** e-mail: pdimas@mail.ntua.gr*

Introduction

The analysis of dam failure mechanisms and the subsequent propagation of flood waves is critical in understanding the risks associated with hydropower infrastructure. This also includes pumped hydropower storage (PHS) systems, which are, in fact, interconnected infrastructures, and they are pivotal for renewable energy integration. Given the growing significance of PHS, understanding the multidimensional impacts of potential failures on human activities and critical infrastructures downstream, is paramount.

This study focuses on the pumped-storage hydropower system at Sfikia Reservoir, located in the Aliakmon River basin in Greece, which incorporates a series of cascading reservoirs (Ilarionas, Polyfyto, Sfikia, Asomata, Ag. Varvara). The PHS project in hand includes a primary existing reservoir (Sfikia), a proposed upper reservoir at Brava, and associated hydraulic structures. Utilizing advanced simulation tools, combined with empirical approaches, this research examines the potential failure mechanisms, focusing on piping of the upper dam at Brava, and the resulting flood wave dynamics across the entire downstream path, down to the lower dam (Sfikia).

In particular, the study investigates multiple failure scenarios, assesses flood wave propagation through hydrodynamic simulation, and evaluates the impacts on downstream reservoir under the scope of hydrologic routing of the incoming hydrograph and the effects of large-scale wave generation (tsunami phenomenon). This concludes to effective risk mitigation measures, such as early warning systems and preventive interventions, ensuring the safety and sustainability of the integrated PHS system.

Materials and methods

This study integrates: *(a)* dam failure modelling, by using both HEC-RAS (Goodell, 2005) and BASEbreach (Macchione, 2008; Peter, 2017; Peter et al., 2018) in a Monte Carlo context, thus providing a range of potential outflow patterns (Fig. 1a); *(b)* hydrodynamic modelling via HEC-RAS 2D, to assess the impact of dam failure and flood wave propagation between the upper and the lower reservoir; *(c)* a dual approach to model tsunami generation and propagation in Sfikia reservoir, by assuming that the incoming hydrograph generated from the dam break is acting as a landslide, and *(d)* the routing of the hydrograph, combined with upstream inflows, through the control structures of Sfikia dam (turbines and spillway). This scheme ensures a comprehensive evaluation of the *cascade risks* and their potential impacts.

Flood modelling focuses on the propagation of flood waves from the Brava Reservoir to the downstream Sfikia Reservoir in the event of dam failure. Using HEC-RAS 2D, the study simulates flood wave dynamics, including velocity, depth, and timing. Key considerations include: *(i) Dam Breach Parameters*: A number of scenarios of piping failures are modelled using regression-based equations and empirical relationships (e.g., Froehlich, 2008), *(ii) Hydraulic Connectivity*: The hydrological and topographic linkages between the reservoirs are modelled to capture wave movement, *(iii) Flood Wave Transformation*: Flood wave characteristics, i.e. maximum depths, velocities (Fig. 1b) and arrival times, are assessed along the flow path for three specific scenarios (favorable, representative, adverse) accounting for attenuation due to natural and structural barriers. The Tsunami Generation Approaches (Fig. 1c) include: *(a) a Theoretical Approach*, and *(b) a Semi-Empirical Approach*. The first one employs physical principles to predict wave generation dynamics from landslides entering the reservoir. The key factors encapsulate: *(i) Landslide Volume*: total

displaced material entering the water, *(ii) Entry Velocity*: speed of the landslide upon entering the reservoir, *(iii) Slope Angle*: Affects the energy transfer into wave generation. The initial wave height is estimated using the differential equation proposed by Di Risio and Sammarco (2008). Factors such as bottom friction, radial dispersion, and diffraction are included to refine wave height predictions over distance (Goda, 2010), while the last step calculates the run-up at the Sfikia dam crest. The Semi-Empirical approach follows the computational procedure developed by Evers et al. (2019), which utilizes empirical formulae that are calibrated against observations, thus enabling more realistic predictions of wave impact.

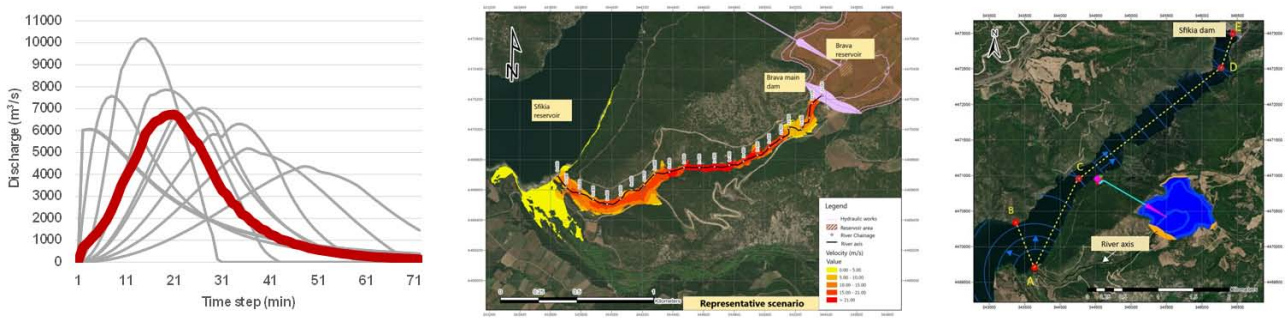


Figure 1. Characteristic elements of the modelling approach (a) outflow hydrographs due to upper dam break (bold line refers to the representative scenario); (b) maximum velocity for the area between Brava and Sfikia reservoirs, and (c) tsunami propagation route.

Results and concluding remarks

The analysis of potential impacts due to upper dam failure highlights significant risks across the PHS system. The modelled flood waves showed peak discharges exceeding 6,500 m³/s at the Sfikia Reservoir under the representative scenario. Flood propagation analyses revealed potential inundation of downstream areas, stressing the importance of integrated risk management. Tsunami modelling demonstrated that landslide-triggered waves could substantially amplify localized water levels within the reservoirs. The semi-empirical approach produced wave heights exceeding 6 m near the landslide impact zone, with attenuation observed downstream due to bottom friction and reservoir geometry. The run-up at the Sfikia dam location is calculated ~1.4 m. The theoretical approach, on the contrary, is producing run-up heights ranging from 1.4 to 3.7 m. Overall, the results highlight the need for enhanced mitigation strategies, including early warning systems, adaptive structural reinforcements, and coordinated reservoir operation plans to strengthen system resilience.

References

Di Risio, M., Sammarco, P., 2008. Analytical modeling of landslide-generated waves. Journal of waterway, port, coastal, and ocean engineering 134, 53–60.

Evers, F., Heller, V., Fuchs, H., Hager, W., Boes, R., 2019. Landslide-generated impulse waves in reservoirs. Basics and Computations. Swiss Federal Office of Energy SFOE. Bern, Switzerland. Laboratory of Hydraulics, Hydrology and Glaciology VAW. ETH Zurich. Zurich, Switzerland.

Froehlich, D.C., 2008. Embankment Dam Breach Parameters and Their Uncertainties. Journal of Hydraulic Engineering 134, 1708–1721. https://doi.org/10.1061/(ASCE)0733-9429(2008)134:12(1708)

Goda, Y., 2010. Random seas and design of maritime structures. World scientific.

Goodell, C.R., 2005. Dam Break Modeling for Tandem Reservoirs — A Case Study Using HEC-RAS and HEC-HMS, in: Impacts of Global Climate Change. Presented at the World Water and Environmental Resources Congress 2005, American Society of Civil Engineers, Anchorage, Alaska, United States, pp. 1–11. https://doi.org/10.1061/40792(173)402

Macchione, F., 2008. Model for Predicting Floods due to Earthen Dam Breaching. I: Formulation and Evaluation. Journal of Hydraulic Engineering 134, 1688–1696. https://doi.org/10.1061/(ASCE)0733-9429(2008)134:12(1688)

Peter, S.J., 2017. Dam break analysis under uncertainy 241. https://doi.org/10.3929/ethz-b-000484484

Peter, S.J., Siviglia, A., Nagel, J., Marelli, S., Boes, R.M., Vetsch, D., Sudret, B., 2018. Development of Probabilistic Dam Breach Model Using Bayesian Inference. Water Resources Research 54, 4376–4400. https://doi.org/10.1029/2017WR021176

Knowledge-based vs. data-driven seasonal precipitation forecasts in the Mediterranean region

A. Senatore[1*], L. Furnari[1], G. Nikravesh[1], F. Cortale[1], C. Lorenz[2], A. Naghibi[3], L.A. Cuartas[3,4], H. Kunstmann[2,5], C. Bertacchi Uvo[3,6], G. Mendicino[1]
[1] Department of Environmental Engineering, University of Calabria, Rende (CS), Italy
[2] IMK-IFU, Karlsruhe Institute of Technology (KIT), Campus Alpin, Garmisch-Partenkirchen, Germany
[3] Department of Water Resources Engineering, Lund University, Lund, Sweden
[4] National Center for Monitoring and Early Warning of Natural Disasters, Brazil
[5] Institute of Geography, Augsburg University, Augsburg, Germany
[6] Marine and Freshwater Solutions, Finnish Environment Institute (Syke), Helsinki, Finland
* e-mail: alfonso.senatore@unical.it

Introduction

Water scarcity and drought in a warming climate are particularly challenging threats that are expected to increase their potential to harm the economy and society, especially in climate change hotspots such as the Mediterranean Basin. In an efficient water resources management system, forecasting the onset of such phenomena in due time is a key requirement to allow the organization of effective and efficient countermeasures. Seasonal forecasts are the right tool to support proactive response to water scarcity and drought risk. Their reliability increased over time, along with the overall capability of physically-based weather modelling systems to provide accurate forecasts at many different lead times. Currently, various centres provide global seasonal ensemble forecasts for up to six months and beyond based on such mechanistic models, which are regularly disseminated by services like the Copernicus Climate Change Service (C3S). Nevertheless, paradoxically (at least seemingly), while knowledge-based seasonal models' skills and reliability are reaching a level of maturity such that they are starting to be used operationally, the rise and success of Artificial Intelligence suggests starting over with a different, data-driven approach that essentially dispenses with previous physically-based knowledge in order to regain it through a learning process activated by efficient machine learning programs (e.g., Roushangar et al., 2021).

This study proposes a comparison between two state-of-the-art versions of seasonal forecasts relying on the knowledge-based and data-driven approaches, respectively. Both the modelling systems are fine-tuned for a southern Italian region, the Calabrian peninsula located in the centre of the Mediterranean basin, and evaluated in terms of forecasting performance in an operational context.

Materials and methods

The core of the knowledge-based approach is the ensemble seasonal forecasts provided by the SEAS5 (Johnson et al., 2019) system of the European Centre for Medium-Range Weather Forecasts (ECMWF), whose predicted precipitation fields are spatially disaggregated up to the resolution of the ERA5-Land (Muñoz-Sabater et al., 2021) dataset (ca. 9 km) and bias-corrected according to the method proposed by Lorenz et al. (2021) to achieve higher-resolution and more consistent probabilistic quantitative precipitation forecasts. Bias correction involves each of the 132 9-km grid cells overlying the study region and is applied to the historical data from 1981 to 2020.

The data-driven approach is based on the monthly time series provided by 134 rain gauges of the regional monitoring network. For each of these gauges, future precipitation up to six months ahead is predicted using different methods, namely Gaussian process regression (GPR), support vector machine (SVM) and feed-forward neural network (FFNN). More in detail, based on several model features' combinations, the best technique is GPR, which is applied with 24 lags and with Variational Mode Decomposition (VMD) over the training period from 1955 to 2020.

The comparison of the systems' performance is performed for the 3-year test period 2021-2023,

evaluating several indices like bias, RMSE, and Pearson correlation coefficient in a spatially distributed way.

Results and concluding remarks

The results demonstrated a strong agreement between the two techniques and their respective adopted reference datasets. As an example, Figure 1 illustrates the correlation coefficient *r* on a monthly scale, comparing the knowledge-based technique (ensemble median) and the data-driven technique with their reference datasets for the validation period 2021-2023. Specifically, the average correlation observed with the knowledge-based technique is 0.67, while the average correlation for the data-driven technique is 0.73.

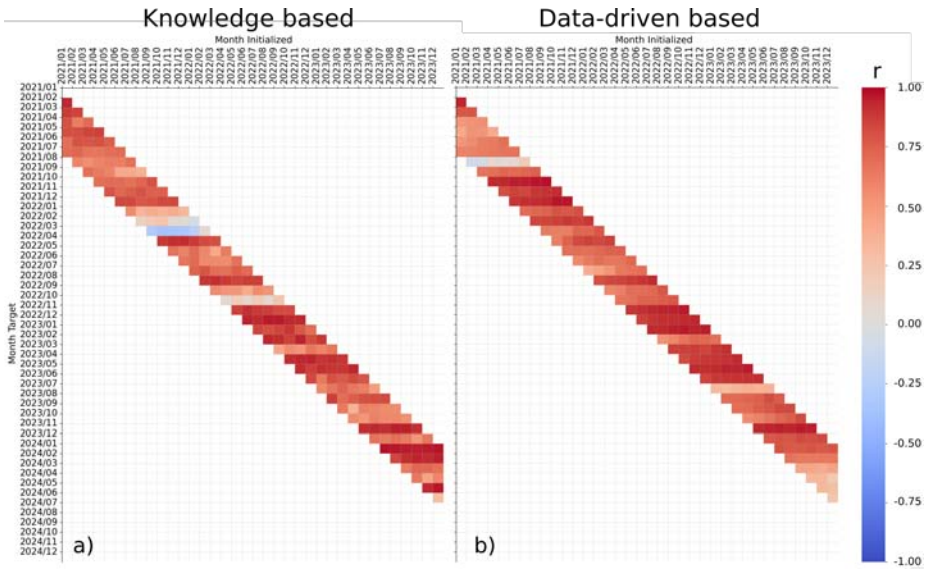


Figure 1. Correlation coefficient r heatmap for the (a) knowledge-based and (b) data-driven models. Each column indicates a different initialization, and each row refers to the target months.

The results achieved highlight the relevant potential for the integrated use of the two approaches, exploiting their respective advantages (e.g., probabilistic forecast and physical consistency with other variables for knowledge-based methods, flexibility and computational efficiency for data-driven models).

Acknowledgments: This study was funded by The Next Generation EU - Italian NRRP, Mission 4, Component 2, Investment 1.5, call for the creation and strengthening of 'Innovation Ecosystems', building 'Territorial R&D Leaders' (DD n. 2021/3277) - project Tech4You - Technologies for climate change adaptation and quality of life improvement, n. ECS0000009; The Research Project of National Interest (PRIN 2022 PNRR) "INnovative FOrecast-informed REServoir operations for sustainable use of water resources and climate change adaptation" (INFORES, CUP H53D23001430006), Italian Ministry of University and Research, The Next Generation EU - Italian NRRP, Mission 4 'Education and Research' - Component C2, Investment 1.1; The Next Generation EU - Italian NRRP, Mission 4, Component 2, Investment 1.3, project WaterWISE - Water Management Strategies and Climate Change Adaptation in Southern Italy, n. PE00000005, CUP D43C22003030002.

References

Johnson S.J., Stockdale T.N., Ferranti L., et al. (2019) SEAS5: the new ECMWF seasonal forecast system. Geosci. Model Dev. 12: 1087–1117. https://doi.org/10.5194/gmd-12-1087-2019

Lorenz C., Portele T.C., Laux P., Kunstmann, H. (2021) Bias-corrected and spatially disaggregated seasonal forecasts: a long-term reference forecast product for the water sector in semi-arid regions. Earth Syst. Sci. Data, 13: 2701–2722. https://doi.org/10.5194/essd-13-2701-2021

Muñoz-Sabater J., Dutra E., Agustí-Panareda A., et al. (2021) ERA5-Land: a state-of-the-art global reanalysis dataset for land applications. Earth Syst. Sci. Data 13: 4349–4383. https://doi.org/10.5194/essd-13-4349-2021

Roushangar K., Ghasempour R., Kirca V. O., Demirel M. C. (2021) Hybrid point and interval prediction approaches for drought modeling using ground-based and remote sensing data. Hydrology Research 52(6): 1469-1489. https://doi.org/10.2166/nh.2021.028

Estimation of flood damage costs due to climate change and storm surge in Busan, South Korea

S. Shin[1], K. Jung[2], J. Kim[1], D. Park[1*]
[1] Department of Civil and Environmental Engineering, Konkuk Univerisity, Seoul 05029, Republic of Korea
[2] Department of Planning and Strategy, Korea Environment Institute, Sejong 30147, South Korea
* e-mail: drpark@konkuk.ac.kr

Introduction

Climate change and urbanization-induced floods have become a great global problem. Busan, inland along the Nakdong River and the coast, was repeatedly damaged by flooding. Additionally, the aging system of drainage also exposes the vulnerability. However, Flood defense policies currently aren't adequately accounting for future climatic and economic shifts.

In this study, we estimated flood damage costs in Busan using an object-based method. Flood damage costs are divided into four categories: building, agriculture, population, and vehicles The scenarios used to estimate damage costs consider storm surge frequencies, projections of climate change, and drainage effectiveness. This approach allows for evaluation of regional damage patterns and damage outcomes by each scenario.

Materials and methods

We estimate flood damage costs using an object-based method with high spatial resolution. The spatial data for four categories were structured into grids by applying a 100m x 100m grid. Each grid contains building, agriculture, human and vehicle information. These data are obtained from governmental sources. After collecting data, we set up 10 scenarios. The scenarios underlying this study are based on 50-year and 100-year storm surge and sea level rise to climate change. The climate change scenarios applied SSP 2-4.5 and SSP 5-8.5. To assess the impact under different drainage efficiencies, we apply drainage efficiencies of 80%, 50%, and 0% to these scenarios.

Damage costs are estimated using depth-damage functions applied to each asset type. All damage functions are based on the KDI report (KDI, 2019). For buildings, structural and content damages are assessed based on flood depths. Building damage costs are calculated using Content-to-Structure Value Ratios (CSVR) to account for depreciation. Agricultural damage costs are calculated by the sum of farmland damage cost and crop damage cost. The farmland damage cost categorizes into burial and loss damage costs. Flood depths over 1 meter indicate farmland damage due to burial or loss.

Human casualties are calculated as the sum of casualty damage cost and displaced person damage cost. The casualty damage cost is associated with deaths and injuries. Exposed population at risk refers to the population geographically exposed to floods. Also, Exposed populations are divided into general and vulnerable. Vulnerable populations include individuals under 5 and over 65, while the general population includes those aged 5 to 64. The vehicle costs within the census block are categorized by vehicle type. The Korea Development Institute provides damage rates and average asset values (residual values) by vehicle type and flood depth. We apply a damage function and vehicle asset based on the reference. Like the human casualties, vehicle damage cost is calculated by damage function based on flood impact rate.

Results and concluding remarks

This study estimates flood damage costs for ten scenarios. As presented in the method section, flood damage costs are calculated for buildings, agriculture, population, and vehicles. The results show higher damage costs due to sea level rise from climate change compared to storm surge of 50-year and 100-year events. In the sea level rise scenario with drainage efficiency, lower drainage efficiency leads to prolonged

flooding, resulting in higher damage costs. Geographically, the scenarios by storm surge and sea level rise result in significant damage along the coast. However, as drainage efficiency decreased, significant damage is observed in inland areas of Busan. These findings suggest the need for region-specific flood defense policies and improvements in drainage systems.

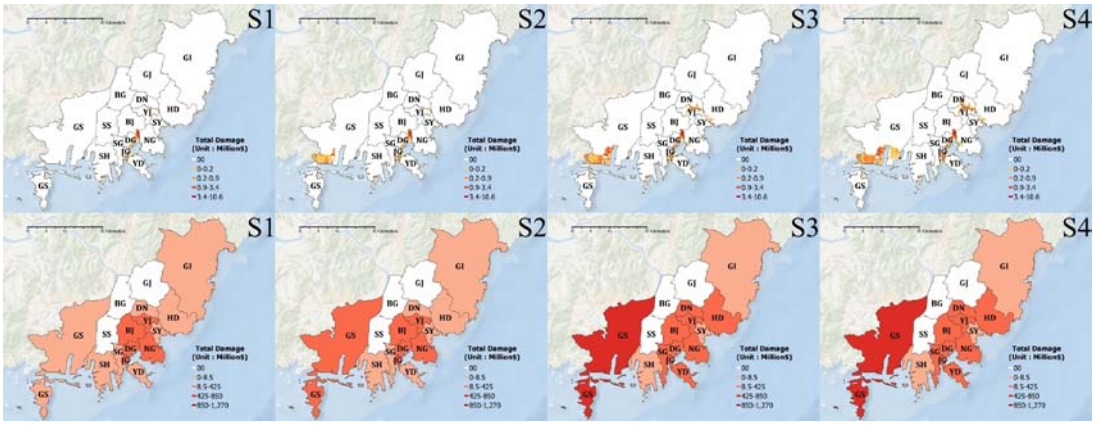


Figure 1. Total flood costs in Scenario 1, 2, 3 and 4.

Acknowledgements: This work was supported by Korea Environment Industry & Technology Institute (KEITI) through R&D Program for Innovative Flood Protection Technologies against Climate Crisis, funded by Korea Ministry of Environment (MOE) (RS-2023-00218973). It was also supported by the National Research Foundation of Korea (NRF) grant funded by the Korean Government (MSIT) (RS-2023-00272933).

References

Korea Development Institute (2019) Study on the Application Criteria of Multidimensional Methods for Calculating Flood Damage Mitigation Benefits. Available online: https://www.kdi.re.kr/research/reportView?&pub_no=16445

Identifying optimal probability distributions for SPI and SPEI drought indices in South Korea

H.J. Kim, E.S. Chung*
Civil Engineering, Seoul National University of Science and Technology, Seoul, South Korea
** e-mail: eschung@seoultech.ac.kr*

Introduction

Drought indices such as the Standardized Precipitation Index (SPI) and the Standardized Precipitation Evapotranspiration Index (SPEI) are widely used in climate research for quantifying and comparing drought conditions (Vicente-Serrano et al., 2010; Beguería et al., 2013). However, the selection of an appropriate probability distribution for these indices can introduce biases, potentially leading to inconsistent results, especially in regions experiencing frequent zero-precipitation events or under changing climate conditions (Stagge et al., 2014).

This study examines multiple candidate distributions for SPI and SPEI across various accumulation periods using long-term observations from 60 weather stations in South Korea. Building on previous studies, it also incorporates regional climatic and topographic features to propose a distribution selection method tailored to the region. Additionally, this work clarifies how different distributions affect drought characteristics—such as severity, duration, and magnitude—ultimately aiding more reliable drought monitoring in a changing climate.

Materials and methods

The study utilized meteorological data from 60 weather stations of the Korea Meteorological Administration's Automated Synoptic Observing System (ASOS). Station selection criteria included continuous data availability for over 30 years with no missing values and ongoing operational status.

The study employed two standardized drought indices: the Standardized Precipitation Index (SPI) and the Standardized Precipitation Evapotranspiration Index (SPEI). Both indices were calculated for accumulation periods of 6, 9, 12, and 24 months to capture different temporal scales of drought phenomena. For SPEI calculation, the climatic water balance was computed as the difference between precipitation and potential evapotranspiration (PET), where PET was estimated using the Penman-Monteith method incorporating net solar radiation based on observed sunshine hours, latitude, and elevation data. The PET calculation was as follows eq (1):

$$PET = (0.408\Delta(Rn - G) + \gamma(900/T + 273)u_2(es - ea))/(\Delta + \gamma(1 + 0.34u_2)) \quad (1)$$

where Rn is net radiation, G is soil heat flux, T is air temperature, u_2 is wind speed, and (es - ea) represents the vapor pressure deficit.

The evaluation methodology and selection of candidate probability distributions followed the framework proposed by Stagge et al. (2015). The assessment was conducted based on two primary criteria: (1) the goodness-of-fit between the observed data and the probability distributions, and (2) the normality of the calculated drought indices. For SPI, seven candidate distributions were evaluated: Gamma, Gumbel, Logistic, Log-Logistic, Lognormal, Normal, Weibull Distributions. For SPEI, four candidate distributions were considered: Generalized Logistic, Generalized Extreme Value (GEV), Normal, and Pearson Type III. Parameter estimation was performed using Maximum Likelihood Estimation (MLE). The optimal distribution selection process employed a comprehensive evaluation framework incorporating: Kolmogorov-Smirnov (K-S) test for goodness-of-fit, Anderson-Darling (A-D) test for distribution fitting, Akaike Information Criterion (AIC) for relative distribution ranking, and Shapiro-Wilk test for normality verification of the resulting indices

Results and concluding remarks

Table 1 presents the optimal probability distribution selection results for drought indices calculated using data from 60 weather stations in South Korea. For SPI, the Weibull distribution showed consistently high adoption rates across all accumulation periods, notably achieving a 90% selection rate for SPI-6. The Gamma distribution generally exhibited lower adoption rates compared to Weibull, peaking at 20% for SPI-12 while showing its lowest rate for SPI-6. The Gumbel distribution was rejected across all cases due to high bias leading to extreme SPI values, with the K-S test results indicating poor fit between the distribution and observed data. Both Log-logistic and Lognormal distributions demonstrated increasing adoption rates as accumulation periods lengthened.

Table 1 Percentage of weather stations where each probability distribution for SPI and SPEI calculations across different accumulation periods. Best results in bold.

SPI					SPEI				
Distributions	**SPI-6**	**SPI-9**	**SPI-12**	**SPI-24**	**Distributions**	**SPEI-6**	**SPEI-9**	**SPEI-12**	**SPEI-24**
Gamma	10(%)	15(%)	20(%)	11.67(%)	Genlogistic	1.67(%)		3.33(%)	10(%)
Gumbel	0	0	0	0	Genextreme		40(%)	**50(%)**	**50(%)**
Logistic	0	0	0	0	Normal				16.67(%)
Loglogistic	0	0	5(%)	11.67(%)	Pearson3	**98.33(%)**	**60(%)**	46.67(%)	23.33(%)
Lognormal	0	3.33(%)	10(%)	5(%)	Total	100(%)	100(%)	100(%)	100(%)
Normal	0		0	1.67(%)					
Weibull	**90(%)**	**81.67(%)**	**65(%)**	**70(%)**					
Total	100(%)	100(%)	100(%)	100(%)					

The results demonstrate distinct distribution preferences for SPI and SPEI in South Korea's climate context. For SPI, the Weibull distribution consistently outperformed other candidates across all accumulation periods, with particularly strong performance for shorter periods (90% adoption for SPI-6).

As accumulation periods increased, other distributions like Gamma, Log-logistic, and Lognormal gained moderate adoption, suggesting that longer temporal scales may benefit from more diverse distribution considerations. For SPEI, a clear transition pattern emerged with Pearson Type III distribution dominating shorter accumulation periods (98.33% for SPEI-6), while the Generalized Extreme Value (GEV) distribution became increasingly prevalent for longer periods (50% for SPEI-24). This transition likely reflects how the incorporation of potential evapotranspiration introduces more complex spatiotemporal patterns that manifest differently across various time scales. These findings emphasize the importance of carefully selecting appropriate probability distributions for drought indices based on both the specific index and its temporal scale to ensure reliable drought monitoring and assessment in South Korea's changing climate.

Acknowledgments: This study was supported by the National Research Foundation of Korea NRF (2021R1A2C2005699).

References

Beguería S, Vicente-Serrano SM, Reig F, Latorre B (2014) Standardized precipitation evapotranspiration index (SPEI) revisited: parameter fitting, evapotranspiration models, tools, datasets and drought monitoring. International Journal of Climatology 34(9): 3001–3023. https://doi.org/10.1002/joc.3887

Stagge JH, Tallaksen LM, Gudmundsson L, Van Loon AF, Stahl K (2015) Candidate distributions for climatological drought indices (SPI and SPEI). International Journal of Climatology 35(13): 4027–4040. https://doi.org/10.1002/joc.4267

Vicente-Serrano SM, Beguería S, López-Moreno JI (2010) A multiscalar drought index sensitive to global warming: the standardized precipitation evapotranspiration index. Journal of Climate 23(7): 1696–1718. https://doi.org/10.1175/2009JCLI2909.1

Nature-based Solutions in catchment scale flood mitigation: mechanisms and limitations

P. Herath[1,2*], R. Prinsley[1], B. Croke[1], J. Vaze[2], C. Pollino[2]
[1] Australian National University, Canberra, Australian Capital Territory, Australia
[2] CSIRO Environment, Canberra, Australian Capital Territory, Australia
* e-mail: Prabhasri.Herath@anu.edu.com

Introduction

Riverine flooding ranks among the most destructive natural hazards globally, causing annual damages exceeding USD 40 billion and threatening lives and infrastructure (OECD, 2016; WMO, 2024). While traditional engineering approaches like levees and dams have provided crucial flood protection, growing evidence suggests the need for complementary solutions that address environmental impacts and adaptation to changing conditions. Nature-based Solutions (NbS), defined as actions that work with and enhance natural processes to deliver multiple benefits, have emerged as promising alternatives for sustainable flood mitigation while providing additional environmental and societal benefits. NbS leverage natural processes to reduce flood impacts through detention, energy reduction, and flow diversion mechanisms.

Current literature lacks a comprehensive synthesis of NbS strategies' effectiveness across different geographical and environmental contexts, particularly regarding their contribution to flood mitigation and implementation challenges. This systematic review addresses this gap by examining diverse NbS types while analysing their hydrological processes and implementation challenges. The discussion presents empirically-grounded findings on NbS interventions, and their categorisation, while identifying critical knowledge gaps and limitations.

Materials and methods

This review adheres to the Collaboration for Environmental Evidence (2013) guidelines, employing systematic searches, filtering, and bibliometric analysis. Literature searches spanning 2000-2023 were conducted across Web of Science, Scopus, PubMed, and Google Scholar, alongside targeted Google searches for grey literature using 32 keywords related to natural flood management, ecosystem-based adaptation, and river restoration. Additional sources included WorldCat, Dimensions, and government websites. After duplicate removal, 8,368 papers were screened using PICO framework criteria and PRISMA guidelines. Studies were excluded if they focused solely on urban/coastal areas, engineered solutions, or lacked quantitative flood mitigation data. Tools like Covidence and Elicit AI narrowed the results to 141 academic and 7 grey literature documents meeting these criteria. Data extraction focused on NbS characteristics, flood mitigation metrics, and co-benefits using bibliometric and content analysis.

Results and concluding remarks

NbS research shows significant geographical bias, with the UK contributing 21.6% of studies due to favourable policies and conditions, while the Global South remains underrepresented. This disparity limits our understanding of NbS effectiveness in diverse socio-ecological contexts where flood risks often disproportionately affect vulnerable populations. The methodological assessment reveals that modelling approaches dominate (53.9% of studies), with field-based methods accounting for 35.5%, highlighting the need to integrate empirical evidence with advanced techniques for validating NbS effectiveness in flood management.

The review categorizes NbS interventions into four types: managing catchment land cover, storing excess water, managing floodplains, and creating alternative routes. NbS for flood management implement

three fundamental strategies (Figure 1), often combining them to address flood risks comprehensively.

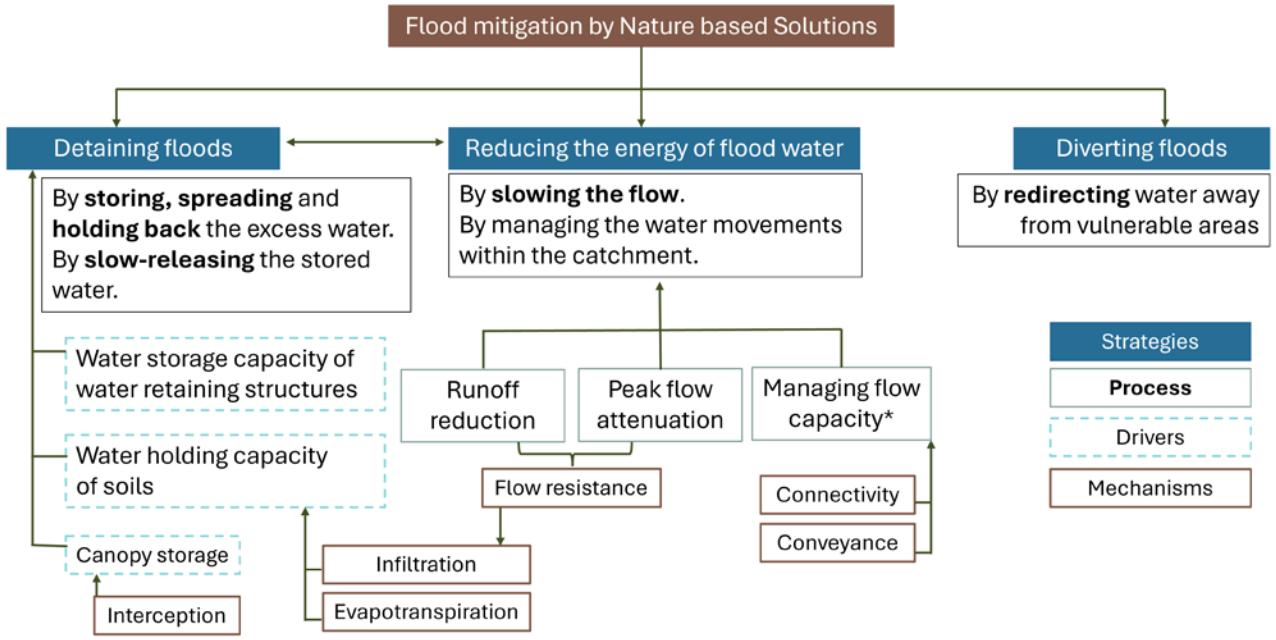


Figure 1. Flood mitigation strategies through Nature-based Solutions: Conceptual framework showing the relationship between fundamental processes, driving mechanisms, and their hydrological impacts.

Detaining floods, involves storing excess water to reduce flood volume and risk through structures like ponds, wetlands, and detention basins. Water-holding capacity depends on soil properties, organic matter content, infiltration rates, and evapotranspiration. Forests and dense vegetation contribute by intercepting rainfall, delaying runoff, and reducing downstream energy, while soil management and land cover conservation improve infiltration and recharge, though effectiveness diminishes in saturated conditions.

Reducing floodwater energy, the second strategy, slows flow velocity using interventions like riparian vegetation, leaky weirs, and afforestation. These increase surface roughness, dissipate kinetic energy and reduce downstream discharge. Extending the time of concentration allows upstream storage but may cause localised flooding, with limited effectiveness during major events.

Diverting floodwater, the third strategy, redirects water from vulnerable areas using modified drainage systems. Restoring palaeochannels, palaeovalleys, bypasses, and secondary channels reduces peak flow and volume, alleviating pressure on main rivers and minimising damage.

Nature-based Solutions face implementation challenges across technical, environmental, social, and economic dimensions at the catchment scale. Technical constraints include reduced effectiveness during extreme events, non-linear benefits across scales, and significant time lags between implementation and functionality. Environmental challenges encompass soil and groundwater constraints, climate variability impacts, and long-term climate change effects. Socio-economic barriers include limited land availability, high initial costs, and maintenance requirements, particularly in areas with competing land-use demands. Addressing these challenges requires integrated planning, adaptive management, and cross-sector collaboration.

References

Collaboration for Environmental Evidence (2013) Guidelines for Systematic Reviews in Environmental Management, Version 4.2. http://www.environmentalevidence.org/wp-content/uploads/2014/06/Review-guidelines-version-4.2-final.pdf.

OECD (2016) Financial Management of Flood Risk. Paris: OECD Publishing. 10.1787/9789264257689-en.

WMO (2024) Floods, World Meteorological Organization. https://wmo.int/topics/floods (Accessed: 13 September 2024).

Hydrological extremes: The New Zealand experience

J. Renwick
School of Geography, Environment and Earth Sciences, Victoria University of Wellington, Wellington, New Zealand
e-mail: james.renwick@vuw.ac.nz

Introduction

New Zealand lies in the Southern Hemisphere mid-latitudes and is surrounded by ocean. The country's climate is broadly described as "maritime", Köppen Classification Cfb. However, because of the country's rugged topography and its interactions with the prevailing westerly wind, regional climates vary strongly, from very wet in the western South Island to semi-arid east of the Southern Alps, to quasi-Mediterranean climates in the eastern North Island (Sturman & Tapper, 2006). All regions of the country are exposed to hydrological extremes, from storms originating over the Southern Oceans and the Tropics, from atmospheric river events, and from slow-moving anticyclones bringing drought conditions.

As the climate changes, New Zealand's water availability is being modified across the whole country, broadly according to the "wet get wetter, dry get drier" paradigm (Douville et al., 2022), regardless of the underlying regional climate. Since New Zealand's economy is strongly agriculture-based, and electricity production is dominated by hydro-electric generation, such changes in precipitation have major implications for land use, water storage, and the siting of infrastructure. This presentation will discuss observed precipitation variability and extremes and how those extremes are changing, with implications for New Zealand society.

Materials and methods

The climate of New Zealand (NZ) will be described using a combination of observational data from the National Institute of Water and Atmospheric Research (NIWA, nd) and large-scale circulation features derived from the ERA5 data set (Hersbach et al., 2020). The key feature of the Southern Hemisphere extra-tropical circulation is the mid-latitude westerly jet, the strength of which over New Zealand is modulated primarily by the El Niño-Southern Oscillation (ENSO; Bhaskaran & Mullan, 2003) and more strongly by the Southern Annular Mode (SAM; Kidston et al., 2009). In particular, the future of the SAM is a major determinant of future NZ regional climate. Its positive trend in recent decades, towards stronger westerlies closer to the Pole, has been driven by a combination of stratospheric ozone depletion and greenhouse gas-induced warming. This has added a warming and a drying trend in many parts of NZ climate since the 1960s (Kidston et al., 2009). As the ozone "hole" recovers, the relative impacts of those two factors on the SAM trend are largely unknown, adding uncertainty to future NZ climates.

Beyond such dynamical effects, direct thermal effects of increasing atmospheric water vapour and increasingly efficient surface evaporation are strongly affecting NZ. Recent rainfall extremes have shown unprecedented precipitation intensities. Storm damage from ex-tropical cyclone Gabrielle in 2023 was made worse through increased rainfall and also increased storm intensity with stronger winds, brought about by the changed climate (World Weather Attribution, 2023). A major drought in 2013 was made worse by the warming already experienced (Harrington et al., 2014). It has been estimated that the climate change-induced components of such extremes cost the NZ economy close to one billion NZ dollars in the decade 2007-2017 (Frame et al., 2020).

Such economic losses look set to increase in the future. Based on analysis of a large ensemble of regional climate model simulations from the weather@home experiment (Massey et al., 2015), it has been shown that all regions of the country are likely to experience increased wet and dry extremes as a result of climate change (Harrington et al., 2024).

Results and concluding remarks

New Zealand's climate is changing through a combination of dynamical and thermodynamical effects. The water cycle over New Zealand is becoming more extreme, with wetter "wets" and drier "drys", as a result of increased atmospheric water vapour and more intense land surface evaporation and associated feedbacks. This is combined with dynamical changes to the average location of the mid-latitude westerly jet and its associated storm track.

Implications for water availability in NZ are significant, from storage requirements in urban areas to land-use for agriculture and effects on the "dry-year risk" for electricity production. Thus far, policy-makers in New Zealand have not responded noticeably to such changes, as has been seen elsewhere (Douville et al., 2022). However, major adjustments are likely to be required by mid-century. My presentation will summarise the state of New Zealand's climate, how aspects of the water cycle are changing, and implications for policy-makers.

References

Bhaskaran, B., & Mullan, A. B. (2003). El Nino-related variations in the southern Pacific atmospheric circulation: model versus observations. Climate Dynamics, 20(2-3), 229-239.

Douville, H., Allan, R. P., Arias, P. A., Betts, R. A., Caretta, M. A., Cherchi, A., Mukherji, A., Raghavan, K., & Renwick, J. (2022). Water remains a blind spot in climate change policies. PLOS Water, 1(12), e0000058. https://doi.org/10.1371/journal.pwat.0000058

Frame, D. J., Rosier, S. M., Noy, I., Harrington, L. J., Carey-Smith, T., Sparrow, S. N., Stone, D. A., & Dean, S. M. (2020). Climate change attribution and the economic costs of extreme weather events: a study on damages from extreme rainfall and drought. Climatic Change, 162(2), 781-797. https://doi.org/10.1007/s10584-020-02729-y

Harrington, L. J., Rosier, S., Dean, S. M., Stuart, S., & Scahill, A. (2014). The role of anthropogenic climate change in the 2013 drought over North Island, New Zealand [in "Explaining Extremes of 2013 from a Climate Perspective"]. Bulletin of American Meteorological Society, 95(9), S45-S48.

Harrington, L. J., Rosier, S. M., Marsh, T. I., & Frame, D. J. (2024). Robust changes to the wettest and driest days of the year are hidden within annual rainfall projections: a New Zealand case study. Environmental Research Letters, 19(7), 074057. https://doi.org/10.1088/1748-9326/ad585a

Hersbach, H., Bell, B., Berrisford, P., Hirahara, S., Horányi, A., Muñoz-Sabater, J., Nicolas, J., Peubey, C., Radu, R., Schepers, D., Simmons, A., Soci, C., Abdalla, S., Abellan, X., Balsamo, G., Bechtold, P., Biavati, G., Bidlot, J., Bonavita, M., De Chiara, G., Dahlgren, P., Dee, D., Diamantakis, M., Dragani, R., Flemming, J., Forbes, R., Fuentes, M., Geer, A., Haimberger, L., Healy, S., Hogan, R. J., Hólm, E., Janisková, M., Keeley, S., Laloyaux, P., Lopez, P., Lupu, C., Radnoti, G., de Rosnay, P., Rozum, I., Vamborg, F., Villaume, S., & Thépaut, J.-N. (2020). The ERA5 global reanalysis. Quarterly Journal of the Royal Meteorological Society, 146(730), 1999-2049. https://doi.org/https://doi.org/10.1002/qj.3803

Kidston, J., Renwick, J. A., & McGregor, J. (2009). Hemispheric-scale seasonality of the Southern Annular Mode and impacts on the climate of New Zealand. Journal of Climate, 22(18), 4759-4770. http://dx.doi.org/10.1175%2F2009JCLI2640.1

Massey, N., Jones, R., Otto, F. E. L., Aina, T., Wilson, S., Murphy, J. M., Hassell, D., Yamazaki, Y. H., & Allen, M. R. (2015). weather@home—development and validation of a very large ensemble modelling system for probabilistic event attribution. Quarterly Journal of the Royal Meteorological Society, 141(690), 1528-1545. https://doi.org/https://doi.org/10.1002/qj.2455

NIWA (nd). https://niwa.co.nz/climate-and-weather/climate-data

Sturman, A. P., & Tapper, N. J. (2006). The Weather and Climate of Australia and New Zealand (2nd ed.). Oxford University Press.

World Weather Attribution (2023). https://www.worldweatherattribution.org/the-role-of-climate-change-in-extreme-rainfall-associated-with-cyclone-gabrielle-over-aotearoa-new-zealands-east-coast/

On the use of TCEV distribution in at-site flood frequency analysis: insights from eastern Australia

V. Totaro[1*], G. Kuczera[2], V. Iacobellis[1]
[1] Dipartimento di Ingegneria Civile, Ambientale, del Territorio, Edile e di Chimica, Politecnico di Bari, Bari, 70125, Italy
[2] School of Engineering, University of Newcastle, Callaghan, 2308, NSW, Australia
* e-mail: vincenzo.totaro@poliba.it

Introduction

Typically, the estimation of a flood quantile relies on fitting a number of three-parameter parent distributions to annual maxima flood peaks series and evaluating their goodness-of-fit. However, in many cases this simple paradigm needs to be revisited in the light of the evidence that flood series can be composed from observations arising from multiple populations. In those cases, evaluating the opportunity of using mixture models represents a promising option, especially when there is clear evidence in lack-of-fit of traditional distributions and the mixture model is consistent with the physical mechanisms responsible for the flood generation processes (Lamontagne et al., 2016; Alila and Mtiraoui, 2002). Unfortunately, mixed distributions are generally characterized by four or more parameters and their limited use in at-site flood frequency analysis can be attributed both to computational issues in parameter estimation and to difficulties in the identification of compounding populations.

The Two-Component Extreme Value distribution (TCEV) was proposed by Rossi et al. (1984) and belongs to the family of compound mixture models. Despite application of TCEV mainly limited to regional frequency analysis of rainfall and floods, several studies have highlighted that this distribution could represent a suitable alternative in at-site analysis (e.g., Totaro et al., 2024a,b). In particular, Totaro et al. (2024b) proposed a robust Bayesian framework to support parameter estimation even in those cases where degeneracy occurs and highlighted how the choice of TCEV could be justified by physical evidence of underlying hydrological mechanisms.

In this work we systematically applied the TCEV distribution to all annual maximum flood series in eastern Australia with record lengths of at least 50 years. The objective is to expand the findings of Totaro et al. (2024b) and hence contribute to the scientific debate on the use of mixture probability distributions in flood frequency analysis and in the study area.

Materials and methods

The Two-Component Extreme Value distribution has the following cumulative distribution function:

$$F(x) = exp\left(-\Lambda_1 exp\left(-\frac{x}{\theta_1}\right) - \Lambda_2 exp\left(-\frac{x}{\theta_2}\right)\right), x \geq 0 \quad (1)$$

where the two components are respectively characterized by the parameter couples (Λ_1, θ_1) and (Λ_2, θ_2). The physical basis of TCEV distribution assumes that the annual number of exceedances of each component is Poisson distributed with related exceedances following an exponential distribution. Λ_1 and Λ_2 are the mean annual number of peaks and θ_1 and θ_2 as the mean amplitude of components 1 and 2.

As the method of L-moments is known to fail for TCEV, we use the Bayesian framework described in Totaro et al. (2024b) to infer TCEV parameters. We use Markov chain Monte Carlo sampling to sample the posterior. This was demonstrated to be robust and provided adequate diagnostics for handling component degeneracy.

We present an application to 158 annual maximum flood peak series of Queensland and New South Wales (Australia) with at least 50 years of data. Sites are homogeneously distributed along the eastern

coast of Australia and with catchment sizes ranging from 6.7 to 4929 km^2.

Results and concluding remarks

With respect to TCEV parameter inference, the robustness of the Bayesian framework was confirmed. Diagnostics provided valuable support in handling the degeneracy issues, confirming advantages of the Bayesian approach with respect to maximum likelihood or L-Moment.

TCEV distribution also provided a good fit in a significant number of series characterized by the so-called "dog-leg", a signature of the presence of multiple populations (Potter, 1958). Furthermore, when compared with the recommended approach of fitting flood series with the Log Pearson type III distribution in which potentially influential low flows are censored, the TCEV was found to produce significantly narrower confidence intervals than LP3 for high quantiles. Our findings are generally in line with those provided by Totaro et al. (2024b). In addition, dependence of parameters of the second component on catchment area and distance from the sea was investigated, revealing interesting dependences related to the physical mechanisms responsible for floods generation.

Results of this study confirmed the suitability of TCEV distribution for at-site flood frequency analysis, providing additional elements in the need of integrating physical considerations for supporting the choice of a probability distribution when fitting flood series.

Acknowledgments

The authors thank Mark Babister and Monique Retallick for their advice and access to LP3 results for a range of Australian catchments.

References

Alila Y, Mtiraoui A. (2002) Implications of heterogeneous flood-frequency distributions on traditional stream-discharge prediction techniques. Hydrological Processes 16, 1065–1084. https://doi.org/10.1002/hyp.346

Lamontagne, J. R., Stedinger, J. R., Yu, X., Whealton, C. A., & Xu, Z. (2016). Robust flood frequency analysis: Performance of EMA with multiple Grubbs-Beck outlier tests. *Water Resources Research*, *52*(4), 3068-3084.

Potter WD (1958) Upper and lower frequency curves for peak rates of runoff. Eos, Trans Am Geophys Union 39:100–105. https://doi.org/10.1029/TR039i001p00100

Rossi F, Fiorentino M, Versace P (1984) Two-component extreme value distribution for flood frequency analysis. Water Resources Research. 20(7): 847-856. https://doi.org/10.1029/ WR020i007p00847

Totaro V, Gioia A, Kuczera G, Iacobellis V (2024a). Modelling multidecadal variability in flood frequency using the Two-Component Extreme Value distribution. *Stochastic Environmental Research and Risk Assessment*, 38, 2157–2174. https://doi.org/10.1007/s00477-024-02673-8

Totaro V, Kuczera G, Iacobellis V (2024b) Goodness-of-fit, identifiability and extrapolation: Can the Two-Component Extreme Value distribution be used in at-site flood frequency analysis?. *Journal of Hydrology*, *640*, 131590. https://doi.org/10.1016/j.jhydrol.2024.131590

Non-stationary flood frequency analysis – the role of physical covariates and flood generating mechanisms

M.N. Khaliq
Ocean, Coastal, and River Engineering Research Centre, National Research Council Canada, Ottawa, ON, Canada
e-mail: Muhammad.Khaliq@nrc-cnrc.gc.ca

Introduction

Flood frequency analysis (FFA) is commonly used to derive design flow values for sizing various hydraulic structures, such as culverts, bridges, small dams, and levees, in addition to informing hydraulic procedures of floodplain mapping/delineation and water resources management-related activities. For the classical FFA, long sequences of observed flood flows are generally employed and it is often assumed that these sequences are realizations of a stationary process. However, this assumption is being increasingly questioned due to the anticipated climate change that could potentially alter their timing, magnitude, and frequency (e.g., Khaliq et al. 2006; Sushama et al. 2006; Katz 2010; Kundzewicz 2011; Wasko et al. 2021). To overcome this limitation, scientists have introduced non-stationary FFA approaches, where it is explicitly assumed that the parameters of the controlling probability distribution function are dependent on the state of a few pre-selected covariates, such as time, indicators of large-scale atmospheric circulations, seasonal precipitation amounts, etc. A large number of studies have used time as the sole covariate for non-stationary FFA (Islam et al. 2024). This choice lacks physical justification, given the diverse evolution of flood determining factors in many regions of the world, and therefore other flood-relevant physical covariates are required to be investigated.

The objective of this study was to examine the role of flood-relevant physical covariates, representing various flood generating mechanisms, for conducting non-stationary FFA and to support flood-vulnerability assessments of critical water infrastructure across Canada. The various insights discussed here are driven mainly by the work of Maria et al. (2024) and the ideas distilled from the literature on non-stationary FFA. The outcomes of the study are expected to help plan resilience enhancement strategies for water infrastructure against climate-related future flood risks.

Materials and methods

Annual maximum river flows, derived from a five-member ensemble of continuous streamflow simulations performed with an integrated climate-hydrology regional modelling system (Teufel and Sushama 2021; Maria et al. 2024) for the 1950–2099 period, are used in this study. These simulations were driven at the lateral boundaries by five different members of an initial condition ensemble of the second-generation Canadian Earth System Model, following the Representative Concentration Pathway 8.5 (RCP8.5) scenario. The generalized extreme value (GEV) distribution, with the maximum likelihood parameter estimation method, is used for FFA. The GEV distribution has a strong theoretical basis and is often used for the analysis of extreme values in hydrology and water resources within both the stationary and non-stationary contexts (Coles 2001; Khaliq et al. 2006; Katz 2010). Given that snowmelt and rainfall and/or their combination are primarily responsible for floods in Canada, the physical covariates considered in this study are: (1) annual maximum snow water equivalent (SWE), (2) average annual temperature (AAT), (3) rainfall for the spring-summer (March-August; SSR) period, and (4) rainfall for the fall-winter (September-February; FWR) period. Based on these co-variates and their combinations, ten non-stationary GEV models, with the location parameter being dependent on the state of various co-variates, are considered. The information about covariates is derived from the same ensemble of climate model simulations as for the annual maximum flows. To explore the utility of non-stationary models driven by physical covariates, a stationary GEV model and another non-stationary GEV model with time as the sole covariate are also considered. From the set of these twelve competing models, the best performing model

is identified based on a corrected form of the Akaike Information Criterion, AICc (Burnham et al. 2004).

Results and concluding remarks

After fitting all non-stationary GEV models and evaluating their relative performance based on the AICc values, it is found that the spatial patterns of selected physical covariates are consistent with the commonly understood flood generating mechanisms across various regions of Canada. Additionally, insignificant support is found for the stationary FFA and non-stationary FFA with time as a covariate, compared to the non-stationary FFA with physical covariates.

From the set of four physical covariates, SSR and SWE are found as the most frequently selected covariates. A clear spatial pattern emerged for the eastern regions, while a complex pattern is noted for other parts of the country, reflecting diversity in hydro-climatic controls, with SWE being a major factor. For the east and west coastal regions, FWR is found as the dominant factor, which is consistent with the prevalent flood generating mechanisms in these regions. AAT-based models are found as the preferred option for the northern and west-central regions of Canada.

The non-stationary models outperformed the stationary model with lower AICc values noted for over 80% of grid cells covering the whole country, highlighting the inability of the stationary approach in capturing the full range of climate induced flood risks. This observation suggests that the stationary approach might underestimate future flood risks, which could be critical for regions with aging infrastructure, requiring appropriate adaptation and re-enforcement strategies. Thus, future studies should enhance the conventional approaches of FFA by integrating physical factors responsible for generating flood flows than merely relying on stationary approaches, which may result in under preparedness for future flood risks, particularly as climate patterns continue to evolve due to anthropogenic activities.

Acknowledgments: This work was funded through the National Research Council Canada's Climate Resilient Built Environment (CRBE) initiative, which is supported through Infrastructure Canada, and Government of Canada's National Adaptation Strategy. These funding sources and the leadership of CRBE are gratefully acknowledged.

References

Burnham KP, Anderson DR (2004) Multimodel inference: understanding AIC and BIC in model selection. Sociological Methods and Research 33(2): 261–304. https://doi.org/ 10.1177/0049124104268644

Coles S (2001) An Introduction to Statistical Modelling of Extreme Values, Springer, London, UK

Islam MR, Fereshtehpour M, Najafi MR, Khaliq MN, Khan AA, Sushama L, Nguyen VTV, Elshorbagy A, Roy R, Wilson A, Perdikaris J, Masud MB, Khan MS (2024) Climate-resilience of dams and levees in Canada: a review. Discover Applied Sciences 6(4), 174, https://doi. org/10.1007/s42452-024-05814-4

Katz RW (2010) Statistics of extremes in climate change. Climatic Change 100(1): 1–76, https://doi.org/10.1007/s10584-010-9834-5

Khaliq MN, Ouarda TBMJ, Ondo JC, Gachon P, Bobee B (2006) Frequency analysis of a sequence of dependent and/or non-stationary hydro-meteorological observations: A review, Journal of Hydrology 329(3): 534–552. https://doi.org/ 10.1016/j.jhydrol.2006.03.004

Kundzewicz ZW (2011) Nonstationarity in water resources – central European perspective, Journal of American Water Resources Association 47(3): 550–562. https://doi.org/ 10.1111/j.1752-1688.2011.00549.x

Maria D, Sasmito A, Sushama L, Khaliq MN (2024) Non-stationary analysis of future floods using physical covariates and implications for dams across Canada. Results in Engineering 24, 103645. https://doi.org/10.1016/j.rineng.2024.103645

Sushama L, Laprise R, Caya D, Frigon A, Slivitzky M (2006) Canadian RCM projected climate-change signal and its sensitivity to model errors, International Journal of Climatology 26(15): 2141–2159. https://doi.org/10.1002/joc.1362

Teufel B, Sushama L (2021) 2°C vs. high warming: transitions to flood-generating mechanisms across Canada. Water 13(11), 1494. https://doi.org/10.3390/ w13111494

Wasko C, Westra S, Nathan R, Orr HG, Villarini G, Villalobos Herrera R, Fowler HJ (2021) Incorporating climate change in flood estimation guidance, Philosophical Transactions of the Royal Society A 379, 20190548. https://doi.org/10.1098/rsta.2019.0548

Is ERA5 dataset adequate for drought characterisation? The case of river basin areas of Peloponnese, Greece

P. Golfinopoulou[1], I.M. Kourtis[1], D. Tigkas[1,2], H. Vangelis[1*]
[1] Laboratory of Reclamation Works and Water Resources Management, School of Rural, Surveying and Geoinformatics Engineering, National Technical University of Athens, Athens, Greece
[2] Directorate of Land Reclamation and Soil-Water Resources, Ministry of Rural Development and Food, Athens, Greece
* e-mail: harrivag@central.ntua.gr

Introduction

It is widely accepted that drought is a natural hazard directly affected by the balance between rainfall and evapotranspiration. As new datasets are becoming available, mainly based in reanalysis satellite data, it is crucial to investigate the accuracy of these datasets in drought identification.

In this paper, the use of rainfall and evapotranspiration data from the widely available ERA5 dataset, towards accurate drought identification, is inspected. The concept is that if gauged data, which precisely represent the conditions of a small area, indicate the same drought category (i.e., mild, severe, extreme) as the ERA5 data, which represent a large area (0.25° x 0.25°) without taking into account the specific conditions produced by the, sometimes intense, topographic relief, the ERA5 dataset can be considered accurate for drought identification and monitoring. To explore the concept, four drought indices are used to assess drought in Peloponnesian river basin areas, utilising both gauged and reanalysis datasets.

Materials and methods

The analysis is based in gauged data recorded by the Hellenic National Meteorological Service (HNMS) at 7 meteorological stations: Astros, Andravida, W. Achaia, Pyrgos, Tripoli, Kalamata and Methoni (Argiriou et al., 2023). The meteorological stations are located in both mountainous and lowland areas, scattered in the three river basin areas of Peloponnese, representing the entire rugged topographic relief of the area.

The dataset which is evaluated against the gauged data was obtained by the ERA5 satellite reanalysis database (Hersbach et al., 2023), through the Climate Data Store, in NetCDF4 file format. A MATLAB code was used to transfer the data in appropriate formats for the conducted analysis. As a 12-month temporal scale is selected for the analysis, the data are compiled in hydrological year monthly timeseries for the period 1960-2010.

Four drought indices are used for this analysis, namely the Standardised Precipitation Index – SPI (McKee et al., 1993), the Reconnaissance Drought Index – RDI (Tsakiris and Vangelis, 2005), the Agricultural Standardized Precipitation Index – aSPI (Tigkas et al., 2019) and the Effective Reconnaissance Drought Index – eRDI (Tigkas et al., 2017).

The analysis of the drought indices is facilitated by the DrinC software (Tigkas et al., 2022). DrinC is also used for the assessment of effective precipitation (P_e) required by aSPI and eRDI and for the calculation of evapotranspiration (PET) required by RDI and eRDI.

Results and concluding remarks

The well-known drought event of 1989-1990 is indicated by all the drought indices utilised in this study. It is interesting, though, that the ERA5 dataset underestimates drought severity in the specific hydrological year, although there is no significant pattern of underestimation for the rest of the calculation period. Although in mild drought conditions the two datasets report differences in drought severity, however, within the same drought category, significant disagreement is presented in the few (one or two, depended on the specific meteorological station) extreme events reported in the entire period.

To further explore these discrepancies, the coefficient of determination, between the drought indices values estimated for each dataset, was calculated in all the examined stations, for the entire period under

study and for each drought index, as presented in Table 1. The coefficient reveals that in most cases a "weak relationship" exists between the two datasets. A "very strong relationship" is indicated mainly in Pyrgos station, where the two indices based on P_e perform better than their corresponding original indices.

Table 6. Coefficient of determination (R^2) between the two datasets for the calculated drought indices.

	Astros	Andravida	Western Achaia	Pyrgos	Tripoli	Kalamata	Methoni
SPI	0.277	0.450	0.486	0.603	0.421	0.544	0.425
aSPI	0.216	0.655	0.542	0.715	0.391	0.577	0.444
RDI	0.299	0.027	0.367	0.572	0.425	0.512	0.461
eRDI	0.252	0.038	0.338	0.679	0.372	0.508	0.467

Significant disagreement is also detected in the spatial scale, as indicated by maps developed for the visualisation of drought conditions. In the second most intense drought episode in the examined period, which was detected during the hydrological year 2006-2007, the difference in the spatial coverage of the extreme conditions between the two datasets is obvious in Figure 1.

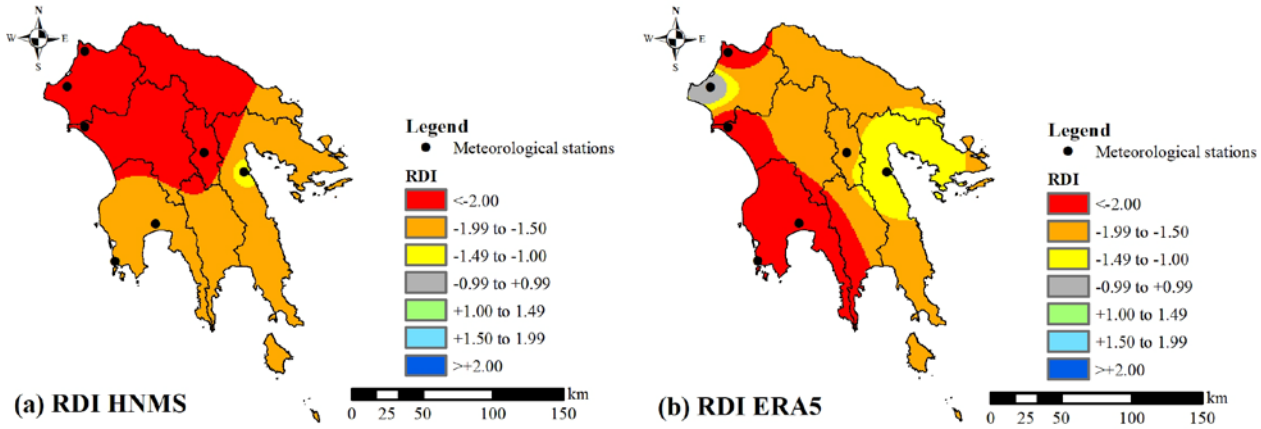


Figure 1. Indicative visualisation of RDI conditions using HNMS and ERA5 datasets for the hydrological year 2006-2007.

It may be concluded that ERA5 dataset may be considered useful for the rough estimation of regional drought conditions. However, special care should be taken in case of drought identification in specific areas, since significant differences are detected in relation to gauged data, especially in the case of severe drought episodes.

References

Argiriou AA, Li Z, Armaos V, Mamara A, Shi YL, Yan ZW (2023) Homogenised monthly and daily temperature and precipitation time series in China and Greece since 1960. Advances in Atmospheric Sciences 40(6): 1326–1336. https://doi.org/10.1007/s00376-022-2246-4

Hersbach H, Bell B, Berrisford P, Biavati G, Horányi A, Muñoz Sabater J, Nicolas J, Peubey C, Radu R, Rozum I, Schepers D, Simmons A, Soci C, Dee D, Thépaut J-N (2023) ERA5 monthly averaged data on single levels from 1940 to present. Copernicus Climate Change Service (C3S) Climate Data Store (CDS) 10: 252–266. https://doi.org/10.24381/cds.f17050d7

McKee TB, Doesken NJ, Kleist J (1993) The relationship of drought frequency and duration to time scales. In Proceedings of the 8th Conference on Applied Climatology, Anaheim, CA, USA, 17–22 January 1993, pp. 179–183.

Tigkas D, Vangelis H, Tsakiris G (2017) An enhanced effective reconnaissance drought index for the characterisation of agricultural drought. Environmental Processes 4(Suppl 1): 137–148. https://doi.org/10.1007/s40710-017-0219-x

Tigkas D, Vangelis H, Tsakiris G (2019) Drought characterisation based on an agriculture-oriented standardised precipitation index. Theoretical and Applied Climatology 135(3-4): 1435–1447. https://doi.org/10.1007/s00704-018-2451-3

Tigkas D, Vangelis H, Tsakiris G (2022) Incorporating aSPI and eRDI in Drought Indices Calculator (DrinC) software for agricultural drought characterisation and monitoring. Hydrology 9(6): 100. https://doi.org/10.3390/hydrology9060100

Tsakiris G, Vangelis H (2005) Establishing a drought index incorporating evapotranspiration. European Water 9/10: 3–11. https://ewra.net/ew/pdf/EW_2005_9-10_01.pdf

Effects of the flood event of August 2023 on the design discharge values in Slovenia

N. Bezak*, M. Šraj
Faculty of Civil and Geodetic Engineering, University of Ljubljana, Ljubljana, Slovenia
** e-mail: nejc.bezak@fgg.uni-lj.si*

Introduction

Between August 4 and 8, 2023, an extreme flood event occurred in Slovenia (Bezak et al. 2023), causing direct and indirect damages totalling almost EUR 10 billion (i.e., around 15% of Slovenia GDP) (Bezak et al., 2023). Unusual summer hydrologic conditions combined with high air and sea temperatures of the Mediterranean and Adriatic Sea and high antecedent soil moisture were the main causes of the most extreme flood event in Slovenia in recent decades (Bezak et al., 2023). Between 150 and 200 mm of rainfall was measured in 6 to 12 hours at multiple precipitation stations across Slovenia. The estimated return period of precipitation was more than 250 years in several places. In July 2023, the monthly amount of precipitation was around two to three times higher than the long-term average for July (Bezak et al., 2023). Moreover, several severe thunderstorms with extreme wind occurred in May-July period, which triggered a lot of small landslides, soil slips and caused forest damage. The result of all factors was extensive and devastating flood event with significant torrential characteristics (Bezak et al., 2023). The estimated runoff coefficients were around 0.5 or even more for typical forested torrential catchments. The estimated return periods of the peak discharges were also above 250 years at several water level gauging stations.

Reconstruction after such a devastating flood event requires the estimation of new values for the design discharges. Therefore, the main objective of this contribution is to assess the impact of the August 2023 flood event on the design discharges for more than 30 water level gauging stations in Slovenia.

Materials and methods

A total of 33 water level gauging stations were selected for the analysis. Continuous data is available for these stations for the 1961-2023. Based on the continuous discharge data, the annual maximum (AM) sample was extracted for each gauging station. The flood frequency analysis (FFA) was performed for every gauging station using two samples: 1961-2022 (62 years of data) and 1961-2023 (63 years of data). Eight distribution functions were selected and tested: Pearson distribution type 3, Log-Pearson distribution type 3, Generalized Extreme Value distribution, Gumbel distribution, 3-parameter log-normal distribution (LN3), Gamma distribution, Generalised Logistic Distribution, Exponential distribution. The distribution parameters were estimated using the method of L-moments (Hosking and Wallis, 1997). The best fitting distribution for each gauging station was selected based on the Akaike Information Criterion (AIC) and Kolmogorov-Smirnov test was used to determine if selected distribution is able to adequately describe the AM sample.

The catchment areas of selected stations ranged from 9 to 4821 km^2 with an average value 636 km^2. The water level gauging stations were distributed relatively evenly across Slovenia (Figure 1). The specific discharge values calculated based on the peak discharges for the August 2023 event ranged from 0.14 to 3.8 with an average value of 0.95 $m^3/s/km^2$. A comparison of the specific discharge values with some commonly used empirical envelope curves showed that the flood event of August 2023 can be considered extreme, but theoretically even higher flood events could occur in the future (Bezak et al., 2023). The measured 24h rainfall amounts were equal to around 35% of the probable maximum rainfall in the northern (most affected) part of the country (Figure 1). Moreover, rainfall erosivity of August 2023 event at some precipitation stations in Slovenia exceeded 200 % of long-term average annual rainfall erosivity and at the majority of stations the ratio (compared to the long-term rainfall erosivity) was higher than 100% (Bezak et al., 2023).

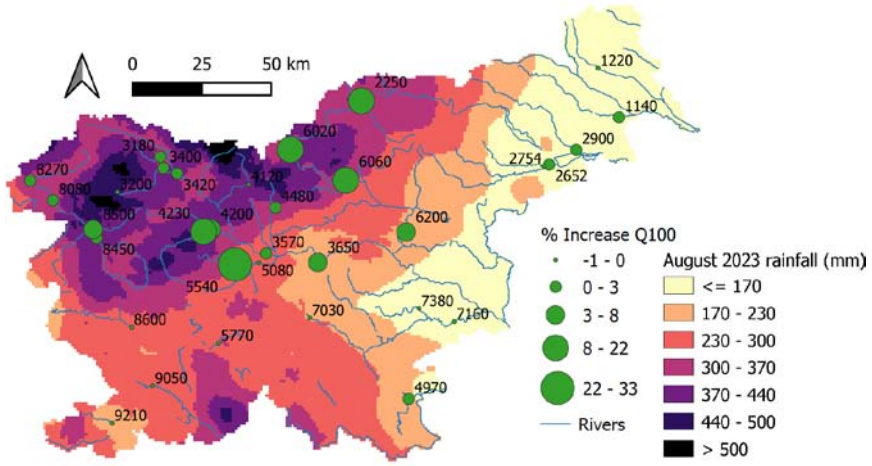


Figure 1. Differences in the design discharges between 1961-2023 and 1961-2022 for a return period of 100 years (Q100). The monthly precipitation totals for August 2023 are shown as a background. Green circles indicate locations of 33 water level gauging stations and numbers indicate station's IDs.

Results and concluding remarks

Flood frequency analysis (FFA) was performed for 33 water level gauging stations for two samples. In order to determine the effects of the 2023 flood peak on the results of the FFA, FFAs were carried out with and without the 2023 peak discharge. It should be noted that at some stations the 2023 flood peak was not measured at the time of the August event, but in other months (e.g., May, October, November, December). These stations were mostly located in southern part of the country (Figure 1). The results (Figure 1) show that the 2023 event at the individual gauging stations increases the design discharges with a 10-years return period by up to 9 %, the discharges with a 100-years return period by up to 33 % and the discharges with a 500-years return period by up to 57 %. The average increase (for 33 discharges gauging stations) was 2 %, 5 % and 7 % for the 10-, 100- and 500-years return periods, respectively. Considering only the gauging stations that were most affected during the August 2023 event (i.e., stations in the Drava, Savinja and Sora catchment areas), the average increase was 4%, 10% and 15% for the 10-, 100- and 500-years return periods, respectively.

The results of the study show that the influence of a single extreme flood event on the design discharges can be relatively large, which is why it is advisable and necessary to take confidence intervals into account when determining the design discharges and their application in practise. In fact, the design discharges with 100- and 500-year return periods for the period 1961-2023 were within the confidence intervals of the design discharges with 100- and 500-year return periods for the period 1961-2022 at 32 of the 33 gauging stations.

Therefore, the determination of design discharges must be updated regularly and the results of older studies (i.e., older than 10-15 years) should not be used for practical applications. After hydrologically very wet years, the design discharges should always be recalculated, as even a single year can have a considerable influence on the relationship between discharge and return period.

Acknowledgments: This work was financially supported by the Slovenian Water Agency (DRSV) and Slovenian Research and Innovation Agency (ARIS) through grants "P2-0180", "N2-0313" and "J6-4628".

References

Bezak N, Panagos P, Liakos L, Mikoš M (2023) Brief communication: A first hydrological investigation of extreme August 2023 floods in Slovenia, Europe. Natural Hazards and Earth System Sciences 23: 3885-3893. https://doi.org/10.5194/nhess-23-3885-2023.

Hosking J R M, Wallis J R (1997) Regional frequency analysis: an approach based on L-moments. Cambridge University Press, Cambridge.

Flood forecasting in the Kosi basin (India): A comparative study of singular and hybrid NARX models utilising satellite rainfall products

A.K. Singh*, V. Singh, T. Roshni
Department of Civil Engineering, National Institute of Technology, Patna 800005, India
** e-mail: adityass.ph21.ce@nitp.ac.in*

Introduction

Floods are among the most devastating natural disasters, causing loss of life, property damage, and degradation of ecological systems. Therefore, a reliable flood forecasting and warning system is crucial for mitigating the severe impacts of floods. However, the accuracy of flood forecasts can be significantly compromised by inadequate rain gauge networks and the lack of real-time rainfall data, particularly in remote and inaccessible regions (Singh and Singh 2024). The increasing availability of real-time satellite-based rainfall products offers a promising solution to these limitations. By integrating these satellite products with advanced data-driven models, the accuracy and reliability of real-time flood forecasting (RTFF) can be greatly enhanced (Yeditha et al.2022 ; Kumar and Singh 2024). This study first evaluates the performance of satellite rainfall products (SRPs) from Integrated Multi-Satellite Retrievals for Global Precipitation Measurement (IMERG) using statistical metrics to assess their reliability for flood forecasting. Secondly, it develops a data-driven model, the nonlinear autoregressive with exogenous inputs (NARX) model, and compares it to the hybrid wavelet-based nonlinear autoregressive with exogenous inputs (W-NARX) model using satellite rainfall products (SRPs) to predict water level (WL) at multiple lead times.

Materials and methods

The study focuses on the Kosi River basin, a region highly prone to frequent flooding, resulting in significant loss of life and economic damage annually. To evaluate the accuracy of the SRPs, daily rainfall data from eight strategically located ground-based rain gauge (RG) stations in the Kosi basin were collected from the India Meteorological Department (IMD), while the IMERG dataset can be accessed at https://giovanni.gsfc.nasa.gov/giovanni/ for the period 2001–2020. Additionally, daily water level data from the Baltara gauging station were acquired from the Water Resources Division, Patna, for the same period. For the IMERG dataset, the grid cell corresponding to each RG station was identified, rainfall data were extracted from the grid, and subsequently compared with the observed RG data. To account for the varying grid size of the IMERG dataset (0.10° × 0.10°), bilinear interpolation was applied (Singh and Singh 2024). Furthermore, the Thiessen Polygon technique was used to calculate the mean precipitation over the entire basin for both the observed RG data and the IMERG dataset. Subsequently, the Probability of Detection (POD) and False Alarm Ratio (FAR) were employed to assess the daily performance of IMERG in comparison with RG data. These metrics are used to evaluate the alignment of observed data with SRPs in detecting rainfall events (Kumar and Singh 2023). Lag components were further identified using the Auto Correlation Function (ACF) for water level (WL) and the Cross Correlation Function (CCF) for both water level and satellite rainfall products (SRPs). Based on the results of the lag analysis, NARX and W-NARX models were developed, employing a 70:30 training-testing split to predict water level (WL) at lead times of 1 and 3 days. The architectural framework for both models can be referred from Nanda et al. (2016). The performance of the models was assessed using four statistical indicators: the coefficient of correlation (R), Root Mean Square Error (RMSE), Nash-Sutcliffe efficiency (NSE), and Mean Absolute Error (MAE).

Results and concluding remarks

For the contingency test, the POD and FAR values were evaluated, and the results show that the IMERG dataset performed effectively in capturing rainfall events within the basin, with a POD of 78.03% and a FAR

of 24.85%. The studies conducted by Nanda et al. (2016), Yeditha et al. (2022), and Kumar and Singh (2024) have demonstrated that SRPs with a POD above 70% are considered effective for flood assessment. At the Baltara gauging station, the Highest Flood Level (HFL), Danger Level, and Warning Level are 36.40 m, 33.85 m, and 32.85 m, respectively. The model's efficacy was validated using flood event from 2020. Based on the ACF and CCF analysis, the optimal lag for SRPs was determined to be four days for model development. Table 1 demonstrates the model's performance during training and testing. As the lead time increased, the performance of the models declined, resulting in reduced R and NSE values along with greater RMSE and MAE values. Figure 1 shows the model's simulation results for the 2020 flood event at 1-day and 3-day lead times. However, the W-NARX outperformed the singular NARX model when utilizing the IMERG dataset. Its efficacy is due to its adaptive use of wavelet transform for feature extraction, facilitating a multi-resolution analysis that successfully identifies both high-frequency and low-frequency patterns in rainfall data. Additionally, the smooth combination of wavelet and NARX allows the W-NARX model to attain improved forecasting accuracy. Therefore, the W-NARX model was recognized as a reliable RTFF technique due to its ability to provide accurate forecasts using the IMERG dataset. Nevertheless, the applicability and accuracy of the SRPs, as well as the effectiveness of the proposed models, require additional validation and support. This can be accomplished through practical applications in different river basins with diverse climate conditions and catchment features.

		Training				Testing			
Model	**Lead Time**	**R**	**RMSE**	**NSE**	**MAE**	**R**	**RMSE**	**NSE**	**MAE**
NARX	1 Day	0.95	0.76	0.90	0.47	0.90	0.91	0.80	0.61
	3 Days	0.81	1.70	0.61	0.98	0.68	1.61	0.49	1.22
W-NARX	1 Day	0.97	0.65	0.92	0.38	0.92	0.86	0.82	0.55
	3 Days	0.86	1.51	0.74	0.94	0.78	1.57	0.62	1.18

Table 1. Evaluation of Model Performance in Training and Testing.

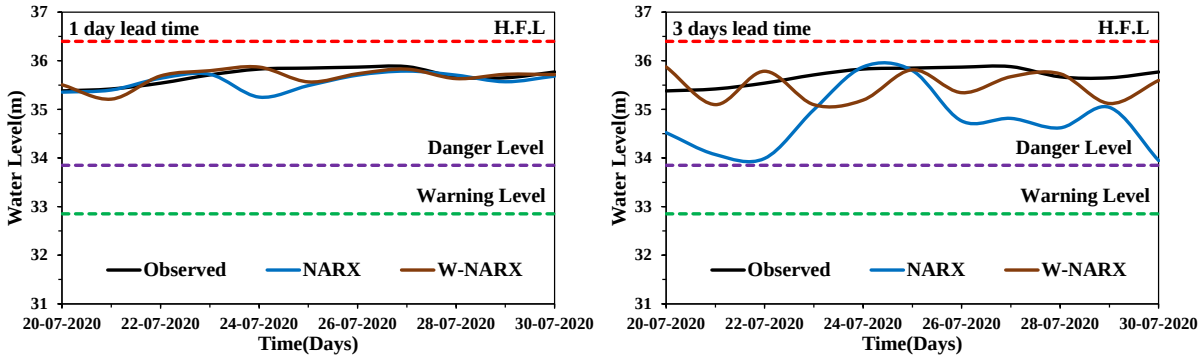


Figure 1. Forecasted water levels for the 2020 flood event at 1-day and 3-day lead times.

References

Kumar A, Singh, V (2024) Real-time flood forecasting using satellite precipitation product and machine learning approach in Bagmati river basin, India. Acta Geophysica. https://doi.org/10.1007/s11600-024-01332-4.

Kumar A, Singh V (2023) Comparative analysis of gridded rainfall datasets over the Bagmati river basin,India. Water Practice and Technology, 18(12): 31413163. https://doi.org/10.2166/wpt.2023.206.

Nanda T, Sahoo B, Beria H, Chatterjee C (2016) A wavelet integrated non-linear autoregressive with exogenous inputs (WNARX) dynamic neural network model for real-time flood forecasting using satellite-based rainfall products. Journal of Hydrology, 539: 57-73.

Singh A K, Singh V (2024) Assessing the accuracy and reliability of satellite-derived precipitation products in the Kosi River basin (India). Environmental Monitoring and Assessment 196(7): 671.

Yeditha P K, Rathinasamy M, Neelamsetty S S, Bhattacharya B, Agarwal A (2022) Investigation of satellite precipitation product driven rainfall-runoff model using deep learning approaches in two different catchments of India. Journal of Hydroinformatics 24(1): 16-37.

Stochastic rainfall simulation at sub-daily scales preserving IDF curves

F. Cappelli[1], E. Volpi[2], A. Langousis[3], R. Deidda[4], A. Perdios[3,4], S. Grimaldi[1]
[1] Dipartimento di Innovazione nei sistemi Biologici, Agroali-mentari e Forestali, Università degli Studi della Tuscia, Italy
[2] Dipartimento di Ingegneria Civile, Informatica e delle Tecnologie Aeronautiche, Università degli Studi Roma Tre, Italy
[3] Department of Civil Engineering, University of Patras, Patras, Greece
[4] Dipartimento di Ingegneria Civile, Ambientale ed Architettura, University of Cagliari, Cagliari, Italy
* e-mail: elena.volpi@uniroma3.it

Introduction

Rainfall simulation is essential in a wide range of environmental and hydrological studies. Despite substantial research efforts and the development of several modelling approaches (e.g. Volpi et al., 2024), practical applications remain limited because of model's diversity and the absence of standards for specific applications, as no universal optimal model/calibration strategies exist. Further, calibration of rainfall models relies on continuous-time data, which are often too short to support rigorous modelling procedures.

To address these challenges, we propose a two-step approach incorporating statistical information from different temporal resolutions; it relies on first modelling daily rainfall and then disaggregating it at sub-hourly scales. This allows to (i) maximize the available information for the daily rainfall model, (ii) capture correlation structures and extreme events distribution, (iii) extend daily models to multisite implementations mitigating the underestimation of the spatial correlation. Focusing on rainfall disaggregation, we illustrate here a parsimonious calibration procedure based on a multifractal approach that matches the theoretical and empirical Intensity-Duration-Frequency (IDF) curves (Cappelli et al., 2025).

Materials and methods

The multifractal modelling approach assumes that the rainfall process exhibits scale invariant properties in ranges of scales of interest for hydrological applications, i.e. $I_d \overset{dist}{=} A_r I_{rd}$, where A_r is a non-negative log-infinitely divisible unit-mean random variable, $r > 1$ is a contraction factor and $\overset{dist}{=}$ stands for equality in all finite dimensional distributions. We use a beta-lognormal model for A_r such that

$$A_r = \begin{cases} 0 & \text{with probability } 1 - r^{-C_\beta} \\ r^{C_\beta} \exp\left(-C_{LN} \ln r + Q\sqrt{2C_{LN} \ln r}\right) & \text{with probability } r^{-C_\beta} \end{cases} \quad (1)$$

where $A_r = A_{\beta,r}\, A_{LN,r}$. $A_{\beta,r}$ is a discrete RV equal to 0 or 1 with probability $1 - r^{-C_\beta}$ and r^{-C_β}, respectively; $A_{LN,r}$ (independent from $A_{\beta,r}$) is a continuous RV that follows a lognormal distribution with log-mean $m_{A_{LN,r}} = (C_\beta - C_{LN}) \ln r$, and log-variance $\sigma^2_{A_{LN,r}} = 2C_{LN} \ln r$. Q ~ $N[0, 1]$ is standard normal random variable and (C_β, C_{LN}) are non-negative parameters satisfing $C_\beta + C_{LN} < 1$. The beta component (i.e. A_β) models the alternation of dry and wet periods, while the lognormal component (i.e. A_{LN}) describes the intensity of the fluctuations when it rains.

The proposed disaggregation model belongs to the class of discrete Multiplicative Random Cascades (MRC) based on a canonical downscaling scheme. Here we preserve exactly the intensity value and control the generation of zeros at the last level of the cascade, departing from exact canonical MRC construction; this introduces deviations of the statistics of the simulated series from those theoretically prescribed. The model takes advantage of a simple theoretical approximation to the IDF curves (Langousis et al., 2009)

$$\frac{i_{d,T}}{\bar{I}} = \begin{cases} \left(r\, r_0\right)^{C_\beta - C_{LN}} e^{\sqrt{2C_{LN} \ln(r\, r_0)}\, \phi^{-1}\left[1 - \frac{(r\, r_0)^{C_{\beta_D}}}{8760\, rT}\right]} & T \le T_r^* \\ i_r^* \left(\frac{8760\, T}{T_r^*}\right)^{C_{LN}/(1 - C_\beta)} & T > T_r^* \end{cases} \quad (2)$$

where $i_{d,T}$ [mm/h] is the rainfall intensity averaged over duration d [h] with return period T [yr], $\bar{I}$ [mm/h] is the mean rainfall intensity, D [h] is the maximum temporal scale of multifractality, $r = D/d$ is the contraction factor, r_0 is a function of the parameter set (C_β, C_{LN}) approximating the dressing effect, $\phi^{-1}[.]$ is the quantile of the standard normal distribution and $i_r^* = (r\, r_0)^{2-C_{LN}-C_\beta}$. Furthermore

$$T_r^* = d\sqrt{4\pi \ln(r\, r_0)\frac{(1-C_\beta)^2}{C_{LN}}}\,(r\, r_0)^{\left[\frac{(1-C_\beta)^2}{C_{LN}}+C_\beta\right]}\ \text{[h]} \tag{3}$$

The model can be calibrated to reproduce empirically derived IDFs usually met in the form $i_{d,T} = a(T)d^{n-1}$, where n [-] is a positive constant with $0 < n < 1$, and $a(T)$ [mm/h^n] is a scale (i.e. d) independent growth curve. The proposed parsimonious calibration method is assessed through the large regional dataset of the Arno River basin, which comprises 70 rainfall time series observed at 15-min intervals.

Results and concluding remarks

The canonical disaggregation cascade procedure can be applied starting from the calibrated parameter values and the observed daily time series. To ensure a thorough evaluation, we disaggregated each of the 70 observed daily rainfall time series 100 times to a terminal 15-min resolution. These synthetic time series were then compared and evaluated against the observed rainfall time series at the same resolution.

The statistical evaluation focuses on key metrics relevant to flood-related applications: IDFs exponent n and dry-frequency, three percentiles (97.5th, 99th, and 99.9th) of the rainfall intensity distribution, two autocorrelation coefficients (at lag equal to 1 and 10) at the 15-min temporal resolution. As an example Fig. 1 compares the value of exponent n estimated from the empirical records (x-axis) to those estimated from the 100 synthetic realizations of disaggregated (to 15 min) historical daily rainfall totals (whisker plots). Results are promising, as the simulated series are almost aligned with the benchmark values. Further investigation is necessary to explore the full range of properties of the simulated time series.

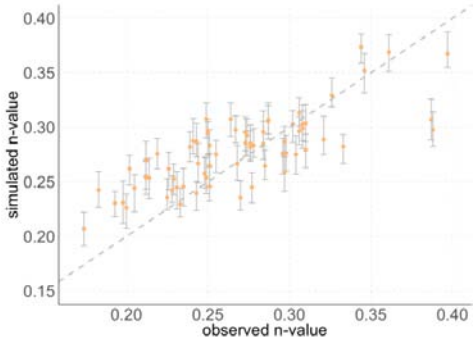


Figure 1. Comparison between the values of exponent n estimated from observations (x-axis), and those obtained from the ensemble of 100 synthetic timeseries (whisker plots) from the 70 raingauges (y-axis). The diagonal dashed line resembles the perfect matching condition. Figure selected from Cappelli et al. 2024.

Acknowledgments: This study was carried out within the RETURN Extended Partnership and received funding from the European Union Next-GenerationEU (National Recovery and Resilience Plan – NRRP, Mission 4, Component 2, Investment 1.3 – D.D. 1243 2/8/2022, PE0000005). This work was performed as part of the IAHS HELPING Working Group on “Hydrologic Design: Solutions and Communication".

References

Cappelli F., E. Volpi, A. Langousis, R. Deidda, A. Perdios, S. Grimaldi (2025). Rainfall simulation based on parsimonious calibration of a multifractal canonical disaggregation scheme in the Arno River basin, Italy. Journal of Hydrology: Regional Studies, 59: 102447, https://doi.org/10.1016/j.ejrh.2025.102447

Langousis, A., D. Veneziano, P. Furcolo, C. Lepore (2009). Multifractal rainfall extremes: Theoretical analysis and practical estimation, Chaos, Solitons and Fractals, 39 (3): 1182-1194, doi: 10.1016/j.chaos.2007.06.004

Volpi, E., S. Grimaldi, et al. (2024). The legacy of STAHY: Milestones, achievements, challenges, and open problems in statistical hydrology, Hydrological Sciences Journal, https://doi.org/10.1080/02626667.2024.2385686

Urban flood management considering a Bayesian approach to analyse extreme rainfall events

C. Iliadis[1,2*], P. Galiatsatou[3,4], J.P. De La Fuente Cusicanqui[1], L. Vasiliades[5], V. Glenis[1,2], C. G. Kilsby[1]
[1] School of Engineering, Newcastle University, Newcastle Upon Tyne, NE1 7RU, UK
[2] Willis Research Network, 51 Lime St., London, EC3M 7DQ, UK
[3] Hydraulics Laboratory, School of Civil Engineering, Aristotle University of Thessaloniki (AUTh), 54124 Thessaloniki, Greece
[4] Executive Division of Strategic Planning, Hydraulic Works & Development, Thessaloniki Water Supply and Sewerage Company S.A. (EYATH S.A.), 54622 Thessaloniki, Greece
[5] Laboratory of Hydrology and Aquatic Systems Analysis, Department of Civil Engineering, School of Engineering, University of Thessaly, 38334 Volos, Greece
* e-mail: chris.iliadis@newcastle.ac.uk

Introduction

Urban floods, being among the most widely distributed natural hazards, refer to the inundation of a densely populated area due to excess rainfall of a continuous and impervious stretch of land, and are accountable for loss of human lives, damage to infrastructure, and economic losses. These floods mostly arise due to an inadequate capacity of the drainage system and reduced infiltration rate in urban areas. Climate change and urbanisation are expected to increase urban flood risk, contributing to different components of the flooding system (Iliadis et al. 2023).

Intensity-Duration-Frequency (IDF) curves are usually constructed based on annual maximum rainfall intensities and depths for time periods of 5min, 10min, 15min, 30m, 1h, 2h, 6h, 12h and 24h. For sites lacking in long series of such short-duration rainfall measurements, the resulting IDF curves can lead to an unreliable assessment of the related flooding hazard. This research develops a methodology based on a Bayesian approach to estimate extreme rainfall events (Galiatsatou et al. 2008), to assess IDF curves. The inference is performed within a Bayesian framework, offering significant advantages especially in terms of inherent uncertainty in the model parameter estimation process.

Materials and methods

The study area of this research is the historic centre of Thessaloniki city in Greece. Short-duration annual maximum rainfall intensities and depths at Mikra station (in the eastern part of the city), made available from the National Meteorological Service (NMS) of Greece, cover two quite short and non-successive periods of 25 years (1963-1987) and 16 years (2007-2022). Available datasets also include daily rainfall at Parko AUTh station (in the city centre) for a long period of 64 years (1958-2021), obtained from the database of the School of Geology, AUTh. A Bayesian approach is applied in this work (Galiatsatou et al. 2008) to annual maximum rainfall data at Mikra station, using the most recent dataset to construct informative priors for the different rainfall durations. The daily rainfall series at the city centre is also analysed using Extreme Value Theory (EVT) to predict rainfall return levels associated with defined return periods and is then subjected to a simple scaling approach (Iliadis et al. 2023; Galiatsatou and Iliadis 2022) to assess IDF curves at the city centre.

Storm events corresponding to defined return periods and storm durations are then constructed and used as input to a high-resolution hydrodynamic model to assess and finally manage the flooding hazard. The City Catchment Analysis Tool – CityCAT (Glenis et al. 2018), developed at Newcastle University, is a unique hydrodynamic model, able to simulate fully coupled surface and pipe network flows, it can represent natural drainage systems and built-up areas, with explicit representation of buildings, and different types of Blue-Green Infrastructure (BGI) (Iliadis et al. 2024).

In this research, a novel '*source-receptor*' flood analysis (Iliadis et al. 2024) is applied to identify areas at

high flood risk of the study area that contribute the most to flooding (sources), as well as buildings and locations at high flood risk (receptors). The '*source-receptor*' includes dividing the study area into approximately equal cells and classifying buildings by type. The CityCAT model simulates flood depths for different storm scenarios, followed by a max capture assessment by removing rainfall from individual cells. Flood damages are calculated, and interventions (BGI) are introduced into intervention cells. A cost-benefit analysis compares baseline and intervention scenarios to determine the most effective flood mitigation strategies for the study area.

Results and concluding remarks

Figure 1 illustrates the modelled flood depths and flow captured by inlets in a zoomed-in area of the city centre of Thessaloniki under two storm scenarios generated using the proposed Bayesian approach. The simulations, conducted for a 50-year return period storm with durations of (a) 60 min and (b) 120 min, depict water depth (in blue) and flow through storm inlets (in red) over the urban layout. Higher water depths, exceeding 0.50 m in some locations, are observed in low-lying areas and along major road networks, indicating inadequate drainage capacity. Comparing both scenarios, the extended storm duration (b) results in increased water accumulation and more extensive inundation, particularly in areas 9, 11, 12, and 18. The catchment division highlights these key areas for further analysis, supporting the identification of targeted adaptation solution to improve flood resilience in dense urban areas.



Figure 1. Example of flood depth and flow captured by the synthetic inlets drains for two different storm events in the city centre of Thessaloniki: a) a 50-year storm with 60min duration; b) a 50-year storm with 120min duration.

Acknowledgments: This work has been funded by DAFNI (Data & Analytics Facility for Nation Infrastructure), I4C (Impetus 4 Climate) and the Willis Research Network.

References

Iliadis C., Galiatsatou P., Glennis V., Prinos P., Kilsby C. (2023) Urban flood modelling under extreme rainfall conditions for building-level flood exposure analysis. Hydrology, 10(8), 172. https://doi.org/10.3390/hydrology10080172

Iliadis C., Glenis V., Kilsby C. (2024). A cost-benefit 'source-receptor' framework for implementation of Blue-Green flood risk management. Journal of Hydrology, 634, 131113. https://doi.org/10.1016/j.jhydrol.2024.131113

Galiatsatou, P., Prinos, P., Sanchez-Arcilla, A. (2008). Estimation of extremes: conventional versus Bayesian techniques. Journal of Hydraulic Research, 46(S2), 211-223. https://doi.org/10.1080/00221686.2008.9521955

Galiatsatou, P., Iliadis, C. (2022). Intensity-duration-frequency curves at ungauged sites in a changing climate for sustainable stormwater networks. Sustainability, 14(3), 1229. https://doi.org/10.3390/su14031229

Glenis, V., Kutija, V., Kilsby, C. (2018). A fully hydrodynamic urban flood modelling system representing buildings, green space and interventions. Environmental Modelling and Software, 109, 272-292. https://doi.org/10.1016/j.envsoft.2018.07.018

Multi-objective algorithms to improve urban flood resilience

C. Iliadis[1,2*], J. Mckenna[1], V. Glenis[1,2]
[1] School of Engineering, Newcastle University, Newcastle Upon Tyne, NE1 7RU, UK
[2] Willis Research Network, 51 Lime St., London, EC3M 7DQ, UK
* e-mail: chris.iliadis@newcastle.ac.uk

Introduction

Storm events are becoming increasingly frequent and intense due to the impacts of climate change, significantly amplifying urban flooding risks globally. This issue is further exacerbated by the proliferation of impervious surfaces, inadequate drainage systems, and urban expansion, all of which disrupt the natural hydrological cycle and heighten flood vulnerability (Sörensen & Emilsson, 2019). Addressing these challenges requires advanced flood management approaches, integrating hydrodynamic modelling and multi-objective optimisation to predict, mitigate, and manage stormwater impacts effectively. Hydrodynamic models, such as CityCAT (Glenis et al., 2018), when coupled with optimisation techniques, such as evolutionary algorithms, provide robust tools for the design and spatial optimisation of Blue-Green-Grey Infrastructure (BGGI) interventions. This study presents a comparative analysis of multiple Genetic Algorithms for the purpose of automating the optioneering of the placement of BGGI within the context of nature-based flood risk management.

Materials and methods

The city centre of Newcastle upon Tyne, UK, (Figure 1a) is highly susceptible to flooding, particularly during extreme storm events, such as the locally infamous '*Toon Monsoon*' on June 28, 2012. Its unique mix of historic and commercial buildings, combined with significant green spaces like the Town Moor and Leazes Park, makes it an ideal case study for urban flood risk research. Recent advancements, such as a framework by Iliadis et al. 2024, enable systematic identification of high-risk areas by dividing catchments into equal cells and selectively assessing their flood contributions under varying storm intensities. This approach is further enhanced by integrating multi-objective optimisation tools to automate the selection of optimal locations for BGGIs interventions.

The presented research utilises CityCAT, an advanced hydrodynamic flood modelling tool capable of simulating surface and sub-surface flows while explicitly accounting for detailed urban features, including buildings, drainage systems, and BGGIs. Through coupling of the high-resolution data produced by CityCAT, with a novel exposure analysis tool developed by Bertsch et al. 2022, the proposed optimisation tool is capable of performing the accurate property scale flood vulnerability and hazard analyses required to optimise the placement of BGGI. This integration enables robust, data-driven planning for urban flood resilience via explicit modelling of BGGI features.

The proposed optimisation tool optimises the placement of BGGI with respect to the bi-objective minimisation of the cost of implementation and a chosen flood risk metric (either the expected cost of damages or the number of buildings at high risk of flooding). By leveraging the high-resolution outputs produced by CityCAT coupled with an efficient evolutionary algorithm, specifically designed to maximise solution quality with respect to the number of hydrodynamic simulations required, the tool enables an efficient exploration of potential solutions. Specifically, the proposed evolutionary algorithm utilises ε-dominance concepts, seeding of the initial archive population using domain-specific knowledge, adaptive population sizing, population preconditioning, and a self-termination criterion to promote rapid convergence to optimal solutions in a computationally efficient and automated manner, requiring minimal parameter calibration. Together, CityCAT's hydrodynamic modelling capabilities, the exposure calculator and evolutionary optimisation strategy enable a systematic approach to reducing urban flood risk through optimally placed interventions.

Results and concluding remarks

The proposed evolutionary search strategy is first validated using a test case derived from the exhaustive search of a tractable search space. The NSGA-II (Deb et al. 2000) and SPEA 2 (Zitzler et al. 2001) evolutionary algorithms, representing popular second-generation evolutionary algorithms, are used to benchmark the performance of the proposed algorithm. A second, more realistic, test case is then presented which considers the installation of permeable paving and detention basins across the catchment, as shown in Figure 1a. As this search space is intractable, inter-algorithm comparisons are used as the basis for analysis.

Through use of performance indicators, it is shown that the proposed algorithm provides a superior convergence rate and spread of solutions with respect to the benchmark second generation evolutionary algorithms. The comparative quality of the approximation of the set of optimal solutions produced by the respective algorithms is showcased in Figure 1b. Within Figure 1b, which shows the respective fronts for the three algorithms following termination after ~3000 hydrodynamic simulations for test case II, it can be seen that, in the most extreme cases, the solutions found by the proposed algorithm (referred to as ε-MOEA (Laumanns eta al. 2002)) offer the same expected cost of damages at a cost of ~£20m less with respect to the benchmark algorithms.

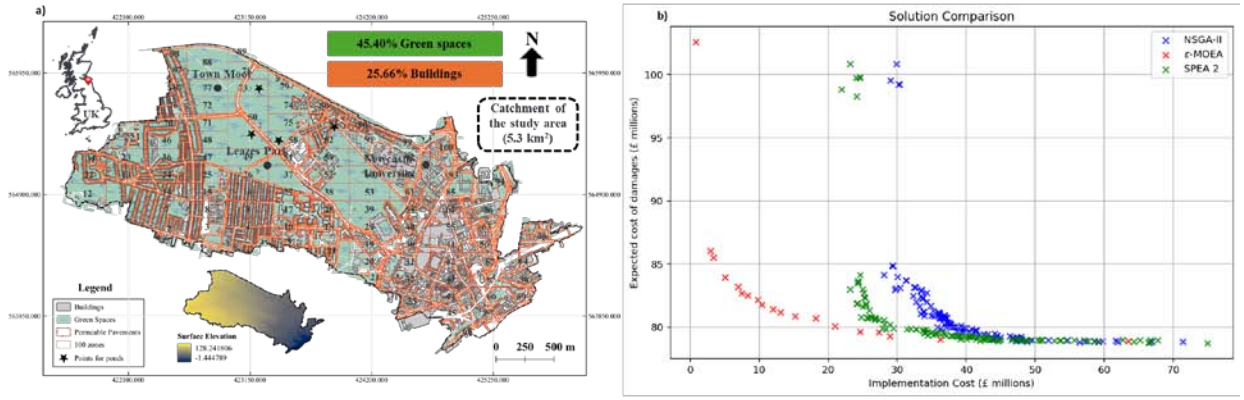


Figure 1. a) Overview of the study area in Newcastle Upon Tyne, UK; b) Comparison between the solutions produced by three evolutionary algorithms for a validation test case.

Acknowledgments: This work has been funded by DAFNI (Data & Analytics Facility for Nation Infrastructure), I4C (Impetus 4 Climate) and the Willis Research Network.

References

Bertsch R., Glenis V., Kilsby C. (2022). Building level flood exposure analysis using a hydrodynamic model. Environmental Modelling & Software, 156, 105490. doi: 10.1016/j.envsoft.2022.105490

Deb K., Agrawal S., Pratab A., Meyarivan T. (2000). A fast elitist non-dominated sorting genetic algorithm for multi-objective optimization: NSGA-II, in: M. e. a. Schoenauer (Ed.), Proceedings of the Parallel Problem Solving from Nature VI Conference, Springer, pp. 849–858.

Glenis, V., Kutija, V., Kilsby, C. (2018). A fully hydrodynamic urban flood modelling system representing buildings, green space and interventions. Environmental Modelling and Software, 109, 272-292. doi: 10.1016/j.envsoft.2018.07.018

Iliadis C., Glenis V., Kilsby C. (2024). A cost-benefit 'source-receptor' framework for implementation of Blue-Green flood risk management. Journal of Hydrology, 634, 131113. doi: 10.1016/j.jhydrol.2024.131113

Laumanns M., Thiele L., Deb K., Zitzler E. (2002). Combining Convergence and Diversity in Evolutionary Multiobjective Optimization, Evolutionary Computation, 10(3), 263–282. doi: 10.1162/106365602760234108

Sörensen, J., Emilsson, T. (2019). Evaluating Flood Risk Reduction by Urban Blue-Green Infrastructure Using Insurance Data. Journal of Water Resources Planning and Management, 145(2), 04018099. doi: 10.1061/(ASCE)WR.1943-5452.0001037

Zitzler E., Laumanns M., Thiele L. (2001), SPEA2: Improving the strength pareto evolutionary algorithm for multiobjective optimization, in: K. C. Giannakoglou, D. T. Tsahalis, J. Périaux, K. D. Papailiou, T. C. Fogarty (Eds.), Evolutionary Methods for Design Optimization and Control with Applications to Industrial Problems, International Center for Numerical Methods in Engineering (CMINE), Athens, Greece, pp. 95–100.

Unravelling the paradox of a flash flood event in northern Greece

S.P. Stefanidis[1*], N.D. Proutsos[2], P.S. Stefanidis[3], D. Tigkas[4], I. Tsevreni[5]
[1] Forest Research Institute, Hellenic Agricultural Organization -DIMITRA, Thessaloniki, Greece
[2] Institute of Mediterranean Forest Ecosystems,Hellenic Agricultural Organization -DIMITRA, Athens, Greece
[3] School of Forestry & Natural Environment, Aristotle University of Thessaloniki, Greece
[4] Centre for the Assessment of Natural Hazards and Proactive Planning & Lab. of Reclamation Works and Water Resources Management, School of Rural and Surveying Engineering, National Technical University of Athens, Greece
[5] Department of Early Childhood Education, University of Thessaly, Volos, Greece
* e-mail: sstefanidis@elgo.gr

Introduction

Flash floods occur within a few minutes or hours of intense rainfall when the volume of water exceeds the ground's ability to absorb it. These sudden events are among the most widespread and destructive natural disasters with devastating effects on local communities and infrastructure (Ali et al. 2017). In the context of climate change, such extreme weather events are becoming more frequent and severe. Coupled with increased urbanization and population growth, more people and assets are now exposed to the risks of flash floods, escalating the challenges of flood management and mitigation (Stefanidis et al. 2022). In Mediterranean countries, as Greece, the occurrence of flash floods has increased during the last decades, raising concerns about the adequacy of current forecasting and mitigation strategies (Giannaros et al. 2022).

On June 21, 2020, a flash flood hit the city of Serres, Northern Greece damaging more than 100 houses. The fact that there was no rainfall reported at the meteorological station close to the city made this event exceptional. Instead, a sudden downpour in the nearby mountainous region channeled large volumes of water and sediment into the city (https://www.youtube.com/watch?v=JIXXp87To-w), through local torrents, showing that flash floods are unpredictable and life-threatening events, particularly in areas with complex relief. The present study investigates the unusual flash flood event, focusing on the meteorological factors that contributed to the disaster. By analyzing the prevailing rainfall conditions, this research provides insights into the challenges of operational flood nowcasting.

Materials and methods

The main watercourse passing through the city of Serres (Northern Greece) is the Agion Anargiron torrent which has historically led to frequent flooding in the area. Its watersheds cover an area of 77 Km^2 (Figure 1), with mean watershed and mainstream slopes 39.5 % and 5%, respectively (Sapountzis 2011). Moreover, due to the intense torrential environment of the watershed numerous technical and agrotechnical works implemented in the watershed mitigate the effects of torrential flow.

To investigate the cause and mechanism of the flood event of 21 June 2020, we conducted a field visit to the study area the day after the event to track the pathways of floodwaters through the urban area. Additionally meteorological data from ground stations in the winder area were analyzed. One station near the city center at the racing circuit (32 m a.s.l, $41^0$09'54'' N, $23^0$33'21 E) is operated by National Observatory of Athens (NOA), while another, located approximately 11 km away in the mountainous area of Chrysopigi (605 m a.s.l., $41^0$09'54'' N, $23^0$33'21 E) is operated by the Forest Research Institute of Thessaloniki (FRI).

Results and concluding remarks

The flood event was driven by an intense, short-duration (2 hours) rainfall in the mountainous region on 21 June 2020. Data from the Chrysopigi station showed high-intensity precipitation, with 22.2 mm/h recorded at 15:00 and 24 mm/h at 16:00. This is a significant amount, especially considering that no rainfall was recorded at the lowland station, highlighting the high spatial variability typical in complex,

mountainous topography. This variability emphasizes the necessity for establishing a dense network of meteorological stations to cover both plain and mountainous areas, enhancing the ability to monitor and predict such localized events. The meteorological stations network could be used to promote environmental awareness through environmental, science, and citizen science education activities. Furthermore, human activities within plain stream beds such as cafes, recreational facilities, and leisure parks, aggravate flood impacts. Our visits to the area confirmed that the interventions led to the narrowing of the stream beds exacerbating the risk of flooding.

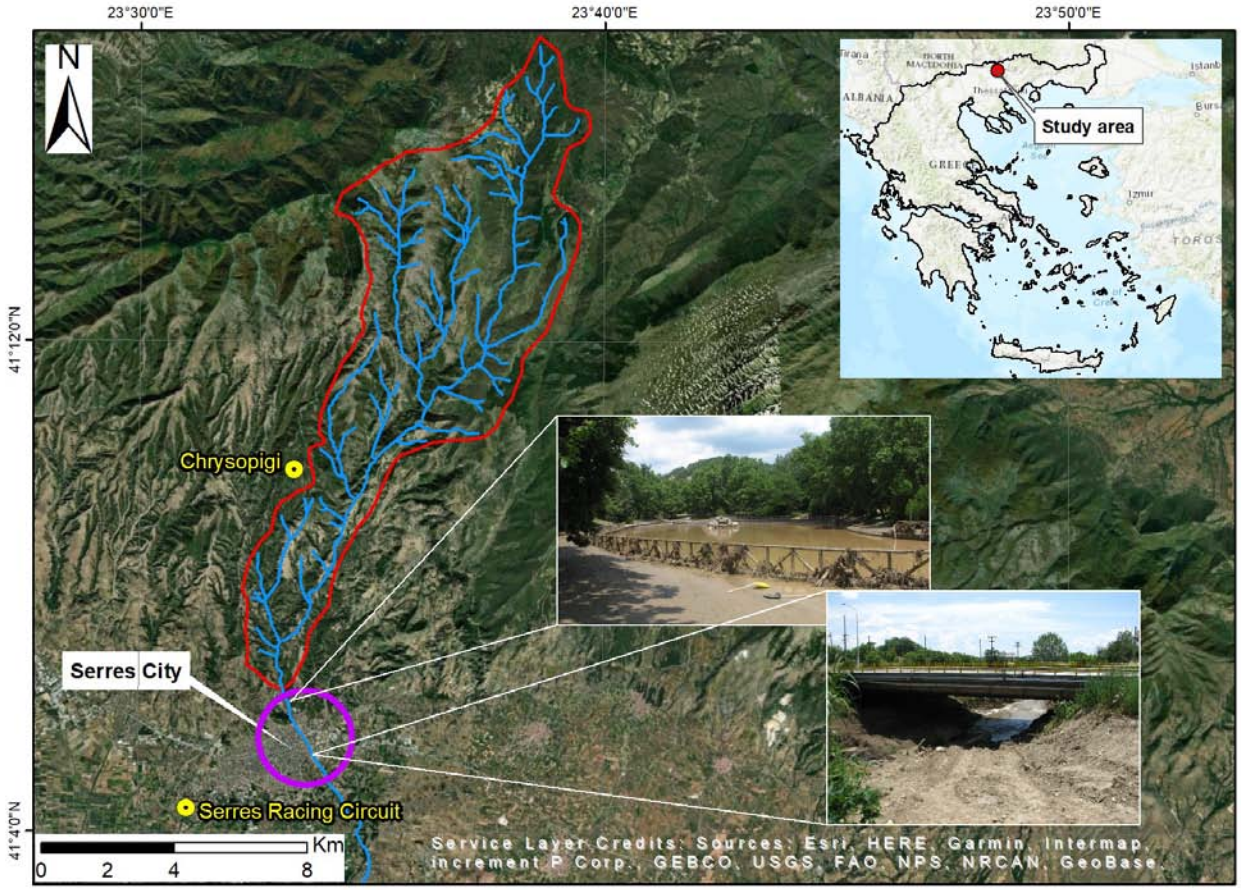


Figure 1. The study area, showing the watershed boundaries (red polygon), hydrographic network (blue lines), location of the meteorological stations (yellow dot), and areas where damages have been recorded (purple circle).

It is important to note that rainfall intensities exceeding 20 mm/h can trigger floods, even in regulated watersheds. This is particularly important for small watersheds, as their steep slopes and short concentration times make them more susceptible to rapid water accumulation and increased specific discharge ($m^3/sec/km^2$).

Acknowledgments: This work is supported by the project "Research on Forest Hydrology Parameters in Mountainous Watersheds of Greece" funded by the OMIKRON S.A. The authors are grateful to the National Observatory of Athens and the Forest Research Institute, for providing the meteorological data.

References

Ali K, Barataria RM, Raut N (2017) Advances and challenges in flash flood risk assessment: A review. Journal of Geography & Natural Disasters 7(2): 1-6. http://dx.doi.org/10.4172/2167-0587.1000195

Giannaros C, Dafis S, Stefanidis S, Giannaros TM, Koletsis I, Oikonomou C (2022) Hydrometeorological analysis of a flash flood event in an ungauged Mediterranean watershed under an operational forecasting and monitoring context. Meteorological Applications 29(4): e2079. https://doi.org/10.1002/met.2079

Sapountzis M (2011) The torrent potential of the area of Sidirokastro and of Serres in Northern Greece and the effectiveness of the torrent control systems. Wildbach-und Lawinenverbau 170: 293-299.

Stefanidis S, Alexandridis V, Theodoridou T (2022) Flood exposure of residential areas and infrastructure in Greece. Hydrology 9(8): 145. https://doi.org/10.3390/hydrology9080145

The PRIME Index: Prioritization of cultivated Regions IMpacted by drought in agriculturE

L. Cappellato[1*], B. Moccia[1], E. Ridolfi[1], D.D. Chiarelli[2], F. Russo[1], F. Napolitano[1], M. C. Rulli[2]
[1] Department of Civil, Building, and Environmental Engineering, Sapienza Università di Roma, Rome, Italy
[2] Department of Civil and Environmental Engineering, Politecnico di Milano, Milan, Italy
* e-mail: lorenza.cappellato@uniroma1.it

Introduction

Drought is one of the major challenges for Italian agriculture, with significant repercussions on food production, the economy, and water security (Liu et al. 2025). As part of the Mediterranean Basin, Italy is particularly vulnerable to climate change, experiencing rising average temperatures and decreasing precipitation levels (Leijnse et al. 2024). Within the framework of the CASTLE project, aimed at identifying areas where small reservoirs for irrigation are essential for sustaining the agricultural sector, this research focuses on targeting Italy's most drought-affected agricultural regions to mitigate economic losses and crop failures.

The key innovation of this study lies in the development of the "PRIME index," an integrated assessment tool combining climatic and agricultural data. This index classifies the Italian territory into ten priority intervention classes, providing policymakers with a scientifically robust yet operationally simple instrument to guide mitigation actions both in the present and the future. Unlike conventional drought assessments that primarily focus on analysing drought events and their impacts, the "PRIME index" serves as a practical decision-making tool designed for ease of use and direct application, thereby enabling strategic water storage solutions to support agriculture under prolonged drought conditions.

Materials and methods

This research integrates the Standardized Precipitation Evapotranspiration Index (SPEI) (Vicente-Serrano et al. 2010) at multiple time scales, computed between 1951 and 2024, with crop sowing and harvest dates to identify Italy's agricultural drought-exposed areas. The analysis of the 6-month SPEI, commonly used to assess agricultural drought, reveals a significant increase in the frequency, duration, and intensity of drought events, indicating progressively worsening drought-prone conditions.

To evaluate the impact of drought on the Italian agricultural sector, the study considers the sowing and harvesting months for each crop. Specifically, the SPEI magnitude at the time of harvest is assessed using a water deficit accumulation period (D), where D = precipitation – evapotranspiration, corresponding to the months between sowing and harvesting. This methodology, allows the identification of water shortages during critical growth stages, thereby determining the potential risk of yield loss (Liu et al. 2025).

For each crop, we initially determine the severe drought threshold exceedance frequency during the 74-year observation period. This analysis, combined with the percentage of cultivated area per grid cell and the economic value of the selected crops, leads to the development of the "PRIME Index," an innovative tool capable of ranking intervention priorities by considering both spatial extent and economic impact.

Once these results are obtained, the procedure is repeated using future climate projections up to 2100 (CMCC, 2025), considering both the most severe Shared Socioeconomic Pathway (SSP5-8.5) and the sustainability scenario (SSP1-2.6) (Riahi et al. 2017). This analysis provides insights into how climate change will affect Italian agriculture, contributing to an early warning system framework for risk assessment and mitigation planning.

Results and concluding remarks

The evaluation of the SPEI index highlights a rise in agricultural drought occurrence, while dually

revealing a marked expansion of drought-affected regions over the past two decades, highlighting not only the intensification and increased frequency of drought events but also a broader geographic impact. By accounting for both the agricultural area extent and crop economic value, the “PRIME index” allows the identification of the areas at the highest risk, underscoring the urgent need for tailored mitigation strategies to enhance the resilience of agriculture to climate change.

Given the ease of computation of the “PRIME Index” and the availability of climatic and agricultural datasets at the European level, future research will extend this analysis beyond national borders. Additionally, we aim to enhance the reliability of the index by incorporating annual crop-specific irrigation volumes, yearly crop yields, crop resilience to drought-induced shocks, drought event magnitude, and the strategic value of crops in terms of production importance. By refining and expanding this framework, we strive to provide a more comprehensive tool for policymakers and stakeholders, fostering proactive and data-driven adaptation strategies for a more sustainable agricultural future.

References

CMCC (2025) CMIP6 Stat Downscaled Over Italy. https://doi.org/https://doi.org/10.25424/cmcc-75s8-a308

Leijnse M, Bierkens M F P, Gommans K H M, Lin D, Tait A, Wanders N (2024) Key drivers and pressures of global water scarcity hotspots. Environmental Research Letters, 19(5). https://doi.org/10.1088/1748-9326/ad3c54

Liu Z, Lv A, Li T (2025) Intensified Drought Threatens Future Food Security in Major Food-Producing Countries. Atmosphere 16, 34. https://doi.org/10.3390/atmos16010034

Riahi K, Vuuren D, Kriegler E, Edmonds J, O’Neill B, Fujimori S, Bauer N, et al. (2017) The Shared Socioeconomic Pathways and their energy, land use, and greenhouse gas emissions implications: An overview. Global Environmental Change 42. https://doi.org/10.1016/j.gloenvcha.2016.05.009

Vicente-Serrano, S. M., Beguería, S., & López-Moreno, J. I. (2010) A multiscalar drought index sensitive to global warming: The standardized precipitation evapotranspiration index. Journal of Climate, 23(7), 1696–1718. https://doi.org/10.1175/2009JCLI2909.1

Evaluation of Survivability from Droughts Index (SDI) with EO-based indicators

M.C. Gunacti*, C.P. Cetinkaya
Dokuz Eylul University, Faculty of Engineering, Department of Civil Engineering, Izmir, Turkey
** e-mail: mert.gunacti@deu.edu.tr*

Introduction

Droughts are among the most severe natural hazards affecting water resources, agriculture, and socio-economic stability, particularly in semi-arid and arid regions (Willhite, Svoboda, and Hayes 2007). Drought monitoring and analyses developed by researchers have increased our understanding of droughts and resilience of the drought-stricken communities. Traditional drought indices primarily focus on meteorological and hydrological parameters; however, the newly developed Survivability from Droughts Index (SDI) provides an integrative perspective by assessing the ability of a system to endure and recover from drought events (Gunacti, 2024). This study aims to evaluate the applicability and robustness of the SDI by comparing it with the commonly used EO-based indicators such as the Normalized Difference Vegetation Index (NDVI), Normalized Difference Moisture Index (NDMI), and Land Use map of the related period (Horler and Ahern 1986; Mishra and Sarkar 2020). The study focuses on the Gediz River Basin located in the West of Turkey, an agriculture-intensive basin within the boundaries of the Mediterranean region where the impacts of anthropogenic influences and climate change experienced severely. By juxtaposing SDI and mentioned EO-based indicators, identifying drought-prone regions within the Gediz Basin is aimed, thereby informing targeted water resource management strategies.

Materials and methods

The SDI was calculated using a combination of environmental, social, and economic indicators, including drought risk, water availability, access to market ratio, and land-use characteristics, derived from historical records and conducted surveys spanning 1960–2023. The collected indicators feed into four main sub-indices of SDI, which are Perception, Adaptability, Vulnerability, and Recoverability according to the min-max normalization of inputs and point allocation weighting of indicators and sub-indices. Along with the quantitative data, several qualitative data have been collected through Value-Attitude-Perception (VAP) Surveys conducted with farmers and stakeholder engagement meetings.

The EO-based indicators, on the other hand, were computed based on the Sentinel-2A/2B satellite imagery of the European Space Agency (ESA). The land use map of the related period was acquired from the CORINE program data. The calculation of EO-based indicators was based on the following equations,

$$NDVI = (NIR-RED)/(NIR+RED) \quad (1)$$

$$NDMI = (NIR-SWIR)/(NIR+SWIR) \quad (2)$$

where, NIR is the Near Infra-Red band, RED is the red band, and SWIR is the Short Wavelength Infra-Red band. Spatial interpolation techniques were employed to map the SDI distributions across the basin, and the overlay of the indices was evaluated. High-resolution geospatial datasets and statistical tools were used to determine regions exhibiting significant similarities between SDI and EO-based indicators, highlighting areas where water resource planning is most critical.

Results and concluding remarks

Preliminary findings indicate a complementing relationship between SDI (Fig. 1a) and EO-based indicators across the basin. Where regions with high NDVI (Fig. 1b) and low NDMI (Fig. 1c) values, indicate agricultural lands (Fig. 1d) with water stress which is also highlighted by the SDI map. On the other hand,

areas with low NDVI and high NDMI, meaning areas with less intensive agriculture and higher moisture are marked as having higher SDI values. Notably, the NDVI and NDMI maps confirm the intensive agricultural activities and low moisture rates in the basin. In the central Gediz, areas subjected to low SDI and NDMI and high NDVI can be marked to focus on sustainable water management.

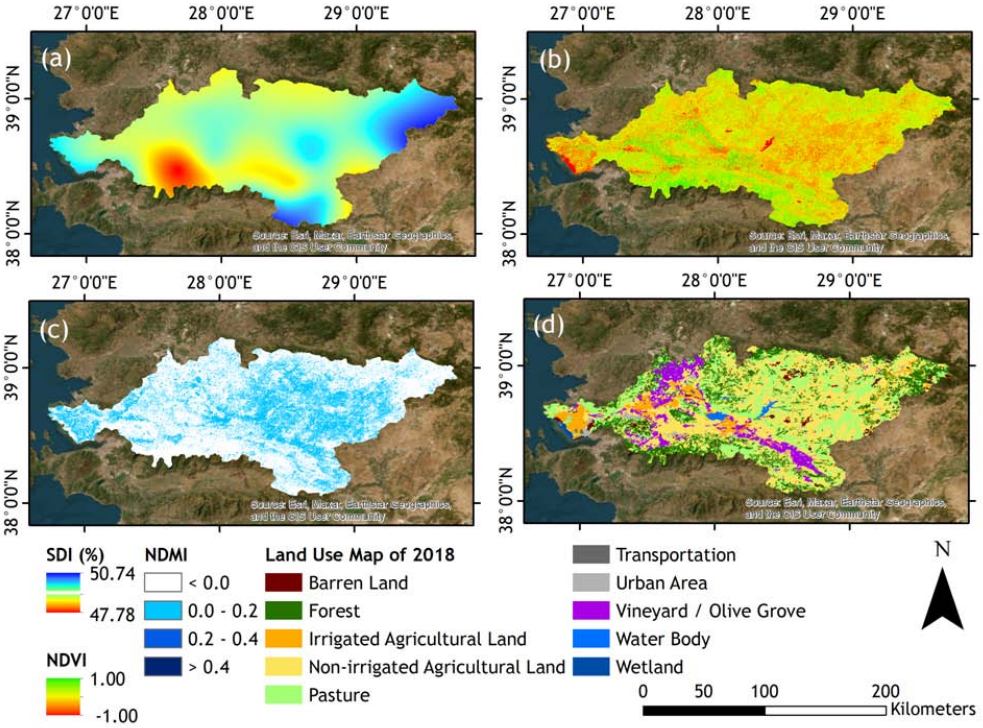


Figure 1. (a) SDI, (b) NDVI, (c) NDMI, and (d) LU maps of Gediz River Basin.

The presented study highlights the importance of qualitative data including drought index, SDI, and its compatibility with other EO-based indicators. Although the SDI examines a broad variety of indicators established by the stakeholders, its overlay with even more indicators helps locate drought-prone areas in a more precise manner. The results of the study present a tool for the stakeholders and decision-makers of the hydrological systems to increase their survivability from droughts.

Acknowledgments: This study has been supported by the UNIMED Project (Project No:122N412), which is funded by the Bilateral Cooperation Program of TUBITAK and Xjenza Malta, and PRIMA Foundation. The authors also thank IRMCo Ltd. of Malta, Dirk de Ketelaere, and Anna Spiteri for their valuable contributions to the presented study.

References

Gunacti MC (2024) Assessment of a survivability index for drought management in river basins. (Doctoral thesis, Dokuz Eylul University). Turkey.

Horler DNH, Ahern FJ (1986) Forestry information content of thematic mapper data. International Journal of Remote Sensing, 7(3), 405 – 428. https://doi.org/10.1080/01431168608954695

Mishra M, Sarkar T (2020) A multistage hybrid model for landslide risk mapping: tested in and around mussoorie in uttarakhand state of india. Environmental Earth Sciences 79(19):1–24. https://doi.org/10.1007/s12665-020-09180-3

Wilhite DA, Svoboda MD, Hayes MJ (2007) Understanding the complex impacts of drought: A key to enhancing drought mitigation and preparedness. Water Resources Management, 21, 763–774. https://doi.org/10.1007/s11269-006-9076-5

Assessment of drought by precipitation variability in Mediterranean coastal countries using entropy-based analysis

F. Barbaros[1*], D. De Ketelaere[2], F. Vargun[3], M.C. Gunacti[1], C.P. Cetinkaya[1]
[1] Dokuz Eylül University, Faculty of Engineering, Department of Civil Engineering, Izmir, Turkey
[2] Integrated Resources Management Company Ltd. Senglea, Malta
[3] Dokuz Eylül University, The Graduate School of Natural and Applied Sciences, Izmir, Turkey
* e-mail: filiz.barbaros@deu.edu.tr

Introduction

The Mediterranean region is susceptible to climate change as intensive as worldwide, experiencing increasing drought frequencies and intensities (Singh 2013). The analysis of long-term hydro-meteorological data is crucial for water resources management and studies on the impacts of climate change. Understanding the probabilistic nature of drought occurrences is also essential for sustainable water resources management. Utilizing historical rainfall data of multiple locations, the research applied entropy methods to quantify uncertainty and detect trends in precipitation patterns.

This study employs entropy-based statistical methods to analyze rainfall data of coastal Mediterranean countries (Shannon 1948), aiming to assess drought by precipitation variability and forecast potential trends, evaluating percent changes in rainfall by assessing long-term historical data to manage future basin management strategies. Maps were generated to visualize the spatial distribution of rainfall uncertainty across the Mediterranean basin, including information on percentage changes in rainfall from 1960 to 2020. These maps serve as a critical tool for understanding drought-prone areas and their future potential development with the information they include. Furthermore, entropy maps visually represent rainfall uncertainty, enhancing the interpretability of results and identifying critical drought-prone regions (Singh 2024).

Materials and methods

Historical monthly rainfall data from 29 stations across Mediterranean coastal countries (Algeria, Cyprus, France, Greece, Italy, Lebanon, Malta, Spain, Tunisia and Turkey) were collected and divided into two periods covering 30 years each, i.e. 1960-1990 and 1990-2020. Then data was processed to determine percent changes in rainfall for the two specified periods. Following on this, the rainfall data has been analyzed using entropy-based method to assess the drought by precipitation variabilities. Entropy-based variability was quantified using the Intensity Disorder Index (IDI), which is determined by subtracting the entropy (H) of a given time series from the maximum possible entropy (maxH) based on the occurrence frequencies, as given in Eq. 1 (Barbaros 2022). A higher IDI value signifies the greater variability.

$$\text{IDI} = (\max H) - H \quad (1)$$

When a variable has a uniform distribution, its Shannon entropy reaches its maximum value (Mishra et al. 2009).

Results and concluding remarks

Percentage change values in rainfall between the two periods were calculated. The obtained results are given in Figure 1 (top) showing decreasing and increasing changes. Here, the regions with high decreasing changes were identified as regions more susceptible to drought and marked as larger circles. When the percentage changes in the overall Mediterranean are examined, in the east, only at the Aegean part of Turkey and in the west, higher decreasing change at the west of the Mediterranean are observed. The highest change was observed at Menemen station, followed by Spain with 1 station and Algeria with 4 stations. In particular, the study focuses on examining the correlation between locations with high negative changes in precipitation percentage and locations with high rainfall variability.

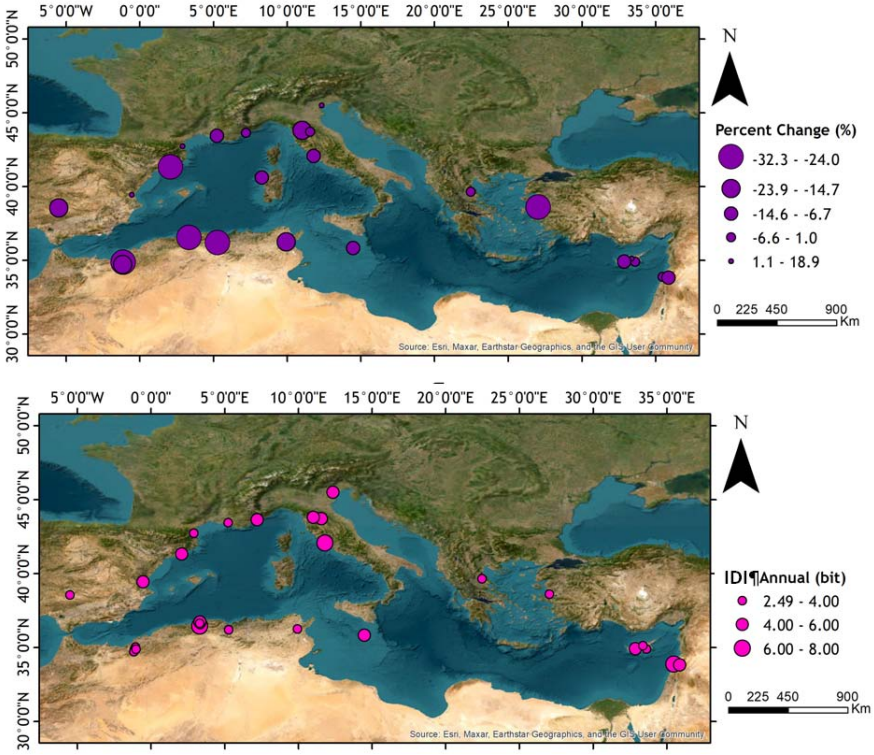


Figure 1. Percent changes in rainfall (top) and calculated IDI values for the annual period (bottom) in across the Mediterranean.

The entropy analysis revealed heterogeneous rainfall patterns, with certain regions exhibiting significantly higher variability. Analysis has been carried out for annual and seasonal periods. The entropy-based maps, obtained from calculations made with annual and seasonal data, were generated, and the annual IDI values are presented in Figure 1 (bottom). IDI values were found to have the highest values in the 4 stations of Italy and in Algeria, Lebanon, and Cyprus. The locations which merit a primary focus and are to be evaluated first in terms of drought planning efforts are the locations with the highest decreasing percentage changes and highest IDI values, which correspond to areas with high negative trends of precipitation and high uncertainty of drought risk.

Entropy-based forecasting suggests a continued decline in precipitation levels, with increasing risks of prolonged drought events. The entropy maps clearly illustrate regions where rainfall patterns are becoming more unpredictable, aiding in identifying high-risk drought zones. These maps serve as an essential tool in visually communicating climate risks and assisting in policy planning. Additionally, cross-comparison with historical drought records further validates the predictive capacity of entropy-based assessments.

Acknowledgments: This study has been supported by the UNIMED Project (Project No:122N412), which is funded by the Bilateral Cooperation Program of TUBITAK and Xjenza Malta, and PRIMA Foundation. The authors also thank Anna Spiteri from IRMCo Ltd. of Malta for her valuable contributions to the presented study.

References

Barbaros F (2022) Batı Karadeniz Havzası yağış değişkenliklerinin entropi tabanlı bir yaklaşımla değerlendirilmesi. Gümüşhane Üniversitesi Fen Bilimleri Dergisi, 12(1), 344-356. https://doi.org/10.17714/gumusfenbil.995514

Shannon CE (1948) A mathematical theory of communication. The Bell System Technical Journal, 27, 379-423.

Singh VP (2013) Entropy theory and its applications in environmental and water engineering. John Wiley & Sons.

Singh VP (2024) Entropy Theory of Hydrologic Systems, Journal of Hydrologic Engineering, 29(6), 04024039-1-15, ASCE. https://doi.org/10.1061/JHYEFF.HEENG-6259

Mishra AK, Özger M, Singh VP (2009) An entropy-based investigation into the variability of precipitation. Journal of Hydrology, 370(1–4):139-154. https://doi.org/10.1016/j.jhydrol.2009.03.006

Advancing the detection of multi-sector drought impacts via feature extraction and multi-task learning

M. Merlo*, M. Giuliani, A. Castelletti
Dept. Electronics, Information, and Bioengineering, Politecnico di Milano, Milano, Italy
** e-mail: martina.merlo@polimi.it*

Introduction

Drought indices are essential tools for quantifying drought conditions by integrating multiple variables into a single measure that represents its characteristics, such as intensity, duration, and severity (Mishra et al. 2010). These indices play a key role in real-time monitoring, forecasting, and supporting risk management actions (Zargar et al. 2011). However, traditional statistical indices often fail to account for the complex interactions between drought precursors and their socio-economic and environmental impacts. Moreover, given the absence of a universally accepted drought definition, no single index is applicable to all drought types, climate conditions, or affected sectors (Svoboda et al. 2016).

In this study, we aim to improve traditional drought detection by defining new impact-based combined drought indices through Machine Learning algorithms. These indices are designed to better link the observed impacts of extreme droughts across different sectors with their potential drivers, including climatic, meteorological, and hydrological variables, analyzed across multiple spatial and temporal scales. The methodology is applied to the case study of the Adda River basin, focusing on the multisectoral impacts of drought on agricultural production, hydroelectric generation, and recreational and ecosystem services.

Materials and methods

The definition of impact-based drought indices relies on the FRamework for Index-based Drought Analysis (FRIDA; Zaniolo et al. 2018), which is structured in three main steps:

- Identification of basin characteristics
- Feature extraction
- Drought index modelling

The initial step involved selecting a target variable (a representative proxy for drought impacts within the basin) and gathering potential predictor variables. The predictor dataset comprises candidate features to replicate the target variable, including observed hydro-meteorological variables across various spatial and temporal scales (e.g. water levels, snow depth, temperature). Regarding the target variables, 3 variables are used as proxy of drought impacts across 3 different sectors: the deficit between the lake release and the maximum water allocated to the run-of-the-river hydropower plants for the hydropower sector; the water lake level deficit for the recreational sector; the Fraction of Absorbed Photosynthetically active radiation ANomaly (FAPAN) index for the agricultural sector. All the data are resampled to 1-month temporal resolution and the length of the time series is equal to 216 samples (monthly values between 2001 and 2018).

The second step focused on selecting relevant subsets of variables that best explained the target variable. This was achieved using an advanced feature extraction algorithm, specifically the Wrapper for Quasi-Equally Informative Subset Selection (W-QEISS; Karakaya et al. 2015). A multi-objective evolutionary algorithm was employed to recursively explore the input space of candidate predictors and identify Pareto-efficient subsets based on four objectives: (i) accuracy, (ii) cardinality, (iii) relevance, and (iv) redundancy. A regression model was used to compute the predictive accuracy of each subset, with the iterative process continuing until the termination criterion (number of iterations) was met. Low-accuracy solutions were discarded, resulting in a set of quasi-equally accurate subsets from the W-QEISS algorithm.

After selecting the preferred efficient solution within the set of quasi-equally accurate subsets, an appropriate model is fitted to the sample of selected inputs and target variable. Two classes of models

were explored: linear models and Artificial Neural Networks (ANNs). For the ANNs, hyperparameters were tuned via trial and error for determining the best architecture in terms of number of nodes and layers: in the case of hydropower and recreation sectors, we used a 3-layers network with five nodes in each layer; conversely, for the agricultural sector, we preferred a single-layer architecture with 30 nodes.

Results and concluding remarks

Our findings indicate that FRIDA has produced indices that accurately capture the drought impacts. Indeed, as shown by Table 1, when considering ANN as model structure, the Pearson correlation coefficient (PCC) between observations and model's outputs remains consistently above 0.6, with values reaching 0.97 and 0.99 for the hydropower and recreation sectors, respectively.

Table 7. Performance in cross-validation of the FRIDA indices with alternative model structures across the three considered sectors.

	HYDROPOWER		RECREATION		AGRICULTURE	
Model	**PCC**	**R^2**	**PCC**	**R^2**	**PCC**	**R^2**
Linear	0.88	0.77	0.53	0.28	0.25	0.04
ANN	0.97	0.95	0.95	0.90	0.59	0.15

Additionally, it is noteworthy that the inputs selected by the algorithm vary depending on the sector being considered, shedding light on sector-specific connections between drivers and impacts. For instance, the selected variables for the agricultural sector are the following: $inflow_3$ (inflow to the lake aggregated over 3 months), $prec_3$-up (precipitation in the upstream area, aggregated over 3 months), $temp_1$-down (monthly mean temperature in the downstream area) and snow $depth_1$-down (monthly mean snow depth in the downstream area). The first two variables are likely capturing the water availability for irrigation, while the temperature and snow information in the downstream area are directly influencing crop growth processes. It is important to highlight that in this case the final performance of the FRIDA index is much lower than for the two other sectors. This anomaly can be explained by the considered impact variable, i.e. the FAPAN index derived from satellite information, which is less connected with the available candidate predictors.

Ongoing experiments are investigating the potential for further improving our results by adopting a multi-task model for better handling the interdependencies across the impacted sectors with respect single-task models that identify individual indices independently for the different sectors.

Acknowledgments: This study was carried out within the RETURN Extended Partnership and received funding from the European Union Next-GenerationEU (National Recovery and Resilience Plan – NRRP, Mission 4, Component 2, Investment 1.3 – D.D. 1243 2/8/2022, PE0000005). This research was also partially supported by the EU-funded Climate Intelligence (CLINT) project (grant agreement ID: 101003876) and the SAHARA project (ID: P20227NPLW) funded by PNRR MUR – M4C2 – Investimento 1.1 – Fondo per il Programma Nazionale della Ricerca (PNR) e Progetti di Ricerca di Rilevante Interesse Nazionale (PRIN).

References

Karakaya, Galelli, Ahipaşaoğlu, Taormina (2015) Identifying (quasi) equally informative subsets in feature selection problems for classification: a max-relevance min-redundancy approach. IEEE transactions on cybernetics, 46(6), 1424-1437.

Mishra, Singh (2010) A review of drought concepts. Journal of hydrology, 391 (1-2):202–216.

Svoboda, Fuchs (2016) Handbook of drought indicators and indices (Vol. 2). Geneva, Switzerland: World Meteorological Organization.

Zaniolo, Giuliani, Castelletti, Pulido-Velazquez (2018) Automatic design of basin-specific drought indexes for highly regulated water systems. Hydrology and Earth System Sciences, 22(4):2409–2424.

Zargar, Sadiq, Naser, Khan (2011) A review of drought indices. Environmental Reviews, 19(NA), 333-349.

Using lagged ERA5-Land soil moisture data and Artificial Neural Networks for identifying landslide triggering conditions

N. Palazzolo*, D.J. Peres, G. Buonacera, A. Cancelliere
Department of Civil Engineering and Architecture, University of Catania, Catania, Italy
** e-mail: nunziarita.palazzolo@unict.it*

Introduction

Landslides triggered by rainfall are among the numerous natural hazards responsible for loss of human life and severe consequences. Between 2004 and 2016, it is estimated that 55997 people lost their lives in 4862 landslides worldwide (Froude and Petley, 2018), highlighting the ongoing global threat of landslides which continue to cause casualties. Within this framework, landslide prediction is crucial for the development of landslide early warning systems (LEWSs), which are essential for mitigating this risk. Traditionally, LEWSs are based on rainfall thresholds modeled using a power-law relationship between event duration (D) and intensity (I), at a regional scale. Thus, such models overlook the possibility to exploit information on other hydrological variables more directly related to the triggering mechanism, such as soil moisture. Enhancing the predictive accuracy of these systems requires advanced methodologies such as artificial neural networks (ANNs) that can dynamically assess landslide-triggering conditions. Thanks to their ability to analyze large datasets and identify potential patterns, ANNs can learn and model complex relationships among multiple variables. Thus, several scholars started to focus on the possibility to use different machine learning algorithms to tackle the challenge of landslide prediction (Mondini et al. 2023). Among these, Distefano et al. (2023) demonstrated improved prediction accuracy when ANNs were fed with precipitation and multilayered soil moisture data from ERA5-Land at the onset of rainfall events. However, ERA5-Land data are usually available with a delay of approximately five days, making their direct application to real-time prediction systems challenging. Therefore, this study explores the feasibility of using lagged ERA5-Land soil moisture data for real-time landslide prediction and assesses its impact on predictive performance. The proposed methodology is tested in Sicily, a region highly susceptible to rainfall-induced landslides.

Materials and methods

The proposed methodology is schematized by the flow chart in Figure 1. Once the historical landslides have been collected (FraneItalia project by Calvello and Pecoraro, 2018), as well as the rainfall data, the CTRL-T research code (Melillo et al. 2018) is employed to reconstruct both triggering and non-triggering rainfall events. Then, multi-layered reanalysis soil moisture data are assigned to each rainfall event. Specifically, soil moisture information for each rainfall event is assigned starting back to up 15-days before its beginning. The most interesting case is that of a 5 days lag, as ERA5-Land data are released with such a delay. After the dataset has been created, the ANNs model is developed. In more detail, the following input variables were considered: (i) precipitation duration *D*, (ii) cumulative precipitation *E*, (iii) volumetric soil water content *S* at different depths retrieved from ERA5-Land reanalysis at different lag times. For details on the ANN architecture, see Distefano et al. (2022). To optimize performance, a heuristic approach was applied, varying the number of hidden neurons between 5 and 20, while each network was trained 30 times to evaluate the impact of random data splitting in training, validation and test. Finally, ROC statistics are used to assess the performance at varying time lag.

Results and concluding remarks

Results showed that lagged soil moisture data have a low impact on prediction accuracy. With a 5-day lag, TSS decreased slightly from 0.78 to 0.72, while at a 15-day lag, performance declined further to 0.67.

These results suggest that ERA5-Land multilayered soil moisture data can be effectively integrated into operational LEWSs, even with lagged datasets, offering potential for real-time applications.

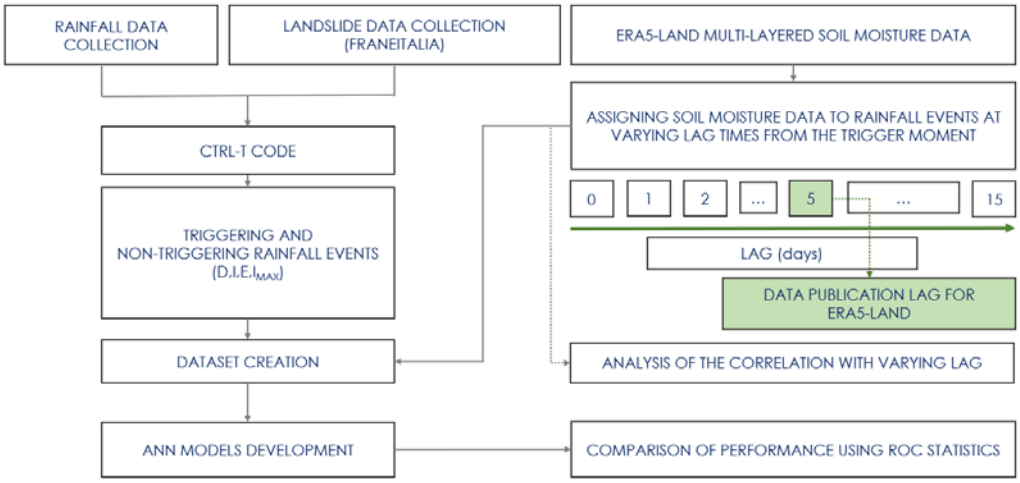


Figure 1. Flow chart of the methodology

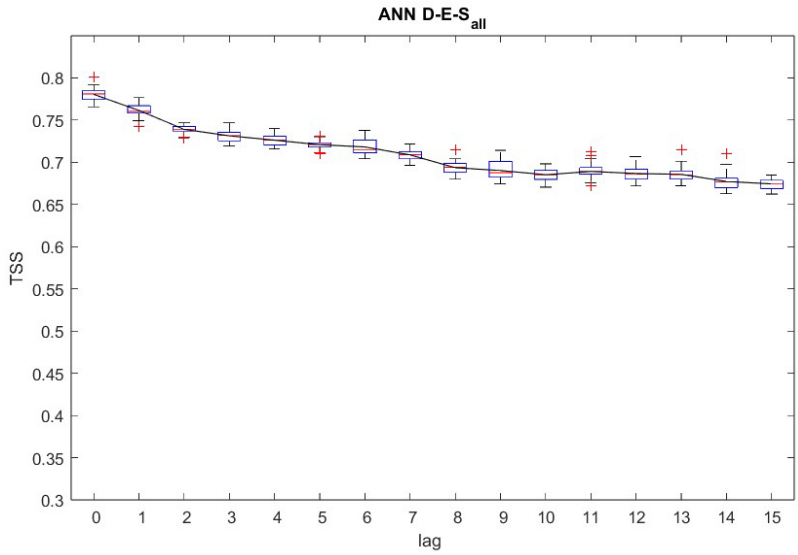


Figure 1. Boxplot of the TSS carried out using D-E-S$_{all}$

Acknowledgments: The authors acknowledge the funding support from the PRIN 2022 "Prediction of Rainfall-INduced landslides – Improving multi-scale TerritoriAL Early warning through aRTificial intelligence (PRIN-ITALERT)" project, funded by the Ministry of University and Research (code 202248MN7N, CUP E53D23004150006).

References

Calvello M, Pecoraro G (2018) FraneItalia: a catalog of recent Italian landslides. Geoenvironmental Disasters 5, 1–16. https://doi.org/10.1186/S40677-018-0105-5/FIGURES/11

Distefano P, Peres DJ, Piciullo L, Palazzolo N, Scandura P, Cancelliere A (2023) Hydro-meteorological landslide triggering thresholds based on artificial neural networks using observed precipitation and ERA5-Land soil moisture. Landslides 20, 2725–2739. https://doi.org/10.1007/S10346-023-02132-5/TABLES/6

Froude MJ, Petley DN (2018) Global fatal landslide occurrence 2004 to 2016. https://doi.org/10.5194/NHESS-2018-49

Melillo M, Brunetti MT, Peruccacci S, Gariano SL, Roccati A, Guzzetti F (2018) A tool for the automatic calculation of rainfall thresholds for landslide occurrence. Environ. Model. Softw. 105, 230–243. https://doi.org/10.1016/J.ENVSOFT.2018.03.024

Mondini AC, Guzzetti F, Melillo M (2023) Deep learning forecast of rainfall-induced shallow landslides. Nat. Commun. 2023 141 14, 1–10. https://doi.org/10.1038/s41467-023-38135-y

Comparative assessment of drought characteristics obtained using gridded and station datasets from India Meteorological Department (IMD) in a semi-arid basin of India

A. Gupta[1,2], M.K. Jain[1*], R.P. Pandey[1], D.M. Hannah[2,3]
[1] Department of Hydrology, Indian Institute of Technology Roorkee, Roorkee, India
[2] School of Geography, Earth and Environmental Sciences, University of Birmingham, Birmingham, United Kingdom
[3] Birmingham Institute for Sustainability and Climate Action, University of Birmingham, Birmingham, United Kingdom
* e-mail: manoj.jain@hy.iitr.ac.in

Introduction

Information on climate and weather are vital for understanding the impacts of droughts on various aspects of agriculture production. Long-term datasets on precipitation and temperature are required to study the impact of climate change (Piyoosh & Ghosh, 2016). However, the availability of good quality datasets from meteorological observatories at any location remains a challenge, as most of the station data lack spatio-temporal continuity over a more extended period. Also, the directly measured station datasets are often limited and restricted in access. Gridded weather datasets are readily available and prepared from interpolating ground-based or satellite-based rainfall products, which provide essential weather information in any region. The gridded precipitation and temperature datasets are continuous and can also be used for regions lacking with observational datasets. However, gridded datasets have inherent limitations as they are prepared using interpolation. Many studies have conducted the comparison of different meteorological datasets which are generated by various sources. However, just a few research have compared station data with gridded precipitation datasets (Chakraborty et al., 2018).

Therefore, to understand the characteristics and constraints of gridded datasets, a comparative analysis of gridded datasets (precipitation, maximum and minimum temperature) with that of manually observatory point datasets was conducted to check the reliability of the datasets for the estimation of drought characteristics in the semi-arid Krishna River Basin of Peninsular India.

Materials and Methods

The meteorological variables, namely precipitation, maximum and minimum temperature, from gridded datasets of India Meteorological Department (IMD) were analysed and compared with that of the observed point datasets obtained from IMD in the Krishna Basin of India. For the comparison, IMD grid points and 21 rain-gauge stations nearest to grid falling on the stream networks are considered in the study. The meteorological drought was estimated using the Standardised Precipitation Index (SPI) and the Standardised Precipitation Evapotranspiration Index (SPEI) for 3-month timescale. The drought characteristics such as average drought duration (months), average drought severity and the total number of drought months for all the grid points and their corresponding rain-gauge stations was checked using the run theory approach (McKee et al., 1993). To better understand the reliability of gridded dataset with respect to point dataset, the statistical parameters like coefficient of variation, mean, median, maximum, and minimum value, standard deviation, and skewness were checked at seasonal (south-west monsoon and north-east monsoon) and annual scale for all the grid points and their corresponding rain-gauge stations.

Results and concluding remarks

Good quality datasets for any region are the initial step towards the estimation and mitigation of drought. Hence, it is important to check the reliability of gridded and point datasets for the drought estimation and its characteristics. The comparison of drought characteristics such as average drought duration, severity and total drought months using SPI-3 and SPEI-3 at three gridded and their

corresponding manually observatory point locations are shown in Figure 1 below for reference (out of 21 locations selected for the study).

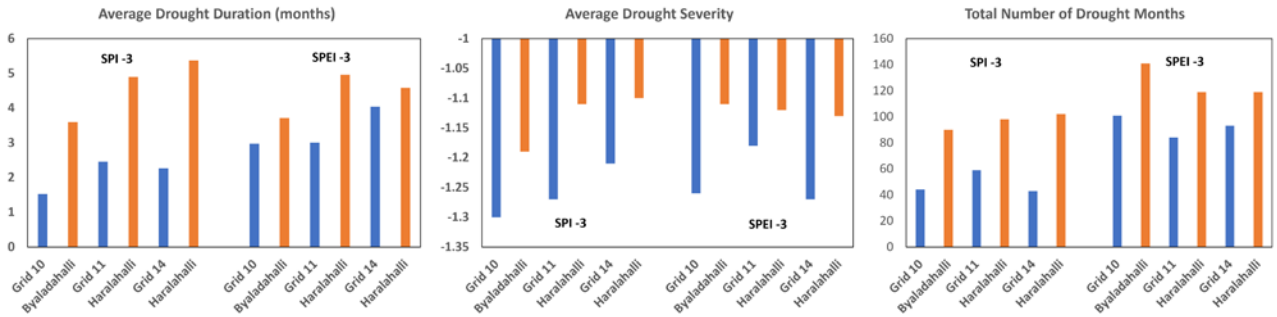


Figure 1 The average drought duration (months), average drought severity and the total number of drought months obtained using SPI-3 and SPEI-3 at three gridded and its corresponding point locations.

From this study, the following conclusion can be drawn:

1. In case of south-west monsoon, the gridded rainfall dataset shows notably higher rainfall in the range of 33.5 mm to 4156.38 mm compared to the observed point rainfall in the range of 21.3 mm to 2690.6 mm at corresponding rain gauge station.
2. In case of north-east monsoon, there is no significant difference between the gridded rainfall dataset compared to the observed point rainfall at corresponding rain gauge station.
3. In case of annual scale, the reported gridded rainfall is significantly more in the range of 153.53 mm to 4390.51 mm than the corresponding point rainfall in the range of 156.3 mm to 3435 mm particularly in higher rainfall areas.
4. The drought characteristics obtained for both SPI and SPEI at 3-month timescale, indicates that a smaller number of drought duration, severity and drought months are captured from gridded rainfall datasets when compared with point datasets.
5. At SPI 3-month timescale, the total number of drought months captured were less from gridded datasets at seasonal and annual scale, and for severe drought category, except for moderate and extreme drought category, when compared with that of point datasets.
6. At SPEI 3-month timescale, the total number of drought months captured were almost same from gridded datasets at seasonal and annual scale, and for severe drought category when compared with point datasets, whereas the total number of drought months captured were less for moderate and extreme drought category, when compared with that of point datasets.

Thus, the analysis results indicates that the gridded datasets could not capture all the moderate, severe, and extreme drought months during the study period. The reason may be simply because the gridded rainfall datasets has been estimated using interpolation of observed rainfall in the stations in the vicinity of the given grid. On the other hand, the observed point datasets captured most of the drought months more realistically. Thus, it is important to note that the station rainfall datasets yield a more realistic assessment of drought months. Therefore, the station datasets should be preferred over gridded ones for better accuracy of drought forecasting and early warning systems.

References

Chakraborty, D., Sehgal, V. K., & Dhakar, R. (2018). Comparison of Gridded Weather Datasets with Point Datasets over Three Locations of India Comparison of Gridded Weather Datasets with Point Datasets over Three Locations of India. Journal of Agricultural Physics, 18(2), 218–223.

McKee, T. B., Doesken, N. J., & Kleist, J. (1993). The relationship of drought frequency and duration to time scales. Proceedings of the 8th Conference on Applied Climatology, 17(22), 179–183.

Piyoosh, A. K., & Ghosh, S. K. (2016). A comparative assessment of temperature data from different sources for Dehradun, Uttarakhand, India. Journal of Meteorological Research, 30(6), 1019–1032. https://doi.org/10.1007/s13351-016-6031-0

Parameter sensitivity in network-based clustering: Implications for regional frequency analysis of extreme rainfall

M. Billios, L. Vasiliades*
Laboratory of Hydrology and Aquatic Systems Analysis, Department of Civil Engineering, School of Engineering, University of Thessaly, 38334 Volos, Greece
** e-mail: lvassil@gmail.com*

Introduction

Extreme rainfall events have significant social and economic impacts, which are expected to intensify with climate change. Reliable statistical methods, such as Regional Frequency Analysis (RFA), are essential for estimating high quantiles of extreme rainfall; however, the identification of statistically homogeneous regions remains a challenge due to data limitations and other uncertainties. These regions are typically delineated based on climatic, geographical, or topographical boundaries. However, this method does not always ensure statistical homogeneity, as rainfall characteristics can vary significantly within seemingly continuous regions.

Recently, Billios and Vasiliades (2025) propose an iterative network-based clustering approach. By optimizing the modularity index (Newman, 2018), in a rainfall station network created by stacking multiple delineations possibilities of their study area, they were able to define adequate homogeneous regions while minimizing subjectivity in covariate selection. This study builds upon previous research, focusing on sensitivity analysis to evaluate the influence of clustering parameters on network creation.

Materials and methods

The approach employs the network-based clustering method, developed in a previous study (Billios and Vasiliades, 2025), to ensure statistical homogenous regions, a critical step in Regional Frequency Analysis (RFA) based on L-moments as proposed by Hosking and Wallis (1997). The dataset consists of daily annual maximum rainfall records obtained from 55 rainfall stations across Thessaly, Greece. The study area is characterised by the central Thessalian plain that get surrounded by mountainous regions from all sides.

Using six station covariates (annual mean rainfall, longitude, latitude, elevation, mean maximum annual precipitation, and L-skewness) all possible combinations were generated, selecting two to five variables at a time. This process resulted in a total of 56 unique combinations. Each combination, after getting pre-processed by Principal Component Analysis (PCA variant) or not (non PCA variant), is then used as input for the k-means clustering algorithm. Choosing two (2) to seven (7) k-means clusters (K parameter), unique regions are formed. To establish networks, stations that belong to the same cluster at least 50 (threshold parameter T) out of 56 times are connected, ensuring robust clustering and independence of specific covariates or the number of them. Finally using the igraph package in R, communities are then formed by maximizing the modularity measure (Newman, 2018). These communities are subsequently tested for heterogeneity, and suitable ones are used for regional frequency analysis. Cluster evaluation is performed by applying the heterogeneity test (Hosking and Wallis, 1997). When a region has is $H1<1$ is considered as "acceptably homogeneous" if $1 \leq H1<2$ "possibly heterogeneous" and "definitely heterogeneous" if $H1 \geq 2$. The sensitivity analysis performed in this study explores the K parameter in the k-means algorithm and the threshold number T used to filter the co-occurrence matrix. The differences between the PCA and the Non-PCA (Figure 1) variants are also analysed and compared.

Results and concluding remarks

Starting with the K parameter the values analysed range from two to seven. A smaller value leads to fewer, but larger communities, which often do not meet the homogeneity requirement due to greater

variability. On the other hand, a larger value creates smaller clusters that are more likely to satisfy the homogeneity test but may include too few stations to be useful. This balance between cluster size and homogeneity is also affected by the threshold T in the same way. Lower values of T starting from zero create fewer but bigger heterogenous clusters, and higher values, up to 50, create more homogenous clusters with smaller station population. Higher k values generally improve homogeneity mainly because of the station number per cluster decreasing, with T value having a secondary role. Both PCA and non PCA variants maximize their community number for the maximum K value studied i.e seven and for threshold values T around 40. Specifically, in both variants most communities appear for K values 5 to six 7 and T values from 35 to 40. When examining lower thresholds (T = 5) heterogeneity prevails for both PCA and Non-PCA variants, with almost none of the communities passing the test. However, as T increases, the number of homogeneous clusters increases sharply. At T = 50, PCA variant maintains a higher proportion of homogeneous clusters per total clusters, compared to lower rates for the Non-PCA variant, which on the other hand, utilizes a bigger number of total stations. For that reason, further analysis will continue for threshold value T=50 and for varying K values.

In the non-PCA variant, a similar pattern emerges with clusters of low population, particularly those containing only 2 or 3 stations. Almost all of these clusters have H<2, but their small size makes them unsuitable for RFA. In contrast, for K values from 2 to 4, there is always at least one cluster with a moderate population. These clusters consist of different combinations of stations located at the center of the study area, which is characterized by uniform terrain and low altitudes. The largest cluster, encompassing all stations, forms when K=2 (14 stations). This cluster is also acceptably homogeneous, with H <1.

Similarly, in the PCA variant, most small clusters remain homogeneous. The largest cluster also appears at K=2, representing the central study area, but with a key difference: it splits into two equal parts. Regarding the mountainous regions, both methods generate similar clusters, with the PCA variant incorporating more stations while achieving comparable results in the heterogeneity test.

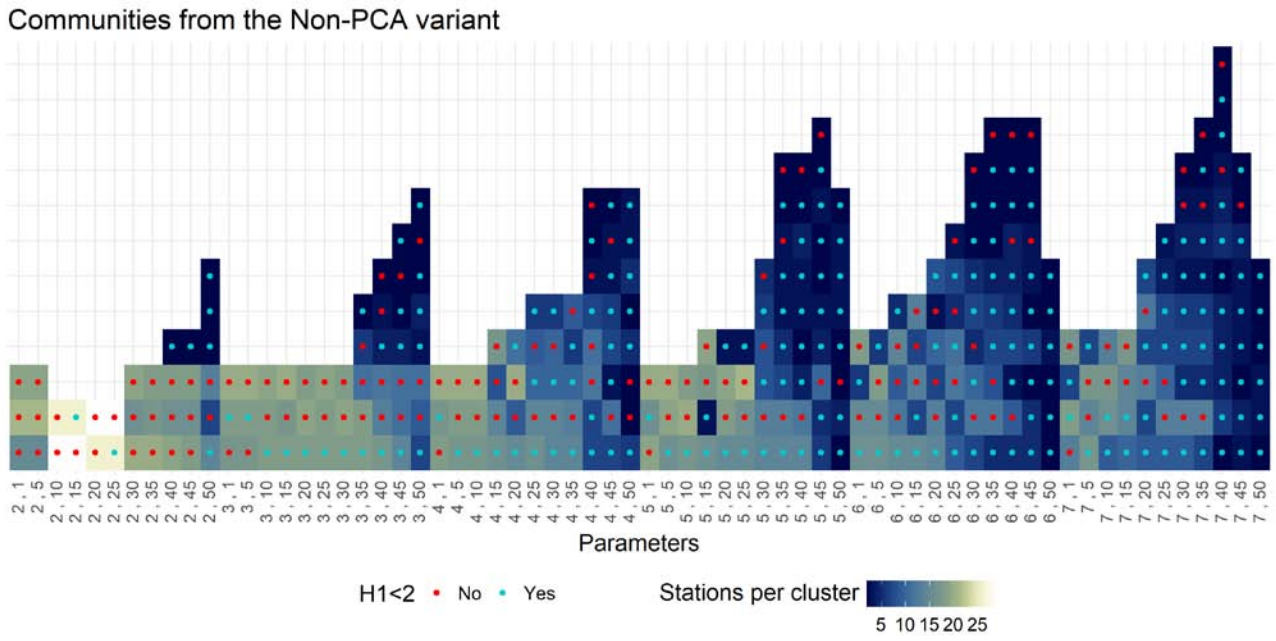


Figure 1. Community structures from the Non-PCA variant are shown, with the heatmap indicating the number of stations per cluster (darker colors for fewer stations, lighter for more). Red and cyan dots represent whether the condition H1<2 is not met or met, respectively. In the x-axis the first number represents the K parameter value and the second number the T parameter value.

References

Billios, M., Vasiliades, L., 2025. A Network-Based Clustering Method to Ensure Homogeneity in Regional Frequency Analysis of Extreme Rainfall. Water 17, 38. https://doi.org/10.3390/w17010038

Hosking, J.R.M., Wallis, J.R., 1997. Regional Frequency Analysis: An Approach Based on L-Moments, 1st ed. Cambridge University Press. https://doi.org/10.1017/CBO9780511529443

Newman, M., 2018. Networks, Second Edition, Oxford University Press, Oxford, New York.

Assessing critical soil moisture to demarcate terrain stability

J. Thomas[1*], L.V. Noto[2], R.L. Bras[3], E. Arnone[1]
[1] University of Udine, Polytechnic Department of Engineering and Architecture, Udine (UD), ITALY
[2] University of Palermo, Department of Engineering, Palermo (PA), ITALY
[3] Georgia Institute of Technology, School of Earth and Atmospheric Sciences, Atlanta (GA), USA
*e-mail: juby.thomas@uniud.it

Introduction

Changes in rainfall patterns and the increased frequency of extreme rainfall events can significantly impact terrain stability in areas prone to rainfall-induced landslides. The spatial variability of terrain stability is closely related to the dynamics of soil moisture and the groundwater level, as both reflect the intensity and duration of precipitation events. Thus, soil moisture and groundwater level can effectively serve as proxies for assessing the stability of vulnerable terrains. Deriving critical maps of soil water content (*SWC*) for hazard initiation can significantly aid authorities, and emergency responders in risk management.

Several studies have focused on delineating conditionally and unconditionally stable areas, in 'partially saturated' soils based on topography, mechanical properties, and a steady state wetness index (*WI*) or height of groundwater level (Montgomery and Dietrich, 1994). However, this approach does not account for the transient and unsaturated conditions of soils, both in the stability index and at the infiltration front (Lepore et al., 2013). To address this, the present study proposes a method for demarcating conditionally and unconditionally stable areas by incorporating both 'unsaturated' and 'partially saturated' conditions. Within the conditionally stable areas, we derive critical maps of landslide initiation.

Materials and methods

The present study implements two equations to assess the stability index, known as the factor of safety (*FoS*): eq. 1 for saturated conditions at the failure surface (Arnone et al., 2011; Montgomery and Dietrich, 1994), and eq. 2 for unsaturated conditions along the soil column (Arnone et al., 2016; Lepore et al., 2013). The former equation computes the *FoS* as a function of groundwater level and the hydro-mechanical properties of the soil over the slope, ω. The latter incorporates the matric suction (or pressure head if positive), $\psi(\theta)$, and the volumetric water content, θ:

$$FoS = \frac{c}{\gamma_s h \sin\omega} - \frac{\gamma_w}{\gamma_s} \cdot \frac{h_w}{h} \cdot \frac{\tan\phi}{\sin\omega} + \frac{\tan\phi}{\tan\omega} \quad (1)$$

$$FoS = \frac{c}{\gamma_s h \sin\omega} - \frac{\gamma_w \psi(\theta)}{\gamma_s h} \cdot \frac{\theta-\theta_r}{\theta_s-\theta_r} \cdot \frac{\tan\phi}{\sin\omega} + \frac{\tan\phi}{\tan\omega} \quad (2)$$

where c and ϕ are the cohesion and internal friction angle of the soil, γ_w and γ_s are the unit weight of water and soil, h is the depth where FoS is computed (≈depth of failure surface) and h_w the height of the saturated water column (≈height of groundwater level from failure surface), respectively. The residual and saturated water content of the soil are θ_r and θ_s. Forcing *FoS* to a critical value of 1, at given h, eq. 1 and eq. 2 are inverted to delineate the unconditionally and conditionally stable areas with respect to slope ω, in terms of critical groundwater level (*CGL*) and critical soil moisture (*CSM*), respectively. Specifically, assuming the entire soil column to be saturated, i.e., $h_w = h$, eq. 1 provides the critical slopes, ω^*, which separates the unconditionally stable area (below which the terrain remains stable regardless the saturation) from the conditionally stable area (Figure 1a). Assigning the maximum water content of the soil, θ_s, to θ, eq. 2 determines a second critical slope, ω^{**}, which divides the 'partially-saturated-conditionally' stable areas from the 'unsaturated-conditionally' stable areas. This indicates that in the region between ω^* and ω^{**} instabilities occur under partially saturated conditions, due to the groundwater; above ω^{**} instabilities occur under unsaturated conditions. The corresponding failure initiation values either of groundwater level or soil moisture represent the *CGL* and *CSM*, respectively.

The methodology is being applied to the But stream basin (327 km²), located in the Friuli Venezia Giulia region (Italy), where many shallow rainfall-induced landslides have been observed, according to the IFFI (ISPRA, 2024) catalogue. To produce efficient and easy-to-interpret maps, we identified Homogeneous Soil Units (HSUs) defined by a unique combination of slope and hydro-mechanical properties. The critical value of CGL or CSM is determined for HSUs at the potential failure surfaces h.

Results and concluding remarks

The results are presented below as part of methodology demonstration, assuming loam soil parameters homogenous across the study area. Figure 1 (a) shows the terrain stability at different slopes for a depth of 2.5m. Unconditionally stable areas are those below 14° (ω^*). The region between 14° (ω^*) and 28.8° (ω^{**}) is stable depending on the CGL, in a linear way from 0 to 2.5m (right Y-axis). Stability of areas steeper than 28.8° depends on the critical soil moisture values reported in the left Y-axis of Figure 1 (a), ranging from 0 to 0.46. The steeper the areas, the lower the *CSM* enough to trigger a possible movement. Hydro-mechanical properties and depth at which the *FoS* is calculated determine ω^* and ω^{**} and, consequently, the critical water content values. The variation of *CSM* and *CGL* with depth is further illustrated in Figure 1 (b) for different slope angles. CSM varies non linearly with depth, it quickly approaches values close to saturation (i.e., θ_s = 0.46 and CGL = 0) for shallower depths. Variation of CGL is again linear, with more rapid changes for the gentler angle (30°).

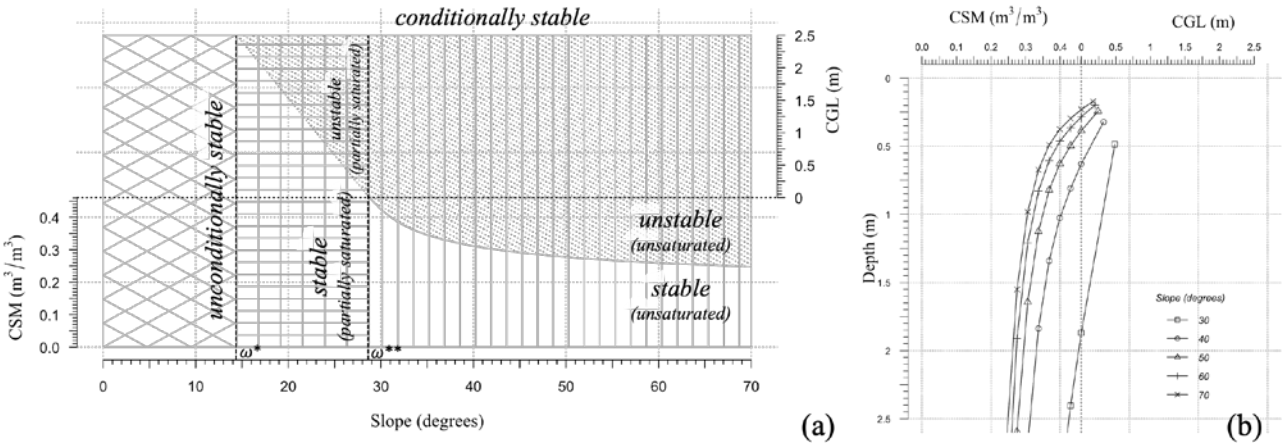


Figure 1 (a) Unconditionally and conditionally stable areas, along with critical soil moisture (CSM) and critical groundwater level (CGL), at varying slopes and a depth of 2.5m for loam soil parameters (b) Corresponding variation of CSM and CGL with depth for different slope angles.

Acknowledgments: This research was supported by the PRIN 2022 project "INTENSE – raINfall exTremEs and their Impacts: from local to national Scale", PNRR M4.C2.1.1 - PRIN 2022 – Codice 2022ZC2522 - CUP G53D23001400006.

References

Arnone, E., Caracciolo, D., Noto, L. V., Preti, F., Bras, R. L. (2016). Modeling the hydrological and mechanical effect of roots on shallow landslides. Water Resources Research, 52(11), 8590–8612. https://doi.org/10.1002/2015WR018227

Arnone, E., Noto, L. V., Lepore, C., Bras, R. L. (2011). Physically-based and distributed approach to analyze rainfall-triggered landslides at watershed scale. Geomorphology, 133(3–4), 121–131. https://doi.org/10.1016/j.geomorph.2011.03.019

ISPRA. (2024, December 16). IFFI – Inventory of Landslide Phenomena in Italy. https://www.progettoiffi.isprambiente.it/

Lepore, C., Arnone, E., Noto, L. V., Sivandran, G., Bras, R. L. (2013). Physically based modeling of rainfall-triggered landslides: a case study in the Luquillo forest, Puerto Rico. Hydrology and Earth System Sciences, 17(9), 3371–3387. https://doi.org/10.5194/hess-17-3371-2013

Montgomery, D. R., Dietrich, W. E. (1994). A physically based model for the topographic control on shallow landsliding. Water Resources Research, 30(4), 1153–1171. https://doi.org/https://doi.org/10.1029/93WR02979

Red flags on the map: Exceptional rainfall and temperature events in Portugal (1980/1981 – 2023/2024)

L.A. Espinosa[1*], M.M. Portela[2]
[1] Associação do Instituto Superior Técnico para a Investigação e Desenvolvimento (IST-ID), Civil Engineering Research
[2] Instituto Superior Técnico (IST), CERIS; Portugal
*e-mail: luis.espinosa@tecnico.ulisboa.pt

Introduction

Extreme weather events, including exceptional rainfall and temperature, have intensified due to climate change, profoundly impacting hydrological forecasting, human health, disaster risk management, and infrastructure planning. Understanding the spatiotemporal distribution of these extremes is critical for raising climate change awareness and developing effective climate adaptation policies. This paper summarises key findings from two studies based on reanalysis data that utilised severity heat maps (as proposed by Espinosa et *al*., 2024) to analyse exceptional rainfall and temperature events in mainland Portugal. The country is characterised by diverse topography and climatic variations, and has experienced noticeable shifts in extreme rainfall and temperature patterns over recent decades. These changes pose substantial risks to water resources, infrastructure, agriculture, and ecosystem stability. The findings highlight the intensification of extreme weather events throughout the past four decades and provide insights into their regional impacts.

Material and methods

The study used the ERA5-Land reanalysis daily dataset of continuous rainfall data and maximum daily temperature spanning from 1 October 1980 to 30 September 2024 (44 hydrological years) at 1,012 grid points, evenly distributed over mainland Portugal. The extreme events were identified based on three high empirical non-exceedance probability thresholds, namely Q99.0, Q99.5, Q99.9, regarding daily rainfall, and Q90.0, Q99.0, Q99.9, in what concerns daily maximum temperature.

The results are presented in the form of severity heat map (Espinosa *et al.*, 2024), generated from a 2 × 2 matrix that combines two characteristics of extreme events, related to the number and magnitudes of the occurrences, and compares their values in two consecutive 22-year sub periods or phases: a late one (1 October 1980 to September 2002) *versus* a recent one (October 2002 to 30 September 2024).

Results and concluding remarks

Figure 1 displays severity maps showing Portugal's spatial susceptibility to changes in the occurrence and magnitude of extreme events of precipitation and maximum temperature (Tmax), based on the comparison between the two 22-year phases. Higher values of both variables (occurrences of exceptional rainfall and cumulative rainfall above threshold for upper figures, and occurrences of exceptional maximum temperature and relative temperature excess for the lower figures), in the case of in the most recent period compared to the first indicate a worsening of extreme hydrological events (red areas in the figure); conversely, lower values of both variables suggest no worsening of such events (green areas). The intermediate categories accounted for the type of phenomena being analysed. For extreme rainfalls, an increase in rainfall amount was considered potentially more damaging (orange areas) than an increase in the number of occurrences (yellow areas), as it better reflects the expected effects from climate change, where exceptional rainfall events may become less frequent but more intense. Regarding maximum daily temperature, higher temperatures, even if less frequent (orange areas), were considered more harmful, namely in terms of human health, than lower but longer lasting temperature (yellow areas).

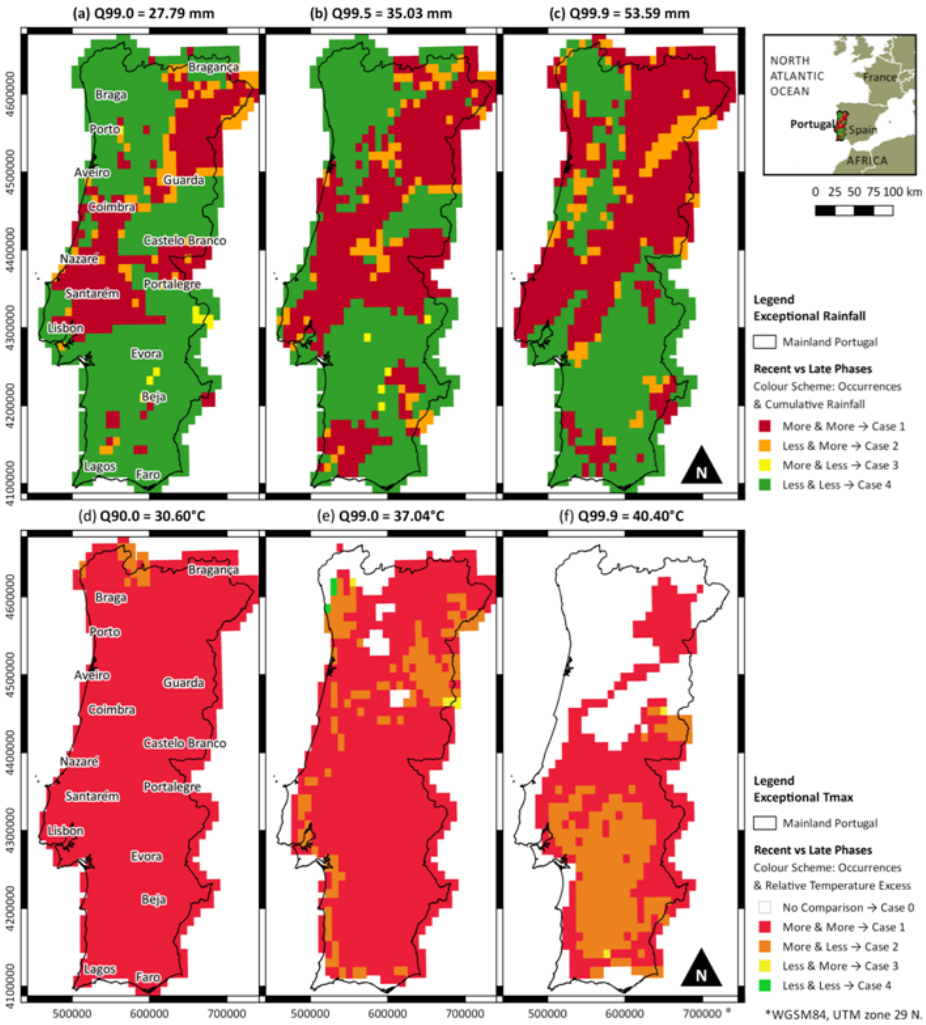


Figure 1. Severity heat maps of extreme rainfall (upper figures) and maximum daily temperature, Tmax (bottom figures) events from late (October 1980 to September 2002) and recent (October 2002 to 30 September 2024) phases.

The results regarding changes in the occurrence and magnitude of extreme rainfall from the earlier to the more recent period highlight the greater susceptibility of Portugal's northern regions, with this susceptibility becoming more pronounced as events become more extreme. Certain areas, including the urban regions of Lisbon and Porto, show a clear increase in both the frequency and magnitude of exceptional rainfall events exceeding the threshold in the recent phase.

Regarding maximum daily temperatures, the northern and central regions experienced the most significant increases in both the frequency of extreme events and temperature excess. In contrast, some areas, primarily in the south, saw a rise in frequency but a lower temperature excess at higher thresholds. A few regions exhibited a decrease in either occurrences or temperature excess, indicating localized conditions that are more favourable over time. Climate change is undeniably reshaping Portugal's hydrological and temperature patterns, intensifying both extreme rainfall and temperature events. Severity heat maps offer valuable insights into these evolving trends. To mitigate risks associated with extreme weather, policymakers, engineers, and scientists must collaborate to enhance resilience, promote sustainable water and climate governance, and develop adaptive strategies.

Acknowledgments: This research was supported by Fundação para a Ciência e Tecnologia (FCT) through funding UIDB/04625/2020 from the research unit CERIS, and the EU Horizon 2020 programme SCORE (Grant No. 101003534).

References

Espinosa L.A., Portela M.M., Gharbia S. (2024). Assessing Changes in Exceptional Rainfall in Portugal Using ERA5-Land Reanalysis Data (1981/1982– 2022/2023). Water, 16(5): 628. http://doi.org/10.3390/w16050628

Spatiotemporal drought patterns and their impact on water resources: A case study of Thessaly, Greece

A. Psilovikos[1], V. Leivadiotis[1], T. Papathanasiou[1], S. Sakellariou[2], N. Alpanakis[2], M. Spiliotopoulos[2], G. Tziatzios[2], I. Faraslis[2], N. Dalezios[2]
[1] *Department of Ichthyology & Aquatic Environment, Laboratory of Ecohydraulics & Inland Water Management, University of Thessaly, Fytokou St., 38446, N. Ionia Magnisias, Greece*
[2] *Department of Civil Engineering, Laboratory of Hydrology and Aquatic Systems Analysis, University of Thessaly, Pedion Areos, 38221, Volos, Greece*
** e-mail: psiloviko@uth.gr*

Introduction

Drought is a critical environmental hazard affecting agricultural productivity and water resource management, especially in semi-arid regions like Thessaly, Greece. Climate variability has intensified drought frequency and severity, posing significant risks to water-dependent sectors (Dai, 2011; IPCC, 2012). The Mediterranean region has experienced an increasing trend in drought occurrence due to global warming, leading to significant environmental and socioeconomic consequences (Hoerling et al., 2012; Williams et al., 2013). Recent studies have highlighted that drought in Europe are becoming more prolonged and severe, affecting both water resources and agricultural production (Caloiero et al., 2018; Pietrapertosa et al., 2023).

This study provides a spatiotemporal drought assessment using the Standardized Precipitation Index (SPI) over a 40-year period (1981-2020) (Sakellariou et al., 2024) to identify drought trends and extreme events. The novelty of this study lies in integrating remote sensing data (CHIRPS) with SPI for improved drought monitoring, enabling more effective water management strategies. The use of satellite-derived data, such as CHIRPS, instead of conventional meteorological data enhances the accuracy and spatial coverage of drought assessments (Climate Hazards Center, 2022).

Materials and methods

The study area, Thessaly, is one of Greece's most agriculturally significant regions, highly susceptible to water shortages. Drought conditions were analyzed using the SPI at multiple timescales (seasonal and annual) based on precipitation data from CHIRPS. The methodology involved calculating SPI values and mapping drought severity across different sub-regions using geostatistical techniques. Validation was conducted by comparing SPI-derived results with historical meteorological records, achieving a coefficient of determination (R^2) of 0,67, confirming the reliability of satellite-based drought assessments.

Results and concluding remarks

The results indicate that Thessaly experienced two extreme drought events (1988–1989 and 1989–1990), with SPI values reaching as low as -2.26. Conversely, the region faced extremely wet conditions in 2002–2003 (SPI = 2,1), followed by 2009 – 2010 (SPI = 1,15) which have led to another hydrological year with wet conditions. The eastern and central parts of Thessaly showed the highest vulnerability to drought. The findings highlight the importance of adopting targeted water conservation policies, such as precision agriculture and adaptive irrigation strategies, to mitigate drought impacts. Future research should explore forecasting models for drought prediction under changing climate scenarios.

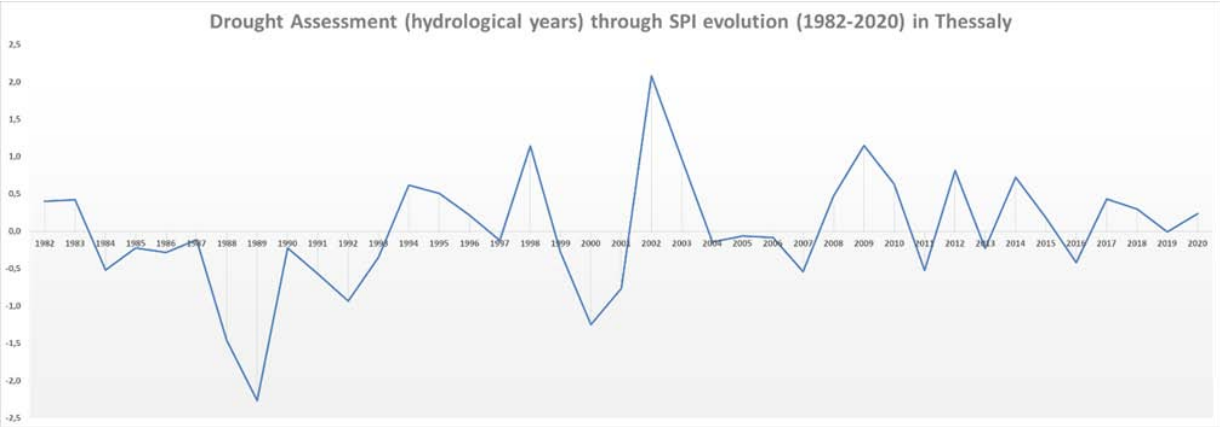


Figure 1. Drought assessment in Thessaly region, Greece from 1982 to 2020

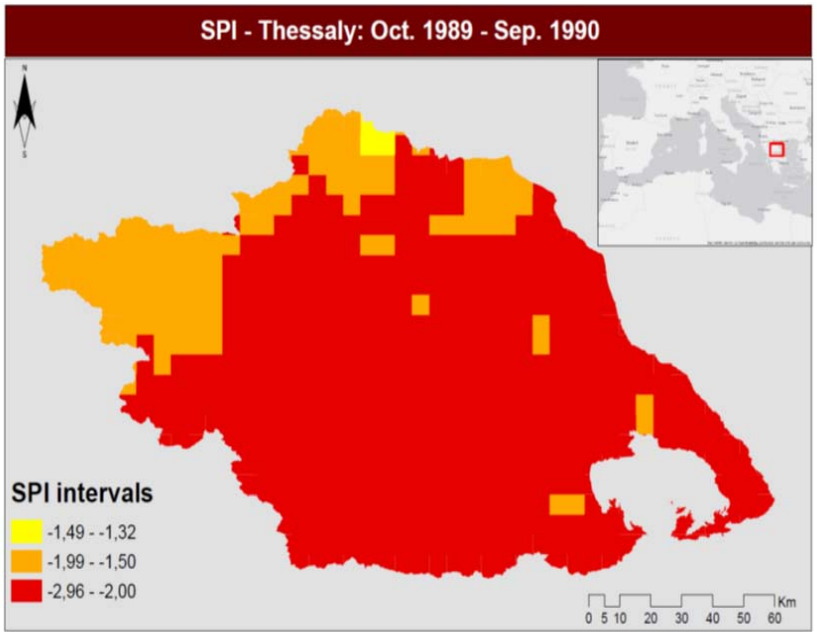


Figure 2. Spatial distribution of drought intensity in the driest hydrological year (1989 – 1990) in Thessaly region

Acknowledgments: The research is sponsored and funded by the "National Research Network for Climate Change and Its Effects – CLIMPACT", in which we co-operate as members of University of Thessaly

References

Caloiero, T., Veltri, S., Caloiero, P., & Frustaci, F. (2018). Drought analysis in Europe and in the Mediterranean Basin using the Standardized Precipitation Index. Water, 10(8), 1043.

Climate Hazards Center. (2022). CHIRPS: Rainfall Estimates from Rain Gauge and Satellite Observations. Retrieved from https://www.chc.ucsb.edu/data/chirps.

Dai, A. (2011). Drought under global warming: A review. Wiley Interdisciplinary Reviews: Climate Change, 2(1), 45-65.

Hoerling, M.P., Quan, X.W., Eischeid, J.K., & Perlwitz, J. (2012). On the increased frequency of Mediterranean drought. Journal of Climate, 25(6), 2146-2161.

IPCC (2012). Managing the Risks of Extreme Events and Disasters to Advance Climate Change Adaptation. Cambridge University Press.

Pietrapertosa, F., Olazabal, M., Simoes, S., Salvia, M., Fokaides, P., et al. (2023). Adaptation to climate change in cities of Mediterranean Europe. Cities, 140, 104452.

Sakellariou, S., Spiliotopoulos, M., Alpanakis, N., Faraslis, I., Sidiropoulos, P., et al. (2024). Spatiotemporal Drought Assessment Based on Gridded Standardized Precipitation Index (SPI) in Vulnerable Agroecosystems. Sustainability 2024, 16, 1240. https://doi.org/10.3390/su16031240

Williams, A.P., Allen, C.D., Macalady, A.K., Griffin, D., Woodhouse, C.A., et al. (2013). Temperature as a potent driver of regional forest drought stress and tree mortality. Nature Climate Change, 3, 292-297.

A combined methodology to address the frequency of extreme discharge and precipitation: Muriaé river basin case study (Brazil)

C.L.F. Silva*, M.M. Portela, J.P. Matos
Instituto Superior Técnico, Universidade de Lisboa. CERIS - Civil Engineering Research and Innovation for Sustainability
**carla.larissa.silva@tecnico.ulisboa.pt*

Introduction

Exceptional hydrological events can have significant economic, social, and environmental impacts, making it crucial to study them in the context of climate change and human-induced stressors, with emphasis on urbanization that may increase their frequency, magnitude and consequences. Among these events, extreme precipitation is particularly significant, underscoring the need for thorough investigation to understand its role in flooding and associated impacts. A deeper understanding of such occurrences is therefore crucial for water resource managers and users to improve resource management and minimize risks effectively.

One of the most common approaches to characterizing extreme hydrological events is frequency analysis. Among the sampling methods required for that analysis, the partial duration series or peaks over threshold (POT) approach offers advantages over the traditional annual maximum sampling method. Specifically, it allows for larger and more comprehensive samples, enabling the study of a greater number of events and, most relevant, of its frequency.

In Brazil, the Muriaé River Basin is a relatively urbanized watershed particularly vulnerable to extreme precipitation and flooding. For this reason, it was selected as a case study with the aim of exemplifying the suitability and added value of the POT approach combined with a Kernel Occurrence Rate Estimator (KORE) in non-stationary flood analysis, specifically in detecting changes in the frequency of those extreme events over time.

Materials and methods

The study area, the Muriaé River Basin (covering approximately 8,126 km², with a centroid located at WGS coordinates 21.09°S and 42.07°W), is situated in southeastern Brazil. It includes parts of the Minas Gerais and Rio de Janeiro states, and is a sub-basin of the Paraíba do Sul River.

To obtain the POT samples required for the frequency analysis, daily discharge and precipitation data were retrieved from the Hidroweb Portal of the National Water and Basic Sanitation Agency (ANA) (https://www.snirh.gov.br/hidroweb/serieshistoricas).

Four river gauging stations with continuous daily discharges were selected, namely Patrocínio do Muriaé (58920000), Carangola (58930000), Porciúncula (58934000), Cardoso Moreira station (58960000), along with eight rain gauges with influence in the basin, according to the Thiessen polygon method. Missing data in the rainfall series were filled using the Multivariate Imputation by Chained Equations (MICE) method (Van Buuren, Groothuis-Oudshoorn, 2011).

The application of the POT technique requires confirmation of the temporal independence of peaks (Cunnane, 1979; Silva et al., 2012). To achieve this for daily discharge data, two conditions were imposed: the minimum discharge between two consecutive peaks had to be less than or equal to one-third of the first peak's discharge, and the peaks had to be separated by at least three times the time to peak, approximated using the time of concentration of the analyzed river basins (Engecorps, 2011). For precipitation peaks, the selection criteria required peaks separate by at least three consecutive days without precipitation. Additionally, for both discharge and precipitation samples, a minimum average of two exceedances per year was imposed, the absence of correlation at lag 1 and lag 2 was verified, and the selected threshold was confirmed to lie within an approximately linear segment of the mean excess residual plot, as required.

After obtaining the POT series for discharge and precipitation, the Kernel Occurrence Rate Estimator (KORE) was used to assess the frequency of the peaks. To prevent distortions at the beginning and end of the time interval, pseudo-data were generated using the reflection method for a time interval on both sides of three times the bandwidth.

Results and concluding remarks

Figure 1 shows the occurrence rates of peak discharge (continuous black lines) and extreme rainfall events (dashed colored lines). The fact that, at each river gauging station, the curves for both types of samples follow the same pattern (albeit with different frequencies) confirms that the basin is largely under natural conditions.

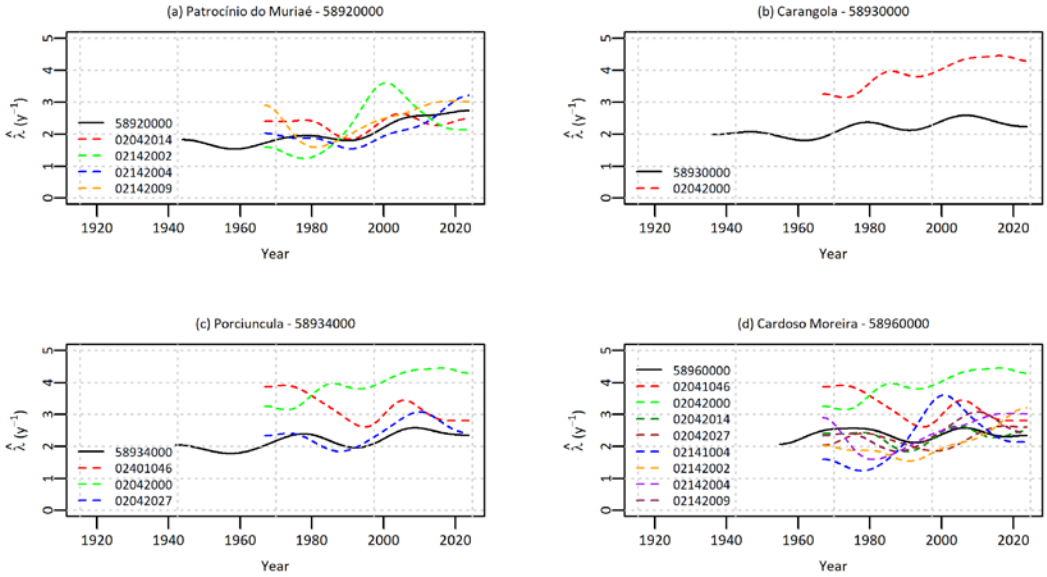


Figure 1. Estimated occurrence rates of peak discharge and extreme rainfall. The river gauging station to which each graph relates as well as the rain gauges that were assigned to the same are identified in the graph.

Regarding the river gauging stations, the peak discharges at Patrocínio do Muriaé - 58920000, Carangola - 58930000, and Porciuncula - 58934000, show a positive trend in frequency (i.e., more occurrences over time) while the Cardoso Moreira station - 58960000 exhibits a stationary behavior. Such an increase in the frequency also applies to peak precipitation except for 02041046 rain gauge, which shows an opposite trend, possible due to data quality issues, including those related to the gap filling procedure.

The work presented exemplifies a robust methodology for analyzing extreme hydrological events, leveraging the capabilities of the partial duration series (PDS) or peaks over threshold (POT) sampling technique, namely in terms of its suitability to be combined with frequency descriptors.

Acknowledgments: The research was carried out at the CERIS – Civil Engineering Research and Innovation for Sustainability (CERIS), a registered unit in the Fundação para a Ciência e a Tecnologia (FCT), UIDB/04625/2020. Additionally, the first author was supported by FCT under grant number 2023.04248.BD.

References

Cunnane C (1979) A note on the Poisson assumption in partial duration series models. Water Resources Research 15(2): 489-494. http://doi.org/10.1029/WR015i002p00489.

Engecorps (2011) Previsão de Eventos Críticos na Bacia do Rio Paraíba do Sul, R31 – Papel dos Afluentes nas Cheias e Pontos Críticos para o SIEMEC. ANA, SUM/SPR, Brasília, 51 p.

Silva AT, Portela MM, Naghettini M (2012) Nonstationarities in the occurrence rates of flood events in Portuguese watersheds. Hydrology and Earth System Sciences 16(1): 241-254. https://doi.org/10.5194/hess-16-241-2012.

Van Buuren S, Groothuis-Oudshoorn K (2011). mice: Multivariate imputation by chained equations in R. Journal of Statistical Software, 45: 1-67. https://doi.org/10.18637/jss.v045.i03.

A non-stationary GEV-based bias correction method

M. Onderka[1,2*], J. Pecho[1,2], M. Garaj[1,2], V. Rattayová[1,2]
[1] Department of Climate Services, Slovak Hydrometeorological Institute, Jeséniova 17, Bratislava, Slovakia
[2] Regional Climatological Institute, Plavecký Štvrtok 794, 900 62 Slovakia
* e-mail: milan.onderka@shmu.sk

Introduction

Rainfall projections from Regional Climate Models (RCMs) provide information on how rainfall extremes may evolve in the future. RCM climate simulations usually show systematic biases that have to be reduced before further applications. Bias correction approaches counteract the tendency of RCM simulations to overestimate or underestimate downscaled variables. One of the assumptions in fitting a distribution function to rainfall intensities is that the time series is strictly stationary. However, this assumption is not satisfied in changing climate conditions. Under non-stationary conditions, using simple quantile mapping approach may not be adequate for preserving trends. Since traditional bias-correction techniques (e.g., quantile mapping, delta quantile mapping, etc.) are fundamentally designed to correct the entire distribution function, the resulting bias-corrected data are inevitably skewed by the dominance of non-extreme data. To avoid this problem, we propose a novel technique based on a non-stationary form of the GEV distribution that allows us to map quantiles from the upper tail of the GEV distribution where all the extremes are located.

Materials and methods

Most bias correction approaches replicate the probability distribution of a model to observations using variations of the quantile mapping approach. Quantile mapping can be mathematically described as a transfer function:

$$q_{m,p}(t) = F_{o,h}^{-1}\{F_{m,t_1}[x_{m,p}(t)]\} \quad (1)$$

where $q_{m,p}(t)$ is the bias-corrected quantile of the annual maximum series modelled for a time t within some projected period (denoted by the subscript m and p); $F_{o,h}^{-1}$ is the inverse cumulative distribution function (CDF) of the historical observations; F_{m,t_1} is the CDF of the modelled projected data for time t1; and $x_{m,p}(t)$ is a modelled value at time t within some projected period. Since traditional bias-correction techniques (e.g., quantile mapping, delta quantile mapping, etc.) are fundamentally designed to correct the entire distribution function, the resulting bias-corrected data are inevitably skewed by the dominance of non-extreme data. To avoid this problem, we propose a novel technique based on a non-stationary form of the GEV distribution that allows us to map quantiles from the upper tail of the GEV distribution where all the extremes are located. The mathematical framework is based on the non-stationary formulation of the GEV distribution. The location parameter μ was allowed to vary over time. Allowing the location parameter μ to vary over time, and assuming the parameters σ and ξ are kept constant, the quantile of the nonstationary GEV distribution matches the quantile of the stationary GEV distribution precisely at the series' central point. This property is depicted in an example where we sought to correct bias from regional climate models (Fig. 1 - upper section), where the non-stationary quantile intersects the stationary quantile at the midpoint of the 1991-2021 period. In other words, the value of the non-stationary quantile at the midpoint of the 1991-2021 period corresponds to the stationary quantile derived for the entire 1991-2021 period. However, it is important to note that this equivalence would not hold if the σ and ξ parameters were permitted to vary over time or if the location parameter μ(t) was handled as a nonlinear function. The stationary quantiles were computed using the historical rain gauge observations according to Eq. 2. Having the estimated stationary quantiles from the historical 1991-2021 period, we can move forward with the quantile mapping (Figure 1):

$$q_{m*,p,non-stat} = F_{o,h,stat}^{-1}\{F_{m*,p,non-stat}[x_{m,p,non-stat}]\} \quad (2)$$

where $q_{m*,p,non-stat}$ is the bias-corrected quantile of the value modelled at the centre of the observational period (i.e., 2006, for the observational period starting in 1991 and ending in 2021); $F^{-1}_{o,h,stat}$ is the inverse CDF of the historical 'stationary' observations; $F_{m*,p,non-stat}$ is the CDF of the modelled value at time t1; and $x_{m,p,nan-stat}$ is the predicted value modelled at a future time t.

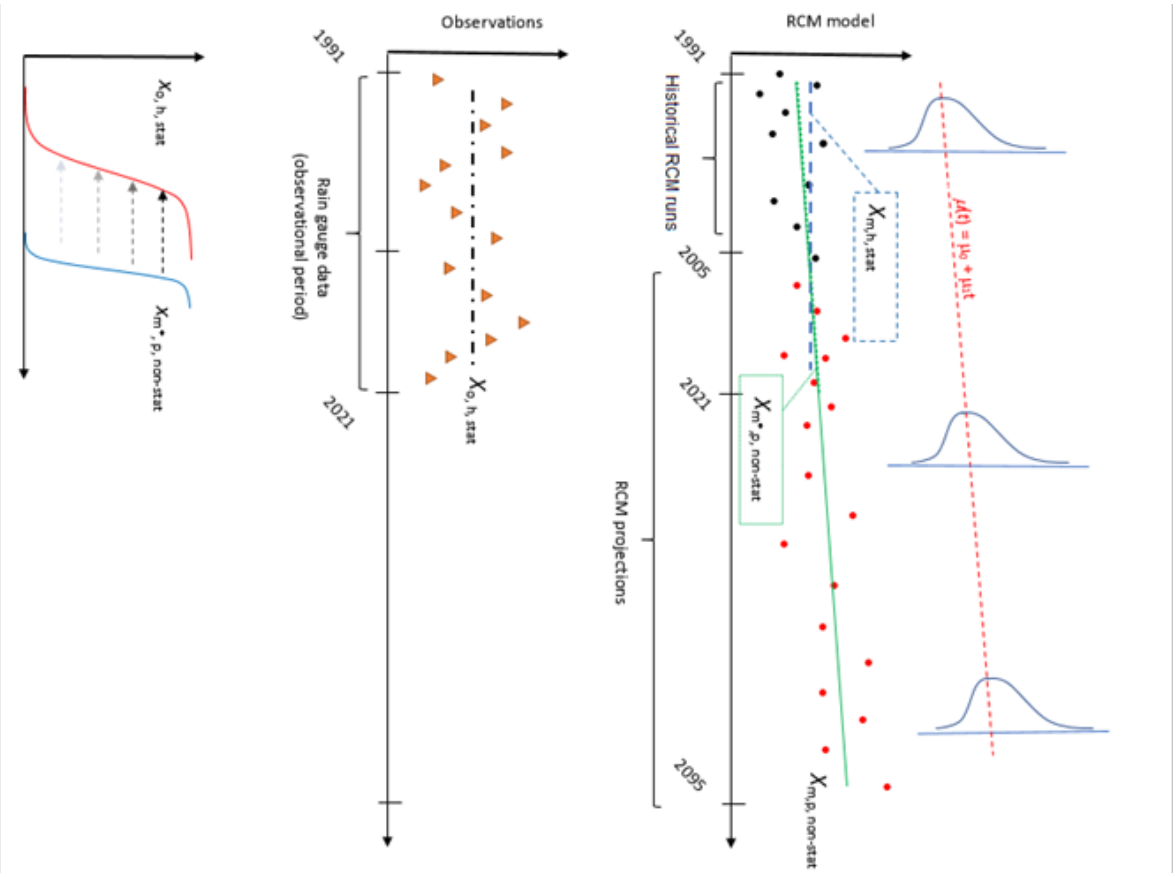


Figure 1. Conceptual representation of a non-stationary series featuring the time-dependent location parameter of the GEV distribution, denoted as μ(t) = μ_0 + μ_1t. The upper section displays a non-stationary hypothetical quantile derived from RCM simulations, combining both the historical RCM runs ($x_{m*,p,non-stat}$) and the RCM projections ($x_{m,p,non-stat}$), where the term $x_{m,h,stat}$ equals the $x_{m*,p,non-stat}$ exactly at the centre of the historical time series. The middle section illustrates a stationary model portraying a hypothetical quantile based on the data observed during the period 1991-2021 ($x_{o,h,stat}$). The lower section illustrates the principle of the simple quantile mapping of $x_{m*,p,non-stat}$ into $x_{o,h,stat}$.

Results and concluding remarks

The main results of this paper can be summarized as follows:

- a novel procedure has been described that permits correcting extreme values (e.g. the upper tails of the GEV distribution function), while preserving the trend in projected short-term rainfall extremes,
- the linear form of the non-stationary GEV distribution permits to calculating quantiles for any future horizon,
- the bias correction technique presented preserves trends, i.e., it enables maintaining physical scaling with temperature projections through the CC-scaling relationship,

Acknowledgments: This work was supported by the Slovak Research and Development Agency no. APVV-23-0332.

References

Onderka M., Pecho J., Szolgay J., Kohnová S., et al. (2024). Applying a time-varying GEV distribution to correct bias in rainfall quantiles derived from regional climate models. Journal of Hydrology and Hydromechanics, 499-512. https://doi.org/10.2478/johh-2024-0025

Comparing modelling approaches to estimate the impact of check dams as a Nature-Based Solution against flooding

C. Ouzounis*, G.Sylaios, V. Bellos
Department of Environmental Engineering, Democritus University of Thrace, Xanthi, Greece
** e-mail: couzouni@env.duth.gr*

Introduction

Flood risk management usually focuses on large-scale, catastrophic flood events. However, smaller to medium recurrent flood events with a cumulative impact on local communities over time, are often omitted due to low prioritizing over cost-benefit analysis. That said, in the last decade, Nature-Based Solutions (NbS) emerged as a cost effective, viable technical alternative to traditional grey engineering (Lupp et al. 2021). Today, there is an ongoing effort to raise political and research awareness for NbS, in an effort to deal with problems such as floods and other natural hazards or even ecosystem recovery. Moreover, it is now widely recognized that NbS should represent an evolving process based on balance between local society, developmental strategies and nature (Gomez Martin, 2021).

In this work we focus on the technical aspect of NbS structures and the understanding of their actual impact on water flow mechanisms, within the framework of water management (Ata et al., 2022; Emiroglu et al., 2025; Liu et al., 2023). More specifically, we explore three different modelling approaches to estimate the effectiveness of small gabions dams as a Nature Based Solution against flooding in a catchment located in the region of Kavala (Greece): a) Empirical hydrological rainfall-runoff models, b) hydrological rainfall-runoff model informed from physics-based hydrodynamic model, and c) physics-based hydrodynamic models.

Materials and methods

The study area is a small, ungauged catchment covering approx. 50 km^2, located west of Kavala city, in North Greece. The area is characterized by a granitic mountainous region that transitions into an alluvial coastal lowland, predominantly agricultural, with a few settlements of various sizes. Relatively intensive tourism activity, is also present along the coast. The Curve Numbers (CN) for the area were chosen from the pan-European Curve Number dataset developed by Kourtis et al. 2023. Infiltration rates were defined based on the values of Hydrologic Soil Groups (HSG).

Design rainfall for the study was estimated from the Intensity-Duration-Frequency (IDF) curves provided by the Greek Ministry of Environment and Energy (https://floods.ypeka.gr/sdkp-lap/maps-2round/). Also, Alternating Block Method (ABM) (Chow et al., 1988) was applied for rainfall temporal distribution.

As NbS structures for water flow control and against flooding, we chose small dams of height up to 5m, representing actual check dams constructed from gabions or geotextile tubes. In that way, it is expected that small reservoirs formed upstream would contribute to a) concentration time increase in each subbasin, and eventually b) flood peak reduction.

To evaluate the impact of the above NbS structures, three modelling approaches were applied:

1. Rainfall-runoff hydrological model (HEC-HMS software); time concentration is estimated from empirical formulas based on catchment characteristics. Simulation provides metrics such as the flood hydrograph at the catchment outlet and the reduce of flood peak after the NbS implementation.
2. Rainfall-runoff hydrological model informed by Hydrodynamic Model (HEC-HMS and HEC-RAS software); time concentration is estimated from using hydrodynamic models, with and without NbS implementation. As previously, simulation provides metrics such as the flood hydrograph at the catchment outlet and the reduce of flood peak after the NbS implementation.
3. Fully Hydrodynamic model (HEC-RAS software); Rain on Grid (RoG) method applied to an integrated

2D hydrodynamic model using a detailed Digital Terrain Model. Simulation provides metrics such as the inundated area, maximum water depths and flow velocities.

Results and concluding remarks

The results in all three approaches showed that small dams contributed to both flood peak reduction and increase in concentration time for rainfall events with low return periods, as expected. Empirical hydrological model provided an overview, while its informed version with integrated hydrodynamic data improved the results accuracy. On the other hand, physics-based hydrodynamic model provided detailed insights of the actual flood impact on the terrain.

In conclusion, with this work we focus on the designing for NbS implementation, contributing to a better understanding of their potential impact and moreover, provide a solid basis for stakeholders to evaluate their role within the framework of NbS projects.

Acknowledgments: This work was supported by DesirMED project (Grant Agreement No. 101112972).

References

Alsubih, M., Ahmed, M., Alqadhi, S. et al. (2023). Gabion water barrier structures as a sustainable approach to water and land conservation. Environ Sci Pollut Res 30, 126057–126071. https://doi.org/10.1007/s11356-023-31040-3

Asare, P., Atun, F., Pfeffer, K. (2023). Nature-Based Solutions (NBS) in spatial planning for urban flood mitigation: The perspective of flood management experts in Accra. Land Use Policy, Volume 133. 106865. ISSN 0264-8377. https://doi.org/10.1016/j.landusepol.2023.106865.

Ata, A., Kaywan Othman, A., Yahya, P. et al. (2022) The Effects of Check Dams on the Amount and Pattern of Flood using Hydrological Modeling, preprint (Version 1) available at Research Square. https://doi.org/10.21203/rs.3.rs-1992312/v1

Emiroglu, M.E., Ikinciogullari, E., Yalcin, E.E. et al. (2025). Investigation of the flow characteristics of slit check dams using novel models. Appl Water Sci 15, 14. https://doi.org/10.1007/s13201-024-02344-7

Gomez Martin, E., Manez Costa, M., Egerer, S., Schneider, U.A. (2021). Assessing the long-term effectiveness of Nature-Based Solutions under different climate change scenarios. Science of The Total Environment, Volume 794. 148515. ISSN 0048-9697. https://doi.org/10.1016/j.scitotenv.2021.148515.

Johnson, B.A. et al. 2022. Nature-based solutions for climate change adaptation: A systematic review of systematic reviews. Nature-Based Solutions, 2. 100042. ISSN 2772-4115. https://doi.org/10.1016/j.nbsj.2022.100042.

Liu, J., et al. (2023). Suitability Assessment of Small Dams' Location as Nature-Based Solutions to Reduce Flood Risk in Mataniko Catchment, Honiara, Solomon Islands. Sustainability, 15(4), 3313. https://doi.org/10.3390/su15043313

Lupp, G., et al. 2021. Stakeholder Perceptions of Nature-Based Solutions and Their Collaborative Co-Design and Implementation Processes in Rural Mountain Areas—A Case Study From PHUSICOS, Frontiers in Environmental Science, 9. doi: 10.3389/fenvs.2021.678446

Pérez-Corredor, L., Hume, S. E., Alivio, M. B., & Bezak, N. (2024). Exploring the Impact of Nature-Based Solutions for Hydrological Extremes Mitigation in Small Mixed Urban-Forest Catchment. Applied Sciences, 14(24), 11813. https://doi.org/10.3390/app142411813

Piton, G., et al. (2017) Why do we build check dams in Alpine streams? An historical perspective from the French experience. Earth Surf. Process. Landforms, 42: 91–108. doi: 10.1002/esp.3967.

Rosmadi, H. S. B., Ahmed, M. F., Mokhtar, M. B., Halder, B., & Scholz, M. (2024). Nature-Based Solutions (NbS) for Flood Management in Malaysia. Water, 16(24), 3606. https://doi.org/10.3390/w16243606

Yazdi, J., Sabbaghian Moghaddam, M. & Saghafian, B. (2018) Optimal Design of Check Dams in Mountainous Watersheds for Flood Mitigation. Water Resour Manage 32, 4793–4811. https://doi.org/10.1007/s11269-018-2084-4

A multi-source methodological framework for drought monitoring: Integration of remote sensing and meteorological indicators

C. Chatzichristaki[1*], A. Moumtzidou[1], K. Karystinakis[1], I. Gialampoukidis [1], S. Vrochidis[1], I. Kompatsiaris[1], M. Bügelmayer-Blaschek[2], T. Tötzer[2], D. Havlik[2]
[1] Information Technologies Institute (ITI), Centre for Research and Technology Hellas (CERTH), Thessaloniki, Greece
[2]Austrian Institute of Technology (AIT) GmbH, Center for Energy, Vienna, Austria
* e-mail: xrysxat@iti.gr

Introduction

Drought is a prolonged dry period within the natural climate cycle, marked by a lack of precipitation that leads to water shortages, with significant impacts on health, agriculture, economies, and ecosystems (WHO). The impact of drought is expected to gradually increase under global warming prompting numerous in-depth studies on drought conducted in recent years (Cheng et al., 2023). Unlike other natural disasters, drought's impacts are gradual, widespread, and non-structural, resulting in substantial economic and environmental costs (Naumann et al., 2015). Specifically, the Mediterranean countries are particularly vulnerable to drought, with the threat expected to intensify due to the climate crisis.

Research on drought, its severity, and its impact across various fields such as agriculture, forestry, urban trees, and the natural environment has become increasingly important due to climate change. Drought monitoring using remote sensing-derived vegetation indices has been extensively studied. Various vegetation indices serve as crucial tools for monitoring drought conditions. These indices assess vegetation health, water stress, and soil moisture. Additionally, meteorological drought indices are essential tools for measuring and evaluating drought conditions. Meteorological indices are developed using precipitation and evapotranspiration as key inputs and provide information about climatic factors, one more step in determining drought severity and understanding its effects on ecosystems, agriculture, and water resources. Together, these tools provide a solid framework for drought monitoring across multiple domains and time scales, enabling effective decision-making and adaptation strategies.

Materials and methods

Numerous studies have explored the effectiveness of various indices to assess drought conditions in different domains like agriculture and forestry. There are two main categories of indices, spectral and meteorological. Vegetation indices (VIs) provide data on vegetation health and water stress. On the other hand, meteorological indices assess drought from climatic parameters such as precipitation, evapotranspiration, and atmospheric moisture.

The calculation of these indices relies on different data sources. VIs benefit from satellite imagery and particularly from Sentinel-2 data, which are widely used offering high spatial resolution and a revisit time of 5 days. On the other hand, meteorological indices utilize either ground-based observations or reanalysis datasets, such as ERA5 and CERRA, which are widely used due to the lack of a dense network of meteorological stations. Both types of indices have the advantage of being applicable to past and current conditions, enabling retrospective and real-time drought assessments. An overview of the most widely used drought assessment indices, based on their ability to detect drought, is presented in Table 1 (Du et al., 2018; WMO and GWP, 2016).

Table 1. Proposed vegetation and meteorological drought assessment indices.

Vegetation	Meteorological
Normalized Difference Vegetation Index (NDVI)	Standardised Precipitation Evapotranspiration Index (SPEI)
Vegetation Condition Index (VCI)	Vapour-Pressure Deficit (VPD)
Normalized difference water index (NDWI)	Keetch-Byram Drought Index (KBDI)
Land Surface Water Index (LSWI)	
Normalized Difference Drought Index (NDDI)	

Results and concluding remarks

Comprehensive monitoring of drought conditions in rural landscapes requires integrating multi-source data. In recent decades, the ever-growing data availability and the well-established use of geospatial technologies have made large-scale spatiotemporal drought assessment feasible. Our proposed methodological framework is based on Copernicus EO data (Sentinel, reanalysis) and is highly transferable, as it relies on open-access datasets with pan-European coverage.

The main advantage of this approach is its ability to integrate diverse data sources and indicators, providing a multi-dimensional perspective on drought conditions. The VIs are grouped into two categories: greenness and water-related. In terms of greenness indices, NDVI has been widely applied to detect drought by measuring the difference between near-infrared and red reflectance, whereas VCI enhances drought stress assessment by normalizing NDVI values with historical data to determine drought severity in a given region. Water-related VIs such as NDWI, LSWI and NDDI assess moisture availability in vegetation and soil. NDWI assesses water content in vegetation and is considered complementary to NDVI. LSWI, on the other hand, captures changes in vegetation water content and monitors the temporal evolution of flash droughts, providing early warning of water stress. Additionally, NDDI combines NDVI and NDWI to assess vegetation health and water content, quantifying drought intensity.

The meteorological indices (SPEI, VPD and KBDI) provide useful insights on drought monitoring. Specifically, SPEI reflects the impact of temperature on water availability. It is multi-scalar, meaning it can assess drought severity over different time scales (Minea et al., 2022). This flexibility allows it to capture both short-term agricultural droughts and long-term hydrological droughts, making it a valuable tool for monitoring climate-induced changes in water balance. VPD measures the difference between the actual moisture content in the air and the amount it could hold at full saturation; therefore, dry conditions, as indicated by high VPD values, affect plant growth and can lead to reduced yields, lower-quality production, forest tree mortality and increased wildfire occurrences. To that end, it is valuable for agriculture, irrigation scheduling and ecosystem management. As for KBDI, it is a continuous reference scale used to estimate the dryness of the soil and duff layers. It represents the net effect of evapotranspiration and precipitation in producing a cumulative moisture deficiency in deep duff or upper soil layers. Moreover, it has been used for wildfire prediction and is especially linked to the availability of large dead fuels and the increased likelihood of high-severity fire events due to prolonged fuel drying.

Combining vegetation and meteorological indices offers a holistic approach to drought monitoring and assessment, capturing drought dynamics from atmospheric conditions to soil moisture and plant stress. Meteorological indices highlight the predisposition to drought due to climatic factors, while vegetation indices enable the detection of affected, stressed vegetation, offering real-time insights into ecosystem response. The integration of these indices into a technological platform enhances decision-making, providing policymakers and stakeholders with a robust tool for mitigating drought impacts at regional or even national scale.

Acknowledgments: This work was supported by the Horizon research and innovation programme under grant agreement No. 101112728 ClimEmpower.

References

Cheng Y, Zhang K, Chao L, Shi W, Feng J, Li Y. (2023) A comprehensive drought index based on remote sensing data and nested copulas for monitoring meteorological and agroecological droughts: A case study on the Qinghai-Tibet Plateau. Environmental Modelling & Software, 161, 105629. https://doi.org/10.1016/j.envsoft.2023.105629

Du TLT, Bui DD, Nguyen MD, Lee H (2018) Satellite-based, multi-indices for evaluation of agricultural droughts in a highly dynamic tropical catchment, central Vietnam. Water 10(5): 659. https://doi.org/10.3390/w10050659

Minea I, Iosub M, Boicu D (2022) Multi-scale approach for different type of drought in temperate climatic conditions. Natural Hazards 110(2), 1153-1177. https://doi.org/10.1007/s11069-021-04985-2

Naumann G, Spinoni J, Vogt JV, Barbosa P (2015) Assessment of drought damages and their uncertainties in Europe. Environmental Research Letters 10(12): 124013. https://doi.org/10.1088/1748-9326/10/12/124013

World Meteorological Organization (WMO) and Global Water Partnership (GWP), 2016 Handbook of Drought Indicators and Indices. Integrated Drought Management Programme (IDMP), Integrated Drought Management Tools and Guidelines Series 2. Geneva. ISBN 978-92-63-11173-9. http://www.droughtmanagement.info

13th World Congress on Water Resources and Environment (EWRA 2025)
"New challenges in understanding and managing water-related risks in a changing environment"
Palermo, Italy, 24 - 28 June 2025

Development and implementation of a regional flood regression model in Pieria, Greece

S. Bouzos, A. Bournas*, E. Baltas
Department of Water Resources and Environmental Engineering, School of Civil Engineering, National Technical University of Athens, 5 Iroon Polytechniou, 157 80, Athens, Greece
** e-mail: abournas@chi.civil.ntua.gr*

Introduction

Floods and flash floods are becoming an even more concurrent danger. To examine the impact of such events, a complete hydrological analysis is required based on typical principles of rainfall-runoff mechanics. Although recent advances have allowed for more complex and detailed modeling, the complicated nature of the required models and the quantity and quality of the required datasets have made them less attractive for operational usage. Moreover, in cases such as in Greece, where many small ungauged basins are formed due to the extensive coastline, applying typical rainfall-runoff methodology is discouraged mainly because proper calibration of the models cannot usually be performed. To address these issues, this research re-introduces the classical regression modeling analysis, where key flood parameters, such as discharge peak, time to peak, and flood volume, can be estimated using easily accessible variables of a selected basin (Pandey and Nguyen 1999). The model was developed and implemented in the administrative region of Pieria, in northern Greece. The methodology applied can lead to powerful equations that can quickly assess a region's flood susceptibility (Smith et al. 2015) and a quick and accurate estimation of possible incoming rainfall threats, acting as an early warning system tool.

Materials and methods

The study area is the Pieria administrative region near Olympus Mountain in Northern Greece, as shown in Figure 1. The region is susceptible to flooding, with recent floods affecting mainly the lowland areas near the coast. The impact of Olympus Mountain and its proximity to the sea makes it difficult to analyze since it causes many steep, small-scaled basins with quick response. In this analysis, 15 basins were examined to develop the regional regression model, shown in Figure 1. The basin areas range from 8 to 135 km^2, with a mean size of 60 km^2. Basins 1 to 9 are found on the Olympus Mountain foothills, featuring a mean area of 21.2 km^2 and a slope of 55%, whereas basins 10 to 15 are found on the west and northern side, with 102 km^2 and 27% mean area and slope respectively. The largest basin is basin 10, which is 387 km^2.

For each basin, the following rainfall-runoff methodology is applied. First, the geomorphological analysis of each basin is performed to calculate the Unit Hydrograph (UH) of each basin. The Soil Conservation Service (SCS) dimensionless UH is used, where the main parameter required is the basin's lag time, usually taken as 60% of the basin's time of concentration (TC). The Giandotti equation was used to calculate the TC, which performs well in Greece, even though some basins are small for the method. This issue, however, is expected to have a limited impact since the basin size is included in the regression model, and consistency is preferred. Following this, the SCS-Curve Number (CN) is calculated for each basin based on the hydrological soil group map and land use datasets. Concerning the design storm, the rainfall height is calculated for a given return period and duration through the state-wide known intensity-duration-frequency (IDF) equations, and the alternating block method was used to derive the hyetograph. Finally, the HEC-HMS software was used to simulate the design storm and evaluate the flood hydrographs for each case. For each hydrograph, the three parameters, i.e., the flood peak, time to peak, and flood volume, were selected for regression analysis. The regression analysis followed an in-depth analysis to identify the most crucial characteristics to extract the above variables. The mathematical expression used is non-linear in the form of a power-form function, as shown in eq.1,

$$X = \alpha_0 A_1^{\alpha 1} A_2^{\alpha 2} A_3^{\alpha 3} \ldots A_v^{\alpha v} \varepsilon_0 \quad (1)$$

where X, the variable in question, α_0, α_1, α_2…., α_v are the model parameters, A_0, A_1, A_2…., A_v are the selected characteristics and ε_0 is the multiplicative error term. The independently selected characteristics examined were the basin area (A), mainstream length (L), the mean elevation, Hmean, rainfall intensity (i), rainfall height (h), the CN value, the mean slope, and the time of concertation (tc). The analysis was performed for the return period T=50. Finally, random basins were selected as a "calibration" set, whereas two non-neighboring basins were selected as the "validation" set.

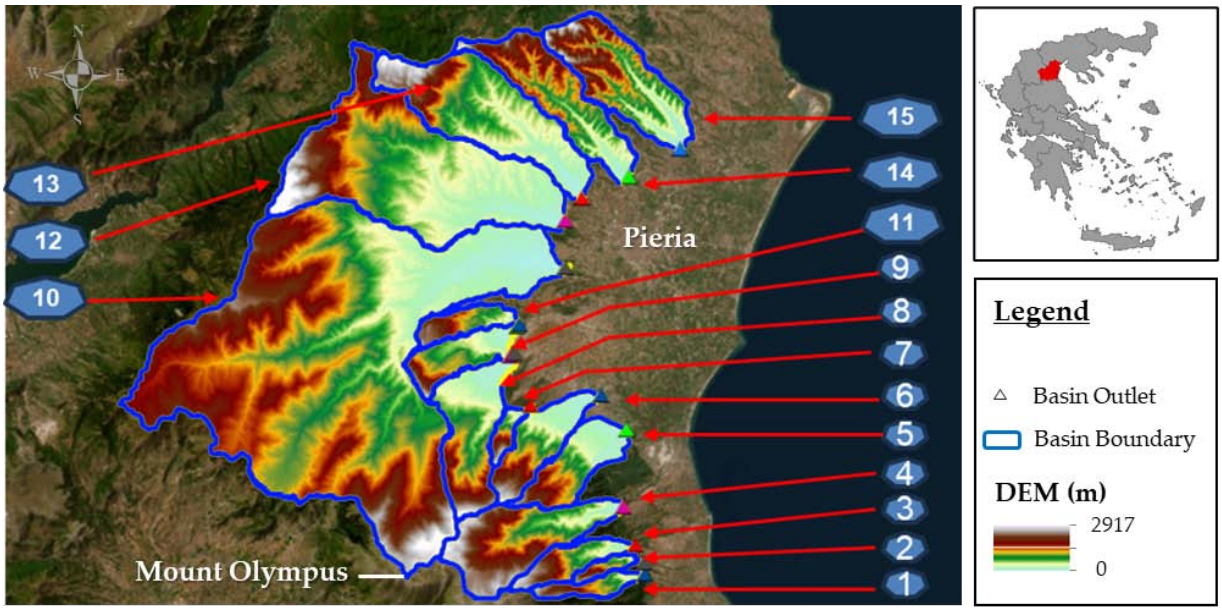


Figure 1. Study Area and the basins examined.

Results and concluding remarks

The hydrological analysis led to the calculation of the crucial variables. While in almost all basins, the rainfall intensity was equal to approximately 18mm/h, the peak discharge, excluding basin 10, ranged from 3.50 to 420 m^3/s, while the time to peak ranged from 1.25 to 5.75 hours, and the flood volume ranged from 24 to 9000 hm^3. Basin 10 featured the highest numbers with a peak discharge of 1051 m^3/s, time to peak of 5.45 h, and 24310 hm^3 flood volume. Overall, the "Olympus" basins featured a unit discharge (Qpeak/Area) of 0.4-4 $m^3/s/km^2$, whereas the rest featured a unit discharge of 4 $m^3/s/km^2$ on average.

Finally, the following equations were extracted through the regression analysis, which featured the least possible characteristics and highest statistical scores.

$$Q_{max} = A^{1,5248} * H_{mean}{}^{(-0,9125)} * i^{1,2502} * CN^{0,2921} \quad (2)$$

$$t_{up} = A^{0,0871} * H_{mean}{}^{(-0,1525)} * i^{(-0,8084)} * CN^{0,9659} \quad (3)$$

$$V_{disch} = A^{1,5417} * H_{mean}{}^{(-0,8544)} * i^{0,7172} * CN^{1,1999} \quad (4)$$

The R-squared was calculated to be 0.80, representing a good fit, while the RMSE exhibited to the validation basins were only 14%, 7%, and 13% for peak discharge, time to peak, and flood volume, respectively. Overall, the regional model exhibited good results in both the calibration and validation set, which makes it a valuable tool for estimating the key flood characteristics of any other basin size in the region and is useable for early warning system applications.

References

Pandey GR, Nguyen V-T-V (1999) A comparative study of regression based methods in regional flood frequency analysis. Journal of Hydrology 225:92–101. https://doi.org/10.1016/S0022-1694(99)00135-3

Smith A, Sampson C, Bates P (2015) Regional flood frequency analysis at the global scale. Water Resources Research 51:539–553. https://doi.org/10.1002/2014WR015814

HAMR system: seasonal discharge prediction

A. Vizina[1,2*], P. Pavlík[1,2], M. Hanel[1,2], I. Georgievová[1,2], A. Beran[1,2]
[1] T.G. Masaryk Water Research Institute, Prague, Czech Republic,
[2] Czech Univerity of Life Sciences, Faculty of Environment, Prague, Czech Republic
* e-mail: adam.vizina@vuv.cz

Introduction

Water scarcity and drought events are increasing in the Czech Republic and globally, often reaching disaster levels. Their frequency, particularly in Central Europe, is linked to climate change, affecting even regions previously unaffected by drought. Although water consumption has halved since 1990, this mitigating trend is fading. In 2015, Czech municipalities faced water supply issues, with droughts affecting agriculture, forestry, and industry. The number of moisture-deficient days has risen, threatening future water availability and quality. Over the past decade, research institutions have focused on drought prediction, leading to the development of a forecasting tool.

System and seasonal predictions play a crucial role in managing natural resources, including water. Predicting hydrological and meteorological conditions enables proactive planning to mitigate risks associated with droughts, floods, and water scarcity. The HAMR (Hydrological, Agronomical, Meteorological, and Retention) system represents an advanced example of integrated prediction systems that assess and forecast drought conditions and discharges across various domains. The results are available on website hamr.chmi.cz.

Materials and methods

The HAMR (Vizina et al., 2018) tool is based on a combination of a soil moisture balance model SoilClim (Hlavinka et al., 2011), a hydrological balance model BILAN (Vizina et al., 2015; Melišová et al., 2020), and a model of water management systems of river basins WATERES (Georgievová et al., 2023), its purpose being to produce models of probable developments of the hydrological situation approximately eight weeks ahead. The system´s structure is shown in Figure 1. Its components are described in detail below. The system´s name is HAMR, which is an abbreviation containing all the components of the system, namely: Hydrology, Agronomy, Meteorology, and Retention.

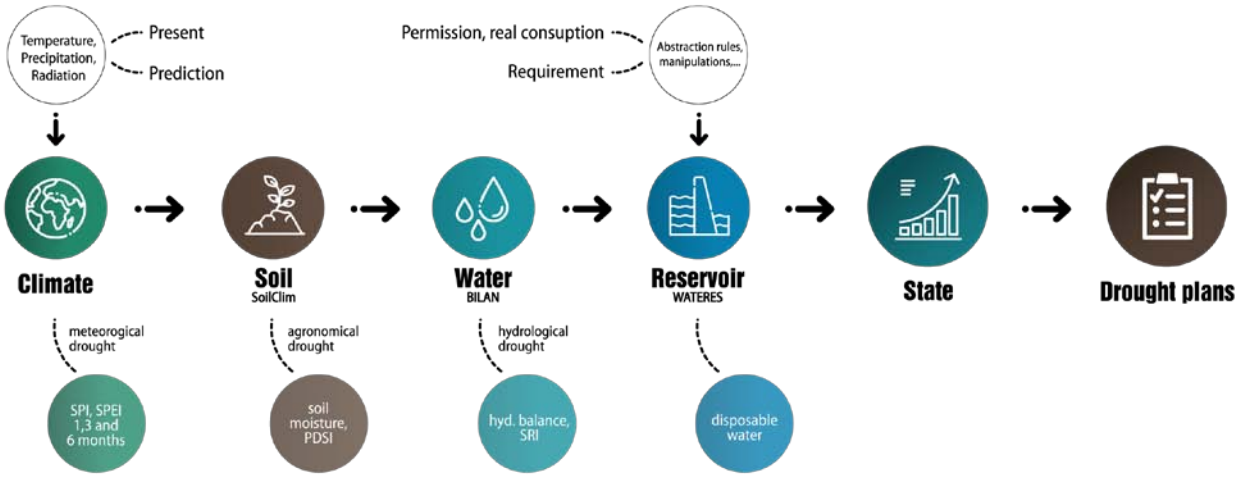


Figure 1. HAMR scheme

The climate short term forecast is based on five prediction models: IFS – European Centre for Medium-Range Weather Forecasts (ECMWF); GFS – Global Forecast System of the U.S. National Center for Atmospheric Research; GEM (CMC) – Model of the Canadian Meteorological Centre; UK (GUM) – Global model of the UK Met Office; and ARPEGE – Model of the French Meteorological Service. Long-term prediction (16 weeks) is based on statistical methods using historical climate time series.

Results and concluding remarks

The natural runoff heights for individual water bodies are converted into the SRI (Standardized Runoff Index), analogous to SPEI (Standardized Precipitation Evapotranspiration Index). Water availability for specific water bodies is shown in Figure 2. These values are modeled using the WATERES model, adjusted based on current observations. The forecast is then generated for an sixteen-week period (see Figure 2, which also displays the time series with predictions). Additionally, water availability can be viewed based on M-day flows.

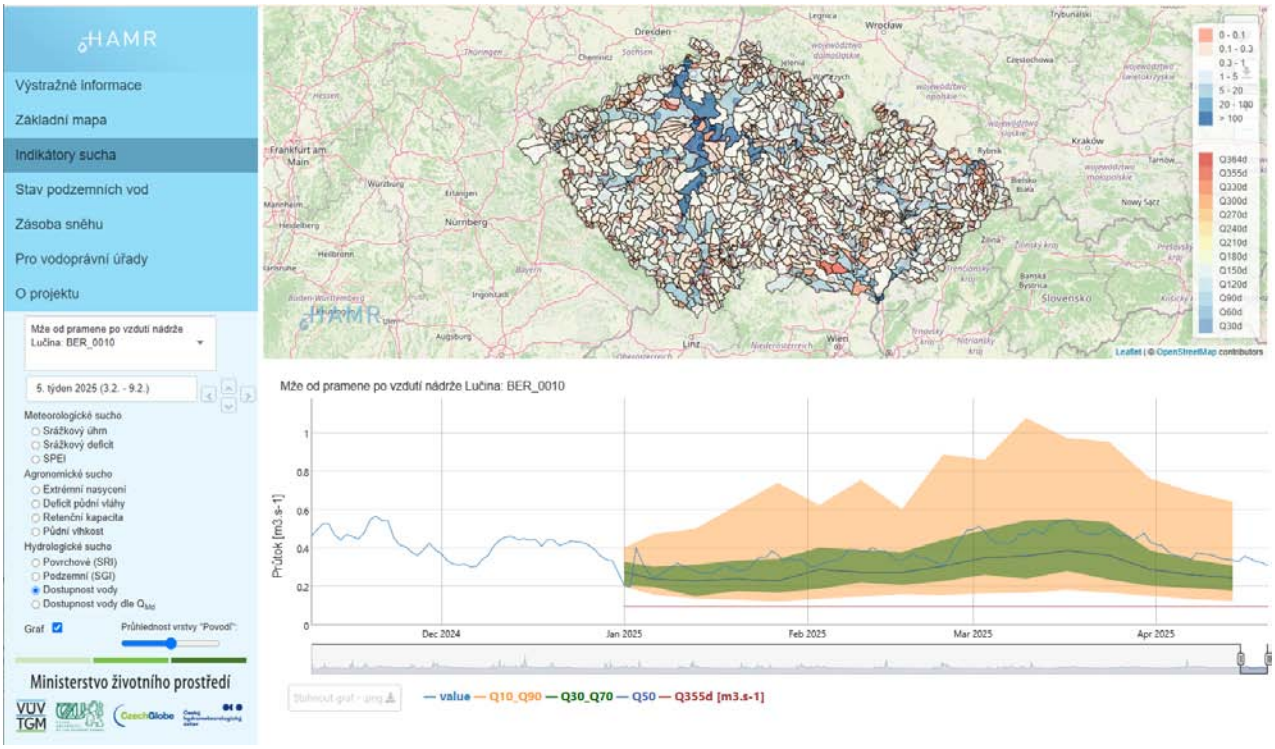


Figure 2. Map window and prediction of water availability

Acknowledgments: This research was supported by projects SS02030040 “Prediction, Evaluation and Research for Understanding National sensitivity and impacts of drought and climate change for Czechia (PERUN)” and SS02030027 “Water systems and water management in the Czech Republic under climate change conditions (Water Centre)” funded by the Technology Agency of the Czech Republic.

References

Georgievová, Irina, et al. Streamflow simulation in poorly gauged basins with regionalised assimilation using Kalman filter. Journal of Hydrology, 2023, 620: 129373.

Hlavinka, P. et al. Development and evaluation of the SoilClim model for water balance and soil climate estimates. Agricultural Water Management, 2011, 98.8, p. 1249–1261.

Melišová, Eva, et al. The role of hydrological signatures in calibration of conceptual hydrological model. Water, 2020, 12.12: 3401.

Vizina, A., Horáček, S. A Hanel, M. Nové možnosti modelu Bilan. VTEI, 2015. 55:. 4–5.

Vizina, A., Hanel, M., Trnka, M., Daňhelka, J., Gregorievová, I., Pavlík, P., and Heřmanovský, M. Hamr: Online drought management system – operational management during a dry episode. Water Management Technical and Economical Information Journal, 2018, 60(5): 22–28.

Meteorological drought assessment using gridded data: Case study of Croatia

J.F. Santos[1*], L. Tadic[2], M.M. Portela[3,4], T. Brlekovic [2], L. Espinosa[5]
[1] CREATE – Center for SciTech Research in Earth System and Energy, Polytechnic Institute of Beja, Portugal
[2] Faculty of Civil Engineering and Architecture, University of Osijek, Croatia
[3] Instituto Superior Técnico, Universidade de Lisboa, Portugal
[4] CERIS – Civil Engineering Research and Innovation for Sustainability Research, Lisboa, Portugal
[5] Association of the Instituto Superior Técnico for Research and Development (IST-ID)
* e-mail: joaof.santos@ipbeja.pt

Introduction

Droughts have been increasing in the Balkan region, with unusual hydro-climatological conditions that clearly differ from the rest of Europe. Some studies have been carried out in Croatia, notably the work of Cindrić et al. (2016) who analysed an extreme drought by examining its severity using the Standardised Precipitation Index (SPI) (McKee et al., 1993) with a secular dataset or the work of Brleković & Tadić (2022) who compare the SPI, Standardized Precipitation Evapotranspiration Index (SPEI) (Vicente-Serrano et al., 2010) and the Standardized Groundwater Level Index (SGI) (Bloomfield & Marchant, 2013) on different time-scales. Due to the insufficient number of observation records of long time series of climatic variables covering the continuum of Croatia, the use of a highly dense and complete set of gridded meteorological data could clearly contribute to overcoming these limitations and greatly benefit the assessment of drought characteristics.

Following the works of Santos et al. (2010), Espinosa & Portela (2022) for Portugal and more recently Di Nunno & Granata (2023) for southern Italy, that allowed the identification of well-distinguished homogeneous regions with different spatial and temporal patterns of drought, the main contribution of this research is the realisation of a long-term analysis, using well-established and validated methodologies, to investigate the phenomenon of drought in Croatia, representing the first case in which complete long-term data has been used for this purpose. The results are intended to be of practical value for water resources planning and management activities, providing information that can be used to create risk-based drought management plans, but also to understand the link between drought risk and climate variability.

Materials and methods

By considering the monthly precipitation and temperature time series obtained from the E-OBS dataset, the SPEI at 6 and 12 month time scales were calculated over a period of 73 years, from September 1950 to July 2022.

A comprehensive characterisation of droughts in Croatia is achieved by using a combined set of classification methods, such as Principal Component Analysis (PCA) and Cluster Analysis (K-means), to determine the spatial variability of drought characteristics, temporal behaviour by examining changes in the annual occurrence rate of drought events with a kernel occurrence rate estimator (KORE) and the characterisation of trends which was approached based on the modified Mann-Kendall test (MMK). All this was done using robust techniques that are commonly used in the fields of climatology and hydrology.

Results and concluding remarks

Some of the study's main conclusions, presented in Figure 1, are: (1) PCA and K-means shows three homogeneous drought regions: Central North region (D1), Eastern region (D2) and Southern region (D3); (2) D1 and D2 showed an upward trend in the percentage of areas affected by drought, but in D3 a negligible trend was obtained for SPEI6 and a downward trend for SPEI12. Both zones D1 and D2 have large tracts of rainfed agricultural land and pastures, resulting in high ecological vulnerability; (3) D1 experiences an

increase in the drought occurrence rate till 2010 and some decrease in the last 10 years period. D2 exhibits a generalized continuous increase in the drought occurrence rate in the study period, in all drought categories and SPEI time-scales. In the D3, a decrease in the drought occurrence rate was obtained. An increase in the number of drought occurrences over the years means progressively more periods of time with negative water balances which induces to bigger challenges on water management practices; (4) A generalised shift towards greater susceptibility to drought conditions in most areas of D1 and D2 was obtained with the MMK test with strong statistical significance in both SPEI's. Given the Sen´s slope values obtained from the trend analysis, more intense drought events are expected in those areas. In D3, the trend into less susceptibility to drought conditions spatially follow the mountainous areas of the Dinarides but with less statistical significance (Istria and some coastal parts of Zadar and Sibenik-Knin are the exceptions).

In general terms, the west is becoming less susceptible to drought while the east is tending to become more prone to have an intensification of drought events, showing a greater increase in the areas affected by drought and an increasing rate of occurrence of the number of annual droughts. Although the Mediterranean region is usually at the center of drought research, it is in the mainly agricultural mainland of Croatia that drought conditions seems to have worsened.

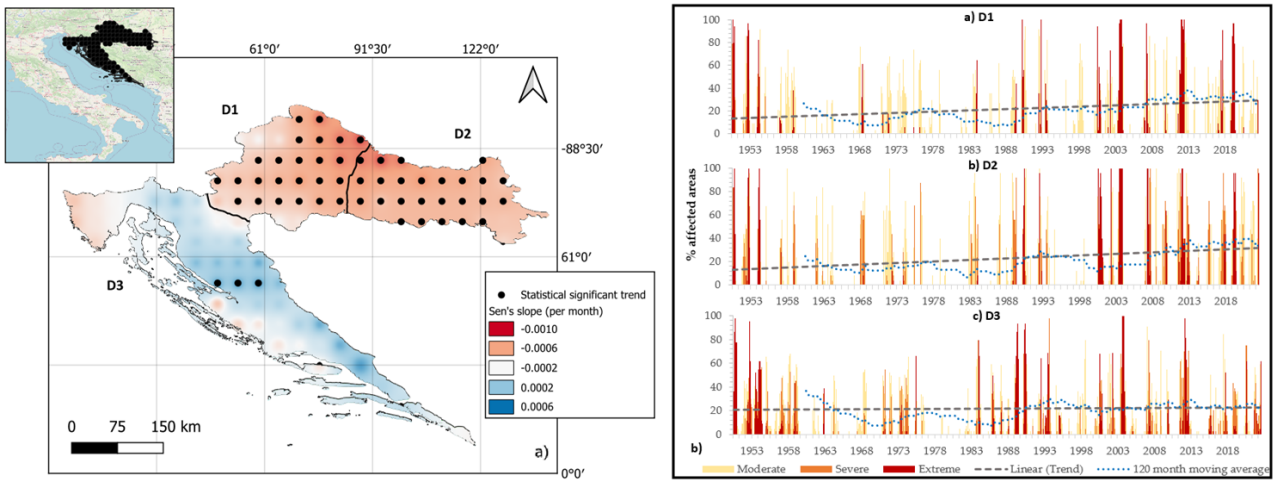


Figure 1. Spatio-temporal results for SPEI6. a) Drought trends based on the MMK test. Black dots represent the statistically significant trends at the 0.05 significance level. b) Temporal evolution of the percentage of area affected by different drought categories in each of the homogeneous regions.

References

Bloomfield, J.P., Marchant, B.P. (2013) Analysis of groundwater drought building on the standardised precipitation index approach. Hydrology and Earth System Sciences, 17(12), 4769–4787. https://doi.org/10.5194/hess-17-4769-2013

Cindrić, K., Telišman Prtenjak, M., Herceg-Bulić, I., Mihajlović, D., & Pasarić, Z. (2016) Analysis of the extraordinary 2011/2012 drought in Croatia. Theoretical and Applied Climatology, 123(3–4), 503–522. https://doi.org/10.1007/s00704-014-1368-8

Di Nunno, F., & Granata, F. (2023) Spatio-temporal analysis of drought in Southern Italy: A combined clustering-forecasting approach based on SPEI index and artificial intelligence algorithms. Stochastic Environmental Research and Risk Assessment, 37(6), 2349–2375. https://doi.org/10.1007/s00477-023-02390-8

Espinosa, L. A., & Portela, M. M. (2022) Grid-Point Rainfall Trends, Teleconnection Patterns, and Regionalised Droughts in Portugal (1919–2019). Water, 14(12), 1863. https://doi.org/10.3390/w14121863

McKee, T. B., Doesken, N. J., & Kleist, J. (1993) The relationship of drought frequency and duration to time scales. Volume 17, 179–183.

Santos, J. F., Pulido-Calvo, I., & Portela, M. M. (2010) Spatial and temporal variability of droughts in Portugal. Water Resources Research, 46(3). https://doi.org/10.1029/2009WR008071.

Vicente-Serrano, S. M., Beguería, S., & López-Moreno, J. I. (2010) A Multiscalar Drought Index Sensitive to Global Warming: The Standardized Precipitation Evapotranspiration Index. Journal of Climate, 23(7), 1696–1718. https://doi.org/10.1175/2009JCLI2909.1

Brleković, T., & Tadić, L. (2022) Hydrological Drought Assessment in a Small Lowland Catchment in Croatia. Hydrology, 9(5), 79. https://doi.org/10.3390/hydrology9050079.

Cynefin categories meet ensemble forecasting: A novel framework for forecast analysis

Z. Bovermann*, J. Dietrich
Institute of Hydrology and Water Resources Management, Leibniz University Hannover, Hannover, Germany
** e-mail: bovermann@iww.uni-hanover.de*

Introduction

Ensemble forecasting plays a crucial in flood management by providing multiple equally probable scenarios, which help to assess uncertainty and inform decision-making processes. Yet, the devastating floods in Europe, including those in the Ahr Valley (June 2021) and Valencia (October 2024), have highlighted persistent challenges in effectively utilizing these predictions when disseminating warnings.

In this research, we address these challenges by incorporating the Cynefin framework, a decision-making model that categorizes scenarios into "clear," "chaotic," "complex," and "complicated" domains (French, 2013). This framework is used to better understand and act in situations of high risk and high uncertainty. By defining these categories clearly from the outset, the aim is to enhance sense-making for decision-makers (Constable et al., 2022). Additionally, this approach builds upon existing methodologies of clustering techniques for ensemble forecast to derive thresholds for landslides (e.g., Sajinkumar et al., 2020).

Unlike traditional statistical methods, such as the Fractions Skill Score or the Brier Score, which primarily focus on systemic performance, our approach integrates behavioural insights to uncover decision-relevant patterns within ensemble forecast analyses. The intention is to provide a more nuanced evaluation of forecast usability, thereby improving the skill assessment of forecast products from a decision-maker's point of view as suggested by Speight et al. (2023).

The findings aim to reshape decision-making processes in flood risk management, aligning forecast information more closely with human risk perception and response.

Materials and methods

The study area, the Ahr Valley features a descending V-shaped landscape from 300 to less than 180 meters, extending southwest to northeast. Influenced by Devonian greywacke-slate, its width and steepness fluctuate, featuring narrow rocky sections that give way to a broad plain near the Rhine. The slopes are mainly forested, while the valley floor supports grasslands and vineyards, transitioning to arable land towards the Rhine.

This study focuses on the ICON-D2 ensemble rainfall forecasts with 48 hours lead-time, for the notable flood event that occurred in the Ahr Valley in July 2021. This event was selected for its significant impact and because prior research has explored its predictability, providing a comprehensive backdrop for our analysis (Saadi et al., 2023).

The ICON-D2 forecasts, developed by the German Weather Service (Deutscher Wetterdienst – DWD), consist of 20 ensemble members updated every three hours. For this study, these forecasts were regridded onto a regular rectangular grid and normalized.

Subsequently, threshold-based radial clustering was applied to categorize forecasts within the Cynefin framework's context, focusing on "clear," "chaotic," "complex," and "complicated" categories. The "confused" category, deemed indistinct, was excluded from automated categorization and left to expert judgment as necessary. This categorization aims to illuminate patterns in forecast uncertainty and usability that traditional metrics might overlook. The clustering is guided along radii. This results in a semi-circular or fan-like distribution of the data points, with the "clear" category concentrated near the origin and the other categories radiating outward.

Results and concluding remarks

Mapping the cluster results unveils regions where decision-making is more challenging. By examining clusters adjacent to chaotic areas, the map facilitates operational planning and decision-making.

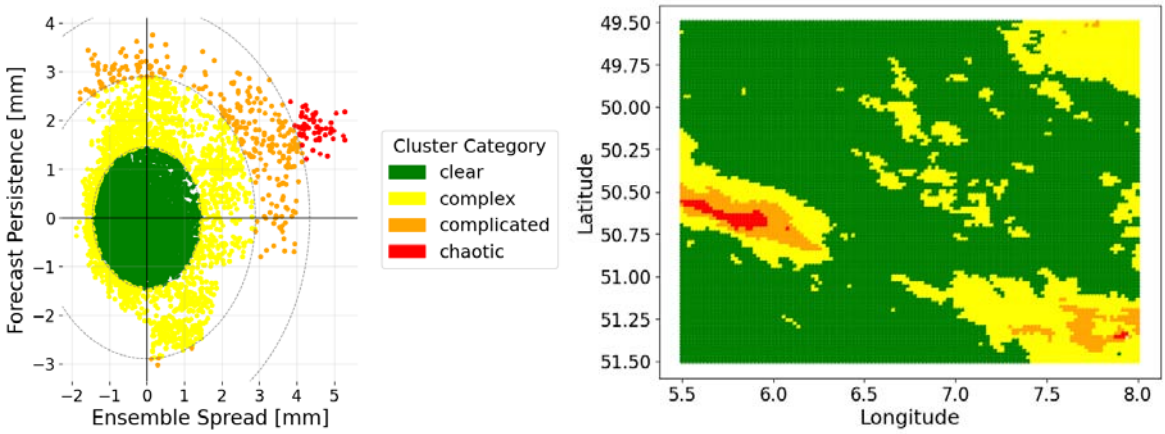


Figure 1. Clustering results for the last timestep using ICON-D2 rainfall forecast from 2021-07-13 00:00 until 2021-07-13 18:00 (left) and the spatial distribution (right).

Figure 1 illustrates the clustering results for the last timestep using the ICON-D2 rainfall forecast from 2021-07-13 00:00 to 2021-07-13 18:00. This moment represents a critical decision point for planners contemplating evacuations before the flood expected on July 14, 2021.

The clustering analysis reveals a high density of data points in the "clear" (green) region, which gradually decreases through the "complicated," "complex," and into the "chaotic" (red) regions.

Regions marked in red indicate "chaotic" conditions and are characterized by a high forecast spread and persistence, suggesting difficult to interpret forecasts in these areas. This difficulty necessitates special attention or contingency plans, potentially through adaptive strategies. Importantly, the non-random distribution of clusters highlights that forecast uncertainties are linked to specific geographic or meteorological patterns.

By integrating clustering results with spatial visualization, stakeholders can readily identify zones of consistent forecast reliability and areas with prominent difficulty to make decisions. This enhanced understanding aids in making well-informed decisions related to emergency preparedness, resource distribution, and targeted forecast improvements, such as investing in additional observations or modelling efforts in regions marked by high uncertainty.

Next, engaging with decision-makers to discuss their perception of these clusters could further guide the categorization process. Understanding their challenges and decision-making criteria will be crucial for transforming current practices to a more effective decision-making framework, especially in managing the risks associated with "chaotic" conditions.

References

Constable AJ, French S, Karoblyte V, Viner D (2022) Decision-Making for managing Climate-Related risks: Unpacking the decision process to avoid “Trial-and-Error” responses Frontiers in Climate 4. https://doi.org/10.3389/fclim.2022.754264

French, S (2013) Cynefin, Statistics and Decision Analysis. J. Operat. Res. Soc. 64: 547–561. https://doi.org/10.1057/jors.2012.23

Saadi M, Furusho-Percot C, Belleflamme A, Trömel S, Kollet S, Reinoso-Rondinel R (2023) Comparison of three Radar-Based precipitation nowcasts for the extreme July 2021 flooding event in Germany. Journal of Hydrometeorology 24(7): 1241–1261. https://doi.org/10.1175/jhm-d-22-0121.1

Sajinkumar KS, Rinu S, Oommen T, Vishnu CL, Praveen KR, Rani VR, Muraleedharan C (2020) Improved rainfall threshold for landslides in data sparse and diverse geomorphic milieu: a cluster analysis based approach. Natural Hazards 103(1): 639–657. https://doi.org/10.1007/s11069-020-04004-w

Speight L, Stephens E, Hawker L, Baugh C, Neal J, Cloke H, Grey S, Titley H, Marsden K, Sumner T, Ficchi A, Prudhomme C, Archer L, Bazo J, Dambo J, Dolan S, Huhn AL, Moschini F, Savage J, Smith A, Towner J, Wanzala M (2023) Recommendations to improve the interpretation of global flood forecasts to support international humanitarian operations for tropical cyclones. Journal of Flood Risk Management 18(1). https://doi.org/10.1111/jfr3.12952

An integrated strategy for improving drinking water supply system resilience to regional drought

F.Zanello*, P.Martinis, V. Baù, D. Russo
Idrostudi S.r.l.,Trieste, Italy
** e-mail: zanello@idrostudi.it*

Introduction

Over the past few years, the increasing frequency of droughts in Friuli Venezia Giulia region, Italy, has caused significant depletion in springs discharges and groundwater levels in several wells, leading to an urgent and serious water security crisis. Notably, the severe drought of 2022 had a substantial impact on the agricultural sector, and its effect on the drinking water system, though minimal, requires future attention (ARPA, 2023, Lippi et al., 2023). Drought has become a significant global issue, exacerbating water scarcity and amplifying existing risks to sustainable development. Climatic variations and unsustainable water usage are contributing to the increasing frequency of drought conditions (e.g., Bevacqua et al., 2024), highlighting the need for accurate drought prediction and strategic interventions.

To effectively address potential future water crises in the Friuli Venezia Giulia region, it is essential to develop an integrated strategy that enables pre-emptive management and monitors the water resources usage, ensuring a reliable drinking water supply while preserving water quality in response to drought conditions. This study paves the way to a strategic plan with swift, practical measures that local institutions and integrated water service managers should implement in the near future to prepare for drought events and enhance the drinking water supply resiliency.

Materials and methods

For establishing a robust and shared approach to safeguard drinking water resources, an evaluation of the current technical regulations, existing plans in Italy, and the scientific literature on water security was carried out. This was followed by a review of the general and specific characteristics of the regional territory and of the water supply and distribution systems of concern.

Subsequently, a statistical analysis of the available hydrologic data was performed, along with a thorough assessment of the feasibility of calculating the Standardized Precipitation Index (SPI) (WMO, 2012), the Standardized precipitation evapotranspiration index SPEI (Beguería et al, 2013), the Standardized Groundwater Level Index (SGI) (Bloomfield and Marchant, 2013) and the return periods of past drought events given the available databases for the examined territories.

To identify the types of water usages to prioritize in case of an emergency, it is crucial to implement specific selection criteria that consider the most significant customers in terms of service continuity needs, strategic importance of functions, and potential water demand. Therefore, after reviewing the regional water supply systems, a critical analysis of water management practices was also undertaken, analysing both alert and criticality scenarios. The critical socio-economic and political stakes tied to proactive planning were also highlighted.

Based on these analyses and insights, a proposal for an Operational Plan for a Drinking Water Crisis was then developed, outlining rules, strategies, and responsibilities for monitoring and responding to the impacts of drought on the Integrated Water Service in the regional territory.

Results and concluding remarks

Though not immediately critical, the impact of drought on the drinking water system of Friuli Venezia Giulia Region warrants future attention. The findings of the study highlight that the complex, non-stationary nature of drought precludes the straightforward application of extreme value analysis, which is

commonly used in engineering practice to determine return periods for rainfall data.

Therefore, the results encourage water supply systems managers and experts to embrace a methodological shift that starts with redesigning the current hydrological monitoring system for the assessment of Standardized Indexes for specific sites. The application of advanced methods for time series analysis, new hydrogeological studies, comprehensive evaluation of key water springs, climate modelling and pollution monitoring are also deemed necessary to further improve the knowledge of the system and enhancing preparedness.

Additionally, a thorough risk assessment based on quantitative data is essential in order to establish tiered alert levels corresponding to the severity of drought conditions. The risk assessment gives rise to a plan for drinking water security, centred on a scalable monitoring system (i.e., regular, increased and emergency monitoring) that adjusts according to drought severity and water availability (Figure 1). The involvement of stakeholders in a coordinated effort to enhance water infrastructure is both envisioned and recommended, together with public awareness campaigns on drought and sustainable water usage. All these initiatives will support advanced measures like legal restrictions and system integrations in critical scenarios to build a resilient, integrated drinking water system that warrants sustainable water use and long-term water security.

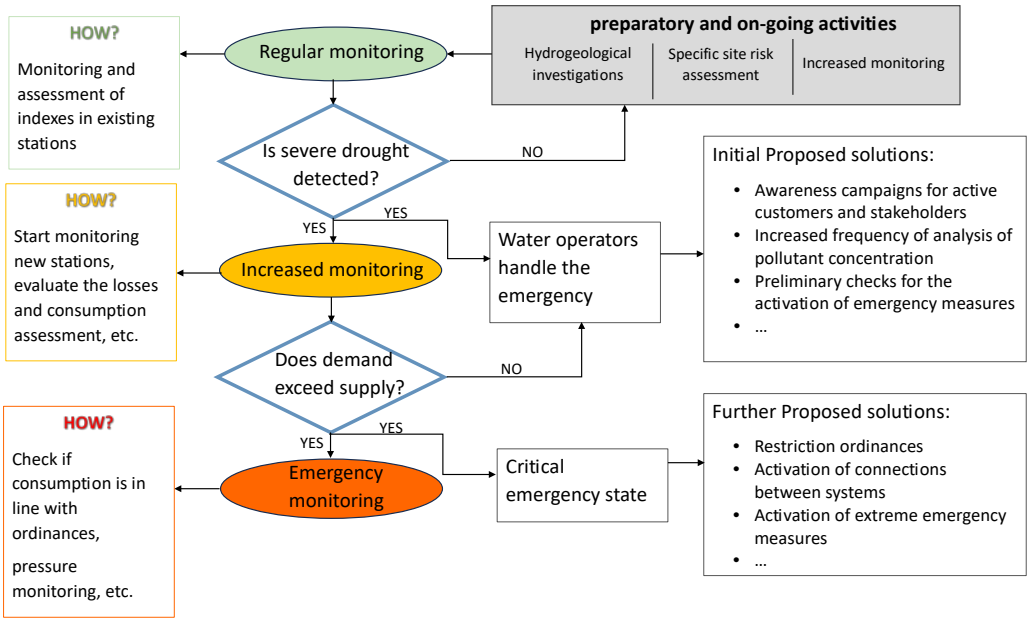


Figure 1. Multi-pronged approach for an integrated drinking water system based on an action plan with tiered alert levels to assess drought quantitatively and dynamically respond to the fluctuation of water management demand in a changing climate.

It would be valuable to extend the application of the methodology proposed in the present study to other contexts, as it could serve as a cornerstone for re-evaluating current engineering methodologies and setting new standards for the resilience of water infrastructure against drought conditions

References

ARPA FVG. (2023). METEO.FVG Report n.13/2022 – Riepilogo Anno 2022, ARPA FVG

Beguería, S., Vicente-Serrano, S. M., Reig, F. and Latorre, B. (2014), Standardized precipitation evapotranspiration index (SPEI) revisited: parameter fitting, evapotranspiration models, tools, datasets and drought monitoring. International Journal of Climatology. 34(10):3001-3023. https://doi.org/10.1002/joc.3887

Bevacqua, E., Rakovec, O., Schumacher, D.L. et al. (2024) Direct and lagged climate change effects intensified the 2022 European drought. Nat. Geosci. 17, 1100–1107. https://doi.org/10.1038/s41561-024-01559-2

Bloomfield, J. P. and Marchant, B. P. (2013): Analysis of groundwater drought building on the standardised precipitation index approach, Hydrol. Earth Syst. Sci., 17: 4769–4787. https://doi.org/10.5194/hess-17-4769-2013.

Lippi, F., Iervolino, D., and Casagrande G. (2023). Stato delle Risorse idriche in Friuli Venezia Giulia. Technical report, Servizio Gestione Risorse Idriche, Regione Autonoma Friuli Venezia Giulia.

World Meteorological Organization, (2012) Standardized Precipitation Index User Guide, World Meteorological Organization (WMO), Geneva.

Evaluation of agro-hydrological sub-seasonal forecasting within two extremely wet and dry seasons in Northern Germany 2017/2018

E. Fallah-Mehdipour, J. Dietrich*
Leibniz University Hannover, Institute for Hydrology and Water Resources Management
** e-mail: dietrich@iww.uni-hannover.de*

Introduction

Irrigation advise for farmers in Northern Germany today relies on short-term weather forecasts, typically with one week lead time, which limits their ability to prepare for longer extreme events. Sub-seasonal to seasonal (S2S) climate forecasts extend the lead time but show higher uncertainty. S2S and its capacities have been discussed and developed in literature, e.g., Kolachian and Saghafian (2019), Musonda et al. (2021), Graham et al. (2022) and Malik and Mishra (2024). Most of the mentioned literature on the application of S2S in water management focuses on a single climate variable or several climate variables separately. However, many natural phenomena are inherently dependent on multiple climate factors. In these phenomena, not only the uncertainty of a single type of variable is important, but also the uncertainties of other climate variables may accumulate.
Agricultural modelling in water management is affected by uncertainties in climate variables, especially in forecasting irrigation water demand. In this study, the uncertainty of irrigation estimations with S2S forecasts was investigated for an experimental agricultural field (Hamerstorf), which serves as test area for developing irrigation advises for the Federal State of Lower Saxony. In this field, different crops are planted, fertilized and irrigated with different irrigation scenarios. Figure 1 shows the annual crop yield of winter wheat for irrigated and non-irrigated scenarios. The two years 2017 and 2018 faced extreme conditions with 2017 being very wet, where irrigation did not increase yield (was not necessary), and with 2018 being very warm and dry, where there is a significant difference (55 percent) between the crop yields of the irrigation and no irrigation scenarios. The main research question is how accurate irrigation water demand can be forecasted by a chain of an S2S meteorological and an agro-hydrological model with lead times of one to six weeks in 2017 and 2018 as the two most extreme years of the experimental records.

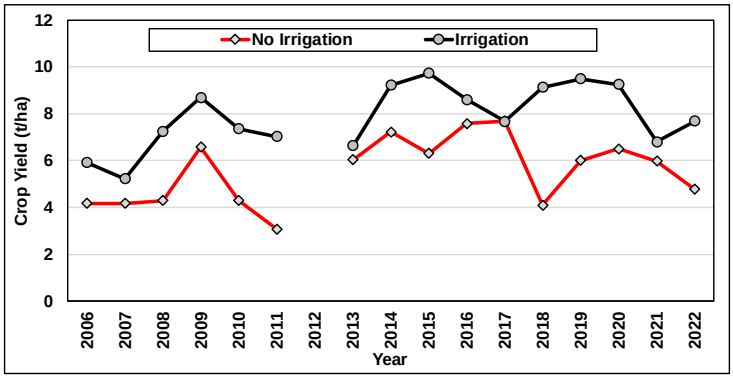


Figure 1. Annual winter wheat yield for the irrigated and non-irrigated scenarios (data source: Fachverband Feldbewässerung)

Materials and methods

The soil, water, atmosphere and plant (SWAP) model was calibrated by using data from the experimental field, including time of sowing and harvesting, time and amount of fertilizing, different irrigation scenarios and crop yield for 2006-2022. The auto-irrigation option of SWAP was used. The model was calibrated to minimize the differences between simulated and observed irrigation and simulated and observed soil moisture. Thus, the calibrated model can be applied to forecast irrigation based on climate.

Then, SWAP was driven by ECMWF S2S reforecast ensembles to simulate soil moisture, crop growth and irrigation water demand with lead times of up to six weeks. Different from previous studies evaluating S2S forecasts, we investigated precipitation, dew point temperature, minimum and maximum temperature, solar radiation, and wind speed to determine irrigation schedules and volumes. The results obtained were analysed using error criteria, such as the percent bias (Equation (1)) between observed and modelled irrigation for winter wheat for the extremely wet year 2017 and the dry year 2018.

$$PBIAS_w = \frac{\sum_{e=1}^{NE} \frac{\sum_{t=1}^{NT} SI_{t,e} - I_t}{\sum_{t=1}^{NT} I_t}}{NE} \qquad \forall w = 1, \dots, 6 \quad e = 1, \dots, NE \tag{1}$$

in which, *PBIASw* = percentage of bias for each week ahead (*w*=1, …, 6), $SI_{t,e}$ = simulated irrigation at time step t in the irrigation season for ensemble member *e*, I_t = Observed irrigation at time step *t* in the irrigation season, *NT* and *NE* = number of time steps and ensemble members, respectively.

Results and concluding remarks

By using the combination of the SWAP and the S2S ensemble with daily time steps for 6 weeks ahead and updating the ensembles weekly, the PBIAS of irrigation estimation in 2017 and 2018 is increasing with lead time (Figure 2). However, for the wet year, future irrigation water demand was overestimated and for the dry year it was underestimated by the S2S model prediction. Where it is obvious that the accuracy of simulated irrigation significantly declines with increasing lead time, the opposite direction of the PBIAS in wet and dry years confirms that the S2S models tend to simulate climatology well when reaching out to the period after the ca. two weeks covered by weather forecast. Even though it might be seen as a desired behaviour, it indicates that forecasting irrigation water demand particularly in humid regions during years with extreme climate still has limited capabilities for operational real-time services. Further work will investigate if better information can be extracted from the ensembles by selecting subsets of the members.

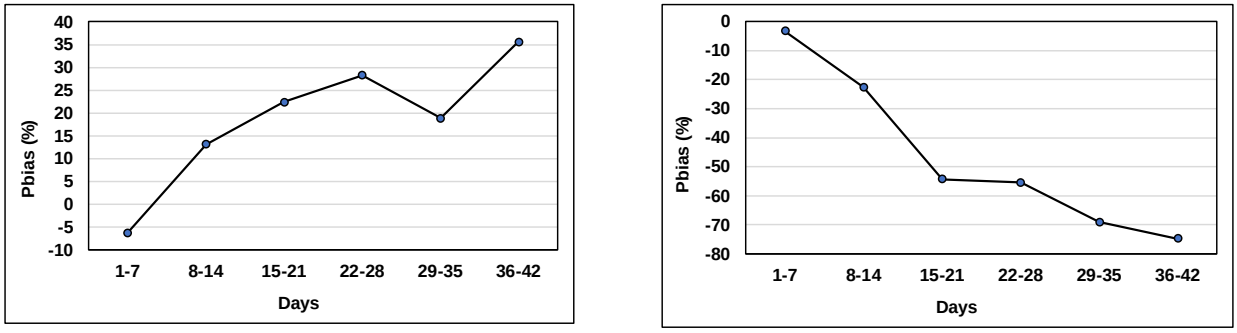


Figure 2. PBIAS of S2S-SWAP in irrigation estimation in 2017 (left) and 2018 (right)

Acknowledgments: The study was performed within the project “Improving the agro-hydrological simulation of irrigation in catchments under extreme climatic conditions by using ensembles (ICEE)”, funded by Deutsche Forschungsgemeinschaft (DFG). Experimental data were provided by the Fachverband Feldbewässerung.

References

Graham RM, Browell J, Bertram D, White CJ (2022) The application of sub-seasonal to seasonal (S2S) predictions for hydropower forecasting. Meteorological Applications 29(1): e2047. https://doi.org/10.1002/met.2047

Kolachian R, Saghafian B (2019) Deterministic and probabilistic evaluation of raw and post-processed sub-seasonal to seasonal precipitation forecasts in different precipitation regimes. Theoretical and Applied Climatology 137:1479–1493. https://doi.org/10.1007/s00704-018-2680-5

Malik I, Mishra V (2024) Sub-seasonal to seasonal (S2S) prediction of dry and wet extremes for climate adaptation in India. Climate Services 34: 100457. https://doi.org/10.1016/j.cliser.2024.100457

Musonda B, Jing YS, Nyasulu M, Mumo L (2021) Evaluation of sub-seasonal to seasonal rainfall forecast over Zambia. Journal of Earth System Science 130(1): 47. https://doi.org/10.1007/s12040-020-01548-0

Flood damage assessment: A methodological approach using AI-based flood mapping

J. Saavedra Navarro[1*], R. Zhuang[1], C. Albertini[1], C. Samela[2], S. Chaturvedi[1], S. Riccardi[3], P. Macciacchera[3], L. Luzietti[3], G. Murchio[3], S. Manfreda[1]
[1] *Dipartimento di Ingegneria Civile, Edile e Ambientale (DICEA), Università degli Studi di Napoli Federico II, Napoli, Italy*
[2] *Istituto di Metodologie per le Analisi Ambientali (IMAA), Consiglio Nazionale delle Ricerche (CNR), Tito Scalo (PZ), Italy*
[3] *e-GEOS, Rome, Italy.*
** e-mail: jorgeandres.saavedranavarro@unina.it*

Introduction

Floods are among the most impactful natural disasters, causing significant economic and social damage worldwide. This study integrates machine learning techniques with satellite-derived flood inventories to enhance flood hazard mapping over a large scale and consequently assess potential damages. The proposed approach enables more efficient flood damage evaluations, particularly in ungauged areas with limited hydrological data. The predicted flood-prone areas were compared with flood hazard maps developed by ISPRA (*Istituto Superiore per la Protezione e la Ricerca Ambientale*) (Lastoria et al., 2021).

Materials and methods

The methodology integrates multiple data sources into a machine Learning approach**.** A Random Forest (RF) model was used to predict flood-prone areas based on a rich flood inventory database that includes historical flood data from satellite imagery (Copernicus Emergency Mapping Service) and exposure variables. The RF algorithm is trained using a combination of hydrological and geomorphological indicators such as the Geomorphic Flood Index (GFI), elevation, and proximity to rivers, climate and land use variables, including precipitation records, Normalized Difference Vegetation Index (NDVI), and lithology. In addition, floodwater depth was estimated using digital elevation models (DEMs) to assess the severity of the inundation and its impact on affected buildings and agricultural land. Raster files were provided at ~90 meters resolution.

The considered methodology to evaluate flood-induced damage is the depth-damage curves developed by the Joint Research Center (JRC, European Commission, 2016) for Europe. Vulnerability metrics derived from the floodwater depth and exposure classification were computed based on building characteristics, such as the category and function (e.g., residential, commercial, industrial) and agricultural land (crops). Building data was extracted from DBSN (DataBase di Sintesi Nazionale) and agricultural land from the Corine Land Cover 2018. Due to scarce historical records in Italy, the validation of damage analysis was not considered in this study.

Results and concluding remarks

The preliminary findings indicate that the AI-based approach accurately identifies flood-prone areas, with an AUC of 0.94. The proposed methodology effectively classifies exposure levels across different asset categories, enabling a more detailed assessment of flood-induced damage. The potential economic losses reached 1.8 and 3.6 million euros in industrial (27) and residential (992) buildings in the AOI, respectively. According to the agricultural land, the potential losses reached 3.6 million euros, affecting 6.1 km2 (Figure 1).

Uncertainties remain due to the lack of direct association with specific return periods and water depth estimation. Future work will focus on refining exposure classification models, validating depth-damage functions for the Italian case, and incorporating additional socio-economic indicators to improve flood damage estimation.

This study underscores the potential of AI-driven methodologies to enhance flood risk assessment and damage evaluation. The results provide a basis for more effective risk management strategies and policy development in flood-prone regions.

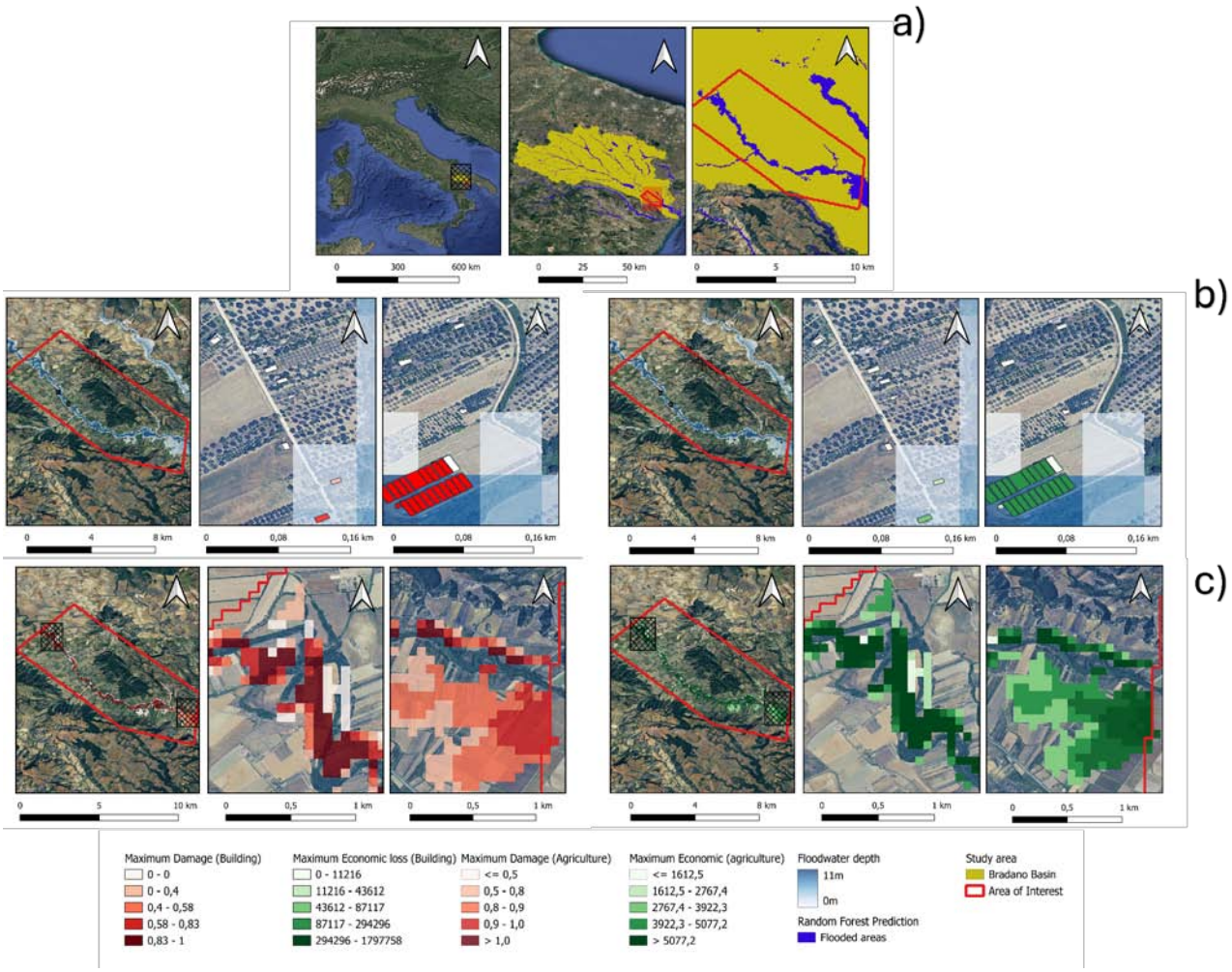


Figure 1. Flood damage analysis. a) Study area, AOI and flood-prone areas by the Random Forest model. b) Floodwater depth and building impacts. c) Agricultural land impact.

Acknowledgements: This study was carried out within the RETURN Extended Partnership and received funding from the European Union Next-Generation EU (National Recovery and Resilience Plan -NRRP, Mission 4, Component 2, Investment 1.3 -D. D. 1243 2/8/2022, PE0000005).

References

European Commission. Joint Research Centre. (2016). Global flood depth-damage functions: Methodology and the database with guidelines. Publications Office. https://data.europa.eu/doi/10.2760/16510

Lastoria, B., Bussettini, M., Mariani, S., Piva, F., & Braca, G. (2021). Rapporto sulle condizioni di pericolosità da alluvione in Italia e indicatori di rischio associati. Istituto Superiore per la Protezione e la Ricerca Ambientale, Rapporti 353/21, Roma. www.isprambiente.gov.it

Manfreda, S., & Samela, C. (2019). A digital elevation model based method for a rapid estimation of flood inundation depth. Journal of Flood Risk Management, 12(S1), e12541. https://doi.org/10.1111/jfr3.12541

Priest et al., (2007). Building a model to estimate risk to life for European flood events – Final report. FLOODsite.

Samela et al., (2017). Geomorphic classifiers for flood-prone areas delineation for data-scarce environments. Advances in Water Resources, 102, 13–28. https://doi.org/10.1016/j.advwatres.2017.01.007

Investigation of uncertainties in flood risk assessment under climate change in urban cities in South Korea

J.Y. Song[1], Y.H. Song[2], E.S. Chung[3*]
[1] Department of Civil Engineering, National Korea Maritime and Ocean University, Busan, South Korea
[2] Department of Applied Artificial Intelligence, Seoul National University of Science and Technology, Seoul, South Korea
[3] Department of Civil Engineering, Seoul National University of Science and Technology, Seoul, South Korea
* e-mail: eschung@seoultech.ac.kr

Introduction

Flooding in urban areas significantly impacts human society and the economy, and is expected to occur more frequently and severely in the future due to urbanization and climate change. To assess the future urban flood vulnerability, this study incorporates multiple general circulation models (GCMs), shared socioeconomic pathway (SSP) scenarios, weight determination methods, and multi-criteria decision making (MCDM) techniques, where uncertainty inevitably arises throughout these processes. Therefore, this study ranked the future urban flood risk for urbanized cities in South Korea, considering all combinations of the aforementioned multiple sources, and investigated the contributing sources of uncertainties through an analysis of variance (ANOVA) test.

Materials and methods

The driving force-pressure-state-impact-response (DPSIR) framework was utilized in this study (European Environment Agency, 1999), and a number of indicators related to urban flooding were selected and categorized into social, economic, and environmental factors. Weighting values were determined using different methods such as equal weight, entropy, Delphi, fuzzy, and grey approaches (Kang et al., 2023; Shannon and Weaver, 1947). These weightings were then applied in different MCDM methods (weighted sum method, VIKOR, TOPSIS, etc.) (Hwang and Yoon, 1981). The urban flood vulnerability assessments were carried out based on the combinations of different uncertainty sources including GCMs, SSP scenarios, weight determination methods, and MCDM techniques. The rankings for each city were compiled to analyze the variation in flood vulnerability based on different methodologies and identify the contributing sources of uncertainty using an ANOVA test.

This study was applied to selected big and medium cities where synoptic weather observation centers exist in South Korea (Figure 1). The GCM data, which have varying spatial resolutions, were downscaled to a compatible resolution (0.25 degrees) using linear interpolation. Additionally, the inverse distance weighting method was used for spatial interpolation to simulate point climate data for the study area based on the downscaled GCM grid data. Bias correction was performed using the quantile mapping method, which is a widely used technique for this purpose. A number of GCMs under different SSP scenarios were utilized, and a number of combinations for future monthly precipitation cases were applied as the driver component in the environmental factor.

The ANOVA test is used to assess whether there are significant differences between the means of two or more groups. It evaluates if the group means are equal or if the variance between them exceeds what would be expected by random chance. The strength of ANOVA lies in its ability to quantify uncertainty related to each individual source and analyze the uncertainty resulting from the interactions among these sources (Yip et al., 2011). In this study, the flood vulnerability rankings derived from the assessment were considered, rather than the mean values, to examine whether different sources affect the urban flood vulnerability rankings.

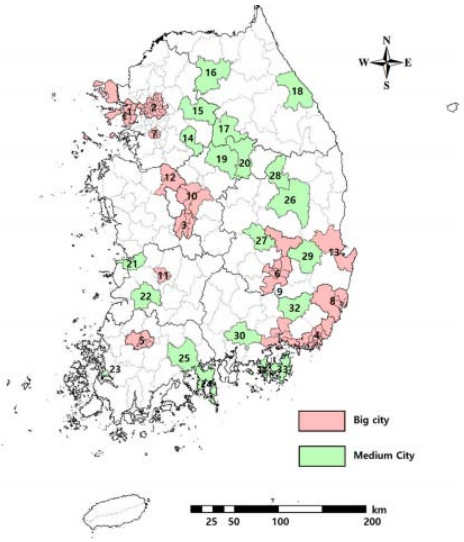


Figure 1. Selected cities in the study area.

Results and concluding remarks

The city with the highest proxy value was ranked 1st, indicating the highest vulnerability to urban flooding, while the city with the lowest proxy value was ranked 33rd, indicating the lowest vulnerability (Figure 2). Comparing city sizes showed that bigger cities are generally more vulnerable to flooding.

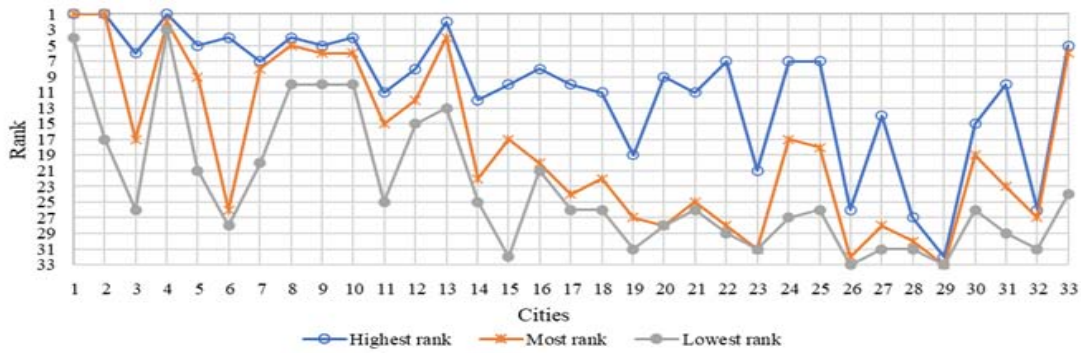


Figure 2. Ranks (highest, most frequent, and lowest) of urban flood vulnerability for each city.

This study can find the most significant factor contributing to variations in urban flood vulnerability rankings is the weighting value, followed by MCDM method and the combination of weight determination method and MCDM technique. This emphasizes the importance of considering all potential methods to better understand and communicate flood vulnerability uncertainties to decision-makers and stakeholders.

Acknowledgments: This work was supported by National Research Foundation of Korea funded by the Ministry of Education (RS-2023-00249547).

Reference

European Environment Agency (1999) Environmental Indicators: Typology and Overview, Copenhagen, Denmark.

Hwang, C.-L. and Yoon, K. (1981) Multiple Attribute Decesion Making; Springer: Berlin/Heidelberg, Germany; New York, NY, USA.

Kang, H.-Y., Chae, S.T., and Chung, E.-S. (2023) Quantifying Medium-Sized City Flood Vulnerability Due to Climate Change Using Multi-Criteria Decision-Making Techniques: Case of Republic of Korea. Sustainability, 15, 16061. https://doi.org/10.3390/su152216061

Shannon, C.E. and Weaver, W. (1947) The Mathematical Theory of Communication; University of Illinois Press: Urbanan, IL, USA.

Yip, S., Ferro, C.A.T., Stephenson, D.B., and Hawkins, E. (2011) A Simple, Coherent Framework for Partitioning Uncertainty in Climate Predictions. Journal of Climate, 24(17): 4634–4643. https://doi.org/10.1175/2011JCLI4085.1

Addressing the effects of storm Daniel floods on land reclamation works in Thessaly, Greece: aftermath and restoration management

D. Tigkas[1,2*], D. Papalexis[1], N. Proutsos[3], G. Sofou[1], H. Vangelis[2], K. Stournaras[1], G. Tsakiris[2]
[1] Directorate of Land Reclamation and Soil-Water Resources, Ministry of Rural Development and Food, Athens, Greece
[2] Centre for the Assessment of Natural Hazards and Proactive Planning & Lab. of Reclamation Works and Water Resources Management, School of Rural, Surveying and Geoinformatics Engineering, National Technical University of Athens, Greece
[3] Institute of Mediterranean & Forest Ecosystems, Hellenic Agricultural Organization "DEMETER", Athens, Greece
* e-mail: ditigas@mail.ntua.gr

Introduction

The proper management of land reclamation works (irrigation and drainage systems, rural road networks, etc.) is essential for ensuring suitable cultivation conditions, adequate water availability and water efficiency in agriculture. Apart from providing the means for enhancing the agricultural yield, land reclamation works also serve for reducing the vulnerability of a region to extreme events, such as floods and droughts (Tigkas et al. 2023). The preventive maintenance of the water systems is necessary for their reliability and decreased disruption of service (Tsakiris et al. 2011), and crucial for the robustness and resilience of irrigation and drainage networks for appropriate functionality, especially during the critical periods of crops development. In spite of the above, reclamation works are susceptible to floods, which may cause significant impacts to the relevant infrastructure. In such cases, the prompt restoration is particularly important for supporting the jeopardized agricultural production and consequently the local and regional economy and society.

Thessaly plain is one of the major agricultural production areas in Greece. The collective land reclamation works, which have been implemented by the central and regional state authorities since the 1960s, have played a significant role in the development of the area. Due to its special topographic and climatic characteristics, the region has a high agricultural yield potential, though with many challenges involved. Indicatively, it is crucial to retain the proper operation of irrigation systems for establishing high yield crops, due to the arid and semi-arid conditions that dominate in the region. Also, there are many low-altitude plains, drained swamps and lakes, susceptible to flooding, in which the drainage systems are essential for maintaining the agricultural production capacity.

The current paper focuses on the impacts of the extreme floods caused by the Mediterranean cyclone 'Daniel' during September 2023 in the region of Thessaly. Many areas of the same region have also been severely impacted by flood events due to the Mediterranean Cyclone 'Ianos' (September 2020). The damages on collective irrigation and drainage systems of this region are examined, along with the restoration actions that have been taken for assisting the timely relief of agriculture.

Materials and methods

The Copernicus EMS Rapid Mapping service was triggered by the Greek authorities on September 2023 to monitor and provide mapping and estimations on the flood caused by Daniel storm. The monitoring of the event produced data and reports on the severity, duration and spatial extent of the flood event and estimations of the affected population (Figure 1) (CEMS 2023). Other ground-based and remote sensing monitoring tools were also available for acquiring information on the affected areas and assessing the corresponding damages.

Regarding the collective irrigation and drainage systems, technical reports on the damages were prepared by the Regional Authorities and the Land Reclamation Organisations (LRO), which are the responsible bodies for managing the collective land reclamation works in the area of their jurisdiction. A comprehensive methodology was followed for assessing the urgent restoration actions in the affected areas.

Results and concluding remarks

The rainfall occurred in the overall basin varied spatially, though the amounts were very high in most of the cases, estimated to have a return period up to 150 years for the overall event (Dimitriou et al. 2024). The total inundated area was approximately 1150km ^{2}, while about 70% of this area was agricultural land (He et al. 2024). The affected population by the damages was approximately 38,000 people, located mostly in the prefectures of Magnesia, Larissa and Karditsa (CEMS 2023).

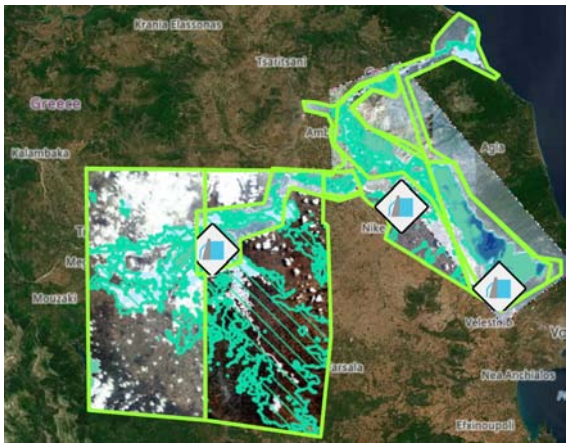


Figure 1. Delineation monitoring of Daniel flood event in Thessaly region (CEMS 2023)

The damages on the irrigation and drainage systems included extended breakages and sedimentation at irrigation canals and the drainage ditches, electromechanical damages in pumping stations and destruction of rural roads. In some cases, the age of the infrastructure (50-60 years old) and the poor maintenance were additional factors increasing the susceptibility that might have magnified the severity of the damages.

The overall cost of the damages on the aforementioned infrastructure under the management of LROs was estimated at approximately 180 million €. Considering the fact that there were also serious problems with the condition of the arable land in many parts of the basin, along with the significant loss of the agricultural production of the region, the prompt restoration of irrigation and drainage networks emerged as an urgent issue. To this end, the immediate measures for restoring the principal hydraulic and electromechanical infrastructure for each LRO to operational conditions were determined. Approximately 10 million € were provided by state funds before the beginning of the forthcoming irrigation period for the repairing tasks.

To confront the impacts of the increasing severe flood events, apart from proper flood control projects, suggestions are made for implementing sustainable risk management strategies tailored to the local specific environments, such as nature-based solutions and small-scale interventions in mountainous areas.

References

CEMS - Copernicus Emergency Management Service (2023) Flood in Greece EMSR692 - Situational reporting. Available online: https://rapidmapping.emergency.copernicus.eu/EMSR692/reporting

Dimitriou E, Efstratiadis A, Zotou I, Papadopoulos A, Iliopoulou T, Sakki G-K, Mazi K, Rozos E, Koukouvinos A, Koussis AD, Mamassis N, Koutsoyiannis D (2024) Post-Analysis of Daniel Extreme Flood Event in Thessaly, Central Greece: Practical Lessons and the Value of State-of-the-Art Water-Monitoring Networks. *Water* 16(7): 980, https://doi.org/10.3390/w16070980

He K, Yang Q, Shen X, Dimitriou E, Mentzafou A, Papadaki C, Stoumboudi M, Anagnostou EN (2024) Brief communication: Storm Daniel flood impact in Greece in 2023: mapping crop and livestock exposure from synthetic-aperture radar (SAR). Nat. Hazards Earth Syst. Sci. 24: 2375–2382, https://doi.org/10.5194/nhess-24-2375-2024

Tigkas D, Proutsos N, Sofou G, Papalexis D, Kitsos A, Vangelis H, Tsakiris G, Papadiamantopoulou E, Stournaras K (2023) Extreme hydrometeorological events and the role of reclamation works and irrigation - drainage systems in the era of climate crisis. In: Proceedings of 12th World Congress of EWRA 'Managing Water-Energy-Land-Food under Climatic, Environmental and Social Instability', 27 June - 1 July 2023, Thessaloniki, Greece

Tsakiris G, Vangelis H, Tigkas D, Stathaki A, Sofotasios D, Toprak S et al. (2011) Urban water distribution systems: Preventive maintenance. Water Utility Journal 1: 41-48

Improvement of early warning systems for flood risk with a distributed hydrological model and an analog-based precipitation forecast

M.C. Llasat[1,4], R. Marcos Matamoros[1], C. Guzzon[1], J. Arzaibar[2], A. Cabañas[2], D. Carril Rojas[3], A. Díaz Guilera[4,5], L. Garrote[3], M. Llasat-Botija[1], D. Marinelli[1,4], L. Mediero[3], O. Varela[6]
[1] *Department of Applied Physics, Universitat de Barcelona, Spain*
[2] *CUBIT, Spain*
[3] *Department of Civil Engineering: Hydraulics, Energy and Environment, Universidad Politécnica de Madrid, Spain*
[4] *UBICS, Universitat de Barcelona, Spain*
[5] *Department of Condensed Matter Physics, Universitat de Barcelona, Spain*
[6] *IBERCIVIS, Spain*
** e-mail: carmell@meteo.ub.edu*

Introduction

The Spanish Mediterranean region is frequently impacted by catastrophic floods, driven by intense convective rainfall, the presence of torrential basins, rapid urbanization in flood-prone areas, and potential aggravation due to climate change. The recent catastrophic flash flood event in Valencia (Spain) in October 2024 that produced 224 fatalities and 3 missing people is an example. In November 2022, the UN Secretary General launched the call for 'Early Warning for All', with the commitment that everyone should have access to an early warning system (EWS) by 2030. An EWS is a system from beginning to end, based on four pillars: knowledge of the phenomenon, forecasting and monitoring, communication and emergency management, and the population's response capacity. Although the knowledge and forecasting of very intense and heavy rainfall is complex and subject to improvement, the floods in the Valencian Community revealed the main weaknesses in the last two pillars (Llasat, 2024). It is possible that a better communication and adequate response by the population would have prevented most of the deaths. Improving these pillars requires raising awareness of the risk of flooding. One of the possible tools for this is citizen science (Craglia and Granell 2014), which in this case involves the active participation of citizens in taking measures, such as the level of the river, or in the generation of a participatory proposal for better communication and action in the event of an emergency.

The improvement of the first two pillars can be carried out by studying previous cases and supporting decision-making. In Catalonia (Spain) it exists the INUNGAMA database (Barnolas and Llasat 2007), that contains all the flood events recorded since 1900 in this region. The major part of them are flash floods, that are produced by intense and short-duration rainfalls in basins of less than 2000-3000 km^2 (Amponsah et al. 2018). Despite advances in weather forecasting models, this type of episode is still difficult to predict, both in terms of intensity and location. In this case, any additional information can be useful for decision-making. An example is the prediction of the rainfall field by an analog-based method (Ben Daoud et al. 2016) adjusted to the study area from a selection of previous flood cases. This type of forecasting is useful to feed and generate a probabilistic prediction of the flow in order to detect whether the alert threshold will be exceeded to warn the emergency services, as well as the population. The use of a distributed model such as RIBS (Garrote and Bras 1995a, 1995b) is especially useful in this type of study, while the use of platforms such as Delft-FEWS (https://oss.deltares.nl/web/delft-fews/) offer the possibility of using this type of hydrometeorological chain operationally.

Materials and methods

INUNGAMA is a comprehensive impact-based flood datasets that have been manually assembled from press news archives (La Vanguardia) for more than 20 years. INUNGAMA covers the episodes in the autonomous region of Catalonia (Spain) for the period 1900-2020 and contains 435 flooding episodes. From it, the flood episodes that have affected the Francolí River Basin have been selected. For these episodes,

the geopotential height fields at high altitude (500 hPa) and near the surface (1000 hPa) and the precipitation fields have been obtained from ERA5 reanalysis. A comparative analysis of different analog-based methods (AM) has been made, starting from the simple comparison of predictors using a metric distance, progressing to the incorporation of the definition of weather types, and further enhanced by introducing a post-hoc seasonal standardization of the predicted precipitation field. The accuracy of the methods has been assessed for both moderate precipitation events, using a total of 3746 days with recorded precipitation, and for 230 days associated with past flood occurrences. The performance of the tested methods has been compared against the numerical GFS model.

The spatially distributed precipitation forecasts obtained from the analogues has been used as input data to the calibrated RIBS model in the Francolí catchment. A set of five past events has been used as an ensemble for generating a probabilistic precipitation field forecast for the region. The accuracy and reliability of the analog forecasts has been assessed comparing the hydrological model outputs with the streamflow and precipitation observations at the gauging stations considered in the study. At the same time, the analogue identification method has been introduced into the FEWS platform for operational running on a daily basis.

On the other hand, after the 2019 floods in Francolí, a citizen science campaign was developed that provided information on the depth of the flood as well as on the response of the population during the emergency, which was subsequently completed with different awareness-raising activities.

Results and concluding remarks

Results show that AM with seasonal standardization and the Perfect Prognostic hypothesis outperform GFS forecasts with a 24-hour lead time, particularly in capturing peak precipitation values and spatial accuracy. The Nash–Sutcliffe Efficiency coefficient shows good agreement between observed and simulated hydrographs for some events with values in the range 0.6179-0.9114. The introduction of analogues allows obtaining a probabilistic distribution of the expected flow rate which, in general, better captures the possibility of exceeding the warning threshold. The study highlights the potential of AM's using weather types as a good complement to numerical weather models, offering enhanced forecasting capabilities for extreme weather events and contributing to more effective flood risk management.

Results also show for the 2019 floods, that, although the protocols of the warnings and alerts chain were well-defined, the messages reached the citizens with difficulty, who often didn't know how to act. In some cases, there were delays between the official warnings and local warnings or recommendations. It would be necessary to define a local emergency plan with the participation of the community, who know the area best, with protocols adapted to the local reality and means that include the care of dependent people and newcomers.

Acknowledgments: This study has been supported by the projects C3RiskMed (PID2020-113638RB-C22), funded by the Ministry of Science, Innovation and Universities (Spain) and Flood2Now (Grant PLEC2022-009403 funded by MICIU/AEI/ 10.13039/501100011033 and by the "European Union-NextGenerationEU/PRTR").

References

Amponsah W, Ayral PA, Boudevillain B, et al. (2018) Integrated high-resolution dataset of high-intensity European and Mediterranean flash floods Earth Syst. Sci. Data, 10, 1783–1794. https://doi.org/10.5194/essd-10-1783-2018.

Barnolas M, Llasat MC (2007) A flood geodatabase and its climatological applications: The case of Catalonia for the last century. Nat. Hazards Earth Syst. Sci., 7(3), 271–281.

Ben Daoud A, Sauquet E, Bontron G, Obled C, Lang M (2016). Daily quantitative precipitation forecasts based on the analogue method: Improvements and application to a French large river basin. Atmosph. Res., 169:147–159.

Craglia M, Granell C (2014) Citizen Science and smart cities-Report of summit, Ispra 5–7 Feb. JRC Technical Report.

Garrote L Bras RL (1995 a) A distributed model for real-time forecasting using digital elevation models. J. Hydrol., 167, 279–306.

Garrote L Bras RL (1995 b) An integrated software environment for real-time use of a distributed hydrologic model. J. Hydrol., 167, 307–326.

Llasat MC (2024) Spain's flash floods reveal a desperate need for improved mitigation efforts. World View, 26 November 2024 Nature 635, 787. https://doi.org/10.1038/d41586-024-03825-0

An erosive Sicilian beach: a multidisciplinary approach to study the coastal dynamic effects

G. Manno, F. Capodici, P. Scala*, G. Ciraolo
Department of Engineering, University of Palermo, Viale delle Scienze, Bd. 8, 90128 Palermo
** e-mail: corresponding pietro.scala@unipa.it*

Introduction

In recent decades, Mediterranean beaches have undergone a radical transformation due to significant population growth. The anthropogenic pressure of these coastal areas is linked to the development of commercial zones, the expansion of tourism-related activities, and the corresponding growth of the road network. The increase in all these activities has encouraged rapid expansion, often occurring under inadequate urban and environmental planning. As a result, several coastal areas are nowadays complex systems in which the evolution of the beach is driven by two main forces: natural processes (sediment transport, waves, tides, etc.) and coastal engineering (ports, groynes, breakwaters, river dams, etc.).

The Sicilian coastline extends for 1,400 km; about 395 km are natural and/or human-altered beaches. This research focuses on a beach located on the southern Sicilian coast which was affected by severe coastal dynamics due to anthropogenic changes affecting both the emerged and submerged beach areas. The objective of this study was to analyse the dynamics of this beach by means of an interdisciplinary approach; thus, by integrating various techniques from different disciplines.

Materials and methods

The study was conducted on a Sicilian erosive beach identified through an historical change analysis. The beach was characterized by describing its morphology and sediment composition.

Quantitative assessment of shoreline movement involved the use of various measurement techniques and data analysis methods to track and quantify changes in the position of a shoreline over time. This process included the use of satellite imagery, aerial photographs, *in situ* stable-video monitoring, and geographic information systems (GIS) to detect shifts in the coastline. By analysing these changes, erosion rates (End Point Rate -EPR, Linear Regression Rate, Shoreline Change Envelope SCE, etc.) were assessed by means of *ad hoc* QGIS plug-in, developed by some of the authors affiliated to the Engineering Department of the University of Palermo (Scala et al. 2024).

The coastal armouring coefficient was computed to evaluate the impact of the coastal structures on the beach. This refers to stretches of coastline that are "covered" by various types of maritime structures (ports, groynes, breakwaters, etc.). Indeed, these structures allow to protect a stretch of coastline, on the other hand, they also create a sediment imbalance in the nearby areas.

A maritime hydraulic study was crucial to assess the impact of atmospheric forces on the shoreline position. Wave significant heights, and tidal variations were analysed using both the tide gauge and the re-analysis wave data from the ECWMF (European Centre for Medium-Range Weather Forecasts). Seasonal variations and extreme weather events were assessed to determine their impact on beach morphology. This study, combined with the calculation of sediment input from the nearby catchment, was essential for assessing longshore sediment transport. The latter was calculated using the well-known formula of the Coastal Engineering Research Center - CERC (Komar, 1979, List et al. 2007).

To better understand the physical phenomena that control the beach, an *in situ* stable-video monitoring was deployed. This system comprises two cameras mounted to 15 meters above ground and approximately 70 meters from the shoreline. Hourly averaged snapshots were daily computed by the acquisition system and processed to monitor morphological information such as the shoreline position evolution.

Due to large amount of averaged snapshot an automatic processing algorithm (Fig. 1) allowed determining the daily automatic coastline (AD) position via the k-means classification (MacQueen, 1967).

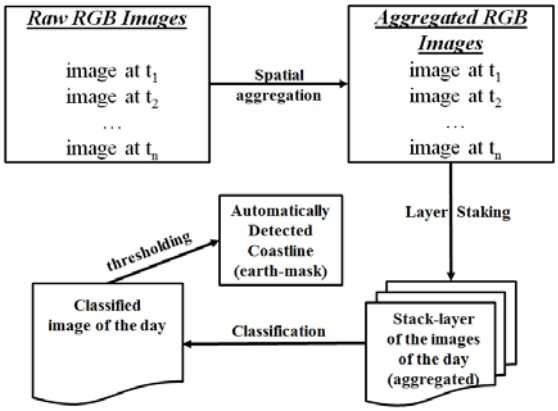


Figure 1. Flow chart of the AD coastline detection using daily images collected by the available video-system.

Results and concluding remarks

The analysed beach shows visible signs of land loss and transformation due to natural and human-induced forces. In this area, coastal erosion is a dynamic process driven by factors such as wave action, tides, currents, and storms, which gradually remove sediment from the shoreline. Over time, this erosion leads to the retreat of the beach, affecting both the landscape and the ecosystems dependent on it. Human activities, such as coastal development and the construction of protective structures, have exacerbated the problem by disrupting natural sediment transport. In some areas of this beach, the coastline has become more vulnerable to flooding, habitat loss, and damage to infrastructure. Effective coastal management is crucial to mitigating the impacts of erosion and protecting both the environment and human settlements.

The AD extraction algorithm allowed monitoring the dynamics of the shoreline (Figure 2).

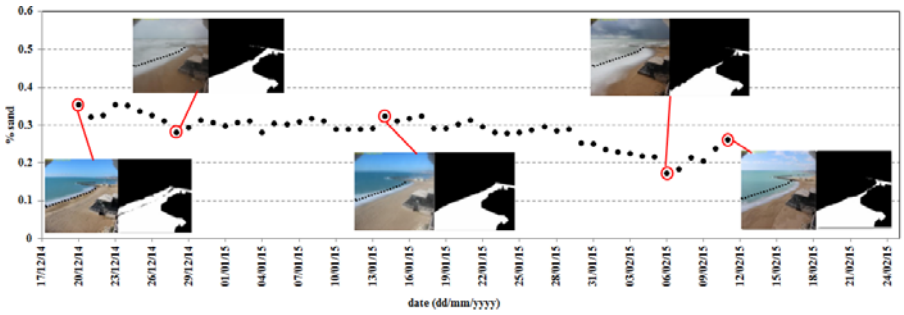


Figure 2. Time series of the percentage of sand detected in earth-mask images; original snapshots and corresponding earth-mask image are shown for selected days; the black-dotted line shows the reference shoreline position at the beginning of the video monitoring experiment.

Acknowledgments: This study was carried out within the RETURN Extended Partnership and received funding from the European Union Next-GenerationEU (National Recovery and Resilience Plan – NRRP, Mission 4, Component 2, Investment 1.3–D.D. 1243 2/8/2022, PE0000005).

References

Komar PD (1979). Beach-slope dependence of longshore currents. Journal of the Waterway, Port, Coastal and Ocean Division, 105(4), 460-464. https://doi.org/10.1061/JWPCDX.0000169

List JH, Hanes DM, Ruggiero P (2007). Predicting longshore gradients in longshore transport: Comparing the CERC formula to Delft3D. In Coastal Engineering 2006: (In 5 Volumes) (pp. 3370-3380). https://doi.org/10.1142/9789812709554_0284

MacQueen, J. (1967). Some methods for classification and analysis of multivariate observations. Proceedings of the Fifth Berkeley Symposium on Mathematical Statistics and Probability, 1, 281-297

Scala P, Manno G, Ciraolo G (2024) Coastal dynamics analyzer (CDA): A QGIS plugin for transect based analysis of coastal erosion. SoftwareX, 28, 101894. https://doi.org/10.1016/j.softx.2024.101894

Reliable estimates of the probability of record-breaking weather extremes through the Metastatistical approach

M. Marani*, S. Andria, M.F. Caruso, P. Devò
Department of Civil, Environmental, and Architectural Engineering, University of Padua, Padua, Italy
** e-mail: marco.marani@unipd.it*

Introduction

Methods to quantify the probability of occurrence of record-breaking extremes are the focus of much attention, e.g. in engineering practice, where infrastructure must be designed to withstand events that have not yet been observed. However, methodologies based on traditional extreme value theory do not make good use of the available observations and are not specifically designed to be applied under changing climatic conditions. Here we illustrate the Metastatistical Extreme Value Distribution (MEVD), an approach that uses all available observations, rather than relatively few large values. We examine here how the MEVD significantly improves our ability to estimate the probability of occurrence of events that are not present in the observational record. Illustrative examples are drawn from the unprecedented flood event in the Romagna Region (Italy) in May 2023 and extreme Atlantic Hurricanes.

Materials and methods

The MEVD (Marani and Ignaccolo, 2015), as applied to rainfall, expresses the cumulative probability distribution of the maximum yearly rainfall depth as:

$$G(x) = \frac{1}{T}\sum_{j=1}^{T}\left[1 - exp\left(\frac{x}{C_j}\right)^{w_j}\right]^{n_j} \quad (1)$$

based on the assumption of a Weibull distribution for the ordinary rainfall, with parameters C_j and w_j, while n_j is the number of events in each year. T is the number of years on record. Parameter values are estimated based on all the observed ordinary events, rather than just on yearly maxima, as for the Generalized Extreme Value distribution (GEV), leading to a better use of the available information.

The Metastatistical approach was applied by Hosseini et al. (2020) to the HURDAT2 record of Atlantic Hurricanes, by adopting for the hurricane intensity a Generalized Pareto Distribution, such that the MEVD cumulative distribution of the most intense hurricane in a year is expressed as:

$$G(x) = \frac{1}{T}\sum_{j=1}^{T}\left[1 - \left(1 - k_j\frac{(x-u)}{\sigma_j}\right)^{\frac{1}{k_j}}\right]^{n_j} \quad (2)$$

This formulation was shown to reduce by about 70% the uncertainty in the estimation of extreme quantiles with respect to GEV distribution.

Results and concluding remarks

The application of the MEVD formulation to rainfall observations in the Lamone River basin shows the robustness of MEVD estimates of the probablity associated with the catastrophic event occurred in the Romagna region on May 16th 2023. MEVD estimates, based on a large number of observations, are insensitive to the inclusion of the event itself in the sample used for the estimation. The GEV method estimates a return period of 640 yrs, when the 16-May event is included, which is reduced to 320 years when the event is included in the sample (Figure 1).

Event intensity and occurrence appear separately in the MEVD formulation. This allows using the entire HURDAT2 dataset to estimate the probability of hurricanes of various intensity hitting Hispaniola (Figure 2).

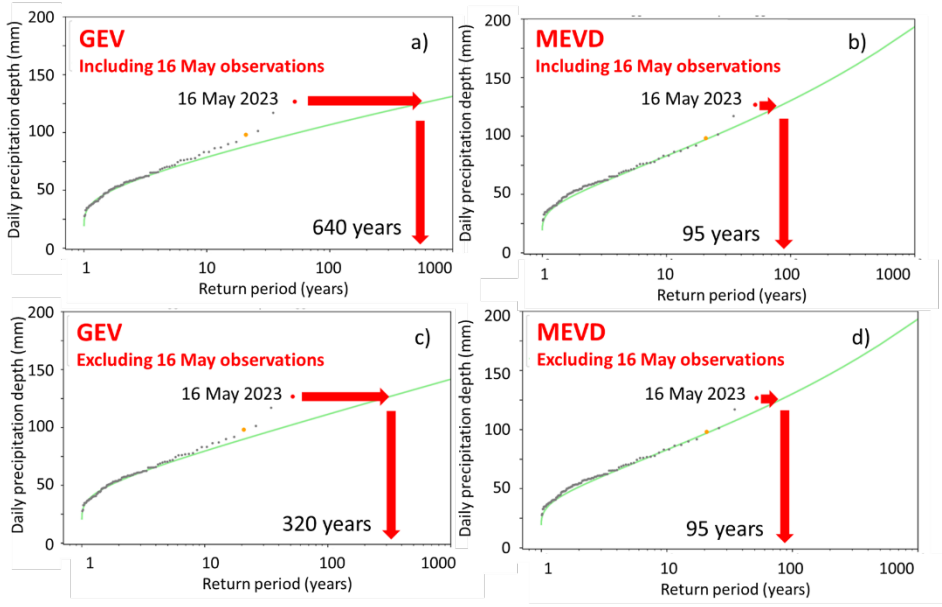


Figure 1. GEV-estimated return period of the 16 May 2023 event in the Lamone River basin in the Romagna Region (panels a and c). MEVD estimates, making better use of observations, are not similarly sensitive to the inclusion or exclusion of the largest observed value (panels b and d).

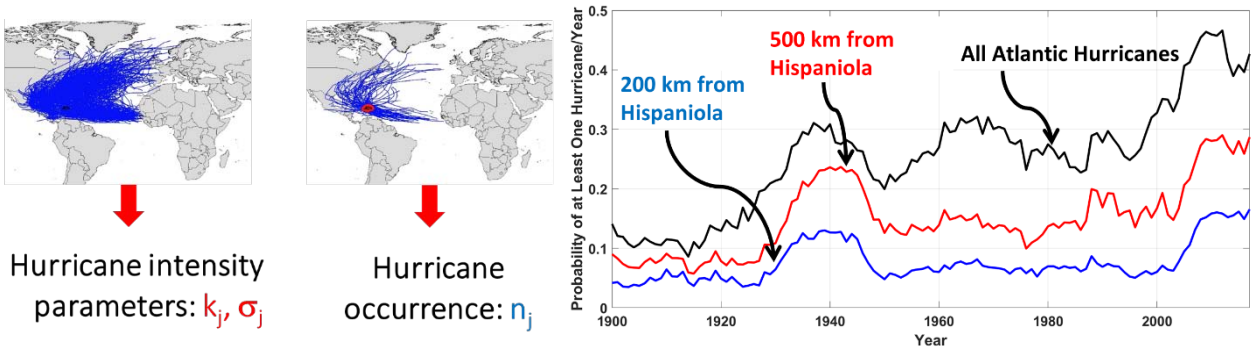


Figure 2. MEVD separates the roles of the probability distribution of ordinary events and of event occurrence process and thus permit the estimation of GPD parameters from all observed hurricanes in the HURDAT2 dataset. The frequency of hurricanes hitting close the island of Hispaniola is simply obtained by counting them in the observations. Estimates on sliding windows of 30 years highlights the probability of observing at least one cat. 5 hurricane/year over time.

Estimates in Figure 2 would not be feasible using traditional approaches, which may only rely on the few hurricanes historically hitting the island.

These examples illustrate how the MEVD better uses observational information with respect to traditional approaches, reduces estimation uncertainty, and yields more robust estimates of unprecedented extremes.

Acknowledgments: This study was carried out within the RETURN Extended Partnership and received funding from the European Union Next-GenerationEU (National Recovery and Resilience Plan, Mission 4, Component 2, Investment 1.3 – D.D. 1243 2/8/2022, PE0000005). It was also supported by the INTENSE project (raINfall exTremEs and their impacts: from the local to the National scalE) funded by the Next GenerationEU Program through Progetti di ricerca di Rilevante Interesse Nazionale - grant 2022ZC2522).

References

Hosseini, S. R., Scaioni, M., & Marani, M. (2020). Extreme Atlantic hurricane probability of occurrence through the Metastatistical Extreme Value Distribution. Geophys. Res. Lett., 47, doi:10.1029/2019GL086138.

Marani, M., and M. Ignaccolo (2015). A Metastatistical Approach to Rainfall Extremes, Adv. Water Resour., 79, 121–126, doi:10.1016/j.advwatres.2015.03.001.

Estimates of point rainfall extremes from satellite precipitation products: application and testing in Northeastern Italy

C.A. Sanchez Pena[1*], F. Marra[2], M. Marani[1]
[1] University of Padova, Department of Civil, Environmental and Architectural Engineering, Padova, Italy
[2] University of Padova, Department of Geosciences, Padova, Italy
* e-mail: cesararturo.sanchezpena@unipd.it

Introduction

The extensive available historical rainfall record from rain gauges allows the derivation of extreme precipitation probabilities at gauged locations. However, gauged areas present vast gaps, such that rainfall extremes are virtually unknown in many areas of the world. A detailed understanding of the spatial variability of extreme rainfall remains elusive, particularly in regions with strong climatological gradients, such as areas with variable orography and coastal areas. As a contribution to addressing these limitations, here we integrate national-scale observations from rain gauges and satellites towards the production of a spatially-explicit description of rainfall extremes at the national scale, using recent metastatistical analyses of extremes (Marani and Ignaccolo 2015; Marra et al. 2020). A key step in our approach is the use of a statistical downscaling method (Zorzetto and Marani 2018), which establishes a link between point rainfall statistics, as observed through a rain gauge, and the statistics derived from satellite/reanalysis products representing rainfall averaged over scales of tens of kilometers.

Materials and methods

We used six datasets from different satellites: IMERG (3 hour), CMORPH (3 hour), ERA5 (1 day), PERSIANN (1 day), MSWEP (3 hour), and SM2RAIN (1 day). The data cover a time period from 2002 to 2023. We focus on the Veneto Region, in northeastern Italy, stretching from the Dolomite Mountains to the Adriatic Sea. In the same area we used hourly rainfall observations from the "Agenzia Regionale per la Prevenzione e Protezione Ambientale del Veneto" (ARPAV) at a total of 171 stations for the study period. We used a statistical framework for downscaling extreme rainfall statistics proposed by Zorzetto and Marani (2019). This method provides the probability of daily precipitation at a point scale (a rain gauge) based on satellite estimates with a coarser spatial resolution. By defining a neighborhood centered on the pixel of interest, the wet fraction at the satellite and point scales is calculated. Additionally, the autocorrelation among the remotely-sensed pixels within the neighborhood is analyzed to recover the spatial correlation. Finally, the downscaling process is completed by determining the statistical properties of a point within the satellite tile (Zorzetto and Marani 2019).

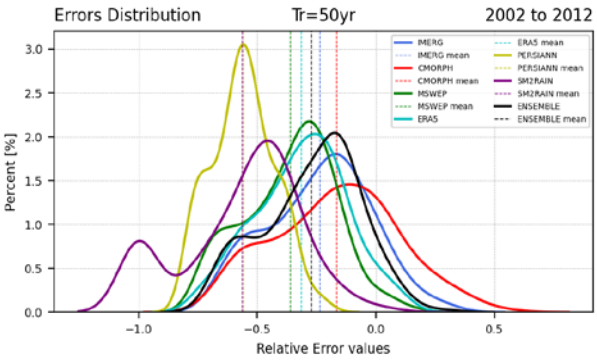
Results and concluding remarks

The findings shown in Figure 1a indicate that among the satellite products, IMERG, MSWEP, and ERA5 demonstrated the lowest relative error when compared to observed data, while CMORPH showed moderate error, being the one that presented the greatest dispersion. In contrast, PERSIANN and SM2RAIN exhibited the poorest performance.

In Figure 2, the scatter plots reveal an underestimation of quantiles for a 50-year return period, with IMERG, MSWEP, and ERA5 yielding slightly more favorable results than CMORPH, mainly due to its dispersion. SM2RAIN showed a strong underestimation that intensified at higher quantile values. PERSIANN displayed extremely low spatial variability, resulting in the least accurate estimates. Given that some products demonstrated promising performance, the next step involves applying a bias correction to the downscaling results. This includes adjustments for the number of wet days, as well as the scale and shape parameters of the Weibull distribution used in our approach. The Figure 2 shows a previous result for a

comparison between before and after IMERG quantiles correction.

Relative error values.



Scatter plot of quantiles.

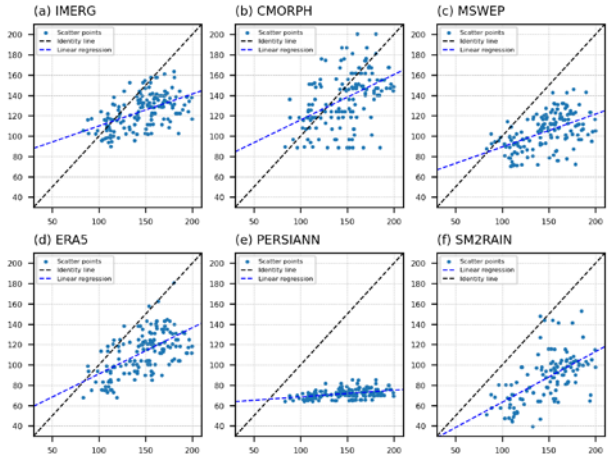


Figure 1. Results of satellite products compared with rain gauge stations for quantiles corresponding to a 50-year return period.

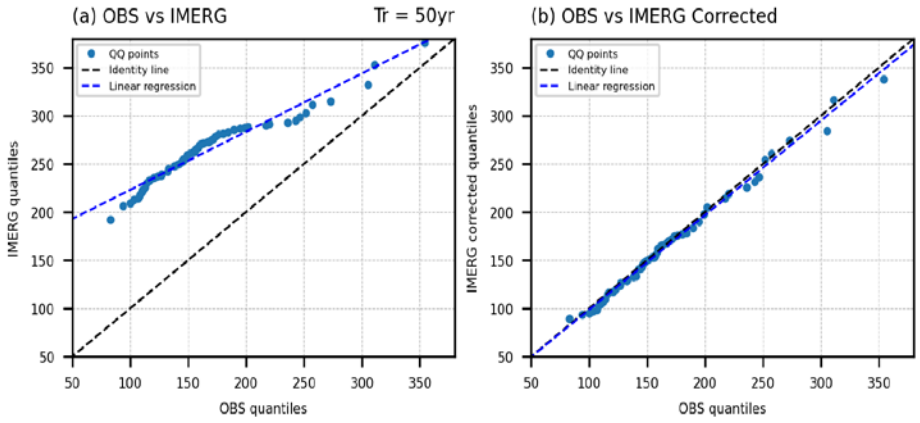


Figure 2. Quantile-Quantile plots comparing (a) observed data with IMERG and (b) with IMERG after bias correction.

The latest results led to more favorable outcomes. However, it is necessary to apply cross-validation to obtain a reliable assessment of the performance of the presented framework.

Acknowledgments: This research was supported by the "raINfall exTremEs and their impacts: from the local to the National ScalE" (INTENSE) project, funded by the European Union - Next Generation EU in the framework of PRIN (Progetti di ricerca di Rilevante Interesse Nazionale) programme (grant 2022ZC2522).

References

Marani M, Ignaccolo M (2015) A Metastatistical Approach to Rainfall Extremes. Advances in Water Resources 79(2015): 121-126. http://dx.doi.org/10.1016/j.advwatres.2015.03.001

Marra F, Borga M, Morin E (2020) A Unified Framework for Extreme Subdaily Precipitation Frequency Analyses Based on Ordinary Events. Geophysical Research Letters 47: 1-8. https://doi.org/10.1029/2020GL090209

Zorzetto E, Marani M (2018) Downscaling of Rainfall Extremes From Satellite Observations. Water Resources Research 55(1): 156-174. http://doi.org/10.1029/2018WR022950

Extreme precipitation in Italy: detection of changes and trends in satellite data

M. Darienzo[1*], M. Marani[1], F. Marra[2]
[1] Department of Civil, Environmental, and Architectural Engineering, University of Padua, Padua, Italy
[2] Department of Geoscience, University of Padua, Padua, Italy
* e-mail: matteo.darienzo@unipd.it

Introduction

Several studies derived past changes in the probability of occurrence of extreme precipitation over Italy using historical rainfall records from rain gauges (e.g. Libertino et al. 2019; Dallan et al. 2022). However, rain gauges alone cannot adequately sample the spatial variability of extreme rainfall, especially in areas with strong climatological gradients, such as the Italian orographic and coastal regions (Marra et al. 2022). To improve the spatial understanding of extreme rainfall and to identify hotspots of extreme rainfall across Italy, we use precipitation estimates from a long-recording satellite precipitation product.

Before assessing trends, however, it is critical to assess the homogeneity of the time series, as the presence of change-points in the data may introduce spurious trends. This is particularly important for satellite products, as diverse sensors and data correction have been used to produce them over the years. To avoid this pitfall, we propose a two-step analysis framework based on (i) classical homogeneity tests and a probabilistic segmentation procedure to detect past change points, and (ii) trend analysis tests to assess the presence of statistically significant trends in the series. We focus on the annual maximum daily precipitation, the cumulative annual precipitation and the three largest daily precipitation amounts in each year. We are mainly interested in identifying macro spatial patterns of these discontinuities.

In a further stage, non-stationary models will be implemented for the frequency analysis (e.g. MEVD, Marani and Ignaccolo 2015, and SMEV, Marra et al. 2020) to search for causative relationships between trends in extremes and trends in intensity and/or occurrence frequency of ordinary values.

Materials and methods

We analyse daily precipitation data estimated across Italy by the satellite product CHIRPS (Funk et al. 2015, pixel size of 5566 m, from 1981 to 2023), which dates back to the first geostationary satellites and is the longest satellite record available. For each grid cell, we study the following rainfall depth statistics: annual maximum, annual total accumulation, and annual three-largest values. For each variable we apply:

1. three homogeneity tests (at the 5% of significance level): the Pettitt, the Buishand's Range, and the Standard Normal Homogeneity tests, using R package *trend* (Pohlert 2023).
2. A probabilistic multi-changepoint segmentation method based on Bayesian/MCMC framework (Darienzo et al. 2021), which provides the uncertainty on each estimated change time.
3. Mann-Kendall and Sen's Slope trend tests (at the 5% significance level) using R package *trend* (Pohlert 2023), which provide indications on the existence and magnitude of trends.
4. The analysis of the autocorrelation function to explore data independence.

Results and concluding remarks

Figure 1 shows that for all three variables a few areas are affected by statistically significant discontinuities and/or trends. However, most of the areas with discontinuities are consistent with those showing trends (e.g. South-Eastern Italy, alpine North-Eastern Italy, Sardegna). The pdfs of all change times show poor informative results with slightly multimodal behaviour (three main modes near 1985-1994, 2001 and 2014), but affected by very large uncertainty covering almost the whole period, suggesting the discontinuities are not due to instrumental changes but probably to the trends or to seldom and local

anomalies (e.g. a few years particularly dry/wet in some regions). Moreover, the analysis of the autocorrelation function (not shown) indicates poor autocorrelation across Italy, suggesting data independence. The analysis will be then performed on other available products despite their shorter time coverage. After further validation, we will proceed with the frequency analysis using SMEV non-stationary models accounting for the trends.

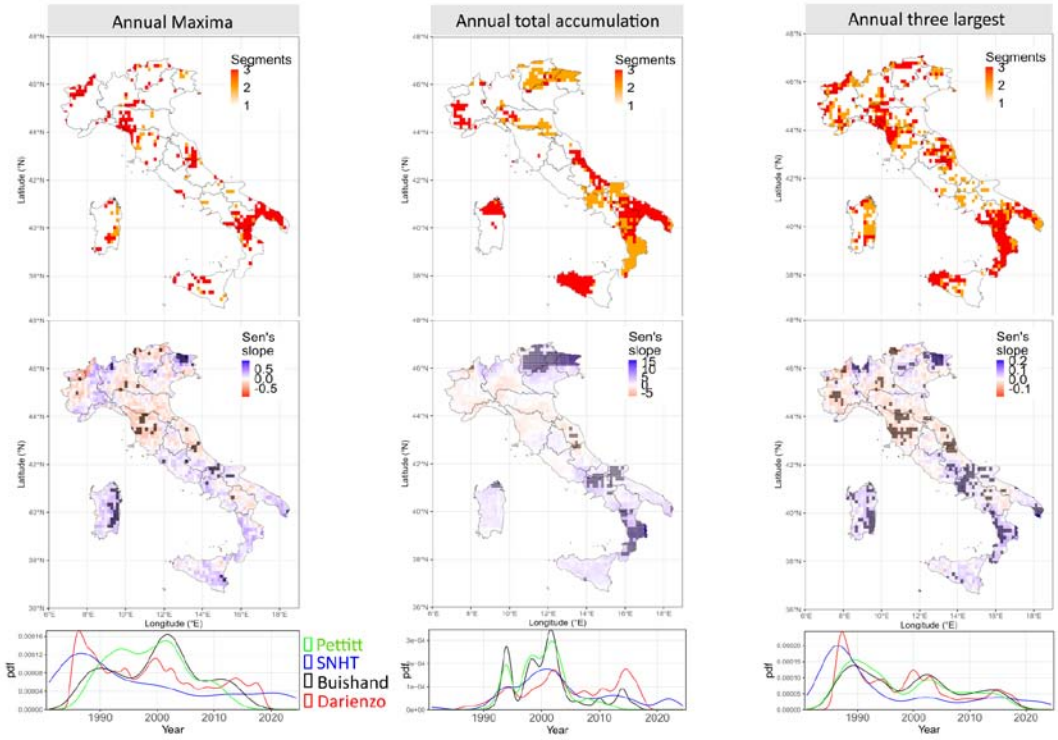


Figure 1. Results for CHIRPS (on Italy) for three different variables. On the top, segmentation results (when at least two of the four methods show a change); in the middle, Sens' Slope from red (decreasing trend) to blue (increasing trend) and black dots for significant Mann-Kendall trends; on the bottom, the pdfs of all detected change times.

Acknowledgments: This research has been supported by the INTENSE project (raINfall exTremEs and their impacts: from the local to the National ScalE) funded by the European Union - Next Generation EU in the framework of PRIN (Progetti di ricerca di Rilevante Interesse Nazionale) programme (grant 2022ZC2522).

References

Dallan E, Borga M, Zaramella M, Marra F (2022) Enhanced summer convection explains observed trends in extreme subdaily precipitation in the eastern Italian Alps. Geophysical Research Letters, 49, e2021GL096727. https://doi.org/10.1029/2021GL096727

Darienzo M, Renard B, Le Coz J, Lang M (2021) Detection of stage-discharge rating shifts using gaugings: A recursive segmentation procedure accounting for observational and model uncertainties. Water Resources Research, 57, e2020WR028607. https://doi.org/10.1029/2020WR028607

Funk C, Peterson P, Landsfeld M, Pedreros D, Verdin J, Shukla S, Husak G, Rowland J, Harrison L, Hoell A, Michaelsen J (2015) The climate hazards infrared precipitation with stations—a new environmental record for monitoring extremes. Sci Data 2, 150066. https://doi.org/10.1038/sdata.2015.66

Libertino A, Ganora D, Claps P (2019) Evidence for increasing rainfall extremes remains elusive at large spatial scales: The case of Italy. Geophysical Research Letters, 46, 7437–7446. https://doi.org/10.1029/2019GL083371

Marani M, Ignaccolo M (2015) A metastatistical approach to rainfall extremes. Advances in Water Resources, Volume 79, Pages 121-126, ISSN 0309-1708. https://doi.org/10.1016/j.advwatres.2015.03.001

Marra F, Borga M, Morin E (2020). A unified framework for extreme subdaily precipitation frequency analyses based on ordinary events. Geophysical Research Letters, 47, e2020GL090209. https://doi.org/10.1029/2020GL090209

Marra F, Armon M, Morin E (2022) Coastal and orographic effects on extreme precipitation revealed by weather radar observations, Hydrol. Earth Syst. Sci., 26, 1439–1458. https://doi.org/10.5194/hess-26-1439-2022

Pohlert T (2023) Trend: Non-Parametric Trend Tests and Change-Point Detection. R package version 1.1.6. https://CRAN.R-project.org/package=trend

Using agent-based modeling to address climate change in coastal areas: The case of Vouliagmeni, Greece

C.N. Roukounis*, V.A. Tsihrintzis
Center for the Assessment of Natural Hazards and Proactive Planning & Laboratory of Reclamation Works and Water Resources Management, School of Rural, Surveying and Geoinformatics Engineering, National Technical University of Athens, 9 Heroon Polytechniou St., 15780 Zographou, Athens, Greece
** e-mail: roukchar@mail.ntua.gr*

Introduction

Erosion and flooding are serious threats to coastal areas worldwide, affecting both public and private infrastructure, including ports, airports, power plants, residences, hotels, and wastewater treatment plants (Giannakidou et al. 2020; Stamou et al. 2024). Agent-based modeling (ABM) captures how diverse stakeholders adapt to economic and regulatory challenges in climate change. It simulates dynamic decision-making, policy impacts, and economic trade-offs, offering scenario-based insights that traditional models often miss. To investigate potential relationships between economic growth, energy dynamics, and climate change at the regional, national, and international levels, a new generation of agent-based models has emerged in recent years (e.g. Fouladvand 2024).

In this study, we evaluate the degree of resilience for various socioeconomic scenarios using the previously created Coastal Resilience Agent-Based Model (CRes-ABM) (Roukounis et al. 2025) and Coastal Resilience Index (CResI) (Roukounis et al. 2023), using the GAMA Platform (Taillandier et al. 2019). At both the individual (household) and governmental levels, CRes-ABM assesses the immediate impacts of these environmental changes and emphasizes the effectiveness of different adaptation and mitigation strategies. The region of Vari-Voula-Vouliagmeni, Attica, Greece, is chosen for application of the model.

Materials and methods

In order to evaluate the local resilience of coastal urban and suburban areas to coastal flooding, CResI (Roukounis et al. 2023) provides a single, unitless aggregated value, incorporating nineteen coastal parameters. A CResI value of 1.00 indicates very high resilience, while a value of 5.00 indicates very low resilience. To ensure a comprehensive representation of the parameters influencing coastal resilience, the model integrates information on sea-level rise projections, population demographics, and wave climate.

Depending on the complexity that needs to be handled, the number of agents can be changed. In the present study, the model took into account three different kinds of agents: one governmental agent serving as the primary decision-maker, household agents representing individual households, and cell agents, representing the coastal environment. The model incorporates a set of adaptation measures that were assessed by experts in earlier research (Roukounis and Tsihrintzis 2024). Data and agent decisions within the model are updated and mapped in each time-step (1 year). Household agents adapt to environmental changes, policies, and community norms, making decisions about property insurance and flood protection. The governmental agent makes decisions to protect community safety and sustainability, such as launching awareness campaigns, and implementing protection measures or retreat plans.

Results and concluding remarks

Three climate change scenarios were chosen. Current and historical conditions (from 1976 to 2005), as well as the scenarios "Symphony of Disintegration" (GR-SSP2xRCP4.5) and "For Whom the Storm Tolls" (GR-SSP5xRCP8.5). Two maps are produced, one with and without adaptation measures (CResI-Adapt), displaying the CResI values under each scenario. In contrast, it is less evident how vulnerability is reduced in scenario GR-SSP5xRCP8.5 following adaptation. Moreover, the total number of cells with CResI values greater than 4.0 is tracked. Additionally, since both insurance and awareness status continue to grow at a

positive rate throughout the experiment, we draw important conclusions about the timing of the governmental decisions and actions. The "For whom the storm tolls" scenario is the most challenging due to continued fossil fuel development and reliance on unsustainable measures like quay walls and breakwaters. In all scenarios managed retreat was not feasible due to high costs and advanced tourism activity in the area.

Model outcomes demonstrated that agent interactions have a substantial impact on each region's degree of resilience. In addition to the typical coping strategies, like installing hard protection (breakwaters, etc.), the resilience is largely shaped by easier choices. The resilience of regions is significantly influenced by decisions about insurance coverage and awareness initiatives. The behavioral simulation, which was based on social and economic conditions in addition to physical data, generally showed various profiles of how people and communities react to natural hazards.

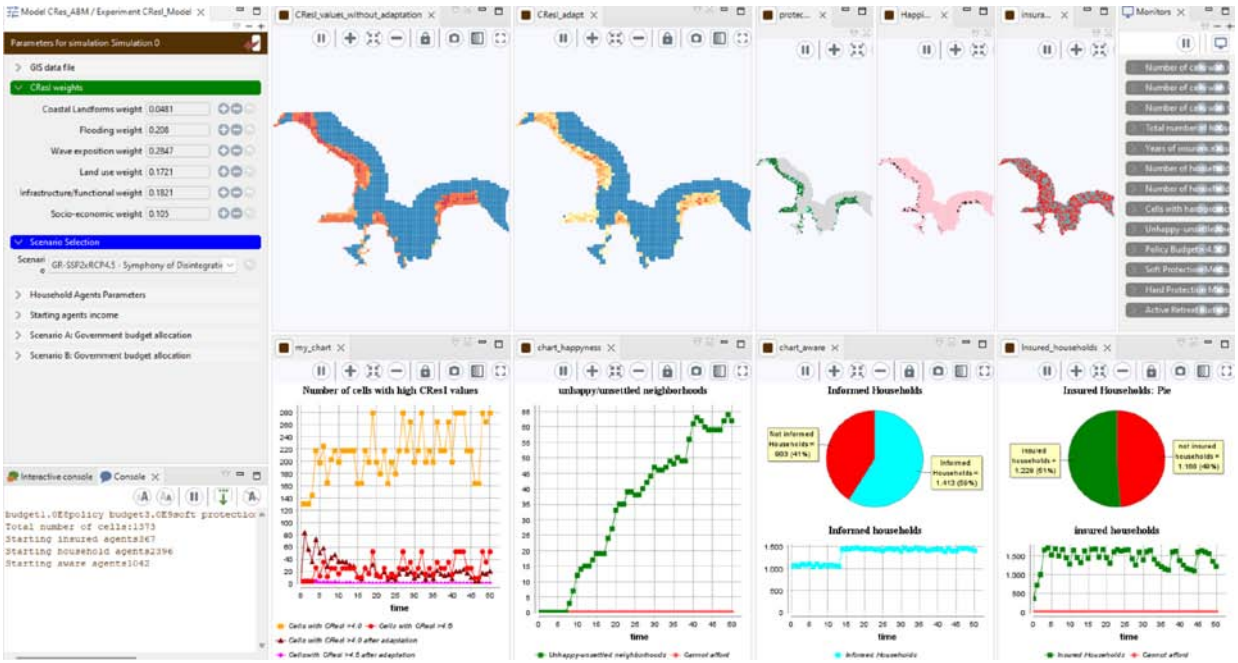


Figure 1. Indicative screenshot of the output of the model for year 2090 – Scenario "Symphony of Disintegration".

References

Filatova T, Verburg P, Parker DC, Stannard CA (2013) Spatial agent-based models for socio-ecological systems: Challenges and prospects. Environ. Modell. Software 45:1-7 http://dx.doi.org/10.1016/j.envsoft.2013.03.017

Fouladvand J (2024) Why and how can agent-based modelling be applied to community energy systems? A systematic and critical review. Energy Res Soc Sci 114:103572. https://doi.org/10.1016/j.erss.2024.103572

Giannakidou C, Diakoulaki D, Memos CD (2020) Vulnerability to Coastal Flooding of Industrial Urban Areas in Greece. Environ Process 7:749–766. https://doi.org/10.1007/s40710-020-00442-7

IPCC (2023) Summary for Policymakers. In: Climate Change 2023: Synthesis Report. Contribution of Working Groups I, II and III to the Sixth Assessment Report of the Intergovernmental Panel on Climate Change [Core Writing Team, H. Lee and J. Romero (eds.)]. IPCC, Geneva, Switzerland, pp. 1-34.

Roukounis CN, Chondros M, Tsoukala VK, Tsihrintzis VA (2025) Agent-Based Modeling Under Climate Uncertainties: The Coastal Resilience (CRes-ABM) Model. J Geovis Spat Anal 9(11). https://doi.org/10.1007/s41651-024-00210-3

Roukounis CN, Tsihrintzis VA (2024) Climate Change Adaptation Strategies for Coastal Resilience: A Stakeholder Surveys. Water (Basel) 16:1519. https://doi.org/10.3390/w16111519

Roukounis CN, Tsoukala VK, Tsihrintzis VA (2023) An Index-Based Method to Assess the Resilience of Urban Areas to Coastal Flooding: The Case of Attica, Greece. J Mar Sci Eng 11:1776. https://doi.org/10.3390/jmse11091776

Stamou A, Mitsopoulos G, Koutroulis A (2024) Proposed Methodology for Climate Change Adaptation of Water Infrastructures in the Mediterranean Region. Environ Process 11:12. https://doi.org/10.1007/s40710-024-00691-w

Taillandier P, Gaudou B, Grignard A, et al (2019) Building, composing and experimenting complex spatial models with the GAMA platform. Geoinformatica 23:299–322. https://doi.org/10.1007/s10707-018-00339-6

Assessment methodology of flash flood susceptibility for the river basins of Sardinia (Italy)

J. Napolitano[1*], D. Caracciolo[2], A. Cera[1], S. Frongia[2], G. La Gumina[1], S. Liberatore[2], A. Carletti[1,3]
[1] CINSA - Interdepartmental Center for Engineering and Environmental Sciences, University of Cagliari, Italy
[2] ARPAS - Regional Agency for Environmental Protection of Sardinia, Cagliari, Italy
[3] DICAAR - Department of Civil, Environmental Engineering and Architecture, University of Cagliari, Italy
* e-mail: jacopo.napolitano@unica.it

Introduction

In the forthcoming decades, the most significant impacts resulting from the combined effects of rising temperatures, increased frequency of extreme weather events, reduced average annual precipitation, and decreased annual river discharge are expected to manifest primarily through alterations in the hydrological regime. These changes may further increase the risk of landslides, debris flows and flash floods.

Flash flood events are typically characterized by intense rainfall and short durations, usually few hours (Doswell 2015). These events occur in basins with low storage capacity and produce highly unpredictable effects with limited lead time (Terti et al. 2015). According IPCC report (2012), the incidence of climate change has made these phenomena more frequent, particularly in specific territorial contexts characterized by "small basins" (Karkani et al. 2021), with very short concentration times and meteorological event durations on the order of few hours or less.

Such phenomena occur in areas with poorly permeable soils or inadequate drainage systems, where the hydrological input is unable to infiltrate the soil rapidly, thus contributing almost entirely to surface runoff. In hydrological processes related to runoff formation, the land cover, morphometric, and geopedological characteristics of the river basin play a crucial role (Santangelo et al. 2011). These factors are particularly significant in Mediterranean basins, such as those in Sardinia, which are often small basins in size, have shallow soil profiles (Rinat et al. 2018), and exhibit low attenuation of hydrometric phenomena.

In hydraulic terms, the rapid growth phase (or concentration) of the flood, where the peak can occur shortly after precipitation begins, and the dynamics of the flow (Marchi et al. 2016), create the conditions for sudden overflow and potential damage to people and infrastructures. The speed at which these phenomena develop makes it difficult for the relevant authorities to implement timely civil protection measures. Therefore, proactive actions (European Commission 2007) such as weather forecasting activities and mapping with classification of the flash floods susceptibility over different river basins are crucial for the protection of these susceptible areas.

Materials and methods

In the framework of the methodologies for the study of flash floods susceptibility, the "Arno" method (Distretto Idrografico dell'Appennino Settentrionale 2010) has been proposed to be applied on all Italian territory, establishing guidelines for this kind of assessment. It is based on the identification and evaluation of three parameters assumed as indicators of the predisposition to flash flood phenomena for the hydrographic basins. This method has a comparative nature; indeed, it allows to evaluate the susceptibility of the basin through the normalization and the comparison of the three "forecasting" parameters: basin area (A_B in km²), the lag time (T_{LAG} in hours) which represents the rapidity of the flood development and the return time (T_R in years) of the expected recurrence of critical rainfall events (50 mm hour^{-1}), considered as the "critical rainfall threshold" for the Arno basin.

This methodology was developed and validated based on empirical evidence related to the specific characteristics of the Arno River basin. The application of this approach in other contexts, such as the basins in the Sardinia region, suggested a critical review of the method highlighting the need to introduce new descriptive parameters in order to adequately account for the differences and homogeneities among

basins, while also considering the main flash floods influencing factors found in the literature (Marchi et al. 2010; Elghouat et al. 2024), such as topography, vegetation cover, land use, geology and pedology.

This study presents an enhancement to the Arno methodology by identifying a new set of parameters for assessing the flash floods susceptibility of river basins. Specifically, in addition to the morphometric, hydrological, and pluviometric characteristics used in the original methodology, a novel set of descriptive parameters have been incorporated, including slope, potential infiltration coefficient, and normalized difference vegetation index (NDVI), aimed at improving and generalizing the representation of flash floods susceptibility.

Results and concluding remarks

The proposed methodology is based on a critical review of the Arno methodology, with the objective of generalizing its applicability to a broader and more heterogeneous territorial context. This has been achieved through the integration of a new set of influencing factors for flash floods, with promising results in terms of identifying, with a high level of detail, the areas susceptible to flash flood events.

The model developed, based on accessible data and easily applicable by no expert users, will provide a strategic tool for decision-making authorities. The main output consists of flash flood susceptibility maps for river basins and sub-basins, depicted through a simple and readable categorization into four classes (low, medium, high, and very high).

Acknowledgments: This study was supported by the Hydrographic District Regional Board of Sardinia (ADIS) and the Regional Agency for Environmental Protection of Sardinia (ARPAS).

References

Distretto Idrografico dell'Appennino Settentrionale (2010) Metodologia per la definizione della predisposizione al verificarsi di fenomeni tipo Flash Flood nel bacino del fiume Arno (a cura di M. Brugioni e B.Mazzanti).

Doswell CA (2015) Flooding. In: Encyclopedia of Atmospheric Sciences, 2nd edn In: (North, G. R., Pyle, J. & Zhang, F., eds.). Academic Press, Oxford, pp. 201–208. https://doi.org/10.1016/B978-0-12-382225-3.00151-1.

Elghouat A, Algouti A, Algouti A, Baid S, Ezzahzi S, Kabili S, Agli S (2024) Integrated approaches for flash flood susceptibility mapping: spatial modeling and comparative analysis of statistical and machine learning models. A case study of the Rheraya watershed, Morocco. Journal of Water and Climate Change 1 August 2024; 15 (8): 3624–3646. doi: https://doi.org/10.2166/wcc.2024.726.

European Commission (2007) EU directive 2007/60 on the assessment and management of flood risks. Official Journal of the European Union. https://eur-lex.europa.eu/legal-content/EN/TXT/HTML/?uri=CELEX:32007L0060.

IPCC (2012) Managing the Risks of Extreme Events and Disasters to Advance Climate Change Adaptation; Field, C.B., Barros, V., Stocker, T.F., Qin, et al., Eds.; Cambridge University Press: Cambridge, UK.

Karkani A, Evelpidou N, Tzouxanioti M, Petropoulos A, Santangelo N, Maroukian H, Spyrou E, Lakidi L (2021) Flash Flood Susceptibility Evaluation in Human-Affected Areas Using Geomorphological Methods—The Case of 9 August 2020, Euboea, Greece. A GIS-Based Approach. GeoHazards, 2(4), 366-382. https://doi.org/10.3390 /geohazards204002.

Marchi L, Borga M, Preciso E, Gaume E (2010) Characterisation of selected extreme flash floods in Europe and implications for flood risk management. Journal of Hydrology. 349: 118-133. https://doi.org/10.1016 /j.jhydrol.2010.07.017.

Marchi L, Cavalli M, Amponsah W, Borga M, Crema S (2016) Upper limits of flash flood stream power in Europe. Geomorphology, 272: 68-77. https://doi.org/10.1016/j.geomorph.2015.11.005.

Rinat Y, Marra F, Zoccatelli D, Morin E (2018) Controls of flash flood peak discharge in Mediterranean basins and the special role of runoff-contributing areas. Journal of Hydrology. https://doi.org/10.1016/j.jhydrol.2018.08.055.

Santangelo N, Santo A, Di Crescenzo G, Foscari G, Liuzza V, Sciarrotta S, Scorpio V (2011) Flood susceptibility assessment in a highly urbanized alluvial fan:the case study of Sala Consilina (southern Italy). Natural Hazards and Earth System Sciences, 2765-2780. DOI: 10.5194/nhess-11-2765-2011.

Terti G, Ruin I, Anquetin S, Gourley J (2015) Dynamic vulnerability factors for impact-based flash flood prediction. Natural Hazards, 1481–1497. https://doi.org/10.1007/s11069-015-1910-8.

Climate change impact on compounding streamflow flood and drought characteristics in Europe

R.A. Odongo*,T. Koenen, P. Reija Zamora, S.J. Sutanto
Earth Systems and Global Change, Environmental Sciences, Wageningen University, Netherlands
** e-mail: rhoda.odongo@wur.nl*

Introduction

Droughts and floods are among the most devastating natural hazards, causing substantial economic, social, and environmental consequences worldwide (He, 2019). While these events have traditionally been studied in isolation (e.g., Van Loon, 2015), recent evidence suggests that compound flood and drought (CFD) events—where a flood is followed by a drought or vice versa—can result in far greater impacts (de Ruiter et al., 2020; Matanó et al., 2024). Climate change is expected to alter the frequency, duration, and severity of both floods and droughts, thereby influencing CFD occurrences (Cammalleri et al., 2020; Roudier et al., 2016). However, studies on compounding events that have an opposite nature of hazards, such as CFD, are still very limited. Furthermore, to our knowledge there is no studies in Europe exploring the effects of climate change on CFD events.

This study aims to investigate how the characteristics of single flood and drought events, as well as their return periods, evolve under different climate scenarios in European river basins (the Danube, Rhine, Rhone, and Tagus), with a specific focus on the changes in characteristics of CFD by using daily streamflow simulations from the Community WaterModel (CWatM). We assess changes in the return periods of high- and low-flow events under two climate change scenarios: SSP1-2.6 (low-emission scenario) and SSP5-8.5 (high-emission scenario). By addressing these aspects, the research provides insights into how water resource management strategies should adapt to mitigate future compound risks associated with shifting hydrological extremes.

Materials and methods

Study Area

The selected river basins represent a diverse range of climatic and hydrological conditions across Europe and over different Köppen-Geiger climate zones: 1) *Danube Basin:* the second-largest river basin in Europe, covering central and eastern Europe, with a mix of temperate and continental climates (ICPDR, 2010). 2) *Rhine Basin:* a major western European river that experiences both glacial and rainfall-fed hydrological regimes (Uehlinger et al., 2009). 3) *Rhone Basin:* a predominantly Alpine river, strongly influenced by snowmelt dynamics (Olivier et al., 2022). 4) *Tagus Basin:* a Mediterranean river basin characterized by seasonal variability and prolonged drought periods (Britannica, 2023).

Data and Methods

- *Hydrological Model:* Daily streamflow data were obtained from the CWatM for the historical period (1981-2010) and projected future periods (2041-2070) under SSP1-2.6 and SSP5-8.5.
- *Flood and Drought Identification:* Threshold-based methods were applied, using the 95th percentile for floods and the 15th percentile for droughts. Flood and drought characteristics were defined as flood/drought frequency, flood/drought duration, flood magnitude, flood volume, and drought volume.
- *CFD Definition:* A CFD event occurs when a flood is followed by a drought (F-D) or vice versa (D-F) within a 7-month transition period (Rezvani et al., 2023). CFD characteristics were analysed based on frequency, duration, transition time, and empirical compound severity index.
- *Statistical Analysis:* Gumbel's extreme value distribution was used to estimate return periods of high- and low-flow events. These return periods were calculated using the annual maxima and minima streamflow.

Results and concluding remarks

Changes in Flood and Drought Characteristics

- *Floods:* Under SSP1-2.6, floods are projected to become more frequent and severe, particularly in the Rhine and Rhone basins. In contrast, under SSP5-8.5, flood frequency decreases but severity increases, particularly in the Tagus and Danube basins.
- *Droughts:* Drought severity is expected to increase across all basins under both scenarios, with the Tagus and Danube basins experiencing the largest increases in drought duration and intensity.

Changes in High- and Low-Flow Events

- In the Rhine and Tagus basins, high-flow events will generally be less extreme under both climate scenarios. In contrast, high-flow events in the Rhone basin will be more extreme. In the Danube basin, high-flow events will be more extreme under SSP1-2.6 but less extreme under SSP5-8.5.
- Low-flow events in the Rhine and Tagus basins are expected to be generally less extreme under both climate scenarios. In the Rhone basin, low-flow events will not change significantly under SSP1-2.6 but will be more extreme under SSP5-8.5. In the Danube basin, low-flow events will be less extreme under SSP1-2.6 and more extreme under SSP5-8.5.

Changes in Compound Flood and Drought Events

- *CFD Frequency:* Varies greatly depending on the climate scenarios and basin. The Rhine and Rhone basins will experience an increase in CFD events, while the Danube basin will see a decline. The Tagus basin CDF events will remain constant under both scenarios.
- *Transition Time:* The Rhone basin will experience shorter transition times between floods and droughts, exacerbating the risks associated with rapid shifts in hydrological extremes, with the Rhine basin seeing slightly longer transition times.
- *Impact of Baseflow:* Rivers with lower baseflow (e.g., Tagus) exhibit more extreme CFD variations due to their reliance on variable precipitation inputs.

Acknowledgments: This work was supported by the European Union's Horizon Europe MSCA Staff Exchanges programme under grant agreement No. 101131220 (ClearClimate) and by the Earth Systems and Global Change research group, Wageningen University.

References

Britannica. (2023). Tagus River. Tagus River. Encyclopedia Britannica. Https://Www.Britannica.Com/Place/Tagus-River.

Cammalleri, C., Naumann, G., Mentaschi, L., Bisselink, B., Gelati, E., De Roo, A., & Feyen, L. (2020). Diverging hydrological drought traits over Europe with global warming. Hydrology and Earth System Sciences, 24(12), 5919–5935. https://doi.org/10.5194/hess-24-5919-2020

de Ruiter, M. C., Couasnon, A., van den Homberg, M. J. C., Daniell, J. E., Gill, J. C., & Ward, P. J. (2020). Why We Can No Longer Ignore Consecutive Disasters. Earth's Future, 8(3). https://doi.org/10.1029/2019EF001425

He, X. (2019). Droughts and floods in a changing environment natural influences. Human Interventions, and Policy Implications.

ICPDR. (2010). River basin. Https://Www.Icpdr.Org/Danube-Basin/Danube-River-Basin.

Matanó, A., Berghuijs, W. R., Mazzoleni, M., de Ruiter, M. C., Ward, P. J., & Van Loon, A. F. (2024). Compound and consecutive drought-flood events at a global scale. Environmental Research Letters, 19(6), 064048. https://doi.org/10.1088/1748-9326/ad4b46

Olivier, J.-M., Carrel, G., Lamouroux, N., Dole-Olivier, M.-J., Malard, F., Bravard, J.-P., Piégay, H., Castella, E., & Barthélemy, C. (2022). The Rhône River Basin. In Rivers of Europe (pp. 393–453). Elsevier. https://doi.org/10.1016/B978-0-08-102612-0.00011-0

Rezvani, R., RahimiMovaghar, M., Na, W., & Najafi, M. R. (2023). Accelerated lagged compound floods and droughts in northwest North America under 1.5–°C 4 °C global warming levels. Journal of Hydrology, 624, 129906. https://doi.org/10.1016/J.JHYDROL.2023.129906

Roudier, P., Andersson, J. C. M., Donnelly, C., Feyen, L., Greuell, W., & Ludwig, F. (2016). Projections of future floods and hydrological droughts in Europe under a +2°C global warming. Climatic Change, 135(2), 341–355. https://doi.org/10.1007/s10584-015-1570-4

Uehlinger, U., Arndt, H., Wantzen, K. M., & Leuven, R. S. E. W. (2009). The Rhine River Basin. In Rivers of Europe (pp. 199–245). Elsevier. https://doi.org/10.1016/B978-0-12-369449-2.00006-0

Van Loon A. F. (2015) Hydrological drought explained. WIREs Water 2(4): 359–392. https://doi.org/10.1002/wat2.1085

The characteristics of flash droughts across Thessaly, Central Greece, from 1990 to 2024

V. Leivadiotis, A. Psilovikos*
Laboratory of Ecohydraulics & Inland Water Management (ECO–HYDRO Lab), Department of Ichthyology & Aquatic Environment, University of Thessaly, Fytoko St., 384 46, N. Ionia Magnisias, Greece
** e-mail:* psiloviko@uth.gr

Introduction

Traditional droughts are typically slow-developing events, taking months or years to peak (Raposo et al., 2023). However, recent studies highlight "flash droughts," characterized by rapid onset and intensification, often triggered by atmospheric anomalies (Osman et al., 2022). Flash droughts are defined by their short duration or rapid decline in conditions, with soil moisture (SM) anomalies serving as key indicators. Indices like the Evaporative Demand Drought Index (EDDI) and the Evaporative Stress Index (ESI) have been developed to identify these events. Globally, research on flash droughts is often localized, focusing on specific basins or countries. In Europe, comprehensive studies remain scarce, and no research has examined flash droughts in Greece, a Mediterranean region heavily reliant on agriculture. This study explores flash drought dynamics in Thessaly, Greece's key agricultural hub, to enhance understanding and support early warning systems.

Materials and methods

The ERA5-Land dataset (Muñoz-Sabater et al., 2019) provides high-resolution global data on land-based water and energy cycles. This study uses soil moisture data (0–7 cm, 7–28 cm) from 1990 to 2024, aggregated into pentad averages. Flash droughts are identified when soil moisture drops from above the 40th percentile to below the 20th within three consecutive pentads, with a decline rate exceeding the 5th percentile threshold (Otkin et al., 2018). Events last 3–12 pentads, excluding short-term anomalies, distinguishing them from conventional droughts (Yuan et al., 2019).

Results and concluding remarks

Based on ERA5 soil moisture data and flash drought identification criteria, the spatial distribution of flash drought frequency in Thessaly (1990–2024) reveals significant variability. Frequencies range from 18.4% to 57.5%, with the western region showing the lowest frequency (~25%), the eastern region averaging 35%, and the northern region peaking at 45% (Figure 1). On average, Thessaly experiences a flash drought frequency of 27.1%, with an annual average frequency of 0.8%. The average duration of events is 6 pentads (30 days), though central and northern regions experience longer events (35 days). Soil moisture decline rates range from 0.6% in the north to 1.4% in the southwest, averaging 1.01%. Event magnitude varies, with the lowest values (0.35) in the north and east and the highest in the west. Intensity values range from 5.56% in the northeast to 10.56% in the southwest, averaging 7.85%. Seasonally, flash droughts occur most in the fall (43.3%), followed by spring (32.0%), summer (21.1%), and winter (3.6%) (Figure 2). Decline rates are lowest in winter (0.30%) and highest in summer (1.2%). Event magnitude is consistent across winter, spring, and fall (0.5) but lower in summer (0.32). Intensity peaks in fall (8.9%) and is lowest in summer (5.1%). The analysis highlights significant spatial and seasonal variability in flash drought characteristics across Thessaly, emphasizing the region's susceptibility to rapid-onset drought events. The findings indicate that the northern and eastern parts of Thessaly are more frequently affected, while the southwestern areas experience the highest soil moisture decline rates and event intensities. Seasonal trends reveal a concentration of flash drought events in the fall, aligning with periods of agricultural vulnerability in this agriculturally significant region. These results provide valuable insights into the spatial

and temporal dynamics of flash droughts, which can inform targeted mitigation strategies and early warning systems. By identifying areas with higher frequencies, intensities, and durations, stakeholders can prioritize resource allocation and risk management efforts. The study underscores the need for continued monitoring and refinement of drought prediction tools to address the challenges posed by flash droughts in a changing climate, particularly in regions heavily reliant on agriculture.

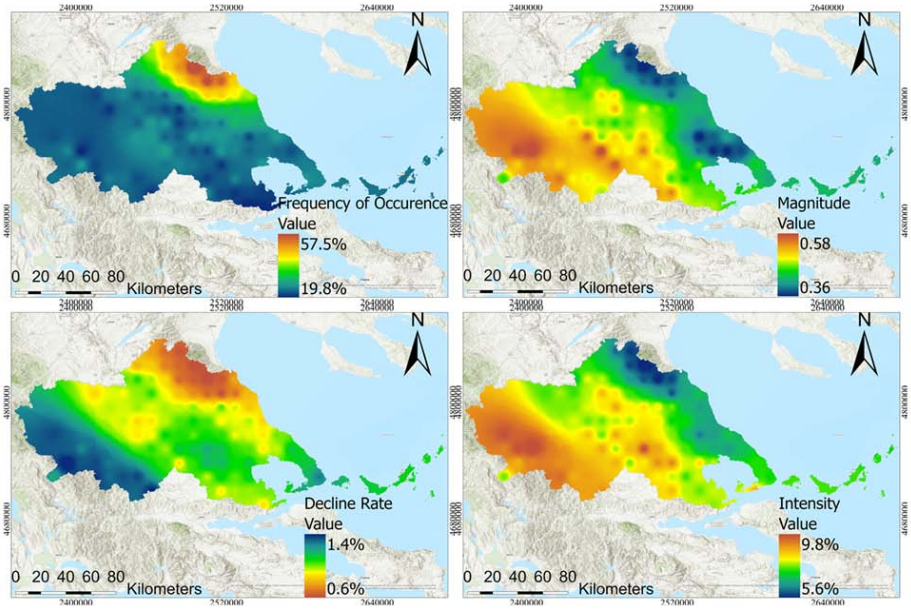


Figure 1. Spatial distribution of flash drought characteristics

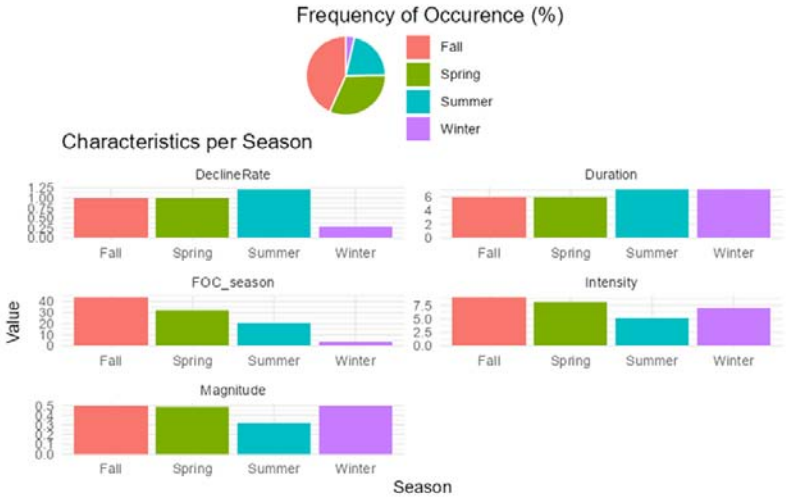


Figure 2. Seasonal characteristics of flash droughts

References

Raposo, V. D. M. B., Costa, V. A. F., & Rodrigues, A. F. (2023). A review of recent developments on drought characterization, propagation, and influential factors. Science of The Total Environment, 898, 165550. https://doi.org/10.1016/j.scitotenv.2023.165550

Osman, M., Zaitchik, B. F., Badr, H. S., Otkin, J., Zhong, Y., Lorenz, D., Anderson, M., Keenan, T. F., Miller, D. L., Hain, C., & Holmes, T. (2022). Diagnostic Classification of Flash Drought Events Reveals Distinct Classes of Forcings and Impacts. Journal of Hydrometeorology, 23(2), 275-289. https://doi.org/10.1175/JHM-D-21-0134.1

Muñoz Sabater, J. (2019): ERA5-Land hourly data from 1950 to present. Copernicus Climate Change Service (C3S) Climate Data Store (CDS). DOI:10.24381/cds.e2161bac

Otkin, J. A., Svoboda, M., Hunt, E. D., Ford, T. W., Anderson, M. C., Hain, C., & Basara, J. B. (2018). Flash droughts: A review and assessment of the challenges imposed by rapid-onset droughts in the United States. Bulletin of the American Meteorological Society, 99(5), 911-919.

Yuan, X., Wang, L., Wu, P., Ji, P., Sheffield, J., & Zhang, M. (2019). Anthropogenic shift towards higher risk of flash drought over China. Nature Communications, 10(1), 1-8. https://doi.org/10.1038/s41467-019-12692-7.

Using complex networks in Reconnaissance Drought Index (RDI) non-stationary estimation

H. Vangelis[1*], K. Spiliotis[2], K. Voudouris[3], M. Spiliotis[4]
[1] Laboratory of Reclamation Works and Water Resources Management, School of Rural, Surveying and Geoinformatics Engineering, National Technical University of Athens, Athens, Greece
[2] Laboratory of Mathematics and Informatics (ISCE), Department of Civil Engineering, Democritus University of Thrace, Xanthi, Greece
[3] Laboratory of Engineering Geology and Hydrogeology, School of Geology, Aristotle University of Thessaloniki (AUTh), Thessaloniki, Greece
[4] Division of HydraulicWorks, Department of Civil Engineering, Democritus University of Thrace, Xanthi, Greece
* e-mail: harrivag@central.ntua.gr

Introduction

Drought is a global phenomenon, exhibiting, however, significant regional variation, and thus, understanding its response to climate change and accurately assessing its patterns and tendencies is important at global, regional, and local scales (Asadi Zarch et al., 2015). In most regions around the globe, future droughts seem to present an increasing trend compared to historical periods (e.g., Wu et al., 2024). Moreover, due to global warming, hydrometeorological processes do not retain a stationary behaviour. Studies on future climate conditions imperatively recommend the use of non-stationarity in drought assessment (e.g., Zhang et al., 2022).

Global warming has also increased precipitation (P) and temperature sensitivity (Giorgi and Bi, 2005), with increasing temperature leading to potential evapotranspiration (PET) increase, due to the amplified surface vapour pressure deficits (Zhao and Dai, 2022). This impact has shifted the focus from precipitation to evapotranspiration as a key influencer of drought (Wang et al., 2021). Therefore, drought indices which can reflect the deficit between P and PET, such as the Reconnaissance Drought Index (RDI) proposed by Tsakiris and Vangelis (2005), are considered more accurate in drought assessment.

In this paper, Complex Networks Theory is applied to the initial value a_k of RDI, thus, overriding the problem of stationarity, since Complex Networks do not use statistical measures such as the mean and standard deviation. The outcome is compared to the timeseries produced through the typical standardisation of RDI, based on the gamma probability distribution.

Materials and methods

The analysis is based on gauged data of precipitation and temperature recorded by the Department of Meteorology of Cyprus, at the meteorological station of Nicosia (Lefkosia), the capital and largest city of Cyprus, reflecting the conditions of Eastern Mediterranean region.

A complex network is constructed from the time series of the initial value a_k of RDI, as presented by Tsakiris and Vangelis (2005), based on the visibility algorithm by Lacasa et al. (2008). According to the visibility algorithm, nodes correspond to time (years in our case), and edges are created in proportion to the intensity of the yearly drought value. To understand the structure of the resulting network, characteristic measures of connectivity are proposed, indicating the importance (centrality) of the vertices in the network. According to Spiliotis et al. (2025), the following measures should be used: (a) betweenness centrality, expressing the importance of a node in terms of the number of paths passing through it (large values of betweenness centrality correspond to important nodes), (b) closeness centrality, estimating the importance of a node in terms of the average minimum path of the node in relation to the other nodes (smaller values of the average minimum path imply higher closeness of the node), and (c) network communities detection and modularity, proposing the organization of drought into specific periods (color code in Figure 1, numbers are years: 1 corresponds to 1971-72, etc.).

Results and concluding remarks

Applying the visibility algorithm to the available time series of a_k for the 39 hydrological years of the period 1971-72 to 2009-10, the Complex Network of Figure 1 is produced.

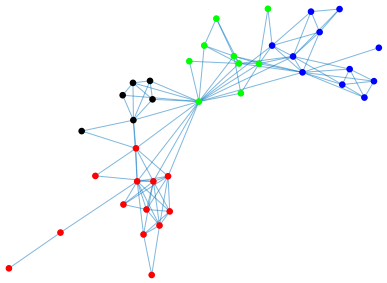


Figure 1. Complex Network by applying the Lacasa et al. (2008) visibility algorithm.

As presented in Figure 2, betweenness centrality captures the droughts events of 1972–73, 1977–78, 1990–91 and 2007–08, emphasizing in the extreme drought of 1990–91. On the other hand, closeness centrality presents a high correlation with standard RDI calculation, with a correlation coefficient of ρ=0.76.

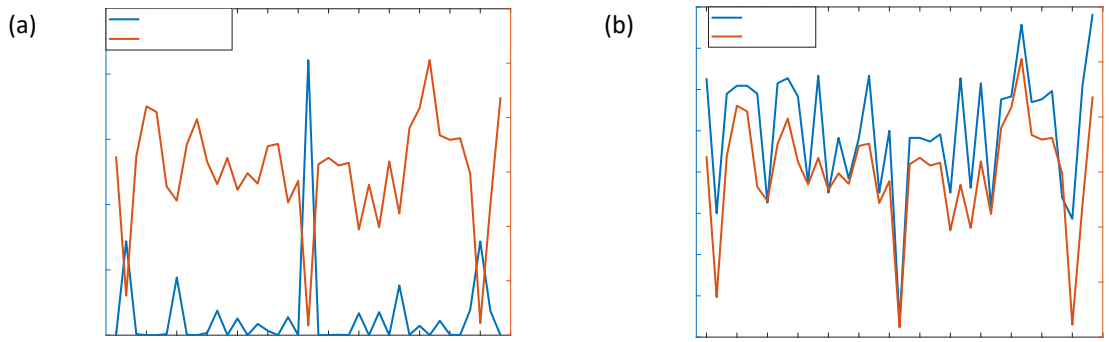


Figure 2. Measures of connectivity of the Complex Network: (a) betweenness centrality, and (b) closeness centrality.

It may be concluded that the proposed methodology can override the stationarity issue in drought assessment, identifying accurately the drought occurrences, while the closeness centrality can also provide a measure of the intensity of each drought episode.

References

Asadi Zarch MA, Sivakumar B, Sharma A (2015) Droughts in a warming climate: a global assessment of Standardized precipitation index (SPI) and Reconnaissance drought index (RDI). Journal of Hydrology 526: 183–195. https://doi.org/10.1016/j.jhydrol.2014.09.071

Giorgi F, Bi X (2005) Updated regional precipitation and temperature changes for the 21st century from ensembles of recent AOGCM simulations. Geophysical Research Letters 32: L21715. https://doi.org/10.1029/2005GL024288

Lacasa L, Luque B, Ballesteros F, Luque J, Carlos Nuno J (2008) From time series to complex networks: The visibility graph. Proceedings of the National Academy of Sciences of the USA 105 (13): 4972–4975. https://doi.org/10.1073/pnas.0709247105

Spiliotis K, Voudouris K, Vangelis H, Spiliotis M (2025) Analysis of Annual Drought Episodes Using Complex Networks. Sustainability 17(4): 1441. https://doi.org /10.3390/su17041441

Tsakiris G, Vangelis H (2005) Establishing a drought index incorporating evapotranspiration. European Water 9/10: 3–11. https://ewra.net/ew/pdf/EW_2005_9-10_01.pdf

Wang T, Tu X, Singh VP, Chen X, Lin K (2021) Global data assessment and analysis of drought characteristics based on CMIP6. Journal of Hydrology 596: 126091. https://doi.org/10.1016/j.jhydrol.2021.126091

Wu D, Chen J, Xiong L, Lee J-H, Kim J-S, Moon H-T (2024) Assessing global drought conditions under climate change: A comparison of stationary and non-stationary approaches and identification of hotspot regions. Journal of Hydrology 640: 131663. https://doi.org/10.1016/j.jhydrol.2024.131663

Zhang X, Hao ZC, Singh VP, Zhang Y, Feng SF, Xu Y, Hao FH (2022) Drought propagation under global warming: characteristics, approaches, processes, and controlling factors. Science of the Total Environment 838(2): 156021. https://doi.org/10.1016/j.scitotenv.2022.156021

Unravelling the role of temperature for convective storms in Sicily

G. Patti*, D. Treppiedi, A. Francipane, L.V. Noto
Department of Engineering, University of Palermo, Palermo, Italy
** e-mail: giorgia.patti@unipa.it*

Introduction

Convective precipitation events are frequently associated with the occurrence of lightning, which serves as an indicator of the electrical activity typically present in more intense thunderstorm systems. In this context, air temperature plays a crucial role in influencing the intensity of extreme precipitation. According to the Clausius–Clapeyron relationship, the air's capacity to hold water vapor increases by approximately 7% per degree Celsius of warming, suggesting that extreme precipitation events may intensify under climate change. Recent studies, such as the one by Molnar et al. (2015) conducted in Switzerland, have shown that precipitation intensities during lightning-associated storm events tend to increase at higher rates than those without lightning. However, the scaling rate observed in the presence of lightning strikes is lower than what is obtained considering all events together. Starting from this evidence, we questioned if these dynamics are also relevant for the Sicilian context, where other studies have verified the presence of CC scaling values tending towards super-CC (i.e., approximately 14%/°C), especially in areas particularly affected by convective phenomena induced by orographic uplift (Treppiedi et al., 2023, 2025).

Materials and methods

Following the methodological approach proposed by Molnar et al. (2015), an empirical analysis was conducted using observational data from several meteorological stations located in Sicily, with the aim of investigating the relationship between air temperature, extreme precipitation intensity, and the presence of lightning as an indicator of convective activity. The definition of precipitation events was based on the criteria described by Marra et al. (2020), which involve identifying ordinary rainfall events based on consecutive wet periods separated by dry periods, rather than fixed time intervals. This event-based approach allows for a more realistic characterization of precipitation phenomena, especially when it comes to taking into account the type of event, namely distinguishing between convective or stratiform events. For data processing, we used the agrometeorological network of SIAS (i.e., *Servizio Informativo Agrometeorologico Siciliano*), which provides high-resolution measurements of precipitation (10 minutes) and air temperature (1 hour). Lightning data were obtained from the Italian Air Force's lightning detection system, which allowed for the classification of rainfall events according to the presence or absence of atmospheric electrical activity —a key element for identifying convective precipitation. In particular, for each meteorological station, a surrounding area with a radius of 30 km was defined as the lightning search zone, ensuring that the analysis focused exclusively on atmospheric electrical activity directly associated with the rainfall events observed at each station.

Results and concluding remarks

We associated the maximum 10-minute precipitation intensity with the number of lightning strikes recorded during each event. As an example, for the Maletto station we observed that the most intense rainfall episodes tend to be accompanied by a greater number of lightning strikes, despite the presence of lightning across a broad range of precipitation intensities (Figure 1a). This confirms the convective nature of such storms and highlights the complex and variable relationship between lightning and rainfall, with several lightning-rich events also occurring at moderate precipitation levels.

To investigate the role of temperature, events were classified as convective or stratiform based on lightning presence, and scaling relationships were assessed using a semi-logarithmic quantile regression approach. The results reveal a clear distinction in how precipitation intensity scales with air temperature

depending on storm type. For the Maletto station, the empirical Clausius–Clapeyron (CC) scaling rate is highest when all events are analyzed together (black line), reaching approximately 12.13% $°C^{-1}$. This rate is significantly higher than those calculated for lightning (red line) and non-lightning (blue line) events separately: 10.75% $°C^{-1}$ and 7.81% $°C^{-1}$, respectively (Figure 1b).

This pattern aligns with the results obtained by Molnar et al. (2015) for Swiss stations, where mixing stratiform and convective events leads to an overestimation of the overall scaling rate. Stratiform events are typically less intense and more frequent at lower temperatures, while convective ones are more intense and associated with higher temperatures. Although the Maletto station is shown here as an example, the results suggest that even in Mediterranean regions with complex orography like Sicily, storm type and temperature are crucial factors influencing extreme precipitation scaling. These results suggest the importance of distinguishing between convective and stratiform events in temperature–precipitation scaling analyses to avoid misleading interpretations in climate change studies.

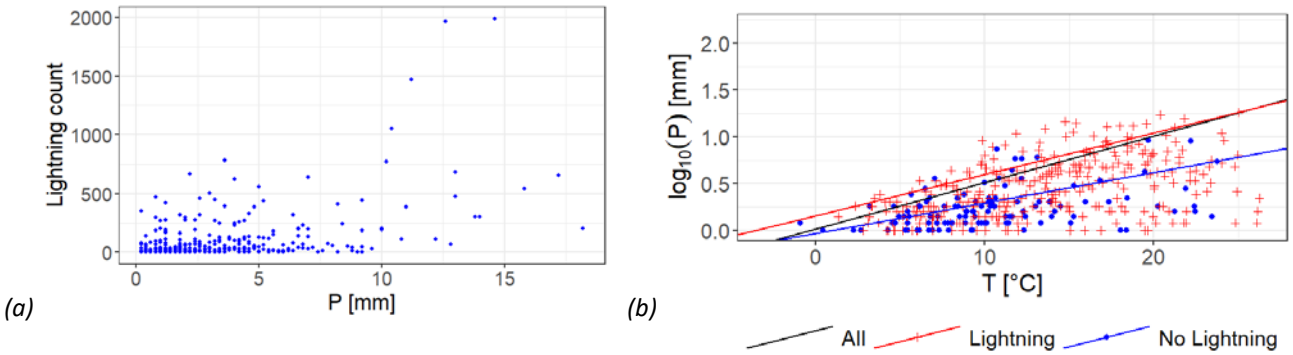


Figure 1. (a) Relationship between total precipitation and number of lightning strikes recorded during individual events at the Maletto station. (b) Example of the estimates of scaling slopes by the quantile regression method for the Maletto station.

Acknowledgments: We acknowledge the Italian Air Force Meteorological Service for providing lightning data.

References

Marra F, Borga M, Morin E (2020) A unified framework for extreme subdaily precipitation frequency analyses based on ordinary events. Geophysical Research Letters, 47,e2020GL090209. 9. https://doi.org/10.1029/2020GL090209

Molnar P, Fatichi S, Gaál L, Szolgay J, Burlando P (2015) Storm type effects on super Clausius–Clapeyron scaling of intense rainstorm properties with air temperature. Hydrol. Earth Syst. Sci., 19, 1753–1766. https://doi.org /10.5194/hess-19-1753-2015

Treppiedi D, Cipolla G, Noto LV (2023) Convective precipitation over a Mediterranean area: From identification to trend analysis starting from high-resolution rain gauges data. International Journal of Climatology, 43(1), 293-313.

Treppiedi D, Francipane A, Noto LV (2025) Projecting Depth-Duration-Frequency Curves for Future Climate: a Case Study in the Mediterranean Area. Water Resources Management, https://doi.org/10.1007/s11269-025-04162-1

Where floodwater meets mobility: A GIS approach to bridge risk and rerouting in the Flood@Road project

L. Pavesi[1], F. Nardi[1*], M. Amaddii [2], C.B. Amirehsan[2], A. Carboni[3], F. Castelli[2], P. Claps[3], F.P. Deflorio[3], M. Ferraro[3], P. Mazzoglio[3], F. Vagnon[3], C. Arrighi[2]
[1] *Department of Civil and Environmental Engineering, University of Rome Tor Vergata, Rome, Italy*
[2] *Department of Civil and Environmental Engineering, University of Florence, Florence, Italy*
[3] *Department of Environmental, Land and Infrastructure Engineering (DIATI), Polytechnic University of Turin, Turin, Italy*
** e-mail: fernando.nardi@uniroma2.eu*

Introduction

Flood events increasingly threaten the functionality and safety of transport infrastructure, particularly in riverine regions where bridges represent critical nodes. Bridge overtopping not only endangers drivers but also causes significant disruptions in mobility, emergency response, and logistics. While traditional flood risk assessments focus on hydrological scenarios, they often overlook geomorphological predisposition and cascading effects on traffic (Pregnolato et al., 2017, Shahdani et al., 2022).

This work presents an integrated approach developed within the FLOOD@ROAD project, combining overtopping risk screening with traffic impact simulation. A key innovation lies in the use of a web-based GIS platform that visualizes at-risk bridges and evaluates the consequences of their closure on regional mobility through dynamic rerouting simulations.

Materials and methods

The proposed methodology combines large-scale geospatial screening and dynamic traffic simulation to assess the risk of bridge overtopping and its systemic impacts on road network performance. The case study focuses on the Magra River basin in north-western Tuscany (970 km²), one of Italy's rainiest and most flood-prone regions.

The first phase involves catchment-scale screening using LiDAR-derived DSM and DTM, OpenStreetMap (OSM) road data, and hydrographic layers. Each road–river intersection is identified via GIS and analyzed morphometrically. The intersection height (Hi)—the difference between road level and river thalweg—is computed, while a Terrain Ruggedness Index (TRI) is applied to filter DSM noise caused by vegetation and artifacts.

The cross-section height (Hs) is extracted through unsupervised classification (Iso Cluster) of morphometric indicators such as profile curvature and elevation variance. Intersections with Hi < Hs are classified as overtopping-prone (Figure 1). Field surveys at selected locations validate Hi estimates, with error analysis stratified by TRI and Strahler stream order.

In the second phase, traffic disruption scenarios are modeled in SUMO (Simulation of Urban Mobility). A baseline network, built using ISTAT and AISCAT mobility data, is compared with flood scenarios in which at-risk bridges are removed. SUMO computes rerouting effects and quantifies travel time increases, detour lengths, and accessibility losses. Macroscopic simulations support the vulnerability assessment through indicators like Weighted Cost and Accessibility Index.

Simulation results are reintegrated into GIS, providing spatial insight into disruption patterns and supporting targeted, resilient infrastructure planning in the Magra River basin (Figure 2).

Results and concluding remarks

The methodology was applied to the Magra River basin (970 km²), identifying 231 road–river intersections. About 30% showed Hi < Hs, indicating high overtopping susceptibility under flood conditions.

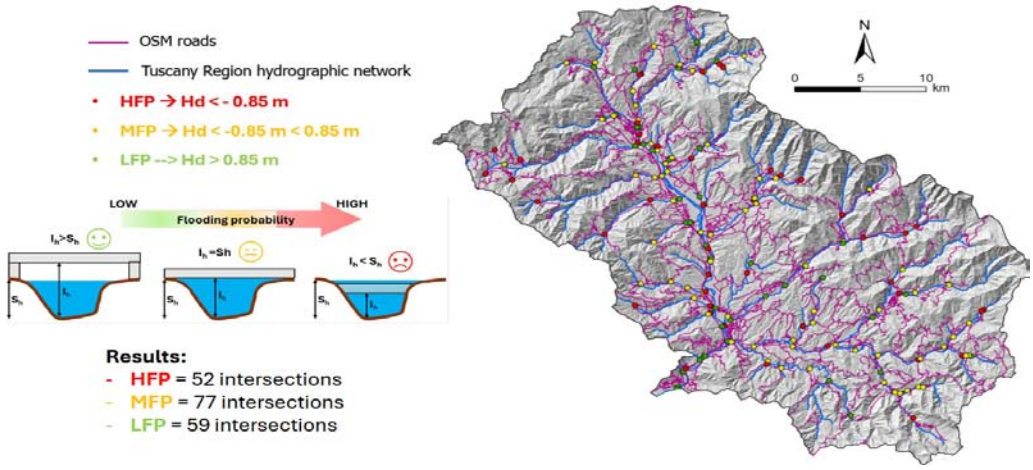


Figure 1. Flood overtopping risk at road–river intersections in the Magra River basin, based on morphometric screening (Hi < Hs).

Field validation showed that the accuracy of remotely sensed Hi varies with stream scale. For Strahler < 4, the median error (Δhe) was ~2 m (40%), due to vegetation and misalignment in narrow channels. For Strahler > 3, accuracy improved significantly, with Δhe ~0.4 m (12%), consistent with the DTM's 0.3 m resolution and typical stream widths (~35 m).

These findings (Figure 2) confirm the method's suitability for large-scale, low-cost screening of overtopping risk using only geometric and morphometric data. It effectively prioritizes critical sites for further hydraulic and traffic impact analysis, offering a replicable framework for flood-prone areas and supporting early warning, risk-informed planning, and resilience strategies.

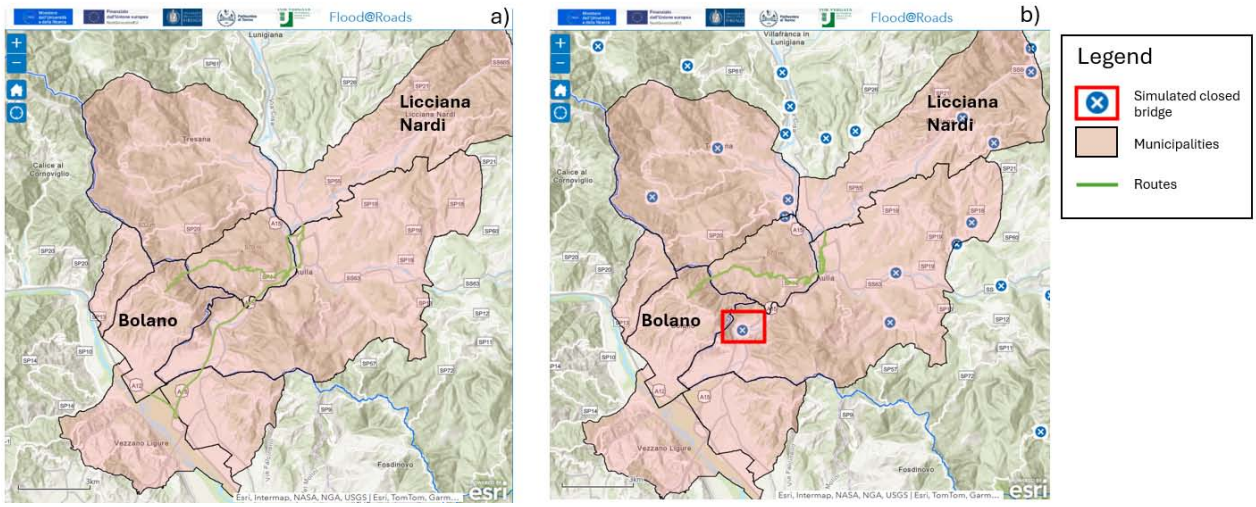


Figure 2. Web GIS app output of traffic network under flood scenarios; panel a) baseline condition, panel b) impact of single bridge closure due to overtopping.

Acknowledgment: This study was funded by the European Union – Next Generation EU through the PRIN 2022 initiative, within the project "FLOOD@ROAD" (Prot. 202257JJSJ).

References

Pregnolato, M., Ford, A., Wilkinson, S. M., & Dawson, R. J. (2017). The impact of flooding on road transport: A depth disruption function. Transportation Research Part D: Transport and Environment, 55, 67–81. https://doi.org/10.1016/j.trd.2017.06.020

Shahdani, F.J.; Santamaria-Ariza, M.; Sousa, H.S.; Coelho, M.; Matos, J.C. Assessing Flood Indirect Impacts on Road Transport Networks Applying Mesoscopic Traffic Modelling: The Case Study of Santarém, Portugal. Appl. Sci. 2022, 12, 3076. https://doi.org/10.3390/app12063076

An observational quality-controlled hourly precipitation database for Italy

D. Treppiedi[1*], E. Arnone[2], M. Darienzo[3], A. Ezeaba[4], A. Francipane[1], U. Khan[3], M. Marani[3], F. Marra[5], L.V. Noto[1], R. Paranunzio[6], C.A. Sanchez Pena[3]
[1] Department of Engineering, University of Palermo, Palermo, Italy
[2] Polytechnic Department of Engineering and Architecture, University of Udine, Udine, Italy
[3] University of Padova, Department of Civil, Environmental and Architectural Engineering, Padova, Italy
[4] Department of Land Environment Agriculture and Forestry, University of Padova, Padova, Italy
[5] Department of Geosciences, University of Padova, Padova, Italy
[6] Institute of Atmospheric Sciences and Climate (CNR-ISAC), National Research Council, Torino, Italy
* e-mail: dario.treppiedi@unipa.it

Introduction

Although we are living in a data-rich era, the availability of high-temporal-resolution precipitation data from rain gauges is still limited and highly spatially fragmented. While several satellite, radar, and reanalysis products are available, they often suffer from significant biases, particularly when it comes to intense precipitation events. The development of high-resolution observational datasets faces several challenges, most of which are related to data management or the lack of centralized institutions able of overseeing and integrating large-scale monitoring networks. In Italy, for example, hourly precipitation data are collected and managed independently by regional or sub-regional authorities. This results in a fragmented system and the absence of a unified, national-scale hourly precipitation dataset.

In this short paper, we present a first attempt to create an hourly precipitation dataset derived from rain gauges distributed throughout Italy. To ensure its reliability, we also apply different quality control algorithms designed to identify and correct potential inconsistencies and gross measurement errors.

Materials and methods

We start collecting sub-hourly and hourly rain gauge data from different regional agencies in Italy (i.e., Regional Civil Protection, Regional Agency for Environmental Protection, Agrometeorological services). In a first phase of pre-processing, we exclude all those gauges that are repeated among the different regional database or for which coordinates are not available. We then aggregate the data to the same temporal resolution (i.e., hourly) and refer the timing to the same time zone (i.e., UTC). Some of the quality checks defined in literature (Blenkinsop et al., 2017, Lewis et al, 2021) are then modified to suit the climatic characteristics of the Italian regions and applied to this homogenized dataset.

Results and concluding remarks

We collected data from approximately 3,000 rain gauges evenly distributed across the Italian mainland and the two main islands (i.e., Sicily and Sardinia) (Fig. 1a). From a temporal perspective, some of the time series begin in the early 1980s, but the highest gauges density covers a period ranging from the early 2000s to 2024 (Fig. 1b).

Figure 1c shows an example of the application of some quality control checks. Specifically, the Montemaggiore station in Friuli-Venezia Giulia (Fig. 1c) exhibits significant issues during the early years of sensor operation. Anomalous values are observed at a fixed time of day, likely due to the daily total being erroneously recorded as a single hourly value in the database. Other common errors include suspiciously high values (identified using extreme percentile thresholds) that occur after extended periods of missing data, potentially due to sensor instability when measurements resume.

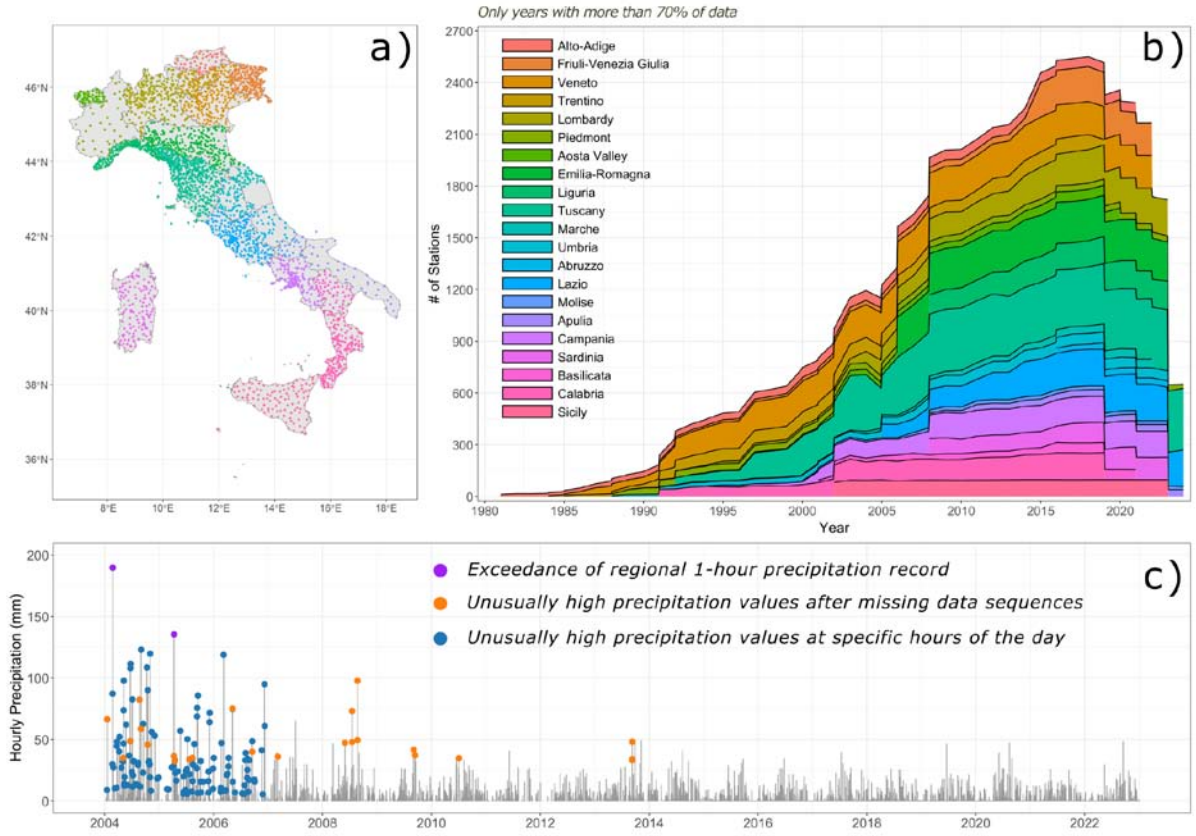


Figure 1. Spatial distribution of rain gauges collected at the national scale (a). Yearly hourly data availability (b); only years with more than 70% of available data were considered. Example of the quality control procedure for the Montemaggiore station (Friuli Venezia Giulia) (c). Colored dots indicate suspect values identified for removal to ensure data consistency.

The availability of this dataset can serve several purposes, including improving our understanding of hourly precipitation events and their spatio-temporal evolution across Italy. Furthermore, it can contribute to the validation of high-resolution climate projections (e.g., those from Convection Permitting Models) by investigating the characteristics of convective events. Finally, it can support efforts related to hydrological modelling, providing high-resolution input data that are essential for accurately simulating runoff processes, calibrating and validating hydrological models, and assessing the impact of extreme rainfall events at the catchment scale.

Acknowledgments: This research received funding from European Union NextGenerationEU – National Recovery and Resilience Plan (PNRR), Mission 4, Component 2, Investiment 1.1 - PRIN 2022 – 2022ZC2522 - CUP G53D23001400006. The authors gratefully acknowledge the Regional Agencies and Civil Protection Departments for providing rainfall data used in this study, including: ARPA Emilia-Romagna, ARPA Friuli-Venezia Giulia, ARPA Lombardia, ARPA Piemonte, ARPA Sardegna, ARPA Veneto, Centro Funzionale Regionale Regione Autonoma Valle d'Aosta, Meteo Trentino, Osservatorio Meteo Idrologico Reg. Liguria (OMIRL), Provincia Autonoma di Bolzano, Servizio Idrografico Regione Umbria, Servizio Idrologico della Regione Toscana, Protezione Civile Abruzzo, Protezione Civile Basilicata, Protezione Civile Calabria, Protezione Civile Campania, Protezione Civile Marche, Protezione Civile Molise, Protezione Civile Lazio, Protezione Civile Puglia, Servizio Informativo Agrometeorologico Regione Sicilia

References

Blenkinsop, S., Lewis, E., Chan, S. C., Fowler, H. J. (2017) Quality-control of an hourly rainfall dataset and climatology of extremes for the UK. International Journal of Climatology, 37(2), 722-740

Lewis, E., Pritchard, D., Villalobos-Herrera, R., Blenkinsop, S., et al. (2021) Quality control of a global hourly rainfall dataset. Environmental Modelling & Software, 144, 105169

Image-based surface velocity mapping in rivers: study case and calibration by ADCP data

P. Peykani*, D. Termini
Department of Engineering, University of Palermo, Palermo, Italy
** e-mail: peyman.peykani@unipa.it*

Introduction

Accurate estimation of river flow discharge is crucial for forecasting models, especially under the increasing threat of extreme hydrological events. Flow discharge is commonly calculated as the product of mean velocity and cross-sectional area, making precise velocity data essential. While field measurement instruments like Acoustic Doppler Current Profilers (ADCP) can be used in measuring full-depth velocity profiles, their deployment becomes difficult and risky during high-flow events due to turbulence, debris, and operator safety concerns. To address these challenges, non-contact image-based velocimetry technique has emerged as viable alternative for measuring surface velocities. Starting from the free-surface velocity distribution, the application of Entropy theory can be used to estimate the velocity profiles (e.g., Termini and Moramarco 2017).

Image-based technique, often supported by fixed-camera, offers spatially distributed, high-resolution velocity data. Recent comparative assessments demonstrate the practical value of this technique across a range of river environments and flow conditions, especially when calibrated against field measurements (Perks et al. 2016; Le Coz et al. 2010; Wijaya et al. 2023). A key challenge in applying image-based techniques is accurately assessing the error in surface velocity estimation, as this uncertainty is influenced by numerous factors related both to the measurement environment and the data processing approach (Termini and Di Leonardo 2018). To this aim detailed measured data should be used.

In this study, image-based technique is used to estimate free surface velocity distribution in selected reaches of Oreto River (Italy) and ADCP measurements are used for calibration and validation processes.

Materials and methods

Flow velocity measures were obtained during field campaigns conducted along a selected reach of the Oreto River in Palermo, Italy (Figure 1), by using an ADCP instrument mounted on a GPS-equipped boat. The boat traversed 13 cross-sectional transects, systematically collecting three-dimensional velocity data across the full water column. Multiple transects over the same cross-section have been performed in order to minimize random errors and improve the reliability of the measured velocity field.



Figure 1. Overview of the study area and field campaign

Post-processing of ADCP data included quality control filtering and transformation from instrument coordinates to river-aligned coordinates. Detailed vertical velocity profiles were obtained along two selected cross-sections.

The image-based technique has been implemented by using a Camera Nikon D5300, with high-resolution images (1920×1080 px, 30 fps), opportunely positioned over a bridge to capture the investigated

area. The recorded images sequences were then processed using PIVLab, an open-source particle image velocimetry (PIV) toolbox implemented in MATLAB. This software estimates surface flow velocity by identifying and tracking the movement of tracers between couples of consecutive images frames, by applying a cross-correlation algorithm to small interrogation windows across the image pairs. On the contrary to classical LSPIV procedures, in this work the image-based technique has been applied only by using moving grains and natural tracers and applying a procedure optimizing the selections of the interrogation area.

Results and concluding remarks

To assess the performance of the image-based technique, surface velocity measurements obtained from images analysis were compared with ADCP data collected along the selected cross sections of the river. A preliminary calibration has been operated by adjusting the software settings to minimize the discrepancy between the image-based estimates and ADCP measurements in the first cross-section. Then, the procedure has been validated by comparing image-based technique results to ADCP data in the second cross-section. Figure 2 presents a contour plot of the image-derived surface velocities and the comparison of the cross-sectional velocity profile obtained with ADCP data in this last section. The image-based method accurately captured the transversal distribution of flow velocity along the considered section. Discrepancies between the two methods remained within acceptable bounds.

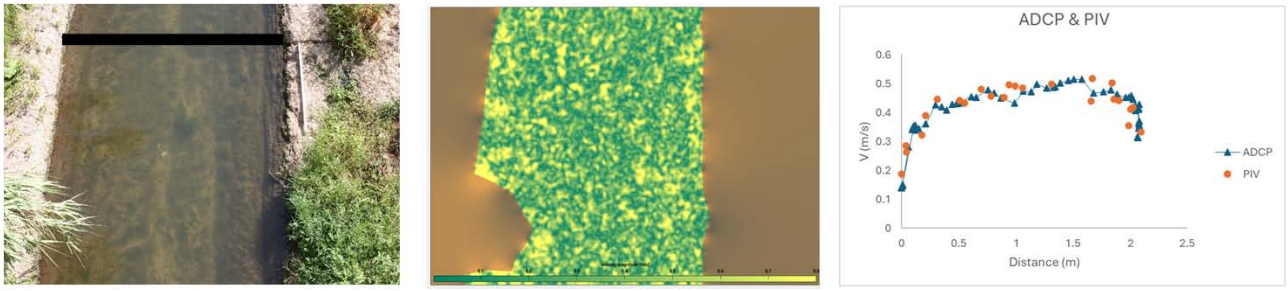


Figure 2. Comparison of velocity determined by image analysis with ADCP measure

These findings confirm that, with a proper calibration, image-based methods can serve as effective tool for flow monitoring by using only natural tracers, especially in scenarios where traditional instruments are impractical or unsafe. Further analyses will include sensitivity analyses related to image resolution and integration area to further improve image-based technique applicability.

Acknowledgments: This study funded by the European Union- Next Generation EU, Mission 4 Component 2 Project RETURN CUP B73C22001220006.

References

Le Coz, J., Hauet, A., Pierrefeu, G., Dramais, G., Camenen, B. (2010). Performance of image-based velocimetry (LSPIV) applied to flash-flood discharge measurements in Mediterranean rivers. Journal of hydrology, 394(1-2), 42-52. https://doi.org/10.1016/j.jhydrol.2010.05.049

Perks, M. T., Russell, A. J., Large, A. R. (2016). Advances in flash flood monitoring using unmanned aerial vehicles (UAVs). Hydrology and Earth System Sciences, 20(10), 4005-4015. https://doi.org/10.5194/hess-20-4005-2016

Termini, D., Di Leonardo, A. (2018). Efficiency of a digital particle image velocimetry (DPIV) method for monitoring the surface velocity of hyper-concentrated flows. Geosciences, 8(10), 383. https://doi.org/10.3390/geosciences8100383

Termini, D., Moramarco, T. (2017). Application of entropic approach to estimate the mean flow velocity and Manning roughness coefficient in a high-curvature flume. Hydrology Research, 48(3), 634-645. https://doi.org/10.2166/nh.2016.106

Wijaya, F., Liu, W. C., Huang, W. C. (2023). Comparative assessment of different image velocimetry techniques for measuring river velocities using unmanned aerial vehicle imagery. Water, 15(22), 3941. https://doi.org/10.3390/w15223941

III. Data and Models for Environmental, Social, and Governance (ESG) Risk Assessment

Bayesian analysis in assessing water quality: lessons learned from case studies

Z. Srđević, M. Ilić-Paunić*, B. Srđević
Department of Water Management, Faculty of Agriculture, University of Novi Sad, Novi Sad, Serbia
** e-mail: milica.ilic@polj.uns.ac.rs*

Introduction

Bayesian networks (BNs), also known as belief networks or causal probabilistic networks, are directed acyclic graphs that model the cause-and-effect relationships of system variables using conditional probabilities (Jensen, 1996; Heckerman, 2008). BNs are adept at integrating diverse system components, handling data from various sources, managing missing data, and incorporating uncertainty, making them ideal for these assessments. BNs are particularly useful when datasets are small or incomplete, offering a significant advantage when evaluating irrigation water quality. This paper aims to present and discuss the experience of the authors in applying BNs in two case studies: for the classification/prediction of water quality and assessment of water fitness for irrigation.

Materials and methods

Bayesian networks (BNs) consist of nodes (system variables), links (causal relationships), and Conditional Probability Tables (CPTs) that quantify the strength of these relationships. Nodes can be discrete or continuous, and links point from cause to effect. For instance, if nodes A and B influence node C, A and B are "parent" nodes, and C is their "child."

Each node has a CPT that specifies probabilities for every combination of its parent nodes' states. Conditional probabilities determine how states propagate through the network, updating other nodes' probabilities when new information becomes available. Changes in one node affect all connected nodes, directly or indirectly, as probabilities are updated iteratively using Bayes' theorem.

Root nodes, like A and B in this example, are not caused by other nodes and are associated with unconditional probabilities. BNs rely on Bayesian principles to revise probabilities as new evidence emerges, transitioning from prior (initial) probabilities to more reliable posterior probabilities through the iterative application of the Bayesian formula.

Naïve Bayes model proposed in Ilic et al. (2022b) is based on nine water quality parameters: temperature, pH value, electrical conductivity, oxygen saturation, biological oxygen demand, suspended solids, nitrogen oxides, orthophosphates, and ammonium. It is created in the software Netica and tested and verified using the data covering the period 2013-2019 from five locations in Vojvodina Province, Serbia. The model trained on forty-eight samples is then used to classify 68 water samples.

Assessment of irrigation water fitness for varying natural and management conditions should preferably, but usually not possible, include all influential factors and their complex interdependence. An approach based on the FAO guidelines and Bayesian Network (BN) modelling (Ilic et al. 2022a) included fifteen factors recommended by FAO in a network to assess irrigation water fitness. Seven nodes in the network belong to the FAO-defined water quality variables, one node to "Soil Texture," and two for plant tolerance: "Salt Sensitivity" and "Sensitivity to Toxic Ions." These serve as parent and root nodes. Child nodes represent potential issues from water use: "Miscellaneous Effects," "Salinity," "Water Infiltration Rate," and "Specific Ion Toxicity," each with three quality states (I, II, III). These nodes are parents to the final node, "Degree of Restriction on Use." The usability of the BN was tested on two water samples from two measuring points in Vojvodina Province, Serbia.

Results and concluding remarks

Some variables in water fitness assessments are known (e.g., soil and plant characteristics), some are easily measured (e.g., pH and EC), while others are costly or time-consuming to obtain. The Bayesian network created by Ilic et al. (Ilic et al., 2022a) proved that can provide accurate results even with limited data and can be expanded by adding nodes for factors like irrigation methods, crop water needs, and additional water quality parameters. They can also include decision nodes to support management actions. However, expanding a BN requires adjustments to child nodes and a strong understanding of the network structure. Knowledge of water quality and irrigation management is crucial, particularly for constructing CPTs.

BNs are limited by their inability to incorporate feedback loops, unlike Naïve Bayes (NB), which assumes variable independence. While NB is unsuitable for correlated irrigation data, it excels in classification tasks, handling large datasets with minimal preprocessing and robustness to missing data. Effectiveness of the NB NB in classification tasks is demonstrated by Srđević and Srđević (2020) and Ilić et al. (2022b) in water quality prediction, where it correctly classified water samples in 64 out of 68 cases despite missing data – example showing the differences between classification based on Serbian Water Quality Index (SWQI) and NB predicted water quality classes for sampling location at River Danube is given in Figure 1. However, its simplicity can lead to biases in complex datasets and challenges in capturing intricate dependencies.

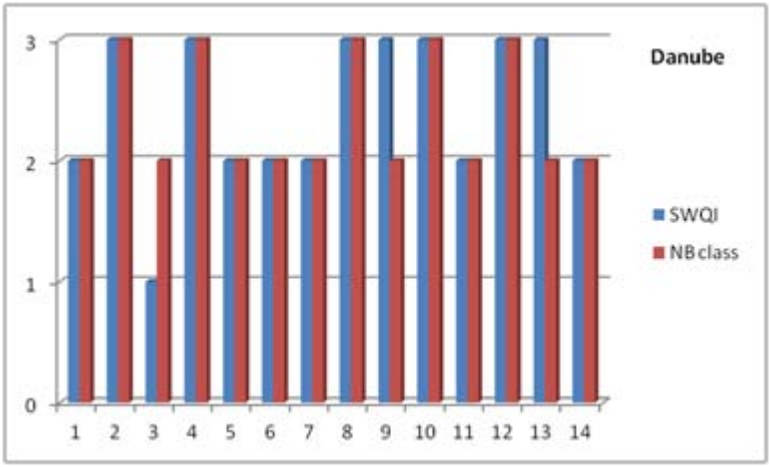


Figure 1. The differences between SWQI-based water quality classes and predicted by NB (Ilić et al. (2022b).

Both BN and NB have unique strengths and limitations for water quality assessment or similar types of problems. The choice between them depends on the specific problem to be solved, the data's complexity and availability, available computational resources, desired interpretability, scalability, etc.

Acknowledgments: Ministry of Science, Technological Development and Innovation of Serbia, Grant No. 451-03-137/2025-03/ 200117 and 451-03-136/2025-03/ 200117.

References

Heckerman, D (2008). A Tutorial on Learning with Bayesian Networks. In: Holmes, D.E., Jain, L.C. (eds) Innovations in Bayesian Networks. Studies in Computational Intelligence, vol 156. Springer, Berlin, Heidelberg.

Ilić M, Mutavdžić B, Srđević Z, Srđević B (2022a) Irrigation water fitness assessment based on Bayesian network and FAO guidelines. Irrigation and Drainage, 71 (3), 665-675.

Ilić M, Srđević Z, Srđević B (2022b) Water Quality Prediction Based on Naïve Bayes Algorithm. Water Science and Technology 2022; wst2022006.

Jensen FV (1996) Bayesian network basics. AISB quarterly, 9-22.

Srđević Z, Srđević B (2020) Procena klase kvaliteta voda primenom algoritma Naivni Bajes (Water quality class prediction using Naïve Bayes algorithm). Vodoprivreda, 52(303-305), 125-134. (In Serbian)

An engineering model based on the renovation times of impacted building for estimating indirect damage to residential properties

S. Molica*, G. Brigandì, G.T. Aronica
Department of Engineering, University of Messina, Messina, Italy
** e-mail: salvatore.molica@studenti.unime.it*

Introduction

One of the main challenges in flood risk management is understanding the various phases that form the post-disaster recovery (PDR) process. Understanding recovery mechanisms through modelling recovery time phases is crucial as it can help predict losses, effectively manage the recovery process, and design mitigation measures for more resilient communities (Ali & Mannakkara, 2024). Despite its growing importance, the recovery phase of individual households has been understudied, with most literature focusing on large-scale indirect damages related to economic activities. In this regard, existing studies on estimating post-event recovery time for residential properties lack logical engineering approaches and are primarily based on post-event observational data, making them difficult to transfer to other contexts (see, for example, FloodSite data 2007). This study proposes an engineering-based method to take advantages of direct damage data to model the restoration time of impacted housing units (as done by Almufti et al. 2013 in the case of earthquakes). The restoration time, combined with the event duration, constitutes the medium-term recovery phase, which can be used both for a rapid estimation of possible post-event indirect damages and to model the recovery time of an impacted community.

Materials and methods

The main idea of the model proposed in this work is to correlate the concept of recovery time with that of direct damage to assess possible indirect impacts (evacuation costs, temporary housing, and extra costs) immediately after a flood. This is done by estimating the restoration duration of damaged housing units and, consequently, the post-evacuation return duration. To determine the post-event restoration duration, the model uses the concept of direct damage, which represents a snapshot of the necessary repair work after an event. The direct damage data is integrated with the man-day parameter to estimate the hypothetical duration of the restoration work. The model thus provides an engineering-based estimate of the recovery duration that allows for use regardless of the case study, as it solely presupposes the availability of damage functions calibrated on reconstruction costs.

The proposed methodology is structured in several phases. First, it is assumed that direct damage represents a snapshot of the necessary repair work. The direct damage and the amount of repair work are then estimated. Subsequently, the existence of a typical work crew, corresponding to the minimum necessary crew, is assumed. The labour incidence relative to the total work is extrapolated based on public price lists to estimate the restoration duration. Finally, it is considered that the duration of the repair work, combined with the event duration and the flood's persistence time, corresponds to the evacuation duration. This duration is then linked to temporary housing costs and extra costs to determine the flood's indirect impact.

This procedure allows modelling the time required for returning to damaged buildings after the flood and thus linking this time with extra costs incurred by impacted families, such as temporary housing costs, temporary job loss, travel extra costs, and general expenses.

Results and concluding remarks

The proposed procedure was applied to the case study of the town of Barcellona Pozzo di Gotto (Sicily, Italy) which is crossed by the Longano torrent. On 22 November 2011, the town centre was affected by a large flooding with water levels ranging from 0.7 to 2.0 metres caused by an extreme rainfall event which a

duration of approximately 11 hours and, a cumulative volume of 348 mm.

Direct damages, used as input for the application of the described methodology, were estimated for return periods ranging from 10 to 300 years, using specific damage functions derived by Naso et al. (2016) using surveyed reconstruction costs, and micro-scale exposure maps. through a market analysis conducted on the basis of data available from real estate agencies in the area, and ISTAT (National institute of Statistics) data processing, the costs of temporary accommodation and board were estimated at approximately €425 per week per person (excluding travel expenses due to additional distances, job loss, etc.).

By putting together restoration times with the event duration and the flood persistence time (derived from a two-dimensional flood inundation model) it was allowed to derive the average restoration time curve for a typical 100 m^2 buildings (Figure 1, left side). The estimation of direct and indirect damage is, instead, summarised in the curves of Figure 1 (right side), where the expected annual average damage with and without indirect costs is shown.

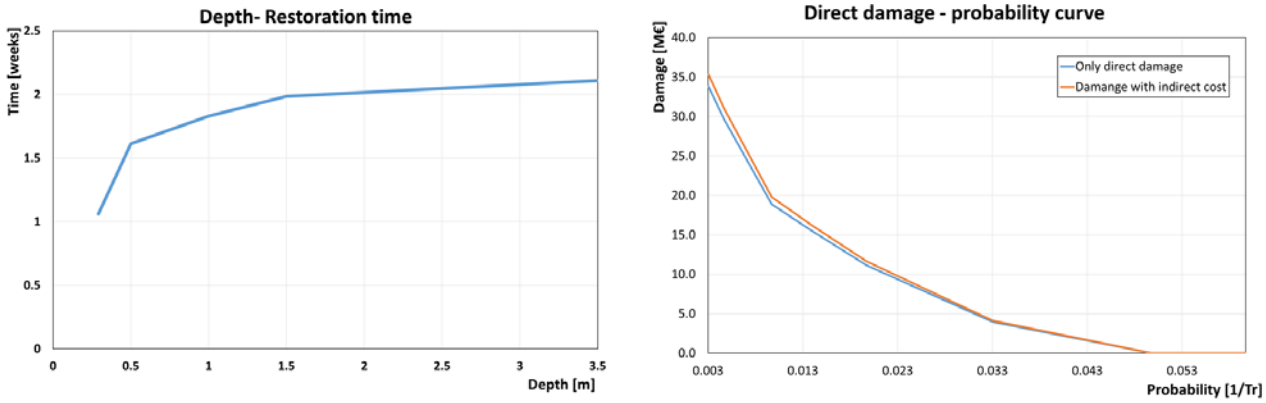


Figure 1. (left side) Depth restoration curve for a standard residential building; (right side) expected annual damage

These results indicate that indirect damage represents an amplification of approximately 5% of direct damage. However, the methodology tends to underestimate both the recovery time, (which ranges between 1 and 2 weeks, as it does not consider possible delays in the execution of works due to factors such as the limited financial capacity of affected residents, difficulties in sourcing materials and labour), and indirect costs, (excluding all extra costs that might affect impacted families).

Despite this general underestimation, an amplification factor of about 5% highlights the need for further investigation, especially considering current transitions in the field of risk mitigation interventions, which predict a more widespread use of individual self-protection systems compared to traditional large-scale control measures.

References

Ali R. A., Mannakkara S. (2024) Phased post-disaster recovery challenges: 2016–2017 floods and landslides in Colombo and Kalutara, Sri Lanka. International Journal of Disaster Risk Reduction, 111. https://doi.org/10.1016 /j.ijdrr.2024.104728

Almufti I., Williford M. (2013) REDi™ Rating System: Resilience-based Earthquake Design Initiative for the Next Generation of Buildings. Guidelines. https://doi.org/10.13140/RG.2.2.20267.75043

FLOODSite (2007) Vulnerability and flooding: a re-analysis of FHRC data. Report T11-07-11, Integrated Flood Risk Analysis and Management Methodologies. ResearchGate, (1) Vulnerability and Flooding: a Re-analysis of FHRC Data

Keyvanfar A., Shafaghat A., Ya'Acob N., Roslan A. (2021) Sustainable post-disaster settlement (sps) assessment model for evaluating performance of construction management in post-flood risk-reduction and recovery. Journal of Sustainability Science and Management, 16(5), 174–199. https://doi.org/10.46754/JSSM.2021.07.013

Naso S., Chen A. S., Aronica G. T., Djordjevic S. (2016) A novel approach to flood risk assessment: the Exposure-Vulnerability matrices. E3S Web of Conferences 7 FLOODrisk 2016 - 3rd European Conference on Flood Risk Management, 08007 (2016). https://doi.org/10.1051/e3sconf/201 60708007

Estimating sediment concentration, fluxes and trends in selected tributaries of the Illinois River

E. Getahun
Praire Research Institute, University of Illinois, Champaign, USA
e-mail: egetahun@illinois.edu

Introduction

Soil erosion and sedimentation have been a major water quality problem in Illinois, threatening agricultural productivity and resulting in water quality impairment (Getahun, et al. 2019). One of the objectives of the 1997 Illinois Integrated Management Plan (IMP) has been to achieve a measurable reduction in sediment entering the Illinois River and its tributaries. In Illinois River basin (IRB), 60% of its sediment flux is deposited in the river and its tributaries. This could be mitigated through adoption of key strategies for reducing sediment loads such as stream stabilization and effective restoration techniques involving sediment removal from backwater lakes and side channels and reuse in areas with distressed topsoil (Duane et al. 2017). Long term monitoring programs such as the Illinois Benchmark Sediment Monitoring Network (BSMN) allows accurate estimation of sediment loads and their trends in IRB for effective water resource planning and environmental protection. In this study, sediment concentration, flux and their respective trends are estimated at selected monitoring sites in IRB, providing a comprehensive picture of sediment transport dynamics in the major tributaries of the Illinois River.

Materials and methods

Long-term suspended sediment samples collected by Illinois State Water Survey (ISWS) at the five BSMN sites, covering a total drainage area of 10,764 sq. km., were used in this study. The BSMN sites are also U.S Geological Survey (USGS) sites for which continuous daily discharge data is available. Land uses of the drainage areas are predominately agricultural, with some forested and urban areas. Soils are primarily silt loam and silt clay loam, and slopes are generally low to moderate, typical of agricultural lands in the region. The WRTDS (Weighted Regressions on Time, Discharge, and Season) method employs weighted regressions to estimate concentrations and fluxes using time, discharge, and season as explanatory variables (Hirsh et al. 2010). As the coefficients of WRTDS can vary across the data's domain, it helps achieve a better fit to the observed data. Five WRTDS models were developed using 20 years of data at each site and sediment concentration, flux and their trends were estimated for water year, winter, spring, summer and fall seasons. In addition, WRTDS-K method (Hirsh et al. 2015), which enhances WRTDS by incorporating a Kalman filter is used to improve accuracy of sediment concentration and flux.

Results and concluding remarks

The WRTDS analysis of sediment concentration and flux trends for Illinois River tributaries reveals distinct annual and seasonal patterns. Table 1 presents the estimated changes and likelihoods of annual concentration and flux trends for the five sites. The Vermilion River near Leonore (site 122) shows a significant downward trend in both concentration (-28 mg/L) and flux (-161.8 million kg/year), with a 98.8% likelihood of a downward trend in flux. In contrast, the Spoon River at London Mills (site 229) exhibits a strong upward trend, with concentration increasing by 186 mg/L and flux by 107.6 million kg/year, with a likelihood of at least 93%. The La Moine River at Ripley (site 245) displays a significant upward trend in both concentration (122 mg/L) and flux (330.9 million kg/year), with a 97.1% likelihood of an upward trend in concentration. Conversely, the La Moine River near Colmar (site 242), upstream of site 245, shows a downward trend in concentration and an upward trend in flux, with a likelihood of less than 72%. Downward trends in both concentration (-28 mg/L) and flux (-22.7 million kg/year) are observed at the

Sangamon River at Monticello (site 249), with a 93.1% likelihood for flux trend. Figure 1 illustrates sediment concentration, fluxes, and their trends using flow-normalized estimates with a 90% confidence interval (CI).

Table 8.Estimated changes and likelihood of trends in sediment concentration and flux (water year 2003 to 2022)

Station name (ID)	Drainage area (sq. km.)	Sediment concentration (mg/L)			Sediment flux (x 10^6 kg/yr)		
		Change	90% CIs	Likelihood	Change	90% CIs	Likelihood
Vermilion R. (122)	3,240	-28.	-64.8 – 8.9	89.%	-161.8	-249—76.2	98.8%
Spoon R. (229)	2,751	186	99.5 – 249.4	99.%	107.6	-4.9—491.7	93.1%
LaMoine R. (242)	1,696	-50.8	-163.1 – 28	86.3%	9.8	-30.4— 65.1	71.3%
LaMoine R. (245)	3,349	122.0	21.7 – 170.4	97.1%	330.9	-64.1 – 466	93.1%
Sangamon R. (249)	1,425	-28	-55.5 – 17.6	89.2%	-22.7	-42.4 – 6.1	93.1%

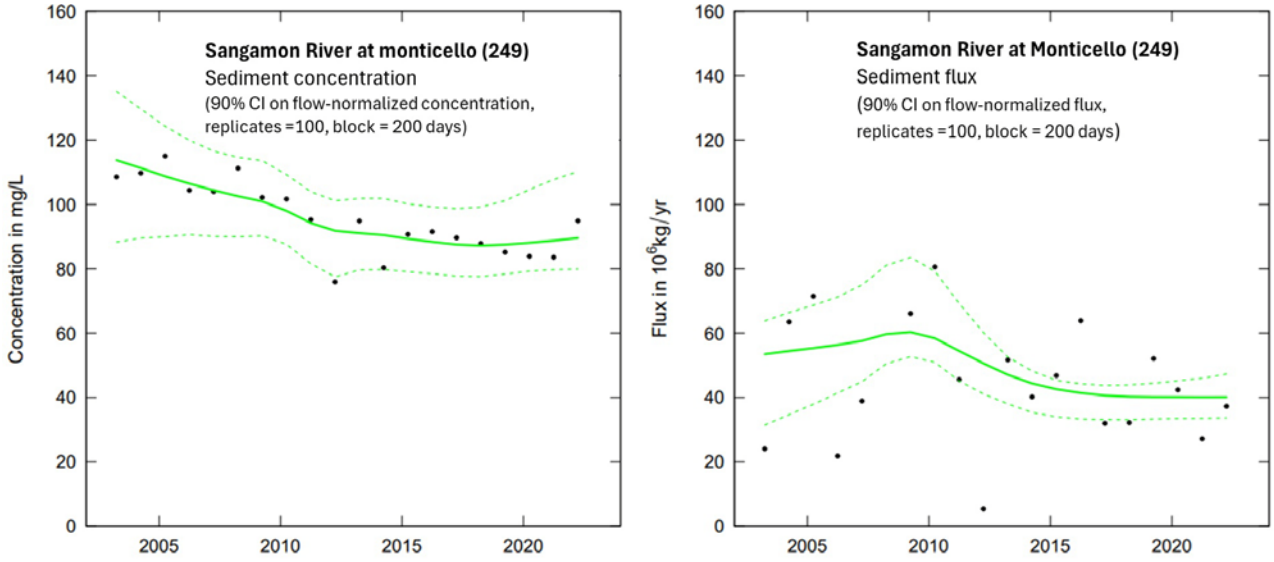


Figure 1. Sediment concentration and flux trends for Sangamon River at Monticello

The seasonal sediment concentration and flux trends also show distinct patterns across the five tributaries of the Illinois River. Site 122 exhibits a general downward trend across all seasons, with winter and spring experiencing the most significant decreases in flux. In contrast, site 229 shows a general upward trend, particularly in winter and fall. During winter and spring, a mixed pattern with downward trends in concentration but slight upward trends in flux is exhibited at site 242. Site 245 demonstrates a consistent upward trend in both concentration and flux, especially in spring and summer. Lastly, site 249 indicates a general downward trend, with the most pronounced decreases in flux during winter and concentration during summer. In addition, WRTDS-k is employed for each site, resulting in improved estimates of sediment concentration and flux. These findings underscore the importance of continued monitoring and analysis for effective management of the river. Understanding these trends could aid in developing targeted strategies to mitigate sediment-related issues and improve water quality.

References

Duane Esarey D, Nancy Holm N, Keefer LL, Meschewski E, Phillips A, Stein J, Winkel R (2017) Assessing Progress on the 1997 Integrated Management Plan for the Illinois River Watershed, Prairie Research Institute, Champaign

Getahun, E, Keefer, LL, Crowder DW, Demissie, M, Chandrasekaran, S, Allgire, RL (2019) Benchmark Sediment Monitoring Program for Illinois Streams: Analysis of 36 Years of Sediment Data (Water Years 1981-2016), Illinois State Water Survey, Champaign

Hirsh RM, Archfield SA, De Cicco, LA (2015) A bootstrap method for estimating uncertainty of water quality trends. Journal of Environmental Modelling 73: 148-166. https://doi.org/10.1016/j.envsoft.2015.07.017

Hirsh RM, Moyer DL, Archfield SA (2010) Weighted regressions on time, discharge, and season (WRTDS) with an application to Chesapeake Bay River inputs J. Am. Water Res. Assoc. 1–24. doi:10.1111/j.1752-1688.2010.00482.x

Identification of critical source areas related to diffuse pollution in an agricultural watershed – using SWAT model

F.N. Dogan, G. Capar*
Water Management Institute, Ankara University, Ankara, Turkey
** e-mail: gcapar@ankara.edu.tr*

Introduction

Agricultural watersheds are increasingly facing environmental challenges related to diffuse pollution, particularly nutrient loading from nitrogen and phosphorus sources (NPS). These nutrients, primarily originating from agricultural practices such as fertilizer application, livestock management, and land-use intensification, pose significant risks to water quality, ecosystem health, and human well-being. The complex interactions between land management, hydrological processes, and nutrient dynamics make comprehensive assessment and mitigation strategies critical for sustainable watershed management. NPS pollution is a major contributor to water quality degradation especially in agricultural watersheds due to uncontrolled and excess fertilization usage (Wang et al., 2022). Excess nitrogen and phosphorus can lead to eutrophication of water bodies, causing algal blooms, oxygen depletion, and disruption of aquatic ecosystems. Moreover, NPS pollution contaminate groundwater and surface water resources, potentially impacting drinking water quality and agricultural productivity. Understanding the spatial and temporal distribution of nutrient loads within a watershed is essential for developing targeted conservation and management approaches. The hydrological and water quality play a crucial role in nutrient pollution control by providing insights into the movement of water and associated nutrients through watersheds, water bodies, and ecosystems (Fang et al., 2024)

This study aims to comprehensively assess nutrient pollution dynamics in Ankara River Watershed by utilizing the Soil and Water Assessment Tool (SWAT) model to i) quantify spatial and temporal variations in nitrogen and phosphorus loading ii) identify critical source areas (CSAs) contributing to diffuse pollution iii) provide insights for developing watershed-specific nutrient management strategies. By mapping and analyzing the critical zones prone to diffuse pollution, this research seeks to contribute valuable knowledge for sustainable agricultural practices and water resources management.

Materials and methods

The Ankara River Watershed is situated in Ankara as a sub-basin of Sakarya River Basin which is one of the major watersheds of Turkey. It is located in the south-west part of Ankara (31° 47' - 40° 08' E - 40° 33' - 39° 20' N) with a total area of 7.178 km^2.

The SWAT model is a semi-distributed, continuous-time watershed-scale model that operates on a daily time step and divides watersheds into multiple hydrological response units (HRUs), which are defined by unique combinations of land use, soil type, and slope characteristics. SWAT employs a comprehensive approach to nitrogen cycling that encompasses multiple transformations and transport mechanisms. Mineral nitrogen inputs were characterized through fertilizer applications, atmospheric deposition, crop residue contributions and organic matter mineralization. Nitrogen transformation processes simulate the mineralization, nitrification, denitrification, plant uptake and immobilization and lateral and surface transport mechanisms. SWAT's phosphorus modelling distinguishes between organic and inorganic phosphorus pools, tracking their dynamics across terrestrial and aquatic systems. Phosphorus inputs were quantified through fertilizer applications, organic matter contributions and sediment-associated phosphorus. The model simulates organic phosphorus mineralization, inorganic phosphorus sorption and desorption, sediment-associated phosphorus transport, dissolved phosphorus leaching and plant phosphorus uptake as transformation mechanisms.

The ArcSWAT 2012 version was used for the hydrological and water quality (nutrient) modelling. The

calibration and validation of the model outputs was performed by SWAT-CUP automatic calibration programme.

Results and concluding remarks

The SWAT model demonstrated satisfactory performance in simulating streamflow dynamics within the watershed. Model calibration and validation yielded Nash-Sutcliffe Efficiency (NSE) values of 0.76 and 0.72, respectively.

The average annual nitrogen loads to the Ankara River were 0.290 kg/ha, while phosphorous loads were 0.01 kg/ha with substantial spatial heterogeneity. The spatial analysis revealed significant variability in nitrogen and phosphorus losses across the watershed. High nutrient loads were predominantly associated with agricultural zones characterized by intensive fertilizer application, particularly in sub-basins with steep slopes and poorly drained soils. Nitrogen loads were highest in the northern sections, with average annual losses reaching 8.607 kg/ha/year. Similarly, phosphorus hotspots were concentrated in lowland areas near waterbodies, with losses of 1.047 kg/ha/year.

CSAs contributing to nutrient pollution exhibited a combination of low soil infiltration rates, and proximity to surface water. Nutrient transport was highly seasonal, with peak loads observed during the rainy months (Figure 1). These peaks corresponded to high rainfall events and the period of fertilizer application. Nitrogen and phosphorus exports were dominated by deposition in soil in the watershed.

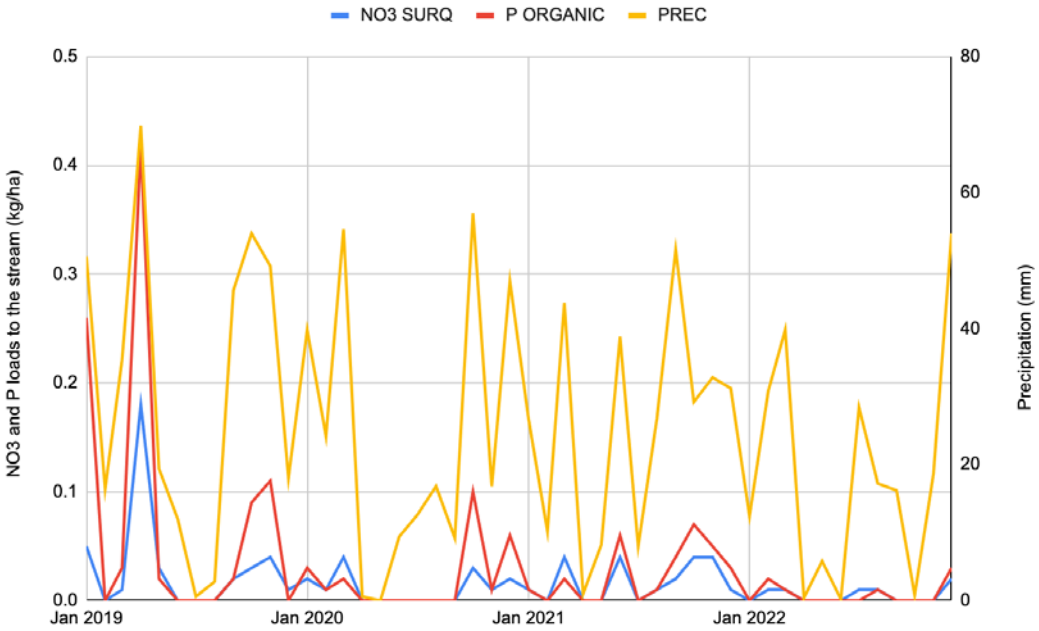


Figure 1. Monthly change of nitrogen (NO_3 in surface water) and phosphorous (P organic) loads to the Ankara River from 2019-2022 period

Acknowledgments: Funding for this research was provided by the TUBITAK (The Scientific and Technological Research Council of Turkey) via 2218 - National Postdoctoral Research Fellowship Program.

References

Fang, S., Deitch, M. J., Gebremicael, T. G., Angelini, C., & Ortals, C. J. (2024). Identifying critical source areas of non-point source pollution to enhance water quality: Integrated SWAT modeling and multi-variable statistical analysis to reveal key variables and thresholds. Water Research, 253, 121286. https://doi.org/10.1016/j.watres.2024.121286

Wang, M., Chen, L., Wu, L., Zhang, L., Xie, H., & Shen, Z. (2022). Review of Nonpoint Source Pollution Models: Current Status and Future Direction. Water, 14(20), 3217. https://doi.org/10.3390/w14203217

Machine learning-enhanced flood risk assessment model for local government-level decision support

H. Park[1*], H.W. Jee[2], S.B. Seo[2]
[1] Institute of Urban Science, University of Seoul, South Korea
[2] International School of Urban Science, University of Seoul, South Korea
* e-mail: watergis@uos.ac.kr

Introduction

Climate change has increased the global frequency of natural disasters, with floods causing the most severe human casualties and economic losses. The IPCC's Sixth Assessment Report emphasizes the importance of local-level capacity in climate change adaptation. While regression models based on historical data have effectively quantified economic damage from natural disasters, they become unreliable when historical data is limited. Regional Regression Analysis, using physical and socioeconomic characteristics as independent variables and regression coefficients as dependent variables, has been widely applied in hydrology for ungauged basins (Abdulla & Lettenmaier, 1997). This methodology evolved into a framework linking flood damage functions with regional coefficient functions. Kim et al. (2012) evaluated flood damage using logistic growth functions, which reflect minimal initial damage, rapid increase beyond thresholds, and maximum limitation based on infrastructure capacity. Recent studies have applied this approach to estimate flood damage under provincial-level mitigation policies (Jee et al., 2023; Seo et al., 2024). Our study downscales this framework to assess flood damage based on local level policies, enabling targeted decision-making.

Materials and methods

As shown in Figure 1, This study constructed a flood risk assessment model by applying regional regression analysis methodology to 228 basic local governments nationwide, enabling the reflection of regional characteristics and policy effects. The first regression equation, the flood damage function (step 2 in Figure 1), is based on a logistic growth function and was constructed for each local government using daily maximum rainfall as an independent variable and actual damage costs as a dependent variable.

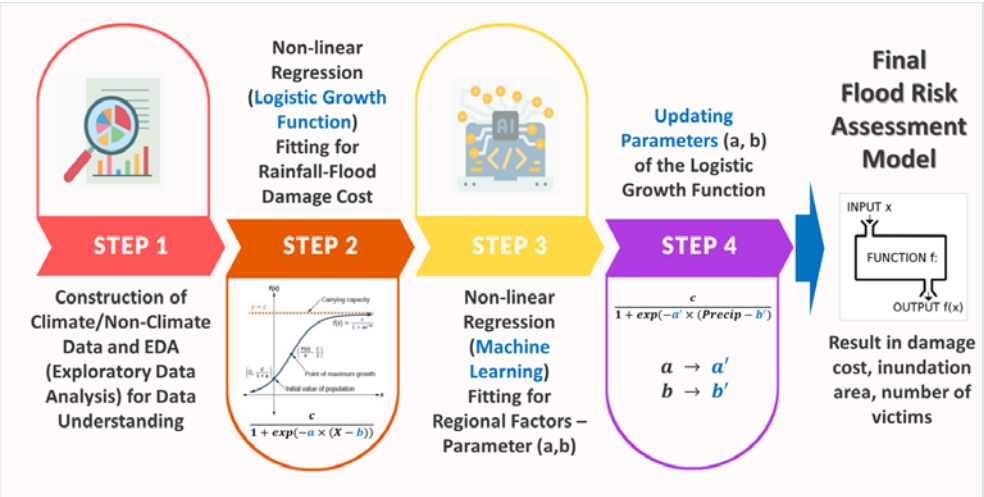


Figure 1. Process of the machine learning-based flood risk assessment model

The second regression equation, the regional coefficient function (step 4 in Figure 1), is a nonlinear regression equation using the coefficients of the flood damage function as dependent variables and regional characteristic factors such as retention area ratio, river improvement rate, and pumping capacity

as independent variables. Among twenty machine learning algorithms compared, Ridge Regression was identified as the most suitable approach. The retention area ratio, river improvement rate, and pumping capacity, all normalized by administrative area, showed significant correlations with the flood damage function coefficients.

To verify the model's applicability, flood damage reduction effects were analyzed by local government using a ten-year hypothetical policy scenario. The results showed varying damage reduction effects across regions despite identical policy implementation, attributed to differences in physical characteristics and existing infrastructure levels.

Results and concluding remarks

Our simulation results (Figure 2) demonstrated a shift in the logistic growth function's coefficient b after implementing new flood mitigation policies over a 10-year period, indicating a quantifiable reduction in flood damage. The magnitude of this coefficient shift varied across local governments, reflecting different regional characteristics and policy effectiveness. The model developed in this study is expected to serve as a crucial decision-support tool in establishing climate change adaptation measures for basic local governments. Particularly, it can assist in selecting optimal adaptation measures within limited budgets by enabling quantitative pre-evaluation of policy implementation effects. Future research expanding the model to incorporate more diverse flood reduction policies is expected to provide more sophisticated decision-making support.

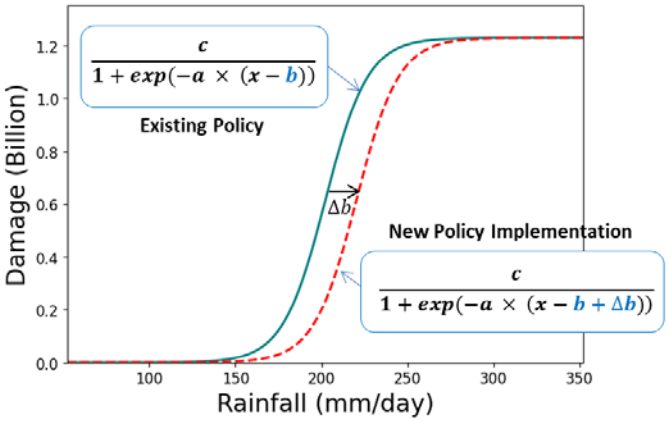


Figure 2. Changes in coefficients before and after policy implementation

Acknowledgments: This work was supported by Korea Environment Industry & Technology Institute (KEITI) through Climate Change R&D Project for New Climate Regime, funded by Korea Ministry of Environment(MOE) (grant number RS-2022-KE002152).

References

Abdulla, F. A., & Lettenmaier, D. P. (1997). Development of regional parameter estimation equations for a macroscale hydrologic model. Journal of Hydrology, 197(1–4), 230–257. https://doi.org/10.1016/S0022-1694(96)03262-3

Kim, Y.-O., Seo, S. B., & Jang, O. J. (2012). Flood risk assessment using regional regression analysis. Natural Hazards, 63(2), 1203–1217. https://doi.org/10.1007/s11069-012-0221-6

Jee, H. W., Seo, S. B., Ko, K. M., Cho, J., & Chae, Y. (2023). Macroscale impact assessment of flood damage reduction from climate change adaptation policies. Journal of Flood Risk Management, July 2023, 1–16. https://doi.org/10.1111/jfr3.12969

Seo, S. B., Jee, H. W., Cho, J., Oh, C., Chae, Y., Jo, S., & Hur, J. (2024). Assessment of the flood damage reduction effect of climate change adaptation policies under temperature increase scenarios. Mitigation and Adaptation Strategies for Global Change, 29(1), 1–22. https://doi.org/10.1007/s11027-024-10105-9

A spatially explicit risk assessment of future climate change on ecosystem services provided by surface irrigation in the Veneto region, Italy

A. Santini[1*], S. Balbi[2], Y. Casali[2], M. Masiero[1]
[1] Department of Land, Environment, Agriculture and Forestry (LEAF), University of Padova, 35020 Legnaro, Italy
[2] Basque Centre for Climate Change (BC3), 48940 Leioa, Spain
* e-mail: alessandra.santini@phd.unipd.it

Introduction

Beyond food production, irrigated agroecosystems – in particular those served by traditional gravity-fed surface irrigation systems - provides multiple ecosystem services (ES) (e.g., Oyonarte et al., 2022; Ricart et al., 2019) that are beneficial for society and also contribute to mitigate negative environmental effects of agriculture. However, the increase in climate change-induced extreme events, such as floods and droughts are threatening the capacity of irrigated agroecosystems to deliver and sustain these ES.
The objective of this study is to assess climate change risks to determine the likelihood of future climate hazards and their potential impacts on the ES delivered by surface irrigation. Our research focuses on the case study area of the Veneto Region (located in northeastern Italy) served by a dense gravity-fed surface irrigation network comprising 18,000 km of water canals.
A spatially explicit and integrated risk model has been developed to map hotspot where future floods and droughts will impact ES with the aim of informing decision-makers on critical areas where adaptation strategies (such as nature-based solutions) will be required to cope with the impact of climate change. The novelty provided by our research is double. To date, the literature is missing studies that have analysed the risks of climate change on ES provided by surface irrigation. Additionally, through the use of integrated modelling and artificial intelligence we were able to map risk using the irrigation water canals as a spatial unit, providing a unique and novel overview of risk mapping.

Materials and methods

Risk has been calculated as a function of hazard, vulnerability and exposure following the framework proposed by IPCC (2014). In the model, selected hazards are flood and droughts. Since we were interested in assessing the future climate risk, we made use of climate projections considering the mean ensemble from different regional and global climate models. The data were downloaded from "Piattaforma Proiezioni Climatiche per il Nord-Est" provided by ARPA Veneto (https://clima.arpa.veneto.it/) and subsequently downscaled to the case study area. For each hazard, we have aggregated seasonal climate projections in 2050 and in 2100, considering both 4.5 and 8.5 RCPs scenarios. Exposure has been defined as the spatial presence of the ES ecosystem services supplied by the irrigation water canal network. Spatial data mapping ES has been provided by the Veneto Region. Lastly, for accounting vulnerability, we have considered two variables: the anthropic pressure index (Regione del Veneto, 2024) and soil erosion (Borrelli et al., 2017).

The risk model developed in this study utilizes the integrated modelling approach of ARtificial Intelligence for Environment and Sustainability (ARIES; https://aries.integratedmodelling.org/, last accessed: 12 December 2024). ARIES integrates a network of web-accessible data, models, and other resources while adhering to the FAIR principles (Findable, Accessible, Interoperable, Reusable). This integration has been achieved through the k.LAB (Knowledge Laboratory) software, which facilitates interoperability from data sources to the resulting models (Villa et al., 2017).

Results and concluding remarks

The results mapped the spatial distribution of risk by identifying hotspots for future flood and drought events in the case study area, projected for 2050 and 2100 (Figure 1) Preliminary results highlight risk

hotspots for both droughts and floods are predominantly located in irrigation canals that are closer to large basins or to major urban centers and industrial districts meaning that in both area ES are particularly prone to hazards impacts. Other relevant hotspots have been found just outside the boundaries of regional parks, suggesting that these areas may also require additional protection for the maintenance of the ES.

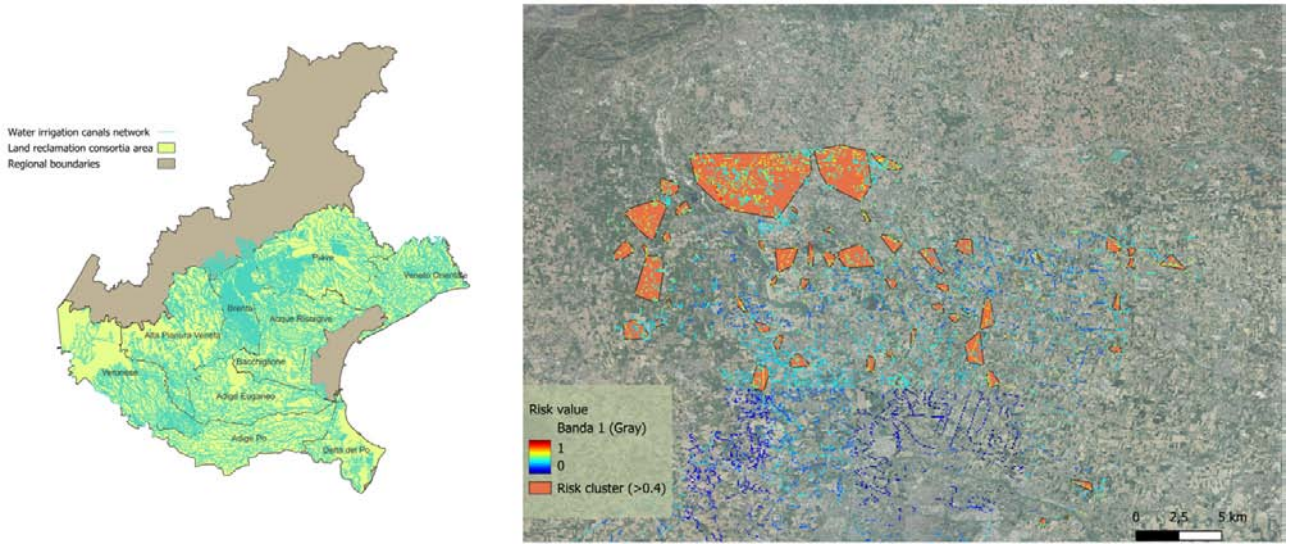


Figure 1. Map of the study (left) and an example of risk assessment map and cluster on Padua province of Veneto region (right)

References

Borrelli, P., Robinson, D. A., Fleischer, L. R., Lugato, E., Ballabio, C., Alewell, C., Meusburger, K., Modugno, S., Schütt, B., Ferro, V., Bagarello, V., Oost, K. Van, Montanarella, L., & Panagos, P. (2017). An assessment of the global impact of 21st century land use change on soil erosion. Nature Communications, 8(1), 2013. https://doi.org/10.1038/s41467-017-02142-7

IPCC (2014). AR5 Synthesis Report: Climate Change. IPCC, 218(2). https://www.ipcc.ch/report/ar5/syr/

Oyonarte, N. A., Gómez-Macpherson, H., Martos-Rosillo, S., González-Ramón, A., & Mateos, L. (2022). Revisiting irrigation efficiency before restoring ancient irrigation canals in multi-functional, nature-based water systems. Agricultural Systems, 203, 103513. https://doi.org/10.1016/j.agsy.2022.103513

Regione del Veneto. (2024). "Valutazione economica dei servizi ecosistemici degli agrosistemi irrigui gestiti dai Consorzi di bonifica del Veneto". Venezia Me.

Ricart, S., Kirk, N., & Ribas, A. (2019). Ecosystem services and multifunctional agriculture: Unravelling informal stakeholders' perceptions and water governance in three European irrigation systems. Environmental Policy and Governance, 29(1), 23–34. https://doi.org/10.1002/eet.1831

Villa, F., Balbi, S., Athanasiadis, I. N., & Caracciolo, C. (2017). Semantics for interoperability of distributed data and models: Foundations for better-connected information. F1000Research, 6, 686. https://doi.org/10.12688/f1000research.11638.1

Wilkinson, M. D., Dumontier, M., Aalbersberg, Ij. J., Appleton, G., Axton, M., Baak, A., Blomberg, N., Boiten, J.-W., da Silva Santos, L. B., Bourne, P. E., Bouwman, J., Brookes, A. J., Clark, T., Crosas, M., Dillo, I., Dumon, O., Edmunds, S., Evelo, C. T., Finkers, R., … Mons, B. (2016). The FAIR Guiding Principles for scientific data management and stewardship. Scientific Data, 3(1), 160018. https://doi.org/10.1038/sdata.2016.18

Impact of climate change on water supply systems vulnerability to drought events: a methodological framework to assess uncertainty

E. Romano[1], F. Ercolani[1], E. Volpi[2], N. Guyennon[1], S. Passaretti[3], C. Mineo[3], E. Boscariol[3], A. Trotta[3], A.B. Petrangeli[1]

[1] *National Research Council of Italy, Water Research Institute, IRSA-CNR, Rome, Italy*

[2] *Roma Tre University, Department of Civil, Computer Science and Aeronautical Technologies Engineering, Rome, Italy*

[3] *ACEA Ato2 SpA, Department of Water Resource Protection, Rome, Italy*

** e-mail: emanuele.romano@cnr.it*

Introduction

The observed and forecasted increase of drought events in the Mediterranean area poses serious concerns on reduction of water resources available for different uses, included the environmental ones. However, the assessment of the impact of climate change on water supply systems to develop mitigation strategies over mid- to long-term horizons, from years to decades, is challenging, also due to the uncertainty on the future scenarios provided by climate models at global and regional scales. In this paper a methodological framework to evaluate the uncertainties related to the complex modelling chain from the global atmosphere circulation models (GCM) under different "Shared Socioeconomic Pathways" (SSP) to impact on the water supply systems is presented. The main goal is to explore, using a real case study in Central Italy, if the uncertainties are small enough to provide robust information to design reliable mitigation measures to cope with future water scarcity issue.

Materials and methods

The modelling chain adopted to assess the future vulnerability of water supply systems (WSS) to drought events includes the following steps have been performed (Figure 1):

- Four Global Circulation Models with different spatial resolution (CMCC-ESM2, CNRM-ESM2.1, CNRM-CM6-1-HR and INM-CM5) have been selected from the Coupled Model Intercomparison Project (CMIP6), considering three SSPs for each of them (SSP1, SSP2 and SSP5). The related precipitation scenarios have been obtained applying a quantile mapping downscaling procedure over the historical period 1950-2014.

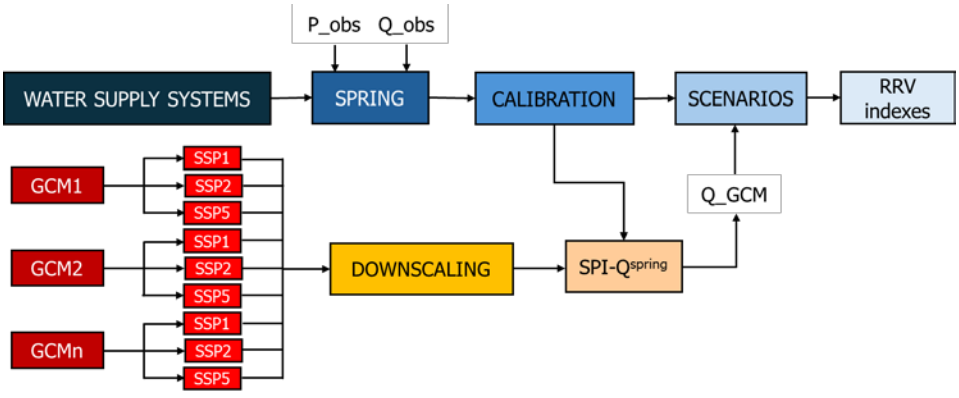


Figure 1. Overview of the adopted modelling chain

- The ability of the historical scenarios from the different GCMs (hindcast) to reproduce the observed climate in terms of drought characteristics has been evaluated based on the Standardized Precipitation Indexes computed at different time scales (SPI3, SPI6, SPI12, SPI24). In particular, the changes in occurrence and duration of drought episodes defined as SPIn < -1 have been evaluated comparing the period 1953-1981 to the period 1982-2014. The same metrics have been adopted to

compare the output from the different GCMs and future scenarios.

- The observed and simulated precipitation time series have been used as input to the SPI-Q^{spring} model (Guyennon et al. 2024) to simulate the outflow regime of 8 karst springs located in Central Italy, each of them connected to WSSs intended for civil purposes.
- Finally, the entire modelling chain has been applied to each WSSs case study to evaluate the future risk of water shortage, defined as the ability of each system to meet the connected water needs. Such risk has been assessed using a customized Reliability-Resilience-Vulnerability (RRV) metrics (Romano et al., 2017).

Results and concluding remarks

The results can be summarized as follows:

1. The reliability of the different GCMs in reproducing the observed precipitation regime in terms of drought events strongly depends on the model (Figure 2): in central Italy, CMCC-ESM2 appears the most suitable to simulate the hydrological processes mainly led by the inter-annual variability of the seasonal precipitation (SPI3 and SPI6), whereas CNRM-CM6-1-HR better simulates the processes led by long-term oscillation of the precipitation regime (SPI12 and SPI24). As the analysed spring mainly respond to precipitation deficit cumulated over some months (approximately from 4 to 7 months), the CMCC-ESM2 model appears to be recommended for impact studies in the analysed context.

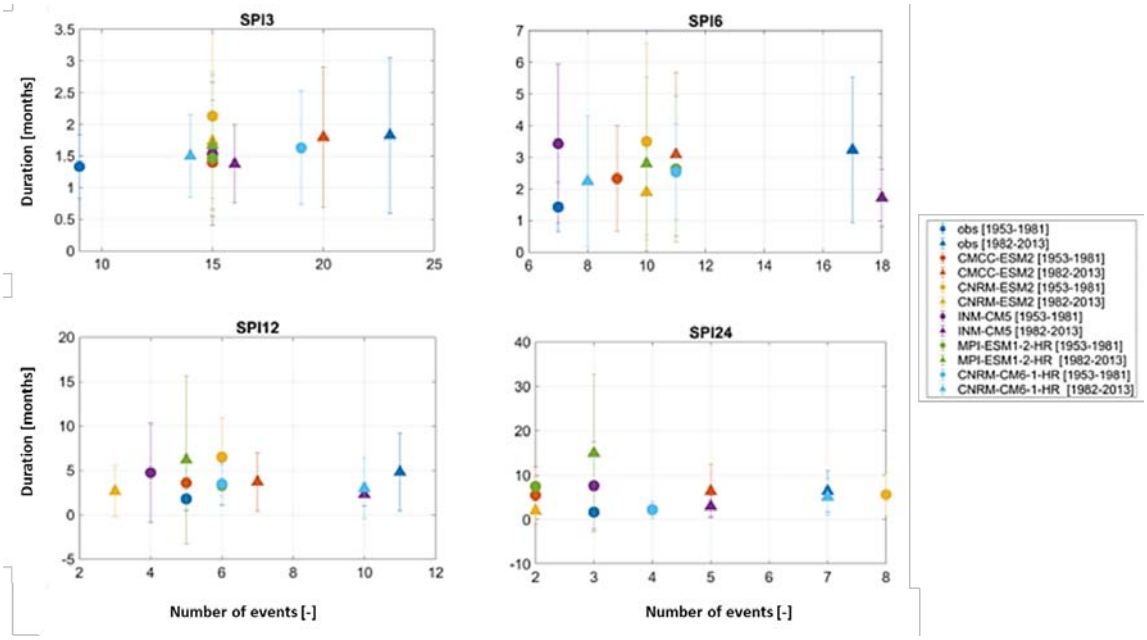


Figure 2. Statistics of the drought events over the periods 1953-1982 (circles) e 1983-2012 (triangles).

2. The outcomes from CMCC-ESM2 indicate a sensitivity to the SSPs with a worsening of the reliability and vulnerability indexes and a stationarity of the resilience. In general, the implementation of the other models leads to less clear changes in comparison to the past, pointing out the importance to conveniently select the GCMs to start the modelling chain for impact studies. However, the uncertainty on the SSPs scenarios appears higher than uncertainty related to the GCM's choice.

References

Guyennon N, Passaretti S, Mineo C, Boscariol E, Petrangeli AB, Varriale A, Romano E (2024) A parsimonious model for springs discharge reconstruction and forecast for drought management: Lessons from a case study in Central Italy. Journal of Hydrology – Regional studies 56:102021. http://10.1016/j.ejrh.2024.102021

Romano E, Guyennon N, Del Bon A, Petrangeli AB, Preziosi E (2017) Robust method to quantify the risk of shortage for water supply systems. Journal of Hydrologic Engineering 22(8):04017021 http://10.1061/(ASCE)HE.1943-5584.0001540

Forests and wetlands as Nature-Based Solutions to address resource costs in water management: a case study in the Brenta river area

M. Masiero[1], L.F. Esse-Villa[1*], S. Iacopino[1], G. Amato[2], G. Laghetto[2], G. Cristofani[3], P. Gatto[1]
[1] Department of Land, Environment, Agriculture and Forestry (LEAF), University of Padova, Padova, Italy;
[2] ETIFOR | valuing nature;
[3] Consorzio di Bacino Brenta
* e-mail: luisa.esse@unipd.it

Introduction

The acceleration of climate change and the increasing pressure on water resources is causing significant threats to ecosystems worldwide, the provisioning of ecosystem services (ES), and water security (Sterling et al., 2013; Schulz et al., 2024). Water management approaches have traditionally relied on engineering solutions (Wolfe et al., 2016). However, Nature-based Solutions (NbS) are emerging as innovative strategies for managing water-related risks while providing multiple environmental and social benefits (EC, 2019). Despite their potential, quantifying the benefits of NbS and assessing their cost-effectiveness remain critical research areas in the literature. Doing so allows for a comparative analysis of alternative strategies (e.g., business as usual, alternative grey solutions, blended solutions), which ultimately guides decision-makers in developing, financing, and implementing effective water management projects (Gómez-Baggethun & Barton, 2013; Le Coent et al., 2021).

This study addresses this knowledge gap by developing a multi-criteria assessment framework to evaluate the effectiveness of NbS in water resource management, using the middle River Brenta area in North-Eastern Italy as a case study. Our approach combines stakeholder engagement, scenario modelling, and cost-effectiveness analysis to quantify the impact of different NbS scenarios on water infiltration, carbon sequestration, and habitat conservation. The main objectives of the research are to assess the economic and ecological potential of various NbS scenarios compared to current land use practices (business as usual) and evaluate their effectiveness in managing water-related risks. This study represents the first case in Italy aimed at establishing an environmental fund for mitigation/compensation interventions addressing negative impacts caused by the Integrated Water Service, financed through water tariffs.

Materials and methods

The study area is the middle River Brenta area in North-Eastern Italy, a site that serves as a critical water source, supplying approximately 1.5 million people annually. The area, partially designated as a Natura 2000 site, faces significant challenges from intensive agriculture, water extraction, and habitat fragmentation, making it an ideal location for testing NbS.

Our methodological approach centered on developing and assessing the effectiveness of three types of NbS: Conservation Agriculture (CON), Constructed Wetlands (WET), and Forest Infiltration Areas (FIA) (Figure 1). We first created detailed suitability maps for each NbS type using land-use classification data, environmental parameters, and socio-economic factors. Based on these maps, we developed six scenarios: a baseline representing current conditions, three scenarios implementing each NbS type independently, and two blended scenarios combining multiple NbS interventions in different configurations (MIX 1 and MIX2). These scenarios were assessed by evaluating three key ES: water infiltration, carbon storage and sequestration, and habitat quality as a proxy for biodiversity. Finally, we conducted a cost-effectiveness analysis comparing the development and maintenance costs of each NbS scenario against their ES delivery.

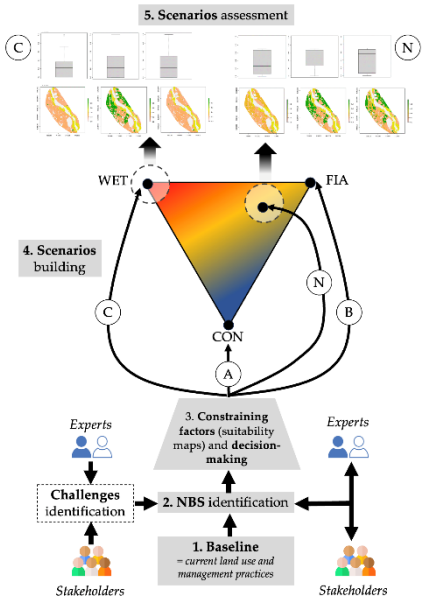


Figure 1. Conceptualization of the methodological approach (A: conservation agriculture, B: forest infiltration areas, C: constructed wetlands, N: blended NbS scenario).

Results and concluding remarks

Our analysis of NbS showed diverse performance patterns across the evaluated scenarios. Forest infiltration areas demonstrated the highest increase in water infiltration and carbon sequestration, while constructed wetlands are the most effective NbS in improving habitat quality. The blended scenario combining multiple NbS (MIX1) emerged as the most balanced solution, showing significant improvements across all ES. The cost-effectiveness analysis revealed that conservation agriculture proved most cost-efficient, though it had modest environmental benefits (low effectiveness). Constructed wetlands showed the highest costs, while forest infiltration areas maintained moderate cost-effectiveness. The blended scenario (MIX1) achieved balanced cost-effectiveness.

Our findings support recent research highlighting the effectiveness of mixed NbS solutions in managing environmental risks (Debele et al., 2023). We offer helpful insights for water resource managers and policymakers looking to increase system resilience by implementing NbS.

Acknowledgments: This study was carried out within the BIOFIN project (GA 101135476) and the Life Brenta 2030 (LIFE18 NAT/IT/000756) funded by the European Union.

References

Debele, S. E., Leo, L. S., Kumar, P., Sahani, J., Ommer, J., Bucchignani, E., Vranić, S., Kalas, M., Amirzada, Z., Pavlova, I., Shah, M. A. R., Gonzalez-Ollauri, A., & Di Sabatino, S. (2023). Nature-based solutions can help reduce the impact of natural hazards: A global analysis of NBS case studies. Science of The Total Environment, 902, 165824. https://doi.org/10.1016/J.SCITOTENV.2023.165824

European Commission. (2019). Fitness Check of the Water Framework Directive and the Floods Directive.

Gómez-Baggethun, E., & Barton, D. N. (2013). Classifying and valuing ecosystem services for urban planning. Ecological Economics, 86, 235–245.

Le Coent, P., Graveline, N., Altamirano, M. A., Arfaoui, N., Benitez-Avila, C., Biffin, T., Calatrava, J., Dartee, K., Douai, A., & Gnonlonfin, A. (2021). Is it worth investing in NBS aiming at reducing water risks? Insights from the economic assessment of three European case studies. Nature-Based Solutions, 1, 100002.

Schulz, C., Wolf, L. J., Martin-Ortega, J., Glenk, K., & Gischler, M. (2024). Valuing water: A global survey of the values that underpin water decisions. Environmental Science & Policy, 153, 103685.

Sterling, S. M., Ducharne, A., & Polcher, J. (2013). The impact of global land-cover change on the terrestrial water cycle. Nature Climate Change, 3(4), 385-390.

Wolfe, M. L., Ting, K. C., Scott, N., Sharpley, A., Jones, J. W., & Verma, L. (2016). Engineering solutions for food-energy-water systems: it is more than engineering. Journal of Environmental Studies and Sciences, 6, 172–182

Risk-based design of hydraulic infrastructures for flood risk mitigation using cost-benefit analysis

G.T. Aronica[1*], G.M.Sechi[2], M.L.V. Martina[3], G. Brigandì[1], C. Arena[4], A. Candela[4], M. Arosio[3], M. D'Ayala[3], J. Napolitano[2], I. Scolaro[2]

[1] *Department of Engineering, University of Messina, Messina, Italy*
[2] *Department of Civil, Environmental and Architecture Engineering, University of Cagliari, Cagliari, Italy*
[3] *Department of Science, Technology and Society, University School for Advanced Studies IUSS, Pavia, Italy*
[4] *Department of Engineering, University of Palermo, Palermo, Italy*
** e-mail: garonica@unipa.it*

Introduction

Traditional infrastructure design methodologies for flood risk mitigation based on the concept of return time are now challenged by climate change, increased public attention towards the social and environmental impacts of this type of works and ultimately by the relevant financial costs required. While the use of appraisal tools such as Cost-Benefit-Analysis (CBA) is largely invoked to justify and prioritize large flood mitigation initiatives at a river basin scale (EU Flood Directive, 2007), the use of CBA as a design tool is far less widespread and accepted. This explains the favorable reception and the subsequent funding by the Italian Ministry of the Environment of the RIDES project, a two-year (2020 – 2022) research initiative carried out by three Italian Universities to develop and demonstrate risk-based methodologies for the optimal choice of structural interventions to mitigate hydraulic risk. The core of the methodology is a cost-benefit analysis, which unlike traditional design methodologies uses the flood flow rate as the decision variable - instead than as a parameter– of an optimization problem where the objective function Is the maximization of net benefits, i.e. the difference between the benefits generated by the infrastructures in terms of reduction of expected damage (NRC. 2000, Tsakiris 2014) and the internal (investment, operation and maintenance) and external (environmental) costs to build the infrastructure.

This paper summarizes the main outcomes of the project concerning the design methodology; however, the project also included an extended survey of the most widespread structural interventions in Italy and their classification by area of application (urban, peri-urban, river, mountain) and by type of flood event (urban flood, river flood, pluvial flood) that was carried out using the RENDIS database. In addition, the project has produced a probably unique nation-wide database of investment cost appraisals for the construction or implementation of many types of structural elements such as embankments, concrete channels, gabion mattresses, large-section excavation, whose combination gives rise to mitigation infrastructures such as levees, large off-stream retention tanks etc. Costs of the more complex elements such as channels and embankments were appraised by typifying the element and developing an analytical assessment based on its geometry and on the prices of the inputs required (labour, machinery, materials). These results are available for the ten largest Italian regions and highlight some significant differences in unit prices, due to different costs of some inputs.

Materials and methods

The methodology to design the infrastructure that maximizes the present net social benefit can be summarized as follows:

a) Use hydraulic simulation to obtain flooded areas for different non-exceedance probabilities (return periods) and overlay these flooded areas, in a GIS environment, with land use categories. In the case study illustrated below the 2D HEC-RAS 6.0 simulation tool of the USACE was used considering 8 different flood hydrographs corresponding to 8 different non-exceedance probabilities (Figure 1 (a)).
b) Estimate the expected tangible flooding damage starting from parametric "damage curves" providing damage (in €) as a function of water depth and/or speed. In the case study, the curves developed by

the EU Joint Research Centre (Huizinga et al., 2017) were used.

c) Identify the different mitigation alternatives.
d) Estimate total costs of the project alternative for different dimensions (e.g. different heights of an embankment protection of a given length). Costs were obtained using the already mentioned appraisal procedures and databases developed in the RIDES project.
e) Simulate flooded areas for different mitigation and project alternatives.
f) Estimate benefits as the avoided damage by subtracting the expected, residual damage in the situation with the alternative in place from the expected damage in the situation without the alternative.
g) Identify the alternative that determines the maximum present value by discounting the flow of net benefits (benefits – costs) along a planning horizon of, say 30 years, also accounting for a salvage value at the end of the planning period using an appropriate discount rate. Annual costs of maintenance must be also considered and added to the other costs.

Results and concluding remarks

The procedure was demonstrated through two case studies: a real one, located in the lower part of the Carboj river basin, a 230 km^2 river basin located in south-western Sicily, and a synthetic one obtained from the real one by partially modifying the actual land use so to include an urban area around the river mouth.

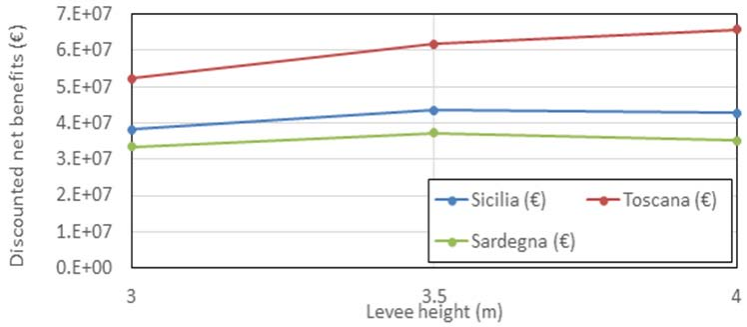


Figure 1. Discounted net benefits associated to the construction of levees considering the actual current land use.

Figure 1 shows the effect of different unit levee costs on the optimal levee height. While levee costs for Sicily and Sardinia determine a maximum discounted net benefit at a levee height of 3.5 m, levee height in Tuscany could easily be 4 metres or higher due to lower unit levee costs in that regions. A similar pattern could also be observed in the synthetic case, featuring higher damage values due to the presence of an urban area regardless, of the unit costs of levees. Overall, the toolkit developed in the RIDES project can assist administrations and professional alike to move from traditional to more comprehensive, risk-based design methodologies especially when planning of large, basin-wide mitigation systems is required.

Acknowledgements: Research funding for this study was provided by the RIDES-IDRO project, (Risk-based design delle opere idrauliche per la mitigazione del rischio di inondazione), funded by Italian Ministry for Environment, Sea and Land Protection

References

Huizinga J, De Moel H, Szewczyk W. (2017) Global flood depth-damage functions: Methodology and the database with guidelines, EUR 28552 EN, Publications Office of the European Union, Luxembourg, ISBN 978-92-79-67781-6, doi:10.2760/16510, JRC105688

National Research Council (2000) Risk analysis and uncertainty in flood damage reduction studies. National Academy Press, Washington, D.C.

Tsakiris A (2014) Flood risk assessment: concepts, modelling, applications. Natural Hazards and Earth System Sciences Discussions 2, 261–286. doi:10.5194/nhessd-2-261-2014

Data-driven high-resolution rainfall reconstruction of 85-year Atlas: A two-tier approach integrating occurrence probability and magnitude

N. Beikahmadi*, A. Francipane, D. Treppiedi, L.V. Noto
Dipartimento di Ingegneria, Università degli Studi di Palermo, Palermo, Italy
** e-mail: niloufar.beikahmadi@unipa.it*

Introduction

Precipitation gridded products derived from station-based records are crucial for hydrological modelling, uncertainty quantification in reanalysis/remote sensing products, and applications such as flood forecasting. Numerous methodologies exist for precipitation reconstruction, ranging from neighbouring station weighting and geostatistical approaches to advanced machine learning techniques (Serrano-Notivoli & Tejedor, 2021). However, their performance depends on factors such as regional heterogeneity, network density, and target resolution. To account for rainfall's dual nature (i.e., occurrence and magnitude), our study draws inspiration from previous studies on dry-event frequency classification (Barancourt et al., 1992) and magnitude variability (Berndt & Haberlandt, 2018). We propose a two-step, data-driven approach that independently models occurrence and magnitude. The resulting product offers high spatiotemporal resolution (i.e., daily maps of precipitation at 2 km resolution) over a long temporal period (from 1940 to present), addressing critical needs in hydrological applications.

Materials and methods

Rainfall records from an extensive gauge network in Sicily (i.e., 372 stations) were retrieved from the Regional Department of Civil Protection website. The data, consisting of hourly measurements from 2022 to 2025, were aggregated into daily accumulations and pre-processed.

In the occurrence modelling phase, daily data were classified into three classes based on the frequency, F, of dry events (F0–25, F25–75, F75–100). A lower class (e.g., F0-25) indicates a widespread presence of wet events across the island, whereas a higher class (e.g., F75-100) signifies that many stations recorded no rainfall across the island. For each class, an experimental variogram was computed from the binary (rain/no rain) data and fitted with several theoretical models, including Spherical, Exponential, Gaussian, Matérn, and Wave Effect models. The optimal model was selected via the lowest AIC (Akaike's Information Criterion; Akaike H., 1998) value. Indicator kriging was then applied at a 2km resolution to interpolate the probability of occurrence, which was subsequently converted into a binary map using a class-based, data-driven cutoff threshold. Additionally, monthly class frequencies were analyzed to refine default variogram parameters for each month.

In the magnitude modelling phase, daily rainfall heterogeneity was characterized by computing statistical spatial descriptors: daily mean, maximum, standard deviation, and the coefficient of variation. Days were then classified into rainfall magnitude groups according to standard Mediterranean ranges (e.g. "Light", "Light–Moderate", "Moderate–Heavy", and "Torrential", following (Alpert et al., 2002)). For each group, an experimental variogram was derived from actual rainfall amounts, and the best theoretical model was chosen based on the AIC metric. The group-specific variogram parameters were subsequently used in ordinary kriging to interpolate rainfall magnitudes at unsampled locations. The resulting fields were masked with the binary occurrence maps, and any negative interpolation artifacts were set to zero.

Finally, to assess model uncertainty and ensure the robustness of the final gridded products leave-one-out cross-validation (LOOCV) was carried out on both occurrence and magnitude interpolated maps. This initial analysis, leveraging the dense 2022–2025 dataset, establish the spatial structure of precipitation, offering a detailed calibration of the two-step approach. In a subsequent phase, these findings will be used to guide and refine the interpolation of long-term historical precipitation (1940 to present), where only sparse records are available.

Results and concluding remarks

Figure 1a shows a day classified under the F25–75 dryness frequency, with light rainfall amounts and highly localized rainfall event, whereas(Figure 1b represents a day featuring moderate – heavy precipitation (i.e., F0–25). In both cases, the two-step scheme clearly distinguishes between rainfall occurrence (left panels in the bottom row) and magnitude estimation (right panels in the bottom row). The kriged probability fields align well with station-level data, effectively delineating rainy versus dry areas, w hile the interpolated rainfall magnitudes accurately capture the spatial distribution of precipitation.

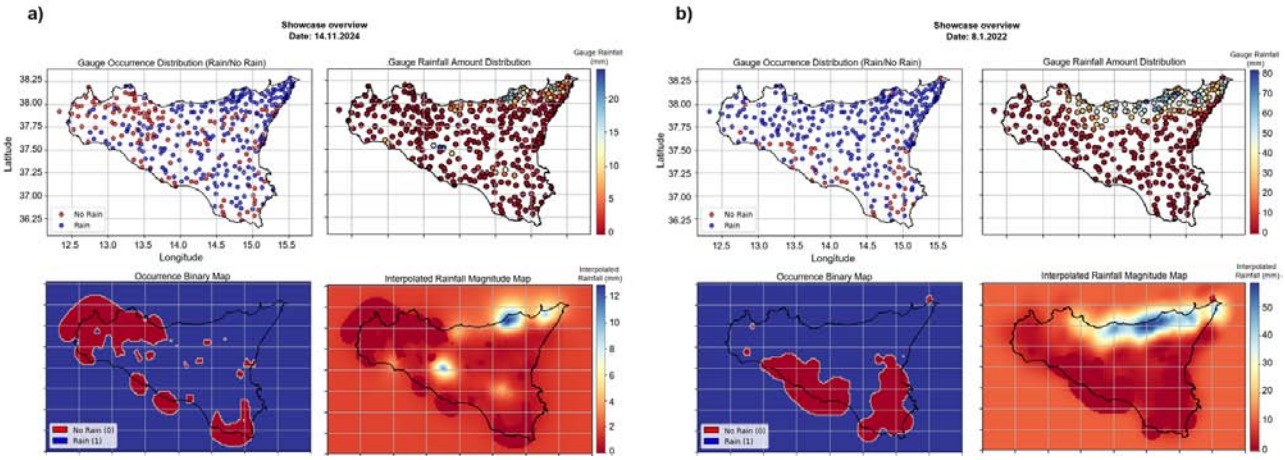


Figure 1. Example outputs from the two-step interpolation approach for two contrasting days. The top panels show gauge-based occurrence (rain vs. no rain) and measured rainfall amounts, while the bottom panels display the corresponding binary occurrence map and kriged rainfall magnitude fields, respectively.

In conclusion, the two-phase approach described here yields robust, high-resolution rainfall maps over Sicily by first classifying dry/wet events into three frequency categories — thereby enabling the extraction of distinct indicator variograms with optimal model selection via AIC — and then by categorizing rainfall magnitude using daily mean, maximum, and CV to derive well-defined variogram models. This integrated framework outperforms conventional single-step methods and offers promising applications for regions with sparse gauge networks and complex climatic regimes. Future work will extend this approach to real-time forecasting and hydrological simulations.

References

Alpert P, Ben-Gai T, Baharad A, Benjamini Y, Yekutieli D, Colacino M, Diodato L, Ramis C, Homar V, & Romero R (2002) The paradoxical increase of Mediterranean extreme daily rainfall in spite of decrease in total values. Geophysical research letters, 29(11), 31-31-31-34.

Barancourt C, Creutin J, & Rivoirard J (1992) A method for delineating and estimating rainfall fields. Water Resources Research, 28(4), 1133-1144.

Berndt C, & Haberlandt U (2018) Spatial interpolation of climate variables in Northern Germany—Influence of temporal resolution and network density. Journal of Hydrology: Regional Studies, 15, 184-202.

Serrano-Notivoli R, & Tejedor E (2021) From rain to data: A review of the creation of monthly and daily station-based gridded precipitation datasets. Wiley Interdisciplinary Reviews: Water, 8(6), e1555.

Geostatistical methods for temperature estimation: A high-resolution Atlas of daily temperatures in Sicily

C. Mattina*, D. Treppiedi, A. Francipane, L.V. Noto
Department of Engineering, University of Palermo, Palermo, Italy
** e-mail: calogero.mattina01@unipa.it*

Introduction

Daily maximum and minimum temperature data are essential for different applications, such as climate change detection studies and the assessment of hydrological processes. These variables are generally obtained from meteorological stations, satellite products or reanalysis-based dataset. However, it is now well known that each of these products has limitations that compromise their use and/or reliability. As an example, reanalysis products generally provide datasets with very coarse spatial resolution, and their reliability may be affected by biases due to data availability during the assimilation processes. Even when statistical or dynamical downscaling techniques are used to improve their spatial resolution, computational resources and the high amount of observational data required limit these datasets to the last 20 years (Cornes et al. 2018). In contrast, ground stations offer a much more robust measurement but are often characterized by significant temporal discontinuities and limited spatial coverage.

To address the lack of spatial and temporal coverage of ground-based temperature observations, several geostatistical techniques have been developed and used over time. For instance, Holdaway (1996) used the Ordinary Kriging (OK) method on monthly temperatures in Minnesota, USA, highlighting a temperature trend in some months. Wu and Li (2013) adopted the Residual Kriging (RK) method in the United States to interpolate monthly mean temperatures, demonstrating that the inclusion of elevation as an external drift improves the estimate. Di Piazza et al. (2015) compared different spatial interpolation methods in Sicily including OK and RK for estimating annual mean temperatures, finding that RK outperforms OK. Moving to the daily scale, Sekulić et al. (2019) developed a regression kriging model on daily average temperatures in Croatia at a spatial resolution of 1 km. They compare the outcomes with the MODIS land surface temperatures, founding reliable results.

Here we propose a spatial interpolation methodology, based on geostatistical methods, for reconstructing a daily maximum and minimum temperature ATLAS for Sicily with a high spatial resolution (~2km) and for the period 1980-2024.

Materials and methods

Sicily, which is the largest island in the Mediterranean Sea and characterized by a semi-arid climate, exhibits a feature that is common in Italy and other parts of the world: the presence of two different measurement networks, covering different periods and characterized by varying station density. The first network is managed by the Osservatorio delle Acque (OA) and cover the period 1924 – 2018. It is important to specify that, although some stations have been measuring temperature since the 1920s, their number decreases significantly going further back in time. At the same time, the presence of gaps in the time series increases significantly. For these reasons, we limit the reconstruction starting from 1980. The second network is managed by the Servizio Informativo Agrometeorologico Siciliano (SIAS), which provides data from 2002 to 2022, ensuring a high temporal continuity of the historical series.

For the reconstruction of daily temperatures, we used the Ordinary Kriging (OK) method combined with the Near Surface Lapse Rate (NSLR). In particular, the NSLR is derived for each day of the year through linear regression between the temperature values from both measurement networks and their respective elevations. This helps to take into account for the effect of elevation on temperature and, at the same time, for its seasonal behaviour. Since there is a period of overlap between the two networks (i.e., 2002 – 2018), we initially validated the methodology through point interpolation with the OA-ARRA datasets on the SIAS

network stations. By doing so, it is possible to compare the observed SIAS series with the reconstructed OA-ARRA series. This allows us to verify the reliability of the methodology while simultaneously obtaining daily estimation errors associated with it. These errors are interpolated onto the same 2 km grid used for the interpolation of the OA data for the period 1980-2002. Their combination ensures the temporal consistency of the entire dataset.

Results and concluding remarks

We used the daily temperatures from the two datasets to estimate the NSLR for each day of the year. Our analyses highlighted the critical role of the daily NSLR in capturing the seasonality of temperatures. We then validated our approach through point interpolation during the overlapping period from 2002 to 2018, where we found that the proposed method produced accurate results. As an example, the comparison between the observed SIAS series and the reconstructed OA-ARRA dataset for the Canicattì station is shown in Figure 1.

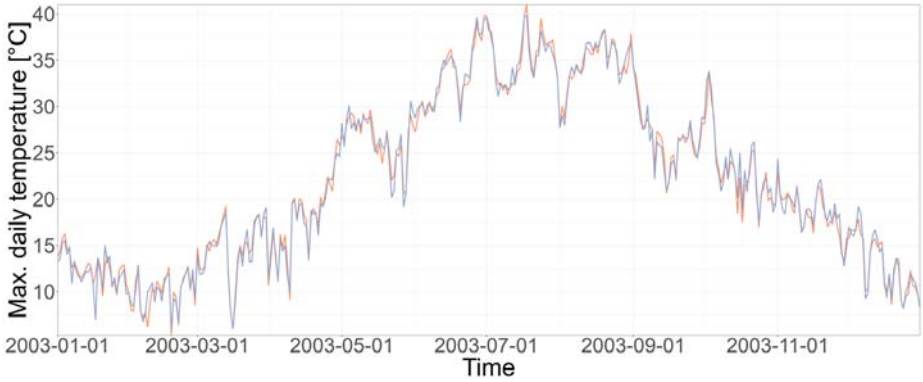


Figure 1. Example of a comparison between the daily maximum temperatures in 2003 from the OA-ARRA interpolated network (orange line) and SIAS recorded values network (blue) (Canicatti station).

While our methodology guarantees a good accuracy in estimating daily maximum and minimum temperatures, it is important to note that the two measurement networks may introduce some biases due to differences in the instruments used. However, the interpolation in the estimated errors obtained in the overlapping period is useful minimize these biases, ensuring more reliable and consistent results across the whole 1980-2024 period. This atlas, resulting from our methodology, represents a valuable tool for further research in the fields of climate change and hydrological modelling. By providing high-quality, interpolated temperature data, it facilitates a more accurate understanding of regional climate dynamics and supports the evaluation of hydrological processes. Furthermore, it serves as an important starting point for future studies that require consistent and robust temperature data at both a spatial and temporal scale.

References

Cornes R.C., van der Schrier G., van den Besselaar E. J., Jones P. D. (2018) An ensemble version of the E temperature and precipitation data sets. Journal of Geophysical Research: Atmospheres, 123(17), 9391-9409. https://doi.org/10.1029/2017JD028200

Holdaway M. R. (1996) Spatial modeling and interpolation of monthly temperature using kriging. Climate research, 6(3), 215-225. https://doi.org/10.3354/cr006215

Piazza, A. D., Conti, F. L., Viola, F., Eccel, E., Noto, L. V. (2015) Comparative Analysis of Spatial Interpolation Methods in the Mediterranean Area: Application to Temperature in Sicily. Water, 7(5), 1866-1888. https://doi.org/10.3390/w7051866

Sekulić A., Kilibarda M., Protić D., Tadić M. P., Bajat B. (2020) Spatio-temporal regression kriging model of mean daily temperature for Croatia. Theoretical and applied climatology, 140(1), 101-114. https://doi.org/10.1007/s00704-019-03077-3

Wu T., Li Y. (2013) Spatial interpolation of temperature in the United States using residual kriging. Applied Geography, 44, 112-120. https://doi.org/10.1016/j.apgeog.2013.07.012

Retrospective analysis of the accuracy of SEAS5 ECMWF seasonal forecasts and their bias correction: An application to Sicily

F. Castaldo[1,2*], A. Francipane[1], D. Treppiedi[1], L.V. Noto[1]
[1] Department of Engineering, University of Palermo, Palermo, Italy.
[2] IUSS Pavia, Pavia, Italy.
* e-mail: francesco.castaldo@unipa.it

Introduction

Nowadays, seasonal forecasts (SFs) have become indispensable tools in many fields of life and science, including hydrology, hydraulic risk mitigation, and water resource management; their ability to forecast climate variables up to six months in advance is more valuable than ever since the presence of the effects of climate change. SFs play a crucial role not only in predicting floods and droughts but also in the water resource management, where they enhance decision-making processes, mitigate risks, optimize resource use, and secure water supplies, particularly in areas vulnerable to water scarcity and climate variability (Francipane et al. 2023).

Despite their importance, the reliability of SFs remains a key concern. Biases inherent in climate models can compromise forecast accuracy, making retrospective analyses essential for evaluating forecasts by comparing them with observed values. When systematic errors are detected, various bias correction techniques, such as quantile mapping, linear regression, mean bias correction, the MOS-Analog method, and mean and variance adjustment, can be applied to adjust the forecasts (Marcos et al. 2018). In addition to the previous methods, this study also explores an innovative approach using Artificial Neural Networks (ANN), which may offer superior performance by capturing the nonlinear relationships (Moghim and Bras 2017).

Here ECMWF SEAS5 SFs relative to monthly precipitation, P, and temperature, T, have been analyzed on different areas of Sicily, which include four river basins whose reservoirs serve the Palermo metropolitan area's water system, specifically Piana degli Albanesi, Rosamarina, Poma, and Scanzano; for these river basins the SFs have been compared with observed precipitation and temperature data provided by the Sicilian regional basin authority (AdB).

Materials and methods

The accuracy of ECMWF SEAS5 forecasts for precipitation and temperature has been evaluated by comparing SFs with observational data from AdB across all the case studies over the period from 1995 to June 2023.

Different bias correction (BC) methods have been used to improve forecast accuracy and reliability. These include a range of techniques applied at both monthly and annual scales to improve the accuracy of SFs. Quantile mapping (QM) utilizes a non-parametric cubic spline function to adjust the modeled distribution, ensuring it aligns more closely with observed data. Linear regression (LR) applies a zero-intercept fit to correct systematic biases, while mean bias correction (MBC) eliminates the average forecast error by simple offsetting. The MOS-Analog (MOS) method refines predictions by identifying and averaging past forecast analogs, whereas Mean and Variance Adjustment (MVA) ensures that the corrected forecasts match the statistical properties of the observations. Additionally, an innovative monthly-scale approach was used, exploiting an ANN with the month and raw SF data as inputs and the observed data as the output. For the ANN approach, two experimental trials have been carried out: one covering the entire period from 1995 to 2023, including retrospective forecasts known as Hindcasts (SHs) and Seasonal Real-Time forecasts (SRTs), and another focusing on the period from 2017 to June 2023, considering only SRTs and excluding SHs.

Results and concluding remarks

For all case studies, SFs exhibit a systematic error (i.e., bias), with an overestimation of lower observed temperatures and a consistent underestimation of higher observed precipitation. The normalized Taylor diagram in Figure 1 evaluates the quality of raw SF and their bias-corrected counterparts at lead time zero (LT0) against observations for precipitation (on the left) and temperature (on the right) for Poma reservoir. The diagram captures the distance between forecasts and observations in terms of normalized standard deviation (STD), correlation coefficient (CC), and normalized root mean square difference (RMSD), with STD and RMSD normalized by the observed standard deviation. The black dot on the x-axis represents perfect agreement between forecasts and observations (STD = 1, CC = 1, RMSD = 0). Forecasts closer to this point indicate higher accuracy and reliability. For precipitation across all reservoirs, and particularly for Poma as shown in Figure 1, bias correction using ANN on SRTs yields the most accurate overall results (green symbols in Figure 1). Notably, ANN with SRTs outperforms other methods, although MVA and QM also effectively preserve the observed data's variability on both annual and monthly scales. This is especially important because the raw SFs exhibit lower variability, primarily due to their inability to predict precipitation values exceeding a certain threshold (160 mm), which is frequently surpassed in the observed data. However, despite restoring variability, QM compromises temporal consistency, leading to higher RMSD values than the raw SFs. This aspect is due to the fact that matching the ECDFs does not ensure the correct temporal sequence of events. In terms of CC and RMSD, the ANN applied to SRTs outperforms all other methods, demonstrating its ability not only to correct bias but also to capture both the temporal and spatial variability of precipitation data more effectively than other approaches**.** For temperature across all reservoirs, and particularly for Poma as shown in Figure 1, ANN yields the best results. However, monthly-scale results are also satisfactory, and some annual-scale methods (QM and MVA) perform well. This is due to the difference in variability and prediction between temperature and precipitation.

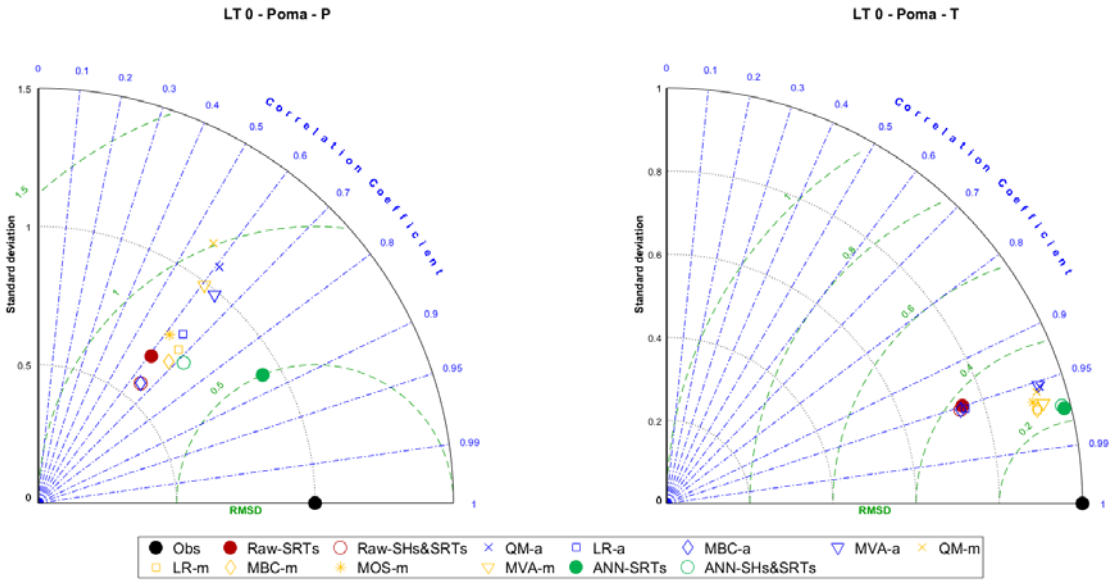


Figure 1. Normalized Taylor diagrams. The black dot represents observations. Solid markers indicate bias correction conducted considering only SRTs, while empty markers represent bias correction applied considering both SHs and SRTs. Blue symbols refer to the annual approach, whereas orange symbols refer to the monthly approach.

References

Francipane A. Arnone, E., Noto L.V., 2023. Combining a data-driven approach with seasonal forecast data to predict reservoir water volume in the Mediterranean area. Hydrol. Sci. J. 68, 764–781. https://doi.org/10.1080/02626667.2023.2189521

Marcos R., Llasat M.C., Quintana-Seguí P., Turco M., 2018. Use of bias correction techniques to improve seasonal forecasts for reservoirs — A case-study in northwestern Mediterranean. Sci. Total Environ. 610–611, 64–74. https://doi.org/10.1016/j.scitotenv.2017.08.010

Moghim S., Bras R.L., 2017. Bias Correction of Climate Modeled Temperature and Precipitation Using Artificial Neural Networks. J. Hydrometeorol.

The theoretically derived probability distribution of water level in detention dams

A. Avino[1*], F.D. Pacia[1,2], S. Manfreda[1]
[1] Department of Civil, Architectural and Environmental Engineering, University of Naples Federico II, Naples, Italy
[2] University School of Advanced Studies IUSS Pavia, Pavia, Italy
* e-mail: angelo.avino@unina.it

Introduction

During the last decades, there has been a perceived global rise in flood hazards due to the catastrophic effects of several floods, resulting in damage and losses to the environment and communities (Merz et al. 2021). Therefore, the increasing frequency and severity of floods (Bertola et al. 2020) has underscored the need to identify dynamic solutions for flood mitigation. In this context, detention basins can be effective tools for attenuating peak discharges. However, the proper design of a detention system is extremely challenging due to its impact on the hydrological response of the basin.

With this aim, several approaches have been developed to interpret the functional relationships between inflows and expected outflows from dams. In particular, Manfreda et al. (2021) defined a theoretically derived probability distribution of the peak outflows from in-line detention basins. This framework was further explored by Albertini et al. (2022) to design a flood detection system in a river basin in southern Italy.

However, these approaches tend to neglect the reservoir pre-filling from previous flood events, leading to an underestimation of storage volume (Raimondi and Becciu 2015). With this aim, an analytical-probabilistic approach to theoretically derive the distribution of the water level in the reservoir has been developed.

Materials and methods

By exploiting the theory of theoretically derived distributions (TDD, Benjamin and Cornell 2014), the distribution of water level in detention dams has been obtained by combining the stage-storage capacity curve and the probability density function (pdf) of water volume in the reservoir, p_w.

In detail, the water balance equation for the water accumulated in the detention basin has been used to derive the pdf of water volume in the reservoir, p_w, by exploiting the approach of Manfreda and Fiorentino (2008). Specifically, the proposed water balance equation at the daily scale is:

$$dW(t) = R(t) - L \tag{1}$$

where: R *[m³]* represents the daily runoff: $R = \varphi A_b I$ (φ is the coefficient of infiltration, A_b *[m²]* is the area of the upstream river basin and I *[mm/day]* is the mean daily rainfall); L *[m³]* is the water losses (withdrawal) and $W(t)$ *[m³]* is the volume accumulated in the reservoir (function of the water level, $H(t)$, through the stage-storage capacity curve).

Specifically, by considering the mass conservation equation of the water volume in the reservoir, the rainfall forcing is considered as an additive noise (modelled by a sequence of instantaneous pulses that occur in a Poisson process of time rate λ), while the water losses (water withdrawal) are assumed to be constant over time. Therefore, the probability density function of water volume, p_w, has been derived following the approach of Rodriguez-Iturbe et al. (1999).

Ultimately, the TDD of the water level has been obtained by combining the stage-storage capacity curve and the probability density function of water volume (p_w). The expression of the TDD is:

$$p(H) = \left|\frac{d\, f^{-1}(H)}{d\, H}\right| p_W(f^{-1}(H)) \tag{2}$$

where $f^{-1}(H) = W = w_1 h^n$ is the inverse of the stage-storage capacity curve (w_1 $[m^{3-n}]$ is the parameter of the curve, h $[m]$ the water level in the reservoir and n $[-]$ the exponent influenced by the shape of the control volume).

Results and concluding remarks

In the current work, a numerical simulation of the dam operation was carried out using the same rainfall forcing (sequence of instantaneous pulses that occur in a Poisson process of time rate λ) adopted for the proposed TDD. The comparison between the TDD of the water level (continuous blue line) and the empirical probability density function (pdf) obtained via numerical hydraulic simulation (orange dots) helps in understanding the reliability of the proposed methodology and quantifying the impact of the approximations adopted. Results are reported in the following Figure 1.

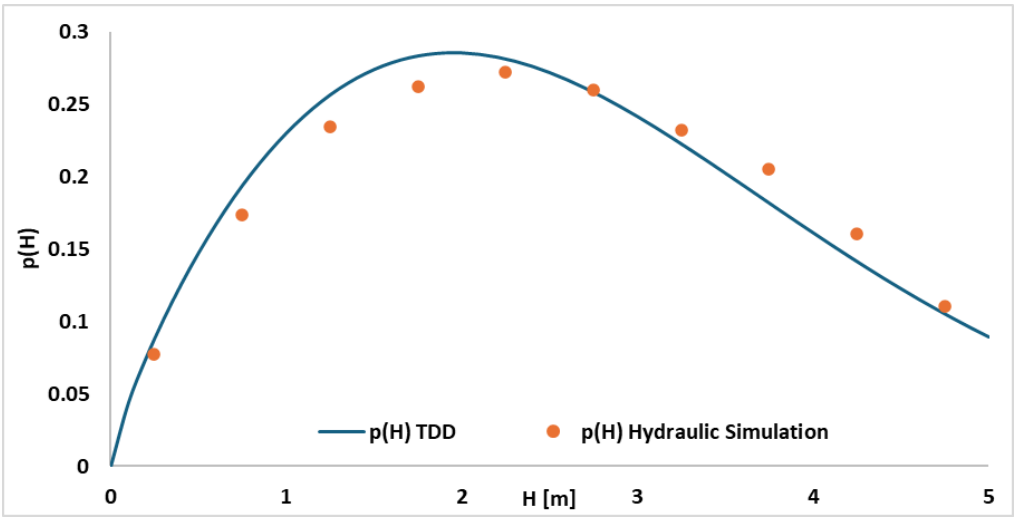


Figure 1. Comparison between the theoretically derived distribution (TDD) of the water level (continuous blue line) and the empirical probability density function (pdf) obtained via numerical hydraulic simulation (orange dots).

The numerical simulation was carried out at the daily scale by considering a dam with the following characteristics: h_s = 5 m; w_1 = 5000 m^3, n = 1.78, A_b = 10 km^2, φ = 0.5. In addition, the daily withdrawals (L) are assumed to be 30% of the incoming discharge, while the inflow is modelled as a sequence of instantaneous pulses that occur in a Poisson process of time rate λ = 0.2 and main daily rainfall of 5 mm.

Acknowledgments: This study was carried out within the RETURN Extended Partnership and received funding from the European Union Next-GenerationEU (National Recovery and Resilience Plan - NRRP, Mission 4, Component 2, Investment 1.3 - D.D. 1243 2/8/2022, PE0000005).

References

Albertini C, Miglino D, Bove G, et al. (2022) Integration of a Probabilistic and a Geomorphic Method for the Optimization of Flood Detention Basins Design. Environmental Sciences Proceedings, 21(1).

Benjamin JR, Cornell CA (2014) Probability, statistics, and decision for civil engineers. Courier Corporation, New York.

Bertola M, Viglione A, Lun D, Hall J, Blöschl G (2020) Flood trends in Europe: are changes in small and big floods different? Hydrology and Earth System Sciences, 24(4): 1805-1822.

Manfreda S, Fiorentino M (2008) A stochastic approach for the description of the water balance dynamics in a river basin. Hydrology and Earth System Sciences, 12: 1189-1200.

Manfreda S, Miglino D, Albertini C (2021) Impact of detention dams on the probability distribution of floods. Hydrology and Earth System Sciences, 25: 4231-4424.

Merz B, Blöschl G, Vorogushyn S, Dottori F, Aerts JCJH, Bates P, Bertola M, Kemter M, Kreibich H, Lall U, Macdonald E (2021). Causes, impacts and patterns of disastrous river floods. Nature Reviews Earth & Environment, 2.

Raimondi A, Becciu G (2015) On pre-filling probability of flood control detention facilities. Urban Water Journal, 12(4): 344-351.

Rodrıguez-Iturbe I, Porporato A, Ridolfi L, Isham V, Cox DR (1999) Probabilistic modelling of water balance at a point: The role of climate, soil and vegetation. Proceedings of the Royal Society of London Series A, 455: 3789-3805.

A Digital Twin for the management of the urban drainage system and flooding events in the city of Palermo

M. Avanti*, A. Francipane, L.V. Noto
Dipartimento di Ingegneria, Università degli Studi di Palermo, Palermo, Italy
** e-mail: marco.avanti@unipa.it*

Introduction

Assessing and managing flood risk in cities, especially those with large historical centers where interventions are often challenging or prevented by highly constrained contexts, is essential, especially considering the increase in the frequency of extreme rainfall events in recent years. A powerful tool that opens up a range of possibilities to address these critical issues can be the implementation of a Digital Twin (DT) that integrates the interaction between hydraulic models, internet-connected sensors, remote control organs of the systems, updating from GIS sources and the address of physical interventions by technicians on the physical system. The DT evolves with the physical system and addresses the managing infrastructures under both ordinary and critical situations, such as urban floods.

In this study, a DT of the urban drainage system of the city of Palermo was developed using data and information provided by the Municipal Waterworks of Palermo (*Azienda Municipalizzata Acquedotto di Palermo*, AMAP), alongside the hydraulic solver InfoWorks ICM (Integrated Catchment Modeling). This effort aims to create a tool for analysing system responses, identifying hydraulic criticalities under different conditions and providing mitigation measures.

Materials and methods

The urban drainage system of Palermo is highly complex. The evolution of its sewer network is closely linked to the many changes that the city has undergone over its millennia-long history. Since the Arab period, the Kemonia and Papireto streams served as natural drainage channels until they were covered in the 16th century in an attempt to prevent flooding. Between 1860 and 1886, urban growth led to the haphazard construction of numerous pipes, further increasing the complexity of the network. The 1930 plan attempted to rehabilitate the network by reorganizing it into three basins and aiming to reduce discharges into the Cala. However, subsequent uncontrolled urban expansion made the mapping and the management of the urban drainage network increasingly difficult, especially in the historic centre, where the overlapping of old collectors and new infrastructure has made its configuration challenging to identify.

The starting point for the creation of the DT was the information on the physical system provided by AMAP. This data includes a geodatabase consisting of 963 km of pipes, 22,431 nodes, 43 lifting plants, 26,337 drains, various overflow structures, retention works, and water treatment plants. The data and parameters were implemented within the commercial software InfoWorks ICM, an advanced software developed by Autodesk that integrates hydrological and hydrodynamic components to simulate the drainage system comprehensively, even during flood events. The peculiarities of the software include easy modeling of sewerage structures such as spillways, lifts, siphons, sluice gates, pumping stations etc. The combined 1D and 2D hydraulic modeling capabilities enable the simulation of both sewer networks and surface water movement in urban areas and watercourses, offering a holistic view of the system.

In addition to the implementation of the drainage network based on AMAP data, the topography of the area is modelled using LIDAR data with a spatial resolution of 2 meters. Buildings footprints are excluded from the 2D computational mesh, as they are considered insurmountable obstacles. Rainfall that falls on the rooftops is directly routed into the drainage system, while wastewater flows are assigned to nodes and calculated based on per-capita flow rates, time use design profiles, and population density obtained from the Italian National Institute of Statistics (*Istituto Nazionale di Statistica*, ISTAT) website. Surface modeling is carried out directly on the 2D computational mesh, while hydrological losses are calculated using a

modified version of the SCS-CN method that considers only infiltration losses. Furthermore, an updated Curve Number (CN) map for Sicily was used.

Figure 1 shows a detailed view of the Cala area of Palermo within the digital twin model, highlighting various elements of the drainage system.



Figure 1. Example of the digital twin model representing the Cala area of Palermo.

Results and concluding remarks

The creation of a DT for Palermo's urban drainage system represents a significant advancement in understanding, managing, and optimizing the city's complex sewer network, providing a robust, data-driven framework for informed decision-making, flood risk management, and land use planning, ultimately contributing to the resilience and adaptability of Palermo's drainage system in the face of evolving environmental and urban challenges.

The DT will allow for the identification of key areas where performing specific inspections to progressively fill the information gaps of the system, developing strategies to minimize management costs and to identify more effectively improvement interventions to be carried out on the drainage system (Wright et al., 2017). it also will play a crucial role in evaluating, forecasting, and managing pluvial flood events by analysing system responses and identifying hydraulic criticalities during high intensity meteorological events (Montestruque et al., 2015).

Despite its advantages, the effectiveness of the digital twin will depend on continuous data updates (Mashaly, M. 2021). Integrating real-time sensor data, improving model parameterization, and addressing uncertainties in historical infrastructure records will be essential for maintaining accuracy and reliability.

References

Mashaly M. (2021) Connecting the twins: A review on digital twin technology & its networking requirements. Procedia Computer Science, 184, 299-305

Montestruque L., Lemmon M. D. (2015) Globally coordinated distributed storm water management system. In Proceedings of the 1st ACM International Workshop on Cyber-Physical Systems for Smart Water Networks (pp. 1-6)

Wright J., Marchese D. (2018) Briefing: Continuous monitoring and adaptive control: the 'smart'storm water management solution. Proceedings of the Institution of Civil Engineers-Smart Infrastructure and Construction, 170(4), 86-89

Comparative analysis of data-driven techniques for spring yield prediction

G. Gullotti*, C. Arena, M. Cannarozzo, L.V. Noto
Dipartimento di Ingegneria, Università degli Studi di Palermo, Palermo, Italy
**e-mail: giorgio.gullotti@unipa.it*

Introduction

The primary objective of this research is to compare various data-driven techniques for predicting spring yields, including multiple regression, Evolutionary Polynomial Regression (EPR) and neural networks. In recent years, the integration of artificial intelligence (AI) techniques in hydrology and water resources management has seen significant progress (Chang et al. 2023). Modern computational tools are used in this research to address the need for generating hydrological scenarios of water availability based on climate change forecasts. These hydrological scenarios will become the input of simulation models of complex, regional water resources systems needed to implement both investment planning and system management (Arena et al. 2014). The use of data-driven models is particularly suitable for springs, where the complex phenomena of groundwater circulation often make it impractical to use physically based models.

Materials and methods

This study focuses on springs located in Sicily, Italy. The dependent variable data, i.e., spring yields, were provided by a local water utility on a monthly scale for the period from January 1958 to December 2018. The data for the independent variables, areal rainfall and temperature, were obtained on a monthly scale by processing data from the BIGBANG hydrological model database developed by ISPRA (Braca et al. 2021), freely accessible online, for the period from 1951 to 2023. Areal precipitation was calculated considering recharge areas from the regional water resources plan (Piano di Tutela delle Acque della Sicilia, 2008).

MATLAB software was used for data processing and the Regression Learner, a tool integrated within MATLAB, was employed to efficiently calibrate several machine learning models. In this tool these techniques can be easily executed by selecting the appropriate options in the application interface.

Among the different available regression models in the Regression learner, traditional regression, assisted by stepwise techniques, and Artificial Neural Networks (ANN) were tested and compared. Another model used, for which specific code was developed, is the Evolutionary Polynomial Regression (EPR).

Conventional regression models available in the tool include linear and quadratic regression as well as regressions with interactions and can be calibrated even using a stepwise approach. Stepwise regression is a technique that allows the choice of predictors of a conventional regression model through an automatic procedure. The stepwise regression starts with no predictors in the model. During the forward selection phase, predictors are added one by one: at each step, the predictor that provides the most significant improvement to the model is included. This is followed by the backward elimination phase, where the least significant predictor is removed at each step until only statistically significant predictors remain.

Another technique tested for the comparison is the Evolutionary Polynomial Regression (EPR). EPR is an advanced regression technique that combines elements of polynomial regression with evolutionary algorithms to enhance the accuracy of predictive models. EPR utilizes a polynomial to represent the relationship between independent variables and the dependent variable. Each term in the polynomial is given by the product of a coefficient and all the independent variables, each raised to its own exponent. The evolutionary aspect of EPR involves using genetic algorithms to optimize the coefficients and the exponents, leading to an expression that minimizes an objective function, i.e. the mean squared error, MSE. This combination allows for the creation of complex and adaptable models that can better capture the dynamics of the data compared to traditional regression methods. The technique is particularly effective in handling complex and nonlinear data, as demonstrated by Giustolisi & Savic (2006). Their research applied

EPR to the prediction of groundwater levels, showcasing its potential in managing intricate hydrological data.

ANN were also experimented. ANN are computational models inspired by the structure and function of the human brain. They consist of interconnected units called neurons, organized in layers: an input layer that represents the sample data, one or more intermediate (or "hidden") layers that process the data, and an output layer that provides the results. Each neuron transmits a numerical signal called input to the connected neurons of the next layer. The receiving neuron assigns a weight to each input received, determining its importance; the receiving neuron also has an activation function that introduces non-linearity by transforming the sum of inputs and an additional parameter, called bias, into output. Training a neural network involves optimizing weights and biases using algorithms like backpropagation to minimize the error between predicted and actual outputs. ANN have various practical applications, including regression tasks, where they are used to predict numerical values.

Results and concluding remarks

The study experimented the above-mentioned models. Additionally, the models were tested by aggregating the dependent and independent variables at different time scales (monthly, quarterly, and annually). The results are overall encouraging and indicate that some models perform better than others (Figure 1). An aspect that should not be overlooked when evaluating the prediction potential of these models is their ability to provide some insights into the dynamics of the hydrological process leading to spring yield: for instance, conventional regression is able to measure formally the significance of each of the covariates in explaining the dependent variable, while is much less the case for other techniques. These aspects are related to the issue of parameter parsimony, a well-known topic in data-driven models.

The findings underscore the potential of data-driven techniques in predicting spring yields and highlight the importance of selecting the appropriate model for accurate and physically interpretable predictions.

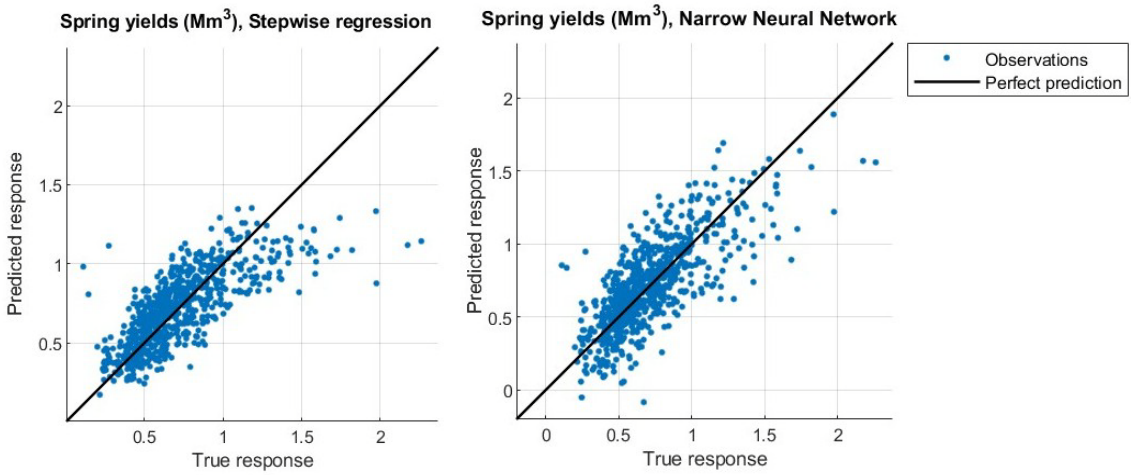


Figure 1. Predicted vs Actual plots of a linear regression model and an ANN model for Risalaimi spring's flows on a monthly scale

References

Arena C, Cannarozzo M, Mazzola MR (2014) Screening Investments to Reduce the Risk of Hydrologic Failures in the Headwork System Supplying Apulia (Italy) – Role of Economic Evaluation and Operation Hydrology. Water Resour Manag 28:1251–1275. https://doi.org/10.1007/s11269-014-0539-9

Braca G, Bussettini M, Lastoria B, et al (2021) Il Bilancio Idrologico Gis BAsed a scala Nazionale su Griglia regolare – BIGBANG: metodologia e stime. Rapporto sulla disponibilità naturale della risorsa idrica. Istituto Superiore per la Protezione e la Ricerca Ambientale, Rapporti 339/21, Roma.

Chang F-J, Chang L-C, Chen J-F (eds) (2023) Artificial Intelligence Techniques in Hydrology and Water Resources Management. MDPI - Multidisciplinary Digital Publishing Institute, Basel

Giustolisi O, Savic DA (2006) A symbolic data-driven technique based on evolutionary polynomial regression. J Hydroinformatics 8:207–222. https://doi.org/10.2166/hydro.2006.020b

A novel Data Cube framework for environmental and climate change monitoring in coastal areas

I. Kavouras[1], G. Kopsiaftis[2*], I. Rallis[1], N. Bakalos[1], A. Doulamis[1], N. Doulamis[1], D. Kalogeras[3]
[1] Laboratory of Photogrammetry, School of Rural, Surveying and Geoinformatics Engineering, NTUA, Greece
[2] Laboratory of Reclamation Works and Water Resources Management, School of Rural, Surveying and Geoinformatics
[3] Institute of Communications & Computer Systems (ICCS), NTUA. Greece
* e-mail: gkopsiaf@survey.ntua.gr

Introduction

Environmental hazards and climate change significantly impact coastal regions, particularly those with intensive industrial activities such as ports and shipyards. These areas are highly vulnerable to pollution and extreme weather events, requiring continuous monitoring to mitigate their effects. Earth Observation (EO) technologies, including satellite imagery and aerial climate measurements, offer a robust mechanism for tracking environmental changes. However, the heterogeneous nature of EO datasets—arising from differences in spatial resolution, format, and source—poses a challenge for effective data integration and analysis.

Data Cube (DC) frameworks have emerged as a solution for harmonizing and homogenizing large-scale EO datasets. By structuring data into multidimensional arrays, DCs enable comprehensive spatiotemporal analyses of environmental phenomena. A DC framework is primarily used for applications related to big data storage and online analytical processing. Existing implementations, such as the Australian Geoscience Data Cube (Lewis et al., 2017) and the Earth Observation Swiss Data Cube (Poussin et al., 2019), have demonstrated the potential of DC architectures for processing EO data. These frameworks primarily focus on organizing and querying large-scale satellite datasets for various applications, including water observations, coastal erosion, and forest and snow cover changes. Temenos et al. (2024) proposed an adaptive, context-aware DC framework for environmental monitoring and mitigation of climate change impacts, integrating remote-sensing techniques, machine learning (ML), and deep learning (DL) methods for automated data classification and harmonization. This paper introduces a DC framework, enhanced by ML and DL methods, to facilitate climate change and disaster monitoring in port and coastal regions. The proposed framework integrates EO data from multiple sources, applies standardization techniques, and generates ready-to-use analysis products for environmental management.

Materials and methods

The primary goal of the proposed DC framework is to harmonize and homogenize diverse remote sensing and climate data products (EO data) sourced from multiple providers, such as USGS, Copernicus, and NASA. Additionally, non-EO data, including geographical boundaries of the area of interest, can be incorporated into the processing pipeline. This data integration forms the initial stage of the framework's architecture, as shown in Figure 1.

The data harmonization and homogenization step is fundamental to the DC framework, ensuring standardization and interoperability. Initially, EO products are reprojected into a common Coordinate Reference System (CRS) to standardize spatial alignment, allowing for the seamless integration of data from different sources such as Landsat-8 and Sentinel-2. Subsequently, the data are pre-processed to focus on the area of interest, minimizing file sizes. All image data are resized and resampled to achieve a unified spatial resolution and to perform accurate raster calculations within the DC. Additionally, widely used remote sensing indices, such as those derived from optical, near-infrared, and shortwave infrared bands are computed when relevant, further enhancing the analytical capabilities of the framework.

The proposed DC framework is implemented using open-source Python libraries suitable for handling EO data. The final output is a NetCDF file, a widely adopted format in Geographic Information Systems (GIS)

that ensures compatibility with various analytical tools. This DC framework can also integrate non-EO data, such as drone imagery, to create advanced cartographic products and support environmental monitoring applications. Additionally, machine and deep learning techniques could be incorporated to automate data pre-processing, optimize remote sensing product generation, and enhance feature extraction, thereby improving the efficiency and accuracy of environmental monitoring efforts.

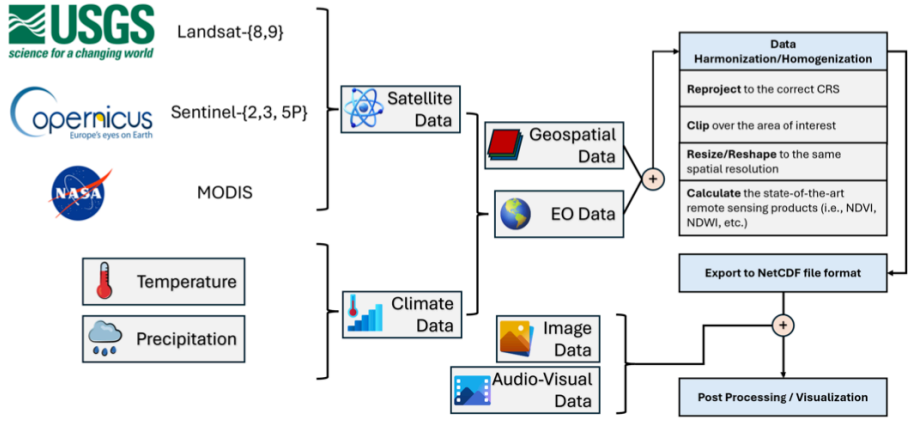


Figure 1. The overall architecture of the data cube implementation.

Results and concluding remarks

The effectiveness of the DC framework is demonstrated through several case studies in coastal areas. The framework successfully generated a 4D Data Cube, enabling time-series analysis enhanced by ML and DL techniques for data classification, anomaly detection, and predictive modeling. The results highlighted the spatiotemporal advantages of integrating multi-source EO data within a unified NetCDF product, revealing critical patterns in environmental changes over the affected area. The DC framework offers a scalable and automated solution for harmonizing and homogenizing diverse EO datasets, supporting both long-term environmental monitoring and disaster response applications. In addition to the coastal and marine ecosystems, the framework will also expand its applicability to various environmental challenges, such as deforestation, flooding, and climate change. The use of harmonized and analysis-ready data led to faster and more accurate identification of affected areas and improved the response time in post-disaster assessments. End-users, including environmental agencies and local authorities, benefited from ready-to-use outputs that could be directly visualized and analyzed in common GIS platforms, promoting informed decision-making without the need for extensive preprocessing.

Acknowledgments: This work is part of the "OCEANIDS, "User-driven applications and tools for Climate-Informed Maritime Spatial Planning and integrated seascape management, towards a resilient & inclusive Blue Economy" project. This project has been funded by the European Union through the Horizon 2020 research and innovation programmes under Grant Agreement No. 101112919.

References

Harinarayan, V., Rajaraman, A., & Ullman, J. D. (1996). Implementing data cubes efficiently. Acm Sigmod Record, 25(2), 205-216.

Lewis, A., Oliver, S., Lymburner, L., Evans, B., Wyborn, L., Mueller, N., Raevksi, G., Hooke, J., Woodcock, R., Sixsmith, J., Wu, W., Peter Tan, Li, F., Killough, B., Minchin, S., Roberts, D., Ayers, D., Bala, B., Dwyer, J., Dekker, A., Dhu, T., Hicks, A., Ip, A., Purss, M., Richards, C., Sagar, S., Trenham, C., Wang, P., Wang, L. W. (2017). The Australian geoscience data cube—foundations and lessons learned. Remote Sensing of Environment, 202 (pp. 276-292).

Poussin, C., Guigoz, Y., Palazzi, E., Terzago, S., Chatenoux, B., & Giuliani, G. (2019). Snow cover evolution in the Gran Paradiso National Park, Italian Alps, Using the earth observation data cube. Data, 4(4), 138.

Temenos, A., Temenos, N., Tzortzis, I. N., Rallis, I., Doulamis, A., & Doulamis, N. (2024). C2A-DC: A context-aware adaptive data cube framework for environmental monitoring and climate change crisis management. Remote Sensing Applications: Society and Environment, 34, 101171.

IV. Geo-information and Water Resources

Assessment of potentially vulnerable glacial lakes of the Eastern Himalayan region

A.K. Shukla[1], I. Ahmad[1*], S.K. Jain[2]
[1] Department of Civil Engineering, National Institute of Technology Raipur, India
[2] Centre of Excellence in Disaster Mitigation and Management, Indian Institute of Technology Roorkee, India
* e-mail: iahmad.ce@nitrr.ac.in

Introduction

The Eastern Himalayas, particularly in Sikkim, are witnessing the rapid expansion of glacial lakes due to the retreat of glaciers, a process driven by climate change. One of the most significant examples is South Lhonak Lake, which has grown from around 17.5 hectares in 1977 to over 80 hectares in recent decades (Racoviteanu et al., 2015; Sattar et al., 2019), a result of accelerated glacial melting and increased precipitation. The region's vulnerability to Glacial Lake Outburst Floods (GLOFs) is heightened by the presence of over 14 potentially dangerous lakes, with a 24% increase in the total surface area of glacial lakes between 1975 and 2017 (Hazra & Krishna, 2021; Meraj & Kumar, 2024). A recent GLOF event in October 2023, triggered by the breach of South Lhonak Lake, caused catastrophic flooding along the Teesta River basin, destroying infrastructure and homes and claiming at least 40 lives (Sattar et al., 2019; Meraj & Kumar, 2024). This event underscores the urgent need for enhanced monitoring and early warning systems to mitigate GLOF hazards, alongside continuous risk assessment and adaptive management strategies to address the growing threats posed by climate-driven glacial lake expansion in Sikkim (Hazra & Krishna, 2021).

Materials and methods

To identify potentially dangerous lakes, LANDSAT 5 imagery (1993, 2003) and LANDSAT 8 imagery (2013, 2023) were utilized to observe changes in glacial lakes over time. The Randolph Glacier inventory was also used for glacier mapping, providing additional context to assess glacial lake dynamics. Additionally, the Digital Elevation Band is used for slope and other parameters with GUI-based Arc Map software.

Method of Identification of glacial lakes and glacier boundary:

1) Pixel-based interpretation is particularly powerful for identifying glacial lakes and glacier boundaries by leveraging the distinct spectral signatures of ice, snow, water, and surrounding terrain in satellite imagery. For glacial lakes, the method capitalizes on water's strong absorption of near-infrared radiation (appearing very dark in these bands) contrasted against the high reflectance of surrounding ice and snow, making lake boundaries clearly distinguishable. 2) Google Earth Engine with Multiple Wate Indices: Lake detection by leveraging cloud computing to process multiple water indices (NDWI, MNDWI, AWEI) simultaneously across large temporal datasets of satellite imagery. This multi-index approach enhances detection accuracy by accounting for varying lake conditions like turbidity and ice cover, while effectively distinguishing lakes from shadows and snow in complex mountain terrain. 3) Pixel and Feature-Based Classification: This combines pixel-based methods with machine learning classifiers that consider both pixel-level features (like color or spectral signature) and higher-level features (like texture or spatial context). This approach would help refine identification of potentially dangerous lakes by classifying water bodies based on their characteristics, such as size, shape, and surrounding landforms.

Identification of potentially dangerous lakes:

Method 1: Characteristics-based Assessment (evaluates lakes based on area, elevation, and dam type)

Area: Larger lakes may pose a greater flood risk, as they contain more water; Elevation: Higher elevation lakes, particularly those located in steep valleys or moraine-dammed lakes, tend to be more unstable and prone to outbursts; Dam Type: The type of moraine dam (whether ice or debris-dam) and its stability is crucial in determining the risk. Weak or undercut dams are more likely to fail, leading to potential GLOFs.

Method 2: Scenario-based Approach (Mathematical and pervious study)

Scenario 1 (Quantitative): A quantitative GLOF risk assessment integrates precise measurements of lake dimensions, including area (derived from satellite imagery), volume (estimated through empirical relationships or bathymetric surveys), and elevation (from digital elevation models). This data-driven approach enables the development of statistical models that can assign probability scores to GLOF hazards, helping prioritize high-risk lakes for monitoring and mitigation measures. Scenario 2 (Semi-Quantitative): A semi-quantitative GLOF risk assessment integrates historical GLOF records and measured parameters to create a comprehensive hazard evaluation framework. This approach combines quantitative measurements (lake area, volume, expansion rate) with qualitative factors such as dam stability and ice avalanche potential, while also incorporating past GLOF events to identify common trigger patterns and risk factors, to classify lakes into different risk categories (high, medium, low) while accounting for both measurable data and site-specific conditions that may not be fully quantifiable. Scenario 3 (Qualitative): This approach examines documented disasters to recognize common trigger mechanisms, such as ice/rock avalanches into lakes or rapid lake expansion patterns that preceded past GLOFs. The analysis focuses on visual interpretation of lake growth dynamics, evaluating changes in lake area and elevation through satellite imagery time series.

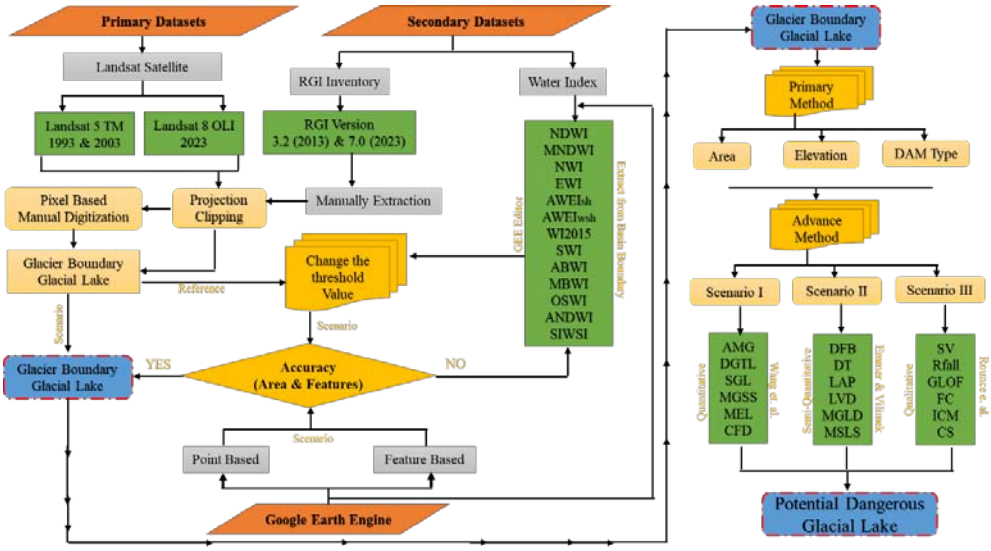


Figure 1. Methodology for identification of potentially dangerous lakes

Results and concluding remarks

In 2023, a comprehensive study of glacial lakes in Sikkim identified 14 lakes as potentially dangerous due to their rapid expansion and growing vulnerability to Glacial Lake Outburst Floods (GLOFs). These lakes, formed by the retreat of glaciers in the Eastern Himalayas, have seen a marked increase in their surface area, primarily driven by accelerated glacier melting and changing climatic conditions. Among these, South Lhonak Lake has emerged as a significant concern, having expanded dramatically from 17.5 hectares in 1977 to over 80 hectares in recent years. This alarming growth is accompanied by an increased risk of GLOFs, particularly as the region experiences more frequent and intense precipitation events. The study underscores the urgent need for proactive measures to mitigate the risks associated with GLOFs.

References

Hazra, S., & Krishna, A. (2021). Glacial Lake Outburst Floods in the Eastern Himalayas: Vulnerabilities and Risk Assessment. Journal of Himalayan Research, 18(2), 112-130.

Meraj, K., & Kumar, V. (2024). Impacts of Climate Change on Glacial Lake Dynamics in Sikkim, India. Environmental Change and Adaptation, 10(3), 205-220.

Racoviteanu, A., et al. (2015). Glacier Retreat and Glacial Lake Expansion in the Eastern Himalayas: A Historical and Contemporary Analysis. Himalayan Journal of Earth Science, 22(4), 185-202.

Sattar, M. A., et al. (2019). South Lhonak Lake and the October 2023 GLOF Event: Impacts and Lessons Learned. Journal of Glacial Studies, 13(1), 76-89.

DATASET: GrounDwater sAlinizaTion and pollution AsseSsmEnt Tool: a holistic approach for coastal areas

G. Busico[1*], D. Potrykus[2,3], M. Mastrocicco[1]
[1] Di.S.T.A.Bi.F., University of Campania "Luigi Vanvitelli", Via A. Vivaldi 43, 81100 Caserta, Italy
[2] Faculty of Civil and Environmental Engineering, Gdansk Tech, Narutowicza 11/12, 80-233 Gdansk, Poland
[3] Polish Geological Institute – NRI, Marine Geology Branch, Koscierska 5, 80-328 Gdansk, Poland
* e-mail: gianluigi.busico@unicampania.it

Introduction

Coastal areas are invaluable ecosystems, providing crucial resources for economic and societal development. However, salinization processes (SP) of freshwater resources represent one of the most alarming and widespread issues affecting coastal regions (Mastrocicco et al., 2021). This situation, coupled with the intensive agricultural practices characteristic of fertile coastal plains, has significantly heightened water resource stress, frequently leading to groundwater pollution due to agricultural leaching (AGL). SP and AGL often coexist in low-lying areas worldwide (Busico et al., 2018), such as deltas, where persistent and ubiquitous interactions between surface and groundwater bodies occur. Within this context, assessing aquifer vulnerability to AGL and SP is a crucial preventive measure for ensuring the sustainable management of groundwater resources. Rating methods, which can be readily implemented within GIS environments, are often scalable to large domains (regional or national levels) using freely available global-scale open databases (Rama et al., 2022). However, these methods are inherently static, frequently influenced by subjectivity, and may overlook critical parameters. Despite these limitations, the use of groundwater vulnerability assessment (GVA) and particularly rating methodologies has grown in response to the increasing pressure of SP and AGL phenomena (Machiwal et al., 2018). The novelty of DATASET lies in its implementation of a holistic approach to quantify the vulnerability of coastal areas to both SP and AGL, encompassing all contributing processes. Moreover, DATASET aims to deeply investigate the direct and side effects of climate change and land-use change on SP and AGL to provide effective solutions not only for actual sustainable management but even for future scenarios.

Materials and methods

The *DATASET index* incorporates some of the pre-existing parameters typical of the standard GVA indices. Only the parameters with the highest impact and weight, and available on open repositories among local and global databases have been selected as suitable for the DATASET index. The main drawback of rating methods is their high sensitivity to scores and weights. Thus, scientific research in the field needs to objectify and challenge assumptions with mathematical procedures, such as sensitivity and uncertainty analysis. To correctly identify all parameters responsible for SP and AGL that have been used in previous applications along with their assigned weights, two detailed Systematic Reviews have been performed as the first screening phase of the DATASET methodology. This allows us to consider a wide range of applications, with a worldwide extension, and a huge variety of different hydrogeological settings.

Results and concluding remarks

Systematic reviews were conducted to address the following questions: "Which parameters used in weight-and-rate index methods influence GVA to anthropogenic pollution?" and "Which hydrogeological factors influence SP and AGL?" The primary objective was to rank the most frequently used parameters in the literature, from highest to lowest importance. To achieve this, literature on standard and modified applications of DRASTIC, SINTACS, GOD, and GALDIT was reviewed and analyzed. Statistical analysis of the weights assigned to each parameter produced two rankings. The findings emphasize the critical importance of depth to water, topography, and recharge for AGL, and height of the groundwater level above sea level,

distance from the shore, and hydraulic conductivity for SP (Table 1). Conversely, parameters such as vadose zone, aquifer media, groundwater occurrence, and existing status of SWI showed very low impacts. This is attributed to their high intrinsic subjectivity and limited ability to fully represent the complexities of SP.

Table 1. Final ranking of Parameters for AGL and SP.

Parameters (AGL)	Ranking	Parameters (SP)	Ranking
Depth to water	1	Height of the GW level above sea	1
Topography	2	Distance from the shore	2
Recharge	3	Aquifer hydraulic conductivity	3
Hydraulic conductivity	4	Thickness of the aquifer	4
Impact of vadose media	5	Groundwater occurrence	5
Aquifer media	6	Impact on existing status of SWI	6
Soil Texture	7		

Building on these findings, the new DATASET index was developed to enable a dual GVA approach, allowing for the activation or deactivation (ON/OFF) of significant parameters. No qualitative parameters are included in the formula. The method is designed to facilitate two levels of assessment: a simplified screening using only 3 to 4 parameters and a detailed screening incorporating up to 7 parameters. Other parameters, coming from the two systematic reviews were proposed as new or replaced one to allow a better representation of GVA (Figure 1).

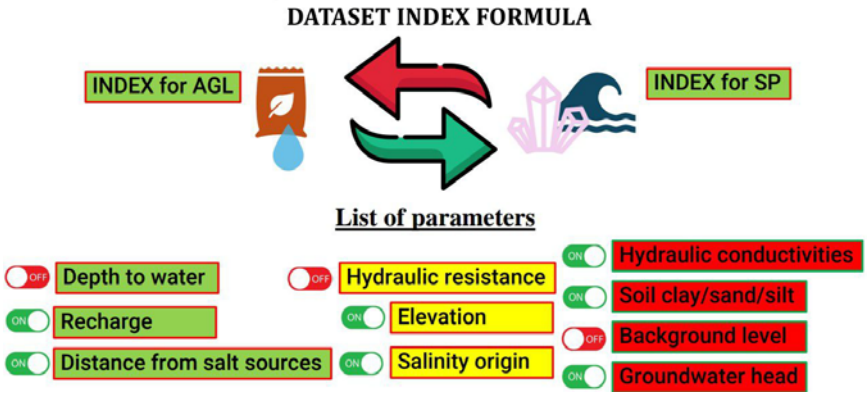


Figure 1. DATASET index scheme.

Acknowledgments: The authors would like to thank the European Commission and MUR for funding in the frame of the collaborative international consortium DATASET (Groundwater salinization and pollution assessment tool: a holistic approach for coastal areas, Water4All_00084), financed under the 2022 Joint call of the European Partnership 101060874 - Water4All.

References

Busico G, Cuoco E, Kazakis N, Colombani N, Mastrocicco M, Tedesco D, Voudouris K (2018) Multivariate statistical analysis to characterize/discriminate between anthropogenic and geogenic trace elements occurrence in the Campania Plain, Southern Italy. Environmentak Pollution. 234, 260-269. https://doi.org/10.1016/j.envpol.2017.11.053.

Machiwal D, Cloutier V, Güler C, Kazakis N (2018) A review of GIS-integrated statistical techniques for groundwater quality evaluation and protection. Environmental Earth Science. 77, 681. https://doi.org/10.1007/s12665-018-7872-x

Mastrocicco M, Gervasio MP, Busico G, Colombani N (2021) Natural and Anthropogenic Factors Driving Groundwater Resource Salinization for Agriculture Use in the Campania Plains (Southern Italy). Science of the Total Environment. 2021, 758, 144033. https://doi.org/10.1016/j.scitotenv.2020.144033

Rama F, Busico G, Arumi JL, Kazakis N, Colombani N, Marfella L, Hirata R, Kruse EE, Sweeney P, Mastrocicco M (2022). Assessment of intrinsic aquifer vulnerability at continental scale through a critical application of the drastic framework: The case of South America. Science of the Total Environment. 823, 153748. https://doi.org/10.1016/j.scitotenv.2022.153748.

Dam break assessment and flood hazards mapping of Minimata Bango dam

G. Sahu, I. Ahmad*
Department of Civil Engineering, National Institute of Technology Raipur, India
** e-mail: iahmad.ce@nitrr.ac.in*

Introduction

The Hasdeo Bango Dam, situated on the Hasdeo River in Chhattisgarh, represents a critical water infrastructure that requires comprehensive safety assessment due to its significant storage capacity and the downstream population at risk. Dam break analysis has emerged as an essential tool for evaluating potential flood hazards and developing emergency action plans for large dams worldwide (Basheer et al., 2017). The potential failure of the Hasdeo Bango Dam, with its storage capacity of 3.28 billion cubic meters, could pose catastrophic risks to downstream communities, agricultural lands, and infrastructure in the Korba and Janjgir-Champa districts (Central Water Commission, 2018). Recent advancements in computational hydraulic modeling and geographic information systems (GIS) have enabled more accurate predictions of flood wave propagation and inundation patterns following hypothetical dam failure scenarios (Chandel et al., 2016). Understanding these dynamics is particularly crucial for the Hasdeo Bango Dam, given its location in a region experiencing increasing rainfall intensity and changing precipitation patterns due to climate change (Kumar et al., 2020). This analysis aims to develop detailed flood hazard maps and assess potential impacts through hydraulic modeling, providing essential information for emergency preparedness and dam safety management strategies to protect the vulnerable downstream populations and assets.

Materials and methods

The dam break analysis for the Hasdeo Bango Dam was conducted using HEC-RAS 2D modeling software, incorporating multiple failure scenarios and uncertainty analysis. The methodology consisted of several sequential steps to ensure accurate flood hazard mapping and risk assessment, shown in Figure 1.

Data Acquisition and Terrain Model Development: - The development of the terrain model began with the selection of PRISM 3D Digital Elevation Model (DEM) as the primary terrain data source, chosen for its superior accuracy and resolution compared to other available DEMs. To enhance the model's accuracy in representing the reservoir characteristics, detailed bathymetry data was incorporated into the terrain model, ensuring precise representation of the storage-elevation relationship. The dam structure itself was then integrated into the model using HEC-RAS's inline structure tool, maintaining all actual dimensions and specifications of the Hasdeo Bango Dam to ensure the most accurate representation of the physical structure for subsequent analysis.

Dam Break Scenario: - The dam break analysis considered four failure scenarios for both earthen and concrete sections of Hasdeo Bango Dam. For the earthen section, overtopping failure (progressive crest erosion) and piping failure (internal erosion at FRL) were analyzed. The concrete section scenarios included complete structural failure through piping (instant collapse) and spillway gate washout, increasing discharge capacity. Breach parameters were calculated using Froehlich's (2017) empirical equations, ensuring a comprehensive assessment of both catastrophic and partial failure modes for flood risk evaluation.

Uncertainty and Sensitivity Analysis: - The analysis applied Froehlich's 2017 methodology using the delta method for estimating standard errors and prediction intervals of breach parameters, providing rigorous uncertainty quantification. Sensitivity analysis varied breach parameters to assess impacts on peak outflow and inundation extent. HEC-RAS 2D unsteady flow simulations were conducted with an optimized mesh,

land use-based Manning's coefficients, a PMF hydrograph as the upstream boundary, and normal depth as the downstream boundary.

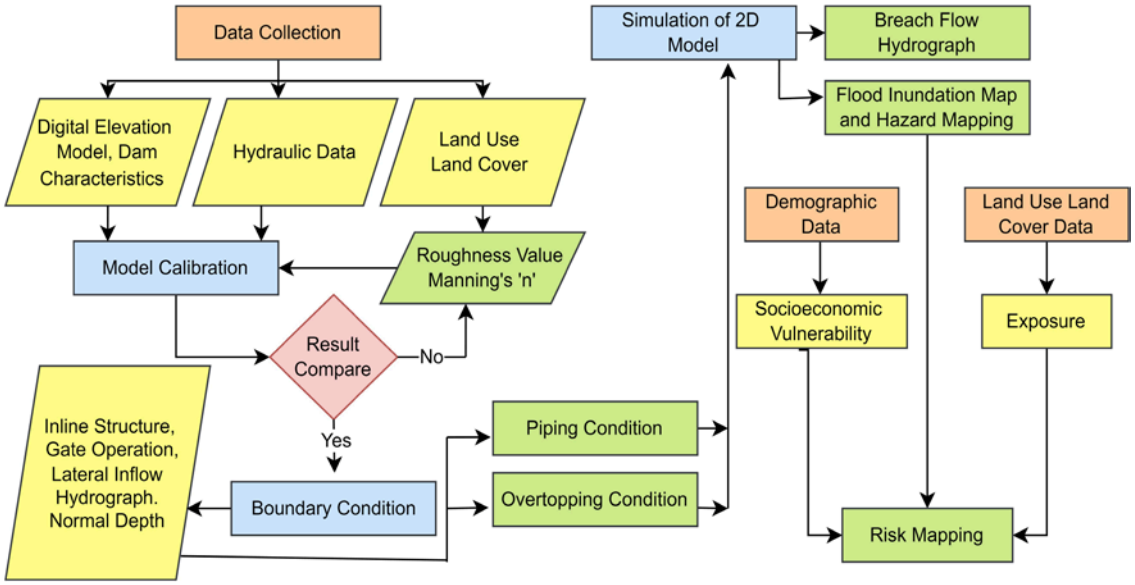


Figure 1. Methodology for Dam break analysis and flood hazard mapping

Results and concluding remarks

A comprehensive dam break analysis was conducted for the Hasdeo Bango Dam, addressing both earthen and concrete sections using HEC-RAS 2D unsteady flow simulation. For the earthen section, two failure scenarios were examined: overtopping and piping. The overtopping scenario, characterized by progressive erosion of the dam crest, resulted in a peak discharge of 69,185.6 cumecs. The piping scenario, simulating internal erosion, produced a peak discharge of 31,626.2 cumecs. Sensitivity analysis for the piping scenario involved varying breach parameters to evaluate their impact on peak discharge and inundation extent. For the concrete section, two failure scenarios were analyzed: complete structural failure through piping and an emergency spillway gate washout. Breach parameters were estimated using Froehlich's (2017) empirical equations, and uncertainty analysis was conducted using the delta method to provide prediction intervals for key parameters. Flood hazard maps were created to visualize inundation extents and potential impact areas for each failure scenario. These maps are critical for risk assessment and emergency planning, highlighting the most vulnerable areas. The simulation results underscore the necessity of detailed hydraulic modeling and comprehensive analyses in dam safety evaluations. Enhanced monitoring, early warning systems, and adaptive management strategies are essential to mitigate risks and safeguard downstream communities from potential flood hazards.

References

Brunner G. W. (2014) Using HEC-RAS for Dam Break Studies. Hydrologic Engineering Center.

Froehlich D. C. (2017) Embankment Dam Breach Parameters and Their Uncertainties. Journal of Hydraulic Engineering, 143(8), 04017020.

Ponce V. M., Tsivoglou E. C. (1981) Modeling Gradually Varied Flow in Dam-Break Flood Waves. Journal of Hydraulic Research, 19(1): 47-61.

U.S. Army Corps of Engineers (2016) HEC-RAS River Analysis System: Hydraulic Reference Manual. Hydrologic Engineering Center.

Wahl T. L. (1998) Prediction of Embankment Dam Breach Parameters: A Literature Review and Needs Assessment. U.S. Department of the Interior, Bureau of Reclamation.

Assessment of snow water equivalent reanalyses and improving snow process simulations in rainfall-runoff model across Northern Italy

G. Sarigil[1*], M. Neri[1], F. Avanzi[2], E. Toth[1]
[1] *University of Bologna, Civil, Chemical, Environmental, and Materials Engineering - DICAM , Bologna, Italy*
[2] *CIMA Research Foundation, Savona, Italy*
** e-mail: gokhan.sarigil2@unibo.it*

Introduction

Snow plays a critical role in the Mediterranean mountainous region by storing winter precipitation and releasing meltwater during spring and summer, which helps regulate water resources. However, direct measurements of Snow Water Equivalent (SWE), crucial for mountain hydrology and water management, are often limited. Due to these limitations, alternative approaches such as large-scale reanalysis products and rainfall-runoff models are commonly used, though both methods face significant challenges. Large-scale reanalysis products face several limitations including sparse data assimilation, coarse spatial resolution, and simplified orographic precipitation. Similarly, rainfall-runoff models encounter challenges with input data accuracy, precipitation-phase determination, and simplified snow thermodynamics. This study follows a two-phase approach to validate and improve snow monitoring in Northern Italy. First, we evaluate the reliability of SWE estimates from multiple large-scale reanalysis products and a streamflow-calibrated rainfall-runoff model against a high-resolution national reference dataset (IT-SNOW). Second, we explore various strategies for integrating SWE data into model calibration to improve SWE simulations.

Materials and methods

This study evaluates SWE estimates across more than 100 catchments in Northern Italy for the period 2010-2020. We used the IT-SNOW dataset (Avanzi et al., 2023) as reference, which provides SWE estimates at 500 m resolution through comprehensive assimilation of satellite and in-situ measurements. Against this dataset, we evaluated three reanalysis products derived from land-surface models (Table 1) and the SWE simulation by the GR6J-CemaNeige rainfall-runoff model (Coron et al., 2017; Valéry et al., 2014) calibrated with streamflow observations. Comparisons were performed both at the gridded and catchment scale.

Table 9. Main characteristics of the reanalysis datasets used in this study.

Dataset	Coverage	Resolution	Atmospheric model	Land surface model	Produced by
IT-SNOW (Avanzi et al., 2023)	Italy, 2011- present	0.5 km, Daily	Station data + Radar merge	S3M	CIMA
ERA5-Land (Muñoz-Sabater et al., 2021)	Global, 1950-present	9 km, Hourly	IFS (ERA5 atmospheric forcing)	CHTESSEL	ECMWF
Cerra-Land (Verrelle et al., 2022)	Europe, 1984-2020	5 km, Hourly	HARMONIE-AROME (CERRA atmospheric forcing)	SURFEX	COPERNICUS
VHR-REA_IT (Raffa et al., 2021)	Italy, 1981-2023	2.2 km, Hourly	COSMO-CLM	TERRA-URB	CMCC

In the second part of the analysis, to improve the SWE simulations with the GR6J-CemaNeige model, we implemented three distinct calibration strategies using both streamflow and IT-SNOW data with the Kling-Gupta Efficiency (KGE) as objective function: i) a sequential approach where the CemaNeige snow parameters are first optimized with SWE data, followed by GR6J calibration of the other parameters based on streamflow observations, ii) a NSGA-II multi-objective optimization to identify Pareto front solutions, and iii) a weighted objective function combining streamflow and SWE fitting. These multi-objective calibration strategies aimed to optimize both streamflow (KGE_Q) and snow water equivalent (KGE_SWE) simulations, and compare their relative performance and optimal parameter distributions.

Results and concluding remarks

The evaluation of reanalysis products revealed significant variations in SWE estimates, in both snow cover extent and magnitude (Figure 1a). ERA5-Land showed the closest alignment with the IT-SNOW reference dataset at lower elevations (0-1200m), while the streamflow-calibrated CemaNeige-GR6J model showed the best estimates in regions above 1200 m (Figure 1b). CERRA-Land showed strong agreement with reference dataset in high-elevation winter conditions, but overestimated SWE during summer months (Figure 1b). VHR-REA underestimates SWE across all elevation bands throughout the year.

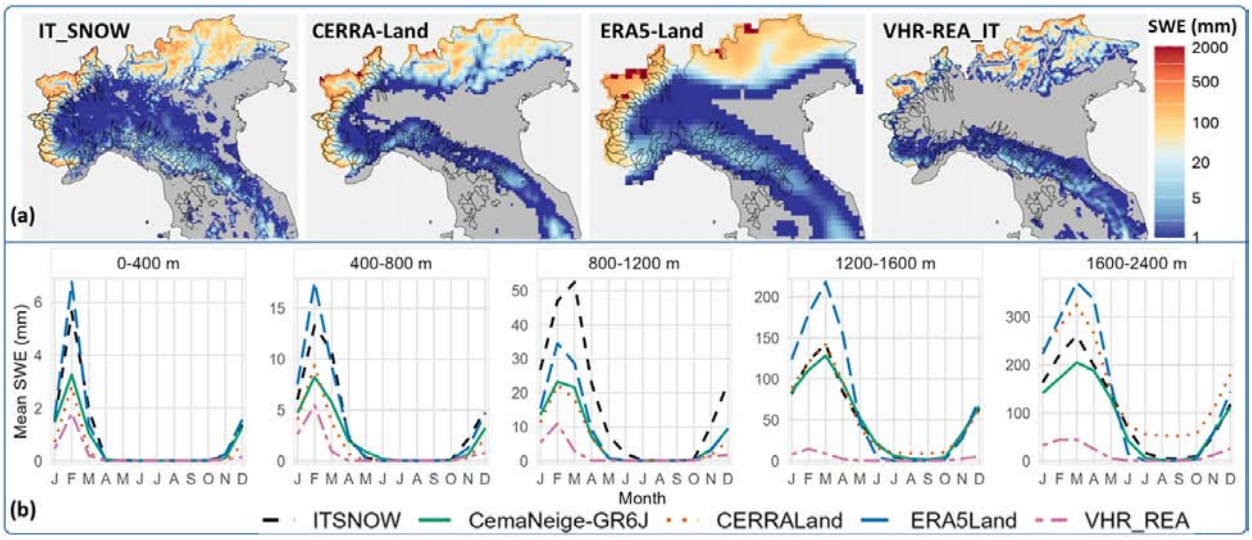


Figure 1. Spatial and seasonal patterns of SWE in Northern Italy (2010–2020). (a) Mean annual SWE distribution of gridded reanalysis products; (b) Monthly SWE seasonality averaged over catchments within each elevation band.

On the other hand, the integration of IT-SNOW data into the rainfall-runoff model calibration process significantly improved SWE simulations while maintaining high-quality streamflow simulations, demonstrating the value of incorporating multiple data sources. Future research will focus on parameter equifinality and uncertainty quantification across these catchments. This analysis will advance regionalization studies by enhancing parameter transferability to ungauged basins, particularly valuable given the sparsity of SWE observations in many regions.

Acknowledgments: This study was carried out within the RETURN Extended Partnership and received funding from the European Union Next-GenerationEU (National Recovery and Resilience Plan – NRRP, Mission 4, Component 2, Investment 1.3 – D.D. 1243 2/8/2022, PE0000005).

References

Avanzi F, Gabellani S, Delogu F, Silvestro F, Pignone F, Bruno G, ... , Ferraris L (2023) IT-SNOW: a snow reanalysis for Italy blending modeling, in-situ data, and satellite observations (2010–2021). Earth System Science Data Discussions, 2022, 1-30. https://doi.org/10.5194/essd-15-639-2023

Coron L, Thirel G, Delaigue O, Perrin C & Andréassian V (2017) The suite of lumped GR hydrological models in an R package. Environmental modelling & software, 94, 166-171. https://doi.org/10.1016/j.envsoft.2017.05.002

Muñoz-Sabater J, Dutra E, Agustí-Panareda A, Albergel C, Arduini G, Balsamo G, ... & Thépaut J N (2021) ERA5-Land: A state-of-the-art global reanalysis dataset for land applications. Earth system science data, 13(9), 4349-4383. https://doi.org/10.5194/essd-13-4349-2021

Raffa M, Reder A, Marras G F, Mancini M, Scipione G, Santini M & Mercogliano P (2021) VHR-REA_IT dataset: very high-resolution dynamical downscaling of ERA5 reanalysis over Italy by COSMO-CLM. Data, 6(8), 88. https://doi.org/10.3390/data6080088

Valéry A, Andréassian V & Perrin C (2014) 'As simple as possible but not simpler': What is useful in a temperature-based snow-accounting routine? Part 2–Sensitivity analysis of the Cemaneige snow accounting routine on 380 catchments. Journal of hydrology, 517, 1176-1187. https://doi.org/10.1016/j.jhydrol.2014.04.058

Verrelle A, Glinton M, Bazile E, Le Moigne P, Randriamampianina R, Ridal M, ... & Mladek R (2022) CERRA-Land sub-daily regional reanalysis data for Europe from 1984 to present. Copernicus Climate Change Service (C3S) Climate Data Store (CDS): Reading, UK. DOI: 10.24381/cds.a7f3cd0b

AQUADMC: Smart solutions for a sustainable aquaculture value chain

V. Santarsiero[1*], D. Iasillo[1], G. Ceriola[1], L. Martino[1], C. Rossignoli[1,2], L. Longobardi[2], A. Aiello[1]
[1] Planetek Italia
[2] Worldfish
* e-mail: santarsiero@planetek.it

Introduction

Aquaculture is a rapidly growing sector worldwide, essential for food security and local economies, but faces challenges in identifying sustainable sites, especially in developing countries. Traditional aquaculture methods, based on limited data, can lead to inefficient exploitation of resources, environmental degradation and logistical problems. Therefore, policy makers, investors and local authorities need reliable tools to ensure that aquaculture meets ecological criteria, market needs and community well-being [1].

Earth Observation technology, utilising powerful satellites, offers a game-changing approach to monitoring vast areas. It is particularly valuable in identifying suitable locations for coastal aquaculture, considering both environmental and logistical factors.

The AQUADMC (Optimising AQUAculture Development and Market Connectivity) project uses satellite remote sensing technologies and geospatial data to improve aquaculture development by identifying suitable freshwater and coastal sites in areas of Bangladesh and Kenya. Without satellite data, namely Copernicus data, decisions are based on incomplete or out-of-date information, making it difficult to achieve sustainability goals. The AQUADMC project is using Copernicus satellite data to address these challenges by integrating environmental, socio-economic and logistical factors into a comprehensive platform for decision making.

Materials and methods

The methodology employs advanced satellite technologies to monitor water quality parameters in rivers, lakes and coastal areas. Indicators such as turbidity, chlorophyll-a concentrations, salinity and surface temperature are analysed to evaluate environmental suitability for aquaculture activities.

Satellite images support the identification of existing and potential aquaculture sites, with an emphasis on their location, water quality, and proximity to essential resources. For example, high- and mid-resolution satellite imagery and sensors such as Sentinel-2 and Sentinel-3 are used to map potential sites by assessing factors such as chlorophyll-a concentrations, sediment loads, and thermal regimes.

Water quality data obtained through the application of algorithms on satellite imagery are complemented by historical, socio-economic data tracing the evolution of aquaculture practices in the analysed regions. These data sources provide critical information on various surface water quality parameters, including chlorophyll-a concentration, total suspended matter, turbidity, water transparency, and sea surface temperature [2,3]. The data processing and analysis phase consists of several key steps, starting with the acquisition and pre-processing of satellite images. The first step involves the daily processing of satellite imagery to extract measurements at a spatial resolution of 10 and 300 meters for most parameters and 1 kilometre for sea surface temperature. This pre-processing includes radiometric and atmospheric corrections, georeferencing, and resampling to ensure data consistency and accuracy. Quality control measures is applied to filter out clouds, shadows, and other noise, ensuring the reliability of the data.

After pre-processing, various water quality parameters were extracted using advanced algorithms. For example, chlorophyll-a concentration is estimated through an AI-based algorithm, while total suspended matter and turbidity is derived using reflectance models calibrated for the specific regions of interest. Water transparency is assessed using Secchi disk depth proxies obtained from satellite imagery. Sea surface temperature is retrieved from thermal infrared bands. The temporal analysis component focuses on the

detection of seasonal and inter-annual variations in water quality parameters. Statistical methods are employed to identify significant patterns and anomalies, including time series analysis and trend detection. This analysis will help to understand long-term trends and seasonal variations, which are crucial for making informed decisions on aquaculture site selection.

The land-based analysis focus on assessing the connectivity of potential aquaculture sites to markets. This includes an assessment of existing infrastructure, including road networks and/or cold chain logistics, which are essential to maintain the quality of perishable aquaculture products during transport.

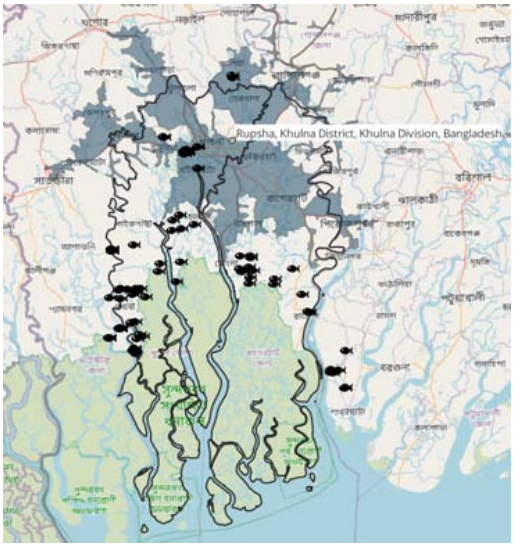


Figure 1. The map shows an example of accessibility analysis in the 60-minute isochrone between the main fish market of Khulna District and the main aquaculture sites present.

Satellite imagery is used to extract information on land cover and recent changes to the landscape, such as new developments, road alterations and/or natural events such as floods or landslides. This analysis provides a detailed understanding of accessibility and travel times to urban markets, helping to identify potential bottlenecks and areas to improve.

The socioeconomic impact assessment evaluates how aquaculture development could benefit local employment and contribute economically to surrounding communities. This assessment collects socioeconomic data from secondary sources, including government reports, census data, and local surveys.

Results and concluding remarks

The project aims to improve the logistical efficiency of aquaculture operations and facilitate the timely and quality delivery of products to markets by ensuring efficient connectivity.

The AQUADMC project offers significant benefits along the entire aquaculture value chain, from policy makers to local communities and the environment. It provides accurate, real-time data to public administrations to guide strategic planning and ensure compliance with sustainability policies. It simplifies decision-making by integrating environmental, logistical and socio-economic information, saving time and reducing costs compared to traditional methods. The project is aligned with the Sustainable Development Goals, contributing to climate resilience and economic stability by monitoring water quality parameters such as turbidity and chlorophyll levels, which help maintain healthy aquatic environments.

References

Ceriola, G., Drimaco, D., Aiello, A., Bollanos, S. (2019) From SST measurements to actionable information for public and private users: Rheticus services. Proceedings of the GHRSST XX SCIENCE TEAM MEETING, pp. 144-148

Gephart, J. A., Golden, C. D., Asche, F., Belton, B., Brugere, C., et al. (2020) Scenarios for global aquaculture and its role in human nutrition. Reviews in Fisheries Science & Aquaculture, 29(1), 122-138. https://doi.org/10.1080/23308249.2020.1782342

Sarelli, A., Ceriola, G., Iasillo, D., Aiello, A., (2019) Coastal Eutrophication estimation for SDG 14: innovative algorithm and novel provision approach based on the exploitation of large EO time series and a cloud-based application platform. ESA Living Planet Symposium 2019

High resolution agricultural water demands on refined crop-specific spatializations

N. Galli, H. Nanesha, A. Tolazzi*, D.D. Chiarelli, M.C. Rulli
Department of Civil and Environmental Engineering, Politecnico di Milano, Milano, Italy
** e-mail: arianna.tolazzi@polimi.it*

Introduction

Agriculture accounts for about 70% of all the freshwater consumption in the world, making it not only the biggest consumer, but also the sector that is affected the most by water scarcity. In a world where the 4 billion people suffering from water scarcity are projected to increase, the impacts climate change and water management have on agriculture and on water availability and scarcity are a primary object of investigation (FAO, 2018). This makes refined assessments of water demand in agriculture a research priority, and models that can help keeping track of agricultural water use and water needs are gaining importance.

In Italy, agriculture plays a critical role in environmental conservation, economic structure, and cultural heritage. In 2023, Italy exported agro-food products worth €64 billion, accounting for approximately 10% of its total exports (ISTAT, 2024). This success largely stems from high-quality products strongly tied to regional identities. However, the sector is highly vulnerable to hydroclimatic fluctuations, as demonstrated by the 2022 drought, which resulted in estimated losses of €6 billion (Coldiretti, 2022). Addressing such challenges requires advanced models to quantify agricultural water consumption with spatial and temporal precision while capturing local specificities of cultural and economic importance.

Here, we create a detailed, harmonized crop mapping dataset and use it to inform a spatially distributed agro-hydrological model, producing refined spatial quantifications of water demands in agriculture for Italy.

Materials and methods

The main input for crop mapping is EUCROPMAP2022 (JRC,2022), a high-resolution (10m) cropland classification over Europe. We supplement this dataset with CORINE Land Cover (Bontemps et al., 2009) (100m) especially for permanent crops, which have a more refined classification in CORINE than in EUCROPMAP. For crops for which the two datasets do not provide sufficiently reliable results we integrate municipal statistics from ISTAT (2024). To separate irrigated and rainfed croplands we allocate irrigated extent according to GMIE (Tian et al., 2024) and GMIA (Siebert et al., 2013) datasets to different crops following a prioritization based on the most irrigated crops in Italy. The harmonization between the datasets is performed onto a 30-arcsecond (~750m) resolution grid. The result is a set of maps detailing the fractional distribution of irrigated and rainfed crops across Italy. These maps are validated against ISTAT provincial statistics.

Integrating this crop mapping into the agro-hydrological WATNEEDS model (Chiarelli et al., 2020) enables the evaluation of crop water needs met by rainfall (green water) and irrigation (blue water). WATNEEDS is used on the period from 2013 to 2023 and adapted to compute evapotranspiration based on the Hargreaves-Samani formulation, using MERIDA data as climatic inputs (Bonanno et al., 2019). WATNEEDS solves the soil water balance equation at a daily timestep separately for each of the crop covers present within a pixel.

Results and concluding remarks

In over 80% of the areas, the crop maps present strong correlation (>75%) and low error (<20%) when validated against subnational statistics of cropped area. Preliminary results indicate that Italy's 23 main crops require an annual water volume of 43.25 km³, with 35.67 km³ provided by precipitation and 7.58 km³

from irrigation. Key crops such as wheat, corn, and legumes exhibit the highest water demands, particularly in regions like Emilia-Romagna, Lombardy, Veneto, and Puglia, where irrigation is crucial to offset summer evapotranspiration peaks. Ongoing improvements focus overcoming limitations from input data, hydrological assumptions, and regional agricultural practices and further harmonizing the crop dataset with regional cultivation plans, incorporating higher-resolution meteorological inputs, and refining soil parameters and agricultural calendars. These enhancements aim to provide stakeholders with actionable tools to address environmental and climatic challenges, ensuring sustainable water resource management and agricultural resilience in Italy. This integrated framework serves as a robust foundation for informed policymaking and resource planning, critical to mitigating water scarcity impacts and sustaining Italy's agricultural economy.

Acknowledgments: This study was carried out within the RETURN Extended Partnership and received funding from the European Union Next-GenerationEU (National Recovery and Resilience Plan NRRP, Mission 4, Component 2, Investment 1.3 D.D. 1243 2/8/2022, PE0000005).

References

Bontemps, S., Defourny, P., Van Bogaert, E., Weber, J. L., & Arino, O. (2009). GlobCorine - A joint EEA-ESA project for operational land dynamics monitoring at pan-European scale. Proceedings, 33rd International Symposium on Remote Sensing of Environment, ISRSE 2009, 289–292.

Chiarelli, D. D., Passera, C., Rosa, L., Davis, K. F., D'Odorico, P., & Rulli, M. C. (2020). The green and blue crop water requirement WATNEEDS model and its global gridded outputs. Scientific Data, 7(1), 273. https://doi.org/10.1038/s41597-020-00612-0

Coldiretti (2022) Clima: 6mld di danni dalla peggiore siccità da 500 anni. https://www.coldiretti.it/meteo_clima/clima-6-mld-di-danni-dalla-peggiore-siccita-da-500-anni

European Commission, Joint Research Centre (JRC) (2022): EUCROPMAP 2022. European Commission, Joint Research Centre (JRC) [Dataset] PID: http://data.europa.eu/89h/555e5d1d-1aae-4320-a716-2e6d18aa1e7c

FAO (2018) The future of food and agriculture. Alternative pathways to 2050.

ISTAT (2024) Istituto Nazionale di Statistica, https://www.istat.it/it/.

Siebert, S., Henrich, V., Frenken, K., & Burke, J. (2013). Global Map of Irrigation Areas version 5. Retrieved from https://www.fao.org/aquastat/en/geospatial-information/global-maps-irrigated-areas/latest-version

Tian, F., Wu, B., Zeng, H., Zhang, M., Zhu, W., Yan, N., et al. (2024). GMIE-100: a global maximum irrigation extent and irrigation type dataset derived through irrigation performance during drought stress and machine learning method. Earth System Science Data Discussion, 2024(February), 1–33. https://doi.org/10.7910 /DVN/HKBAQQ

Estimation of soil runoff in a fire affected mountain landscape

F. Diana, G. Busico*, M. Mastrocicco. S. Castaldi
DiSTABiF – Department of Environmental, Biological and Pharmaceutical Sciences and Technologies, Campania University "Luigi Vanvitelli", Via Vivaldi 43, 81100 Caserta, Italy
** e-mail: gianluigi.busico@unicampania.it*

Introduction

Fires can be considered as an abiotic and natural ecological factor whose characteristics differ according to the various terrestrial ecosystems. Wildfires represent a globally important and a fundamental process of many ecosystems, such as the Mediterranean area, playing a key role in ecosystem dynamics, and in the retention of species that have evolved in response to fire (Pausas et al. 2019). At the same time, wildfires are common sources of disturbance in the Mediterranean ecosystems, because they affect a substantial amount of the forest cover, especially in concomitance with summer drought. By causing a general reduction in the forest understory and tree crown cover and changes in physical, chemical, and biological properties of soil, wildfires can adversely affect soil functions. Indeed, soil alteration induced by fire could favour erosive processes and nutrient loss, thus affecting nutrient cycling (Rodríguez et al. 2017), microbial activity, and CO_2 emission from soil (Fierro et al. 2007). To understand soil runoff behaviour in a wildfire-affected region, the Universal Soil Loss Equation (USLE) (Wischmeier and Smith, 1978) was applied to a mountainous area within Maiella National Park. This area has experienced frequent wildfires over the past five years. Data from field campaigns and open databases were collected and analysed to produce the results.

Materials and methods

Soil runoff can be measured in the field using permanent plots or estimated through models. In this study, the Universal Soil Loss Equation (USLE) was employed to estimate soil runoff:

$$SE = R * K * LS * C * P \quad (1)$$

where SE represents the average annual soil loss (tons of soil/ha/year), R is the rainfall erosivity index, K is the soil erodibility factor, LS is the topographic factor (L for slope length and S for slope steepness), C is the cropping factor, and P is the conservation practice factor. The USLE was applied to estimate actual soil runoff for the year 2024, considering two scenarios in the same mountainous area: unburned and burned. To project soil runoff, certain input parameters were adjusted in the USLE calculation. Specifically, the C and K parameters were modified to reflect changes in land use resulting from fire severity. For the unburned scenario, the forest canopy coverage was considered greater than 75%, while for the burned scenario, it decreased to less than 25% following wildfire events.

Results and concluding remarks

Most of sampled soils exhibit textures ranging from clay loam to silty loam, with soil organic matter content higher than 5% in nearly all samples collected under both burned and unburned conditions and high rock fragment percentage. Infiltration rates vary between 7 and 15 mm/hour.

The results of the USLE equation have been averaged considering 36 soil samples and grouped into three slope categories: 20–35%, 35–45%, and >45% (Figure 1), to highlight the primary differences in soil erosion SE behavior. Under the unburned scenario, SE mainly increases following the increase of rock fragment % and ranging from 0.23 t/ha/year on lower and moderate slope to 0.11 t/ha/year on steeper slopes. In this scenario, where soil remains largely unchanged, tree cover (evergreen and deciduous tree) and rock fragments are dominant factors influencing SE.

In contrast, the burned scenario shows a far more worrying situation. SE values are up to 100 times

higher compared to the unburned scenario, with the lowest SE calculated at 20.3 t/ha/year and the highest reaching 51 t/ha/year. In this case the reduction of canopy cover of more than 70%, along with ash deposition have a significant impact on calculation spotlighting the effect of fire on soil erosion dynamics.

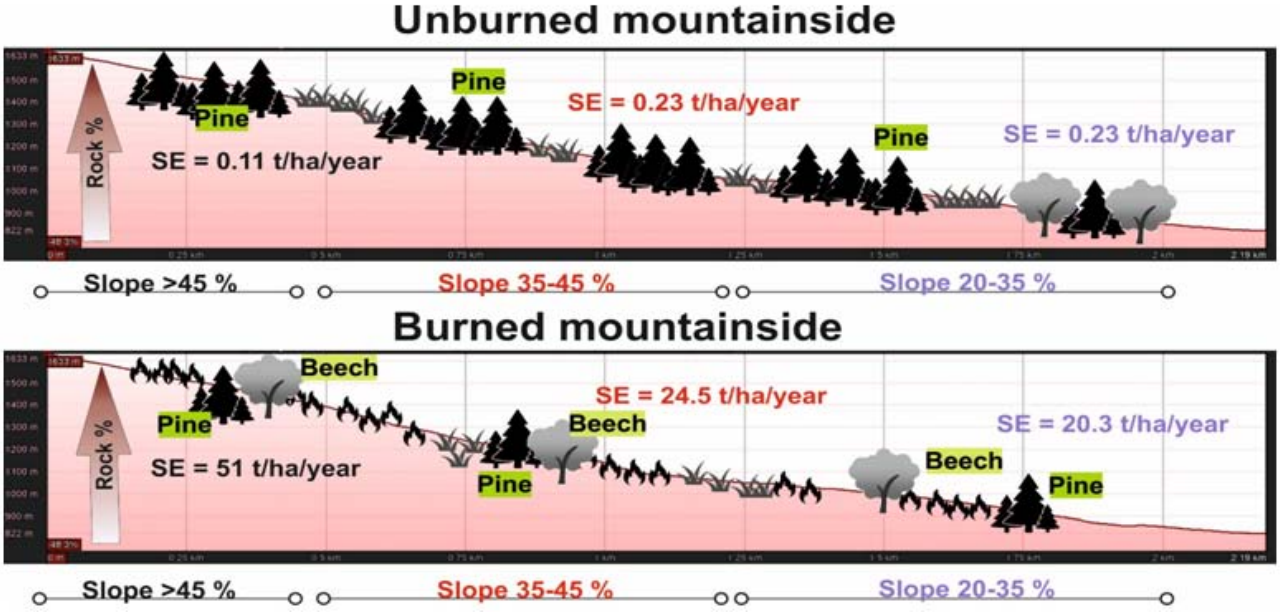


Figure 1. Conceptual scheme of calculated SE at different slope intervals

Acknowledgments: Project BIOSFeR^{3}a: BIOdiversita' Specifica e Funzionale per la Resistenza, Resilienza e Recupero ai disturbi ed al cambiamento climatico funded by the "National Biodiversity Future Center - NBFC", Project code CN_00000033, under the National Recovery and Resilience Plan (NRRP), Mission 4 Component 2 Investment 1.4.

References

Busico G, Grilli E, Carvalho S.C.P, Mastrocicco M, Castaldi S (2023). Assessing Soil Erosion Susceptibility for Past and Future Scenarios in Semiarid Mediterranean Agroecosystems. Sustainability. 15(17): 12992. https://doi.org/10.3390/su151712992

Fierro A, Rutigliano FA, De Marco A, Castaldi S, Virzo De Santo A (2007) Post-fire stimulation of soil biogenic emission of CO2 in a sandy soil of a Mediterranean shrubland. International Journal of Wildland Fire 16: 573–583. https://doi.org/10.1071/WF06114

Pausas J.G, Keeley J.E. (2019) Wildfires as an ecosystem service. Frontiers in Ecology and the Environment 17:289–295. https://doi.org/10.1002/fee.2044

Rodríguez J, González-Pérez JA, Turmero A, Hernández M, Ball AS, González-Vila FJ, Arias ME (2017) Wildfire effects on the microbial activity and diversity in a Mediterranean forest soil. Catena 158: 82–88. https://doi.org/10.1016/j.catena.2017.06.018

Rutigliano FA, De Marco A, D'Ascoli R, Castaldi S, Gentile A., Virzo De Santo A (2007) Impact of fire on fungal abundance and microbial efficiency in C assimilation and mineralisation in a Mediterranean maquis soil. Biology and Fertility of Soils 44: 377–381.

Assessment of potential evapotranspiration formulas at catchment scale for rainfall-runoff modelling around the globe

G. Selleri*, M. Neri, E. Toth
Department of Civil, Chemical, Environmental, and Materials Engineering, University of Bologna, Bologna, Italy
** e-mail: giovanni.selleri4@unibo.it*

Introduction

The combined effect of evaporation and transpiration plays a key role in the water balance for hydrological modelling at catchment scale. However, the direct measurement of these processes is very challenging, and a formula based on meteorological variables is typically used to estimate the potential evapo-transpiration (PET), i.e. the maximum rate of water leaving the catchment to the atmosphere in ideal conditions.

Many rainfall-runoff models take the PET as input, and improving the quality of the PET data can directly enhance the performance of the model. Moreover, PET is a crucial factor to characterize the hydrological behavior and to find similarities between basins.

Multiple PET formulas have been proposed and several of them are commonly used with excellent results, but the choice is up to the single researcher, that each time must decide based on the input data available and their personal preferences.

Here we analyze the differences between several formulas in the estimated values, obtained for a large set of catchments in different parts of the world, aiming at providing insights on which PET formulas could be more suited for the use in rainfall-runoff modelling and for a PET-based classification of basins.

Materials and methods

PET formulas foundation lays on the meteorological forcing data which influence the two processes of evaporation and evapotranspiration. In order to consider in the analysis a large set of catchments around the world, with homogenous data availability of the needed meteorological variables, we selected more than three thousand basins from the recently released dataset Caravan (Kratzert F et al. 2023). Caravan gathers streamflow daily timeseries and attributes for thousands of catchments from previous national or regional datasets, in addition to thirty-eight meteorological daily timeseries at catchment scale, derived from global reanalysis products. In this study we used the most recent Caravan timeseries, with continuous daily data from 1950 to 2023. The Caravan catchments considered in this study are located in US, Brazil, Chile, Australia, UK, and Central Europe.

Among the many PET formulas, we selected and applied eight of the most widely used in rainfall-runoff modelling literature, presenting here only the results for four of them, for sake of brevity:

- Thornthwaite formula, the less data-demanding one that requires only the mean daily temperature (Thornthwaite 1948).
- Hargreaves formula, which uses mean daily temperature and the difference between maximum and minimum daily temperature (Hargreaves et al. 1985).
- Priestley-Taylor formula, which requires mean daily temperature and net radiation (Priestley et al. 1972).
- Penman-Monteith formula in the FAO version (Allen R et al. 1998), that is often used as benchmark in the literature and describes all the main physical processes involved in the evaporation and transpiration, and it is based on dewpoint, minimum, maximum and mean daily temperature, wind speed, pressure and net radiation.

For every catchment we calculated the daily values of PET for each formula, then we computed the cumulated annual values and compared graphically the results to identify the main differences.

Additionally, based on the PET estimates and the streamflow (Q) and precipitation (P), the catchments data are plotted in the Budyko diagrams.

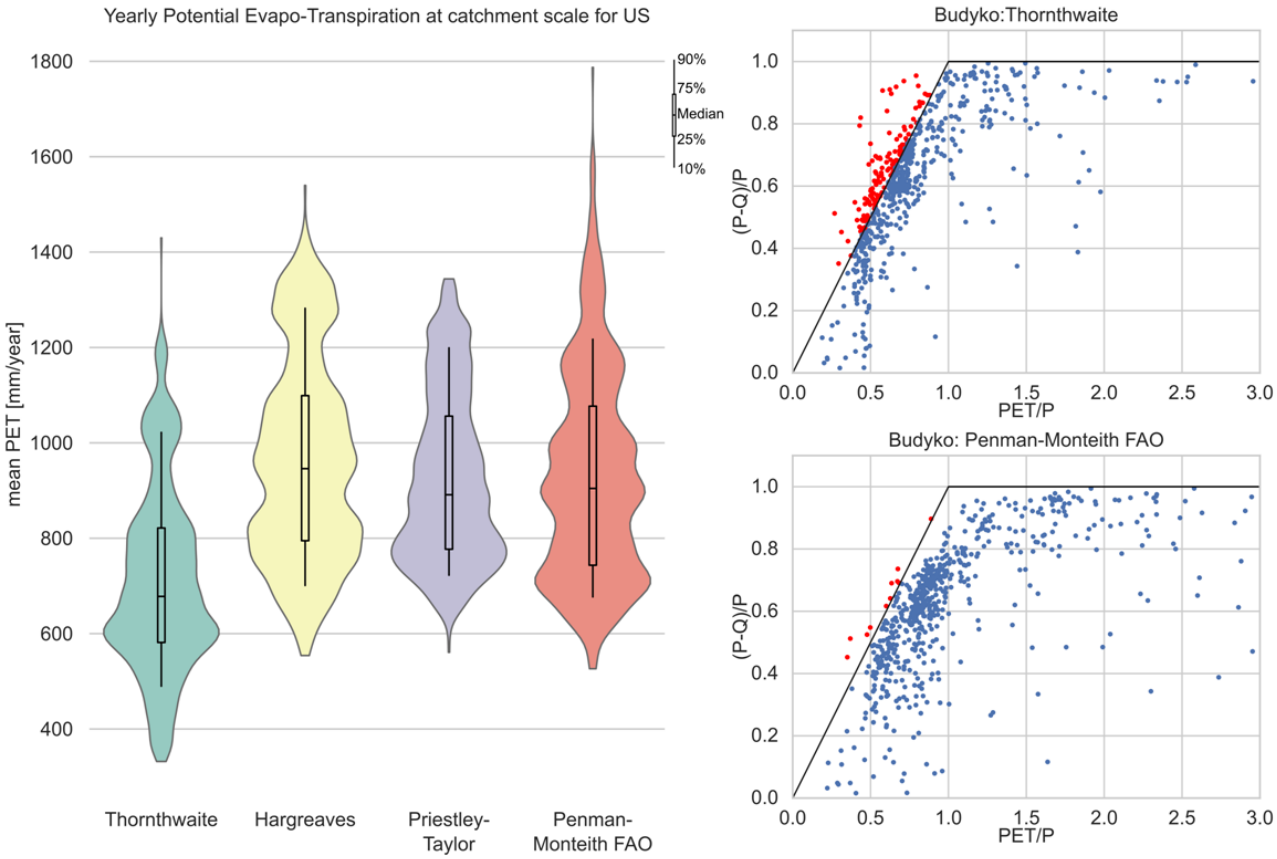


Figure 1. Mean yearly cumulated PET values in the US from four different formulas and Budyko diagrams for Thornthwaite and Penman-Monteith FAO

Results and concluding remarks

The results illustrated in the violin plots in Figure 1 show that Thornthwaite formula strongly underestimates the PET with respect to the Penman-Monteith, while Hargreaves appears to be slightly overestimated. Priestley-Taylor values look similar to Penman-Monteith, but their range is lower especially for the higher values. The Budyko plots are presented only for the Thornthwaite and Penman-Monteith formulas, showing that catchment positions are significantly influenced by the PET formula used.

These differences suggest that the choice of the PET formula could have an important effect on the water balance and on the catchment aridity classification.

References

Allen R, Pereira L, Raes D, et al. (1998) FAO Irrigation and drainage paper No. 56. Rome: Food and Agriculture Organization of the United Nations. 56. 26-40.

Hargreaves G, Samani Z (1985) Reference Crop Evapotranspiration from Temperature. Applied Engineering in Agriculture, 1(2), 96–99. https://doi.org/10.13031/2013.26773

Kratzert F, Nearing G, Addor N, et al. (2023) Caravan - A global community dataset for large-sample hydrology. Sci Data 10, 61. https://doi.org/10.1038/s41597-023-01975-w

Priestley C H B, Taylor R J (1972) On the Assessment of Surface Heat Flux and Evaporation Using Large-Scale Parameters. Monthly Weather Review, 100(2), 81–92. https://doi.org/10.1175/1520-0493(1972)100

Thornthwaite C W, (1948) An Approach toward a Rational Classification of Climate. Geographical Review 38, no. 1: 55–94. https://doi.org/10.2307/210739

AMAPGeo: Smart water infrastructure for water management

T. Borruso
AMAP S.p.A., Palermo, Italy: Technical Service PLC Unit
e-mail: tiziana.borruso@amapspa.it

Introduction

AMAP S.p.A., the operator of the integrated water service for ATO 1 PA, has revolutionized its infrastructure knowledge management and archiving system following the expansion of its corporate structure by initiating the development of the GIS platform "AMAPGeo." The core of the system is the network infrastructure database.

In 2023, as part of the React-EU projects, the platform's functionalities were enhanced by upgrading hardware for the production and utilization of cartographic data and by integrating modules for leak monitoring, asset management of linear infrastructures, and real-time hydraulic modeling.

The collected data, related to water and sewage infrastructures, is transformed into information, forming the essential knowledge base for managing water both as a resource and as a potential threat.

The first critical issue encountered in implementing this knowledge-building process concerns the collection, analysis, and reconstruction of infrastructure data, which is often no longer visible. However, through mathematical model simulations, it can be interpreted as accurately as possible. As a result, reality is represented at a 1:1 scale through an iterative process of knowledge refinement cycles.

Another challenge is the significant commitment of resources—both human and physical—required to maintain and manage the platform. This aspect is often underestimated in corporate contexts. However, the *digitalization of networks* is the operational tool that optimizes the management of the integrated water service using the industry's best technologies. It is also a fundamental requirement for achieving the sustainable and optimal use of available resources.

Materials and methods

Since 2018, the transformation of the management structure, along with the obligations imposed by the national regulatory authority, has required a rapid acceleration in the recovery of management efficiency.

To rebuild and enhance knowledge of the managed water and sewage infrastructures, the company chose to use ESRI products to define its integrated system, *AMAPGeo*.

AMAPGeo is AMAP's GIS, developed in an ESRI Client-Server environment and accessible via the Web with Geocortex (now VertiGIS) and Portal. It includes all the networks and facilities of the Integrated Water Service for the municipalities within the Palermo ATO currently managed by AMAP.

AMAPGeo serves as a knowledge base and support platform for the mathematical model (developed with Mike Urban) used for analysis, calculation, and hydraulic simulation.

The core of the system is a central database organized on both territorial and local scales, composed of the following data types:

- *Cartographic data* (base maps and thematic layers)
- *Alphanumeric data* (tables, relationships, domains of physical assets)

To meet the need for greater digitalization of the networks, it was necessary to enhance the corporate GIS system by enriching it with new functionalities and increasing its computational capacity.

First, the system architecture was modified by adding a *middleware* component for data transfer across various information systems. The middleware serves as an intermediate repository where the information layer is stored, containing basic data from company databases, processed and aggregated to be usable for feeding simulation applications. The proposed *DBMS* for managing this repository is *SQL Server*.

At the same time, three modules were developed using *DHI applications:*

- *Digital Twin (WNA+WDO)* – The *Digital Twin* is the software application that enables real-time

decision-support systems, allowing for automatic updates of simulation models and the execution of real-time or scenario-based simulations.

- *Leakage Monitor* – The *Leakage Monitor* is an application that supports active district monitoring by providing the necessary tools for optimizing the network, both from a *technical-energy* perspective and an *economic* perspective.
- *NOP* – The *NOP* module for the *Asset Management System*, building upon existing data processing on network knowledge, will enable the full operation of a decision-support system for prioritizing interventions on AMAP S.p.A.'s networks.

AMAPGeo infrastructure offers fast information access from anywhere in the system. The system's accessibility to share information has also been designed to comply with *privacy and cybersecurity regulations*.

Regarding resource utilization, *PNRR funding* has provided new momentum for network digitalization and has initiated a long-term *cultural shift* aimed at efficiency and sustainability—objectives that can only be fully achieved through the use of the most *advanced technologies*.

The following table indicates the key parameters of the digitization process.

Table 1. Digitalization of networks

Operating areas	Municipality	Networks (km)	Utility junction	Models	Leak detection	Remote control	Smart meter
Western operational area	23	1.036*	36.773*	16*	21	No/partial	15.000*
Western operational area	24	962*	38.178*	16*	1	No/ partial	22.000*
Operational area of Palermo	1	1.319	39.540*	1	1	yes	17.000*

**ongoing*

The main issues to address are:

- Updating and aligning data
- Sharing data in compliance with cybersecurity rules
- Managing material and human resources
- Managing change

Results and concluding remarks

Through network digitalization and hydraulic modeling based on ESRI products and DHI applications, AMAPGeo provides a comprehensive and integrated system for monitoring, analyzing, and planning the water network. This tool not only enhances AMAP's operational efficiency but also serves as a model of innovation and sustainability for companies in the water sector. It can successfully addresses the complexities of rotational supply networks and contributes to greater transparency in data transmission to regulatory authorities. However digitalizzation presents not only advantages but also barriers inside organizations.

References

Alegre H, Cohelo ST (2012) Alegre Systems in: Water Supply Infrastructure Asset Management of Urban Water System in: Water Supply System Analysis - Selected Topics, Avi Ostfeld (Ed.), InTech, DOI: 10.5772/52377

Hamilton S, Charalambous B (2020) Leak Detection: Technology and Implementation, IWA Publishing

Kozarkiewicz A (2020) General and specific: the impact of digital transformation on project processes and management methods Foundations of Management, Vol. 12 DOI: 10.2478/fman-2020-0018

Zekri S, Jabeur N, Gharrad H (2022) Smart water management using intelligent digital twins. Computing and Informatics 41(1): 135-153, doi: 10.31577/cai 2022 1 135

Assessment of flood vulnerable areas in the river basin district of Thrace

C.S. Pantoulas, I.M. Kourtis*, H. Vangelis, I. Nalbantis, V.A. Tsihrintzis
Center for the Assessment of Natural Hazards and Proactive Planning & Laboratory of Reclamation Works and Water Resources Management, School of Rural, Surveying and Geoinformatics Engineering, National Technical University of Athens, 9 Heroon Polytechniou St., 15780 Zographou, Athens, Greece
** e-mail: gkourtis@mail.ntua.gr*

Introduction

Mapping flood vulnerable areas is crucial in mitigating risks associated with increasingly frequent and intense flooding events driven by climate change. In the present work, we present a tool for the assessment of flood vulnerable areas, at the scale of River Basin District (RBD), employing a multi-criteria analysis method and a Geographical Information System (GIS). Seven criteria were used to assess flood vulnerable areas, which were classified into five distinct categories. Then, a comparison was made with the Areas of Potential Significant Flood Risk (APSFR) of the Flood Risk Management Plans (Directive 2007/60) using an appropriate index as well as an assessment of the flood vulnerable areas after two fires. Such approaches can effectively and timely provide vital insights for sustainable water resource management and adaptive planning in regions highly susceptible to hydrological and/or environmental hazards.

Materials and methods

The study area is the RBD of Thrace (EL12). Approximately 50% of the RBD lies at an altitude of up to 200 m, followed by the part between 200–600 m with a percentage of 30%, while the remaining 20% exceeds 600 meters in elevation.

The criteria used to assess flood vulnerable areas were: (i) ground elevation, (ii) ground slope, (iii) precipitation approximated through the Modified Fournier Index (MFI) based on monthly reanalysis rainfall data (i.e., ERA5), (iv) land use, (v) flow accumulation, (vi) soil type, and (vii) distance from the nearest stream. Weights of the criteria were estimated using the Analytical Hierarchy Process (AHP) method (Saaty (1987)). AHP constitutes one of the most widely used methods of multi-criteria analysis and provides a rational and integrated framework for structuring a problem.

In order to find the optimal selection of the weights of the criteria, seven scenarios were developed, one for each criterion, in which the primary criterion and its corresponding weight were altered. Finally, the influence of forest fires on flood vulnerability of the study region was evaluated. The fire events that occurred on 21/07/2022 and 23/08/2023 were studied with fire data obtained from the Copernicus Emergency Management service (https://emergency.copernicus.eu/). Flood hazard was classified into 5 classes (Kourgialas and Karatzas 2017): (i) Very low = 1; Low = 2; (iii) Moderate = 5; (iv) High = 8; and (v) Very high = 10.

For the validation of the procedure, APSFR of the RBD of Thrace according to the Flood Risk Management Plan was used as the baseline. Specifically, from each scenario, only the categories of high and very high flood vulnerable areas were extracted and used for the comparison. For this, the following equation, proposed by Horitt and Bates (2002), was used.

$$F = ((SmodO Sobs)/(SmodU Sobs)) *100 \quad (1)$$

where: S_{mod} is the area of flood-prone areas estimated by the proposed approach and S_{obs} is the area according to the APSFR.

Results and concluding remarks

The moderate flood vulnerable areas occupy the largest area of the RBD of Thrace with an average percentage of 28% and a range of 23% to 33%, depending on the scenario considered. The class of high

flood vulnerable areas had an average coverage rate (across all scenarios) of about 27%, ranging from 18% to 31%. Low flood vulnerable areas showed an average rate of 22%, ranging from 18% to 27%. The category of very low flood vulnerable areas was estimated to an average coverage rate of approximately 13% and ranging from 8% to 20%. Finally, the least covered areas were at the class of very high flood vulnerability whose average coverage rate was approximately 11% and their values ranged from 7% to 16%. Indicatively, Figure 1 presents the flood-vulnerable areas for the RBD of Thrace according to Scenario 7.

The correspondence of the APSFR with the flood vulnerable areas highlighted by the scenarios was satisfactory. Scenarios 3, 4, 6, and 7 best represented the areas of increased flood risk, and in particular, scenario 7 presented the greatest correspondence. A smaller correspondence of flood vulnerable areas with Potentially High Flood Risk Zones was presented by scenario 5.

Finally, based on the proposed methodology, the change in flood vulnerable areas was evaluated before and after the forest fires that occurred on 21/07/2022 and 23/08/2023. Indicatively, Figure 2 presents the comparison for the event on 23/08/2023. The incinerated area was estimated at about 0.94 km^2, and it came from the combination of two fires, one that started from the Forest of Dadia and the second from Alexandroupolis. The northern side of the incinerated area, prior to the event, was classified as moderate flood vulnerable area with parts of low to very low vulnerability. Some areas were classified in the very high class. After the fire events, the flood vulnerable areas were classified to the high and very high classes.

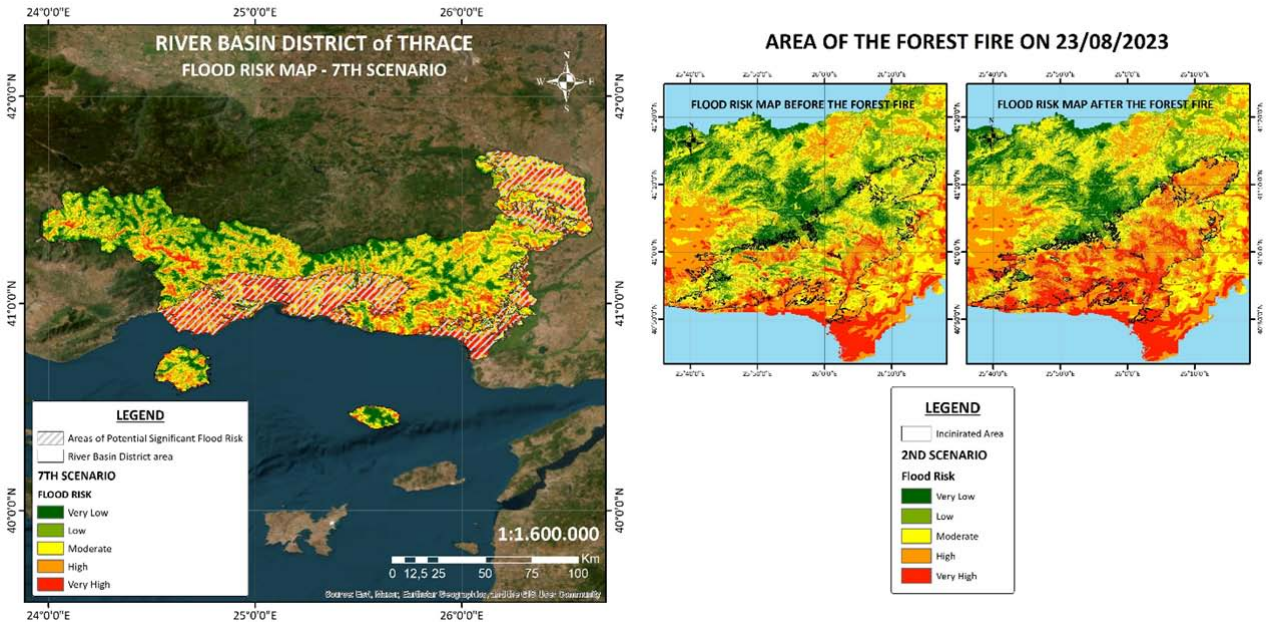


Figure 1. Flood Risk map for RBD of Thrace according to Scenario 7 (left); and comparison of flood vulnerable areas before and after the forest fire on 23/08/2023 (right)

For the RBD of Thrace, lowland areas are potentially high flood risk areas, and areas close to water surfaces showed a particularly increased flood risk. The North side of the district was shown as low risk. The island regions, and especially Thassos, presented danger mainly in coastal areas and in sections of streams.

References

Horritt M, Bates PD (2002). Evaluation of 1D and 2D numerical models for predicting river flood inundation. Journal of Hydrology 268(1–4): 87–99. http://dx.doi.org/10.1016/S0022-1694(02)00121-X

Kourgialas N, Karatzas G (2017). A national scale flood hazard mapping methodology: The case of Greece – Protection and adaptation policy approaches. Science of the Total Environment 601–602: 441–452.

Saaty, R (1987). The Analytic Hierarchy Process – What it is and how it is used. Journal of Mathematical Modelling 9(3-5): 161-176.

Evaluation of the effectiveness of satellite data in hydrological modeling using SWAT model

S.N. Yeşilyurt[1*], G. Onuşluel Gül[2]
[1] Graduate School of Natural and Applied Sciences, Dokuz Eylul University, Izmir, Turkey
[2] Department of Civil Engineering, Dokuz Eylul Unıversity, Izmır, Turkey
* e-mail: sefanur.yesilyurt@deu.edu.tr

Introduction

Hydrological modeling in data-scarce regions is crucial for effective water resources management, environmental analysis, and climate change impact assessments. The reliability of models under such constraints is essential for informed decision-making. Reliable models can only be built with robust data sources. When ground-based observations are insufficient or inaccessible, satellite data is a valuable alternative for hydrological modeling. The Soil and Water Assessment Tool (SWAT) is a widely used open-source model that enables comprehensive hydrological simulations, supporting sustainable water management efforts. Its versatility has enabled its application in various hydrological contexts, including rainfall-runoff simulations (Janjic and Tadic, 2023), hydrological assessments in data-scarce mountainous regions (Marahatta et al., 2021), and watershed-scale modeling in diverse climatic and topographic conditions (Iresh et al., 2021). This study explores the applicability of satellite-derived datasets in hydrological modeling, with a specific focus on the Büyük Menderes Basin in Turkey. Initially, observational datasets were utilized to calibrate and validate the SWAT model. Subsequently, satellite data were employed to develop an alternative modeling approach. Model calibration was performed using SWAT-CUP in conjunction with the Sequential Uncertainty Fitting Version 2 (SUFI-2) algorithm to optimize parameter estimation. The results highlight the potential of satellite datasets in addressing the limitations associated with in situ observations, thereby enhancing the reliability of hydrological simulations. Furthermore, this research provides a methodological framework for the broader integration of satellite data in hydrological assessments, especially in the context of climate variability and land-use change, contributing to more sustainable water resources management strategies.

Materials and methods

The Soil and Water Assessment Tool (SWAT), developed by the USDA, is a widely used open-source hydrological model designed to simulate long-term physical processes in watersheds. It operates at a watershed scale, with Hydrologic Response Units (HRUs) representing unique combinations of land use, soil type, and slope. Its adaptability and integration with GIS platforms, such as ARCSWAT for data preparation and spatial analysis, make it effective for diverse applications, including water resource management and climate change assessment.

This study focused on the Büyük Menderes Basin, Turkey, characterized by a Mediterranean climate, utilizing observational data from 1994 to 2017 (1994 as warm-up). Daily meteorological data such as precipitation, maximum and minimum temperature, wind speed and relative humidity were obtained from the Turkish State Meteorological Service (MGM-Station 17886), but solar radiation data was derived by aggregating hourly ERA5 data. Streamflow data was sourced from the General Directorate of State Hydraulic Works (DSI-Station D07A001). The Digital Elevation Model (DEM) from USGS and the SWAT US SSURGO Soils Database supported soil data preparation. All meteorological data for the model to be established with satellite data were acquired from NASA POWER (Estimation of World Energy Resources, https://power.larc.nasa.gov/). The agreement between NASA POWER data and observed data was evaluated, and a correlation coefficient of at least 0.84 was obtained depending on the variables examined. Model calibration and uncertainty analysis were performed using the SUFI-2 algorithm in SWAT-CUP, which optimizes parameter ranges through an objective function. Model performance was evaluated using

statistical metrics such as Nash-Sutcliffe Efficiency (NSE), Kling-Gupta Efficiency (KGE), and Coefficient of Determination (R^2). The SWAT and SWAT-CUP manuals provided further details on these metrics.

Results and concluding remarks

The SWAT model for the Büyük Menderes Basin was developed with initial parameters and observed meteorological data. Model performance improved through calibration and uncertainty analysis using the SUFI-2 algorithm in SWAT-CUP. Of 38 parameters, iterative calibration with 500 sets per iteration improved model accuracy in basin hydrology. Performance metrics (Table 1) confirm its reliability, with the observed data-based model achieving NSE values of 0.83 during calibration and 0.93 during validation (Model 1). Furthermore, the satellite-derived meteorological dataset enabled an alternative SWAT model using calibrated parameters derived from the Model 1, achieving NSE values of 0.70 during calibration and 0.62 during validation (Model 2). Despite lower performance, the satellite-driven model effectively captured hydrological processes and streamflow dynamics. A different model was also created in which the calibration and validation processes were based only on satellite observations (Model 3). Table 1 demonstrates the relative reliability of three models. The model provided reasonable accuracy in estimating monthly and seasonal discharge trends, supporting its potential as a feasible alternative for hydrological simulations in data-scarce basins. Figure 1 compares observed and simulated streamflow, illustrating model accuracy and performance differences between the two datasets.

Table 1. Statistical Performance metrics of calibration and validation process

	Model 1			Model 2			Model 3		
Calibration -	NSE	KGE	R^2	NSE	KGE	R^2	NSE	KGE	R^2
Validation	0.83-0.93	0.85-0.92	0.84-0.93	0.70-0.62	0.67-0.42	0.79-0.91	0.80-0.88	0.84-0.85	0.81-0.89

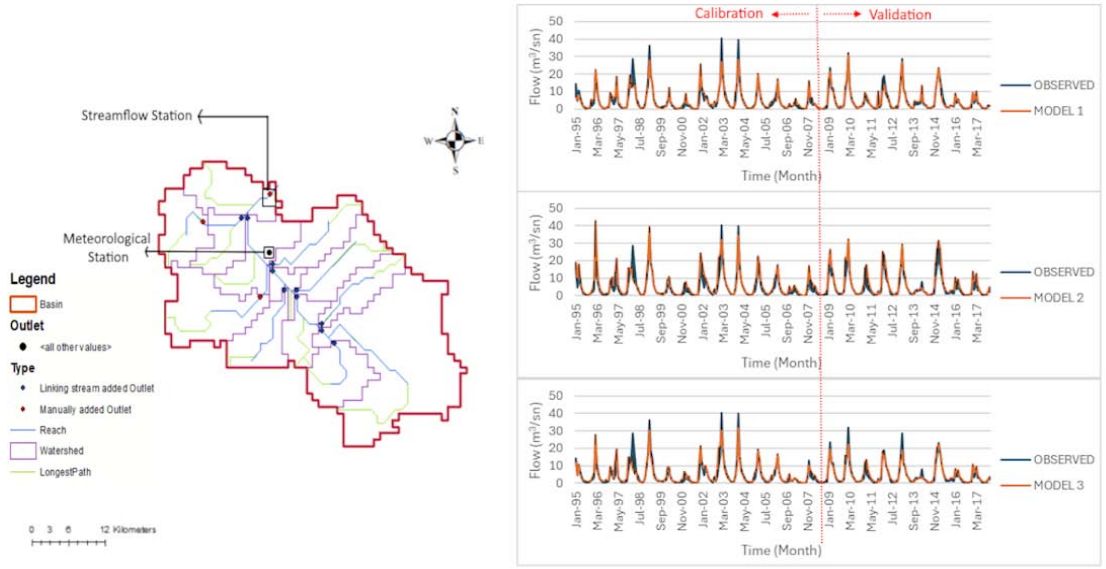


Figure 1. SWAT model and model calibration and validation results

This study highlights the SWAT model's robustness in hydrological modeling and its adaptability to basin-scale applications. The calibrated observational and satellite-based models provide reliable frameworks for future hydrological research. These findings emphasize the potential of remotely sensed data as a viable alternative for hydrological modeling, particularly in regions with limited ground-based observations.

References

Iresh ADS, Marasingha AGNS, Wedanda AMTSH et al (2021) Development of a hydrological model for Kala Oya basin using SWAT model. Engineer: Journal of the Institution of Engineers, Sri Lanka 54(1).

Janjić J, Tadić L (2023) Fields of application of SWAT hydrological model—a review. Earth, 4(2): 331-344.

Marahatta S, Devkota LP, Aryal D (2021) Application of SWAT in the hydrological simulation of complex mountainous river basin (Part I: Model development). Water 13(11): 1546

GEOframe: A first attempt of regionalization on Sicilian basins

D. Ciriminna[1*], G. Formetta[2], A. Francipane[1], L.V. Noto[1]
[1] Department of Engineering, University of Palermo, Palermo, Italy.
[2] Department of Civil, Environmental and Mechanical Engineering, University of Trento, Trento, Italy
* e-mail: diego.ciriminna@unipa.it

Introduction

The necessity to quantify and manage available water resources has become a common priority in recent years, especially in light of the increasing occurrence and severity of phenomena such as dry spells, driven in part by climate change and human activities, which are significantly impacting socio-economic life. Several cases worldwide have shown that these climatological events can occur repeatedly, even in the same regions but at different times of the year.

This study focuses on Sicily (Italy), the largest island in the Mediterranean Sea, which has been particularly affected by dry spells in recent years. One of the main challenges in managing water resources in Sicilian basins is due to a sparse flow monitoring network; not all basins have sufficient stream gauging stations, and not always data are consistently recorded. Additionally, river flow rates are often outdated. In such a context, it is crucial to have a modelling framework capable to correctly deal with those basins where observed flow data are unavailable, making the hydrological model calibration impossible.

In this study, Sicilian basins with available flow data have been modelled using the GEOframe system, a framework developed at the University of Trento and widely applied in several hydrological basin studies. The main objective is the regionalization of the hydrological model parameters estimated in gauged basins (see Figure 1) to ungauged basins. This will enable the application of GEOframe across the entire island as a tool to support the management of present and future estimated water resources at different time scales.

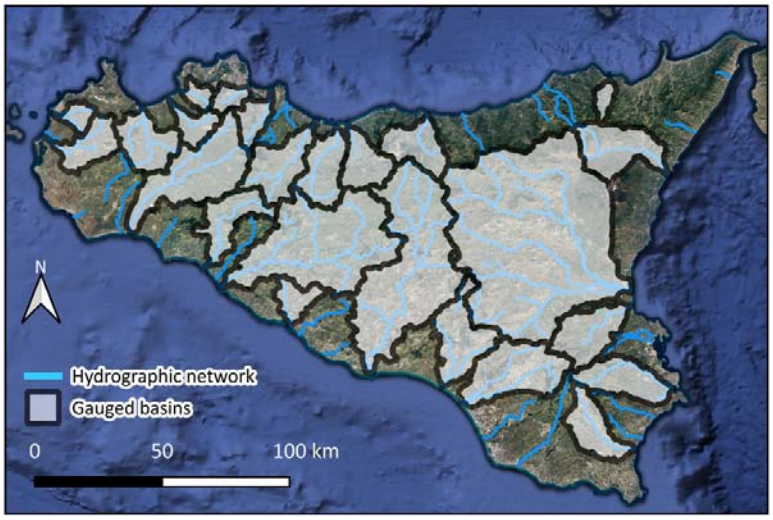


Figure 1. Gauged basins in Sicily.

Materials and methods

Water resources modelling is done using and extending the open-source GEOframe system (Formetta 2014; Morlot et al., 2024). GEOframe tests multiple hypotheses with its flexible architecture, modifying model structures, parameterizations, and observations. It is a semi-distributed system based on hillslope-link partitions, with hillslope response units (HRUs) sized between 0.01 and 0.1 km². The model solves energy and water balances for each HRU and performs discharge routing for each river reach. GEOframe components, including meteorological interpolation (Bancheri et al., 2019), radiation balance (Formetta et

al., 2013), evapotranspiration, snow dynamics, infiltration, groundwater storage, runoff production, and river routing, have been used for various research projects from small to large catchments (e.g., the Blue Nile).

For the calibration of the model across different basins, a multiple-objective, stepwise, automated procedure is adopted. This approach, known as LUCA (Let US Calibrate, Hay and Umemoto, 2007), is widely applied in hydrological model calibration. It utilizes the Shuffled Complex Evolution global search algorithm to calibrate any model compiled with the U.S. Geological Survey's Modular Modelling System.

Regionalization consists of transferring model parameters from gauged to ungauged basins, where direct calibration is not possible, based on catchments characteristics. These characteristics are easily measurable basin properties from both geomorphological (e.g., area, slope, maximum and minimum elevation, hydrological characteristics of soils, and land use, or their combinations such as the CN) and climatic (e.g., annual and seasonal precipitation and temperature mean) perspectives. By leveraging this knowledge, relationships are established to estimate parameters for ungauged basins using calibrated parameters from gauged basins.

Different regionalization approaches will be explored, including the Donor-Basin method, which identifies the most similar gauged basins for each ungauged basin and transfer weighted mean parameters from selected donor (Su et al., 2024), the multi-objective-regional calibration method (MORC) (Bastola et al., 2008), the regression-based method (Oudin et al., 2008), and the spatial interpolation technique (Samuel et al., 2011).

Results and concluding remarks

In this work, we present the results of calibration of GEOframe for the Sicilian gauged basins, which yielded reasonable results. The simulated hydrographs showed an agreement with observed data, as evaluated using Kling-Gupta Efficiency (KGE) and Nash-Sutcliffe Efficiency (NSE) metrics. As an illustrative example, the KGE was 0.55 for the Oreto basin and 0.6 for the San Leonardo Basin. Additionally, we report results on the initial attempts of regionalization across the entire Sicily.

The regionalization results will support a decision-making system designed to assist authorities responsible for evaluating and managing water resources on the island. This system will help them make informed decisions and adopt the best strategies to address critical periods, such as dry spells, across different time scales.

References

Bancheri, M., Serafin, F., Bottazzi, M., Abera, W., Formetta, G., & Rigon, R. (2018). The design, deployment, and testing of kriging models in GEOframe with SIK-0.9. 8. Geoscientific Model Development, 11(6), 2189-2207.

Bastola, S., Ishidaira, H., Takeuchi, K., 2008. Regionalisation of hydrological model parameters under parameter uncertainty: A case study involving TOPMODEL and basins across the globe. J. Hydrol. 357, 188–206. https://doi.org/10.1016/j.jhydrol.2008.05.007

Formetta, G., Antonello, A., Franceschi, S., David, O., & Rigon, R. (2014). Hydrological modelling with components: A GIS-based open-source framework. Environmental Modelling & Software, 55, 190-200.

Formetta, G., Rigon, R., Chávez, J. L., & David, O. (2013). Modeling shortwave solar radiation using the JGrass-NewAge system. Geoscientific Model Development, 6(4), 915-928.

Hay, L.E., Umemoto, M., 2007. Multiple-Objective Stepwise Calibration Using Luca (No. 2006–1323), Open-File Report. Geological Survey (U.S.). https://doi.org/10.3133/ofr20061323

Morlot, Martin, Riccardo Rigon, and Giuseppe Formetta. "Hydrological digital twin model of a large anthropized italian alpine catchment: The Adige river basin." Journal of Hydrology 629 (2024): 130587.

Oudin, L., Andréassian, V., Perrin, C., Michel, C., Le Moine, N., 2008. Spatial proximity, physical similarity, regression and ungaged catchments: A comparison of regionalization approaches based on 913 French catchments. Water Resour. Res. 44. https://doi.org/10.1029/2007WR006240

Samuel, J., Coulibaly, P., Metcalfe, R.A., 2011. Estimation of Continuous Streamflow in Ontario Ungauged Basins: Comparison of Regionalization Methods. J. Hydrol. Eng. 16, 447–459. https://doi.org/10.1061/(ASCE)HE.1943-5584.0000338.

Su, L., Lettenmaier, D.P., Pan, M., Bass, B., 2024. Improving runoff simulation in the Western United States with Noah-MP and variable infiltration capacity. Hydrol. Earth Syst. Sci. 28, 3079–3097. https://doi.org/10.5194/hess-28-3079-2024

IHACRES model regionalization for water resource management in Sicily

C. Alonzo*, F. Alongi, A. Francipane, L.V. Noto
Department of Engineering, University of Palermo, Palermo, Italy
** e-mail: caterina.alonzo@unipa.it*

Introduction

Hydrological rainfall-runoff models are important tools for understanding and predicting how watersheds respond to precipitation and other meteorological inputs, considering processes such as infiltration, surface runoff, evapotranspiration. These models are crucial in a variety of hydrological analyses, including water resources management, flood forecasting, and flood risk assessment. Regardless of their type, rainfall-runoff models rely on specific parameters that must be calibrated using historical data. Calibration involves adjusting model parameters to match observed runoff values as closely as possible, ensuring that the model can accurately simulate real-world hydrological conditions. The quality and availability of historical data play a crucial role in this process.

For gauged basins with available historical data, calibration is performed using observed data. However, for ungauged basins, traditional calibration is not possible. In such cases, model parameters may be estimated based on regional data, analogies to nearby gauged basins, or other indirect methods. This approach, which typically introduces additional uncertainty, uses some regionalization techniques for models' parameters to overcome the lack of local data. These methods usually transfer calibrated parameters from gauged to ungauged basins, based on similarities in physical and climatic characteristics, making it possible to establish statistical relationships between basins' characteristics and models parameters.

Materials and methods

The analysis presented in this work was conducted using the lumped conceptual rainfall-runoff model *IHACRES* (*Identification of Hydrographs And Components from Rainfall Evaporation and Streamflow*; Jakeman & Hornberger, 1993). The model was designed with a flexible structure to ensure its applicability to a variety of watersheds and climatic contexts. It is suitable for basins within arid and semi-arid climates and ephemeral flows, characteristics typically found in Mediterranean areas. The model consists of a nonlinear loss module, which converts precipitation into effective rainfall, and a linear transfer module, which transforms effective rainfall into runoff (Ye et al., 1997; Lotfirad et al., 2019). A comprehensive dataset from gauged basins located throughout Sicily (Italy) was used for model calibration and validation (Figure 1). The dataset includes precipitation, temperature, and runoff records spanning the period 1951 - 1997, made available by the River Basin Authority of the Hydrographic District of the Sicily Region.



Figure 1. Spatial distribution of the gauged and ungauged basins across the Sicily region.

The selected gauged basins, characterized by a range of physical and morphological attributes, were used to create a comprehensive dataset for each basin, providing a detailed description of the study area. To understand the dependencies between IHACRES parameters and physical characteristics of each basin, a correlation analysis will be performed. For ungauged basins, different regionalization methodologies will be tested to estimate the model parameters, including the *regression-based approach* (*RBA*), *spatial proximity approach* (*SPA*), and *physical similarity approach* (*PSA*). These methods aim to improve transferability of IHACRES parameters to regions lacking monitoring data. The best regionalization method will be identified by evaluating performance through statistical metrics (e.g., Nash-Sutcliffe Efficiency, NSE; Mean Absolute Error, MAE; Root Mean Square Error, RMSE; coefficient of determination, R^2), providing a comprehensive understanding of the predictive accuracy of each method (Mihret et al., 2025).

Figure 2 presents the flowchart outlining the procedure used to identify the optimal regionalization method for IHACRES across Sicily.

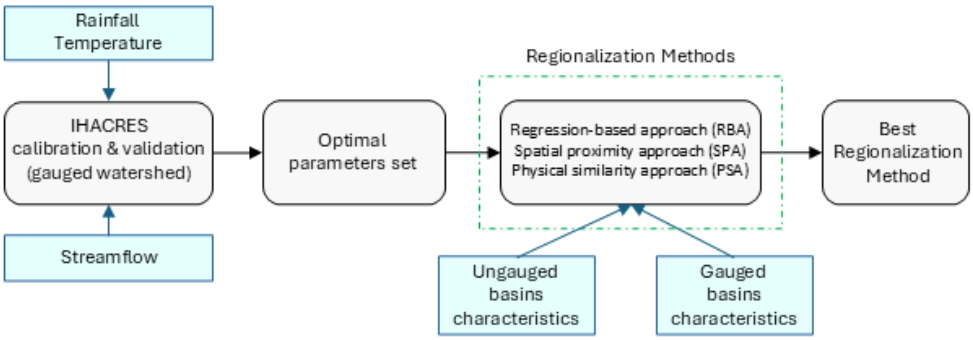


Figure 2. Flowchart of IHACRES regionalization.

Results and concluding remarks

The calibration and validation of the IHACRES model for gauged basins in Sicily showed a good agreement between observed and simulated runoff, confirming the model's ability to accurately represent the hydrological response of the selected basins. Model performance was assessed using the Kling-Gupta Efficiency (KGE), with values ranging from 0.65 to 0.85. The correlation analysis between the model parameters and basins characteristics revealed strong dependencies, suggesting that certain basin attributes are key factors influencing the model parameters.

Regarding regionalization, the comparison of the different methodologies (RBA, SPA, PSA) will determine which approach ensures the most effective transferability of IHACRES parameters to ungauged basins. The explored regionalization techniques explored will offer valuable tools for extending the model's application to ungauged basins, improving the reliability of hydrological predictions in data-scarce regions and supporting water resource management in Sicily.

References

Jakeman, A. J., & Hornberger, G. M. (1993). How much complexity is warranted in a rainfall-runoff model? Water Resources Research, 29(8), 2637–2649. https://doi.org/10.1029/93WR00877

Lotfirad, M., Salehpoor Laghani, J., & Ashrafzadeh, A. (2019). Using the IHACRES model to investigate the impacts of changing climate on streamflow in a semi-arid basin in north-central Iran. Journal of Hydraulic Structures, 5(1). 10.22055/jhs.2019.27816.1090

Mihret, T. T., Zemale, F. A., Worqlul, A. W., Ayalew, A. D., & Fohrer, N. (2025). Unlocking watershed mysteries: Innovative regionalization of hydrological model parameters in data-scarce regions. Journal of Hydrology: Regional Studies, 57, 102163. https://doi.org/10.1016/j.ejrh.2024.102163

Ye, W., Bates, B. C., Viney, N. R., Sivapalan, M., & Jakeman, A. J. (1997). Performance of conceptual rainfall-runoff models in low-yielding ephemeral catchments. Water Resources Research, 33(1), 153–166. https://doi.org/10.1029/96WR02840

V. Climate and Land Use Changes

An integrated method for the characterization of climate change scenarios

J. Kim[1*], M.H. Lee[1], J.H. Ahn[1], S.B. Seo[2]
[1] Devision of Integrated Water Management, Water and Land Research Group, Korea Environment Institute, Republic of Korea
[2] International School of Urban Sciences, University of Seoul, Seoul, Republic of Korea
* e-mail: jykim@kei.re.kr

Introduction

Developing climate change adaptation strategies for water environments requires projections of future conditions, but achieving a single projection is challenging due to randomness and uncertainty. To address this, various combinations of GCMs (Global Climate Models) and SSPs (Shared Socioeconomic Pathways) are used, though this incurs significant computational and time costs. The Coupled Model Intercomparison Project Phase 6 (CMIP6) offers over 120 GCMs and numerous SSP-RCP combinations, necessitating optimal selection for efficiency. Traditional approaches focus on models that accurately reproduce historical climates or plausibly project future conditions. Methods like change rate analysis, clustering, extreme climate indices (ECI), and the Katsavounidis-Kuo-Zhang (Katsavounidis et al., 1994; KKZ) algorithm have been applied, but challenges such as high-dimensional data complexity and redundancy persist.

This study proposes a novel integrated approach that consolidates high-dimensional datasets, including regions, time periods, and indices, into a single dimension. This integration captures the variability and extremeness of climate scenarios, simplifying the understanding of each scenario's characteristics. By analyzing the distribution range of these quantified values, the method offers insights into future climate impacts, facilitating the development of effective climate change adaptation strategies.

Materials and methods

This research identifies suitable GCM-SSP combinations for water environment climate assessments, utilizing seven GCMs (CanESM5, EC-Earth3, GFDL-ESM4, IPSL-CM6A-LR, MIROC6, MPI-ESM1-2-LR, and MRI-ESM2-0) and five SSP scenarios (SSP119, SSP126, SSP245, SSP370, and SSP585), through a systematic five-step process. First, a representative site with stable historical climate data is selected using Entropy Analysis (Shannon, 1948). Second, ECIs with high multicollinearity are excluded to optimize the indicators. Third, future ECI variability is quantified for each combination using Entropy-based methods, while the fourth step quantifies ECI extremeness through frequency analysis of extreme events. Finally, the KKZ algorithm integrates these results to identify optimal GCM-SSP combinations, effectively managing uncertainty and reducing the need for exhaustive scenario analysis.

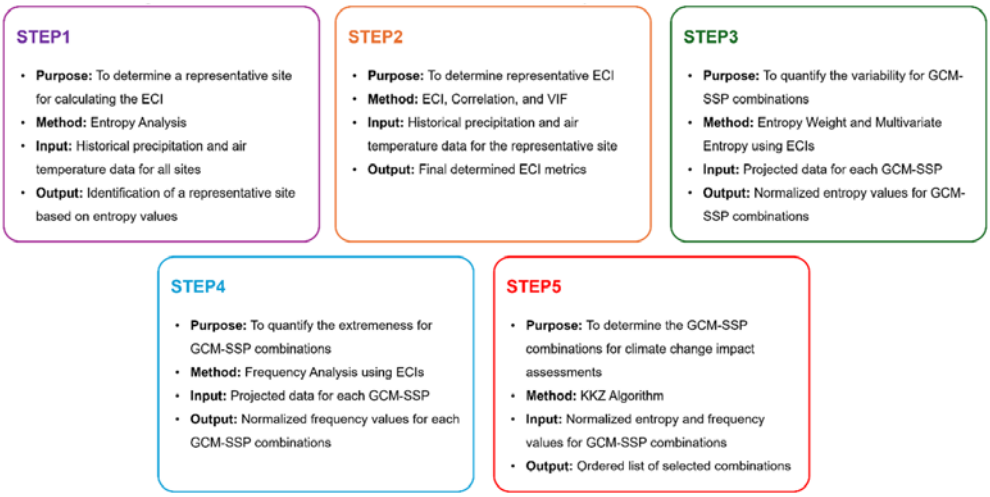


Figure 1. Frameworks for identifying suitable GCM-SSP combinations.

Results and concluding remarks

Figure 2 illustrates the integrated results of variability and extremeness for each GCM-SSP combination. High scores reflect greater informational richness and the presence of extreme weather conditions. While variability and extremeness generally increase under severe global warming scenarios, this trend is not always consistent. Integrated values above the median show an increasing trend from SSP119 to SSP585, but below the median, this pattern is less pronounced, with cases like MIR6 showing higher values under SSP119 or SSP126. These findings suggest that SSP scenarios are more distinct under high variability and extremeness, while their differences are less apparent under lower conditions.

Figure 2-(C) highlights the six selected GCM-SSP combinations. MPI-SSP119 was chosen as the first model for its proximity to the centroid of the model ensemble, representing the average behavior of all models. Can5-SSP585, the second model, and MIR6-SSP370, the third, were selected to represent the maximum and minimum extremes, respectively, making them the most distinctive combinations in terms of variability and extremeness. These three combinations effectively capture the full range of precipitation and air temperature variability and extremes across climate scenarios, while also reflecting average conditions. The fourth, fifth, and subsequent combinations provide complementary insights, bridging the gap between the variability and extremeness represented by the second and third models.

This study primarily focused on precipitation and air temperature but demonstrates potential for extension to variables such as wind speed and solar radiation. The integrated approach captures diverse climate scenarios, offering valuable insights into projected climates across different regions and timescales. By reducing high-dimensional data to a single dimension, it simplifies interpretation and facilitates the identification of GCM-SSP combinations tailored for effective climate adaptation strategies.

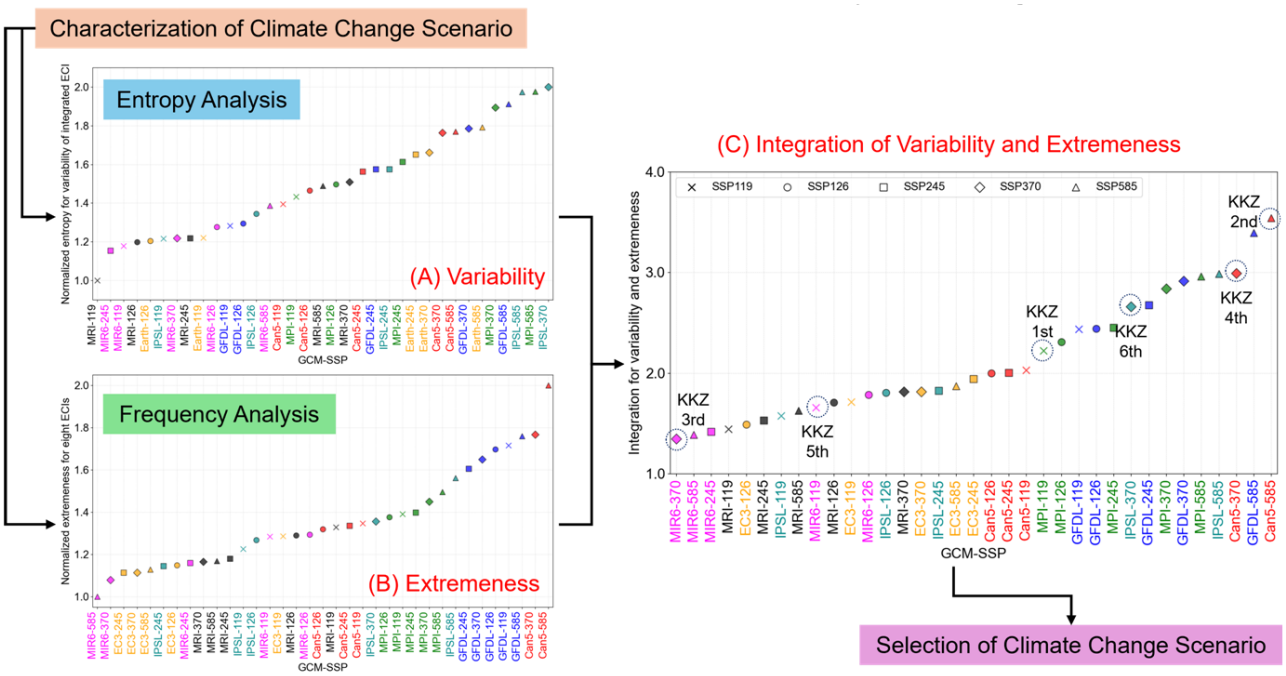


Figure 2. Characterization and selection of climate change scenarios. The process includes: (A) analysis of variability, (B) assessment of extremeness, and (C) integration of variability and extremeness.

Acknowledgments: This work was supported by Korea Environment Industry & Technology Institute (KEITI) through Climate Change R&D Project for New Climate Regime, funded by Korea Ministry of Environment (MOE) (RS-2022-KE002152).

References

Katsavounidis, I., Kuo, C.-C.J., Zhang, Z (1994) A new initialization technique for generalized Lloyd iteration. IEEE Signal processing letters 1(10), 144-146. https://doi.org/10.1109/97.329844.

Shannon, C.E. (1948) A mathematical theory of communication. The Bell system technical journal 27(3), 379-423. https://doi.org/10.1002/j.1538-7305.1948.tb01338.x

Water storage strategies to adapt to climate change: the case of Val d'Orcia, Central Italy

L. Villani[1*], G. Castelli[1,2,3], E. Forzini[1], I. Bouizrou[1], L. Piemontese[1], G. Bertoli[4], M. Lompi[4], A. Giuliano[4], T. Pacetti[4], E. Caporali[4], E. Bresci[1]

[1] Department of Agriculture, Food, Environment and Forestry (DAGRI), University of Florence, Florence, Italy
[2] Environmental Governance and Territorial Development Hub (GEDT), University of Geneva, Geneva, Switzerland
[3] UNESCO Chair in Hydropolitics, University of Geneva, Geneva, Switzerland
[4] Department of Civil and Environmental Engineering, University of Florence, Florence, Italy
* e-mail: lorenzo.villani@unifi.it

Introduction

In many Mediterranean areas such as Val d'Orcia, increasing temperatures and more erratic rainfall patterns are forcing the farmers to consider the installation of irrigation systems for crops which were typically rainfed such as olive and grapevine. Increasing water storage either through the construction of small/large reservoirs or the restoration of existing Small Agricultural Reservoirs (SmARs) is among the preferred solutions to cope with water scarcity (Aminzadeh et al., 2024). The rural landscape of Central Italy already features thousands of SmARs which are currently largely underutilized or abandoned (Casadei et al., 2019). Moreover, recent droughts encouraged institutions and water authorities to reconsider abandoned projects of a large dam in the upper Val d'Orcia. Within the activities of the PRIMA AG-WaMED project, we aim to study various aspects related to non-conventional waters, and in the Italian Living Lab – the Val d'Orcia – we are evaluating SmARs from agro-hydrological, economic, social and legislative perspectives. In this study, we present the results of the hydrological modelling carried out with the Soil and Water Assessment Tool Plus (SWAT+, Bieger et al., 2017). We first set up the models aiming at the best representation of the two types of water storages considered (namely SmARs and the large dam). After calibration and validation, we force SWAT+ with five bias-corrected General Circulation Models (GCMs) to understand future characteristics and trends related to the climate, hydrological fluxes at the catchment scale, the planned large dam and SmARs.

Materials and methods

We set up alternative SWAT+ models for calibration and validation and to represent SmARs and the planned large dam. All the setups are prepared with the same input data. The DEM (10 m resolution) and river network provided by the Tuscany Region were used to delineate the watershed with QSWAT+. The Corine land use map and soil map elaborated from data of the Tuscany Region (see Villani et al., 2024) were used to create the Hydrological Response Units, with three slope classes (0-5%, 5-20%, >20%). Olive, grapevine and general agricultural land were split to obtain a more accurate representation of the irrigated and rainfed cropland. Representing SmARs is challenging in SWAT+ since most of them are small and are not directly placed on the channel network. Hence, we prepare SWAT+ setups in which we consider only the SmARs on the channel network but also one in which we move some SmARs to the closest channel (see Forzini et al., 2024). Then, we calibrate and validate the model considering monthly streamflow and catchment monthly actual evapotranspiration retrieved from remote sensing using the statistics and performance criteria of Moriasi et al. (2007). After the model set-up, calibration and validation, we simulate future climate by considering the five bias-corrected GCMs of the ISIMIP3b experiments (Lange, 2019). We use all the variables needed for the Penman-Monteith method to calculate potential evapotranspiration and we select the Shared Socioeconomic Pathway 585 (SSP585), the one with the highest additional radiative forcing of 8.5 W/m² by the end of the century. We run simulations combining historical and future climates from 1981 to 2100 and we then evaluate the trends in annual precipitation, average temperature, evaporation and seepage losses from reservoirs, and flow stored in the reservoirs with linear regression

and Mann-Kendall test. We also compare the ensemble means of the annual average values of the far future (2071-2100) and historical (1987-2014) periods to quantify the absolute and percentage changes.

Results and concluding remarks

The SWAT+ was successfully calibrated and validated according to the performance criteria selected for this study. For all the GCMs, the increasing trends in average temperature and evaporation from reservoirs, as well as the decreasing trends for precipitation, seepage from reservoirs and flow stored in reservoirs, are always significant. The ensemble mean of the annual average temperature increases by 4.9 °C (34.7%), while the ensemble mean yearly precipitation decreases by 156 mm (-18.8%). The ensemble mean of the total flow stored in the reservoirs is reduced by 1.46E+06 m^3 (-6.2%, Fig. 1a). Conversely, annual average evaporation from reservoirs is expected to increase by 1.16E+05 ha-m (8.7%, Fig. 1b). Understanding future climatic conditions and the projected hydrological fluxes is crucial for improved planning and management of water resources. Increased evaporation losses (Aminzadeh et al., 2024) and reduced seepage and groundwater recharge from water storage infrastructures are additional challenges caused by climate change.

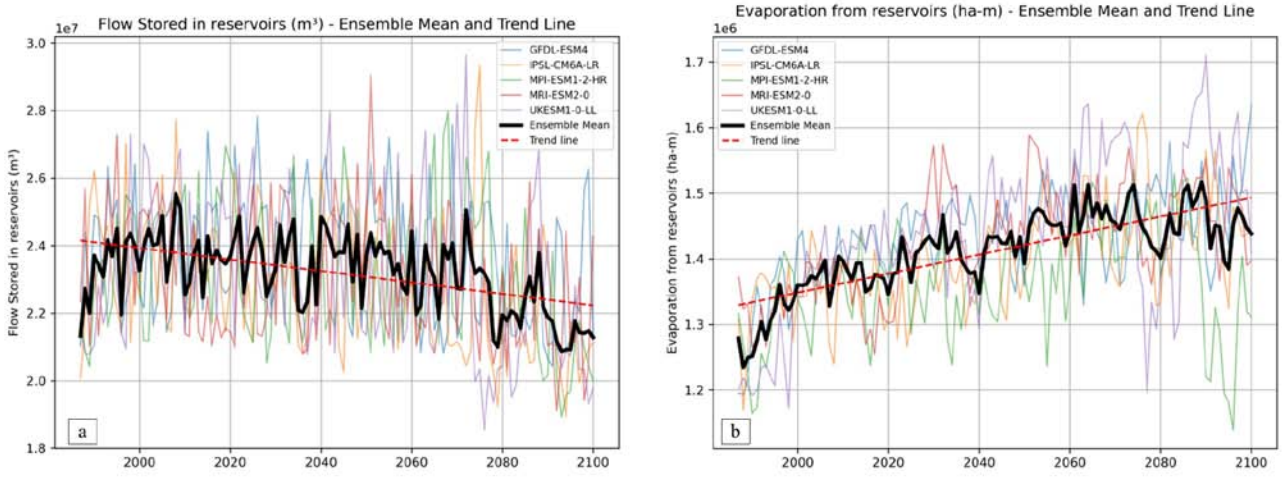


Figure 1. Flow stored (a) and evaporation from reservoirs (b) for the 5 GCMs and the ensemble mean.

Acknowledgments: This research was carried out within the AG-WaMED project, funded by the Partnership for Research and Innovation in the Mediterranean Area Programme (PRIMA), an Art.185 initiative supported and funded under Horizon 2020, the European Union's Framework Programme for Research and Innovation, Grant Agreement Number No. [Italy: 391 del 20/10/2022, Egypt: 45878, Tunisia: 0005874-004-18-2022-3, Greece: ΓΓΡ21-0474657, Spain: PCI2022-132929; Algeria: N° 04/PRIMA_section 2/2021].

References

Aminzadeh M, Friedrich N, Narayanaswamy S, Madani K, Shokri N (2024). Evaporation Loss From Small Agricultural Reservoirs in a Warming Climate: An Overlooked Component of Water Accounting. Earth's Future, 12(1).

Bieger K, Arnold JG, Rathjens H, White MJ, Bosch DD, Allen PM, ... Srinivasan R (2017) Introduction to SWAT+, a completely restructured version of the soil and water assessment tool. JAWRA Journal of the American Water Resources Association, 53(1), 115-130.

Casadei S, Di Francesco S, Giannone F, Pierleoni A (2019) Small reservoirs for a sustainable water resources management. Adv. Geosci. 49, 165–174.

Forzini E, Villani L, Castelli G, Bresci E (2024) Participatory modeling of small agricultural reservoirs in the Orcia watershed, Italy. AIIA 2024: biosystems engineering promoting resilience to climate change (Mid-Term 2024 AIIA)

Lange S (2019) Trend-preserving bias adjustment and statistical downscaling with ISIMIP3BASD (v1.0), Geoscientific Model Development, 12, 3055–3070.

Moriasi DN, Arnold JG, Van Liew MW, Bingner RL, Harmel RD, Veith TL (2007) Model evaluation guidelines for systematic quantification of accuracy in watershed simulations. Transactions of the ASABE, 50(3), 885-900.

Villani L, Castelli G, Yimer EA, Chawanda CJ, ... Bresci E (2024) Impacts of climate change and vegetation response on future aridity in a Mediterranean catchment. Agricultural Water Management, 299, 108878

The impact of hydraulic-hydrological model calibration on SuDS assessments: preliminary analyses

R. D'Ambrosio*, A. Longobardi
Department of Civil Engineering, University of Salerno, Via Giovanni Paolo II, 132, 84084 Fisciano, SA, Italy
** e-mail: robdambrosio@unisa.it*

Introduction

Hydraulic and hydrological models are essential tools for evaluating stormwater management strategies, including the implementation of Sustainable Drainage Systems (SuDS). Accurate calibration of these models is critical to ensuring their reliability in assessing SuDS effectiveness. However, the lack of monitoring data often presents significant challenges for model calibration, as highlighted in key studies (Krebs et al. 2014; Zhang et al. 2022). While uncalibrated models are widely used in scenario analyses, offering preliminary insights to support sustainable urban runoff management planning (D'Ambrosio et al. 2022), their reliability in interpreting specific phenomena remains a key question. This study focuses on the case study area of Sesto Ulteriano (MI), managed by the water and wastewater utility Gruppo CAP, with the objective of investigating the differences between calibrated and uncalibrated hydraulic-hydrological models in defining SuDS performance at the urban catchment scale (Figure 1). Leveraging a flow monitoring campaign conducted by the water and wastewater utility Gruppo CAP, this analysis further examines the broader impact of discharge monitoring data availability on urban water management strategies.

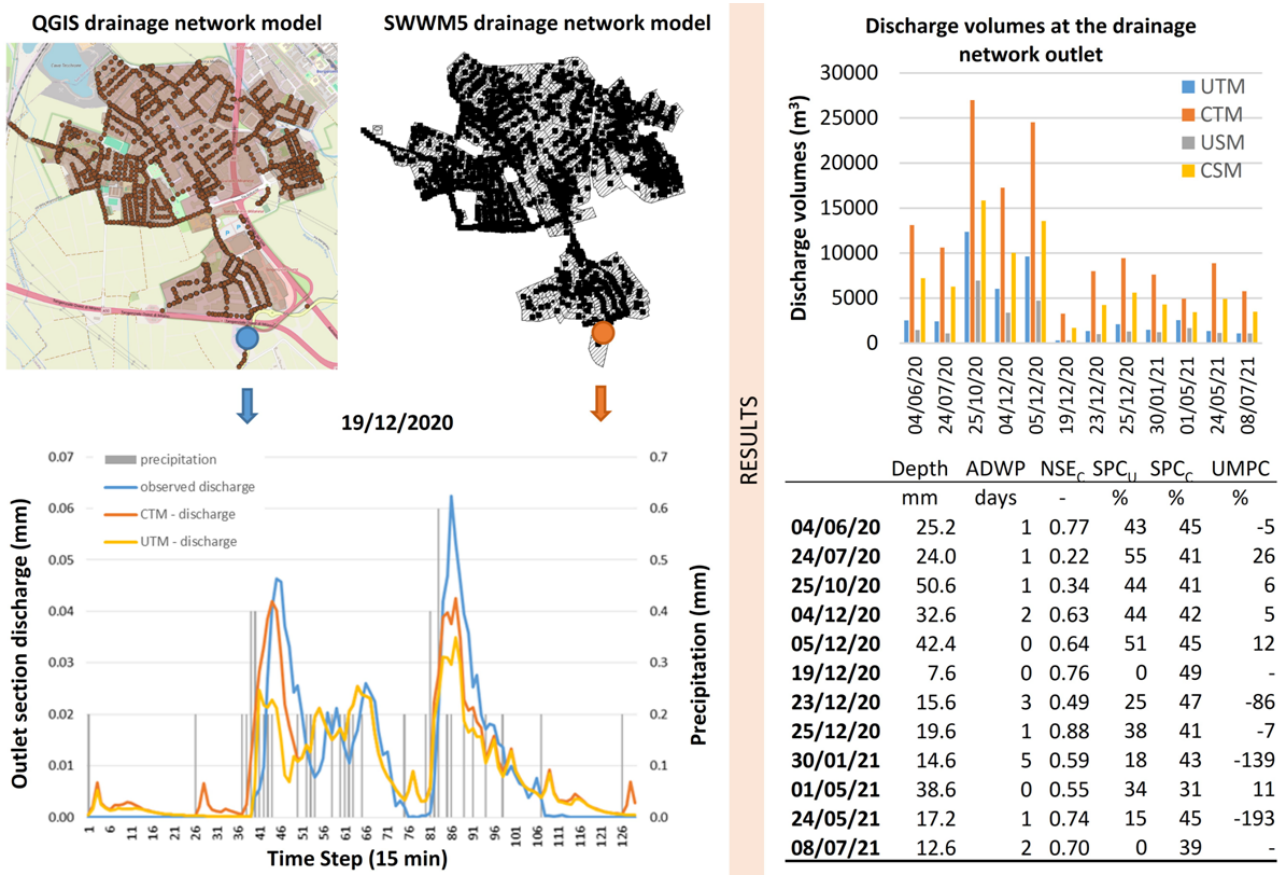
Materials and methods

The case study area, located in the municipality of San Giuliano Milanese (MI), spans approximately 290 hectares with varying land uses, predominantly industrial (73%). The area, characterized by a combined sewer network and extensive impervious surfaces, exhibits typical challenges of urbanized catchments and has been the focus of previous researches (D'Ambrosio et al. 2022; D'Ambrosio et al. 2023). Flow observations from the drainage network, recorded between June 2020 and July 2023 by Gruppo CAP, were used to calibrate and validate a SWMM5 hydraulic-hydrological model of the existing drainage network (Calibrated Traditional Model - CTM). The Curve Number and the depression storage of subcatchments were chosen as calibration parameters (Rossman and Huber, 2016) and the Nash-Sutcliffe Efficiency (NSE) was employed as metric to assess model accuracy. A Calibrated SuDS Model (CSM) was subsequently developed by implementing 24 hectares of SuDS (rain gardens, infiltration trenches, and pervious parking lots) into the CTM. However, this resulted in a partially calibrated model, as the absence of flow measurements for the design scenario prevented a complete calibration. The stormwater discharge volume at the outlet section, obtained from the CSM simulation for several precipitation events occurred between 2020 and 2023, was compared with that of the CTM, used as a benchmark. This comparison resulted in an indicator, the SuDS Performance Coefficient from the calibrated model (SPC_C), expressed as a relative difference and representing the capacity of SuDS to mitigate volumes discharged into the drainage network. The same procedure was subsequently applied to the uncalibrated SWMM5 hydraulic-hydrological models (Uncalibrated Traditional Model - UTM; Uncalibrated SuDS Model - USM). Simulations were performed using identical rainfall inputs and observing the same output variable, allowing for the calculation of additional SPC, this time corresponding to the uncalibrated models (SPC_U). To evaluate the impact of calibration on estimating SuDS effectiveness, an additional indicator, the Uncalibrated Model Performance Coefficient (UMPC), was calculated. This metric represents the ability of the uncalibrated hydraulic-hydrological model to predict the SPC: UMPC (%) = $[(SPC_U - SPC_C)/SPC_U]\cdot 100$. UMPC values close to zero indicate that the uncalibrated model predicts the SPC with similar accuracy to a calibrated model. Positive values suggest that the uncalibrated model overestimates SuDS performance, while negative values indicate an underestimation.

Results and concluding remarks

Preliminary results suggest that calibrating hydraulic-hydrological models generally has a minimal impact on the assessment of SPC, as evidenced by the relatively low UMPC values (Figure 1). However, specific cases (i.e. the rainfall-runoff event that occurred on May 24th 2021) show significant differences between assessments performed with calibrated and uncalibrated models (higher UMPC values). Overall, no consistent behavior is observed: in some rainfall-runoff events, the uncalibrated model tends to overestimate the SPC (positive UMPC values), while in others, it underestimates it (negative UMPC values). This may be influenced by event-specific characteristics, including precipitation depth, the Antecedent Dry Weather Period (ADWP), and the adaptability of the calibrated model. Additionally, the selection of calibration parameters can also play a significant role.

The absence of monitoring data for SuDS design scenarios poses inherent limitations, as the calibration is restricted to the traditional drainage network. Expanding the analysis to include a larger sample of rainfall-runoff events could provide deeper insights into the behavior of uncalibrated models.



	Depth	ADWP	NSE_C	SPC_U	SPC_C	UMPC
	mm	days	-	%	%	%
04/06/20	25.2	1	0.77	43	45	-5
24/07/20	24.0	1	0.22	55	41	26
25/10/20	50.6	1	0.34	44	41	6
04/12/20	32.6	2	0.63	44	42	5
05/12/20	42.4	0	0.64	51	45	12
19/12/20	7.6	0	0.76	0	49	-
23/12/20	15.6	3	0.49	25	47	-86
25/12/20	19.6	1	0.88	38	41	-7
30/01/21	14.6	5	0.59	18	43	-139
01/05/21	38.6	0	0.55	34	31	11
24/05/21	17.2	1	0.74	15	45	-193
08/07/21	12.6	2	0.70	0	39	-

Figure 1. Sesto Ulteriano drainage network: modeling and results.

References

D'Ambrosio R, Balbo A, Longobardi A, Rizzo A (2022) Re-think urban drainage following a SuDS retrofitting approach against urban flooding: A modelling investigation for an Italian case study. Urban Forestry & Urban Greening 70, 127518. https://doi.org/10.1016/j.ufug.2022.127518

D'Ambrosio R, Longobardi A (2023) Adapting drainage networks to the urban development: An assessment of different integrated approach alternatives for a sustainable flood risk mitigation in Northern Italy. Sustainable Cities and Society 98, 104856. https://doi.org/10.1016/j.scs.2023.104856.

Krebs G, Jacobsen P, Einfalt T (2014) Influence of calibration data and model complexity on urban drainage modelling. Journal of Hydrology 510, 555-563. http://doi.org/10.1080/1573062X.2013.847464

Rossman L, Huber W, 2016. Storm Water Management Model Reference Manual Volume III – Water Quality. U.S. EPA Office of Re-search and Development, Washington, DC. EPA/600/R-16/093

Zhang K, Chui TFM, Cheng KH (2022) Evaluating the performance of SuDS under different climate and land use scenarios using calibrated hydrological models. Water Research 221, 118720. http://doi.org/10.1016/j.watres.2022.118720

Land use and solar power: Maximizing photovoltaic potential in Singapore

S. Maroufpoor, X.S. Qin*
School of Civil and Environmental Engineering, Nanyang Technological University, Singapore
** e-mail: xsqin@ntu.edu.sg*

Introduction

The depletion of fossil fuels and the rising greenhouse gas emissions have posed formidable challenges in recent years. Renewable energy could be considered the sustainable solution to these challenges. The International Energy Agency (IEA) recognizes photovoltaic (PV) systems as among the most economically competitive means of electricity generation in a majority of nations. Furthermore, these systems alone constituted three-quarters of the expansion in global renewable energy capacity during the year 2023 (IEA, 2024). PV technology uses solar radiation which can be converted directly into current electricity, and the lack of moving mechanical parts characterizes this process. This lack eliminates the need for regular mechanical maintenance, which is a considerable operational advantage (Adefarati and Bansal, 2019). Beyond the intensity of solar radiation, a primary constraint on the energy output of photovoltaic (PV) systems is the quantity and characteristics of land that can be utilized for installation. The goal of this research is to determine the capacity for photovoltaic (PV) system implementation in Singapore, specifically within the context of existing land use constraints.

Materials and methods

This study used hourly temperature and solar radiation data for Singapore. The data were collected from the Meteorological Service Singapore (MSS) for three weather stations, including Changi Airport (1° 22' 4.08'' N, 103° 58' 56'' E), Sentosa Island (1° 15' 1.08'' N, 103° 49' 39'' E), and Choa Chu Kang (1° 22' 22'' N, 103° 43' 20'' E). Solar radiation and temperature hourly data from April 2011 to December 2023 were analyzed, with a focus on the daylight hours between 8 AM and 8 PM. To address data uncertainties, cumulative distribution functions (CDFs) including normal, log-normal, gamma, Gumbel, and Weibull, were tested, and the best-fitting model was used to generate exceedance levels ranging from 5 to 95%. PV output was subsequently determined based on established equations (Crook et al., 2011).

$$PVOUT = Ra \times E_c \tag{1}$$

$$\frac{E_c}{E_{ref}} = 1 - \alpha(T_C - T_{ref}) + \lambda Log_{10}(Ra) \tag{2}$$

$$T_C = a_1 + (a_2 T_a) + (a_3 Ra) \tag{3}$$

where PVOUT is the output of the PV system ($W.m^{-2}$), E_c and E_{ref} are the calculated and reference efficiencies of the PV cells, respectively. Ra and T_a are the solar radiation ($W \cdot m^{-2}$) and the average air temperature (°C). T_c and T_{ref} are the PV cell temperature and the reference condition temperature, where T_{ref} is 25°C according to Cork et al (2011). The equation parameters for the monocrystalline silicon module were α=0.0045, λ=0.1, C_1= -3.75 °C, C_2= 1.14 and C_3=0.0175 $°C \cdot m^2 \cdot W^{-1}$ (Zuluaga et al., 2022).

This study assessed PV output potential while accounting for several land-use restrictions, using data from the World Bank Group (WBG, 2024). Areas excluded were those with high elevation variations, large water bodies (with exceptions for floating PV potential within 1km of coastlines), dense forests (over 50% cover), remote areas (>25 km from settlements), high urbanization areas (over 50% density), all protected areas, and croplands. Thiessen polygons linked meteorological stations to specific regions, and PV output potential was then quantified at both 75% and 30% exceedance probability levels to represent common and maximum energy output respectively.

Results and concluding remarks

Figure 1 illustrates the duration curves for PVOUT measured at three different stations, highlighting clear variations in energy generation. It also shows PVOUT (50% exceedance level) without land use constraints. The Sentosa Island station produced higher PVOUT (kWh/m²) than the others due to recording higher solar radiation

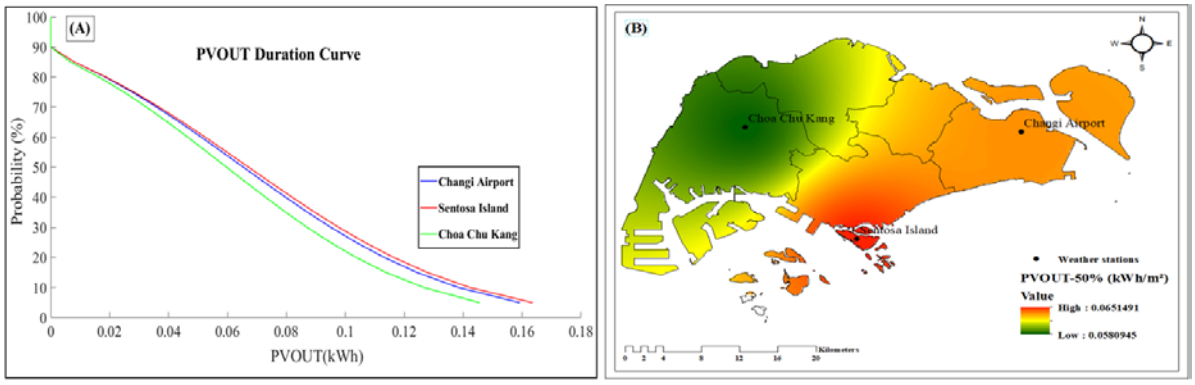


Figure 1. Duration curves (A) and 50% exceedance probability map (B) of solar photovoltaic output.

To further investigate the feasibility of PV system implementation, land use restrictions were integrated into a spatial analysis. This analysis employed two probability levels—75% and 30%—to identify areas with suitable energy production potential (Figure 2). Overall, the study found a concentration of potential sites in the northern and northwestern portions of the study area, with these regions exhibiting higher overall production capabilities. These areas showed an energy output range of 60-200 kWh at the 75% probability level, increasing to a range of 200-700 kWh at the 30% probability level.

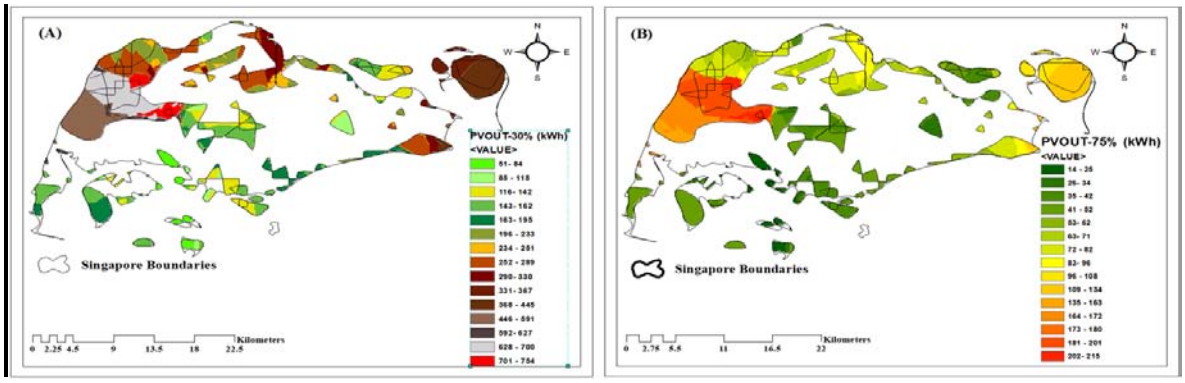


Figure 2. Solar photovoltaic output based on land use restrictions at 30% (A) and 75% (B) probability of exceedance

Acknowledgments: This research is supported by the National Research Foundation, Singapore, and the National Environment Agency, Singapore, under its Climate Impact Science Research (CISR) Programme (project ID NRF-000413-01). Any opinions, findings and conclusions or recommendations expressed in this material are those of the authors and do not reflect the views of the National Research Foundation, Singapore, the National Environment Agency, Singapore.

References

Adefarati, T., & Bansal, R. C. (2019). Energizing renewable energy systems and distribution generation. In Pathways to a smarter power system (pp. 29-65). Academic Press.

Crook, J. A., Jones, L. A., Forster, P. M., & Crook, R. (2011). Climate change impacts on future photovoltaic and concentrated solar power energy output. Energy & Environmental Science, 4(9), 3101-3109.

IEA [International Energy Agency]. (no date). Solar - Fuels & Technologies. https://www.iea.org/fuels-and-technologies/solar [Accessed December 30, 2024].

WBG [World Bank Group]. (no date). Global Photovoltaic Power Potential. https://datacatalog.worldbank.org/search/dataset/0038379 [Accessed December 20, 2024].

Zuluaga, C. F., Avila-Diaz, A., Justino, F. B., Martins, F. R., & Ceron, W. L. (2022). The climate change perspective of photovoltaic power potential in Brazil. Renewable Energy, 193, 1019-1031.

Monitoring soil sealing in the Mediterranean: The ESA Ulysses project for sustainable land management

D. Iasillo[1*], V. De Pasquale[1], P. Di Lauro[1], V. Santarsiero[1], W. De Simone[1], L. Congedo [2], M. Munafò[2]
[1] Planetek Italia
[2] Italian Institute for Environmental Protection and Research;
* e-mail: iasillo@planetek.it

Introduction

Soil sealing, a human-driven process, alters soil permeability through the application of artificial materials and compaction. This process is also known as impermeability, has significant environmental impacts, including changes in urban climates, heat exchange, soil permeability, water infiltration, and groundwater recharge. Soil sealing reduces the capacity of soil to absorb rainwater, increasing the risk of flooding and compromising soil ecological functions. In addition, this phenomenon contributes to the formation of urban heat islands, exacerbating climate change-related risks. Understanding the shift from natural to artificial land use and land cover is essential to understanding the relationship between human activities and the environment.

The impacts and implications of land use have been widely studied and documented in the scientific literature [1,2,3,4,5]. In many regions, urban sprawl is widespread, resulting in extensive sealing of the land [1,3]. These dynamics underline the urgent need for sustainable land management and planning to mitigate its negative effects.

Nowadays, satellite data are essential to quantify and monitor these changes as they provide detailed information and an overview of the characteristics of changes in urban and rural areas. Numerous studies have addressed the issue of soil sealing using different applications, multispectral data and classification methods [1,6]. The ESA Ulysses project focuses on the strategic challenges of monitoring land take and sustainable development in the Mediterranean region, where soil sealing is a significant environmental problem. The project, supported by the European Space Agency (ESA), is part of a broader effort to exploit advanced Earth observation (EO) technologies to better understand and manage environmental problems in the Mediterranean. Improving the monitoring of soil sealing dynamics, urbanization and related environmental impacts in the Mediterranean basin is the main objective of the initiative. The aim is to help regional and local authorities develop and implement effective land management policies that mitigate the negative effects of soil sealing.

Materials and methods

The methodology uses Sentinel-2 images to estimate soil sealing with a spatial resolution of 10 meters, detecting minimal variations of 1 m². The analysis accounts for mixed pixels and the spectral similarity between natural soil and artificial surfaces. From the images, the annual NDVI, monthly cloud-free composites, and a series of spectral indices useful for describing urban and natural characteristics, such as NDTI, MNDWI, and NDBI, are calculated. The soil sealing mapping phase uses a tool called "Broceliande" in combination with machine learning algorithms, such as the Random Forest classifier, to classify pixels as sealed or unsealed[7]. The result is a raster map with a spatial resolution of 10 meters, representing the degree of soil sealing (from 0 to 100%) within an area up to 20 km from the coastline. Validation was conducted using stratified random sampling, estimating thematic accuracy for sealed areas, and assessing the correlation between the estimated values and the degree of soil sealing.

Several soil consumption indicators have been calculated, including the percentage of sealed soil relative to the total area of a given administrative level, providing insights into the degree of urbanization and its environmental effects. Soil sealing in coastal areas within the Mediterranean region and in the countries of Italy, France, Spain, and Greece at the national level is analysed through buffers of 500, 1000,

and 2000 meters, allowing for an evaluation of urban development impacts. A similar approach is applied to waterways, where the percentage of sealed soil within buffers of 500 and 1000 meters is calculated to examine the consequences of urbanization along riverine areas. The application also integrates metrics dedicated to protected areas and seismic risk zones, highlighting the impact of human activities in ecologically and seismically sensitive regions. These indicators are calculated annually for the period 2018-2024, enabling a temporal analysis of soil sealing trends both at the administrative level and within protected areas and river buffers.

Results and concluding remarks

Soil sealing increases the vulnerability of urban areas to natural disasters, particularly floods. Monitoring soil sealing dynamics and linking them to disaster risks allows authorities to develop targeted risk reduction strategies, such as sustainable drainage systems, green spaces, and stricter regulations on impervious surfaces in high-risk areas. Data from the Ulysses project can be used by national and international policymakers to promote sustainable land use practices, reduce impervious surfaces, and incentivize the rehabilitation of sealed areas.

Furthermore, the Ulysses project raises public awareness about the environmental impacts of soil sealing through outreach programs and by engaging local communities in adopting sustainable practices. By integrating with other environmental monitoring initiatives in the Mediterranean region, Ulysses creates synergies among different datasets and approaches, providing a more comprehensive understanding of environmental dynamics. This integrated perspective helps address multiple environmental challenges simultaneously, improving land management and conservation efforts.

The project also supports the development of climate resilience strategies by identifying areas where soil sealing could exacerbate the impacts of climate change, such as rising temperatures or water scarcity. By combining these data with climate models, authorities can better prepare for future challenges and make cities and communities more resilient.

In summary, the ESA Ulysses Project plays a vital role in monitoring and managing soil sealing in the Mediterranean region. By providing essential data and tools, it helps mitigate environmental impacts, supports sustainable planning, and fosters climate resilience, protecting coastal ecosystems and enabling sustainable development for the future.

References

EEA. Technical specifications for implementation of a new land-monitoring concept based on EAGLE . Public Consultation document for CLC+ Core. EEA.(2020)

European Commission. Proposal for a DIRECTIVE OF THE EUROPEAN PARLIAMENT AND OF THE COUNCIL on Soil Monitoring and Resilience (Soil Monitoring Law) COM(2023) 416. Commission Of The European Communities, Brussels, (2023)

Fiorini, Lorena, et al. "Land take and landscape loss: Effect of uncontrolled urbanization in Southern Italy." Journal of Urban management 8.1 (2019): 42-56. https://doi.org/10.1016/j.jum.2018.09.003

Friedl, Mark A., and Carla E. Brodley. "Decision tree classification of land cover from remotely sensed data." Remote sensing of environment 61.3 (1997): 399-409. https://doi.org/10.1016/S0034-4257(97)00049-7

Marquard, Elisabeth, et al. "Land consumption and land take: enhancing conceptual clarity for evaluating spatial governance in the EU context." Sustainability 12.19 (2020): 8269. https://doi.org/10.3390/su12198269

Merciol, F., Pham, M. T., Santana Maia, D., Masse, A., & Sannier, C. (2020). BROCELIANDE: a comparative study of attribute profiles and feature profiles from different attributes. The International Archives of the Photogrammetry, Remote Sensing and Spatial Information Sciences, 43, 1371-1377. https://doi.org/10.5194/isprs-archives-XLIII-B3-2020-1371-2020

Santarsiero, Valentina, et al. "Remote sensing and spatial analysis for land-take assessment in Basilicata Region (Southern Italy)." Remote Sensing 14.7 (2022): 1692. https://doi.org/10.3390/rs14071692

Evaluation of heat stress in a Mediterranean watershed under the influence of climate change

H. Boyacioglu[1*], M.C. Gunacti[2], F. Barbaros[2]
[1] Dokuz Eylül University, Faculty of Engineering, Department of Environmental Engineering, Izmir, Turkey
[2] Dokuz Eylül University, Faculty of Engineering, Department of Civil Engineering, Izmir, Turkey
* e-mail: hulya.boyacioglu@deu.edu.tr

Introduction

Heat stress is a major consequence of climate change, affecting human health, agriculture, infrastructure, and ecosystems. As global temperatures rise due to increased greenhouse gas emissions, extreme heat events are becoming more frequent, intense, and prolonged. Air temperature and relative humidity are the key meteorological variables in assessing heat stress. The Heat Index (HI), incorporates both variables and is useful for evaluating thermal conditions. It provides a more accurate representation of how hot it actually feels to humans, rather than just relying on air temperature alone (Li et al. 2024).

Recent research from 2020 to 2025 has extensively examined the implications of climate change on heat stress in the Mediterranean basin, utilizing simulations from the Coupled Model Intercomparison Project Phase 6 (CMIP6). Studies indicate a significant rise in the HI across the Mediterranean by the end of the 21st century. Under the SSP5-8.5 scenario, strong upward trends of approximately 1°C per decade are anticipated, with the most pronounced increases during summer months, especially along coastal areas. By employing specific indices, heat-prone regions that may face heightened risks due to escalating temperatures and associated heat stress were pinpointed (Alvarez et al 2024; Tejedor et al. 2024). Collectively, the studies done by Urdiales-Flores et al. (2024), Anav et al. (2024), Tuel and Eltahir (2021), emphasize the rising heat stress in the Mediterranean region due to climate change, highlighting the necessity for adaptive strategies to mitigate potential health risks and socioeconomic impacts.

This study aims to create a novel approach for formulating strategies by establishing a connection between the heat index and climate change in the Gediz River Basin in Western Turkey, which is a mixed land-use watershed dominated by intensive agricultural activities and struggles with water scarcity within the Mediterranean region.

Materials and methods

This study examined climate data from the ERA5-Land Program of the Gediz River Basin from 1994 to 2024 to better understand HI patterns. The basin is well-suited for analysing how climate factors contribute to heat stress under increasing pressure from climate change. For the calculations, daily maximum temperature and relative humidity data recorded simultaneously in July—the warmest month of the year throughout the study period—were used (Eq. 1) (Rothfusz 1990; Blazejczyk et al. 2012).

$$HI=-8.784695+1.61139411xT+2.338549xRH-0.14611605xTxRH-1.23080894x10^{-2}xT^{2}-1.6424828x10^{-2}xRH^{2}-2.211732x10^{-3}xT^{2}xRH+7.2546x10^{-4}xTxRH^{2}-3.582x10^{-6}xT^{2}xRH^{2} \quad (1)$$

where, T is the air temperature in °C, and RH is the relative humidity in %. HI is valid for air temperatures above 20°C. Potential changes in the HI for the Gediz River Basin in Turkey were examined using simulations from the CORDEX regional climate model data under the RCP 8.5 future scenario. Moreover, the overlay of the HI maps and CORINE program land cover maps were evaluated. By juxtaposing HI of different periods and land cover maps the interrelations between these variables have been examined.

Results and concluding remarks

The land use map of 2006 represents the mid-period of the HI analysis. As seen in Figure 1 (above) the basin is dominated by intensive agricultural lands, both irrigated and non-irrigated. On the other hand, as

given in Figure 1 (below) to plot the HI map, the 95th percentile of each data pixel timeseries of the period 1994-2024 have been calculated. Spatial interpolation techniques were employed to map the calculated HI values. When the HI map with the land use map is examined together, a strong connection of agricultural lands and high HI values have been observed. Moreover, a similar connection can be indicated for the water bodies and high HI values and forested areas and low HI values in the reference period.

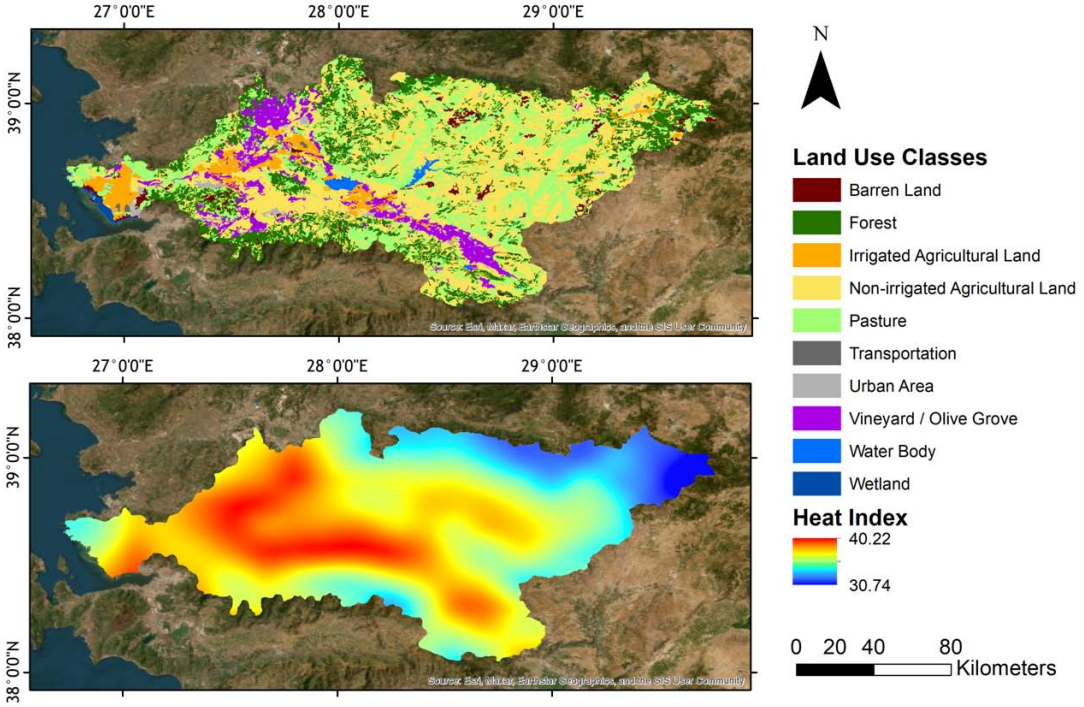


Figure 1. Land cover map of the year 2006 (above), and HI map according to the 95th percentile of the period 1994-2024 (below)

In the case of future periods, similar relationships are to be expected with higher HI values in the basin due to climate change effects. The higher HI values are a threat to human health and the environment in general. The correlation between the HI values and land use classes presents a tool for the communities and decision-makers in the basin to prioritize and focus on the HI-prone areas to mitigate its adverse effects beforehand.

References

Alvarez I, Diaz-Poso A, Lorenzo MN, Roye D (2024) Heat index historical trends and projections due to climate change in the Mediterranean basin based on CMIP6, Atmospheric Research, 308, 107512.

Anav A, Antonelli M, Calmanti S, Carillo A, Catalano F, Dell'Aquila A, Iacono R et al. (2024) Dynamical downscaling of CMIP6 scenarios with ENEA-REG: an impact-oriented application for the Med-CORDEX region. Clim Dyn 62, 3261–3287. https://doi.org/10.1007/s00382-023-07064-3.

Blazejczyk K, Epstein Y, Jendritzky G, Staiger H, Tinz B (2012) Comparison of UTCI to selected thermal indices. Int J Biometeorol 56, 515–535. https://doi.org/10.1007/s00484-011-0453-2.

Li F, Yigitcanlar T, Nepal M, Nguyen K, Dur F, Li W (2024) Assessing heat vulnerability and multidimensional inequity: Lessons from indexing the performance of Australian capital cities, Sustainable Cities and Society, 115, 105875, ISSN 2210-6707. https://doi.org/10.1016/j.scs.2024.105875.

Rothfusz, LP (1990) The heat index equation (or, more than you ever wanted to know about heat index), Fort Worth, Texas: National Oceanic and Atmospheric Administration, National Weather Service, Office of Meteorology, 90-23.

Tejedor E, Benito G, Serrano-Notivoli R, et al. (2024) Recent heatwaves as a prelude to climate extremes in the western Mediterranean region. npj Clim Atmos Sci 7, 218. https://doi.org/10.1038/s41612-024-00771-6.

Tuel A, Kang S, Eltahir EA (2021) Understanding climate change over the southwestern Mediterranean using high-resolution simulations. Climate Dynamics 56(3):985-1001. https://doi.org/10.1007/s00382- 020-05516-8.

Urdiales-Flores D, Zittis G, Hadjinicolaou P, Cherchi A, Alessandri A, Peleg N, Lelieveld J (2024) A global analysis of historical and future changes in mediterranean climate-type regions. Int J Climatol, 44: 5607-5620. https://doi.org/10.1002/joc.8655.

From IDF curves to urban drainage systems parameters in the context of climate change: an application on Vilnius, Lithuania

L.A. Gomez-Mogollon[1], L. Napolitano[1], G. Rianna[1*], R. Padulano[2], K. Virsilaite[1]
[1] CMCC Foundation - Euro-Mediterranean Center on Climate Change, Italy
[2] Department of Civil, Architectural and Environmental Engineering, Università degli Studi di Napoli "Federico II", Napoli, Italy
* e-mail: guido.rianna@cmcc.it

Introduction

Design of sewer networks is usually conducted so that a partial filling ratio is achieved in every pipe under a design extreme rainfall event whose duration depends on the drainage basin characteristics, and whose return period is usually in the range 3-10 years, depending on the specific municipal regulations. The "design storm" is usually estimated from local or regional Intensity-Duration-Frequency (IDF) curves (Kourtis & Tsihrintzis, 2022). The expected increase in frequency and magnitude of extreme precipitation events due to climate change can increase the frequency of the network reaching surcharge conditions, with significant impacts for local communities (Hathaway et al., 2024). Update of IDF curves under climate change is challenging for two main reasons: current weaknesses in climate modelling (raw precipitation outputs need to be bias-corrected for informing decisions at local scale); uncertainties in the future societal development pathways (considering multiple different scenarios is required). Despite its technical relevance, potential variations in IDF curves, and their uncertainty, are difficult to communicate in a decision-making framework and it is necessary to "translate" them into design parameters that are easily interpreted by practitioners and local decision-makers. In this work, we propose "translating" the expected changes of IDF curves into pipe sizes required to ensure a proper disposal of the surface runoff. Then, these results are compared with the current drainage infrastructure to identify under which scenarios the system operates under surcharge conditions and may lead to an increase in the frequency of overflow events. The analysis is carried out for Vilnius Old-Town (Lithuania) where overflow events are particularly critical due to the historical relevance of the area.

Materials and methods

The proposed framework is presented in Figure 1. Future IDF curves are defined using information from 14 modelling chains of the Euro-CORDEX project. Three climate altering gases scenarios (RCP2.6, RCP4.5, and RCP8.5) and three 30-years periods throughout the 21st century are considered in the analysis. Three statistical bias-correction techniques are implemented under the assumption that modelling results are affected by systematic biases (Maraun, 2016): Quantile-Quantile Downscaling (QQD), Detrended Quantile Mapping (DQM), and Quantile Delta Mapping (QDM) (Padulano et al., 2025). For bias correction, IDF curves obtained from observed precipitation close to the city of Vilnius are used as reference.

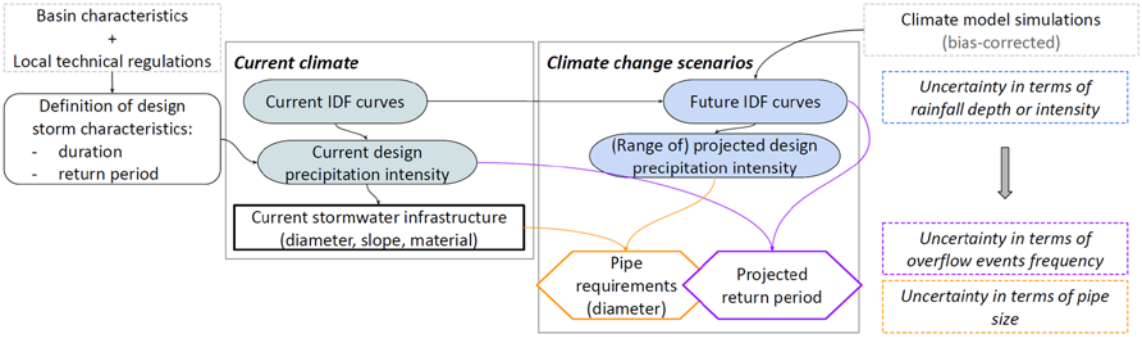


Figure 1. Methodological approach.

Information of terrain elevation, land use, and the drainage system in Vilnius Old-Town is obtained from open access sources and local entities. These physical parameters are used to define the duration of the design storm, about 40 minutes, while the design return period is defined according to the recommendations of local technical regulations, as 5 years. Precipitation intensity values with design return period are retrieved from the current and future bias-corrected IDF curves. Then, the rational method and Manning's equation (consistent with the local design criteria) are used to calculate the required pipe size for each precipitation value. In addition, to analyse changes in the frequency of overflow events, new return periods associated with the current design intensity are obtained from the future IDF curves.

Results and concluding remarks

This study provides preliminary results regarding the analysis of climate change impacts on the urban drainage system of the Old-Town in Vilnius. Figure 2 depicts the IDF curves under climate change and the calculated pipe size (ensemble median, 10th and 90th -tile) required for future design precipitation intensity on a specific "proof of concept" conduit of the system. The range of variability of extreme precipitation is significant, having that the 40-minutes storm with a return period of 5 yrs is projected to range between 29 and 50 mm/h, that represents a reduction of -9% or an increase up to +56% compared to current climate. On the other hand, results expressed in terms of required pipe size show that i) the current infrastructure can manage the median variation projected under most of the scenarios for early in the century; ii) the next larger commercially available diameter is enough to cover most of the projected variations up to the end of the century (in some cases, it may even be too large); and iii) for 2010-2039, RCP2.6 projects higher rainfall intensities and, then, larger design pipe size, whereas RCP8.5 provides larger impacts in 2070-2099. The latter reflects the uncertain relationship between interannual "natural" variability superimposed to anthropo-induced climate change.

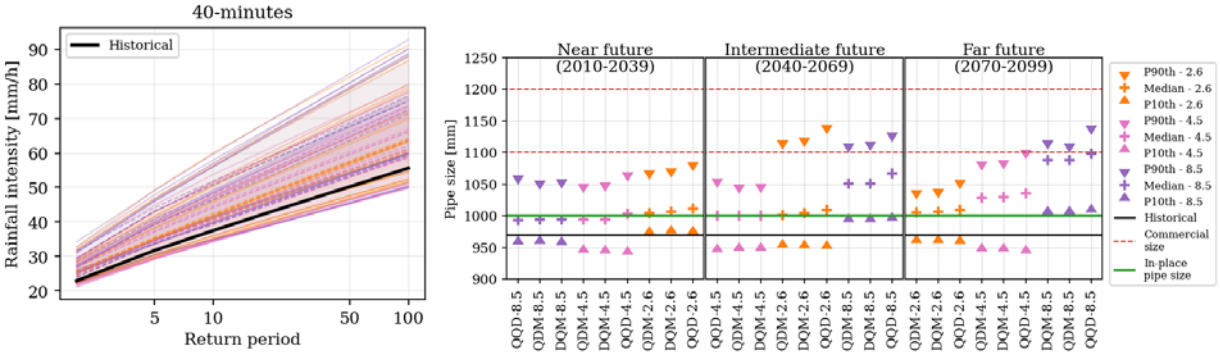


Figure 2. Climate change impacts in terms of IDF curves and required pipe size for a specific conduit.

Despite all the conceptual limitations, this approach offers a practical assessment of the impacts and repercussions of climate change on urban drainage design. Further analyses will show the effect of future design storms on the filling ratio of the current drainage network, to showcase the resilience of the infrastructure and the ability to cope with a more severe extreme rainfall regime.

Acknowledgments: The authors would also like to acknowledge The HuT Project funded by the Horizon Europe Framework Programme with Grant Agreement No. 101073957.

References

Hathaway, J. M., Bean, E. Z., Bernagros, J. T., et al. (2024). A Synthesis of Climate Change Impacts on Stormwater Management Systems: Designing for Resiliency and Future Challenges. Journal of Sustainable Water in the Built Environment, 10(2), 04023014. https://doi.org/10.1061/JSWBAY.SWENG-53

Kourtis, I. M., Tsihrintzis, V. A. (2022). Update of intensity-duration-frequency (IDF) curves under climate change: a review. Water Supply, 22(5), 4951-4974. https://doi.org/10.2166/ws.2022.152

Maraun, D. (2016). Bias correcting climate change simulations-a critical review. Current Climate Change Reports, 2(4), 211-220. https://doi.org/10.1007/s40641-016-0050-x

Padulano, R., Gomez-Mogollon, L.A., Napolitano, L., Rianna, G., (2025). Quantile-based bias-correction of extreme rainfall: Pros & cons of popular methods for climate signal preservation. Journal of Hydrology, https://doi.org/10.1016/j.jhydrol.2025.132814

Climate and land-uses changes contribute to water scarcity in a rural basin

A. Yfanti*, I. Kourtis, M.P. Papadopoulou
School of Rural, Surveying and Geoinformatics Engineering, National Technical University of Athens, Athens, Greece
** e-mail: annaifanti2@gmail.com*

Introduction

The sustainable management of water resources in a rural region is expected to be affected not only by climate change but also by land-uses especially those related to the anthropogenic activities. The aim of this work was to study the water use rates for different land uses and to assess the impact of different climate change scenarios in a rural area where agricultural, tourist and energy production activities are among the main water-users. To this end, a water resources management model employing WEAP software (e.g., Dau et al. 2021; Obahoundje et al. 2021), was developed for the basin, downstream an electricity production dam (Platanovrisi dam). The area of interest represents the largest concentration of agricultural activity within the watershed (Nestos river basin) including the Delta area (30%), which is predominantly composed of cultivable land, where other land-uses are forested land (48%), pastures (15%) and a small portion of urban zones (2%). Thus, the majority of water withdrawals are directed towards meeting the growing irrigation demands (97% of water demand), while smaller quantities are used to fulfill the water needs of urban areas (2.9%) and livestock (0.1%). Future climate scenarios, Representative Concentration Pathway (RCP2.6 – a moderate scenario for carbon dioxide emissions mitigation & RCP8.5 – a scenario of increased emissions), were considered in relation to water withdrawals for the same land uses. Finally, a scenario for a new irrigation project is being examined, which aims to expand the irrigated area by approximately 50% by withdrawing significant volumes of water from the river.

Materials and methods

Data collection and analysis process started with the delineation of the study area at the southern part of the Nestos River basin, downstream the Platanovrisi dam. After an assessment of land uses within this area was made, surface and subsurface runoff data were estimated. Subsequently, in order to calculate the irrigation needs and withdrawals, the area of interest was divided into two catchment areas and all crops were grouped into five distinct categories. Meteorological data (i.e., rainfall and temperature), were collected from Chrysoupolis Meteorological Station for the period spanning from 1984 to 2022. The meteorological data were used to estimate evapotranspiration employing the Blaney-Criddle method (Blaney and Criddle 1950). In addition, an estimation of the quantity of water needs and withdrawals, not only for irrigation, but also for livestock and domestic use, considering system losses for water transportation, distribution and application was performed. Projected temperature and precipitation data were collected from the application "DEAR Clima" for the period 2021 – 2100. The future climate data were used to calculate projected evapotranspiration values and develop annual time series which were subsequently used for modeling future water demand using WEAP software under the two aforementioned RCPs scenarios. For the scenario of the new irrigation project, the new irrigated area was included defining an increase in the required irrigation withdrawals.

Results and concluding remarks

The results of the water resources management model showed total water withdrawals of about 233 hm^3 per year, distributed per land use (agricultural 97%, urban 2.9%, livestock 0.1%). As it is expected, irrigation constitutes the largest water consumer as the water stored in the dam is used for energy production primarily, irrigation purposes and securing an yearly ecological flow for the river. Monthly

results revealed significantly increased water needs for irrigation purposes compared to the other land uses, especially during the summer months. The irrigation water needs of the area of interest are closely linked to the increased agricultural activity, as different types of crops and soil management require varying amounts of water to ensure production. Results also indicated that the majority of the water demand is met using surface water resources and only a small percentage is met using the groundwater resources. The results are in accordance with the results presented in the corresponding River Basin Management Plan (Ministry of Environment and Energy, 2020). Indicatively results for the future climate scenarios and the scenario of the new irrigation project, compared to the reference scenario are presented in Figure 1. Results suggested that under climate change conditions the monthly withdrawals in the area of interest will be higher under the RCP8.5 scenario, especially in the months of July and August and lower under the RCP2.6 scenario. The increased water demands under the RCP8.5 scenario are expected due to the negative impacts of climate change associated with high greenhouse gas emissions and a continuously rising global temperature, whereas the RCP2.6 scenario predicts significantly lower emissions, leading to comparatively reduced water demands. The scenario for the new irrigation project poses a significant increase of water withdrawal volumes, given the increase in irrigated area by 5,600 ha, while the allocation of water to land use attributes 97.7 % to irrigation, 2.2 % to water supply and only 0.1 % to livestock. The expansion of agricultural land on this scale directly impacts the region's irrigation needs, as the more cultivable land utilizes water from the area's finite natural resources, the higher the water volumes required to satisfy these needs. Efficient management of water resources is crucial in light of increased agricultural activity and potential climate change scenarios, which are expected to drive significant changes in water demand and may further strain already limited water supplies. Overall, it can be concluded that robust and holistic approaches are needed for the sustainable management of water resources under anthropogenic and environmental changes (climate and land use changes).

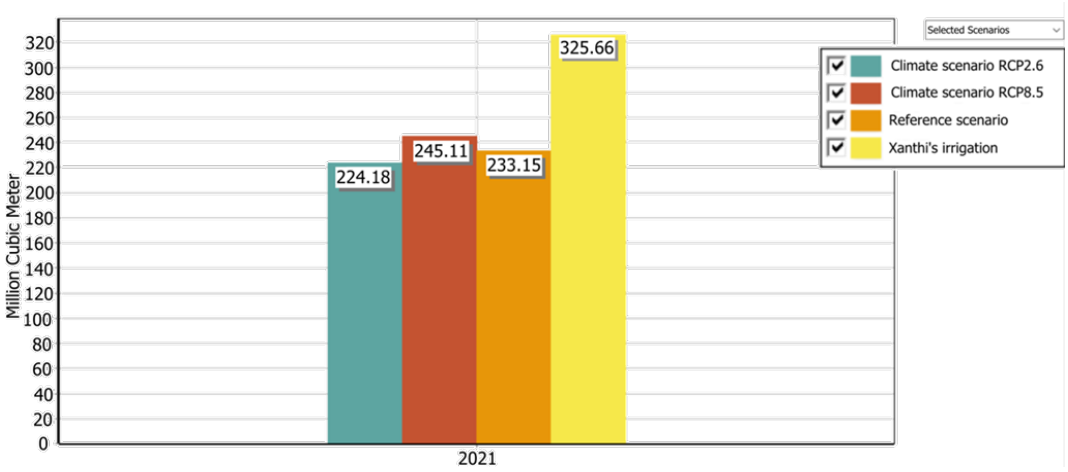


Figure 1. Estimated annual water withdrawal (hm³/year) per scenario.

Acknowledgments: This work was conducted in the frame of H2020 NEXOGENESIS project funded by the European Union's Horizon 2020 Innovation Action programme (GA No. 101003881). Also special thanks belong to "*ENVIRONPLAN S.A.*" for providing the primary data.

References

Blaney HF, Criddle WD (1950) Determining water requirements in irrigated areas from climatological data. U.S. Department of Agriculture, Soil Conservation Service Technical Paper No. 96.

Dau QV, Kuntiyawichai K, Adeloye AJ (2021) Future Changes in Water Availability Due to Climate Change Projections for Huong Basin, Vietnam. Environmental Processes 8: 77–98. https://doi.org/10.1007/s40710-020-00475-y

Ministry of Environment and Energy (Greece) (2020). Strategic Development and Land Allocation Plan (SDLAP). Ministry of Environment and Energy. https://wfdver.ypeka.gr/el/home-gr/

Obahoundje S, Youan Ta M, Diedhiou A, Amoussou E, Kouadio K (2021) Sensitivity of Hydropower Generation to Changes in Climate and Land Use in the Mono Basin (West Africa) using CORDEX Dataset and WEAP Model. Environmental Processes 8: 1073–1097 (2021). https://doi.org/10.1007/s40710-021-00516-0

Using uncertain rainfall projections in hydrological models: An approach to collate practical insights for decision-making under climate change

F.M. Mourot[1,2*], D.J. Irvine[1,2], T.A. Remenyi[3,4], L.B. Hutley[1], R.S. Crosbie[5], C.R. Moore[6]
[1] Research Institute for the Environment and Livelihoods, Charles Darwin University, Northern Territory, Australia
[2] National Centre for Groundwater Research and Training, Adelaide, Australia
[3] Acclimatised Pty Ltd, Hobart, Australia
[4] Eratos Australia Pty Ltd, Melbourne, Australia
[5] CSIRO, Environment, Waite Campus, Adelaide, Australia
[6] GNS Science, Lower Hutt, New Zealand
* e-mail: frederique.mourot@cdu.edu.au

Introduction

Climate change projections are, in essence, uncertain. These projections are usually based on theoretical scenarios (e.g., the Shared Socioeconomic Pathway (SSP)– Representative Concentration Pathway (RCP) scenarios, van Vuuren & Carter 2014). In addition to uncertainties from the different pathways, further uncertainty is also introduced by the simplifications and hypotheses of Global Climate Models (GCMs) used to project future climate variables and by natural climate variability.

Hydrological models commonly use GCM ensemble-derived climate variables as inputs to project future impacts of climate change on water resources to capture some of these uncertainties (Crosbie et al. 2013). GCM ensemble-derived climatic and hydrological variables often present large inter-model differences, with low model agreement on projected variables for certain regions (e.g., see Douville et al. 2022). In this context, the use of hydrological projections to guide water management is particularly challenging.

Using a case study in Northern Australia, where future rainfall projections are uncertain (Srikanthan et al. 2022), here we present an approach to collate hydrological model outputs that can effectively support decision-making (theoretical approach presented by Mourot et al. (2025).

Materials and methods

To encompass future rainfall projection uncertainty, we used three scenarios (SSP1-2.6, SSP2-4.5 and SSP3-7.0). For each scenario, we used an ensemble of 15 high-resolution GCM members from the latest Coupled Model Intercomparison Project (CMIP6), collated and dynamically downscaled by Chapman et al. (2023). Our projections were developed from 1960 to 2100, covering a historical period and two future horizons (mid-century and end-century).

We applied our approach to the Daly River catchment (53,700 km^2) in Northern Australia, which has a tropical monsoonal climate. The Daly River catchment has limited surface water resources available for water use, owing to water management approaches in the region. This catchment heavily relies on groundwater and is the object of increasing water demand. Accordingly, we focused our hydrological modeling on groundwater recharge (GWR), a crucial component of the hydrological cycle that can be significantly impacted by climate change and human activities (Smerdon 2017). We selected a simple lumped recharge model (LUMPREM, Doherty 2020) to alleviate the computational burden associated with the use of multiple scenarios and GCM climate variables and to test as many future climate scenarios as possible. Hydrogeomorphic units (HGUs) with similar climate, hydrogeology, soil characteristics and land use were used to report future GWR and to provide further efficiencies for the numerical modelling.

We used Python to prepare LUMPREM inputs, run the simulations and assess the output files, providing projected changes in groundwater recharge.

Results and concluding remarks

Projected changes in GWR point to differences according to GCM members. For instance, for SSP3-7.0, GWR changes between the historical period and the end of the century are projected to be limited when using NorESM2-MM and more significant when using CNRM-CM6 and ACCESS-CM2 (Figure 1).

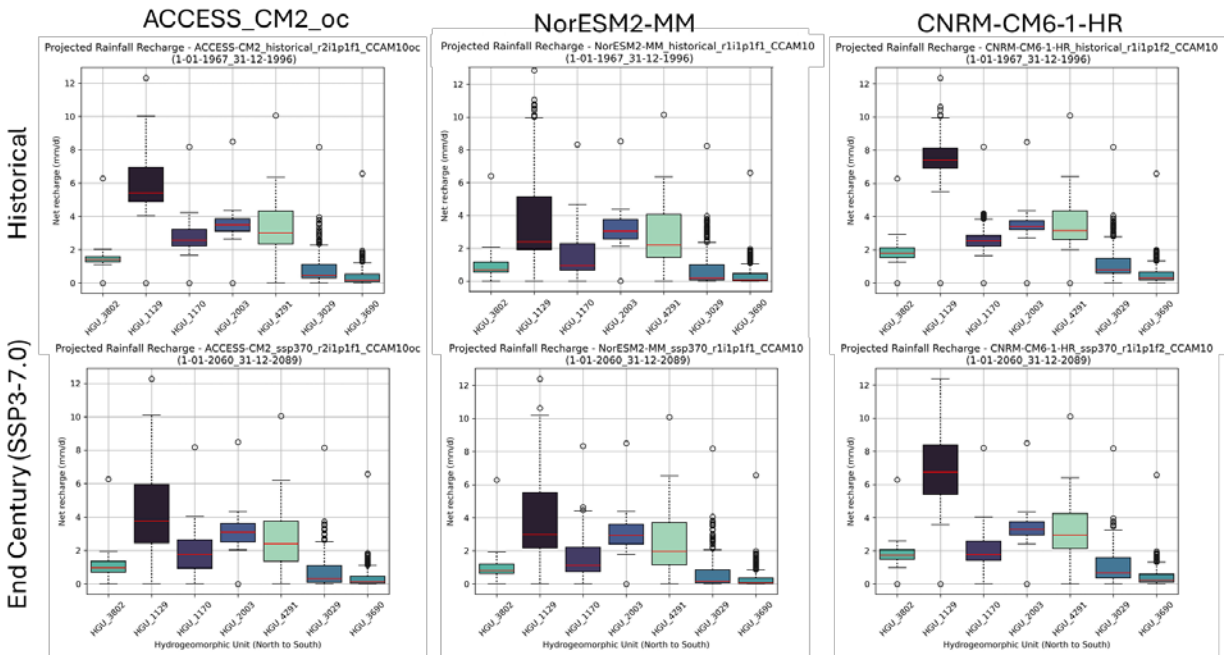


Figure 1. Groundwater recharge projections for exemplar hydrogeomorphic units in the Daly River catchment.

Spatial differences are also projected with GWR that greatly varies between HGUs. In addition to climate change, land use changes are projected to have significant impacts on GWR in the catchment. Results from the numerous numerical simulations tested with different scenarios, GCM members and land use changes will support water management decisions to help maintain water security in the Daly River catchment.

Acknowledgments: This research has been supported by the Cooperative Research Centre for Developing Northern Australia (Water Security Program, Grant no. AT.7.2223014). Additional support has also been provided by the Australian Government Research Training Program.

References

Chapman S, Syktus J, Trancoso R, Thatcher M, Toombs N, Wong KKH, & Takbash A. (2023). Evaluation of dynamically downscaled CMIP6CCAM models over Australia. Earth's Future, 11, e2023EF003548. https://doi. org/10.1029/2023EF003548

Crosbie RS, Scanlon BR, Mpelasoka FS, Reedy RC, Gates JB, & Zhang L. (2013). Potential climate change effects on groundwater recharge in the High Plains Aquifer, USA. Water Resources Research, 49(7), 3936 3951. https://doi.org/10.1002/wrcr.20292.

Doherty J. (2020). A simple lumped parameter model for unsaturated zone processes (p. 31). Watermark Numerical Computing. https://gmdsi.org/blog/tutorial-lumprem/

Mourot FM, Irvine DJ, Remenyi TA, Hutley LB, Crosbie RS, & Moore C. Producing Hydrological Projections under Climate Change: A Groundwater-inclusive Practitioners' Guide. Authorea Preprints. 2025 Jan 11. http://doi.org/10.22541/essoar.173655360.06047722/v1

Smerdon BD. (2017). A synopsis of climate change effects on groundwater recharge. Journal of Hydrology, 555, 125-128. https://doi.org/10.1016/j.jhydrol.2017.09.047

Srikanthan S, Bende-Michl U, Oke A, Hope P, Vjekoslav M, Kahn Z, Thomas S, Sharples W, Kociuba G, Peter J, Vogel E, Wilson L, & Turner M. (2022). Monsoonal North-National Hydrological Projections Assessment report. p. 72. Bureau of Meteorology, AU.

van Vuuren DP & Carter TR. (2014). Climate and socio economic scenarios for climate change research and assessment: Reconciling the new with the old. Climatic Change, 122(3), 415-429. https://doi.org/10.1007/s10584-013-0974-2

Evaporation fraction presented in a climatic energy balance diagram illustrates climate change and its consequences

L. Báder
Budapest University of Technology and Economics, Department of Hydraulic and Water Resources Engineering, Faculty of Civil Engineering, H-1111 Műegyetem rkp. 1. Budapest, Hungary.
** e-mail: laszlo.bader@edu.bme.hu*

Introduction

The impact of global warming on the hydrological cycle has become an area of intensive research. The Danube basin loses 1km^3 of water per year (Báder et. al 2023a). Evaporative forcing increases with warming (driving more evaporation where water is available), but potential evaporation increases faster (Báder & Szilágyi 2023). The availability of moisture for evaporation may become critical (Jung et al., 2010), consequently the function of evaporation in distributing climatic energy may also become critical. Further research is urged to study the role of vegetation in surface cooling (Ellison et al. 2024).

Evaporation is seen more and more as a key ecological service for sustainability of landscape environmental conditions. Recently it is converging towards a more complex functional view from the traditional interpretation of evaporation as a loss factor in the hydrological cycle (Báder et. al 2023b). The objective of this study is to contribute to the paradigm shift with an easy to use visualisation tool and promote evaporation fraction as an easy to use indicator to assess the status of land surface cover.

Materials and methods

Data used are from the ECMWF ERA5-Land reanalysis database with spatial resolution of 0.1° × 0.1°. Monthly averaged data were downloaded for net short- and long-wave radiation parameters to get net radiation (Rn = „ssr" + „str") and rolled up to annual values. Evaporative Fraction (EF) is the portion of net radiation that is absorbed by evaporation (parameter "e") and removed from the surface as latent heat and is calculated as EF = e/Rn. All flux measurement units were converted to water-depth equivalents via the latent heat of vaporization (2.48 MJkg^{-1}). Average value of the evaporation fraction in the Danube region is around 0.7 with no significant trend of the overall annual averages. Spatial analysis grid point by grid point, however, uncovers remarkable changes (Fig. 1.), in several areas with significant trends (Báder 2025).

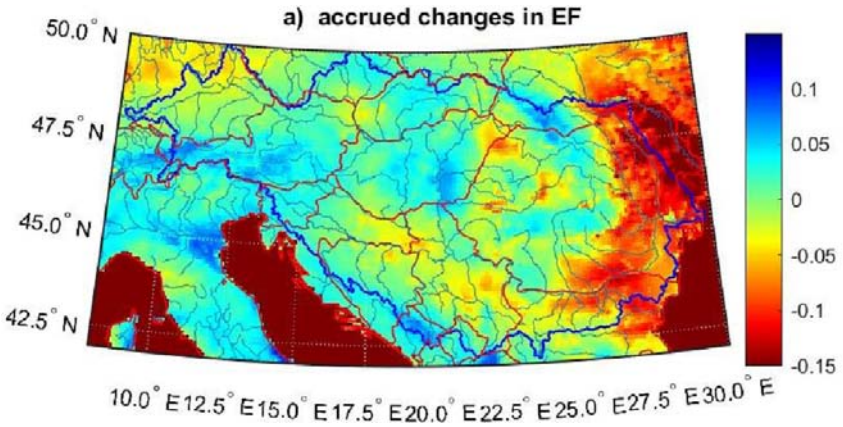


Figure 1. Spatial distribution of accrued changes in annual evaporative fraction in the Danube region in 1991–2020.

Evaporative fraction can be interpreted as an efficiency indicator of the energy distribution process on the land surface. Using the simplified energy balance equation Rn = ET + H, where H is the thermal energy flux (sensible heat), the values determine a "working point" and can be plotted on the ET-H plane. Smaller terms of a more complex energy balance equation, such as ground heat flux, stored energy, etc., are

neglected at first approximation as they average out over several years. Based on the balance equation Rn = ET + H, the ET and H points meet on the 45° traverse line. The plot can be called Climatic Energy Balance Diagram (CEBD) and can be prepared with absolute values and in normalized form, values rated to Rn.

Results and concluding remarks

The Climatic Energy Balance Diagrams are shown for the Danube region and demonstrated for 2 other areas in Fig 2. The CEBD with annual average absolute values shows that the annual working points of the Danube region are in a relatively close range (in red and blue). Notable that despite the huge difference of the available energy for evaporation between Danube region and the Amazon rainforests (in green), the latter one can still keep sensible heat level low. Analysing the amount of sensible heat remaining on the surface in Danube region and central Spain (in yellow), it is almost the double compared to that of the Amazon region.

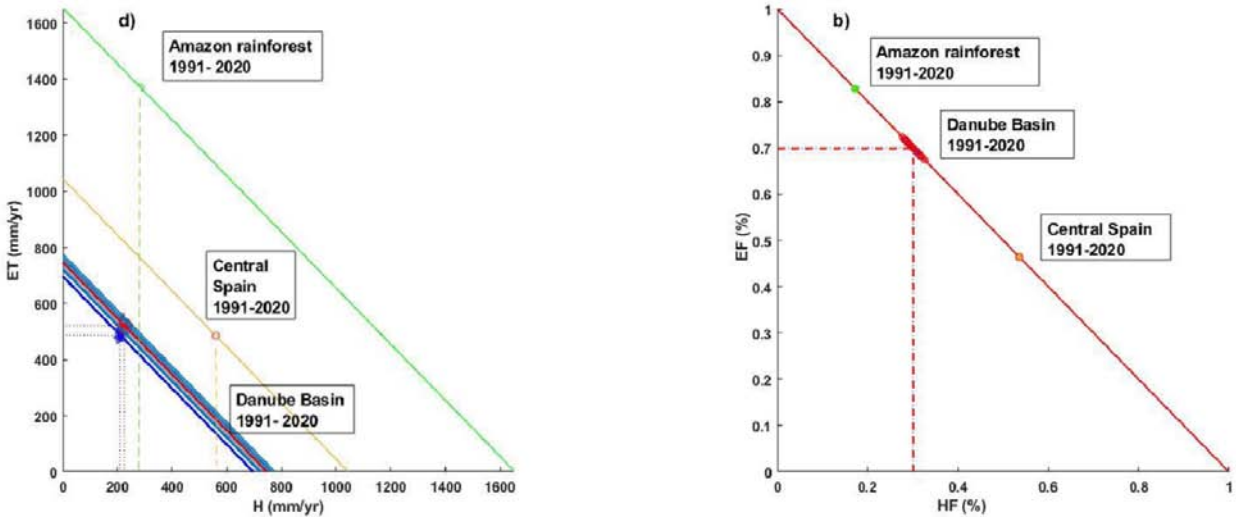


Figure 2. Climatic Energy Balance Diagram (CEBD) for 3 different regions in 1991-2020. Left: annual average absolute values demonstrate the energy levels involved in the process. Right: normalized version allows comparison of areas in different climatic zones.

The benefit of the CEBD diagram is that it is easy to create from a few parameters (or reuse Bowen rate data from earlier studies), and the interpretation is intuitive. Visualization helps to point to the fundamental process, to the energy dissipation process and the importance of availability of water in the landscape. Further analysis is in progress to address the role of vegetation and surface cover.

Acknowledgments The research was funded by the Sustainable Development and Technologies National Program of the Hungarian Academy of Sciences (FFT NP FTA)

References

Báder, L., (2025) The Climatic Energy Balance Diagram (CEBD) highlights changes in the hydrological cycle of the Danube River basin. J. Hydrol. Hydromech., 73, 2025, 1, 24–33 https://doi.org/10.2478/johh-2025-0001

Báder, L., Szilágyi, J., (2023) Widening Gap of Land Evaporation to Reference Evapotranspiration Implies Increasing Vulnerability to Droughts in Hungary. Periodica Polytechnica Civil Engineering. https://doi.org/10.3311/PPci.21836

Báder, L, Szilágyi, J., Négyesi, K., Nagy, E., Földváry, L., (2023a) Changes and trends in the climatic water balance of the Danube River basin based on meteorological, hydrological, and gravimetric data for the period 1961-2020. In: Proc. HydroCarpath Conference, Vienna Austria, 9. Nov. 2023. https://doi.org/10.35511/978-963-334-505-4

Báder, L., Szilágyi, J., Négyesi, K., (2023b) Freshwater paradox: will saving of water help in mitigating climate change or increase the instability of the hydrological cycle? In: Proc. EMS Annual Meeting 2023, Bratislava, Slovakia, 4–8 Sep 2023, EMS2023-528. https://doi.org/10.5194/ems2023-528

Ellison, D., Pokorný, J., Wild, M., 2024. Even cooler insights: On the power of forests to (water the Earth and) cool the planet. Global Change Biology, 30, e17195. https://doi.org/10.1111/gcb.17195

Jung, M., Reichstein, M., Ciais, P. et al., 2010. Recent decline in the global land evapotranspiration trend due to limited moisture supply. Nature, 467, 951–954. https://doi.org/10.1038/nature09396

Flood frequency analysis of two Mediterranean river basins by using convection-permitting model projections and a rainfall-runoff model

M. Lompi[1*], J. El Jeitany[1], O. Boulariah[2], F. Viola[2], M. Borga[3], R. Deidda[2], E. Caporali[1]
[1] Department of Civil and Environmental Engineering, University of Florence, Florence, Italy
[2] Department of Civil Engineering and Architecture, University of Cagliari, Cagliari, Italy
[3] Department of Land, Environment, Agriculture and Forestry, University of Padova, Padova, Italy
* e-mail: marco.lompi@unifi.it

Introduction

Changes in extreme precipitation are expected in a warmer climate with possible impacts on the frequency of flood events. Assessing the expected changes in the flood frequency distributions is essential for adaptation strategies. The impact of climate change on flood events is usually evaluated using climate projections of Regional Climate Models (RCM) in rainfall-runoff models. However, RCM projections often lack the resolution needed to accurately describe convective storms, leading to underestimating the intensity of extreme precipitation events, which are typically responsible for flash floods in small river basins. This study aims to analyse the future flood frequency in two river basins in the Mediterranean context with bias-corrected convection-permitting model projections, which have been demonstrated to increase the performance in capturing extreme precipitation.

Materials and methods

The methodology applied in this work is shown in the flowchart in Figure 1.

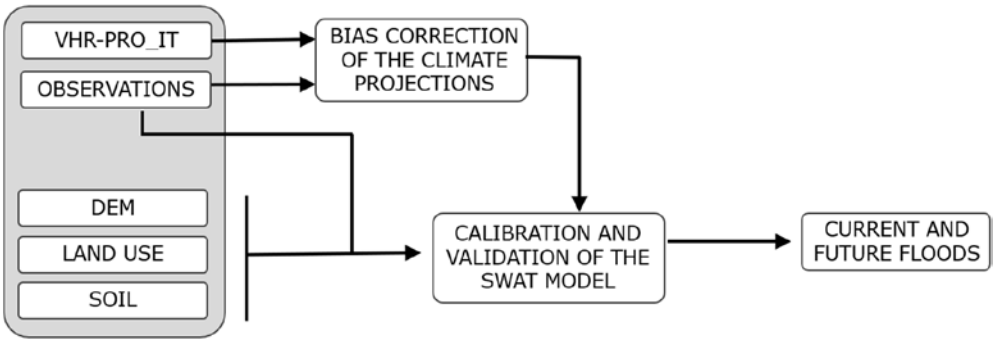


Figure 1. Flowchart of the methodology to assess the impact of climate change on the flood frequency distribution.

Digital Elevation Model (DEM), land use, and soil data are used to prepare the Soil and Water Assessment Tool Plus (SWAT+), a semi-distributed and continuous hydrological model (Arnold et al., 1998). Observation from rain gauges, thermometers, and hydrometers are used to calibrate and validate the model and assess the flood frequency distribution under the current climate. Ground observations from rain gauges and thermometers are also used to bias-correct the climate projections. The projections are derived from VHR-PRO_IT, Very High-Resolution Projections over Italy (Raffa et al., 2023). These projections have a spatial resolution of 2.2 km and a temporal resolution of 1 hour, spanning 90 years from 1981 to 2070 under two emission scenarios: RCP 4.5 and RCP 8.5. The bias correction of precipitation projections is performed using a parametric approach (Mamalakis et al., 2017), which adjusts the frequency distribution of daily precipitation events. In contrast, temperature projections are corrected using a more straightforward method based on the linear scaling of monthly average temperatures. The bias-corrected projections are the input of the SWAT model, enabling a 90-year continuous simulation. The annual maximum series are extracted from simulated daily discharge in the two scenarios. Then, a Generalized Extreme Value Distribution is used to fit the cumulative distribution of the maximum discharge to assess the flood frequency in three-time windows with a 30-year length: 1981–2010 (Historical), 2011–2040 (Near

Future), and 2041–2070 (Far Future).

The methodology is applied in two Mediterranean river basins: the Arno River and the Allai Creek catchments (Figure 2). The Allai catchment, with a river basin area of 780 km^2, is located in Sardinia and is part of the Tirso basin. The other case study is the Arno River basin upstream of the Ponte a Signa hydrometer. The outlet is slightly downstream of the city centre of Florence and the river basin area is about 4640 km^2.

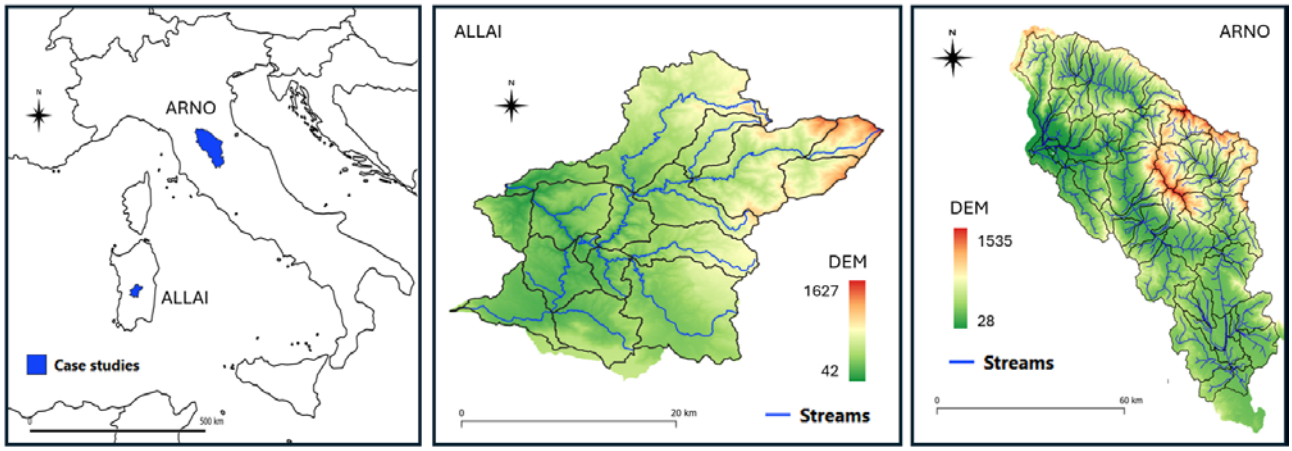


Figure 2. The Allai catchment and the upstream part of the Arno River basin are chosen as case studies.

Results and concluding remarks

The results show how the VHR-PRO_IT projections underestimate the observed precipitation and how the bias correction was necessary to adjust the total rainfall and the frequency of the extreme events in the two river basins. The calibration and validation of the SWAT+ model show a good performance based on Moriasi et al. (2015) in describing the discharges in the two case studies. The flood frequency distributions of the two river basins show an increase in the flood quantiles, especially in the RCP 8.5 scenario in the far future, highlighting the importance of adaptation measures to consider an increase in the flood hazard.

Acknowledgements: The research is carried out within the RETURN – multi-Risk sciEnce for resilienT comUnities undeR a changiNg climate Extended Partnership and received funding from the European Union Next-GenerationEU (National Recovery and Resilience Plan – NRRP, Mission 4, Component 2, Investment 1.3 – D.D. 1243 2/8/2022, PE0000005).

References

Arnold JG, Srinivasan R, Muttiah RS, Williams JR (1998) Large area hydrologic modeling and assessment Part I: model development. Journal of the American Water Resources Association, 34, pp. 73-89, https://doi.org/10.1111/j.1752-1688.1998.tb05961.x

Raffa M, Adinolfi M, Reder A, Marras GF, Mancini M, Scipione G, Santini M, Mercogliano P (2023) Very High Resolution Projections over Italy under different CMIP5 IPCC scenarios. Scientific Data, 10, 238. https://doi.org/10.1038/s41597-023-02144-9.

Mamalakis A, Langousis A, Deidda R, Marrocu M (2017) A parametric approach for simultaneous bias correction and high-resolution downscaling of climate model rainfall. Water Resources Research, 53:2149–70. http://doi.wiley.com/10.1002/2016WR019578

Moriasi D, Gitau M, N. Pai N, P. Daggupati P (2015) Hydrologic and Water Quality Models: Performance Measures and Evaluation Criteria. Transaction of the American Society of Agricultural and Biological Engineering, 58, 1763-1785, https://doi.org/10.13031/trans.58.10715

Hydrologic and hydraulic modeling of an urban area using SWMM: climate change and land use impacts

A.V. Tsihrintzis[1*], I.M. Kourtis[2], E. Baltas[1]
[1] *Department of Water Resources, School of Civil Engineering, National Technical University of Athens, 9 Heroon Polytechniou St., 15780 Zographou, Athens, Greece*
[2] *Center for the Assessment of Natural Hazards and Proactive Planning & Laboratory of Reclamation Works and Water Resources Management, School of Rural, Surveying and Geoinformatics Engineering, National Technical University of Athens, 9 Heroon Polytechniou St., 15780 Zographou, Athens, Greece*
** e-mail: tsihrin@gmail.gr*

Introduction

Hydrologic and hydraulic modeling of urban areas is of utmost importance to determine areas of increased flooding risk, in an effort to avoid human life fatalities and reduce economic losses. Recent studies indicate increases in flood intensities and frequencies of extreme rainfall events (e.g., Kourtis et al. 2023). This study presents the hydrologic and hydraulic modeling of a sub-catchment area of the combined sewer system of Athens using the Storm Water Management Model (SWMM) developed by USEPA.

Materials and methods

The study area is the sub-catchment Z2 (0.66 km^2) of the combined sewer system of Athens, which is part of a larger area of 12 sub-catchments ultimately draining in Kifisos river (Fig. 1). The drainage system of area Z2 is shown in Fig. 1 (Tsihrintzis 2023).

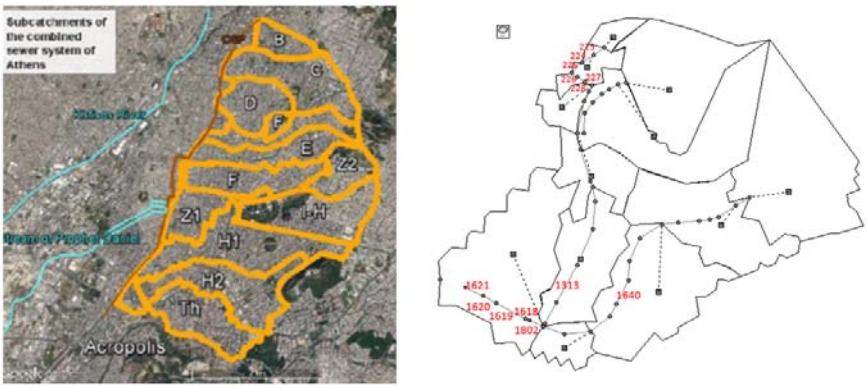


Figure 1. Location of the study area Z2 (left). Drainage system of area Z2 (right).

The hydrologic-hydraulic model of the study area was configured employing SWMM software. Manual calibration was based on a historical rainfall episode (1/1/2005) for which there were actual measurements of runoff hydrographs at two points (conduits 1313 and 1640) and comparison with model results using statistical coefficients (NSE, RMSE, NOF, PBIAS, etc). Calibration parameters included the: Curve Number (CN), percent of imperviousness, slope and width of each sub-area, and Manning coefficients for impervious and pervious areas and the storm sewers.

Runoff hydrographs were produced for various return periods (2, 5, 10, 25, 50 and 100 years) and rainfall duration of 1 hour using the alternate block method and current and future (under climate change) Intensity-Duration-Frequency (IDF) curves. Three future IDF curves were considered (Kourtis et al. 2023), and included mean, upper and lower limit climate change projections for year 2100. Scenarios of increase of the studied historical rainfall from 7% to 25% were also tested using the model. A hypothetical scenario of land use change was also examined by changing a part of a park to continuous urban fabric. The significance of these changes on the flow magnitude were statistically tested by the Student t-test at a 5% confidence level.

Results and concluding remarks

Model calibration showed good results with NSE values of 0.897 (Conduit 1313) and 0.545 (Conduit 1640).

When the current IDF curves were used, the capacity of the system outlet conduit is adequate in carrying runoff for rainfalls up to 100 years (Fig. 2). When using the future IDF curves for the mean climate change projections, flooding occurs for return periods of more than 50 years (Fig. 2), while for the upper limit projection, the capacity is exceeded to the 10-year storm (Fig. 3).

Furthermore, the model response to the possibility of higher rainfall depths (7% to 25% increase in the historical hyetograph) revealed non-significant increase in the runoff hydrograph.

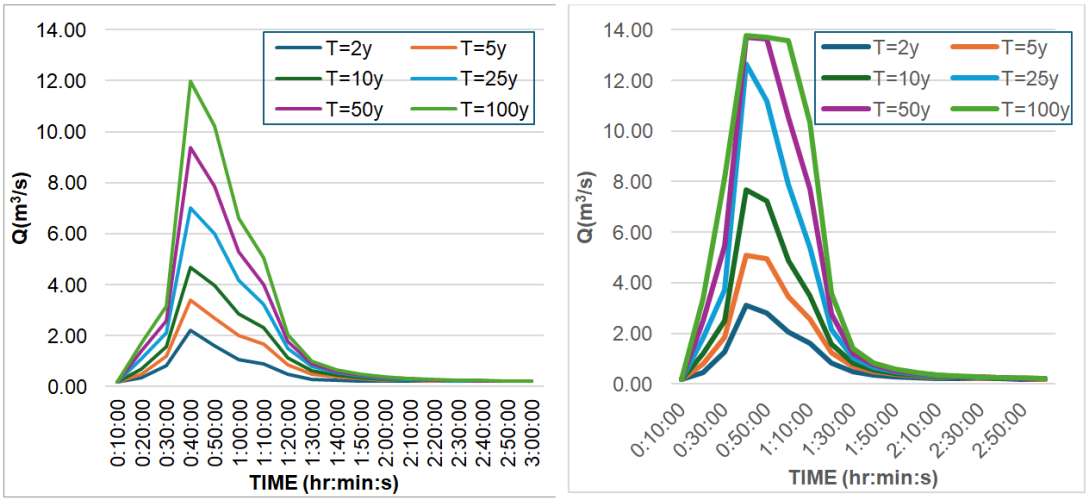


Figure 2. Predicted hydrographs of the sewer network outlet for return periods of 2, 5, 10, 25, 50 and 100 years: current IDF curves based on the Flood Risk Management Plan for Attica River Basin District (EL06 - 2017) (left); future IDF curves of the mean projection for year 2100 (right).

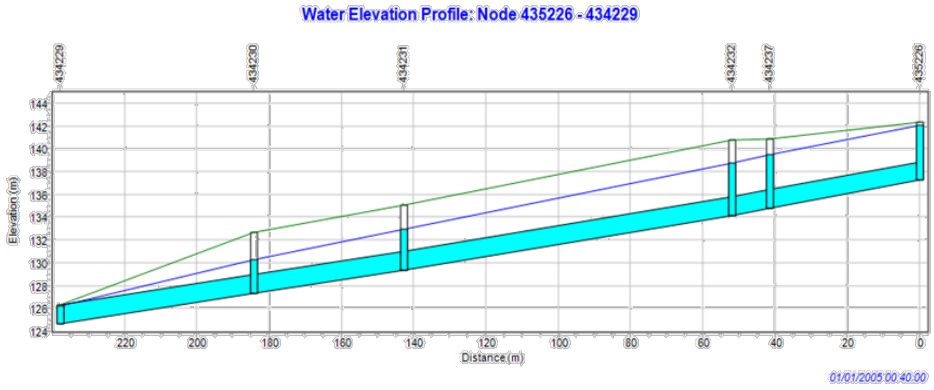


Figure 3. Profile of system conduits 1802, 1618, 1619, 1620, and 1621 for return periods of 10 years at the time of the peak of the hydrograph for the future IDF curves of the upper limit climate change projections. Surcharge is indicated. Line code: Conduits (black), water (blue), storm sewer (black), piezometric line (purple), ground surface (green), and catch basin laterals (vertical lines).

References

Kourtis IM, Nalbantis I, Tsakiris G, Psiloglou B, Tsihrintzis VA. (2023). Updating IDF Curves under Climate Change: Impact on Rainfall-Induced Runoff in Urban Basins. *Water Resources Management* 37(6-7):2403–2428. https://doi.org/10.1007/s11269-022-03252-8.

Tsihrintzis A. (2023). Hydrological and Hydraulic Modeling Using the SWMM Model in the Area of Attico Alsos Under Changing Conditions, Post-graduate Thesis, Graduate Program “Science and Technology of Water Resources”, National Technical Univeristy of Athens, Zographou, Athens, Greece (in Greek)

A long-term analysis for changes in temperature regime over Sicily

D. Treppiedi*, C. Mattina, N. Scinta, A. Francipane, L.V. Noto
Department of Enigneering, University of Palermo, Palermo, Italy
** e-mail: dario.treppiedi@unipa.it*

Introduction

During the last ten years, global temperature records have been continuously broken, with each year ranking among the hottest ever recorded. In this context, the 2024 is particularly significant since it marked the first year where the global average temperature surpassed 1.5 °C above pre-industrial levels (Tollefson, 2025), established as the critical limit for avoiding severe climate disasters by the Paris Agreement. Human activities have played, continue to play, and will probably play, a dominant role in driving global warming. The impacts of this changes are evident in many areas of the world, with increased frequency and intensity of extreme weather events, rising sea levels, and the destruction natural ecosystems.

The Mediterranean area has been identified as a "hotspot" for global warming, being particularly responsive to rising temperatures (Lionello and Scarascia, 2018). Several studies have shown that this area is warming at a faster rate than the global average, and this trend will probably continue also in the future. This is expected to have profound implications for the region's climate system, affecting precipitation patterns, evapotranspiration rates, and, consequently, water availability. Many areas within the Mediterranean basin are already experiencing a growing water scarcity, which in turn threatens agricultural productivity, biodiversity, and so on. The combination of rising temperatures and declining water availability is likely to drive an increasing process of aridification, with severe environmental, economic, and social impacts for millions of people.

In this context, it is essential to move from a macro-regional spatial perspective to a more detailed, in order to better understand how different areas within the Mediterranean basin are responding to global warming. This helps to identify the most vulnerable areas and develop specific adaptation strategies to mitigate the effects of climate change.

Materials and methods

We focus our analysis on Sicily Island, which lies in the hearth of the Mediterranean Sea. The island is characterized by a hot-summer Mediterranean climate, which is representative of a large portion of the Mediterranean area. Moreover, due to its position, it represents a transition between the arid climate of North Africa and the temperate climate of continental Europe.

To examine the potential changes in the island's climate, we use observed time series of maximum and minimum temperatures recorded by various meteorological stations managed by the Sicilian Autorità di Bacino (Adb). These records span almost 100 years (i.e., 1924 to 2021), providing a long-term dataset for assessing temperature trends and variability over the past century. Since time series can be affected by uncertainty and data gaps, especially in the early years of the network's life, the dataset used in this study has been restricted to the most temporally homogeneous records. Only time series with minimal interruptions and no evident breakpoints (generally caused by station relocations) were considered to ensure data reliability and consistency in the analysis.

To gain a thorough understanding of the potential changes, we computed various indicators from the daily maximum and minimum temperatures. We focus on different ETCCDI indices (Peterson et al., 2001), as well as on the definition of heatwaves events (HWs). Regarding the latter, different methodologies exist for their identification. Among all, we focused on two specific criteria:

- Exceedances of the 95th percentile of daily maximum temperatures, calculated over the 1961–1990 climatological normal, using a 10-day moving window (five days before and five days after the given Julian day), for at least three consecutive days (Stefanon et al., 2012).

- Exceedances of the daily mean temperature for the 1961–1990 climatological normal by at least 5°C (computed using the same 10-day window) for at least three consecutive days (Frich et al., 2001).

For both methods, HWs separated by just one day were considered part of the same event. We then analyzed the key characteristics of the identified HW events, including their start and end dates, duration, mean intensity, and peak intensity. For all the ETCCDI indices and HW characteristics, we applied various statistical tests (e.g., Poisson regression, Mann-Kendall test, etc.) to assess the presence of significant trends over time at different temporal scales (e.g., annual, seasonal, and monthly).

Results and concluding remarks

The obtained results show that changes over time in daily maximum and minimum temperatures are both evident and statistically significant, confirming that Sicily is experiencing the effects of global warming. For most of the stations examined, the observed trends align with those identified at a broader spatial scale for the Mediterranean region. As an example, Figure 1 shows a statistically significant increase in the annual frequency of HW events for the Licata station (southwestern Sicily), especially during the last decades.

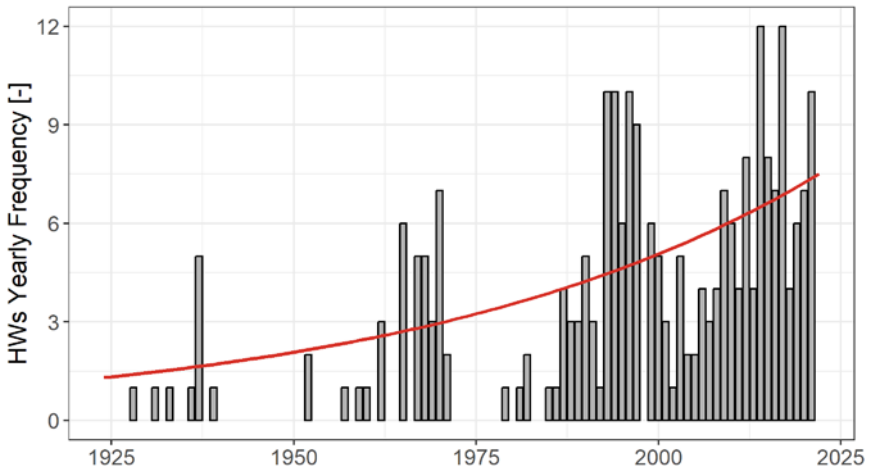


Figure 1. Annual trend in the frequency of heatwaves (HWs) for the Licata station.

Further analyses will aim to identify potential correlations between the observed trends and major large-scale atmospheric circulation mechanisms, such as the Atlantic Multidecadal Oscillation (AMO), the North Atlantic Oscillation (NAO), and the occurrence of blocking anticyclones. Understanding these connections could enhance the comprehension of the warming dynamics in Sicily.

References

Frich, P. A. L. V., Alexander, L. V., Della-Marta, P., Gleason, B., Haylock, M., Tank, A. K., & Peterson, T. (2002). Observed coherent changes in climatic extremes during the second half of the twentieth century. Climate research, 19(3), 193-212.

Lionello, P., & Scarascia, L. (2018). The relation between climate change in the Mediterranean region and global warming. Regional Environmental Change, 18, 1481-1493.

Peterson, T., Folland, C., Gruza, G., Hogg, W., Mokssit, A., & Plummer, N. (2001). Report on the activities of the working group on climate change detection and related rapporteurs (p. 143). Geneva: World Meteorological Organization.

Stefanon, M., D'Andrea, F., & Drobinski, P. (2012). Heatwave classification over Europe and the Mediterranean region. Environmental Research Letters, 7(1), 014023.

Tollefson, J. (2025). Earth breaches 1.5° C climate limit for the first time: what does it mean?. Nature, 637(8047), 769-770.

A semi-analytical approach for drainage network sizing and verification

D. Martino*, D. Pirone, A. D'Aniello, L. Cimorelli, D. Pianese
Department of Civil, Architectural and Environmental Engineering, University of Naples Federico II, Naples, Italy
** e-mail: daniele.martino2@unina.it*

Introduction

The design and verification of sewer networks are essential for urban water management, influencing flood risk mitigation and infrastructure resilience. Traditional methods often rely on oversimplified assumptions, such as neglecting surface runoff (Keifer and Chu, 1957) or using empirical parameters with little physical significance (Supino, 1947), leading to inaccurate drainage system sizing. Additionally, some approaches fail to fully exploit Intensity-Duration-Frequency (IDF) curves, missing critical insights for peak flow estimation (Chow, 1962). To overcome these limitations, this study proposes a semi-analytical approach that accurately models upstream runoff and optimally utilizes IDF curves through a variational method. This approach ensures more precise and efficient sewer network design by identifying critical peak inflow conditions while maintaining computational speed and transparency.

Overall, the proposed methodology provides a reliable alternative to traditional techniques, enhancing sewer network performance and adaptability to changing urban and climatic conditions.

Materials and methods

The proposed Semi-Analytical Approach evaluates the maximum flow in a sewer pipe of defined characteristics (i.e., diameter, slope, etc.). It models the basin upstream of the sewer pipe as a linear reservoir, which requires the lag time as a design parameter, and considers the rational method to evaluate the effective inflow discharge, thus the fraction of precipitation that reaches the basin as surface runoff. Then, the approach exploits all the information from the IDF curve (expressed as $i_{d,T}=a_T\ d^{\beta-1}$) through a variational method that searches for the critical rainfall duration that maximises the incoming flow in the sewer pipes (Cimorelli et al., 2015). In this way, the incoming flows, thus the Flow Duration Reduction (FDR) curves, are analytically linked to the IDF curves parameters and upstream basin parameters (Equations 1).

$$Q_{D,d^*} = p_{d^*} \frac{k}{D}\left\{\frac{d^*}{k} - \ln\left[1 - e^{-\frac{D}{k}}\left(1 - e^{\frac{d^*}{k}}\right)\right]\right\} \quad (1)$$

where D is the flow duration, d* is the rainfall duration that maximizes, for each D considered, the maximimum mean discharge entering the sewer pipe, and k is the "lag time" needed to characterize the way the whole basin upstream contributes to the formation of discharge Q_D.

Finally, the approach exploits all the information from the FDR curve through a maximizing approach that searches for the critical flow duration D* that maximises the peak flow Q_u outflowing the sewer pipe (Pirone et al., 2025). In fact, knowing sewer pipe characteristics, such as length, cross-section shape, slope, etc., the uniform hydrographs over the durations D are propagated using a kinematic model (Equation 2),

$$q_u = \frac{1}{n_M} R^{\frac{2}{3}} \sigma\, i^{\frac{1}{2}} \approx \mu\, \omega^{\alpha} = \mu \left(\frac{w}{L}\right)^{\alpha} = \frac{\mu}{L^{\alpha}} w^{\alpha} \Leftrightarrow w = \frac{L}{\mu^{\frac{1}{\alpha}}} q_u^{\frac{1}{\alpha}} \Leftrightarrow w = c\, {q_u}^{v} \quad (2)$$

whose approximate solution for the maximum discharge Q_u leaving the sewer pipe is analytically known (Pirone et al., 2025). Then, coupling this analytical solution with a maximizing procedure (given by the COBYLA algorithm; Powel, 2007), the maximum discharge ${Q_u}^*$ leaving the sewer pipe is obtained very quickly.

Therefore, the method requires the basin parameters (area, runoff coefficient, and lag time), the IDF curve parameters and pipe parameters (length, cross-section, slope, and material). They are all known values except for the lag time, which can be evaluated according to existing formula (Desbordes, 1974). Moving downstream within the network, it is assumed that all elements upstream (pipes+basins) can be schematised as a linear reservoir.

Furthermore, this work offers two formulations for estimating the lag time by correlating it to physical parameters such as basin upstream area (A), rational coefficient (φ), travel time (t_p).

$$\widehat{k_1} = 10^{(c+m_1 \log t_p + m_2 \log \varphi_{averaged} + m_3 \log A)} \quad (3)$$

$$\widehat{k_2} = a\, t_p + k_0 \quad (4)$$

The proposed formulas for the lag time have been obtained by implementing the procedure in the software SWMM (Stormwater Management Model) on seven synthetic sewer networks, setting the slope of the basins variable in the range 0.05% - 0.5% and the coefficient of Manning equal to 0.02 $s \cdot m^{-1/3}$. Specifically, the hydrological module of SWMM allowed for the evaluation of the FDR curves, which were used to calibrate the k value in Eq. 1, and then to obtain the "true" lag times. Then, these were correlated with the aforementioned parameters to obtain Eqs.3 and 4.

Results and concluding remarks

The following results (Figure 1) compare the peak flows in each pipe of the sewer networks computed using the numerical method (Q_{NA}) coupled to the "maximizing approach" with those obtained by: a) the S-AA (Semi-Analitycal Approach), carried out by considering, in Eq. 1, the "true" lag time ($Q_{S\text{-}AA\text{-}C}$), b) the S-AA carried out by considering, in Eq. 1, the k values obtained by Eq. 3 ($Q_{S\text{-}AA\text{-}R1}$), and c) the S-AA carried out by considering, in Eq. 1, the k values obtained by Eq. 4 ($Q_{S\text{-}AA\text{-}R2}$).

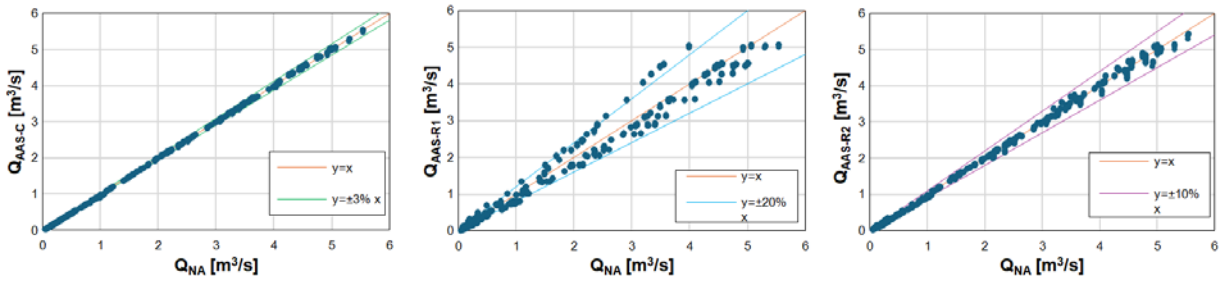


Figure 1. Maximum outflow discharge - Comparison between NA and S-AA.

The proposed Semi-Analytical Approach offers a computationally efficient alternative to a fully numerical model (Fig. 1), showing errors within ± 3% and ± 20%. Comparison shows that the approach based on Eq. 4 is better. While numerical methods provide detailed simulations of sewer network performance, they require significant computational resources and extensive calibration efforts. On the other hand, the Semi-Analytical Approach offers a streamlined solution that retains the essential hydrological and hydraulic complexities while reducing computational demands. This makes it particularly suitable for preliminary design and rapid assessment scenarios, where quick and reliable estimates are needed to guide decision-making.

One of the primary advantages of the semi-analytical approach is its ability to integrate detailed hydrological information without relying on oversimplified assumptions. By systematically analysing the IDF curve and employing a variational optimisation technique, this method identifies the most critical rainfall and flow duration, leading to a more accurate estimation of peak flows in the sewer pipes. Despite its advantages, the proposed method also presents some challenges that warrant further investigation.

References

Chow, V.T. (1962). Hydrologic design of culverts. Journal of Hydraulic Division, ASCE, 88 (2), 39-55.

Cimorelli, L., Cozzolino, L., D'Aniello, A., Morlando, F., Pianese, D. (2015). A simplified Approach for Stormwater Drainage Networks Sizing. J Climatol Weather Forecasting 3: 136. https://doi:10.4172/2332-2594.1000136

Desbordes, M. (1974). Reflections on the calculation methods for urban storm water systems. Thesis D.I., 224 pp., CNRS A0 9125, University of Sciences, Montpellier.

Keifer C.J. , Chu, H.S. (1957). Synthetic Storm Pattern for Drainage Design Journal of the Hydraulics Division, Vol. 83(4), https://doi.org/10.1061/JYCEAJ.00001

Pirone, D., Cimorelli, L., D'Aniello, A., Pianese, D. (2025). A novel Generalised Semi-Analytical Approach for flood control reservoir design. Under review.

Powell, M. J. D. (2007). A view of algorithms for optimization without derivatives. Cambridge University Technical Report DAMTP 2007

Supino, G. (1947). A few observations on the using of "volume di invaso" method to evaluate the specific flood contribution given by unit drained area (in Italian) 227-231.

VI. Environmental Vulnerability and Risk

Impact of light-absorbing impurities in snow on snowmelt runoff and hydrological processes in the Ili basin, Central Asia

B. Wu[1,2,3], J. Abuduwaili[1,2,3*]
[1] State Key Laboratory of Desert and Oasis Ecology, Key Laboratory of Ecological Safety and Sustainable Development in Arid Lands, Xinjiang Institute of Ecology and Geography, Chinese Academy of Sciences Urumqi 830011, P.R. China
[2] CAS Research Center for Ecology and Environment of Central Asia, Urumqi 830011, Xinjiang, P.R.China
[3] University of Chinese Academy of Sciences, Beijing 100049, P.R.China
* e-mail: jilil@ms.xjb.ac.cn

Introduction

Light-absorbing impurities (LAIs) deposited in snow, including mineral dust (MD), organic carbon (OC), and black carbon (BC), can reduce snow albedo and accelerate snowmelt. It has an important impact on regional water cycle and water resources (Xie et al., 2018; Kang et al., 2022). The Ili Basin has emerged as a significant depositional zone for LAIs owing to its unique geographical location and topography. Snowmelt-induced floods predominantly occur in northern Xinjiang, particularly in the Ili Basin (Sun et al., 2013). Therefore, quantitatively studying the impact of LAIs in snow on snowmelt in the Ili Basin and clarifying their contribution to snowmelt runoff have become urgent issues that need to be addressed. Research on light-absorbing impurities in snow and their impacts in the Ili Basin is still lacking. For example, Ye et al. (2012) measured BC concentrations at 32 sites in Xinjiang but did not investigate their impact on snowmelt. Zhong et al. (2019) analysed the radiative forcing caused by LAIs on snow in northern Xinjiang, but only two samples were taken from the Ili Basin. Liu et al. (2022) analysed the concentration of soluble ions and dissolved arsenic in snow utilised snow samples from 17 sampling points in the Ili Basin without examining the influence of LAIs on snowmelt. Thus, there is an urgent need to enhance the systematic understanding of the impact of LAIs on snowmelt in the Ili Basin.

This study used field sampling, situ monitoring and numerical simulation to shed light on the spatial features of LAIs in the snow and their influence on snowmelt in the Ili Basin in Central Asia. Firstly, this study investigated the spatial distribution of LAIs in snow based on LAIs and observational data of snow samples taken from the Ili Basin. Secondly, SNICAR models are used to quantitatively assess the influence of MD and BC on snow albedo, radiative forcing, and snowmelt duration in the Ili Basin..

Materials and methods

March marks the onset of snowmelt in the Ili Basin, and we selected the sampling period from March 1 to March 8, 2024. A total of 51 sampling points were selected and 297 samples were collected. Simultaneously with the collection of snow samples, parameters such as snow albedo, snow density, water content, snow depth, snow temperature, and snow grain size were measured. The MD concentration in the snow was determined by filtering through a quartz filter, while the BC and OC concentrations were measured using a DRI Model 2015.

The SNICAR model is a one-dimensional heterogeneous multilayer snow and ice model widely used to simulate the albedo of snow and ice surfaces. This study uses the method proposed by Painter et al. (2013) to calculate the radiative forcing caused by LAIs in the snow of the Ili Basin as follows:

$$RF = \sum_{0.325\mu m}^{2.500\mu m} E(\lambda,\theta)\left(\alpha_{(\gamma,\lambda)} - \alpha_{(\gamma,\lambda,imp)}\right)\Delta\lambda \quad (1)$$

where E represents the spectral irradiance (W/m^2), γ represents the diameter of the snow particles (μm), θ represents the solar zenith angle (°), α represents the snow albedo, λ represents the wavelength (μm), and imp represents the concentration of LAIs.

This study simulated the effect of LAI on snowmelt days in the Ili Basin (Schmale et al., 2017).

Results and concluding remarks

The mean concentrations of MD in the top layer (0–5 cm) and subsurface layer (5–10 cm) of snow in the Ili Basin are 77.50 μg/g and 54.69 μg/g, respectively, with higher concentrations found in the eastern Kunes River Basin and central plains. The mean BC concentration is 75.50 ng/g in the top layer and 143.80 ng/g in the subsurface layer, whereas the mean OC concentration is 484.15 ng/g in the top layer and 1903.86 ng/g in the subsurface layer, with higher concentrations occurring mainly in the southwestern Tekes River Basin and eastern mountainous regions.

MD plays a dominant role in reducing snow albedo, and its impact on the absorption of solar radiation by snow is greater than that of BC. MD and BC reduce snow albedo by 0.0399 and 0.0162, contributing 17.87% and 7.45%, respectively, to the reduction. MD and BC lower snow albedo by 0.0515, with a combined contribution of 21.86%. The radiative forcing caused by MD, BC, and MD + BC are 30.17 W/m^2, 12.31 W/m^2, and 39.10 W/m^2, respectively.

MD is the primary light-absorbing impurity responsible for the reduction in snow duration in the Ili Basin. MD reduces snow melt days by 1.81 ± 1.37 to 6.02 ± 4.56 days, whereas BC reduces snow melt days by 0.74 ± 0.97 to 2.45 ± 3.22 days. Under the combined effects of MD and BC, the number of snow melt days decreased from 2.19 ± 1.43 to 7.31 ± 4.76 days.

Table 1. Mean reduction in the number of snowmelt days by BC and MD under different SW and SWE values.

	SWE = 40 mm			SWE = 80 mm		
Shortwave	MD	BC	BD+MC	MD	BC	BD+MC
SW = 120 W/m^2	3.01 ± 2.28	1.23 ± 1.61	3.65 ± 2.38	6.02 ± 4.56	2.45 ± 3.22	7.31 ± 4.76
SW = 160 W/m^2	2.26 ± 1.71	0.92 ± 1.21	2.74 ± 1.79	4.51 ± 3.42	1.84 ± 2.42	5.48 ± 3.57
SW = 200 W/m^2	1.81 ± 1.37	0.74 ± 0.97	2.19 ± 1.43	3.61 ± 2.73	1.47 ± 1.93	4.39 ± 2.86

This study highlights the significant role of MD in reducing snow albedo and accelerating snowmelt in the Ili Basin, with BC also contributing to a lesser extent. The findings emphasize the importance of considering both MD and BC in snowmelt dynamics and regional hydrology. The data provide essential baseline information for future research on LAIs' impact on snowmelt runoff and hydrological processes, offering crucial insights into climate change effects on snow-dependent ecosystems and water resources in Central Asia.

Acknowledgments: This research was funded and supported by the National Natural Science Foundation of China (42307523, 42171014).

References

Kang H, Shang X, Abdumutallip M et al. Accurate observation of black and brown carbon in atmospheric fine particles via a versatile aerosol concentration enrichment system (VACES)[J]. Science of the Total Environment, 2022,837: 155817. https://doi.org/10.1016/j.scitotenv.2022.155817

Liu X, Li Y, Ma K et al. Spatial distribution and potential sources of arsenic and water-soluble ions in the snow at Ili River Valley, China[J]. Chemosphere, 2022,295: 133845. https://doi.org/10.1016/j.chemosphere.2022.133845

Schmale J, Flanner M, Kang S et al., 2017. Modulation of snow reflectance and snowmelt from Central Asian glaciers by anthropogenic black carbon, Scientific Reports, 7, 40501. https://doi.org/10.1038/srep40501

Sun G, Chen Y, Li W et al. Spatial distribution of the extreme hydrological events in Xinjiang, north-west of China[J]. Natural Hazards, 2013,67: 483-495. https://doi.org/10.1007/s11069-013-0574-5

Xie X, Liu X, Che H et al. Radiative feedbacks of dust in snow over eastern Asia in CAM4-BAM[J]. Atmospheric Chemistry and Physics, 2018,18(17): 12683-12698. https://doi.org/10.5194/acp-18-12683-2018

Ye H, Zhang R, Shi J et al. Black carbon in seasonal snow across northern Xinjiang in northwestern China[J]. Environmental Research Letters, 2012,7(4): 044002. https://doi.org/10.1088/1748-9326/7/4/044002

Zhong X, Kang S, Zhang W et al. Light-absorbing impurities in snow cover across Northern Xinjiang, China[J]. Journal of Glaciology, 2019,65(254): 940-956. https://doi.org/10.1017/jog.2019.69

Risk assessment of land-based marine debris in an estuarine ecosystem with high river discharge in South Korea

C.K. Kim[1*], K.S. Kim[1], H.J. Hong[1], K.Y. Bang[2]
[1] Water and Land Research Group, Korea Enviornment Institute, Sejong, Republic of Korea
[2] GeoSystem Research Corp., Gyeonggi, Republic of Korea
* e-mail: ckkim@kei.re.kr

Introduction

Marine debris is a critical environmental challenge that severely affects biodiversity, fisheries, and human activities. In regions experiencing intense rainfall and high river discharge—such as South Korea's monsoonal climate—land-based sources significantly contribute to marine debris.

Approximately 70% of marine debris originates from land sources, primarily consisting of plastics and vegetation (Korea Policy Briefing, 2022; KOEM, 2022). Estuaries, which are vital for biodiversity and socio-economic activities, are particularly vulnerable to debris accumulation. This study investigates the distribution of land-based marine debris and the risks it poses to sensitive estuarine resources in South Korea's high river discharge regions.

Materials and methods

A multi-step framework integrating data collection, modeling, and spatial analysis was developed to assess the risk of land-based marine debris to estuarine ecosystems. Data from 26 dam watersheds (2010–2020) were used to model annual debris inflow (tons/year) based on hydrological parameters. This model was applied to five major river basins to estimate debris transport to downstream estuarine environments. The spatial distribution and movement of debris were simulated using a particle transport model. Model predictions were validated against shoreline debris collection data, providing insights into debris dispersal patterns in estuarine and coastal zones.

The InVEST Habitat Risk Assessment tool (Natural Capital Project, 2024) was utilized to evaluate the risk posed by marine debris to sensitive resources such as seabirds, beaches, ports, and fishing grounds. This approach considered both the level of debris exposure (hazard) and the sensitivity and resilience of each resource. The resulting risk scores were visualized as spatial risk maps to highlight high-risk zones.

Results and concluding remarks

This study found significant variability in debris inflow and associated risk levels across different river basins and estuarine zones. Debris inflow was highest during monsoonal rainfall events, emphasizing the critical role of extreme weather in transporting debris. The risk maps identified estuarine regions where sensitive resources faced high exposure to debris (Figure 1). For example, seabird habitats and coastal beaches were among the most impacted resources, exhibiting high hazard scores coupled with low resilience levels. Climate change, with projected increases in extreme rainfall, is expected to exacerbate debris transport and accumulation, further amplifying risks to coastal ecosystems and biodiversity. These findings underscore the urgent need for targeted management strategies to mitigate the impacts of land-based marine debris on estuarine ecosystems.

Key recommendations include:

1. Improvement of waste management systems: Enhancing waste collection and disposal infrastructure in upstream areas can reduce the volume of debris transported to estuaries.
2. Prioritization of high-risk zones: Risk maps can guide the allocation of resources for debris removal and management, focusing on areas of significant ecological and socio-economic importance.
3. Climate change adaptation: Incorporating climate projections into debris management plans can help address future challenges associated with increased rainfall intensity and other extreme

weather events.

This research provides a robust framework for assessing and managing marine debris risks, with potential applications in other regions facing similar challenges. By integrating spatial risk assessment tools, hydrodynamic modeling, and stakeholder engagement, the study offers actionable insights for sustainable coastal and estuarine management.

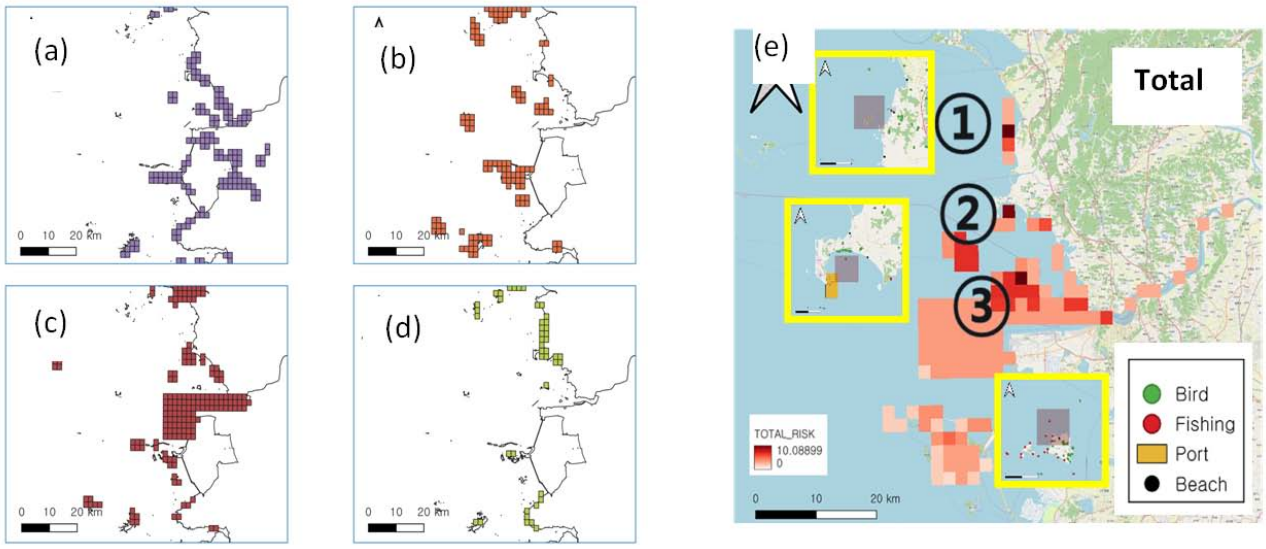


Figure 1. Distribution of sensitive resources and marine debris risk in the Geumgang Estuary, South Korea: (a) Birds, (b) Fishing grounds, (c) Ports, (d) Beaches, (e) Marine debris risk.

Acknowledgments: This research was a part of the project titled “Establishing a smart response platform for marine accidents” (Grant Number 20220463), funded by the Korea Coast Guard, supported by Korea Institute of Marine Science & Technology Promotion. The project was implemented by the Korea Environment Institute (project 2024-007(R), project 2024-008(R)).

References

KOEM (Korean Marine Environment Management Corporation) (2022) Coastal Debris Monitoring https://www.koem.or.kr/site/koem/04/10401070000002019051004.jsp

Korea Policy Briefing (2022). Measures to reduce marine debris. https://www.korea.kr/special/policyCurationView.do?newsId=148899381

Natural Capital Project (2024) InVEST 3.14. Stanford University, University of Minnesota, Chinese Academy of Sciences, The Nature Conservancy, World Wildlife Fund, Stockholm Resilience Centre and the Royal Swedish Academy of Sciences. https://naturalcapitalproject.stanford.edu/software/invest

Water management in disasters: an analysis of recent earthquakes and risks in Turkey

E. Tuncbilek[1], G. Capar[2*]
[1] Dept. of Integrated Water Management, Grad. Sch. of Natural and Applied Sci., Ankara University, Ankara, Turkey
[2] Water Management Institute, Ankara University, Ankara, Turkey
* e-mail: gcapar@ankara.edu.tr

Introduction

Disaster refers to the situations caused by natural, technological, or human-induced events that halt or disrupt the normal flow of life and human activities and also exceed the capacity of society to cope with it. According to AFAD (Disaster and Emergency Management Presidency), disaster is not the event, but its consequences. A hazardous event can be classified as a disaster if it leads to significant damage to life and property, environment, economy and cultural assets.

Earthquake is an elastic and complex wave motion caused by the displacement resulting from the discharge of the deformation energy accumulated on the active faults formed due to the movements of the plates forming the earth's crust, depending on the elastic rebound theory. Earthquakes, one of the most common disasters in Turkey, cause loss of lives and devastating damage to both superstructures and infrastructure, halting socio-economic, demographic and vital activities. In particular, drinking water infrastructure damages can lead to hygiene issues, diseases, and outbreaks; however, literature on water management during disasters remains limited. Hence, providing recommendations for water management before, during, and after the earthquakes is crucial.

The study conducted by the China Earthquake Administration (2023) focuses on analyzing the damage to drinking water infrastructure pipelines located on fault lines during the most recent earthquake in Turkey, which happened in Kahramanmaraş/Pazarcık region on February 6, 2023 (Demir and Dinçer, 2023). The seismic characteristics of these earthquakes, including their magnitude and effects, are detailed, and Peak Ground Displacement (PGD) values are calculated based on these data. As a case study, the drinking water pipeline of Islahiye State Hospital, situated directly on the East Anatolian Fault, is examined to assess the pipeline damages caused by ground displacement. The findings underline the vulnerability of infrastructure on fault zones and emphasize the importance of enhancing resilience in such areas.

Materials and methods

In this study, the active fault maps and database generated by the General Directorate of Mineral Research and Exploration (MTA) and the drinking water pipeline projects carried out by the Provinces Bank (ILBANK; incorporated company affiliated with the Ministry of Environment, Urbanization and Climate Change) were mainly used. First, field observations were made and then risk assessment for drinking water transmission main line was performed.

Within the scope of the field observations, studies were carried out in the provinces of the earthquake zone that experienced the earthquakes of 6 February, 2023 X. Changes in drinking water sources, damages in transmission and distribution (branch) pipelines (Figure 1) and damages in drinking water mechanical and electrical equipment were analysed during field studies. For risk assessment, as a seismic gap, the Yedisu segment of the North Anatolian Fault (NAF) located between east of Erzincan and Bingöl provinces was examined, focusing on the assessment of infrastructure damage in risky areas. It was determined by historical records that the Yedisu segment last generated an earthquake in 1784 with a recurrence interval of 250-300 years (Kürçer and Özalp, 2022), making it a significant seismic gap.

The study specifically evaluated the damage potential of fault lines intersecting water transmission pipelines in the central districts of Bingöl and Altınbaşak in Erzincan. Accordingly, active fault maps prepared by MTA and digital data sets operational projects obtained from İLBANK and municipalities were

analyzed on the Google Earth platform to identify the locations of pipelines intersecting the fault lines and to determine a high probability of post-earthquake damage (Figure 2c).

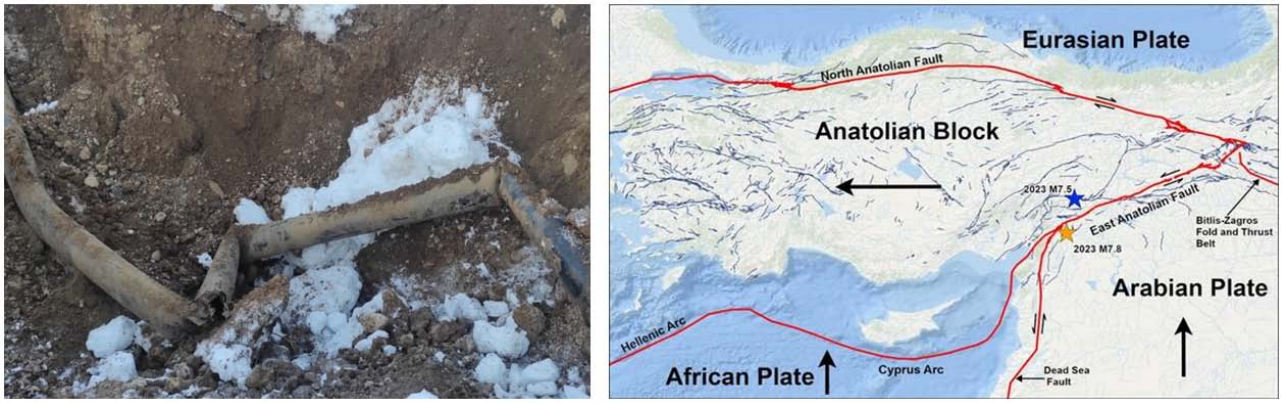


Figure 1. Damages in transmission pipeline occurred by left lateral strike slip fault M_w: 7.8 earthquake

Results and concluding remarks

The following issues have been identified in water bodies located near or intersecting fault lines due to earthquake effects: turbidity in drinking water sources (Figure 2a and 2b), decreases or changes in water flow direction, the emergence of a need for water treatment in areas where it was previously unnecessary, and blockages in dams and mechanical equipment of pipelines caused by water turbidity.

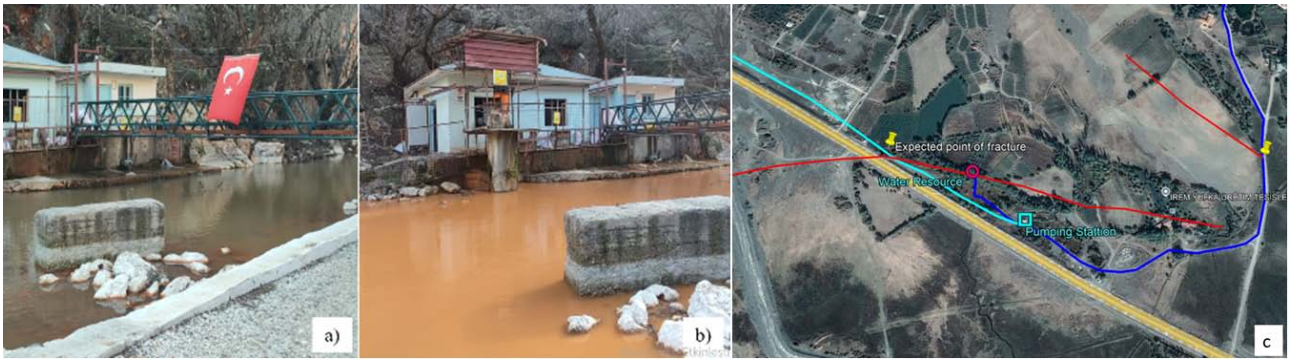


Figure 2. Adıyaman water supply a) before and b) after the earthquake c) Fault line and transmission line intersection

Appropriate water management after an earthquake cover these measures: (1) Fault lines of the region should be analysed while planning drinking water transmission lines and studies should be made according to the types of fractures that may occur in the fault lines and should be passed without intersecting the fault lines at a certain distance, (2) Flexible pipes and movable pipes, which are among the advanced pipe technologies, should be preferred, (3) Pipe and fitting materials suitable for pipe diameter and dimensions should be stocked at the points where ruptures are expected to occur, (4) The nearest public building to the region should be designed as logistic base, (5) Transport plans are necessary for after the disaster, (6) Lists of personnel competent to work in the field should be prepared together with their reserves, (7) Use of fragile type (asbestos, GRP, uPVC, cast iron, etc.) pipes should be avoided in earthquake zones planned to be renewed within the scope of long-term investment.

References

Demir, A., Dinçer, A. E. (2023). Efficient disaster waste management: identifying suitable temporary sites using an emission-aware approach after the Kahramanmaraş earthquakes. International journal of Environmental Science and Technology, 20(12), 13143-13158.

Fan, X., Zhang, L., Wang, J., Ren, Y., Liu, A. (2024). Analysis of faulting destruction and water supply pipeline damage from the first mainshock of the February 6, 2023 Turkey earthquake doublet. Earthquake Science, 37(1), 78-90.

Kürçer, A. Özalp, S. (2022). The paleosysmic history of Yedisu Segment in the last 4000 years (in Turkish), Kuzey Anadolu Fayı, Turkey. Active Tectonics Research Group (ATAG)25th Workshop, 17-18.

Investigating heavy metal contamination in soil-water systems: a case study of Hindon tributary, India

P. Dwivedi, B.K. Yadav*
Department of Hydrology, Indian Institute of Technology, Roorkee, India
** e-mail: p_dwivedi@hy.iitr.ac.in*

Introduction

Heavy metal contamination in soil and water resources, driven by socio-economic activities, results in long-term persistence and accumulation, posing risks to environmental security and human health as they enter the food chain through crops and aquatic organisms (Chen et al. 2024). Therefore, monitoring heavy metals in soil and water is crucial to develop effective remediation strategies. The mobility of pollutants in the combined soil and water system is influenced by chemical and physical properties, such as pH, organic matter, phytoextraction, overland flow, infiltration, water table fluctuations, and hydraulic conductivity (Shokri et al. 2022). Though field-based monitoring of soil and water can only provide the heavy metal levels, it may not fully capture the subsurface distribution and transport pathways of these metals. Non-invasive techniques, such as geophysical surveys, offer a complementary approach to demarcating potential subsurface contamination hotspots. This study conducted a preliminary geophysical investigation using Electrical Resistivity Tomography (ERT) to identify subsurface regions of contamination, followed by systematic sampling of surface water, groundwater, and soil along the Kali River, a tributary of the Hindon basin, India. This approach will comprehensively assess the spatial and depth wise distribution of heavy metals in soil and water systems.

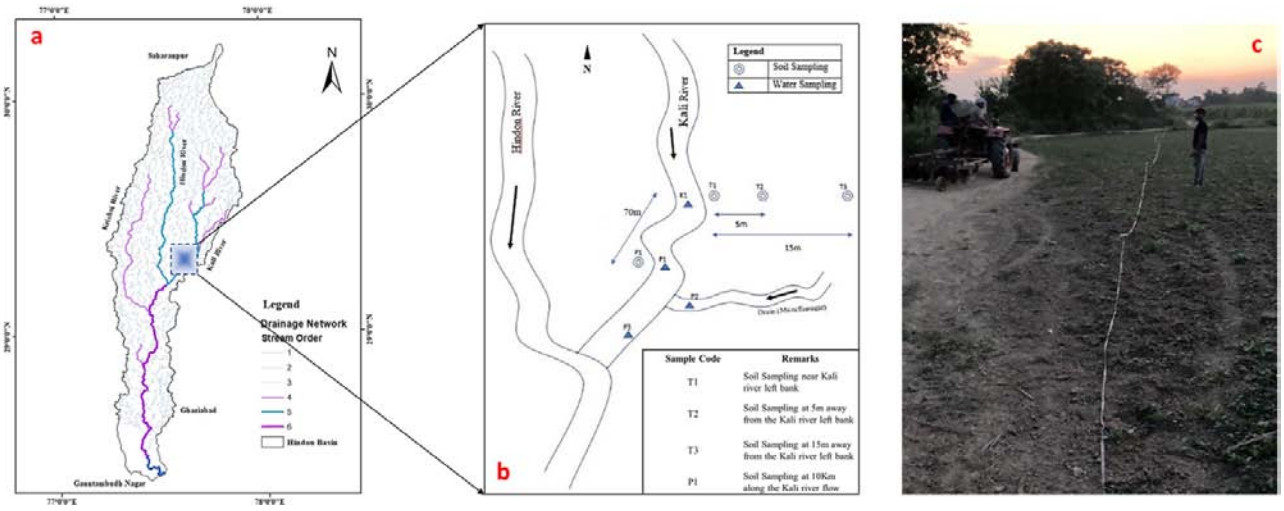


Figure 1. Map showing the location of the study area (a), soil-water sampling sites (b), and ERT survey (c).

Materials and methods

A detailed field investigation was conducted in the pre-monsoon season of 2023 along the Kali River (Figure 1a) to assess heavy metal contamination in surface water, groundwater, and soil. The preliminary ERT geophysical survey was performed along a 300-meter stretch (Figure 1c) parallel to the river to identify potential subsurface hotspots of contamination. The 2D resistivity profile obtained from this survey demarcates areas of low resistivity values indicating saturated and contaminated zones. Also, this survey enables pinpointing the contaminated subsurface locations for further sampling. After the survey, targeted field sampling was conducted in soil and water to validate the findings (Figure 1b). Surface water samples were obtained directly from the Kali River while groundwater samples were collected from India Mark

handpumps within the study area to evaluate the heavy metal concentrations. Subsequently, soil sampling was strategically performed near the riverbank, with samples taken at 30 cm depth intervals up to 1 meter below the surface to study the vertical distribution of heavy metals. Lateral soil sampling was also conducted, with samples taken at 5-meter intervals up to 15 meters from the riverbank, to capture spatial variability in contamination. This approach enabled the tracing of contaminants within the soil and their movement from water to soil. Also, integrated geophysical investigations with targeted field sampling established a robust methodology, enabling a detailed assessment of contamination and its spatial patterns across the Kali River subbasin.

Results and concluding remarks

The findings from this study highlighted the presence of elevated heavy metal concentrations, particularly Cr, Zn, Ni, Pb, Cd, and Cu, across surface water, groundwater, and soil within the Kali subbasin (Figure 2b). A preliminary geophysical investigation using ERT revealed two highly contaminated sites located at 30-40m and 90-100m with shallow low-resistivity zones (11.2–25.8 Ohm.m) at a depth of 0–10 m indicating contaminated sediments influenced by industrial discharges and river seepage. In contrast, deeper high-resistivity zones (45–78 Ohm.m) signify dry or compacted materials that may act as barriers, restricting vertical contaminant migration and facilitating accumulation in shallower layers. In the surface water, the influx of wastewater drains from the Muzaffarnagar region introduces a dilution effect downstream, resulting in a noticeable decrease in heavy metal concentrations in the river. However, in the groundwater, the decline in metal concentrations post-drain confluence may be attributed to groundwater recharge by less polluted drain water and extensive groundwater extraction for irrigation. The soil samples from the contaminated site identified by ERT (30-40m) were rich in metals such as Cr, Zn, Ni, and Cu with concentrations highest within the top 60 cm of soil layers, especially near the riverbank (Figure 2a). Their concentrations diminish further away from the river, suggesting the influence of riverbank saturation and the potential for uptake by plant roots. Beyond the 60 cm depth, the longitudinal distribution showed minimal changes in concentrations, implying accumulation in deeper soil layers due to limited vertical mobility and potential adsorption onto soil particles. The combined results from the ERT survey and field sampling emphasize the interconnected nature of contamination across soil and water resources in the region. These findings highlight the significant impact of anthropogenic activities and the urgent need for targeted pollution mitigation strategies.

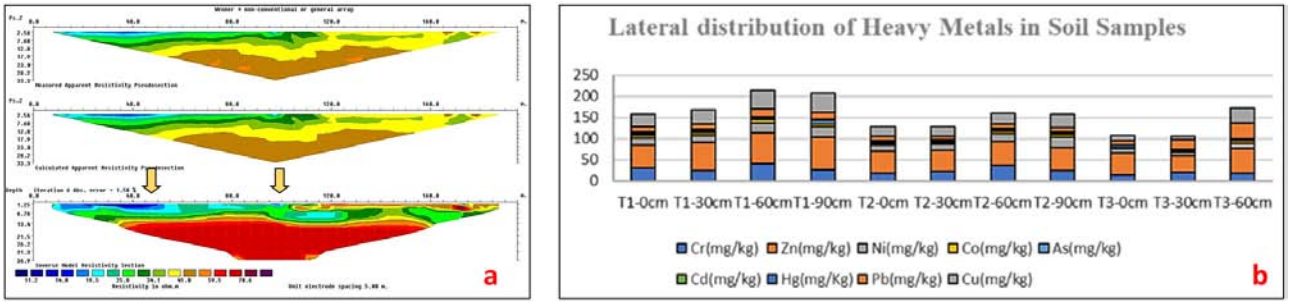


Figure 2. Detailed resistivity distribution showing contaminated sites (a); Lateral distribution of heavy metal in the soil samples (b).

References

Chen X, Fu X, Li G, Zhang J, Li H, Xie F (2024) Source-specific probabilistic health risk assessment of heavy metals in surface water of the Yangtze River Basin. Science of the Total Environment, 926, 171923. https://doi.org/10.1016/j.scitotenv.2024.171923

Shokri M, Gao Y, Kibler KM, Wang D, Wightman MJ, Rice N (2022) Contaminant transport from stormwater management areas to a freshwater karst spring in Florida: Results of near-surface geophysical investigations and tracer experiments. Journal of Hydrology: Regional Studies, 40, 101055. https://doi.org/10.1016/j.ejrh.2022.101055

Assessment of sediment production in transboundary Douro River Basin

M. Ferreira*, J. Mendes, R. Maia
FEUP–Faculty of Engineering of the University of Porto/Hydraulics Water Resources and Environment Division, Portugal
** e-mail: mafalda.araujo.ferreira@gmail.com*

Introduction

Soil erosion, sediment transport, and sedimentation are natural processes that are influenced by a number of factors, including precipitation, runoff, topography, soil type, and vegetation. Global trends indicate a reduction in sediment delivery to coastal areas, with the Mediterranean region exhibiting particular vulnerability due to droughts followed by intense precipitation on unstable slopes. The Douro River basin, a significant sediment source, requires precise sediment quantification for effective resource management (Portela 2008). There has been a decline in annual precipitation in Portugal, in line with trends observed across the Iberian Peninsula. This has resulted in a reduction in sediment production, particularly during periods of prolonged drought (Santos et al. 2019).

In this study, the HEC-HMS model was used to evaluate sediment production in the Douro River Basin from 2002 to 2015, focusing on the effects of average precipitation and extreme weather events. The research addresses data deficiencies and permits forecasting sediment production trends under future climate change scenarios.

Materials and methods

The Douro River basin, the largest in the Iberian Peninsula, covers 97,603 km², of which 80.9% is in Spain and 19.1% in Portugal. The main river runs for 927 km to the Atlantic, of which 597 km is in Spain, 122 km is the international section, and 208 km is in Portugal. The region features steep slopes, with gradients exceeding 40%, at its Portuguese and Spanish extremities, while the central portion, located in the Spanish part, is relatively flat (less than 5%). The western regions near the Atlantic Ocean receive the greatest precipitation, with annual averages of 930 mm in Portugal and 588 mm in Spain and a basin-wide mean of 653 mm. The mean annual temperature is 13.2°C in Portugal and 11.2°C in Spain, with a basin-wide mean of 11.6°C. There has been a decline in rainfall and temperatures since 1988 (APA 2022). The main course of the Douro has 15 dams, 5 in Portugal, 5 in Spain and 5 in the International Stretch, of which 2 are managed by Spain and 3 by Portugal.

The HEC-HMS software employs the Modified Universal Soil Loss Equation (MUSLE) to estimate soil erosion caused by surface runoff. Sediment Production (sed) for a specific day is calculated using the runoff volume (Q_{surf}) and peak flow (q_{peak}), as shown in Eq. (1). The equation incorporates five key coefficients: K_{USLE} (soil erodibility factor), C_{USLE} (soil management and cover factor), P_{USLE} (soil conservation practice factor), and LS_{USLE} (topographic factor).

$$sed = 11.8 * \left(Q_{surf} * q_{peak}\right)^{0.56} * K_{USLE} * C_{USLE} * P_{USLE} * LS_{USLE} \quad (1)$$

To assess soil loss, the K_{USLE} parameter considers soil properties, including particle size, organic matter, permeability, and structure. C_{USLE} evaluates the impact of land use and cover by comparing soil loss under specific conditions to that of bare soil. P_{USLE} examines the influence of conservation practices, such as terracing, on soil loss against unmanaged slopes. LS_{USLE} quantifies the role of topography by comparing soil loss on a given slope to that of a standard slope.

Data for the Douro River basin is limited, which led to the incorporation of derived data from low-resolution European databases. Using Corine Land Cover 2018, the land use classification shows that 48.76% of the area is agricultural, 50.35% is natural vegetation and forests, and 0.89% is urban. Soil characterisation was based on the Infosolo database for Portugal and the FAO database for Spain, with Cambisols being the predominant soil type (82%). Meteorological data for Portugal was sourced from

SNIRH stations, while Spanish data (1951–2019) came from AEMET.

The P_{USLE} factor was estimated using ESDAC values (0.9178 for Portugal, 0.9293 for Spain) in the absence of detailed calculations due to the scale of the basin. The K_{USLE} values for the various soil types were derived from georeferenced data, ranging from 0 to 0.3021. C_{USLE} values, based on land use, were calculated using QGIS and exhibited a range of 0.002 to 0.461. LS_{USLE} values, representing topographic factors, were also calculated in QGIS, with an average range of 0.114 to 5.65 for sub-basins. Given the unavailability of data for the Douro River basin, erosion maps based on models such as RUSLE, including the ESDAC Soil Loss by Water Erosion in Europe map (Panagos et al. 2015), based on the year 2010, offer viable alternative information, with the average soil loss calculated for each sub-basin of the HEC-HMS model. The ESDAC map was used to calibrate the sediment production by adjusting the K_{USLE} and P_{USLE} values within their specified intervals.

Results and concluding remarks

The initial simulation of the HEC-HMS model, based on uncalibrated MUSLE parameters, yielded an estimated average annual sediment production of 4.61×10^{7} tonnes/year for the Douro River basin. These results exceeded the reference values (2.39×10^{7} tonnes/year) by 2.22×10^{7} tonnes/year. Notable overestimations were observed in the northern part of the basin, particularly in the upper reaches of the Esla River and in the headwaters of the Sabor and Tua Rivers. Downstream of the Régua reservoir, located at km 105 of the main channel (about halfway along the Portuguese section (208km)), the model also indicated an increase in sediment production, which was visible in the simulation results but less pronounced in the reference map. These discrepancies reflect MUSLE's greater spatial dispersion of erosion risks compared to RUSLE, as supported by previous studies.

The calibration of the HEC-HMS model involved adjusting the P_{USLE} and K_{USLE} parameters to align simulated sediment production with reference data from the ESDAC soil loss risk. After modifying these parameters, the model's estimated average annual sediment production decreased to 1.61×10^{7} tonnes/year, underestimating the reference value of 2.39×10^{7} tonnes/year by 0.78×10^{7} tonnes/year. Figure 1 presents the final map as well as the reference map by ESDAC.

The RUSLE model was influenced by precipitation anomalies in 2010, a year with unusually high rainfall across Portugal and Spain. In 2010, the model estimated a sediment production of 2.49×10^{7} tonnes/year, with only a 4% discrepancy compared to the ESDAC value. Although map discrepancies were noted, the overall results indicate a promising alignment between the model and reference data.

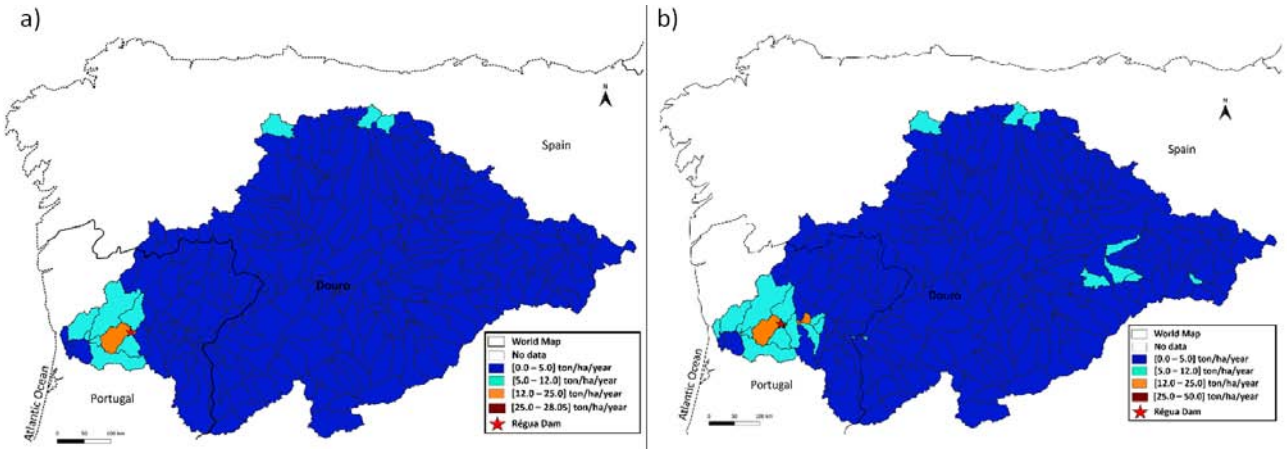


Figure 1. a) Final results for calibration of the HEC-HMS model; b) Map of ESDAC average sediment production values.

References

APA (2022) Plano de Gestão de Região Hidrográfica RH3.

Panagos P, Borrelli P, Poesen J, Ballabio C, Lugato E et al. (2015) The new assessment of soil loss by water erosion in Europe. Environmental Science and Policy 54: 438–47. https://doi.org/10.1016/j.envsci.2015.08.012.

Portela, Luís Ivens. (2008) Sediment transport and morphodynamics of the Douro River estuary. Geo-Marine Letters 28 (2): 77–86. https://doi.org/10.1007/s00367-007-0091-1.

Santos M, Fonseca A, Fragoso M, e João A. Santos (2019) Recent and future changes of precipitation extremes in mainland Portugal. Theoretical and Applied Climatology 137 (1–2): 1305–19. https://doi.org/10.1007/s00704-018-2667-2

On the correlation between earthern leeves' vulnerability to seepage and flood events probability of occurrence

B. Bonaccorsi[1,2*], S. Barbetta[1], L. Ciabatta[1], M. Dionigi[1], G.T. Aronica[2]
[1] Research Institute for Geo-hydrological Protection, National Research Council (IRPI-CNR), 06128 Perugia, Italy
[2] Engineering Department, University of Messina, 98158 Messina, Italy
* e-mail: biancabonaccorsi@cnr.it

Introduction

Earthen levees are one of the main structural measures against flooding in floodplain areas; however, these structures can fail due to different mechanisms. From the risk point of view, the construction of embarkments might paradoxically increase the overall risk because of a general decrease in flood hazard perception by the exposed population and urban planner (Castellarin et al., 2011). For this reason, ample research has been focused on studying the physical process affecting the levees during a flood event, such as overtopping and seepage/piping (Deverel et al.; 2016; Palladino et al.; 2019). Specifically, the piping process is very hazardous because it is not openly visible and, therefore, is hard to identify before the failure. Nevertheless, evaluating the vulnerability to seepage for different flood events affecting the earthen levee is fundamental to support territorial planning and risk management in quasi-real-time.

In this context, the present work proposes a procedure to calculate the correlation between the probability of levee failure due to seepage process and the probability of occurrence of the flood event affecting the embankment. The vulnerability to seepage is quantified by identifying the saturation line location in the levee through a two-dimensional numerical model SEEP/W. The analysis is carried out for flood events characterized by a different probability of occurrence estimated by applying a procedure based on stochastic generation of precipitation and temperature time series and continuous hydrological modelling. The proposed procedure is applied to an experimental levee located along the Tatarena stream, in central Italy.

Materials and methods

For the assessment of the saturation line through a simplified approach, Barbetta et al. (2017) developed a rapid procedure based on hydraulic characteristics of the river (water head h'_0, duration of the flood event D), geometric information of the levee and only two parameters of the soil (soil porosity ξ and hydraulic conductivity K_s).

$$H_x=h_1\,[1-\mathrm{erf}(x/2\,\sqrt{(\xi/(KH_0D))})] \quad (1)$$

where: H_0 is the groundwater depth (Figure 1).

To evaluate the seepage mechanism through a numerical model, useful to simulate real physical process, SEEP/W was used in the present work. SEEP/W, part of GeoStudio software, is a finite element model (FEM) capable to resolve the simple saturated steady state problems and also saturated/unsaturated time dependent problems. The principal quality is due to its ability to allow seepage analysis as a function of time. There are three main parts to a finite element analysis: the first is creating the numerical domain, including the selection of an appropriate geometry and creating the discretized mesh; the second is the specification of material properties and the third is the definition of the appropriate boundary conditions.

Results and concluding remarks

In the comparison between the saturation line evaluated with Marchi's equation and with SEEP/W is clearly noticeable that the finite element model consider better the soil characteristics and the geotechnical parameters, representing different seepage lines when the soil is more saturated or when the

hydraulic conductivity of the soil is very low.

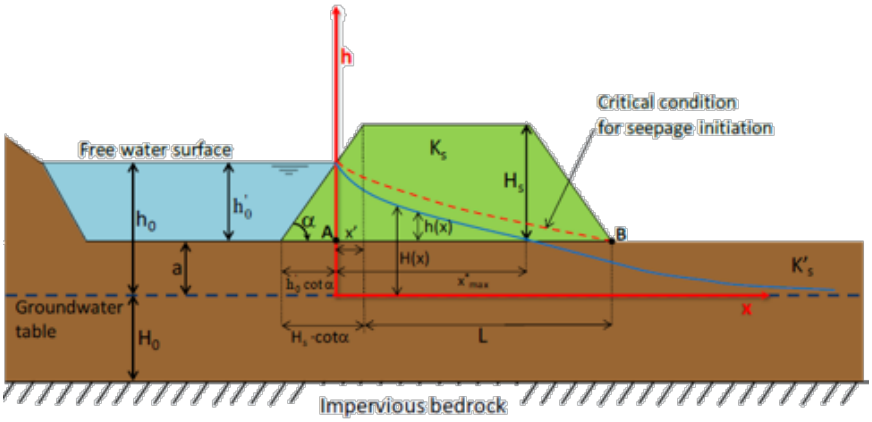


Figure 1. Saturation line for a levee with known geometry (for symbols see text).

Regards the correlation through the probability of levee failure due to seepage process and the probability of occurrence of the flood event, the results show that for almost all water levels and for the four duration of the flood event considered (12, 18, 24, 48 hours), the vulnerability index is negative, i.e., the saturation line is contained in the levee and the earthen embankment is not vulnerable. Only for the duration of 48 hours, for the maximum water level, the vulnerability index was slightly positive.

In conclusion, this result provides a useful tool during the management phase of a flood event, knowing beforehand for certain return period, what is the probability of failure of the levee.

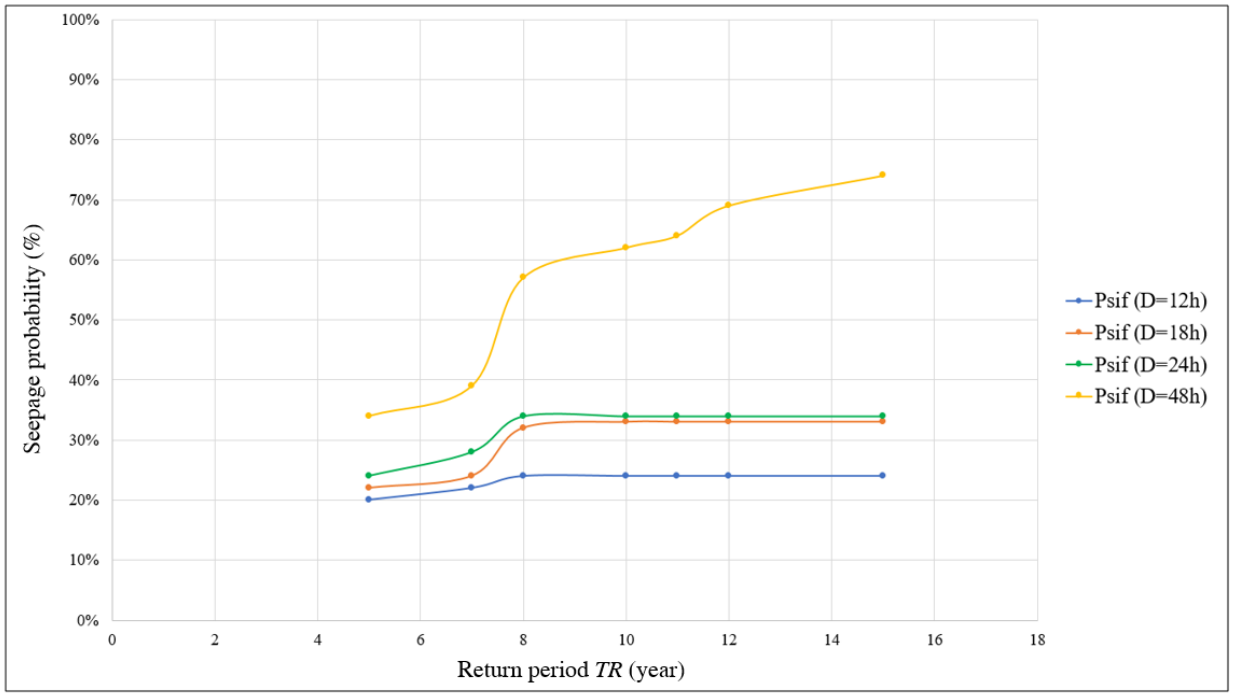


Figure 2. Seepage probability for different water level (TR corresponded), for four durations of the flood event.

References

Castellarin, A., Di Baldassare, G., Brath. (2011) A floodplain management strategy for flood attenuation in the River Po. River Res. Appl. 27 (8), 1037–1047

Deverel, S. J, Bachand, S., Brandenberg, S. J, Jones, C. E, Stewart, J. P, & Zimmaro, P. (2016) Factors and Processes Affecting Delta Levee System Vulnerability. San Francisco Estuary and Watershed Science, 14(4). doi: https://doi.org/10.15447/sfews.2016v14iss4art3.

Palladino M.R., Barbetta S., Camici S., Claps P., Moramarco T. (2020). Impact of animal burrows on earthen levee body vulnerability to seepage. Journal of Flood Risk Management. https://doi.org/10.1111/jfr3.12559.

GIS-based flood vulnerability mapping using fuzzy AHP: An integrated indicator approach

E. Efraimidou*, M. Spiliotis
Department of Civil Engineering, Democritus University of Thrace, University Campus Kimmeria, Xanthi, Greece
** e-mail: iriniefremidou@yahoo.com*

Introduction

Floods are among the most frequent and destructive natural disasters, causing severe socioeconomic and environmental impacts. Their increasing intensity, driven by climate change and urbanization, threatens communities worldwide. Traditional flood vulnerability assessments often fail to capture the complex interplay of hydrological, topographical, and socio-economic factors, limiting their effectiveness in risk management.

This study applies a multi-criteria decision analysis (MCDA) approach, integrating Fuzzy Analytic Hierarchy Process (FAHP) with Geospatial Techniques to enhance flood vulnerability mapping. Expert input was used to determine the relative weights of 17 vulnerability indices, ensuring a data-driven weighting process. The methodology was applied in the Filiouris and Vovsvozis river basins in Rhodope, Greece. Weighted overlay analysis in a GIS environment produced a flood vulnerability map integrating multiple indicators, offering a reliable expert-driven framework for disaster risk reduction and mitigation

Materials and methods

The research was carried out in the neighbouring river basins of Filiouris and Vovsvozis in northern Greece, covering 1,851.4 km². These basins discharge into the Thracian Sea, with Komotini serving as the primary urban centre. The indicators for constructing the Flood Vulnerability Index (FVI) were selected based on their conceptual relevance, demonstrated significance in prior research, and availability of reliable data sources.

For this study, we utilized publicly available georeferenced data and consulted relevant sources for supplementary information. Indicators were standardized into five ordinal categories to enhance cross-dataset comparability. Jenks' Natural Breaks optimization was applied to quantitative indicators to define class boundaries that minimize within-group variance while maximizing inter-group differentiation. For categorical indicators with uniformly absent data, a fixed vulnerability score was assigned, reflecting the lack of mitigation capacity.

Table 1. Vulnerability indices and their weights.

Vulnerability Indices	Weights	Vulnerability Indices	Weights
Population density	0.1218	Industries	0.0431
Civil protection structures	0.0992	Tourist activities	0.0430
Early warning system	0.0954	Agricultural activities	0.0418
National road network, railway lines, airports	0.0895	Power plants	0.0379
Public infrastructures	0.0707	Protected areas for species and habitats	0.0365
Water supply sources	0.0693	Monuments of cultural heritage of international significance	0.0349
Social infrastructures	0.0564	Monuments of cultural heritage of national and regional significance	0.0334
Wastewater treatment facilities	0.0535	Museums	0.0273
Solid Waste Management and Disposal Facilities	0.0464		

A structured questionnaire was developed to obtain expert-based pairwise comparisons of the indicators. A representative group of stakeholders, including academics, municipal authorities, and practitioners, provided valuable input during this process. The triangular fuzzy number approach was

employed to address uncertainty in expert judgments, while fuzzy consistency testing ensured the reliability of the assigned weights. Multi-expert judgments were synthesized using the geometric mean, which is less sensitive to extreme values compared to the arithmetic mean (Liu et al., 2020). Subsequently, the FAHP method, as proposed by Barzilai (1997), was implemented using the fuzzy geometric mean, as shown in Equation (1).

$$\tilde{C}_i = \left(\tilde{C}_{i1} \otimes \tilde{C}_{i2} \otimes \ldots \otimes \tilde{C}_{in} \right)^{1/n}, \; \widetilde{C}_i = \frac{\tilde{C}_i}{\sum_{j=1}^{n} \tilde{C}_j} \quad (1)$$

where *n* the number of the criteria and $\tilde{C}_{ij}$ means the relative (binary) importance of C_i over *Cj.* As $\otimes$ the crisp multiplication is applied but when it being applied to fuzzy numbers.

Notably, the widely used fuzzy extended analysis was excluded due to its tendency to nullify weight values (Liu et al. 2020). Regarding the consistency the CI method proposed by Bulut et al. (2012) was utilized. Finally, the achieved defuzzied values of weights are presented in Table 1.

Standardized and weighted indicators were integrated into ArcGIS 10.8, using 1000-year flood hazard boundaries (T=1000) from the Ministry to create the final flood vulnerability map. Table 1 presents the vulnerability indices and their weights.

Results and concluding remarks

The resulting flood vulnerability map (Figure 1) identifies high vulnerability in urban areas like Komotini and agricultural zones near riverbanks, aligning closely with the patterns shown in the Ministry's map. This consistency validates the methodology used and highlights its reliability in identifying flood-prone areas.

The integration of GIS and Fuzzy AHP demonstrates a powerful approach to flood vulnerability assessment, addressing uncertainties in weight assignment and enhancing decision-making processes. By incorporating a broad range of indicators, the model provides a comprehensive assessment framework. Future research could explore real-time hydrological data assimilation and participatory approaches involving local stakeholders to refine the model.

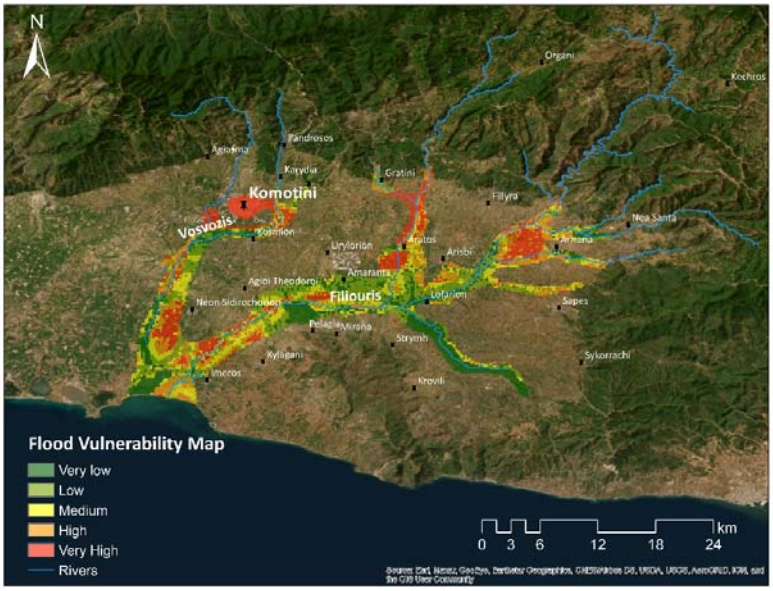


Figure 1 Vulnerability map.

References

Barzilai J (1997) Deriving weights from pairwise comparison matrices. Journal of the Operational Research Society 48: 1226–1232.

Bulut E, Duru O, Keçeci T, Yoshida S (2012) Use of consistency index, expert prioritization and direct numerical inputs for generic fuzzy-AHP modeling: A process model for shipping asset management. Expert Systems with Applications 39: 1911–1923. https://doi.org/10.1016/j.eswa.2011.08.056

Liu Y, Eckert CM, Earl C (2020) A review of fuzzy AHP methods for decision-making with subjective judgements. Expert Systems with Applications 161: 113738. https://doi.org/10.1016/j.eswa.2020.113738

Investigation of the habitats' state in Natura 2000 site coded "GR1410001" in Lake Tavropou area

A. Psilovikos[1*], T. Papathanasiou[1], I. Vergos[1,2]
[1] Laboratory of Ecohydraulics & Inland Water Management (ECO–HYDRO Lab), Department of Ichthyology & Aquatic Environment, University of Thessaly, Fytoko St., 384 46, N. Ionia Magnisias, Greece
[2] Natural Environment and Climate Change Agency (NECCA). Management unit of Protected Areas in Thessaly
* e-mail: psiloviko@uth.gr

Introduction

Lake Tavropos or Plastiras, is a reservoir that was created with the construction of the dam at the southern end of the headwaters of Tavropos River in 1960. It is characterized by competitional uses of water, which are: a) Hydroelectric Production, b) Irrigation, c) Domestic water supply, d) flood protection, e) Ecological Conservation. The wider area is a complicated hydrosystem of natural rivers and artificial dam-lake, grasslands and woodlands. It is rich in biodiversity and that's why it is a natural system of European importance, integrated into the network of Natura 2000 (Psilovikos et al., 2024). The largest percentage rate of the natural environment has been transformed into an anthropogenic one, after the construction of the "N. Plastiras" dam from the Public Power Corporation of Greece (PPC) for hydroelectric production, but also serves the uses above. It is noted that the "N. Plastiras" dam is one of the big reservoirs in Greece, with approximately 400 x 10^6 m^3 of stored water. According to the 90657/5905/30-9-2021 Ministerial Agreement, the protected elements, under the Habitats Directive, of Special Area of Conservation "GR1410001" (EEA, 2024) require monitoring, through the preparation of a specific program, in which various factors (such as "Pressures-Threats", the Perspective, etc.) will be recorded with the aim of evaluating the status of conservation of the protected area. A Monitoring Program Plan took place, for the documentation of these areas, under the cooperation of PPC with ECO–HYDRO Lab (Psilovikos et al., 2024).

Materials and methods

According to the European Environment Agency (EEA, 2024), the classification of the site "GR1410001" has been confirmed as SCI (Site of Community Importance) in 09/2006 and its definition as SAC (Special Area of Conservation) took place in 03/2011 (OGG A΄ 60/31-3-2011). The table below shows all the habitats of the site coded "GR1410001". The site "GR1410001" includes 1 type of priority habitats of Annex I of Directive 92/43/EEC: 9530 – (Sub) Mediterranean pine forests with endemic black pines. It is noted that the relevant SDF (Standard Data Form) also mentions the habitat "92C0", but with zero (0) cover (ha). Concerning the wild fauna, the most important species are: *Barbastella barbastellus*, *Bombina variegata*, *Cerambyx cerdo*, *Lucanus cervus*, *Lutra lutra*, *Testudo graeca*, *Testudo hermanni* and *Testudo marginata* (EEA, 2024). To preserve and protect the habitat types and the landscapes of the area of interest, it is considered valuable to investigate the compatibility of anthropogenic pressures with the legislations of the specific Natura 2000 area, their status and conservation prospects. For this purpose, on-site visits and fieldwork were carried out in the area, using Drone Mavic 2JS II camera, for the photographic documentation, together with analysis of orthophotomaps (time period 2015–2016, 0.5-meter accuracy) and stereoscopic observation of aerial photographs of the National Cadaster, as well as utilization of previous literature. It is emphasized that the anthropogenic pressures of Lake Tavropou Area can be distinguished mainly in agriculture, livestock farming, fishery, tourism, artificial dams, other technical constructions, waste etc. (Paraskevopoulos and CO LP, 2020; Psilovikos et al. 2024).

Table 1. The Description of the habitats found in the site "GR1410001" (EEA, 2024).

Habitats	Description	*Cover (ha)*
3140	Hard oligo-mesotrophic waters with benthic vegetation of *Chara* spp.	*4.2597*
5210	Arborescent matorral with *Juniperus* spp.	*20.3982*
6170	Alpine and subalpine calcareous grasslands	*25.9502*
91M0	Pannonian-Balkanic turkey oak – sessile oak forests	*125.778*
9270	Hellenic beech forests with *Abies borisii-regis*	*343.379*
9530	(Sub-) Mediterranean pine forests with endemic black pines	*22.7349*

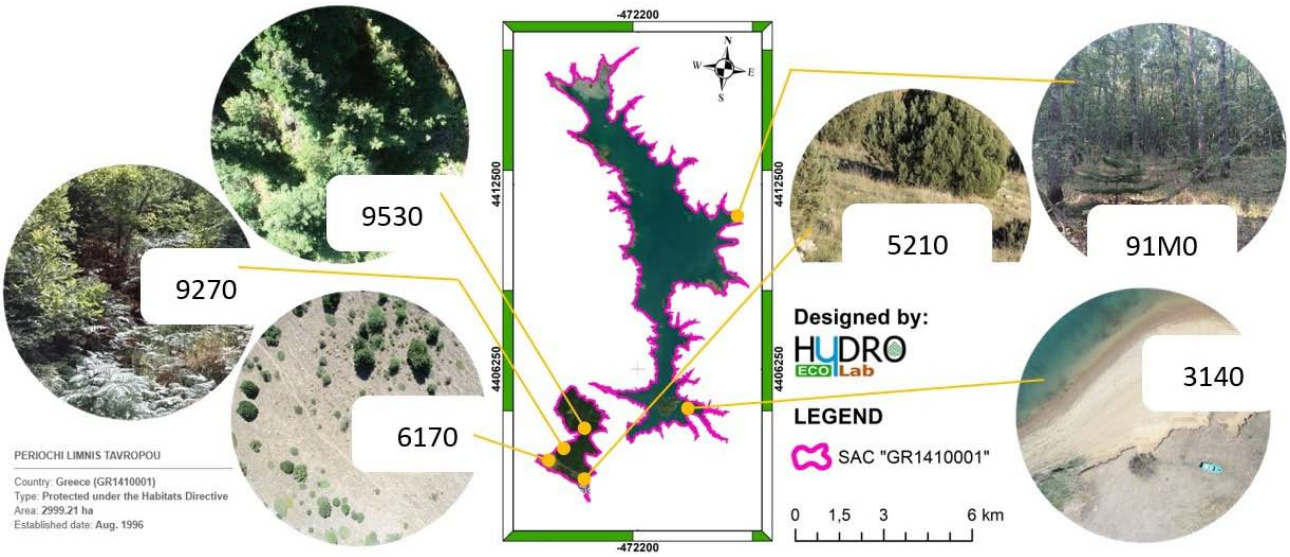


Figure 1. The boundaries of the site "GR1410001" and photographs from representative habitats (Psilovikos, 2024).

Results and concluding remarks

After the field work, the documentation of the habitats and the mapping of the study area, it appears that the current state of Lake Tavropou Area has not been significantly affected and the complicated hydrosystem has reached a dynamic equilibrium between the natural processes combined with the anthropogenic interventions. In Catchment Area of Lake Tavropou, the fluvial processes do not drastically and practically affect the preservation of the habitats (both flora and wild fauna) (Psilovikos et al. 2024). In addition, a stabilized situation appears to have occurred, exactly as described in previous studies and research that preceded it. Non-significant degradation is shown in populations and condition of the habitat types. Moreover, the conditions of the Environmental Flows (maximum & minimum water level of reservoir), have been considered, according to OGG Bʹ 4703/23-10-2020.

References

Decision No 90657/5905/30.09.2021 of the General Director for Environmental Policy. (2021). Renewal of the validity of the Decision on the Approval of Environmental Terms (AEPO) with protocol number: 197254/17-3-2011 of project "Existing N. Plastira Power Plant on the Tavropos River of the Prefecture of Karditsa" of PPC S.A. Ministry of the Environment and Energy.

European Environment Agency (EEA). (2024). N2K GR1410001 Dataforms. Database release: End 2022-12/03/2024. Retrieved from https://natura2000.eea.europa.eu/Natura2000/SDF.aspx?site=GR1410001.

Paraskevopoulos Georgios and CO LP. (2020). Renewal of Environmental Conditions for the Operation of the Existing "N. Plastira" Power Plant on the Tavropos River in the Province of Karditsa. Main Issue.

Psilovikos A. et al. (2024). Preparation of a Monitoring Program of the Protected Areas in the Special Conservation Zone GR1410001 of Lake Tavropos Area, in Accordance with the Environmental Condition 21.2 of the "AEPO" of Plastiras' Hydroelectric Plant, as Amended, Renewed and Validated. Research Program, Public Power Corporation of Greece (PPC). Technical Reports A, B. Research Committee University of Thessaly, Volos, Greece.

Official Government Gazette (OGG) Bʹ 4703/23-10-2020. (2020). Decision No 1392/2020: Determination of the amount of the Maximum and Minimum Security Level in accordance with the provisions of paragraph 3 of article 21 of the Balancing Market Regulation and paragraph 4 of article 18 of Law 4425/2016, as applicable.

Understanding the relationship between ecosystem services and pressures of islands: Fuzzy-cognitive modelling approach

M. Ilić Paunić[1*], R.M.Pacheco[2], A. Moustakas[3], Z. Srđević[1], B. Srđević[1]
[1] Department of Water Management, Faculty of Agriculture, University of Novi Sad, Serbia
[2] Institute of Agrifood Research and Technology - IRTA, Caldes de Montebui, Spain
[3] Natural History Museum of Crete, University of Crete, Heraklion, Crete, Greece
* e-mail: milica.ilic@polj.uns.ac.rs

Introduction

Islands across Europe face growing pressures that threaten their vital ecosystem services (ESs), which are crucial for local livelihoods and regional economies, with the environmental and socio-economic isolation of islands increasing their dependence on them (Balzan et al., 2018). These pressures heighten the vulnerability of these ecosystems, more so than on the mainland (Vogiatzakis et al., 2023). Understanding the relationships between ESs and the pressures acting on them is essential for effective management. These pressures are often interconnected, amplifying each other, and their management is vital for protecting island ecosystems and the services they provide. Any change in one part of the ecosystem can trigger a chain reaction across the system.

Recent research on island ESs (Du et al., 2024a) has shown a steady increase in publications from 2000 to 2023. The field has evolved through three distinct phases: the initial phase (2000–2005), the early development stage (2006–2015), and the period of rapid growth (2016–2023). Despite this growth, studies on ES trade-offs in island terrestrial areas remain limited (Du et al., 2024b). One significant effort to synthesize and strengthen knowledge related to island conservation and ecosystem services is the COST Action (CA21158) titled "Enhancing Small-Medium IsLands resilience by securing the sustainability of Ecosystem Services - SMILES." This initiative aims to enhance the understanding of island ecosystems and their contribution to sustainable development.

This paper presents a fuzzy-cognitive modeling approach to define causal relationships between island ESs and pressures. This approach enables the visualization of "what-if" scenarios of potential impacts from changing pressures on selected ESs, as detailed by Ilić et al. (2024).

Materials and methods

The methodological approach involves three main steps: (1) *Identification of key ESs and pressures* - through participatory processes such as workshops, surveys, or expert interviews, stakeholders prioritize the most relevant ESs, and identify critical pressures; (2) *Building the Fuzzy Cognitive Model (FCM)* - Stakeholders' knowledge is used to quantify the strength and direction of relationships between ESs and pressures. Connections are assigned values ranging from -1 (strong negative impact) to +1 (strong positive impact), with intermediate values capturing weaker associations. Here, the software Mental Modeler is used (Grey et al., 2013); (3) *Simulation and analysis* - The FCM is used to analyze and reveal key interactions and priorities. Simulated results can help identify where interventions would yield the greatest possible benefits. For details, the reader is referred to Ilić et al., 2024.

Results and concluding remarks

Based on the literature review and expert-based assumptions (in the absence of direct stakeholder participation), it is shown here how one can simulate interactions between ESs and pressures, providing an initial approximation of their relationships. As a case example, the assessment is conducted in general for island ES to illustrate the possibilities of using FCM. Ten ecosystem services (Fig. 1, orange boxes) and five pressures (Fig.1, white boxes) were chosen, in this case, based on the available scientific literature on typical island ESs.

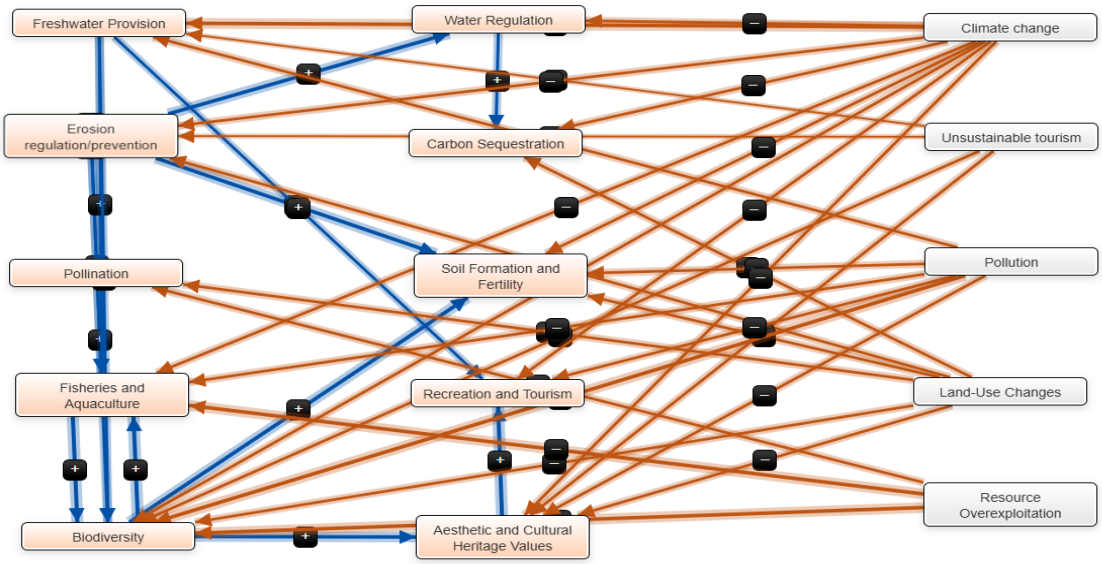


Figure 1. The ecosystem services - pressures relationship network.

The resulting network consists of 15 components (ESs and pressures) connected through a total of 41 links (2.73 connections per component). There are: five drivers of changes (all pressures) not affected by the others (the strongest one is pollution); four receivers (components influenced by the others, but not been influenced) – pollination, carbon sequestration, soil formation and fertility, recreation and tourism. The rest are ordinary components, meaning that have an influence and are influenced by others. The highest centrality (relative importance) has the ES "Biodiversity", meaning that it is the most influential in the system. It is highly affected by all pressures, but it also affects other components. The lowest relative importance has the ES "Pollination".

This methodology highlights the most influential ESs and pressures, providing valuable insights for decision-making and conservation efforts. By integrating participatory modeling with scientific data, it supports more effective policies and adaptive management strategies. Engaging stakeholders from the outset not only streamlines the process but also enhances public acceptance and ensures access to critical firsthand knowledge that would otherwise remain unavailable. Finally, scenario analysis allows for testing changes in individual elements or combined effects, providing a comprehensive view of ecosystem dynamics and informing strategic interventions.

Acknowledgments: This article is based upon work from COST Action 21158 "Enhancing Small-Medium IsLands resiliance by securing the sustainability of Ecosystem (SMILES)", supported by COST (European Cooperation in Science and Technology).

References

Balzan MV, Potschin-Young M, Haines-Young R (2018) Island ecosystem services: insights from a literature review on case-study island ecosystem services and future prospects. International Journal of Biodiversity Science, Ecosystem Services & Management, 14(1): 71-90. https://doi.org/10.1080/21513732.2018.1439103

Du R, Liu B, Chen Z, Xu M (2024b). Exploring the multiscale island terrestrial ecosystem service relationships and coastal vulnerability under the influence of coastal ecosystems. Ocean & Coastal Management, 256, 107267. https://doi.org/10.1016/j.ocecoaman.2024.107267

Du R, Liu B, Xu M (2024a) Current status and trends in island ecosystem services research: A bibliometric analysis from 2000 to 2023. Marine Policy, 163, 106098. https://doi.org/10.1016/j.marpol.2024.106098

Gray SA, Gray S, Cox LJ., Henly-Shepard S (2013) Mental modeler: a fuzzy-logic cognitive mapping modeling tool for adaptive environmental management. In: 2013 46th Hawaii international conference on system sciences 965-973.

Ilić M, Srđević Z, Srđević B, Stammel B, Borgs T, Benka P, Grabić J, Ždero S (2024) The nexus between pressures and ecosystem services in floodplains: New methods to integrate stakeholders' knowledge for water quality management in Serbia. Ecosystem Services, 68, 101643. https://doi.org/10.1016/j.ecoser.2024.101643

Vogiatzakis I, Balzan M, Drakou E, Katsanevakis S, Padoa-Schioppa E, Tzirkalli E, ... & Manolaki P (2023) Enhancing Small-Medium IsLands resilience by securing the sustainability of Ecosystem Services: the SMILES Cost Action. Research Ideas and Outcomes, 9, e116061. https://doi.org/10.3897/rio.9.e116061

Flood exposure of environmental assets in Tuscany, Italy

G. Bertoli*, C. Arrighi, E. Caporali
Department of Civil and Environmental Engineering (DICEA), University of Florence, Firenze, Italy
**e-mail: gabriele.bertoli@unifi.it*

Introduction

In the context of a changing world, assessing environmental vulnerability and risk due to natural hazards is crucial for effective risk management and mitigation. Floods are among the most destructive natural hazards, hitting millions of people and affecting billions of hectares of territory every year all over the world (CRED 2024; UNDRR 2024). Several impacts to the environment, water resources and ecosystems have been related to floods (Arrighi and Domeneghetti 2024), then, flood risk analyses should be extended to environmental assets. As far as we know, there is no standard procedure for flood risk analysis of environmental assets. Risk assessment involves three main elements: Hazard, Exposure and Vulnerability (Crichton 1999). We have developed the EnvXflood method (Bertoli et al. 2024) to improve the exposure assessment of environmental assets, aligning the procedure with the standard applied for other assets (e.g. buildings), going beyond the exposed area indicator commonly used today by including the environmental value of the assets. The ecosystem services (MEA 2005) associated with the assets form the basis of the evaluation process. In the following sections we present some results of the analyses performed for the Tuscany region, highlighting the differences between the various levels of the EnvXflood flood exposure assessment method.

Materials and Methods

The EnvXflood assessment methodology introduced in Bertoli et al. (2024) have been implemented at two different levels of detail: Level 1, and Level 2. Level 1 of the methodology is based on the listing level (local, regional, national, international) of the analysed assets, where international assets are more important than national, which are more important than regional, which are more important than local. Level 2 analysis requires to assess the social and environmental value of the assets and combine this information to the Level 1 ranking. The environmental value has been determined following a participatory approach, based on common Multi-Criteria Decision-Making Analysis (MCDM-A) (Evers et al. 2018; Ferla et al. 2024). A survey was distributed involving the public and selected experts in the field. The outcomes of the participatory analysis are expressed as weights to be applied to the ecosystem services associated to the environmental assets part of the analysis. The resulting values contribute to determine the Environmental Value (EV) for each asset and, subsequently, the Environmental Exposure Value (EEV). According to the definition of Environmental Assets provided in Bertoli et al. (2024), and the associated dataset (Bertoli et al. 2025), the EnvXflood assessment methodology for flood exposure of environmental assets at level 1 and level 2 have been applied to the Tuscany region, Italy.

Results and Concluding Remarks

Level 1 and level 2 results of the analysis are shown in Figure 1.

The Environmental Exposure Value (EEV) for the level 2 analysis from Bertoli et al. (2024) is reported with a red line fading to blue. Red indicates most exposed assets, and blue less exposed assets. The light blue line and the orange line represent the Environmental Value (EV) of level 2 and level 1, respectively. Level 1 EV does not contain the ecosystem services values associated with the assets, therefore being less effective in catching the importance of the assets. The two EV values are anyway comparable in the first positions of the ranking, since water-related assets (rivers, lakes, and wetlands) are highly exposed to floods and provide valuable ecosystem services, thus equalising the level 1 and level 2 results. Yet, the differences between the two levels are more evident for assets that can provide less ecosystem services

(e.g. archaeological areas, karst forms, monumental trees), but are listed at national or international levels. In these cases, the level 2 EV is lower, giving priority to the assets that provide more ecosystem services.

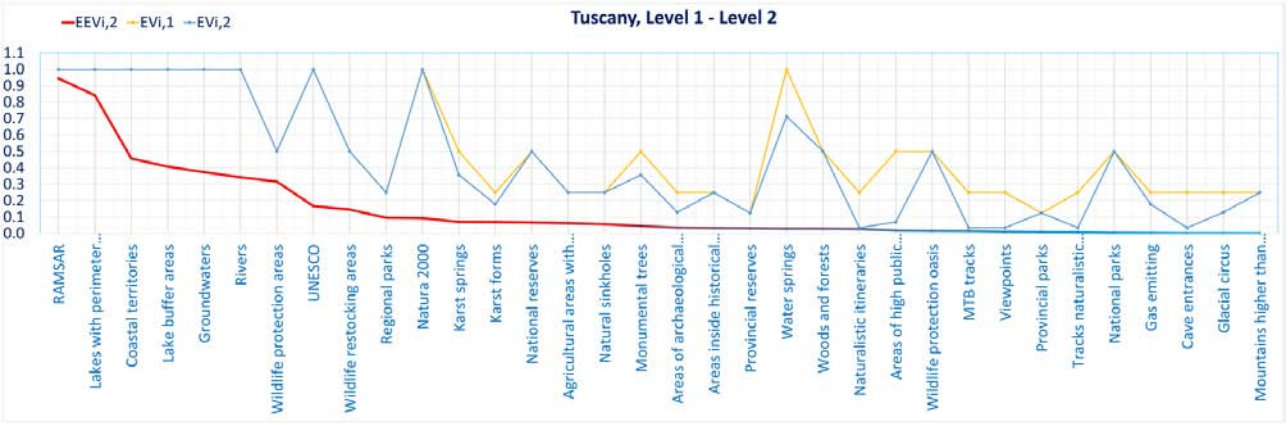


Figure 1. Environmental Exposure Value (EEV, level 2) and comparison of Environmental Value (EV) in level 1 and level 2 Analyses This diagram illustrates the Environmental Exposure Value (EEV) for level 2 analysis (red-to-blue line), alongside the Environmental Value (EV) for level 1 (orange) and level 2 (blue). The shift from level 1 to level 2 highlights how the refined assessment better captures the environmental significance of various assets. While some categories maintain high rankings, others shift, emphasizing the improved ability of level 2 to describe environmental value more comprehensively.

Despite resulting the most exposed to floods, water-related assets are often overlooked in risk assessments, usually assuming that floods have negligible impacts to natural areas. The results of the analysis demonstrate that this practice is no more sufficient for a comprehensive flood risk assessment, as the water-related assets are the most exposed to floods, and human activity introduced new flood-related impacts. This is a first step for an enhanced flood exposure assessment, and future research should direct to improve and validate the participatory approach results, and towards the flood vulnerability assessment of environmental assets.

References

Arrighi, C., A. Domeneghetti (2024) Brief communication: On the environmental impacts of the 2023 floods in Emilia-Romagna (Italy). In: Nat. Hazards Earth Syst. Sci. 24: 673–679. doi: 10.5194/nhess-24-673-2024.

Bertoli, G., C. Arrighi, E. Caporali (2025) Flood exposure of environmental assets. Nat. Hazards Earth Syst. Sci., 25, 565–580, https://doi.org/10.5194/nhess-25-565-2025.

Bertoli, G., C. Arrighi, E. Caporali (2025) GIS data - Flood Exposure of Environmental Assets - Tuscany, Italy. Version V1. doi: 10.17632/55phb4xw5k.1.

CRED (2024) 2023: Disasters in Numbers. Brussels. https://files. emdat.be/reports/2023_EMDAT_report.pdf (accessed: 2024-11-12)

Crichton, D. (1999) The Risk Triangle. In: Natural Disaster Management. Ed. by J. Ingleton. Tudor Rose, pp. 102–103. isbn: 978-0953614011.

Evers, M., A. D. S. Almoradie, M. M. de Brito (2018) Enhancing Flood Resilience Through Collaborative Modelling and Multi-criteria Decision Analysis (MCDA). In: Urban Book Series, Springer, pp. 221–236. doi: 10.1007/978-3-319-68606-6_14.

Ferla, G. et al. (2024) Multi-Criteria Decision Analysis (MCDA) for sustainability assessment in food sector: A systematic literature review on methods, indicators and tools. Sci. Total Environ. 946: 174235. doi: 10.1016/j.scitotenv.2024.174235.

MEA, Millennium Ecosystem Assessment (2005) Ecosystems and Their Services. Island Press.

UNDRR (2024) GAR Special Report 2024 Forensic Insights for Future Resilience Learning from Past Disasters. url: https://www.undrr.org/gar.

Challenges in determining the displacement of anti-personnel landmines by flooding

G. Keve[1*], B. Abonyi[1], S. Krikovszky[1], D. Csátaljay[1], Z. Kovács[2], I. Ember[2], J. Padányi[2]
[1] Faculty of Water Sciences, Ludovika University of Public Service, Baja, Hungary
[2] Faculty of Military Science and Officer Training, Ludovika University of Public Service, Budapest, Hungary
* e-mail: keve.gabor@uni-nke.hu

Introduction

Landmines are among the essential warfare materiel of a force and have a significant impact during combat, as they can destroy enemy troops personnel and combat equipment. Mines are usually deployed in large quantities in a so-called minefield, either manually or by some mechanical means. In a minefield, mines may be placed a few centimetres below the surface of the ground or on the surface of the ground, either in a systematic pattern or in a random, scattered pattern (Kovács 2022).

These lethal devices are still used in many parts of the world. It is estimated that between 65 and 120 million of these landmines are in use in 70 countries around the world, with a further 110 million in stockpiles. In 2023, 4,355 civilians, including 1,498 children, were killed in explosions from mines and other remnants of war (Landmine 2024). According to the Ukrainian government, about 174,000 km^2 of the country's territory are potentially in need of demining. Although this estimate seems exaggerated, mines and unexploded ordnance are a critical problem in a large territory, nearly six million Ukrainians live in vulnerable areas.

A common method of laying anti-personnel landmines is the use of mines that can be dropped from an aerial vehicle and scattered over the surface to quickly and effectively block routes, ***river crossings*** and roads. The PFM-1 anti-personnel mine under consideration (Figure 1) is a well-known and widely used representative of this type of mines. Its ease of deployment, its plastic body, which is difficult to detect with metal detectors, and its sensitivity make it a very dangerous mine.



Figure 1. Tutorial/training version of the mine PFM–1.

These and similar surface mines are often washed away by floodwaters, making them a potential source of danger in other locations. In these areas, mine maps and inventories of known minefields or unexploded ordnance are no longer valid (Baselt 2023).

There is a clear need for more information on the displacement of mines by flooding.

Materials and methods

Hydrodynamic tests were carried out using a glass flume in our Hydraulic Laboratory. The 7 m long

0.5*0.5 m cross-section glass flume with a 20 l/s discharge capacity provided sufficient possibilities for our first tests to wash away a single identical PFM-1 anti-personnel mine model by stream. This model was made by a 3D printer taking care for the proper shape and density.

Although the theory of bodies to move on any surface is quite straightforward, the determination of the frictional force derived from gravity and buoyancy force is far from trivial. It would require a coefficient of friction, which depends on material quality, roughness and even geometric parameters. The design of a specific landmine and the way in which it is placed and the exact conditions in which it is placed (soil conditions, vegetation, etc.) have a fundamental influence on its ability to be moved by drift.

Our tests with safe samples show that in all cases these mines lands on one of the two larger sides. We have defined these as "A" and "B" sides. We then defined 4 locations for each side relative to the direction of flow. In this way, a total of 8 placements were investigated.

Results and concluding remarks

Several tests have been carried out under laboratory conditions to determine the limiting displacement velocities as a function of different surface cover and slope conditions. One of our result can be seen on Figure 2. This figure shows the stream velocity required to move the PFM-1 mines in a grassy floodplain (Vargas-Luna 2015) as a function of slope. The different coloured lines indicate the position of the mines relative to the flow direction. This set of curves provides the basis for calculating the displacement of the PFM-1 using the velocity vector field of the 2D hydrodynamic models already available.

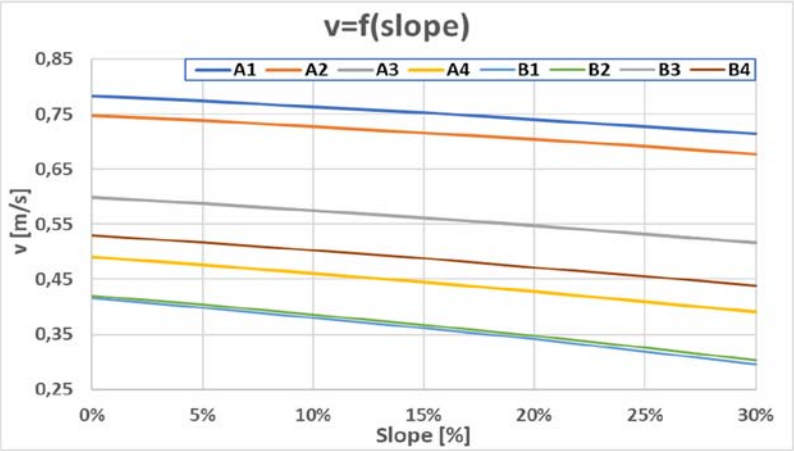


Figure 2. PFM-1 displacement boundary water velocities as the function of slope in grasslands.

Unfortunately, we are not able to calculate the proper relocation of landmines in flood events due to the stochastic nature of the process. However, our investigations can provide a good approximation of their most likely new position. Note, that mines explode under pressure, so they can be activated in a certain depth of water. Driving the mines into deep water by streams could also be a mine clearance method, but this new direction of research is still ahead of us.

References

Baselt I, Skejic A, Zindovic, B, Bender, J (2023) Geologically-Driven Migration of Landmines and Explosive Remnants of War—A Feature Focusing on the Western Balkans. 2023. június 24. Online: https://www.mdpi.com/2076-3263/13/6/178

Kovács Z (2022) Aknatelepítés: Keleten a helyzet jelentősen megváltozott 1. rész. Haditechnika 2022/3. 31-38. (in Hungarian)

Landmine Monitor (2024) International Campaign to Ban Landmines, Landmine Monitor 2024, Geneva: ICBL-CMC, November 2024. 2.

Vargas-Luna A, Crosato A, Collot L, Uijttewaal W.S.J. (2015) Laboratory investigation on the hydrodynamic characterization of artificial grass. In E-proceedings of the 36th IAHR World Congress 28: 728-734.

Effectiveness of emergency postfire rehabilitation treatments in Mediterranean forests: A nature-based solution for erosion control

N. Proutsos[1*], A. Bourletsikas[1], S. Stefanidis[2], A. Solomou[1], P. Michopoulos[1]
[1] Institute of Mediterranean Forest Ecosystems, Hellenic Agricultural Organization - DIMITRA, Athens 11528, Greece
[2] Forest Research Institute, Hellenic Agricultural Organization - DIMITRA, Vasilika 57006 Thessaloniki, Greece
* e-mail: nproutsos@elgo.gr

Introduction

Postfire restoration and forest management are important for the sustainability of Mediterranean terrestrial ecosystems, considering the high numbers of wildfires and the vulnerability of the area as a climate change and biodiversity hotspot. Restoration efforts can ensure the conservation status of the local forests aiming to retain soil material immediately after wildfires. Several types of nature-based solutions are adopted and tailored to the specific characteristics of the forest sites to enhance the effectiveness of the interventions and achieve the main goal, which is the restoration of the terrestrial ecosystems.

Implementation of emergency rehabilitation treatments is imposed in many cases of high-risk burned forests prone to erosion. The significance of such actions is acknowledged, however the research on their effectiveness to reduce the impact of erosion is limited. This study follows previous work by Stefanidis et al. (2024) and aims to enhance knowledge on the behaviour of erosion control structures, by assessing the impact of three types of erosion control structures in three Greek sites, through the analysis of measured volumes of the retained soil material two years after the wildfires and the construction of the works.

Materials and methods

The current study is based on measurements of retained soil material in three Mediterranean forest sites (Parnitha-Attica, Mavrolimni-Corinth and Ancient Olympia-Ilia, Figure 1) that were destroyed by wildfire in 2021, for two years (2022 and 2023) after the implementation of emergency rehabilitation treatments (construction of wooden structures as wattles, log-barriers and log-dams). Specific details of the sites and the forest fire characteristics can be found in http://epadap.web.auth.gr/.



Figure 1. Map of the study sites in Greece and different types of emergency erosion control structures.

The rehabilitation treatments in the burned areas involved the construction of linear wooden structures, including wattles (in moderate or light slopes) and log-barriers (in steep slopes), positioned perpendicular to the slopes, in conjunction with small wooden dams in the streams (Figure 1). The three study sites were

characterized by different soil characteristics. The forest site of Parnitha-Attica is on hard limestone and flysch, Corinth on peridotites-gabbros and deposition cones and Ilia on tertiary deposits. Additionally, different climatic conditions persist among them. In each study site, experimental plots were installed to measure the volumes of the retained soil material. In total, data from 25 plots were analysed including 9 log-dams, 9 log-barriers and 7 wattlets in the three sites. The retained soil volumes were estimated according to Myronidis et al. (2010).

Results and concluding remarks

This study analyses the accumulated deposition volumes by erosion control structure type and research site for two years following the fire and the postfire restoration (Figure 2). Wattles were more effective in retaining soil than log-barriers, which are also linear wooden structures constructed, though, on steeper slopes. Over 2022 and 2023, average accumulated soil retention for wattles was 0.029 m³ per linear m of structure, while for log-barriers, it reached 0.013 m³/m.

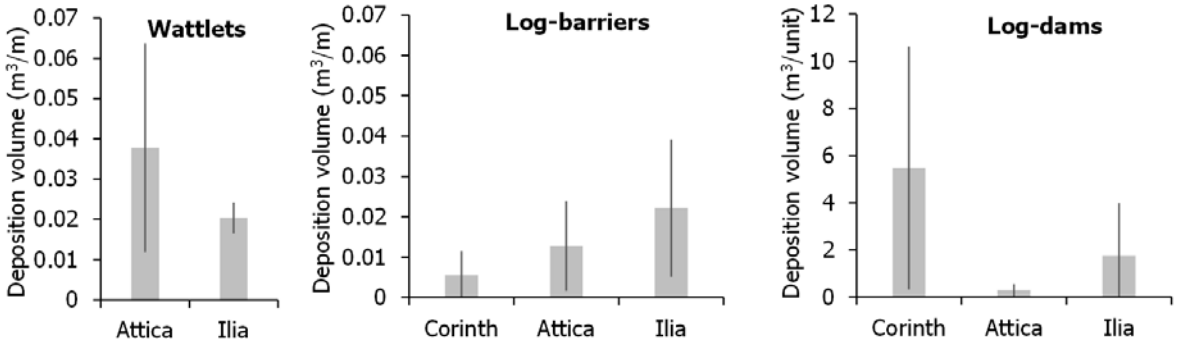


Figure 2. Deposition volumes in Corinth, Attica and Ilia, by type of erosion control structure two years after fire.

There were obvious differences between sites. Two years postfire, the accumulated amount of eroded material retained by wattles was higher in Attica (0.038±0.026 m³/m), whereas in Ilia, it was almost equivalent to that retained by log barriers (0.022±0.004 m³/m). Wattles retained higher amounts of soil than log-barriers in Attica (0.038 m³/m vs. 0.013 m³/m), due to site characteristics (slope, soil type, etc) and rainfall distribution, differences. The maximum total retention for log barriers measured in Ilia at 0.022 m³/m, followed by moderate retention in Attica (0.013 m³/m) and lower in Corinth (0.005 m³/m). In September 2023, the log-dams in Corinth had the highest soil retention per structure unit (5.48 m³/unit) compared to other regions. This was largely due to a significant rainfall event on September 6th (71 mm) which was substantially higher than the rainfall in Ilia and Attica, resulting in soil retention 1.77 and 0.29 m³/unit, respectively.

This study highlights the need to carefully consider variations in seasonal precipitation patterns and structure types when assessing the relative effectiveness of postfire erosion control measures. The success of such structures generally depends on site-specific factors like construction timing and seasonal rainfall intensity. This underscores the importance carefully evaluating site conditions in tailoring erosion control strategies to optimize soil retention and mitigate postfire erosion.

Acknowledgments: This work is supported by the research projects “MoRe Forest: MOnitoring the impact of REstoration works in the post fire Forest environment in Greece” funded by the Hellenic Green Fund, with beneficiary the Directorate General for Forests and Forest Environment and “Research on Forest Hydrology Parameters in Mountainous Watersheds of Greece” funded by OMIKRON S.A.

References

Myronidis DI, Emmanouloudis DA, Mitsopoulos IA, Riggos EE (2010) Soil erosion potential after fire and rehabilitation treatments in Greece. Environmental modeling & assessment, 15, 239-250. https://doi.org/10.1007/s10666-009-9199-1

Stefanidis SP, Proutsos ND, Solomou AD, Michopoulos P, Bourletsikas A, Tigkas D, Spalevic V, Kader S (2024) Spatiotemporal monitoring of post-fire soil erosion rates using earth observation (EO) data and cloud computing. Natural Hazards, 1-22. https://doi.org/10.1007/s11069-024-06907-4

Drought vulnerability parameters: a literature review

A. Theodoroulis*, H. Vangelis, V.A. Tsihrintzis
Centre for the Assessment of Natural Hazards and Proactive Planning, & Laboratory of Reclamation Works and Water Resources Management, School of Rural, Surveying and Geoinformatics Engineering, National Technical University of Athens, 9 Heroon Polytechniou, 15780 Zographou, Athens, Greece
** e-mail: axilleastheodwroulis@gmail.com*

Introduction

Drought is a prolonged period of water shortage, impacting human life and the environment (Wilhite & Glantz, 1985). The main drought types are meteorological, hydrological, agricultural, and socio-economic (Saha et al., 2023a). According to Wolf et al. (2013), vulnerability to drought is referred to as the capacity to anticipate, manage, resist, and recover from drought effects. In the literature, vulnerability parameters are usually grouped into three main groups, namely exposure, sensitivity, and adaptive capacity (e.g., Wolf et al., 2013; Saha et al., 2023b).

The present study aims to identify drought vulnerability parameters, which are commonly used in the literature, and present them in terms of drought types and vulnerability parameter groups. Drought vulnerability parameters may be used for the quantification of drought impacts, and therefore, identifying the most widely used ones is considered essential. In this context, the frequency of appearance of each parameter in the literature, is also recorded. Needless to say that, understanding these parameters is crucial for developing effective mitigation strategies to reduce the adverse effects of drought (Wilhelmi & Wilhite, 2002).

Materials and methods

Studies on drought vulnerability parameters were identified, screened, and reviewed following the PRISMA 2020 guidelines for systematic reviews and meta-analyses (Page et al., 2021). Data from 2002 to 2024 were examined to ensure relatively recent and comprehensive coverage. Searches were conducted using Scopus, Science Direct, Springer, and Google Scholar literature databases, employing the phrase "drought vulnerability parameters". Initially, 103 titles were recorded and scrutinized based solely on their abstracts. If the main content from the abstract was found relevant, the papers were selected for further study. In a next step, duplicates were removed from the record. Finally, 73 titles were excluded based on eligibility criteria, and 35 publications were included in this review.

Results and concluding remarks

The review identified 241 parameters in these 35 publications. Drought vulnerability can be influenced by several parameters across different aspects. Though these parameters could be presented in context-specific parameter significance levels, however, only the most critical parameters were finally selected to be presented followed by their frequency of appearance in the literature (Tables 1 and 2). For the meteorological drought type, the most common vulnerability parameters are rainfall departure from the mean (e.g., Thomas et al., 2016), average rainfall (e.g., Safavi et al., 2014), and drought intensity (e.g., Saha et al., 2023a). Regarding hydrological drought, distance to rivers, groundwater levels, and groundwater availability (e.g., Saha et al., 2023a) are the most common vulnerability parameters, while in agricultural drought, parameters include slope and elevation (e.g., Saha et al., 2023a) and soil type (e.g., Thomas et al., 2016). Socio-economic drought vulnerability is influenced by land use land cover (LULC) (e.g., Thomas et al., 2016), population density (e.g., Saha et al., 2023a), and farm population (e.g., Thomas et al., 2022). In terms of vulnerability parameters groups, sensitivity is affected by slope, elevation, and population density (e.g., Saha et al., 2023a), exposure is determined by LULC (e.g., Yu et al., 2021), farm population (e.g., Thomas et al., 2022), and overall population (e.g., Yu et al., 2021), while, adaptive capacity takes into account the

distance to rivers and irrigated land (e.g., Saha et al., 2023a), and Plant Available Water Capacity (PAWC) (e.g., Wilhelmi & Wilhite, 2002).

Table 1. Three most common drought vulnerability parameters according to drought type

Drought types	1st parameter & frequency (%)	2nd parameter & frequency (%)	3rd parameter & frequency (%)
Meteorological	Rainfall departure (21.74%)	Average rainfall (21.74%)	Drought intensity (17.39%)
Hydrological	Distance to river (30.43%)	Groundwater levels (Depth to groundwater levels) (17.39%)	Groundwater availability (17.39%)
Agricultural	Slope (15.24%)	Elevation (Altitude) (12.38%)	Soil Type (7.62%)
Socio-economic	Land use land cover (17.95%)	Population density (16.67%)	Farm population (11.54%)

Table 2. Three most common drought vulnerability parameters according to vulnerability parameter group

Vulnerability param. groups	1st parameter & frequency (%)	2nd parameter & frequency (%)	3rd parameter & frequency (%)
Sensitivity	Slope (11.35%)	Elevation (Altitude) (9.22%)	Population density (9.22%)
Exposure	Land use land cover (29.17%)	Farm population (18.75%)	Population (10.42%)
Adaptive capacity	Distance to river (19.51%)	Irrigated land (14.63%)	Plant available water capacity (12.20%)

It is concluded that meteorological drought vulnerability parameters could correspond only to exposure and sensitivity parameter groups, as there is no correlation to adaptive capacity parameters. It should also be mentioned, that there seems to be a confusion between drought hazard parameters and meteorological drought vulnerability parameters in the literature. This could be based on the fact that both hazard and meteorological drought vulnerability use many same parameters for different evaluations.

References

Page M J, McKenzie J E, Bossuyt P M, Boutron I., Hoffmann T C, Mulrow C D, Shamseer L, Tetzlaff J M, Akl E A, Brennan S E, Chou R, Glanville J, Grimshaw J M, Hróbjartsson A, Lalu M M, Li T, Loder E W, Mayo-Wilson E, McDonald S, Moher D (2021) The PRISMA 2020 statement: An updated guideline for reporting systematic reviews. BMJ 372: n71. https://doi.org/10.1136/bmj.n71

Safavi H R, Esfahani M K, Zamani A R (2014) Integrated index for assessment of vulnerability to drought, case study: Zayandehrood River basin, Iran. Water Resources Management 28(6): 1671-1688. https://doi.org/10.1007/s11269-014-0576-4

Saha S, Kundu B, Saha A et al. (2023a) Manifesting deep learning algorithms for developing drought vulnerability index in monsoon climate dominant region of West Bengal, India. Theoretical and Applied Climatology 151: 891-913. https://doi.org/10.1007/s00704-022-04300-4

Saha S, Kundu B, Paul G C et al. (2023b) Proposing an ensemble machine learning based drought vulnerability index using M5P, dagging, random sub-space and rotation forest models. Stochastic Environmental Research and Risk Assessment 37: 2513-2540. https://doi.org/10.1007/s00477-023-02403-6

Thomas T, Jaiswal R K, Galkate R, Nayak P C, Ghosh N C (2016) Drought indicators-based integrated assessment of drought vulnerability: A case study of Bundelkhand droughts in central India. Natural Hazards 81(3): 1627-1652. https://doi.org/10.1007/s11069-016-2149-8

Thomas T, Nayak P C, Ventakesh B (2022) Integrated assessment of drought vulnerability for water resources management of Bina basin in Central India. Environmental Monitoring and Assessment 194(9): 621. https://doi.org/10.1007/s10661-022-10300-8

Wilhelmi O V, Wilhite D A (2002) Assessing Vulnerability to Agricultural Drought: A Nebraska Case Study. Natural Hazards 25(1): 37-58. https://doi.org/10.1023/A:1013388814894

Wilhite D A, Glantz M H (1985) Understanding the drought phenomenon: The role of definitions. Water International 10(3): 111-120. https://doi.org/10.1080/02508068508686328

Wolf S, Hinkel J, Hallier M, Bisaro A, Lincke D, Ionescu C, Klein R J T (2013) Clarifying vulnerability definitions and assessments using formalisation. International Journal of Climate Change Strategies and Management 5(1): 54-70. https://doi.org/10.1108/17568691311299363

Yu J, Kim J E, Lee J-H, Kim T-W (2021) Development of a PCA-based vulnerability and copula-based hazard analysis for assessing regional drought risk. KSCE Journal of Civil Engineering 25(5): 1901-1908. https://doi.org/10.1007/s12205-021-0922-z

Vulnerability assessment of wastewater treatment plants using a territorial multi-hazard multi-scale approach

M. Castiglione*, S.F. Corsino, M. Capodici, M. Torregrossa
Department of Engineering, University of Palermo, Palermo, Italy
** e-mail: maria.castiglione01@unipa.it*

Introduction

Extreme natural events are becoming more frequent and intense also due to climate change (Pang et al., 2023). The effects are expected to intensify, resulting in new challenges for infrastructure resilience. In this scenario, waste water treatment plants (WWTPs) are a critical component of the industrial infrastructure (Casson Moreno et al., 2018). These facilities play an essential role in public health and environmental protection, particularly in densely populated areas where large volumes of wastewater are generated. To estimate the effects of extreme events it is certainly important to identify areas (location) and related infrastructures (function) that may be damaged by these events. Most of the scientific studies on hazard assessment methodology have focused on single hazard approaches. This approach is useful to address the risk of a specific hazard, but it has significant limitations when it is applied for overall assessment (Novelli et al., 2024). The objective of this study is to assess wastewater treatment plants vulnerability applying a multi-hazard approach to the Sicilian territory. This approach will provide a more comprehensive understanding of the risks. It will allow for the development of more effective resilience strategies for these critical infrastructures.

Materials and methods

The methodology framework considered five types of natural hazards (j): hydraulic, geomorphological, volcanic, seismic and tsunami. Focusing on the Sicilian region, each hazard map was harmonized so that H1 corresponded to the lowest hazard and H4 corresponded to the highest. The Sicilian territory was divided into a grid with 200 m x 200 m cells. Each cell is identified by an index i. Each cell i is composed of portions that may belong to different hazard classes. The total area of the cell is denoted as Ai (40000 m^2), while the area of the portion of territory associated with class H_k for hazard j is $A_{i,j,k}$.

For every cell, the relative weight of each hazard class is determined by the proportion of the cell's area associated with that class, given by $w_{i,j,k}=A_{i,j,k}/A_i$.

This weight quantifies the contribution of each class to the overall hazard of the cell. To calculate the contribution of a particular class, its relative weight is multiplied by the assigned numerical value H_k.

The sum of the contributions of all classes gives the individual hazard indicator for hazard j within cell i:

$$HI_{i,j} = \sum_{k=1}^{4}(w_{i,j,k} \cdot H_k) \quad (1)$$

Finally, the multi-hazard index (2) for cell i is computed as the weighted sum of individual hazard indicators by assuming an equal weight for each of them:

$$MHI_i = \sum_{j\in\{s,g,h,v,t)} HI_{i,j} \quad (2)$$

A multi-hazard map was created to classify the territory into four distinct hazard levels, representing a gradation of potential threats. Additionally, this hazard map was overlaid with the locations of wastewater treatment plants. A detailed analysis was subsequently conducted at municipal level.

The municipalities of Cefalù and Mascali and their respective WWTPs were considered as case studies.

Results and concluding remarks

Figure 1 illustrates the spatial distribution of the multi- hazard index (MHI) crossed with the location of

wastewater treatment plants. The tables and pie charts summarise the distribution of WWTPs between the various hazard classes, providing a clearer view. It can be observed that most wastewater treatment plants (240) are in low hazard zones (class 1), while 37 WWTPs fall into moderate hazard class (class 2). Focusing on the case studies, it can be observed that in the municipality of Cefalù the predominant hazards are geomorphological and seismic, followed by tsunami hazard. While in the case of Mascali municipality, due to its proximity to Mount Etna, volcanic and seismic hazards predominate.

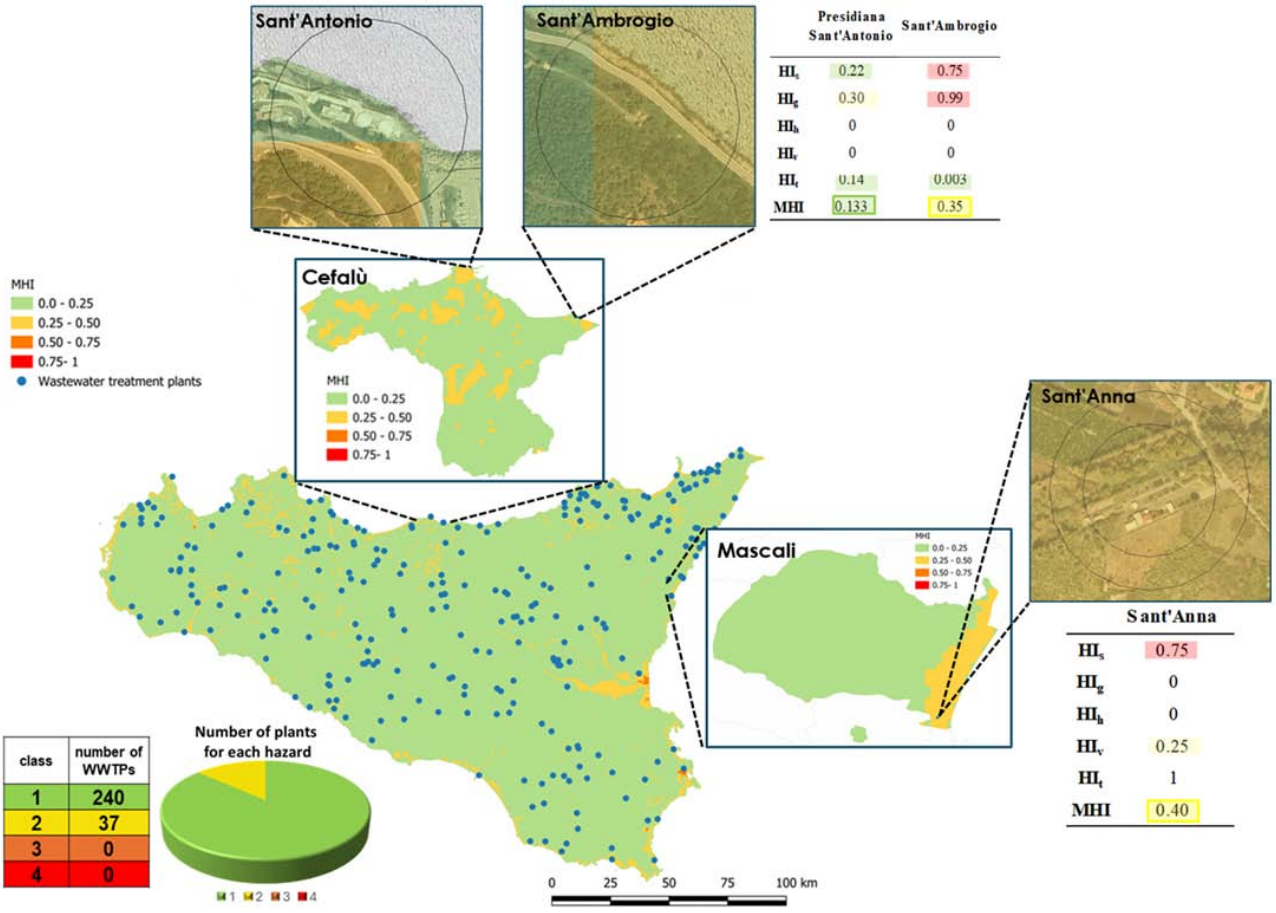


Figure 1. Results from the multi-hazard, multi-scale approach depicting vulnerability between industry and territory.

The developed multi-hazard map significantly impacts the assessment and management of hazards for wastewater treatment plants, addressing several existing gaps in literature. The subsequent identification of possible equipment failures triggered by a natural event, and its potential consequences, can suggest to WWTP managers the correct measures to adopt to increase the resilience of the infrastructure.

Acknowledgments: These topics are investigated within the RETURN project. Specifically, within the Spoke TS2-Multi Risk Resilience of Critical Infrastructures. WP 3 - Dynamic mapping of natural and climatic hazards over the infrastructure systems. T 3.2 – Robust hazard mapping over point critical infrastructures. Sub Task 3.2.2. Natural Hazards classification maps of point-like infrastructures of national relevance.

References

Casson Moreno, V., Reniers, G., Salzano, E., Cozzani, V. (2018). Analysis of physical and cyber security-related events in the chemical and process industry. Process Safety and Environmental Protection 116: 621–631. https://doi.org/10.1016/j.psep.2018.03.026

Novelli, F., Pesce, F., Bubbico, R. (2024). Seismic risk in the chemical process industry: A semi-quantitative methodology for critical equipment identification. J Loss Prev Process Ind 88. https://doi.org/10.1016/j.jlp.2024.105252

Pang, T., Wang, X., Nawaz, R.A., Keefe, G., Adekanmbi, T., 2023. Coastal erosion and climate change: A review on coastal-change process and modeling. Ambio. https://doi.org/10.1007/s13280-023-01901-9

Assessing the Individual Flood Risk index to identify areas with lower risk sustainability

D. Biondi*, G. Capparelli, D. Spina, F. Cruscomagno
Department of Computer, Modeling, Electronics and Systems Engineering (DIMES), University of Calabria, Rende, Italy
** e-mail: daniela.biondi@unical.it*

Introduction

The increasing frequency and intensity of extreme weather events, in the context of global changes, highlights the urgency of understanding and mitigating hydrogeological risks. Accurate identification of areas exposed to potential flooding plays a key role in formulating land management strategies and defining adaptation policies. Within the framework of the PON Governance and Institutional Capacity 2014-2020, a possible definition of Areas with Lower Risk Sustainability (ALRS) was provided: "Areas where critical hydrogeological and hydraulic phenomena could occur, mostly characterized by high kinetic energy, and where conditions of exposure and vulnerability exist that make it difficult to promptly and effectively implement measures to safeguard public and private safety and assets" (Versace et al., 2021a).

This study presents the preliminary results of the Individual Flood Risk (IFR) index evaluation using an empirical, indicator-based approach. The methodology was tested in the urban area of Cosenza, a municipality intersected by a dense hydrographic network, primarily the Crati and Busento rivers.

Materials and methods

The IFR index represents the risk to which an individual is exposed, providing a comprehensive measure of flood-related threats. It can take values between zero and one, with higher values indicating higher risk. The quantitative evaluation of IFR is framed within a broader framework, called QUEST (QUantitative ESTimator) (Versace et al., 2021b). Flood risk is conceptually structured into several components that align with the main terms of the risk equation—hazard, vulnerability, exposure, and coping capacity—building upon the formulation of UNISDR (2009), which expands on that of Varnes (1984):

- Hazard refers to the likelihood of flood related processes that may result in loss of life, injury, or other health impacts, as well as property damage.
- Exposure indicates the presence of people, infrastructure, housing, production capacities and other tangible assets located in hazard-prone areas.
- Vulnerability refers to the susceptibility of communities, assets, or systems to the impacts of hazards, depending on conditions shaped by physical, social, economic, and environmental factors or processes.
- Coping Capacity is a behavioural capacity of people, institutions, organisations and systems, using available skills, values, beliefs, resources, and opportunities, to address, manage and overcome adverse conditions in the short to medium term (UNISDR, 2009).

The scores for hazard, exposure, vulnerability, and coping capacity range from 0 to 1. It should be noted that, in the calculation of flood risk, higher values of the first three factors represent "negative" contributions, meaning they increase the overall risk. Conversely, coping capacity incorporates "positive" indicators into the analysis, helping to mitigate the impact of the event and effectively reducing the risk value. The way in which risk is calculated here, is therefore based on the following formulation:

$$\text{Risk} = \text{Hazard} \times \text{Exposure} \times \text{Vulnerability} \times (1 - \text{Coping Capacity}) \quad (1)$$

The procedure for estimating the IFR index consists of a series of systematic and progressive steps that involve the cascading analysis of indicators (approximately 50, some of which are composite), attributes (24), and domains (8), using a weighted average approach. The process involves estimating the indicators, normalizing them, and assigning weights based on their relevance, with the same methodology applied to

determine the attributes and domains. To calculate the IFR index, the critical scenario associated with a potential river overflow during a flood event with a 500-year return period was considered for the case study. Flood-prone areas were identified using HEC-RAS 6.6 software through hydrodynamic modeling based on the two-dimensional de Saint-Venant equations.

Results and concluding remarks

Figure 1c presents the results of the IFR index evaluation at a 5×5 meter grid scale for the urban area of Cosenza. The index is clipped to the floodable areas, which include historically flooded zones (see Figure 1b), and integrates various indicators related to hazard, vulnerability, exposure and coping capacity. As an example, Figure 1a illustrates the normalized values for a specific indicator, event magnitude (*Magn*), which is part of the Event Intensity attribute within the Hazard domain. The *Magn* indicator is calculated based on a combination of flow depth and velocity, with values assigned to each grid cell according to the most severe conditions. The accuracy of the IFR index assessment is strongly dependent on the availability and quality of the data used to estimate these indicators. This data comes from different sources, including consultations of existing databases (e.g., ISTAT), thematic maps, technical documents, and, when needed, ad hoc surveys and studies.

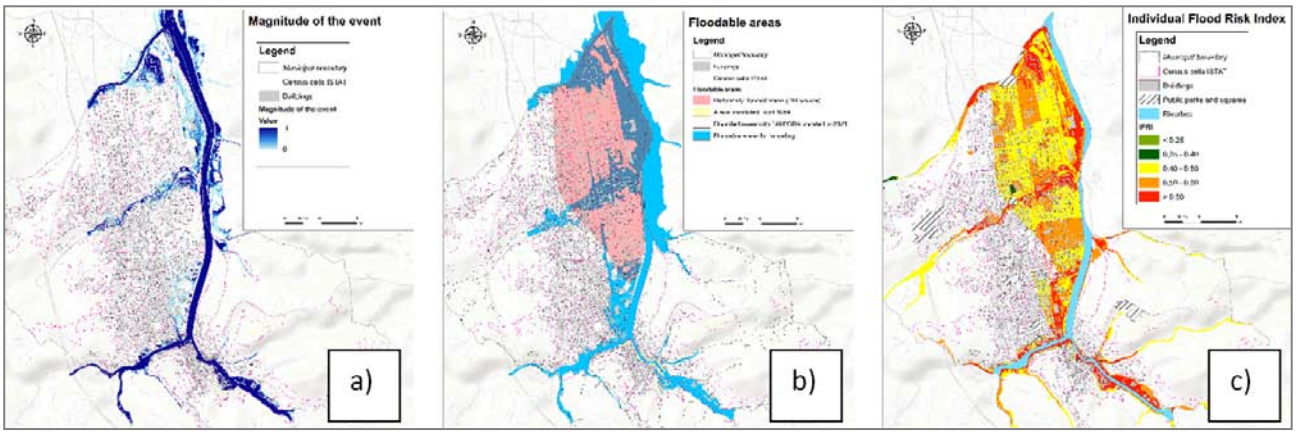


Figure 1. a) Normalized results (0-1) of the 'magnitude of the simulated event' indicator; b) Floodable areas, including historically flooded zones (various sources); c) IFR index at 5×5 grid scale, clipped to the floodable area.

Acknowledgments: This work was funded by the Next Generation EU - Italian NRRP, Mission 4, Component 2, Investment 1.5, call for the creation and strengthening of 'Innovation Ecosystems', building 'Territorial R&D Leaders' (Directorial Decree n. 2021/3277) - project Tech4You - Technologies for climate change adaptation and quality of life improvement, n. ECS0000009. This work reflects only the authors' views and opinions, neither the Ministry for University and Research nor the European Commission can be considered responsible for them.

References

Varnes D. J. (1984) "LSLR: Landslide Risk Assessment." In: Landslides: Analysis and Control, Special Report 176. Transportation Research Board, National Research Council, Washington D.C., pp. 15-33.

Versace P., De Luca D. L., De Santis D., Penna G. & Spina D. (2021a) Linee guida per l'identificazione delle aree a minore sostenibilità del rischio per gli scenari di evento tipici identificati. Report tecnico del "Programma per il supporto al rafforzamento della governance in materia di riduzione del rischio idrogeologico e idraulico ai fini di protezione civile" a valere sul PON Governance e Capacità istituzionale 2014-2020.

Versace P., De Santis, D. Penna, G. Politanò L. & Presta D. (2021b) Definizione di linee guida per un modello di valutazione standard della pianificazione di Protezione Civile comunale e intercomunale. Report tecnico del "Programma per il supporto al rafforzamento della governance in materia di riduzione del rischio idrogeologico e idraulico ai fini di protezione civile" a valere sul PON Governance e Capacità istituzionale 2014-2020.

UNISDR (United Nations International Strategy for Disaster Reduction). (2009). 2009 UNISDR Terminology on Disaster Risk Reduction. United Nations International Strategy for Disaster Reduction (UNISDR). https://www.undrr.org/publication/2009-unisdr-terminology-disaster-risk-reduction

VII. Water-Energy-Food-Ecosystem Nexus

Setting greenhouse gas mitigation targets in the water sector through cost-effective approaches

H. Han*, D. Ahn, B. Hwang
Integrated Water Management, Korea Environment Institute, Sejong, Republic of Korea
** e-mail: hanhj@kei.re.kr*

Introduction

Water facilities contribute significantly to public sector emissions in the Republic of Korea, accounting for 20.8% of the total. Despite the critical role of these facilities, domestic research remains limited regarding the costs of mitigation measures, their impacts on water management functions, and their co-benefits. This lack of data and analysis poses challenges to setting effective and achievable greenhouse gas (GHG) reduction targets.

This study aims to address these gaps by developing a cost-effectiveness evaluation framework tailored specifically for Korea's water sector. This framework evaluates reduction potential, implementation costs, and policy synergies to establish evidence-based national GHG mitigation targets for 2030. The results provide a practical roadmap for aligning water management and climate policy objectives, ensuring effective and sustainable GHG reductions in the water sector.

Materials and methods

This study employs a multi-step methodological framework for GHG mitigation targets and developing a cost-effective implementation roadmap for the water sector. The methodology is structured into six key stages:

1. *Setting Foundational Directions for GHG Mitigation*
   The first step defines the basic principles and scope for GHG mitigation in the water sector. This ensures alignment with both national policies, such as Korea's Nationally Determined Contributions (NDCs), and international frameworks, including the Science Based Targets initiative (SBTi).
2. *Organizational Structure and Operational Boundaries*
   This step establishes organizational boundaries and operational guidelines, which are essential for accurately assessing sectoral emissions. It sets the framework for data collection and scenario development.
3. *Baseline GHG Emissions Assessment*
   The baseline year for GHG emissions is 2018, aligned with Korea's NDCs. Direct emissions include wastewater processes, LULUCF, and fuel use, while indirect emissions cover electricity consumption, calculated using national inventory and IPCC guidelines.
4. *Developing the GHG Mitigation Measures Database (DB)*
   This study builds a database for cost-effective GHG mitigation in the water sector through three steps: collecting data from existing sources, selecting feasible measures based on reduction potential and cost, and classifying them by sub-sector, priority, cost level, technology, and facility type.
5. *Establishing the 2030 Mitigation Scenarios*
   Five scenarios were evaluated: maximum mitigation (Scenario A), renewable energy-focused (Scenario B), maximum facility participation (Scenario C), cost-effective measures (Scenario D), and a hybrid strategy (Scenario E). Scenarios were assessed for reduction potential, cost, and feasibility.
6. *Developing the Roadmap*
   The final step synthesizes the findings into a comprehensive roadmap, outlining actionable steps for achieving the water sector's 2030 mitigation targets. This roadmap provides detailed guidance on implementing prioritized measures, integrating sectoral policies, and aligning with overarching

climate goals.

Results and concluding remarks

The cost-effectiveness analysis of GHG mitigation measures in the water sector reveals a wide range of reduction potentials and associated costs (Figure1).

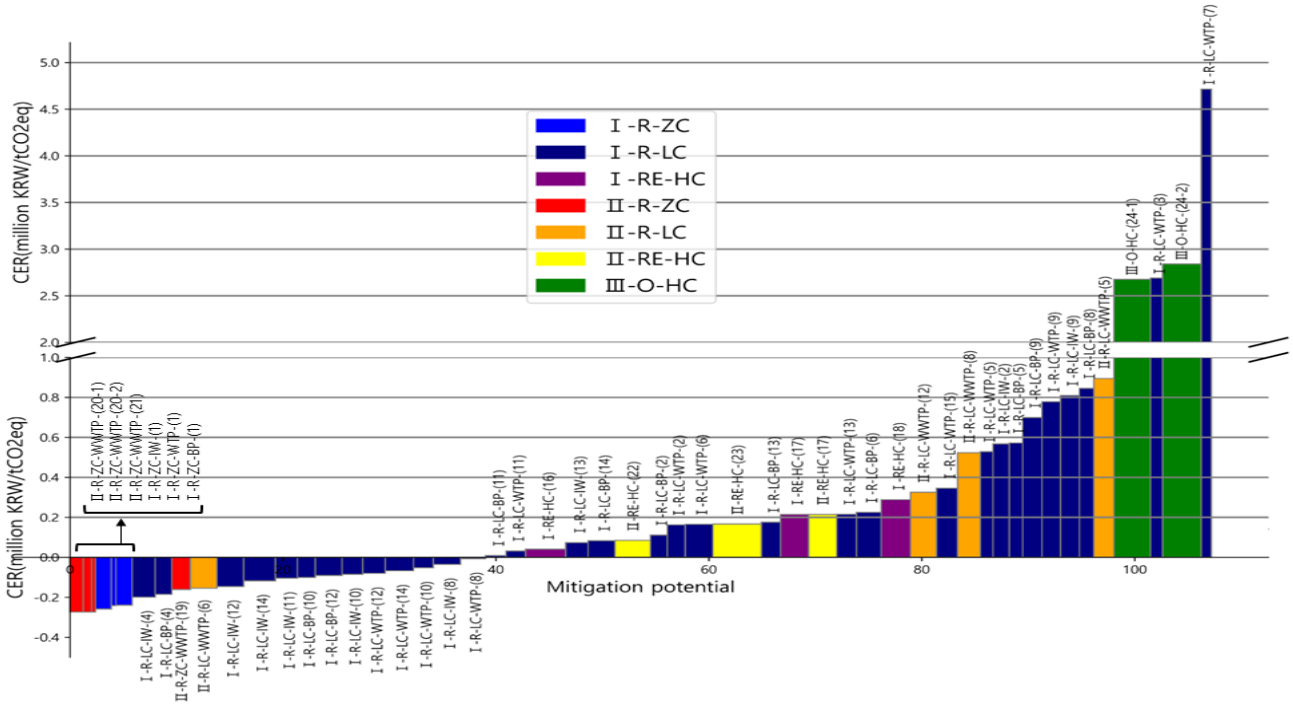


Figure 1. Cost-effectiveness ratios of GHG mitigation measures in the water sector

The five scenarios (A–E) all achieved more than 70% reduction, meeting the criteria for ambition in GHG mitigation. Beyond ambition, Scenario E was selected as the basis for the roadmap due to its balanced performance in cost-effectiveness, policy alignment, and feasibility, making it the most practical and sustainable option for implementation.

Table 1. Results of scenario analysis for GHG mitigation in the water sector

Scenarios	A	B	C	D	E
Mitigation Direction	Maximum reduction	Focus on renewable energy-based reduction	Focus on water facility-based reduction	Focus on zero-cost measures	Hybrid: Renewable energy and cost-effective reduction measures
2030 Reduction Rate (%)	123	76	75	93	71
Marginal Abatement Cost (KRW/ton)	113,335	115,966	64,859	-21	1,0762

This study presents a comprehensive framework for achieving a 70% GHG reduction in Korea's national water sector by 2030. The proposed roadmap is a key strength, offering practical strategies that prioritize energy efficiency in water facilities and transitioning to renewable energy sources. The results provide actionable insights and align with long-term sustainability goals.

However, this study has limitations, such as the absence of a comprehensive water sector database, limited renewable energy options, reliance on cost-effectiveness over marginal abatement cost analysis, and minimal consideration of co-benefits. Future research should expand the database, assess co-benefits, and apply advanced methods to support 2050 carbon neutrality.

References

Han H, et al. (2022) Roadmap Development for Achieving Carbon Neutrality in the Water Sector by 2050. National Water Management Committee, Sejong

Metals concentration in selected fish species available in Polish food markets

P. Biedka, I.A. Tałałaj
Bialystok University of Technology, Faculty of Civil Engineering and Environmental Science, Białystok, Poland
** e-mail: p.biedka@pb.edu.pl; i.talalaj@pb.edu.pl*

Introduction

Heavy metals are pollutants whose harmfulness is related to their persistence and toxicity. Some of these metals, such as zinc, iron, and copper, are considered essential elements that play a key role in biological processes. Others, however, are classified as non-essential elements, as they have no role in biological processes and can produce toxic effects when their concentrations exceed certain thresholds (Ouali et al., 2018). Among these contaminants are metallic trace elements (MTEs), such as lead, cadmium, and mercury, which are known for their toxic properties even at low doses. These elements are not metabolized by living organisms, leading to their accumulation in the food chain (Akhouchal et al., 2021). Heavy metals present in the aquatic environment can accumulate in bottom sediments and penetrate aquatic organisms, including fish, plankton, and benthos (Szymonik and Lach, 2015). The effects of their presence are not immediate, often becoming apparent only after many years or generations, and they remain not fully understood (Romanowska-Duda, 2015). According to the Food and Agriculture Organization of the United Nations (FAO), fish are the most important single source of high-quality protein for humans. Globally, in 2019, fish products accounted for approximately 17 percent of animal protein and 7 percent of all proteins in the human diet. In Poland, marine fish catches between 2011 and 2022 ranged from 203.2 to 162.6 tons annually (GUS, n.d.). Due to the varying and often conflicting information found in press articles regarding the risks of fish consumption in the context of environmental pollution, this article presents the results of research on the content of selected metals, including heavy metals, in the meat of fish available in Polish retail grocery chains (included fish from Polish waters and imported).

Materials and methods

The study included several species of fish, mostly marine, as well as two species of farmed fish bought from several food markets. The Table 1. presents an overview of the species and the fishing areas from which they were obtained. The samples were collected in 2019 and 2024 and tested for the content of metals: Cu, Ni, Cr, Zn, As, Hg, Pb, Cd, and Co. The measurements were performed using AAS.

Table 1. Species of fish studied and fishing areas from which they were sourced.

Fish species	FAO Fishing Areas
Clupea harengus membras	Area 27: Northeast Atlantic, Baltic Sea
Platichthys flesus	Area 27: Northeast Atlantic, Baltic Sea
Gadus morhua callarias[1]	Area 27: Northeast Atlantic, Baltic Sea
Thunnus thynnus	Area 71 – Western Central Pacific
Thunnus thynnus (fish can)	Area 71 – Western Central Pacific
Salmo Salar	Area 27: Northeast Atlantic, Norwegian Sea
Gadus morhua	Area 27: Northeast Atlantic, Norwegian Sea
Pollachius virens	Area 27 – Northeast Atlantic
Merlangius merlangus[1]	Area 27 – Northeast Atlantic
Sebastes norvegicus[1]	Area 27 – Northeast Atlantic
Gadus morhua – liver[2]	Area 27 – Northeast Atlantic
Merluccius hubbsi[2]	Area 41 – Southwest Atlantic
Theragra chalcogramma[2]	Area 61 – Northwest Pacific
Oreochromis niloticus[2]	Fish farming, China
Pangasianodon hypophthalmus[2]	Fish farming, Vietnam

[1] samples collected only in 2019, [2] samples collected only in 2024

Results and concluding remarks

The maximum concentration of metals in the meat of the tested fish is presented in Table 2.

Table 2. Maximum concentration of metals in the meat of the tested fish.

Fish species	Co	Cr	Ni	Cu	Zn	As	Cd	Hg	Pb
					mg/kg fresh weight				
Clupea harengus membras	0.096	0.399	4.124	0.904	17.03	0.867	0.005	0.042	0.269
Platichthys flesus	0.476	0.517	0.555	0.610	30.81	0.525	0.004	0.078	0.476
Gadus morhua callarias	0.075	0.205	0.347	0.324	9.859	n.t.	n.t.	n.t.	0.075
Thunnus thynnus	0.014	0.232	0.377	0.564	7.432	0.296	0.023	0.213	0.186
Thunnus thynnus (fish can)	0.062	0.205	0.218	1.098	7.852	0.861	0.048	0.300	0.324
Salmo Salar	0.008	0.334	0.093	0.776	2.481	1.407	0.006	0.016	0.124
Gadus morhua	0.073	0.152	0.632	0.345	9.800	11.06	0.004	0.026	0.291
Pollachius virens	0.148	0.262	0.275	0.481	5.445	0.996	b.d.l.	0.053	0.148
Merlangius merlangus	0.048	0.112	0.276	0.096	4.683	b.d.l.	n.t.	n.t.	0.048
Sebastes norvegicus	0.016	0.092	0.479	0.066	4.511	b.d.l.	n.t.	n.t.	0.016
Gadus morhua – liver (fish can)	0.015	0.825	0.375	3.376	17.32	4.254	0.896	0.064	0.320
Merluccius hubbsi	0.004	0.119	0.103	1.305	4.452	0.833	0.004	0.009	0.209
Theragra chalcogramma	0.002	0.115	0.231	1.851	4.142	0.387	0.002	0.003	0.169
Oreochromis niloticus	0.010	0.135	1.091	0.974	4.263	0.027	b.d.l.	b.d.l.	0.251
Pangasianodon hypophthalmus	0.004	0.148	0.483	7.951	2.625	0.022	b.d.l.	0.033	0.190

b.d.l. below detection limit, n.t. – not tested

The current regulatory framework within the European Union (Commission Regulation (EU) 2023/915 of 25 April 2023 on maximum levels for certain contaminants in food and repealing Regulation (EC) No 1881/2006) establishes maximum permissible concentrations of heavy metals in fish products, specifically for lead (0.3 mg/kg), cadmium (0.05 mg/kg), and mercury (0.5mg/kg for most fish species, 1 mg/kg – for Thunnus spp.). In the analyzed samples, elevated lead concentrations were detected in the meat of Baltic herring, canned tuna, and canned cod liver, while cadmium levels exceeded the established limits in canned cod liver. Additionally, significant arsenic concentrations were identified in both the meat and liver of the examined cod samples. Notably, no exceedances of metal concentration limits were observed in the meat of selected farmed fish from China and Vietnam.

The mercury and cadmium concentrations observed in the tested samples were lower than those reported in demersal fish from the Mediterranean Sea (Storelli and Barone, 2013), where the authors recorded maximum concentrations of up to 1.98 mg/kg of fresh weight for mercury and 0.13 mg/kg of fresh weight for cadmium. In contrast, higher concentrations of lead were detected in the present study.

Acknowledgments: The research was carried out as part of research work WZ/WB-IIŚ/3/2022 at the Bialystok University of Technology and financed from a subsidy provided by the Ministry of Education and Science.

References

Akhouchal I, Alla AA, Hajji S, Agnaou M, Moukrim A (2021) Assessment of Trace Metal Concentrations in Three Seafood Deep-Sea Fished Caught in the Moroccan Atlantic. J. Ecol. Eng. 87–98. https://doi.org/10.12911/22998993/141480

GUS, n.d. Rocznik Statystyczny Rzeczypospolitej Polskiej 2023 [WWW Document]. stat.gov.pl. URL https://stat.gov.pl/obszary-tematyczne/roczniki-statystyczne/roczniki-statystyczne/rocznik-statystyczny-rzeczypospolitej-polskiej-2023,2,23.html (accessed 10.23.24).

Ouali N, Belabed BE, Zeghdoudi F, Rachedi M (2018) Assessment of metallic contamination in sediment and mullet fish (Mugil cephalus Linnaeus, 1758) tissues from the East Algerian coast. J. Water Land Dev. 38.

Romanowska-Duda Z (2015) Metale ciężkie jako specyficzne zanieczyszczenia środowiska wodnego. Uniw. Łódz. Wydz. Biol. Ochr. Śr. Dostępny Na Www Proakademia Eu.

Storelli MM, Barone G (2013) Toxic Metals (Hg, Pb, and Cd) in Commercially Important Demersal Fish from Mediterranean Sea: Contamination Levels and Dietary Exposure Assessment. J. Food Sci. 2, T362–T366. https://doi.org/10.1111/j.1750-3841.2012.02976.x

Szymonik A, Lach J (2015) Akumulacja metali ciężkich w organizmach ryb, efekt toksyczności. Technol. Wody 66–72.

How farm management can improve the ability of soil to retain water: Adaptation to less water for agriculture in Europe

A. Iglesias[1*], A. Sordo-Ward[2], D. Santillán[2], L. Garrote[2]
[1] Department of Agricultural Economics, Universidad Politécnica de Madrid, Madrid, Spain
[2] Department of Hydraulics, Energy and Environment, Universidad Politécnica de Madrid, Madrid, Spain
* e-mail: ana.iglesias@upm.es

Introduction

The water and agriculture nexus identifies mutually beneficial responses that are based on understanding the synergies of water, energy, and agricultural policies (Iglesias and, Garrote 2015; Trnka et al., 2022). Using water more efficiently and mitigating climate are the main environmental challenges to agriculture in the 21st century. The implications are clear for increasing water for ecosystems and lowering the use of energy for irrigation. Improving the ability of soil to retain water and nutrients is crucial to achieving higher agricultural productivity in dryland cropping systems. In this study we explore the role of agricultural management as significant contributor to soil organic carbon. Practices such as conservation tillage, crop rotation, and the application of organic amendments have been shown to enhance soil carbon storage (Bai et al., 2018). These improvements contribute to reducing greenhouse gas emissions and promoting sustainable farming systems in view of climate change. This study examines the potential for enhancing soil carbon storage as a critical ecosystem service under varying climate and policy scenarios. Using historical records of crop and soil management practices in Europe and advanced modeling tools, it estimates the impacts of future management strategies on soil carbon dynamics.

The study contributes to understand the dynamic interplay between agricultural practices, climate change, and global environmental policies and how these factors collectively influence the water, agriculture and energy nexus.

Materials and methods

The study identifies and characterizes typical farming systems in Europe with seven relevant crop types and four soil management practices in seven agro-climatic regions. The study builds from publicly available datasets on soil, agriculture, physical context and socioeconomic context. These data have been compiled, processes and projected on a common geospatial framework that allows for cross-data analyses. The database includes geographical zones, spatial extent, productivity level and intensity of land and resource use and management practices.

Empirical relationships are applied to characterize the link between agricultural management and soil carbon storage. Bai et al. (2018) evaluated paired response ratios for different soil quality indicators and management practices. In total, 354 paired observations were analysed. The results obtained for the soil quality indicator "Soil Organic Matter" are summarized in Table 1, showing the number of pairs compiled and relevant parameters of the distribution (mean, median and standard deviation). All tested management practices produced a beneficial impact on soil organic matter.

Table 1. Relevant impact of selected management practices on soil organic matter (response ratios, dimensionless). Adapted from Bai et al. (2018).

Management	Mean	Median	Standard Deviation	N
Organic matter addition versus no organic matter input	1.39	1.29	0.33	63
No tillage versus tillage	1.46	1.20	0.69	18
Crop rotation versus mono cultivation	1.41	1.25	0.61	15
Organic farming versus conventional agriculture	1.31	1.12	0.56	22

A methodology was developed for upscaling local information that relate the local results to the continental level. The objective of the upscaling model is to produce maps of improvement of soil carbon storage under different policy scenarios. Functional relations to define the effect of agricultural management practices on soil carbon storage were formulated in qualitative terms, accounting for the particularities of farming systems, agro-climatic zones and crop types. This additional information was derived through personal interviews and through a questionnaire in the context of the iSQAPER project. Therefore, the model accounts for spatially explicit representation of soil processes. The upscaling was based on soil environmental footprint, and it focuses on soil carbon storage as an agricultural ecosystem service.

Results and concluding remarks

The study analysed how choices of farming systems and agricultural management practices in Europe affect soil carbon storage. The upscaling model described above was applied to obtain results of an additional implementation of 10% of the four agricultural management practices in each agro-climatic region. Results were obtained for soil carbon storage in all seven cropping patters. An example of those results is presented on Figure 1, where results obtained for the percent increase of soil carbon storage in the different cropping patterns have been averaged using as weights the area of each cropping pattern in the cell.

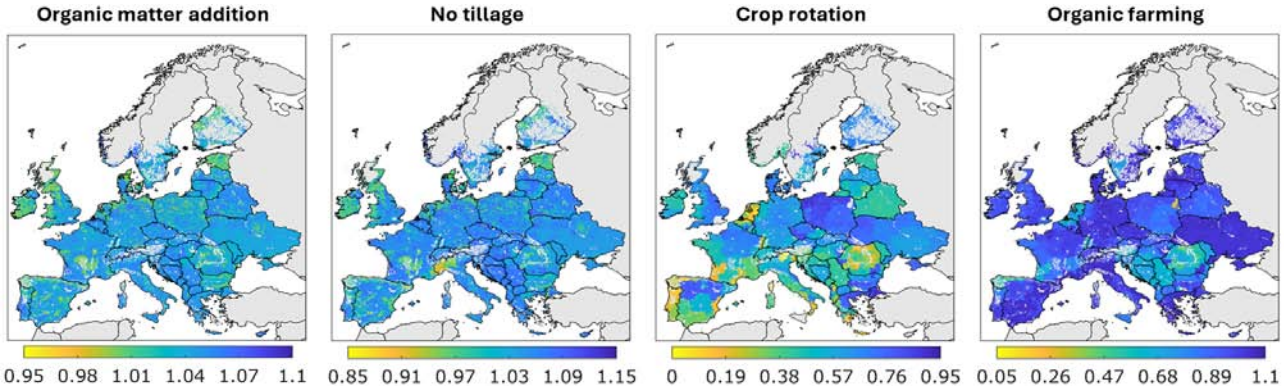


Figure 1. Average effect of a 10% increase of different management practices on soil carbon storage, in percentage.

The results obtained in this study may be used to explore the potential effect of public policies targeted at improving soil environmental footprint supporting adequate agricultural management practices. This knowledge on environmental footprint is valuable to improve production systems, environmental status and adaptation to climate change. Unlike previous research, this work integrates the influence of global environmental and climate policies into its analysis, providing a comprehensive perspective on the future role of soil carbon storage in climate mitigation. By linking historical trends to forward-looking scenarios, the study offers novel insights into the potential of agricultural practices to optimize carbon sequestration, addressing a key challenge in sustainable agriculture and climate policy.

Acknowledgments: The authors wish to acknowledge funding received from the NOVASOIL project (Grant agreement ID: 101091268) to carry out this research.

References

Bai Z, Caspari T, Ruiperez Gonzalez M et al. (2018): Effects of agricultural management practices on soil quality: A review of long-term experiments for Europe and China. Agriculture, Ecosystems and Environment 265, 1-7.

Iglesias A, Garrote L (2015) Adaptation strategies for agricultural water management under climate change in Europe', Agricultural Water Management, 155, pp. 113–124. doi:https://doi.org/10.1016/j.agwat.2015.03.014.

Trnka M et al (2022) Increasing Available Water Capacity as a Factor for Increasing Drought Resilience or Potential Conflict over Water Resources under Present and Future Climate Conditions." Agricultural Water Management, vol. 264, p. 107460, https://doi.org/10.1016/j.agwat.2022.1074

The uncertainty of agricultural production: A case study from Pianura Padana

D.D. Chiarelli[1], E. Volpi[2*], A. Fiori[2], M.C. Rulli[1]
[1] *Dipartimento di Ingegneria Civile e Ambientale, Politecnico di Milano (Italy)*
[2] *DICITA, Roma Tre University (Italy)*
** e-mail:* elena.volpi@uniroma3.it

Introduction

Climate variability and change often challenge agricultural production. Increasingly, we hear about how drought periods are expected to become more intense and prolonged in the future, severely damaging agricultural output. Already in 2022, the Po Valley, one of Italy's breadbaskets, experienced an unprecedented drought, resulting in agricultural production losses of up to 60%. To propose effective and resilient solutions, a deeper understanding of the phenomenon is required; this is achieved here by combining continuous-time simulation of the agro-hydrological system based on WATNEEDS model with in-depth statistical analysis.

Materials and methods

The water requirement for agricultural production is obtained by the following continuous-time simulation procedure:

- synthetic daily rainfall and temperature series are statistically generated for a period of 5000 years by using WeaGets (*Chen et al.,* 2012), calibrated on 30 years of observations;
- rainfall and temperature data are used as input to an agro-climatic model called WATNEEDS (*Chiarelli et al.*, 2020):
- two of the most widespread crops in the area, irrigated maize (planted in April and harvested at the end of September) and winter rainfed wheat (planted in November and harvested at the end of July), are considered for illustrative purposes;
- GW and BW volumes are statistically analysed to estimate their probability distributions.

WATNEEDS allows for solving the vertical water balance in the active soil layer to assess the potential and actual water consumption of crops; to this aim it uses the FAO approach for evaluating plant water requirements and provides as outputs the volumes of Green Water GW (i.e., rainfall water that the plant can utilize) and Blue Water BW (i.e., irrigation water) needed to ensure growth under stress conditions.

The procedure is applied locally in the Po Valley, Pianura Padana region (Northern Italy).

Results and concluding remarks

Results are presented in Figures 1 and 2 for both irrigated maize and winter rainfed wheat. Maize is seed between mid March and mid April and harvested at the end of September; it is generally irrigated during the month of June, July and August. Our model results show that in April and May the maize is mainly rainfed; precipitation is comparable to the water requirement, thus the crop water requirement can be satisfied with green water, as shown in Figure 1a. In June the maize water requirement is larger than the precipitation and green water is greater than precipitation, meaning that the delta to precipitation used by plant comes from the water stored into the soil (Figure 1c). Figure 1c shows that the soil water content during the fall, winter and spring months remains high on average, with values well above the water demand. Soil water content reduces in the months from June to October, when the blue water sustains the process of evapotranspiration. The BW demand is strongly influenced by root zone soil water content (being inversely proportional). BW starts increasing in June, when its variability is significant (the coefficient of variation CV is larger than 1); while the variability is much less in later months, when CV is lower

generally than 0.5.

The probability distribution of the BW demand for irrigated maize varies at the monthly scale between 0 and about 200 (mm), with an increase of about 20% between 10 and 100 years return time (figure not shown). The variability in demand is very different from month to month; for example, between 10 and 100 years the demand more than doubles in June (where CV>1).

The overall water required for the winter rainfed wheat, seed on October and harvested in late July, is much less than for the irrigated maize (Figure 1b). It is almost entirely GW since the vegetative period of the plant does not coincide as for maize with the period of high temperature/evapotranspiration. The CV of the BW is definitely high, which means that in different years the demand might be very different depending on rainfall distribution. The soil humidity should be, on average, smaller than for maize, due to greater use of rainwater (i.e. the soil does not recharge). However, as a consequence of water stress conditions, the active layer of the soil is generally thicker, implying an overall higher water content (Figure 1d). The demand, as premised, is significantly lower, almost half, of that pertaining to maize and the distributions are significantly more variable (figure not shown).

Continuous-time simulation allows for the probabilistic assessment of crop water requirement, especially the BW component that is the fresh surface and groundwater applied with irrigation. This is fundamental for sustainable water management, accounting for the natural variability of freshwater resources.

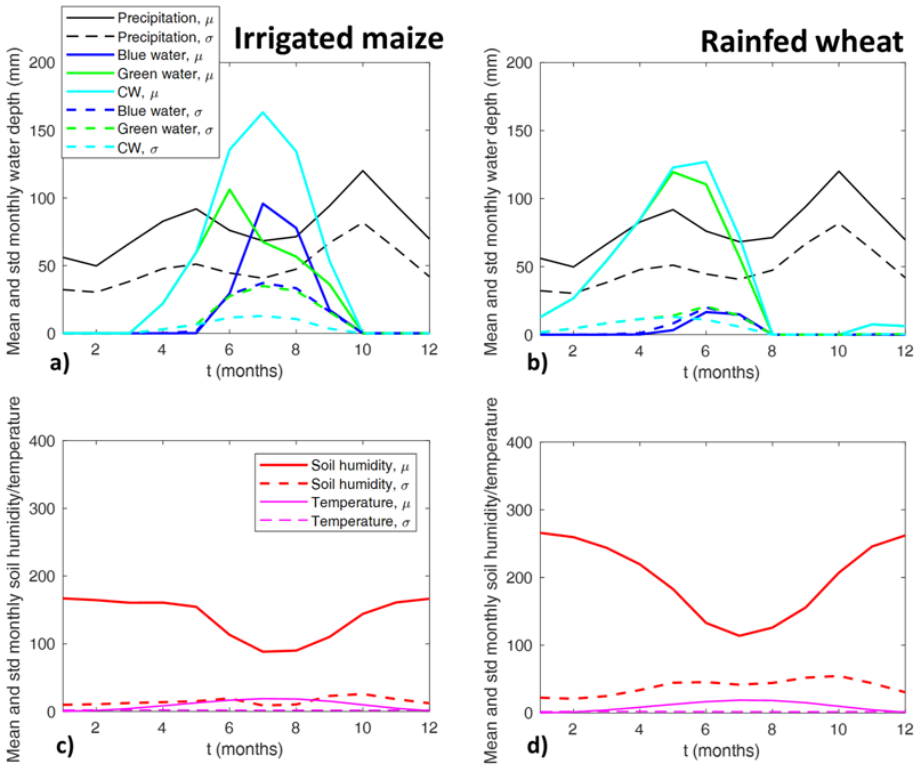


Figure 1. Monthly-scale mean and standard deviation of precipitation, blue water, green water and total water (mm) (a, b), soil humidity (mm) and temperature (C°) (c, d) for irrigated maize (a, c) and winter rainfed wheat (b, d).

References

Chen, J., Brissette, F. P., Leconte, R., & Caron, A. (2012). A versatile weather generator for daily precipitation and temperature. Transactions of the ASABE, 55(3), 895-906.

Chiarelli, D. D., Passera, C., Rosa, L., Davis, K. F., D'Odorico, P., & Rulli, M. C. (2020). The green and blue crop water requirement WATNEEDS model and its global gridded outputs. Scientific data, 7(1), 273.

Integrating a pumped-storage hydropower plant with photovoltaics: impacts on energy production and on the water resource system

D. Micocci[1*], C. Bragalli[1], E. Toth[1], M. Zappa[2]
[1] Department of Civil, Chemical, Environmental and Materials Engineering, University of Bologna, Bologna, Italy
[2] Swiss Federal Institute WSL, Birmensdorf, Switzerland
* e-mail: domenico.micocci@unibo.it

Introduction

Variable renewable energy resources (VRES), including solar photovoltaics (PV), are posing new challenges to the management of the electricity grid (Lund et al. 2015), since their availability is driven by climate-related variables and it is therefore independent from the consumers' demand. Reservoir-based hydropower (HP) is particularly valuable to resolve the mismatch between demand and supply, since it is one of the few renewables whose power output can be set almost on demand. Even higher flexibility is provided by pumped-storage HP, which also allows to absorb energy exceeding the consumers' demand and to store it by pumping water from a lower to an upper reservoir (Guittet et al. 2016).

Integrating PV and HP in a single hybrid power station is seen as a promising solution to get more regular power generation profiles compared to stand alone PV, thus facilitating the introduction of high shares of VRES in the energy mix (Jurasz et al. 2020). On the other hand, complementing an existing reservoir-based HP plant with PV may affect the way the reservoir is operated (François et al. 2014), possibly offering potential for improving the conditions of the downstream water resource system.

For a real Swiss pumped-storage HP plant, we set up a numerical experiment to analyse the impacts of expanding the existing plant through a floating photovoltaic (FPV) plant, installed directly on the reservoir surface. The possibility of increasing downstream environmental releases, using water which is not used for HP purpose thanks to PV production, is also explicitly taken into account.

Materials and methods

Lake Sihl is an important artificial reservoir, located in the Swiss pre-Alpine region (catchment area: 155.5 km^2; average elevation: 1243 m a.s.l.; discharge regime: nivo-pluvial-prealpine). Water collected in the lake is mostly used by the Swiss Federal Railways in the Etzelwerk HP plant, which exploits a difference in elevation of about 480 m between Lake Sihl (upper reservoir) and Lake Zurich (lower reservoir); being a pumped-storage plant, water can also be pumped from Lake Zurich, either to store energy or to refill Lake Sihl when its level is too low. Finally, an environmental release from Lake Sihl is prescribed, depending on downstream flow conditions.

Historical meteorological data (including temperature, precipitation and solar radiation) were available for the study area over the period 1981-2018. A calibrated hydrological model, developed using the semi-distributed modelling system PREVAH (Viviroli et al. 2009), was forced with these data in order to obtain all the necessary hydrological input data (including lake inflow and evaporation losses, and natural runoff downstream of the dam, which triggers the environmental release).

A fictional FPV plant was introduced on Lake Sihl, covering 10 % of the minimum reservoir surface (3.15 km^2 at the minimum pool level) and having almost half of the HP generating capacity (120 MW). The hybrid HP-FPV plant was simulated at an hourly resolution through a modelling chain involving: i) a PV production model, converting input temperature and irradiance timeseries into a timeseries of PV power available; ii) a power demand profile, obtained through a multiple linear regression model calibrated on historical plant production data, taking into account only time-related explanatory variables (month, day, hour); iii) a reservoir operation model, setting the amount of water to be turbined or pumped according to the requirements and the available storage. Specifically, reservoir operations were guided by rule curves deduced from a statistical analysis of historical storage timeseries (1981-2023), which unveiled a target

storage management strategy, particularly from June to October, when the level of the lake is prescribed not to fall below a given threshold to comply with a legal constraint.

Simulations were repeated according to three scenarios: i) NoPV is a reference scenario, with no PV to support HP; ii) in PV1 solar energy, if available, contributes to fulfil the demand and excess PV power is possibly stored through pumping; iii) PV2 is similar to PV1, but including the possibility to release 50 % of the water saved from HP production thanks to PV, so as to increase the legally prescribed environmental flow from May to October.

Results and concluding remarks

The introduction of PV allows to increase by almost 20 % the overall energy production, compared to the base scenario NoPV (Table 1). Interestingly, a similar energy increase has been obtained both for scenario PV1 and PV2, despite additional water releases, which are allowed in the latter. To this regard, between May and October the mean monthly release from Lake Sihl is increased from 14 % (May) up to about 50 % (June to August) in scenario PV2 compared to PV1 (Table 1), possibly contributing also to lower the downstream water temperature, which is a fundamental ecological variable (Rojas-Aguirre et al. 2025).

Table 1. Energy annually produced in each scenario (GWh/year) and mean monthly downstream release (m^3/s). Average values computed over the entire simulation period (1981-2018).

	Energy total	Energy from HP	Energy from PV	Release May	Release Jun	Release Jul	Release Aug	Release Sep	Release Oct
NoPV	256.6	256.6	–	0.47	0.55	0.60	0.63	0.59	0.71
PV1	319.1	257.7	61.4	0.47	0.55	0.60	0.63	0.59	0.71
PV2	315.2	254.1	61.1	0.54	0.85	0.91	0.93	0.81	0.91

The hybrid plant (PV1 and PV2) meets the power demand more often than the conventional HP plant, as portrayed by the reliability index (here defined as the ratio between energy supplied and energy required in the simulation period), which increases from about 90 % in scenario NoPV to about 97 % in PV1 and PV2. This leads to a significant increase of energy annually produced for self-consumption.

In conclusion, according to the results of the numerical experiment, it seems that introducing PV in the selected case study could improve downstream flow conditions (at least to some extent), while also providing benefits in terms of energy production and reliability of supply.

Acknowledgments: This study was carried out within the RETURN Extended Partnership and received funding from the European Union Next-GenerationEU (National Recovery and Resilience Plan – NRRP, Mission 4, Component 2, Investment 1.3 – D.D. 1243 2/8/2022, PE0000005).

References

François B, Borga M, Anquetin S, Creutin JD, Engeland K, Favre AC, Hingray B, Ramos MH, Raynaud D, Renard B, Sauquet E, Sauterleute JF, Vidal JP, Warland G (2014) Integrating hydropower and intermittent climate-related renewable energies: a call for hydrology. Hydrological Processes 28: 5465–5468. https://doi.org/10.1002/hyp.10274

Guittet M, Capezzali M, Gaudard L, Romerio F, Vuille F, Avellan F (2016) Study of the drivers and asset management of pumped-storage power plants historical and geographical perspective. Energy 111: 560–579. https://doi.org/10.1016/j.energy.2016.04.052

Jurasz J, Canales FA, Kies A, Guezgouz M, Beluco A (2020) A review on the complementarity of renewable energy sources: Concept, metrics, application and future research directions. Solar Energy 195: 703–724. https://doi.org/10.1016/j.solener.2019.11.087

Lund PD, Lindgren J, Mikkola J, Salpakari J (2015) Review of energy system flexibility measures to enable high levels of variable renewable electricity. Renewable and Sustainable Energy Reviews 45: 785–807. https://doi.org/10.1016/j.rser.2015.01.057

Rojas-Aguirre AF, Bray EN, Dozier J (2025) Evaluating the effects of climate change on managed lowland rivers in the California Bay Delta Watershed. Journal of Hydrology 647: 132293. https://doi.org/10.1016/j.jhydrol.2024.132293

Viviroli D, Zappa M, Gurtz J, Weingartner R (2009) An introduction to the hydrological modelling system PREVAH and its pre- and post-processing-tools. Environmental Modelling & Software 24: 1209–1222. https://doi.org/10.1016/j.envsoft.2009.04.001

Empowering smart renewable cities through hydropower technology in urban drinking water supply system

Á. Alcaide Royo[1*], C. Sánchez Briones[1], A. Pérez Lleó[1], A. Gamón[2], R. Ponz Carcelén[2], H. Royo[3], M. Pedro Monzonís[4], C. de Diego[4], G. Dasí[4], T. Oltra Benavent[4]
[1] *Empresa Mixta Valenciana de Aguas S.A. (EMIVASA), València, Spain*
[2] *Empresa Mixta Metropolitana S.A. (EMIMET), València, Spain*
[3]*Empresa Municipal de Serveis Públics S.L,. (EMIVASA), València, Spain*
[4] *Aguas de Valencia S. A. (AVSA), València, Spain*
**e-mail: angealro@emivasa.es*

Introduction

Over the past few decades, sustainability and efficiency have assumed utmost importance in the management of urban resources, particularly within the realms of water and energy. The water transport and distribution network, in addition to its supply function, can be considered as an energy transport system in the form of pressure. This approach makes it possible to transform the energy contained in water into usable electrical energy, promoting an efficient use of available resources.

In this context, technologies such as microturbines and power generation equipment based on waste energy recovery have emerged as key tools. These devices convert excess energy, resulting from high pressures in pipelines, into electricity that can be used for self-consumption or public use (Pérez-Sánchez et al. 2020). The AVI TURBINES project (INNEST/2022/196) has been a benchmark in demonstrating the technical and economic viability of these solutions, establishing a significant precedent in the city of València. For its part, the LIFE TURBINES project (101113749 - LIFE22-CCM-ES-LIFE TURBINES) advances along the same lines, integrating advanced technologies in complex urban networks with variable demands and exploring new strategies that contribute to decarbonisation and urban sustainability in a global context.

Materials and methods

València and its Metropolitan Area are supplied by two Drinking Water Treatment Plants (DWTP), 'El Realón' and 'La Presa', which operate at elevations of 92 and 111 metres above sea level respectively. These plants supply water to an urban distribution network that is more than 1,400 kilometres long. Due to the topography of the city of Valencia, the water is transported from the elevated areas where the plants are located to the consumption points, located close to sea level. This process generates pressure surpluses in various sections of the system.

To manage the excess pressure and ensure operational stability, the València distribution network is equipped with more than 68 pressure reduction valves, as well as other devices designed to control flow and pressure. At these points, excess energy is dissipated in the form of heat due to the friction and turbulence generated by pressure reduction, thus resulting in considerable energy loss throughout the drinking water distribution network. This situation highlights a strategic opportunity for the implementation of energy recovery systems using hydraulic turbines, which make it possible to transform the excess pressure into usable electrical energy.

The transformation of this potential and pressure energy into mechanical energy is carried out by means of the mass of water in movement circulating inside the turbine. In turn, the mechanical energy produced in the turbine shaft, coupled to an electric generator, is transformed into electrical energy (Ayza Prats et al. 2017). The power that can be obtained from a hydraulic turbine is expressed by the following equation:

$$P = \eta * g * Q * H \quad (1)$$

where: P (power, kW), η (overall system efficiency, including mechanical and electrical generation losses), g (gravity, 9.81 m/s²), Q (flow rate, m³/s), and H (piezometric head, mwc).

Considering the energy dissipation caused by pressure exceedances, the AVI TURBINES project (INNEST/2022/196) has implemented the installation of three hydraulic turbines at strategically selected locations within the València network. These installations are integrated with advanced control systems that monitor and dynamically adjust the operating conditions according to variations in flow and pressure. All three systems operate in the same way with a turbine in bypass to the main pipeline. The flow is distributed between the turbine and the main to maintain the operating pressure within the set values. Normally the flow passes through the bypass, but when the turbine cannot reach the optimum pressure, part of the flow is diverted through the main pipe, ensuring a stable supply and maximising energy recovery without affecting the network.

At these three locations, the generated energy has been utilized for self-consumption within the supply network, powering drinking water quality control equipment and a public fountain providing filtered and refrigerated water. These solutions enhance the conversion of hydraulic energy into electricity while ensuring full compatibility with the water distribution system.

Results and concluding remarks

The AVI TURBINES project has demonstrated that integrating hydraulic turbines into drinking water distribution networks is a technically and economically viable solution for recovering excess energy and stabilizing pressures in urban supply networks. Through the case studies in València, the ability of these technologies to adapt to dynamic flow and pressure conditions has been proven, generating renewable energy that can be used for self-consumption or public services. This approach not only optimizes the energy performance of supply networks but also establishes a replicable model for other urban and rural contexts.

Building on this experience, the LIFE TURBINES project expands its objectives toward developing an advanced methodology for intelligent energy recovery, optimizing turbine efficiency and promoting renewable energy generation. This will be achieved through a digital tool designed to select and size turbine equipment, maximizing real-time energy recovery. Additionally, the tool will assist network operators in selecting the most suitable equipment and defining the most cost-effective operational model.

LIFE TURBINES will apply these solutions at 13 locations across Spain and Italy, demonstrating that hydroelectric energy production is feasible at any point with a pressure differential. These initiatives are making water supply systems more sustainable and resilient, aligning with the European Green Deal and the REPowerEU strategy, thereby driving the transition towards a cleaner and more autonomous energy system.

Acknowledgments: This project is based on the project funded by the Agència Valenciana de la Innovació (AVI) INNEST/2022/196 and is currently co-financed by the European Union through the LIFE Programme under grant agreement number 101113749 – LIFE22-CCM-ES-LIFE TURBINES.

References

Ayza Prats M, García Casas D, Sanz Tárrega F, Conejos Fuertes P, Hervás Carot M, Lledó J, Ruiz E (2017) Aprovechamiento de la energía de la red mediante turbinación: experiencia en Global Omnium-Grupo Aguas de Valencia S.A. XXXIV Jornadas Técnicas de AEAS: 225–236.

Pérez-Sánchez M, Sánchez-Romero FJ, Ramos HM, López-Jiménez PA (2020) Improved Planning of Energy Recovery in Water Systems Using a New Analytic Approach to PAT Performance Curves. Water 12:468. https://doi.org/10.3390/w12020468

Assessing the water footprint of livestock feed: insights from a global analysis

C. Govoni*, D.D. Chiarelli, M.C. Rulli
Department of Civil and Environmental Engineering (DICA), Politecnico di Milano, Milan, Italy
** e-mail: camilla.govoni@polimi.it*

Introduction

Agriculture accounts for approximately 90% of global freshwater use and nearly 70% of total water withdrawals. The livestock sector alone is responsible for 30-40% of this demand (Heinke et al., 2020; Mekonnen & Hoekstra, 2012) while supplying 16% of the global food supply through meat, eggs, and dairy. The water footprint (WF) of plant-based foods corresponds to the cultivation of primary crops consumed directly by humans. Conversely, the WF of animal-source foods (ASF) includes not only the water used for animal drinking and service but also the substantial indirect water consumption from feed production. The literature consistently reports that feed production accounts for ~98% of the sector water demand (Mekonnen & Hoekstra, 2012). Despite this recognition, few studies have assessed the specific WF of both primary crops and their by- and co-products, and no specific studies were carried out on the WF of animal feeds considering only the fraction of crop products actually ingested by livestock. Research on ASF water use has often focused on specific livestock species at local or regional scales, with only a few studies providing comprehensive global assessments (Heinke et al., 2020; Mekonnen & Hoekstra, 2012). This study addresses these gaps by evaluating the WF of different livestock feeds across countries.

Materials and methods

The analysis covers 262 countries and 140 plant-based feed products using climate data averaged from 2015 to 2019. For feed products derived from crop residues or by-products rather than whole crops, we identified the primary crops they originate from. When multiple co-products stem from a single crop, an allocation method was applied to distribute water use among them (A.Y. Hoekstra et al., 2011). The literature highlights three common allocation methods: mass, energy content, and economic value. While the Water Footprint Assessment Manual (A.Y. Hoekstra et al., 2011) recommends economic allocation, recent studies suggest metabolizable energy (ME) allocation for livestock feed. Economic allocation is subject to price fluctuations, whereas mass and energy allocations remain stable over time. Due to data limitations, energy and economic allocation were applied to oilseeds and their co-products, while mass allocation was used for the main analysis. Indeed, the difference between adopting mass, energy, or economic allocation methods is more relevant for oilseed co-products than for the other feed products.

Water volumes associated with feed production and WF calculations were obtained using the WATNEEDS model (Chiarelli et al., 2020), an agro-hydrological, crop-specific, and spatially distributed model. The model computes the vertical soil water balance at a 5 arc-min resolution to estimate green (GW) and blue water (BW) requirements. Monthly gridded outputs, based on climate and soil data, were aggregated annually using harvested area-weighted averages (SPAM2010, Yu et al., 2020) to derive mean country values for 2015-2019. Crop-specific yields were also averaged based on national harvested areas.

Results and concluding remarks

The WF records for the 140 feed products (Govoni et al., 2024) are available in Figshare (https://doi.org/10.6084/m9.figshare.27324984), categorized by agricultural system and allocation method. Globally, rainwater (GW) constitutes the largest share of WF, as rainfed agriculture covers ~80% of harvested areas and supplies ~60% of crop water requirements (CWR) in irrigated systems. Primary crops exhibit higher GW and BW footprints than by- and co-products, irrespective of the allocation method. Rainfed conditions lead to greater GW footprints due to lower yields compared to irrigated crops.

The WATNEEDS model outputs were validated against estimates by Siebert and Döll (2010) and compared with crop water use (CWU) data for 15 selected primary crops from Mialyk et al. (2024). Our

estimated WFs generally exceed those of Mialyk et al. and Mekonnen & Hoekstra (2010), yet production GW footprints align well when considering increase in total harvested area between the different temporal scales, whereas BW footprints appear smaller despite an increase in irrigated areas.

The findings emphasize that utilizing agricultural by-products as livestock feed can reduce water consumption while keeping agricultural residues within the food chain and reallocating primary crops for direct human consumption. However, the feasibility of this practice depends on factors such as animal species, life stage nutritional needs, production systems, and regional availability of by-products. While by-product use is common in full and semi-extensive systems due to economic advantages, industrial systems could further incorporate these feeds to replace resource-intensive concentrates (Govoni et al., 2023).

Assessing water use in ASF production is crucial to raising awareness among producers and consumers regarding the environmental impact of livestock. Moreover, WF estimates for various feed types can help farmers select water-efficient diets while maintaining sustainability standards. These outputs can also support virtual water assessments, particularly in global feed trade scenarios, such as soybean exports.

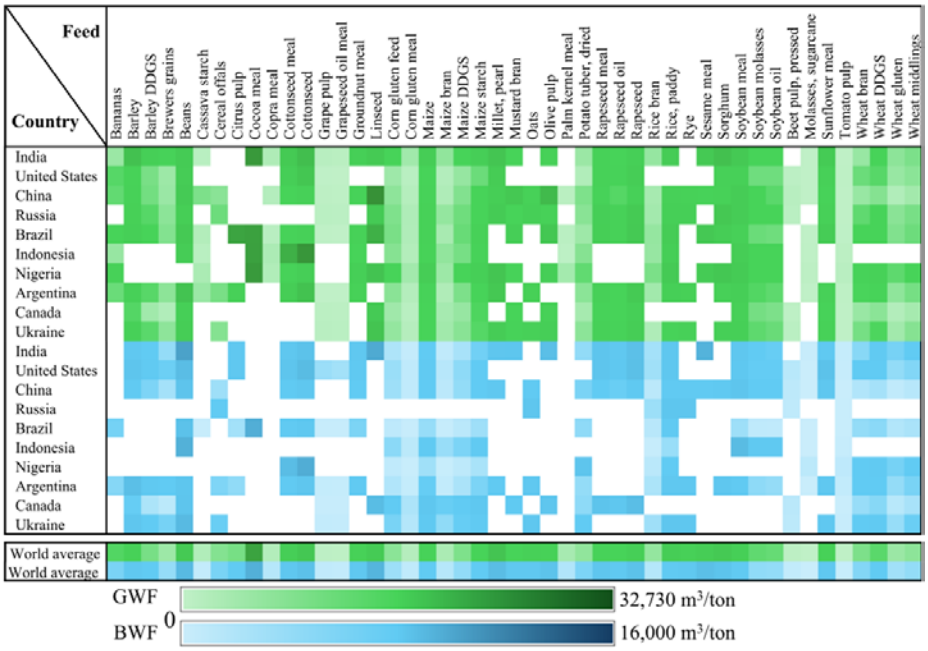


Figure 1. GWF and BWF for the main agricultural producer countries and the most consumed feed products.

References

Chiarelli, D.D., Passera, C., Rosa, L., Davis, K.F., D'Odorico, P., & Rulli, M.C. (2020). The green and blue crop water requirement WATNEEDS model and its global gridded outputs. Scientific Data, 7(1), 273. 10.1038/s41597-020-00612-0

Govoni, C., Chiarelli, D.D., & Rulli, M.C. (2024). A global dataset of the national green and blue water footprint of livestock feeds. Scientific Data, 11(1), 1–12. 10.1038/s41597-024-04264-2

Govoni, C., D'Odorico, P., Pinotti, L., & Rulli, M.C. (2023). Preserving global land and water resources through the replacement of livestock feed crops with agricultural by-products. Nature Food, 4(12), 1047–1057. 10.1038/s43016-023-00884-w

Heinke, J., Lannerstad, M., Gerten, D., Havlík, P., Herrero, M., Notenbaert, A.M.O., Hoff, & H., Müller, C. (2020). Water use in global livestock production—opportunities and constraints for increasing water productivity. Water Resources Research, 56(12). 10.1029/2019wr026995

Hoekstra, A.Y., Chapagain, A.K., Aldaya, M.M., & Mekonnen, M.M. (2011). The Water Footprint Assessment Manual. 10.1080/0969160x.2011.593864

Hoekstra, A.Y., & Mekonnen, M.M (2010). The Green, Blue and Grey Water Footprint of Crops and Derived Crop Products. Volume 1 : Main Report. Value of Water Research Report Series No. 47, 1(16), 80.

Mekonnen, M.M., & Hoekstra, A.Y. (2012). A Global Assessment of the Water Footprint of Farm Animal Products. Ecosystems, 15(3), 401–415. 10.1007/s10021-011-9517-8

Mialyk, O., Schyns, J.F., Booij, M.J., Su, H., Hogeboom, R.J., & Berger, M. (2024). Water footprints and crop water use of 175 individual crops for 1990–2019 simulated with a global crop model. Scientific Data, 11(1), 1–16. 10.1038/s41597-024-03051-3

Siebert, S., & Döll, P. (2010). Quantifying blue and green virtual water contents in global crop production as well as potential production losses without irrigation. Journal of Hydrology, 384(3–4), 198–217. 10.1016/j.jhydrol.2009.07.031

Yu, Q., You, L., Wood-Sichra, U., Ru, Y., Joglekar, A.K.B., Fritz, S., Xiong, W., Lu, M., Wu, W., & Yang, P. (2020). A cultivated planet in 2010-Part 2: The global gridded agricultural-production maps. Earth System Science Data, 12(4), 3545–3572. 10.5194/essd-12-3545-2020

Users perspectives on water access management and technologies in irrigation distribution systems

G. Ferrarese*, D. Troiani, S. Malavasi
Dipartimento di Ingegneria Civile e Ambientale, Politecnico di Milano, Milano, Italy
** e-mail: giacomo.ferrarese@polimi.it*

Introduction

Water management is a critical aspect of sustainable agricultural development, particularly in regions where demand is high and resources are increasingly scarce (Ramos et al. 2022). In Italy, irrigation water distribution is managed by consortia that ensure water access for agricultural users. However, the mechanisms governing water access and distribution vary significantly among these consortia, depending on local regulations, infrastructure capabilities, and user needs (Zucaro 2011). Additionally, technological innovations, such as smart metering and digital water management platforms, are gaining traction as tools that could enhance irrigation efficiency and accessibility (Xu et al. 2022).

In recent years, pressurized irrigation networks have become increasingly widespread due to their higher efficiency in the context of water scarcity and climate change. Unlike traditional open-channel systems, pressurized networks optimize water distribution, reduce losses, and enable precise control of irrigation flows. Furthermore, the adoption of pressurized systems introduces new opportunities for integrating advanced technological solutions that were previously unfeasible (Ferrarese et al. 2021), such as automated remote control, real-time monitoring, and smart irrigation scheduling.

This study aims to investigate current irrigation water access and distribution practices among Italian water consortia, with a focus on the perspectives of both end users and network operators. Specifically, the research explores: (i) the existing modes of water access for agricultural users, (ii) the tools and strategies employed by distribution network managers to deliver irrigation water, and (iii) the willingness of users to adopt innovative technological solutions for monitoring consumption and optimizing water use. By examining these aspects, this study provides insights into the challenges and opportunities associated with modernizing irrigation water management practices in Italy.

Materials and methods

A survey was conducted among several Italian water consortia, targeting both network operators and end users. The survey was designed to collect qualitative and quantitative data on various aspects of water management, including the types of distribution infrastructures in place, user access methods, and the level of digitalization in water service provision. Additionally, respondents were asked about their openness to adopting smart technologies, such as remote water meters and digital access platforms. The collected data were analyzed to identify common trends, regional disparities, and potential areas for improvement.

Results and concluding remarks

Preliminary findings indicate that water access modes vary widely across different consortia, with some relying on traditional infrastructure, while others are gradually incorporating digital solutions. Many network operators still manage water distribution using conventional methods, such as manual meter readings and fixed allocation schedules. However, there is an increasing interest in adopting smart technologies to enhance operational efficiency and ensure fair resource distribution.

From the end-user perspective, there is a growing demand for solutions that offer greater transparency and ease of access. However, the willingness to adopt such technologies depends on factors such as cost, perceived benefits, and trust in the system. While some users express enthusiasm for digital tools that facilitate real-time consumption tracking, others remain skeptical due to concerns about data privacy and

implementation challenges.

This study highlights the diverse approaches to water access and distribution among Italian consortia and underscores the potential for technological advancements to enhance service delivery. The findings suggest that while interest in smart water management solutions is growing, successful implementation requires addressing technical, economic, and social barriers. Future research should focus on pilot projects that test the effectiveness of innovative technologies in real-world settings and explore policy frameworks that support digital transformation in the sector.

By understanding the perspectives of both water providers and end users, this study contributes to ongoing discussions on improving water management efficiency and sustainability in Italy and beyond. The results can inform policymakers, utility providers, and technology developers in designing solutions that meet the evolving needs of water stakeholders.

Acknowledgments: Funding: This study received funding from the European Union - Next-GenerationEU - National Recovery and Resilience Plan (NRRP) – MISSION 4 COMPONENT C2, INVESTIMENT N. 1.1, CALL PRIN 2022 D.D. 104 02-02-2022 – (Project 2022WLW9X8, Equality and Resilience of Agroecosystems through Smart water Management and USe - ERASMUS) CUP N. B53D23006510006.

References

Ferrarese G, Pagano A, Fratino U, Malavasi S (2021) Improving Operation of Pressurized Irrigation Systems by an Off-grid Control Devices Network. Water Resources Management. https://doi.org/10.1007/s11269-021-02869-5

Ramos HM, Morani MC, Carravetta A, et al (2022) New Challenges towards Smart Systems' Efficiency by Digital Twin in Water Distribution Networks. Water 14:1304. https://doi.org/10.3390/w14081304

Xu J, Gu B, Tian G (2022) Review of agricultural IoT technology. Artificial Intelligence in Agriculture 6:10–22. https://doi.org/10.1016/j.aiia.2022.01.001

Zucaro R (2011) Atlante Nazionale dell'Irrigazione. INEA, Roma

Navigating climate change: The water-food nexus and its role in durum wheat production in Mediterranean regions

M. Grosse-Heilmann[1*], E. Cristiano[1], G. Pusceddu[2], M. Marrocu[2], F. Viola[1], R. Deidda[1]
[1] Department of Civil and Environmental Engineering and Architecture, University of Cagliari, Cagliari, CA, Italy
[2] CRS4 Centro di Ricerca, Sviluppo e Studi Superiori in Sardegna
* e-mail: malin.grosseheilmann@unica.it

Introduction

In the coming years climate change and population growth are expected to increase pressure on agricultural systems. In semi-arid environments, like the Mediterranean region where agriculture represents a significant economic pillar, future irrigation conditions are likely to exacerbate challenges related to local water resource management. In this setting, it is essential to understand future variability in crop production, as well as potential implications on water resources resulting from measures taken to stabilize yields. In the framework of the EU Horizon 2020 ARSINOE project, this study analyses the cultivation of durum wheat in Sardinia (Italy), comparing present and future climatic conditions. In the Mediterranean environment, durum wheat is a major C3 crop, thanks to its traditional importance, nutritional benefits and relatively high tolerance to drought conditions. Understanding how future climatic conditions might affect the crop's productivity is complex as some climatic changes, such as rising temperatures and decreasing rainfall, are predicted to constrain future yields, while other factors, such as increasing CO2 concentrations, act as potential drivers for durum wheat productivity (Grosse-Heilmann et al., 2024). This contradiction necessitates analysis on regional and local level to enable policymakers and farmers to adapt accordingly.

Moreover, in Sardinia durum wheat is currently cultivated under rainfed conditions and therefore particularly vulnerable to climatic variations, including drought events. Applying additional irrigation might be a strategy to avoid crop failure under future dryer conditions or even to increase the production in line with the Goal 2 (Zero hunger) of the United Nations (UN) Sustainable Development Agenda 2030. However, in a semi-arid environment like Sardinia effective and fair water resource management is crucial for sustainable development. Irrigation expansion could potentially increase pressure on the system or even result in competition over water resources with other sectors such as the domestic and energy sector. Analysing future impacts from a Nexus perspective can help to identify potential conflict points at an early stage and avoid creating new challenges. Through the lens of the Water-Food Nexus approach this study explores different irrigation scenarios with the objective to understand how and to what extent they might influence the local water resource system.

Materials and methods

The AquaCrop-OpenSource model (Foster et al., 2017), the open-source implementation of the UN Food and Agriculture Organization's crop model AquaCrop, was calibrated to reflect soil, crop cultivar and agricultural management conditions in Sardinia's durum wheat growing regions. The cultivation area, mainly located in the southern area of the island, was derived from the CORINE land cover database on rainfed agriculture (EEA, 2019). Furthermore, the soil composition was taken from the European Soil Database (Ballabio et al., 2016) and used to identify the soil class and corresponding hydraulic properties. Crop parameters with the highest impact on model results were identified via sensitivity analysis and calibrated based on durum wheat yield data from the Italian National Institute of Statistics (ISTAT, 2024).

The future climatic scenarios were derived from the ClimEx-II dataset (Leduc et al., 2019), a comprehensive ensemble of simulations generated running the Canadian Regional Climate Model for Europe and North America on the SuperMUC-NG supercomputer. The aim of these simulations was to assess the impacts of realistic and plausible land-use change scenarios aligned with the Shared

Socioeconomic Pathways (SSPs). Two distinct timeframes were considered: a historical period from 1979 to 2015 and a future one from 2080 to 2100. The model climatic data were bias-corrected applying the linear correction method, using as reference rainfall based on Voronoi averages of daily rainfall records from 1922 to 2023 and temperature with the ERA5, fifth generation of the ECMWF atmospheric reanalysis.

Durum wheat production has been estimated for both timeframes under rainfed and net-irrigation conditions with the calibrated AquaCrop-OS model. Additionally, main climatic influencing factors, such as temperatures, rainfall and CO_2 concentration, were addressed individually to better understand the extent of their influence on future crop yields. Furthermore, different irrigation scenarios were analysed to determine the water volume required to stabilize yields or to even achieve maximum productivity. In a last step these values were compared with the current water volume provided for agricultural irrigation on the island, as well as with the total available water resources.

Results and concluding remarks

Results indicate that durum wheat productivity in Sardinia might become increasingly unstable in the future, with enhanced occurrences of low yield years and total crop failures, requiring early adaption measurements at farm and governmental level. Additionally, a reduction in duration of growing period, largely due to the increasing temperatures, can be noticed. While rising CO_2 concentrations are shown to be a main driver for the crop's productivity, decreasing rainfall and rising temperatures increasingly constrain future yields.

Applying additional irrigation could potentially help to stabilize crop yields. Interestingly, the required irrigation volume, varies strongly among the different zones in Sardinia, indicating that some regions might be better suitable for future durum wheat cultivation. Regional transect in precipitation and soil hydraulic properties are identified as main drivers for additional irrigation needs. Furthermore, stabilizing productivity by means of irrigation is shown to largely increase the water demand of Sardinia's agricultural sector, especially in the case of the irrigation scenario aimed to maximise production. This does not only underline the necessity of an efficient supply system, but also indicates that the additional demand could result in potential competition over freshwater resources with other irrigated crops, such as vegetables, rice and corn. Moreover, this competition could even be expanded to other water using sectors, like domestic, which themselves are predicted to have changed water demands in the face of climate change. These linkages again highlight the importance of investigating Food and Water systems jointly, as changes in one are likely to influence the other as well.

Acknowledgments: This project has received funding from the European Union's Horizon H2020 innovation action programme under grant agreement 101037424 (ARSINOE).

References

Ballabio, C., Panagos, P., & Monatanarella, L. (2016). Mapping topsoil physical properties at European scale using the LUCAS database. Geoderma, 261, 110-123. doi:10.1016/j.geoderma.2015.07.006

EEA. (2019). CORINE Land Cover. Retrieved from https://sdi.eea.europa.eu/catalogue/copernicus/api/records/960998c1-1870-4e82-8051-6485205ebbac?language=all

Foster, T., Brozović, N., Butler, A. P., Neale, C. M. U., Raes, D., Steduto, P., et al. (2017). AquaCrop-OS: An open source version of FAO's crop water productivity model. Agricultural Water Management, 181, 18-22. doi:10.1016/j.agwat.2016.11.015

Grosse-Heilmann, M., Cristiano, E., Deidda, R., & Viola, F. (2024). Durum wheat productivity today and tomorrow: A review of influencing factors and climate change effects. Resources, Environment and Sustainability, 17. doi:10.1016/j.resenv.2024.100170

ISTAT. (2024). Coltivazioni : Cereali, legumi, radici bulbi e tuberi. Retrieved from http://dati.istat.it/#

Leduc, M., Mailhot, A., Frigon, A., Martel, J.-L., Ludwig, R., Brietzke, G. B., . . . Scinocca, J. (2019). The ClimEx Project: A 50-Member Ensemble of Climate Change Projections at 12-km Resolution over Europe and Northeastern North America with the Canadian Regional Climate Model (CRCM5). Journal of Applied Meteorology and Climatology, 58(4), 663-693. doi:10.1175/jamc-d-18-0021.1

Water-Energy-Food-Ecosystem Nexus factors driving global agrivoltaic potential

N.Galli[1*], M. Curioni[1], F. Capone[1], G. Manzolini[2], M.C. Rulli[1]
[1] Department of Civil and Environmental Engineering, Politecnico di Milano, Milano, Italy
[2] Department of Energy, Politecnico di Milano, Milano, Italy
* e-mail: nikolas.galli@polimi.it

Introduction

Thanks to past policies and technological advancements, solar energy stands as a key player in the transition towards clean energy to reduce greenhouse gasses emissions (Nijsse et al., 2023). Utility scale photovoltaic (PV) plants can occupy significant amounts of land, potentially interacting with ecosystem services (Choi et al., 2023) and the food system—a sector under increasing pressure due to climatic, demographic, and economic shifts. Water-Energy-Food-Ecosystem Nexus approaches offer a means to identify such interactions and mitigate them when they come in the form of resource competitions (D'Odorico et al., 2018). Agrivoltaic, i.e., the superposition of croplands and PV plants on the same land, is often presented as a synergistic solution in this sense. However, broad-scale analyses of this solution are still emerging, and could help to better contextualize agrivoltaics in the portfolio of Nexus solutions for climate action (Adeh et al., 2019). Here, we quantify the current competition between ground-mounted photovoltaic systems and agriculture by cross-referencing high quality global datasets. Then we use hydrological and agroecological modelling to simulate water stress and associated agricultural yield dynamics for current and hypothetical agrivoltaic conditions, on global high resolution, crop-specific maps of rainfed and irrigated agricultural areas. From that, we derive spatialized indexes of agrivoltaic performance from a Water-Energy-Food Nexus perspective, that can help identify global clusters of suitable areas for agrivoltaic systems.

Materials and methods

We study the competition between ground-mounted PV plants and agriculture by cross-referencing the PV systems dataset by Dunnet et al. (2020) with cropland maps at different time periods by Potapov et al. (2021). High-resolution hydrological simulations are performed using the dynamic, spatially distributed, crop-specific agro-hydrological model WATNEEDS (Chiarelli et al., 2020), with a daily operative timestep and monthly aggregated results, to identify crops evapotranspiration in traditional and agrivoltaic settings, where agrivoltaic is characterised by a set of reduced radiation scenarios. Then, we obtain variations in yield combining the agroecological method for potential yield estimation by Allen et al. (1998) with the yield response to water stress equation by Doorenbos & Kassam (1979).

Water-stress associated yield variations in each pixel are finally used to find existing or potential agricultural areas where agrivoltaics could mitigate water stress conditions. These areas are further reduced by filtering out those that do not match a set of land use conflict avoidance and biodiversity preservation criteria. By combining radiation scenarios and yield loss thresholds we create high resolution crop-specific datasets of areas that could be converted to agrivoltaics maintaining a synergistic Nexus condition.

Results and concluding remarks

The analysis of PV-cropland competitions shows that up to 16% of ground-mounted PV plants globally are mounted on previous cropland, indicating a preference of PV development towards croplands already present in the literature (Adeh et al., 2019). On the other hand, our global model shows that up to 35% of currently non-irrigated agricultural areas could be suitable for agrivoltaics at least from the point of view of

water stress and the associated yield response. In these areas, mostly located where crop growth is limited by water availability but not by availability of sunlight, agrivoltaics can lead to a reduction of the crop water footprint, and thus to a more efficient use of water resources by the crops, even though often at the cost of (slight) yield decreases. This research presents open development and improvement possibilities, as a more accurate simulation of agrivoltaic microclimate variables and of the associated crop response, as well as a better integration of the PV component and the energy infrastructures development. This will generate more and better high-resolution, spatially disaggregated but globally consistent results, that could potentially aid for further local case study analysis and priority setting of regional policies, bridging the gap between the global scale of the clean energy transition challenge and its local land use and landscape alteration constraints.

Acknowledgments: This study was carried out within the RETURN Extended Partnership and received funding from the European Union Next-GenerationEU (National Recovery and Resilience Plan NRRP, Mission 4, Component 2, Investment 1.3 D.D. 1243 2/8/2022, PE0000005).

References

Adeh, E. H., Good, S. P., Calaf, M., & Higgins, C. W. (2019). Solar PV Power Potential is Greatest Over Croplands. Scientific Reports, 9(1), 1–6. https://doi.org/10.1038/s41598-019-47803-3

Allen, R G; Pereira, L S; Raes, D; Smith, M. (1998). Crop evapotranspiration-Guidelines for computing crop water requirements. FAO Irrigation and Drainage Paper, 56, D05109.

Chiarelli, D. D., Passera, C., Rosa, L., Davis, K. F., D'Odorico, P., & Rulli, M. C. (2020). The green and blue crop water requirement WATNEEDS model and its global gridded outputs. Scientific Data, 7(1), 273. https://doi.org/10.1038/s41597-020-00612-0

Choi, C. S., Macknick, J., Li, Y., Bloom, D., McCall, J., & Ravi, S. (2023). Environmental Co-Benefits of Maintaining Native Vegetation With Solar Photovoltaic Infrastructure. Earth's Future, 11(6). https://doi.org/10.1029/2023EF003542

D'Odorico, P., Davis, K. F., Rosa, L., Carr, J. A., Chiarelli, D. D., Dell'Angelo, J., et al. (2018). The Global Food-Energy-Water Nexus. Reviews of Geophysics, 56(3), 456–531. https://doi.org/10.1029/2017RG000591

Doorenbos, J., Kassam, A. H., Bentvelsen, C., & Uittenbogaard, G. (1979). Yield Response to Water. FAO Irrigation and Drainage Paper, 33. https://doi.org/10.1016/b978-0-08-025675-7.50021-2

Dunnett, S., Sorichetta, A., Taylor, G., & Eigenbrod, F. (2020). Harmonised global datasets of wind and solar farm locations and power. Scientific Data, 7(1), 130. https://doi.org/10.1038/s41597-020-0469-8

Nijsse, F. J. M. M., Mercure, J. F., Ameli, N., Larosa, F., Kothari, S., Rickman, J., et al. (2023). The momentum of the solar energy transition. Nature Communications, 14(1), 1–10. https://doi.org/10.1038/s41467-023-41971-7

Potapov, P., Turubanova, S., Hansen, M. C., Tyukavina, A., Zalles, V., Khan, A., et al. (2021). Global maps of cropland extent and change show accelerated cropland expansion in the twenty-first century. Nature Food 2021 3:1, 3(1), 19–28. https://doi.org/10.1038/s43016-021-00429-z

Enhancing irrigated agroecosystem resilience through a Nexus approach with numerical modelling and multidimensional indicators

V.R. Coletta[1*], U. Fratino[2], N. Lamaddalena[2], S. Mohammedi[2,3], I. Portoghese[1], A. Pagano[2]
[1] Consiglio Nazionale delle Ricerche – Istituto di Ricerca Sulle Acque (CNR-IRSA), Bari, Italy
[2] Politecnico di Bari – DICATECh, Bari, Italy
[3] Università degli Studi di Bari Aldo Moro – DISSPA, Bari, Italy
* e-mail: virginiarosacoletta@cnr.it

Introduction

Improving the efficiency and resilience of irrigated agroecosystems in the Mediterranean region is fundamental to address growing environmental and socio-economic challenges, such as increasing food demand and limited resource availability (Peterson et al. 2018). To achieve this goal, innovative strategies that optimize irrigation systems while also reducing resource consumption and environmental impact are required.

This work, conducted as part of the ERASMUS project (funded under the PRIN 2022 call by the European Union - Next Generation EU), develops an integrated modelling framework to assess the benefits and co-benefits of smart water management technologies in pressurized irrigation systems. A holistic approach based on the "Nexus" concept is adopted to consider the interconnections between water, energy, food, and ecosystems. By combining numerical modelling with multidimensional indicators, the objective is to evaluate the performance of irrigation networks in terms of resource efficiency, operational effectiveness, user satisfaction, and ecosystem resilience. Different scenarios (e.g., the Business-As-Usual scenario and the implementation of smart water management technologies) are analysed and compared using an irrigation consortium in Apulia (Southern Italy) as a case study. The main objective is to quantify the multidimensional impacts of these solutions and support sustainable long-term management practices. A Community of Innovation (CoI) is established to promote knowledge exchange and stakeholder involvement, thus ensuring effective solutions for future irrigation management.

Materials and methods

Two complementary modelling approaches are used: numerical modelling and System Dynamics (SD) modelling. The former analyses irrigation network performance by evaluating key parameters such as water distribution equity, pressure regulation, and energy consumption (Ferrarese et al. 2021). The latter expands this analysis also considering environmental and socio-economic dynamics, represented through aggregated multidimensional indicators (Coletta et al. 2024). This combination of modelling approaches improves the understanding of the impact of different strategies (including smart water management technologies) on irrigation network efficiency and on the long-term sustainability of irrigated agroecosystems.

The numerical modelling approach is based on a Rapid Appraisal Procedure to assess network performance from both a physical and qualitative perspective. Data on cropping patterns and water volumes are gathered through field surveys and then integrated into simulation processes using Clément's model to estimate flow and pressure dynamics. Model calibration, based on field measurements, improves accuracy, thus enabling a detailed assessment of hydrants and networks performance. In this way, inefficiencies and operational gaps are identified, providing suggestions for optimizing resource use and operational reliability (Lamaddalena et al. 2024).

An innovative aspect of this work is the development of multidimensional indicators that combine the results of numerical modelling with other agroecosystem dynamics. In fact, these indicators not only assess network parameters such as reliability, discharge equity, and pressure adequacy, but also resource footprints, personnel performance, user satisfaction, and ecosystem resilience. Using these indicators

provides actionable insights into the operational and environmental benefits of modernizing pressurized irrigation systems. Therefore, this approach aims to support the design of strategies for sustainable water management (Portoghese et al. 2013).

Results and concluding remarks

The proposed methodology has been applied to an irrigation consortium in Apulia to demonstrate its practical application. The CoI has played an active role in modelling activities, fostering stakeholder involvement and ensuring the practical relevance of the research.

The results revealed operational inefficiencies, such as persistent pressure deficits at specific hydrants within District 10. Specifically, the analysis of hydrant Relative Pressure Deficit (RPD) revealed that 38% of the tested configurations experienced pressure deficits, with approximately 15% of hydrants classified in the 'failure' category ($-1 < RPD < 0$) and 5% in the 'danger' category ($RPD < -1$), highlighting the need for targeted hydraulic interventions. Conversely, certain hydrants exhibited a surplus of pressure ($RPD \geq 0$), indicating potential for energy recovery solutions through pressure regulation and energy conversion technologies. Beyond hydraulic performance, the study incorporated additional multidimensional indicators to capture other crucial aspects of the agroecosystem. Stakeholder feedback highlighted that the consortium is actively investing in network upgrades, including staff training initiatives. To reflect this, the Technical Staff Competency indicator was introduced, measuring the proportion of personnel with specialized technical skills relative to the total workforce. This is particularly relevant as modernization efforts require trained personnel to manage and operate the upgraded infrastructure efficiently. Another significant aspect emerging from stakeholder discussions was the strong responsiveness of the consortium's administration to user concerns. The governance structure ensures that any complaints from users are promptly relayed to the technical management teams. To quantify this dynamic, the User Complaint Index was calculated, assessing the number of reported complaints per delivery point. The results indicate that despite occasional operational inefficiencies, the consortium's management framework effectively mitigates prolonged service disruptions by addressing issues swiftly.

The next steps involve: i) finalizing the set of multidimensional indicators, incorporating feedback from stakeholders; ii) integrating these indicators into the SD modelling framework to analyse their interconnections and the combined effect of implementing technological interventions; iii) evaluating how smart water management strategies can improve the network performance and contribute to the long-term resilience of the consortium. This integrated approach ensures that management strategies are selected based on their ability to maximize both operational benefits and environmental sustainability.

Acknowledgments: This study received funding from the European Union—Next-Generation EU, National Recovery and Resilience Plan (NRRP)—MISSION 4 COMPONENT C2, INVESTIMENT N. 1.1, CALL PRIN 2022 D.D. 104 02-02-2022—(Project 2022WLW9X8, Equality and Resilience of Agroecosystems through Smart water Management and Use—ERASMUS) CUP N. B53D23006510006.

References

Coletta VR, Pagano A, Zimmermann N, Davies M, Butler A, Fratino U, Giordano R, Pluchinotta I (2024) Socio-hydrological modelling using participatory System Dynamics modelling for enhancing urban flood resilience through Blue-Green infrastructure. Journal of Hydrology, 636, 131248. https://doi.org/10.1016/j.jhydrol.2024.131248

Ferrarese G, Pagano A, Fratino U, & Malavasi S (2021) Improving Operation of Pressurized Irrigation Systems by an Off-grid Control Devices Network. Water Resources Management, 35(9), 2813–2827. https://doi.org/10.1007/s11269-021-02869-5

Lamaddalena N, Salman M, Pek E, Ahmad W, Lebdi F & Wahaj R (2024) Mapping System and Services for Pressurized irrigation systems – MASSPRES. FAO Irrigation and Drainage Paper, No. 68. Rome, FAO. https://doi.org/10.4060/cd0784en

Peterson CA, Eviner VT, & Gaudin ACM (2018) Ways forward for resilience research in agroecosystems. Agricultural Systems, 162, 19–27. https://doi.org/10.1016/j.agsy.2018.01.011

Portoghese I, D'Agostino D, Giordano R, Scardigno A, Apollonio C, Vurro M (2013) An integrated modelling tool to evaluate the acceptability of irrigation constraint measures for groundwater protection, 46, 90-103. http://dx.doi.org/10.1016/j.envsoft.2013.03.001

Mapping a Water-oriented Energy Food Ecosystems (WEFE) Nexus in the Nestos / Mesta river basin

C. Papadopoulos[1], D. Latinopoulos[1*], M. Karasani[1], I. Kagalou, [1] , C. Stylios[2], M. Spiliotis[1*]
[1] Department of Civil Engineering, Democritus University of Thrace, Kimmeria Campus, 67100 Xanthi, Greece
[2] Department of Informatics and Telecommunications, University of Ioannina, Kostakioi, 47150, Arta, Greece
* e-mail: mspiliot@civil.duth.gr, dlatinop@civil.duth.gr

Introduction

The water-energy-food-ecosystem (WEFE) nexus approach is considered as an appropriate analytical tool in managing and effectively governing river basins because of its inclusive and integrated nature (De Strasser et al. 2016). A nexus analysis, in a transboundary context, can inform, support and promote cooperation helping interlinkages' (and trade-offs) identification among the WEFE sectors and synergies' development to foster WEFE security, and understanding of cooperation benefits (Elsayed et al. 2022; De Strasser et al. 2016). The "nexus thinking" seeks synergies between the sectors attempting a holistic, multisectoral and multidimensional approach. The basic principles of this approach include: i) identifying the WEFE resources' interdependencies, ii) promoting logical and inclusive dialogues in decision- making, focused on sustainability, iii) supporting synergies and eliminating trade-offs across nexus sectors iv) managing the sources and ecosystems as a system (Carmona-Moreno et al. 2017).

Bulgaria and Greece share the waters of Mesta/Nestos River with the downstream part belonging to Greece, holding great social, economic, and environmental values for both countries. Greece officially receives 29% of the total volume generated in Bulgarian territory. The Greek basin economy relies on agriculture, tourism and manufactures and less on energy (non-negligible). Focusing on a Water(-oriented) EFe nexus, intensive irrigation activities and hydropower generation are observed during the past decades along with several water quality and quantity issues (Mooren et al. 2024) and "fragile" ecosystem services. Those aspects are included via targeted indicators within the nexus scheme. Given the complexity of the system, which is nearly impossible to analyze using a purely physics-based approach, the meta-model of Fuzzy Cognitive Maps (FCMs) was selected as the analytical tool. Our research is not targeted on WEFE nexus transboundary governance (Mooren et al. 2024); our focus is more technical on awareness raising, resources' monitoring and co-dependency across water-related sectors. Our aim is to utilize quasi-nonlinear FCM to "translate" the sum of interconnections among the WEFe Nexus pillars, built mostly on Analytical Hierarchy Process (AHP) processes, to ultimately project the current practices in the Greek territory of Nestos River, assisting regional water management.

Materials and methods

A Fuzzy Cognitive Map (FCM) is a semi-qualitative method of system analysis, and it is not primarily a sophisticated or equation-based tool. It leverages the existing knowledge of stakeholders to model the system, making it inherently based on people's perceptions. The FCMs consist of nodes and weighted connections, which indicate the degree of causality between the nodes or, in other words, the interactions among various factors of different natures. The nodes in the graph (Fig. 1a) represent the evaluation of each examined factor, while the initial values of these factors range between -1 and 1: A value of -1 implies that the variable is entirely absent from the system, whereas a value of 1 indicates that the variable is present to its fullest extent. By applying the FCM process, the trend of the existing system can be determined (Tyrovolas et al. 2023). In this work, the quasi-nonlinear reasoning rule is used to analyse the evolution of the examined system, aiming to overcome the limitations of conventional FCM approaches, such as the use of the sigmoid function, outputs 0.5 when its input is zero, allowing nodes without incoming connections to activate. The quasi-nonlinear reasoning rule is mathematically expressed as follows (Nápoles et al. 2023):

$$A_i^{(t+1)} = \varphi f\left(\sum_{\substack{j=1 \\ j\neq i}}^{n} A_j^{(t)} w_{ji}\right) + (1-\varphi) A_i^{(0)} \text{ , where } f\left(\bar{A}_i^{(t)}\right) = \begin{cases} \dfrac{\bar{A}_i^{(t)}}{\left\|\bar{\boldsymbol{A}}^{(t)}\right\|_2}, \bar{\boldsymbol{A}}^{(t)} \neq \vec{0} \\ 0, \quad otherwise \end{cases} : \mathbb{R}^n \to \mathbb{R}^n \quad (1)$$

where $\varphi \in [0,1]$ is a parameter indicating the nonlinearity degree of the reasoning rule and f is the re-scaled activation function. Additionally, $\bar{\boldsymbol{A}}^{(t)} = \left[\bar{A}_1^{(t)}, \bar{A}_2^{(t)}, ..., \bar{A}_n^{(t)}\right]$ is the raw state vector in t^{th} iteration and $\|\cdot\|_2$ denoting the Euclidean norm. However, the design of the FCM requires a lot of information, so, to simplify the decision, formalization of only five nodes was adopted to achieve a first insight. The initial state of the nodes was assessed by using the AHP (Saaty, 1980) incorporating in such way the individual complexity of each factor. For this reason, a group of experts participated. In the case of water quantity, the Water Exploitation Index (WEI^{GR}) (2nd revision of the River Basin Management Plan) was used as a single representative index.

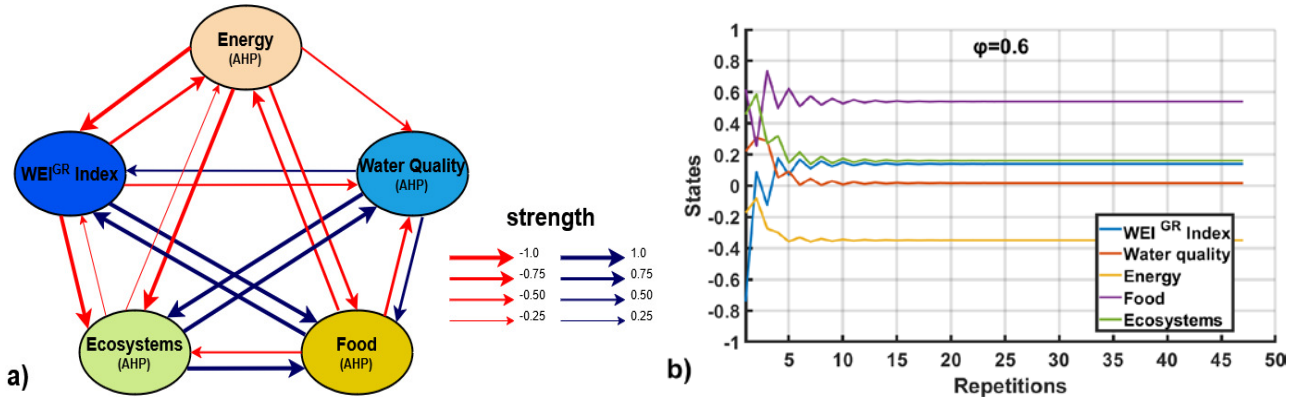


Figure 1. (a) Causal graph and (b)Visual illustration of the FCM's recurrent reasoning process for φ=0.6

Results and concluding remarks

As shown in Fig. 1b, it is evident that the system tends to shift toward a more anthropocentric tendency, which becomes more intensive at higher *φ*-values. Similar findings have been reported in Papadopoulos et al. (2024). Although there is a slight reduction, the node representing the food factor maintains a high value, while the state of the WEI^{GR} increases as a result of the food factor's influence. The states of the ecosystem and water quality factors decrease closer to a neutral state, whereas the state of the energy factor shows a declining trend in an era of energy crisis. Proper monitoring of all water related aspects is critical for resources preservation and structural changes implementation.

References

Carmona-Moreno C, Dondeynaz C, Biedler, M (2019) Position Paper on Water, Energy, Food, and Ecosystem (WEFE) Nexus and Sustainable Development Goals (SDGs). EUR 29509 EN, Publications Office of the European Union, Luxembourg. ISBN 978-92-79-98276-7. http://doi.org/10.2760/5295. JRC114177.

De Strasser L, Lipponen A, Howells M, Stec S, Bréthaut C (2016) A Methodology to Assess the Water Energy Food Ecosystems Nexus in Transboundary River Basins. 2016.Water, 8(2), 59. https://doi.org/10.3390/w8020059.

Mooren E, Munaretto S, Hegger T, Driessen J, La Jeunesse I (2024). Towards transboundary Water-Energy-Food-Ecosystem Nexus governance: a comparative governance assessment of the Lielupe and Mesta-Nestos river basins. Journal of Environmental Policy & Planning, 26(6): 623–642. https://doi.org/10.1080/1523908X.2024.2384582

Papadopoulos C., Bakas T., Tyrovolas M., […] Stylios C (2024) Participatory modelling and scenario analysis for managing Mediterranean river basins using fuzzy cognitive maps (under review)

Saaty TL (1980) The Analytic Hierarchy Process; McGraw-Hill: New York, NY, USA

Tyrovolas M, Liang XS, Stylios C (2023) Information flow-based fuzzy cognitive maps with enhanced interpretability. Granular Computing 8:2021–2038. https://doi.org/10.1007/s41066-023-00417-7

A socio-hydrological analysis of the Water – Energy – Food – Ecosystems Nexus in a meso-scale watershed in Northern Italy

E. Lucca[1], G. Castelli[1,2,3], J. Sušnik[4], J. Wenninger[5], L. Villani[1], L. Piemontese[1], E. Bresci[1]
[1] Department of Agriculture, Food, Environment and Forestry (DAGRI), University of Florence, Firenze, Italy
[2] UNESCO Chair in Hydropolitics, University of Geneva, Genève, Switzerland
[3] Environmental Governance and Territorial Development Hub (GEDT), University of Geneva, Genève, Switzerland
[4] Land and Water Management, IHE Delft, Delft, The Netherlands
[5] Water Resources and Ecosystems, IHE Delft, Delft, The Netherlands
* e-mail: enrico.lucca@unifi.it

Introduction

The Alps are referred to as the "water towers" of Europe because of their role in provisioning and regulating water supply for densely populated and agricultural intensive downstream regions (Viviroli et al., 2007). Although once abundant in water resources, parts of the Alps are experiencing increasingly more frequent water scarcity conditions (Briffa et al., 2009). Water scarcity, i.e., an imbalance between water demand and supply, is determined mainly by how water resources are allocated, used and managed. It is a socio-hydrological phenomenon (Nüsser, 2017). Furthermore, it concerns all sectors that crucially rely on water, including hydropower, agriculture, drinking water supply, and freshwater ecosystems, thus calling for a multi-sectoral approach to water resources management (i.e., the Water-Energy-Food-Ecosystems (WEFE) Nexus). While previous literature using the WEFE Nexus approach to investigate water scarcity have primarily focused on hydrological analysis (e.g., Yin et al., 2022), in this study, we explore both the social and the hydrological aspects of water scarcity. We do so in the Orco watershed, a meso-scale sub-basin of the Po River located in Northern Italy, characterised by significant storage capacity in hydropower reservoirs in the upper part of the basin and large water withdrawals for irrigation in the downstream part. The specific objectives of this study are to 1) identify socio-hydrological processes and their interdependencies across the WEFE Nexus sectors under water scarcity and 2) quantify the trade-offs between the WEFE Nexus sectors in the allocation of water resources.

Materials and methods

This study combines qualitative and quantitative methods to explore how water scarcity developed in the Orco watershed and to assess the resulting trade-offs across the WEFE Nexus. The qualitative analysis consisted of mapping socio-hydrological variables describing the availability and demand of water for hydropower, irrigation, drinking water supply and sustaining ecological flows. The mapping is done through the Causal Loop Diagram (CLD), a system-thinking tool used to graphically represent cause-effect relationships and feedback dynamics, and informed by interviews with local stakeholders. The quantitative analysis consisted of developing a water resources management model of the Orco watershed and simulating alternative water allocation strategies for the period 2011 - 2022. The model is developed within the Water Evaluation and Planning (WEAP) platform, and it integrates the simulation of hydrological processes with a priority-based water allocation module on a weekly timestep. What-if management scenarios referred to the period 2011 – 2022 were built by assigning different priorities to hydropower, upstream and downstream irrigation districts and by changing the values of environmental flow requirements.

Results and concluding remarks

Figure 1 shows the CLD of water availability and demand across the WEFE Nexus sectors in the Orco watershed as mapped through stakeholders' interviews. Trade-offs and synergies were identified in the timing of water releases for hydropower, irrigation and drinking water supply, in the multi-purpose use of

stored water during droughts, between irrigation withdrawals and sustaining ecological flows and between optimal hydropower production and downstream water needs through the so-called hydropeaking.

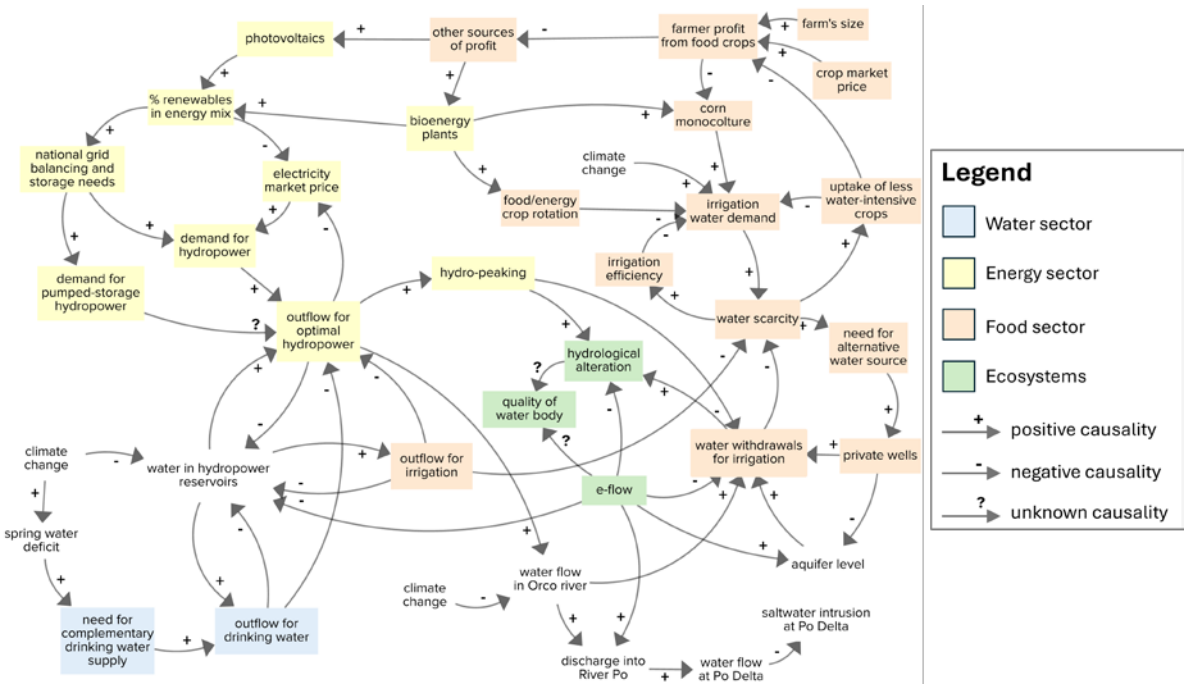


Figure 1. Socio-hydrological processes associated with water demand and supply in the Orco watershed.

The quantitative analysis showed that irrigation needs were fully met only in the years 2013, 2014, and 2018, highlighting an underlying imbalance between water availability and demand in the Orco watershed. The largest unmet irrigation demand of 88 million m3, 29 million m3 and 15 million m3 experienced in 2022, 2021 and 2016, respectively, are comparable with the total storage capacity of upstream hydropower reservoirs, amounting to 90 million m3. As such, trade-offs typically occurred late in the irrigation season, specifically in the last week of July and August. This is when the largest outflows from hydropower reservoirs tor meet downstream irrigation demands would be needed at the expense of hydropower production in winter. If irrigation needs had been prioritised over hydropower production, our study indicates that the annual supply deficits experienced by irrigation districts would have been either drastically reduced or fully compensated throughout the simulated period except from the years 2022 and, partly, 2021. The consequent reduction in hydropower production would have remained within 10% up to 2021 and reached 28 % in 2022. Higher values of the environmental flow requirement would have the most significant impact on the most downstream irrigation district, which would face an increase in the weekly supply deficit up to +70% against an increase lower than +25% for the most upstream one.

Acknowledgments: E. Lucca acknowledges the "PON Ricerca e Innovazione 2014-2020" of the Italian Goverrnment through the PhD scholarship granted to him (scholarship n. DOT137M5SZ n. 2, 2022–2024).

References

Briffa, K.R., Van Der Schrier, G., Jones, P.D., 2009. Wet and dry summers in Europe since 1750: evidence of increasing drought. Int. J. Climatol. 29, 1894–1905. https://doi.org/10.1002/joc.1836

Nüsser, M., 2017. Socio-hydrology: A New Perspective on Mountain Waterscapes at the Nexus of Natural and Social Processes. Mt. Res. Dev. 37, 518–520. https://doi.org/10.1659/MRD-JOURNAL-D-17-00101.1

Viviroli, D., Dürr, H.H., Messerli, B., Meybeck, M., Weingartner, R., 2007. Mountains of the world, water towers for humanity: Typology, mapping, and global significance. Water Resour. Res. 43, 2006WR005653. https://doi.org/10.1029/2006WR005653

Yin, D., Li, X., Wang, F., Liu, Y., Croke, B.F.W., Jakeman, A.J., 2022. Water-energy-ecosystem nexus modeling using multi-objective, non-linear programming in a regulated river: Exploring tradeoffs among environmental flows, cascaded small hydropower, and inter-basin water diversion projects. J. Environ. Manage. 308, 114582. https://doi.org/10.1016/j.jenvman.2022.114582

Analysis of water scarcity through the lens of Water – Energy – Food – Ecosystem (WEFE) Nexus approach at basin scale: A study from Mahi basin, India

G.E. Nagashree, A. Sharma*
Department of Hydrology, Indian Institute of Technology Roorkee, Roorkee, India
** e-mail: ashutosh.sharma@hy.iitr.ac.in*

Introduction

Water scarcity is defined as the point at which the combined demands of all users across sectors, including environmental needs, exceed the available supply or compromise water quality, under the prevailing institutional arrangements. This results in an inability to fully meet the demands of all sectors (Damkjaer and Taylor 2017). It has been reported that approximately 4 billion people globally are currently living under conditions of water scarcity (Mekonnen and Hoekstra 2016). Water scarcity affects all social and economic sectors and threatens the sustainability of the natural resources base. Addressing water scarcity requires an intersectoral and multidisciplinary approach to managing water resources to maximize economic and social welfare equitably without compromising the sustainability of vital ecosystems.

The Bonn 2011 Conference (Hoff 2011) highlights that adopting the Nexus strategy can enhance water, energy, and food security by integrating management across sectors and scales. This supports the transition to a Green Economy, ensuring resource use efficiency and reduced negative externalities. Embracing a Nexus approach minimizes trade-offs and creates synergies, promoting the need to move away from conventional policymaking. Hence in this study, we are adopting the Water-Energy-Food-Ecosystem (WEFE) Nexus to explore the interaction between the driving factors of water scarcity, the sectors that represent the WEFE system, and the water scarcity index from 1995-2010. We have selected the Mahi basin in India as a study area. This basin has been facing water scarcity for a long period, and very few studies have been connected with a holistic approach. With the implementation of WEFE nexus, the basin can be studied in various ways to provide a nexus perspective for policy makers to address water scarcity in the region.

Materials and methods

The Water Scarcity Index (WSI) was calculated based on the ratio of total water withdrawals for irrigation and other sectors to the total blue water availability, above minimum environmental flow requirements (Liu et al. 2022). Indicators for total water consumption, energy consumption, food production, and environmental flow requirement (EFR) were selected to represent each sector in the WEFE framework. A total of twenty indicators were chosen based on previous studies, categorized into economic, demographic, quality, natural water resources, and landscape factors. These categories influence the dynamic changes in the WEFE sectors, ultimately determining the water scarcity of the basin, as represented by WSI. Changes in one factor can directly or indirectly affect the entire system due to interlinkages between these factors.

To explore these interactions and quantify their effects, a simultaneous equation model (SEM) was adopted. For this study, the model consists of five equations, known as behavioral equations, which represent how indicators of each sector are influenced by the factors responsible for the WSI. SEM is used to analyze the joint determination of explanatory variables and dependent variables, identifying interactions and synergy effects in various domains such as economics, urban development, and sustainability (Mclean and Shepherd 1976; Huntington et al. 2021).

Data availability is critical in managing WEFE resources and selecting the nexus research approach. Panel data was constructed by analyzing a spatial resolution of 0.5 arc degree for the period from 1995 to 2010 at

annual timescales from 11 districts in the Mahi basin, which was simulated by two global hydrological models (GHMs), namely LPJmL (Sitch et al. 2003), PCR-GLOBWB (Wada, Wisser, and Bierkens 2014), at a spatial resolution of 0.5 arc degree. The multi-model simulations were archived in the Inter-Sectoral Impact Model Intercomparison Project (ISIMIP) 2a dataset. These GHMs were forced by the global meteorological data, namely WFDEI (Weedon et al. 2014) datasets.

Results and concluding remarks

Key positive factors influencing water scarcity through the WEFE subsystem include total crop sown area (1.184), industrial gross domestic product (GDP) (0.532), and total pasture area (0.977). In contrast, food production (-0.837), total GDP (-0.325), and nitrogen fertilizer use per unit crop area (-0.144) have negative impacts. A 1% increase in urban areas leads to a 0.350% increase in EFR. The analysis identifies the system boundary, four positive feedback loops, and six nexus points. Notably, irrigation water consumption and total GDP are the two nexus points that exert a holistic impact across the WEFE equations. Urbanization enhances water-use efficiency, reducing total water consumption as urban areas replace farmland. Increased domestic water consumption, paired with water-saving practices, lowers energy demand for pumping and treatment. Improved food production efficiency reduces water usage, while economic growth shifts resources from agriculture to industry, decreasing food production. Overuse of nitrogen fertilizers harms soil health, reducing agricultural yields. Increased water consumption worsens water scarcity, but energy-intensive solutions and efficient food systems help mitigate this. Protecting environmental flow requirements ensures sustainable water allocation, preventing over-extraction and promoting long-term water resource sustainability. The findings contribute to a deeper understanding of the WEFE interactions in the Mahi basin to address water scarcity, providing valuable insights for future policy development.

Acknowledgments: The first author acknowledges the support of IIT Roorkee and the Ministry of Human Resource Development, Government of India, through the Prime Minister's Research Fellowship (PMRF) for carrying out this research.

References

Damkjaer S,, Taylor R, 2017. The Measurement of Water Scarcity: Defining a Meaningful Indicator. Ambio 46 (5): 513–31. https://doi.org/10.1007/s13280-017-0912-z.

Hoff, H. 2011. Understanding the Nexus. Background Paper for the Bonn2011 Nexus Conference: Stockholm Environment Institute, no. November: 1–52.

Huntington, H.P., Jennifer I. Schmidt, Philip A. Loring, Erin Whitney, Srijan Aggarwal, Amanda G. Byrd, Subhabrata Dev, et al. 2021. "Applying the Food–Energy–Water Nexus Concept at the Local Scale." Nature Sustainability 4 (8): 672–79. https://doi.org/10.1038/s41893-021-00719-1.

Liu, W., Xingcai L., Hong Y., Philippe C., Yoshihide W. 2022. Global Water Scarcity Assessment Incorporating Green Water in Crop Production. Water Resources Research 58 (1). https://doi.org/10.1029/2020WR028570.

Mclean, M., Shepherd P. 1976. The importance structure Mick McLean and Paul Shepherd, no. February: 40–51.

Mekonnen, M.M., Hoekstra A.Y. 2016. Sustainability: Four Billion People Facing Severe Water Scarcity. Science Advances 2 (2): 1–7. https://doi.org/10.1126/sciadv.1500323.

Sheffield, J., Goteti G, Wood E.F. 2006. Development of a 50-Year High-Resolution Global Dataset of Meteorological Forcings for Land Surface Modeling. Journal of Climate 19 (13): 3088–3111. https://doi.org/10.1175/JCLI3790.1.

Sitch, S., B. Smith, I. C. Prentice, A. Arneth, A. Bondeau, W. Cramer, J. O. Kaplan, et al. 2003. Evaluation of Ecosystem Dynamics, Plant Geography and Terrestrial Carbon Cycling in the LPJ Dynamic Global Vegetation Model." Global Change Biology 9 (2): 161–85. https://doi.org/10.1046/j.1365-2486.2003.00569.x.

Wada, Y., D. Wisser, M. F.P. Bierkens. 2014. Global Modeling of Withdrawal, Allocation and Consumptive Use of Surface Water and Groundwater Resources. Earth System Dynamics 5 (1): 15–40. https://doi.org/10.5194/esd-5-15-2014.

Weedon, G.P, Balsamo G., Bellouin N, et al. 2014. The WFDEI Meteorological Forcing Data Set: WATCH Forcing Data Methodology Applied to ERA-Interim Reanalysis Data. Water Resources Research 50: 7505–14. https://doi.org/10.1002/2014WR015638.Received.

Assessing water scarcity hotspots with refined water demand data for Italy

F. Capone*, N. Galli, C. Govoni, H. Nanesha, D.D. Chiarelli, M.C. Rulli
Department of Civil and Environmental Engineering (DICA), Politecnico di Milano, Milan, Italy
** e-mail: francesco.capone@polimi.it*

Introduction

Water scarcity is quantified through a relatively diversified set of indicators. The common characteristic of these indicators, and the defining trait of water scarcity, is that they all represent an imbalance between water demand and water availability. Two of these indicators can be particularly useful in evaluating how water scarcity propagates and impacts on the food sector, especially if driven by drought: green water scarcity and blue water scarcity. Green water scarcity is the degree by which the evapotranspirative demand of a crop is satisfied by green water, i.e. soil moisture generated by naturally occurring precipitation. It is of prime importance because, following the conceptualization by Dooremboos et al. (1980), it is directly proportional to yield losses caused by water stress. Moreover, evapotranspirative demand is mainly conditioned by temperature, while green water availability is driven by precipitation. Temperature and precipitation are also the two main observed signals in drought characterization (Wada et al., 2011). Thus, green water scarcity, if assessed through a soil water balance modelling that accounts for feedbacks between green water availability and evapotranspiration, can be an efficient indicator of the compound demand- and supply-side impacts of drought on agricultural productivity (Schyns et al., 2019). Blue water scarcity is the ratio between total cross-sectoral blue water demand and blue water availability, net of environmental flow requirements and water used by upstream users. Therefore, it is a useful metric to assess the sustainability of water use when irrigation water is provided. Given that agricultural irrigation water demand typically accounts for the majority of water demand, blue water scarcity incorporates both demand- and supply- driven mechanisms of water scarcity impacts on the food sector (Ingrao et al., 2023). Here we quantify water scarcity impacts on the food sector by using high quality quantifications of blue water flows and demands as inputs to the blue water scarcity index first introduced by Mekonnen and Hoekstra (2016), with a particular focus on the agricultural sector.

Materials and methods

We use irrigation water demands from the AIDA (Agricultural Irrigation Demand Analyzer) product of the WATNEEDS model (Chiarelli et al., 2020), a 30arc seconds simulation between 2013 and 2023 with refined crop maps over Italy. WATNEEDS performs the soil water balance to split the biophysical water demand of agriculture between green water (evapotranspirative demand satisfied by precipitation-driven soil moisture) or blue water (irrigation requirements). WATNEEDS-AIDA provides blue water demands in a spatially distributed way, associating crop-specific water volumes (depending on crop demand and harvested area) to each 30s-resolution pixel. For domestic and industrial uses, we start from the water footprint dataset by Mekonnen and Hoekstra (2011), at nominal 5 arcmin (but actual 0.5°) resolution and downscale it to the model resolution based on the 100m settlements maps by Nieves et al. (2020). In particular, we distribute industrial uses based on the proportion of non-residential settlements in each of the 30arcsec pixels falling within a 5 arcmin pixel and repeat the procedure on residential settlements for domestic uses. We then compute blue water scarcity as the ratio between total water demands and water availability, accounting for locally generated runoff, net of environmental flows, and upstream runoff, net of environmental flows and upstream demands. We compute water scarcity for long-term average inputs in the 2013-2023 period and for each of the years, to be able to characterize year-specific water scarcity deviations from the average and cross-reference them with drought parameters. Finally, we analyze these data based on cropping areas to identify crop-specific drought vulnerability hotspots as regions where

water scarcity is most sensitive to drought.

Results and concluding remarks

Preliminary results show that the main urban areas in Italy, as well as the most densely cultivated regions, are in water scarcity conditions for most if not all the year. These hotspots are mediated by geographical trends that can be traced back to climatic and morphologic gradients across the country, with southern regions and plains having longer water scarcity periods around spring and summer. The Po plain is a significant water scarcity hotspot, mainly due to intensive irrigation. One limitation that arises in this sense is that the water scarcity formulation used here bases water propagation exclusively on natural hydromorphology, thus not accounting for the presence of irrigation infrastructure. Considering this aspect could be done by shifting water demands of irrigation consortia to their withdrawal points, thus potentially highlighting the effect of irrigation withdrawals on river ecosystem flows. The main challenge in this is the lack of information regarding effective irrigation water deliveries within irrigation consortia, which limits the possibility of validating model outputs. Concerning other uses, the impact of downscaling domestic and industrial water demands is evident also in the final results, that present a more accurate spatialization of water scarcity.

Acknowledgements: This study was carried out within the RETURN Extended Partnership and received funding from the European Union Next-GenerationEU (National Recovery and Resilience Plan NRRP, Mission 4, Component 2, Investment 1.3 D.D. 1243 2/8/2022, PE0000005).

References

Chiarelli, D. D., Passera, C., Rosa, L., Davis, K. F., D'Odorico, P., & Rulli, M. C. (2020). The green and blue crop water requirement WATNEEDS model and its global gridded outputs. Scientific Data, 7(1), 273. https://doi.org/10.1038/s41597-020-00612-0

Doorenbos, J., Kassam, A. H., Bentvelsen, C., & Uittenbogaard, G. (1980). Yield Response to Water. In Irrigation and Agricultural Development (pp. 257–280). Pergamon. https://doi.org/10.1016/b978-0-08-025675-7.50021-2

Ingrao, C., Strippoli, R., Lagioia, G., & Huisingh, D. (2023). Water scarcity in agriculture: An overview of causes, impacts and approaches for reducing the risks. In Heliyon (Vol. 9, Issue 8, p. e18507). Elsevier. https://doi.org/10.1016/j.heliyon.2023.e18507

Mekonnen, M. M., & Hoekstra, A. Y. (2011). The green, blue and grey water footprint of crops and derived crop products. Hydrology and Earth System Sciences, 8(1), 763–809. https://doi.org/10.5194/hessd-8-763-2011

Mekonnen, M. M., & Hoekstra, A. Y. (2016). Sustainability: Four billion people facing severe water scarcity. Science Advances, 2(2), 1–7. https://doi.org/10.1126/sciadv.1500323

Nieves, J. J., Sorichetta, A., Linard, C., Bondarenko, M., Steele, J. E., Stevens, F. R., Gaughan, A. E., Carioli, A., Clarke, D. J., Esch, T., & Tatem, A. J. (2020). Annually modelling built-settlements between remotely-sensed observations using relative changes in subnational populations and lights at night. Computers, Environment and Urban Systems, 80, 101444. https://doi.org/10.1016/j.compenvurbsys.2019.101444

Schyns, J. F., Hoekstra, A. Y., Booij, M. J., Hogeboom, R. J., & Mekonnen, M. M. (2019). Limits to the world's green water resources for food, feed, fiber, timber, and bioenergy. Proceedings of the National Academy of Sciences of the United States of America, 116(11), 4893–4898. https://doi.org/10.1073/pnas.1817380116

Wada, Y., Van Beek, L. P. H., & Bierkens, M. F. P. (2011). Modelling global water stress of the recent past: On the relative importance of trends in water demand and climate variability. Hydrology and Earth System Sciences, 15(12), 3785–3808. https://doi.org/10.5194/hess-15-3785-2011

Towards a climate resilient region through systemic solutions and innovations: the Bavarian case study in the ARSINOE project

A. Böhnisch[1*], I. Beck[1], M. Zilker[2], G. Braun[2], R. Ludwig[1]
[1] Department of Geography, Ludwig-Maximilians-Universität München, Germany
[2] Verband Kommunaler Unternehmen – Landesgruppe Bayern
* e-mail: a.boehnisch@lmu.de

Introduction

Climate change impacts show high heterogeneity in terms of type, intensity or frequency across Europe (EEA, 2024). Regionally specific vulnerability and adaptive capacity adds to the challenges of fostering cross-sectoral resilience in the water-energy-food-ecosystem nexus. Hence, diversified strategies that are adapted to local needs are required.

The project "ARSINOE – Climate Resilient Regions Through Systemic Solutions and Innovations", funded under EU's Horizon 2020 – Green Deal call, aims to provide tool boxes for improving resilience. The tool boxes contain innovations and solutions for climate change adaptation. They are designed within nine case study regions, but can be adopted beyond. To reach this goal, ARSINOE combines the Systems Innovation Approach, i.e., a holistic integration of social, economic and environmental factors for developing adaptation pathways, and the Climate Innovation Window, i.e., a marketplace for adaptation tools (https://climateinnovationwindow.eu/). All case study regions establish stakeholder dialogues to discuss and develop regional resilience pathways and innovation packages. These include nature-based solutions, citizen science initiatives, novel technologies or governance schemes and financial instruments.

This contribution illustrates the ARSINOE approach in the case study Main River (southern Germany).

Materials and methods

The Main River is the largest tributary to the Rhine. The ARSINOE case study focuses on the upper 400 km of the Main River. Its catchment covers an area of 21 500 km² with highly diversified land use and urban centres like Nuremberg and Würzburg. Additionally, the Main River catchment is embedded in the complex interregional Main-Danube water transfer system, supporting among others navigation, hydropower and tourism. Water scarcity and competition are identified as key challenges in the region. In particular, climate change and rising demands exert stress on water resources. This raises risks for river and ground water quality and quantity, but also for maintaining ecosystem services and city utility operations.

However, measures to prepare and respond to regional climate change impacts suffer from limited awareness of their severity, slow propagation of method application into practice, and unclear responsibility structures between private and public bodies. The region is thus at risk for being pushed beyond its resilience threshold. The ARSINOE approach addresses these barriers by co-designing science-driven innovations to build new climate-resilient development pathways. Central to this approach is the creation of so-called Living Labs within the case study. A Living Lab creates a platform for exchange between science and stakeholders who are affected by climate change impacts.

In the Living Lab "Bayerischer Main" (Bavarian Main River), three workshops were held for participants from regional enterprises, authorities, NGOs and associations from different sectors of the WEFE-nexus. While the first workshop was dedicated to defining the major challenges that stakeholders face, participants jointly developed a vision for a sustainable future with these challenges having been addressed in the second workshop. In the third workshop, participants formulated transformation pathways for major fields of action within the water-energy-food nexus. These transformation pathways were further assessed in terms of a PESTLE analysis (Morrison, 2013) which addresses *p*olitical, *e*conomic, *s*ocial, *t*echnological, *l*egal and *e*nvironmental factors. Therefore, semi-structured expert interviews were conducted. The transformation pathways also identified gaps where innovations are required. To close the gaps, two open

tenders for innovations were launched, which considered the input of stakeholders on what innovations were most needed. For the Main River Basin, one social-educational and one scientific-technological innovation were selected. These innovations are currently implemented and will be evaluated at a later stage of the project. To provide evidence for climate change related stress on water availability and to offer hydro services for stakeholders, a hydrological model is implemented for the Main River Basin. Using a set-up from the Bavarian project ClimEx (Leduc et al. 2019), the water balance model WaSiM provides a large ensemble of hydrological simulations for assessing climate trends, variability and extreme events until 2099 under a high-emissions scenario (Willkofer et al. 2024).

Results and concluding remarks

Under climate change conditions, mean discharges in the Main River catchment are projected to decrease by 15-25%, most pronounced during summers, with floods and low flow periods becoming more intense, frequent and prolonged. Against this backdrop, stakeholders identified a lack of cooperation or adequate resource governance as drivers for enhancing the already observed competition for water resources. Opposed to these projections, the stakeholders formulated a vision for a sustainable future with a healthy water balance and secured water supply, that recognises interconnections between water, food, energy and ecosystems. From the vision, stakeholders derived goals for the topics „water“, „land use and soils“, „towns and cities“, „public awareness and education“ and identified measures for reaching said goals. They concluded that developing climate resilience does not only require measures like improving soil protection, water efficiency, unsealing soils, or building water storage tanks, but also improved environmental education, restructuring funding programmes, and attracting personnel to key sectors. The PESTLE analysis results indicate that systemic barriers inhibit transformations (e.g., political will, psychological effects, financial risks, competing interests of lobby groups). However, interviewees also identified supporting factors (e.g., existing funding schemes, educational structures, existing expertise) and stressed the potential of building synergies. The innovators selected different gaps in the transformation pathways: Raising awareness for sustainable water use and building water knowledge was pursued by one innovator group who implements a “tap friendly” cycle route along the Main River with water bottle refill stations. The second innovator group provides data-based support for the discussion of irrigation needs in the currently rain-fed agricultural areas in the Main River Basin. As the Living Lab had revealed that many adaptation efforts were based on past experiences, it was followed by workshops and discussions on climate/hydro services with selected stakeholders. Here, a gap between user needs and services currently provided was identified. The development and provision of climate services is still ongoing. Future work will focus on the replicability of the case study results in, and transfer to other regions, particularly regarding modelling tools and data analytics, but also integrative river management (plans).

Acknowledgments: The ARSINOE project has received funding from the European Union’s Horizon H2020 innovation action programme under grant agreement 101037424.

References

European Environment Agency (2024): European Climate Risk Assessment. Publication Office of the European Union, Luxembourg. ISBN 978-92-9480-678-9; doi: 10.2800/8671471

Leduc, M.; Mailhot, A.; Frigon, A.; Martel, J.-L.; Ludwig, R.; Brietzke, G.; Giguère, M.; Brissette, F.; Turcotte, R.; Braun, M.; Scinocca, J. (2019): The ClimEx Project: A 50-Member Ensemble of Climate Change Projections at 12-km Resolution over Europe and Northeastern North America with the Canadian Regional Climate Model (CRCM5). J. Appl. Meteorol. Clim., 58, 663–693. DOI: 10.1175/JAMC-D-18-0021.1

Morrison, M. (2013): Strategic business diagnostic tools: theory and practice. CreateSpace Independent Publishing. (Chapter 3: PESTLE)

Willkofer, F., Wood, R. R., and Ludwig, R. (2024): Assessing the impact of climate change on high return levels of peak flows in Bavaria applying the CRCM5 large ensemble, Hydrol. Earth Syst. Sci., 28, 2969–2989, https://doi.org/10.5194/hess-28-2969-2024

Replacing staple crops with pulses to meet sustainable diet targets while ensuring water savings

L. Ricciardi[1*], P. D'Odorico[2], D.D. Chiarelli[1], M.C. Rulli[1]
[1] Department of Civil and Environmental Engineering, Politecnico di Milano, Milano, Italy
[2] Department of Environmental Science, Policy, and Management, University of California, Berkeley, CA, USA
* e-mail: livia.ricciardi@polimi.it

Introduction

Scientific literature has extensively highlighted how the current global food system negatively impacts both human health and environmental sustainability (Mekonnen and Hoekstra 2016; Willett et al. 2019). In fact, present diets are causing natural resource (e.g., water and land) depletion, while also contributing to the prevalence of diet-related diseases, like micronutrient deficiencies and malnutrition (Willett et al. 2019). Currently, diets are mainly based on high-yielding staple crops (e.g., rice, wheat, and maize), which, while calorically dense, are relatively low in micronutrients compared to other crops such as pulses (Willett et al. 2019). Pulses are nutrient-dense, provide essential micronutrients like iron and zinc, and offer a sustainable alternative to cereals in terms of land and water use (Willett et al. 2019). To address both dietary nutritional deficiencies and environmental sustainability, a shift towards more diversified and sustainable diets is currently needed (Willett et al. 2019). In fact, the adoption of sustainable diets, such as the one promoted by the EAT-Lancet Commission, is currently promoted worldwide (Willett et al. 2019). Overall, literature studies have already demonstrated that by increasing the consumption of micronutrient-rich foods, like pulses, dietary micronutrient intake could be significantly improved while environmental impacts could be reduced (Damerau et al. 2020; Springmann et al. 2018; Davis et al. 2018).

Here, to assess the feasibility of crop shifts at high resolution, we evaluate crop replacement scenarios where cereal production is reduced and pulse production is increased at pixel scale (Ricciardi et al. 2024). We do so in low-to-middle income countries like Pakistan and Nigeria where staple crops are overproduced and overconsumed (FAOSTAT 2019) to enhance the micronutrient availability of local diets. We develop crop replacement scenarios that ensure the intake of the dietary requirement of pulses set by the EAT-Lancet Commission (Willett et al. 2019). As a result, we assess the water savings while shifting crop production and the increase in micronutrient intake among the population.

Materials and methods

This study addresses dietary imbalances in Nigeria and Pakistan by shifting crop production to improve the dietary consumption of micronutrient-rich food. We consider replacing cereals (wheat, maize, and rice), which are locally overproduced and overrepresented in the diet, with pulses, which are locally underproduced and underrepresented in the diet, to meet the nutritional requirements following the EAT-Lancet Commission's recommendations (Willett et al. 2019). To do so, we first evaluate the dietary imbalances, which means we assess how the present diet (PD) from FAO (FAOSTAT 2019) is different from the country-specific healthy diet (HD). HD is computed by scaling the dietary requirements from Willett et al. (2019) to meet the caloric needs (i.e., average dietary energy requirement (ADER) (FAOSTAT 2019)) of the population of each Country. Then, we model different crop replacement scenarios at pixel scale (5 arcminutes resolution), namely: a) scenario A1, where pulses are replaced in areas currently used for cereals (i.e., wheat, rice, maize) production; b) scenario A2, where pulses are replaced in areas used for rice (Nigeria) or cash crops (Pakistan); c) scenario A3, where pulses are replaced avoiding monoculture, which means that cereals and pulses are evenly split in each pixel. Harvested areas are taken from Yu et al. (2020). Crop replacement is happening only in suitable areas for replacement which are computed based on soil suitability (e.g., pH), and crop calendars correspondence. Moreover, we assume that cereals can be replaced with pulses only when there is a reduction in water use. Crop water use, divided into blue water

BW (irrigation) and green water GW (precipitation), is computed through the spatially distributed agro-hydrological model WATNEEDS (Chiarelli et al. 2020) at 5 arcminutes resolution for both cereals and pulses in each country. We also compute the water savings associated with the crop shifts. The change in production (and so consumption) when shifting crops is then computed by using yields from Yu et al. (2020). Then, we also compute how pulse consumption can overcome micronutrient inadequacies in both countries for each scenario. Micronutrient information is from USDA (2019).

Lastly, we also assess the economic feasibility of implementing these crop replacement strategies by considering farmers' ability to redirect production and market conditions for consumers. To do so we assess whether the proposed crop replacements are both environmentally and economically viable.

Results and concluding remarks

Results show that both countries consume cereals in excess compared to the recommended dietary intake (i.e., around 50% of daily calories, much higher than the recommended 32%) while underconsuming pulses (less than 10% of daily calories, below the recommended 17%). As a result, by shifting crop production locally, pulse availability increases in all scenarios. Scenario A1 (monoculture of pulses) shows the most significant increase in pulse supply and water savings. However, in Pakistan, pulses still fall short of the recommended intake in scenarios A2 and A3, while Nigeria can nearly meet the recommendations in all scenarios. Consequently, all the crop replacement scenarios offer water savings. In particular, the highest savings are found in scenario A1, where, for example, it could be possible to save 31% of BW in Pakistan. Moreover, shifting diets toward more pulse consumption improves the availability of essential micronutrients, such as potassium, iron, thiamine, riboflavin, and folate.

While this shift in production could be environmentally feasible, it is difficult to occur because of both the higher prices of pulses and the existing subsidies put in place to boost cereal production rather than pulse production.

References

Chiarelli DD, Passera C, Rosa L, Davis KF, D'Odorico P, Rulli MC (2020) The green and blue crop water requirement WATNEEDS model and its global gridded outputs. Scientific data 7(1): 1-9. https://doi.org/10.1038/s41597-020-00612-0

Damerau K, Davis KF, Godde C, Herrero M, Springmann M, Bhupathiraju SN, Myers SS, Willett W (2020) India has natural resource capacity to achieve nutrition security, reduce health risks and improve environmental sustainability. Nature Food 1(10): 631-639. https://doi.org/10.1038/s43016-020-00157-w

Davis KF, Chiarelli DD, Rulli MC, Chhatre A, Richter B, Singh D, DeFries R (2018) Alternative cereals can improve water use and nutrient supply in India. Science Advances 4(7): 1-12. https://doi.org/10.1126/sciadv.aao1108

FAOSTAT (2019) Food Balance Sheet. https://www.fao.org/faostat/en/#data/FBS

Mekonnen MM, and Hoekstra AY (2016) Four billion people facing severe water scarcity. Science Advances 2(2): 1-12. https://doi.org/10.1126/sciadv.1500323

Ricciardi L, D'Odorico P, Chiarelli DD, Rulli MC (2024) To what extent can agriculture be reshaped to address healthy and sustainable diets by boosting pulse production locally? Global Food Security 40(100734): 1-10. https://doi.org/10.1016/j.gfs.2023.100734

Springmann M, Wiebe K, Mason-D'Croz D, Sulser TB, Rayner M, Scarborough P (2018) Health and nutritional aspects of sustainable diet strategies and their association with environmental impacts: a global modelling analysis with country-level detail. The Lancet Planetary Health 2(10): e451-e461. https://doi.org/10.1016/S2542-5196(18)30206-7

USDA (2019) Food Data Central. https://fdc.nal.usda.gov/

Willett W, Rockstrom J, Loken B, Springmann M, Lang T, Vermeulen S, Garnett T, Tilman D, DeClerck F, Wood A, Jonell M, Clark M, Gordon LJ, Fanzo J, Hawkes C, Zurayk R, Rivera JA, De Vries W, Majele Sibanda L, Afshin A, Chaudhary A, Herrero M, Agustina R, Branca F, Lartey A, Fan S, Crona B, Fox E, Bignet V, Troell M, Lindahl T, Singh S, Cornell SE, Reddy KS, Narain S, Nishtar S, Murray CJL (2019) Food in the Anthropocene: the EAT-Lancet Commission on healthy diets from sustainable food systems. The Lancet 393(10170): 447-492. http://dx.doi.org/10.1016/S0140-6736(18)31788-4

Yu Q, You L, Wood-Sichra U, Ru Y, Joglekar AKB, Fritz S, Xiong W, Lu M, Wu W, Yang P (2020) A cultivated planet in 2010 - Part 2: The global gridded agricultural-production maps. Earth System Science Data 12(4): 3545-3572. https://doi.org/10.5194/essd-12-3545-2020

Assessing flood impact on agriculture: A high-resolution hydrodynamic approach for crop damage evaluation

T. Lucaora[1], A. Annis[2*], F. Nardi[3], M.C. Rulli[1], D.D. Chiarelli[1]
[1] Department of Civil and Environmental Engineering, Politecnico di Milano, 20133, Milano, Italy
[2] Department of Civil, Architectural, and Environmental Engineering, University of Padua, Padua, Italy
[3] Department of Civil Engineering and Computer Science, University of Rome Tor Vergata
* e-mail: antonio.annis@unipd.it.

Introduction

Flooding is a recurring global natural hazard with increasing frequency and intensity due to climate change. While much research has focused on the impact of floods on urban areas, the damage to agricultural lands remains an underexplored field (Lucaora et al., 2025). This study presents a novel methodology for assessing flood-induced crop damage using high-resolution hydrodynamic modelling, applied to the Marta River Basin in central Italy. The methodology involves the adoption of a hydrologic-hydraulic modelling chain to define flood hazard maps for different return periods considering the application of the regional IDF curves (Rossi & Villani, 1994), a lumped physically based rainfall-runoff model (WFIUH, Grimaldi et al., 2012) and a high resolution 2D hydrodynamic model. The outcomes of the model are used as inputs for a crop resistance model to evaluate the potential losses in terms of tons/year and Kcal/year for different crops considering their seasonal stages. Alternative distributions of crop settings are proposed to potentially reduce crop risk. The analysis is aimed to propose a methodology to better agricultural management reducing economic losses due to flood risk.

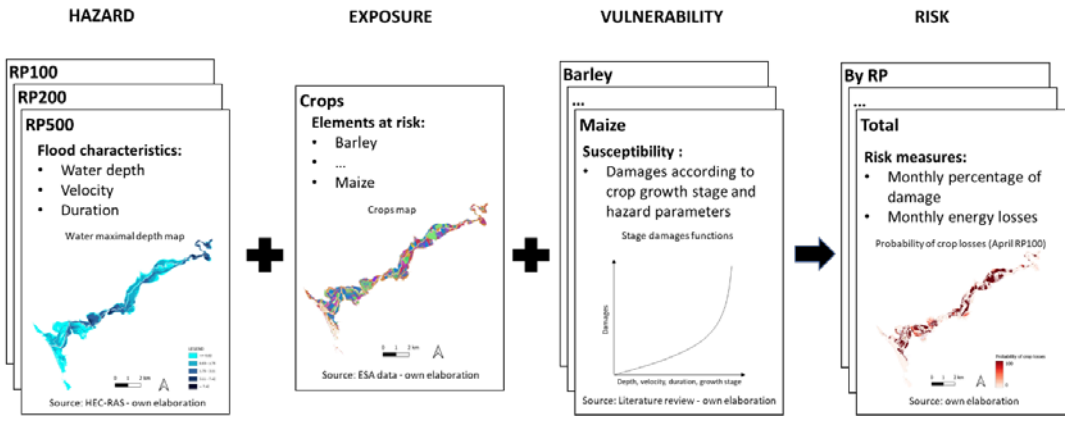


Figure 1. Step diagram explaining the method for determining risk. Flood parameters (hazard) are associated with a crop (exposure) and its susceptibility to flooding (vulnerability), which allows it to determine the risk.

Materials and methods

The study area, the Marta River Basin, spans 1079 km² in central Italy, characterized by croplands, grasslands, and artificial spaces. The research utilizes a high-resolution (1-meter) flood simulation model combined with crop resistance functions. The methodology consists of three main steps depicted in Figure 1:

1. Flood modelling: A 1D-2D hydraulic model simulating flood flow dynamics for 100-, 200-, and 500-year return periods. The model was calibrated and validated in previous studies (Annis et al., 2020)
2. Crop resistance modelling: Evaluating crop vulnerability based on water depth, velocity, submersion duration, and seasonality (Agenais et al., 2013).
3. Crop loss calculation: Estimating caloric losses based on historical crop yield data (D'odorico et al., 2014) and resistance parameters.

Results and concluding remarks

Results are partially shown in Figure 2 and indicate that the month of April exhibits the highest vulnerability due to the prevalence of winter cereals at the flowering stage, leading to significant caloric losses (up to 4.47 × 10^9 kcal for RP200). Alternative cr op scenarios suggest that substituting durum wheat with maize or sunflower could mitigate losses and enhance overall resilience. Although maize was likely to be suitable for the study area because they were also grown there, it should be verified that maize could effectively replace durum wheat in the areas concerned (like quality of the soil). The study highlights the need for adaptive agricultural planning in flood-prone regions to optimize crop selection based on flood exposure and seasonal risks.

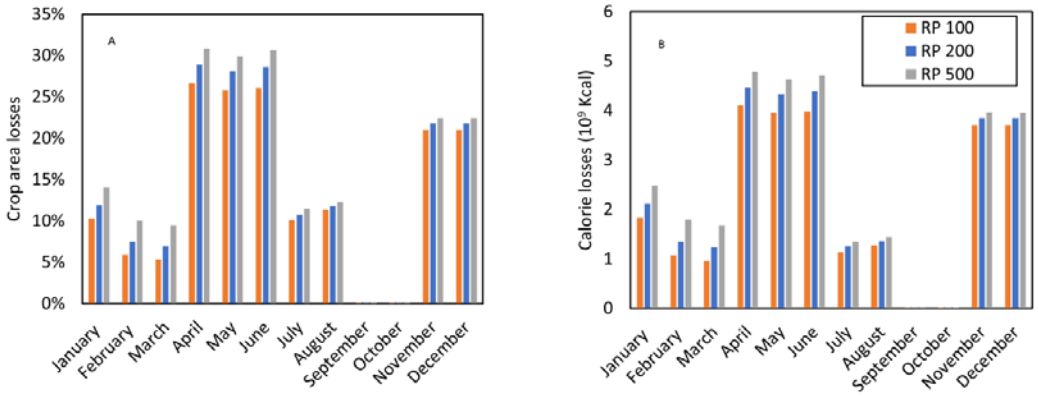


Figure 2. (left panel) Weighted average crop losses (in percent as respect to total production). (Right panel) Absolute damage (in 109 kcal) per month for all crops. Grasslands and fodder crop are not considered in both panels.

Acknowledgments: DDC and MCR were supported by CASTLE project (financed by MUR, project PRIN 2022XSERL4, CUP D53D23004920006); MCR, DDC, FN and AA were supported by the NEXUS NESS project (PRIMA Programme, an Art.185 initiative supported and funded under Horizon 2020, the European Union's Framework Programme for Research and Innovation, with GRANT AGREEMENT n.2042, CUP D49J21005050006). AA is supported by the RETURN Extended Partnership and received funding from the European Union Next-GenerationEU (National Recovery and Resilience Plan – NRRP, Mission 4, Component 2, Investment 1.3 – D.D. 1243 2/8/2022, PE0000005)

References

Agenais, A. L., Grelot, F., Bremond, P., Erdlenbruch, K., (2013). Dommages des inondations au secteur agricole: guide méthodologique et fonctions nationales. https://hal.inrae.fr/hal-02600061

Annis, A., Nardi, F., Volpi, E., Fiori, A. (2020). Quantifying hydrological and hydraulic modeling uncertainty in flood maps. Hydrol. Sci. J. 65(4), 507–523.

D'odorico, P., Carr, J.A., Laio, F., Ridolfi, L., Vandoni, S., (2014). Global food self-sufficiency under sustainable agriculture. Earth's Future 2(9), 458–469.

Grimaldi, S., Petroselli, A., Nardi, F., (2012). A parsimonious geomorphological unit hydrograph for rainfall–runoff modelling in small ungauged basins. Hydrological Sciences Journal, 57 (1), 73–83. doi:10.1080/02626667.2011.636045

Lucaora, T., Annis, A., Nardi, F., Rulli, M. C., Chiarelli, D. D., (2025). Distributed hydrodynamic modelling for assessing flood impacts on crops: Assessing flood-resilient crop management in a coastal basin of central Italy. Agricultural Water Management, 309, 109352.

Rossi, F., Villani, P., (1994). A project for regional analysis of floods in Italy. In: Coping with floods. Dordrecht: Springer, 193–217.

VIII. Water Pollution and Eco-systems Conservancy

Impacts of intensified water pumping on the aquifer and wetlands in a region of the Southern Mediterranean

A. Hani[1*], S. Hani[1], N. Bougherira[1], S. Lallahem[3], H. Chaffai[1], L. Djabri[1]
[1] Laboratory of Water Resources and Sustainable Development, Badji Mokhtar Annaba University, 23000, Algeria
[2] University 8 May 1945 Guelma, Algeria
[3] IXSANE, Parc des Moulins 23 Avenue de la Créativité - 59650 Villeneuve d'Ascq- France
* e-mail: haniazzedine@yahoo.fr

Introduction

In addition to the interest it represents for the water supply of populations, the dune massif of Bouteldja (Algeria) offers a place of wintering and nesting for many species of birds and for the development of flora of internationally recognized wealth. This site is today subject to progressive anthropogenic pressure which is becoming worrying. Indeed, the continuous exploitation of nearly fifty boreholes has led to a deterioration in water quality and has negatively influenced the hydrodynamic balance of the aquifer. It also resulted in a reduction in spring flows and the appearance of salty wedges, threatening even in the short term and the exploitation of the aquifer and the proper functioning of wetlands (Samraoui and de Belair 1998).

In this study, we attempted to use a hydrodynamic and hydrodispersive model:

- To assess the condition of water resources,
- identify sectors vulnerable to marine intrusion, and
- identify the factors responsible for the reduction in flow rates from the main sources and the reduction in the surface area of wetlands in the region.

Materials and methods

The Bouteldja region, located in the North-East of Algeria, is made up of Quaternary aeolian sands containing a free sheet of generally triangular shape with a thickness varying from 25 m in the east to 175 m in the west. To the south, the sands pass laterally to the gravels of the Bouteldja alluvial layer.

The climate of the study area is Mediterranean. The average annual rainfall is around 785 mm. The average annual temperature is 18°C. The average recharge of the aquifer is around 270 mm/year, or nearly 35% of rainfall.

Transmissivity values vary from 3.10^{-5} to 1.10^{-2} $m^2.s^{-1}$. The effective porosity ranges between 9 and 20%. The gravel layer located to the South and the Mediterranean Sea to the North constitute the two main outlets of the layer. Finally, the contact of the reservoir with the Numidian clays forms a watertight boundary in places. The infiltration of precipitation water is estimated at 0.272 m, or nearly 1550 $l.s^{-1}$ passing through a dune surface of 180 km^2. Evaporation at the numerous outcrop areas of the water table (Garâet Khroubzi, Gouréate, etc.), designated under the names of "Néchaât" and "Garâet", also constitutes an important element of the assessment given their extension (near 15 km^2).

MODLFOW (Harbaugh 2005) was used to describe the behavior of groundwater flows by solving the equations using the finite difference method. The aquifer was discretized into 720 active square grids of size 500 m, i.e., a study area of 180 km^2. By combining MT3DMS, it was made possible to simulate the propagation of pollutants in the aquifer. To highlight the vulnerability of the coastal sectors of the aquifer to seawater intrusion, we chose chloride as the characteristic element, which does not undergo adsorption and degradation phenomena during its transport in water.

Results and concluding remarks

The intensification of pumping in the dune aquifer and the regularization of watercourses, via the construction of numerous hydraulic dams, have led to a significant reduction in the flow of springs, a drop in the water table level and a reduction in the surface areas of the wetlands (Figure 1).

The intensive pumping also had the corollary of the appearance of a marine intrusion which threatens the exploitation of this important reservoir, particularly in the western sector near Mafragh. The drop in the piezometric surface can reach up to -30 m and by a fairly significant drop in diffuse emergencies. The drop in spring flow rates goes from 360 $L.s^{-1}$ in 2000 to less than 130 $L.s^{-1}$ in 2014.

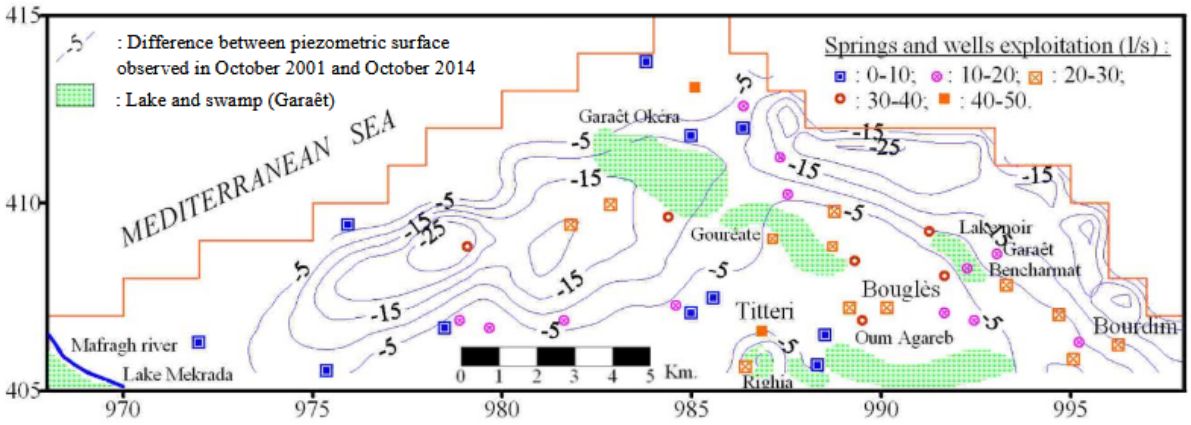


Figure 1. Map of the Bouteldja dune drawdowns.

The results of the hydrochemical balance show that the flow rates of marine waters entering the aquifer are of the order of 0.07 $m^3.s^{-1}$ for all model meshes that are sensitive to seawater invasion. Concentrations vary from 0 to nearly 350 g/s for each of the coastal meshes.

The intensification of pumping has a direct consequence of a modification of the surface area and hydrological regime of wetlands and a deterioration of the water quality of wadis, alder groves and lakes.

References

Harbaugh, A.W. (2005). MODFLOW-2005, the U.S. Geological Survey Modular Ground Water Model the Ground-Water Flow Process. Reston, VA, USA: US Department of the Interior, US Geological Survey. Volume 6.

Samraoui, B., de Belair, G., 1998. Les zones humides de la Numidie orientale. Bilan des connaissances et perspectives de gestion. Revue Synthèse, pub. de l'université de Annaba (Algérie), n°4, 90p.

Persistent organic pollutants as indicators of contamination status in surface waters of western Tianshan Mountains, Kyrgyzstan

B. Shen[1], J. Wu[2*]
[1] College of Environmental Science and Engineering, Yangzhou University, Yangzhou, 225127, China
[2] State Key Laboratory of Lake Science and Environment, Nanjing Institute of Geography and Limnology, Chinese Academy of Sciences, Nanjing 210008, China
* e-mail: w.jinglu@niglas.ac.cn

Introduction

Polycyclic aromatic hydrocarbons (PAHs), categorized as persistent organic pollutants (POPs), exhibit characteristics of toxicity, high persistence, bioaccumulation, and semi-volatility. Low temperatures and efficient snow scavenging at mountain areas facilitate enrichment of semi-volatile PAHs (Wania and Westgate, 2008). Thus, mountain regions are ideal settings to study contaminant transport and behavior along gradients of climate and surface cover. In such areas, water quality is important to pristine high-altitude ecosystems, but also to lowland people who depend on freshwater from mountains. There an accelerated tendency of glacier shrinkage and thawing permafrost may lead to a large release of accumulated PAHs into adjacent aquatic ecosystems. Information about PAHs in alpine aquatic systems, therefore, is essential.

Central Asia, characterized by limited and uneven distribution of water resources, is highly dependent on precipitation and meltwater from snow and glaciers in the Tianshan Mountains. However, PAHs in waters of the Tianshan Mountains would further amplify the uncertainty of water security; therefore, there is need to gain more insight into many aspects of water quality in the Tianshan Mountains. Approximately half the glaciated surface of the Tianshan Mountains is located in Kyrgyzstan, and the glacial contribution accounts for 15%-80% of runoff. Tianshan includes several separate hydrographic systems, such as the Issyk-Kul Basin (IKB), the Son-Kul Basin (SKB) and the Chu River Basin (CRB). In this study, we measured the concentrations of PAHs in surface waters from the western Tianshan Mountains of Kyrgyzstan, identified pollution sources, used hydrochemical and water isotopic (δD and $\delta^{18}O$) compositions to elucidate the behaviour of PAHs and the factors that influence transport pathways, and evaluated their potential risk.

Materials and methods

We carried out this study in the mountain ranges of Issyk-Kul Basin (IKB), Son-Kul Basin (SKB) and the Chu River, located in western Tianshan Mountains, Kyrgyzstan. A total of 59 surface water samples were collected from lakes and rivers in August 2018, including 25 lake water samples and 34 river water samples. The samples covered the major rivers discharged into lakes and highly populated areas.

PAHs in water were extracted by the method of solid-phase extraction (SPE) (Shen et al. 2021a). First, the cartridges were preconditioned by successive elution with 10 mL methanol and 10 mL ultrapure water. Second, 2 L of filtered water was passed through the cartridges, under vacuum. Finally, after eluting subsequently with 10 mL hexane and twice with 20 mL dichloromethane, the latter extracts containing PAHs were dewatered with anhydrous sodium sulphate, and then rota-evaporated and solvent-exchanged to hexane. They were then concentrated to 1 mL under nitrogen flow and stored at -20 °C until analysis. PAHs were analyzed using a high-performance liquid chromatograph (Agilent 1200) with diode array detection (238 nm) and a fluorescence detector, according to ISO 1799 standard (ISO 1799, 2002; Wolska, 2008).

In the field, pH and total dissolved solids (TDS), were measured by an EXO multiparameter water quality sonde (EXO 2, YSI Incorporated), and concentrations of CO_3^{2-} and HCO_3^- were calculated based on acid-base titration of subsamples. The anion concentrations were determined using an inductively coupled plasma-atomic emission spectrometry (ICP-AES, Prodigy, Teledyne Leeman Labs). The concentrations of Cl^- and

SO_4^{2-} were detected by an ion chromatography system (ICS 2000, Dionex). The δD and $\delta^{18}O$ were analyzed by a water vapor isotope analyzer (WVIA, DT100, Los Gatos Research) (Shen et al 2021b). The isotopic values are reported as per mil (‰) from the Vienna Standard Mean Ocean Water (VSMOW; Gonfiatini 1978).

Results and concluding remarks

Total concentration of PAHs (∑PAHs) in waters were between 13.84 ng L^{-1} and 81.57 ng L^{-1}, with a mean value of 42.77 ng L^{-1}. Compared with limited data published on PAH concentrations in waters from mountain regions, the concentrations are lower than values in some lakes impacted by local pollutant emission, but higher than those in remote regions. The discrepancy suggested that PAH concentrations in waters of high-altitude areas differ because of differences in environmental conditions and extent of anthropogenic influence.

PAH concentrations in lake waters were enhanced along with river discharge, reflecting the stronger influence of fluvial inputs. Higher contaminant levels were found along eastern IKB and north-eastern SKB. Karakol, in the eastern IKB, is the oblast capital of the Issyk-Kul oblast, but also a major tourist destination in Kyrgyzstan and an important industrial area in this region. Chon-Ak-suu River in the northern IKB are used as irrigation water sources and may receive contaminant loads from agricultural activities. Moreover, Chong-Kyzylsu River flows through a waste disposal area that is an abandoned Uranium mining site. A highly contaminated site in the SKB is close to a mountain hut. Municipal wastewater discharge, along with industrial and tourism-related activities, therefore, are responsible for enhanced PAH levels in the study area. Moreover, pollution sources were mainly from petroleum and combustion of biomass and coal for domestic heating and agricultural practices, inferred from molecular ratios.

Evaporation encourages volatilization of low-molecular-weight (LMW) contaminants from lake water bodies into the atmosphere, resulting in both isotope enrichment and lower LMW concentrations in the aqueous phase. River waters with high LMW concentrations had the most negative isotope values, implying wet deposition of these gaseous pollutants and the transfer of light PAHs in the snowpack to streamflow. One sample collected from Chu River, however, was isotopically enriched and had high molecular weight (HMW) PAH contents, which is possible due to evaporation of river water from irrigation canals. HMW PAH concentrations in river waters significantly correlated with hydrochemistry, likely suggesting that HMW PAHs were possibility exported from land to aquatic environments during the soil erosion process. These correlations were not found in lake waters, which is supposed to integrate riverine discharge, inputs from surface runoff and atmospheric deposition, and would also experience intensive evaporation.

Risk estimation suggests likely effects of PAHs on ecosystem biota, but negligible non-carcinogenic and carcinogenic effects on humans, from either dermal contact or water ingestion.

Acknowledgments: We thank the CAS Research Center for Ecology and Environment of Central Asia for assistance with this work. The study was supported by the National Natural Science Foundation of China (U2003202, 41671200), the Strategic Priority Research Program of Chinese Academy of Sciences, Pan-Third Pole Environment Study for a Green Silk Road (XDA2006030101).

References

Gonfiatini R (1978) Standards for stable isotope measurements in natural compounds. Nature 271: 534–536.

ISO procedure 1799. (2002) Water quality—determination of 15 PAHs in water by HPLC with fluorescence detection.

Shen B, Wu J, Zhan S, et al. (2021a) Residues of organochlorine pesticides (OCPs) and polycyclic aromatic hydrocarbons (PAHs) in waters of the Ili-Balkhash Basin, arid Central Asia: Concentrations and risk assessment. Chemosphere 273: 129705. https://doi.org/10.1016/j.chemosphere.2021.129705.

Shen B, Wu J, Zhan S, et al. (2021b) Spatial variations and controls on the hydrochemistry of surface waters across the Ili-Balkhash Basin, arid Central Asia. Journal of Hydrology 600: 126565. https://doi.org/10.1016/j.jhydrol.2021.126565.

Wania F, Westgate J N. (2008) On the mechanism of mountain cold-trapping of organic chemicals. Environmental Science and Technology 42(24): 9092–9098. https://doi.org/10.1021/es8013198.

Wolska L (2008) Determination (monitoring) of PAHs in surface waters: why an operationally defined procedure is needed. Analytical and Bioanalytical Chemistry 391: 2647-2652. https://doi.org/10.1007/s00216-008-2173-y.

Evaluating effectiveness of technical interventions on lake health: A case from Bengaluru, India

P. Jamwal
Centre for Enviornment and Development, ATREE
e-mail: priyanka.jamwal@atree.org

Introduction

Bengaluru, once known as the "City of Lakes," faces significant challenges in managing and maintaining healthy lakes. Population growth, rapid urbanization, and poor wastewater treatment infrastructure has caused the rapid deterioration of these water bodies. The government has implemented several programs under various initiatives for lake restoration. However, the technical interventions implemented under various projects—such as diverting inflows, removing silt, clearing shoreline vegetation, and installing artificial islands—have failed to effectively address recurring issues of severe algal blooms, foul odours, frothing, and fish kills. The anecdotal evidence highlights these issues, however lack of consistent, standardized studies that quantifies the impact of such activities on health of water bodies is not available. This study quantifies the impact of technical interventions on water quality of Venkateshpura Lake (V-Lake). It also proposes alternative restoration approach that aims at addressing stakeholder interests, accommodating diverse uses of lake and is feasible within financial and environmental constraints.

Materials and methods

V-Lake is located [13°4'42"N, 77°37'23"E] in the north of Bengaluru city with a water spread area of 2.75 hectares. The lake has two inlets and one outlet. Pre-restoration, Inlet 1 discharged stormwater runoff, while Inlet 2 released 150 m^3/day of primary-treated wastewater. The hydraulic retention time (HRT) of lake was around 120 days. This was estimated by factoring in a daily evaporation loss of 6 mm and a percolation loss of 2 mm in addition to the outflows during monsoons.

Pre-restoration water sampling at the lake began in November 2022, with biweekly collection from five sampling locations across the lake. Restoration activities were initiated in December 2023 and completed in May 2024. Major technical interventions at the lake included, removing shoreline vegetation, diversion of primary treated wastewater by construction of a diversion channel and fencing the inner boundary of the lake. Water quality sampling continued during and after the completion of these activities. The water samples were tested for a range of physical, chemical, and biological parameters, including Secchi depth (SD) which is a measure of water clarity, total nitrogen (TN), total phosphorus (TP) and chlorophyll-a. The Carlson Trophic State Index (TSI) was estimated using samples collected pre- and post-restoration. The overall TSI was determined as the average of individual indices calculated using Eqs. (1) to (3):

$$TSI(SD) = 60 - 14.41 * \ln(SD), \text{ SD in m} \quad (1)$$

$$TSI(Chl\text{-}a) = 9.81 * \ln(Chl\text{-}a) + 30.6, \text{ chlorophyll-a in } \mu g/L \quad (2)$$

$$TSI(TP) = 14.42 * \ln(TP) + 4.15, \text{ TP in } \mu g/L \quad (3)$$

Results and concluding remarks

The technical interventions implemented to restore V-Lake have led to significant changes in key water quality parameters. As shown in Figure 1, Secchi depth (SD) at the outlet of the lake decreased significantly from 0.67 m pre-restoration to 0.17 m post-restoration. This decline in water clarity was accompanied by a substantial increase in chlorophyll-a concentrations, which reached a maximum of 58 µg/L post-restoration (Table 1). Additionally, the average total phosphorus (TP) levels increased significantly from 1.4 mg/L to 4.4 mg/L, indicating elevated nutrient enrichment within the lake system (Figure 1).

Despite measures to mitigate external nutrient loading, including the diversion of 150 m3/d of primary-treated wastewater, the lake transitioned from eutrophic state (average TSI: 74) to hypereutrophic state (average TSI: 98). The presence of severe algal blooms at the lake can be attributed to the removal of shoreline/in-lake vegetation and nutrient release from sediments (anaerobic conditions) driven by increased hydraulic retention time (HRT)(Zheng et al. 2022). The deterioration in water quality post-restoration also highlights the inadequacy of current approach in capturing the complex biogeochemical interactions that govern lake health. To improve outcomes, restoration frameworks in context of developing countries should adopt incremental approach to restoring lake health that considers the ecological, social, and economic dimensions of blue-green ecosystems (Jamwal et al. 2023).

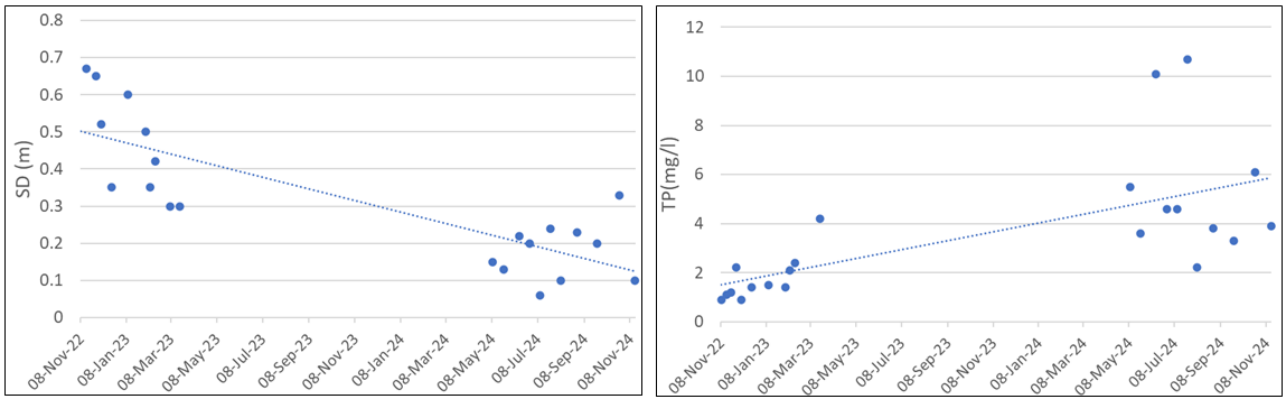


Figure 1. Pre and post restoration SD(m) and TP (mg/l) at the outlet of V-lake

Stakeholder-driven frameworks, such as the stepwise restoration model offer a structured methodology for rehabilitating degraded ecosystems in rapidly urbanising regions (Liu et al. 2024). Additionally, defining restoration targets in collaboration with stakeholders is essential to align ecological interventions with societal expectations and ensure the long-term sustainability of lake management strategies.

Table 1. Pre and Post restoration TSI at V lake

Parameters	Pre restoration	Post restoration
TSI(SD)	67	93
TSI (Chl-a)	54	70
TSI(TP)	102	130
Average TSI	74	98

References

Jamwal, P., Carvalho, L., Bhattacharyya, S., & Muttepawar, P. (2023). The benefits of restoring urban lakes in the tropics. Environmental Monitoring and Assessment, 195(11), 1294. https://doi.org/10.1007/s10661-023-11888-1

Liu, J., Dou, Y., & Chen, H. (2024). Stepwise ecological restoration: a framework for improving restoration outcomes. Geography and Sustainability. https://www.sciencedirect.com/science/article/pii/S2666683924000105. Accessed 20 November 2024

Zheng, X.-N., Wu, D.-X., Huang, C.-Q., Wu, Q.-Y., & Guan, Y.-T. (2022). Impacts of hydraulic retention time and inflow water quality on algal growth in a shallow lake supplied with reclaimed water. Water Cycle, 3, 71–78.

Bacteriostatic activity of ion-exchange samples of the Armenian clinoptilolite as new effective sorbent for aqueous systems purification

L. Harutyunyan[1*], A. Manukyan[2], K. Nazaretyan[3], H. Sargsyan[4], N. Dolaberidze[5], M. Nijaradze[5], N. Mirdzveli[5], V. Tsitsishvili[5,6]

[1] *Department of Biosience and General Chemistry, Armenian National Agrarian University, Yerevan, Armenia*
[2] *Mining and Metallurgy Institute, Yerevan, Armenia*
[3] *Institute of Chemical Physics NAS RA, Yerevan, Armenia*
[4] *Institute of Biochemistry after H. Buniatyan, Yerevan, Armenia*
[5] *Department of Chemistry and Chemical Technologies, Georgian National Academy of Sciences, Tbilisi, Georgia*
[6] *Petre Melikishvili Institute of Physical and Organic Chemistry, I. Javakhishvili Tbilisi State University, Tbilisi, Georgia*
** e-mail: l.harutyunyan@anau.am*

Introduction

Treatment of water used for municipal and industrial purposes refers to the removal of impurities such as dissolved substances, as well as suspended colloids and solids. Among all available water treatment technologies (coagulation, foam flotation, solvent extraction, electrolysis, etc.), adsorption is considered the best option because of convenience, ease of operation, and simplicity of design (Bhatnagar and Sillanpaha 2010). As effective sorbent zeolite-containing tuff from the Nor Kokhb deposit, Armenia, was chosen as one of the main materials for creating new bactericidal zeolite filter materials for purification-decontamination of water from various sources (Tsitsishvili et al. 2022). By application of the metal-containing zeolites it is possible microbiological contamination of zeolite sorbents used in the purification of industrial wastewater. In such cases it is necessary to provide the sorption materials with bacteriostatic properties in order to prevent the growth of microorganisms on their surface (Reeve and Fallowfield, 2018).

Materials and methods

The zeolitic tuff from Nor Kokhb deposit (Armenia), which are characterized as clinoptilolite, was used in this study. "Liquid-phase" ion exchange (LIE) of natural clinoptilolite to obtain silver-, copper- and zinc-containing zeolites was carried out in a combined orbital-linear shaking water bath using aqueous solutions of the corresponding salts.

Bacteriostatic properties of zeolite samples were determined by the disk diffusion (Kirby-Bauer) method in standard conditions using the cultures of Gram-negative bacteria *Escherichia coli* (strain 335-548-23) and *Salmonella enteritidis* (363-619-23), Gram-positive bacteria *Staphylococcus aureus* (485-1071-2) and *Bacillus subtilis* (486-1176-2), fungal pathogenic yeast *Candida albicans* (443-1440-23) and a fungus *Aspergilus niger* (392-1132-2) placed (10^9 CFU/ cm^3) in Mueller–Hinton agar (3 mm deep) poured into 100 mm Petri dishes. Tests were carried out at the testing laboratory Mi Lab (Tbilisi, Georgia).

Results and concluding remarks

Results of the Kirby-Bauer test using gram-negative and gram-positive bacteria, as well as fungal microorganisms are given in Tables 1 to 3. The activity of the silver form against *Escherichia coli* decreases slightly after preheating, and after acid treatment remains only at an "intermediate" concentration (1 N), and against salmonella it increases sharply after heating to 200 °C, and remains unchanged after acid treatment only at high concentration (2 N). The activity of the copper form against *E. coli* is maintained only if the heating temperature does not exceed 200 °C and the concentration of hydrochloric acid does not exceed 0.5 N, and only the form that is not treated with heat or acid is active against *Salmonella*. The zinc form is active only if the zeolite has undergone preliminary acid treatment in a hydrochloric acid solution with a concentration of 0.5 N. With the exception of the zinc forms of the original and heat-treated clinoptilolites, all other forms enriched with biologically active metals are active against gram-positive

bacteria; the zinc forms of samples pre-treated with acid are the most active.

Table 1. Diameter (mm) of zones of inhibition of the growth of gram-negative bacteria by zeolites calcined at various temperatures and then subjected to ion exchange in solutions of bioactive metal salts.

Bacteria		***Escherichia coli***			***Salmonella***		
Bioactive metal		**Ag**	**Cu**	**Zn**	**Ag**	**Cu**	**Zn**
Initial ion-exchanged sample		14	12	0	14	13	0
Calcination temperature, °C	**200**	13	11	0	22	0	0
	300	12	0	0	14	0	0
Concentration of HCl, N	**0.5**	0	12	14	0	0	14
	1	11	0	0	0	0	0
	2	0	0	0	12	0	0

Table 2. Diameter (mm) of zones of inhibition of the growth of gram-positive bacteria by zeolites calcined at various temperatures and then subjected to ion exchange in solutions of bioactive metal salts.

Bacteria		***Staphylococcus aureus***			***Bacillus subtilis***		
Bioactive metal		**Ag**	**Cu**	**Zn**	**Ag**	**Cu**	**Zn**
Initial ion-exchanged sample		15	18	0	13	25	20
Calcination temperature, °C	**200**	14	16	0	13	20	19
	300	15	13	0	13	22	17
Concentration of HCl, N	**0.5**	15	11	20	11	20	24
	1	13	11	16	11	17	21
	2	11	11	15	12	16	20

Table 3. Diameter (mm) of zones of inhibition of the growth of fungal microorganisms by zeolites calcined at various temperatures and then subjected to ion exchange in solutions of bioactive metal salts.

Bacteria		***Candida albicans***			***Aspergillus niger***		
Bioactive metal		**Ag**	**Cu**	**Zn**	**Ag**	**Cu**	**Zn**
Initial ion-exchanged sample		19	0	0	11	22	19
Calcination temperature, °C	**200**	22	0	0	19	0	0
	300	20	0	0	22	0	0
Concentration of HCl, N	**0.5**	0	0	0	23	0	0
	1	16	0	0	21	0	0
	2	16	0	17	22	0	0

Pre-heated silver forms are most active against fungal pathogenic yeast, copper forms do not affect the growth of *Candida albicans* at all, and the zinc form becomes active only after treatment in a concentrated solution of hydrochloric acid (2 N). The activity of the silver form against black fungus increases as a result of preheating and, in particular, pre-acid treatment. As for the enrichment of clinoptilolite with copper and zinc, only the corresponding ion-exchanged forms of the original clinoptilolite have very high activity against *Aspergillus niger*, but any pre-treatment neutralizes the activity.

Acknowledgments: The authors express their gratitude to the International Science and Technology Center (ISTC) for the support of this work under the project GE-2506 “Scientific substantiation of the possibility of creating new bactericidal zeolite filter materials for purification-decontamination of water from various sources”.

References

Bhatnagar A, Sillanpaha M (2010) Utilization of agro-industrial and municipal waste materials as potential adsorbents for water treatment: a review. Chemical Engineering Journal 157: 277-296. http://dx.doi.org/10.1016 /j.cej.2010.01.007

Reeve P, Fallowfield H (2018) Natural and surfactant modified zeolites: a review of their applications for water remediation with a focus on surfactant desorption and toxicity towards microorganisms. Journal of Environmental Management 205: 253-261. https://doi.org/10.1016/j.jenvman.2017.09.077

Tsitsishvili V, Panayotova M, et al. (2022) Characterization of Georgian, Kazakh and Armenian natural heulandite-clinoptilolites. Bulletin of the Georgian National Academy of the Sciences 16(4): 39-46.

Exploring microbial contamination in the Vjosa river: A year-long study

K. Peli[1], B. Parllaku[1], M. Lika[1], A. Lugaj[1], S. Amalfitano[2], E. Hamzaraj[1*]
[1] Department of Biology, Faculty of Natural Sciences, University of Tirana, Tirana, Albania
[2] Water Research Institute, National Research Council of Italy, Rome, Italy
* e-mail: etleva.hamzaraj@fshn.edu.al

Introduction

Rivers frequently receive discharge from wastewater treatment plants (WWTP), untreated wastewater, and pollution from other point and diffuse sources, all of which significantly reduce the hygienic water quality. This problem exists even in areas with advanced wastewater treatment technologies (Kirschner et al., 2017). In less developed areas and countries, the problem is of course worse.

With a total length of 272 km and a catchment area of 6,700 km², the Vjosa River forms a transboundary ecosystem between Albania and Greece and is one of the last free-flowing, wild rivers in Europe (Schiemer et al., 2018). However, little is known about the hygienic conditions within the waters of the Vjosa River main branch. This study aims to investigate the bacteriological water quality of the Vjosa River.

Materials and methods

Seven sampling points were chosen within the Vjosa River main branch. Samples were collected at regular intervals on a monthly basis over a one-year period (January 2023 to March 2024). Sampling procedures and analytical methodologies adhered rigorously to established international standards (ISO 1991; WHO 1984). The evaluation of total coliform bacteria was conducted using the Most Probable Number (MPN) index, following the guidelines prescribed in the aforementioned standards. Heterotrophic bacteria were enumerated utilizing the Plate Count Agar (PCA) method.



Figure 1. The map depicted the Vjosa River catchment and the locations where samples were taken. The black line represents the territorial border between Albania and Greece.

Results and concluding remarks

During the longitudinal survey of the Vjosa River catchment area, faecal indicator bacteria (FIB) exhibited distinct spatial patterns. Notably, site S-07-ARO recorded elevated faecal coliform (FC) levels, reaching a maximum of 46,000 CFU/100 mL in October 2024. These elevated levels are likely linked to the direct discharge of untreated wastewater from the city of Përmet. Similarly, sites S-01-MIF and S-03-POC also reported 46,000 CFU/100 mL in November 2024. These high concentrations may be attributed to agricultural runoff and livestock activities in the surrounding rural areas. Fecal bacteria can enter surface waters through direct deposition of feces or overland runoff, with animal waste identified as a major contributor to water pollution in many regions (Payment et al., 2003). Elevated Enterococci (EF) levels were

observed at site S-06-DRA, with a peak of 9,300 CFU/100 mL in July 2024. The heterotrophic plate count (HPC) at 22°C and 35°C within the main branch of the Vjosa River exhibited considerable variability.

High microbial counts in surface water samples during the summer are often linked to increased nutrient levels due to water concentration caused by evaporation during dry periods (Ouma et al., 2016). Furthermore, reduced precipitation during the summer months can lead to lower volumes of tributary water entering the river. This results in higher relative fractions of wastewater in the river and reduced dilution of contaminants, further exacerbating microbial pollution levels. Based on Kavka et al. (2006) classification system, most of the sampling points within the Vjosa river main branch showed critical to strongly fecal pollution by putting those in III and IV categories based on this classification.

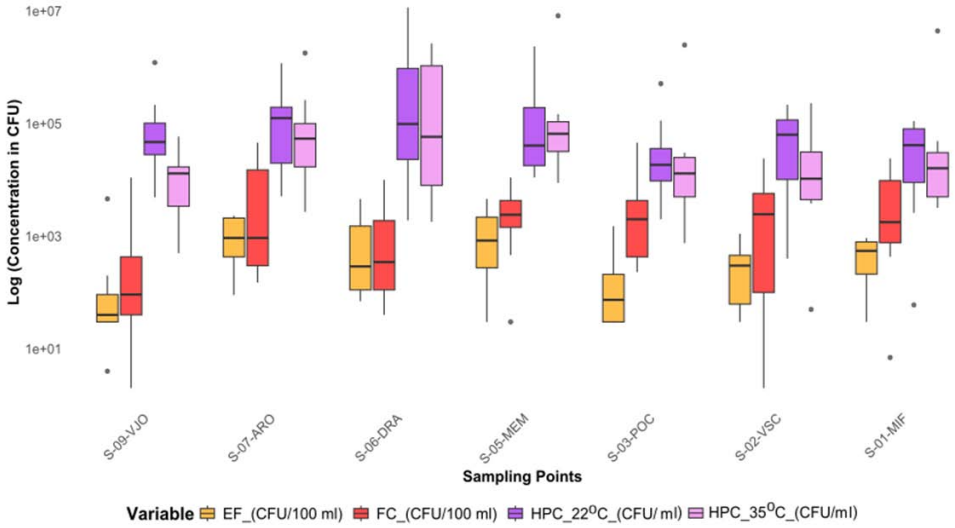


Figure 1. Boxplot of microbial parameters in the sampling points along the Vjosa River.

To gain a more comprehensive understanding of the Vjosa River's water quality, extended sampling over a longer timeframe is recommended. Such monitoring would help capture seasonal variations and provide more accurate insights into the factors influencing microbial water quality.

Acknowledgments: The projects: "VjoSusDev: Environmental assessment of the Vjosa riverscape as the basis for an integrated water management and sustainable catchment development", supported by Austrian Development Cooperation, programme APPEAR, and "SUSPENSE: Microorganisms associated with suspended solids: an emerging quality issue for river waters", supported by Cooperation Program between Italy and Albania.

References

ISO (International Organization for Standardization) (1991) ISO 5667-2:1991(E). Water Quality—Sampling, Part 2: Guidance on Sampling Techniques. Second edition 1991-07-01.

Kavka GG, Kasimir DG, Farnleitner AH (2006) Microbiological water quality of the River Danube (km 2581 - km 15): Longitudinal variation of pollution as determined by standard parameters: Proceedings 36th International Conference of IAD. In Proceedings 36th International Conference of IAD Austrian Committee Danube Research/ IAD, Vienna.

Kirschner AKT, Reischer GH, Jakwerth S, Savio D, Ixenmaier S, Toth E, Sommer R, Mach RL, Linke R, Eiler A, Kolarevic S, Farnleitner AH (2017) Multiparametric monitoring of microbial faecal pollution reveals the dominance of human contamination along the whole Danube River. Water Research, 124: 543–555. https://doi.org/10.1016/j.watres.2017.07.044

Payment I, Waite M, Dufour A (2003) Introducing parameters for the assessment of drinking water quality. In Assessing microbial safety of drinking water: Improving approaches and methods. World Health Organization & Organisation for Economic Co-operation and Development, IWA Publishing, pp. 47-77.

Schiemer F, Drescher A, Hauer C, Schwarz U (2018) The Vjosa River corridor: A riverine ecosystem of European significance. Hydrobiologia 155: 1–40. https://doi.org/10.1007/s10750-018-3577-6

World Health Organization (1984) Microbiological methods for water quality monitoring (2nd ed.). World Health Organization.

Assessing the health of the Erzeni River: a multidimensional approach to water quality

E. Hamzaraj[1*], V. Gjeci[2], B. Parllaku[1], P. Lazo[1], A. Paparisto[1], E. Keçi[3], S. Duka[1], L. Vallja[1]
[1] Department of Biology, Faculty of Natural Sciences, University of Tirana, Tirana, Albania
[2] National Environmental Agency, Tirana, Albania
[3] University "Aleksander Moisiu", Durrës, Albania
* e-mail: etleva.hamzaraj@fshn.edu.al

Introduction

The Erzeni River, located in central Albania, is an essential water source for both domestic and agricultural uses. However, rapid urbanization, industrial growth, and agricultural practices have raised concerns regarding its water quality. The primary concerns include contamination from untreated wastewater, agricultural runoff, and industrial effluents, which significantly impact the river's ecological health and pose potential risks to public health. Assessing the water quality of the Erzeni River is essential for understanding the extent of pollution and its effects on the environment and human well-being.

Microbial indicators such as faecal coliforms, total coliforms, and faecal streptococci are commonly used to assess bacterial contamination in water. Microbiological contamination with faecal bacteria remains a significant concern throughout rivers. Benthic macroinvertebrates are crucial for the functioning of river ecosystems and play a key role in river monitoring (Balderas et al., 2015). These organisms are sensitive to changes in environmental conditions and can provide insights into the health of the river ecosystem over time. (USEPA. 2005). Chemical parameters are fundamental in evaluating the overall water quality and the health of aquatic ecosystems.

As urbanization and industrialization continue to grow in Albania, understanding the river's water quality will be critical for balancing economic development with environmental conservation. Through comprehensive monitoring and data collection, the study of the Erzeni River will inform future policy decisions, guide conservation efforts, and help protect public health, all while promoting environmental stewardship for future generations.

Materials and methods

Samples were collected monthly from October 2023 to October 2024 in three sampling sites along the Erzeni River. The sampling sites were chosen based on their proximity to potential pollution sources. Sterile glass bottles are used to take water samples for microbiological analysis. Samples were taken at a depth of 30-50 cm from the water surface, at a distance of 30 - 100 cm from the river bank and in accordance with all standards for sampling for microbiological analysis (ISO 19458). The Most Probable Number method (ISO 9308-2, ISO 7899-2) is used to determine the concentration of fecal coliforms, *E. coli* and *Enterococcus faecalis*. For the determination of heterotrophs, PCA medium, pour plating method and incubation at 22°C in a biological thermostat for 48 hours are used.

Biological samples for macroinvertebrates were collected using a benthic kick net (0.5 mm mesh) according to Campaioli et al. (1994) and Lenat (1998). Density, TV, and SWRC Biotic Index, which correlates water quality with species tolerance values and densities, is calculated using the formula (1) outlined by McGonigle (2000).

$$[\text{SWRC - Biotic Index }] = \frac{\sum(\text{TV})*\text{d}}{\text{D}} \quad (1)$$

Results and concluding remarks

Bacterial Contamination: The microbiological parameters in Erzeni River water showed important spatial

and temporal fluctuations. High concentrations of faecal coliforms were recorded in sampling station 3 in October 2024 (110000 CFU/100 mL), while low values were recorded in sampling station 1 during spring 2024 (110 to 430 CFU/100 mL). The highest concentrations were observed near wastewater discharge points and agricultural runoff zones, suggesting that untreated wastewater and agricultural practices are major contributors to pollution. According to the classification of Kavka et. Al (2006) the water in stations 2 and 3 is strongly polluted. The concentration of faecal streptococci confirmed that human and animal waste were likely sources of contamination, with higher concentrations near urban settlements.

Macroinvertebrates: Macroinvertebrate diversity was found to be negatively correlated with bacterial contamination. In the more polluted sections of the river, the abundance of pollution-sensitive species, was significantly reduced. The SWRC Biotic Index values suggest that the water quality of the Erzeni River ranges from fair (St. 1, in the upper part of the river) to very poor (St. 3, near river mouth). According to the data, Station 3 exhibits significant organic pollution. These findings confirm that the river's ecological health is compromised in areas with higher levels of contamination, highlighting the importance of macroinvertebrate diversity as a reliable bioindicator of water quality.

Chemical Parameters: All the pH values and electrical conductivity during the study period fall within the recommended and mandatory values according to DIRECTIVE 2006/44/EC of the European Parliament. On the other hand, chemical analysis showed that the water quality of the Erzeni River was adversely affected by elevated levels of nitrates and phosphates. These nutrients are commonly associated with fertilizer runoff and can contribute to eutrophication, leading to oxygen depletion. Dissolved oxygen levels were lower in the more polluted sections of the river, further indicating the impact of organic pollution.

In conclusion, this study provides a comprehensive assessment of the water quality of the Erzeni River, highlighting significant pollution from both anthropogenic and agricultural sources. Elevated levels of bacterial contamination, particularly faecal coliforms and total coliforms, indicate that the river is at risk of waterborne diseases, especially in areas near urban and industrial settlements. The macroinvertebrate community reflects the negative impact of pollution, with reduced biodiversity and the dominance of pollution-tolerant species in heavily contaminated sections. Chemical analysis confirms the presence of excess nutrients and localized heavy metal contamination, which may contribute to ecological degradation.

To improve the water quality of the Erzeni River, it is essential to implement stronger wastewater treatment practices, particularly in urban and industrial areas. Regular monitoring of both microbial and chemical parameters, along with the continued assessment of macroinvertebrate diversity, will be crucial for tracking improvements and informing future water management policies.

Acknowledgments: The project “Effects of microplastics on water quality in the Erzen River and the Adriatic Sea”, supported by University of Tirana, Programme “UT- Research, Excellence and Innovation”.

References

Balderas ECS, Grac C, Berti-Equille L, Hernandez MAA (2016) Potential application of macroinvertebrate indices in bio-assessment of Mexican streams. Ecological Indicators 61: 558–567.

Campaioli S, Gheti PF, Minelli A, Ruffo S (1994) Manuale per riconoscimento dei Macroinvertebrati delle acque dolci italiane (Manual for the recognition of Benthic macroinvertebrates of Italian freshwater). Appa Trento 1: 9–14, 27–190.

Kavka G, Kasimir G, Farnleitner A (2006) Microbiological water quality of the River Danube (km 2581 - km 15): Longitudinal variation of pollution as determined by standard parameters. In: Proceedings 36th International Conference of IAD. Austrian Committee Danube Research/ IAD, Vienna: 415–421

Lenat DR (1988) Water quality assessment of streams using a qualitative collection method for benthic macroinvertebrates. Journal of the North American Benthological Society 7 (3): 222–233.

McGonigle J. 2000 Education: Leaf Packs and Beyond. Stround Water Research Center, USA.

USEPA. 2005 Water Quality Standards Academy: Basic Course. United States Environmental Protection Agency Office of Water, Washington District of Columbia, USA, pp 152

Analysis of transport of selected heavy metals to the Baltic Sea along the continuum of the largest Polish rivers - Vistula River case study

D. Matuszewska[1,2,3*], E. Kiedrzyńska[3,1], M. Kiedrzyński[4]
[1] UNESCO Chair on Ecohydrology and Applied Ecology, 12/16 Banacha Str., University of Lodz, Lodz, Poland
[2] Doctoral School of Exact and Natural Sciences, 21/23 Jana Matejki Str., University of Lodz, Lodz, Poland
[3] European Regional Centre for Ecohydrology of the Polish Academy of Sciences, 3 Tylna Str., 90-364, Lodz, Poland
[4] Department of Biogeography, Paleoecology and Nature Conservation, 1/3 Banacha Str.,University of Lodz, Poland
* e-mail: dominika.matuszewska@edu.uni.lodz.pl

Introduction

Due to the fact that the area of the Baltic Sea catchment is four times larger than the surface of the sea itself and is inhabited by 85 million people, the sea is exposed to a constant supply and accumulation of toxic compounds (Borecka et al., 2015). One of the most dangerous pollutants entering the Baltic Sea ecosystem are heavy metals (HELCOM, 2021). Among the sources emitting their greatest amounts are mining, metallurgy, the exploitation of minerals and fossil fuels, industry and transport, the use of pesticides and fertilizers, as well as wastewater discharges from WWTPs (Piwowarska et al., 2024). Nevertheless, it is worth mentioning that one of the main routes through which pollutants, including heavy metals from the above-mentioned sources, enter the Baltic Sea is via river waters, such as the Vistula (HELCOM, 2021).

Because of the danger posed by the entry of heavy metals into the aquatic environment, compounds such as cadmium (Cd), lead (Pb), mercury (Hg), nickel (Ni) are included in documents establishing strategies to combat water pollution, such as the Water Framework Directive (WFD) 2000/60/EC of the European Parliament and of the Council of 23 October 2000, and Directive 2013/39/EU of the European Parliament and of the Council of 12 August 2013 (European Union, 2000, 2013). These directives provide guidelines for actions in the field of water policy, emphasizing proper water resource management and highlighting the need to monitor a group of hazardous toxic substances that contribute to water pollution.

Despite the restrictions, heavy metals are still detected in both the Baltic Sea and the river waters flowing into it (HELCOM 2021). Therefore, it is important not only to monitor surface water pollution, but also to analyze the transformation of pollutants along the river continuum. This analysis provides crucial insights into the self-purification potential of rivers and the transportation of contaminants along their course. Accordingly, the aim of the presented research was to conduct a holistic spatiotemporal analysis of the monitoring and transportation of heavy metals to the Baltic Sea via the largest Polish river, the Vistula River.

Materials and methods

The preliminary analysis of the Vistula River pollution with heavy metals included in the priority list – cadmium, lead, nickel (European Union, 2000) — along the river continuum was based on data from the Chief Inspectorate for Environmental Protection in Poland (CIEP). To calculate the average annual metal loads, flow data from the Polish Institute of Meteorology and Water Management were also used. For this purpose, the points for which data were obtained and which are located closest to the CIEP points were selected. The analysis covered the period from 2018 to 2020. A map of the Vistula River with CIEP measurement points - W1 (827.39 km of river from the mouth), W2 (417.48 km), W3 (11.2 km) is presented in Figure 1.

Results and concluding remarks

Preliminary analysis of data obtained from the Chief Inspectorate for Environmental Protection (CIEP) showed that out of the four heavy metals listed as EU priority substances, three – cadmium, lead and

nickel, were detected at selected measurement and control points (Figure 1) during the years 2018-2020 (Table 1).

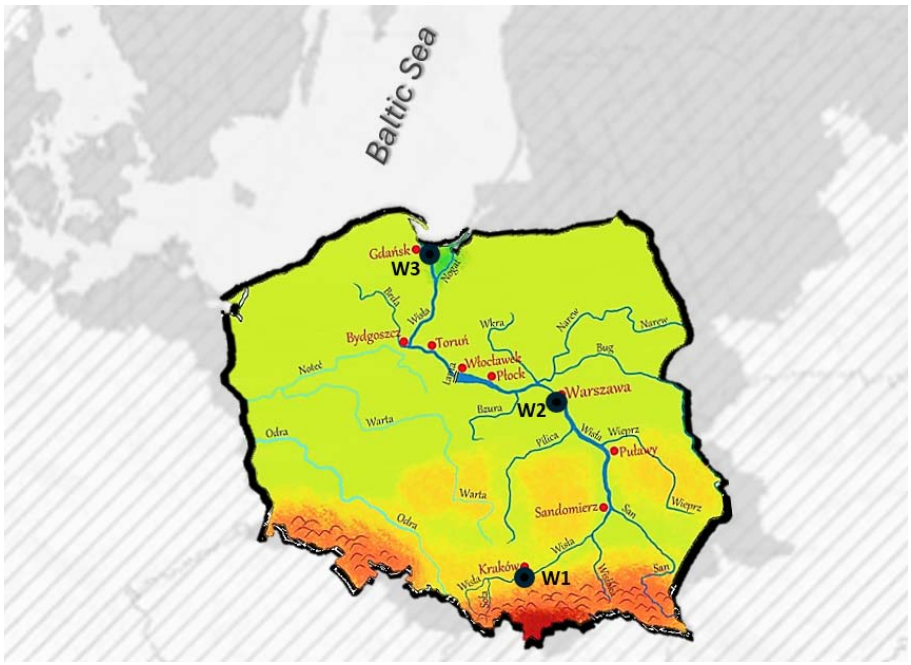


Figure 1. Map of Poland at the background of the Baltic Sea catchment area with heavy metal monitoring points designated along the Vistula River (measurement points of the Chief Inspectorate for Environmental Protection).

Table 1. Average load (t/year) of Cd, Pb and Ni from selected CIEP monitoring points for the period 2018-2020.

	Cd	Pb	Ni
W1	no data	1.02	8.93
W2	0.93	6.41	26.45
W3	0.49	1.90	38.50

Analyses revealed that during the period 2018-2020, no significant decrease in the magnitude of Cd, Pb and Ni loads flowing with Vistula water was observed. Point W2 is located in the centre of a large urban agglomeration, which may explain the increased loads of Cd and Pb in this place. The Ni loads, compared to Cd and Pb, increase along the river continuum.

Results indicate the Vistula's constant exposure to the continuous inflow of pollutants from its catchment areas and highlights not only the ongoing need for monitoring pollution in the Vistula but also the necessity of implementing effective ecosystem remediation methods, which will positively impact not only the condition of the river itself but also of the Baltic Sea.

Acknowledgments: The analysis was conducted as part of the FARMIKRO project, funded by the National Science Centre (NCN), Poland, under Opus 22 – Project No. 2021/43/B/ST10/01076.

References

Borecka M., Siedlewicz G., Haliński Ł.P., Sikora K., Pazdro K., Stepnowski P., Białk-Bielińska A. (2015) Contamination of the southern Baltic Sea waters by the residues of selected pharmaceuticals: method development and field studies. Marine Pollution Bulletin, 94(1-2), 62-71. doi: 10.1016/j.marpolbul.2015.03.008

European Union (EU) (2000) Water Framework Directive 2000/60/EC of the European Parliament and of the Council of 23 October, 2000 establishing a framework for Community action in the field of water policy. Official Journal of the European Union, 43(L 327), 1–51.

European Union (2013) Council Directive 2013/39/EU of the European Parliament and of the Council of 12 August, 2013; amending Directives 2000/60/EC and 2008/105/EC as regards priority substances in the field of water policy. Official Journal of the European Union, 56(L 226), 1–17.

HELCOM (2021) Inputs of hazardous substances to the Baltic Sea. Baltic Sea Environment Proceedings No. 179

Piwowarska D., Kiedrzyńska E., Jaszczyszyn K. (2024) A global perspective on the nature and fate of heavy metals polluting water ecosystems, and their impact and remediation. CREST 1-23. Doi:10.1080/10643389.2024.2317112

A GIS-grid nonpoint pollution and self-purification model for hydropower reservoirs

J.R. Ribas[1*], M.E.A. Fariña[2], J.C.R. Severo[3], L.S. Santos[4] , J.V.F. Guedes[4]
[1] Industrial Engineering Department/Polytechnic School/Universidade Federal do Rio de Janeiro, Rio de Janeiro, Brazil
[2] Industrial Engineering Department/Polytechnic School/Universidade da Coruña/Ferrol, Spain
[3] Fundação para Desenvolvimento de Bauru, Bauru, Brazil
[4] Environment Department/Corumbá Concessões S/A, Brasilia, Brazil
* e-mail: ribas@poli.ufrj.br

Introduction

The surface runoff from fertilized areas and urban areas (incorporating chemicals containing phosphorus), in addition to contributions associated with sewage, can be responsible for the increase in nitrogen and phosphorus levels in aquatic environments (Von Sperling 2014). Point sources refer to the release of urban and industrial effluents. In domestic effluents, nitrogen and phosphorus are associated with organic matter and the use of cleaning products. Among the diffuse release sources, agricultural activities deserve special attention, given the intensive use of phosphate fertilizers to increase crop productivity. A GIS multicriteria method based on the flow path to a water body, the efficiency of runoff generation, and the climatic driving force, was adopted to evaluate the diffuse nitrogen loss potential in a basin in China (Zhang and Huang 2011). The indicators adopted to analyze N and P loss in the Three Gorges Reservoir area in China were crop planting, livestock production, domestic inputs and the water-level-fluctuation zone (Zhong et al. 2020). An indicator called the land use impact coefficient was proposed to assess the impact of land use on the export coefficient of the non-point source pollution (Qian et al. 2021). Here we propose a GIS-grid nonpoint pollution model integrated with a hydrodynamic modeling procedure for self-purification of aquatic bodies. The GIS file is made up of a grid where each cell accounts for organic matter from households and livestock and nutrients from fertilizers. The reservoir pollution scenario is a function of the predicted degree of anthropization for a study horizon of one year.

Materials and methods

In this study, we analyzed the area of influence of the reservoir near the dam of the Corumbá IV hydroelectric plant, as shown in Figure 1, located in the central region of Brazil. The area includes the collection points located downstream of the Descoberto River water treatment plant and the water collection point of the Alagado River, two important tributary rivers. As for the reservoir, a collection point located approximately seven km from the axis perpendicular to the dam defines the boundary of the study. This delimitation assumes that the water body it circumscribes represents a potential effect on the dam and the plant's equipment. Data input consisted of estimating the production of organic matter and nutrients from household sewage, relevant point loads, agricultural fertilizers, and organic matter from livestock. For each of these, the following were evaluated: (i) current occupation, estimated through images captured by Landsat 8 and aerial images obtained by drones; (ii) land use and occupation regulations; (iii) altimetric survey data; and (iv) survey data on roads and tributary rivers. The limits and growth curves were parameterized in all grids. Estimates of pollutant loads, represented here by BOD, N (ammonia, nitrite, and nitrate), and P, were estimated at the collection points. Then the QUAL-UFMG method was used to model the effects of self-purification and contamination levels in the dam.

Results and concluding remarks

This study using the Qual-UFMG model (Von Sperling 2014) on the self-purification capacity of the Corumbá IV reservoir indicated that although domestic effluents and bleach from agricultural fertilizers will be discharged in the rivers that flow towards the dam, no further stretches were detected where BOD

values exceeded the limits established by law. Figure 2 shows that although the volumes of BOD, N and P upstream of the dam reached the aggregate values of 27.75 mg/L, 23.79 mg/L and 4.61 mg/L, respectively, the processes of sedimentation, dissolution and dispersion of nutrients along the course of the rivers and the rest of the reservoir area were sufficient to purify the water, so that the levels that reached the dam were 1.74 mg/L, 1.28 mg/L and 0.01 mg/L, for BOD, N and P, respectively.

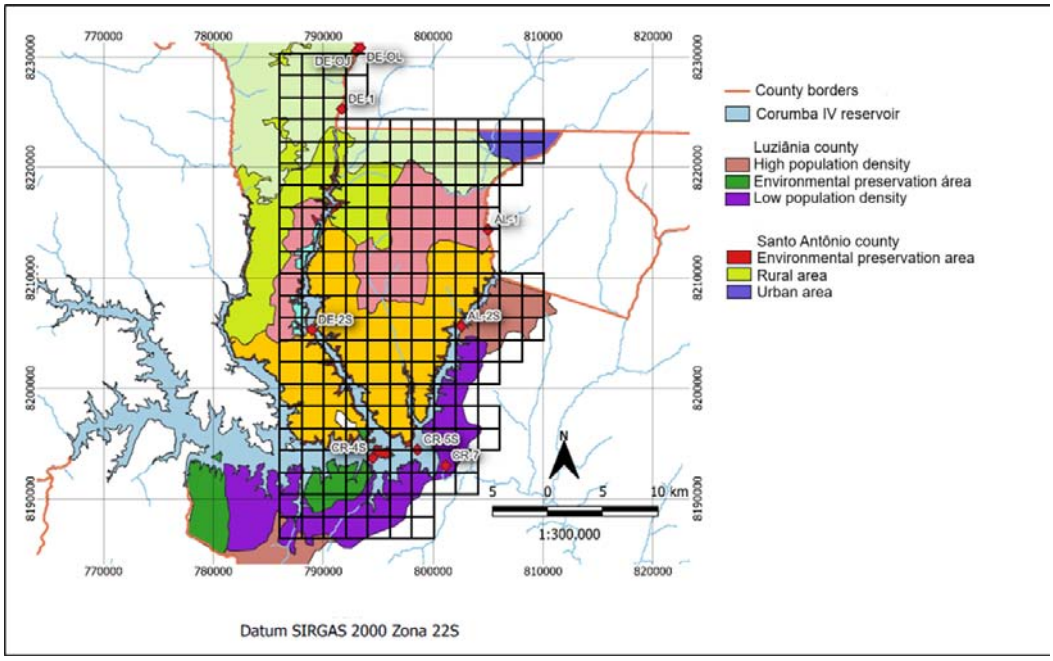


Figure 1. Study area.

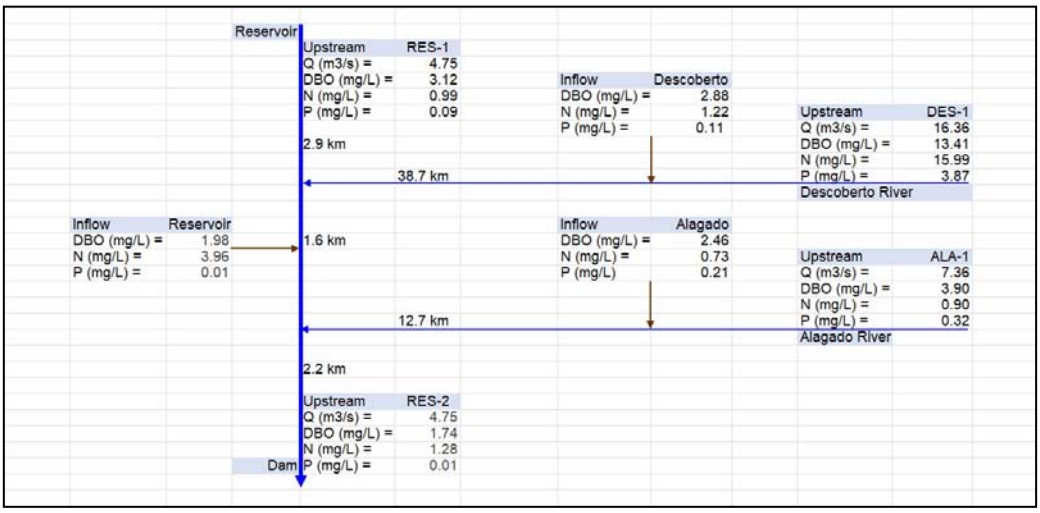


Figure 2. Parameters estimated by the Qual-UFMG model.

Acknowledgments: This research is financed by Corumbá Concessões S/A and ANEEL, as part of the project ANEEL PD-02262-0020/2022, which is executed by Fundeb and Farol Consulting.

References

Qian Y, Sun L, Chen D, et al. (2021) The response of the migration of non-point source pollution to land use change in a typical small watershed in a semi-urbanized area. Science of the Total Environment 785: 147387. https://doi.org/10.1016/j.scitotenv.2021.147387

Von Sperling M (2014) Introdução à qualidade das águas e ao tratamento de esgotos. 4a.ed. Universidade Federal de Minas Gerais, Belo Horizonte.

Zhang H, Huang GH (2011) Assessment of non-point source pollution using a spatial multicriteria analysis approach. Ecological Modelling 222(2): 313-321. https://doi.org/10.1016/j.ecolmodel.2009.12.011

Zhong S, Chen F, Xie D, et al. (2020) A three-dimensional and multi-source integrated technology system for controlling rural non-point source pollution in the Three Gorges Reservoir Area, China. Journal of Cleaner Production 272: 122579. https://doi.org/10.1016/j.jclepro.2020.122579

'Prove to me it's my molecule of nitrogen': Nitrate-sensing technologies and water quality engagement with Australian farmers

A.M. Davis[1*], L. Buono[1], T. Webster[2]
[1] TropWATER, James Cook University, Townsville, Australia,
[2] Commonwealth Scientific and Industrial Research Organisation, Land and Water
* e-mail: aaron.davis@jcu.edu.au

Introduction

Management of diffuse nutrient pollution from agricultural catchments remains an ongoing water resource management challenge in northern Australia's Great Barrier Reef (GBR) catchment area (Waterhouse et al. 2024). Catchment losses of dissolved inorganic nitrogen (DIN) from intensive agriculture specifically remains a key risk to the long-term resilience of the GBR. Decades of investment by different levels of government, farming industries and farmers themselves, have produced only modest progress toward to end-of-catchment DIN reduction targets to the GBR lagoon. Policy and science engagement with key agricultural industries face numerous, long-standing challenges such as stakeholder distrust of 'top-down', government-driven water quality monitoring programs; long reporting timeframes; often large 'end-of-catchment' monitoring scales (encompassing hundreds of farms); limited accessibility of water quality data; and an emphasis on catchment water quality models in reporting, communications and engagement. A common refrain from farmers is 'prove to me it's my molecule of nitrogen, and I'll do something about it'.

With nutrient sensor technology maturing rapidly, provision of accurate, high-frequency observations has emerged as an increasingly attractive and effective tool for water quality monitoring and associated water resource management decisions across multiple spatial scales (Pellerin et. al. 2016). Here we report on several years of recent experiences in use of fine-scale, nitrate-sensing technology networks as an engagement tool with sugarcane farmers, the dominant intensively cultivated crop in GBR catchments.

Materials and methods

Fine-scale water quality monitoring programs co-designed with key agricultural commodities were rolled out in several Reef Plan 2050 'high priority' catchments, with the aim of defining the water quality signal of multiple, discrete land uses such as intensive agriculture (sugarcane and bananas), conservation lands (national parks), and urban areas. Long-term, continuous monitoring over several years was conducted using *in situ*, commercially available optical nitrate sensors, with monitoring stations emphasising rapid on-ground installation and small infrastructure footprints (Figure 1). Data were recorded every 15 minutes and transmitted to online environmental data management portals. A purpose-built, bespoke 'web app' (1622.farm) provided capacity to communicate sensed nitrate-N and stream height data in a form understandable and accessible to farmers in near 'real time'. Qualitative social research was conducted in several catchments with stakeholders (farmers, advisors and researchers) both directly involved, and external, to the process, to appraise attitudinal and behavioural changes (Fielke et al. 2022).

Results and concluding remarks

Provision of very local, targeted, sub-catchment water quality data, in near-real time, has proven a valuable complement to historical catchment water quality monitoring approaches, alleviating many of the historical impediments to meaningful water quality engagement with farming stakeholders (Table 1). Social analyses of several programs indicated having near real time and visual evidence in the 'data' (e.g. nitrate-nitrogen readings, rainfall data and river height at various points in their catchment) led to the articulation of farmer trust and confidence in the water quality science as partners in catchment water quality monitoring. This confidence in interpretation of 'trustworthy' scientific information created the opportunity

for involved growers to share and discuss experiences with neighbours, enabling peer-to-peer leadership and, in some cases, contributing to on-farm practice changes.



Figure 1. Streambank monitoring installation (a) and 1622.farm 'webapp' in use (b).

Social research did, however, also emphasise the need for considered program co-design with catchment stakeholders, the need for social capital, trust frameworks and co-generation of knowledge, and an ongoing investment in science communication to maximise extension-engagement impact (Fielke et al. 2022). There were also a range of emergent challenges associated with these new technologies relating to aspects of QA/QC, data management and archiving, and immediate public availability of collected data (Table 1). Translating this new quantum of sensor data, into a form accessible, coherent and understandable to target stakeholders also represents a significant challenge, requiring input from diverse disciplines (water quality, sensor-telemetry, ICT, user experience etc.). In an increasingly contested science-policy landscape, sensor technologies can provide a powerful tool in facilitating more meaningful engagement with agricultural industries on critical water sustainability issues.

Table 1. Some of the emergent advantages/challenges of nitrate-sensing technologies and real-time water quality data presentation in GBR catchment farming stakeholder engagement programs.

Advantages	Challenges
- sensor accuracy and detection limits often comparable to laboratory alternatives	- QA/QC and catchment stakeholder anonymity-confidentiality considerations around fine-scale data, collected and publicly available in real-time
- capacity for near real-time visualisation of local water quality dynamics to stakeholders	- substantial data management and storage requirements
- industry responsiveness in identification with stakeholders of specific farming practices contributing to DIN losses	- ongoing upkeep requirements to maintain sensor performance easy to underestimate
- capacity for clear visualisation of water quality-land use change relationships (i.e., rainforest vs. sugarcane) in nested monitoring designs	- initial sensor costs (although sensor data progressively become less expensive per data point as sampling of frequency increase)
- high frequency sensor technologies very 'fit-for-purpose' in monitoring the often-transient water quality fluctuations characteristic of GBR sugarcane catchments	-site water quality 'matrix' effects on optical sensor performance (dissolved organics, turbidity, salinity etc.)

Acknowledgments: This project received funding from the Australian Government's National Environmental Science Program and GBRF Reef Trust Program and the CSIRO Digiscape Future Science Platform.

References

Fielke S, Taylor BM, Coggan A, Jakku E, Davis AM, Thorburn PJ, Webster AJ, Smart JCR (2022) Understanding power, social capital and trust alongside near real-time water quality monitoring and technological development collaboration, Journal of Rural Studies 92: 120-131

Pellerin BA, Stauffer BA, Young DA, Sullivan DJ, Bricker SB, Walbridge MR, Clyde GA Jr, Shaw DM (2016) Emerging Tools for Continuous Nutrient Monitoring Networks: Sensors Advancing Science and Water Resources Protection. Journal of the American Water Resources Association 52: 993–1008. https://doi.org/10.1111/1752-1688.12386

Waterhouse J et al. (2024) 2022 Scientific Consensus Statement: Conclusions. In Waterhouse J, Pineda M-C, Sambrook K (Eds) 2022 Scientific Consensus Statement on land-based impacts on Great Barrier Reef water quality and ecosystem condition. Commonwealth of Australia and Queensland Government

Storage of drinking water in underground concrete tanks: The case of Tajoura, Libya

B. Brika*, N. Elaziby, M. Orhuma
Libyan Advanced Center for Chemical Analysis, Libyan Authority for Scientific Research, Tripoli, Libya
** e-mail: bashirforlibya@gmail.com*

Introduction

The municipal water supply is inaccessible to 90% of the Tajoura community. Residents are therefore compelled to either collect, transport and store their water for cooking and drinking or purchase bottled water [Brika et al. 2018]. Furthermore, the city of Tajoura lacks a sewage infrastructure, which means there are no systems in place to manage waste or recycle wastewater for purposes like agriculture. Untreated urban wastewater is the main cause of groundwater contamination. This absence of services not only creates difficulties for the residents but also poses significant health hazards. Due to the lack of a municipal sanitation system, the residents of Tajoura have been compelled to establish their sanitation solutions, which include constructing black wells.

Although the number of people who depend on drinking water delivery trucks is not well known, several Libyan cities, including Tajoura, use this option to serve their citizens who are not linked to the public distribution system. Approximately 81% of locals buy drinking water in bottles or via truck delivery from specialized water purification [Brika et al. 2018]. Furthermore, about 54% of Tajoura households have their underground water storage tanks, which are known locally as Majin or Faskia [Figures 1 a, b]. The study aimed to investigate the chemical and microbial quality of water of households stored in underground tanks in Tajoura.

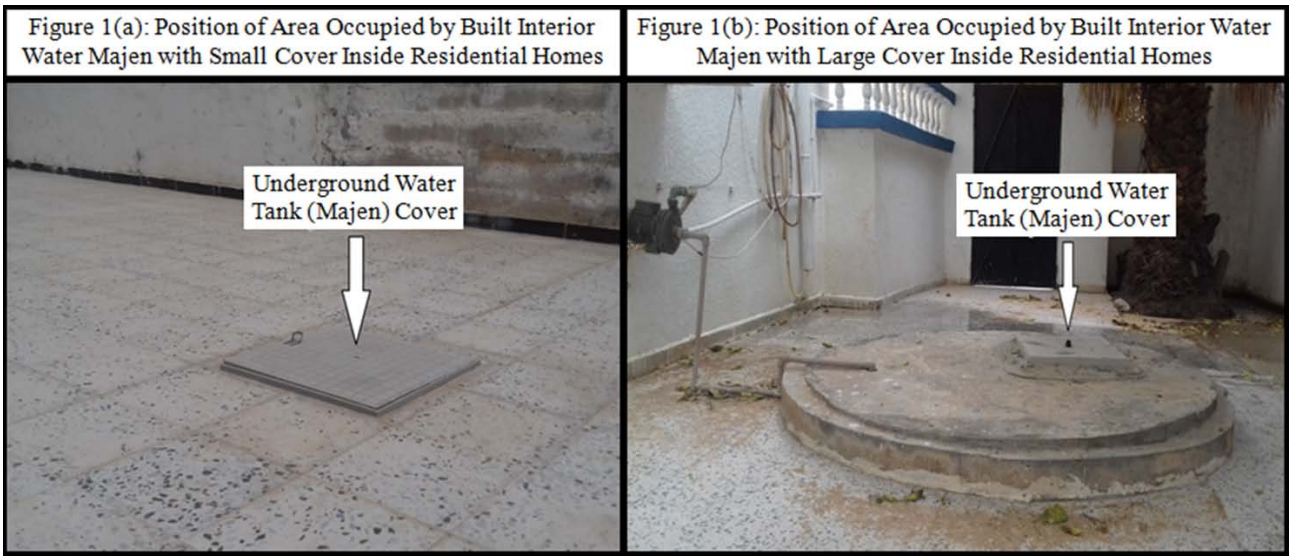


Figure 1. Positions (a) and (b) of water Majens inside residential home

Materials and methods

Between April and November 2019, fifteen water samples were taken from about eight districts in the city of Tajoura. Face-to-face interviews were used to collect data on water collection, use, and storage habits. Taps that were attached to the tank were used to collect samples. Before the sample was taken, the samples were transported to a nearby laboratory for analysis.

Conductivity, total dissolved solids (TDS), sodium (Na+), potassium (K^+), calcium (Ca^{2+}), nitrate ($NO3^-$). Samples for bacteriological analysis were gathered in sterile, labelled glass bottles and were analysed

within four hours of collection. The testing for total coliforms and E. coli was conducted using membrane filtration and m-coli blue 24 (HachR, Loveland, CO), which facilitates the simultaneous detection of E. coli and total coliforms [USEPA, 2002, USEPA. 2004].

Results and concluding remarks

One of the most important chemical indicators of drinking water quality for consumers is its taste, which results from the amount of TDS in water [Fhelboom and Brika 2020, Sarda and Sadgir 2015]. Based on that, the findings of this study indicated that the TDS in drinking water stored in underground tanks varied from 103 to 546 mg/l. Every sample tested was determined to be within the acceptable standard limit. Furthermore, because the underground tanks are situated in a convenient depression and feature walls constructed from concrete and bricks, there is a possibility that some metals may leach from the composition of the wall materials into the water, ultimately leading to a rise in TDS. This could be a contributing factor to the increase in TDS observed in water that has been stored for extended periods. To prevent the release of materials from occurring again, it is advisable to coat the walls with a layer of non-soluble plastic insulation.

Results indicated that the distance from the underground tank to the black well (pit latrine) in one house typically lies between 8 and 30 meters. This could lead to microbial transfer from the black sewage well to the underground tank if the underground tank is not constructed according to certain standards. Additionally, the risk of bacteriological contamination may be increased if the underground storage tanks store drinking water for long periods (more than seven months).

Because of the unavailability of drinking water supplies, rising population, along insufficient water service infrastructure, it was unavoidable that families in certain regions of rural Tripoli would construct underground tanks for the storage of drinking water.

Based on the findings of this study, even when no chemicals were added for disinfection, E. coli counts were absent from underground storage tanks that were cleaned twice or more annually. However, to maintain the highest degree of drinking water quality, proper disinfection is necessary. Additionally, this study offered proof that as the water is transported from farms or a brackish water desalination facility to underground storage tanks via tanker trucks, E. coli and total coliform counts in water may arise either from the initial water source or the transport vehicle.

References

Brika B, Ghuila H, Mosbah H (2018), Municipal water shortage and related water issues in the city of Tajoura: A case study to raise public awareness. Water Conservation and Management, 2(2): 31-33.

Fhelboom R and Brika B (2020), Bottled water sold in the Tripoli markets: Challenges and shortcomings. Water Conservation and Management, 4(2): 65-69.

Sarda, P and Sadgir P (2015), Assessment of multi parameters of water quality in surface water bodies-A review, International Journal for Research in Applied Science & Engineering Technology (IJRASET), 331-336.

US EPA, 2002 “Method 1603: Escherichia coli (E. coli) in Water by Membrane Filtration Using Modified Membrane-Thermotolerant Escherichia coli Agar (Modified m- TEC),” US EPA Office of Water, Washington DC, 2002.

US EPA, 2004. Results of the Interlaboratory Validation of EPA Method 1603 (modified mTEC) for E. coli in Wastewater Effluent. EPA-821-R-04-009. December 2004.

Numerical study of the formation of water pollution zones from various industrial emissions

A. Issakhov*, A. Sabyrkulova, A. Abylkassymova
Kazakh British Technical University, Almaty, Republic of Kazakhstan
** e-mail: alibek.issakhov@gmail.com*

Introduction

Pollution of rivers by industrial emissions poses a serious environmental and social threat, especially in the context of growing production and expansion of industrial zones. Water is a key resource that maintains healthy ecosystems and human well-being, and its pollution not only reduces the quality of life, but also threatens biodiversity, sustainable agriculture and the economy. Hazardous substances such as benzene often enter rivers from industrial sources, causing toxic effects on living organisms and creating long-term risks to human health. This problem is especially significant for transboundary water systems such as the Ural River, where the impact on adjacent ecosystems and bioresources of the Caspian Sea affects the interests of several countries.

Numerical modeling methods are widely used to assess the impacts of pollution and develop effective treatment strategies. In this context, the use of computational fluid dynamics (CFD) allows for a detailed analysis of pollutant dispersion and impacts on water resources, which supports water quality management and environmental safety efforts. Examples of such studies demonstrate how numerical models help understand complex pollution processes and toxic substance dispersion (Wei et al. 2023; Amiri et al. 2019; Liu et al. 2021; Bai et al., 2023; Montazeri et al., 2022).

This study analyzes the impact of industrial benzene pollution on water quality in the Ural River and the adjacent Caspian Sea, Kazakhstan. In particular, it aims to develop methods for assessing and predicting pollution using CFD modeling that takes into account the real coastal contour. Determining the impact of hydrodynamic and natural conditions on benzene transfer processes in the river and in the lake. To achieve the stated objectives, a non-stationary numerical model based on the Navier-Stokes equations and the concentration equation was developed for the Ural River, which flows into the Caspian Sea. The Navier-Stokes equations describe the movement of a fluid taking into account such factors as flow velocity and viscosity, while the concentration equation allows modeling the spread of pollutants in a reservoir.

Materials and methods

A two-dimensional system of Navier-Stokes equations is used to model the spread of oil products that form a film on the surface of water due to their lower density compared to water. The model takes into account equations for velocity, concentration and temperature. The flow is considered incompressible, non-stationary and turbulent, which allows for the complex dynamics of mixing. A turbulent k-ω SST model is used to close the system of Reynolds-averaged equations.

$$\frac{\partial u_i}{\partial x_i} = 0 \tag{1}$$

$$\frac{\partial u_i}{\partial t} + \frac{\partial (\rho u_i u_j)}{\partial x_j} = \frac{\partial \left(-\rho \overline{u_i' u_j'}\right)}{\partial x_j} - \frac{\partial P}{\partial x_i} + \frac{\partial}{\partial x_j}\left(\mu \left(\frac{\partial u_i}{\partial x_j} + \frac{\partial u_j}{\partial x_i}\right)\right) \tag{2}$$

$$\frac{\partial T}{\partial t} + \frac{\partial (\rho u_j T)}{\partial x_j} = \frac{\partial \left(-\rho \overline{u_j' T'}\right)}{\partial x_j} + \frac{\partial}{\partial x_j}\left(D \frac{\partial T}{\partial x_j}\right) \tag{3}$$

$$\frac{\partial C}{\partial t} + \frac{\partial (\rho u_j C)}{\partial x_j} = \frac{\partial \left(-\rho \overline{u_j' C'}\right)}{\partial x_j} + \frac{\partial}{\partial x_j}\left(D \frac{\partial C}{\partial x_j}\right) \tag{4}$$

where u – is the mean velocity vector, u_i' – are the turbulent velocity fluctuations, μ is the viscosity, ρ is the density, P is the fluid pressure, D is the diffusion coefficient, $\overline{u_i' u_j'}$ is the Reynolds stress tensor, $\overline{u_j' T'}$ – are the turbulent heat fluxes, $\overline{u_j' C'}$ are the turbulent concentration fluctuations.

This study focuses on the spread of benzene pollution in the Ural River and the Caspian Sea, originating from industrial discharges occurring near the mouth of the river, in the immediate vicinity of the city of Atyrau, known for its oil industry. The study covers the northern part of the Caspian Sea, where the impact of such spills may be most significant. The Ural River originates on the slopes of the Uraltau Range in the Southern Ural Mountains, Russia. The river is 2428 km long and flows through the territories of two countries, Russia and Kazakhstan, making it the third longest river in the region. The Ural River plays an important role in the ecosystem and is a significant source of fresh water for the region. It is used for shipping, agricultural irrigation, and water supply.

Results and concluding remarks

Numerical modeling by CFD allows us to estimate how each emission rate affects the distribution of pollutant concentration in the river. The modeling covers a period of 12 hours, which is sufficient to analyze the short-term and medium-term effects of the emission. In the initial stages, from the moment of emission to 4 hours, a predominantly linear spread of the pollutant along the river can be seen. In this case, the main movement of benzene is directed downstream, in the western direction. The contour plots (Figure 1), presented for different discharge rates, clearly show the effect of velocity on the distribution of benzene concentration. The study demonstrates the importance of modeling the process of pollutant spreading in rivers for assessing environmental risks and developing effective emission management strategies. The results show that an increase in the emission rate significantly affects the nature of the spread and concentration of benzene in water. Numerical modeling confirms the need to implement measures to control the velocity and frequency of emissions, as well as to monitor and protect localized zones subject to high pollution. These results serve as a basis for developing environmentally friendly emission management methods and improving water quality in water resources.

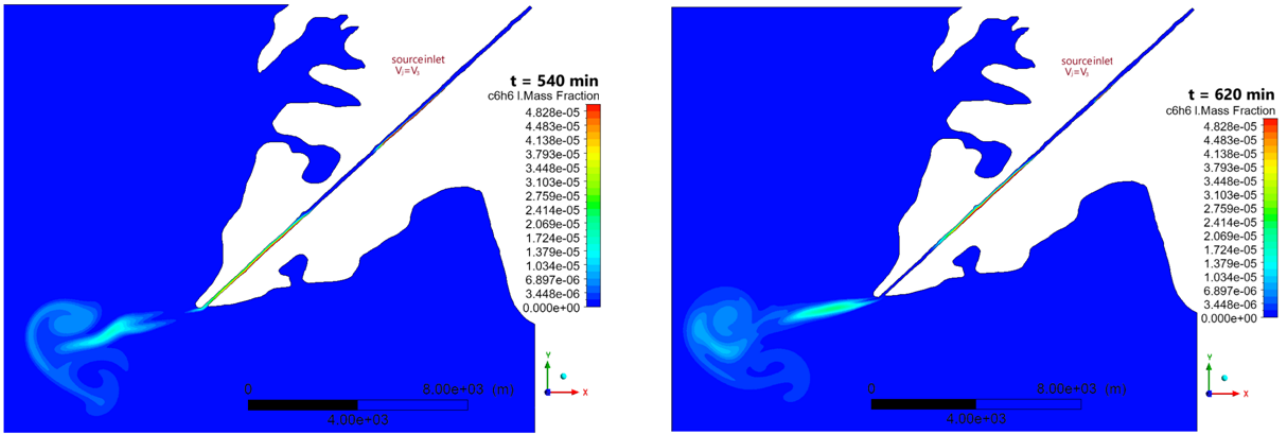


Figure 1. Distribution of concentration in different time intervals.

Acknowledgments: This work is supported by grant from the Ministry of Science and Higher Education of the Republic of Kazakhstan (AP23489948).

References

Amiri S, Mazaheri M, Samani JMV. (2019) Introducing a general framework for pollution source identification in surface water resources (theory and application). Journal of Environmental Management. 248:109281. doi:10.1016/j.jenvman.2019.109281

Bai Y, Zhao Y, Huang L, Shen D, Sun G. (2023) Numerical simulation of velocity distribution and pollution retention in flexible submerged vegetated channel. Journal of Hydrology. 626:130265. doi:10.1016/j.jhydrol.2023.130265

Liu H, Chen J, Zhang L, Sun K, Cao W. (2021) Simulation effects of clean water corridor technology on the control of non-point source pollution in the Paihe River basin, Chaohu lake. Environmental Science and Pollution Research. 28(18):23534-23546. doi:10.1007/s11356-020-12274-x

Montazeri A, Abedini A, Aminzadeh M. (2022) Numerical investigation of pollution transport around a single non-submerged spur dike. Journal of Contaminant Hydrology. 248:104018. doi:10.1016/j.jconhyd.2022.104018

Wei S, Fu D, Wang D, Yu G, Luo Y, Xu H. (2023) Tracer study of CDOM for nitrogen and phosphorus pollution in the offshore Leizhou Peninsula, China. Ecological Indicators. 148:110019. doi:10.1016/j.ecolind.2023.110019

Numerical investigation of air and air-water jets in two-layer stratified flow

E. Budak Cotel
Civil Engineering Department, METU, Ankara, Turkiye
e-mail: ezbudak@metu.edu.tr

Introduction

Submerged jets which can be water, air, or air-water mixtures play a crucial role in various environmental and engineering applications. These jets interact with different ambient conditions such as stagnant water, stratified flow, or crossflow. Their behavior is influenced by multiple factors as jet momentum, buoyancy effects, and the ambient fluid properties.

One of the fundamental studies on submerged water jets in crossflow was conducted by Hirst (1972) and focused on understanding jet behavior in crossflows. Later, Maxwell et al. (1975) extended this analysis to include both stratified and non-stratified flow environments. Several studies have investigated the dynamics of air jets and air-water jets in different ambient conditions (e.g., Zhang & Zhang (2022), Dong et al. (2020). and others). Despite the extensive research on submerged jets, relatively few studies have specifically examined the jet behavior in two-layer stratified environments. This study aims to address this gap by analyzing the penetration characteristics of submerged air jets and air-water jets in a two-layer stratified flow. This study is conducted numerically with simulations performed using the OpenFOAM software. Understanding how stratification thickness and jet velocity influence penetration behavior is crucial for applications such as aeration systems and industrial fluid mixing.

Materials and methods

The simulations in this study were conducted using OpenFOAM, an open-source computational fluid dynamics software. The interMixingFoam solver is employed that is for multiphase flow with phase mixing and volume of fluid method. For turbulence modeling, the k-ω SST RANS model is selected due to its ability to accurately capture flow separation, shear layers, and near-wall effects. The k-ω SST model combines the advantages of the k-ε RANS and k-ω RANS models. This makes it a suitable choice for stratified flows where turbulence dynamics vary across different regions of the flow domain.

Velocity-inlet boundary conditions are applied for the hot and cold inlets, as well as for the jet inlet. The total pressure at the top boundary is specified as zero. zeroGradient boundary conditions are applied at the outlet for both pressure and velocity. No-slip boundary conditions and wall functions are used at the walls. Alpha fractions are specified to distinguish between different jet compositions. For example, for pure air, it is set as 1 at the jet inlet, while for air-water jets, air and water are defined with volume fractions of 0.5 each. A plate is inserted between the hot and cold inlets and the outlet to prevent direct mixing of the inlet and outlet flows. The simulations are performed in 2D domain. A mesh independence study is conducted, and based on the results, the total number of mesh elements is determined as 153257. The domain dimensions and patch names are provided in Figure 1.

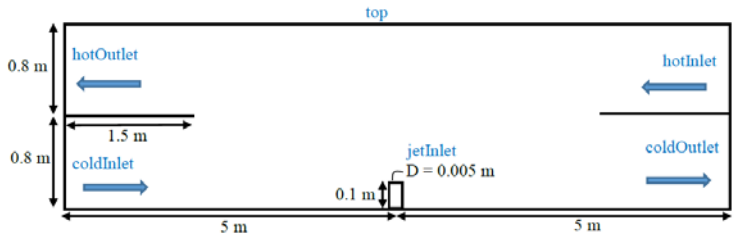


Figure 1. A representative sketch showing the model dimensions and patch names.

Results and concluding remarks

The validation of the conducted model was performed using submerged water jets in crossflow with the study of Hirst (1972). After successful validation, the study proceeded to analyze the penetration of air and air-water jets into a two-layer stratified flow under different stratification conditions. Before analyzing the jet behavior, stratification is first established in the simulations. The stratification thickness is observed to vary with different density and velocity differences between the hot and cold layers. As density and velocity differences increased, the stratification thickness also increased which leads to decrease in the Richardson number. A lower Richardson number corresponds to stronger stratification, making jet penetration more difficult. This trend is demonstrated in Figure 2.

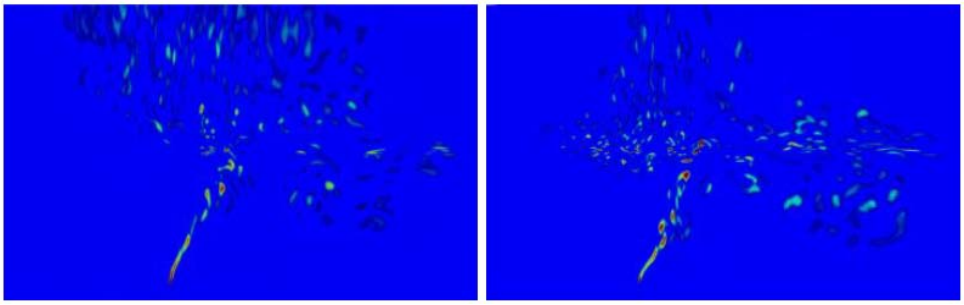


Figure 2 Air penetration figures for higher (left) and lower (right) density differences.

Air jets tend to rise more easily in crossflow environments compared to water jets in the literature. The simulations in this study confirm this behavior, showing that the air phase penetrates through the stratified layer more effectively than water jets. Furthermore, it was observed that air-water jets travel through the ambient fluid more quickly than pure water jets. This behavior is illustrated in a figure that compares penetration patterns for different jet compositions.

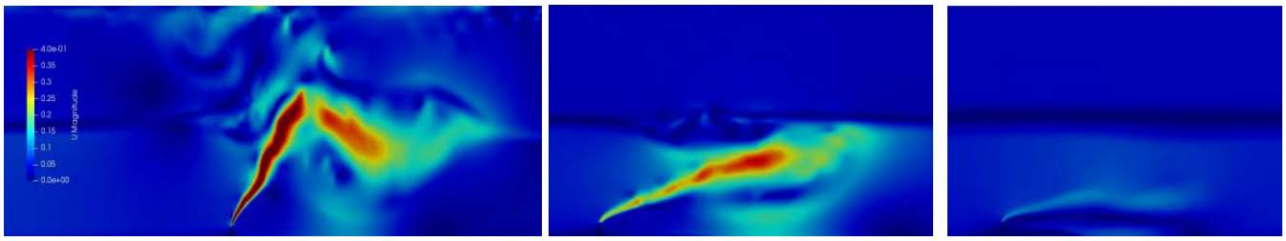


Figure 3. Pure air jet (left), air-water mixture jet (middle) and pure water jet (right) at the same ambient condition.

These findings show how different jet compositions interact with stratified flows and contribute to a better understanding of jet penetration mechanisms under varying stratification conditions.

References

Dong, P., Lu, B., Gong, S., & Cheng, D. (2020). Experimental study of submerged gas jets in liquid cross flow. Experimental Thermal and Fluid Science, 112. https://doi.org/10.1016/j.expthermflusci.2019.109998

Hirst, E. (1972). Buoyant Jets with Three-Dimensional Trajectories. Journal of the Hydraulics Division, 98(11).

Maxwell, W. H. C., Holley, E. R., Lin, C.-Y., & Tekeli, S. (1975). Study of Stratified Overflows and Underflows. In University of Illinois Water Resources Center (Issue 98).

Zhang, H., & Zhang, W. (2022). Numerical simulation of bubbly jets in crossflow using OpenFOAM. Physics of Fluids, 34(12). https://doi.org/10.1063/5.0116853

Bacterial communities of water and sediment of an artificial reservoir in Mexico: their metabolic inference and biotechnological potential

J. Cordovillo-Armijo[1], M.J. Aguilar-Méndez[2], N.G. Rojas-Avelizapa[1], A.M. Rivas-Castillo[1*]
[1] Centro de Investigación en Ciencia Aplicada y Tecnología Avanzada Unidad Querétaro, Instituto Politécnico Nacional, Querétaro, México
[2] Unidad Profesional Interdisciplinaria de Ingeniería Campus Guanajuato, Instituto Politécnico Nacional, Guanajuato, México
* e-mail: amrivasc@ipn.mx

Introduction

Aquatic ecosystems of natural origin have been widely explored worldwide. However, artificial ones, have awakened interest only in recent years; specifically, in developing countries like Mexico, artificial aquatic systems have been scarcely explored despite their importance for socioeconomic activities, and the few studies reported are focused on monitoring the quality of water and sediments, and the presence of pollutants (Rubio-Arias et al. 2013). Thus, physicochemical techniques have been mainly used to study these environments, although the incorporation of next-generation sequencing (NGS) approaches, like metagenomics, has allowed the exploration of the microbial communities therein (Zhou et al. 2023). Particularly, the study of bacterial communities from environmental systems is crucial for understanding ecosystem functions, biodiversity, microbial succession, and adaptation mechanisms. Therefore, the present work focused on analyzing the bacterial communities of water and sediment from an artificial reservoir by 16S rRNA gene sequencing to reveal their structure and diversity and, even more, to unravel their metabolic pathways and potential biotechnological capabilities presumably linked to the environmental conditions of the ecosystem and that may be useful to envision future sustainable processes.

Materials and methods

Water and sediment samples were collected in September 2023 from Santa Catarina Dam, Querétaro, Mexico (820°48'8"N, 100 27'2"W), at 40 cm depth from the water surface and from superficial sediment. Water temperature, pH, and electrical conductivity were determined *in situ* using a portable multiparameter meter, while total phosphorus and total nitrogen were analyzed following Mexican standards. Conversely, the sediment sample was dried and ground using a mortar and pestle, and subsequently sieved with a #35 mesh for further analysis of pH, total phosphorus, total nitrogen, and organic matter content, following also Mexican regulations. DNA extraction was performed with the ZymoBIOMICS DNA Miniprep kit and quantified using a Nanodrop (2000c, Thermo Fisher Scientific) (Simbolo et al. 2013). Sequencing services and library preparation were provided by Zymo Research®, using an Illumina NextSeq sequencer with the amplification of the V3-V4 region of 16S rRNA. The sequences were processed with Quantitative Insights in Microbial Ecology (QIIME 2 v.2024.2) (Callahan et al. 2016). DADA2 was used in the steps of trimming, removal of PCR adaptors and chimeras, and noise elimination, to obtain the Amplicon Sequence Variants (ASVs). Taxonomic classification was performed using Silva 138 SSURef NR99 database, both the pre-trained database of full-length sequences and the taxonomy, to guarantee 99% accuracy. Additionally, the Alpha (α) diversity index was calculated with QIIME 2, determining α diversity values by Shannon and Simpson indices. Additionally, the metabolic profiles were predicted using Phylogenetic Investigation of Communities by Reconstruction of Unobserved States (PICRUSt) v2.5.3, normalizing the data before processing and using the automatic script metagenome_pipeline.py with MetaCyc and KEGG databases in a non-stratified manner to allow a global view of the metabolic functions (Douglas et al. 2020). The most abundant of these metabolic functions were determined and analyzed, and those pathways potentially related to biotechnological applications were identified. The metabolic pathway

plots were performed using the statistical test G-test (w/Yates) + Fisher´s with the program Statistical Analysis of Taxonomic and Functional Profiles (STAMP v2.1.3).

Results and concluding remarks

The water presented a pH of 9.52, a temperature of 23.89°C, an electrical conductivity of 750 µS/cm, and total nitrogen and total phosphorus of 58.10 mg/L and 0.61 mg/L, respectively. The sediment showed a pH of 7.82, total nitrogen of 840 mg/Kg, available phosphorus of 66.61 mg/Kg, and an organic matter content of 68.63%. The alkaline level of water, together with the nutrients and temperature, favor cyanobacterial blooms commonly occurring in eutrophic or hypereutrophic water bodies (WHO, 1998). In sediment, the pH level remained close to a neutral value possibly due to the proper buffering mechanisms of sediments (Herlihy & Mills, 1986). The high organic matter content is considered a primary factor influencing nutrient exchange and structures of prokaryotic communities. Besides, the metagenomic analysis showed a total of 28 bacterial phyla distributed 7.14% in water and 53.57% in sediment, whereas both samples shared 39.29%. The top five most abundant phyla in both water and sediment were Proteobacteria (29.01% and 14.82%), Bacteroidota (22.32% and 9.77%), Chloroflexi (3.61% and 19.31%), Actinobacteriota (18.61% and 4.15%) and Planctomycetota (9.44% and 2.87%). Moreover, the Shannon and Simpson indices of the samples revealed a high bacterial diversity prevailing in sediments, and dominance of specific bacterial groups in the communities. Regarding the metabolic inference, the most abundant metabolic hierarchy in both communities was the *Generation of precursor metabolites and energy,* that contained the Aerobic respiration I (cytochrome c) pathway, which is associated with the phyla Proteobacteria, Actinobacteria, and Chloroflexi, found in surface layers of waters and sediments, of which their energy generation routes can be related to aerobic mechanisms (Graças et al. 2011). The identified pathways with biotechnological potential are related to the biosynthesis of pharmaceuticals and the degradation of toxic organic compounds, reflecting the polluted status of the system and the bacterial adaptative mechanisms. The findings of the present work set precedence on the use of metagenomic analysis to decipher the functional metabolic profiles and potential biotechnological applications of bacterial communities from polluted water bodies, for further envisioning sustainable processes.

Acknowledgments: The authors deeply thank the Centro de Investigación y Desarrollo de Tecnología Digital of the Instituto Politécnico Nacional de México (CITEDI IPN) for the computing resources needed for this study. The project was supported by the funds granted to Projects SIP No. 20231513 and 20241515 of the Instituto Politécnico Nacional de México.

References

Callahan BJ, McMurdie PJ, Rosen MJ, Han AW, Johnson AW, Holmes SP (2016) Dada2: High-resolution sample inference from Illumina amplicon data. Nature Methods 13(7): 581-583. https://doi.org/10.1038/nmeth.3869

Douglas GM, Maffei VJ, Zaneveld, JR, Yurgel SN, Brown JR, Taylor CM, Huttenhower C, Langille MG (2020) PICRUSt2 for prediction of metagenome functions. Nature Biotechnology 38(6): 685–688. https://doi.org/10.1038/s41587-020-0548-6

Graças DA, Miranda PR, Baraúna RA, McCulloch JA, Ghilardi R, Schneider MP, Silva A (2011) Microbial Diversity of an Anoxic Zone of a Hydroelectric Power Station Reservoir in Brazilian Amazonia. Microbial Ecology 62(4): 853-861. https://doi.org/10.1007/s00248-011-9906-8

Herlihy AT, Mills AL (1986) The pH regime of sediments underlying acidified waters. Biogeochemistry 2(1): 377-381.

Rubio-Arias H, Ochoa-Rivero JM, Quintana RM, Saucedo-Teran R, Ortiz-Delgado RC, Rey-Burciaga NI, Espinoza-Prieto JR (2013) Development of a Water Quality Index (WQI) of an Artificial Aquatic Ecosystem in Mexico. Journal of Environmental Protection 04(11): 1296–1306. https://doi.org/10.4236/jep.2013.411151

Simbolo M, Gottardi M, Corbo V, Fassan M, Mafficini A, Malpeli G, Lawlor RT, Scarpa A (2013) DNA Qualification Workflow for Next Generation Sequencing of Histopathological Samples. PLoS ONE 8(6): 1-8 https://doi.org/10.1371/journal.pone.0062692

WHO (1998) Guidelines for drinking-water quality. World Health Organization, Geneva

Zhou X, Lennon JT, Lu X, Ruan A (2023) Anthropogenic activities mediate stratification and stability of microbial communities in freshwater sediments. Microbiome 11(1): 1–19. https://doi.org/10.1186/s40168-023-01612-z

Circular economy and biodiversity in the treatment of wastewater using an industrial waste - LIFE RENATURWAT

M. Añó*, P. Almenar, J. Macián-Cervera
Empresa Mixta Valenciana de Agua, S.A.(EMIVASA) - Grupo Global Omnium, València, Spain
**miaso@globalomnium.com*

Introduction

Due to the insufficient water resources on the Mediterranean basin and the probable intensification of extreme events caused by climate change, the generation of water resources from non-conventional sources in a sustainable manner is an option that should become a priority. Treated wastewater is a water resource that with appropriate post-treatment can be suitable for maintaining the environmental quality of rivers and wetlands or be used for productive activities such as agricultural uses.

Returning water to nature in conditions similar to those in which it reaches us is vital to promote its reuse and help maintain biodiversity. In this sense, the European project LIFE RENATURWAT- LIFE19 ENV/ES/000197, presented in this work, aims to demonstrate that the integration of circular economy and biodiversity is possible in obtaining reclaimed water by combining Nature Based Solutions (NBS) and industrial waste from the water purification process.

Materials and methods

When producing drinking water, one of the main wastes is the sludge from the physical-chemical treatment of water, which is sent to landfills. The intrinsic characteristic of these "hydroxide sludges" is their high concentration of aluminium (7-17%), originating from the coagulation process, where aluminium- based coagulants are added to remove suspended particles.

The concentration of total aluminium opens the way for recovery to obtain a "low-cost active substrate" that can be applied in NBS such as artificial wetlands, helping to eliminate nutrients such as phosphorous or pollutants such as pesticides, drugs or metals (Benlalla et al. 2015). In this way, the project proposes to use this waste, previously conditioned, as the basis for constructed wetlands that function as a refining treatment at the outlet of small Wastewater Treatment Plants (WWTP). The aim is to improve the performance of phosphorus removal from wastewater effluent by replacing part of the classic granular medium (gravel and sand) with dehydrated sludge, improving the quality of treated water and thus optimising the useful life of the waste.

In the generation of a low-cost material to create active beds in NBS that is integrated within the concept of circular economy, the characteristics of the material must be studied in depth, not only in the elimination of phosphorus, but also its microporosity, its hydraulic operation with respect to the correct granulometry that determines the load losses and the clogging of the filtering bed itself.

The line followed up involves carrying out a study with filter columns in the laboratory to analyse the phosphorus adsorption capacity and the percentage of saturation of the substrate over time and at different particle sizes and phosphorus concentrations, satisfying the hydraulic and chemical needs. The solution proposed by the project consists of two types of constructed wetlands in combination. The first is a vertical flow constructed wetland with active substrate as a filter medium. The second is a free-flowing surface constructed wetland. This results in a wastewater effluent with a very low phosphorus concentration, without additional consumption of reagents (aluminium salts), addressing one of the main problems faced by wastewater treatment plant managers, which is the eutrophication of the natural environment and compliance with phosphorus discharge limits.

Within the framework of this project, two case studies have been deployed, one in the Valencian town of Carrícola, and the other in the Los Monasterios housing development (Puçol), which act as tertiary treatment for the two existing eco-treatment plants in these municipalities.

The RENATURWAT project is in its last year of development and, during this time, 60 m2 of wetland and two lagoons have been constructed in the Los Monasterios urbanisation and two 20 m2 wetlands in the town of Carrícola.



Figure 1. Sludge drying, sludge grinding and wetland constructed in Monasterios.

Results and concluding remarks

The treatment flow of the wetlands is about 60 m3/day. At the Carrícola wetland the effluent concentration has been reduced from 6 to 1 mg/l phosphorus, while at the Monasterios wetland it has been reduced from 3 to 0.6 mg/l phosphorus. Microbiological values for Escherichia coli have also been reduced.

The sludge that forms the bed of these wetlands was obtained in the Drinking Water Treatment Plant (DWTP) of La Presa (Manises, València). A total of 356 tonnes of sludge were extracted and spread out on the drying beds until it reached at least 90% dryness, a necessary condition for grinding in the sand mill. The grinding process consists of a portable impactor with an output of 80 Tn/hour and a sieving machine. Although it was found in the laboratory that the best phosphorus adsorption capacity was for particle sizes between 0.83-2.83 mm so as not to produce too much by-product in the form of fines, this has been increased to a range of 1-3.5 mm. In the end, more than 100 Tn of material was obtained for filling the wetlands.

With a maximum phosphorus adsorption capacity ranging from 11.7 to 16.13 mg/g, this material ranks as significant when compared to other adsorbents reported in scientific literature, positioning it in an intermediate performance range. Beyond its use as an active layer in constructed wetlands for the renaturation of treated urban water, it shows potential for application as an adsorbent in biological treatment processes or as a substrate in wetlands treating industrial or runoff water. An added advantage lies in giving a second life to a material typically treated as waste.

The sludge generated, being free of metals and rich in organic matter with a high active surface area, presents significant potential for reuse in agricultural applications or as a substrate in constructed wetlands, thereby contributing to a more eco-friendly and circular approach to water treatment.

Acknowledgments: LIFE RENATURWATis a project co-financed by the European Commission (LIFE19 ENV/ES/000197) through the Environmental and Climate Action financial instrument (LIFE).

References

Benlalla A, Elmoussaouiti M, Cherkaoui M, Ait L, Assafi M (2015) Characterization and valorization of drinking water sludges applied to agricultural spreading. In: Proceedings of the International Conference on Water, Energy and Environment (ICEWE), 26–28 March 2015, Agadir, Morocco.

Impacts of long-term poultry manure applications on subsurface drain water quality under continuous corn production systems

S. Lenka[1], N. Hoover[2], M. Soupir[2], D. Anderson[2], R. Kanwar[2*]
[1] Indian Institute of Soil Science, ICAR, Bhopal, India
[2] Department of Agricultural and Biosystems Engineering, Iowa State University, Ames, Iowa 50011, USA
* e-mail: rskanwar@iastate.edu

Introduction

Nitrogen and phosphorus loss from agricultural production systems with subsurface drainage is of regional concern throughout the Midwest of United States of America and globally. Agricultural practices, especially nutrient management, are vital for sustaining global food production and ensuring food security. However, these practices can also have adverse environmental impacts, including contaminating water bodies with nutrients such as nitrogen (N) and phosphorus (P). Excessive nutrient application, particularly fertilizers and manure, can lead to nutrient losses resulting in water quality degradation and ecosystem disruption.

Spring and fall application of manure is a common farmer's practice in agricultural regions of Iowa and the US Midwest. Spring-applied manure is environmentally better, however, fall applications of poultry manure have traditionally been a common practice due to manure storage limitations and availability of time for farmers after harvest. Fall application of manure provides farmers with a broader application window compared to the busy spring planting season. Previous research has shown that long-term fertilization significantly contributes to nutrient pollution. To mitigate these environmental concerns, transitioning from long-term spring to fall poultry manure application has gained attention as a potential nutrient management strategy. Hydrological factors, such as rainfall patterns and drainage characteristics, were also found to influence nitrate losses. Liu et al. (2021) reported that switching from a fall application to a majority spring application resulted in changes from 67% to 52% in subsurface NO3-N loads. It is, therefore, essential to assess the impact of timing on the potential trade-offs between nutrient loss reduction and crop productivity for optimizing nutrient management strategies. In this study, we hypothesized that shifts from 17 years of long-term spring manure application to fall poultry manure application at different application rates would result in substantial loss of nutrients in the tile drains with subsurface drainage, especially during high rainfall events, compared to spring-applied inorganic N (UAN).

Materials and methods

Ten Chisel Plow field plots from a long-term study were used for this study (Chinkuyu et. al., 2001). Each plot (ranging in size from 0.22 ha to 0.44 ha) was drained by single subsurface tile drain installed in the middle of the plot at a depth of 1.20 m. Subsurface drainage water samples were collected from eight of the ten plots and data on soils and crop yield results were collected from all ten plots.

The long-term poultry manure study was initiated in 1998 continued until 2009 with a corn-soybean (CS) rotation system. To understand the impact of poultry manure on continuous-corn (CC) system, adapt to changing landscape trends, the study design was switched to continuous corn (CC) from 2010 to 2017. In both CS and CC phases, poultry manure was applied at two different application rates, while only one application rate was used for UAN, resulting in 3 treatments in each phase (Hoover et al., 2015, 2019; Huy et al., 2013). Then, a three-year study (2018-2020) evaluated the impacts of switching changing from a long-term from the spring poultry manure application practice management to a fall poultry manure application in from 2017, the transition base year. The UAN continues to be applied in the spring, consistent with standard farming field practices in Iowa, while the poultry manure was applied in the fall to early winter. There were three replicates of the poultry manure treatments for the CP plots and four replicates of the UAN treatment for the CP plots during this three-year period of the study. Fall poultry

manure application treatments were made at a target full agronomic N rate for continuous corn (PM: 224 kg N ha^{-1}) or at a half rate (PM0.5: 112 kg N ha^{-1}). UAN was applied in the spring at the full agronomic recommended rate (224 kg N ha^{-1}). The UAN plots were additionally treated with phosphorus and potassium maintenance applications in 2017 and 2020.

Subsurface drainage water samples were collected throughout the crop growing period at least once per week while the tiles were flowing to evaluate for nutrient (NO3-N and PO4-P) concentrations in subsurface drain water.

Corn was harvested (after the crop had reached maturity, and the grain moisture contents reached at acceptable levels on October 17 (2018), November 5 (2019), and September 21 (2020). Grain yields and moisture content values were measured and recorded in the field at the time of harvest. Reported yield values were corrected to 15.5% moisture content.

Results and concluding remarks

Three-year (2018-2020) data from study has clearly shown that transitioning from long-term farming practice of spring applications of poultry manure to continuous-corn production to fall poultry manure applications can significantly increase corn yields as well as resulted in higher PO4–P and NO3–N concentrations in subsurface drain water. Unlike our previously reported results of spring application of poultry manure in the corn-soybean phase (1998-2009; Nguyen et al., 2013) and corn-corn phase (2010-2017; Hoover et al., 2015, 2019), the shift to fall manure application increased nitrate nitrogen (NO3-N) and PO4-P concentrations in tile drains for the poultry manure applied at agronomic N application rates (cf. UAN and PM0.5). Also, it was found that by reducing the poultry manure applications to half the rate of N applications, PO4–P and NO3–N concentrations in subsurface drain water decreased and came to closed acceptable water quality levels in comparison with UAN treatments. The higher yields observed in the PM and PM0.5 treatments, particularly in the challenging year of 2020, suggest the potential benefits of long-term manure application in enhancing soil health and improving crop resilience. Hydroclimatic conditions influenced tile drain flow rates, but there was no significant effect of nutrient treatment on sub-surface tile discharge rates. Further research is needed to investigate additional factors contributing to the differences in NO3-N dynamics between spring and fall manure application and to develop effective management strategies that balance nutrient availability and environmental concerns.

Acknowledgments: Authors acknowledge the research funding provided by the USDA-FAS scientific exchange program on climate-smart agriculture and the Iowa Egg Council to conduct this study.

References

Chinkuyu AJ, Kanwar RS, Lorimar J, Xin H, Bailey TB (2002) Effects of laying hen manure application rate on water quality. TRANSACTIONS of the ASABE 45(2):299-308.

Hoover NL, Kanwar RS, Soupir ML, Pederson C (2015) Effects of poultry manure application on phosphorus in soil and tile drain water under a corn-soybean rotation. Water, Air, and Soil Pollution 226 (5): 138-150.

Hoover NL, Law JY, Long LAM, Kanwar RS, Soupir ML (2019). Long-term impact of poultry manure on crop yield, soil and water quality, and crop revenue. J. Environ. Manage. 252, 109582. https://doi.org/10.1016/j.jenvman.2019.109582.

Liu W, Yuan Y, Koropeckyj-Cox L (2021) Effectiveness of nutrient management on water quality improvement: A synthesis on nitrate-nitrogen loss from subsurface drainage. TRANSACTIONS of the ASABE 64, 675–689. https://doi.org/10.13031/TRANS.14078

Nguyen HQ, Kanwar RS, Hoover NL, Dixon P, Hobbs J, Pederson C, Soupir ML (2013) Long-term effects of poultry manure application on nitrate leaching in tile drain water. TRANSACTIONS of the ASABE 56, 91–101.

Investigation of microplastics in five natural Greek lakes

G. Kehayias[1*], P. Kanellopoulou[2], A. Kechagias[1], A.E. Giannakas[1], C.E. Salmas[3]
[1] Department of Food Science & Technology, School of Agricultural Sciences, University of Patras, Agrinio, Greece
[2] Department of Sustainable Agriculture, School of Agricultural Sciences, University of Patras, Agrinio, Greece
[3] Department of Materials Science and Engineering, School of Engineering, University of Ioannina, Ioannina, Greece
* e-mail: gkechagi@upatras.gr

Introduction

Although microplastics (MPs) are widely distributed in various aquatic environments worldwide, most of their studies accounted for the marine environments, while the first investigations on lake microplastic pollution are considerably lesser and started to publish after 2011 (Bowszys 2022). In Europe, the number of the available references on the microplastic contamination in freshwater remains small considering the overall number of lakes in this continent. There are only a few studies on this issue from the southern Europe and there are no reports on any of the lakes in Greece.

Thus, the main objectives of the present study are: i) to investigate the existence and the abundance of MPs in five natural lakes of Greece with various levels of morphometric characteristics, productivity and proximity to human activities. ii) To compare the results concerning the surface samples with those taken vertically, to access the magnitude of the sinking MPs in the overall pollution levels. iii) To compare the five lakes attempting to reveal the possible drivers of the microplastic pollution levels in these waterbodies.

Materials and methods

The study was conducted in five natural lakes situated in western Greece and having certain differences (Table 1). In each lake water samples were taken horizontally and vertically in three sampling sites using 200 μm nylon planktonic nets during September to October 2024. The horizontal tows were performed with a pair of rectangular nets attached in both sides of a small boat which was moving at speed of 1 knot. The nets were filtered the upper 20 cm of the water, and the volume was estimated using a Hydrobios flowmeter. The vertical samples were taken using a conical net (1.5 m length, 50 cm mouth diameter) which was vertically towed bottom to surface. The samples were stored in glass bottles in formalin. In the laboratory, the samples were examined under a 45X stereomicroscope, and the microplastic fibres and fragments were recovered and counted, while their shape and colour were recorded. The identification of their types is going to be accessed using FTIR spectrometry during the next few months.

Table 1. Morphometric characteristics, productivity and proximity to human activities of the five natural lakes.

LAKES	Area (km^3)	Catch. area (km^3)	Maximum depth (m)	Trophic condition	Distance from town	Anthropogenic activities
Ziros	0.4	0	56	Oligotr.	14	-
Ozeros	9.5	59	6	MesoEutr	13	A, F, H
Lysimachia	13.1	246	8	Eutrophic	4.5	A, F, H
Trichonis	95.8	400	58	OligoMeso	5.5	A, F, H, WS
Pamvotis	19.5	531	5	Eutrophic	0	A, F, H, WS, MW, BT

(A: agriculture, F: fishing, H: hunting, WS: water sports, MW: municipal waste, BT: boat transportation)

Results and concluding remarks

The total number of fibres and fragments in the surface samples was 2715 and 673, respectively. These findings accounted for an average abundance that ranged between 0.60 in Lake Ziros to 19.57 items/m^3 in Lake Pamvotis (Table 2). The respective values for the fragments were 0.0 to 4.93 items/m^3 in the same lakes. There was a positive correlation (Pearson coefficient R^2=0.9977) among the mean abundance of fibres and fragments recorded in the sampling sites of the five lakes (p=0.001). The black colour accounted

for the 28.5 % of total fibres, followed by blue (23.6 %), and transparent (15.7 %). The length of fibres ranged between 0.5 mm and up to 15 mm, with those of 2 - 3 mm accounting for 44.7 %. There were no statistically significant differences between the three sampling sites considering the abundance of fibres or fragments (Kruskal-Wallis test, $p>0.05$)

The present investigation revealed that most of the microplastic pollution was not floating in the surface but sunk in greater depths. Indeed, the total number of fibres and fragments recovered from the vertical samples were 946 and 53, respectively. The fibres abundance in the vertical axis were from 10 to more than 60 times greater than in the surface, while this was also true as the fragments are concerned (Table 2). The transparent colour was accounted for the 32.9 % of total fibres, followed by red, black, blue and purple in similar percentages. The length of fibres ranged between 0.1 mm and up to 10 mm, with those of 2 - 3 mm accounting for 40.6 %.

Table 2. Mean abundance (items/m³) of microplastic fibres and fragments revealed from surface and vertical samples in the five natural lakes. The Standard Error (±SE) is given the in parentheses.

Lakes	Fibres		Fragments	
	Surface	Vertical	Surface	Vertical
Ziros	0.60 (±0.15)	6.27 (±3.87)	0.00 (±0.00)	0.00 (±0.00)
Ozeros	0.65 (±0.08)	40.34 (±22.51)	0.08 (±0.03)	0.00 (±0.00)
Lysimachia	2.33 (±1.17)	68.79 (±21.67)	0.31 (±0.16)	1.84 (±0.37)
Trichonis	1.02 (±0.29)	28.87 (±9.52)	0.25 (±0.07)	2.38 (±1.16)
Pamvotis	19.57 (±8.61)	159.66 (±46.54)	4.93 (±2.02)	6.54 (±2.70)
Total avg	4.83 (±2.06)	60.79 (±20.82)	1.11 (±0.45)	2.15 (±0.85)

Comparisons of the present results with other lakes of the southern Europe are not easy due to the lack of consistent sampling methodology (Bowszys 2022). Moreover, in some cases the concentrations of MPs were reported per unit of water surface of lakes, or per volume of water filtered, depending on the gear used to collect the MPs. The net porosity of 200 μm used in the present study was smaller than the 300 μm that is the most popular sampling porosity for surface samples (Sighicelli et al. 2018).

In all cases, Lake Pamvotis was the most polluted. This lake is in contact with the town of Ioannina, having a population of more than 100,000 residents. The human activities include intense agriculture around the lake, fishing, hunting, water sports (mainly rowing), inputs of municipal waste, and daily boat transportation to the island of the lake. In contrast, Lake Ziros is expected to be the least polluted, as it is a small oligotrophic lake away from residential areas, surrounded by a forest and the only human activity that is allowed is canoeing. The other three lakes are situated in close distances between them in lowland agricultural areas of the western Greece and the main anthropogenic activities are hunting and fishing. In Like Trichonis there was a small fleet of commercial boats exercising fishing of *Atherina boyeri* using the purse seine method. The present results agree with Tanentzap et al. (2021), who studied 67 European lakes and focused on the factors determining the levels of pollution. Their findings suggested that lakes in urban catchments are more exposed to microplastic accumulation since this is where there is high potential for microplastic emissions, high population density, and high waste production and wastewater discharge.

References

Bowszys, M. 2022. Microplastics in the waters of European lakes and their potential effect on food webs: a review. Polish Journal of Natural Sciences, 37(3): 345–364. DOI: 10.31648/pjns.8040

Sighicelli M., Pietrelli L., Lecce F., Iannilli V., Falconieri M., Coscia L., Di Vito S., Nuglio S,. Zampetti G. 2018. Microplastic pollution in the surface waters of Italian Subalpine Lakes. Environmental Pollution, 236: 645–651.

Tanentzap A.J., Cottingham S., Fonvielle J., Riley I., Walker L.M., Woodman S.G., Kontou D., Pichler C.M., Reisner E., Lebreton L. 2021. Microplastics and anthropogenic fibre concentrations in lakes reflect surrounding land use. PLoS Biology., 19(9): e3001389

Distribution, sources and risk assessment of polycyclic aromatic hydrocarbons (PAHs) in waters of Amu Darya Basin, Uzbekistan

M. Jin[1,2], J. Wu[1,2*], S. Zhan[1,2], S. Shakhimardan[3]
[1] State Key Laboratory of Lake and Watershed Science for Water Security, Nanjing Institute of Geography and Limnology, Chinese Academy of Sciences, Nanjing 211135, China
[2] University of Chinese Academy of Sciences, Beijing 1000409, P.R.China
[3] Berdakh Karakalpak State University, Nukus, Uzbekistan
* e-mail: w.jinglu@niglas.ac.cn

Introduction

The Amu Darya is the largest inland river in Central Asia in terms of water volume, and it serves as one of the two major water sources for the Aral Sea and the primary water source within Uzbekistan. The river is utilized for various purposes, including industrial, agricultural, and domestic activities. Research has indicated the presence of pesticides and heavy metals in the water of the Amu Darya River and in the bodies of nearby residents, with concentrations exceeding the upper limit concentrations set by the World Health Organization. The situation of water pollution cannot be ignored. Polycyclic aromatic hydrocarbons (PAHs), as persistent organic pollutants closely associated with human activities, have garnered widespread attention. However, research on PAHs pollution levels in the Aral Sea basin, particularly in water bodies, remains limited. This study analyzed the concentrations, distribution patterns and sources of PAHs in the waters of the Amu Darya River region in Uzbekistan and evaluated their potential risks. A comprehensive understanding of the composition characteristics of PAHs in different environmental regions, along with the factors influenced by human activities and ecological conditions, can provide a scientific foundation for the comprehensive assessment of water resources and human ecological environment in this region.

Materials and methods

The study area covered the lower reaches of the Amu Darya River and the Amu Darya River Delta within Uzbekistan. A total of 50 water sampling points were collected. The concentrations of 16 priority controlled PAHs in the samples were determined by high performance liquid chromatography - diode array - fluorescence detector (HPLC-DAD-FLD).

Results and concluding remarks

The results indicated that the total PAHs concentration in the surface water of Amu Darya Basin ranged from 3.19 to 779 ng/L with an average value of 98.4 ng/L. The monomer concentration of PAHs ranged from 0 to 333 ng/L, and the monomer PAH with the highest concentration was Acy. The five monomer PAHs of Flu, Ant, Fla, Pyr and Chr had the detection rate of 100% and the monomer BbF had the highest total amount. The PAHs of 2-4 rings had a similar concentration with the PAHs of 5-6 rings, while they had significant differences in each sampling site. The areas with relatively high concentrations of the sample are mainly concentrated in urban areas, agricultural irrigation zones and the near-Caspian Sea region of the Amu Darya River Delta. Compared with surface waters in the world, the PAHs concentration in the Amu Darya Basin was at a medium level (Aziz F et al. 2014; Montuori P et al. 2016; Shen BB et al. 2021). According to the relative abundance, molecular diagnostic ratios and positive matrix factorization analysis (Hijosa-Valsero M et al. 2015; Matlyuba M et al. 2019), the PAHs in the Amu Darya Lower stream area mainly came from biomass combustion and the PAHs in the Amu Darya Delta came from the biomass combustion pollution, combustion source and traffic pollution, affected by human activity. This study simultaneously employed the Kalf risk entropy method in combination with relevant research, using negligible concentrations (NCs) and maximum permissible concentrations (MPCs) as reference concentrations for the 16 PAH monomers calculate ecological risks (Li Y et al. 2021). The results indicated

that Nap, Ace, Phe and Ant had a low ecological risk and other monomer PAHs were at a moderate risk, but BbF had a relatively high-risk level. Overall, the ΣPAHs were at the relatively low ecological risk in the study area while there were still 12 and 8 sampling sites at the moderate risk2 and the high-risk level, appropriate control measures should be considered to prevent further pollution.

Acknowledgments: The study was supported by the National Natural Science Foundation of China (U2003202, and 41671200).

References

Aziz F, Syed JH, Malik RN et al. Occurrence of polycyclic aromatic hydrocarbons in the Soan River, Pakistan: Insights into distribution, composition, sources and ecological risk assessment. Ecotoxicology and Environmental Safety, 2014, 109: 77-84. DOI: 10.1016/j.ecoenv.2014.07.022.

Hijosa-Valsero M, Bécares E, Fernández-Aláez C et al. Chemical pollution in inland shallow lakes in the Mediterranean region (NW Spain): PAHs, insecticides and herbicides in water and sediments. Science of the Total Environment, 2016, 544: 797-810. DOI: 10.1016/j.scitotenv.2015.11.160.

Li Y, Liu M, Hou LJ et al. Geographical distribution of polycyclic aromatic hydrocarbons in estuarine sediments over China: Human impacts and source apportionment. Science of the Total Environment, 2021, 768: 145279. DOI: 10.1016/j.scitotenv.2021.145279.

Matlyuba M, Nekqadam N, Nilufar A. Results of research on the study of the chemical composition of the Amu Darya River's water in the dynamics. American Journal of Medicine and Medical Sciences, 2019, 9(7): 270-274. DOI: 10.5923/j.ajmms.20190907.09.

Montuori P, Aurino S, Garzonio F et al. Distribution, sources and ecological risk assessment of polycyclic aromatic hydrocarbons in water and sediments from Tiber River and estuary, Italy. Science of the Total Environment, 2016, 566/567: 1254-1267. DOI: 10.1016/j.scitotenv.2016.05.183.

Shen BB, Wu JL, Zhan SE et al. Residues of organochlorine pesticides (OCPs) and polycyclic aromatic hydrocarbons (PAHs) in waters of the Ili-Balkhash Basin, arid Central Asia: Concentrations and risk assessment. Chemosphere, 2021, 273: 129705. DOI: 10.1016/j.chemosphere.2021.129705.

Use of machine learning tools in predicting contaminant removal in full-scale coal mine water treatment schemes

A. Almpanis[1*], V.G. Ioannidou[2*]
[1] *School of Engineering, University of Warwick, Coventry, United Kingdom*
[2] *School of Built Environment, Engineering and Computing, Leeds Beckett University, Leeds, United Kingdom*
** e-mail: atolgrp@gmail.com; v.ioannidou@leedsbeckett.ac.uk*

Introduction

Prediction and effective monitoring of the contamination levels of metals and other associated to mine drainage contaminants in abandoned MWTS is regarded indispensable, to improve their operational and maintenance features and practices, as well as retrofitting of existing treatment units or construction of new ones. However, the effectiveness of the use of predicting tools has not been systematically researched and documented in the field of full-scale systems treating mine drainage (Ahmed et al., 2019; Avila et al., 2018; Ilyas et al., 2021; Xie et al., 2021). Conducting regression analyses on long-term datasets is envisaged to offer a better understanding on the relationships between all the physicochemical parameters, removal efficiencies and the design aspects of the treatment system (Ilyas et al., 2021; Xie et al., 2021).

This study is one of the limited studies currently available that employs data arising from full-scale passive MWTS, offering also an assessment of the factors that affect iron removal. To achieve these aims, random forest regression (RFR), a machine learning tool, was employed.

This study attained to assess the treatment performance of the MWTS, further investigating the influence of physicochemical parameters on iron removal from mine water discharge lagoons and wetlands.

This research contributes to knowledge by providing sound scientific basis for lagoons and wetlands design engineers, research scientists, and MWTS operators to make informed decisions in MWTS management.

Materials and methods

Data from five UK locations of passive MWTS has been analysed. It corresponds to ten settlement lagoons receiving outflow from adjacent abandoned mines. These five sites have been chosen for the common time period when chemical data was collected as well the variation of lagoon features. The data collection period spanned over twelve years. The dataset contains monthly records of ferric iron (Fe^{3+}). Design aspects of the MWTS (i.e. aspect ratio, shape, depth) were obtained from topographic maps.

Preprocessing of the data (removing missing values and NaN entries) and subsequent analysis was carried using python on Jyputerlab (Kluyver et al., 2016). Preprossecing also involved the conversion of categorical variables into numerical ones using the LabelEncoder function of scikit-learn (Pedregosa et al., 2011) and data normalization. Statistical tests for correlation (ANOVA, Kruskal-Wallis, pairwise comparison) was conducted with SciPy. Linear regression model was fitted using statsmodels, and subsequently using machine learning with scikit-learn. The latter was also used for the Random Forest Regression (RFR) analysis. RFR was chosen due to its resistance to outliers and to non-linearity. Shapley Additive Explanations (SHAP) was applied on the model predictions in order to show the contribution of each feature to the model's output.

Results and concluding remarks

The dataset comprised of 1065 entries, corresponding to Fe^{3+} records from five distinct sites. A preliminary analysis demonstrated significant differences between the sites, suggesting that local parameters (e.g. design of the lagoon, environment) had an influence on the profiles of Fe^{3+} removal. A simple heatmap confirmed this, indicating a correlation between aspect ratio, volume, and area with Fe^{3+}

removal. An ANOVA test for the influence of the lagoon shape on iron removal was conducted, giving an F-statistic of 41.75 ($p < 3.52e-18$). Kruskal-Wallis test (non-parametric alternative to ANOVA) resulted in an F-statistic of 66.18 ($p < 4.26e-15$). Tuckey test showed that oval shape was the best regarding Fe^{3+} removal. Rectangle and trapezium were close to each other, with a significantly worse performance.

Ordinary least squares regression (OLS) model explained 29.7% of the variance in Fe^{3+} removal (0.295 adjusted, or 29.5%) (F-statistic 149.4, $p < 8.85e-81$). The residuals showed signs of non-normality and autocorrelation, suggesting room for improvement. RFR explained approximately 67% of the variation (R^2 0.668, MSE 267.445), a significant improvement over the linear regression or the OLS. Residuals were better distributed than in the linear regression, but still showed some bias. Feature-wise, the most important indication for Fe^{3+} removal was the aspect ratio of the lagoon. With respect to the shape, oval-shaped lagoons performed markedly better. The importance of aspect ratio and oval shape was confirmed by running a SHAP test.

Both the statistical tests and the regression models indicated that there is a strong correlation between aspect ratio and shape of a MWTS lagoon with its capacity for efficient Fe^{3+} removal. The best model implemented (random forest) managed to explain approximately 67% of the variance observed in the data, an indication that more parameters need to be incorporated into the model. It was confirmed that our results were not noisy or imbalanced, so that a high confidence level is put in the RFR analysis.

References

Ahmed, U., Mumtaz, R., Anwar, H., Shah, A.A., Irfan, R., García-Nieto, J., 2019. Efficient Water Quality Prediction Using Supervised Machine Learning. Water 11, 2210.

Avila, R., Horn, B., Moriarty, E., Hodson, R., Moltchanova, E., 2018. Evaluating statistical model performance in water quality prediction. J. Environ. Manage. 206, 910–919.

Bowell RJ, Bamforth S, Walton J, Brabham P (2023) An assessment of the current operation of the Coal Authority Six Bells Mine Water Treatment Scheme, South Wales. In: IMWA 2023 – "The Future." Presented at the IMWA 2023 Conference, Wales, England. 17-21 July 2023, pp 77–82 https://www.imwa.info/docs/imwa_2023/IMWA2023_Bowell_77.pdf

Ilyas, H., Masih, I., van Hullebusch, E.D., 2021. Prediction of the removal efficiency of emerging organic contaminants in constructed wetlands based on their physicochemical properties. J. Environ. Manage. 294, 112916.

Kluyver, T., Ragan-Kelley, B., Fernando Perez, Granger, B., Bussonnier, M., Frederic, J., … Willing, C. (2016). Jupyter Notebooks – a publishing format for reproducible computational workflows. In F. Loizides & B. Schmidt (Eds.), Positioning and Power in Academic Publishing: Players, Agents and Agendas (pp. 87–90).

Pedregosa, F., Varoquaux, Ga"el, Gramfort, A., Michel, V., Thirion, B., Grisel, O., … others. (2011). Scikit-learn: Machine learning in Python. Journal of Machine Learning Research, 12(Oct), 2825–2830.

Rinder T, Dietzel M, Stammeier JA, Leis A, Bedoya-González D, Hilberg S (2020) Geochemistry of coal mine drainage, groundwater, and brines from the Ibbenbüren mine, Germany: A coupled elemental-isotopic approach. Appl Geochemistry 121. https://doi.org/10.1016/J.APGEOCHEM.2020.104693

Xie, X., Wu, T., Zhu, M., Jiang, G., Xu, Y., Wang, X., Pu, L., 2021. Comparison of random forest and multiple linear regression models for estimation of soil extracellular enzyme activities in agricultural reclaimed coastal saline land. Ecol. Indic. 120, 106925.

Roles of riverine wetlands in diffusive greenhouse gas emissions: Comparative insights from before and after wetland destruction

W. Zhang[1,2], H. Li[1,2*]
[1] Key Laboratory of Lake and Watershed Science for Water Security, Nanjing Institute of Geography and Limnology, Chinese Academy of Sciences, Nanjing 211135, China
[2] Key Laboratory of Watershed Geographic Sciences, Nanjing Institute of Geography and Limnology, Chinese Academy of Sciences, Nanjing 211135, China
* e-mail: hpli@niglas.ac.cn

Introduction

While wetland construction and restoration are widely employed as nature-based solutions to achieve various eco-environmental goals, their roles in affecting diffusive greenhouse gas emissions (GHG) remain poorly understood. In this study, we investigated the monthly and diurnal dynamics of diffuse GHG emissions in a headwater river, which initially contained a series of constructed wetlands but were later destroyed. We sought to address the following questions: (i) What changes occurred in monthly and diurnal patterns of the GHG concentrations and fluxes following wetland destruction? (ii) What role do wetlands play in influencing environmental conditions for GHG emissions?

Materials and methods

To elucidate the roles of wetlands in mediating diffusive GHG emissions, we implemented two sampling schemes: monthly and diel sampling. Both schemes were conducted comparatively, covering periods both with and without wetlands.

During all sampling visits, samples for measuring water quality and dissolved GHG concentrations were collected simultaneously.

Concentrations of GHG in excess of their saturated solubilities in water were calculated. Emission fluxes of GHG were also estimated by the water-air exchange equation. To elucidate the impact of environmental factors on each GHG during periods with or without wetlands, we ranked variable importance using factor importance analysis (FIA) based on the random forest algorithm.

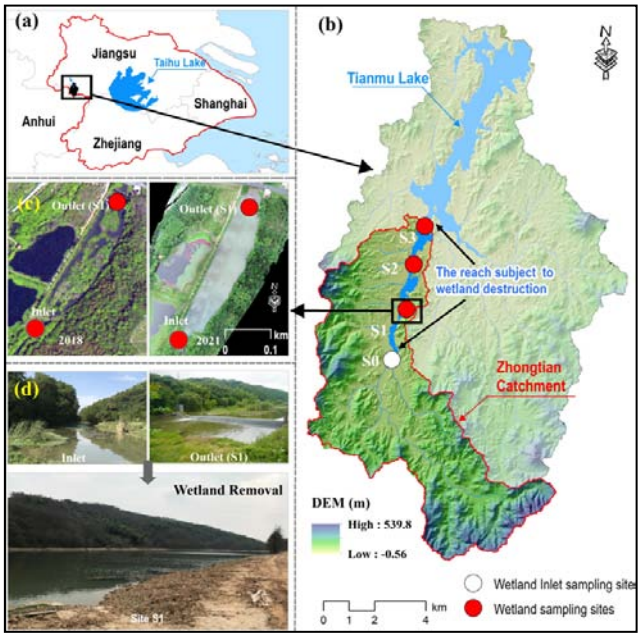


Figure 1. Location of the sampling sites

Results and concluding remarks

This study aimed to elucidate the impacts of riverine wetlands on GHG emissions. By directly measuring monthly and hourly dissolved GHG concentrations in the water column of a headwater river that previously contained constructed wetlands, which were later removed, we revealed a reduction in GHG emissions, ranging from 16.08% to 22.97% following the removal of the wetlands. Our results highlight a paradox: wetland destruction, typically viewed as environmentally detrimental, is associated with a decrease in GHG emissions. However, despite the observed reduction in GHG emissions after wetland destruction, our study does not support the conclusion that constructed wetlands can significantly enhance global warming potential. Instead, our findings alleviate concerns about wetlands significantly contributing to GHG emissions, indicating that their restoration might have only a marginal effect on global warming. Overall, our comparative results provide compelling scientific evidence that can guide the understanding of wetland restoration's effects on GHG emissions and emphasize the need for a balanced approach that considers the various ecosystem services provided by wetlands alongside their potential impact on GHG emissions, ensuring ecologically and climatically sound wetland management strategies.

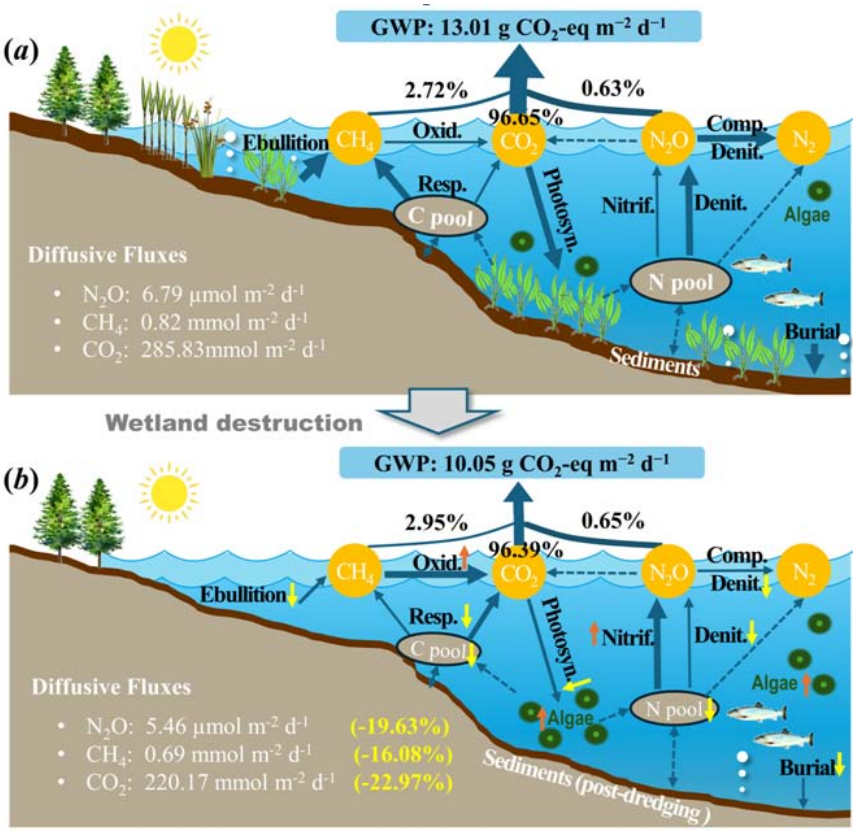


Figure 2. Schematic diagram illustrating changes in the processes responsible for GHG emissions in the lower reach of the Zhongtian River: (a) before and (b) after wetland destruction.

Acknowledgments: This study was financially supported by the National Natural Science Foundation (42071143), the Youth Innovation Promotion Association of CAS (2023330), the Science and Technology Planning Project of NIGLAS (NIGLAS2022TJ16 and NlGLAS2022GS03).

References

Wangshou Zhang, Hengpeng Li, Dawei Xu, Tianyu Xia, 2024. Wetland destruction in a headwater river leads to disturbing decline of in-stream nitrogen removal, Environmental Science & Technology 58: 2774-2785

Wangshou Zhang, Hengpeng Li, Bing Li, 2022. Whole-system estimation of hourly denitrification in a flow-through riverine wetland. Journal of Hydrology. 618:129132

Are combined sewer overflows from wastewater treatment plants a critical source of microplastics discharge into water bodies?

G. Beringheli*, S.F. Corsino, M. Capodici, M. Torregrossa
Department of Engineering, University of Palermo, Palermo, Italy
** e-mail: giuseppe.beringheli@unipa.it*

Introduction

Microplastic (MPs) pollution has emerged as a significant environmental concern due to its widespread presence in aquatic ecosystems (Yang et al., 2022). Wastewater treatment plants (WWTPs) could play a crucial role in mitigating microplastic contamination, with removal efficiencies ranging from 60% and 99.9% (Krishnan et al., 2023). However, substantial amounts of MPs can still enter the environment, especially during combined sewer overflow (CSO) events. CSOs occur when intense rainfall exceeds the capacity of WWTPs, leading to the direct discharge of untreated wastewater into the environment. Precipitation events can significantly influence the concentration and composition of microplastics in wastewater, as stormwater runoff mobilizes plastic debris from urban surfaces while resuspension processes within the sewer network further contribute to their abundance. Nevertheless, few studies are available about this topic. Understanding the impact of CSO events on microplastic contamination is essential for assessing the environmental risks associated with untreated stormwater discharges. For this purpose, this study investigated the variations in MPs concentrations under different weather conditions, highlighting the role of CSOs in amplifying their presence in wastewater discharges.

Materials and methods

The experimental campaign lasted one year, from September 2023 to August 2024. Samples were collected at the Municipal WWTP that treats wastewaters produced in Palermo (Italy). The plant has a potential close to 440.000 PE and the average daily flow is 78,000 m^3/day. According to the WWTP design operation, the CSO activation occurred under rainy event when the flow rate overcomes of five times the average daily flow rate. Wastewater samples were collected from the influent flow in different weather conditions: dry weather, wet weather with or without CSO activation, and from the effluent of the WWTP. A summary of the samples collected during the experiment is reported in Table 1.

Table 1. Samples of wastewater collected for microplastics analysis.

Sample/Weather conditions	Type of sample	N. samples
Influent wastewater		35
Dry weather	24-h composite	19
Wet weather without CSO	24-h composite	8
Wet weather with CSO	Instantaneous	8
Effluent wastewater	24-h composite	23

All samples were stored at 4°C to prevent degradation. Microplastics were isolated from wastewater using a multi-step approach (Yang et al., 2022). First, 500 mL of sample was filtered through a stainless-steel screen (5 mm), to remove larger particles. Hereafter, the organic material was removed by adding 10 mL of 30% H_2O_2 to the 500-mL sample and heating to 65°C while mixing at 100 rpm for 12 hours. MPs were separated by adding 50 mL of saturated NaCl solution following by 24 hours of settling. The supernatant was then filtered through a nylon filter with 20 µm mesh size. Then, MPs were let dried at 40 °C in an oven for 24 hours. The MPs were analyzed using a stereomicroscope (Olympus) with 20-80x magnification. The number of microplastics were manually counted and then classified by shapes into 4 classes: spheres, fibers, fragments, and films. Finally, the MPs concentrations were expressed as number of elements per L.

Results and concluding remarks

Figure 1 shows the average MPs concentrations obtained from the collected samples under different weather conditions.

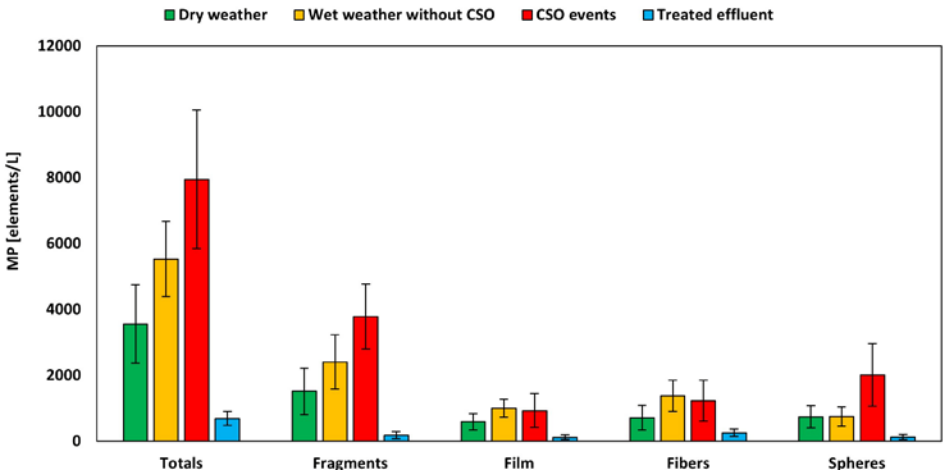


Figure 1. Concentration of MPs in the collected samples distinguished by total and shape

The highest MPs concentration in the WWTP influent was found in CSO samples (7950 ± 2100 elements/L), followed by rain event samples without CSO activation (5527 ± 1140 elements/L) and dry weather samples (3556 ± 1185 elements/L). In contrast, the MPs concentration in the WWTP effluent was significantly lower, averaging 685 ± 209 elements/L, indicating a good efficiency of the WWTP in removing microplastics. Overall, MPs concentration in CSO samples was almost twice that during dry weather condition and approximately 50% higher than rainy event without CSO activation. This result pointed out the influence of urban runoff to microplastic pollution in wastewater. Indeed, during precipitation events, urban runoff washes out microplastics accumulated on road surfaces during dry weather, increasing the presence of MPs in the wastewater. Interestingly, when the intensity of the meteorological event increased to the point of triggering CSO activation, the concentration of MPs becomes even higher. This was certainly due, on one hand, to the more intense runoff phenomenon, but also to the possible resuspension of sediments containing microplastics within the sewer collectors. Fragments were the most represented MPs in the WWTP influent samples, followed by fibers, spheres, and films. In contrast, fibers were the most abundant in the effluent WWTP samples. In more detail, the concentration of fragments during rain events without CSO activation increased by approximately 50% compared to dry weather conditions, while a further significant increase was observed in CSO samples. This result suggested that the concentration of fragments increased with the intensification of the meteorological event. No significant differences were observed in terms of films and fibers abundance, while a significant increase in spheres was observed only during CSO events. The higher presence of fragments and spheres during extreme weather events can be attributed to the runoff from road surfaces, leading to a greater input of microplastics into the sewer system from the degradation of primary plastics (e.g., plastic waste accumulation and tires wear).

It was interesting to note that MPs concentration in CSO samples was found to be approximately 12 times higher compared to effluent samples, suggesting that CSO events could represent a not negligible source of microplastic pollution. It should be pointed out that the release of microplastics through the WWTP effluent occurs continuously, but with relatively low concentrations. In contrast, although less frequent, CSO events could represent a not negligible source of microplastic, considering both the higher volume of water and MPs concentration released into the environment.

References

Krishnan, R., Manikandan, S., & Subbaiya, R. (2023). Recent approaches and advanced wastewater treatment technologies for mitigating emerging microplastics contamination – A critical review. Science of the Total Environment, 858: 159681. https://doi.org/10.1016/j.scitotenv.2022.159681

Yang, F., Li, D., Zhang, Z., Wen, L., Liu, S., Hu, E., Li, M., & Gao, L. (2022). Characteristics and the potential impact factors of microplastics in wastewater originated from different human activity. Process Safety and Environmental Protection, 166: 78–85. https://doi.org/10.1016/j.psep.2022.07.048

IX. Sustainable and Adaptive Water Resources Management

Questioning efficiency targets at river basin scale: A practical assessment in southern Spain

A. Expósito[1*], C. Gutiérrez-Martín[2], F. Delgado[3], J. Berbel[2]
[1] WEARE research group and Universidad de Málaga, Spain
[2] WEARE research group and Universidad de Córdoba, Spain
[3] Universidad de Granada, Spain
* e-mail: aexposito@uma.es

Introduction

In the current context of increasing water scarcity and the effects of climate change in regional availability of renewable water resources, the idea of enhancing efficiency in the use of water resources is acquiring greater political and social sound. With this aim, different administrations are promoting the development of water efficiency indicators as a tool to monitor efficiency targets at basin scale and facilitate inter-basin (and inter-regional) comparative analyses. Specifically, the Blueprint for Water report (European Commission, 2012) calls for the development of basin-specific efficiency targets by river basin authorities, emphasising the importance of considering the broader impact of individual measures at the river basin level. This work aims to contribute towards the discussion on the appropriateness of basin-wide efficiency targets (and indicators) for guidance and information on water policy with the goal of achieving environmental objectives (e.g., good status of water bodies, as set by the EU WFD). With this aim, we carry out a practical assessment in the case study of the Guadalquivir river basin (GRB) in Spain by using a hydro-economic model to assess basin efficiency changes in alternative scenarios.

Materials and methods

The Guadalquivir river basin (GRB) is located in southern Spain and it is one of the longest rivers in southern Europe. Using our hydro-economic model for the GRB and real data, we test how increases in water use efficiency by the irrigation sector (at basin and sub-basin scales) affect basin-wide efficiency. Water requirements and efficiencies have been obtained from CHG (2023). The average application efficiencies are 61% for flood irrigation, 67% for sprinkler irrigation and 77% for drip irrigation. These figures include losses in the transport (90% efficiency) and distribution (90% efficiency) of water. Therefore, although this efficiency is often referred to as application or on-farm efficiency, it should be understood as a broader measure encompassing the entire process from water extraction to its application in the field. To avoid confusion with basin-level efficiency, we will refer to it as local efficiency.

The Guadalquivir hydro-economic model is a holistic approach that integrates elements of hydrological and agro-economic models. It consists of a network of interconnected nodes that adhere to the principle of water mass balance at each node. These nodes represent key points within the general basin scheme, such as urban and agricultural demand points, reservoirs, and gauging stations. The economic component consists in a group of models that simulate the behaviour of agricultural zones. Each agricultural area is calibrated using Positive Mathematical Programming (PMP). The PMP model comprises an objective function that maximises the gross margin of a zone, subject to technical and resource constraints. The model can accurately reproduce crop areas for the reference year. Another advantage is that it provides smooth responses to changes in initial conditions (such as variations in applied or consumed water, changes in water application efficiency, and shifts in crop prices and costs) and simulates the adaptive behaviour of farmers by adjusting cultivated areas. The complete model is described in greater detail in Martínez-Dalmau et al. (2023).

Results and concluding remarks

As shown in Table 1, if the local efficiency is increased by an additional 5%, one would expect a final

average local efficiency of 76.2%, since less water would be applied for the same consumption. However, the basin efficiency only increases by 3.5%, from 80.7% to 84.2%. This illustrates the fact that an increase of local efficiency does not translate to the same increase of basin efficiency, illustrating the complexities of targeting basin-wide efficiency through sectoral or individual actions.

Table 1. Water flows (hm^3) and efficiencies for different scenarios

	Local efficiency increase				
	Baseline	**5%**	**10%**	**15%**	**20%**
Inflow	3,526	3,526	3,526	3,526	3,526
Water applied	3,468	3,238	3,037	2,860	2,702
Water consumption	2,468	2,468	2,468	2,468	2,468
Return flow (recoverable)	409	307	217	137	66
Return flow (total)	1,000	770	569	392	234
Water abstraction	3,059	2,931	2,820	2,723	2,636
Avg. local efficiency	71.2%	76.2%	81.3%	86.3%	91.3%
Basin efficiency	80.7%	84.2%	87.5%	90.7%	93.6%

Source: Own elaboration.

Successive 5% increments in local efficiency result in less than 5% increases in basin efficiency. In fact, at the basin level, efficiency gains diminish progressively (3.5%, 3.3%, 3.1%, and 3.0% for local efficiency improvements of 5%, 10%, 15%, and 20%, respectively). For example, a 15% increase in local efficiency (from 71.2% to 86.3%), produces just 10% increase of basin efficiency (from 80.7% to 90.7%). Thus, the higher the local efficiency, the closer the difference with respect to basin efficiency.

Practical evidence shows that not all return flows are recoverable downstream. Transport and distribution losses, as well as irrigation return flows, can be directed to destinations that are not reusable, such as wild vegetation, evaporation from canals, or confined or saline sinks. Under these conditions, local efficiency improvements would have a greater impact at the basin level by reducing non-recoverable return flows. Our analysis shows that even when reuse efficiency is lower than 100%, efficiency changes at basin scale remain similar. In summary, results demonstrate that increments in local efficiencies result in smaller increases in basin-wide efficiencies, being negligible at basin scale if return flows are reused by downstream users.

This study contributes to the discussion on the appropriateness of basin-wide efficiency targets (and indicators) to guide and inform water policy with the ultimate goal of achieving environmental objectives (e.g., good status of water bodies, as set by the EU WFD). We describe and discuss a theoretical example to highlight the constrains of setting a basin-wide efficiency target and apply a practical assessment of basin-wide efficiency to the case study of the GRB. The use of a hydro-economic model shows that an increase in water-use efficiency at sectoral or individual level does not translate to an increase of basin efficiency, thus illustrating the complexity of setting basin-wide efficiency targets. As discussed, measuring and evaluating basin-wide efficiency constitutes a complex exercise due to the need of taking into account multiple social, environmental, technical and policy aspects.

References

CHG (2023) Plan Hidrológico de la demarcación hidrográfica del Guadalquivir (2021-2027) Confederación Hidrográfica del Guadalquivir, Gobierno de España, Madrid.

European Commission (2012) A blueprint to safeguard Europe's water resources. T. C. Communication from the Commission to the European Parliament, the European Economic and Social Committee and the Committee of the Regions, Brussels.

Martínez-Dalmau J, Gutiérrez-Martín C, Kahil T, Berbel J (2023) Impact of alternative water policies for drought adaptation in the Guadalquivir Mediterranean River basin, southern Spain. Journal of Hydrology: Regional Studies 47: 101444. https://doi.org/10.1016/j.ejrh.2023.101444

Recovery of metals from livestock bio-sludge with acetic acid extraction followed by biosorption of baker's yeast

J.J. Su[1,2,3*], K.W. Yen[1], W.C. Chen[1]
[1] Dept. of Animal Science and Technology, National Taiwan University, Taipei, Taiwan, R.O.C.
[2] Bioenergy Research Center, College of Bio-resources and Agriculture, National Taiwan University, Taipei, Taiwan
[3] Agricultural Net-Zero Carbon Technology and Management Innovation Research Center, National Taiwan University, Taipei, Taiwan
* e-mail: jjsu@ntu.edu.tw

Introduction

Applications of zinc- or copper-rich livestock compost to fields can lead to high residues in the soil, violating limits for land use. Livestock bio-sludge was treated with acetic acid (1N, 2N, and 4N) and hydrogen peroxide (H_2O_2) over varying periods (4, 24, and 48 hours) to investigate zinc and copper extraction efficiency. Results showed that 2% H_2O_2 significantly improved removal efficiency ($p < 0.01$). The best results were 40% copper and 70% zinc removal with 4N acetic acid in 48 hours. Filtrated supernatant at different pH levels (4.5, 5.0, and 5.5) was tested with baker's yeast for bio-absorption. Adding molasses supported yeast growth, achieving over 90% zinc and 50~90% copper removal at pH 5.5 within 4 hours. This study's combination approach effectively reduces and recycles heavy metals in livestock sludge, suggesting future development of machinery for this purpose.

Materials and methods

This study investigates the effects of pH levels and inoculation ratios on the removal efficiency of heavy metals, copper, and zinc by yeast in acetic extract supernatant, based on a previous study by Yen et al. (2024). Commercial baking yeast (Quick-rise yeast, Sunright Foods Co., Ltd., Taiwan) was cultured in YPD broth (Gibco™) at 28°C for 24 hours, purified, and checked for contamination. The yeast was stored on slant agar at 4°C and inoculated into a liquid medium a day before use. The optical density (OD) was measured to determine yeast concentration. Experiments were conducted with three pH groups (4.5, 5.0, 5.5) and different inoculation ratios (2.5%, 5.0%, 10%). The pH was adjusted using 1N sodium hydroxide, with a yeast concentration of 3.59 mg/L and a 5% inoculation ratio. For inoculation ratio tests, the pH was set at 5.5, with a yeast concentration of 2.05 mg/L. Yeast was cultivated in a shaker incubator (Shakers, Orbital Shaking, D9FF-S101, FIRSTEK, Taiwan) at 28°C and 100 rpm, comparing copper and zinc concentrations before and after bio-adsorption.

The acetic extract supernatant was obtained using acetic acid (2N) and hydrogen peroxide (2%) for 24 hours, then centrifuged at 3,000 rpm and filtered using No.1 filter paper. The pH of the supernatant was adjusted to 4.5, 5.0, and 5.5 using 1N sodium hydroxide. Both 45 mL of the supernatant and 2.5 mL of molasses (diluted 50 times) were placed in 125 mL Erlenmeyer flasks and autoclaved as the medium for this study. The OD of the 2.5 mL yeast culture was measured before adding it to the sterile mixture of supernatant, bringing the final volume to 50 mL (inoculation ratio = 5%), and then incubated at 28°C with shaking at 100 rpm. After 4 hours of incubation, the solution was filtered using a 0.2 μm cellulose nitrate membrane filter, and the filtrate was collected for analysis. Copper and zinc concentrations in the filtrate were measured using atomic absorption spectroscopy before and after bio-adsorption to calculate removal efficiency. Ion chromatography was used to analyze ion concentration changes, predicting ions required or interfering during bio-adsorption. To test yeast bio-adsorption, a one-way ANOVA analyze the effects of pH and yeast inoculation ratio on biological adsorption. Removal rate data were converted using angle conversion in Tukey's HSD and compared in pairs if significant differences were found. Data show mean and standard error, marking significant differences at $p < 0.01$.

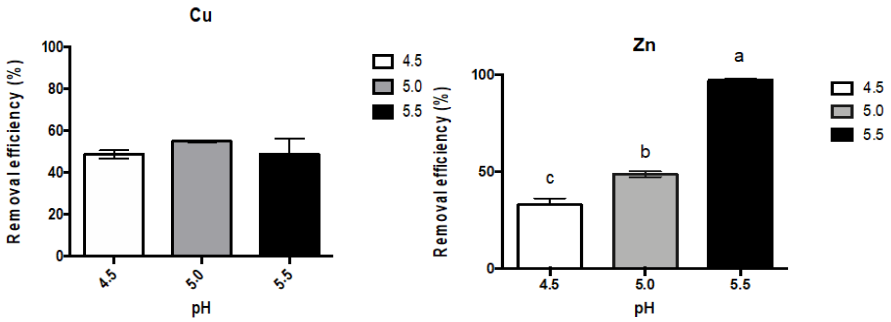


Figure 1. Removal efficiency of copper and zinc from the supernatant of acidic extracts by yeast under various pH values.

Results and concluding remarks

Before biosorption, 1N sodium hydroxide was used to divide the pH into three groups: 4.5, 5.0, and 5.5. The removal efficiency of copper from the supernatant by yeast showed little variation across different pH levels (Fig. 1). The highest removal rate was in the pH 5.0 group, at approximately 54.9 ± 1.6%. However, there were no significant differences at the 5% level among the three groups. The removal rates were 48.8 ± 2.6% for pH 5.5 and 48.6 ± 4.8% for pH 4.5.

In contrast, the ability of yeast to adsorb zinc from the supernatant increased significantly with higher pH levels (Fig. 1). At pH 5.5, the removal rate reached 97.3 ± 2.9%, significantly higher than the rates at pH 5.0 (49.4 ± 6.69%) and pH 4.5 (32.9 ± 8.1%). Although the removal efficiency of copper and zinc is 48.8% and 97.3%, respectively, an environmentally friendly approach is applied by using acetic acid and hydrogen peroxide as the solvents to extract copper and zinc from the concentrated sludge, instead of sulfuric acid or HCl.

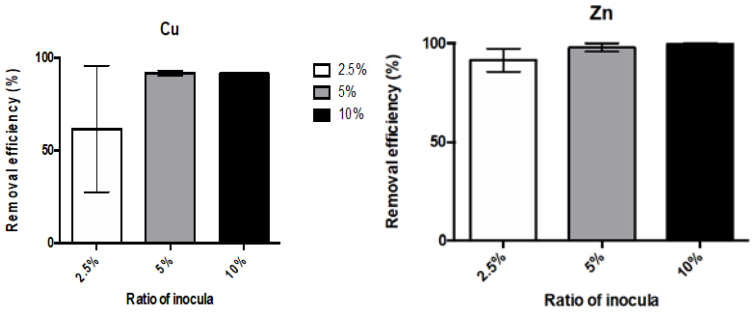


Figure 2. Removal efficiency of copper and zinc from the supernatant of acidic extracts by yeast under various inoculation ratios.

In the groups with 2.5%, 5% and 10% yeast inoculation, the copper removal rates were 60.3%, 91.5% and 91.3%, respectively, showing no significant difference (Fig. 2). For zinc, the removal rates were 91.5%, 98.7%, and 99.6% for the 2.5%, 5%, and 10% inoculation groups, also indicating no significant differences (Fig. 2. However, there is a slight increasing trend in removal efficiency with higher inoculation rates, suggesting that the yeast was sufficient at these concentrations, and further increases did not significantly enhance removal efficiency. In the 2.5% copper group, one repeat experiment showed that the yeast did not absorb any copper from the supernatant, possibly due to the biotoxicity of copper ions to microorganisms.

Acknowledgments: This work was funded by grants (No. MOST 111-2313-B-002-061-MY3) from the National Science and Technology Council (NSTC), Executive Yuan, Taiwan.

References

Yen KW, Chen WC, Su JJ (2024) Recovery of copper and zinc from livestock bio-sludge with an environmentally friendly organic acid extraction. Animals 14: 342. https://doi.org/doi:10.3390/ani14020342.

Rainwater harvesting system as a solution for increasing the water self-sufficiency of road infrastructure facilities

A. Stec*, D. Słyś
Department of Infrastructure and Water Management, Rzeszów University of Technology, Poland
** e-mail: stec_aga@prz.edu.pl*

Introduction

Rainwater harvesting systems (RWHS) can be a valuable alternative water resource and one of the elements of sustainable water management strategies in urban and rural areas (Thapa et al. 2022). Their implementation in buildings brings many environmental, financial and social benefits (Stec 2023, de Sa Silva 2022). It should be emphasized that RWHS operating as decentralized systems not only reduce the exploitation of natural water resources but also significantly increase local water security (Słyś and Stec 2020, Stephan and Stephan 2017). Using rainwater as an alternative water source is also a promising way to achieve several of the 17 Sustainable Development Goals established by The United Nations (UN). Rainwater is a valuable water source because, unlike greywater, it is characterized by a relatively low degree of pollution (Zdeb et al. 2020). However, due to the existence of many technical, climatic and financial factors influencing the effectiveness of RWHS, it is necessary to conduct detailed analyses for each facility. Rainwater harvesting systems are mainly implemented in residential, service, industrial or sports buildings. They are relatively rarely used in road infrastructure facilities, such as rest areas. One of these is rainwater collected from building roofs, which is relatively low in pollutants. Rainwater can be particularly important in these areas because they are often located in areas far from urban or rural development, where there are problems with network infrastructure.

Taking the above into account, comprehensive research was carried out, the aim of which was to determine the possibilities of implementing a sustainable water system that increases the self-sufficiency of road infrastructure facilities.

Materials and methods

One of the rest areas located along the S19 expressway, which is part of the trans-European transport corridor Via Carpatia, was selected for the study. The studied object Rest Area Stobierna (RAS) (50°9'48"N, 22°5'11"E) covers an area of 5.5 ha and includes a building with toilets and showers, five garden gazebos, a playground, parking lots and access roads.

The research was carried out as part of an inter-university research project covering several stages: (1) research on meteorological conditions; (2) research on the quantity and quality of water flowing from building roofs (physical, chemical and bacteriological indicators); (3) development of a concept for a new compact device for pre-treating rainwater; (4) construction of a prototype of this device and (5) laboratory tests of the efficiency of the developed prototype of the device. Samples for testing were collected from April 2023 to May 2024 after the occurrence of rainfall events. The following were determined: colour, turbidity, pH; general indicators: TOC, alkalinity; ions: ammonium, nitrates, phosphates, bacteriological indicators: total number of psychrophilic and mesophilic bacteria, Escherichia coli and Enterococci. The next stage of the research included the analysis of the qualitative research results and the development of a new solution for a device for pre-treating these waters for non-potable uses. The project assumes that the purified rainwater will be used for flushing toilets and cleaning work within the RAS area.

Based on the data obtained from the RAS manager, the actual water consumption in the facility was determined to be an average of 7.17 m^3/day, with a maximum of 8.33 m^3/day. This data was necessary to assess the efficiency of the RWHS for the analyzed facility. For this purpose, a simulation model developed by Słyś (Słyś 2009) was used. The model's algorithm is based on the daily mass water balance and is described by the YAS (Yield After Spillage) operating rules. It can be generally described by the formula (1):

$$V_i = I_i + V_{i-1} - U_i - Z_i \quad (1)$$

where: V_i – the volume of rainwater retained in the tank at the end of the i-day, I_i – the volume of rainwater flowing from the roof to the tank on the i-th day, m^3; V_{i-1} – the volume of rainwater remaining in the tank from the previous day, m^3; U_i – the volume of rainwater collected on the i-th day from the reservoir, m^3; Z_i - the volume of excess rainwater discharged from the tank to the sewage system on the i-th day, m^3.

Results and concluding remarks

The research results allowed for a detailed analysis of the physical, chemical and bacteriological parameters of the collected rainwater and its seasonal variability over a period of 14 months. The tested rainwater is characterized by a slightly alkaline reaction, high colour and turbidity (lack of physical stability) and very low hardness and alkalinity, which gives it a corrosive character (lack of chemical stability). The value of the biogenic substances (TOC, nitrogen and phosphorus compounds) indicates a lack of biological stability. The results of this analysis were the basis for determining the suitability of rainwater for its economic use, as well as for developing an innovative device for its pre-treatment. The compact design of this device and the possibility of building various water treatment technologies into its chambers allow it to be adapted to any local conditions, which constitutes its universality.

Despite the results confirming the usefulness of the studied rainwater for its economic use, the simulation studies of the RWHS for the analyzed facility showed that its implementation in the RAS area is not financially profitable. This is primarily due to the small roof area from which rainwater is collected, which in turn determines the amount of water flowing into the reservoir. The designed RWHS covers only about 3% of the annual water demand. This means that to increase the water self-sufficiency of the RAS, it would be necessary to consider other water sources, such as greywater or groundwater. This study can be a significant contribution to the development of water resources management strategies in remote and non-urbanized areas and those where there are problems with the network infrastructure.

Acknowledgments: The research leading to these results has received funding from the commissioned task entitled "VIA CARPATIA Universities of Technology Network named after the President of the Republic of Poland Lech Kaczyński," under the special purpose grant from the Minister of Science, contract no. MEiN/2022/DPI/2578 action entitled "ISKRA – building inter-university research teams."

References

Stec A (2023) Rainwater and Greywater as Alternative Water Resources: Public Perception and Acceptability. Case Study in Twelve Countries in the World. Water Resources Management 37(13):1-23. http://dx.doi.org/10.1007/s11269-023-03594-x.

de Sá Silva A, Bimbato A, Balestieri J, Vilanova M (2022) Exploring environmental, economic and social aspects of rainwater harvesting systems: A review. Sustainable Cities and Society 76, 103475. https://doi.org/10.1016/j.scs.2021.103475.

Thapa A, Khanal G, Mahapatra S, Devkota N, Mahato S, Paudel U (2022) Identifying determinants of sustainable water management at the household level through rainwater harvesting systems in Nepal. Water Policy 24 (10):1676–1691. https://doi.org/10.2166/wp.2022.113.

Stephan A, Stephan L 2017 Life cycle water, energy and cost analysis of multiple water harvesting and management measures for apartment buildings in a Mediterranean climate. Sustainable Cities and Society 32:584-603. https://doi.org/10.1016/j.scs.2017.05.004.

Słyś D, Stec A (2020) Centralized or Decentralized Rainwater Harvesting Systems: A Case Study. Resources 9(1), 5. https://doi.org/10.3390/resources9010005.

UN 2024. The United Nations, & The Division for Sustainable Development Goals. Sustainable development goals. https://sdgs.un.org/goals (accessed on 27 November 2024).

Słyś D (2009) Potential of rainwater utilization in residential housing in Poland. Water and Environment Journal 23:318–25. https://doi.org/10.1111/j.1747-6593.2008.00159.x.

Zdeb M, Zamorska J, Papciak D, Słyś D (2020) The Quality of Rainwater Collected from Roofs and the Possibility of Its Economic Use. Resources 9, 12. https://doi.org/10.3390/resources9020012.

Impact of LID area segments and design storms on optimal LID combinations

J.H. Lee, S.T. Chae, I. Park, E.S. Chung*
Faculty of Civil Engineering, Seoul National University of Science and Technology, 232 Gongneung-ro, Nowon-gu, Seoul 01811, Korea
** e-mail: eschung@seoultech.ac.kr*

Introduction

The changes in rainfall patterns and intensities caused by climate change are leading to severe flood damage in various regions. The Low Impact Development (LID) is a concept for managing stormwater within watersheds, aiming to restore the natural hydrological cycle to pre-development conditions by increasing the permeable areas in urban watersheds. Various studies have demonstrated the flood mitigation effectiveness of individual LID measures (Li et al. 2019; Chae et al. 2024), but their efficiency can be further maximized through optimal combinations (Gao et al. 2021).

When determining the optimal LID combination, each LID measure may have upper and lower bounds for the allocable area, and the optimal area for each measure in the combination can be derived within this range (Yang et al. 2023). However, the area ranges of individual LIDs for the optimal combination can be determined differently based on the land use characteristics and cost efficiency of the study area. Previous studies have analyzed the optimal LID combinations under specific design storm conditions and within the area ranges of LID practices. However, varying area ranges can directly affect the effectiveness of individual LID measures in restoring the water cycle, thereby influencing the results of the optimal LID combination. For the same reason, an increase in the return period of the design storm can also be a key factor that reduces the efficiency of LID measures. Therefore, this study aims to comprehensively analyze the impact of the varying area ranges of individual LID facilities, divided into segments, and the magnitude of the design storm on the optimal LID combination.

Materials and methods

Optimization algorithm

Differential evolution (DE) algorithm was used for calibrating the storm water management model (SWMM) and optimizing the design parameters of five LID measures (BC, GR, IT, PP, and RG) The DE algorithm generates trial mutations (Vi,g) using three randomly selected parameter vectors (xro,g, xr1,g, and xr2,g), leading the parameter values to converge toward the optimal solution through the mutation process. The F is the differential weighting factor, which takes a value between 0 and 1.

$$V_{i,g}=x_{ro,g}+F(x_{r1,g}-x_{r2,g}) \quad (1)$$

Design rainfall

The design storm for the study area was determined based on rainfall intensities for each return period specified in the Comprehensive Watershed Management Report. The design storm considered 10-, 30-, and 50-year return periods, and the Huff dimensionless curve was used to distribute the rainfall over a 6-hour duration. The rainfall intensity (I) for a 10-year return period with a 6-hour rainfall duration (t) can be calculated as below:

$$I=1666.1/(t+64.8)^{0.7171} \quad (2)$$

Selection of optimal LID combination

The optimal LID combinations were determined to minimize total runoff and peak runoff within the watershed. For each sub-catchment, weights (Wj) for LID measures were set from 0 to 1 in increments of 0.1, and only combinations with a total weight of 1 were considered, resulting in 921 scenarios. The

assignable area for each LID measures (ALID,j) was calculated based on budget cases (Btot) (C1-C11) and unit installation costs for each facility (CLID,j)as below:

$$A_{LID,j}=w_j B_{total}/C_{LID,j} \quad (3)$$

Since the areas of the 31 sub-catchments vary, the assignable area ranges for each LID facility differed across sub-catchments and budget cases. For all 921 scenarios, total runoff and peak runoff were calculated, and the scenario with the lowest average of the normalized values was selected as the optimal combination. To achieve this, a total of 28,551 simulations were conducted for the 31 sub-catchments.

Results and concluding remarks

The optimal LID combinations were derived based on 31 sub-catchments and 11 cost cases, resulting in a total of 341 combinations. Each case was assigned a number, ordered by the increasing upper bounds of LID areas.

While the upper bounds of LID areas increased with the case numbers, the optimal combinations varied, indicating that specific thresholds (area ranges) exist where individual LID measures achieve their highest efficiency. The 341 cases were classified into three area segments, S1, S2, and S3, based on these thresholds (see Table 1). In S1, IT and PP dominated, with minimal contributions from RG and BC. In S2, RG's influence increased, and in S3, BC became a significant part of the optimal combination. These thresholds tended to shift to higher values as the design storm return period increased.

The findings of this study provide comprehensive insights into the impact of varying area ranges and design storms on the optimal LID combinations.

Table 1. The dominant LID in the optimal LID combination selected from the area range of LID measures

Design Rainfall	Segment	Case No	Dominant LID in combination	Maximum installation area % of LIDs				
				BC	GR	IT	PP	RG
10yr6hr	S1	1	IT,PP	0.14	0.21	0.19	0.35	0.21
	S2	122	RG	1.63	2.44	2.22	4.08	2.5
	S3	246	RG,BC	5.05	7.58	6.9	12.66	7.77
	>S3	322	PP	15.79	23.68	21.56	39.58	24.29
30yr6hr	S1	1	IT,PP	0.14	0.21	0.19	0.35	0.21
	S2	208	RG	3.51	5.26	4.79	8.8	5.4
	S3	302	RG,BC	10.27	15.41	14.03	25.76	15.81
	>S3	330	PP	22.03	33.04	30.09	55.24	33.89
50yr6hr	S1	1	IT,PP	0.14	0.21	0.19	0.35	0.21
	S2	226	RG	4.11	6.16	5.61	10.3	6.32
	S3	318	RG,BC	14.21	21.31	19.41	35.62	21.86
	>S3	322	PP	15.79	23.68	21.56	39.58	24.29

Acknowledgments: This research was also supported by Korea Environment Industry & Technology Institute (KEITI) through R&D Program for Innovative Flood Protection Technologies against Climate Crisis Program (or Project), funded by Korea Ministry of Environment (MOE) (RS-2023-00218873).

References

Chae ST, Chung ES, Jiang J (2024) Enhancing Water Cycle Restoration through LID Practices Considering Climate Change: A Study on Permeable Pavement Planning by an Iterative MCDM Model. Water Resources Management 38: 3413-3428. https://doi.org/10.1007/s11269-024-03821-z

Gao J, Li J, Li Y, Xia J, Lv P (2021) A distribution optimization method of typical LID facilities for sponge city construction. Ecohydrology & Hydrobiology 21(1): 13-22. https://doi.org/10.1016/j.ecohyd.2020.09.003

Li C, Peng C, Chiang P-C, Cai Y, Wang, Yang Z (2019) Mechanisms and applications of green infrastructure practices for stormwater control: A review. Journal of Hydrology 568: 626-637. https://doi.org/10.1016/j.jhydrol.2018.10.074

Yang B, Zhang T, Li J, Feng P, Miao Y (2023) Optimal designs of LID based on LID experiments and SWMM for a small-scale community in Tianjin, north China. Journal of Environmental Management 334: 117442. https://doi.org/10.1016/j.jenvman.2023.117442

Modelling scenarios for sustainable water supply and demand in Annaba city, Algeria

S. Hani[1], I.E. Bouznad[2], N. Guezgouz[3], A. Hani[1], S. Lallahem[4]
[1] Laboratory of Water Resources and Sustainable Development, Badji Mokhtar Annaba University, 23000, Algeria
[2] University 8 May 1945 Guelma, Algeria
[3] Mohamed Cherif Mesaidia Souk Ahras University, Algeria
[4] IXSANE, Parc des Moulins 23 Avenue de la Créativité - 59650 Villeneuve d'Ascq- France.
* e-mail: samir.hanidz@gmail.com

Introduction

The Annaba region is currently facing a serious water shortage. It is also distinguished by numerous conflicts of use between farmers, manufacturers and drinking water distribution services. In addition, the demand for water continues to increase due to its significant demographic and socio-economic growth (Berredjem and Hani 2017; Berredjem et al. 2023 ; Hamlat et al. 2012 ; Choi et al. 2012 ; Daifallah et al. 2018). This research involves taking into consideration the upcoming operation of a desalination plant and the start-up of a wastewater treatment plant. It also involves comparing water resources and demands using the WEAP model according to several scenarios and over a period from 2010 – 2050.

Materials and Methods

The site studied corresponds to the Annaba region, located in the North-East of Algeria. Covering an area of 1439 km^2, the region is characterized by a Mediterranean climate marked by a mild and humid winter as well as a hot and dry summer. The annual rainfall is around 660 mm. The population of Annaba is approximately 630.000 inhabitants (2010 census). The useful agricultural areas extend over 48.177 hectares. Industries, concentrated around the town of Annaba, include steel, chemical fertilizers, tomato processing, metal processing and dairy products. ... In this research, WEAP software is used. It makes it possible to compare resources and needs according to several management scenarios. Beforehand, it is necessary to enter data relating to:

- Domestic demand sites, corresponding to the number of inhabitants for the reference year (2010), the growth rate and the allocation of 150 liters/day/inhabitant.
- Agricultural demand sites represented by the areas of irrigated land (2010) and the allocation of 5000 m^3/hectare/year.
- Industrial demand sites corresponding to the annual water consumption rate of industrial areas.
- Conventional water resources represented by surface water resources (El-Tarf dams and hill reservoirs) and underground water resources (drillings, wells and springs).
- Unconventional water resources including the K. Eddraouche Desalination Plant, SDEM, and the Allélick Wastewater Treatment Plant, STEP.

Furthermore, the application of WEAP requires the development of key scenarios and hypotheses:

- Reference scenario (S-R): with a population increase of 1% and an increase in irrigated areas and industrial units of 1%.
- Resource pressure scenario (S-PR): with a population growth rate of 3% and an increase of 2% in irrigated areas and 2% in industrial water needs.
- Seawater desalination scenario (S-DEM): with a future contribution of 160,000 m3/d for AEP in the Annaba region (early 2025).
- Demand Management Scenario (S-GD): with a reduction in leakage rates of 20%, a water saving of 20% for AEP and AEI, and 30% for irrigation. Reuse water from the STEP for industry and agriculture.
- Combined Scenario (S-PR-GD-DEM): by combining all the scenarios.

Results and concluding remarks

Calibration was performed by mapping flow data into the model Recorded at the Meerbeek station for the period 1984-1999. To validate the model, Nash and correlation coefficients were used Applied.

The Nash-Sutcliffe coefficient, NSE, is 0.86, which represents the difference between simulation and simulation Low measurement. The correlation coefficient is 0.93. The results obtained

Thus show good performance of the model. WEAP perfectly simulates the hydrological response of the basin.With a growth rate of 1%, the population would increase from 628.565 (2010) to 899.491 inhabitants (2050) and with 3%, it would reach 2.050.402 inhabitants. Irrigated areas increase from 4.528 hectares (2010) to 6.742 hectares (2050) with a growth rate of 1% and to 10.000 hectares (2050) with a rate of 2%.

The histogram of unmet demand in Figure 1 shows that if no action is taken by managers, the deficit would increase from 17 million m^3 (2010) to 170 million m^3 (2050). According to the results of the simulation of the seawater desalination scenario (S-DEM), the drinking water supply (AEP) of the region would no longer pose a major problem as soon as the desalination plant starts up, early 2025.

Furthermore, the demand management scenario (S-GD) showed the efficiency of the use of water from the STEP for industrial water supply by demonstrating total satisfaction of its water demand, unlike the agricultural needs which require additional supply from the future Mahcha water tank, currently under construction.

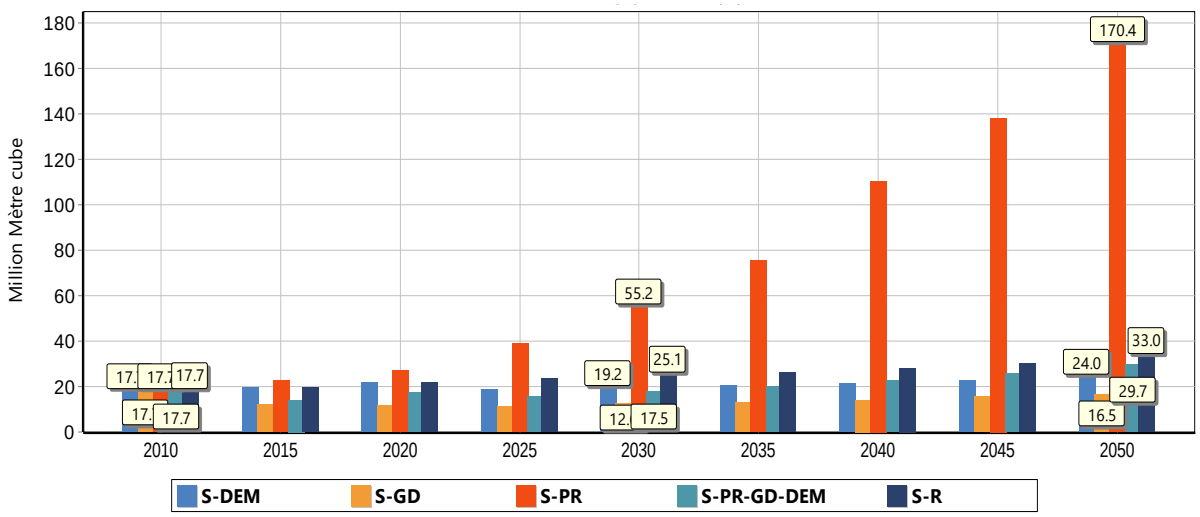


Figure 1. Evolution of global Unmet Demand (DNS).

Acknowledgments: We thank the Annaba Integrated Water Resources Management Agency for their assistance and all the data provided.

References

Berredjem AF, Hani A (2017) Modelling current and future supply and water demand in the northern region of the Seybouse Valley. Journal Of Water And Land Development. 2017, No. 33 (IV–VI): 31–38. DOI: 10.1515/jwld-2017-0016

Berredjem AF, Boumaiza A, Hani A (2023) Simulation of current and future water demands using the WEAP model in the Annaba province, Northeastern Algeria: a case study. AQUA — Water Infrastructure, Ecosystems and Society Vol 72 No 9, 1815 doi: 10.2166/aqua.2023.118

Choi S-J, Kim J-H, Lee D-R (2012) Decision of the Water Shortage Mitigation Policy Using Multi-criteria Decision Analysis, KSCE Journal of Civil Engineering, Volume 16, Issue 2, pp 247-253,

Daifallah T, Hani A (2018) Water Demand Management is Solution of Water Stress? A Case Study of the Kebir-West River Basin in Northern Algeria. Water and energy international. Pp. 62-69.

Hamlat A, Errih M, Guidoum A (2012) Simulation of water resources management scenarios in western Algeria watersheds using WEAP model. Arabian Journal of Geosciences. Volume 6, Issue 7, pp 2225-2236.

RICHWATER nutrients calculation tool for water and fertilizers sustainable and adaptive management

A.M. Lorenzo-López[1,2*], R. Casielles[1], Á. García[1]
[1] BIOAZUL SL, Málaga, Spain
[2] Universidad de Córdoba & WEARE research group, Spain
* e-mail: alorenzo@bioazul.com

Introduction

This research aims to advance sustainable agricultural practices in La Axarquía (Spain), a region facing severe water scarcity. In recent years, reclaimed water has been increasingly used as an irrigation source. Compared to conventional irrigation water, reclaimed water contains higher levels of nutrients, offering the potential to reduce the use of chemical fertilizers. However, inadequate nutrient management may result in unintended environmental impacts. This study evaluates the potential benefits of optimized fertilization for mango crops using reclaimed water.

Materials and methods

The RICHWATER fertilizer optimization tool was developed within the BONEX project and tested in autumn 2024 using data from an experimental mango plot in Algarrobo, a municipality in the La Axarquía region of Málaga (Southern Spain). This area has a hot, dry Mediterranean climate (Köppen-Geiger classification Csa), with an average annual temperature of 18 °C and annual precipitation of 471 mm, concentrated mainly in winter (IFAPA, n.d.). The 200 m² experimental plot is located at 14 m above sea level (36°45'11"N, 4°2'55"O).

The RICHWATER tool is designed to optimize fertilizer application and minimize diffuse pollution by aligning crop nutrient needs with the nutrient content of reclaimed water used exclusively for irrigation. It considers three key variables: (i) the crop's nutritional demand, based on monthly fertilization plans provided by TROPS, a regional cooperative; (ii) nutrient inputs from reclaimed water, determined through regular laboratory analyses and standardized for consistency across different chemical forms and units; and (iii) the composition of commercial fertilizers, selected from a regional database with consideration for cost and electrical conductivity constraints. Together, these components enable precise nutrient balancing and adaptive fertilization strategies.

Weekly or monthly adjustments are possible, allowing adaptation to seasonal changes in water quality. The tool also considers cost and salinity constraints, supporting sustainable nutrient management in water-scarce agroecosystems.

Results and concluding remarks

Optimized fertilization plans have been developed using the RICHWATER tool by combining reclaimed water with commercial fertilizers to meet the nutritional needs of the crop. These plans significantly reduce the need for chemical fertilizers, resulting in lower costs and contributing to the reduction of diffuse pollution caused by over-fertilization.

Figure 1a shows the percentage of crop nutrition supplied by reclaimed water relative to the nutritional demands of the mango crop. This percentage depends on both the nutrient requirements of the plants and the volume of reclaimed water used for irrigation.

As illustrated in Figure 1b, there is an overall reduction in environmental contamination. During the fertilization period (April - September), nutrient surplus is eliminated. However, some unavoidable nutrient excess persists during the months when the crop does not require fertilization but nutrients are still introduced through reclaimed water irrigation. In summary, pollution is minimized as much as possible.

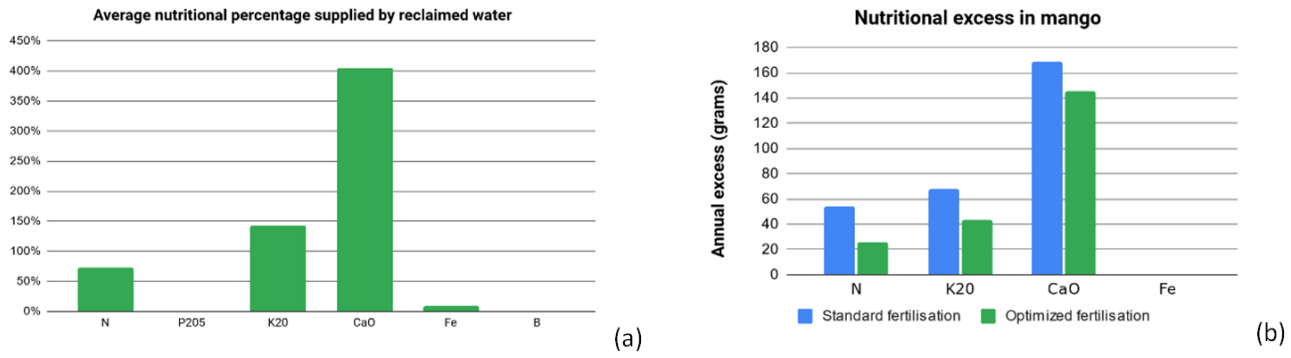


Figure 1. (a) Average nutritional content supplied by reclaimed water (%); (b) Nutritional excess comparison in mango

Table 1 shows the savings comparing standard (T1) and optimized (T2) fertilization schemes.

Table 1. Saving by using reclaimed water for mangoes irrigation.

Mango	T1 (€/tree)	T2 (€/tree)	Saving (%)
April	0.111	0.033	71
May	0.111	0.032	71
June	0.069	0.047	33
July	0.026	0.000	100
August	0.026	0.004	87
September	0.026	0.004	86
Total	**0.370**	**0.119**	

Based on the work conducted, the following conclusions can be drawn:

- The use of the RICHWATER tool significantly reduces dependence on chemical fertilizers by providing optimal fertilization plans when irrigating with reclaimed water. This results in average cost savings of 75%, enhances the competitiveness of the agricultural sector, and lowers CO_2 emissions associated with chemical fertilizer production.
- Optimized fertilization plans minimize nutrient excess during fertilization periods and reduce environmental contamination throughout the year. Although some nutrient surpluses persist, the overall impact of nutrient runoff is substantially mitigated, supporting more sustainable farming practices.
- The tool's adaptable design allows for its application across various crops and regions. Its successful implementation in La Axarquía, a water-scarce area, demonstrates its potential to foster sustainable agricultural practices globally.

Acknowledgments: this study is supported by PRIMA Programme, as part of the BONEX project "Boosting Nexus Framework Implementation in the Mediterranean", grant agreement 2141, financed by Horizon 2020 (European Union). The authors would like to thank TROPs for the provided information.

References

Chojnacka K., A. Witek-Krowiak, K. Moustakas, D. Skrzypczak, K. Mikula, M. Loizidou, A transition from conventional irrigation to fertigation with reclaimed wastewater: Prospects and challenges, Renewable and Sustainable Energy Reviews, Volume 130, 2020, 109959, ISSN 1364-0321, https://doi.org/10.1016/j.rser.2020.109959.

Instituto de Investigación y Formación Agraria y Pesquera. Estación Meteorológica de Vélez-Málaga. IFAPA. https://www.juntadeandalucia.es/agriculturaypesca/ifapa/riaweb/web/estacion/29/2

Maestre-Valero J.F., M.J. Gonzalez-Ortega, V. Martinez-Alvarez, B. Gallego-Elvira, F.J. Conesa-Jodar, B. Martin-Gorriz, Revaluing the nutrition potential of reclaimed water for irrigation in southeastern Spain, Agricultural Water Management, Volume 218, 2019, Pages 174-181, ISSN 0378-3774, https://doi.org/10.1016/j.agwat.2019.03.050.

Vivaldi G.A., Zaccaria D., Camposeo S., Pasanisi F., Salcedo F P., Portoghese I. (2022). Appraising water and nutrient recovery for perennial crops irrigated with reclaimed water in Mediterranean areas through an index-based approach. Science of the Total Environment, 820, 152890., https://doi.org/10.1016/j.scitotenv.2021.152890

Comparative models of sustainable urban drainage systems in a watershed in central Mexico

L. Lizárraga-Mendiola[1*], O.S. Areu-Rangel[1], G.A. Vázquez-Rodríguez[2], J.R. Pérez-Hernández[1], C.M. López-León[1]
[1] Area Academica de Ingenieria y Arquitectura, Universidad Autonoma del Estado de Hidalgo, Pachuca, Mexico
[2] Area Academica de Quimica, Universidad Autonoma del Estado de Hidalgo, Pachuca, Mexico
* e-mail: mendiola@uaeh.edu.mx

Introduction

Urban runoff management in highly urbanized watersheds is a critical challenge in adapting to climate change and accelerated urban growth. This challenge has led to exploring alternatives, such as sustainable urban drainage systems (SUDS) based on the natural water cycle in urban environments (Courty, 2021). In an urbanized area of central Mexico, recurrent flooding has exposed the ineffectiveness of traditional drainage systems. This work proposes two approaches to promote infiltration into the subsoil and mitigate runoff by implementing SUDS. The first approach evaluates green roofs and permeable pavements in isolation and in combination. As our research shows, these solutions are not just theoretical concepts but practical tools in the fight against urban flooding. In addition, alternatives are proposed for selecting spaces where these proposals are more suitable, depending on the distribution of rainfall intensity throughout the watershed. The second approach considers multiple SUDS that can be adapted in public spaces and roadways, such as infiltration trenches, rain gardens, and permeable pavement. In the second case, their hydraulic feasibility was evaluated by modeling using the software SWMM V.5.2 (EPA, 2023). Our main objective was to evaluate and compare the effectiveness of both SUDS implementation approaches in the watershed to mitigate flooding through sustainable urban runoff management.

Materials and methods

The study area is located between parallels 19°30′ and 19°35′ north latitude and meridians 99°05′ and 99°15′ west longitude, at an altitude between 2200 and 2800 meters above sea level (INEGI, 2010). The watershed area was delimited (6,194,211 m^2), and the average slope was 6.5% with an NW-SE orientation (Figure 1). 98% of its surface is mainly urbanized (5,626,018 m^2), and 2% is considered permeable (568,193 m^2).

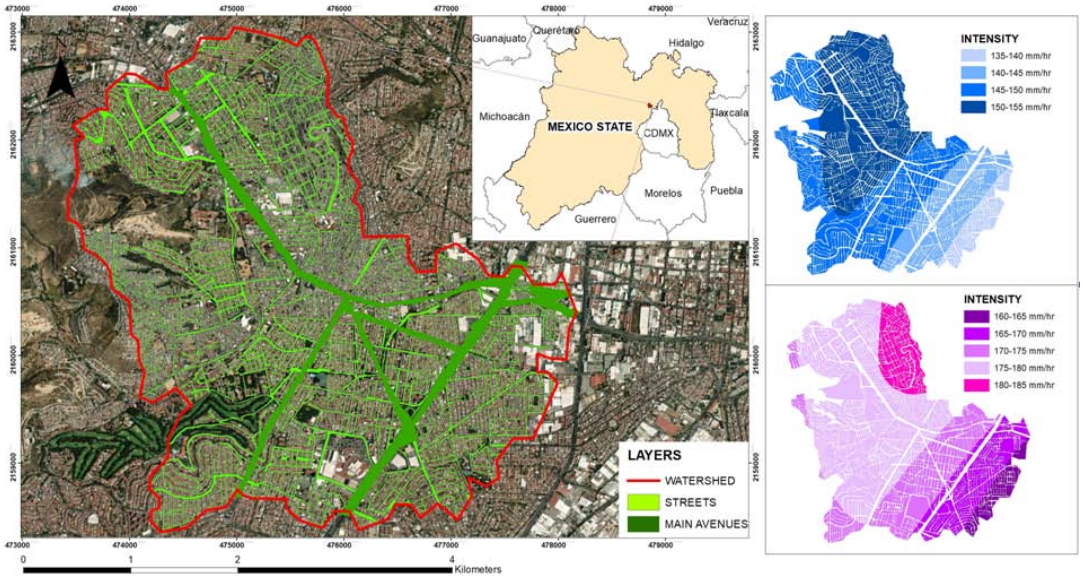


Figure 1. Location of the study area and delimitation of the watershed.

The predominant climate is temperate and sub-humid, with an average humidity of 16.71%. Annual rainfall ranges between 500 and 800 mm, and the average annual temperature is 16.5 °C (CLIMA, 2020). A hydrological analysis of the natural behavior of runoff in the watershed was performed. The watershed (Figure 1) was obtained using the Global Mapper V.19.0 software and the SIATL V.4 platform (INEGI, n.d.). The SUDS most easily adaptable to the available land uses were selected, as well as the criteria for their design (for example, area, thickness, infiltration coefficient, vegetation type, local slope, and Manning's coefficient, among others). In the first approach, rainfall intensity distribution was evaluated for a return period (R_p= 10 years) suggested for urban hydraulic works (CONAGUA, 2019). The hydraulic feasibility was evaluated based on such distribution to select suitable SUDS and their most appropriate location. The second approach simulated a storm event for the same 10-year R_p. Employing SWMM V.5.2 software (EPA, 2023), the hydraulic efficiency of the proposed SUDS to manage peak discharge was evaluated. The runoff behavior was compared with the current conditions, and the proposed hydraulic infrastructure distributed in the watershed and its flood mitigation potential were evaluated.

Results and concluding remarks

The following is a synthesis of the most relevant findings and a comparative analysis of the proposals.

Approach 1: For a R_p= 10 years and rainfall intensity of 175-180 mm/h (1 hour event), if only green roofs were implemented, the ideal zone would be the central-northern part of the watershed. This zone covers an area of 20.70% of the total surface and can intercept up to 51.43% of the rainfall volume. If permeable pavement is chosen for secondary roads, the suitable zone for adaptation is the center-northwest, which covers 26.94% of the total area of the watershed and can manage 51.83% of the runoff through infiltration. Finally, if both proposals are combined in the central-northwest zone. In that case, it is possible to intercept 52.97% of the total volume in an effective surface area equivalent to 52.14% of the watershed area. The combination of SUDS represents the best alternative regarding spatial distribution, available surface area in the watershed, and its capacity to mitigate flooding. In another research, authors have demonstrated that the interconnection of SUDS through their spatial distribution along the predominant runoff path is a key factor in mitigating floods (Ma et al., 2022).

Approach 2: Based on the simulated runoff model for the same R_p (1 hour event), it is observed that the SUDS proposals (infiltration trenches, rain gardens, among others) located in public spaces, such as green areas, medians, and secondary roads with slopes, can manage 4.76% of the total volume of rainfall analyzed in this study. This volume represents 0.74% of the cumulative volume of the watershed, so their capacity to mitigate flooding and promote infiltration could increase if other sustainable intervention measures are proposed (Jaca-Pozzi and Angheben, 2023). Individually, these SUDS' cumulative volume can intercept is equivalent to 3.83%, while the volume infiltrated through the permeable areas is 0.93%. As we can interpret from these two approaches, if a preliminary evaluation is carried out to identify areas where it is more viable to implement these sustainable proposals, it is possible to maximize their hydraulic efficiency.

Conclusions: This work's limitations included evaluating the watershed generally since the mapping was done digitally, and the parameters used to design SUDS may not be accurate. Moreover, the evaluation results may vary significantly if the design of SUDS is tailored more closely to the specific characteristics and spatial variability of the available land and existing infrastructure. Therefore, these limitations should be carefully considered when interpreting the findings of this study.

References

CONAGUA (Comisión Nacional del Agua) (2019) Manual de agua potable, alcantarillado y saneamiento-Drenaje Pluvial Urbano. ISBN: 978-607-626- 019-7.

CLIMA (2020) Clima Tlalnepantla de Baz-México. Access from: https://es.climate-data.org/america-delnorte/mexico/mexico/tlalnepantla-766169/#google_vignette

Courty LG (2021) Hacia una gestión de las aguas urbanas basada en la naturaleza. Perspectivas IMTA, 6: 1-3.

EPA (Environmental Protection Agency) (2023) Storm Water Management Model (SWMM). Access from: https://www.epa.gov/water-research/storm-water-managementmodel-swmm

INEGI (s.f.) Simulador de flujos de agua de cuencas hidrográficas. Access from: https://antares.inegi.org.mx /analisis/red_hidro/siatl/

Jaca-Pozzi G, Angheben E (2023) Diseño de un sistema de desagües urbanos sostenibles (SUDS) en un barrio del Conurbano Bonaerense. En VII Jornadas de Investigación, Transferencia y Extensión de la Facultad de Ingeniería (La Plata, 25 al 27 de abril de 2023).

Ma Y, Xia X, Liang Q, Wan H (2022) Investigating the Impact of Spatial Distribution of Sustainable Drainage System (SuDS) Components on Their Flood Mitigation Performance in Communities with High Groundwater Levels. Water, 14(9): 1367.

River velocity distribution and discharge estimation using entropy theory: an application at river site in Central Apennines (Italy)

E. Boscariol[1], S. Passaretti[1], M. Lapomarda[1], E. Volpi[2], C. Mineo[1*], A. Trotta[1]
[1] ACEA Ato2 SpA, Department of Water Resource Protection, Rome, Italy
[2] Department of Engineering, University Roma Tre, Rome, Italy
* e-mail: claudio.mineo@aceaspa.it

Introduction

A major challenge in monitoring water availability is the collection of time-continuous river discharge series. Traditional methods of measuring river discharge, such as the definition of stage-discharge curve, can present several practical problems, both due to the changing characteristics of the river site and the feasibility of consistent wading measurement (Bahmanpouri et al., 2024). Even the use of remote sensors may not be effective if the river site exhibits changes in hydraulic regimes and channel morphology over time (Fulton et al., 2020). These issues are of interest to a wide range of stakeholders whose goal is the provision of water resources while preserving natural ecosystems. In addition, an accurate assessment of river flow has become a key issue in research due to the increasing interest in modelling drought and water scarcity events.

In recent years, researchers have focused on flow estimation methods that combine the use of in situ instruments with probabilistic analyses, such as entropy theory (Chiu, 1987). Efforts have been concentrated on defining algorithms that require fewer input parameters and mainly differ in the method of estimating the dip phenomenon along the cross-section (Moramarco et al., 2004; Moramarco et al., 2017; Bahmanpouri et al., 2022; Kumar Vyas et al., 2024).

We moved from these studies to implement the process and to estimate river discharge in real-time, relying only on a single pair of surface velocity and stage measurements. According to entropy theory, the hydraulic characteristics of a river site (i.e. surface velocity profile, bathymetry profile, dip distribution) are statistically evaluated by serial measurements obtained with a current meter, while the maximum surface velocity and the associated water depth are continuously provided by in situ instruments. Finally, a discharge abacus is defined within the observation range of the historical data to provide continuous time series of discharge.

Materials and methods

The study focuses on the Rio Peschiera site, which rises from the Peschiera springs fed by Nuria-Velino Mts regional aquifer in the Central Apennines (Italy). Peschiera springs are one of the largest karst springs in Europe and the major spring system of the water supply system managed by ACEA Ato2 SpA, a water utility which operates in Central Italy supplying drinking water to approximately 4 million users in the city of Rome and its hinterland. With the aim of operating sustainable management of water resources, ACEA Ato2 SpA monitors Rio Peschiera through periodic stream discharge measurements by wading. In the recent past, attempts have been made to calibrate stage flow curves or use sensors to calculate flow, but neither method has proved sufficiently reliable. This includes the continuation of wading measurement campaigns, which have proven to be a useful monitoring tool, but do not allow for continuous recording of discharge values. Therefore, the aim of this study is to overcome these problems and implement a reliable flow measurement system for the river section under consideration.

The proposed method for evaluating river discharge is based on entropy-based velocity distribution equation such as simplified by Moramarco et al. (2004). A surface velocity instrument (i.e. a flowmeter) is installed near the mid-channel where the maximum velocity occurs. For the selected river stage, the flowmeter provides continuous measurements of surface velocity and water depth.

Historical dataset consists of monthly wading measurements recorded over the course of one year,

during which different hydraulic regimes were sampled due to variations in flow and riparian vegetation. Pairs of mean flow and maximum flow velocity records allowed the calibration of the entropic parameter: this has been shown to represent an equilibrium constant, invariant under flow conditions (Moramarco et al., 2017). Therefore, we propose an iterative approach that minimizes the error in the entropic parameter for reconstructing the cross-sectional velocity distribution and subsequently determining the river discharge using the velocity-area method starting only from measured surface velocity and water level.

Results and concluding remarks

Figure 1 presents a comparison between the current meter data and the proposed method results. Considering all the wading measurements carried out, the mean percentage error in estimating the discharge is approximately 4%. By extending the application of the method to pairs of surface velocities and water levels within the respective historical ranges, it is possible to infer an abacus that allows real-time discharge estimation for operational purposes.

Nowadays the method is calibrated on a limited number of wading measurements: the prosecution of the study is envisaged to evaluate the reliability of the model to monitor the effectiveness of the continuous flow estimate.

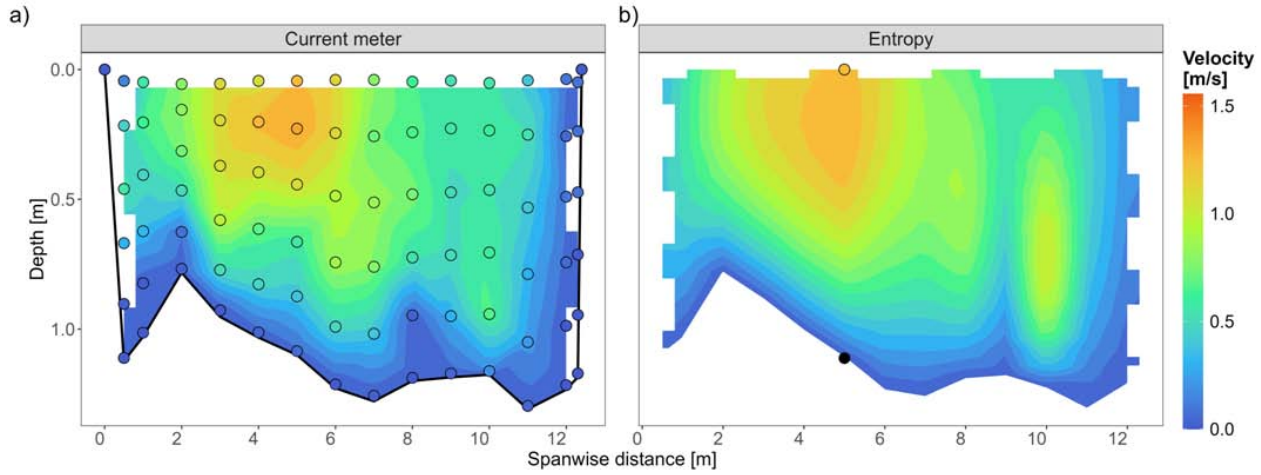


Figure 1. Cross-sectional velocity distribution of Rio Peschiera (a) sampled and (b) entropy theory reconstructed. In (a) circles represent the point where velocity is sampled at each stage of the cross section by means of current meter. In (b) circles represent the point where the superficial velocity and the water depth are evaluated by means of flowmeter.

Acknowledgments: Authors are grateful to Silvia Bernardini for her valuable contribution to the acquisition of the wading measurement data.

References

Bahmanpouri, F., Eltner, A., Barbetta, S., Bertalan, L., & Moramarco, T. (2022). Estimating the Average River Cross-Section Velocity by Observing Only One Surface Velocity Value and Calibrating the Entropic Parameter. Water Resources Research, 58(10). https://doi.org/10.1029/2021WR031821

Bahmanpouri, F., Lazzarin, T., Barbetta, S., Moramarco, T., & Viero, D. P. (2024). Estimating velocity distribution and flood discharge at river bridges using entropy theory - Insights from computational fluid dynamics flow fields.

Chiu, C. L. (1987). Entropy and probability concepts in hydraulics. Journal of Hydraulic Engineering, 113(5), 583-599.

Fulton, J. W., Mason, C. A., Eggleston, J. R., Nicotra, M. J., Chiu, C. L., Henneberg, M. F., Best, H. R., Cederberg, J. R., Holnbeck, S. R., Lotspeich, R. R., Laveau, C. D., Moramarco, T., Jones, M. E., Gourley, J. J., & Wasielewski, D. (2020). Near-field remote sensing of surface velocity and river discharge using radars and the probability concept at 10 U.S. geological survey streamgages. Remote Sensing, 12(8). https://doi.org/10.3390/RS12081296

Kumar Vyas, J., Perumal, M., & Moramarco, T. (2024). Non-contact discharge estimation at a river site by using only the maximum surface flow velocity. Journal of Hydrology, 638. https://doi.org/10.1016/j.jhydrol.2024.131505

Moramarco, T., Barbetta, S., & Tarpanelli, A. (2017). From surface flow velocity measurements to discharge assessment by the entropy theory. Water (Switzerland), 9(2). https://doi.org/10.3390/w9020120

Moramarco, T., Saltalippi, C., Singh, V. P. (2004). Estimation of Mean Velocity in Natural Channels Based on Chiu's Velocity Distribution Equation. Journal of Hydrologic Engineering, 9(1), 42-50. https://doi.org/10.1061/ASCE1084-069920049:142

Supervised approaches for a sustainable water resources management: Forecasting and "similarity" procedure

S. Passaretti[1], N. Guyennon[2], C. Mineo[1*], E. Boscariol[1], A.B. Petrangeli[2], A. Varriale[1], E. Romano[2]
[1] ACEA Ato2 SpA, Department of Water Resource Protection, Rome, Italy
[2] National Research Council of Italy, Water Research Institute, IRSA-CNR, Rome, Italy
* e-mail: claudio.mineo@aceaspa.it

Introduction

The assessment of water availability is a key issue in a water supply system because of increasing drought and water scarcity events. Analysing and predicting the dynamic behaviour of karst aquifers is challenging to conceptualize and model, especially in poorly-monitored systems.

To characterize the hydrogeological features of karst aquifers and to quantify spring discharge in relation to meteo-climate drivers, one can distinguish between physically-based and empirical (or semi-empirical) approaches or the most recent data-driven models. However, these approaches present some drawbacks limiting their use, especially for management purposes: (i) the limited number of discharge data prevent for a robust calibration; ii) the large number of parameters to estimate poses serious uncertainty concerns related to over-parametrization; (iii) the large amount of data necessary to drive the learning phase.

In a context of participative management, it is worth noting that simpler approaches based on linear or multi-linear relations are advisable. These approaches rely on the estimation of the time-dependent cross-correlation between precipitation or recharge and discharge to define the system response (Fiorillo and Doglioni 2010). Advantages of such an approach are mainly attributed to the possibility of implementing automatic and robust procedures, fostering the use of these models by users with a limited background in modelling techniques (Romano et al. 2017).

We moved from these considerations to propose a parsimonious model based on linear regression between the monthly spring discharge time series and Standardized Precipitation Index (SPI) (Guyennon et al. 2024).

The model developed for long-term monitored springs is used to reconstruct the observed hydrographs and to make predictions for poorly monitored springs with similar properties, exploiting the "similarity principle" (Barthel et al. 2021). Moreover, the tool is used to test forecast performance enabling water managers to develop a monthly early-warning system fostering a sustainable water resource exploitation and limiting the critical issues of the water supply system, especially during drought periods. The model is conceived to be adopted in a context of participative water management, mainly addressed to water utilities, who can take advantage from an initial knowledge of the aquifer's hydrological regime, and to foster the involvement of different stakeholders.

Materials and methods

The study focuses on twelve karst springs located in Central Apennine carbonate hydro-structure. Most of the springs are managed by ACEA SpA, a multiutility company which operates mainly in Central Italy, supplying drinking water to more than 9 million users in five Italian regions, including the Umbria region, the city of Rome and a large part of its hinterland.

The model (hereinafter SPIQspring) is based on the simple assumption that the monthly discharge of a karst spring is linearly related to the SPI. The application of SPIQspring implemented by maximizing the Pearson correlation can be considered as "unsupervised" approach (fully automatic and without any explicit operator guidance). Then, two "supervised" applications of the model (user-driven techniques) are performed.

Firstly, a clustering analysis (k-means technique) is performed on the monthly hydrographs of the twelve springs to group them in similar clusters.

The first application explores the possibility to take advantage from the "similarity principle", using a known dataset to assign the calculated parameters (i.e. aggregation SPI scale and delay), to a target spring with a limited number of data and make predictions. The underlying hypothesis is that the degradation of the model's performance is less when using coefficients calibrated on springs belonging to the same cluster rather than using those calibrated on spring itself using a limited amount of data. The second application, hereinafter "forecast approach", allows to select manually the SPI scale and delay based on the correlation matrix between SPIs and observed discharge to optimize the advance in forecasting the low-regime outflow for planning over a time horizon of few months.

Results and concluding remarks

Results from the application of the "similarity principle" point out that when few data (i.e. less than 10 years) are available, it is better to rely on a similar spring for the SPI scale and delay calibration, without reaching the performance obtained by the original SPIQspring applied to the complete dataset.

Results from the application of the "forecast approach" are reported in Figure 1: a manual selection can improve the forecast, with a minimum decrease of the model performance, as illustrated by the black arrow in Figure 1a. This supervised step of calibration aims to both increase and simplify the forecast procedure, as illustrated in Figure 1b for the San Giovenale spring. In fact, by manually adjusting the delay it is possible to forecast at a given month (May in the example of Figure 1b) the spring discharge for the months covering the full period of the expected minimum (September, October and November in Figure 1b).

The use of SPIQspring as forecast tool can constitute a sound basis for the development of early-warning systems of water shortage events, allowing water managers to operate in advance during dry periods, fostering a sustainable water resource exploitation and limiting the critical issues of the water supply.

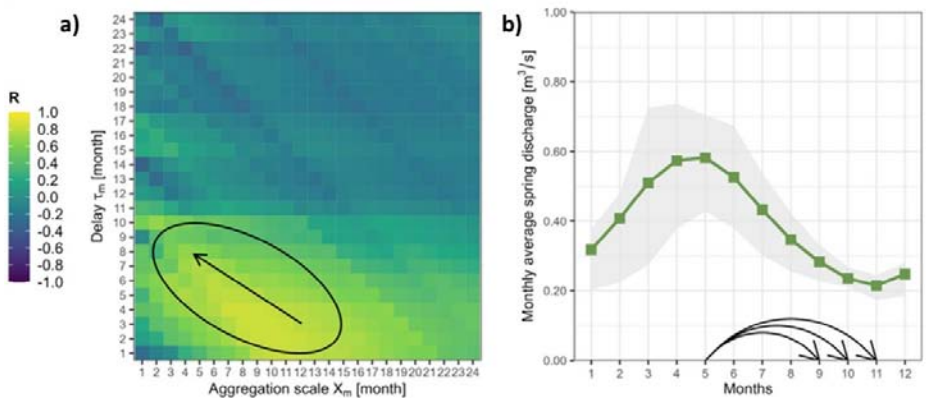


Figure 1. a) correlation matrix between SPI scale (Xm) and delay (τm) to select the best combination while accepting a minimum loss in model performance; b) monthly average hydrograph (grey area represent the range between the 25th and the 75th percentile of the monthly spring discharge time series) and the predictive ability (black arrows).

Acknowledgments: The authors are grateful to Umbra Acque SpA for providing information about the water supply system managed. The research was funded through the agreement "ADAPT - Acea Drought Adaptation Program and knowledge Transfer" between ACEA Ato2 SpA and Water Research Institute, National Research Council of Italy.

References

Barthel R., Haaf E., Giese M., Nygren M., Heudorfer B., Stahl K. (2021). Similarity-based approaches in hydrogeology: proposal of a new concept for data-scarce groundwater resource characterization and prediction. Hydrogeol. J. 29. https://doi.org/10.1007/s10040-021-02358-4

Fiorillo F., Doglioni A. (2010). The relation between karst spring discharge and rainfall by cross-correlation analysis (Campania, southern Italy). Hydrogeol. J. 18 (8), 1881–1895. https://doi.org/10.1007/s10040-010-0666-1.

Guyennon N., Passaretti S., Mineo C., Boscariol E., Petrangeli A. B., Varriale A., Romano E. (2024) A parsimonious model for springs discharge reconstruction and forecast for drought management: Lessons from a case study in Central Italy. Journal of Hydrology: Regional Studies, 56, 102021. https://doi.org/10.1016/j.ejrh.2024.102021

Romano E., Guyennon N., Del Bon A., Petrangeli A.B., Preziosi E. (2017). Robust method to quantify the risk of shortage for water supply systems. J. Hydrol. Eng. 22 (8). https://doi.org/10.1061/(asce)he.1943-5584.0001540

Estimation of the current and future potential sediment transport capacity of the Ebro River

L. Garrote[1*], D. Santillán[1], F. Martin-Carrasco[1], A. Iglesias[2]
[1] Department of Hydraulics, Energy and Environment, Universidad Politécnica de Madrid, Madrid, Spain
[2] Department of Agricultural Economics, Universidad Politécnica de Madrid, Madrid, Spain
* e-mail: l.garrote@upm.es

Introduction

The Ebro Basin, located in the northeastern region of the Iberian Peninsula, spans an area of 85,534 km^2 and is home to around 3.2 million people. The basin's water resources are essential for providing fresh water to the population and sustaining various socioeconomic activities, including industry, agriculture, livestock farming, hydroelectric power generation, refrigeration, aquaculture, navigation, and recreational uses. Over the past decades, human interventions such as dam construction, river channel modifications, and changes in land use have significantly disrupted the natural sediment transport in the Ebro River. These disruptions have led to cascading impacts on the ecological and geomorphological stability of both the Ebro River and its delta. Understanding the complex dynamics of sediment movement within the Ebro River system is crucial for designing effective management strategies to restore sediment flow and mitigate adverse impacts. This study investigates the sediment transport capacity of the Ebro River under historical and projected hydrological conditions. By integrating numerical simulations with historical flow data and estimates of natural flow scenarios, the research evaluates the effects of past and potential future management strategies within the Ebro Basin on the river's sediment transport capacity. The findings enhance understanding of the dynamic relationship between hydrological regimes and sediment transport processes, providing valuable insights for developing strategies to restore sediment flow and improve the ecological balance of the Ebro River.

Materials and methods

The processes of erosion, sediment transport, and sediment deposition in the Ebro River were analyzed through numerical simulations. River simulations were performed with the Iber code (Cea et al. 2007). Hydrodynamic calibration of the model was performed with observation taken during two controlled flood episodes. Sediment transport was calibrated using data compiled by Ibàñez et al. (1996). They provided estimates of the annual transport of suspended sediments for several flow ranges in the Ebro. Data were obtained from Gorria's experiments, conducted in 1877, well before the dam construction period. These data imply a total annual flow 17.38 km^3/yr and sediment transport of 28.1 Mton/yr. Numerical simulations were run for the identified flow regimes, estimating sediment transport parameters to fit the observed data until good agreement was obtained.

The low transport rate currently observed in the Lower Ebro River is due to the lack of availability of sediments. The potential sediment transport that would be available was estimated based on observed flow data and on the sediment transport rating curve derived from numerical simulations. Flow data under actual conditions were obtained from the Tortosa gauging station. Flow data under natural conditions are obtained from the results of the SIMPA model. Estimates of potential sediment transport for future scenarios were obtained using climate projections. The hydrological regime of the Ebro basin was taken from the results of global hydrological models H08 and CWatM, available in the ISIMIP repository. An estimate of the expected future flow of water in the Ebro River under altered conditions was obtained from the results of the AgWaMed project (Garrote et al. 2023). In this project, the potential water availability in the Ebro basin was evaluated in the different climate scenarios. To this end, a simulation model of the management of water resources in the basin was built, in which the maximum demand that could potentially be met at each point was considered. The flow of water circulating through the lower Ebro in

this hypothesis allows us to estimate a lower level of the river's transport capacity, since it assumes the maximum use of the water resources available in each climate scenario.

Results and concluding remarks

Potential sediment transport was estimated by applying the sediment transport rating curve to the monthly flows corresponding to the scenarios. The results obtained in the different scenarios examined are presented in Table 1. The table shows potential sediment transport in the Lower Ebro River in recent (1980-2019) and future time windows (2020-2059 and 2060-2099) under three emission scenarios (SSP1-2.6, SSP3-7.0 and SSP5-8.5). The average potential sediment transport computed with the observed flow in the Tortosa gauging station is 8.96 Mton/yr, much larger than the currently observed sediment flow. This is due to lack of sediment availability, since it is currently trapped in the reservoirs. Ongoing and future efforts for mobilizing sediment transport would allow to increase the sediment flow rate up the obtained upper limit. The estimate of potential sediment transport obtained with the SIMPA model in the last 40 years is 22.68 Mton/yr under natural conditions and 6.26 Mton/yr under altered conditions, a 72% reduction. Global climate models provide an estimate of potential sediment transport between 23.24 Mton/yr (H08) and 38.11 Mton/yr (CWatM). These values get dramatically reduced to 5.97 Mton/yr (a 74% reduction) and 8.98 Mton/yr (a 76% reduction) under altered conditions, respectively.

Table 1. Results of potential sediment transport capacity, in Mt/yr, for the different scenarios examined

Source of flow	obsclim 80-19	ssp126 20-59	ssp370 20-59	ssp585 20-59	ssp126 60-99	ssp370 60-99	ssp585 60-99
Natural SIMPA	22.68						
Natural H08	23.24	15.17	9.93	12.61	16.14	9.38	6.76
Natural CWatM	38.11	36.41	29.26	30.08	37.31	28.35	23.75
Observed in Tortosa	8.91						
Altered SIMPA	6.26						
Altered H08	5.97	4.21	3.21	5.37	4.66	2.68	2.13
Altered CWatM	8.98	9.19	7.16	9.39	10.18	7.37	6.86

The projected reductions in mean annual flow under climate scenarios would dramatically reduce the sediment transport capacity of the Ebro River under natural conditions, due to the nonlinearity of the sediment transport rating curve. Although the H08 and CWatM models produce different absolute figures, the relative projected evolution is similar in both models. In the most likely scenario, SSP3-7.0, the expected reduction in the first period, 2020-2059, ranges between 23% and 57%. The effects for altered conditions are like those for natural flow, but with larger spread between hydrologic models and climate scenarios. In the most likely scenario, SSP3-7.0, the expected reductions projected by H08 model for the first period, 2020-2059, are 46.3%. The reductions projected by the CWatM model are 20.3%. The analysis carried out has made it possible to estimate the effect of the hydrological regime of the Ebro River on the potential capacity of sediment transport. Future projections show a highly uncertain scenario. The main sources of uncertainty of the analysis carried out are the variations between the emission scenarios and between the climate models, the limitations of the hydrological models to capture the real hydrology of the basin and the non-linearity of the relationship between flow and sediment transport capacity.

Acknowledgments: The authors wish to acknowledge funding received from the RESTCOAST project to carry out this research.

References

Cea L., Puertas J., Vázquez-Cendón M.E. (2007) Depth Averaged Modelling of Turbulent Shallow Water Flow with Wet-Dry Fronts. Arch. Comput. Methods Eng., 14, 303–341.

Garrote, L.; Sordo-Ward, A.; Iglesias, A.; Bianucci, P.; Javandel, N. Martin-Carrasco, F. (2023): Assessment of blue and green water availability for agriculture in the Mediterranean. AgWaMed Deliverable 5.1.

Ibàñez C., Prat N., Canicio A. (1996) Changes in the hydrology and sediment transport produced by large dams on the lower Ebro river and its estuary. Regulated Rivers: Research and Management, 12, 51-62.

Sustainable adaptation of urban areas: the case of a Hamburg neighbourhood

A. Bornancin[1], N. Manojlovic[2], A. Marzadri[1*], G. Formetta[1]
[1] Department of Civil, Enviornmental and Mechanical Engineering, University of Trento, Italy
[2] Department Hamburg University of Technology, Hamburg, Germany
* e-mail: alessandra.marzadri@unitn.it

Introduction

Water-related challenges such as: river flooding, stormwater overflow, storm surges and the rising of groundwater levels, triggered by climate change (i.e., with the intensification of the precipitation) have increased the vulnerability of urban areas worldwide (Ferdowsi et al., 2024).

To examine some of this water-climate related stressor and possible adaptation strategies, the present study focuses on the area of Lohbrügge, a neighbourhood of the city of Hamburg (Germany). By its environmental and geographical locations (i.e., located to the Elbe Estuary and thus subject to the tides), the study area is subject to a variety of climate-related hazards and corresponding risks including those of coastal and inland cities. Specifically, to address the need for a resilient urban drainage system able to control the correct functioning of the stormwater sewer during storm surges and urban flooding, a pluvial drainage system has been designed by using Sustainable Urban Design Systems (SuDS, Woods Ballard et al., 2015) elements such as green roofs, permeable pavements, rain barrels and retention basins through the software SWMM (Storm Water Management Mode, Rossman and Simon, 2022). The capability of the integrated drainage network in improving the flood management has been assessed in terms of: stormwater peak flow reduction, increase of soil infiltration and harvest-reuse of rain water for non-potable uses.

Materials and methods

To design the urban drainage system we select a return period of 10 years and through the QGIS plugin "Generate_SWMM_inp" (Schilling and Tränckner, 2022) we generate the SWMM input file. This latter is built in order to contain all the information regarding: the layout of the stormwater system (i.e., junction nodes, outfall nodes, conduits), the characteristics of the sub-catchments where the runoff is generated (i.e., area, width, slope, land use land cover and relative infiltration and soil parameters), the data of the precipitation (German Weather Service provides precipitation data organized by duration and return periods) and the parameters of the numerical solver (i.e., routing model and associated parameters).

A first series of simulations are performed in order to evaluate the critical time of precipitation that maximize the peak flow. This maximum flow is then used to estimate the commercial diameters of the pipes and to verify their correct hydraulic functioning both in terms of routing and in terms of self-cleaning. This configuration represents a Scenario 0 (S0) in which no SuDS have been implemented to simulate the performance of the traditional drainage system.

A second series of simulations are performed in order to evaluate how, through the selection of appropriate SuDS (implemented in SWMM as storage units or Low Impact Development, LID techniques), the drainage system is able to reduce and delay in time the volume of water conveyed by the system. Considering that the 32.38 hectares covered by the study area are residential and consists primarily of small housing units, a few residential complexes, and areas designated for vehicle parking, three types of SuDS elements have been chosen for implementation: extensive green roofs, permeable pavements and rain barrels. The selected SuDS are the result of an assessment that takes into account effectiveness in terms of runoff reduction and feasibility of application. In order to evaluate the performance of the modifications made to the urban drainage system the following Scenarios are created and analyzed: Scenario 1 (S1) implements extensive green roofs for 0.98 ha (3% of the study area), Scenario 2 (S2)

implements permeable pavements for 2.19 ha (6.77 % of the study area), Scenario 3 (S3) includes the rainwater harvesting storing and reusing water for non-potable use for 13204 m^3 per year and Scenario 4 (S4) implement two detention basin (in the drainage sectors referring to outfall 1 and outfall 2) together with all the measures in the Scenario S1, S2 and S3.

To evaluate the performance of the implemented SuDS, we compared the peak reduction and the total volume of water conveyed at the four outfalls in the different Scenarios S1, S2 and S3 respect to the traditional drainage system scenario S0. The percentage difference of total volume (ΔV_{outj}) and peak flow ($\Delta Q_{p,outj}$) are evaluated through Equation (1) and Equation 2, respectively (in both cases outj=1, 2, 3 and 4 represent the j-th outfall and Si=1, 2, 3 and 4 represent the i-th scenario):

$$\Delta V_{outj} = (V_{So}-V_{Si})/V_{S0} \times 100 \quad (1)$$

$$\Delta Q_{p,outj} = (Q_{p,S0}- Q_{p,Si})/ Q_{p,S0} \times 100 \quad (2)$$

Results and concluding remarks

Analyzing and comparing the results of the different scenarios, we can observe that the different SuSD solutions are able to reduce the total volume and the peak flow consistently with the area covered and the combination of multiple techniques. Introducing the rain barrels for the reuse of water and the storage unit for lamination purposes strongly impact the volume removed from the outlet 1 and 2. A brief summary of the performance of the various scenarios compared to the traditional drainage system is shown in the Table 1.

Table 1. Performance summary in terms of the percentage of reduction of the total runoff volume ΔV_{outj} and peak flow reduction $\Delta Q_{p,outj}$ at the different outfalls (j=1,2,3 and 4) in the different scenarios S1-S4 compared to S0.

	ΔV_{out1} (%)	ΔV_{out2} (%)	ΔV_{out3} (%)	ΔV_{out4} (%)	$Q_{p,out1}$ (%)	$Q_{p,out2}$ (%)	$Q_{p,out3}$ (%)	$Q_{p,out4}$ (%)
Scenario 1 (S1)	4.46	10.18	17.22	23.86	1.85	8	16.61	24.18
Scenario 2 (S2)	5.32	9.24	3.16	2.75	3.70	6.45	3.14	3.85
Scenario 3 (S3)	27.77	10	17.28	11	29.63	9.68	19.75	11
Scenario 4 (S4)	32.56	43.24	-	-	40.74	87.9	-	-

Results of this study aims to highlight how the combination of grey (i.e., the classical urban strormwater system composed by pipes, gutter, manhole, lamination tanks, etc.) and green/blue SuDS techniques (i.e., green roof, permeable pavements and rain barrels) represent a significant opportunity to address emerging issues related to water-related challenges in the context of climate change.

Acknowledgments: A. M. and G. F. acknowledge funding from the Italian Ministry of Education, University and Research (MUR) in the framework of the project DICAM-EXC (Departments of Excellence 2023-2027, grant L232/2016).

References

Ferdowsi A, Piadeh F, Behzadian K, Mousavi SF, Ehteram M (2024) Urban water infrastructure: A critical review on climate change impacts and adaptation strategies. Urban Climate 58. http://doi.org/10.1016/j.uclim.2024.102132

Rossman L, Simon M (2022) Storm Water Management Model User's Manual Version 5.2. U.S. Environmental Protection Agency, Washington, DC, EPA/600/R-22/030

Schilling J, Tränckner J, (2022) Generate_SWMM_inp: An Open-Source QGIS Plugin to Import and Export Model Input Files for SWMM. Water 2022, 14, 2262. http://doi.org/10.3390/w14142262

Woods Ballard B, Wilson S, Udale-Clarke H, Illman S, Scott T, Ashley R, Kellagher R (2015) The SuDS Manual. CIRIA Report C753. Published by CIRIA, Griffin Court, 15 Long Lane, London UK

Development of resilient and adaptable drainage system through the integration of multiple SuDS techniques

R.N. Nyawo[1,2*], T.T. Tanyimboh[1]
[1] School of Civil and Environmental Engineering, University of the Witwatersrand, Johannesburg, South Africa
[2] Johannesburg Roads Agency, Johannesburg, South Africa
* e-mail: thulirose19@gmail.com

Introduction

Sustainable drainage systems (SuDS) help create areas that mimic "pre-development" dynamics, safeguard water quality and encourage ecosystem development whilst providing an amenity to urban residents (McGrane 2016). The adoption of any SuDS technique is determined by the unique characteristics of the site under consideration. Therefore, the aim of the investigation was to determine and ascertain the characteristics and features of a greenfield site earmarked for a government-subsidised residential housing development.

The study area was a greenfield site located in Soweto, Johannesburg, South Africa, with no temporary or permanent structures. The extent of the total site was 7.15 ha. The plot of land was subdivided by the Golden Highway (R553) into two stands. The Golden Highway formed the southern boundary for Stand 1 (4.50 ha) and the northern boundary for Stand 2 (2.65 ha). The development will be made up of three-storey structures comprising 780 units in total. Stormwater management for the residential complex aimed to prioritise controlling and treating stormwater runoff as close to the source as possible (Armitage et al. 2013). The candidate SuDS techniques considered included green roofs, rainwater harvesting, pervious pavements, soakaways and detention ponds.

Materials and methods

The investigation entailed an evaluation of the site characteristics, along with the hydrological analyses to determine the catchment peak flows. The key features of the site for which data were required comprised the locality, proposed land use, current use of the site and any adjacent properties, soil type, existing natural drainage patterns, climate, site topography, etc. The site characteristics and features were investigated and ascertained using the cadastral and building plans for the proposed residential complex, plus the site services, geotechnical and topographical survey, and traffic impact assessment reports. The SCS (Soil Conservation Service) soil groupings A to D throughout South Africa (Schulze 2012) was employed to classify the soil type.

The Rainfall.jar software (Smithers and Schulze 2002) that is used for estimating design rainfall depths at selected stations in South Africa was employed to generate rainfall data. It contains rainfall depths for durations ranging from 1-7 days, estimated at 3,945 daily rainfall stations in South Africa. The stormwater peak flows were calculated using the Rational Method, due to the small catchment size (SANRAL 2013). Also, a conventional drainage system was designed using the Civil Designer software, which yielded the required pipe sizes of the proposed conveyance infrastructure and peak runoff flow rates.

Results and concluding remarks

The natural form of stormwater drainage is sheet flow over the surface area and no formal stormwater drainage systems existed within the site. The planned social housing development would alter the natural form of drainage and the total surface area that would be made impermeable (roofs and paving) was approximately 59 per cent. The site was surrounded by industrial developments on the northern extents and low-to-medium residential developments on the southern parts. The site was covered with vegetation comprising short grass, bushes and shrubs, and characterised by a prominent slope of 4% to 12% towards

the southwest direction as well as rock outcrops towards the southwestern portions.

The site's in-situ material classification was gravel-soil (G10) (DoT 1996). This material is prone to differential movement on pavements and roads as it exhibits medium active/expansive clays and, therefore, classified as poor for road building and pavement construction. The general soil type for the project area was "Group C" which translates to material with a high runoff potential when thoroughly wet, high clay content, low infiltration rates, and poorly drained (Schulze and Schütte 2023). Groundwater was encountered in none of the excavated test pits.

The nearest weather station to the site was the Klipspruit weather station, 1.8 km from the site, and the mean annual precipitation at this station was 680 mm. The calculated pre-development runoff co-coefficients based on the above-mentioned site characteristics for rainfall return periods of 2, 5, 10, 25, 50 and 100 years were 0.225, 0.248, 0.270, 0.315, 0.374 and 0.450, respectively. The corresponding calculated pre-development peak stormwater flows were 0.275, 0.419, 0.551, 0.789, 1.107 and 1.539 m^3/s, respectively. The achieved post-development peak flows for the design rainfall of 1:5 years (minor) and 1:25 years (major) for the conventional drainage system were 1.224m^3/s and 2.033m^3/s, respectively. Thus, the peak stormwater flows of the undeveloped conditions would be increased by 292% and 258%, respectively.

Therefore, the results of the investigation revealed that implementation of SuDS was necessary to reduce the post-development peak flows to the pre-development levels. Soakaways are not recommended for sites with impermeable soils and minimum depths to the water table of less than 1 m. Permeable pavements are not recommended for site areas with slopes of more than 5% and minimum depths to the water table of less than 1 m. The average depth of the site's test pits ranged from 0.6 m to over 2.2 m and seepage was not encountered, thus it was concluded that the water table was not less than 1m deep. Therefore, soakaways and permeable pavements were not suitable for implementation at the site due to the poor infiltration (impermeable soil) and surface slope greater than 5% for a large portion of the site.

The building plans indicated an IBR roof sheeting design, which could not cater for the 40-60 kg/m^2 of additional weight required for green roof component materials and expected water detention volumes. Thus, the roof's structural design did not cater for the construction of green roofs.

Therefore, it was concluded that rainwater harvesting was the only applicable SuDS technique at the source control level. The applicable SuDS technique at the local control level were on-site detention ponds. Finally, it was recommended that the various combinations of these two techniques be investigated in detail, potentially to reduce the stormwater runoff to pre-development conditions.

References

Armitage, N., Vice, M., Fisher-Jeffes, L., Winter, K., Spiegel, A., Dunstan, J. (2013). Alternative Technology for Stormwater Management: The South African Guidelines for Sustainable Drainage Systems. Water Research Commission. South Africa.

DoT (Department of Transport). (1996). Technical Recommendations for Highways Draft TRH4. Pretoria, South Africa.

McGrane, J.M. (2016). Impacts of urbanisation on hydrological and water quality dynamics, and urban water management: a review. Hydrological Sciences Journal 61(13): 2296-2311.

Schulze, R.E. (2012). Mapping hydrological soil groups over South Africa for use with the SCS-SA Design Hydrograph Technique: Methodology and results. Proceedings, 16th South African National Hydrology Symposium, University of Pretoria.

Schulze, R.E., Schütte, S. (2023). Mapping SCS hydrological soil groups over South Africa at terrain unit spatial resolution. Journal of the South African Institute of Civil Engineering 2023:65(4), Art. #0806, 8 pages. http://dx.doi.org/10.17159/2309-8775/2023/v65n4a1

Smithers, J.C., Schulze, R.E. (2002). Design rainfall estimation for South Africa. Water Research Commission. South Africa.

South African National Roads Agency Limited (SANRAL). (2013). Drainage Manual, 6th Edition. Pretoria, South Africa.

Enhancing water availability in Mediterranean basins through improved reservoir management

P. Bianucci*, A. Sordo-Ward, L. Garrote
Department of Civil Engineering: Hydraulic, Energy and Environment – Universidad Politécnica de Madrid, Spain
** e-mail: paola.bianucci@upm.es*

Introduction

The study described here was performed in the framework of the PRIMA funded AGWAMED Project. The hydroclimatic conditions (semi-arid) of the Mediterranean region are conducive to drought or water scarcity episodes (Olden et al. 2020). Climate change scenarios predict an increase in the number and intensity of these events (IPCC 2022). Thus, a sustainable water management policy is essential to meet water demands, especially the water resources needed to ensure food production. In this sense, it is decisive to have an adequate knowledge of the impact that this expected reduction in natural resources would have on the water availability to meet demands (Bianucci et al. 2024). It is important to analyse the available water resources considering the concept of *system*, represented mainly through the river basins. The way the systems are connected and manged may affect water availability. This study assessed the potential enhancement of water availability in Mediterranean basins provided by different management strategies.

Materials and methods

Mediterranean basins present diverse socio-economic realities; however, they deal with similar water availability problems and climate change challenges. To assess the water availability at basin scale, we employed a high-resolution GIS-based model named Water Availability and Adaptation Policy Analysis (WAAPA Sordo et al. 2019). We employed datasets from different sources to characterise them, allowing us to obtain a rigorous water system representation:

- Basin delimitation and river network definition were based on detailed topographical model provided by the Hydrosheds dataset (Lehner et al. 2008).
- Reservoir data was extracted from WRD-ICOLD (ICOLD 2003), complemented with GRanD (Lehner et al. 2011) and GOODD (Mulligan et al. 2020) datasets.
- Meteorological and hydrological data were derived from the ISIMIP3b project (data.isimip.org/).
- Three past scenarios (obsclim, picontrol, historical) and six future scenarios (SSP126, SSP370, SSP585, and two time-horizons for each) from ISIMP. Data from two hydrological models (included in ISIMP) were used: H08 and CWatM.
- Baseline model: 40 years analysis period, mixed demand (20% urban supply and 80% irrigation), usually specified for irrigation reliability criteria, no ecological flows imposed, local management.

WAAPA model analyzes reservoir flow regulation and water allocation in a water resources system, its basic components are reservoirs, inflows and demands. These components are linked to nodes of the river network. WAAPA model was run to obtain potential water availability in two scenarios. Potential water availability is defined as the maximum water demand that can be supplied at a given abstraction point of the network, addressing a certain reliability and constraints, with a given regulation capacity and management. Two management methods were applied: local and global strategies. Under local management, reservoirs are managed to supply local demands only. Under global management, all reservoirs in the upstream basin are jointly operated to supply all demands in the region. The comparison of results between these two scenarios provides an estimate of the enhancement of water availability that can be obtained from improved management of the systems.

Results and concluding remarks

We applied the methodology for all river basins directly draining into the Mediterranean Sea, excluding the Nile River basin. Figure 1 shows the increase in water availability for the 34 largest basins in the Mediterranean, excluding the Nile, when switching from a local to a global management strategy. Although the improvement obtained by increasing the level of interconnection of the system (greater and more efficient development of infrastructures) varies from one basin to another (form 3-4% for Hmeimat to 45-47% for Maritsa), it results evident in all cases (average increase of 14% for H08 and 19.5% for CWatM). The shift from local to joint management requires densification of the transport network.

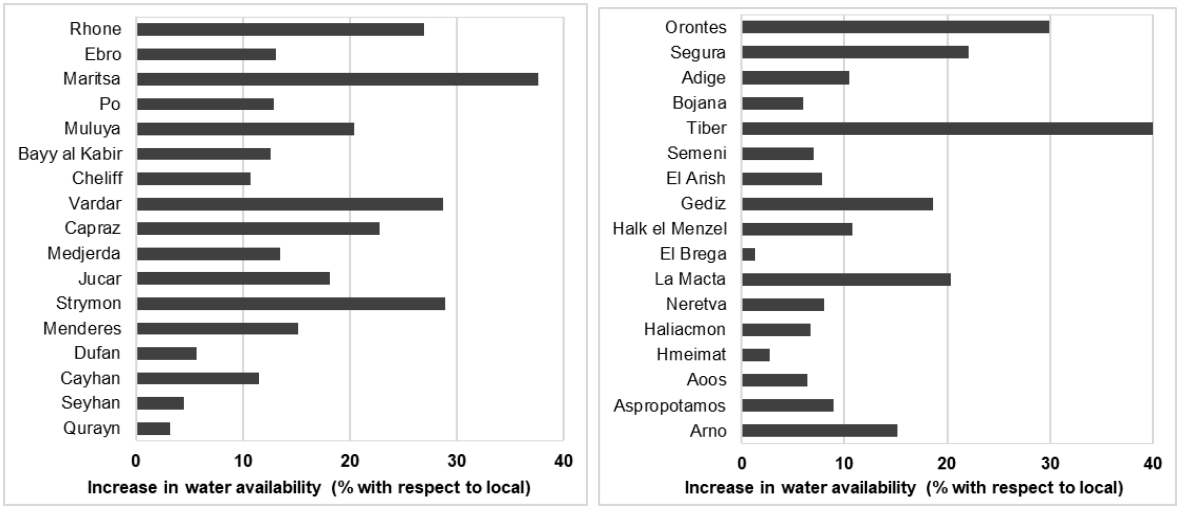


Figure 1. Increase in water availability per basin obtained in the simulations of the global management model run with respect to the local management model run (in percentage). Obsclim scenario.

The role of water infrastructure is essential to reduce the vulnerability of water systems. The proposed analysis helps in decision making regarding the prioritisation of investments in water infrastructure.

Acknowledgments: The research was carried out within the AG-WaMED project, funded by the Partnership for Research and Innovation in the Mediterranean Area Programme (PRIMA), an Art. 185 initiative supported and funded under Horizon 2020, the European Union's Framework Programme for Research and Innovation, Grant Agreement Number: PCI2022-132929.

References

Bianucci P, Sordo-Ward A, Lama-Pedrosa B, and Garrote L (2024) How do environmental flows impact on water availability under climate change scenarios in European basins?. The Science of the total environment. 911. 168566. 10.1016/j.scitotenv.2023.168566.

ICOLD (2023) World Register of Dams. Available at http://www.icold-cigb.net/

IPCC (2022) Climate Change 2022: Impacts, Adaptation, and Vulnerability. Contribution of Working Group II to the Sixth Assessment Report of the Intergovernmental Panel on Climate Change, H.-O. Pörtner et al. (eds.), Cambridge University Press. Cambridge University Press, Cambridge, UK and New York, NY, USA, 3056 pp., DOI:10.1017/9781009325844.

Lehner B, Verdin K, Jarvis A (2008) New global hydrography derived from spaceborne elevation data. Eos, Transactions, American Geophysical Union, 89(10): 93–94. DOI: 10.1029/2008eo100001.

Lehner B, Reidy Liermann C, Revenga C, Vörösmarty C, Fekete B, Crouzet P, Döll P, Endejan M, Frenken K, Magome J, Nilsson C, Robertson JC, Rodel R, Sindorf N, and Wisser D (2011) High-Resolution Mapping of the World's Reservoirs and Dams for Sustainable River-Flow Management. Frontiers in Ecology and the Environment 9 (9): 494-502. DOI: 10.1890/100125.

Mulligan M, van Soesbergen A and Sáenz L (2020) GOODD, a global dataset of more than 38,000 georeferenced dams. Scientific Data, 7(1), pp.1-8.

Olden JD, et al. (2020) Ecological implications of climate-induced alterations in hydrology for riverine ecosystems. Ecohydrology, 13(4), e2229.

Sordo-Ward A, Granados I, Iglesias A, Garrote L (2019) Blue Water in Europe: Estimates of Current and Future Availability and Analysis of Uncertainty. Water, 11(420):1-18.

Traditional Water Management Systems (TWMS) for climate change adaptation: Case study of Jaipur, India

K. Bimrah*, I. Saizen
Laboratory of Regional Planning, Graduate School of Global Environmental Studies, Kyoto University, Japan
** e-mail: kanika.bimrah.24e@st.kyoto-u.ac.jp*

Introduction

Water, a vital resource, is essential for urban growth, community development, and environmental sustainability. The traditional knowledge and practices around water management are deeply rooted in human history, as substantiated by the fact that many ancient civilizations flourished near water bodies (Sharma & Ji, 2024). Traditional Water Management Systems (TWMS) are community-based approaches developed over generations to sustainably manage water resources, often integrating local knowledge with specific environmental such as Qanat systems developed by ancient Persians, Yakhchal found across Iran and stepwells in Indian subcontinent. Our ancestors have adapted to climate change by utilizing traditional systems to secure water access, as shifting precipitation patterns and increasing temperatures threaten water availability. These effects of climate change will worsen in future. (Jiang & Arnold, 2023). The objectives of this research are (1) Analyze the effects of changing precipitation patterns and rising temperatures on Jaipur's groundwater levels and land surface temperature (2) Emphasize the role of TWMS in enhancing resilience against climate change. The study area, Jaipur is located in the semi-arid region of Indian subcontinent. It is characterized by erratic rainfall, but has an extensive history of innovative water management systems (Jawaid, Sharma, Pipralia, & Kumar, 2017).

Materials and methods

A comprehensive research methodology was implemented, as illustrated in Figure 1, detailing the methods, materials, and data sources utilized for each parameter. The study focused on:

- *Groundwater Level Analysis:* Inverse Distance Weighting (IDW) interpolation technique used for analysis.
- *Land Surface Temperature (LST):* Thermal bands of Landsat 8 imagery were used in the equation below.

$$LST = T_B / [1+w(T_B/ p) \ln(\varepsilon)] \quad (1)$$

where, w = 11.5µm is the wavelength of the emitted radiance, p = 1.438×10−2 mK−1 is a constant value, T_B = Brightness Temperature, ε = emissivity (Sultana & Satyanarayana, 2019)

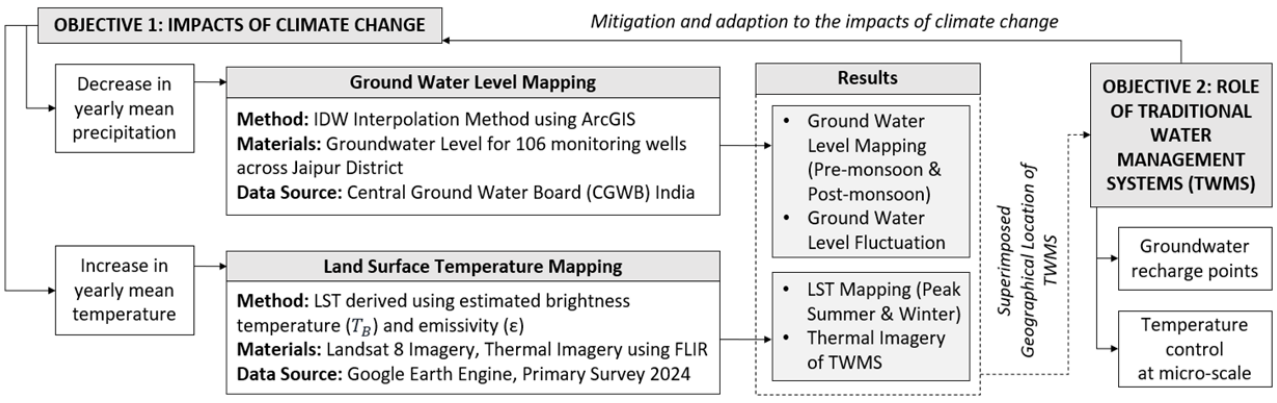


Figure 1. Research methodology

Results and concluding remarks

1. *Groundwater Level Mapping:* From 2020 to 2022, localized or monsoonal recharge had slightly improved maximum groundwater depths, but mean groundwater levels had significantly declined from 43.52 to 45.01 MBGL pre-monsoon and from 29.21 to 37.54 MBGL post-monsoon.

On superimposing the geographical location of TWMS with groundwater level fluctuation, it was observed that these systems are predominantly situated in areas experiencing high groundwater fluctuation (Figure 2). This emphasizes on the importance of restoring and reintegrating these traditional systems into modern water management strategies to mitigate groundwater depletion and support aquifer recharge.

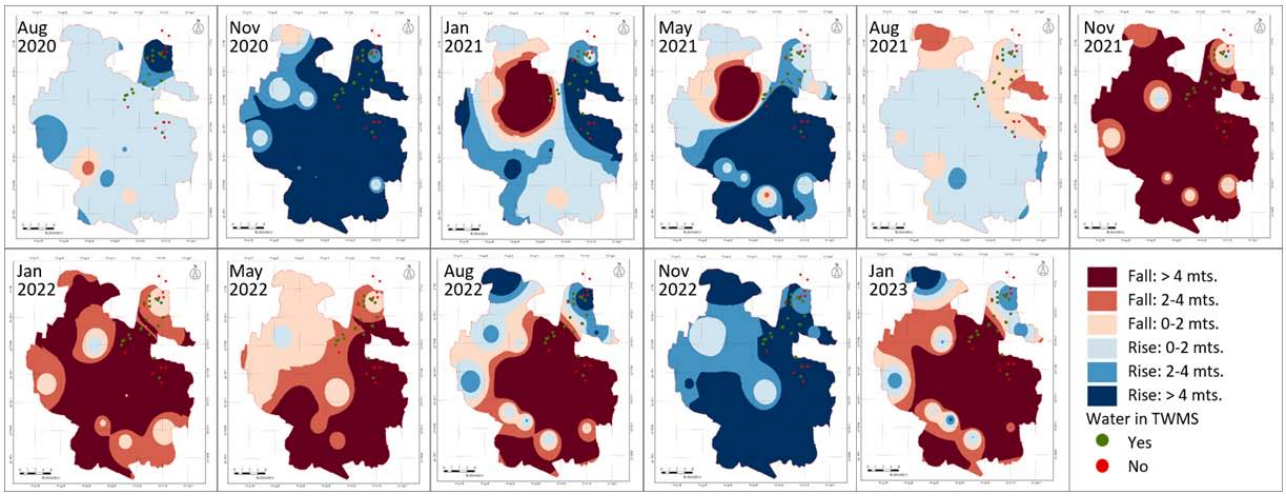


Figure 2. Groundwater Level Fluctuation Map with TWMS in Jaipur

2. *Land Surface Temperature Mapping:* Extreme variations across seasons can be observed, ranging from below 16°C in peak winter to over 56°C during the height of summer. However, analysis of spatial temperature distribution does not reveal any significant patterns across the urban landscape.

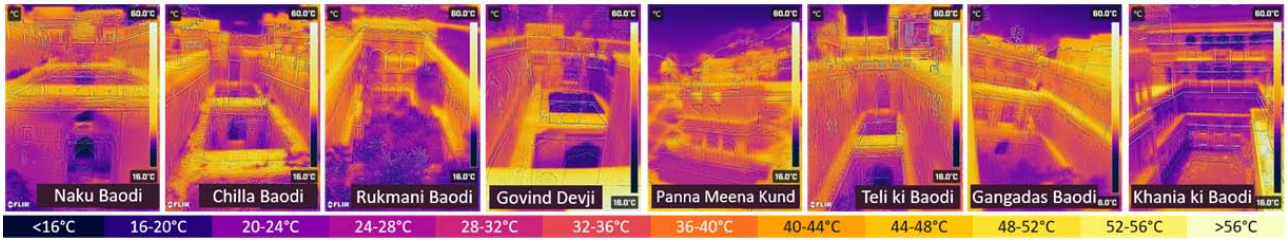


Figure 3. Thermal Imagery of TWMS in Jaipur (Collected during Primary Survey conducted in July 2024)

It was observed that TWMS exhibit minimal impact on surrounding temperatures at macro scale; but have significant influence at micro-scale, particularly within their immediate vicinity as shown in Figure 3. This localized cooling effect suggests the potential to provide thermal comfort to individuals, especially during high temperatures.

Acknowledgments: Sincere gratitude to JSPS KAKENHI for their grant (Grant Number 21KK0014).

References

Jawaid, M., Sharma, M., Pipralia, S., & Kumar, A. (2017). City profile: Jaipur. Cities, 63-81.

Jiang, Y., & Arnold, H. (2023). TraditionalWater Systems Informing Sustainable Contemporary Drylands Design: Documentation, Extraction, and Deployment. Sustainability.

Sharma, A., & Ji, S. (2024). Linkages between Traditional Water Systems (TWS) and Sustainable Development Goals (SDGs): A case of Govardhan, India. Social Sciences & Humanities Open, 1-14.

Sultana, S., & Satyanarayana, A. (2019). Impact of urbanisation on urban heat island intensity during summer and winter over Indian metropolitan cities. Springer Nature.

Floating Photo Voltaic on reservoirs: a sustainable solution with challenges

F. Viola[1*], M. Lo Iacono[2], F. Lo Iacono[2]
[1] Dipartimento di Ingegneria Civile, Ambientale e Architettura, Università di Cagliari, Italy
[2] Liceo Scientifico Felicia e Peppino Impastato, Partinico, Italy.
* e-mail: viola@unica.it

Introduction

Floating solar Photo Voltaics (FPV) are increasingly recognized as a promising technology for renewable energy generation, particularly in areas where land is scarce or valuable.

One such location is the Diga Jato, a large reservoir in Sicily, Italy, where deploying floating solar panels could simultaneously help reduce reliance on fossil fuels and preserve water resources from direct evaporation. However, the potential benefits of FPV systems in the region must be weighed against the challenge of sediment accumulation in reservoirs, which necessitates costly and environmentally impactful dredging operations. This paper explores the technical, economic, environmental, and social implications of installing floating solar panels, with a particular focus on the optimal positioning of the panels and its impact on dredging operations.

Materials and methods

Solar energy has emerged as one of the most prominent sources of renewable energy globally, driven by the need to combat climate change and reduce greenhouse gas emissions. While solar panels are traditionally installed on land, the rapid urbanization and increasing competition for land have made it difficult to find sufficient space for large-scale solar farms. Floating solar panels offer a viable solution by utilizing the vast, untapped surface area of lakes, reservoirs, and other water bodies for energy generation.

FPV systems are mounted on floating platforms that hold solar panels above the water surface. These systems are typically deployed on large bodies of water, such as hydroelectric reservoirs, agricultural reservoirs, or even industrial wastewater ponds. Floating solar systems are seen as a promising way to address land scarcity while also providing unique environmental benefits, such as improving water quality and reducing evaporation from water bodies (Sahu et al., 2016).

A typical FPV system is composed of several key components. Floating platforms form the base, providing support for the solar panels and keeping them afloat while being designed to withstand forces from wind, waves, and water currents. The solar panels, made from silicon-based photovoltaic cells, are mounted on these platforms to optimize sunlight exposure and convert it into electricity. Inverters play a crucial role by transforming the direct current (DC) electricity generated by the solar panels into alternating current (AC) electricity, which is suitable for use by the grid or local consumers. Cabling and electrical connections link the solar panels to the inverters and the grid, ensuring the smooth transmission of electricity. Finally, anchoring and mooring systems keep the floating platforms securely in place, preventing them from drifting due to water currents or winds.

Water reservoirs are critical for irrigation, water supply, and hydropower generation. However, large bodies of water are subject to evaporation, which can lead to the loss of significant amounts of water. Floating solar panels can help mitigate this by covering the water surface, reducing evaporation rates. This can be especially important in arid and semi-arid regions where water conservation is a critical concern. By reducing evaporation, floating solar panels can help preserve water resources for agriculture, drinking water, and power generation (Majumder et al. 2021).

Solar panels typically perform better in cooler temperatures. The presence of water underneath the floating solar panels can help keep them cooler compared to land-based systems, where the heat absorbed by the ground can increase the temperature of the panels and reduce their efficiency. In addition, the

reflective surface of the water can enhance the amount of sunlight that reaches the solar panels, improving their energy output. Studies have shown that floating solar panels can achieve higher efficiency compared to traditional land-based systems, particularly in hot climates.

Floating solar panels can also have positive environmental impacts. For example, they can help improve water quality by limiting the growth of algae. Algae blooms often occur when water bodies are exposed to direct sunlight, which accelerates the growth of algae. The floating panels block sunlight from reaching the water surface, thereby reducing the potential for harmful algae growth and improving water quality. This is particularly important for water bodies used for drinking water, irrigation, and recreation.

Sedimentation is a natural process that occurs when water in a reservoir slows down, causing suspended particles, such as soil, sand, and organic matter, to settle at the bottom of the water body. Over time, sediment accumulation can reduce the storage capacity of reservoirs, affect water quality, and impede the operation of hydroelectric turbines and other infrastructure. In the Mediterranean region, which is characterized by a semi-arid climate, sedimentation can be particularly problematic in reservoirs due to limited rainfall and high evaporation rates.

The Diga Jato is not immune to the issues of sedimentation. The reservoir, which is primarily used for urban water supply and irrigation, is prone to sedimentation due to runoff from the surrounding catchment area. Sediment buildup in a reservoir can pose several challenges to the deployment of floating solar panels. First, it reduces the water depth, which can hinder the stability of floating platforms that require a certain depth to function effectively. Second, excessive sediment accumulation can interfere with anchoring systems, making it harder to securely anchor the platforms and increasing the risk of drifting or instability. Lastly, sediment and organic material may impact water quality, diminishing the water's cooling effect on the solar panels. This can result in higher operating temperatures and lower panel efficiency. Furthermore, sediment buildup can promote algae growth, which may obstruct sunlight and compromise the performance of the solar panels.

Results and concluding remarks

Integrating floating solar systems into a reservoir that undergoes regular dredging presents several challenges. Dredging operations, which often involve heavy machinery, may necessitate the temporary removal or repositioning of floating solar panels, leading to operational disruptions, downtime, and increased costs for relocating the arrays. Proper sediment disposal is another concern, as it requires careful planning to ensure that the disposal process does not interfere with the floating platforms, cables, or maintenance of the solar panels. Additionally, dredging can increase water turbidity, reducing the sunlight available to the panels and potentially impacting their performance. The disturbances caused by dredging could also harm the aquatic ecosystem, potentially diminishing the cooling effect of the water and further affecting the efficiency of the solar panels.

In this study, optimal panel placement solutions are examined, taking into account the actual position of the dam, spillways, and the recreational activities carried out within the water body. Sediment management technologies, such as sediment traps and selective dredging techniques, which offer innovative solutions to reduce the amount of sediment requiring removal, will be also evaluated. By capturing sediment before it accumulates can decrease the frequency and intensity of dredging operations, making sediment management more efficient and less disruptive.

References

Majumder A., Innamorati R., Frattolillo A., Kumar A., Gatto G. (2021) Performance analysis of a floating photovoltaic system and estimation of the evaporation losses reduction. Energies 14 (24), art. no. 8336. DOI: 10.3390/en14248336

Sahu A., Yadav N., Sudhakar K., (2016) Floating photovoltaic power plant: A review. Renewable and Sustainable Energy Reviews 66:815-824. DOI: 10.1016/j.rser.2016.08.051

Retrospective analysis of water availability in Sardinian reservoirs

F. Viola*, P. Corongiu, C. Jakomin, R. Deidda
DICAAR, University of Cagliari, Cagliari, Italy
** e-mail: viola@unica.it*

Introduction

This study aims to perform a retrospective analysis on the interaction between accumulated storage volumes and water demand (Wisser et al, 2013) in Sardinian dams. While dam design typically involves the evaluation of several features, including historical and future water availability, storage capacity, and delivery capacity for various uses (Ahmad et al, 2014), this work adopts a different perspective, focusing on past dynamics: in a real scenario where the infrastructure is already operational and the resource is readily available, the goal is to assess how effectively the resource is being utilized (Sophocleous, 2004).

The analysis focuses on Sardinian reservoirs, specifically on the first order moments of the stored water volumes. We want to investigate potential relationships between accumulated storage and simple meteoclimatic and water supply data. The objective is to gain deeper insights into operational management practices and the performance of these systems.

Materials and methods

Using the daily reservoir levels provided by ENAS (Ente Acque della Regione Sardegna) for the Sardinian dams, the corresponding storage volumes were calculated using the storage curve included in the Operational and Maintenance Condition Sheets (Foglio Condizioni per l'Esercizio e la Manutenzione, *FCEM*) for each dam. To facilitate comparisons across different reservoirs, the daily storage volumes were first adjusted by subtracting the dead storage volume and then made dimensionless relative to the useful regulation volume, yielding the variable *X(t)*.

From the resulting dimensionless variable *X(t)*, the mean, the coefficient of variation (*CV*) and variance were computed to explore potential relationships with five dimensionless parameters defined in equations [1] through [5]. These parameters were formulated based on normalized water supplies and rainfall values relative to the catchment areas of the reservoirs:

$$Par_1 = P_y A/D_y \quad (1)$$

$$Par_2 = P_w A/D_s \quad (2)$$

$$Par_3 = P_s A/D_s \quad (3)$$

$$Par_4 = P_s A/D_w \quad (4)$$

$$Par_5 = P_y A/D_s \quad (5)$$

Here, P_y denotes the mean annual rainfall, P_w the mean winter rainfall (October to March), and P_s the mean summer rainfall (April to September). Similarly, D_y represents the mean annual water supply, while D_s is the mean summer water supply.

The calculation of these parameters required an accurate determination of the catchment areas associated with each dam. Special attention was given to accounting for interconnected basins, using information from the *FCEM* and the hydraulic schemes of Sardinia. Proper adjustments were also made to ensure accurate accounting of outflows from the reservoirs.

Finally, all possible combinations of moment-parameter and CV-parameter relationships were systematically examined. Regression lines were fitted, and their corresponding coefficients of determination (R^2) were calculated to identify and visualize potential correlations between the statistical properties and the dimensionless parameters.

Results and concluding remarks

The described methodology was applied to a dataset comprising eighteen dams in Sardinia, for which detailed records of water supplies and the extent of their respective catchment areas, including any connected basins, were available. For each dam, the dimensionless variable allowed the assessment of key statistical properties mean, coefficient of variation, and variance. The latter were systematically correlated with each of the dimensionless parameters defined in the *Materials and methods* section (Eqs 1-5).

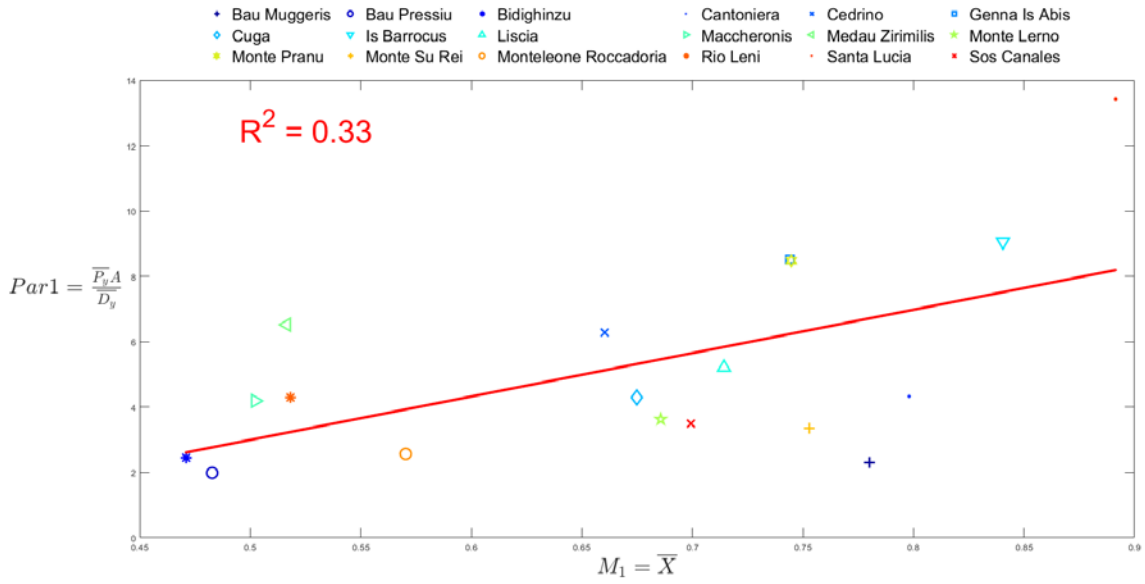


Figure 1. Comparison between parameter 1 [Eq.1] and the first-order moment (mean) of the distribution of the dimensionless variable X(t), extracted from the comparisons performed between parameters and moments. The symbols used for each analyzed dam are shown above the figure.

An interesting interpretation of the results regards the Parameter 1, which represents the inverse of the inflow rate allocated for water supply (World Commission on Dams, 2000). Higher values for parameter 1 indicate that the reservoir is frequently near its full capacity, with water supply representing only a small fraction of water incoming into the dams. On the contrary, low values of parameter 1 are associated with overexploited water resources, which in turns are triggered by high water supply not supported by natural flow.

This study enhances our understanding of the dynamics of resource exploitation in relation to the factors that determine the actual volumes stored in the analyzed reservoirs.

Predicting trends in stored volume using data from variables such as rainfall and water releases would be of critical importance, especially in the context of ongoing climate change, which poses an additional challenge in the management of water resources (Kondolf and Yi, 2022).

References

Ahmad A, El-Shafie A, Razali S.F.M. et al (2014) Reservoir Optimization in Water Resources: a Review. Water Resources Management 28: 3391–3405. https://doi.org/10.1007/s11269-014-0700-5

Kondolf M, Yi J (2022) Dam Renovation to Prolong Reservoir Life and Mitigate Dam Impacts. Water 2022, 14(9), 1464. https://doi.org/10.3390/w14091464

Sophocleous M. (2004) Global and Regional Water Availability and Demand: Prospects for the Future. Natural Resources Research 13, pp 61–75. https://doi.org/10.1023/B:NARR.0000032644.16734.f5

Wisser D, Frolking S, Hagen S, Bierkens M.F.P. (2013) Beyond Peak reservoir storage? A global estimate of declining water storage capacity in large reservoirs. Water Resources Research. https://doi.org/10.1002/wrcr.20452

World Commission on Dams (2000) Dams and Development. Earthscan publications Ltd, London.

Adapting reservoir operating rules in a changing climate for a sustainable management of drinking water sources

M. Neri*, E. Toth
Department of Civil, Chemical, Environmental, and Materials Engineering, University of Bologna, Bologna, Italy
** e-mail: mattia.neri5@unibo.it*

Introduction

An effective and integrated management of available drinking-water resources requires the assessment of the impacts of water scarcity, related to periods of hydrological drought. In a context of growing concern about the impacts of climate change on water availability, sustainable and integrated management of drinking water sources is crucial to ensure resilience of water supply systems. Under these circumstances, the implementation of numerical models of the water systems, aimed at the optimal management of water supply reservoirs, is of fundamental importance (e.g. Giuliani et al., 2021; Macian-Sorribes & Pulido-Velazquez, 2020). Within the broad spectrum of approaches for defining optimal reservoir management rules, the parametrization–simulation–optimization strategy (PSO, Koutsoyiannis & Economou, 2003) is particularly effective for reproducing the complex nature of real-world systems.

Starting from the beginning of the century, water resources analysts have been considering future climatic change scenarios in planning reservoir operation and adaptation strategies. In particular, it is important to evaluate the effectiveness of reservoir management rules, typically optimized based on historical hydro-climatic variability, for meeting demand under future climatic stress conditions. Several studies have tested the resilience of current operational reservoir rules (i.e. designed for historical hydro-meteorological conditions) by forcing the system with one or more regional climate scenarios (e.g. Padiyedath Gopalan et al., 2021), while other research studies have gone a step further by trying to find adaptive management rules and by comparing the results of optimizations conducted on historical or future hydro-climatic series (e.g. Zhang et al., 2017).

This study presents a methodology for the sustainable management of water resources in a coastal region of Northern Italy under climatic change, aimed to optimize the operational management of a water supply reservoir, which represents the main and the most sustainable water source of the system.

Materials and methods

The methodology includes the sequential use of historical meteorological forcings and the outputs of a large ensemble of 10 CORDEX GCM-RCM climate projections, hydrological modelling, and reservoir water balance modelling applied in a water system of Northern Italy. The study area is the Romagna region, one of the most economically developed areas in Europe, characterized by an extremely profitable seaside tourist industry. Its water supply network is served by multiple water sources: major sources are wellfields all across the lowlands, and the Ridracoli reservoir in the Apennines, which is the most environmentally sustainable and least energy-demanding source in the system. The reservoir system is complex since the lake is fed not only by the catchment closed at the dam but also by four additional nearby catchments connected to the reservoir with a system of intakes and tunnel pipes. The first phase of the work focused on developing the simulation model of the entire system, including i) rainfall-runoff modelling of the basins feeding the reservoir and ii) a model for the management of the entire system consisting of intakes, tunnel-pipe, reservoir, release and withdrawal controls. A specific analysis of historical water demand in the Romagna region, aimed to assess the minimum monthly volumes required from the reservoir, was also performed. Then, following a PSO approach, reservoir withdrawal rules are defined at the monthly scale by means of a multi-objective optimization algorithm, with the aim of i) maximizing the withdrawal volumes over the entire observation period, and at the same time, ii) minimizing water deficit volumes, defined as the volumes of resource that, although requested by the downstream network (in particular by areas of the

region that do not have alternative water sources), it is not possible to withdraw and deliver to the users. The PSO approach is applied multiple times by providing as input different meteorological forcings and optimizing the withdrawal operating policies over different historical or future periods. Specifically, 21 optimization runs are considered, including i) 11 optimizations during the historical period (by forcing the system with either observed or each of the 10 GCM-RCM meteorological fields) and ii) 10 optimizations during the long-term future time horizon 2071-2100 by providing as input each of the GCM-RCM scenarios.

Results and concluding remarks

The study successfully modelled the multi-basin water supply system and management of the Ridracoli reservoir, optimizing its operational withdrawal rules under both historical and future meteorological forcings to reduce system failure while maximizing overall supplied water volumes from the reservoir (reducing stress on other, less sustainable, and more energy-demanding regional sources). As an example of the results, Figure 1 shows the obtained Pareto frontiers for the observed historical run (blue) and for each of the future scenarios (orange): on average, future Pareto fronts correspond to worse values of the objective functions, therefore confirming a decreasing water availability in future decades.

Moreover, it was possible to quantify relative changes between withdrawal rules optimized during historical and future scenarios, and to estimate the corresponding expected pattern of withdrawal volumes and water deficit volumes, i.e., the total volumes of user demand that would have to be supplied by other sources (unless water shortages occur). In general, the outcomes show how the more conservative management policies may require frequent revisions of the withdrawal rules along the future decades, and result in a remarkable reduction in total supplied volumes. Conversely, management policies that involve a greater risk of incurring in deficit conditions (and thus an increased water stress on alternative sources when necessary) are better adapted to different climatic regimes and limit the future decrease of overall withdrawal volumes.

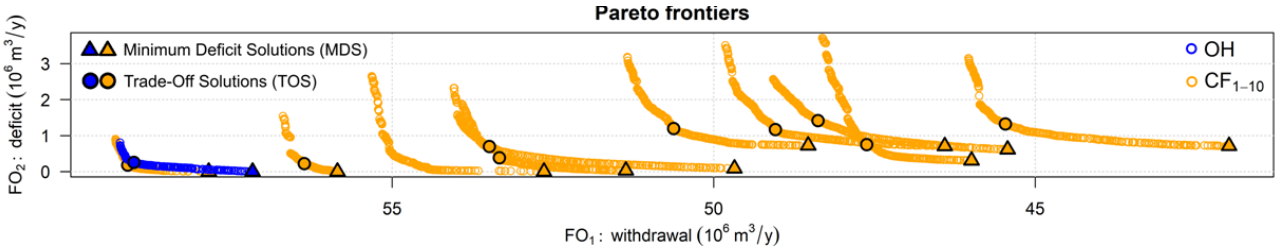


Figure 1. Pareto frontiers obtained for the observed-historical run (OH, blue dots) and for the ten CORDEX-future scenarios (CF_{1-10}, orange dots). Minimum Deficit Solutions (MDS) and Trade-Off Solutions (TOS) are also highlighted.

Acknowledgments: This study was carried out within the RETURN Extended Partnership and received funding from the European Union Next-GenerationEU (National Recovery and Resilience Plan – NRRP, Mission 4, Component 2, Investment 1.3 – D.D. 1243 2/8/2022, PE0000005).

References

Giuliani M, Lamontagne JR, Reed PM, Castelletti A (2021) A State-of-the-Art Review of Optimal Reservoir Control for Managing Conflicting Demands in a Changing World. Water Resources Research 57(12): e2021WR029927. https://doi.org/10.1029/2021WR029927

Koutsoyiannis D, Economou A (2003) Evaluation of the parameterization-simulation-optimization approach for the control of reservoir systems. Water Resources Research 39(6): 2003WR002148. https://doi.org/10.1029/2003WR002148

Macian-Sorribes H, Pulido-Velazquez M (2020) Inferring efficient operating rules in multireservoir water resource systems: A review. WIREs Water 7(1): e1400. https://doi.org/10.1002/wat2.1400

Padiyedath Gopalan S, Hanasaki N, Champathong A, Tebakari T (2021) Impact assessment of reservoir operation in the context of climate change adaptation in the Chao Phraya River basin. Hydrological Processes 35: e14005. https://doi.org/10.1002/hyp.14005

Zhang W, Liu P, Wang H, Chen J, Lei X, Feng M (2017) Reservoir adaptive operating rules based on both of historical streamflow and future projections. Journal of Hydrology 553: 691-707. https://doi.org/10.1016/j.jhydrol.2017.08.03

Degradation testing of PET bottles as floating covers in reservoirs

V. Benjaoran[1*], L. Raksaksri[2], J. Settakhumpoo[1]
[1] School of Civil Engineering, Suranaree University of Technology, Nakhonratchasima, Thailand
[2] School of Polymer Engineering, Suranaree University of Technology, Nakhonratchasima, Thailand
* e-mail: vacharapoom@sut.ac.th

Introduction

Water scarcity is a pressing global issue. Evaporation significantly contributes to water loss in reservoirs, and floating covers have been proposed as an effective solution. Lehmann et al. (2019) used floating balls and discs of different colors, sizes, and materials. They found that when the balls covered up to 91% of the water surface, the evaporation reduction was 70% for the balls and 80% for the floating discs. The color of the material significantly affected the evaporation rate. Simon et al. (2016) proposed using polyethylene terephthalate (PET) bottles as an alternative to plastic balls, achieving approximately 40% evaporation reduction. Recently, Benjaoran et al. (2023) proposed using recycled PET bottles filled with opaque materials as an economical and sustainable alternative for floating covers. The research evaluates the evaporation suppression efficiency of PET bottles under various conditions, including the type of filled opaque materials, cover area, floating patterns, and submerged depth. This approach not only addresses water conservation but also provides a solution for plastic waste management.

However, the long-term environmental impact and degradation of PET bottles in such applications remain understudied, raising concerns that may limit their widespread adoption. Various environmental factors, including exposure to sunlight, water contact, acids, bases, and microorganisms, can contribute to plastic deterioration. This study explores the use of recycled polyethylene terephthalate (PET) bottles filled with opaque materials as an economical and sustainable alternative for floating covers and aims to assess the evaporation suppression efficiency of PET bottles under various configurations. The focus is on investigating the degradation of PET bottles over time using Fourier Transform Infrared Spectroscopy (FTIR) and Differential Scanning Calorimetry (DSC) to ensure their long-term viability and environmental safety, offering insights into their service life as floating covers.

Materials and Methods

This study used 600 mL PET drinking water bottles (24 cm tall, 6 cm diameter) in various configurations, either empty or filled with assorted plastic bags (APB) or laminated aluminum foil (LAF) to create opaque floating covers. These filling materials, made from other single-use plastic container bags, help reflect light, thereby reducing sunlight penetration. The experiment was arranged to evaluate key parameters, including floating cover area, floating patterns, and submerged depth to evaluate their impact on evaporation suppression efficiency and identify the optimal configuration. The bottles were deployed in a controlled reservoir environment using experimental cylindrical ponds (2.84 m² surface area, 0.6 m in depth). The evaporation rate was determined by measuring the daily decrease in water level across all ponds.

Key methods for evaluating plastic deterioration include mechanical property testing, chemical composition analysis, thermal analysis, and physical characteristic evaluation. In this study, FTIR and DSC were selected as primary techniques. FTIR analyzes the absorption of infrared light by a material, enabling the identification of its chemical composition and molecular structure. The functional groups of interest, including C=O (1715 cm^{-1}), C-O (1245 cm^{-1} and 1100 cm^{-1}), and C-H (870 cm^{-1} and 730 cm^{-1}), were analyzed. DSC measures variations in a material's heat capacity as a function of temperature, providing insights into phase transitions, melting points, glass transition temperature, crystallization behavior, and thermal stability. The floating PET bottles lay horizontally and remained stationary for 18 months, with the upper side exposed to sunlight and the lower side submerged in water. For FTIR analysis, samples were collected at 6, 12, and 18 months, with each time point including three sets: empty, APB-filled, and LAF-filled. Each bottle was divided into two sections, one exposed to sunlight and the other submerged in water. For DSC analysis, only samples from the 18-month time point were examined, totaling six specimens.

Table 1. DSC results of PET bottles at 18 months.

Samples	Glass trans. temp. (ºc)	Melting point onset (ºc)	Melting point peak (ºc)	Melting point endset (ºc)	Crystallinity (%)
Control (untreated)	83.6	237.7	251.0	257.4	27.3
Light_Empty 18M	82.6	233.6	250.3	258.2	24.2
Hydro_Empty 18M	83.0	236.4	250.2	256.9	28.7
Light_APB 18M	83.8	235.3	251.3	258.8	28.0
Hydro_APB 18M	83.3	236.4	251.2	258.5	28.6
Light_LAF 18M	81.6	241.5	257.2	264.8	28.3
Hydro_LAF 18M	87.4	239.7	255.8	263.3	24.9



Figure 1.(a) Empty, APB-filled, and LAF-filled bottles; (b) Some experimental ponds.

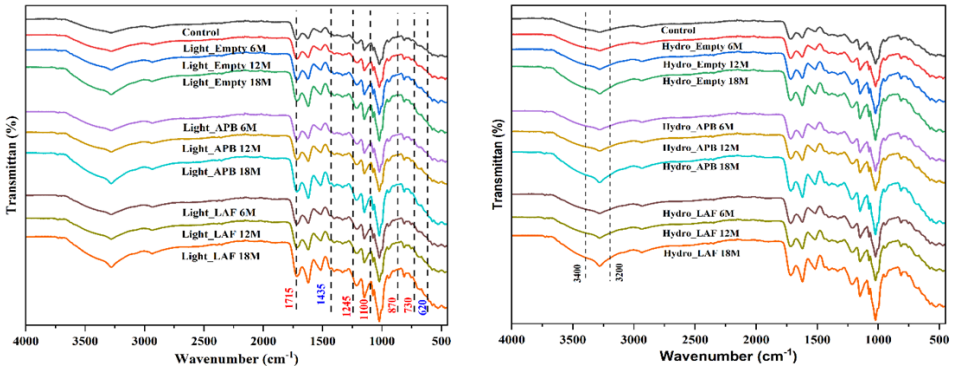


Figure 2. FTIR spectra of PET bottles exposed to sunlight and submerged side, APB, LAF-filled at 6, 12, and 18 months.

Results and concluding remarks

FTIR and DSC analyses showed minimal degradation of PET bottles after 18 months of exposure to sunlight and water. FTIR revealed no significant changes in key functional groups (C=O, C-O, CH2), indicating stable chemical structure. DSC confirmed thermal stability, with melting points between 250–257°C and a slight increase in crystallinity, suggesting improved polymer stability. These results demonstrate that PET bottles remain chemically and thermally stable under prolonged environmental exposure.

This study highlights the feasibility of using recycled PET bottles filled with opaque recycled plastic bags as floating covers to reduce water evaporation in reservoirs. LAF-filled PET bottles exhibited the highest performance, with raft-floating designs at a 3.0 cm submerged depth achieving the greatest evaporation suppression efficiency. FTIR and DSC analyses confirmed the durability of PET bottles over 18 months, revealing no significant degradation or thermal instability. These findings support the viability of recycled PET bottles filled with plastic waste as a sustainable, cost-effective, and long-term solution for water conservation. Further research could explore extending their service life and scaling the approach for larger reservoirs.

References

Benjaoran V, Raksaksri L, Settakhumpoo J (2023) Experimentation of Evaporation Reduction by a Use of Plastic Bottles Covering. Water Conservation and Management 7(2): 114-121. https://doi.org/10.26480/wcm.02.2023.114.121

Lehmann P, Aminzadeh M, Or D (2019) Evaporation suppression from water bodies using floating covers: laboratory studies of cover type, wind, and radiation effects. Water Resources Research 55(6): 4839-4853. https://doi.org/10.1029/2018WR024528

Simon J, et al. (2016) Evaporation Reduction Using PET Bottles: A Sustainable Approach. Journal of Water Conservation 12(4): 234-245.

A decision support tool for rainfed rice cultivation: Integrating rainfall patterns and ENSO predictions

T. Supriyasilp[1*], K. Pongput[2], N. Nongharnpitak[3], A. Sapet[3], J. Khiripet[4]
[1] Department of Civil Engineering, Faculty of Engineering, Chiang Mai University, Chiangmai, Thailand
[2] Department of Water Resources Engineering, Faculty of Engineering, Kasetsart University, Bangkok, Thailand
[3] Land Development Department, Bangkok, Thailand
[4] National Electronics and Computer Technology Center, Pathum Thani, Thailand
* e-mail: thanaporn@eng.cmu.ac.th

Introduction

Determining optimal sowing period for rice can help alleviate damage caused by crop water deficiency, especially in regions relying solely on rainwater for irrigation and during years of low/delayed rainfall. Studies attempting to identify optimal sowing dates for rice belong to three main categories: (i) field experiments, conducted under various periods with the optimal window selected based on yield (Cerioli et al. 2021); (ii) crop models, often in conjunction with future climate scenarios (Dharmarathna et al. 2014; Kim et al. 2021); and (iii) rainfall onset, which does not utilize modeling (Supriyasilp and Pongput 2021). Supriyasilp and Pongput (2021) established a relationship between the El Niño-Southern Oscillation (ENSO) and rainfall characteristics to aid crop planning for rainfed agriculture, particularly under dry conditions. The present study extends concepts built upon by these authors by considering a suitable planting period based on rainfall patterns and climate, soil water balance, and crop evapotranspiration at different growth stages. The study aimed to determine suitable sowing periods for direct seeding of rice in northern Thailand and relate it with ENSO to predict future sowing periods. A prototype was created to illustrate suitable sowing periods. This prototype can be integrated into the Agri-Map online platform, the official platform of the Ministry of Agriculture and Cooperatives of Thailand.

Materials and methods

Three provinces from the upper northern region of Thailand were selected as case studies, covering a rice cultivation area of approximately 2,364.2 km^2. Meteorological data from the Thai Meteorological Department comprised daily rainfall and climate data, including minimum and maximum temperatures, relative humidity, average wind speed, and sunshine duration. This study used Khao Dawk Mali 105 (Thai jasmine rice), a photosensitive rice grown using the direct seeding method. CROPWAT 8.0, a widely used program developed by the FAO, was used to calculate crop evapotranspiration, soil water balance, and percentage yield reduction when water was insufficient for crops. Real-time ENSO forecasts from 2003–2022 were provided by the International Research Institute for Climate and Society of Columbia University Climate School.

The appropriate sowing dates for rice during the rainy season were assessed by considering past rainfall patterns and weather conditions from 1991–2022 and available soil moisture content and crop growth stages. These factors were then input into the CROPWAT model under the condition that only rainwater is used for cultivation throughout the crop growth period. Sowing dates that yielded the best results for that year were selected and appropriate dates were summarized by analyzing the probability of different periods when crops would receive sufficient rainfall throughout their growth.

To develop a tool for government officials responsible for advising farmers on cultivation enabling them to forecast the start of planting days in advance, especially in drought-prone-predicted years, we analyzed rainfall patterns concerning the ENSO and categorized them based on their probability of occurrence into ENSO codes. The ENSO codes use a three-letter coding system to represent ENSO phases for March-April-May (MAM), April-May-June (AMJ), and August–September–October (ASO), respectively, and were assigned to each year. The first two letters of the code correspond to the onset of the rainy season in Thailand. In contrast, the third letter is associated with the reproductive stage of photosensitive rice cultivated in the study area. Sowing dates for each year were then classified according to the ENSO codes.

The results were used to develop a prototype that displayed suitable sowing dates for different areas at the subdistrict level on the Agri-Map online platform, which can be accessed at specific URLs. According to the ENSO code for that year, the results displayed on the Agri-Map online platform will change no later than early April. Most areas of Thailand enter the rainy season in May.

Results and concluding remarks

Figure 1 depicts the prototype when selecting planting date during June 1 to 10, 2024. Districts that are highly and moderately suitable to plant rice during specified dates are in green and yellow, respectively.

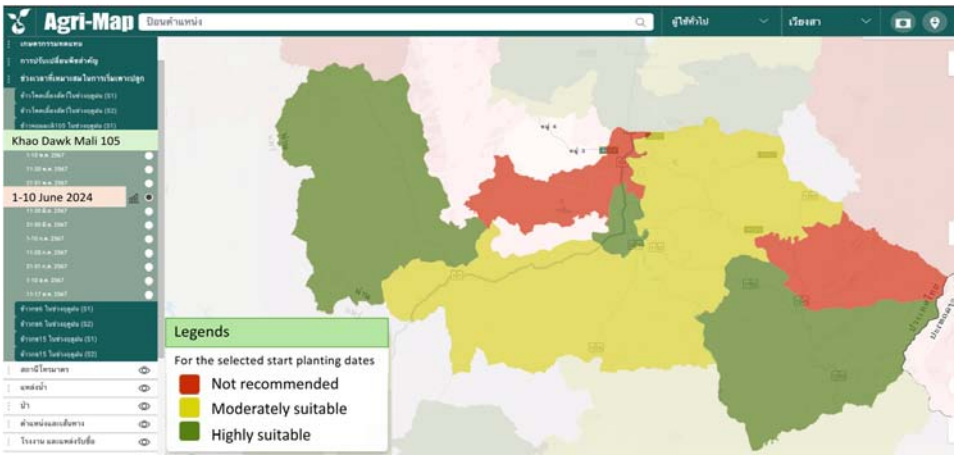


Figure 1. The prototype displayed the areas that can plant rice during the selected planting dates.

For analyzing the appropriate sowing start dates mentioned above, climate and rainfall data from 1991–1999 and data from 2020–2022 were used for validation. Validation results showed that deviation in planting start dates was 17.50, 18.75, and 11.11% of the total 120 cases for 2020, 2021, and 2022, respectively. The main factor that may affect the accuracy of a suitable planting date is rainfall pattern, and climate change has been reported to cause variations in rainfall patterns. This analysis predicted the appropriate planting start date based on past rainfall patterns corresponding to the ENSO codes. When analyzing the rainfall patterns of 2020 and 2021, which had ENSO codes NNN and LNN, respectively, it was found that delayed onset of the rainy season had never occurred in the past for those ENSO codes, resulting in a high level of discrepancy when verifying the accuracy.

In conclusion, the approach presented in this study can be used as a guideline for considering suitable sowing dates for rice and other crops. Sowing dates derived from this approach were simulated using only rainwater for cultivation to reduce the damage from insufficient rainfall during the growth period in rainfed areas. This study did not consider issues related to plant diseases, agronomic methods, or other environmental factors beyond the variables used as input data. If, in the future, data on the relationship between climatic conditions and plant diseases are available and used to improve the analysis results, the results could enhance the accuracy of the proposed planting dates and reduce damage from plant diseases.

Acknowledgments: This research was supported by the Agricultural Research Development Agency (ARDA) under Project No. PRP6605030220. The authors thank ARDA for funding this research, the Thai Meteorological Department for providing climate data, and the Land Development Department of Thailand for their support during our research.

References

Cerioli T, Gentimis T, Linscombe SD, Famoso AN (2021) Effect of rice planting date and optimal planting window for Southwest Louisiana. Agronomy Journal 113:1-10. https://doi.org/10.1002/agj2.20593

Dharmarathna WRSS, Herat S, Weerakoon SB (2014) Changing the planting date as a climate change adaptation strategy for rice production in Kurunegala district, Sri Lanka. Sustainability Science 9: 103-111. https://doi.org/10.1007/s11625-012-0192-2

Kim D-H, Jang T, Hwang S, Jeong H (2021) Paddy rice adaptation strategies to climate change: Transplanting date shift and BMP applications. Agricultural Water Management 252. https://doi.org/10.1016/j.agwat.2021.106926.

Supriyasilp T, Pongput K (2021) El Niño-Southern Oscillation and rainfall characteristics in Northern Thailand: Implications for adaptation in rainfed farms. Regional Environmental Change 21: 123. https://doi.org/10.1007/s10113-021-01852-5

Enhancing streamflow prediction using hydroclimatic variables and machine learning: A case study of the N'fis basin, Morocco

M. Naim[1,2*], B. Bonaccorso[2]
[1] University School of Advanced Studies of Pavia, Italy
[2] Department of Engineering, University of Messina, Italy
* e-mail: mohamed.naim@iusspavia.it

Introduction

Accurate streamflow forecasting is crucial for managing water resources. The primary objective of this study is to strengthen streamflow forecasting data in the N'fis Basin, Morocco, a semi-arid region with high hydrological variability (Zkhiri et al. 2019), enabling more efficient reservoir management and the timely implementation of mitigation measures to minimize drought impacts. To this end, machine learning (ML) techniques are applied for streamflow forecasting. Given the complex interactions between hydroclimatic drivers, we integrate teleconnection indices, and meteorological and hydrological variables to enhance predictive accuracy (Lee et al. 2020; Ayana et al. 2023; Sharma and Goel 2024).

Materials and methods

The N'fis Basin, part of the Tensift River hydraulic system in Morocco (30.5°–31.2°N, 7.55°–8.40°W), is a semi-arid region covering 1,707 km². Figure 1 highlights the high interannual, monthly and seasonal intra-annual streamflow variability, reflecting the basin's hydrological sensitivity to climatic fluctuations. The watershed includes the Yacoub Al Mansour and Lalla Takerkoust dams, which are crucial in irrigation, drinking water supply, and hydroelectric production. Hydroclimatic and remote sensing data from 1982 to 2021 were collected from multiple sources, including in-situ observations and satellite datasets. The dataset comprises streamflow, rainfall, inflow, soil moisture, teleconnection indices (NAO, ENSO, PDO, AO, AMO, AAO), and drought indices (SPI3, SSI3).

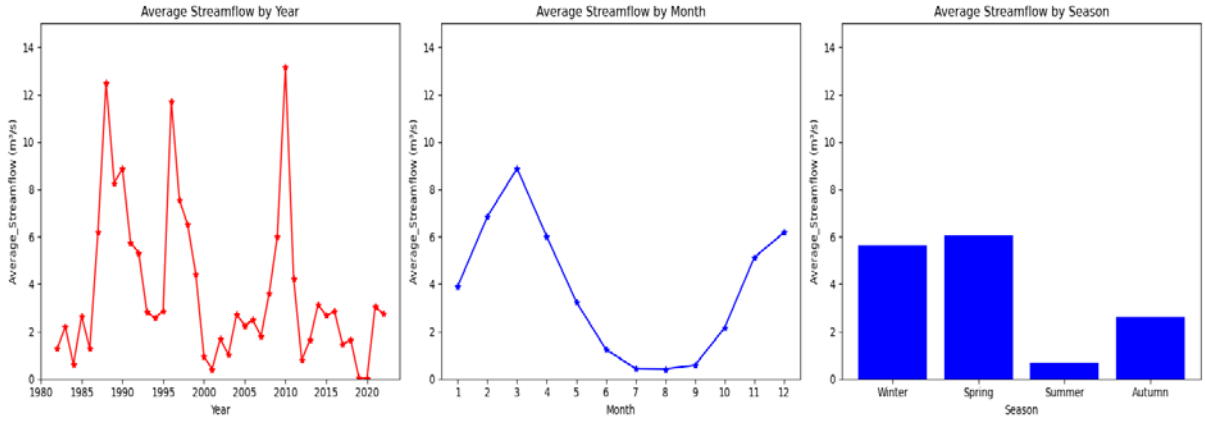


Figure 1. Inter-annual, and monthly and seasonal intra-annual streamflow variability

This study employs a data-driven ML approach to improve monthly streamflow forecasting in the N'fis Basin, Morocco. The methodology consists of the following key steps:

1) Hydroclimatic and teleconnection data were collected and preprocessed by extracting monthly time series, handling missing values, and generating lagged predictors (t-1 to t-6 months) to account for delayed hydrological responses.
2) A correlation-based feature selection was applied, where Pearson correlation analysis identified significant predictors ($p < 0.05$) for each month and lag.
3) Three machine learning models—Random Forest (RF), Support Vector Regression (SVR), and XGBoost (XGB)—were trained using 5-fold cross-validation to assess generalization performance.

Models were evaluated based on Root Mean Square Error (RMSE), Mean Absolute Error (MAE), and R^2 Score, selecting the best-performing model for each month-lag combination.

Results and concluding remarks

Preliminary results indicate that machine learning models for monthly streamflow forecasting reveal significant variability in model performance across different months and lag configurations (Table 1). As expected, larger lags have a major impact on the performance of the SVR, RF, and XGB models (Figure2).

Table 1. Best models per month

Month	Lag	Model	Num Sig Predictors	RMSE	MAE	R2
1	1	SVR	9	4.33	2.93	0.21
2	2	SVR	4	8.64	5.21	0.06
3	1	SVR	8	9.20	6.33	-0.02
4	1	RF	8	3.88	2.91	**0.39**
5	1	RF	8	1.95	1.52	**0.56**
6	1	RF	8	1.09	0.79	**0.51**
7	1	RF	8	0.27	0.17	**0.61**
8	4	SVR	5	0.41	0.27	-0.02
9	4	SVR	1	0.64	0.48	0.11
10	4	SVR	1	2.14	1.59	-1.06
11	1	SVR	4	6.44	3.77	-0.08
12	1	SVR	2	9.90	5.75	-0.13

RF works best for short-term predictions (e.g., 1-month lag), achieving strong results in summer months (e.g., Month 5, Lag 1: R^2 = 0.563). However, its performance drops significantly for longer lags. Although less accurate, SVR handles longer lags better, making it a good option for medium-term forecasts. XGB occasionally performs well (e.g., Month 6, Lag 3: R^2 = 0.466), often failing badly at longer lags. The number of significant features (predictors strongly related to streamflow) also plays a key role. When many features are significant, RF performs well (e.g., Month 4, Lag 1: R^2 = 0.393 with 8 significant features). However, when few features are significant, all models struggle (e.g., Month 12, Lag 1: R^2 = -1.787 with only 2 significant features).

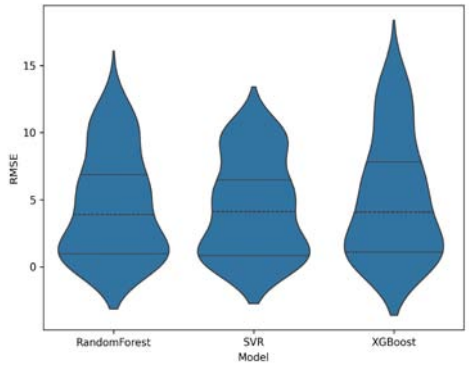


Figure 2. RMSE Distribution by each model

These preliminary results highlight the importance of lag-sensitive modeling, as well as the need to improve feature selection for better performance in challenging conditions. RF is recommended for short-term forecasts, while SVR is a viable option for longer lags. Further research is ongoing on hybrid modeling approaches and dynamic hyperparameter tuning to address these challenges and enhance forecasting accuracy across all seasons and lag configurations.

References

Ayana Ö, Kanbak DF, Kaya Keleş M, Turhan E (2023) Monthly streamflow prediction and performance comparison of machine learning and deep learning methods. Acta Geophys 71(6):2905–2922. https://doi.org/10.1007/s11600-023-01023-6

Lee D, Kim H, Jung I, Yoon J (2020) Monthly reservoir inflow forecasting for dry period using teleconnection indices: A statistical ensemble approach. Appl Sci 10(10). https://doi.org/10.3390/app10103470

Sharma B, Goel NK (2024) Streamflow prediction using support vector regression machine learning model for Tehri Dam. Appl Water Sci 14(5). https://doi.org/10.1007/s13201-024-02135-0

Zkhiri W, Tramblay Y, Hanich L, Jarlan L, Ruelland D (2019) Spatiotemporal characterization of current and future droughts in the High Atlas basins (Morocco). Theor Appl Climatol 135(1–2):593–605. https://doi.org/10.1007/s00704-018-2388-6

Modeling and projecting hydropower production across the Upper Colorado River Basin

F. Marconi[1*], G. Villarini[2], T. Kim[2], H. Kim[2], E. Ridolfi[1], F. Russo[1], C. Veatch[3], W. Veatch[4], F. Napolitano[1]

[1] *Department of Civil, Constructional and Environmental Engineering, Sapienza University of Rome, Rome, Italy*
[2] *Civil and Environmental Engineering & High Meadows Environmental Institute, Princeton University, Princeton, United States*
[3] *Supervisory Hydropower Control Systems Engineer*
[4] *US Army Corps of Engineers, Headquarters, Jacksonville, United States*
** e-mail: flavia.marconi@uniroma1.com*

Introduction

The Colorado River is the primary water source in the western United States, supplying water to 30 million people, irrigating over 16,000 km² of agricultural land, and generating more than 8 billion kilowatt-hours of hydroelectric power annually. In the Upper Colorado River Basin (UCRB), which spans approximately 293,570 km², the Glen Canyon Dam impounds Lake Powell, one of the largest reservoirs in the United States, playing a crucial role in water supply, flood risk management, and hydropower production.

This study investigates the impacts of climate change and extreme events on future hydropower production in the UCRB. By providing insights into these challenges, it aims to support sustainable water resource management and inform decision-making to enhance hydropower resilience.

Materials and methods

The reference precipitation data are obtained from the Parameter Elevation Regression on Independent Slopes Model (PRISM) products, which provide a 4-km gridded climatological dataset spanning from 1981 to 2022 (Daly et al. 2002). Climate model outputs are sourced from the Coupled Model Intercomparison Project Phase 6 (CMIP6), which includes daily outputs from 21 Global Climate Models (GCMs) with spatial resolutions ranging from 25 km to 200 km (Eyring et al. 2016). Additionally, daily inflow, elevation and hydropower production data for Lake Powell are obtained from the U.S. Bureau of Reclamation, (USBR, 2015).

Using data from the common period 2005–2022, we calculate the Spearman correlation coefficient (ρ) on a monthly scale. We then identify the optimal temporal aggregation window, expressed in weeks, that maximizes the correlation between monthly hydropower production and antecedent basin-averaged precipitation. The aggregation period ranges from a minimum of 4 weeks to a maximum of 156 weeks (3 years), beyond which correlation coefficients stabilize.

Then, we model the relationship between spatially and temporally averaged precipitation across the basin and monthly hydropower production at the Glen Canyon Dam using the Generalized Additive Model in Location, Scale, and Shape (GAMLSS) (Rigby and Stasinopoulos 2005).

We compute basin-averaged daily precipitation outputs from 21 CMIP6 climate models and apply bias correction and downscaling using the Empirical Quantile Mapping (EQM) method (Amengual et al 2012). The bias-corrected basin-averaged precipitation projections (Kim and Villarini 2024) are then used as inputs for the identified statistical models to assess potential changes in hydropower production under four CMIP6 future scenarios (SSP1-2.6, SSP2-4.5, SSP3-7.0, SSP5-8.5) over the 2015-2100 period. A GCM is considered viable if it correctly reproduces the statistical significance (at the 5% level) of Kendall's tau (i.e., whether the trend is significant or not) and, in the case of significant trends, the correct sign.

We then compute the ensemble mean across the selected models for each SSP scenario. Finally, we evaluate long-term trends in hydropower production by calculating Kendall's tau across temporal windows

of variable length (minimum of 10 years) from 2005 to 2100, using a significance level of 5%.

Results and concluding remarks

We evaluate the temporal aggregation scale that maximizes the Spearman correlation coefficient (ρ) between monthly hydropower production and antecedent basin-averaged precipitation over the period 2005-2022. The correlation values (ρ) range from 0.4 to 0.8, depending on the month. On average, the optimal aggregation window is approximately 2.5 years, except for March, which is excluded from further analyses. Notably, in March, the highest correlation is observed with a 9-week aggregation window, likely due to the influence of snowmelt during this period.

The Generalized Additive Model for Location, Scale, and Shape (GAMLSS) further confirms precipitation as a key driver of hydropower production, highlighting its critical role in shaping monthly output variability.

To ensure the robustness of future projections, an initial set of 21 Global Climate Models (GCMs) was screened, selecting 16 models that consistently reproduce observed monthly trends in hydropower production. This refined selection enhances confidence in assessing long-term changes in hydropower generation.

Higher-emission scenarios (SSP3-7.0 and SSP5-8.5) project stronger positive trends, particularly in the warmer months, indicating amplified hydropower responses to increasing temperatures. Conversely, lower-emission scenarios (SSP1-2.6) exhibit weaker trends and reduced variability. In high-emission scenarios, long-term trends suggest more consistent increases in spring and summer hydropower production as warming intensifies.

Overall, these findings underscore the need for effective water resource management strategies to address extreme events and changing precipitation patterns under future climate conditions.

Acknowledgments: This work is supported by the RETURN Extended Partnership and received funding from the European Union Next-GenerationEU (National Recovery and Resilience Plan – NRRP, Mission 4, Component 2, Investment 1.3 – D.D. 1243 2/8/2022, PE0000005). This project is developed within the framework of Fulbright-Enel Foundation scholarship on climate change.

References

Amengual A, Homar V, Romero R, Alonso S, Ramis C (2012) A statistical adjustment of regional climate model outputs to local scales: Application to Platja de Palma, Spain. Journal of Climate 25: 939–957. https://doi.org/10.1175/JCLI-D-10-05024.1

Cannon AJ, Sobie SR, Murdock TQ (2015) Bias correction of GCM precipitation by quantile mapping: How well do methods preserve changes in quantiles and extremes? Journal of Climate 28: 6938–6959. https://doi.org/10.1175/JCLI-D-14-00754.1

Daly C, Gibson WP, Taylor GH, Johnson GL, Pasteris P (2002) A knowledge-based approach to the statistical mapping of climate. Climate Research 22: 99–113. https://doi.org/10.3354/cr022099

Eyring V, Bony S, Meehl GA, Senior CA, Stevens B, Stouffer RJ, Taylor KE (2016) Overview of the Coupled Model Intercomparison Project Phase 6 (CMIP6) experimental design and organization. Geoscientific Model Development 9: 1937–1958. https://doi.org/10.5194/gmd-9-1937-2016

Kim T, Villarini G (2024) Projected changes in daily precipitation, temperature and wet-bulb temperature across Arizona using statistically downscaled CMIP6 climate models. International Journal of Climatology 44: 1994–2010. https://doi.org/10.1002/joc.8436

Rigby RA, Stasinopoulos DM, Lane PW (2005) Generalized additive models for location, scale and shape. Journal of the Royal Statistical Society Series C: Applied Statistics 54(3): 507–554. https://doi.org/10.1111/j.1467-9876.2005.00510.x

U.S. Bureau of Reclamation (USBR) (2015) Bureau of Reclamation, Upper Colorado Region. Available at: https://www.usbr.gov/rsvrWater/HistoricalApp.html (accessed Jul 2024).

Investigation of a river basin water potential use under climate change and demand management scenarios

C.P. Cetinkaya[1*], E. Mammadli[2]
[1] Dokuz Eylül University, Faculty of Engineering, Department of Civil Engineering, Izmir, Turkey
[2] Dokuz Eylül University, The Graduate School of Natural and Applied Sciences, Izmir, Turkey
* e-mail: cem.cetinkaya@deu.edu.tr

Introduction

Climate change, considered one of the most significant challenges in the last decades, has substantially impacted water resources. To minimize these effects and ensure a sustainable water supply for future generations, it is crucial to manage water resources in a balanced and well-planned manner. Reservoirs play a key role in regulating river flows, hydropower generation, flood control, and water supply (Bisselink et al. 2018). The effective use of stored water for different purposes depends on the efficient management of reservoirs in line with their design objectives. Various simulation models have been developed to assess reservoir operations and support water resources management.

In this study, the generalized reservoir simulation program HEC-ResSim, developed by the U.S. Army Corps of Engineers (USACE) Hydrologic Engineering Center (HEC), was utilized to analyze reservoir operations. The study focuses on the Çine River sub-basin, located within the Büyük Menderes River Basin, and specifically examines the operation of the Adnan Menderes Dam. Büyük Menderes River Basin is one of the agriculture-intensive basins of Turkey, dominated by Mediterranean climate conditions, experiencing water scarcity exacerbated by anthropogenic influences and climate change. Through simulations based on predefined operational rules, system's behavior was analyzed to evaluate its performance under different conditions.

Materials and methods

In this study, the hydraulic and operational characteristics of the Adnan Menderes Dam were analyzed using HEC-RAS (Brunner 1997) and HEC-ResSim, two widely used models developed by the U.S. Army Corps of Engineers (USACE) Hydrologic Engineering Center (HEC). Daily meteorological data of period 2012-2014 period were utilized. HEC-RAS was employed to simulate the hydrodynamic behavior of the reservoir and downstream river reaches, while HEC-ResSim was utilized to evaluate reservoir operation under different management scenarios. The modeling process consisted of the following steps, (i) Data Collection & Preprocessing – Historical flow records, precipitation, evaporation, and reservoir characteristics (e.g., storage-elevation curve, outlet structures) were compiled, (ii) HEC-RAS Hydrodynamic Modeling – The dam and river system were represented within HEC-RAS to analyze water surface profiles and flow dynamics, (iii) HEC-ResSim Reservoir Simulation – Operational rules, inflow series, and demand scenarios were integrated into HEC-ResSim to simulate reservoir behavior under different conditions, (iv) Model Calibration & Validation – Simulated results were compared against observed data to ensure model reliability, (v) Scenario Analysis – Various operational strategies were tested to assess reservoir performance under different hydrological conditions.

Results and concluding remarks

The developed HEC-RAS hydrological model presents a basis to examine the baseline conditions and also the future meteorological conditions altered by climate change effects, and the demand management scenarios that the stakeholders and the experts of the region have generated together (Figure 1). The preliminary outcomes of the model simulations have been evaluated by the basin's stakeholders for further improvement of the scenarios.

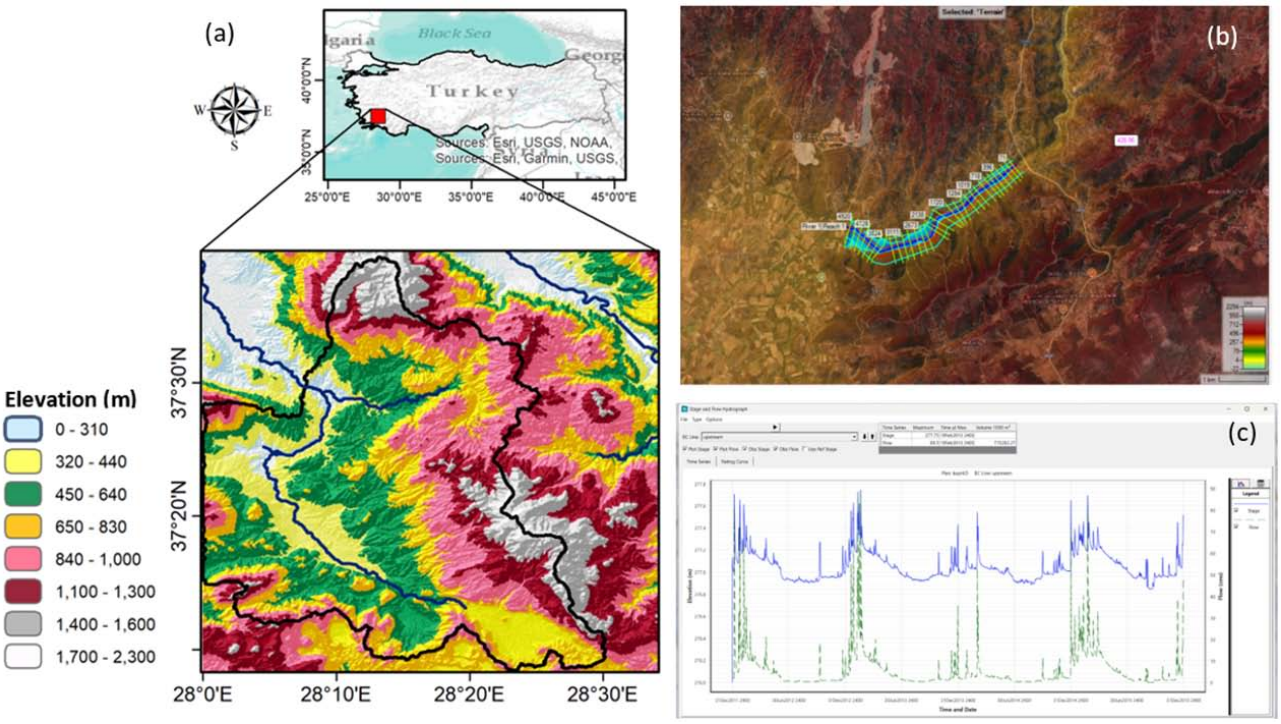


Figure 1. (a) Study area, (b) HEC-RAS model, (c) model outputs for the baseline period.

The results of the study present a valuable tool for both stakeholders and decision-makers of the Büyük Menderes River Basin, as well as for other similar basins that experience semi-arid to arid conditions and are characterized by intensive agricultural activities. This approach presents a tool that provides a comprehensive method to address the challenges faced in such regions, taking into account not only the economic and social dimensions but also the environmental aspects that are crucial for ensuring long-term sustainability.

An additional strength of this study is the inclusion of stakeholder engagement, which ensures that diverse perspectives and priorities are considered in the decision-making process. By involving representatives from various sectors—including policymakers, agricultural producers, local communities, and water resource managers—the study captures the complex and interconnected nature of water management challenges. Furthermore, the active participation of academic institutions and non-governmental organizations (NGOs) has contributed to a well-rounded framework that integrates scientific knowledge with practical, on-the-ground insights.

This multi-dimensional approach fosters sustainable development by balancing economic growth with ecological preservation, ultimately promoting a more resilient and adaptive management strategy for the Büyük Menderes River Basin and similar regions facing comparable climatic and agricultural pressures. The findings of this study provide actionable insights that can guide policy formulation, infrastructure planning, and resource allocation, ensuring that future water management strategies align with both human and environmental needs.

References

Bisselink B, de Roo A, Bernhard J, Gelati E (2018) Future projections of water scarcity in the Danube River Basin due to land use, water demand and climate change. Journal of Environmental Geography, 11(3-4), 25-36. https://doi.org/10.2478/jengeo-2018-0010

Brunner, GW (1997) HEC-RAS river analysis system. Hydraulic reference manual. Version 1.0. 84, 339-348. https://doi.org/10.1016/j.envsoft.2016.06.026

Mirdashtvan M, Najafinejad A, Malekian A, Sa'doddin A (2021) Sustainable water supply and demand management in semi-arid regions: optimizing water resources allocation based on RCPs scenarios. Water Resources Management, 35, 5307-5324. https://doi.org/10.1007/s11269-021-03004-0

Guiding SmAR placement: The role of irrigation water demand

H. Nanesha[1*], M. Lompi[2], M.S. Goodarzi[2], N. Galli[1], E. Caporali[2], M.C. Rulli[1], D.D. Chiarelli[1]
[1] Dipartimento di Ingegneria Civile e Ambiantale, Politecnico di Milano, Milan, Italy
[2] Dipartimento di Ingegneria Civile e Ambientale, Università degli Studi di Firenze, Florence, Italy.
* e-mail: harsh.harsh@polimi.it

Introduction

Water scarcity is an increasing challenge for agriculture in Italy, where recurrent droughts and growing competition for resources threaten productivity. Past water shortages, such as those in 2002, 2003, and 2006 (Altobelli et al., 2015), have underscored the need for more efficient water management strategies. A key issue is the mismatch between water availability and peak agricultural demand, which limits the effectiveness of existing irrigation systems. While previous studies have explored solutions like improved land management and irrigation efficiency (Biemans et al., 2010), there is growing interest in small agricultural reservoirs (SmARs) as a means to enhance water storage and supply stability (Piemontese et al., 2020; Casadei et al., 2019). However, despite global assessments of agricultural water needs (Chiarelli et al., 2020), there remains a lack of high-resolution spatial data to support site selection for SmAR, limiting their potential impact.

This study addresses this gap by identifying the best sites for SmAR from a water demand perspective, comparing spatial patterns of agricultural water demand with available water resources. By integrating hydrological modelling with high-resolution spatial analysis, we aim to determine optimal locations where SmAR can maximize water-use efficiency and drought resilience. The novelty of this research lies in its data-driven approach, bridging the gap between theoretical assessments and practical implementation. The findings will provide actionable insights for policymakers and stakeholders, supporting more sustainable and adaptive water management strategies in the face of increasing climate variability.

Materials and methods

A comprehensive assessment of agricultural water demand and water availability is essential for the sustainable management of water resources, particularly in regions prone to water scarcity. This study quantifies the spatial and temporal variation in irrigation water needs and available water resources to support the optimal siting of SmARs. By identifying areas where demand exceeds supply, this approach facilitates strategic interventions to enhance agricultural resilience against droughts.

To estimate agricultural water demand, spatial datasets on crop distribution and irrigation extent were integrated. Crop type data from EUROCROPMAP (2022) and irrigation extent data from Tian et al. (2024) were combined to delineate irrigated areas for each crop across Italy. This integration allows for a high-resolution assessment of irrigation water demand based on crops, soil properties, and climate conditions.

Crop water requirements were determined using the WATNEEDS model (Chiarelli et al., 2020), which simulates daily vertical soil water balance at a 1 km resolution. Agricultural water demand was quantified as actual evapotranspiration (ETa), derived from potential evapotranspiration (PET), estimated using Hargreaves-Samani method and adjusted using crop-specific coefficients (Allen et al., 1998). Data for precipitation and temperature were obtained from ERA5-Land dataset.

Water availability in SmAR was assessed using remote sensing and empirical models. Multispectral indexes were used to identify water bodies from Sentinel-2 images. Sentinel-2 multispectral indexes were used to identify water bodies, while an area-volume relationship, derived from field campaigns in Tuscany (Giambastiani et al., 2020) was applied to estimate SmAR volumes based on surface area. The feasibility of SmAR was evaluated by identifying suitable locations for supplementary water storage, aimed at mitigating seasonal water shortages.

Results and concluding remarks

This study aimed to identify optimal locations for Small Agricultural Reservoirs (SmARs) by analyzing the spatial and temporal mismatches between water demand and availability across Italy. The findings reveal a significant dependency on irrigation, with approximately 60% of cultivated areas requiring supplemental water, particularly in regions like Emilia-Romagna, Lombardy, Veneto, and Puglia. Among the 23 analyzed crops, wheat and maize demonstrated the highest water requirements, consuming 2.52 km³ and 8.72 km³ per year, respectively, with green water contributing 80% of the total demand. However, irrigation remains essential to compensate for evapotranspiration losses, especially during the summer months (June–September).

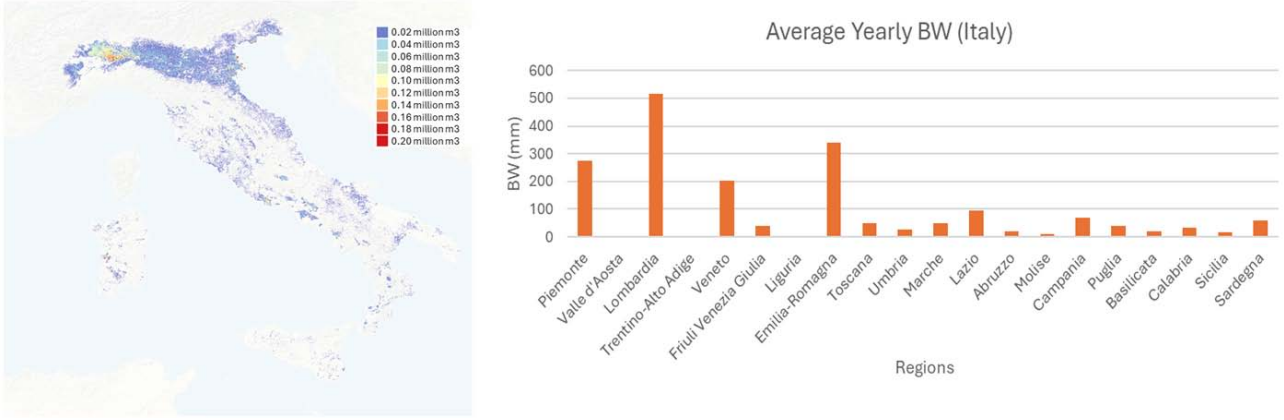


Figure 1. Average yearly BW demand at 1km resolution (left) and average yearly BW demand per region (right) .

Hydrological simulations revealed that water demand often peaks when natural availability is at its lowest, underscoring the need for additional storage infrastructure. Strategic placement of SmARs in regions experiencing chronic water shortages could significantly improve irrigation efficiency, particularly in areas where excess rainfall in wetter months could be harnessed to alleviate seasonal deficits.

Future work will focus on integrating the best siting selection along with vulnerability index and economic feasibility assessments. Stakeholder perspectives will be incorporated to ensure the practical implementation of SmAR solutions at a national scale.

Acknowledgments: This research was developed as a part of project “CASTLE” (PRIN 2022 - CASTLE - cod prog. 2022XSERL4 - CUP D53D23004920006) which is funded by MUR.

References

Allen, R. G., Pereira, L. S., Raes, D., & Smith, M. (1998). Crop evapotranspiration-Guidelines for computing crop water requirements. FAO Irrigation and Drainage paper 56.

Altobelli, F., D'Urso, G., & Del Giudice, T. (2015). Irrigated Agricultural Systems in Italy: Demand And Supply Of Water Management Instruments. Calitatea, 16(S1), 65.

Casadei, S., Di Francesco, S., Giannone, F., and Pierleoni, A.: Small reservoirs for a sustainable water resources management, Adv. Geosci., 49.

Chiarelli, D. D., Passera, C., Rosa, L., Davis, K. F., D’Odorico, P., & Rulli, M. C. (2020). The green and blue crop water requirement WATNEEDS model and its global gridded outputs. Scientific data.

Giambastiani Y., Giusti R., Cecchi S., Palomba F., Manetti F., Romanelli S., Bottai L. 2020. Volume estimation of lakes and reservoirs based on aquatic drone surveys: The case study of Tuscany, Italy. Journal of Water and Land Development. No. 46 (VII–IX) p. 84–96. DOI: 10.24425/jwld.2020.134200.

Muñoz Sabater, J. (2019): ERA5-Land hourly data from 1950 to present. Copernicus Climate Change Service (C3S) Climate Data Store (CDS). DOI: 10.24381/cds.e2161bac

Piemontese, L., Castelli, G., Fetzer, I., Barron, J., Lininger, H., Harari, N., Bresci, E., Jaramillo, F. (2020). Estimating the global potential of water harvesting from successful case studies. Global Environmental Change. https://doi.org/10.1016/j.gloenvcha.2020.102121

Tian, F., Wu, B., Zeng, H., Zhang, M., Zhu, W., Yan, N., Lu, Y., and Li, Y. (2024): GMIE-100: a global maximum irrigation extent and irrigation type dataset derived through irrigation performance during drought stress and machine learning method, Earth Syst. Sci. Data Discuss. https://doi.org/10.5194/essd-2023-536.

Multi-site stochastic precipitation scenarios for water management

A. De Vera*, R. Terra
Department of Fluid Mechanics and Environmental Engineering (IMFIA), School of Engineering (FIng), Universidad de la República (UdelaR), Montevideo, Uruguay
** e-mail: adevera@fing.edu.uy*

Introduction

The Santa Lucía River Basin (SLRB), located in the south of Uruguay, is one of the most critical water sources in Uruguay, it supplies drinking water for the 60% of Uruguayan population (including the capital, Montevideo, and its Metropolitan Area). In addition to anthropic pressures, the basin faces a challenge due to increasing climate variability, with recent periods of severe droughts and extreme rainfall events affecting water availability and quality. In this context, integrated and effective tools for water resource management are essential to ensure its sustainable use.

This work aims to generate climatic scenarios for meteorological variables, in particular precipitation, which then are used as input for an integrated modelling (hydrological and water resources management) framework to assess water supply in a changing climate. The proposed methodology is based on stochastic weather generators (WGs), which have been widely used in decision support systems for risk-based planning and management of natural resources, linked to different process models.

Materials and methods

We use a four-parameter model, which has been previously applied for the generation of synthetic rainfall series in Uruguay (MVOTMA, 2017; De Vera & Terra, 2018). This WG is based on a first-order, two-state Markov chain to simulate the occurrence of daily precipitation (> 0 mm) and a gamma distribution to compute the nonzero daily precipitation amounts. We incorporate the mean annual cycle of the model parameters to capture the seasonal variation. A separate set of parameters is estimated for each calendar day (and geographical point) using a centred moving window of +/-30 days.

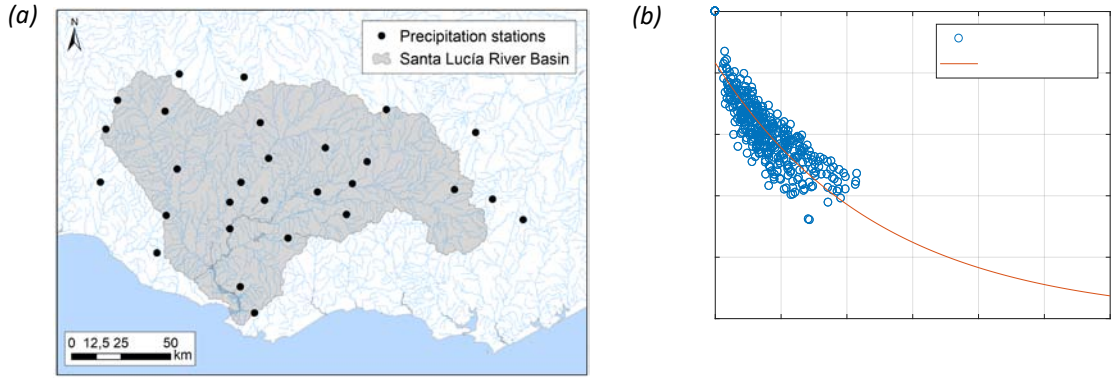


Figure 1. (a) SRLB delimitation and 28 precipitation stations; (b) Correlation of daily amounts as a function of distance.

The daily precipitation dataset considered consists of 28 stations belonging to the INUMET, INIA and UTE, during the period 1998 to 2020 (Figure 1a). Considering the extension of the SLRB (13.500 km^2), the single-point WG was extended to a multi-point model following Wilks (1998), which preserves the observed spatial correlations (shown in Figure 1b as a function of distance). Simulation at multiple locations is achieved with a collection of individual models fed by temporally independent but spatially correlated random numbers (from a multivariate normal distribution). Because the marginal distributions are the same as in the single-point model, the individual behaviour of the local models are preserved.

We simulated 100-years synthetic series of daily precipitation for each station and scenario: the "*baseline scenario*" obtained from the original model parameters without any adjustments, and two other

scenarios, both focused on water deficit situations (which are the most relevant for water management).

The first scenario, called *"dry scenario"*, is obtained decreasing by 5% the current value of model parameters. It was found that the relative magnitudes of multi-annual variation are very similar in the four parameters (of the order of +/- 10% in eight-year moving windows). Based on this result, the amplitude for the sensitivity analysis was taken as 5% for each parameter, considering the simultaneous variations in all parameters, which amplifies the signal, hence the reduction of the amplitude (same as in MVOTMA, 2017).

The second scenario, called *"perpetual La Niña"*, incorporates climate conditioning, selectively resampling the historical data to produce synthetic sequences consistent with a cold phase of the El Niño–Southern Oscillation (ENSO) phenomenon, which is associated with lower-than-normal precipitation in the region (Aceituno, 1992). The conditioning variable used is the Niño-3.4 monthly index (Trenberth, 1997) averaged in quarter November–January (NDJ) for September–August "ENSO years".

Results and concluding remarks

The multi-site precipitation generator effectively captures the observed spatial correlations in the synthetic series. Additionally, the model satisfactorily reproduces the frequency of wet days and the average wet-day amount. It also captures the climatological seasonal cycle of precipitation and the ENSO signal on precipitation, including its seasonality (see Figure 2a). However, it is well known that these models tend to underestimate the interannual variance of aggregated quantities (i.e. annual precipitation, see Figure 2b).

Mean annual basin-integrated precipitation in the "*dry scenario*" is approximately 200 mm lower than in the "*baseline"* one. The "*perpetual Niña*" scenario is intermediate in terms of annual mean totals and, in addition, has the seasonal structure of the signal characteristic of the ENSO phenomenon.

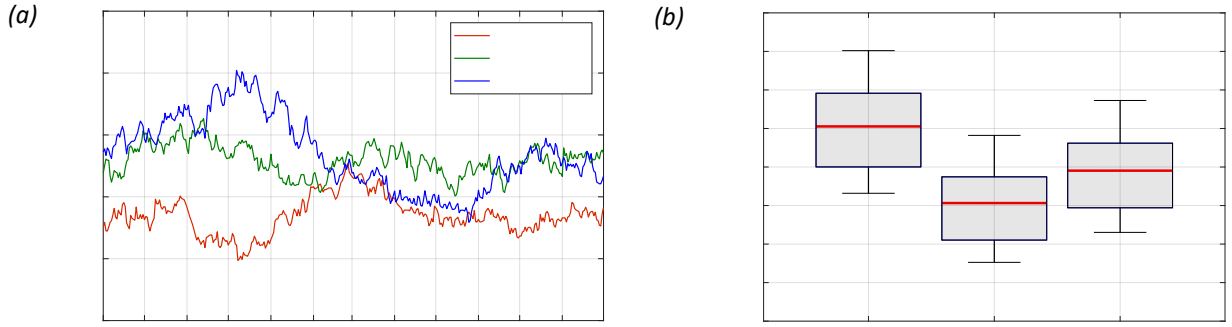


Figure 2. (a) Mean annual cycle of Markov dry-to-wet transition probability according to ENSO phase (Florida station); (b) Distribution of annual precipitation in three scenarios (box: percentile 25-50-75 and whiskers: 10-90).

The impact of these precipitation scenarios on streamflow and, in turn, water security was evaluated with an integrated modelling framework in the context of a collaboration with the water Administration.

Acknowledgments: This work was conducted in the framework of the EUROCLIMA project with DINAGUA.

References

Aceituno P. (1992). El Niño, the Southern Oscillation, and ENSO: Confusing names for a complex ocean–atmosphere interaction. Bull. Amer. Meteor. Soc., 73, 483-485. https://doi.org/10.1175/1520-0477-73.4.483

De Vera A., Terra R. (2018). A Stochastic Precipitation Generator Conditioned by a Climate Index. J. Appl. Meteor. Climatol., 57, 2585–2603, https://doi.org/10.1175/JAMC-D-17-0307.1

MVOTMA (2017). Plan Nacional de Aguas, Uruguay. ISBN: 978-9974-658-31-8. Available on: https://www.gub.uy/ministerio-ambiente/politicas-y-gestion/planes/plan-nacional-aguas

Trenberth K.E. (1997). The definition of El Niño. Bull. Amer. Met. Soc., 78, 2771-2777. https://doi.org/10.1175/1520-0477(1997)078<2771:TDOENO>2.0.CO;2

Wilks D.S. (1998). Multisite generalization of a daily stochastic precipitation generation model. Journal of Hydrology, 210, 178-191. https://doi.org/10.1016/S0022-1694(98)00186-3

Assessment of urban stormwater quality by informing a hydrologic-hydraulic model with microscopic traffic simulations.

G. Formetta*, A. Marzadri, M. Guerrieri
Department of Civil, Environmental and Mechanical Engineering, University of Trento, Trento, Italy
** e-mail: giuseppe.formetta@unitn.it*

Introduction

As urbanization continues to increase and transportation networks expand with many more vehicles on the roads, cities are facing growing challenges, including longer commuting distances, higher rates of traffic accidents, increased pollution from traffic along with reduction of green spaces. When a rainfall event occurs after a dry period, the so-called first flush phenomenon generates (Sartor and Boyd, 1972). It indicates the effect of the first and faster stormwater runoff, which, by washing over impervious surfaces such as roads, gather together pollutants, like particulate matter, nutrients, bacteria and heavy metals. Without proper water treatment measures, this contaminated flow represents one of the major causes of drainage systems and water bodies quality deterioration (e.g., Barbosa and David, 2012). Several studies pointed out a clear correlation between the increase of the contamination level of stormwater runoff from roads and the number of vehicles (e.g., Barrett et al., 1998) or the average daily traffic density (Hares and Ward, 1999). However, the lack of reliable data of stormwater quality together with the costs and difficulties in performing regular monitoring campaigns of traffic in different locations and for different pollutants (i.e., heavy metals, particulate matter, total suspended solids, nitrogen oxides, etc.), have hindered the possibility to quantify the level of contamination.

To overcome some of these obstacles, this study combines two modelling procedures that simulates the traffic related emissions by using AIMSUN (Advanced Interactive Microscopic Simulator for Urban and Non-Urban Networks, AIMSUN 2024), a well-known integrated traffic and emission model, and the relative build-up, wash-off and transport throughout the drainage system by using the Storm Water Management Model (SWMM, Huber 1985). AIMSUN and SWMM were used to characterize the wash-off and fate of particulate matter generated by traffic (hereafter PM) and its possible reduction by the introduction of a first-flush tank in a roundabout of the city of Trento (Italy). The study also explores several alternative layouts to an existing roundabout in order to identify the optimal one from a combined environmental and traffic management perspective.

Materials and methods

The estimates of the measure of effectiveness (MOEs) and traffic PM emissions were obtained through microscopic traffic simulations in the AIMSUN software under high traffic demand (total inflow QT = 3600 vehicles/hour) over the different roundabout layouts (Tollazzi, 2015). This allows the possibility to take into account the existing condition (Layout 1: the so-called "Caduti di Nassiriya" roundabout in Trento) as well as to analyse the behaviour of improved layouts: i) single-lane roundabout (1+1, named Layout 2 with one entry lane for each arm and one circulating lane), ii) single-lane roundabout (1+2, named Layout 3 with one entry lane for each arm and one circulating lane), iii) double-lane roundabout (2+2, named Layout 4, with two entry lanes for each arm and two circulating lanes), iv) flower roundabout (i.e. Layout 5, with stop-controlled right-turn lanes, and iv) basic turbo roundabout (Layout 6).

The traffic model was calibrated considering real traffic data of the roundabout into operation in Trento Municipality and then was applied to all the roundabout types under consideration. Also, drivers' psychotechnical parameters were assessed from real traffic samples. The output of the calibrated AIMSUN model in terms of production of PM for each layout scenario have been used in input the SWMM water quantity/transport model.

The fate of the emitted PM was characterized by using SWMM under a synthetic and constant

precipitation event generated by computing the intensity duration frequency curves (IDF) derived using measured data of annual maximum precipitation depth for a return period of TR=10 years. The drainage system layout near the roundabout was designed by modelling the water infiltration losses via the Curve Number method (NRCS, 1986), assuming pipes with circular cross-section made of concrete, and including the possibility to introduce a first-flush tank to improve the water quality.

In the designed drainage system, the stormwater pollution due to the washed PM was schematised by modelling the three main processes: i) the gradual accumulation on permeable/impermeable surfaces (build-up modelled as a growth curve which asymptotically approaches a maximum limit), ii) the washed off by intense rain after dry periods (wash-off modelled as an exponential decay function), and iii) the mix and transport with stormwater surface runoff.

Results and concluding remarks

Analysing and comparing the results of traffic PM emissions in the different roundabout configurations, we can observe that the layout responsible for a major emission of PM is Layout 5 with an emission of PM=149 gr.

To attenuate the concentration of PM conveyed by the drainage system a possible mitigation strategy consists in introducing a first-flush tank plunged below the roundabout. The volume of the first-flush tank was estimated considering 5 mm of precipitation over the contributing area and an inflow coefficient equal to 0.5 and the volume for the sedimentation of the PM and other settleable solids (Wtank equals to 185 m^3).

After the introduction of the first-flush tank we observe a reduction of the amount of PM conveyed by the system by a 27%. Results of this study aims to highlight how, through the combination of modelling software (such as AIMSUM and SWMM), is possible to analyse in a quantitative way the important linkage between traffic emissions and stormwater pollution. In particular, the applicability of the proposed methodology to different roundabout types allows the design of a first-flush tank to attenuate the pollution along the drainage system. This simple case study can be used as a prototype for possible implementation at larger scales (involving multiple roundabouts) and also combining fist-flush tanks with nature-based solutions or lamination strategies.

Acknowledgments: the authors acknowledge funding from the Italian Ministry of Education, University and Research (MUR) in the framework of the project DICAM-EXC (Departments of Excellence 2023-2027, grant L232/2016). GF and AM acknowledge the project iNEST (Interconnected North-Est Innovation Ecosystem) funded by the European Union NextGenerationEU (PNRR – Missione 4 Componente 2, Investimento 1.5-D.D. 1058 23/06/2022, ECS_00000043)

References

Aimsun (2024). Aimsun Next 24 User's Manual, Aimsun Next Version 24.0.0, Barcelona, Spain.

Barbosa A E, Fernandes JN, David LM (2012). Key issues for sustainable urban stormwater management. Water Res. 46 (20), 6787e6798.

Hares R J, Ward N I (1999). Comparison of the heavy metal content of motorway stormwater following discharge into wet biofiltration and dry detention ponds along the London Orbital (M25) motorway. Science of the Total Environment, 235(1-3), 169-178.

Huber W C (1985). Storm Water Management Model (SWMM). Environmental Research Laboratory, Office of Research and Development, U.S. Environmental Protection Agency. Athens, Ga.

Natural Resource Conservation Service (NRCS), Urban Hydrology for Small Watersheds, Technical Release 55, Second Ed., U.S. Department of Agriculture, Washington, DC, June, 1986.

Sartor J D, Boyd G B (1972). Water pollution aspects of street surface contaminants (Vol. 2). US Government Printing Office.

Tollazzi T (2015). Alternative Types of Roundabouts. An Informational Guide. Springer.

Towards digital twin for sustainable irrigation water management in Mediterranean agriculture

A. Borgo[1,2*], M. Debolini[2], G. Rianna[2], S. Mereu[2,3]
[1] Department of Agriculture, University of Sassari, Viale Italia 39A, Sassari, 07100, Italy
[2] CMCC Foundation – Euro-Mediterranean Centre on Climate Change, Italy
[3] Institute of BioEconomy, Italian National Research Council, Italy
* e-mail: a.borgo@studenti.uniss.it

Introduction

Agriculture is the sector with the highest water demand in the Mediterranean, accounting for 64-69% of total water withdrawals, and exceeding 80% in most arid and semi-arid countries (MedECC, 2020). The situation is expected to be further exacerbated by climate change, which poses a significant threat to water resources by accelerating evapotranspiration rates and altering precipitation patterns, resulting in more frequent heavy rainfall and extended drought periods (IPCC, 2023). Therefore, improving irrigation efficiency through governance tools referring to the widely consolidated Integrated Water Resource Management (IWRM) framework becomes essential for minimizing water conflicts (Agarwal et al., 2000). Digitalizing the irrigation sector can provide a strategic solution to address water scarcity by incorporating advanced technologies, such as the Internet of Things (IoT) and innovative water and weather sensors, into conventional irrigation systems (Abbasi et al., 2022). Although numerous models already exist to estimate irrigation demand based on crop growth (SIMETAW, Mancosu et al., 2016; CROPWAT, Smith, 1992; AQUACROP, Steduto et al., 2009), most of them fail the step to become tool "operationally" adopted by farmers. This work aims to develop and implement a real-time irrigation model that serves as a decision-support tool for precise irrigation management in Mediterranean environments. By integrating sensor-based data (soil moisture sensors, water meters, and weather stations), weather forecasts (from meteorological models), and user inputs (related to crop, soil, and irrigation management), the model provides accurate scheduling for irrigation events, giving users a comprehensive understanding of crop water requirements.

Materials and methods

The irrigation model, developed on the R programming platform, is a tool trained and tested on both annual and perennial crops across different climatic environments (pilots): Mediterranean (Sardinian pilot), semi-arid (Lebanon), and arid (Tunisian pilot and Jordan pilots). The model primarily follows FAO principles (Allen et al., 1998) for computing crop water requirements and is designed to rely on a limited and easily accessible set of input data, making it user-friendly for farmers. Inputs are divided into four categories: atmosphere forcing, soil, crop and irrigation data, sourced from sensors, FAO tables, and user indications. Climate inputs include hourly temperature, relative humidity, solar radiation, precipitation, and wind speed from both sensors (for historical data) and weather forecast APIs (for predictions). Soil inputs, such as percentages of sand, silt, and clay, bulk density, and saturated hydraulic conductivity, are essential for estimating soil water characteristic parameters. Crop parameters (e.g., crop coefficients, phenological stage durations, depletion factors, root depths, and deficit irrigation settings) are documented separately based on FAO guidelines and stakeholder feedback from each pilot. Additional historical data on soil moisture at various depths and irrigation water flow, together with the irrigation system specifications (e.g., irrigation method, emitter flow rate and spacing, and drip line length) are required.

The model runs every 12 hours, estimating hourly irrigation demand patterns (Irr_{full}), deficit irrigation (Irr_{def}), and the actual soil moisture (SM), updating its results iteratively. Each run covers a two-week hourly-scale time frame, with one week of historical data preceding the time step of the run *i* and one week of forecast data following the step *i*. The model reconstructs the historical evolution of Irr_{full}, Irr_{def}, and SM

from field sensor data and calculates the soil water balance to predict the future dynamics, helping users understand changes without irrigation. Based on scenarios of optimal irrigation (Early), moderate (Late), and high (Limit) water stress, the model schedules irrigation events for both full and deficit irrigation strategies.

Results and concluding remarks

The implementation of a real-time irrigation model across Mediterranean and arid areas can demonstrate promising outcomes in enhancing irrigation management in water-scarce regions. Its intuitive architecture, requiring minimal and easily obtainable input data, enables accessible management and clear visualization of the model's outputs. The model's capacity to integrate sensor-based data, weather forecasts, and user inputs allows dynamic and accurate scheduling of irrigation events for diverse environmental, crop and irrigation management conditions. By checking the presence of deep percolation events or water deficit in the lowest level of the soil profile, the model calibrates future irrigation events from the performance of past irrigations. Moreover, its ability to predict soil moisture dynamics and identify the evolution of irrigation demand supports users to flexibly schedule irrigation events according to water availability, avoiding crop water stress and reducing percolation. This flexibility constitutes valuable support for stakeholders, considering the future water availability challenges in arid and Mediterranean environments.

Acknowledgments: The work is financed by the PRIMA-founded project ACQUAOUNT (Adapting to Climate change by QUantifying optimal Allocation of water resOUrces and socio-ecoNomic inTerlinkages - https://www.acquaount.eu/)

References

Abbasi, R., Martinez, P., & Ahmad, R. (2022). The digitization of agricultural industry – a systematic literature review on agriculture 4.0. Smart Agricultural Technology, 2, 100042. https://doi.org/10.1016 /j.atech.2022.100042

Agarwal, A., S. delos Angeles, M., Bhatia, R., Chéret, I., Davila-Poblete, S., Falkenmark, M., Villarreal, F. G., Jønch-Clausen, T., Kadi, M. A., Kindler, J., Rees, J., Roberts, P., & Rogers, P. (2000). TAC background Papers No.4: Integrated Water Resources Management. In Global Water Partnership (Issue 4). https://doi.org/10.4337 /9781788974912.I.43

Allen, R.G., Pereira, L.S., Raes, D., & Smith, M. (1998). FAO Irrigation and Drainage Paper No. 56 - Crop Evapotranspiration (Issue 56). FAO - Food and Agriculture Organization of the United Nations, Rome

IPCC (2023). IPCC, 2023: Summary for Policymakers. In: Climate Change 2023: Synthesis Report. Contribution of Working Groups I, II and III to the Sixth Assessment Report of the Intergovernmental Panel on Climate Change. https://www.unep.org/resources/report/climate-change-2023-synthesis-report

Mancosu, N., Spano, D., Orang, M., Sarreshteh, S., & Snyder, R. L. (2016). SIMETAW# - A model for agricultural water demand planning. Water Resources Management, 30(2), 541–557. https://doi.org/10.1007/s11269-015-1176-7

MedECC (2020). Current situation and risks for the future First Mediterranean Assessment Report. https://zenodo.org/record/4768833

Smith, M. (1992). CROPWAT: a computer program for irrigation planning and management. Food and Agriculture Organization (FAO).

Steduto, P., Hsiao, T. C., Raes, D., & Fereres, E. (2009). AquaCrop—The FAO Crop Model to Simulate Yield Response to Water: I. Concepts and Underlying Principles. Agron. J., 101, 426–437. https://doi.org/10.2134/agronj2008.0139s

Integrating multimodal seasonal forecasts with SWAT to predict seasonal water availability in the Imera Meridionale river basin, Sicily

S. Lemma Tekle[1,2,3*], B. Bonaccorso[2], P. Block[3]
[1] Scuola Universitaria Superiore Pavia - IUSS Pavia, 27100 Pavia, Italy
[2] Dipartimento di Ingegneria, Università Degli Studi di Messina, Messina, Italy
[3.] Department of Civil and Environmental Engineering, University of Wisconsin-Madison, USA
* e-mail: shewandagn.tekle@iusspavia.it

Introduction

Seasonal forecasts have the potential to inform water resources decision-making and support planning and risk management strategies through benefits across social, economic, and ecological dimensions (Block et al., 2009; Jackson-Blake et al., 2022). These systems provide advanced expectations of water availability, and when coupled with infrastructure, can guide allocations, including for environmental flows, for local and regional managers to make timely decisions for their key stakeholders. However, reliable and accurate seasonal climate and streamflow forecasting remains challenging and continues to be the focus of ongoing research (Arnal et al., 2018; Baker et al., 2019; Whateley et al., 2015).

In this study, we evaluate the performance of seasonal reservoir inflow forecasts by integrating multimodal precipitation forecasts with the Soil and Water Assessment Tool (SWAT) (Grillakis et al., 2018; Sehgal et al., 2018) in a drought-prone river basin in central Sicily. The main objective of this study is to develop hydroclimatic forecast systems to assist local managers in making climate-informed decisions. Moreover, this study will pave the way for the development of basin-wide real-time operational forecasting systems in our future research.

Materials and methods

We evaluate three methodologies—dynamical models, and two statistical models (Figure 1b)—for estimating seasonal inflows to the Olivo and Villa Rosa reservoirs in the Imera Meridionale River Basin (IMRB, Figure 1a & b). Specifically, we derive seasonal climate forecasts of precipitation and temperature from dynamical models and feed them into SWAT to simulate expected reservoir inflow. Raw ensemble mean forecasts were retrieved from the Copernicus climate data store from three modeling centers: the European Centre for Medium-Range Weather Forecasts (ECMWF), the Environment and Climate Change Canada (ECCC), and the Japan Meteorological Agency (JMA). The raw forecasts were downscaled and bias-corrected conditioned on observed data from local stations using five different quantile mapping techniques (Chadwick et al., 2023).

This process involved the following steps:

1. Multi-model selection and acquisition of seasonal forecast datasets for Sicily Island
2. Downscaling and bias correction of the raw forecasts
3. Calibration and validation of SWAT using observed climate and hydrologic data
4. Running the calibrated SWAT model to generate pseudo streamflow data for the period 1993 to 2023.
5. Running the calibrated SWAT model using as input the multi-model ensemble mean forecast data to estimate seasonal water availability.
6. Evaluating the performance of the multi-model systems by comparing monthly and seasonal streamflow forecasts against pseudo streamflow data (see pt. 4) through statistical metrics

Results and concluding remarks

Results indicate that forecasts from all three modeling centres, when integrated with SWAT, can generate statistically significant inflow predictions (Table 1) for the Villa Rosa (subbasins 7 & 30) and Olivo

(subbasin 32) reservoirs (Figure 1a), although performance varies. For example, predicted and observed streamflow are strongly correlated (>0.6) considering monthly time steps, however much of this is attributable to simply capturing the seasonal cycle; performance is relatively poor in capturing peaks in the wintertime months (rainy season). Likewise, performance is also limited when assessing the aggregated wintertime seasonal total precipitation and mean streamflow. It should be noted that seasonal evaluation is based on a relatively small sample size, either 23 or 25 years, depending on the model, and may be influenced more by random noise in the data. Regardless, the dynamical climate models appear to have inherent limitations in capturing climate extremes. Although prediction performance does decrease with lead time, it is noteworthy that this drip is minimal for monthly predictions when comparing one-month and five-month leads (Table 1). In general, the JMA model performs poorly compared to the ECMWF and ECCC models and tends to significantly underpredict the wintertime inflow.

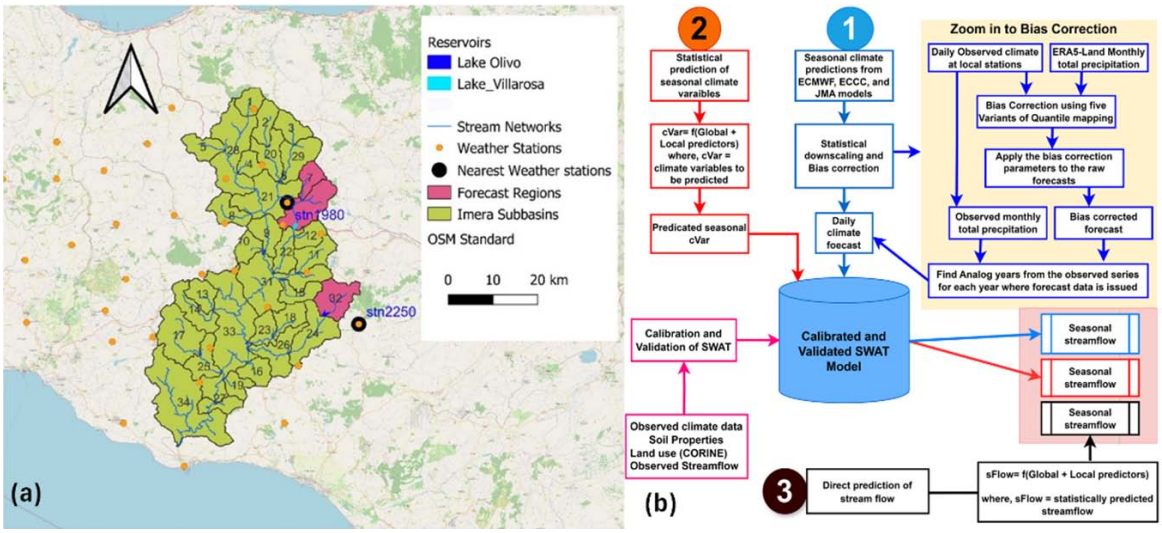


Figure 1. (a) location of study area, (b) general framework of the methodology

Table 1. Correlations of mean winter (DJF) and monthly streamflow predictions. Note: Sbn = Subbasins

	Winter, lead time 1m			Winter, lead time 5m			Monthly, lead time 1m			Monthly, lead time 5m		
	Sbn7	**Sbn30**	**Sbn32**	**Sbn7**	**Sbn30**	**Sbn32**	**Sbn7**	**Sbn30**	**Sbn32**	**Sbn7**	**Sbn30**	**Sbn32**
ECMWF	0.34	0.33	0.43	0.17	0.15	0.22	0.72	0.70	0.76	0.68	0.66	0.68
ECCC	0.42	0.40	0.61	0.08	0.07	-0.01	0.74	0.72	0.75	0.70	0.68	0.69
JMA	0.19	0.18	0.33	0.16	0.14	0.42	0.65	0.62	0.66	0.63	0.60	0.64

In summary, dynamical models show potential for forecasting monthly precipitation predictions at various lead times, however, they struggle to capture monthly and seasonal peak seasons, a critical attribute for water availability in the basin. This motivates the investigation of other forecast approaches, such as statistical and machine-learning models.

References

Arnal L, Cloke HL, Stephens E, et al. (2018) Skilful seasonal forecasts of streamflow over Europe? Hydrology and Earth System Sciences, 22(4), 2057–2072. https://doi.org/10.5194/hess-22-2057-2018

Baker SA, Wood AW, Rajagopalan B (2019) Developing Subseasonal to Seasonal Climate Forecast Products for Hydrology and Water Management. https://doi.org/10.1111/1752-1688

Chadwick C, Gironás J, González-Leiva F, Aedo S (2023) Bias adjustment to preserve changes in variability: the unbiased mapping of GCM changes. Hydrological Sciences Journal, 68(8), 1184–1201. https://doi.org/10.1080/02626667.2023.2201450

Grillakis M, Koutroulis A, Tsanis I (2018). Improving seasonal forecasts for basin scale hydrological applications. Water (Switzerland), 10(11). https://doi.org/10.3390/w10111593

Sehgal V, Sridhar V, Juran L, Ogejo JA (2018) Integrating climate forecasts with the Soil and Water Assessment Tool (SWAT) for high-resolution hydrologic simulations and forecasts in the Southeastern U.S. Sustainability (Switzerland), 10(9). https://doi.org/10.3390/su10093079

Whateley S, Palmer RN, Brown C (2015) Seasonal Hydroclimatic Forecasts as Innovations and the Challenges of Adoption by Water Managers. Journal of Water Resources Planning and Management, 141(5). https://doi.org/10.1061/(asce)wr.1943-5452.0000466

Hydrologic conditions quantification for sustainable water resources management of ungauged river basin

B. Matić[1*], B. Karleuša[2]
[1] Educons University, Sremska Kamenica, 21208, Serbia
[2] Faculty of Civil Engineering University of Rijeka, Rijeka, 51 000, Croatia
*e-mail: branislava.matic@educons.edu.rs

Introduction

Misunderstanding of hydrometeorological events frequency spatial and temporal distribution might result in water resources mismanagement (Viessman and Lewis, 1996) with numerous adverse effects on society regardless the hydrologic unit (HU) area (from small catchment to large river basin). An increase in average global temperature will very likely alter hydrological cycle and affect the frequency of extreme events Houghton et al. (2001). Increase in these events (floods, droughts, etc) over the world are evident with expected trend continuity in the future (Liu et al., 2021) but the exact magnitude and spatio-temporal future characteristics are uncertain (Pratap and Markonis,2022).

Extension of the river basin capacity to retain precipitation increase their discontinuity with runoff generation (Jevđević, 1956). Low runoff potential indicates good hydrologic conditions (Chin, 2000) and natural and hydrologic features specifically for small river basins have to be evaluated (Žugaj, 2010). Improved retention capacity is a favourable contribution to adaptive and sustainable water resources management. This paper presents methodological framework for ungagged river basin runoff curve number (CN) quantification to assess the potential maximum retention capacity of the catchment (S) and the depth of runoff (Q_o).

Materials and methods

Runoff Curve-number (CN) model developed by Natural Resources Conservation Services (formerly named Soil Conservation Service) as a function of hydrologic soil group (HSG), land cover, hydrologic conditions, etc., is widely used both for small rural and urban catchments. The general equation for runoff estimation (NRCS, 2004) based on the catchment potential maximum retention (S) capacity as a function of CN for different HSG (A, B, C, D) initial abstraction (Ia=0.2 S) and rainfall event (P>0.2 S) is:

$$Q_o=\frac{(P-0.2S)^2}{P+0.8S}\ (mm),\ S=25.4\left(\frac{1000}{CN}-10\right)(mm) \quad (1)$$

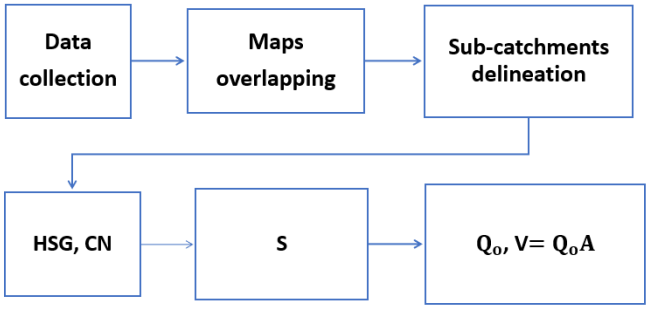
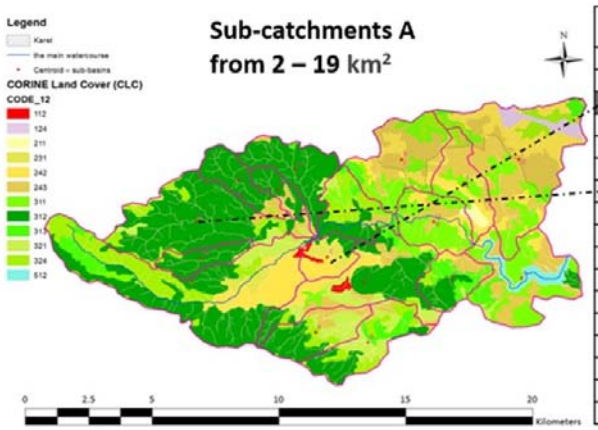


Figure 1. Methodological framework for CN quantification and S and Qo estimation

Water quantity V at the outlet from contributing drainage area (A) is applied for calculated CN values validation, and CN and S for normal dry and wet antecedent runoff condition (ARC) are estimated based in equations available in hydrologic literature. Rainfall data sets from the meteorological station with shortest distance to watershed centroid are used for runoff depth (Q_o) calculation.

Results and concluding remarks

The CN quantification and S and Q_o estimation was conducted by using accepted statistical and hydrological methods, ArcGIS tools and applied to the multipurpose ungauged Vrutci reservoir drainage area (146 km^2) on Đetinja river, located in upper part of Western Morava River basin in Serbia (Matić, 2019). For CN quantification Corine Land Cover, Hydrogeological map and Digital elevation model are overlapped. For comprehensive evaluation and accurate data 17 sub-catchments are delineated (Figure 2).



Sub Catchment	A (km^2)	CN ARC II
A	11	78
B	6	70
C	3	80
D	7	70
E	13	71
F	24	69
G	16	68
H	6	78
I	6	72
J	10	77
K	5	78
L	4	72
M	3	69
N	2	71
O	19	82
P	5	76
R	6	76

Figure 2. Sub-catchments delineation map and CN for normal -ARC II (source: Matić, 2019)

Majority (70%) of sub-catchments has poor hydrologic conditions and moderate to low potential maximum retention capacity (Figure 2) with CN values from 68 to 80 for ARC II (normal condition). The comparison of pre-development water quantity observed at the drainage area outlet and water quantity (V) based on methodology for CN number quantification generates high correlation (R^2= 0. 9883) that indicates sufficient level of results certainty and their applicability in more comprehensive S and runoff estimation based on natural features (slope, catchment shape coefficient, forest cover coefficient, etc) that will allow the consideration of measures for improved water management.

Acknowledgments: This research and publication of this article was partially funded by the University of Rijeka within project: Implementing innovative methodologies, technologies and tools to ensure sustainable water management (uniri-iskusni-tehnic-23-67).

References

Chin A. David (2000) Water – Resources Engineering. Prentice – Hall Inc., Upper Saddle River, New Jersey.

Houghton, Y. Ding, D.J. Griggs (Eds.) (2001) The Scientist Basis, Inter Governmental Panel on Climate Change (IPCC) Cambridge University Press, 881 pp. https://www.ipcc.ch/site/assets/uploads/2018/03/WGI_TAR_full_report.pdf

Jevđević V (1956) Hidrologija I Deo. special ed, book 4, Hidrotehnički institut "Ing. Jaroslav Černi", Beograd

Liu X, Li Z and Attarod P (2021) Editorial: Understanding Hydrological Extremes and Their Impact in a Changing Climate: Observations, Modeling and Attribution. Front. Earth Sci. 8:632186. doi: 10.3389/feart.2020.632186

Matić B. Branislava 2019. Rainfall impact on river basin retention capacity and water management, Ph.D. Dissertation, FTN University of Novi Sad. National Repository of Dissertations in Serbia, Author reprint. Available from: https://nardus.mpn.gov.rs/handle/123456789/11418

Natural Resources Conservation Services (2004) Estimation of direct runoff. Part 630 - National Engineering Handbook, USDA, Washington D.C, USA.

Pratap, S., Markonis, Y. (2022) The response of the hydrological cycle to temperature changes in recent and distant climatic history. Prog Earth Planet Sci 9, 30. https://doi.org/10.1186/s40645-022-00489-0

Viessman Jr. Warren, Knapp W. John, Lewis L Garry, Harbaugh E. Terence (1996) Introduction to Hydrology, 4th edition. Thomas Y.Crowell Company, Inc., New York, New York.

Žugaj, Ranko (2010) Velike vode malih slivova (Small basins high waters), Rudarsko-geološko-naftni fakultet, Zagreb, Hrvatska.

Water scarcity and future management scenarios assessment in Naxos island, Cyclades, Greece

S. Mike[1], M. Ntoi[1], A. Lyra[1], G. Tziatzios[1], N. Mylopoulos[1], A. Loukas[2], L. Vasiliades[1], P. Sidiropoulos[2*]

[1] *Laboratory of Hydrology and Aquatic Systems Analysis, Department of Civil Engineering, School of Engineering, University of Thessaly, 38334 Volos, Greece*

[2] *Laboratory of Hydraulic Works and Environmental Management, School of Rural and Surveying Engineering, Aristotle University of Thessaloniki, 54124 Thessaloniki, Greece*

** e-mail: pasidirop@topo.auth.gr*

Introduction

Naxos, the largest island of the Cyclades, faces increasing water management challenges due to rising water demand for tourism, agriculture, and urban expansion. This study aims to assess the current state of water resource management on Naxos Island and simulate and evaluate future projected scenarios, using the WEAP software. Effective water planning is crucial to ensure long-term water security for Naxos Island.

Materials and methods

The methodology of this study involves data collection and hydrological analysis to evaluate water resource management in Naxos Island. Precipitation and temperature data were analyzed using gradient-based methods to calculate mean surface rainfall and temperature from local gauge stations. Evapotranspiration was estimated using the Thornthwaite method. Water demand was categorized into domestic, industrial, livestock, and agricultural water needs, analyzed over two time periods, 1985–2001 and 2001–2021. Domestic water needs were estimated based on population growth and tourism trends, while industrial and livestock water demands were evaluated considering economic activities and agricultural expansion. Special attention was given to irrigation needs, which are crucial for the island's agricultural sector, with calculations based on historical land use changes and crop water requirements (Mike and Ntoi 2022).

To model and predict water resource availability and management scenarios, the WEAP (Water Evaluation and Planning) software was employed (Sieber 2006). The WEAP model was structured for Naxos Island based on the Water Resources Management Plan by the district of South Aegean Region (South Aegean Region 2005). The model is structured by defining watersheds, rivers, groundwater sources, reservoirs, and demand nodes. Hydrological processes such as runoff, infiltration, and discharge to the sea have been simulated. Runoff and infiltration processes are linked to surface and subsurface hydrological systems to capture interactions between rainfall, soil moisture, and groundwater recharge. Reservoir nodes are established to reflect surface water storage capacity, while water demand sites are defined to represent sector-specific water consumption. Transmission links are introduced to simulate the movement of water from water supply sources to water demand nodes, ensuring a realistic representation of water distribution across island.

The study evaluates multiple water management scenarios for Naxos Island using the WEAP model to assess future water demand and availability. These scenarios aim to capture the potential impacts of external factors such as climate change, economic activities, and demographic shifts on water resources.

- Scenario 1: COVID-19 Impact – Calculated increased domestic water demand due to COVID-19 pandemic outbreak (+20% from 2019-2024) based on the study by Antwi et al (2021).
- Scenario 2: Tourism Growth – Calculated rising tourist arrivals leading to higher water consumption (20% increase (2019–2024), 30% (2025–2029), and 50% (2030–2034)) based on the study by Ganosi (2018).
- Scenario 3: COVID-19 and Tourism Growth – Combined effects of pandemic-related water demand

and tourism surge.

- Scenario 4: Increased Irrigation Needs – Assumed expansion of cultivated land increasing agricultural water demand (10% increase (2019–2024), 20% (2025–2029), and 30% (2030–2034)).
- Scenario 5: Drought Conditions – Assumed reduced rainfall and groundwater recharge simulating climate change impact.
- Scenario 6: COVID-19 and Drought – Combined effects of increased domestic demand coinciding with reduced water availability.
- Scenario 7: Tourism Growth and Drought – Combined effects of peak seasonal water demand under dry conditions.
- Scenario 8: Combined effects of increased irrigation needs and drought.

Results and concluding remarks

Figure 1 presents the annual water deficits derived from various WEAP simulation scenarios for urban and irrigation water demands between 2019 and 2034. Urban water deficits rise notably under COVID-19 impacts (Scenario 1), tourism growth (Scenario 2), and their combination (Scenario 3). Irrigation deficits show sharp variability under increased irrigation needs (Scenario 4) and are exacerbated by drought conditions in Scenarios 5–8.

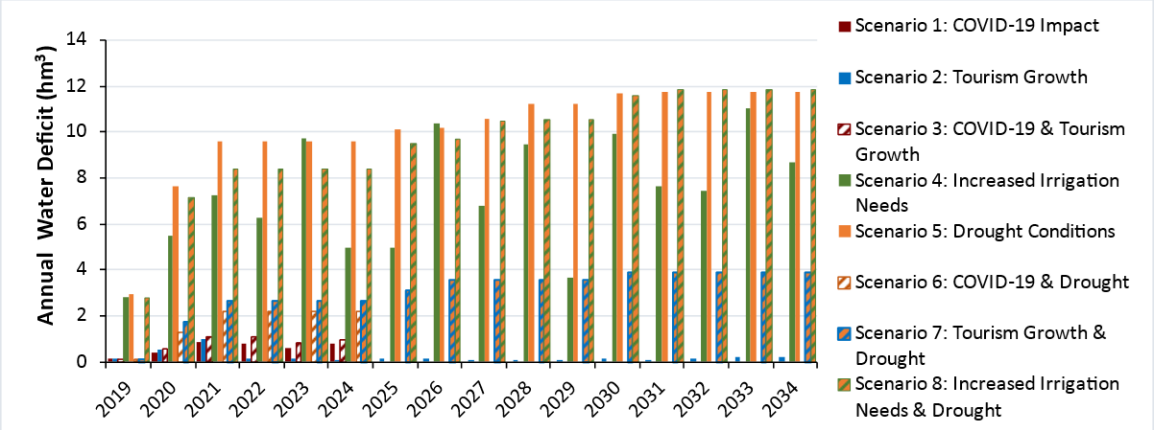


Figure 1. Annual water deficits for urban and irrigation demands on Naxos Island (2019–2034) under various simulated WEAP scenarios.

The analysis highlights the growing concern of water scarcity on Naxos Island, driven by increasing demands from urban growth, tourism expansion, and agricultural needs, especially under drought scenarios. Effective water resource management strategies, including conservation, improved infrastructure, and sustainable planning, are essential to mitigate these challenges and secure water availability for future generations.

References

Antwi, S, Getty, D, Linnane, S, Rolston, A (2021) COVID-19 water sector responses in Europe: A scoping review of preliminary governmental interventions. Science of the Total Environment, 762, 143068. https://doi.org/10.1016/j.scitotenv.2020.143068

Ganosi, M (2018) Modern Tourism in Greece. (Bachelor's Thesis). University of Piraeus, Piraeus. (In Greek).

Mike, S, Ntoi, M (2022). Watershed Management Plan and Integrated Water Resources Management Using WEAP Software: The Case of the Naxos Basin, Cyclades (Diploma thesis). University of Thessaly, Volos. (In Greek).

Sieber, J (2006) WEAP water evaluation and planning system. International Congress on Environmental Modelling and Software.

South Aegean Region (2005) Development of Systems and Tools for the Management of Water Resources in the Water Division of the Aegean Islands. Cyclades Prefecture, South Aegean Region.

Improved methodology for closing water balances and modeling water levels in a reservoir-lake system: Application to Lake Velence, Hungary

M. Chappon, K. Bene*, A. Kálmán
National Laboratory for Water Science and Water Security, Széchenyi István University, Department of Transport Infrastructure and Water Resources Engineering, Győr, Hungary
** e-mail: benekati@sze.hu*

Introduction

Lakes and reservoirs are among Earth's most vital freshwater reserves, playing a key role in water supply, ecosystems, and climate regulation. Understanding the factors influencing their water balance is crucial for predicting the impacts of climate change and human interventions. Minimizing uncertainties and correcting systematic errors in water balance calculations are essential for accurately assessing long-term lake level fluctuations and improving water resource management (Somogyvári et al., 2024). This study presents a methodology to calculate and close a freshwater system's joint, continuous water balance comprising two upstream reservoirs and a downstream lake. The calculations rely on monthly data from 1998 to 2022. Hydrological assessments rely on changes in water levels, which, combined with bathymetric data, enable accurate water balance calculations. Measurement limitations, such as the exclusion of groundwater inflow (Fowe et al., 2015) and uncertainties in evaporation estimates (Dorigo et al., 2021), pose challenges to model accuracy. Prior studies indicate that water balance closure often requires additional storage and groundwater exchange considerations. Improved model-data integration at local and regional scales is essential for advancing water balance modeling (Safeeq et al., 2021). This paper evaluates the application of two different Multiple Linear Regression (MLR) models to close the joint water balance of the water system of Lake Velence and its two regulating reservoirs simultaneously.

Materials and methods

Lake Velence, a shallow lake in Central Hungary, has a catchment area of 602.3 km², primarily fed by the Császár-víz stream. The lake spans 24.2 km², with water levels recorded since 1931, showing significant fluctuations over the decades. Two upstream reservoirs, built in the 1970s to regulate inflow, have become eutrophic due to fish farming and agricultural runoff, limiting their effectiveness for lake replenishment. A prolonged drought (2020-2022) led to record-low water levels, prompting pressure from tourism stakeholders and local authorities for intervention. Recent water management efforts included emptying the Zámolyi reservoir (2021), controlled water release from the Pátkai reservoir (2023-2024) following heavy rainfall, and constructing a bypass channel around Pátkai in 2024. Currently, both reservoirs serve as empty storage areas.

Since 1986, the Water Directorate has calculated Lake Velence's monthly water balance while reservoirs remain unassessed. Errors, averaging -70 lake-mm/year, are retrospectively adjusted across precipitation, evaporation, and surface inflow, suggesting measurement inaccuracies or a missing factor. A weak negative correlation with precipitation implies rainfall underestimation, but seasonal patterns suggest another influence, especially in winter and spring. Recent research estimates groundwater inflow at 47 lake-mm/year, potentially reducing errors, though its dynamics remain unclear. This study applies multiple linear regression to close the continuous water balance of Lake Velence and its two upstream reservoirs over the 1998-2022 period. The refined time series will then be used to model alternative reservoir management scenarios. The methodology follows six key stages:

- Model-A (Baseline): Uses raw measurement data to calculate monthly lake levels.
- Model-B (Regression): Applies uniform regression coefficients to correct systematic errors.
- Model-C (Seasonal): Adjusts errors only from December to May, using raw data for June–November.
- Evaluation: Residual analysis and adjusted R^2 assess model accuracy.

- Error Redistribution: Residuals are proportionally allocated to balance the system.
- Scenario Simulation: Five management scenarios assess impacts on lake levels and storage.Results and concluding remarks

The analysis revealed that the water balance components, apart from inflow (Qin) and outflow (Qout), were uncorrelated. Since Qout, measured at the outflow structure, had lower uncertainty compared to Qin, it was excluded from the multiple linear regression (MLR) model. The Student-T test validated this choice, showing that Qout contributed less significantly than Qin. When using the raw time series to assemble a continuous water balance model for the lake and reservoirs, the results showed an imbalance in the reservoirs and an unrealistic downward trend in Lake Velence's water levels, which did not match the observed data. By applying the revised methodology, which redistributed residual errors and considered seasonal patterns in the inflows, the water balance was more effectively closed, leading to realistic water level simulations for both the lake and the reservoirs (Figure 1).

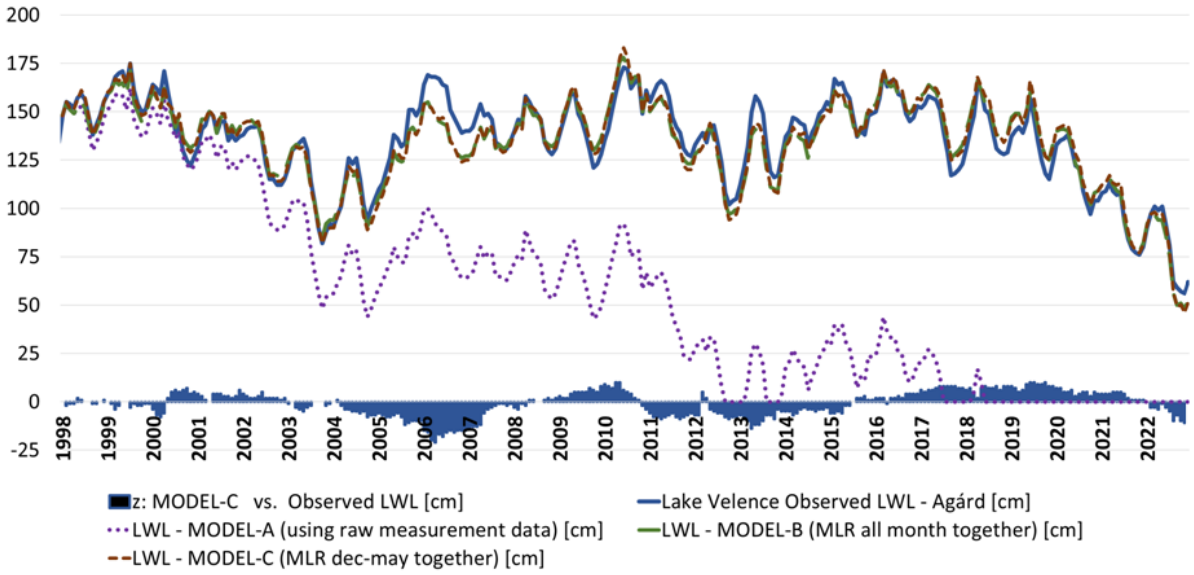


Figure 1. Lake Velence observed vs. modeled Lake Water Level (LWL) times series.

The method proved scalable across the three water bodies, offering a straightforward approach for closing the water balance in larger water systems. This technique utilized raw and error time series, making it a valuable tool for improving water management decisions and modeling in complex freshwater systems.

Acknowledgments: The research presented in the article was carried out within the framework of the Széchenyi Plan Plus program with the support of the RRF 2.3.1 21 2022 00008 project.

References

Dorigo W, and Coauthors (2021) Closing the Water Cycle from Observations across Scales: Where Do We Stand?. Bull. Amer. Meteor. Soc., 102: 1897–1935. https://doi.org/10.1175/BAMS-D-19-0316.1.

Fowe T, Karambiri H, Paturel J-E, Poussin J-C, Cecchi P (2015) Water balance of small reservoirs in the Volta basin: A case study of Boura reservoir in Burkina Faso. Agricultural Water Management, Volume 152: 99-109. https://doi.org/10.1016/j.agwat.2015.01.006.

Safeeq M, Ryan R B., Norman F P., Singh Ch. K., Dralle D. N., Hartsough P., Wagenbrenner J. W. (2021) How realistic are water-balance closure assumptions? A demonstration from the southern sierra critical zone observatory and kings river experimental watersheds. Hydrological Processes, 35 (5) 1099-1085. http://dx.doi.org/10.1002/hyp.14199.

Somogyvári M, Scherer D, Bart F, Fehrenbach B, Okujeni A, Krueger T (2024) A hybrid data-driven approach to analyze the drivers of lake level dynamics. Hydrology and Earth System Sciences 28(18): 4331–4348. https://doi.org/10.5194/hess-28-4331-2024

A self-assessment tool for climate adaptation in urban water management: the water sensitive cities index

T. Pilevneli[1], G. Ozerol[2], G. Capar[1*]
[1] Water Management Institute, Ankara University, Ankara, Turkey
[2] Faculty of Behavioural, Management and Social Sciences, University of Twente, The Netherlands
* e-mail: gcapar@ankara.edu.tr

Introduction

Climate change is a major problem affecting rural and urban areas, particularly cities, which have become a key player in climate action. However, cities are disproportionally affected by the climate change risks, i.e., sea level rise, floods, droughts, and water scarcity, depending on their location, infrastructure, population, and socio-economic conditions. Therefore, the level of vulnerability to climate change is different in each city. Additionally, cities contribute to climate change due to their spatial concentration of assets, people, and economic activities. As a result, urban areas play an important role in climate change adaptation (CCA), and urgent actions are needed to adapt the cities to the relevant impacts. Figure 1 depicts the urban water transition framework from a water supply city to a water sensitive city (Chesterfield et al., 2016). Regarding the cumulative socio-political drivers, intergenerational equity and resilience to climate change are the desired level. Service delivery functions are required to reach the level of adaptive, multifunctional infrastructure and urban design reinforcing water sensitive values and behaviours. The principles of the framework were adopted to support Turkish cities in integrating CCA with urban water management (UWM).

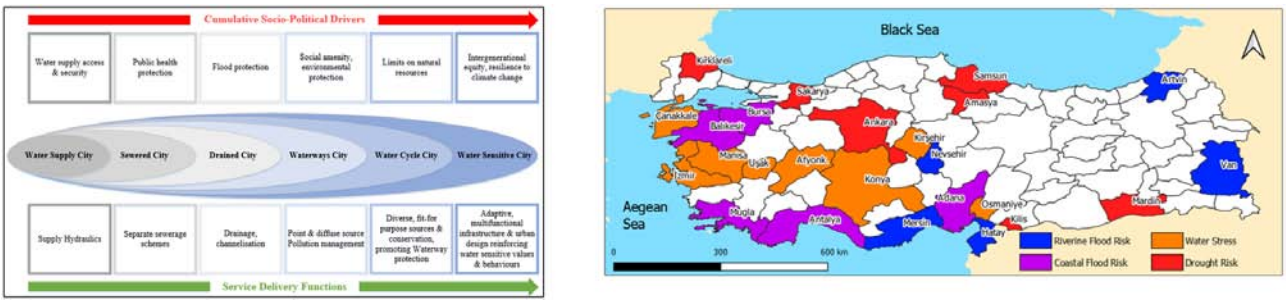


Figure 1. (a) City-state continuum of the Urban Water Transitions Framework, (b) Map of target cities in Turkey and their major climate risks

This study aims to support local authorities in understanding their climate vulnerabilities, focusing on water and wastewater management sectors. Therefore, a set of self-assessment indicators under the water sensitive cities (WSC) index were developed for Turkish cities, building on existing methods and tailoring them to the context of CCA in Turkey. Six pilot cities have been reached initially to apply the index and the study will cover 25 cities in total (Figure 1).

Materials and methods

The themes, targets and related indicators under the Water Sensitive Cities Index were examined through a literature review (Rogers et al., 2020). The indicator set, consisting of 21 unique indicators, was developed as a self-assessment tool specific to Turkish municipalities, which covered three pillars and seven targets (Table 1). Each target was measured by using two to six indicators. Some indicators were further divided into sub-categories to collect additional information, where the level of detail regarding current practices had to be increased, and the total number of indicators reached 30 in the final indicator set. The index was applied to six pilot cities with varying climate risks, and the municipalities gave scores from 1

(lowest) to 6 (highest) for each indicator.

Table 1. Water sensitive cities index for Turkish cities

Pillar	Goal
Pillar 1: Cities as water sensitive communities and networks	Goal 1: Ensure good water sensitive governance Goal 2: Increase community capital Goal 4: Improve productivity and resource efficiency Goal 6: Ensure quality urban space Goal 7: Promote adaptive infrastructure
Pillar 2: Cities as water sensitive catchments	Goal 3: Achieve equity of essential services Goal 4: Improve productivity and resource efficiency Goal 5: Improve ecological health Goal 6: Ensure quality urban space
Pillar 3: Cities as providers of ecosystem services	

Results and concluding remarks

The WSC index was applied to the municipalities of six pilot cities in Turkey and Figure 2 shows the minimum, average and maximum results for six cities. The red line shows that the average scores were between 2.5 and 3.5 for all targets. The dotted line shows minimum scores, and the dashed line shows maximum scores. Among seven goals, "Ensure quality urban space", "Improve productivity and resource efficiency" and "Improve ecological health" had the lowest scores, respectively. The highest variation was observed in indicators regarding improving ecological health, increasing community capital and ensuring quality urban space. The lowest variation was observed in indicators regarding achieving equity of essential services, promoting adaptive infrastructures and improving productivity and resource efficiency. These scores show that the pilot cities focus on traditional water and wastewater services in the cities such as water supply, sewerage, water & wastewater treatment and flood protection. The data indicates that the integration of CCA practices to UWM in pilot cities require adaptive and multifunctional infrastructures, which promote ecological health and quality urban spaces. Therefore, the pilot municipalities need to improve their capacities to provide climate adaptive water and wastewater services to their citizens.



Figure 2. Water sensitive cities index scores of pilot cities

Acknowledgments: Funded by the EU-CCAGP via the project "An Urban Water Resilience Approach to Enhancing Climate Change Adaptation in Turkish Cities (EuropeAid /170484/ID/ACT/TR/CCAGP311)" & TÜBİTAK 2224-A - Grant Program for Participation in Scientific Meetings Abroad.

References

Chesterfield, C., Rogers, B., Beck, L., Brown, R., Dunn, G., Haan, F., Lloyd, S., Urich, C. Wong, T. (2016) A Water Sensitive Cities Index to support transitions to more liveable, sustainable, resilient and productive cities.

Rogers, B. C., Dunn, G., Hammer, K., Novalia, W., de Haan, F. J., Brown, L. et al. (2020) Water Sensitive Cities Index: A diagnostic tool to assess water sensitivity and guide management actions. Water Research, 186: 116411

The "Cistern City Concept" for climate change coping (the 3 for 3 Cs): an integrated solution related to water resources management in cities

F. Megdiche-Kharrat[1,3*], F. Belcadhi[2,3]
[1] Department of Horticulture/Higher Institute of Agronomy of Chott-Meriem, University of Sousse, Sousse, Tunisia
[2] Department of Architecture/National School ofArchitecture and Urbanism, University of Carthage, Carthage, Tunisia
[3] Laboratory Governance, Ambiances and Development of Cities GADEV/UMRAN (ENAU-EDSIA)
* e-mail: feirouzmekdish@gmail.com

Introduction

Ancestral practices in water management date back to Antiquity. They allowed societies to overcome harsh environmental conditions, such as those of Middle Eastern arid and North African semi-arid areas, to settle and upgrade to a superior stage of civilization; societies of Central Iran, Northern Oman and Central and Southern Tunisia being among the best examples. They developed appropriate techniques of water acquisition and harvesting and set up ad hoc rules to manage the resource eco friendly and with integrity, thus insuring the sustainability of the resource and the social structure built around water. Qanats in Iran are sustainable ancestral constructions providing fresh water to communities of users by draining groundwater from aquifers through underground tunnels. On their path are connected watermills, dwellings and urban facilities such as water reservoirs and religious edifices. The aflaj of Oman are historic environmentally friendly water acquisition and irrigation systems conveying groundwater, rainwater and runoff water through gravity. These water community-based managements involve specific social structure and adapted ad hoc rules. In Tunisia, the traditional cities of regions with limited rainfall have adapted by integrating rainwater harvesting systems into domestic and public buildings, known as *mwajel* (*majel* in the singular), which are, in most cases, underground structures built under the patios. In the central part of the country, the medina of Kairouan is a major home for such systems; besides, the city is distinguished by its *extra muros* hydraulic structures displaying the four circular open sky basins of the Aghlabids. For this, the city used to be named in the past as the "city of reservoirs". In the South, and precisely in Toujane, a Berber village backing onto the mountain, *Joussours* are earthen structures in the form of dykes formed against the slope of the land, retaining water to irrigate the cultivated terraces.

In the current context of climate change and the induced challenges societies have to cope with, learning from the past would bring solutions for the present and the future. Indeed, when it comes to water, some urban societies are facing water scarcity and/or flash flooding due to extreme weather conditions. Many research works around water resources have been conducted to explore and understand the indigenous knowledge inherited through generations and still in use nowadays; such as (Smith 1953), (Wessels 2005), (Yazdi and Khaneiki 2013), (Megdiche-Kharrat *et al*. 2018), (Megdiche-Kharrat *et al*. 2020). This paper introduces a new concept as an all-in-one solution in response to the water related challenges cities are facing.

Materials and methods

The study was conducted on ancestral techniques of water acquisition and management mainly in the MENA region including a PhD on the hydraulic societies of the Middle-East relaying on antique water acquisition systems and their associated built environments (first author's PhD project), and a research project on rainwater managing techniques in the Tunisian South (authors' research laboratory project). General data was collected from literature review and specific data was collected through site visits, site investigations and interviews with various stakeholders. Interviews targeted public authorities, managing bodies and the communities of users of the systems; it focused on the management processes and the social structures built around the resource, beside local communities' involvement. Investigations have been conducted for various case studies (in Iran, in Oman and in Tunisia), geographically distinct but

presenting similarities regarding the ancestral techniques they developed to overcome the aridity of their climate. Site investigations relayed on photographic documentation, observation of used materials and matters, reporting of working processes and updating of general states. The analysis of these ancestral techniques and their integration within different urban contexts led to the development of an innovative approach to water management, which is presented in the following section as the “Cistern City Concept”.

Results and concluding remarks

The “Cistern City Concept” is the key finding of more than a decade of field research in many countries of the MENA region. The concept is presented as an integrated solution for cities related to the management of its waters in order to adapt to climate change and overcome its negative effects.

A city, following the “Cistern City Concept” operates as a self-managed embedded systemic mechanism when it comes to the supply and governance of its waters. This implies, to a certain extent, an autonomous mode of water management suitable with the political trend towards decentralisation and the empowering of local authorities’ role in territorial management; thus, the whole is managed locally with involving the various stakeholders, and specifically citizens. Water is governed at various levels in a Cistern City. Indeed, the latter is perceived as an iceberg, a floating mass of freshwater, with a visible part and an invisible one. The visible part, emerging above sea level, represents the seen architectural and landscape components and infrastructure for harvesting, storing and distributing freshwater. The invisible one, diving below sea level, represents the unseen ones. This submerged part of the iceberg is also layered and offers in its deeper parts an access to the natural reservoirs. For this, the Cistern City must be a porous entity allowing the supply of aquifers, as does a “Sponge City” (a concept set and developed by Kongjian Yu). Also, a “Cistern City” takes advantage of its produced waters (urban wastewaters) by operating an effective management, including treatment relaying on low-cost natural methods, that maintains public health and protects the environment, besides contributing in the local economic development.

To conclude, a “Cistern City” is a sustainable self-managed urbanised entity relaying on “human-friendly” and eco-friendly built systems (Watson and Adams 2011), besides nature-based solutions (Conrad and Voraakhom 2024) to insure a continuous supply with freshwater for its inhabitants, as well as preventing from water related risks, such as flash floods, by its capacity of absorbing runoff water and mitigating extreme weather conditions.

References

Conrad, P., & Voraakhom, K. (2024). Works with Nature: Low Carbon Adaptation Techniques for a Changing World. Climate Positive Design.

Megdiche-Kharrat, F., Moussa, M., & Ragala, R. (2020). Dans A. Alehashemi, J.-F. Coulais, & G. Hubert, Water and City: Hydraulic Systems and Urban Structures (pp. 117-127). Paris, France: Editions l'Oeil d'Or et Jean-Luc André d'Asciano.

Megdiche-Kharrat, F., Moussa, M., & Rejeb, H. (2017). Aflaj’ water management in Oman: the case of falaj Al-Khatmeen in Birkat Al-Mouz, Wilayat Nizwa. Dans M. Ouessar, D. Gabriels, A. Tsunekawa, & S. Evett (Éds.), Water and Land Security in Drylands (pp. 119-128). Springer International Publishing. doi:10.1007/978-3-319-54021-4_12

Megdiche-Kharrat, F., Ragala, R., & Moussa, M. (2018, May). Promoting a Sustainable Traditional Technique of Aquifers' Water Acquisition Common to Arid Lands: The Case of Ghassem Abad Qanat in Yazd Province (Iran). Water Scineces & Technology: Water Supply. doi:10.2166/ws.2018.098

Megdiche-Kharrat, F., Zheng, X. Y., Moussa, M., Famin, Z., & Angelakis, A. N. (2020). Historic Hydraulic Works: paradigms of traditional water governance, integrity and sustainability. Water Supply, 20(7), 2484-2498. doi:10.2166/ws.2020.146

Moussa, M. (2005). “Foggara” Inventory, Analysis and Valorization of Traditional Water Techniques of European and Saharan Drainage Tunnels, ICA3-2002-10087. Institut des Régions Arides, Médenine, Tunisie.

Semsar Yazdi, A. A., & Labbaf Khaneiki, M. (2013). Veins of Desert. A Review on the Technique of Qanat/ Falaj/ Karez (éd. 2ème). Iran: Iran Water Resources Management Company IWRMC.

Smith, A. (1953). Blind White Fish in Persia. New York: E. P. Dutton & Co., Inc.

Watson, D., & Adams, M. (2011). Design for Flooding. Hoboken, New Jersey: John Wiley & Sons.

Wessels, J. I. (2005). Criteria for renovating and using ancient qanats in Syria-case studies. Proceedings of the International Frontinus Symposium, 2-5 October 2003 (pp. 249-262). Walferdange, Luxemburg: Frontinus-Gesellschaft.

Generating synthetic wind speed time series: An analysis of Negra et al., Weibull, Haar and Daubechies Wavelets approaches

S. Skroufouta*, E. Baltas
School of Civil Engineering, National Technical University of Athens, Athens, Greece
** e-mail: sofiaskroufouta@chi.civil.ntua.gr*

Introduction

Renewable energy, especially wind energy, is crucial for the global shift to sustainable energy. Accurate wind speed data is vital for the design and operation of wind farms, yet many regions face challenges due to incomplete or limited historical data. Synthetic wind speed generation and forecasting provides a solution by creating time series that mirror real wind patterns, enabling robust analyses and informed decision-making. This paper evaluates four models for synthetic wind speed data generation: Negra et al.'s model (2008), the Weibull distribution, and wavelet-based methods (Haar and Daubechies wavelets). The Haar wavelet captures sharp changes with simplicity, while the Daubechies wavelets (DB4 and DB8) offer smoother representations. By comparing these models, the study aims to identify the best approach for various wind energy applications.

Materials and methods

This study utilizes historical hourly wind speed data from Karpathos Island, Greece, as the basis for calibrating and validating the models under comparison. The dataset exhibits an average wind speed of 6 m/s with a standard deviation of 2 m/s, providing a robust benchmark for evaluating the accuracy and reliability of synthetic wind speed generation methods.

Models Compared:

- *Negra et al. Model:* This stochastic model uses historical wind speed data to calculate monthly transition probabilities between discrete wind speed states. Synthetic time series are generated by simulating transitions and durations based on these probabilities.
- *Weibull Distribution:* The two-parameter Weibull distribution (μk and λ) models wind speed as: Synthetic data is generated by sampling from this distribution, ensuring that its mean and variance match historical data.
- *Haar Wavelet:* The Haar wavelet is a simple yet powerful mathematical tool for capturing abrupt changes in wind speed by breaking down the time series into piecewise constant segments. By decomposing historical wind speed data into wavelet coefficients and modifying them with stochastic noise, synthetic wind speed time series can be reconstructed while preserving short-term variability.
- *Daubechies Wavelets (DB4 and DB8):* The Daubechies wavelets offer a more sophisticated approach by providing smoother approximations of wind speed patterns while maintaining both local fluctuations and long-term trends. The DB4 wavelet captures moderate smoothness, while the DB8 wavelet provides an even finer resolution, making it suitable for preserving complex wind speed dynamics.

The accuracy and reliability of synthetic wind speed models are evaluated using four key metrics: (a) Mean Absolute Error (MAE), which quantifies the average absolute deviation between observed and synthetic wind speeds; (b) Root Mean Squared Error (RMSE), which emphasizes larger errors by squaring deviations before averaging; (c) Mean Absolute Percentage Error (MAPE), which expresses error as a percentage of observed values for relative comparisons; and (d) Coefficient of Determination (R^2), which measures how well the synthetic data explains variance in actual wind speeds.

Results and concluding remarks

The performance of the five synthetic wind speed models was assessed using statistical metrics and distributional characteristics. The shape (k = 1.9956) and scale (λ = 8.3656) parameters of the Weibull distribution provide a baseline representation of the wind speed distribution on Karpathos Island. However, a closer comparison of the models shows big differences in each model's abilities in replicating characteristics of the observed wind speed. The minima and maxima of historical wind speed stand at 0.51 m/s and 46.3 m/s, respectively. Out of the models, Negra et al.'s series have a narrow range of 1.0 – 19.0 m/s and don't capture the extremes which fell under observation for the historical series. The Weibull model is capable of producing only a wider range from 0.01 to 30.97 m/s and underestimates the maximum wind speeds. Improved results are derived by the application of the Haar wavelet model, showing an increased range of 0.003 to 37.95 m/s. The closest approximation to observed extremes is performed by Daubechies wavelet models-0.007 to 46.68 m/s and 0.01 to 46.56 m/s, correspondingly. These findings testify that wavelet-based models-precisely, Daubechies wavelet models work better in the generation of synthetic wind speed time series.

These models not only capture the full range of wind speed variability but also exhibit the lowest errors and highest explanatory power. Both the Negra et al. and Weibull models provide useful broad estimations but cannot preserve critical statistical properties, and thus they yield significant deviations from the observed data, as evident from Table 1 and Figure 1.

Table 1. Quantitative Comparison of the Models

Metrics	Negra	Weibull	Haar	DB4	DB8
MAE (m/s)	4.65	4.37	1.09	0.34	0.33
RMSE (m/s)	34.50	30.12	2.22	0.18	0.18
MAPE (%)	93.12	92.77	21.38	6.78	6.75
R^2	-1.27	-0.98	0.85	0.99	0.99

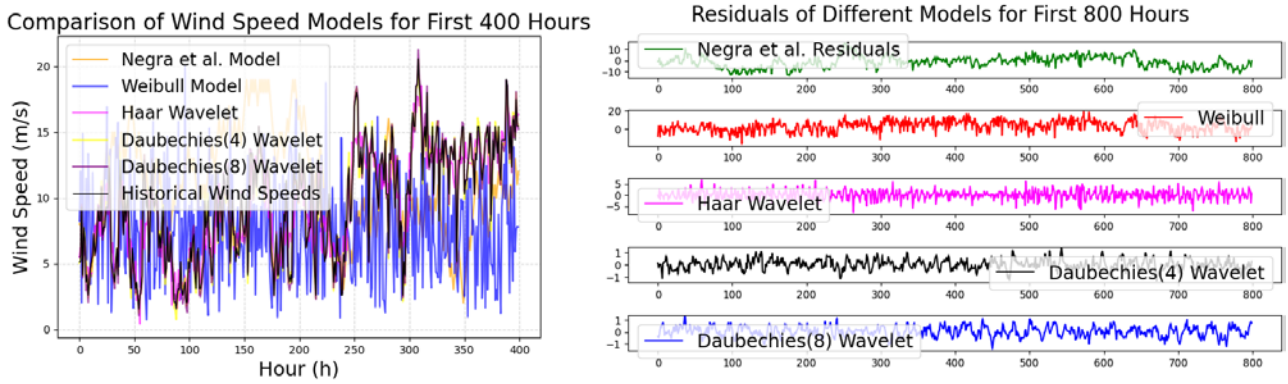


Figure 1. a) Comparison of the Generated Wind Speed Timeseries, b) Residuals of the under study models

Given these results, Daubechies wavelets are recommended for applications requiring high-fidelity synthetic wind speed data, such as wind forecasting and energy system simulations. The Haar wavelet, while an improvement over conventional models, may be suitable for scenarios where computational simplicity is prioritized over absolute accuracy.

References

Burton, T., Sharpe, D., Jenkins, N., & Bossanyi, E. (2011). Wind Energy Handbook. Wiley.

Carapellucci, R., & Giordano, L. (2013). A methodology for the synthetic generation of hourly wind speed time series based on some known aggregate input data. Applied Energy, 101, 541-550.

Chen, J., & Rabiti, C. (2017). Synthetic wind speed scenarios generation for probabilistic analysis of hybrid energy systems. Energy, 120, 507–517. https://doi.org/10.1016/j.energy.2016.11.103

Monteiro, C., Bessa, R. J., Miranda, V., Botterud, A., Wang, J., & Conzelmann, G. (2009). Wind power forecasting: State-of-the-art 2009. Argonne National Laboratory.

Negra, N. B., Holmstrøm, O., Bak-Jensen, B., & Sørensen, P. (2008). Model of a synthetic wind speed time series generator. Wind Energy, 11(2), 193–209

Application of nanobubbles on growth and quality of lettuce (*Lactuca Sativa L.*) under variable salinity water range in hydroponic systems

K. Zoukidis[1,2*], A. Gertsis[1], C. Kissoudis[1], E. Mouratidou[2], V. Hantzara[2], R. Kosheleva[3], A. Apostolidis[1], G. Strouthopoulos[1], A. Giannakoula[2]
[1] *Dept. of Sustainable Agriculture and Management, Perrotis College, Thessaloniki, Greece*
[2] *Dept. of Agriculture, International Hellenic University, Thessaloniki, Greece*
[3] *Hephaestus Laboratory, Department of Chemistry, Democritus University of Thrace, Kavala, Greece*
** e-mail: kzouki@afs.edu.gr*

Introduction

The demand for water resources is rising daily due to the world's population growth and the social economy's quick development. In some arid or semi-arid areas, groundwater is the most important source of freshwater for agriculture. The problem of groundwater salinization increases due to excessive exploitation of groundwater. Saline groundwater irrigation creates many problems. In order to reduce the problems of salinity except the desalinization, the researchers have found that mixed irrigation of saline and fresh water improved the irrigation water quality (Sang et al., 2020). Many researchers have found that salinity stress assumes that responses in hydroponics mimic those in soil. Plant growth and productivity reductions were greater under hydroponics systems than in soil at similar electrical conductivity values (Tavakkoli et al., 2010). Lettuce (*Lactuca sativa L.*) promotes numerous health advantages through vitamins, micro- and macronutrients, phenolic compounds, phytochemicals and secondary metabolites against many chronic diseases (Kim et al., 2016). The innovative and inexpensive technology of Agro-nanobubbles technology is an emerged solution to mitigate climate change and environmental challenges, reduce cost and energy in industrial processes. Nanobubbles (NBs) have found applications in different sectors such as agricultural, medical and environmental and special on water and wastewater treatment. Application of nanobubbles in hydroponics have positive impact in soilless cultivation (Foundas et al., 2023). The objectives of this study were to evaluate various salinity water ranges levels of irrigation water (E.C.i ~1 - 14 dS/m) enriched with nanobubbles with generator of Agro-nanobubbles (Agro-NBs) in floating disk hydroponic system for productivity and the influence of salts on various agronomic parameters and the quality of specific lettuces varieties (Lollo Rosso and Butterhead).

Materials and methods

The research was developed from March to May 2024 in the greenhouse at Perrotis College/American Farm School, with geographic coordinates of latitude 40^{o} 34' N, longitude 22^{o} 59' E) Thessaloniki, Greece. More growing cycles with different leafy vegetables are in progress.

In this experimental design, hydroponic system of floating disc cultivation was used, lettuce variety Lollo Rosso and Butterhead, were planted in plastic containers (6 plants per plastic container, dimension 60 x 18 x 40 cm, filled with 30 liters volume) with nutrient solution (50% of Hoagland solution). The treatments of the first group included 21 containers not enriched with NBs, at 3 replications of 7 salinity levels E.C.i : ~1, 2, 4, 6, 8, 10 and 12 dS/m). In the second group of the experiment, lettuces were grown in 24 plastic containers under a range of saline water (E.C.i: ~1, 2, 4, 6, 8, 10, 12, and 14 dS/m) and were enriched with NBs every 3 days, for each variety.

The goal of this experiment was to evaluate the influence of lettuce growth enriched with NBs and without NBs on various agronomic traits and quality parameters. Various vegetable agronomic parameters, plant tissue parameters, water (nutrition solution) parameters and quality parameters were measured and environmental conditions inside in the greenhouse were continuously recorded.

Results and concluding remarks

This study demonstrated the advantage of the enriched of nanobubbles generator of Agro-nanobubbles under variable salinity water range in floating systems in lettuce production. Most of the treatments of Lollo Rosso and Butterhead lettuces (E.C.i: ~1, 2, 4, 6, 8, 10, 12, and 14 dS/m) enriched with NB, have shown the maximum agronomic parameters (Table 1) and demonstrate statistically significant difference from the regular tap water treatment (E.C.i: ~1, 2, 4, 6, 8, 10 and 12 dS/m). Plant tissue analysis and quality parameters confirmed the trend shown in agronomic parameters of lettuces.

Table 1. Various agronomic parameters of Lollo Rosso and Butterhead lettuce (g/plant), by water treatment. Note in Table. Treatment not connected by same letter are significantly different.

	Fresh green biomass (g/plant)	**Fresh root weight (g/plant)**	**Fresh green biomass (g/plant)**	**Fresh root weight (g/plant)**
Main treatment	**Lollo Rosso Lettuce**		**Butterhead Lettuce**	
Control - tap water (E.C. <1 dS/m)	84,39 AB	6,62 DEF	92,26 B	8,61 BC
Control - tap water (E.C. 2 dS/m)	78,67 BCD	6,23 DEF	92,40 ABC	8,73 ABCD
Control - tap water (E.C. 4 dS/m)	74,67 CD	4,67 DEFG	83,033 D	7,40 BCD
Control - tap water (E.C. 6 dS/m)	67,33 DE	4,80 DEFG	63,67 F	6,83 CD
Control - tap water (E.C. 8 dS/m)	44,33 F	4,33 EFG	43,00 G	6,33 CD
Control - tap water (E.C. 10 dS/m)	7,57 H	3,07 FG	17,10 H	5,10 D
Control - tap water (E.C. 12 dS/m)	0,00 H	0,00 G	0,00 J	0,00 E
Tap water (E.C. <1 dS/m) + NB	88,61 A	10,38 ABC	95,61 A	10,48 A
Tap water (E.C. 2 dS/m) + NB	84,33 AB	10,42 AB	94,39 AB	10,68 A
Tap water (E.C. 4 dS/m) + NB	79,39 BC	11,32 A	88,99 C	10,34 A
Tap water (E.C. 6 dS/m) + NB	76,00 CD	8,36 BCD	81,22 D	10,85 A
Tap water (E.C. 8 dS/m) + NB	73,36 D	7,63 DE	77,49 E	10,47 A
Tap water (E.C. 10 dS/m) + NB	71,58 D	7,84 CDE	75,83 E	10,39 A
Tap water (E.C. 12 dS/m) + NB	62,18 E	7,16 DE	60,65 F	10,11 AB
Tap water (E.C. 14 dS/m) + NB	29,36 G	5,94 EF	9,19 I	7,89 CD

Moreover, the use of nanobubbles, is highly recommended for sustainable grow of leafy vegetables under hydroponic floating disk systems. This study is continued with evaluation in different vegetable species, in different growing seasons, in different hydroponic systems, to further evaluate the potential of the innovative system used in high salinity levels.

Acknowledgments: The authors express their sincere gratitude to two companies provided the HAM Systems (https://shop.hamsystems.eu/pages/smart-agriculture) for the sensors and nurseries of Sporofyta Vasilikon (https://sporofytavasilikon.gr/) in Greece .

References

Foudas, A. W., Kosheleva, R. I., Favvas, E. P., Kostoglou, M., Mitropoulos, A. C., & Kyzas, G. Z. (2023). Fundamentals and applications of nanobubbles: A review. Chemical Engineering Research and Design, 189, 64-86.

Kim, M. J., Moon, Y., Tou, J. C., Mou, B., & Waterland, N. L., (2016). Nutritional value, bioactive compounds, and health benefits of lettuce (Lactuca sativa L.). Journal of Food Composition and Analysis, 49, 19–34.

Sang, H., Guo, W., Gao, Y., Jiao, X., & Pan, X. (2020). Effects of alternating fresh and saline water irrigation on soil salinity and chlorophyll fluorescence of summer maize. Water, 12(11), 3054.

Tavakkoli, E., Rengasamy, P., & McDonald, G. K. (2010). The response of barley to salinity stress differs between hydroponic and soil systems. Functional Plant Biology, 37(7), 621-633.

Balancing water scarcity and stakeholder interests: A study on water management challenges and solutions in the Lake Velence area

A. Kálmán, M. Chappon, K. Bene*
National Laboratory for Water Science and Water Security, Széchenyi István University, Department of Transport Infrastructure and Water Resources Engineering, Győr, Hungary
** e-mail: benekati@sze.hu*

Introduction

The adverse effects of climate change have intensified water-related conflicts in the rapidly developing Lake Velence catchment area in Central Hungary. The growing demand for water-related services and declining availability have put increasing pressure on local water resources. To address these challenges, equitable and economically efficient water allocation among stakeholders is crucial for mitigating conflicts and adapting to climate change (Filippelli et al., 2024). An online survey conducted in the summer of 2024 gathered 840 anonymous responses from three stakeholder groups: residents, holiday-home owners, and visitors (Kálmán, 2024). The survey explored participants' concerns, perspectives, and values related to water services in the area, focusing on their willingness to pay for improved water quality and levels. The results highlighted widespread recognition of water scarcity, with nearly two-thirds of respondents willing to financially contribute to enhancing water quality and availability.

The value and utility of water vary depending on its nature, location and intended use, which is influenced by its classification as an economic good and the balance between supply and demand (Ahmed et al., 2018). Water can range from a private good, like bottled mineral water, where ownership and consumption are exclusive, to a public good, like lake water, where use does not reduce availability for others (White, 2015). When water demand exceeds available resources, such as in the studied area, water is not a pure public good but a common good with mixed properties. This shift in water's role highlights the complex dynamics of resource management, especially in water-scarce regions (Zeder, 2024).

These findings underscore the need for a strategic approach to water management that balances economic, social, and environmental priorities (Asif et al., 2024). This approach would address the challenges of water scarcity while promoting sustainable development and equitable water allocation in the region.

Materials and methods

Lake Velence, located in Hungary's Central Transdanubia region near Székesfehérvár and Budapest, is a small but ecologically diverse catchment area spanning 602.3 km². The region features hilly and flat landscapes, with some of Hungary's oldest rocky mountains, and the leveling datum for height measurements is situated near the lake at Nadap. The lake is shallow, saline, and experiences large water level fluctuations, with a surface area of 24.2 km² and an average depth of 150 cm. Despite an annual average water level decline of 1 cm from 1986 to 2020, recent droughts have led to significant drops in the lowest recorded level of just 53 cm in September 2022. This ongoing decline in water levels is a concerning trend for the lake's ecosystem and water availability and is, thus, the source of many conflicts.

The research aimed to assess the current water-related challenges in the Lake Velence catchment area by gathering perspectives from locals and visitors on water and ecosystem services. The survey utilized the "willingness to pay" method and economically evaluated water-related services across various stakeholders. Despite being available online for just two weeks (July 26th to August 11th, 2024), the survey attracted significant attention, reflected in the high number of responses from 89 settlements. A total of 840 respondents participated, with 57.4% identifying as local residents and 42.6% as temporary visitors, including holiday-home owners and tourists. The active engagement and detailed feedback underscored the importance of addressing the future of the lake and its surrounding environment.

Results and concluding remarks

Lake Velence's waterfront offers opportunities but faces challenges from climate change and competing water demands. Respondents rated water-related services as average, with low scores for beaches and water sports facilities. While kite surfing was rated better, swimming and fishing suffered due to water quality concerns. Shallow lake levels and resource scarcity have fueled conflicts, with calls for improved water quality and quantity. Though water is considered a public good, funding shortages hinder service improvements, creating tensions in the area. While the lake's role is viewed as both a natural habitat and a recreational space, water storage in the lake has become a priority, leading to support for policies to restore water levels. This priority has contributed to further stakeholder conflicts, especially for non-lake water users who face serious consequences and water restrictions that are not sustainable. One potential solution is the economic valuation of water, particularly using the "willingness-to-pay" method, which gauges how much users are willing to contribute to improved services (Figure 1). By analyzing the willingness-to-pay responses, the study offers valuable insights into how different user groups value water resources and ecosystem services, aiding in developing better water management strategies. Climate change has significantly disrupted the water cycle, intensifying challenges in the Lake Velence catchment. However, the survey demonstrates that most water users are willing to financially support water quality and availability improvements, underscoring the need for fair and balanced resource allocation. Analyzing these willingness-to-pay responses allows for determining the optimal balance between economic, ecological, and social factors to address water scarcity and reduce stakeholder conflicts.

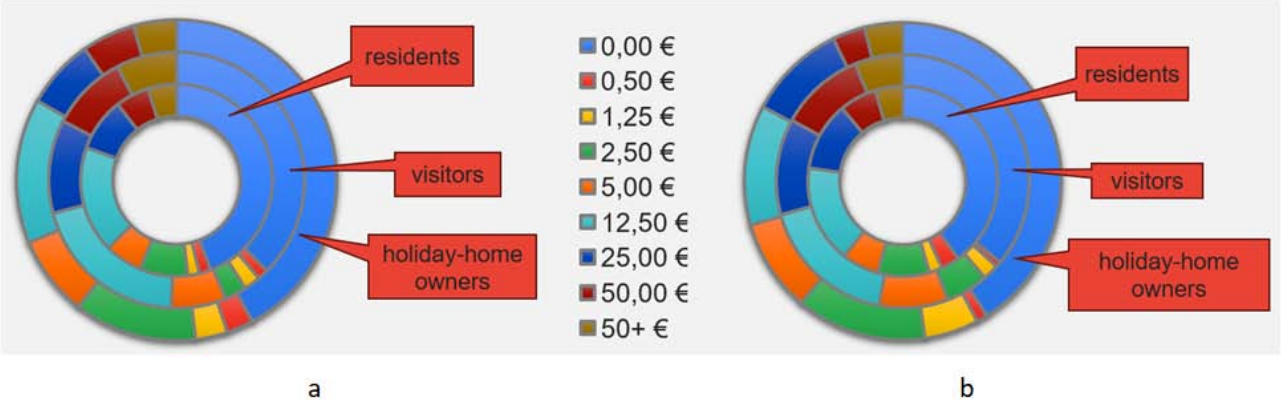


Figure 1. Distribution of payment willingness (a) for higher water levels (quantity) and (b) for better water (quality) among the three stakeholder groups

Acknowledgments: The research presented in the article was carried out within the framework of the Széchenyi Plan Plus program with the support of the RRF 2.3.1 21 2022 00008 project.

References

Ahmed N., Ward J.D., Thompson S., Saint C.P. & Diana J.S. (2018). Blue-Green Water Nexus in Aquaculture for Resilience to Climate Change, Reviews in Fisheries Science & Aquaculture, 26:2, 139-154, DOI: 10.1080/23308249.2017.1373743

Asif, Z., Chen, Z., Sadiq, R., Zhu, Y. (2023) Climate Change Impacts on Water Resources and Sustainable Water Management Strategies in North America, Water Resources Management, 37, 2771–2786, DOI: 10.1007/s11269-023-03474-4

Filippelli R., Termansen M., Hasler B., Holbach A., Timmermann K., Konrad M., Levin G. (2024) Integrated environmental-economic modelling for cross sectoral water policy evaluation, Water Resources and Economics, 47, 100245, DOI: 10.1016/j.wre.2024.100245

Kálmán A. (2024). VELENCEI-TÓ: ÉRTÉKEK, PROBLÉMÁK ÉS JÖVŐKÉP, online survey on Lake Velence, Széchenyi Egyetem, https://www.facebook.com/KozlekedesepitesiTanszekSZE

White C. (2015). Understanding water markets: Public vs. private goods, April 27th, 2015, https://www.globalwaterforum.org/2015/04/27/understanding-water-markets-public-vs-private-goods/

Zeder R. (2024). The Four Different Types of Goods, Quickonomics, https://quickonomics.com/different-types-of-goods; accessed December 27th 2024

Application of nanobubbles irrigation technology, in combination with biostimulants, in leafy vegetables production using hydroponic grow bags

K. Zoukidis[1,2*], M.T. Chatziathanasiou[1], A. Gertsis[1], C. Vasilikiotis[1], A. Apostolidis[1], A. Varoutoglou[4], E.P. Favvas[3]

[1] *Dept. of Sustainable Agriculture and Management, Perrotis College/American Farm School, Thessaloniki, Greece*
[2] *Dept. of Agriculture, International Hellenic University, Thessaloniki, Greece*
[3] *Hephaestus Laboratory, Department of Chemistry, Democritus University of Thrace, Kavala, Greece*
[4] *Institute of Nanoscience and Nanotechnology, NCSR "Demokritos", Attica, Greece*
** e-mail: kzouki@afs.edu.gr*

Introduction

Agro-industries, have applied recent technological developments in nanotechnology and nanobubbles (NB) systems, because of their excellent and useful results and distinctive qualities (Liu et al., 2012). Horticulture is one of the most important sectors of agriculture and nanobubbles technology has shown remarkable results in this sector (Foudas et al., 2023). Many reports have been done for the beneficial results of biostimulants application for plant production in the field or in hydroponic systems under protected structures. Many studies have shown potential for the use of biostimulants in agriculture sector for alleviating different biotic and abiotic stresses (i.e. drought, high temperatures, high salinity, or nutrient deficiencies) (Gómez, S., & Gómez, C., 2022). The objectives of this study were to evaluate the combination of Biostimulants and irrigating with nutrient solution (50% of Hoagland solution) enriched with nanobubbles (NB), with a generator of Agro-nanobubbles (Agro-NBs) in hydroponic grow bags with a mixture of coconut substrate with pumice, for productivity of specific lettuces varieties [Cos and Green Leaf (curly)]. Currently, there are not studies available to evaluate the interaction of Biostimulant and NBs in irrigation water.

Materials and methods

This study is evaluating the effect of Agro-nanobubbles (Agro-NBs) and foliar fertilizer application on agronomic characteristics, and the yield of two lettuce varieties [Cos and Green Leaf (curly)]. The Null Hypothesis (Ho) is that the various treatments will not significantly affect the average yield and other measured properties, while the Alternative Hypothesis (Ha) is that the treatments will significantly affect yield and agronomic characteristics. It is worthy to mention that it was two years, repeated study on Perrotis College's greenhouse laboratories. The main experimental treatments consisted of irrigation with nanobubbles with generator of Agro-nanobubbles and irrigation with tap water (Figure 1). The secondary treatments (within each main one) were different doses of foliar application of a commercial biostimulant (SANOVITA/STEFES; https://www.stefes.eu/) plus the untreated (Control).

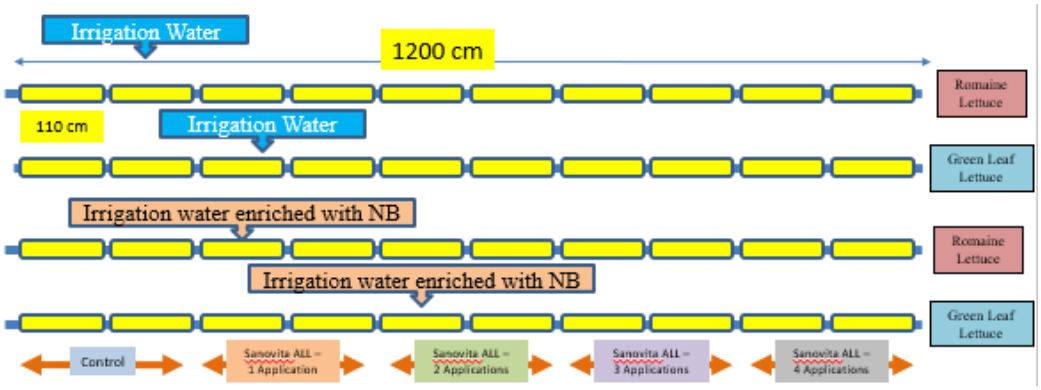


Figure 1. Experimental design of hydroponic system

Results and concluding remarks

Nowadays, farmers are using precision agriculture for sustainable and efficient management. Thus, by the use of nanobubbles technology will be decreased several problems that farmers are facing. Nanobubbles technology is the fifth revolutionary technology of the 21st century. The results (Table 1) have shown that in the hydroponic system different applications of Biostimulants produce an increase in all parameters studied (Tables 1 & 2).

Table 1. Various agronomic parameters of Green Leaf (curly) lettuce by biostimulant (Sanovita-STEFES) application rate.

Biostimulant Rate	Fresh weight (g)		Length (cm)		SPAD		NDVI	
4x	443.00	a	25	a	54	a	0.74	a
3x	378.95	ab	24	ab	51	ab	0.72	ab
2x	353.53	ab	22	bc	49	bc	0.69	b
1x	278.12	bc	21	c	46	c	0.57	c
Control	205.02	c	20	c	45	c	0.52	d

Table 2. Various agronomic parameters of Cos lettuce by biostimulant (Sanovita) application rate.

Biostimulant Rate	Fresh weight (g)		Length (cm)		SPAD		NDVI	
4x	400.13	a	23	a	53	a	0.74	a
3x	373.80	a	23	a	52	ab	0.72	ab
2x	343.22	ab	20	b	48	b	0.69	b
1x	247.92	bc	17	c	38	c	0.57	c
0x	172.78	c	17	c	37	c	0.52	d

Levels not connected by same letter are significantly different.

The effect was observed under both tap water and Agro-NBs, with the Agro-NBs having a significant higher result in all parameters tested. Therefore, the system performed very satisfactorily and represents a new tool for achieving higher and more sustainable lettuce production, it remains to be tested for additional crop species and hydroponic systems.

Acknowledgments: The authors express their sincere gratitude to two companies provided the generator of Agro-nanobubbles (NB) (Hephaestus Lab, Department of Chemistry, Democritus University of Thrace) and nurseries of Sporofyta Vasilikon (https://sporofytavasilikon.gr/) in Greece.

References

Foudas, A. W., Kosheleva, R. I., Favvas, E. P., Kostoglou, M., Mitropoulos, A. C., & Kyzas, G. Z. (2023). Fundamentals and applications of nanobubbles: A review. Chemical Engineering Research and Design, 189, 64-86.

Gómez, S., & Gómez, C. (2022). Evaluating the Use of Biostimulants for Indoor Hydroponic Lettuce Production. HortTechnology, 32(4), 348-355.

Liu, S., Enari, M., Kawagoe, Y., Makino, Y., and Oshita, S. 2012. Properties of the water containing nanobubbles as a new technology of the acceleration of physiological activity. Chem. Eng. Sci., 93, 250–256.

Evaluation of irrigation with nanobubble-enriched water in combination with Biostimulants on lettuce production (*Lactuca sativa L.*)

K. Zoukidis[1,2*], M.T. Chatziathanasiou[1], A. Gertsis[1], C. Vasilikiotis[1], A. Apostolidis[1], A. Varoutoglou[4], E.P. Favvas[3]

[1] *Dept. of Sustainable Agriculture and Management, Perrotis College/American Farm School, Thessaloniki, Greece*
[2] *Dept. of Agriculture, International Hellenic University, Thessaloniki, Greece*
[3] *Hephaestus Laboratory, Department of Chemistry, Democritus University of Thrace, Kavala, Greece*
[4] *Institute of Nanoscience and Nanotechnology, NCSR "Demokritos", Attica, Greece*
** e-mail: kzouki@afs.edu.gr*

Introduction

Green leafy vegetables are considered to play important role in food and nutritional security (Natesh et al., 2017). Lettuce (*Lactuca Sativa L.*) is one of the most popular vegetables produced in commercial indoor farms (vertical farms) and hydroponics production. (Gómez and Gómez, 2022).

Use of biostimulant products have many reported benefits in agriculture, by helping to improve various plant processes in the field or using hydroponic systems in greenhouses. Also, biostimulants offer many opportunities to reduce global challenges with climate, food, and water security. Some biostimulants (special these that contain humic and fulvic acids), helps the metabolic activity of soil microbes and effects in plants and improve macro- and micronutrient uptake in many crop species and increase antioxidant activity, chlorophyll content, photosynthesis, and nucleic acid synthesis in various crops (Gómez and Gómez, 2022).

Nanobubbles' (nano-scaled bubbles) properties are so different from those of mill-scaled bubbles and Micro-bubbles and they have many applications. (Marui, 2013). Nanobubbles potential uses have spread to high-value applications, from engineering, fishery and agriculture to pharmacy and medicine (Favvas et al., 2021).

Materials and methods

The objective of this study was to evaluate irrigation with NB-enriched water with the use of Agro-nanobubbles (Agro-NBs) for growing lettuce in Perrotis College Shade house. The first part of experiment was the irrigate without enriched with NBs (Control) and irrigation enriched with NBs to evaluate productivity of specific lettuces varieties [Lollo Rosso, Cos/Romaine and Green Leaf (curly)]. The second part of experiment was to apply foliar fertilizer with Biostimulants in different doses, such as the 1st group was the control, 2nd group was with one application of foliar fertilizer, 3rd was with two applications of foliar fertilizer and 4th was with 3 applications of foliar fertilizer (Figure. 1).

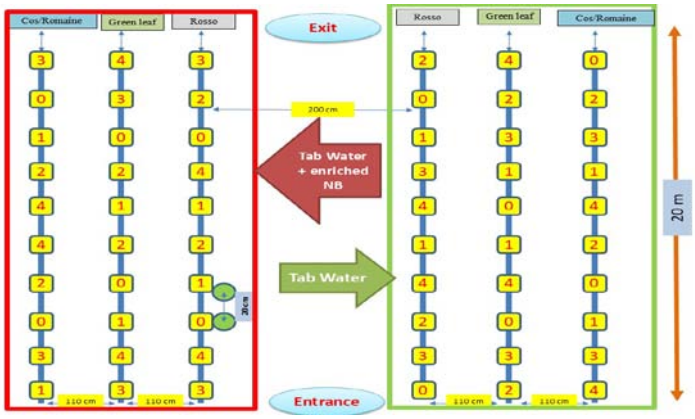


Figure 1. Experimental Design of all treatments

Results and concluding remarks

The results (Table 1) have shown that applications of Biostimulants increased the fresh weight of lettuces with increasing number of applications compared with the control, but only in Lollo rosso and Green leaf the differences were statistically significant. In all three lettuce varieties, irrigation with NB-enriched water resulted in increased fresh weight and the differences were statistically significant (Table 1).

Table 1. Effect of irrigation and biostimulant application rate on Cos, Lollo Rosso and Green Leaf (curly) lettuce (fresh weight, g/plant)

Treatment	Cos		Lollo Rosso		Green leaf	
NB enriched - 4x	343.14	a	296.53	a	378.84	a
NB enriched - 3x	338.58	a	260.20	ab	359.94	ab
NB enriched - 2x	329.23	a	252.72	b	352.44	abc
NB enriched - 1x	312.20	a	244.65	bc	314.14	abcd
NB enriched - 0x	305.32	a	233.48	bcd	292.91	bcd
Tap Water - 4x	228.87	b	255.33	b	304.95	bcd
Tap Water - 3x	205.40	b	213.17	cde	284.85	cd
Tap Water - 2x	185.89	b	205.50	de	279.58	d
Tap Water - 1x	181.23	b	196.00	de	275.70	d
Tap Water - 0x	173.98	b	183.18	e	272.33	d

Therefore, the system performed very satisfactorily and represents a new tool for achieving higher and more sustainable lettuce production, it remains to be tested for additional crop species and hydroponic systems.

Acknowledgments: The authors express their sincere gratitude to two companies provided the generator of Agro-nanobubbles (NB) (Hephaestus Lab, Department of Chemistry, Democritus University of Thrace) and nurseries of Sporofyta Vasilikon (https://sporofytavasilikon.gr/) in Greece.

References

Favvas, E. P., Kyzas, G. Z., Efthimiadou, E. K., & Mitropoulos, A. C. (2021). Bulk nanobubbles, generation methods and potential applications. Current Opinion in Colloid & Interface Science, 54, 101455.

Gómez, S., & Gómez, C. (2022). Evaluating the Use of Biostimulants for Indoor Hydroponic Lettuce Production. HortTechnology, 32(4), 348-355.

Marui, T. (2013). An introduction to micro/nano-bubbles and their applications. Systemics, Cybernetics and Informatics, 11(4), 68-73.

Natesh, H. N., Abbey, L., & Asiedu, S. K. (2017). An overview of nutritional and antinutritional factors in green leafy vegetables. Horticulture International Journal, 1(2), 58-65.

Formulation of an optimization framework for pumped storage with floating photovoltaics integration: Towards smart hydropower

P. Dhawan[1,2*], M. Righetti[1], A. Puchkova[3], M. Herrera[2]
[1] Faculty of Agricultural, Environmental and Food Sciences, Free University of Bozen-Bolzano, Bolzano, Italy, 39100
[2] School of Engineering, Newcastle University, Newcastle Upon Tyne, United Kingdom
[3] Dept. of Engineering, University of Cambridge, Cambridge, United Kingdom
* e-mail: pranav.dhawan@student.unibz.it

Introduction

Pumped storage hydropower (PSH) systems are one of the most well-established solutions for large-scale energy storage (Rehman et at, 2015), providing grid stability and flexibility in electricity markets (Qudaih et al, 2023), making it an essential component of resilient energy infrastructure. These systems operate by storing energy in the form of water, which is pumped from a lower reservoir to an upper reservoir during periods of low electricity demand and lower prices. When energy demand and electricity prices rise, the stored water is released back through turbines to generate electricity. PSH plays a crucial role in integrating renewable energy sources, such as solar and wind, by mitigating their intermittency and ensuring a reliable energy supply (Ramos et al, 2024).

Effective management of PSH systems is essential for optimizing performance and ensuring long-term sustainability. To achieve this, bi-level optimization is employed for hierarchical decision-making (Caselli et al, 2024), where the upper level focuses on economic planning while the lower level manages hydropower scheduling, enabling coordinated and efficient operations. Additionally, probabilistic optimization accounts for uncertainties (Riaz et al, 2022) in inflows and electricity prices, ensuring a more resilient and adaptive operational strategy. Other approaches, such as metaheuristic methods (e.g., Genetic Algorithms, Particle Swarm Optimization) and machine learning-based models, offer alternative solutions for improving scheduling efficiency and adaptability in complex PSH operations.

This study develops an optimization framework for a PSH system, integrating a lower reservoir and Floating Photovoltaics (FPV). By leveraging real-time electricity prices, hydrological forecasts, and FPV generation, the model optimizes pumping and generation schedules for economic and operational efficiency. The novelty lies in dynamically optimizing operations based on day-ahead prices on a multi-scale temporal resolution, incorporating FPV as an additional energy source.

Materials and methods

To optimize the operation of this system, a multi-scale temporal resolution approach will be adopted, addressing both short-term (hourly to daily) and long-term (seasonal and annual) decision-making. A bi-level optimization framework will be applied to coordinate high-level economic objectives with detailed hydropower scheduling. Additionally, probabilistic optimization techniques will account for variations and uncertainties in electricity prices, inflows, and hydrological conditions. Other optimization methods, including Mixed-Integer Linear Programming, metaheuristic approaches such as Genetic Algorithms and Particle Swarm Optimization and other techniques will also be applied and compared to determine the most effective approach. The integration of Floating Photovoltaics (FPV), with reservoir coverage scenarios ranging from 10% to 50% surface area, will be evaluated to assess its impact on energy efficiency, contributing to sustainable and adaptive water resource management.

Results and concluding remarks

The proposed optimization framework is applied to a conventional hydropower plant in Northern Italy. The study explores the feasibility of converting this plant into a PSH system by integrating a lower reservoir and a pumping mechanism. Currently, the plant operates without energy storage, releasing water directly

into the downstream river after power generation. In the proposed system, water will be released for electricity generation when prices are high, while surplus energy during low-price periods will be used to pump water back to the upper reservoir. Several constraints influence system operation, including seasonal water level restrictions for both the upper and lower reservoirs, minimum environmental flow, and inflows from the catchment due to precipitation and snowmelt.

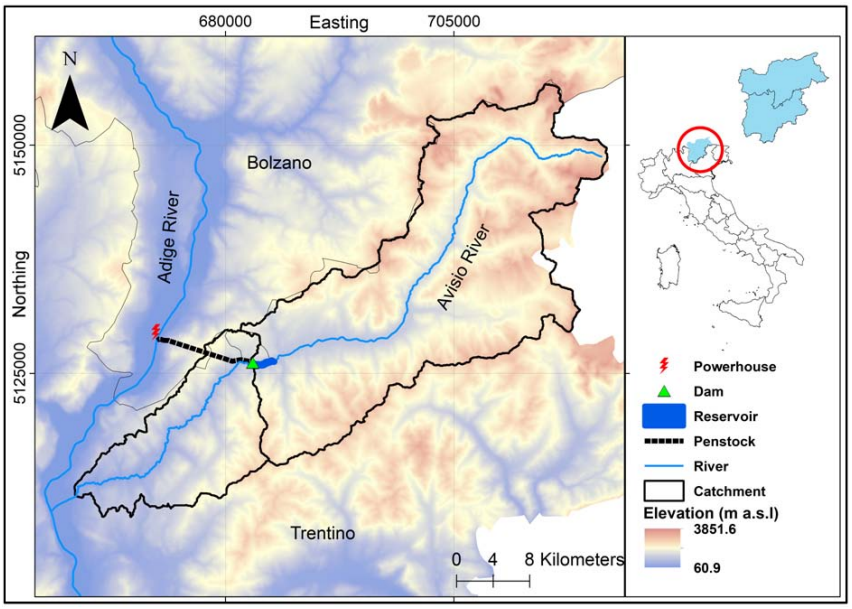


Figure 1. (a) Study area in Northern Italy

As this study serves as a proof of concept, the optimization framework will be tested under various operational scenarios to evaluate the feasibility of converting the conventional hydropower plant into a PSH system. A detailed simulation of multiple multi-scale temporal resolutions (short-term and long-term decision-making) will help determine the most efficient scheduling strategy for energy generation and water storage under fluctuating market conditions. The optimization framework will assess how electricity price fluctuations, hydrological variability, and FPV integration levels impact the overall system performance, helping understand the economic and operational feasibility of the proposed approach.

The results are expected to demonstrate the technical and economic viability of the PSH-FPV hybrid system while highlighting the advantages of adaptive hydropower operation. By incorporating various constraints such as seasonal water levels in both reservoirs, inflows into the reservoir, and electricity prices, the study aims to contribute to the broader field of sustainable and adaptive water resource management.

Building on these findings, future work will focus on refining the optimization models using real-world data and conducting sensitivity analyses to account for uncertainties in electricity prices, inflows, among others. Furthermore, climate change scenarios will be incorporated to assess long-term water availability and its impact on PSH operations, ensuring system resilience. Additionally comparative studies between different optimization techniques will be performed to identify the most effective approach for enhancing energy efficiency and profitability.

References

Caselli G., Iori M., & Ljubić I. (2024). Bilevel optimization with sustainability perspective: a survey on applications. arXiv preprint arXiv:2406.07184.

Qudaih M., Engel B., Truijen D. PK., De Kooning J. DM., Stockman K., Hoffstaedt J., Jarquin-Laguna A., Ruiz R. A., Goseberg N., de Vilder L.} (2023). The contribution of lowhead pumped hydro storage to grid stability in future power systems. IET Renewable Power Generation, 17(14), 3594-3608.

Ramos H. M., Sintong J. E., & Kuriqi A. (2024). Optimal integration of hybrid pumped storage hydropower toward energy transition. Renewable Energy, 221, 119732.

Rehman S., Al-Hadhrami L. M., & Alam, M. M. (2015). Pumped hydro energy storage system: A technological review. Renewable and Sustainable Energy Reviews, 44, 586-598.

Riaz M., Ahmad S., Hussain I., Naeem M., & Mihet-Popa L. (2022). Probabilistic optimization techniques in smart power system. Energies, 15(3), 825.

X. Remote Sensing, Artificial Intelligence, and New Technologies in Water Sciences

How digital revolution is reshaping water resources management? Insights from Spain

A. Expósito[1], E. Díez-Cebollero[2]
[1] WEARE research group and Department of Applied Economics, University of Malaga, Málaga, Spain
[2] French Research Agency and Water JPI Secretariat, Paris, France
* e-mail: aexposito@uma.es

Introduction

The water sector is currently transitioning into its so called 'Digital Revolution' by reshaping its management and decision-making tools (Damman et al., 2023). This study offers insights on how this digital revolution is reshaping water resources management and aims to contribute to the discussion on its impacts on complex water systems. Following the efforts deployed by the European Commission to strengthen Europe's digital sovereignty and leadership (Stein et al., 2022), Spain is determined to lead the digitalization transformation of the water sector though the implementation of an ambitious national program 'Water-Cycle Digitalization Strategic Projects for Economic Recovery and Transformation' (WCD-SPERT) (Spanish Ministry for the Ecological Transition, 2022) to promote digital water projects across the country. With the aim to offer practical insights from the Spanish experience, this study offers valuable information based on semi-structured interviews with water management decision-makers from different sectors (e.g., urban, agriculture) and management levels (e.g., river basin, region).

Materials and methods

Data has been obtained from two sources: 1) Semi-structured interviews with representatives and decision-makers from different sectors (agricultural and urban) and institutions related to the management of water resources at different administrative levels: Spanish Ministry for the Ecological Transition, regional water agencies, basin authorities and municipal utilities; 2) Information gathered from the WCD-SPERT program on the financed digitalization initiatives.

Results and concluding remarks

Based on the gathered information, main aspects of water management impacted by water digitalization are discussed, allowing to obtain useful insights for decision and policy makers. Among the multiple transformative impacts identified, the following can be highlighted.

Digitalization facilitates data collection and real-time monitoring. Smart water networks are being implemented in cities like Madrid, Seville and Barcelona, providing detailed insights into consumption and leakages. In some cases, such technologies have reduced water loss by up to 20% (Spanish Institute of Statistics, 2025), contributing directly to more sustainable water use in urban areas. Additionally, digital monitoring and sensors are providing an accurate and dynamic picture of water systems, improving predictive analytics for droughts, floods, or over-extraction. This precision helps ensure better compliance with sustainability and environmental principles. Further, different initiatives in the Canary Islands (and other Spanish regions) are also implementing the use of GIS-based solutions and IoT sensors to monitor its desalination plants and distribution systems, reducing water loss significantly and allowing for real-time adjustments. The Automated Hydrologic Information Systems (SAIH) used by several Spanish River Basin Authorities are being upgraded with the use of these digital technologies to improve forecasting and predictive capacities. SAIH integrates data from thousands of sensors across the basins, sending continuous updates on water flow and quality.

An example of the functionalities of digital tools in monitoring and real-time feedback is smart irrigation systems, which are gaining ground in Spanish agriculture, dynamically adjust water usage based on real-

time soil moisture data. Since this type of adaptability measures are crucial for optimizing water resources, especially in drought-prone regions, the Spanish Ministry for Agriculture is financing 190 initiatives for irrigation modernization, affecting 700 thousand hectares with a budget of 2400 million euros in the period 2022-2027. In the urban sector, predictive analytics powered by big data are being used to forecast water supply and demand patterns in many Spanish cities. The Valencia water utility company, Aguas de Valencia, has developed a digital tool called GoAigua, which uses predictive models to optimize water distribution across the city based on real-time demand and weather forecasts. These systems allow the utility to adjust water pressure dynamically, ensuring that water is distributed efficiently while minimizing waste.

Digital tools are also transforming the way hydroclimatic extreme events—such as floods and droughts—are managed. Advanced digital technologies, including artificial intelligence (AI), big data analytics, and the Internet of Things (IoT), are being integrated into hydrological forecasting models, significantly enhancing early warning systems. These innovations allow authorities to anticipate extreme weather conditions and implement proactive mitigation strategies.

Efficiency and resource allocation enhancement is also identified as a significant impact. Smart irrigation systems, such as the examples of IDRICA in Valencia, the Digital Data Farm platform (developed by the Polytechnic University of Cartagena in Murcia) or the AGROW digital platform developed at University of Malaga (Andalusia), use data from sensors and AI algorithms to predict and optimize the amount and timing of water applied, reducing overuse and conserving water. At river basin scale, the system SIMPA (a rainfall-runoff simulation tool developed by a public research center, CEDEX) provides accurate predictions of rainfall, runoff, and water availability. Segura and Jucar river basin authorities have long experience in the use of these decision-support system to manage water resources during dry periods. In the case of urban water supply systems, smart water networks based on AI and Blockchain solutions facilitate real-time monitoring and non-revenue water reduction, while constantly improving the supply management and business models of different Spanish water utilities. Smart platforms, such as Aquadvanced (Barcelona) and Aquasig (Seville) are enabling water utilities to make proactive and better-informed decisions.

Additionally, digital technologies are being used to enhance the flexibility of water storage, such as the automation of water reservoirs and distribution networks. For example, in the Guadalquivir River Basin (southern Spain), the project Guadalquivir 4.0 will be able to dynamically manage water storage and release in response to real-time data. This digital tool will allow for better water retention during periods of heavy rainfall and more efficient distribution during dry periods, enhancing the system's ability to cope with climate-induced variability and protecting the environmental value of the Doñana national park.

Regarding water quality monitoring, digital tools, such as automated monitoring stations, are playing a critical role, allowing for immediate action when contamination is detected. In the Guadalquivir basin, as in other Spanish river basins, real-time water quality monitoring systems are being used to track pollutants, ensuring compliance and the identification of pollution sources. In the case of Seville city, the water utility (EMASESA) is implementing the Aquasig project, a tool that simulates different scenarios in the drinking water network in terms of water quality. This system models variables such as chlorine concentration and detects possible contamination events, ensuring safe and clean water for residents.

Finally, advanced digital monitoring systems are facilitating water circularity and reuse. Regions like Murcia are now able to treat wastewater more efficiently and reuse it in agricultural and industrial applications, reducing extraction pressures on natural water reserves. Further, the ability to integrate desalination with reclaimed water reuse increases climate resilience of water systems. With this objective, several projects, such as Circular Toolkit developed by the CETAQUA technological centre or the AQUATIM project promoted by the water utility Aqualia, aim to improve water circularity in different Spanish regions.

References

Damman S, Schmuck A, Oliveira R, Koop SSH, do Céu Almeida M, Alegre H, Ugarelli RM (2023) Towards a water-smart society: Progress in linking theory and practice. Utilities Policy 85: 101674. https://doi.org/10.1016/j.jup.2023.101674

Spanish Ministry for the Ecological Transition (2022) Water-Cycle Digitalization Strategic Projects for Economic Recovery and Transformation, Madrid.

Spanish Institute of Statistics (2025) Statistics of water supply and sanitation, INE, Madrid.

Stein U, Bueb B, Englund A, Elelman R, Amorsi N, et al. (2022) Digitalisation in the Water Sector Recommendations for Policy Developments at EU Level; European Commission, Brussels.

Remote sensing and direct monitoring of plant salinity stress in a coastal back-barrier environment in Volturno Licola Falciano natural reserve

E. Giuditta[1*], L. Alessandrino[1], N. Colombani[2], M. Mastrocicco[1]
[1] DiSTABiF – Department of Environmental, Biological and Pharmaceutical Sciences and Technologies, Campania University "Luigi Vanvitelli", Via Vivaldi 43, 81100 Caserta, Italy;
[2] SIMAU – Department of Materials, Environmental Sciences and Urban Planning, Polytechnic University of Marche, Via Brecce Bianche 12, 60131 Ancona, AN, Italy
* e-mail: elisabetta.giuditta@gmail.com

Introduction

Coastal dune landscapes are dynamic and complex ecosystems located at the interface between land and sea (Van Der Maarel 2003). In the Mediterranean region, these ecosystems, particularly sand dunes, have suffered significant degradation in recent decades. Pine forests within these coastal zones are especially at risk, with their decline posing a severe threat to biodiversity and habitat stability. These forests play a crucial role in global biogeochemical cycles, soil protection, and climate regulation (Conte et al. 2022). Growing environmental and human pressures underscore the need for effective tools to monitor the health of pine forests. Remote sensing (RS) offers valuable capabilities for ecosystem monitoring by providing large-scale data on vegetation characteristics in a consistent and repeatable manner (Lawley et al. 2016). Despite its strengths, traditional field studies remain essential for identifying the specific causes of plant stress or disease (Sun et al. 2023). This study focuses on the pine forest decline in the "Volturno Licola Falciano Natural Reserve" aiming to: (i) analyze the causes and dynamics of this decline; (ii) evaluate salinity as a stressor for both old and newly planted pines; and (iii) assess the effectiveness of combining direct field investigations with RS techniques to identify the primary stressors in Mediterranean coastal dune ecosystems. Furthermore, this study builds upon the findings of Alessandrino et al. 2024.

Materials and methods

The study area, covering an area of 0.6 km² (coordinates: 40°38'14"N, 13°58'4.17"E), is situated within the "Volturno Licola Falciano Natural Reserve" on the Campania Plain (CP) along the Tyrrhenian coast in Southern Italy. The plant community primarily consists of an 80-year-old afforested pine forest dominated by stone pine (*Pinus pinea* L.), alongside maritime pine (Pinus pinaster Aiton.). Additional species include Aleppo pine (*Pinus halepensis* Mill.), holm oak *(Quercus ilex* L.), and Mediterranean scrub vegetation. A direct (in situ) monitoring program was implemented to study the factors contributing to pine salinity stress. This effort was complemented by Sentinel-2 L2A satellite data, specifically using the EVI, Barren Soil, and SAVI indices provided by the EU Copernicus service. These indices were used to assess plant health and evaluate stress levels. Additionally, Actual Evapotranspiration (AET) and Potential Evapotranspiration (PET) data were retrieved from NASA's EARTHDATA platform (https://www.earthdata.nasa.gov/) using the Moderate Resolution Imaging Spectroradiometer (MODIS) instrument. MODIS plays a key role in developing validated, global, interactive Earth system models to predict global changes and support informed environmental policymaking. The vadose zone and shallow groundwater were continuously monitored using logging probes. Soil samples were collected from five depth intervals (0–20 cm, 20–40 cm, 40–60 cm, 60–80 cm, and 80–100 cm) during October and December 2023 to construct comprehensive soil salinity profiles. To ensure statistical reliability, three replicates were taken for each depth, resulting in 45 samples per sampling date. Total Dissolved Solids in porewater (TDSpw) were analyzed through batch extractions using the saturation soil extraction method (Schuwirth et al., 2006). To monitor precipitation chemistry, bulk dry and wet deposition samplers (Nesa srl, Vidor, Treviso, Italy) were installed near each piezometer, with samples collected quarterly.

Results and concluding remarks

Remote sensing (RS) monitoring using Sentinel-2 L2A imagery has proven effective in detecting the gradual decline of the older pine forest. The EVI index clearly highlighted the unhealthy condition and persistent water stress of the pines, while Barren Soil and SAVI indices successfully captured the reduction in forest canopy coverage. The high level of water stress led to a progressive decline in canopy activity starting in 2017, with further evidence provided by MODIS AET data showing a notable decrease in 2020. Shallow groundwater monitoring revealed low salinity levels (0.35–0.4 g/L) near the shoreline, facilitated by the rapid infiltration of rainwater through the dune environment, which prevented seawater intrusion. In contrast, salinity levels increased inland, peaking at the end of summer with values reaching up to 2.8 g/L. Although not the primary factor, salinity stress added pressure to the ecosystem. This study demonstrated that RS was highly effective in pinpointing areas of gradual stress and decline within the mature pine forest using EVI, Barren Soil, and SAVI indices. However, RS alone was insufficient for detecting vegetation stress in newly planted pines. This limitation, highlighted by the accuracy assessment, stemmed from the influence of Mediterranean shrub growth on the main indices. Consequently, RS data must be validated with field-based measurements to address potential biases and prevent misinterpretation. RS is particularly suited for monitoring mature, resilient forests, where sufficient time exists to plan interventions and mitigate stress impacts. Conversely, during vulnerable stages such as early growth, RS should be combined with field-based monitoring to promptly identify emerging issues. The proposed integrated monitoring approach could be widely applied to identify the primary drivers of salinity stress in coastal ecosystems.

Acknowledgments: The authors would like to thank the European Commission and MUR for funding in the frame of the collaborative international consortium DATASET (Groundwater salinization and pollution assessment tool: a holistic approach for coastal areas, Water4All_00084), financed under the 2022 Joint call of the European Partnership 101060874 - Water4All.

References

Alessandrino L, Giuditta E, Faugno S, Colombani N, Mastrocicco M (2024) Direct and Remote Sensing Monitoring of Plant Salinity Stress in a Coastal Back-Barrier Environment: Mediterranean Pine Forest Stress and Mortality as a Case Study. Remote Sensing 16: 3150. https://dx.doi.org/10.3390/rs16173150

Conte A, Zappitelli I, Fusaro L, Alivernini A, Moretti V, Sorgi T, Recanatesi F, Fares S (2022) Significant Loss of Ecosystem Services by Environmental Changes in the Mediterranean Coastal Area. Forests 13: 689. https://doi.org/10.3390/f13050689

Lawley V, Lewis M, Clarke K, Ostendorf B (2016) Site-Based and Remote Sensing Methods for Monitoring Indicators of Vegetation Condition: An Australian Review. Ecological Indicators 60: 1273–1283. https://doi.org/10.1016/j.ecolind.2015.03.021

Moderate Resolution Imaging Spectroradiometer (MODIS). Available online: https://www.spiedigitallibrary.org/conferenceproceedings-of-spie/1939/0000/Moderate-Resolution-Imaging-Spectroradiometer-MODIS/10.1117/12.152835.short#_=_ (accessed on 1 of May 2024).

Schuwirth N, Hofmann T (2006) Comparability of and Alternatives to Leaching Tests for the Assessment of the Emission of Inorganic Soil Contamination. Journal of Soil and Sediments 6: 102–112. https://doi.org/10.1065/jss2005.10.149

Sun C, Liu Y, Zhao S, Li H, Sun J (2017) Saltmarshes Response to Human Activities on a Prograding Coast Revealed by a Dual-Scale Time-Series Strategy. Estuaries and Coasts 40: 522–539. https://doi.org/10.1007/s12237-016-0157-2

Van Der Maarel E (2003) Some Remarks on the Functions of European Coastal Ecosystems. Phytocoenologia 33: 187–202. https://doi.org/10.1127/0340-269X/2003/0033-0187

Validation of ET interpolation for the new Landsat Provisional Actual Evapotranspiration (ETa) product in semi-arid climate

J.M. Carricondo-Antón[1], A. Garcia-Prats[1*], M.A. Jiménez Bello[1], J. Manzano Juarez[2], V. Jiménez[3], Ll. Simón[3], F. Montoya[3], M.Pulido-Velazquez[1]

[1] *Research Institute of Water and Environmental Engineering (IIAMA), Universitat Politècnica de València, Camino de vera s/n, 46022 Valencia, Spain*

[2] *Centro Valenciano de Estudios sobre el Riego (CVER), Universitat Politècnica de València, Camino de vera s/n, 46022 Valencia, Spain*

[3] *Instituto Técnico Agronómico Provincial de Albacete, ITAP. Parque empresarial Campollano, 2ª Avenida, 02007 Albacete 61, Spain*

** e-mail: agprats@upv.es*

Introduction

Understanding the spatial distribution of crop evapotranspiration (ET) is essential for planning and managing water resources at both plot and watershed scales. Methods such as the Surface Energy Balance Algorithm for Land (SEBAL model) by (Bastiaanssen et al., 1998a, 1998b) and Mapping EvapoTranspiration at High Resolution with Internalized Calibration (METRIC model) by Allen et al., (2007) have been developed to estimate ET over large areas. Today, the United States Geological Survey (USGS, https://www.usgs.gov) provides ET data for free through its Landsat Provisional Actual Evapotranspiration (ETa) product, derived from Landsat satellite imagery. This study primarily aims to validate the new ETa product in a semi-arid climate and perform temporal interpolations using different methodologies between satellite overpass dates. Two additional objectives derived from this include evaluating these interpolations and deriving monthly coefficients to improve ETa estimated compared to observed values.

Materials and methods

ETa images with a maximum cloud cover of 10% for the years 2020, 2021 and 2022 are obtained from Tiles 199033, 200032 and 200033 covering the surface of the Jucar River Basin located in eastern Spain. Using the Penman Monteith methodology described in FAO56 (Allen et al., 1998) and a system of multiple regressions developed in the work of Garcia-Prats et al., (2023) y Vicente-Serrano et al., (2007), the ETo and daily net radiation (Rn) are determined for the Jucar basin area for the 3 years of study. The quotient between the value of the ETa determined in each pixel and the value of ETo of each pixel (both 100x100m) determines the ET Fraction (ETrF) for each of the images obtained by the Landsat 8 and 9 satellites, following the equation, in line with the work of Jimenez-Bello et al. (2015):

$$ETrF=ETa \cdot ETo^{-1} \quad (1)$$

where the ETrF is obtained between the hourly net radiation at the time where the satellite passes and the Rn, the ET FractionRn (ETrFRn) was determined by the quotient between the ETa and the Rn using the following equation:

$$ETrFRn=ETa \cdot Rn^{-1} \quad (2)$$

Four different interpolation methods are used. First, a Simple ETrF is used based on the fact that the ETrF on each image acquisition date remains constant until a new image is obtained. In the Linear method, the ETrF is linearly interpolated between the ETrF of two consecutive image acquisition dates. The third interpolation method used is Cubic Spline interpolation (CS) following the methodology of Gerald and Wheatley, (2004). Finally, the Radiation method keeps the ETrFRn constant until the date of acquisition of a new image. Once the ETrF and ETrFRn are obtained, the ET between satellite overpass dates is obtained by multiplying the ETrF by ETo of each overpass day ($ET = ETrF * ETo$) and $ETrF_{Rn}$ by Rn of each overpass day ($ET = ETrF_{Rn} * Rn$).

To validate this product, data from meteorological stations near 20 golf courses are used, since golf courses with irrigation systems have an ET similar to ETo, since their ET Fraction ≈1. In addition, observed data from a lysimeter located in a 1.68ha alfalfa plot (39°03'37"N 2°05'59"W) in Albacete, Spain, are used.

Results and concluding remarks

In this study, four interpolation methods (Simple, Linear, CS and Radiation) and ETa satellite images are evaluated. The interpolated methods show better results than when only ETa images are determined, especially in golf. The Linear method obtained an R^2 of 0.38 for golf courses, while in the lysimeter the values are lower, even negative in some cases, indicating that the model has a performance where it is better to use the mean of the observed values as a prediction. In terms of MAE, Simple and Linear present the lowest errors with 1.17 and 1.18 mm for golf. Monthly coefficients between ETa and observed values (Coefficient=ETa· observed^{-1}) varied depending on the interpolation model. In golf, coefficients ranged from 0.39 to 0.85, indicating better correspondence than in the lysimeter (the closer to 1 the less adjustment the ETa would need), whose values ranged from 0.31 to 0.56. This suggests that ETa values better represent golf conditions than those in the lysimeter.

Table 1. Monthly adjustment coefficient.

	Jan	Feb	March	April	May	June	July	Aug	Sept.	Oct.	Nov.	Dec.
Golf coefficient	0.85	0.39	0.48	0.4	0.58	0.6	0.67	0.66	0.6	0.71	0.73	0.67
Lysimeter coefficient	0.31	0.31	0.39	0.56	0.42	0.33	0.47	0.48	0.43	0.38	0.33	0.34

Adjusting the interpolated data with monthly coefficients significantly improves the metrics. The R^2 reach 0.81 and the MAE is reduced, reaching a value of 0.67 with the Linear in Golf method. In addition, the percentage bias error decreases significantly. These results demonstrate that monthly normalization improves accuracy and corrects systematic deviations. This study demonstrates that interpolation methods, particularly the Linear method, allow generating ETa images between satellite overpass dates with good precision and adjustment when applying correction coefficients. With monthly coefficients, the Linear method achieve an R^2 of 0.80 in golf and 0.84 in lysimeter, with MAE of 0.67 and 0.81, respectively, evidencing its consistency. These results confirm that the Landsat Provisional Actual Evapotranspiration product is useful for irrigation applications, although it requires local adjustments using coefficients to improve its precision according to the characteristics of the area studied.

Acknowledgments: This study has received funding from the European Union's Horizon Europe research and innovation programme under the SOS-WATER project (GA no. 101059264); and from the subvencions del Programa per a la promoció de la investigación científica, el desenvolupament tecnològic i la innovació a la Comunitat Valenciana (PROMETEO) under the WATER4CAST 2.0 project.

References

Allen, R.G., Pereira, L.S., Raes, D., Smith, M., et al. (1998) Crop evapotranspiration-Guidelines for computing crop water requirements-FAO Irrigation and drainage paper 56. Fao, Rome 300, D05109.

Allen, R.G., Tasumi, M., Trezza, R., (2007) Satellite-Based Energy Balance for Mapping Evapotranspiration with Internalized Calibration (METRIC)-Model. Journal of Irrigation and Drainage Engineering 380–394. https://doi.org/10.1061/ASCE0733-94372007133:4380

Bastiaanssen, W.G.M., Menenti, M., Feddes, R.A., Holtslag, A.A.M., (1998a) A remote sensing surface energy balance algorithm for land (SEBAL) 1. Formulation. J Hydrol (Amst) 212–213, 198–212.

Bastiaanssen, W.G.M., Pelgrum, H., Wang, J., Ma, Y., Moreno, J.F., Roerink, G.J., Van Der Wal, T., (1998b) A remote sensing surface energy balance algorithm for land (SEBAL) 2. Validation. J Hydrol (Amst) 212–213, 213–229.

Garcia-Prats, A., Carricondo-Anton, J.M., Jiménez-Bello, M.A., et al. (2023) Dynamic procedure for daily PM56 ETo mapping conducive to site-specific irrigation recommendations in areas covered by agricultural weather networks. Agric Water Manag 287. https://doi.org/10.1016/j.agwat.2023.108415

Gerald, C.F.., Wheatley, P.O.., (2004) Applied numerical analysis. Pearson/Addison-Wesley.

Jimenez-Bello, M.A., Castel, J.R., Testi, L., Intrigliolo, D.S., (2015) Assessment of a Remote Sensing Energy Balance Methodology (SEBAL) Using Different Interpolation Methods to Determine Evapotranspiration in a Citrus Orchard. IEEE J Sel Top Appl Earth Obs Remote Sens 8, 1465–1477. https://doi.org/10.1109/JSTARS.2015.2418817

Vicente-Serrano, S.M., Lanjeri, S., López-Moreno, J.I., (2007) Comparison of different procedures to map reference evapotranspiration using geographical information systems and regression-based techniques. International Journal of Climatology 27, 1103–1118. https://doi.org/10.1002/joc.1460

Mapping irrigated farms using actual evapotranspiration and machine learning for woody crops

M.A. Jiménez Bello*, J.M. Carricondo-Antón, A. Garcia-Prats, E. López-Pérez, J. Huertas-Bastidas
Research Institute of Water and Environmental Engineering (IIAMA), Universitat Politècnica de València, Camino de vera s/n, 46022 Valencia, Spain
** e-mail: mijibar@dihma.upv.es*

Introduction

The expansion of irrigation in arid and semi-arid regions, together with the scarcity of resources, promotes water use by users who do not have rights to it. This occurs mainly through extracting the resources from aquifers, causing overexploitation, conflict between users, and difficulty for the authorities to know the extractions as they cannot be monitored (Molle and Closas, 2020). Due to the large extensions of irrigated areas, traditional control using inspections is very expensive, and it should be carried out with a high temporal frequency.

Remote sensing offers the possibility of detecting these areas because the spectral response between the same irrigated and non-irrigated crops can differ in different phenological phases (Massari *et al.*, 2021). This is easily detectable in horticultural crops from planting to senescence (Ballester-Berman et al., 2013).

Distinguishing between an irrigated or non-irrigated farm is more complicated for woody crops. In the same irrigation district, there may be farms of the same crop with different sizes, making it difficult to distinguish which ones are irrigated since trees of different sizes can transpire the same amount. In addition, there is the possibility that farmers carry out different irrigation strategies, such as controlled deficit irrigation, for the same type of crop.

Until now, the methodologies used to detect irrigated areas used a time series of satellite images that studied the temporal evolution of vegetation indices or vegetation indices and temperature throughout an irrigation campaign and applied an artificial intelligence method to distinguish irrigated farms from those that are not (Bastiaanssen, 2000; Allen, Tasumi and Trezza, 2002).

This work proposes using actual evapotranspiration calculated by energy balance under the starting hypothesis that plots of the same crop with the same leaf area index should transpire the same if they follow similar irrigation treatments. To do this, the actual evapotranspiration was calculated from the series of Landsat 8 and 9 images, and, together with climatic data, the actual evapotranspiration was calculated for an irrigation campaign. Once the study area was sampled, an artificial intelligence methodology (i.e., random forest classifier) was applied to determine which farms of each crop were irrigated.

Materials and methods

The study area is the municipality of Tarazona de la Mancha (39.2167° N, -1.9167° W) located in the central Spanish plateau. It has a total area of 21,254 ha. 90.5% is agricultural land and 27.4% permanent crops. These are nuts and vineyards. Officially only 5% of woody crops would be irrigated.

The information has been extracted from the SIGPAC (Ministerio de Agricultura, Pesca y Alimentación, n.d.). For the field sampling, a simple random sampling method was applied among the plots to be classified. These plots were inspected on-site for several days to document the actual conditions of the land. The areas of the sampled plots varied between a minimum of 130 m^2 and a maximum of 20 ha, ensuring an adequate representation of the entire area. In total, 836 plots were sampled: 269 irrigated and 567 rainfed.

Actual evapotranspiration (ET) was obtained from LANDSAT 8 and 9 images. Actual evapotranspiration was calculated using the SEBAL method (Bastiaanssen, 2000; Allen, Tasumi and Trezza, 2002). A total of 42 cloud-free days were used throughout 2023. For each available day, the crop coefficient for each plot is extracted, which relates the actual evapotranspiration to the reference evapotranspiration. The Normalized

Difference Vegetation Index (NDVI) and Normalized Difference Water Index (NDWI) indices are also calculated.

From the SIAR data available for the Tarazona de la Mancha agroclimatic station, the daily data is interpolated for the date periods between satellite visits (Jimenez-Bello *et al.*, 2015).

The Random Forest Classifier algorithm implemented in Random Forest in ML.NET is trained to be able to distinguish, week by week, whether a farm of a given crop has been irrigated or not, comparing the actual evapotranspiration of each of them according to the development of the crop indicated by the NDVI. At the end of the year, it is decided whether the plot has been irrigated, considering the number of weeks it has been classified as irrigated or rainfed. In this way, the precision or degree of certainty with which a plot has been classified can be quantified.

Results and concluding remarks

The overall precision of the process was 92.58% for the sampled population. According to the crop type, vineyard, and nuts, the precision was 91.85% and 94.32%, respectively.

Performing a visual inspection of the poorly classified plots, it was detected that they were sampled as irrigated due to having an installation. However, the estimated evapotranspiration was very low throughout all the weeks compared to those of the same size, so the presence of the installation does not guarantee use.

In the absence of being extrapolated to other areas, the results of the method based on actual evapotranspiration are highly reliable, determining the precision of the classification, avoiding confusion caused by rainy episodes, in addition to determining the actual evapotranspiration of the farms.

References

Allen, R., Tasumi, M. and Trezza, R. (2002) 'SEBAL (Surface Energy Balance Algorithms for Land)–Advanced Training and Users Manual–', Idaho: Implementation, pp. 1–98.

Ballester-Berman, J.D., Vicente-Guijalba, F. and Lopez-Sanchez, J.M. (2013) 'Polarimetric sar model for soil moisture estimation over vineyards at C-band', Progress in Electromagnetics Research, 142, pp. 639–665. Available at: https://doi.org/10.2528/PIER13071702.

Bastiaanssen, W.G.M. (2000) 'SEBAL-based sensible and latent heat fluxes in the irrigated Gediz Basin, Turkey', Journal of Hydrology, 229(1–2), pp. 87–100. Available at: https://doi.org/10.1016/S0022-1694(99)00202-4.

Gobierno de Castilla-La Mancha. (n.d.). SIAR: Sistema de Información Agroclimática para la Región de Castilla-La Mancha. Recuperado de https://www.castillalamancha.es/web/agricultura/siar

Jimenez-Bello, M.A. et al. (2015) 'Assessment of a Remote Sensing Energy Balance Methodology (SEBAL) Using Different Interpolation Methods to Determine Evapotranspiration in a Citrus Orchard', IEEE Journal of Selected Topics in Applied Earth Observations and Remote Sensing, 8(4), pp. 1465–1477. Available at: https://doi.org/10.1109/JSTARS.2015.2418817.

Massari, C. et al. (2021) 'A review of irrigation information retrievals from space and their utility for users', Remote Sensing, 13(20), p. 4112. Available at: https://doi.org/10.3390/RS13204112/S1.

Ministerio de Agricultura, Pesca y Alimentación. (n.d.). SIGPAC: Sistema de Información Geográfica de Parcelas Agrícolas. Gobierno de España. Recuperado de https://sigpac.mapama.gob.es/fega/visor/

Molle, F. and Closas, A. (2020) 'Why is state-centered groundwater governance largely ineffective? A review', Wiley Interdisciplinary Reviews: Water, 7(1), p. e1395. Available at: https://doi.org/10.1002/WAT2.1395.

Modernizing the Hydroclimatic Atlas: Building for transparency, robustness and sustainability

G. Rondeau-Genesse[1*], L. Arnal[1], L.P. Caron[1], E. Mailhot[2], J. Pelletier-Dumont[2], R. Turcotte[2], R. Arsenault[3], J.L. Martel[3]
[1] *Climate scenarios and services, Ouranos, Montreal, Canada*
[2] *MELCCFP, Government of Quebec, Quebec, Canada*
[3] *Construction Engineering department, École de Technologie Supérieure, Montreal, Canada*
** e-mail: rondeau-genesse.gabriel@ouranos.ca*

Introduction

Integrating new developments into operational products poses significant challenges, particularly when these innovations originate from external research projects involving diverse programming languages or computational frameworks. These challenges were evident during the production of the 2022 version of the Hydroclimatic Atlas of Southern Quebec (Malenfant et al., 2024), which highlighted the limitations in the existing infrastructure. The difficulty in efficiently coordinating external contributions within the current system prompted a reevaluation of the entire production process and the supporting tools.

To address these challenges, efforts have been made to establish a more robust computing infrastructure for the next version of the Hydroclimatic Atlas. A central component of this initiative is the development of an open-source Python library, *xHydro*, which is being created through collaboration among stakeholders in hydrology research and development in Quebec, including the Government of Quebec, Ouranos, Hydro-Québec, and academic researchers. This library consolidates scientific methods previously integrated into the Atlas production workflow, facilitates the inclusion of external scientific developments, and introduces tools for incorporating multiple hydrological models into the analyses. The Atlas production workflow itself has been reworked into a separate GitHub repository, leveraging *xHydro* functionalities and incorporating a workflow manager to automate calculations. Ultimately, this initiative aims to improve the transparency, robustness, and sustainability of the Hydroclimatic Atlas, enhancing its capacity to support water management practices resilient to climate change, while fostering improved collaboration among involved organizations.

Materials and methods

The development of the new version of the Hydroclimatic Atlas follows these key components:

- The integration of a new hydrological model, the Raven-emulated *HBV-EC* (Craig et al., 2020), to strengthen the reliability of hydroclimatic projections already being produced by the operational Hydrotel model (Fortin et al., 2001). This will be further complemented by machine learning-based hydrological projections using Long Short-Term Memory (LSTM) models.
- The creation of the *xHydro* Python library to house the scientific methods used in the Hydroclimatic Atlas production, as well as other functions useful in hydrology. The library will support the calibration and execution of hydrological models, optimal interpolation techniques for reconstructing historical hydrology in both gauged and ungauged basins, the computation of hydrological indicators (e.g., n-day peak and low flow), frequency analyses, the assessment of climate change impacts on hydrological data, and more.
- The modernization and translation of the Atlas production pipeline from MATLAB to Python, housed within a separate GitHub repository, complemented by a workflow manager (*SnakeMake*) to automate calculations on computer clusters.

Results and concluding remarks

A significant portion of the work has focused on ensuring compatibility between the Hydrotel and Raven-emulated HBV-EC hydrological models. This involved extensive adjustments to basin properties, such as computation units, soil categories, lakes, and other landscape features, ensuring coherence between the hydrological networks of both models. These adjustments are crucial for enabling direct comparisons between model outputs and creating more robust ensemble projections for future streamflow indicators. Concurrently, efforts to integrate machine learning-based hydrological projections using an LSTM network are progressing. Model configurations are being tested for their ability to accommodate future climates and changes on hydrological regimes, as well as the consistency of predicted streamflow for frequency analyses (Martel et al., 2024a-b). While still in the testing phase, early results are promising, and LSTMs could become a powerful tool for predicting future hydrological behaviour alongside traditional models.

The development of *xHydro* has fostered active collaboration among stakeholders and has served as a platform for interorganizational cooperation, supporting joint efforts in methodology development and comparison. The library is currently available on both PyPI and conda-forge and adheres to Python development best practices, including complete unit testing and a comprehensive bilingual documentation. The library is undergoing further refinement and is being integrated into the new Atlas production pipeline, which has been successfully translated into Python and automated using *SnakeMake*. Early tests are underway, with full operational capacity expected by the end of 2025 or early 2026. This automation will streamline the Atlas production process, reduce human error, and facilitate the integration of new climate simulations. Furthermore, the separation of *xHydro* from the production pipeline is anticipated to accelerate the incorporation of new scientific developments, improving the reliability and flexibility of hydroclimatic projections in future iterations of the Atlas.

As the Hydroclimatic Atlas of Southern Quebec becomes an increasingly important tool for water management and climate resilience in Quebec, this project lays the foundation for a more robust infrastructure that will allow for more efficient and streamlined updates and could serve as an example for similar initiatives. This will enable the Government of Quebec to integrate new scientific advancements, developed in-house and in universities, more swiftly and add new features as necessary, ultimately contributing to more informed decision-making in the face of ongoing climate challenges.

Acknowledgments: The INPACT project was supported by the Government of Quebec through the INFO-Crue research program.

References

Craig, J.R., G. Brown, R. Chlumsky, W. Jenkinson, G. Jost, K. Lee, J. Mai, M. Serrer, M. Shafii, N. Sgro, A. Snowdon, and B.A. Tolson, Flexible watershed simulation with the Raven hydrological modelling framework, Environmental Modelling and Software, 129, 104728, doi:10.1016/j.envsoft.2020.104728, July 2020

Fortin, J.-P., Turcotte, R., Massicotte, S., Moussa, R., Fitzback, J., and Villeneuve, J.-P.: Distributed Watershed Model Compatible with Remote Sensing and GIS Data. I: Description of Model, Journal of Hydrologic Engineering, 6, 91–99, https://doi.org/10.1061/(ASCE)1084-0699(2001)6:2(91), 2001.

Malenfant, C., Lavigne, M.-P., Mailhot, E., El-Housni, H., Pelletier-Dumont, J., and Lachance-Cloutier, S.: Rapport technique de l'Atlas hydroclimatique du Québec méridional, Government report, Government of Quebec (MELCCFP), Quebec City (QC), Canada, 2024.

Martel, J.-L., Arsenault, R., Turcotte, R., Castañeda-Gonzalez, M., Brissette, F., Armstrong, W., Mailhot, E., Pelletier-Dumont, J., Lachance-Cloutier, S., Rondeau-Genesse, G., and Caron, L.-P.: Exploring the ability of LSTM-based hydrological models to simulate streamflow time series for flood frequency analysis, EGUsphere [preprint], https://doi.org/10.5194/egusphere-2024-2134, 2024.

Martel, J.-L., Brissette, F., Arsenault, R., Turcotte, R., Castañeda-Gonzalez, M., Armstrong, W., Mailhot, E., Pelletier-Dumont, J., Rondeau-Genesse, G., and Caron, L.-P.: Assessing the adequacy of traditional hydrological models for climate change impact studies: A case for long-short-term memory (LSTM) neural networks, EGUsphere [preprint], https://doi.org/10.5194/egusphere-2024-2133, 2024.

Regional frequency analysis for design flood estimation using EANN and GAM models with sensitivity analysis in South Korea

J. Kim[1], K. Jung[2], S. Shin[1], D. Park[1*]
[1] Department of Civil, Environmental and Plant Engineering, Konkuk University, Seoul, South Korea
[2] Department of Planning and Strategy, Korea Environment Institute, Sejong 30147, South Korea
* e-mail: drpark@konkuk.ac.kr

Introduction

Accurate flood quantile estimation is essential for the design of hydraulic structures. However, in South Korea, the available streamflow records are typically limited, necessitating reliable methods for hydrological prediction under data-scarce conditions. Regional Frequency Analysis (RFA) is a widely used method for hydrological predictions under data-scarce conditions. This study utilizes RFA to estimate flood quantiles across 67 catchments in South Korea. The selected models, Ensemble Artificial Neural Networks (EANN) and Generalized Additive Models (GAM), are well-suited for this purpose. EANN excels in capturing nonlinear and complex relationships, while GAM is effective for modeling nonlinear hydrological phenomena, particularly when data deviate from Gaussian distributions (Wood, 2006). Since Shu (2007) demonstrated that Canonical Correlation Analysis (CCA) enhances RFA model performance, this study also applies CCA to evaluate its impact on model accuracy. Additionally, sensitivity analysis is conducted to assess the importance of geomorphic and meteorological variables, contributing to more efficient variable selection for future RFA applications.

Materials and methods

This study conducted a regional frequency analysis (RFA) for 67 watersheds across South Korea. Daily maximum discharge data for these watersheds were collected and preprocessed using the Grubbs-Beck method to eliminate outliers. The preprocessed data were used to estimate the probability distribution of each watershed, employing Akaike Information Criterion (AIC) and Bayesian Information Criterion (BIC), which provided the basis for calculating design floods corresponding to return periods of 10, 50, and 100 years.

Six watershed factors were selected for analysis: basin area(AREA), main basin slope(MBS), main channel slope(MCS), main channel length(MCL), precipitation(AMP), and temperature(AMT). The first four factors were derived from Digital Elevation Model (DEM) data, while precipitation and temperature were obtained from the Korea Meteorological Administration.

Canonical Correlation Analysis (CCA) was adopted to enhance the relationship between geomorphic and meteorological variables and the design flood estimates. The canonical variables (V) obtained through CCA, along with the original design flood values (Y), were used as input data for Ensemble Artificial Neural Networks (EANN) and Generalized Additive Models (GAM). The GAM model was applied to two sets of variables: one processed through CCA and the other comprising the original six watershed factors, enabling an evaluation of CCA's effectiveness.

Sensitivity analysis using the trained EANN model was conducted after modeling, employing the Morris method to assess the effect of input parameters on model output.

Results and concluding remarks

The following are the model performance results. It is confirmed that applying CCA improves the model's performance. While the NSE values of EANN and GAM are similar, GAM exhibits smaller errors and biases, indicating that the GAM model outperforms EANN.

Table 1. The results of EANN and GAM with and without the application of CCA.

	With CCA						Without CCA		
	EANN			GAM			GAM		
	10-y frequency	50-y frequency	100-y frequency	10-y frequency	50-y frequency	100-y frequency	10-y frequency	50-y frequency	100-y frequency
NSE	0.856	0.850	0.842	0.860	0.841	0.835	0.829	0.787	0.776
rRMSE	39.625	42.446	41.613	37.074	39.733	40.500	38.501	41.547	42.278
rBIAS	-4.923	-7.981	-7.224	-5.565	-6.450	-6.704	-6.637	-7.810	-8.072

As a result of the Morris sensitivity analysis, the order of influential factors remains consistent across the three three frequencies: AREA > MCS > AMT > AMP > MCL > MBS. Among these, AREA is identified as the most influential factor, MCS has a moderate level of influence, while the remaining factors have minimal impact on the model. However, the Morris sensitivity analysis has limitations in accurately identifying interactions between factors and analyzing nonlinear relationships. Nevertheless, this analysis provides valuable insights by consistently confirming the ranking of factor importance.

Acknowledgments: This work was supported by Korea Environment Industry & Technology Institute (KEITI) through R&D Program for Innovative Flood Protection Technologies against Climate Crisis, funded by Korea Ministry of Environment (MOE) (RS-2023-00218973). It was also supported by the National Research Foundation of Korea (NRF) grant funded by the Korean Government (MSIT) (RS-2023-00272933)

References

Alobaidi, M.H., Marpu, P.R., Ouarda, T.B.M.J., Chebana, F., 2015. Regional frequency analysis at ungauged sites using a two-stage resampling generalized ensemble framework. Adv. Water Resour. 84, 103–111. https://doi.org/10.1016/j.advwatres.2015.07.019

Aziz, K., Rahman, A., Fang, G., Shrestha, S., 2014. Application of artificial neural networks in regional flood frequency analysis: a case study for Australia. Stoch. Environ. Res. Risk Assess. 28, 541–554. https://doi.org/10.1007/s00477-013-0771-5

Jung, K., An, H., Lee, M., Um, M.-J., Park, D., 2024. Assessment of non-linear models based on regional frequency analysis for estimation of hydrological quantiles at ungauged sites in South Korea. J. Hydrol. Reg. Stud. 52, 101713. https://doi.org/10.1016/j.ejrh.2024.101713

Shu C, Ouarda TBMJ (2007) Flood frequency analysis at ungauged sites using artificial neural networks in canonical correlation analysis physiographic space. Water Resources Research 43: W07438. http://doi.org/10.1029/2006WR005142

Wood SN (2006) Generalized Additive Models: An Introduction with R. CRC Press, Boca Raton. http://doi.org/10.1201/9781420010404

Lab-on-a-chip system for real-time monitoring of emerging contaminants in water and sewage systems

R. La Cognata[1], S. Piazza[2*], G. Freni[2]
[1] Department of Civil Engineering and Architecture, University of Catania, Piazza Università, 2, 95131, Catania, Italy
[2] Department of Engineering and Architecture, University of Enna "Kore", Cittadella Universitaria, 94100, Enna, Italy
* e-mail: stefania.piazza@unikore.it

Introduction

In recent years, technology for monitoring water quality in water systems (Piazza et al., 2020) and sewer systems (Sambito et al., 2022) has seen significant innovation, with portable devices and IoT platforms offering cost-effective solutions (Kumar et al., 2019). Technologies such as Arduino, Raspberry Pi, and lab-on-a-chip enable real-time detection of emerging contaminants (CEC), overcoming many limitations of traditional methods. Thio et al. (2022) developed a Lab-on-Smartphone platform for microbiological monitoring via colorimetric analysis, although limited by hardware accuracy.

Zhao et al. (2021) created a portable system for total nitrogen (TN) detection in 36 min, with a cutoff of 1.2 mg/L, which however needs further validation. Hong et al. (2022) proposed an Arduino-IoT system to monitor the turbidity of water filters, but it is affected by lighting conditions. Lim et al. (2021) developed advanced sensors for mercury, integrating artificial intelligence and 3D printing, showing high sensitivity but vulnerability to complex environments.

Silva et al. (2020) developed a paper-based microfluidic device for parameters such as hardness and total phenols, accurate but limited for very low concentrations.

Ankushavali et al. (2020) presented an IoT system for continuous nitrate detection, but sensitive to temperature variations.

Materials and methods

The review was conducted using the web tool "Ryann Research", to analyze papers from different research portals and simplify the comparative analysis. Four keywords (Arduino, Raspberry Pi, lab-on-a-chip, Raman spectrometry) were selected to identify relevant articles on the monitoring of emerging contaminants.

Results and concluding remarks

The reviewed studies allowed to describe the state of the art on advanced technologies for monitoring emerging contaminants (CEC) in water and sewer networks, combining different cutting-edge methodologies. First, digital sensors integrated in IoT (Internet of Things) systems, such as Arduino and Raspberry Pi platforms, were used for real-time water monitoring, ensuring continuous and decentralized data collection. These devices allowed to collect key information on water quality, including physical parameters such as pH, turbidity and conductivity. For the analysis of contaminants, lab-on-a-chip systems were used, which allowed to perform chemical tests directly in the field, significantly reducing costs and analysis times. Raman spectrometry was used, an advanced technique that exploits the interaction of light with molecules to accurately and rapidly identify contaminants at the molecular level, even in complex samples. The study highlights how the integration of advanced technologies, such as IoT sensors and lab-on-a-chip systems, improves the monitoring of emerging contaminants (CEC) in water and wastewater networks. Portable devices enable real-time detection of pollutants with high precision, while techniques such as Raman spectrometry identify molecular contaminants in complex samples, reducing time and costs compared to traditional methods. Lab-on-a-chip systems offer a cost-effective and efficient alternative, enabling rapid analysis in the field without specialized laboratories.

Technical challenges remain, such as optimizing sensor selectivity, reagent stability, and reliability under variable conditions. Despite progress in total nitrogen and nitrate detection, environmental factors such as pH require further refinement. However, integrated solutions offer timely and precise monitoring of water quality, with potential benefits for public health and the environment, especially through the use of cloud platforms for more efficient and decentralized management.

Future research should focus on increased sensitivity and reliability, making technologies accessible at scale, even in resource-limited settings. The integration of advanced sensors, IoT, and artificial intelligence promises intelligent systems for water quality management, with reduced operating costs and improved emergency response.

References

Ankushavali, M., Divya, G., Akhila, N.s. (2020). Automatic Nitrate Level Recognition in Agriculture Industry. In: Solanki, V., Hoang, M., Lu, Z., Pattnaik, P. (eds) Intelligent Computing in Engineering. Advances in Intelligent Systems and Computing, vol 1125. Springer, Singapore. https://doi.org/10.1007/978-981-15-2780-7_43.

Hong, M., Kim, K., & Hwang, Y. (2022). Arduino and IoT-based direct filter observation method monitoring the color change of water filter for safe drinking water. Journal of Water Process Engineering, 49, 103158. https://doi.org/10.1016/j.jwpe.2022.103158

Kumar, M. J. V., & Samalla, K. (2019). Design and Development of Water Quality Monitoring System in IoT. International Journal of Recent Technology and Engineering (IJRTE), 7(5S3), 527-533.

Lim, Ji Won, Kim, Tai-Yong, & Woo, Min-Ah. (2021). Trends in sensor development toward next-generation point-of-care testing for mercury. Biosensors and Bioelectronics, 183, 113228. Disponibile online dal 7 aprile 2021. DOI: 10.1016/j.bios.2021.113228

Piazza, S., Blokker, E. J. M., Freni, G., Puleo, V., & Sambito, M. (2020). Impact of diffusion and dispersion of contaminants in water distribution networks modelling and monitoring. Water Supply, 20 (1): 46–58. https://doi.org/10.2166/ws.2019.131

Sambito, M., Piazza, S., & Freni, G. (2022). Bayesian Identification of Brackish Water Infiltration by Lagrangian Sensors. Proceedings of the IAHR World Congress, pp. 3718–3720. https://doi.org/10.3850/IAHR-39WC252171192022432

Silva, V. A. O. P., Freitas, R. C. de, Oliveira, P. R. de, Moreira, R. C., Marcolino-Júnior, L. H., Bergamini, M. F., Coltro, W. K. T., & Janegitz, B. C. (2020). Microfluidic paper-based device integrated with smartphone for point-of-use colorimetric monitoring of water quality index. Measurement, 108085. https://doi.org/10.1016/j.measurement.2020.108085

Traina, F., Piazza, S., & Freni, G. (2022). State of the art of technology in urban drainage water quality sensors. AIP Conf. Proc. 2611, 060009. https://doi.org/10.1063/5.0119393

Thio, S. K., Bae, S. W., & Park, S.-Y. (2022). Lab on a smartphone (LOS): A smartphone-integrated, plasmonic-enhanced optoelectrowetting (OEW) platform for on-chip water quality monitoring through LAMP assays. Sensors & Actuators: B. Chemical, 358, 131543. Available online February 8, 2022. https://doi.org/10.1016/j.snb.2022.131543

Zhao, C., Chen, L., Zhong, G., Wu, Q., Liu, J., & Liu, X. (2021). A portable analytical system for rapid on-site determination of total nitrogen in water. Water Research, 202, 117410. https://doi.org/10.1016/j.watres.2021.117410

Integrating weather forecast into a physics-based model for short-term soil moisture and temperature prediction

M. Hájková*, M. Kuráž
Department of Water Resources and Environmental Modeling, Faculty of Environmental Sciences, Czech University of Life Sciences Prague, Kamýcká 129, Praha 6 - Suchdol, 165 21, Czech Republic
** e-mail: hajkovamariana@fzp.czu.cz*

Introduction

As global water resources face increasing stress, the optimization of irrigation practices has become a critical focus in sustainable agriculture. One potential solution is the implementation of Decision Support Systems (DSS), which integrate advanced models and real-time data to assist in managing irrigation (Rinaldi and He, 2014). However, direct measurements of key variables such as soil moisture and evapotranspiration are often costly and technologically demanding. Model-based approaches offer an effective alternative with physics-based models in particular offering highly accurate descriptions of soil water and energy dynamics. These models typically rely on the solution of the Richards equation, and their accuracy is strongly dependent on the appropriate specification of initial and boundary conditions, as well as the soil hydraulic and thermal properties. The upper boundary condition is usually obtained by solving the surface energy balance, which requires meteorological data as input (Saito et al., 2006). The governing equations of the energy balance components are fundamentally based on physical laws. However, many of the parameters within these equations are described by empirical relationships derived from experimental observations. Therefore, proper calibration of these parameters can help improve the accuracy of the model by adjusting the empirical relationships to better reflect the characteristics of the study area.

The objective of this study is to integrate weather forecasts into a fully calibrated version of the open-source numerical model DRUtES, which has previously been applied to simulate capillary barriers and contaminant transport (Kuráž et al., 2013). By incorporating forecasted meteorological data into a physics-based model, this work aims to enable short-term predictions of soil moisture and temperature.

Materials and methods

The model will be calibrated for a study area located at agricultural site Amálie, Lány, Czech Republic. The calibration will be conducted in two stages to ensure accurate representation of both subsurface and surface processes. In the first step, soil moisture data from TDR measurements will be used to estimate key soil properties including the saturated hydraulic conductivity and the parameters defined by van Genuchten (1980).

In the second stage, calibration will focus on parameters governing energy exchange processes. Soil thermal conductivity will be parameterized using the model proposed by Chung and Horton (1987). The calibration of the upper boundary conditions will involve atmospheric emissivity and surface albedo, both of which influence the calculation of net radiation, a major component of the surface energy balance. The final calibrated parameter will be the soil surface resistance, which controls the evaporation rate, which serves as the upper boundary condition for water flow. For this stage, the observation data will be obtained from the eddy covariance station located at the pilot site.

The goal of the calibration is to minimize the difference between simulated and observed data through the process of inverse modeling and differential evolution optimization. For this, the R package DEoptim will be utilized. Following calibration, the model will be validated using historical data.

For soil moisture and temperature prediction, weekly weather forecasts from Yr.no and Meteoblue.com, including variables such as air temperature, humidity, wind speed, and precipitation, will be integrated into the model as input for the energy balance equation. The overall methodology is summarized in Figure 1.

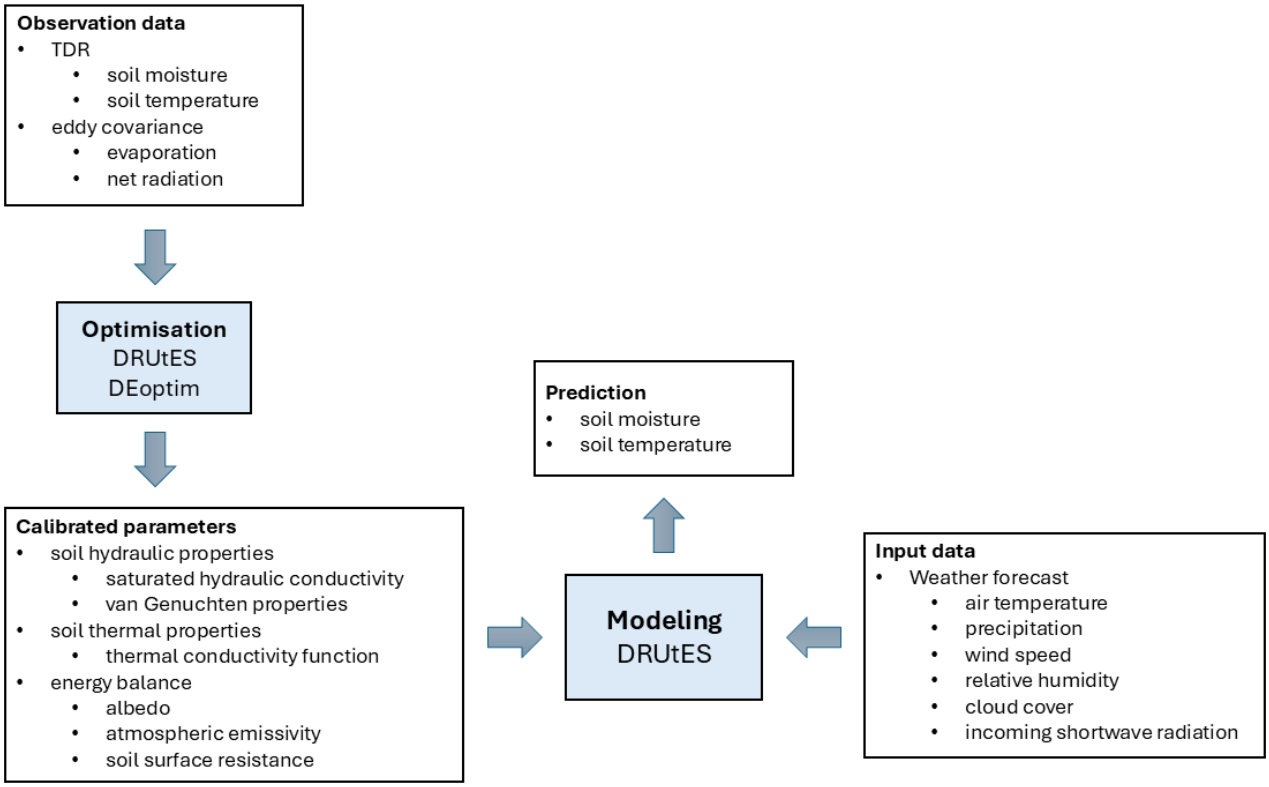


Figure 1. Model calibration and prediction workflow.

Results and concluding remarks

The study is currently in progress and preliminary stages, such as calibration and model setup, are ongoing. The expected outcomes include a calibrated and validated DRUtES model capable of accurately predicting short-term soil moisture and temperature dynamics. The integration of weather forecasts and the validation of energy balance components with eddy covariance data aim to ensure the model's replicability for similar climate regions. Once completed, the results are anticipated to demonstrate the utility of physics-based models in supporting sustainable irrigation practices by providing a groundwork for the development of an interactive Decision Support System.

Acknowledgments: The project was supported by IGA Faculty of Environmental Sciences CZU Prague "Integrating Weather Forecast into a Physics-Based Model for Short-Term Soil Moisture and Temperature Prediction".

References

Chung S-O, Horton R (1987) Soil Heat and Water Flow with a Partial Surface Mulch. Water Resources Research 23(12): 2175–86. https://doi.org/10.1029/WR023i012p02175

Kuráž M, Mayer P, Havlíček V, Pech P, Pavlásek J (2013) Dual permeability variably saturated flow and contaminant transport modeling of a nuclear waste repository with capillary barrier protection. Applied Mathematics and Computation 219(13): 7127–7138. https://doi.org/10.1016/j.amc.2011.08.109

Rinaldi M, He Z (2014) Chapter Six - Decision Support Systems to Manage Irrigation in Agriculture. In: Sparks DL (eds) Advances in Agronomy, Academic Press, Foggia, pp 229–79. https://doi.org/10.1016/B978-0-12-420225-2.00006-6

Saito H, Šimůnek J, Mohanty BP (2006) Numerical Analysis of Coupled Water, Vapor, and Heat Transport in the Vadose Zone. Vadose Zone Journal 5(2): 784–800. https://doi.org/10.2136/vzj2006.0007

van Genuchten, M Th (1980) A Closed-Form Equation for Predicting the Hydraulic Conductivity of Unsaturated Soils. Soil Science Society of America Journal 44(5): 892–98. https://doi.org/10.2136/sssaj1980.03615995004400050002x

Enhancing rainfall monitoring in urban areas by integrating crowdsourced personal weather stations into official networks

B. Moccia[1], P. Mazzoglio[2*], E. Ridolfi[1], F. Russo[1], P. Claps[2], F. Napolitano[1]
[1] Department of Civil, Constructional and Environmental Engineering, Sapienza University of Rome, Rome, Italy
[2] Department of Environment, Land and Infrastructure Engineering, Politecnico di Torino, Torino, Italy
* e-mail: paola.mazzoglio@polito.it

Introduction

Measuring rainfall accurately represents a significant challenge due to its high variability in space and time (Kidd et al. 2017). Recent technological innovations, such as Personal Weather Stations (PWS), leverage crowdsourced Internet-of-Thing (IoT) technologies to share local precipitation data on online platforms (McCabe et al. 2017). These low-cost tipping bucket rain gauges are installed by citizens for home automation and could be exploited as a promising tool for rainfall data collection. However, their non-standardized installation and user-maintained nature pose challenges regarding data quality and accuracy (de Vos et al. 2017; Bardossy et al. 2021; Chen et al. 2021). One of the leading PWS platforms is Netatmo (https://www.netatmo.com/it-it/smart-weather-station), whose rain gauge communicates with an internal module and transmits data to it through wireless technologies. Rainfall records measured by PWSs are sent every five minutes to a cloud service that collects and stores such data, allowing users to retrieve them through an API.

Given the potential of these widely distributed stations, the research question that guides this study is: are those stations reliable enough to obtain rainfall estimates suitable for hydrological modelling in urban areas? In this work, we try to answer this question by processing raw PWS rainfall data and integrating them with official networks to increase the spatial resolution of rainfall patterns.

Materials and methods

In this work, we selected 11 Italian cities as case studies, retrieving both official meteorological data and Netatmo PWS observations at hourly resolution in the October 2020 – September 2024 period. These cities provide a diverse range of climatic and topographical conditions that can affect rainfall patterns and are characterized by differences in the data densities.

In a first step, measurements from the two networks are compared to capture the correlation and deviations in recorded precipitation. Each PWS station is here compared to the closest official station. The comparison is performed using raw observations at hourly resolution, followed by an analysis of key precipitation metrics, including annual average rainfall, annual 1-hour maxima, and the probability of dry.

In a second step, by synthesizing and refining existing quality-control methods from scientific literature and adapting them to the diverse geographical and climatic conditions of Italy, we aim to provide, assess and improve the reliability of PWS rainfall observations.

Then, we evaluated the added value of this crowdsourced information in the spatial representation of rainfall extremes by considering two different intense rainfall events occurred during the analysed period that produced major pluvial flooding. In these case studies, we performed spatial interpolations using both datasets to assess the capacity of PWS data to improve spatial rainfall estimates. By comparing interpolated rainfall fields, we aimed to identify the extent to which quality-controlled PWS data can enhance spatial resolution and provide insights into rainfall variability within urban areas, especially when intense and localized rainfall events are considered.

Results and concluding remarks

The comparison between the raw observations and the precipitation metrics of the two datasets and

the subsequent application of the quality-control procedure highlighted a modest agreement among them but also allowed us to identify unreliable stations that should be discarded, whose low accuracy is probably induced by incorrect installation or poor maintenance performed by non-expert owners. It is interesting to note that PWSs exhibit both overestimations and underestimations of precipitation depth, and this behavior appears to vary not only between different stations but also across different years.

The inclusion of quality-controlled PWS data allowed us to refine the spatial representation of rainfall extremes in the two selected case studies, providing high rainfall amounts in ungauged areas that are consistent with information reported in the news.

Our final aim is to develop a guideline for hydrologists, engineers and regional hydrological agencies on how to treat such a huge and promising collection of rainfall data for hydrological applications, providing a step-based procedure that does not require the needs of other sources of data. This would help practitioners in retrieving rainfall observations at high spatial and temporal resolution without facing data fragmentation problems induced by the decentralization of the Italian rain gauge network. The development of a QC methodology can make the rapidly growing network of PWSs a more useful resource for hydrologic applications, greatly improving the knowledge of rainfall patterns in areas with dense PWSs, and providing also additional information in poorly gauged regions.

Acknowledgments: This research has been supported by the RETURN Extended Partnership and received funding from the European Union NextGenerationEU (National Recovery and Resilience Plan – NRRP, Mission 4, Component 2, Investment 1.3 – D.D. 1243 2/8/2022, PE0000005 – Spoke TS2).

References

Bardossy A, Seidel J, El Hachem A (2021) The use of personal weather station observations to improve precipitation estimation and interpolation. Hydrology and Earth System Sciences, 25: 583-601. https://doi.org/10.5194/hess-25-583-2021

Chen AB, Behl M, Goodall J (2021) Assessing the trustworthiness of crowdsourced rainfall networks: a reputation system approach. Water Resources Research, 57: e2021WR029721. https://doi.org/10.1029/2021WR029721

de Vos LW, Leijnse H, Overeem A, Uijlenhoet R (2017) The potential of urban rainfall monitoring with crowdsourced automatic weather stations in Amsterdam. Hydrology and Earth System Sciences, 21: 765-777. https://doi.org/10.5194/hess-21-765-2017

Kidd C, Becker A, Huffman GJ, Muller CL, Joe P, Skofronick-Jackson G, Kirschbaum DB (2017) So, how much of the Earth's surface is covered by rain gauges? Bulletin of the American Meteorological Society 98: 69-78. https://doi.org/10.1175/BAMS-D-14-00283.1

McCabe MF, Rodell M, Alsdorf DE, Miralles DG, Uijlenhoet R, Wagner W, Lucieer A, et al. (2017) The future of Earth observation in hydrology. Hydrology and Earth System Sciences 21: 3879-3914. https://doi.org/10.5194/hess-21-3879-2017

From coarse to fine: Relative humidity downscaling using AI model

S.K. Jha*, V. Gupta
School of Civil and Environmental Engineering, Indian Institute of Technology, Mandi, India
** e-mail: d23065@students.iitmandi.ac.in*

Introduction

Relative humidity (RH) is crucial to the understanding of atmospheric processes. Hydrological cycles and climate dynamics depend on it. Global climate models often provide coarse RH data. Its use in local studies is limited. Studies have used various methods to improve downscaling accuracy for meteorological variables like temperature, humidity, and wind speed. Bai et al. (2023) proposed a GAN-based statistical downscaling model (GSDM) to downscale relative humidity (RH) data, using air temperature and observed RH data as auxiliary inputs to improve results. Wu et al. (2023) used random forest (RF) to downscale temperature-humidity index (THI) from 6 to 1 km resolution, proving RF's superiority. Hernanz et al. (2023) found that machine learning SDMs outperformed regional climate models (RCMs) in most metrics for European climatic variables. CNN-based downscaling for temperature data over Egypt by Kheir et al. (2023) yielded high accuracy for future climate scenarios. This research uses U-Net, an advanced deep learning architecture (Ronneberger et al., 2015). U-Net is a convolutional neural network, it was originally designed for image segmentation application. The U-Net architecture is characterized by the encoder-decoder path that are connected by skip connections. But later there were many applications of it in the image super resolution task (eg. Hu et al., 2019; Zhang et al., 2020), which then got transferred to the task of climate downscaling applications. Lin et al. (2023) downscaled East Asian climate data using U-Net to create high-resolution meteorological variable datasets. Sha et al. (2020) improved UNet for downscaling surface temperature in complex terrain by integrating elevation data, improving generalization and performance. Adapted U-Net architectures are used in this field to learn complex spatial patterns and relationships present in climate data. This super-resolution model downscales and enhances RH data spatial resolution by scale of 10. We assessed performance using peak signal-to-noise ratio (PSNR), structural similarity index metric (SSIM), coefficient of determination (R2), root mean square error (RMSE) and mean absolute error (MAE).

Materials and methods

This study employed a U-Net architecture to downscale 2m relative humidity data from the Indian Meteorological Data Assimilation and Analysis (IMDAA) dataset spanning 1979 to 2023 (https://rds.ncmrwf.gov.in/). The model was trained on data spanning 1979 to 2008, validated using data from 2009 to 2013, and tested with data from 2014 to 2023. The U-Net features an encoder-decoder architecture with skip connections. The encoder extracts feature via convolutional and pooling layers, whereas the decoder reconstructs high-resolution data utilizing upsampling and concatenation layers. The output is a single band image (Relative humidity data), depicting the downscaled relative humidity. This method significantly enhances the spatial resolution of climate data for subsequent analysis.

Results and concluding remarks

The model attained an average PSNR of 30.70 dB and an average SSIM of 0.8582 during the testing period from 2014 to 2023. The PSNR signifies high prediction quality with negligible noise, whereas the SSIM illustrates substantial structural similarity between the predicted and original data, underscoring the model's proficiency in capturing precise and detailed information.

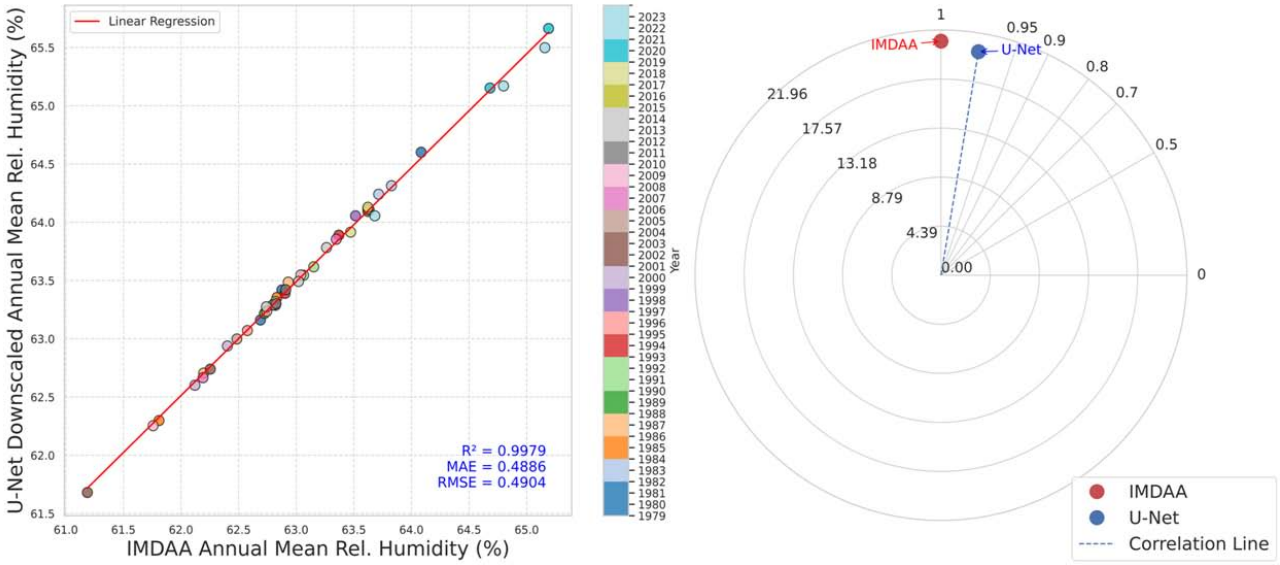


Figure 1. (a) (left) Annual mean relative humidity comparison between IMDAA and U-Net downscaled predictions (1979–2023), with a linear regression line and R², MAE, and RMSE values; (b) (right) Taylor diagram comparing IMDAA ground truth and U-Net downscaled RH (Testing period: 2014–2023), showing standard deviation, correlation, and RMSE.

The Taylor diagram (Figure 1-b) for 2014–2023 shows that U-Net downscaled RH data matches IMDAA ground truth with a small standard deviation difference (IMDAA: 20.9642, U-Net: 20.3031), indicating accurate variability capture. High correlation of 0.9863 indicates a linear relationship between predicted and observed data, while low RMSE of 3.4734 indicates minimal prediction errors. U-Net provides accurate downscaled RH data by replicating ground truth. The U-Net downscaling model accurately predicted annual mean RH values from 1979 to 2023, with a R^2 = 0.9976, explaining 99.76% of variance. MAE = 0.4886 and RMSE = 0.4904 show minimal error, demonstrating the model's accuracy and reliability in replicating RH data. These results (Figure 1-a) demonstrate U-Net's climate data downscaling accuracy.

References

Bai, B., Shi, C., Yang, L., Ge, L., Yue, L., & Liu, G. (2023). A Deep Learning Method for Statistical Downscaling of CLDAS Relative Humidity with Different Sources of Data: Sensitivity Analysis. Journal of Meteorological Research, 37(6), 878-895.

Hernanz, A., Correa, C., Domínguez, M., Rodríguez-Guisado, E., & Rodríguez-Camino, E. (2023). Comparison of machine learning statistical downscaling and regional climate models for temperature, precipitation, wind speed, humidity and radiation over Europe under present conditions. International Journal of Climatology, 43(13), 6065-6082.

Hu, X., Naiel, M. A., Wong, A., Lamm, M., & Fieguth, P. (2019). RUNet: A robust UNet architecture for image super-resolution. In Proceedings of the IEEE/CVF Conference on Computer Vision and Pattern Recognition Workshops (pp. 0-0).

Kheir, A. M., Elnashar, A., Mosad, A., & Govind, A. (2023). An improved deep learning procedure for statistical downscaling of climate data. Heliyon, 9(7).

Lin, H., Tang, J., Wang, S., Wang, S., & Dong, G. (2023). Deep learning downscaled high-resolution daily near surface meteorological datasets over East Asia. Scientific Data, 10(1), 890.

Ronneberger, O., Fischer, P., & Brox, T. (2015). U-net: Convolutional networks for biomedical image segmentation. In Medical image computing and computer-assisted intervention–MICCAI 2015: 18th international conference, Munich, Germany, October 5-9, 2015, proceedings, part III 18 (pp. 234-241). Springer International Publishing.

Wu, D., Yao, Z., Wu, L., Luo, X., Sun, S., He, B., & Zhang, Y. (2023). Downscaling the Midsummer Temperature-Humidity Index Based on Multiple Machine Learning Methods. IEEE Journal of Selected Topics in Applied Earth Observations and Remote Sensing.

Zhang, K., Gool, L. V., & Timofte, R. (2020). Deep unfolding network for image super-resolution. In Proceedings of the IEEE/CVF conference on computer vision and pattern recognition (pp. 3217-3226).

Comparison of machine learning methods for the prediction of Water Quality Index

Ç. Coskun Dilcan[1*], H.T. Gültaş[2], Y. Ahi[1], D.D. Köksal[3]
[1] Water Management Institute, Ankara University, Ankara, Turkey
[2] Department of Biosystems, Faculty of Agricultural and Natural Sci., University of Bilecik Şeyh Edebali, Bilecik, Turkey
[3] Earth Systems and Global Change Group, Wageningen University and Research, the Netherlands
* e-mail: coskunc@ankara.edu.tr

Introduction

The water quality index (WQI) is a widely used metric to evaluate and summarize the overall water quality. The prediction of effluent water quality is crucial for its reuse purposes and control of wastewater treatment plants (WWTPs) in the context of effective water management. The application of machine learning models in predicting WQI contributes to this goal by providing actionable insights that can guide water management strategies, particularly in regions facing water scarcity.

Machine learning (ML) techniques have emerged as a promising approach for WQI prediction (Torky et al., 2023). Several studies have demonstrated the effectiveness of various ML algorithms, such as support vector machines (SVM) (Rahu, 2023), decision trees (Yu et al., 2018), random forest (Sha et al., 2021), and ensemble learning (Liu et al., 2020), in accurately predicting the WQI and other effluent water quality parameters. These ML-based approaches have shown promising results for improving the management and control of WWTPs (Torky et al., 2023). This study will compare various machine learning methods to assess their performance in predicting water quality index of effluent water.

Materials and methods

The study utilized effluent data from the Kırklareli Domestic Wastewater Treatment Plant for the years 2018 and 2019. Located in the Thrace Region, this facility is classified as a medium-sized urban wastewater treatment plant. To ensure proper operation and maintain the facility's efficiency, data is regularly monitored through periodic sampling in wastewater treatment plant. The dataset comprises 192 entries, including measurements of pH, conductivity (EC, mg/L), salinity (TDS, mg/L), dissolved oxygen (DO, mg/L), chemical oxygen demand (COD, mg/L), total nitrogen (N, mg/L), ammonium (NH_4, mg/L), nitrate (NO_3, mg/L), total phosphorus (P, mg/L), and total suspended solids (TSS, mg/L) parameters. Using this dataset, the water quality index (WQI) was calculated based on the National Sanitation Foundation (NSF) water quality index method (Brown et al., 1972).

For ML algorithms, Regression Learner in MATLAB 2017b program was used and 5-fold cross-validation was applied. The WQI data, derived from Köksal's (2020) study, were analyzed, and compared with the outcomes of machine learning models. The results were further subjected to statistical analysis, and the applicability of these findings was critically evaluated.

Results and concluding remarks

The study assessed the performance of various machine learning (ML) models for predicting the Water Quality Index (WQI) of effluent water. Table 1 presents the descriptive statistics of the input and output data, along with the weights assigned to the input parameters. The output parameter, WQI, ranged from 62.3 to 682.1 across the years 2017, 2018, and 2019. According to the classification ranges outlined by İbrahim (2019), these values correspond to categories of "very poor water (76-100)" and "water unsuitable for the intended use (>100)."

Table 2 highlights the error metrics of four ML algorithms—Medium Tree, Linear SVM, Boosted Trees, and Gaussian Process—based on RMSE, MAE, and R-squared values.

Table 1. Descriptive statistics and WQI results of data set.

Parameters	Inputs										Output
	Total N	*Total P*	*TSS*	*COD*	*NH4*	*TDS*	*EC*	*DO*	*NO3*	*pH*	*WQI*
Mean	79.6	8.9	98.5	286.3	38.6	5215.5	1046.6	2.0	2.6	7.4	157.4
Standard error	4.1	3.0	5.8	7.6	1.5	59.4	11.4	0.3	1.3	0.0	5.6
Median	59.8	5.4	68.0	282.0	36.5	5100.0	1022.0	1.2	0.7	7.5	136.9
Standard deviation	57.1	41.2	80.0	105.8	21.5	825.5	158.8	4.8	18.7	0.4	78.2
Variance	3265.9	1700.8	6401.2	11188.6	461.2	681423.8	25224.0	23.3	348.5	0.2	6114.8
Kuortosis	2.3	191.8	7.0	1.1	99.8	9.4	9.4	152.6	191.2	5.9	10.3
Skewness	1.8	13.8	2.2	0.7	8.6	2.3	2.3	11.7	13.8	0.1	2.5
Range	266.2	576.2	496.0	623.0	281.4	6600.0	1273.0	65.0	259.7	3.8	619.8
Min	2.8	1.8	6.0	71.0	9.6	3200.0	659.0	0.0	0.3	5.8	62.3
Max	269.0	578.0	502.0	694.0	291.0	9800.0	1932.0	65.0	260.0	9.7	682.1

As seen from Table 2, Gaussian Process (Matern 5/2 Kernel) model outperformed the others, achieving the lowest RMSE (0.13957) and MAE (0.013353), along with an R-squared value approximating 1, indicating excellent predictive accuracy and reliability. The Linear SVM demonstrated strong predictive performance with an R-squared value of 0.97, though its RMSE (13.606) and MAE (4.4124) were higher than the Gaussian Process. Boosted Trees showed moderate accuracy, with an R-squared value of 0.67, while the Medium Tree performed the highest RMSE (48.598) and MAE (21.56) with an R-squared of 0.62.

Table 2. ML algorithms results

Error metrics	*ML algorithms*			
	Tree (Medium Tree)	SVM (Linear SVM)	Ensemble (Boosted Trees)	Gaussian Process (Matern 5/2)
RMSE	48.598	13.606	44.957	0.13957
MAE	21.56	4.4124	16.192	0.013353
R-squared	0.62	0.97	0.67	≈ 1

These results highlight the need to choose ML algorithms suited to the specific nature of water quality datasets, with the Gaussian Process offering significant potential for improving wastewater management. Further research could explore hybrid models or additional input features to enhance predictions.

References

Brown RM, McClelland NI, Deininger RA, O'Connor MF (1972) A Water Quality Index — Crashing the Psychological Barrier. In: Thomas, W.A. (eds) Indicators of Environmental Quality. Environmental Science Research, vol 1. Springer, Boston, MA. https://doi.org/10.1007/978-1-4684-2856-8_15

Ibrahim MN (2019) Effluent Quality Assessment of Selected Wastewater Treatment Plant in Jordan for Irrigation Purposes: Water Quality Index Approach. Journal of Ecological Engineering 20(10): 206-216. http://doi.org/10.12911/22998993/112491

Köksal DD (2020) Evaluation of treated domestic wastewater reuse for agriculture using artificial intelligence methods. Master Thesis of International Centre for Advanced Mediterranean Agronomic Studies (CIHEAM) of Bari

Liu H, Chen X, Zhang H, Zhang F, Huang M (2020). Effluent quality prediction of papermaking wastewater treatment processes using stacking ensemble learning. IEEE Access, 8, 180844-180854.https://doi.org/10.1109/access.2020.3028683

Rahu MA, Chandio AF, Aurangzeb K, Karim S, Alhussein M and Anwar MS (2023) Toward Design of Internet of Things and Machine Learning-Enabled Frameworks for Analysis and Prediction of Water Quality in IEEE Access, vol. 11, pp.101055-101086, doi: 10.1109/ACCESS.2023.3315649

Sha J, Li X, Zhang M, Wang ZL (2021). Comparison of forecasting models for real-time monitoring of water quality parameters based on hybrid deep learning neural networks. Water, 13(11), 1547. https://doi.org/10.3390/w13111547

Torky M, Bakhiet A, Bakrey M, Ismail AA, Seddawy AIB (2023). Recognizing safe drinking water and predicting water quality index using machine learning framework. International Journal of Advanced Computer Science and Applications, 14(1). https://doi.org/10.14569/ijacsa.2023.0140103

Yu T, Yang S, Bai Y, Gao X, Li C (2018). Inlet water quality forecasting of wastewater treatment based on kernel principal component analysis and an extreme learning machine. Water, 10(7), 873. https://doi.org/10.3390/w10070873

Integrating machine learning models to assess treated wastewater quality and agricultural reuse potential

H.T. Gültaş[1*], Y. Ahi[2], Ç. Coşkun Dilcan[2], D.D. Köksal[3]
[1] Department of Biosystems Engineering, Faculty of Agricultural and Natural Sci., University of Bilecik Şeyh Edebali, Bilecik, Turkey
[2] Water Management Institute, Ankara University, Ankara, Turkey
[3] Earth Systems and Global Change Group, Wageningen University and Research, Wageningen, The Netherlands
* e-mail: huseyin.gultas@bilecik.edu.tr

Introduction

In Thrace / TR, surface and ground water reserves are rapidly decreasing and being damaged due to climate change related factors and heavy industrial development. The importance of protection and sustainability of water resources in the region, which has a strong agriculture and today has the opportunity to grow more and more different product groups and whose population continues to increase, is strongly felt not only in the scientific field but also in the field of waste life. Therefore, for the sustainability of the water resources of the region, which are not sufficient and continue to be seriously damaged in terms of quality, the reuse of treated wastewater, which is one of the few alternatives, is especially important in the field of agriculture (Köksal and Ahi 2020). On the other hand, estimation of treated wastewater quality is a non-linear problem and cannot be solved statistically. In this respect, it is of great importance to establish a new method for the estimation of treated wastewater quality and availability rate. The main objective of the study is to evaluate the suitability of machine learning modelling as a valid input-output tool for estimating some effluent parameters at Babaeski Domestic Wastewater Treatment Plant in the Thrace Region of Turkey. To this end, various machine learning techniques were tested to assess the availability of wastewater quality for irrigation in the case study area. This objective combined three artificial intelligence models (Artificial Neural Network - ANN, Adaptive Neuro-Fuzzy Inference System - ANFIS and Fuzzy Logic-Mamdani - FLM) using various scenarios based on inlet and outlet water quality parameters (Sattari et al. 2016, Nadiri et al. 2018). At the same time, an agricultural projection was carried out to assess the reuse potential of municipal treated wastewater for each selected crop.

Materials and methods

Study conducted at Babaeski / Kırklareli of Thrace of Turkey which is one of the most important agricultural production sites of Turkey. The area's climate is described as semi-arid, with warm dry summer and relative dry winter, nowadays. The location of the domestic wastewater treatment plant (DWWTP) at 41.41316 N latitude and 27.09446 E longitude and plant planned capacity of district population is 50000 people about and 5266 m3 / day flow. In this study, the results of the analysis carried out in the laboratory of Kırklareli Institute have been used the study material. The analyses were based the paths and parameters determined by the Ministry of Agriculture of the Republic of Turkey. These parameters are the following: ph, conductivity, salinity, dissolved oxygen, biological oxygen demand, chemical oxygen demand, total N NH4, NO3, NO2, total P for input and output. The pH, conductivity, salinity, and TSS parameters were daily analysed, BOD each 10-day period, COD parameters 3 days per week, and total N, NH4, NO3, and total P 2 days per week in the Kırklareli Institute laboratory, which is affiliated to the Ministry of Agriculture of the Republic of Turkey. The data set covers data for 3 years (2022-2024).

The relief algorithm is a method of selection by filtering the data according to its properties. The relief algorithm first works according to the basis of descending ordering, with weighting according to the characteristics/attributes of each variable. The outputs of this algorithm vary from -1 to +1 (Urbanowicz et al. 2018, Aggarwal et al. 2023). Wastewater quality parameters are predicted with parameters of Babaeski

Wastewater Treatment Plant using ANNs written script in MATLAB R2024. The scenarios obtained by the ReliefF algorithm were prepared separately for 10 input parameters and single output, and then values were normalized. The most important point here is that the number of input layer data sets is constant for all scenarios.

Once the input scenarios are created, the entire data set is randomly divided by written script. The reason for the random division of the data is that periodic increase-decrease in the values of the parameters is observed. This reduces the performance of artificial neural networks, although it is clear in the literature that they provide more accurate results. Different percentages of data set (Training, validation and testing) were used for each ANNs (Abba and Elkiran 2017, Niel and Bastard 2019). In general, random division of the data set was applied between 75-85% for training, 0-10% for validation and 15-20% for testing. In addition, the purpose of using ANFIS in this study is to establish rules by categorizing each different parameters as inputs between 0 and 1 according to FAO recommendations (Ayers and Westcot 1985, Wan et al. 2011, Rajaee et al. 2020).

Results and concluding remarks

The main purpose of this process is focused on areas that can be irrigated with DWWTP discharge. Therefore, irrigation module was calculated for each crop, parallel to this, irrigation requirement for one hectare was found. Finally, in the light of these data, the amount of irrigable area for each individual crop was calculated according to the flow rate of DWWTP. According to the FAO recommendation and Appendix-7 of Turkey, the wastewater quality variables could be categorized into three main groups as know; chemical, physical, and biological. In this study, DWWTP output water quality was examined in order to make recommendations for agricultural irrigation. When the results for general use are evaluated in detail, it is predicted that the treatment plant effluent can be used in agriculture in the range of 57-83%. The results will be presented in detail at the congress, as it is impossible to include large tables in this section.

References

Abba SI and Elkiran G (2017) Effluent prediction of chemical oxygen demand from the wastewater treatment plant using artificial neural network application. Procedia Computer Science, 120: 156–163. doi:10.1016/j.procs.2017.11.223

Aggarwal N, Shukla U, Saxena GJ, Rawat M, Bafila AS, Singh S, Pundir A (2023) Mean based relief: an improved feature selection method based on ReliefF. Applied Intelligence, 53(19), 23004-23028. https://doi.org/10.1007/s10489-023-04662-w

Ayers RS and Westcot DW (1985) Water quality for agriculture. Rome: FAO.

Köksal DD, Ahi Y (2020) Evaluation of treated domestic wastewater reuse for agriculture using artificial intelligence methods. CIHEAM, Bari

Nadiri AA, Shokri S, Tsai FTC, Asghari-Moghaddam A (2018) Prediction of effluent quality parameters of a wastewater treatment plant using a supervised committee fuzzy logic model. Journal of Cleaner Production 180: 539–549. https://doi.org/10.1016/j.jclepro.2018.01.139

Niel O and Bastard P (2019) Artificial Intelligence in Nephrology: Core Concepts, Clinical Applications, and Perspectives. American Journal of Kidney Diseases, 74(6), 803–810. https://doi.org/10.1053/j.ajkd.2019.05.020

Rajaee T, Khani S and Ravansalar M (2020) Artificial intelligence-based single and hybrid models for prediction of water quality in rivers: A review. Chemometrics and Intelligent Laboratory Systems, 103978. doi:10.1016/j.chemolab.2020.103978

Sattari MT, Joudi AR, Kusiak A (2016) Estimation of water quality parameters with data-driven model. Journal - American Water Works Association 108: E232–E239. http://doi:10.5942/jawwa.2016.108.0012

Urbanowicz RJ, Meeker M, La Cava W, Olson RS, Moore JH (2018) Relief-based feature selection: Introduction and review. Journal of biomedical informatics, 85, 189-203. https://doi.org/10.1016/j.jbi.2018.07.014

Wan J, Huang M, Ma Y, Guo W, Wang Y, Zhan, H and Sun X (2011) Prediction of effluent quality of a paper mill wastewater treatment using an adaptive network-based fuzzy inference system. Applied Soft Computing Journal, 11(3), 3238–3246. https://doi.org/10.1016/j.asoc.2010.12.026

Human-AI teaming for water quality documentation analysis with large language models

S. Conrad*, J. Rodriguez, G. Vizarreta Luna
Department of systems engineering, Colorado State University, 6029 Campus Delivery, Fort Collins, CO 80523
** e-mail: steve.conrad@colostate.edu*

Introduction

Water Quality management in urban systems is a complex endeavor reliant on extensive textual and quantitative documentation. Effective management involves testing and documenting the performance of water treatment, distribution, and environmental conditions, alongside regulatory and policy frameworks. Water managers must analyze an extensive array of water quality data, environmental regulations, test reports, and field documents to determine actionable requirements for managing water quality in urban settings. Quantitative data is routinely processed but documentation analysis is time-intensive and exacerbated by workforce limitations. Manual textual analysis by humans is also prone to notable inconsistencies and errors, especially when managing large datasets or working with multiple reviewers (González Canché, 2023). As a result, many textual data sets remain unexamined. Recent advances in large language models (LLMs) offer promising solutions to these challenges by creating a human-AI teaming environment for water quality documentation analysis.

Emerging research underscores the transformative potential of LLMs in qualitative data analysis. For instance, Tai et al. (2023) show applications of LLM with predefined definitions of content can replicate traditional document classification methods. Xiao et al. (2023) explored using GPT-3 for deductive coding in qualitative research. Similarly, Chew et al. (2023) evaluated GPT-3.5 within their LLM-Assisted Content Analysis framework, finding accuracy comparable to human coders. Our study advances this research by conducting a pre- and post-comparative analysis of using memory chunking approaches for coding water quality documentation, revealing how data localization impacts LLM performance. Our study comments on how LLM-assisted workflows have the potential to bring in additional content for water quality management.

Materials and methods

We used open and deductive coding approach to analyze water quality field and test observations. Laboratory tests included pH measurement, turbidity, biochemical oxygen demand, and contaminants such as heavy metals and nitrates. Field observations included flow rate measurements, visual notations on discoloration, and temperature readings. A team of researchers manually reviewed twenty documents discussing these aspects and were asked to code for water quality concerns, such as corrosion, pollutants, and or chemical imbalances. Coding was reviewed by collaborating water quality analysts. The same documents were provided to LLMs, and their performance was assessed using percent agreement, accuracy, precision, recall, and Fleiss' Kappa values.

OpenAI's gpt-4o, gpt-4o-mini, and o1-mini models were employed using a chunking text approach. Texts were pre-processed using optical character recognition to extract content, which was divided into 500-word chunks. We first asked each model to identify water quality concerns. We then provided the LLMs with detailed definitions of these concerns based on standard operating procedures and localized water quality content provided by collaborating water utilities. Results were classified as True if a minimum of one response indicated the presence of a concern. We used a consensus approach where we treated the LLM as an additional rater alongside manual coders to evaluate human-AI teaming. The performance of each approach was assessed and compared for how the process affected internal variance and false positives and negatives. These measures provide a comparison framework for assessing the efficacy of manual versus AI-assisted document analysis.

Results and concluding remarks

Figure 1 presents a comparison of the three LLM models—GPT-4o, GPT-4o-mini, and o1-mini with pre-localized and non-localized prompting strategies for lab data. Across all models, using localized chunked data improves overall accuracies over an open pre-localized approach. These findings suggest that including LLMs in the document analysis process can help with water quality management where large volumes of documentation and textual data must be analyzed. Using text chunking and localized data improves the accuracy of the LLMs. We also found that localized data improves agreement across multiple iterations of analysis and increased true positive rates. Using LLMs alongside human analysts can streamline the interpretive workload and give access to previously unexamined data. LLMs techniques can support water quality managers to identify water quality concerns and direct water quality efforts, ultimately contributing to more informed and efficient water quality management practices.

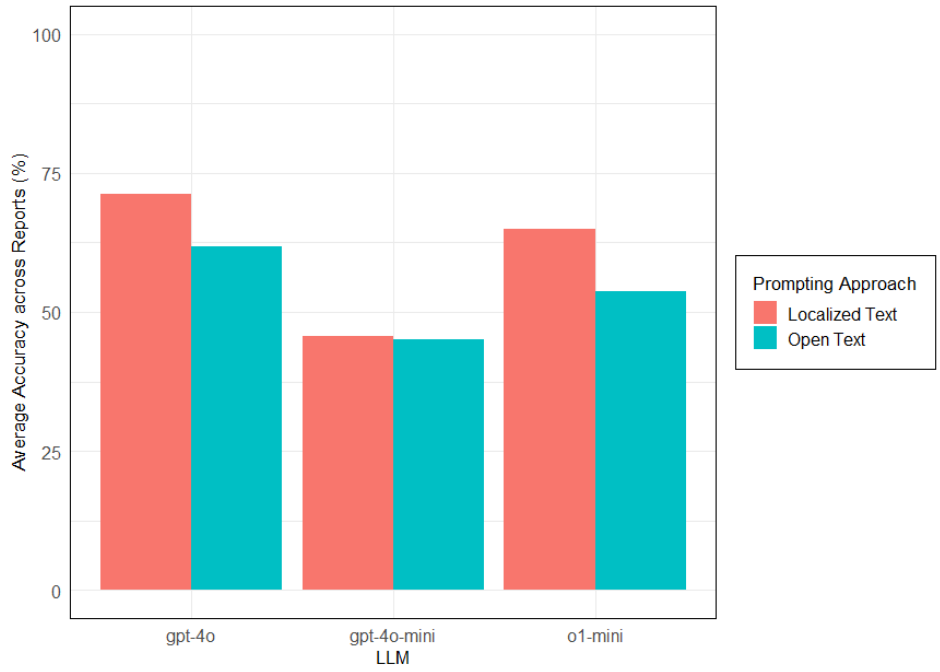


Figure 1. Comparison of Accuracy Across Models and Prompting Strategies

References

Chew, R., Bollenbacher, J., Wenger, M., Speer, J., & Kim, A. (2023). LLM-Assisted Content Analysis: Using Large Language Models to Support Deductive Coding (arXiv:2306.14924). arXiv. https://doi.org/10.48550/arXiv.2306.14924

González Canché, M.S. (2023). Latent Code Identification (LACOID): A Machine Learning-Based Integrative Framework [and Open-Source Software] to Classify Big Textual Data, Rebuild Contextualized/Unaltered Meanings, and Avoid Aggregation Bias. International Journal of Qualitative Methods

Tai, R.H., Bentley, L.R., Xia, X., Sitt, J. M., Fankhauser, S.C., Chicas-Mosier, A.M., & Monteith, B.G. (2024). An Examination of the Use of Large Language Models to Aid Analysis of Textual Data. International Journal of Qualitative Methods

Xiao, Z., Yuan, X., Liao, Q. V., Abdelghani, R., & Oudeyer, P.-Y. (2023). Supporting Qualitative Analysis with Large Language Models: Combining Codebook with GPT-3 for Deductive Coding. 28th International Conference on Intelligent User Interfaces

3D visualization of hydrodynamic models for virtual reality to predict and interpret the level of flood risk for the general public

K. Micko[1*], M. Dobransky[2]
[1] Center for research and innovation in construction, Faculty of Civil Engineering, Technical University of Kosice, Kosice, Slovakia
[2] Institute of technology, economics and management in construction, Faculty of Civil Engineering, Technical University of Kosice, Kosice, Slovakia
* e-mail: kristian.micko@tuke.sk

Introduction

Floods are one of the natural disasters that causes many damages and deaths. There are many ways to predict and minimize the effect of floods on material damage or life victims. Many countries in the world build digital twins of their cities. These digital twins can be helpful for modelling the various types of disasters, including floods, tsunamis, and earthquakes. These models can be useful for many purposes including the evacuation plan, building flood protection barriers or preparing other rescue scenarios (Francesco, Pierfranco, Costanzo, Santis 2019).

The digital twins of cities are helpful for the prediction of the economic consequences after potential climate hazards. The modelling of climate hazards can be visualized via various techniques including virtual reality (VR), augmented reality (AR) or mixed reality (MR). The visualization of climate hazards through VR can be helpful for awareness the risks of losing live or material damages to the public. The public and authorities could prepare the effective scenarios for the resources management in the crisis situation (Vandelli 2024).

Materials and methods

Hydrodynamic models are widely used for simulating flood scenario. The main goal of these models is to represent the level of risk as accurately as possible in the observed area. Many hydrodynamic models are visualised via maps, generated from software such as HEC-RAS, and could be incorrectly interpreted by people, who are not educated properly in the field of study connected to the water management (Figure 1). This study utilizes hydrodynamic modeling and 3D visualization techniques to improve flood risk interpretation for the general public. The methodology follows a structured workflow combining hydrodynamic simulation, geospatial data processing, and VR visualization. *Hydrodynamic modeling* in HEC-RAS was used to simulate flood scenarios. The process involved: (1) Data Preparation: *Collecting digital terrain model (DTM) data from geospatial sources*, (2) Model Configuration: *Defining river flow parameters, flood wave scenarios, and boundary conditions*, (3) Simulation Execution: *Running hydrodynamic simulations to predict water depth, velocity, and flood extent* and (4) Data Export: *Extracting simulation results as HDF5 files, later converted into CSV format*.

The non-scientific public could better understand the level of flood risk predicted via hydrodynamic models via spatial 3D visualisation, which is even more impressive when performed via VR technology. This study proposes to use the game *Cities: Skylines* for deployment of the behavior of potential floods predicted by hydrodynamic models. Scientists and enthusiasts developed suitable plugins, application programming interfaces (APIs) and game modes. These features are user-friendly and do not require advanced programming skills or deep knowledge of game engines (Pinos, Vozelinek, Pavlis 2020). To enhance the accessibility of flood risk data, simulation outputs were **visualized in Cities: Skylines** using a modified workflow: (1) Terrain Import: *The DTM was loaded into the game's terrain editor*, (2) Flood Simulation Overlay: *Processed CSV data containing flood extent was mapped using GeoSkylines mod* and (3) VR Integration: *Using ReShade, a stereoscopic view was created to enable immersive VR visualization via the Meta Quest 2 headset*.

The possibility of modification of the game *Cities: Skylines* is less constrained than other games in that genre. It means that a wide spectrum of mods exists solving issues addressed to the city reconstruction based on geographical data, water hydrodynamic behavior, traffic management system and others.

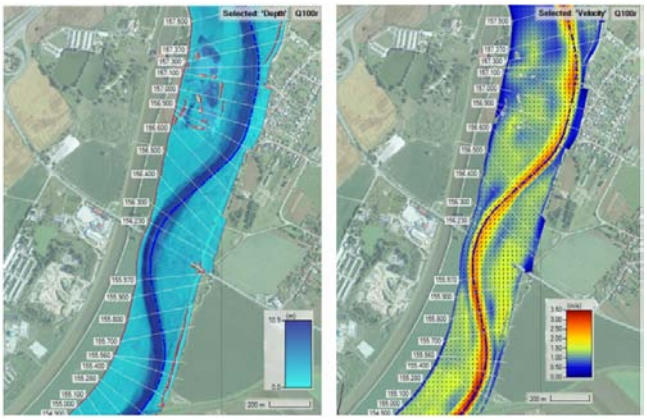


Figure 1. Standard visualisation of hydrodynamic models including the river depth and velocity.

Results and concluding remarks

The integration of hydrodynamic modeling with VR visualization has demonstrated significant potential in enhancing flood risk communication. The study converted hydrodynamic flood simulation data into 3D environment, allowing users to navigate and visually interpret flood scenarios from a 1st person perspective. Results indicate the ability to visualize water depth, velocity, and flood extent in a dynamic, immersive format enhances public awareness and preparedness. Additionally, leveraging existing gaming platforms such as Cities: Skylines provides a cost-effective and accessible way to integrate flood risk data into interactive simulations.

However, challenges remain in terms of data accuracy, real-time simulation capabilities, and user adaptability to different VR platforms. Future work should focus on refining data integration techniques, improving real-time flood modeling within VR environments, and expanding this approach to include more advanced hydrodynamic models. Additionally, testing VR-based flood risk communication in real-world public awareness campaigns could provide valuable insights into its effectiveness in disaster preparedness efforts. This study highlights the potential of game-based visualization for disaster risk management, bridging the gap between technical flood models and public understanding. By making complex hydrodynamic data more accessible, this approach contributes to more informed decision-making and improved resilience against flood events.

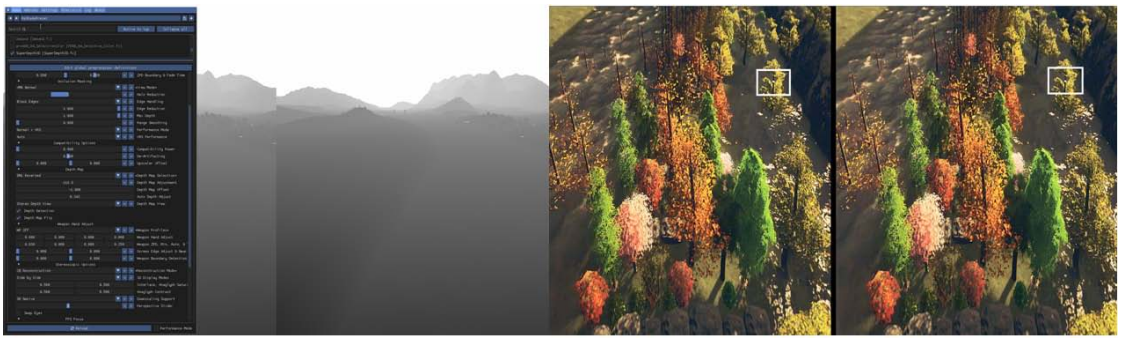


Figure 2. Making stereoscopic view Cities: Skylines to VR headset export.

Acknowledgments: This work was supported by the Slovak Research and Development Agency under the Contract no. APVV-20-0281.

References

Francesco M and et al. (2019) Moving to 3-D flood hazard maps for enhancing risk communication. Environmental modelling & software, 510-522.

Pinos J, Vozelinek V, Pavlis O (2020) Automatic geodata processing methods for real-world city visualizations in cities: Skylines. ISPRS International Journal of Geo-Information, 17.

Vandelli V and et al. (2024) Towards Enhanced Understanding and Experience of Landforms, Geohazards, and Geoheritage through Virtual Reality Technologies in Education: Lessons from the GeoVT Project. Geosciences, 127.

Preliminary results on water quality modelling and mapping in a small river using UAV multispectral imagery

K. Vatitsi[1], K. Bellos[1], D. Latinopoulos[2], C.S. Akratos[2], I. Kagalou[2], V. Tsioukas[1], G. Mallinis[1]
[1] School of Rural and Surveying Engineering, Aristotle University of Thessaloniki, 54124 Thessaloniki, Greece
[2] Laboratory of Sanitary Engineering and Water-Wastewater Quality, Civil Engineering Department, Democritus University of Thrace, 69100 Komotini, Greece
* e-mail: avatitsi@topo.auth.gr

Introduction

Evaluating water quality of inland water bodies involves assessing a range of water quality parameters reflecting the biological, chemical, thermal, and physical characteristics of water. To overcome the limitations of traditional sampling methods, Remote Sensing (RS) provides novel methodologies that facilitate effective and systematic water bodies monitoring, by correlating satellite-recorded reflectance with in-situ observations of water quality parameters. However, satellites spatial resolution is often insufficient for monitoring the entire extent of small-to-medium sized inland water bodies with optically complex waters. Unoccupied Aerial Vehicles (UAVs) provide very high-resolution data, overcoming challenges such as mixed signals presence, by adequately distinguishing land, and water spectral reflectance.

Many studies have leveraged these advantages and estimated water quality parameters of small rivers using machine learning algorithms. The genetic algorithm extreme gradient boosting was used to estimate Chl-a and turbidity among other parameters of an urban river in China (Chen et al. 2021). In order to assess mining-associated water pollution of 12 small water bodies in Spain, scholars used the spectral bands of Micasense RedEdge-MX Dual, mounted on a UAS, combined with in-situ physicochemical data to develop empirical models using regression analysis and estimate water quality parameters including pH, ORP, Al, Cu, Fe and others with high accuracy (Isgro et al. 2022). Another study (Yao et al. 2023) compared the performance of different SVR models to predict Chl-a, total phosphorus, NH3-N, and turbidity in small and micro water bodies, whereas Xiao et al. (2022), used a stacking approach to retrieve four water quality parameters of the Zhanghe River. Yan et al. (2023), built inversion models using a quadrotor to acquire UAV airborne data as well as a portable multi-parameter water quality instrument for sampling, aiming to predict dissolved oxygen and turbidity. In this study, we used multispectral images of a small river in Northeast Greece acquired from UAV combined with in-situ measurements to generate prediction models of turbidity and Chl-a employing machine learning. These data-driven insights support the adoption of informed decisions and reinforce the management and conservation of water resources.

Materials and methods

Two UAV flights equipped with the five-band sensor Micasense RedEdge-MX Dual were conducted, in July 2022 and March 2023, to obtain multispectral images of the Kosinthos river in Thrace, Northeast Greece. Simultaneously, water sampling was carried out, collecting 51 samples across the river, which were then analysed in the laboratory. The mean pixel value within a 5 × 5 pixel window at each sampling site was matched with the corresponding in situ measurement of Chl-a and turbidity respectively. The support vector regression (SVR) algorithm was then employed to analyse the data and model the two parameters, which are strongly correlated with water quality. To derive the SVR models, the algorithm was parameterized employing a grid search method to identify the most appropriate parameter by testing different C values and choosing the one with the highest cross-validation accuracy. The linear kernel, a commonly used kernel function in various studies, was implemented to fit the models. Prior to model execution, datasets were split into training and testing sets in a 7:3 ratio and all the analysis was implemented using R programming language.

Accurate prediction models were then generated, enabling the production of detailed distribution maps of turbidity and Chl-a at a centimetre-scale resolution. In order to assess the accuracy, the prediction models, three accuracy metrics, the coefficient of determination (R^2), root-mean-square error (RMSE), and mean absolute error (MAE), were applied.

Results and concluding remarks

Within the scope of the study, prediction models of two important water quality parameters were developed in order to provide information about the ecological status of a small river in Greece. According to our results (Figure1) the model for Turbidity performed well with R^2 value 0.716, RMSE value 0.677 FNU and MAE value 0.547 FNU. Regarding Chl-a the model's performance was lower achieving R^2 value 0.381, RMSE value 0.234 FNU and MAE value 0.220 FNU.

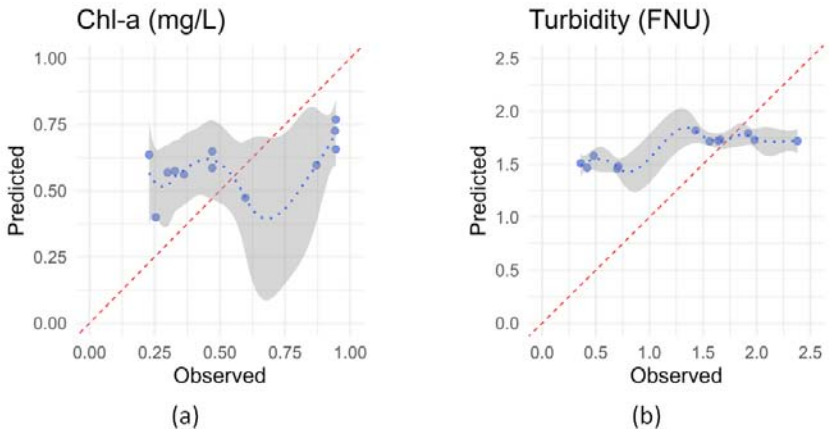


Figure 1. Scatter plots of Chl-a (a) and Turbidity (b) models.

The results demonstrated the significant potential of combining multispectral UAV imagery and machine learning to model these parameters and provide information for the ecological status of small-to-medium river surfaces. Our study contributes to the advancement of monitoring practices for inland water bodies, aligning with the guidelines of European Union environmental legislation. By delivering data-driven insights, empowers informed actions and reinforces strategies for water resource management, ecosystem conservation, and sustainability.

Acknowledgments: We acknowledge the support of this work by the project Eye4Water (MIS 5047246) implemented under the action: "Support for Research Infrastructure and Innovation".

References

Chen, B., Mu, X., Chen, P., Wang, B., Choi, J., Park, H., Xu, S., Wu, Y., & Yang, H. (2021). Machine learning-based inversion of water quality parameters in typical reach of the urban river by UAV multispectral data. Ecological Indicators, 133. https://doi.org/10.1016/j.ecolind.2021.108434

Isgró, M. A., Basallote, M. D., & Barbero, L. (2022). Unmanned Aerial System-Based Multispectral Water Quality Monitoring in the Iberian Pyrite Belt (SW Spain). Mine Water and the Environment, 41(1), 30–41. https://doi.org/10.1007/s10230-021-00837-4

Xiao, Y., Guo, Y., Yin, G., Zhang, X., Shi, Y., Hao, F., & Fu, Y. (2022). UAV Multispectral Image-Based Urban River Water Quality Monitoring Using Stacked Ensemble Machine Learning Algorithms—A Case Study of the Zhanghe River, China. Remote Sensing, 14(14). https://doi.org/10.3390/rs14143272

Yan, Y., Wang, Y., Yu, C., & Zhang, Z. (2023). Multispectral Remote Sensing for Estimating Water Quality Parameters: A Comparative Study of Inversion Methods Using Unmanned Aerial Vehicles (UAVs). Sustainability (Switzerland), 15(13). https://doi.org/10.3390/su151310298

Yao, K., Chen, Y., Li, Y., Zhang, X., Zhu, B., Gao, Z., Lin, F., & Hu, Y. (2024). Water Quality Prediction of Small-Micro Water Body Based on the Intelligent-Algorithm-Optimized Support Vector Machine Regression Method and Unmanned Aerial Vehicles Multispectral Data. Sustainability (Switzerland), 16(2). https://doi.org/10.3390/su16020559

13th World Congress on Water Resources and Environment (EWRA 2025)
"New challenges in understanding and managing water-related risks in a changing environment"
Palermo, Italy, 24 - 28 June 2025

Seamless retrieval of coastal water quality from Landsat-9 and Sentinel-2 imagery based on an AI-enhanced physical model

M. Niroumand-Jadidi[1*], L. Mentaschi[2], S. Silvestri[3]
[1] Interdepartmental Research Center for Environmental Sciences; University of Bologna, Ravenna, Italy
[2] Department of Physics and Astronomy (DIFA), University of Bologna, Bologna, Italy
[3] Department of Biological, Geological, and Environmental Sciences, University of Bologna, Bologna, Italy
* e-mail: milad.niroumand@unibo.it

Introduction

Timely and accurate information about coastal water quality parameters is crucial for monitoring and preserving aquatic ecosystems, ensuring public health, and supporting sustainable coastal development. In this context, remote sensing is a viable means of capturing the spatiotemporal dynamics of water quality parameters such as chlorophyll-a (Chl-a) and total suspended matter (TSM). Despite the availability of various methods for retrieving water quality indicators from optical imagery, achieving a consistent parameter retrieval remains challenging, especially when dealing with multitemporal imagery from different satellite sensors (Arabi et al. 2020). Temporal variabilities from atmospheric effects and sun glint introduce complexities to water quality inversion models. Additionally, differences in spatial, radiometric, and spectral resolutions in multi-sensor analyses add further complexity, potentially hindering the production of consistent and seamless multi-sensor temporal water quality products. Thus, there is a need to further develop and examine models that can be adapted to diverse bio-optical conditions in coastal waters to produce seamless multi-sensor water quality products. This study focuses on consistent water quality retrieval using Landsat-8/9 and Sentinel-2, the primary multispectral satellites providing publicly available imagery with adequate spatial resolution (10–30 m) for coastal studies. These satellites provide different characteristics in terms of spectral and radiometric resolutions that underlines the importance of developing robust methods for seamless retrieval of water quality products (Niroumand-Jadidi et al. 2022).

Physics-based models, which rely on the inversion of radiative transfer models, are sensor-independent and can be adapted to diverse in-water conditions (Giardino et al. 2012, Gege 2014). However, these models often suffer from spectral ambiguity, particularly in optically complex waters (Defoin-Platel and Chami 2007). Additionally, the inversion process is extremely time-consuming, making them less favorable for multi-temporal image analyses. In this study, we explore a new model called WASI-AI (Niroumand-Jadidi and Gege 2025), which integrates artificial intelligence (AI) into the physical inversion process to address the identified issues. We adapt the WASI-AI processing for multitemporal retrieval of TSM and Chl-a concentrations in the optically-complex coastal waters of the Adriatic Sea, using pairs of near-simultaneous Landsat-9 and Sentinel-2 imagery. The analysis provides insight into the effectiveness of this AI-empowered physical inversion model in achieving consistent constituent retrievals using multi-source imagery.

Materials and methods

We build upon WASI-AI model to seamlessly retrieve TSM and Chl-a concentrations from Landsat-9 and Sentinel-2 imagery in coastal waters. WASI-AI (Niroumand-Jadidi and Gege 2025) integrates AI into the physics-based WASI-2D (Gege 2014) model. The integrated approach initially utilizes radiative transfer models of WASI-2D to estimate the water quality parameters for a randomly selected small subset of image pixels. These inverted samples are then divided into training and validation sets. The training samples are employed to train the AI component, which is based on neural networks (NNs). Subsequently, the trained NNs predict the TSM and Chl-a concentration for all water pixels, including the validation set. The agreement between WASI-AI and WASI-2D model retrievals is then quantified using the coefficient of determination (R^2) and root mean square difference (RMSD) using the validation samples. This agreement analysis provides feedback to the physical modeling (i.e., WASI-2D) given that a weak agreement highlights

spectral ambiguity in radiative transfer inverse modeling, suggesting the need for parameter adjustment. Unlike existing machine learning-based approaches, the new WASI-AI model retains all the flexibility of physics-based modeling, allowing it to adapt to various bio-optical conditions and to process any multispectral and hyperspectral data. Meanwhile, the AI integration addresses ambiguity issues and significantly speeds up the inversion process. WASI-AI model also considers a parameter for mitigating the sun glint effects through the inversion process which is of particular importance in multitemporal image analysis.

This study explores the effectiveness of the WASI-AI model in retrieving seamless water quality products from Landsat-9 and Sentinel-2 imagery. The orbital design of Landsat-9 and Sentinel-2 typically permits one or two near-simultaneous acquisitions per month, with only a few minutes time gap between them. We selected a series of near-simultaneous images from these satellites, captured over the west coasts of the Adriatic Sea, to investigate the multi-sensor consistency of the TSM and Chl-a products derived using WASI-AI. The images from both satellites are initially processed using ACOLITE atmospheric correction (Vanhellemont 2019) and subsequently analyzed with WASI-AI under a similar parametrization.

Results and concluding remarks

The results demonstrate a high consistency between the water quality parameters derived from Landsat-9 and Sentinel-2. The TSM and Chl-a retrievals show a strong correlation between these two satellites, with $R^2 > 0.92$ and a normalized RMSD of less than 4%. This highlights the effectiveness of the WASI-AI model in retrieving seamless water quality products for multisensory analysis. The promising results can be attributed to the model's efficiency in adapting to site-specific bio-optical conditions, resolving spectral ambiguity issues, and handling sun glint artifacts. In our study site in the Adriatic coastal waters, the WASI-AI model effectively captured a wide range of water quality conditions, such as TSM concentrations of up to 40 g/m³. While Landsat-9 and Sentinel-2 provided consistent water quality products, the Landsat-9-based maps of TSM and Chl-a exhibited less noise than those of Sentinel-2. This reduced noise can be attributed to the higher signal-to-noise ratio resulting from the enhanced radiometric resolution of Landsat-9 (14-bit) compared to Sentinel-2 (12-bit). In summary, the seamless retrieval of water quality parameters from Landsat-9 and Sentinel-2 satellites using the new WASI-AI model can enhance our understanding of the temporal dynamics of in-water constituents. This approach provides a higher temporal resolution compared to relying on a single satellite.

Acknowledgments: Adriatic coastal areas science-based solutions for climate adaptation (AdriaClimPlus-ITHR0200333) funded by the Interreg Italy-Croatia cooperation program.

References

Arabi B, Salama M.S, Pitarch J, Verhoef W (2020) Integration of in-situ and multi-sensor satellite observations for long-term water quality monitoring in coastal areas. Remote Sensing of Environment. 239, 111632. https://doi.org/10.1016/j.rse.2020.111632

Defoin-Platel M, Chami M (2007) How ambiguous is the inverse problem of ocean color in coastal waters? Journal of Geophysical Research, 112(C3), C03004. https://doi.org/10.1029/2006JC003847

Gege P (2014) WASI-2D: A software tool for regionally optimized analysis of imaging spectrometer data from deep and shallow waters. Computers & Geosciences, 62, 208–215. https://doi.org/10.1016/J.CAGEO.2013.07.022

Giardino C, Candian G, Bresciani M, Lee Z, Gagliano S, Pepe M (2012) BOMBER: A tool for estimating water quality and bottom properties from remote sensing images. Computers and Geosciences, 45, 313–318. https://doi.org/10.1016/j.cageo.2011.11.022

Niroumand-Jadidi M, Bovolo F, Bresciani M, Gege P, Giardino C (2022). Water Quality Retrieval from Landsat-9 (OLI-2) Imagery and Comparison to Sentinel-2. Remote Sensing, 14(18). https://doi.org/10.3390/rs14184596

Niroumand-Jadidi M, Gege, P (2025) WASI-AI: Synergistic Integration of AI and Physics for Retrieving Water Quality and Benthic Parameters from Multi- and Hyperspectral Images, IEEE Journal of Selected Topics in Applied Earth Observations and Remote Sensing (Under Review)

Vanhellemont Q (2019) Adaptation of the dark spectrum fitting atmospheric correction for aquatic applications of the Landsat and Sentinel-2 archives. Remote Sensing of Environment, 225, 175–192. https://doi.org/10.1016/j.rse.2019.03.010

Neural networks for hydrological modelling in Santa Lucía basin, Uruguay

F. Vilaseca[1*], A. Castro[2,3], C. Chreties[1], A. Gorgoglione[1]
[1] Institute of Fluid Mechanics and Environmental Engineering, Faculty of Engineering, University of the Republic, Uruguay
[2] Institute of Computer Science, Faculty of Engineering, University of the Republic, Uruguay
[3] Institute of Electrical Engineering, Faculty of Engineering, University of the Republic, Uruguay
* e-mail: fvilaseca@fing.edu.uy

Introduction

The objective of this work is to evaluate the potential of machine learning based hydrological modelling tools for Santa Lucía watershed, located in south central Uruguay. It is a basin facing intense pressure on its water resources due to the high demand posed by irrigation and drinking water supply. These challenges are amplified by the uncertainty surrounding the actual context due to climate change, thus the importance of generating innovative and robust management tools to face them. Recent years have seen an outstanding increase in the application of machine learning tools to a variety of data related problems, such as hydrological modelling. A common example is the use of machine learning regressors to reproduce river discharge time series from atmospheric (such as rainfall, air temperature, air humidity, etc.) or spatial (land uses, soil moisture distribution, etc.) variables. Neural networks are frequently used for this purpose, due to their usually high performance. In the present study, Artificial Neural Networks (ANNs) and Recurrent Neural Networks (RNNs) are chosen to implement hydrological models with daily step, to simulate the discharge time series at 4 sub-watersheds of the Santa Lucía basin. Results are promising in terms of performance, particularly for RNN based models, which outperform ANNs and several other modelling tools which were utilized for the same watershed in the past.

Materials and methods

Base information was gathered to build the hydrological models. It includes daily time series of accumulated rainfall (P), mean air temperature (T) and mean discharge (Q). Rainfall records were retrieved from 22 rain gauges with influence over the watershed, air temperature from a single meteorological station located in its proximity, and discharges from rating-curve-based measurement stations situated at the closure point of each sub-watershed. All of them cover the period 1981-2023. Original data was processed to generate adequate model inputs. For each sub-watershed, a mean areal precipitation (MAP) time series was generated from the P data recorded at near stations. Also, a series of 7-day-accumulated MAP (MAP_{accum}) was created as a soil moisture proxy to aid model training. Series of 1- and 2-days antecedent discharge (Q_{t-1} and Q_{t-2}) were also built to use as inputs. The selection of these input variables was informed by our previous work (Vilaseca et al., 2023a).

As mentioned in the introduction, the models were built using two different kinds of neural networks: ANNs, which are the most basic configuration, and RNNs whose internal structure provides them with an artificial memory or notion of the past and are widely applied to time series prediction problems. Models were trained using two different sets of input variables: Dataset A consisting of MAP, MAP_{accum}, T, Q_{t-1} and Q_{t-2}, and Dataset B which is the same but excluding the antecedent discharges. Hyperparameters of the algorithms were optimized using the Optuna framework (Akiba et al., 2019), with a training/validation scheme for which the data was divided into 3 subsets: training (70% of the data), validation (15%) and testing (15%). The objective function was the Nash-Sutcliffe Efficiency, and models were evaluated statistically (using percent bias, PBIAS; and the ratio of root mean squared error to standard deviation of the observations, RSR) and graphically (comparative time series, scatter plots and duration curves).

Results and concluding remarks

Table 1 displays the statistical results for all the sub-watersheds, models, and datasets. Graphical results are shown for the sub-watershed with closure point in Florida, using RNNs and Dataset A, as an example (Figure 1).

Table 1. Statistical results for all sub-watersheds, algorithms and datasets.

	ANN						RNN					
	Dataset A			Dataset B			Dataset A			Dataset B		
	NSE	PBIAS	RSR	NSE	PBIAS	RSR	NSE	PBIAS	RSR	NSE	PBIAS	RSR
Florida	0.46	13.7	0.73	0.37	-4.3	0.73	0.69	10.3	0.55	0.75	13.6	0.50
Fray Marcos	0.62	10.4	0.62	0.37	-7.1	0.75	0.77	-0.1	0.48	0.74	10.5	0.51
Picada de Varela	0.88	0.4	0.35	0.54	-25.2	0.76	0.76	-0.3	0.49	0.73	10.4	0.52
Paso Pache	0.87	1.4	0.35	0.54	16.3	0.66	0.84	8.5	0.40	0.82	4.9	0.42

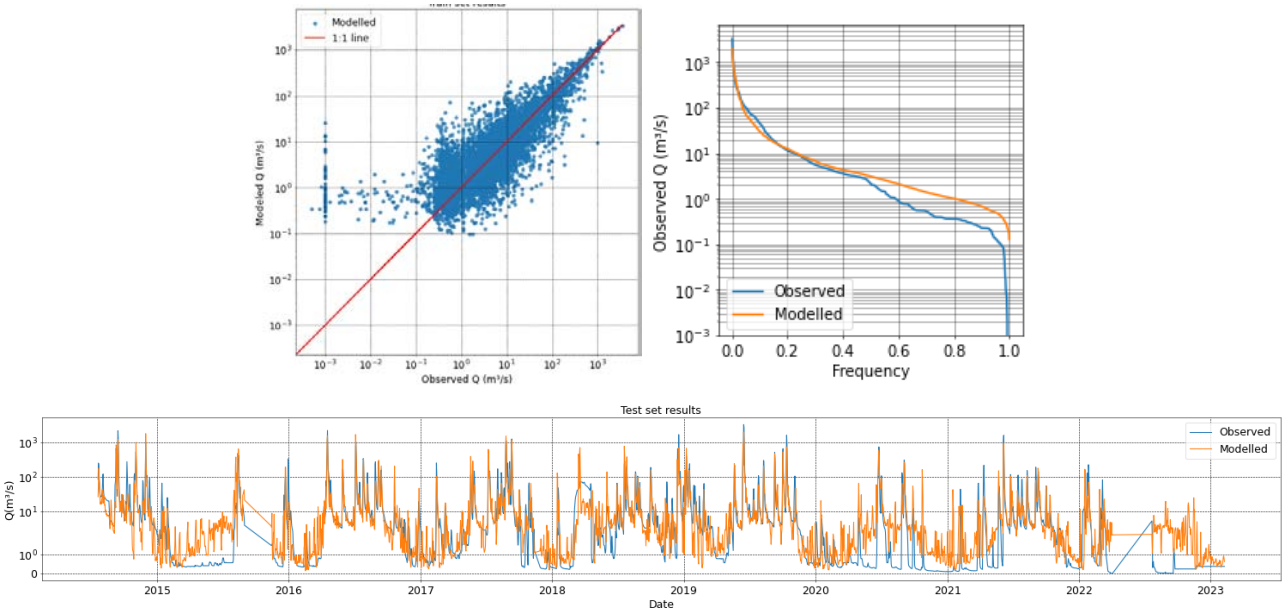


Figure 1. Graphical results for sub-watershed with closure point in Florida, using RNN with Dataset A.

The first thing noticed when looking at the results is that RNN models outperformed those built with ANNs. This is clear in statistical comparisons. Besides that, ANN models show more sensitivity to the input data than RNN models, with a significant descent in performance when using Dataset A as input compared to Dataset B. Applying the standard criterion of Moriasi et al. (2007), all the RNN models can be considered at least satisfactory, while ANN models achieve such ranking only for three watersheds using Dataset A as input, and a single one using Dataset B. The work allowed to conclude that RNNs are promising tools to build robust and accurate hydrological models for Santa Lucía Watershed. They clearly outperform ANNs for this case, requiring less amounts input data (Dataset B) to yield satisfactory results. Compared to other previous studies in the watershed, it is also noted that results with RNNs are also better in general terms than more simple algorithms such as Random Forests or physically based models such as SWAT or GR4J (Vilaseca et al., 2023b).

References

Akiba T, Sano S, Toshihiko Y, Ohta T, Koyama M (2019) Optuna: a next generation hyperparameter optimization framework. In: Proceedings of the 25th ACM SIGKDD international conference on knowledge discovery & data mining, Anchorage, AK, 2623–2631.

Moriasi DN, Arnold JG, Van Liew MW, Bingner RL, Harmel RD, Veith TL (2007) Model evaluation guidelines for systematic quantifica tion of accuracy in watershed simulations. Transactions of the ASABE, 50, 885–900.

Vilaseca F, Castro A, Chreties C, Gorgoglione A (2023a) Assessing influential rainfall–runoff variables to simulate daily streamflow using random forest. Hydrological Sciences Journal, 68(12), 1738–1753.

Vilaseca F, Narbondo S, Chreties C, Castro A, Gorgoglione A (2023b) Simulación del proceso precipitación-escorrentía con paso diario: comparación de los modelos GR4j, SWAT y Random Forests. Ribagua, 10(1), 31–47.

A comprehensive comparative study on potential evapotranspiration in mainland Portugal based on reanalysis data

J.P. Pegas[1*], M.M. Portela[1,2], J.F. Santos[3]
[1] Instituto Superior Técnico, Universidade de Lisboa
[2] CERIS – Civil Engineering Research and Innovation for Sustainability Research
[3] Polytechnic Institute of Beja, CREATE – Center for SciTech Research in Earth System and Energy
*e-mail: joao.pegas @tecnico.ulisboa.pt

Introduction

The study presents a comprehensive comparative analysis of the spatial patterns and magnitudes of potential evapotranspiration (PET) in mainland Portugal. PET data from the GLEAM and ERA5-Land reanalysis databases were analysed alongside PET estimates derived from the Thornthwaite (Thornthwaite, 1948) and the Hargreaves-Samani (Hargreaves, Samani, 1985) empirical models. The input variables for these models were obtained from ERA5-Land database. The period considered in the study spanned from January 1, 1980, to December 31, 2023. Since the reanalysis data and PET empirical estimates have different time scales – daily for the reanalysis data and the Hargreaves-Samani model and monthly for the Thornthwaite model – not all comparisons are feasible. At this stage, only maps of PET long-term annual averages are presented.

PET GLEAM and PET ERA5-Land comparison

The PET maps were generated using 938 points for GLEAM data and 902 points for ERA5-Land data. The difference in the number of grid points is due to the misalignment of the grids in the two datasets. To ensure compatibility, the ERA5-Land data grid was shifted 0.5° north and west. Both maps are shown in Figure 1.

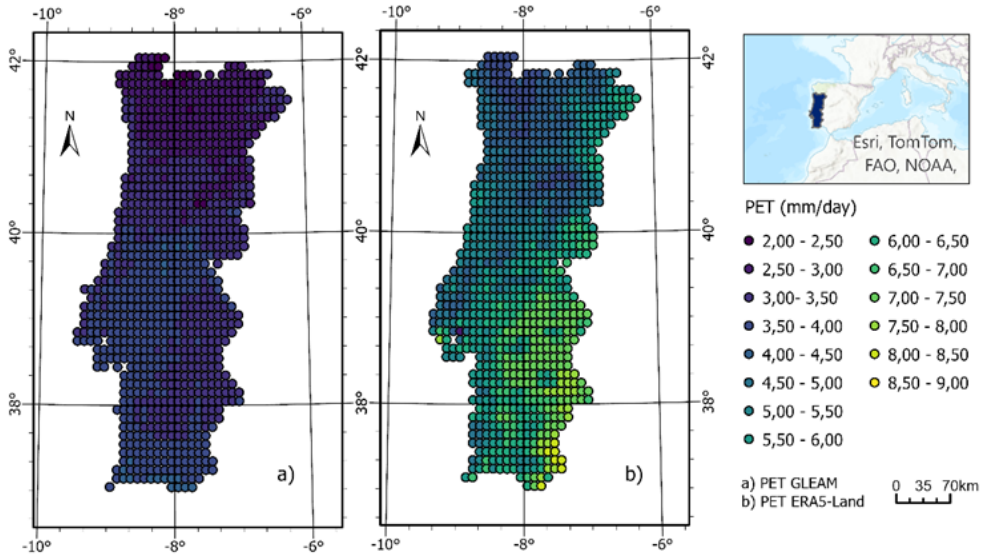


Figure 1. Mean annual daily PET from GLEAM (on the left) and ERA5-Land (on the right) databases.

The Figure 1 suggest that the PET GLEAM database is unsuitable for mainland Portugal. In fact, its spatial variability does not align with the established theoretical knowledge as, for example, it suggests that the hotter, inland southern regions of the country exhibit significantly lower PET than the cooler coastal areas which contradicts the current scientific knowledge. The figure also shows that PET ERA5-Land significantly overestimates PET GLEAM data.

PET Thornthwaite and Hargreaves-Samani models' comparison

The PET empirical models used so far were the Thornthwaite and the Hargreaves-Samani models, given by equations (1) and (2), respectively, applied to temperature data from the ERA5-Land dataset:

$$PET = 1.6\left(10\frac{t_j}{I}\right)^a \quad (1)$$

$$PET = 0.0023\ Ra\ (T + 17{,}8)\ \sqrt{\Delta T} \quad (2)$$

In equation (1), PET represents the evapotranspiration for 30-day month (cm), each day with 12 hours of astronomical insolation, t_j is the monthly mean air temperature (°C), I is the annual thermal index, and α is an empirical exponent. The equation's results need to be correct to account for the actual number of days of each month and for the astronomical insolation as a function of the geographic location. In equation (2), PET is the daily evapotranspiration (mm), Ra is the solar radiation at the top of the atmosphere (mm/day), T is the daily mean temperature, and ΔT is the difference between daily maximum temperatures and T (°C). To enable comparison, PET estimates from Hargreaves-Samani model were accumulated into monthly values – Figure 2. As shown in the figure, both maps exhibit similar and theoretically consistent spatial patterns. However, the Thornthwaite estimates are smoother and lower.

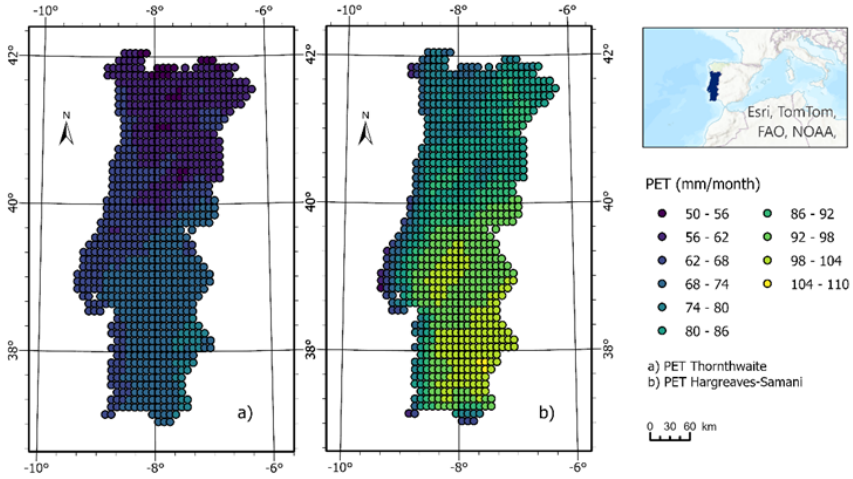


Figure 2. Mean annual monthly PET estimates based on Thornthwaite (on the left) and Hargreaves-Samani (on the right) models.

Concluding remarks

To assess the accuracy of PET values, whether directly extracted from reanalysis datasets or computed using empirical formulas applied to ERA5-Land temperatures, a comparison was made with reference evapotranspiration values from the Penman-Monteith model applied to ground-based data at 20 Portuguese meteorological stations. The comparison confirmed that the PET ERA5-Land significantly overestimates the reference values, whereas the PET GLEAM and the estimates from the applied models with emphasis on the Hargreaves Samani, align closely with them. Further studies are being conducted aiming at an extensive application of other PET empirical formulas to reanalysis data, also with the goal of further evaluating the accuracy of the PET spatial patterns so far obtained.

Acknowledgments: This research was supported by FCT (UIDB/04625/2020) through CERIS and by the EU Horizon 2020 programme SCORE (Grant No. 101003534).

References

Hargreaves, G. H., & Samani, Z. A. (1985) Reference Crop Evapotranspiration from Temperature. Applied Engineering in Agriculture, 1(2), 96-99. https://doi.org/10.13031/2013.26773

Thornthwaite, C. W. (1948) An Approach toward a Rational Classification of Climate. Geographical Review, 38(1), 55-94. https://doi.org/10.2307/210739

13th World Congress on Water Resources and Environment (EWRA 2025)
"New challenges in understanding and managing water-related risks in a changing environment"
Palermo, Italy, 24 - 28 June 2025

Effects of urban green areas on heat islands with large impact on urban water demand

M.B. Akduman[1], A. Gül[2*]
[1] Graduate School of Natural and Applied Sciences, Dokuz Eylül University, Izmir, Turkey
[2] Department of Civil Engineering, Faculty of Engineering, Dokuz Eylul Unıversity, Izmir, Turkey
* e-mail: ali.gul@deu.edu.tr

Introduction

Today, urban areas are intensely experiencing the impacts of climate change, especially with increasing water demand due to water scarcity and high temperatures that put urban water security at risk. Urban heat islands, which can be conceptually explained as an urban area with a high population and built-up areas having higher land surface temperatures than the surrounding or nearby rural areas, increase energy costs in cities (especially due to indoor air conditioning needs), increase air pollution levels, threaten water security due to increases in both utility water and energy needs, and increase heat-related illness and mortality rates. One of the main factors for urban areas to provide a healthy and sustainable environment by mitigating urban heat island effects is urban green spaces. The functions of green areas in cities are vital for maintaining ecological balance for urban areas and their inhabitants. On a case-study selected from the western transect of Turkey struggling with severe impacts of climate change in the Mediterranean basin, the presented study reveals the potential impact of urban green areas on heat islands phenomenon through geospatial analyses of land surface temperatures (LSTs) compared between green and non-green surfaces and for different years in time.

Materials and methods

The presented study primarily considered the distinction of urban morphological zones in order to evaluate the scope of direct impact on heat island formation as a study base, unlike the administrative definition of urban areas. The CORINE Land Cover (CLC) dataset, first produced in 1990 and updated in the years 2000, 2006, 2012, and 2018 was utilized in the UMZ extraction process for the relevant years. CLC offers a comprehensive land cover inventory that categorizes 44 thematic classes, encompassing a diverse range from vast forested areas to individual vineyard plots.

Green areas within the determined urban morphological areas were obtained from satellite images with a method based on spatial analysis. The Landsat 5 data acquired for the years 1999, 2000, 2005, 2006, 2011, and 2012 from USGS public repositories were utilized to delineate green areas across the case-study and extract instantaneous LSTs recorded on the selected dates that represent different indicator periods. Further research in the study involved a series of spatial analyses conducted in successive stages. Different vegetation densities of UMZ analysis grids (i.e. mesh structure with 900x900 cell areas each) were used to investigate the impacts of urban green areas on LSTs (Figure 1). Considering the percentage of green areas within the cells that belong to the UMZs extent, six distinctive classes were identified from the UMZ cells with i. more than 50%, ii. between 10% and 50% , iii. between 5% and 10%, iv. between 2% and 5%, v. between 1% and 2% green space in the cell area, against vi. almost non-green grid cells with less than 1% or no green coverage. LST values were then obtained by systematically converting the digital numbers (DN) representing the resampled thermal image data of the Landsat's thermal band 6. To achieve this conversion, a specific set of formulas were applied to allow for the transformation of the DN values into satellite spectral radiance, denoted as L_λ (Kimothi, et al., 2023). Three classes were defined where LST is the average surface temperature value of the UMZ grid cells that have almost no green coverage (1% or less), LST1 to represent the averages computed from the temperature records coinciding with the green spaces inside the cells involving green area at remarkable rates and LST2 for describing the average temperatures within the same cells with green areas, but this time only considering the non-green portions of the cells.

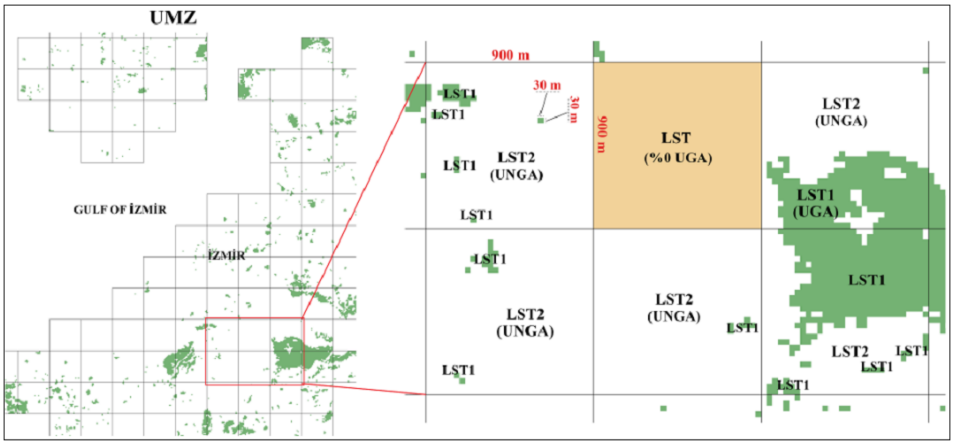


Figure 1. Grid cell analysis units for computing LSTs in the study area.

Results and concluding remarks

The overall findings of the study can help understand the roles and importance of green spaces spatially and seasonally in the urban context. The results show that green coverage significantly influences the change in LST-AT difference. However, a more significant result was seen between the seasons. In summer, the green spaces reveal mitigating impacts on the heat islands as the green ratio increases while conversely in the winter, they have a slightly warming impact of the land surface subject to lower winter air temperatures, providing some insulation and contributing to a slightly warmer urban microclimate (Ge et al. 2024). These positive impacts for the green spaces are also visible from the stand-alone comparison of the LSTs for winter and summer months based on varying rates of green urban coverages (Figure 2).

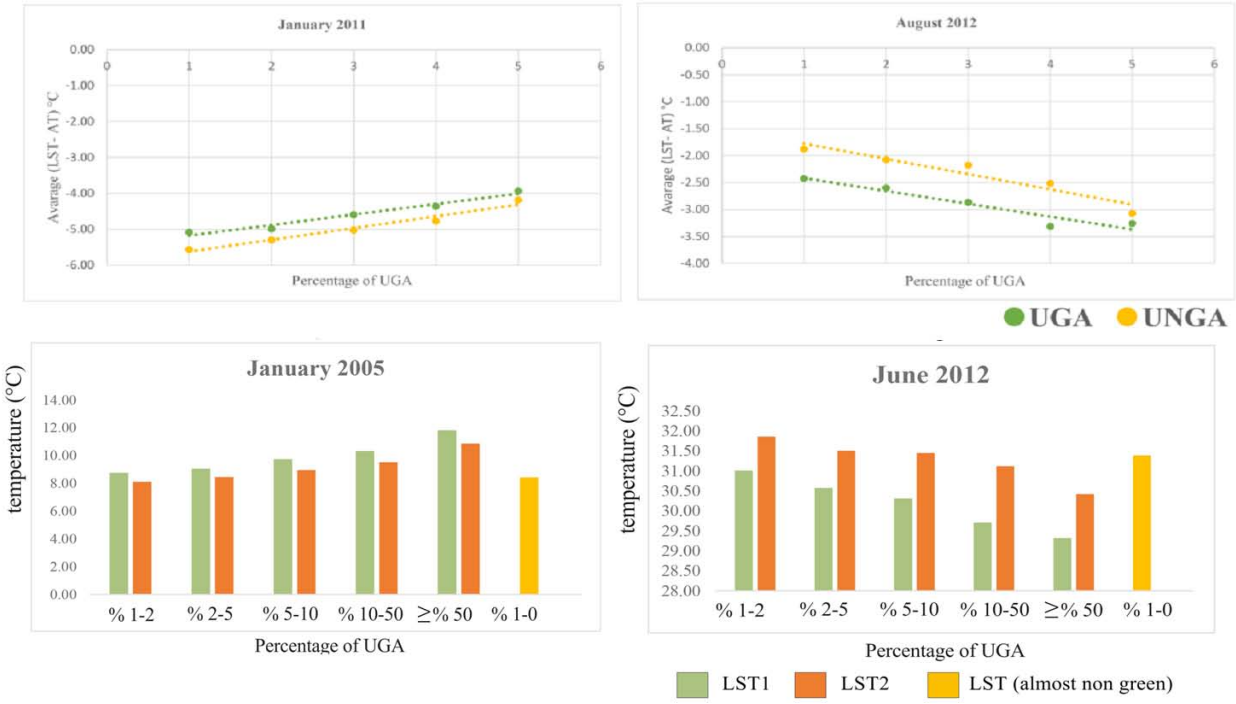


Figure 2. Land surface temperature and air temperature differences for winter and summer months and change of the land surface temperature in winter and summer with respect to green area ratios.

References

Ge J, Wang Y, Zhou D, Gu Z, Meng X (2024) Effects of urban vegetation on microclimate and building energy demand in winter: An evaluation using coupled simulations. Sustainable Cities and Society, 102.

Kimothi S, Thapliyal A, Gehlot A, Aledaily AN, Bilandi N, Singh R, et al. (2023) Spatio-temporal fluctuations analysis of land surface temperature (LST) using Remote Sensing data (LANDSAT TM5/8) and multifractal technique to characterize the urban heat Islands (UHIs). Sustainable Energy Technologies and Assessments 55.

An innovative initiative in water education based on digitalization through extended reality learning environments: WATERLINE

G. Onuşluel Gül[1*], O.C. Doğanlar[2], A. Gül[1], E. Zammit[3], A. Rizzo[3], D. Scerri[3], M. Šťastná[4], D. Prochazka[4], P. Oppeltová[4], M. Ćirić[5], V. Milošević[5], M. Gocić[5], A. Chen[6], M.B. Johns[6], J.H. Körber[7], W. Ravyse[8]
[1] *Department of Civil Engineering, Faculty of Engineering, Dokuz Eylül University, Izmir, Turkey*
[2] *Department of Computer Engineering, Faculty of Engineering, Dokuz Eylül University, Izmir, Turkey*
[3] *Malta College of Arts Science and Technology, Paola, Malta*
[4] *Department of Applied and Landscape Ecology, Faculty of AgriSciences, Mendel University in Brno, Brno, Czechia*
[5] *Faculty of Civil Engineering and Architecture, University of Niš, Niš, Serbia*
[6] *Centre for Water Systems, University of Exeter, Exeter, United Kingdom*
[7] *Faculty of Engineering & Business, Turku University of Applied Sciences, Turku, Finland*
[8] *Futuristic Interactive Technologies research group, Turku University of Applied Sciences, Turku, Finland*
** e-mail: gulay.onusluel@deu.edu.tr*

Introduction

In the field of water resources, which require more effective and capacity-based management as a result of climate and anthropogenic pressures, there is a need for well-trained personnel who can diagnose problems and develop engineering solutions and applications in issues such as the protection of resources, design and operation of water transmission systems, support for technology-based applications like precision agriculture practices, and sustainability of environmental ecosystems. Despite their historically well-established and classical experience-based educational structures, today's higher education institutions, especially those involved in water management studies as a field that requires practical experience through physical learner participation, are negatively affected by periodic interruptions in education (due to natural disasters, epidemics, etc.) in providing learning outcomes to their entirety.

The concerns for higher education institutions which could not keep up with the digital and technological advancements force them to steer away from linear concepts of innovation to more collaborative and co-creative approaches with other external actors, fostering a crucial role for these education institutions within their innovation ecosystems (Reichert 2019). From this point on, the EU HE program project WATERLINE brought to the forefront the objectives of *i.* supporting the consolidation of a digital water higher education alliance while raising the excellence profile of the education partners from the Widening countries, *ii.* building capacity for academics/researchers on digital water education and support topics for academic career development, *iii.* co-creating a portfolio of digital water components for curriculum, and *iv.* sustaining the alliance of extended-reality water emulative centres.

Materials and methods

The project has implemented applications toward digital transformation in water education by supporting the existing emulation infrastructures with assisted reality technologies and/or creating virtual reality learning environments through digital twin development. In the water rig experiment (Fig. 1a), the learning outcomes of understanding a water distribution system, conducting specific network configuration exercises, utilizing monitoring equipment such as flow meters, pressure sensors, and water quality analysers are targeted, while in the pipe losses VR mainly pipe hydraulics principles, major/minor energy losses in pipes and pipe fittings are taught (Fig. 1b).

In the stream course design experiment, the learner abilities for designing watercourse cross-section based on various hydrologic/hydraulic criteria, selecting appropriate cross-sectional parameters and assessing channel surface roughness for different lining materials are targeted. Governing principles of dam failure phenomenon and flood inundation aspects are provided again through VR simulations (Figs. 1c,d).

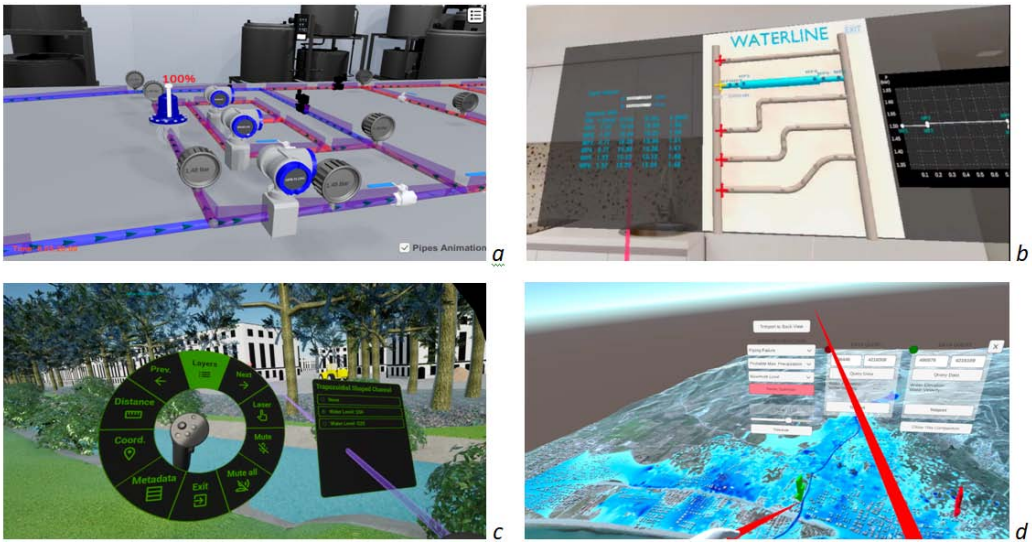


Figure 1. (a) Water distribution rig experiment, (b) pipe losses experiment, (c) stream cross-sectional design experiment and (d) embankment dam break simulation in VR learning environments.

Results and concluding remarks

From across Europe, a total of 142 students from 8 higher education institutions, 33 researchers, and 42 community of practice professionals participated in a series of pilot evaluation studies. User experience and perceived learning data were gathered through the User Experience Questionnaire (UEQ) (Schrepp et al. 2014) and Cognitive Affective Psychomotor (CAP) perceived learning questionnaire (Rovai et al. 2009). The CAP data was collected before (i.e., when students had already attended theoretical coursework) and after experiencing the applications, while the UEQ data was collected immediately after working with the applications. The consolidated UEQ results (Fig. 2a) showed a positive user experience for all applications. Further analysis showed no significant differences between the individual UEQ results of the applications. The CAP perceived learning scores across all applications for all student participants (Fig. 2b) showed an average significant increase from 29.76 to 38.11 after the application.

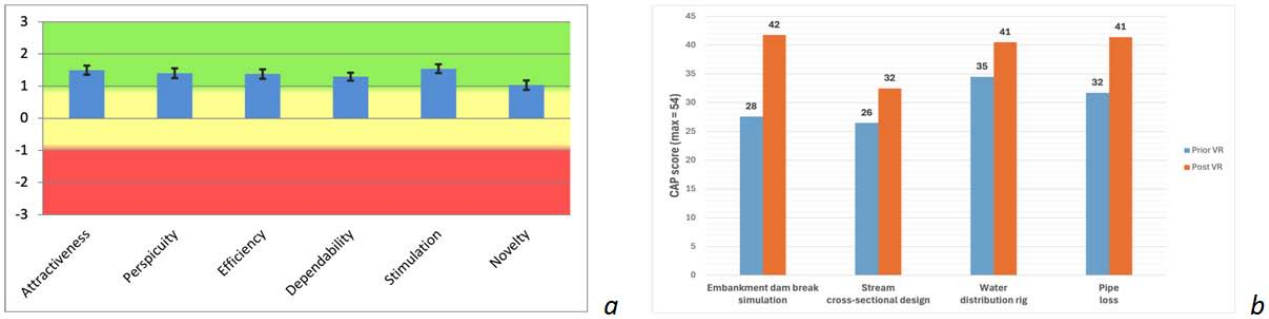


Figure 2. (a) Consolidated UEQ results and (b) CAP results before and after VR experience for each application.

Acknowledgments: This study is presented with the support of the WATERLINE project funded by the EU HE call HORIZON-WIDERA-2021-ACCESS-05 under grant agreement 101071306.

References

Reichert S (2019) The Role of Universities in Regional Innovation Ecosystems. EUA Study, Brussels

Rovai AP, Wighting MJ, Baker JD, Grooms LD (2009) Development of an instrument to measure perceived cognitive, affective, and psychomotor learning in traditional and virtual classroom higher education settings. The Internet and higher education, 12(1): 7-13.

Schrepp M, Hinderks A, Thomaschewski J (2014) Applying the user experience questionnaire (UEQ) in different evaluation scenarios. In: Marcus A (ed) Design, User Experience, and Usability, Springer, NY, pp 383-392

Enhancing the performance of a flood early warning system with the incorporation of SMOS satellite-soil-moisture data

S. Narbondo*, C. Chreties
Instituto de Mecánica de los Fluidos e Ingeniería Ambiental, Facultad de Ingeniería, Universidad de la República, Montevideo, Uruguay
** e-mail: snarbondo@fing.edu.uy*

Introduction

River floods represent one of the most frequent natural emergencies with greatest impact in the world (WMO,2011). The diagnostic studies and evaluation of solutions carried out coincide in general terms, giving priority to non-structural measures over structural ones, such as Flood Early Warning Systems (FEWS) and the implementation of land-use planning policies (WMO, 2011) For FEWS, hydrological and hydrodynamic modelling are key elements, and a good determination of soil moisture (SM) is fundamental for a good representation of the events. In this aspect, satellite SM assimilation into rainfall-runoff models is considered a way to improve their performance.

Satellite SM from products of Soil Moisture and Ocean Salinity (SMOS) mission have a good performance been incorporated in rainfall-runoff models (Lievens et al. 2015, Patil and Ramsankaran 2018), and in Uruguay some work realizes the same with other satellites products and models (Narbondo et al. 2021, Hastings et al. 2024). In this context, the aim of this work is to assess whether the incorporation of SMOS SM observations can enhance the water level simulation of the operational FEWS at Artigas city, Uruguay.

Materials and methods

The study area is the Cuareim Basin (Figure 1), which is a binational basin located in part of the Artigas department in Uruguay and the state of Rio Grande do Sul in Basil. The basin has an extent of 4400 km^2 and an average slope of 4.4%. The average available water is 37 mm, and the concentration time is 50 hours. The primary land use of the catchment is natural pasture (grassland) used for extensive livestock and agricultural land uses also cover a surface of the watershed.

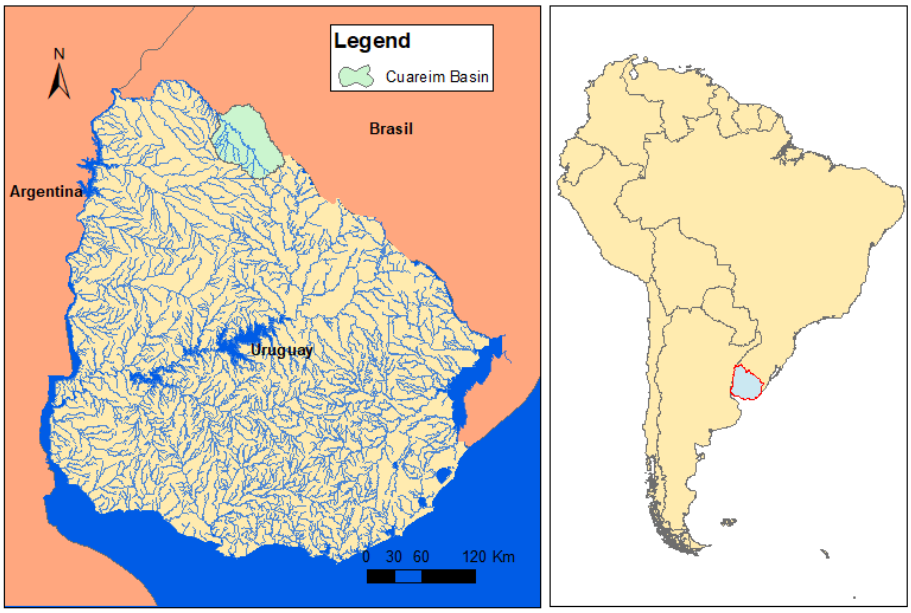


Figure 1. Cuareim basin location.

This work uses the same methodology than Narbondo et al. 2021. That work proposes two blocks, on one, the original FEWS modelling is carried out, the adopted model consisted in divide the basin in subbasin, and coupling the Curve Number (CN) hydrologic model (USDA, 2010) to the hydrodynamic model implemented in HEC-RAS (US Army Corps of Engineers, 2011). And in the other incorporate the satellite SM in the hydrological models, for this work GR4J (Perrin et al. 2003) model is incorporated. Then both approaches are compared. For the incorporation of SM in the CN model the is use the same methodology than Narbondo et al. 2021 and for GR4J use Soil Water Index (SWI) (Wagner et al. 1999, Albergel et al. 2008). For the comparison 8 floods events are examinate and root mean square error (RMSE), the coefficient of determination (R^2), and the absolute difference between observed and simulated values (AbsDif) were adopted for the comparison.

Results and concluding remarks

The results of the 8 events recorded between the years 2010 and 2017, where alert levels were reached in the city of Artigas, are presented in Table 1 for the peak level and the time of peak.

Table 1. Averaged numerical comparison between simulated and measured peak levels and time of the peak levels for the 8 flood events.

Model	Level RMSE (m)	Level R2 (-)	Level DifAbs (m)	Time RMSE (days)	Time DifAbs (days)
Current Model	1.64	0.71	1.09	5.70	2.42
Current Model + SMOS	1.64	0.74	1.04	5.71	2.41
GR4J	1.99	0.83	1.55	1.90	1.28
GR4J + SMOS	2.84	0.31	2.31	3.34	2.15

As in previous works (Narbondo et al. 2021) the results for the event model are better than for the continuous model in terms of peak level, this is to be expected due to the conception and objective of each. However, unlike in the works mentioned above, in this case the improvement of adding SM to the event model is not as significant. In turn, in this case it was found that the results for time to peak are better for the continuous model.

References

Albergel C, Rüdiger C, Pellarin T, Calvet JC, Fritz N, Froissard F, Suquia D, Petitpa A, Piguet B, and Martin E (2008) From Near-Surface to Root-Zone Soil Moisture Using an Exponential Filter: An Assessment of the Method Based on in-Situ Observations and Model Simulations. Hydrology and Earth System Sciences 12 (6): 1323–37. https://doi.org/10.5194/hess-12-1323-2008

Hastings F, Chreties C, Narbondo S, Uriburu M. (2024) Application of the Flood Guidance Model (FG) in the Yi River basin in Uruguay. Agrocienc Urug [Internet]. Feb. 6 27(NE1):e1191. Available from: https://agrocienciauruguay.uy/index.php/agrociencia/article/view/1191

Lievens H, Tomer SK, Al Bitar A, De Lannoy GJM, Drusch M, Dumedah G, ... & Roundy JK (2015) SMOS soil moisture assimilation for improved hydrologic simulation in the Murray Darling Basin, Australia. Remote Sensing of Environment, 168, 146-162.

Narbondo S, Gorgoglione A, Chreties C (2021) Improving the Performance of an Operational Flood Early Warning System with the Assimilation of Satellite-Soil-Moisture Data. In: Gervasi, O., et al. Computational Science and Its Applications – ICCSA 2021. ICCSA 2021. Lecture Notes in Computer Science(), vol 12955. Springer, Cham. https://doi.org/10.1007/978-3-030-87007-2_3

Patil A, Ramsankaran, RAAJ (2018) Improved streamflow simulations by coupling soil moisture analytical relationship in EnKF based hydrological data assimilation framework. Advances in Water Resources, 121, 173–188. https://doi.org/10.1016/j.advwatres.2018.08.010

Perrín C, Michel C, Andreassian V (2003) Improvement of a parsimonious model for streamflow simulation. Journal of Hydrology p 279, 275-289 29.

USDA (2010). Part 630 Hydrology -National Engineering Handbook (NEH). Natural Re-sources Conservation Service, U. S. Department of Agriculture, Washington, D.C.

US Army Corps of Engineers, 2011. HEC-RAS 4.1 Hydraulics Manual. Washington: US Army.

Wagner W, Lemoine G, Rott H (1999) A method for estimating soil moisture from ERS scatterometer and soil data. Remote Sens. Environ. 70:191–207. doi:10.1016/S0034-4257(99)00036-X

WMO, (2011). Manual on Flood Forecasting and Warning. WMO-No. 1072. ISBN 978-92-63-11072-5.

Bridging global teleconnections and local data for subseasonal-to-seasonal forecasting of Lake Como inflows

G. Palcic[1,2*], G. Ascenso[1,2], M. Giuliani[1], A. Castelletti[1,2]
[1] Department of Electronics, Information and Bioengineering, Polytechnic University of Milan, Milan, Italy
[2] CMCC Foundation - Euro-Mediterranean Center on Climate Change, Italy
* e-mail: giulio.palcic@polimi.it

Introduction

Lake Como, Italy, is a regulated sub-alpine lake with an active capacity exceeding 200 Mm^3. Its hydrological regime is characterized by high inflows in spring, driven by snowmelt, and in autumn, influenced by seasonal rainfall, while lower inflows occur in winter and summer. The lake serves multiple purposes, supporting irrigation, hydroelectric power generation, and cooling for thermal power stations.

Recent droughts have severely impacted irrigation, leading to crop failures and increasing conflicts among stakeholders (Anghileri et al., 2013). Low water levels also threaten navigation, recreation, and tourism, while flooding remains a concern, particularly during heavy autumn rainfall and peak snowmelt in late spring. Historically, lake regulation prioritized flood protection and downstream water supply (Denaro et al., 2017). However, the increasing frequency of extreme droughts, driven by climate change (Giudici et al., 2021), presents a significant challenge, making drought management a priority.

Previous research has demonstrated the value of inflow forecasts in optimizing lake operations (Giuliani et al., 2020; Yang et al., 2020). However, effective water management requires longer lead times, and at the basin scale, only a few forecasting products are available. Among them, the European Flood Awareness System (EFAS) provides useful trend information at sub-seasonal lead times but remains limited in accuracy for Lake Como due to a strong dry bias, underestimated inflow variability, and the lack of local calibration in the LISFLOOD hydrological model (Zanutto et al., in press). To address these limitations, we propose a data-driven framework that integrates teleconnection patterns, global climate variables, and meteorological data to predict Lake Como inflows with lead times ranging from one to six months. By offering a robust and scalable solution for medium- to long-term inflow forecasting, this framework represents a significant step forward in integrating machine learning techniques into hydrological prediction.

Materials and methods

The current framework forecasts Lake Como's inflows at 1, 3, and 6 months ahead. The framework consists of three key components. First, it detects the climate state, based on the phase of a selected climate index. For each phase separately, the most informative patterns of the global variables, including Sea Surface Temperature (SST), Mean Sea Level Pressure (MSLP), and Geopotential at 500 hPa (Z500), are identified by applying grid points masks based on mutual information. This filtered dataset is then processed using Principal Component Analysis (PCA) to reduce dimensionality while retaining essential spatial patterns. Second, a feature selection algorithm based on conditional mutual information constructs the combination of candidate input features by combining the principal components of global climate variables with local meteorological data. Finally, a Random Forest model performs regression to predict cumulated inflows (1, 3, and 6 months ahead), based on the selected input features.

Results and concluding remarks

Model performance is evaluated on 2010–2018, aligning with EFAS reforecast benchmarks. The best-performing models are selected based on Mean Absolute Percentage Error (MAPE) and compared to EFAS ensemble median forecasts using a skill score derived from MAPE. For one-month-ahead forecasts, the model achieves a Mean Absolute Percentage Error (MAPE) of 6.73% and a skill score of 0.96. For three-

month-ahead forecasts, it reaches a MAPE of 6.17% with a skill score of 0.98, while for six-month-ahead predictions, the best MAPE is 6.00% with a skill score of 0.85. These results confirm the framework's reliability across lead times, showcasing its strong predictive performance, outperforming the benchmark. The model performs consistently better during the spring and summer seasons, when inflow dynamics are more predictable, whereas its accuracy declines in autumn (October and November) due to higher inflow variability, leading to greater forecast uncertainty.

Beyond its forecasting accuracy, this approach advances automated, data-driven hydrological modeling by integrating a novel combination of filter- and wrapper-based feature selection techniques. A key strength of the framework lies in its ability to select predictive variables that align with established physical and climatological principles, distinguishing between climate-driven long-term variability and meteorological controls on short-term inflows. At longer lead times, the model relies exclusively on large-scale climate signals, which shape hydrological conditions months in advance, while at sub-seasonal scales, it prioritizes local meteorological variables, which exert a more immediate influence on inflows. This consistent and physically meaningful feature selection suggests that the model is not merely optimizing for statistical accuracy but is also capturing fundamental hydrological relationships. By distinguishing between long-term climate influences and short-term weather-driven variability, the framework enhances interpretability and provides a practical tool for improving reservoir management and water allocation strategies.

Acknowledgments: This study was carried out within the RETURN Extended Partnership and received funding from the European Union Next-GenerationEU (National Recovery and Resilience Plan – NRRP, Mission 4, Component 2, Investment 1.3 – D.D. 1243 2/8/2022, PE0000005). This research was also partially supported by the EU-funded Climate Intelligence (CLINT) project (grant agreement ID: 101003876).

References

Anghileri, D., Castelletti, A., Pianosi, F., Soncini-Sessa, R., & Weber, E. (2013). Optimizing watershed management by coordinated operation of storing facilities. Journal of Water Resources Planning and Management, 139, 492–500. doi: https://doi.org/10.1061/(ASCE)WR.1943-5452.0000313

Denaro, S., Anghileri, D., Giuliani, M., & Castelletti, A. (2017). Informing the operations of water reservoirs over multiple temporal scales by direct use of hydro-meteorological data. Advances in Water Resources, 103, 51-63. doi: https://doi.org/10.1016/j.advwatres.2017.02.012

Giudici F., D. Anghileri, A. Castelletti, and P. Burlando (2021). Descriptive or normative: How does reservoir operations modeling influence hydrological simulations under climate change? Journal of Hydrology, 595:125996. ISSN 0022-1694. doi: https://doi.org/10.1016/j.jhydrol.2021.125996

Giuliani, M., Castelletti, A., & Reed, P. M. (2020). Assessing the value of seasonal streamflow forecasts for large-scale water reservoir operations. Hydrology and Earth System Sciences, 24(11), 5891–5905. https://doi.org/10.5194/hess-24-5891-2020

Yang, G., Guo, S., Liu, P., & Block, P. (2020). forecast-informed multiobjective reservoir operations. Resources Planning and Management, 146 (6), 04020038. Integration and evaluation of Journal of Water. doi: https://doi.org/10.1061/(ASCE)WR.1943-5452.0001229

Zanutto, D., Ficchì, A., Giuliani, M., & Castelletti, A. (in press). Reinforcement learning of multi-timescale forecast information for designing operating policies of multi-purpose reservoirs. Water Resources Research.

Comparison of two innovative devices for water treatment in production of nanobubbles under regular and saline water

K. Zoukidis[1,2], A. Gertsis[1*], N. Kasviki[3], R. Kosheleva[3], I. Avdana[1], A. Giannakoula[2]
[1] Dept. of Sustainable Agriculture and Management, Perrotis College, Thessaloniki, Greece
[2] Dept. of Agriculture, International Hellenic University, Thessaloniki, Greece
[3] Hephaestus Laboratory, Department of Chemistry, Democritus University of Thrace, Kavala, Greece
* e-mail: agerts@afs.edu.gr

Introduction

The characteristics of bubbles in the irrigation water affects aspects of nutrient availability, root oxygenation and in general impacts the productivity. Studies have reported the effect of very small bubbles in soil water and in hydroponics with significant effects in plant productivity (Favvas et al., 2021). The MXGROW system was evaluated in studies at Perrotis College and elsewhere at a range of electrical conductivities in irrigation water (Gertsis and Zoukidis, 2019). Both devices were recently studied and results were presented (Zoukidis et al., 2024).

Materials and methods

Two innovative and inexpensive technologies were used (Figure 1). One is the application of a nanobubbles (NBs) and the other is an electronic water treatment system, based on low frequency radiation waves.

MAX GROW (https://maxgrow.tech/) device (MG) is an electronic water treatment system using multiple transmissions of radio frequencies in three different frequency bands simultaneously (ULF/LW/MW) to tackle the problems caused by saline water and water with high concentration of calcium carbonate ions commonly known as limescale. It is extensively used by farmers and researches to manage high salinity irrigation water, with very successful results (References). It improves productivity and the quality of crops. The hypothesis that one more specific characteristic maybe the production of nanobubbles (NBs) by the MG through the process is investigated in this study and compared with the second device which excursively produces NBs in water. The Agro-Nanobubbles system (http://hal.teiemt.gr /index.php/agronb) is a dynamic research group in the cutting edge of NBs technology. Agro-NB generator produce a long stability NB of 150 nm diameter and concentration 5.000.000 NBs/ml. Agro-NBs demonstrate an extended lifetime compared to larger size bubbles Over the last few years, Agro-NBs have drawn great attention due to their exotic properties. Agro-NBs remain stable for extended periods of time and still exist even after several months (~ 1 year) . The NBs system produces very small size water cavities and are defined as: "*Nanoscopic gas cavities in aqueous solutions which diameter is smaller than 1 micron (d<1μm=1000 nm).*" The system includes two pumps connected in row, and they circulate continuously a mixture of gas and water with a pressure of 24 bar. The mixture is forced through a porous plug into the tank containing water. The combination of porosity and the mentioned pressure results in the formation of nanobubbles size ranging from 150 nm to 600 nm.



Figure 1. Generator of Agro-nanobubbles & MAX GROW (Source: My own collection)

The two water qualities reported in this study (regular and saline) were treated by each device separately and data were collected at 5, 10, 15 and 20 min for both waters. Means comparison (pooled data from all time readings) was performed with JMP v 18 (www.jmp.com) considering five replications for each time measurement.

Results and concluding remarks

In treating regular water (EC~ 0.8 dS/m) the NB device produced larger size of nanobubbles and at a higher concentration, both at statistically significant level (Tables 1 and 2). The opposite was shown when the two devices treated a saline water (2 dS/m where the results showed (Tables 3 and 4) that the MG device produced larger size NB and at a higher concentration. However, the general conclusion is that in the saline water both devices reduced the average size of NB and the concentration, as compared to the treatment of regular water. The important concluding remark is that the MG device generated NBs, both in regular and slight saline water. The study is continued with testing the two devices performance in higher salinity levels. The hypothesis for the MG device of being capable to produce NB was confirmed in this study.

Table 1. Analysis of regular water-size (nm) by device.

Device	Mean size of NB (nm) Regular water
Agro-NBs	379 A
MaxGrow	281 B

Table 2. Analysis of regular water-concentration (10^7) by device

Device	Mean NB Concentration (10^7)
Agro-NBs	1.9260500 A
MaxGrow	0.9223492 B

Table 3. Analysis of saline water 2 dS/m -size (nm) by device

Device	Mean NB size (nm)
MaxGrow	258 A
Agro-NBs	123 B

Table 4. Analysis of saline water 2 dS/m-concentration (10^7) by device

Device	Mean NB Concentration (10^7)
MaxGrow	0.68855000 A
Agro-NBs	0.28775000 B

Note in Tables 1-4: Devices not connected by same letter are significantly different ($\alpha<0.05$).

Acknowledgments: The authors express their sincere gratitude to the two companies provided the electronic water treatment system (MAXGROW: https://maxgrow.tech/), and the generator of Agro-nanobubbles (NBs) (Hephaestus Lab, Democritus University of Thrace (https://chem.duth.gr/)

References

Favvas, E.P., Kyzas, G.Z., Efthimiadou, E.K. and Mitropoulos, A.C., 2021. Bulk nanobubbles, generation methods and potential applications. Current Opinion in Colloid & Interface Science, 54, p.101455

Gertsis, A., and K. Zoukidis. 2017. Irrigation with highly saline water: a new innovative water treatment system evaluated for vegetable production in greenhouse. European Water Special Issue III-59. Paper No. 45. EWRA2017 - 10th Word Congress on Water Resources and Environment). http://www.ewra.net/ew/issue_59.htm

Zoukidis, K, Gertsis, A., Apostolidis, A., Strouthopoulos G. and Giannakoula, A. (2024). Innovative technologies (nanobubbles and electronic water treatment) to manage highly saline irrigation water in hydroponic systems. Proceedings of HAICTA 2024, October 17–20, 2022, Samos, Greece. CEUR Workshop Proceedings (CEUR-WS.org).

Laboratory analyses for beach litter detection via remote sensing

L. Corbari[1*], M. Minacapilli[1], G. Ciraolo[1,2], Fulvio Capodici[1,2]
[1] Dipartimento di Ingegneria, Università degli Studi di Palermo, Palermo, Italy
[2] NBFC, National Biodiversity Future Center, Palermo, Italy
*e-mail: laura.corbari@unipa.it

Introduction

Marine litter is "any persistent, manufactured, or processed solid material discarded in marine and coastal environments" (Environment, 2005). Various technologies aim to prevent litter from entering coastal areas and monitor its occurrence.

In-situ sampling, remote sensing, and hydrodynamic modelling are useful tools to deal with the marine litter issue (Bellou et al., 2021). In-situ monitoring campaigns allow to quantify and characterize beach litter (Asensio-Montesinos et al., 2019; Grundlehner et al., 2023) even if these methods are time-consuming, especially over large areas. Remote sensing, particularly using high-resolution data from UAVs, is a more efficient approach to map large/inaccessible areas like dunes and lakes (Manfreda et al., 2018; Andriolo et al., 2022).

Recent studies have examined the limitations of detecting beach litter in sandy backgrounds using proximal remote sensing (Guffogg et al., 2021a), identifying optimal wavelengths for their detection (Guffogg et al., 2021b). Main limitation of remote beach litter detection is the lack of their spectral signature and the absence of a standardized protocol for their acquisition.

This research aims to fill this latter gap by providing spectral libraries of harvested beach litter, employing direct and diffuse illumination setups. Also, the selection of promising spectral bands for outdoor detection is evaluated via the SAM index (Spectral Angle Mapper) between the spectral signature of a sandy background and those of the harvested marine litter.

Outcomes of this research want to contribute to advanced beach litter monitoring via remote sensing which is under continuous development in terms of sensor spectral characteristics and spatial resolutions (*e.g.*, UAV equipped with hyperspectral cameras).

Materials and methods

Marine litter over two Sicilian sandy beaches (Mondello and Isola delle Femmine) have been harvested following the "Guidelines for the monitoring and assessment of plastic litter in the ocean" (GESAMP 2019) protocol.

Totally 221 items were categorized and numbered; excluding the transparent ones, the spectra were acquired for 136 samples in an indoor laboratory experiment. The spectra were collected by placing the samples within a white and a black box, illuminated with diffuse and direct light respectively. Diffuse light was guaranteed using white paint and building the top of the box with a 'cupola' shape; whereas, direct light was ensured with a black painted box. The illumination was provided by two lamps characterized by an irradiance curve that approximates that of the sun. All the spectral signatures were acquired via the FieldSpec 4 Hi-Res spectroradiometer by ASD (Analytical Spectral Devices), able to acquire the reflectance across the entire solar-reflected spectrum (i.e., from 300 to 2500 nm) through a 1.5 m long optical fiber. The employment of an 8° optics ensured pure spectral signature acquisitions of small-sized samples. The different illumination conditions significantly impacted only some of the spectral data acquisition. Finally, the spectral similarity/dissimilarity SAM index was evaluated over the whole wavelength. The more promising wavelengths for marine litter detection were selected by employing a moving window.

Results and concluding remarks

The spectral signature of sand is monotonically increasing in the 350–1350 nm range, showing

absorption peaks around 1400 and 1900 nm to water content. The collected samples show reflectance peaks in the visible range consistently with their colours. Noticeably that, absorption peaks are observed in the NIR (around 950 nm) and SWIR (1200, 1350, 1720 nm) regions.

The comparison of spectra obtained under different illumination conditions highlighted that the illumination setup affected the reflectance data in about 30% of the cases.

The detectability of samples from the sand was difficult (*i.e.*, SAM values below 0.2) for 18% and 15% of the total samples collected in the white and black box respectively. Instead, 21% of the samples in the white box and 37% in the black box exhibited SAM values greater than 0.5, making them moderately highly distinguishable from sand. Overall, SAM values were slightly higher for the spectra acquired in the black box.

The most useful wavelengths for monitoring detection were inferred using a 21 nm moving window across the spectra; the selected bands were in the visible range, around the red-edge (700–770 nm), and near 1230 nm, 1400 nm, and 1720 nm. These results are in agreement with similar findings reported by Salgado-Hernanz et al. (2021) and Guffogg et al. (2021) (reporting both indoor and outdoor experiments). In contrast, bands between 800–1000 nm, 1250–1300 nm, and 1450–1650 nm were ineffective for detecting litter debris (showing SAM values below 0.2).

Acknowledgments: Marine debris and sand samples have been harvested from two Sicilian sandy beaches, the data collection has been conceived and supported by scientists at the Laboratory of Ecology, of the Dipartimento di Scienza della Terra e del Mare (University of Palermo) by applying EU standardize protocols. The activities have been supported by the Interreg Italy Malta territorial cooperation project SenHAR “Campagne di sensibilizzazione per una armonizzazione Italo-Maltese per un buono stato dell’ambiente” C.2-3.1-115.

References

Andriolo U, Garcia-Garin O, Vighi M, et al (2022) Beached and Floating Litter Surveys by Unmanned Aerial Vehicles: Operational Analogies and Differences. Remote Sensing 14:1336. https://doi.org/10.3390/rs14061336

Asensio-Montesinos F, Anfuso G, Williams AT (2019) Beach litter distribution along the western Mediterranean coast of Spain. Marine Pollution Bulletin 141:119–126. https://doi.org/10.1016/j.marpolbul.2019.02.031

Bellou N, Gambardella C, Karantzalos K, et al (2021) Global assessment of innovative solutions to tackle marine litter. Nature Sustainability 4:516–524. https://doi.org/10.1038/s41893-021-00726-2

Environment UN (2005) Marine litter, an analytical overview. In: UNEP - UN Environment Programme. http://www.unep.org/resources/report/marine-litter-analytical-overview. Accessed 5 Jul 2024

GESAMP (2019) Guidelines for the monitoring and assessment of plastic litter and microplastics in the ocean. GESAMP Joint Group of Experts on the Scientific Aspects of Marine Environmental Protection

Grundlehner A, Diepens NJ, Linders T, et al (2023) Towards continuous mass and size distributions for beach plastic litter: Spatiotemporal analyses of abundance and composition. Journal of Hazardous Materials 458:131984. https://doi.org/10.1016/j.jhazmat.2023.131984

Guffogg JA, Blades SM, Soto-Berelov M, et al (2021a) Quantifying Marine Plastic Debris in a Beach Environment Using Spectral Analysis. Remote Sensing 13:4548. https://doi.org/10.3390/rs13224548

Guffogg JA, Soto-Berelov M, Jones SD, et al (2021b) Towards the Spectral Mapping of Plastic Debris on Beaches. Remote Sensing 13:1850. https://doi.org/10.3390/rs13091850

Manfreda S, McCabe MF, Miller PE, et al (2018) On the Use of Unmanned Aerial Systems for Environmental Monitoring. Remote Sensing 10:641. https://doi.org/10.3390/rs10040641

Salgado-Hernanz PM, Bauzà J, Alomar C, et al (2021) Assessment of marine litter through remote sensing: recent approaches and future goals. Marine Pollution Bulletin 168:112347. https://doi.org/10.1016/j.marpolbul.2021.112347

Evaluating the capability of multispectral satellite images in identifying small agricultural reservoirs (SmARs)

M.S. Goodarzi[1*], M. Lompi[1], G. Bertoli[1], N. Mannucci[1], T. Pacetti[1], E. Caporali[1], D.D. Chiarelli[2]
[1] Department of Civil and Environmental Engineering (DICEA), University of Florence, Italy
[2] Department of Civil and Environmental Engineering, Politecnico di Milano, Milan, Italy
* e-mail: mehdi.sheikhgoodarzi@unifi.it

Introduction

Small Agricultural Reservoirs (SmARs) play a crucial role in agricultural resilience by ensuring water availability during dry periods. Their identification and delineation using remote sensing is a remained challenge owning to their limited size, spectral similarities with other water bodies, and varying environmental conditions. This study evaluates the potential of multispectral satellite imagery, particularly Sentinel-2, in detecting SmARs using optical water indices and cartographic datasets. The primary objective is to optimize accuracy estimations while increasing the number of detectable reservoirs.

Methodology

Despite the effectiveness of water detection generally depends on sensor resolution, spectral characteristics, and climatic conditions, thresholding is of crucial importance in this procedure (Kirby et al., 2024). To determine the most suitable water indices for SmAR detection at both local and national scales, we implemented the following methodology:

1. Literature review & index selection: a comprehensive analysis of remote sensing-based water detection methods led to the selection of widely used indices: NDWI, NDVI, MNDWI, EVI, AWEI (both AWEI_sh & AWEI_nsh), WNDWI, WRI, and Sun457 (Yang et al., 2017; Kirby et al., 2024).
2. Implementation in Google Earth Engine (GEE): the indices were applied using Sentinel-2 imagery across the Tuscany region to generate initial water body extractions and preliminary comparisons (see Fig.1).
3. Refinement & false positive removal: misclassified water pixels, such as shadows, streams, and blue infrastructures, were filtered out.
4. Validation of the remotely identified SmAR with performance indicators and ground truth data. Three indices are used to assess the performances: *Probability of Detection (POD)*, *False Alarm Rate (FAR)*, and *Critical Success Index (CSI)* to benchmark the accuracy of different indices. In this context, POD was used to quantify the percentage of SmARs correctly identified, while FAR measured the proportion of non-reservoir water pixels mistakenly classified as SmARs. CSI provided an overall performance metric by integrating both correct detections and false alarms, offering a robust evaluation of each index's effectiveness.

Results and concluding remarks

Preliminary findings indicate that NDWI and MNDWI are the most reliable indices for detecting SmARs in Tuscany, with higher CSI values and reduced false positives, which is in line with Yang et al (2017) findings. Specifically, MNDWI exhibited enhanced performance in areas with urban backgrounds by suppressing built-up land reflectance, while NDWI provided better results in vegetated regions. The AWEI_sh index performed well in shadowed areas but introduced more false positives in agricultural fields; conversely, Su et al (2024) outlined this metric as the second performant indicator of water detection in mixed environments, following the SMBWI (Sentinel Multi-Band Water Index). The integration of OSM data significantly improved classification accuracy by eliminating non-reservoir water bodies, as per definition by law and natural entity, with a notable reduction in FAR.

Index	Threshold	n° SMAR detected	Pearson
AWEI nsh	0	2027	0.781
AWEI sh	0	4719	0.901
EWI	1.8	1895	0.690
NDVI	0.01	2949	0.830
NDWI	0.1	4053	0.798
MNDWI	0.12	2905	0.868
SUM457	0.2	3464	0.864
WNDWI	0.04	3730	0.872
WRI	0.9	3884	0.315

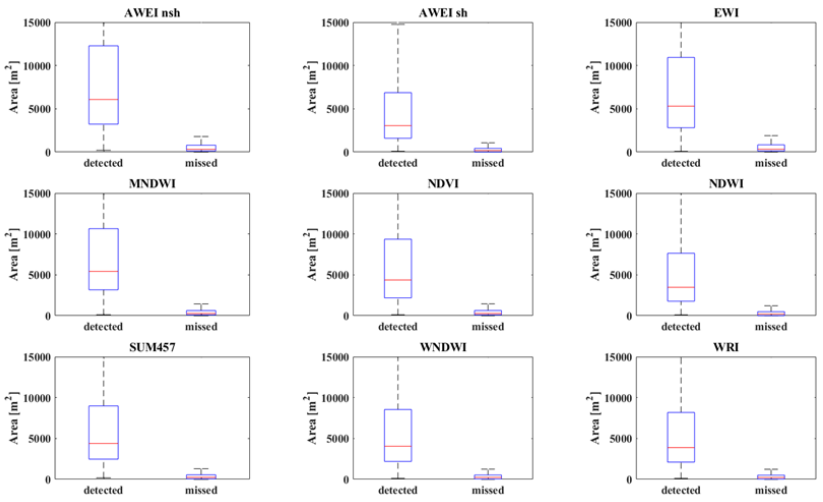


Figure 1. Preliminary SmARs detection

The methodology developed is scalable and can be applied to national-level SmAR mapping, offering a cost-effective alternative to high-resolution commercial imagery. The study underscores the importance of combining spectral indices with cartographic datasets to enhance water body detection in agricultural landscapes, which supports Kirby et al., 2024 remarks.

Acknowledgment: This research was developed as part of the "CASTLE - Creating Agricultural reSilience Through smaLl rEservoirs" project funded by the MUR as part of the PRIN projects - Research Projects of Relevant National Interest - 2022. CASTLE - COD. PROG. 2022XSERL4.

References

Kirby, K., Ferguson, S., D. Rennie, C., Cousineau, J., Nistor, I. 2024. Identification of the best method for detecting surface water in Sentinel-2 multispectral satellite imagery, Remote Sensing Applications: Society and Environment, Volume 36, 2024, 101367, ISSN 2352-9385. doi.org/10.1016/j.rsase.2024.101367.

Mady, B., Lehmann, P., Gorelick, S.M. Distribution of small seasonal reservoirs in semi-arid regions and associated evaporative losses. Environmental Research Communications, 2020 2 (6), Article 061002. Doi.org/10.1088/2515-7620/ab92af.

Su, Z., Xiang, L., Steffen, H., Jia, L., Deng, F., Wang, W., Hu, K., Guo, J., Nong, A., Cui, H., & Gao, P. (2024). A New and Robust Index for Water Body Extraction from Sentinel-2 Imagery. Remote Sensing, 16(15), 2749. https://doi.org/10.3390/rs16152749.

Valerio, F., Godinho, S., Ferraz, G., Pita, R., Gameiro, J., Silva, B., Marques, A. t., & Silva, J. P. 2024. Multi-temporal remote sensing of inland surface waters: A fusion of sentinel-1&2 data applied to small seasonal ponds in semiarid environments. International Journal of Applied Earth Observation and Geoinformation, Volume 135, 2024, 104283, ISSN 1569 8432, https://doi.org/10.1016/j.jag.2024.104283.

Yang, X., Zhao, S., Qin, X., Zhao, N., & Liang, L. (2017). Mapping of Urban Surface Water Bodies from Sentinel-2 MSI Imagery at 10 m Resolution via NDWI-Based Image Sharpening. Remote Sensing, 9(6), 596. https://doi.org/10.3390/rs9060596.

Towards estimating water use efficiency of irrigated orchards from remote sensing: an application to a citrus orchard in Sicily

D. De Caro[1*], O. Merlin[2], V. Rivalland[2], V. Simonneaux[2], G. Boulet[2], M. Ippolito[1], F. Capodici[1], C. Cammalleri[3], G. Ciraolo[1]

[1] *Engineering Department, University of Palermo, Palermo, Italy*
[2] *Centre d'Études Spatiales de la BIOsphère (CESBIO), University of Toulouse, Toulouse, France*
[3] *Department of Civil and Environmental Engineering, Politecnico di Milano, Milano, Italy*
** e-mail: dario.decaro01@unipa.it*

Introduction

Knowledge of actual evapotranspiration (ET_a) and its partitioning into soil evaporation (E_a) and plant transpiration (T_a) can be used to derive water use efficiencies and crop water needs, which are crucial for optimizing water resource management in agriculture (Johnson et al. 2013).

To monitor crop water requirements various data sources are used, such as: *in situ* (meteorological and soil water content data) measurements, gross primary production (GPP) data, reanalysis database, remote sensing observations, and models. These data could be employed as input for three different methods: the Soil Water Balance (SWB), the Surface Energy Balance (SEB), and the Eddy Covariance (EC) tower flux partitioning method.

Within this research, *in situ* or reanalysis meteorological data, GPP estimations, and remotely sensed images are integrated with the aim of discovering synergies between these methods and proposing an operational ET_a estimation in the context of future Thermal InfraRed (TIR) missions (TRISHNA and LSTM).

A SWB model was implemented to estimate daily soil water content (SWC), transpiration (T_a), evaporation (E_a) and, therefore the actual evapotranspiration (ET_a). A SEB model allowed estimating the instantaneous soil (LE_s) and vegetation (LE_v) latent heat fluxes. Finally, the partitioning method allowed the disaggregation of ET_a, into T_a and E_a, at a daily scale. All these approaches were assessed in a Mediterranean citrus orchard.

Materials and methods

Among the available SWBs, the SAtellite Montoring for Irrigation (SAMIR) is a FAO-2Kc-based model (Allen et al. 1998) integrating remotely sensed images of vegetation cover for actual evapotranspiration and water balance spatialization. SAMIR can be forced by irrigation either measured or simulated employing specific rules based on the simulated SWC (Simonneaux et al. 2009).

Alternatively, the Soil Plant Atmosphere and Remote Sensing Evapotranspiration (SPARSE) is a two-source SEB residual model driven by remotely sensed Land Surface Temperature (LST) and vegetation cover (Boulet et al. 2015).

A new and simple method for ET_a disaggregation allowed retrieving T_a and E_a separately; indeed, from EC measurements T_a and E_a are computed via the estimation of soil and canopy conductances; theese latters assumed to be proportional to the GPP (Li et al. 2019).

Both SWB and SEB were investigated by using different combinations of input variables. For SAMIR, two combinations were tested: 1) using *in situ* and 2) using ERA5-Land reanalysis meteorological variables to estimate crop reference evapotranspiration and precipitation depth (both by considering the farmer irrigations and Sentinel-2 NDVI-derived vegetation cover maps). For SPARSE, three combinations were employed: 1) using *in situ* meteorological data, LST, and albedo; 2) replacing LST and albedo with Landsat-8/9 data; 3) replacing *in situ* data with ERA5-Land reanalysis while maintaining Landsat-8/9 inputs.

The partitioning method was implemented using as input data the Net Ecosystem CO_2 Exchange (NEE - CO_2 flux), the ecosystem conductance (G_s), the inferred leaflevel vapor pressure deficit at the ecosystem scale (VPD_{leaf}), and the first layer SWC.

The experiments occurred during seven irrigation seasons, from 2018 to 2024, in a Mediterranean citrus orchard (*Citrus reticulata Blanco* cv. Mandarino Tardivo di Ciaculli), located near Palermo, Italy (38° 4' 53.4'' N, 13° 25' 8.2'' E) in which different irrigation systems and management strategies were applied. The field was equipped with a standard weather station, an Eddy Covariance tower, sap flow sensors, and four "drill and drop" probes to acquire: meteorological variables, energy fluxes, CO_2 concentration, tree transpiration, and SWC.

Results and concluding remarks

SWB and SEB models performance was assessed by comparing their outputs by means of *in situ* data.

SAMIR performance was evaluated year-wise. SAMIR best performance was obtained using the 1-combination with Root Mean Square Error (RMSE) values always less than 0.54 mm d^{-1} and 0.02 cm^3 cm^{-3} for ET_a and SWC, respectively. These metrics were achieved excluding data from 2021 during which worse metrics (ET_a RMSE equal to 0.87 mm d^{-1}) were probably caused by the presence of weeds (due to the lack of maintenance provided by the farmer). The 2-combination provided ET_a RMSE and SWC RMSE less than 0.70 mm d^{-1} and 0.03 cm^3 cm^{-3}, respectively (always excluding 2021 data, ET_a RMSE equal to 0.85 mm d^{-1}). The T_a RMSE for 1-combination, obtained by comparing the output with the sap flow transpiration, was always less than 0.45 mm d^{-1}.

SPARSE performance was evaluated considering all the years. SPARSE best performance for LE (sum of LE_s and LE_v) was obtained using 1-combination with RMSE equal to 53 W m^{-2} when considering all *in situ* data. This value remains unchanged when only data acquired contextually to satellite observations are considered in the performance evaluation. However, 2- and 3- combinations RMSE values were equal to 66 W m^{-2} and 93 W m^{-2}, respectively. The results of 2-combination indicate that implementing the model with satellite-derived LST can effectively provide high-quality spatialized latent heat fluxes.

A comparison between the E_a and T_a obtained from the partitioning method and those achieved by the SAMIR model was evaluated. RMSE resulted always less than 0.54 mm d^{-1} and 0.43 mm d^{-1} for T_a and E_a, respectively. Moreover, partitioned T_a performance was derived considering the sap flow measurement as benchmark. The RMSE resulted always less than 0.41 mm d^{-1}.

The promising achieved results encourage further development of the present work with a focus on synergies between approaches for enhanced transpiration and evaporation estimation separately. Particularly, SWB and SEB models combined with remote sensing technologies represent more scalable and cost-effective approaches to monitoring transpiration and evaporation (and thus the actual evapotranspiration). These models allow for a more accurate and comprehensive assessment of field fluxes, supporting better irrigation management, improving the sustainability of agricultural practices; thus, supporting agriculture practices compliant with climate change scenarios. In this framework, need to be highlighted that the adoption of the presented smart approaches is in agreement with a less environmentally impactful agricultural production.

References

Allen R, Pereira L, Raes D, Smith M (1998) FAO Irrigation and drainage paper No. 56. Rome: Food and Agriculture Organization of the United Nations 56, 26–40.

Boulet G, Mougenot B, Lhomme JP, Fanise P, Lili-Chabaane Z, Olioso A, Bahir M, Rivalland V, Jarlan L, Merlin O, Coudert B, Er-Raki S, Lagouarde, JP (2015) The SPARSE model for the prediction of water stress and evapotranspiration components from thermal infra-red data and its evaluation over irrigated and rainfed wheat. Hydrology and Earth System Sciences 19 (11), 4653–4672. https://doi.org/10.5194/hess-19-4653-2015

Johnson K, Sankaran S, Ehsani R (2013) Identification of water stress in citrus leaves using sensing technologies. Agronomy 3, 747–756. https://doi.org/10.3390/agronomy3040747

Li X, Gentine P, Lin C, Zhou S, Sun Z, Zheng Y, Liu J, Zheng C (2019) A simple and objective method to partition evapotranspiration into transpiration and evaporation at eddy-covariance sites. Agricultural and Forest Meteorology, Volume 265,Pages 171-182, ISSN 0168-1923. https://doi.org/10.1016/j.agrformet.2018.11.017

Simonneaux V, Lepage M, Helson D, Metral J, Thomas S, Duchemin B, Cherkaoui M, Kharrou H, Berjami B, Chehbouni A (2009) Estimation spatialisèe de l'´evapotranspiration des cultures irriguèes par tèlèdètection: application à la gestion de l'irrigation dans la plaine du Haouz (Marrakech, Maroc). Sci. Chang. Planètaires Sècher. 20, 123–130. https://doi.org/10.1684/sec.2009.0177

Tracking water resources in Sicilian reservoirs: A Google Earth Engine application using Sentinel-1 SAR and machine learning

C. Martins Jr*, G. Ciraolo, F. Capodici, M. de Marchis
Dipartimento di Ingegneria, Università degli Studi di Palermo, Palermo, Italy
** e-mail: cicero.martinsjr@unipa.it*

Introduction

Water levels of Sicilian reservoirs are well-monitored using traditional methods, such as limnimetric gauges, which represent a real-time tool for managing the water resources. However, the conversion of the water level into volume is affected by the accuracy of reservoir surface and sedimentation level assessments. Synthetic Aperture Radar (SAR) data from Sentinel-1, with its all-weather capabilities, has proven effective for addressing the reservoir surface estimation for water resource management, particularly in cloud-prone or remote areas (Mullissa et al., 2021). Coupled with machine learning (ML), SAR has demonstrated potential for water body delineation, water volume estimation, and long-term hydrological monitoring (Ghobadi & Kang, 2023).

This study aims to leverage Sentinel-1 SAR data and machine learning techniques within the Google Earth Engine platform (GEE) to estimate the water surface area and volume of 40 Sicilian reservoirs. The proposed workflow combines a Support Vector Machine (SVM) classifier with reservoir-specific surface-to-volume relationships, validated using in situ data from the Autorità di Bacino della Sicilia. While applied to Sicily, the methodology is designed to be scalable, offering a framework for deployment in regions without established monitoring infrastructure, thereby enhancing global water resource management capabilities.

The application can be accessed in: https://ee-ciceromartinsjr.projects.earthengine.app/view/sicilianreservoirsvolume.

Materials and methods

This study employed Sentinel-1 SAR data to monitor the water surface area and volume of 40 reservoirs in Sicily. A Google Earth Engine (GEE) application was developed to automate data processing and visualization, incorporating the following key steps:

- Data Collection: Sentinel-1 SAR (VV and VH bands) images from the COPERNICUS/S1_GRD collection were filtered by spatial resolution (10 m) and the geographic boundaries of each reservoir. Users can define the analysis period, with a default range of one year.
- Classification: A Support Vector Machine (SVM) classifier was trained with labeled water and non-water regions using VV and VH bands. The classifier was validated with a confusion matrix to ensure robust water surface detection.
- Water Mask Refinement: Refinements included speckle noise reduction, masking with data from the JRC Dataset to avoid false positives for water, morphological operations and vectorizing were also used to better retrieve the water body surface.
- Surface Area and Volume Estimation: Water surface areas were calculated from classified masks using GEE's pixelArea function. Volumes were estimated using reservoir-specific area-to-volume equations, derived from Autorità di Bacino della Sicilia datasets.
- Interactive Application: The GEE app allows users to select a reservoir, define time periods, and view water surface and volume time series. Graphs are smoothed using moving averages, and outliers are filtered based on statistical thresholds.



Figure 1. The app displays SAR VV imagery and refined water masks on the map, alongside interactive charts of water area and volume dynamics.

Results and concluding remarks

The SVM classifier effectively delineated the water bodies, with a confusion matrix accuracy of 94.9%. In terms of volume estimation, for instance, significant fluctuations were observed in the monitored reservoirs from 2022 to 2025, as estimated using the GEE model. These results were compared with in situ data from the Autorità di Bacino, showing agreement in terms of trends. For instance, water volumes at Lago Poma ranged from 46 to 18 million m³ during this period (Figure 1), while the Autorità di Bacino reported a range of 56 to 16 million m³. Similarly, Rosamarina, one of the largest reservoirs in Sicily, experienced a decline from 65 million m³ to less than 16 million m³ according to the GEE model, compared to 71 to 10 million m³ reported by the Autorità di Bacino. Lago Pozzillo, the largest reservoir on the island, saw its volume drop dramatically from 57 to less than 2 million m³ in the GEE estimations, but it showed signs of recovery in early 2025, reaching 32 million m³. The Autorità di Bacino recorded similar trends, with volumes ranging from 66 to 2.6 million m³ during the drought and recovering to 23.6 million m³ by February 2025.

While these trends were effectively captured by the GEE model, some uncertainties remain. Variations in accuracy were observed between reservoirs, probably influenced by local characteristics such as soil types and topography. Additionally, the absence of recent bathymetric surveys introduces limitations in the area-to-volume equations, potentially impacting the precision of volume estimates.

To improve the accuracy of volume calculations, future work will explore the use of interferometry to generate digital elevation models (DEMs), leveraging periods of water scarcity, when larger portions of lakebeds are exposed, to refine these estimates. This approach is planned to be validated by employing a bathymetric unmanned surface vehicles (USVs) to measure the actual sedimentation level. This scalable approach could be extended to other drought-prone regions, supporting improved water resource management and climate resilience.

Acknowledgments: The authors express their gratitude to the Autorità di Bacino della Sicilia for providing valuable in situ data on reservoir volumes, which were essential for validating the results of this study.

References

European Space Agency (2023) Sentinel-1 User Guide. https://sentinels.copernicus.eu

Ghobadi F, Kang D (2023) Application of machine learning in water resources management: A systematic literature review. Water 15(620): 1–28. https://doi.org/10.3390/w15040620

Google Earth Engine (2023). Google Earth Engine: A cloud-based platform for planetary-scale environmental data analysis. Available in: https://earthengine.google.com

Martins Jr, C. (2025). Sicilian Reservoirs Volume Application. Available in: https://ee-ciceromartinsjr.projects.earthengine.app/view/sicilianreservoirsvolume

Mullissa A et al. (2021) Sentinel-1 SAR backscatter analysis-ready data preparation in Google Earth Engine. Remote Sensing 13(1954): 1–7. https://doi.org/10.3390/rs13101954

Optimizing image-based surface velocity measurements: sensitivity to graphical enhancement and processing parameters

S.F. Dal Sasso[1], F. Alongi[2], R. Ljubičić[3], D. Pumo[2], L.V. Noto[2]
[1] Department for Humanistic, Scientific, and Social Innovation, University of Basilicata, Matera, Italy
[2] Department of Engineering, University of Palermo, Palermo, Italy
[3] Department of Hydraulic and Environmental Engineering, University of Belgrade, Belgrade, Serbia
* e-mail: silvano.dalsasso@unibas.it

Introduction

Image-based techniques are being increasingly used to monitor natural and artificial rivers due to their advantages over conventional measurement methods. These optical approaches are non-intrusive, allowing data collection without interfering with the flow. Their versatility enables application in diverse conditions, including dangerous situations such as floods, ensuring both operator and equipment safety. By exploiting high-resolution cameras and advanced image processing software, these methods can estimate surface velocity even when traditional techniques are impractical or unsafe. Despite their benefits, the accuracy of image-based measurements depends on several factors. Environmental conditions can affect image quality, leading to potential inaccuracies in velocity estimation. River characteristics (e.g., turbulence, turbidity, vegetation) further influence data capture. Additionally, the effectiveness of these methods relies on proper field acquisition protocols and precise parameterization of the processing software.

Optical techniques follow a three-phase workflow: (i) seeding, (ii) recording, and (iii) processing. The seeding phase involves introducing natural or artificial tracers onto the water surface to track movement. During recording, video sequences are captured using stationary or mobile platforms (Unmanned Aerial Systems, UASs). The final phase consists of three key steps. First, the recorded video undergoes transformations to enhance quality and stability, including stabilization to correct unwanted camera movements, orthorectification for geometric accuracy, and graphical enhancement to improve tracer visibility. Next, surface velocity is estimated using correlation-based algorithms or similar techniques to track the tracers' movement across consecutive frames. Finally, post-processing refines velocity data by filtering noise, interpolating missing information, and generating an average velocity map. Among these steps, graphical enhancement plays a particularly crucial role. By increasing contrast between tracers and background, it improves motion detection and reduces errors in velocity estimation. However, its performance does not solely depend on graphical enhancement; the parametric setup of the processing software is equally critical. Improperly tuned parameters can introduce biases, compromising results.

Materials and methods

This work presents a comprehensive sensitivity analysis, assessing how different graphical enhancement techniques and processing parameters jointly affect measurement accuracy. The study examined the impact of various enhancement methods and algorithmic settings on velocity estimates. The analysis focused on a range of filters, from the traditional ones (e.g., intensity capping, high pass, contrast adjustment) to advanced techniques (e.g., background subtraction, edge detection filters) (Figure 1).

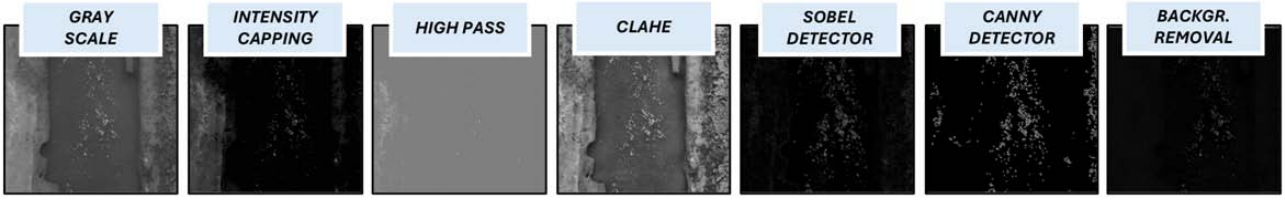


Figure 1. Example of a pre-processed frame with some of the analyzed filters.

The goal was to identify optimal strategies that maximize accuracy while minimizing susceptibility to errors due to environmental and technical constraints.

To achieve this, a dataset of video recordings was collected during discharge measurement campaigns on two Sicilian rivers, conducted over several days to account for a wide range of acquisition conditions. Videos were captured using both UAS platforms (i.e., a small drone) and fixed cameras, ensuring a diverse range of observational conditions. Each video sequence was appropriately stabilized and orthorectified, with only the portions containing an adequate distribution and density of tracers selected for further analysis (Alongi et al., 2023). The tracers were manually introduced by operators onto the water surface to ensure consistent tracking throughout the recordings. The data were processed using PIVlab (Thielicke & Stamhuis, 2014) and SSIMS-Flow (Ljubičić et al., 2024), two widely used software tools for image-based analysis. The study also investigated the key parameters within these software tools that have the greatest influence on the results. The results obtained from these tools were then benchmarked against Acoustic Doppler Current Profiler (ADCP) measurements, which were performed within the recorded area. For these measurements, transects were taken by moving the ADCP from bank to bank, providing a reference for assessing the accuracy of the image-based velocity estimates.

Results and concluding remarks

The findings of this study underscore the critical influence of both graphical enhancement techniques and the optimization of software parameters on the accuracy of velocity estimates in image-based measurements. The results demonstrate that the selection of appropriate enhancement methods can substantially improve tracer detection, reducing tracking errors and enhancing the overall reliability of velocity estimations (Figure 2). Likewise, fine-tuning key processing parameters play a fundamental role in minimizing biases and ensuring that the extracted velocity metrics accurately represent real hydrodynamic conditions.

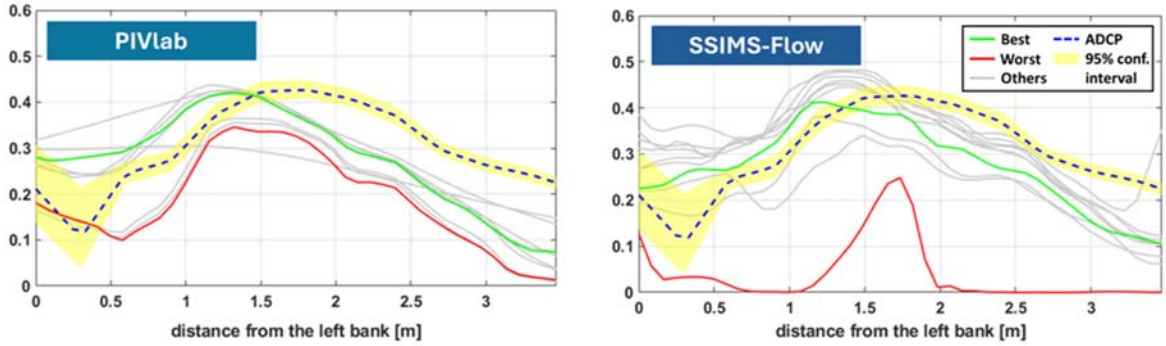


Figure 2. Surface velocity profiles comparison between PIVlab and SSIMS-Flow results and benchmark ADCP. For fixed software parameters, the best profiles (best filter, green line) and the worst profiles (worst filter, red line) are shown.

The study offers valuable insights into the optimal configurations of graphical enhancement and processing strategies, highlighting the importance of adapting these techniques to specific field conditions and operational constraints. These findings further reinforce the potential of image-based methods as powerful tools for hydraulic monitoring, demonstrating their effectiveness in real-world applications.

References

Alongi, F., Pumo, D., Nasello, C., Nizza, S., Ciraolo, G., & Noto, L. V. (2023). An automatic ANN-based procedure for detecting optimal image sequences supporting LS-PIV applications for rivers monitoring. Journal of Hydrology, 626, 130233.https://doi.org/10.1016/j.jhydrol.2023.130233

Ljubičić, R., Dal Sasso, S. F., & Zindović, B. (2024). SSIMS-Flow: Image velocimetry workbench for open-channel flow rate estimation. Environmental Modelling & Software, 173, 105938.https://doi.org/10.1016/j.envsoft.2023.105938

Thielicke, W. & Stamhuis, E. (2014). PIVlab–towards user-friendly, affordable and accurate digital particle image velocimetry in MATLAB. Journal of open research software, 2(1), 30.https://doi.org/10.5334/jors.bl

Physics-informed neural networks for flood modelling: A conceptual framework

M. Herrera[1*], V. Glenis[1], X. Xie[1], B.M. Brentan[2]
[1] School of Engineering, Newcastle University, Newcastle upon Tyne, United Kingdom
[2] School of Engineering, Federal University of Minas Gerais, Belo Horizonte, Brazil
* e-mail: manuel.herrera@newcastle.ac.uk

Introduction

Flood modelling is a critical challenge in hydrology and disaster management, with significant implications for public safety, infrastructure protection, and environmental conservation (Fotovatikhah et al., 2018). Traditional flood modelling approaches, such as hydrodynamic models based on the shallow water equations (SWEs), are computationally expensive and often require high-resolution data (Song et al., 2023). These limitations have spurred interest in data-driven methods, particularly machine learning (ML), to complement or replace traditional techniques. However, purely data-driven ML models often struggle with generalisation, especially in scenarios with limited or sparse data, and they may fail to respect the underlying physical laws governing fluid dynamics.

This paper proposes the use of physics-informed neural networks (PINNs) as a powerful framework to bridge the gap between data-driven models and physics-based models (Raissi et al., 2019). PINNs integrate governing physical equations, such as conservation laws and other fundamental principles, directly into the neural network's loss function, ensuring physically consistent predictions. This hybrid approach leverages the strengths of both data-driven learning and physics-based modelling, making it particularly well-suited for flood management.

Material and methods

PINNs enforce physical consistency by embedding governing equations, typically represented as partial differential equations (PDEs), within neural networks. In flood modelling, the SWEs, such as Equation (1) of mass conservation and Equation (2) and (3) of conservation of momentum, are an instance of the governing PDEs used in this framework,

$$\frac{\partial h}{\partial t} + \frac{\partial (hu)}{\partial x} + \frac{\partial (hv)}{\partial y} = 0 \quad (1)$$

$$\frac{\partial (hu)}{\partial t} + \frac{\partial}{\partial x}\left(hu^2 + \frac{1}{2}gh^2\right) + \frac{\partial (huv)}{\partial y} = -gh\frac{\partial z_b}{\partial x} - ghS_{f_x} \quad (2)$$

$$\frac{\partial (hv)}{\partial t} + \frac{\partial (huv)}{\partial x} + \frac{\partial}{\partial y}\left(hv^2 + \frac{1}{2}gh^2\right) = -gh\frac{\partial z_b}{\partial y} - ghS_{f_y}, \quad (3)$$

where h is the water depth (m), u and v are velocity components (m/s) in the x and y directions, respectively; g is the gravitational acceleration (m/s^2), z_b is the bed elevation (m), and S_{f_x} and S_{f_y} are the friction slopes in the x and y directions.

PINNs modelling process begins with collecting and preprocessing data, such as topographical digital terrain models, hydrological inputs (rainfall events, river flows), and historical flood records. A neural network is then designed to take spatial coordinates (x, y) and time t as additional inputs to estimate water depth h and flow velocities u and v.

The loss function combines data loss (mean squared error, MSE, between predictions and observations), physics loss (residual of SWEs), and boundary/initial condition loss (MSE for constraints), ensuring both data fit and physical consistency. Equation (4) shows the total loss function, L, as a weighted sum of the three components for the PINN: data, physics, and boundary conditions,

$$L = L_{data} + \lambda_1 L_{physics} + \lambda_2 L_{boundary}, \quad (4)$$

where λ_1 and λ_2 are weighting factors that balance the contributions of the physics and boundary/initial condition losses. The network, typically a feed-forward neural network, is trained using gradient-based optimisation, validated against historical or synthetic data, and tested for generalisation. Finally, results are visualised as flood inundation maps, providing information on flood propagation and terrain impacts.

Results and concluding remarks

A synthetic case-study is used as proof of concept to demonstrate the ability of PINNs to model flood dynamics in a simplified 2D domain. The spatial domain is defined as a unit $(x, y) \in [0,1] \times [0,1]$, representing a small area of a floodplain, while the temporal domain spans $t \in [0,1]$, capturing a short period during a flood event. A feed-forward neural network, designed with 3 hidden layers of 50 neurons each and using *tanh* activation functions, takes spatial coordinates and time *t* as additional inputs to predict water depth *h* and flow velocities *u* and *v*. The model enforces the SWEs, Equations (1-3), as physical constraints, ensuring predictions are consistent with the underlying fluid dynamics. Initial conditions are enforced by taking *h* = 1 at *t* = 0, helping to guide the model. Training is performed using the Adam optimiser with gradient clipping to prevent instability (Goodfellow et al., 2016). Figure 1 provides a visualisation of flood dynamics across the spatial domain. Particularly, left-side subfigure highlights areas of high inundation, while the middle and the right subfigures illustrate flow velocity patterns.

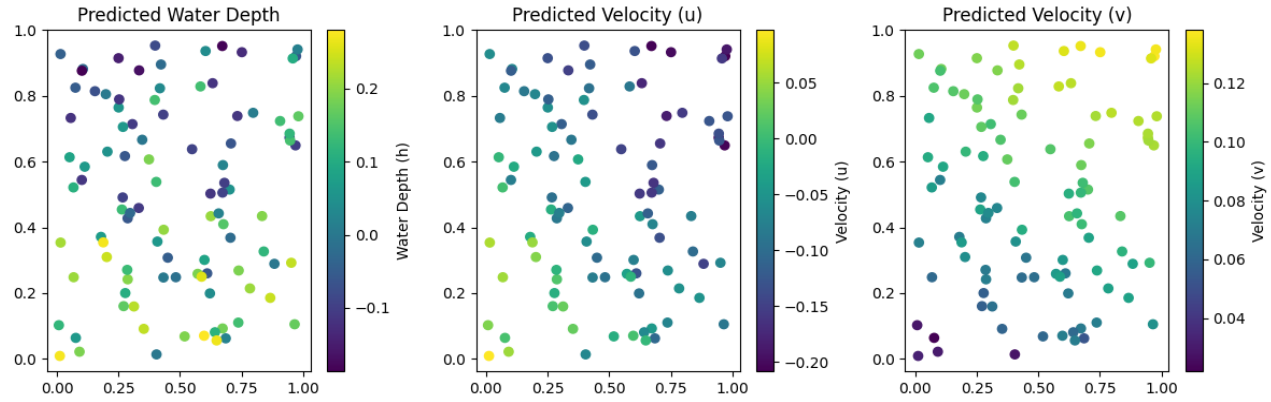


Figure 1. Visualisation of flood dynamics, highlighting areas of inundation and flow velocity.

PINNs provide a data-efficient and physically consistent approach to flood prediction, though challenges remain in computational cost and scalability. The synthetic case study demonstrates their ability to enforce SWEs while accurately estimating water depth and flow velocities. Future work aims to extend this approach to larger domains, integrate real-world topographical and hydrological data, and validate estimations against numerical and experimental benchmarks. Enhancing computational efficiency for real-time applications, refining loss function weighting, and incorporating uncertainty quantification will further improve PINN-based flood modelling for risk management and emergency response.

References

Fotovatikhah F, Herrera M, Shamshirband S, Chau KW, Ardabili SF, Piran MJ (2018) Survey of computational intelligence as basis to big flood management: Challenges, research directions and future work. Eng. Applications of Computational Fluid Mechanics 12(1): 411-437. https://doi.org/10.1080/19942060.2018.1448896

Goodfellow I, Bengio Y, Courville A (2016) Deep learning. MIT Press, Cambridge, MA

Raissi M, Perdikaris P, Karniadakis GE (2019) Physics-informed neural networks: A deep learning framework for solving forward and inverse problems involving nonlinear partial differential equations. Journal of Computational Physics 378: 686-707. https://doi.org/10.1016/j.jcp.2018.10.045

Song Y, Shen C, Liu X (2023) A surrogate model for shallow water equations solvers with deep learning. Journal of Hydraulic Engineering 149(11): 04023045. https://doi.org/10.1061/JHEND8.HYENG-13190

XI. Water Distribution and Water Treatment

13th World Congress on Water Resources and Environment (EWRA 2025)
"New challenges in understanding and managing water-related risks in a changing environment"
Palermo, Italy, 24 - 28 June 2025

Decision support tools for early warning and optimized surveillance of drinking water quality from source to tap

M. Rodriguez[1*], C. Ortiz-Lopez[1], A Carabin[2], A. Ardila[1], G. Pelletier[1], C. Bouchard[1], C. Dorea[2]
[1] NSERC Drinking Water Research Chair, Université Laval, Quebec City, Canada
[2] Department of Civil Engineering, University of Victoria (BC), Canada
* e-mail: manuel.rodriguez@esad.ulaval.ca

Introduction

Decision support tools (DSTs) can play a crucial role in drinking water management, particularly to protect water sources, improve water treatment and optimize water quality monitoring in distribution networks. DSTs are particularly useful when the temporal and spatial variability of water quality is significant. This occurs in many water distribution systems around the world and intensifies due to land use and climate change. The quality of water varies as it flows from the source to the water distribution network due to numerous factors (soil and vegetation, meteorology, anthropogenic activities, treatment operations, network characteristics, pipe materials, hydraulics, etc.). All these factors dynamically alter water quality, sometimes severely degrading it. Influences of all these factors can be interlinked with water quality conditions establishing cause-effect relationships. Based on these relationships, DSTs can be elaborated to help water managers take adequate operational and planning decisions to assure safe drinking water for all, while minimizing operational and management costs (Zhang et al., 2014; Hamouda et al., 2009).

Materials and methods

In recent years and as part of our research activities, we have produced a considerable amount of data on water quality for each of the three components of the supply system (source, treatment, and distribution). These data have considerable value since they represent the temporal and spatial variability of water quality and the operational and infrastructure components of the supply system that may affect it. To develop DSTs, we take into consideration the spatio-temporal data of water quality and information from factors affecting it, using emerging information analysis techniques for prediction and optimization. The use of relevant modelling techniques permits the extraction of knowledge from the data. Such techniques consider the complexity of relationships that exist between the variability of water quality indicators and operational, environmental, hydraulic and infrastructure conditions. In this conference, we present three applications of DSTs, one for each component of the water supply system: DST-1) The anticipation of source water quality to better adjust water treatment; DST-2) The prediction of the formation of disinfection by-products (DBPs) associated with disinfection by chlorine; and DST-3) The optimization of the routine monitoring of water quality in distribution networks. These DSTs are based on spatio-temporal data of water quality, meteorological conditions, operational conditions of water treatment and distribution, and population characteristics within the distribution systems. To effectively model water quality, powerful and relevant data mining and modelling approaches have been used.

Modelling techniques used in these applications comprise machine learning, linear optimization and multivariate logistic regression.

Results and concluding remarks

Sudden changes in source water quality require modifications to water treatment operations. During sudden climatic events, higher organic matter and turbidity levels may occur in raw waters. To adequately adjust the treatment processes in response to sudden raw water quality changes, treatment plant operators must have access to appropriate and timely information. However, there are often delays between climatic events that deteriorate source water quality and the reactions of operators. This situation often occurs with the coagulation process, where optimal conditions are very difficult to establish in situations of changing water quality. DST-1 is an early prediction model for key indicators of raw water

quality: particles and natural organic matter. In particular, turbidity and UV-absorbance levels are predicted based on meteorological and hydrological information (Figure 1).

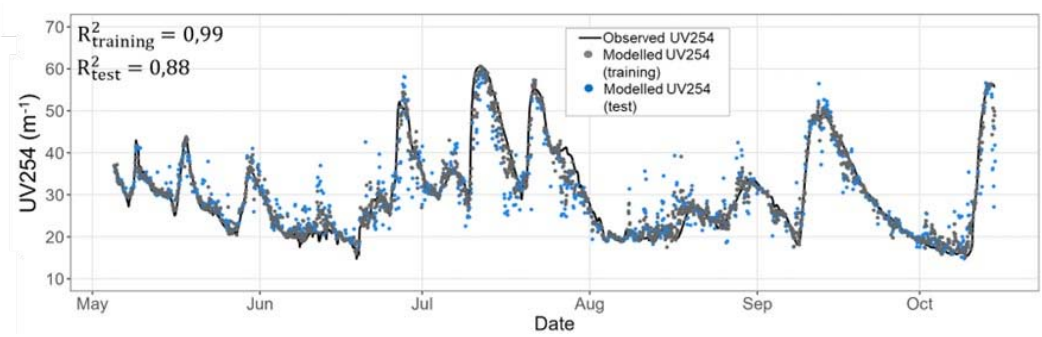


Figure 1. Prediction of UV254 in raw water using a DST based on machine learning techniques (DST-1)

Disinfection by-products (DBPs) derived from water chlorination, the most widely used primary and secondary disinfectant, include numerous species, notably trihalomethanes (THMs) and haloacetic acids (HAAs). These DBPs are subject to regulatory standards in various industrialized countries. Studies conducted over the past years have investigated the formation and evolution of THMs and HAAs in distribution networks (Figure 2a). To identify operational strategies to reduce the formation of these DBPs, a DST was developed to predict their spatio-temporal presence in distribution systems from water quality and operational conditions at the water treatment plant (water temperature, initial DBP levels, residual chlorine concentrations, organic matter indicators, pH and residence time of water within the distribution systems). DST-2 can recommend the best cost-benefit alternative to reduce the levels of DBPs in different locations of the distribution system.

Selecting the appropriate monitoring strategies to routinely monitor water quality in a distribution system is a complicated task. Selecting locations for monitoring requires in-depth knowledge of water quality variability, and infrastructure and population characteristics. DST-3 prioritizes monitoring locations for routine water sampling in a distribution system. This DST is founded on an optimization methodology that focuses on determining the sectors that maximize water quality representativeness by minimizing the spatial variability of key water quality parameters (residual disinfectant, microbiological indicators, and DBPs) and identifying high-risk zones associated with water quality degradation. The methodology also allows for the determination of optimized monitoring locations according to the season (Figure 2b).

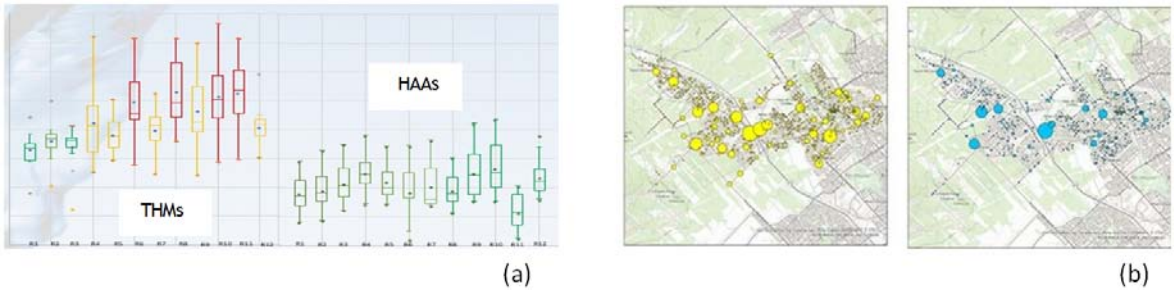


Figure 2. (a) Spatio-temporal variability of THMs and HAAs within a modelled distribution system-DST-2 (box vertical represents temporal variability). Y-axis values vary from 0 to 140ug/L; X-axis represents distribution system location; (b) Prioritization of monitoring locations- DST-3 (left in yellow: summer season; right in blue: winter season. The largest the circle diameter, the higher the location priority)

A detailed description of the development of these three DSTs will be provided during the conference, as well as a discussion of the benefits, challenges and limitations for water utilities to incorporate them in routine and planning decision-making tasks.

References

Hamouda MA, Anderson WB., Huck PM (2009). Decision support systems in water and wastewater treatment process selection and design: a review. Water Science & Technology, 60(7) 1757-1770.

Zhang K., Zargar A, Achari G, Islam SM, Sadiq R (2014). Application of decision support systems in water management. Environmental Reviews, 22, 189-205.

Anomaly detection in water distribution networks based on the analysis of differential pressure values

F. Mazzoni, V. Marsili, S. Alvisi*
Department of Engineering, University of Ferrara, Ferrara, Italy
** e-mail: stefano.alvisi@unife.it*

Introduction

Water distribution networks (WDNs) are complex systems typically featuring thousands of pipes and valves (Marsili et al. 2023), the management of which may be a challenging task for water utilities. In this context, WDN hydraulic models – if properly set up in terms of network features and water-demand patterns – can be useful tools to support water utilities in leakage detection and the identification of anomalies in water consumption (Alvisi 2015, Marzola et al. 2022, Steffelbauer et al. 2022). However, a well calibrated hydraulic model is not always available to water utilities, and sometimes even basic topological or technical aspects (e.g. WDN connectivity, pipe features, etc.) are not perfectly known. Since the last three decades, the advent of WDN digitalization and smart metering has allowed obtaining a large amount of data (e.g. discharge in pipelines, pressure at nodes, water level in storage tanks, etc.) nearly in real-time, opening up new opportunities to water utilities and practitioners. Among these data, pressure measurements may be particularly easy to gather, due to the lower costs of sensors compared to flowmeters, and the possibility of installing them in several sections of the WDN, evenly distributed.

Drawing from the work by Mazzoni et al. (2024), this study investigates the opportunity to exploit pressure data to detect anomalies in WDNs without detailed information about WDN characteristics, and in lack of the hydraulic model. In greater detail, a new methodology – exclusively based on the use of pressure data collected in a series of WDN sections – is presented, allowing the detection of both *hydraulic* anomalies (e.g. unexpected consumption due to unauthorized withdrawal) or *mechanical* anomalies (e.g. breaks, bursts, or gate valves unintentionally left partially or totally closed after maintenance actions) without requiring detailed information on WDN characteristics or the WDN hydraulic model.

Materials and methods

The proposed methodology for anomaly detection exploits pressure data collected through a series of pressure sensors installed in the WDN, and relies on the assumption according to which – under ordinary WDN conditions – the pressure-head distribution varies across WDN nodes and throughout the day based on WDN characteristics and daily fluctuations of water consumption. When an anomaly occurs, a pressure-head alteration is observed in proximity to the area where the anomaly is generated, with nodal-pressure values deviating from related ordinary values. However, variations in nodal pressure may be also related to other factors besides anomalies, e.g. changes in the WDN inlet pressure due to modifications in the controls of pumping systems. To effectively detect anomalies while neglecting other potential causes of pressure variations, the method is based on the analysis of differential pressures calculated in relation to all possible couples of WDN sensors, the ranges of which are expected to deviate from the respective ordinary values only in the case of anomaly occurrence, due to the local pressure-head alteration produced.

Overall, the method is based on six steps: (*i*) identification of a reference period during which the WDN is not affected by anomalies; (*ii*) differential-pressure time series evaluation in relation to all the couples of WDN sensors; (*iii*) definition of reference differential-pressure ranges for each couple of sensors and each hour of the day based on differential-pressure time series of the reference period; (*iv*) comparison of current differential pressures against the respective reference values observed over the same hour; (*v*) alert-level (A) assignment if differential pressure values exceed the respective reference values in the case of at least one couple of sensors; (*vi*) anomaly pre-localization based on the sensor couples related to the highest deviations.

Results and concluding remarks

The proposed method is tested on a real WDN in Northern Italy, featuring around 300 users and provided with a system of 15 pressure sensors collecting data with hourly temporal resolution (Figure 1a). Specifically, a three-week period in relation to which no anomalies are reported by the water utility is considered as a reference, whereas an anomalous event of assigned magnitude (i.e. 0.5 L/s) is generated on the first day of the subsequent week in a given WDN node (i.e. node N1).

Alert levels A produced by the anomaly are shown in Figure 1b-c in relation to the hourly time intervals of minimum and maximum WDN water consumption (i.e. from 3:00 to 4:00 and from 20:00 to 21:00, respectively). Specifically, the anomaly results in the production of alerts (i.e. $A > 0$) in both scenarios, the highest A-values are observed in relation to the couples of sensors in proximity to the area where the anomaly is generated, i.e. sensors S7–S11. This confirms method effectiveness in detecting anomalous events and identifying the area where these events are occurring. At the same time, no alerts are produced due to known water-consumption events of similar magnitude (i.e. about 0.5 L/s) occurring in other areas of the WDN at the same times of the day, due to the fact that these latter events were frequently observed during the reference period, and therefore are not considered as "unexpected" by the approach. In addition, it is worth noting that the maximum A-values obtained at night (up to 8–10 times greater than the width of differential-pressure reference ranges) are much higher than the respective maximum A-values observed throughout the day (1–3 times greater), because differential-pressure reference ranges are typically limited at night due to reduced and constant water consumption.

Overall, the study reveals that: (*i*) the method is effective in detecting and pre-localizing anomalies while disregarding significant (but expected) events; and (ii) method sensitivity varies throughout the day, making it capable of detecting anomalies related to even small water-consumption events at night.

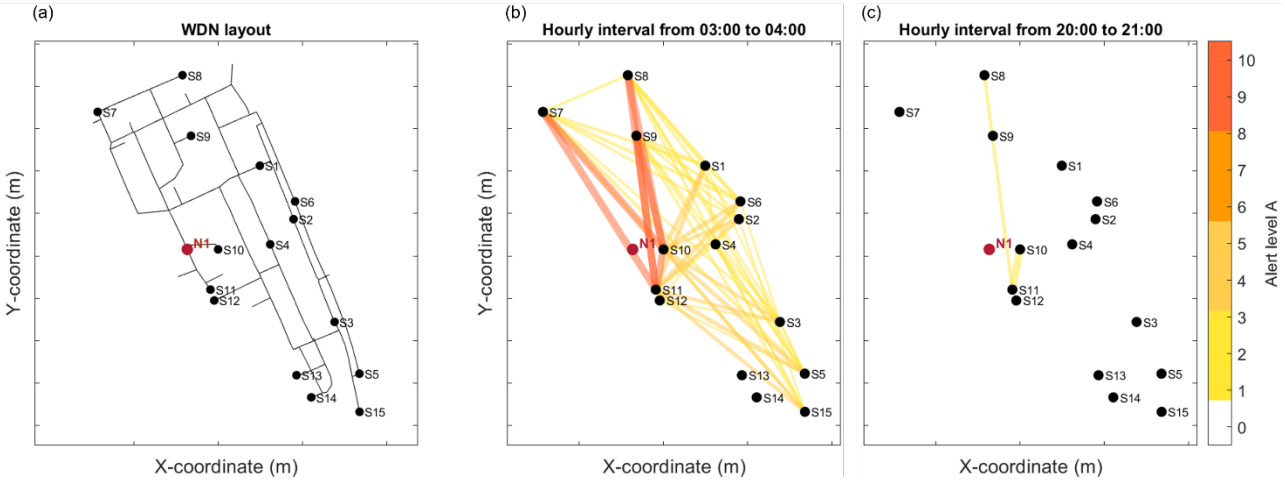


Figure 1. WDN layout (a) and results produced by an anomalous event of assigned magnitude (i.e. 0.5 L/s) in relation to the hourly intervals over which WDN consumption is minimum (b) and maximum (c).

References

Alvisi S (2015). A new procedure for optimal design of district metered areas based on the multilevel balancing and refinement algorithm. Water Resources Management 29(12), 4397–4409. https://doi.org/10.1007/s11269-015-1066-z

Marsili V, Alvisi S, Maietta F, Capponi C, Meniconi S, Brunone B, Franchini M (2023) Extending the Application of Connectivity Metrics for Characterizing the Dynamic Behavior of Water Distribution Networks. Water Resources Research 59(8): e2023WR035031. https://doi.org/10.1029/2023WR035031

Marzola I, Alvisi S, Franchini M (2022) A Comparison of Model‐Based Methods for Leakage Localization in Water Distribution Systems. Water Resources Management, 36: 5711-5727. https://doi.org/10.1007/s11269-022-03329-4

Mazzoni F, Marsili V, Alvisi S, Franchini M (2024) Detection and pre-localization of anomalous consumption events in water distribution networks through automated, pressure-based methodology. Water Resources and Industry 31: 100255. https://doi.org/10.1016/j.wri.2024.100255

Steffelbauer DB, Deuerlein J, Gilbert D, Abraham E, Piller O (2022) Pressure-leak duality for leak detection and localization in water distribution systems. Journal of Water Resources Planning and Management 148(3): 04021106. https://doi.org/10.1061/(ASCE)WR.1943-5452.0001515

Kinetic and isotherm evaluation of simazine adsorption using natural Chilean zeolites: Basis for process optimization

S. Sanzana[1*], A. Fenti[1], P.Iovino[2], A. Panico[1]
[1] Department of Engineering, University of Campania "Luigi Vanvitelli", Via Roma 29, 81031 Aversa (CE), Italy
[2] Department of Environmental, Biological and Pharmaceutical Sciences and Technologies, University of Campania "Luigi Vanvitelli", Via Vivaldi 43, Caserta
* e-mail: silmara.sanzana@unicampania.it

Introduction

The persistence of emerging contaminants (ECs) in water systems and their resistance to traditional wastewater treatment techniques make them an increasing hazard to the environment and public health (Samal et al., 2022). In response, the recent European Directive on Wastewater Treatment mandates the removal of ECs by 2045 for all the plants over 150,000 P.E., thus requiring the implementation of advanced quaternary treatment stages in wastewater treatment plants (WWTPs) to achieve higher water quality standards across Europe. Simazine, a triazine herbicide widely used in agriculture, is one of the most concerning ECs due to its environmental persistence, low biodegradability, and potential toxicity (Gomes et al., 2023). Among all the suitable removal processes, adsorption presents a viable, eco-friendly, and cost-effective alternative for the removal of ECs, particularly when using zeolites as adsorbent materials (Mojiri et al., 2020). Zeolites, with their high surface area and ion-exchange properties, offer significant potential for improving removal efficiency, especially when enhanced through activation techniques and surface modifications. Although zeolites have been investigated for the removal of simazine, existing studies frequently lack a comprehensive analysis of key factors such as cost implications, process optimization, and scalability. This research aims to address these critical gaps by conducting an evaluation and enhancement of zeolite-based adsorption as a highly efficient, sustainable, and scalable approach for simazine removal from aqueous systems. The outcomes of this study are expected to contribute significantly to the advancement of innovative and environmentally sustainable water treatment methodologies, reinforcing their applicability in practical and large-scale scenarios.

Materials and methods

Batch adsorption tests (kinetics and isotherms) in shaking conditions were conducted in 50 mL falcon tubes to evaluate the removal efficiency of Simazine using natural zeolite. Factors such as solution pH (5-7), initial simazine concentration (0.5-4 mg/L) and contact time (1-24 h) were analyzed. Adsorption kinetics (pseudo-first, pseudo-second order, and intraparticle diffusion model) and isotherms (Langmuir and Freundlich) were determined to understand the adsorption behavior and optimize the process.

Results and concluding remarks

In the analysis of adsorption kinetics, the pseudo-second-order model demonstrated the best fit to the experimental data, with R^2 values exceeding 0.95 in most cases. This model suggests that the adsorption process of Simazine onto zeolite is predominantly governed by chemical interactions, involving electron exchange or specific bonding between the adsorbent and the adsorbate. In contrast, while the pseudo-first-order model provided an acceptable fit, its lower R^2 values compared to the pseudo-second-order model indicate that it does not adequately describe the kinetic behavior of the system. The intraparticle diffusion model exhibited the lowest satisfactory fit (R^2<0.9 in some cases), suggesting that internal diffusion resistance is not the primary limiting mechanism in the adsorption process (Revellame et al., 2020). Regarding the adsorption isotherms (see Figure 1), the Freundlich model presented R^2 value of 0.97, while the Langmuir model showed a slightly lower fit (R^2=0.92). This indicates that adsorption does not occur on a homogeneous surface, as proposed by Langmuir, but the adsorption sites are characterized by a wide

heterogeneity, which is consistent with the characteristics of the Freundlich model (Saadie et al., 2015). The results have displayed that the adsorption process can be fine-tuned through changes to the zeolite surface aimed at increasing the adsorption ability under various conditions. These findings lay solid basis for the next stage of the study, which will focus on investigating methods of activation and operation of zeolites to increase their effectiveness in removing Simazine on a large scale.

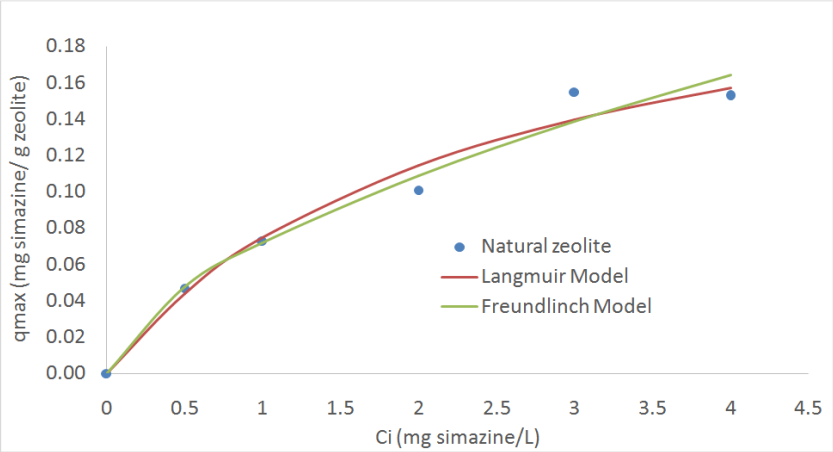


Figure 1. Isotherm models

References

Gomes, F. B. R., Assunção, T. de O. G. de, Dias, Á. C. L., Castro, S. R., Brandt, E. M. F., & Pereira, R. de O. (2023). Assessment of exposure to simazine through drinking waters in Brazil. Environmental Advances, 11(100336), 100336. https://doi.org/10.1016/j.envadv.2022.100336

Mojiri, A., Zhou, J. L., Robinson, B., Ohashi, A., Ozaki, N., Kindaichi, T., Farraji, H., & Vakili, M. (2020). Pesticides in aquatic environments and their removal by adsorption methods. Chemosphere, 253(126646), 126646. https://doi.org/10.1016/j.chemosphere.2020.126646

Revellame, E. D., Fortela, D. L., Sharp, W., Hernandez, R., & Zappi, M. E. (2020). Adsorption kinetic modeling using pseudo-first order and pseudo-second order rate laws: A review. Cleaner Engineering and Technology, 1(100032), 100032. https://doi.org/10.1016/j.clet.2020.100032

Saadi, R., Saadi, Z., Fazaeli, R., & Fard, N. E. (2015). Monolayer and multilayer adsorption isotherm models for sorption from aqueous media. The Korean Journal of Chemical Engineering, 32(5), 787–799. https://doi.org/10.1007/s11814-015-0053-7

Samal, K., Mahapatra, S., & Hibzur Ali, M. (2022). Pharmaceutical wastewater as Emerging Contaminants (EC): Treatment technologies, impact on environment and human health. Energy Nexus, 6(100076), 100076. https://doi.org/10.1016/j.nexus.2022.100076

Supporting regulation and planning in real water distribution systems by water loss performance indicators

S. Ripani[1], S. Piazza[2], L. Berardi[1], D.B. Laucelli[3*], G. Freni[2], O.Giustolisi[3]
[1]University "G. D'Annunzio" of Chieti-Pescara, viale Pindaro, 42, Pescara, Italy
[2] University of Enna "Kore", Cittadella Universitaria, 94100 Enna, Italy
[3] Technical University of Bari, via Orabona, 4, Bari, Italy
*e-mail: danielebiagio.laucelli@poliba.it

Introduction

Water Distribution Networks (WDNs) are vital to supply water to people. Their primary function was to provide water to residents and productive activities, and the main interest was to build aqueducts rather than manage them efficiently. Over the years, with the development of such infrastructures and civil and productive society, the focus has increasingly shifted towards the management of water assets and resources. The technical progress on materials and devices, as well as the greater technical-scientific skills of all operators (engineers, water utilities, academia), fostered the improvement of WDNs efficiency, in terms of efficient water supply of adequate quality, without interruptions, and guaranteeing equal access to water for all users. However, WDNs are affected by water losses, and in some Mediterranean countries their volume can be significant. Water losses in WDNs are generally diffuse dripping due to the combined effect of deterioration and pressure (Farley and Trow, 2015). Pipes deterioration is a natural process that increases over time due to several factors (Kleiner and Rajani, 2001). Pressure is set to supply water to all consumers and depends on spatial and altimetric WDN configuration. Water Loss Performance Indicators (WLPI) (Alegre et al., 2016) have been introduced to evaluate the efficiency in managing WDNs, and adopted by regulatory bodies (e.g., OFWAT, 2013; ARERA, 2017) to evaluate the effects of WDNs operation, planning and maintenance actions.

Materials and methods

This work compares the most adopted WLPIs in the perspective of their use within the water regulation framework and support water companies during the implementation of leakage reduction actions (pressure control, active leakage detection, pipe replacement): the percentage and density water losses performance indicators and the Asset Management Support Indicator (AMSI) (Giustolisi et al., 2024). The density of water losses indicator Dleak [m3/d/km] is the daily volume of leakages normalized to the pipe length of the water system:

$$Dleak = Wleak / L \quad (1)$$

where L [km] is total length of pipes of the water system including private connections, and W_{leak} [m^3/d] is the daily volume of real water losses, that here accounts only for real water losses (depending on pressure-dependent leakage outflows due to pipes deterioration). The percentage water loss indicator $D_{\%}$ is:

$$D\% = 100 \cdot Dleak / (Dleak + Dcons) \quad (2)$$

where D_{cons} [m^3/d/km] is the is the daily volume of consumers demand normalized to the pipe length of the water system. The AMSI is a novel indicator that can be used together with D_{leak} and pressure to better address the investments toward the most efficient leakage management activities among pressure control, pipes replacement plans and active leakage detection. AMSI can be defined at pipe level, DMA level or network level. What follows is for WDN level:

$$AMSI = D_{leak} / (P_{ref})^{\alpha} \quad (3)$$

where P_{ref} is the mean daily pressure and α is the leakage model exponent (Berardi et al., 2025).

Results and concluding remarks

The case study analyses the conditions of 12 WDNs managed by an Italian water company *ex-ante* and *ex-post* the interventions for water loss reduction, and discusses the indications that can be drawn from the application of AMSI, rather than the combined use of D_{leak} and $D_{\%}$. In the limit of this extended abstract, few results will be shown, as summarized in Table 1. The WDNs where optimal DMA design, pressure control and pipe replacement are in light red. Note that the asset management actions has been designed considering the indications given by the AMSI value more than considering only what required by the combined use of D_{leak} and $D_{\%}$, as detailed in Berardi et al. (2025). For example, in WDNs 3-4-11, where there was no margin for pressure reduction to reduce losses, pressure control and DMAs only serve to stabilize and monitor the WDN, while pipe replacement achieves the goal. In the others, it was possible to act on the pressure, as demonstrated by AMSI<1, which indicates that pressure is mostly responsible for water losses.

Table 1. Summary of considered networks ex-ante and ex-post interventions

Network acronym	Ex-ante indicators			Annual recovering required to the water utility [m³]	Work done on the network*	Ex-post indicators			Annual volumes recovered (estimated by hydraulic modelling) [m³]	Replaced Pipes [km]	Compatible pressure [m]
	D_{leak} [m³/km/day]	$D_{\%}$ [%]	AMSI			D_{leak} [m³/km/day]	$D_{\%}$ [%]	AMSI			
WDN-1	13.64	42.0	0.61	49'421	DMA	12.80	40.5	0.58	62'871	0	22.2
WDN-2	4.82	27.7	0.20	2'227	DMA	4.65	26.9	0.20	3'171	0	23.2
WDN-3	13.47	44.0	0.46	8'775	DMA+PC+PR 10%	10.08	37.1	0.34	45'236	3.7	30.1
WDN-4	16.77	56.0	0.74	21'747	DMA+PC+PR 10%	6.43	32.8	0.29	183'221	4.9	21.9
WDN-5	12.54	36.3	0.44	14'921	DMA	11.26	33.9	0.44	31'294	0	25.7
WDN-6	17.23	48.6	0.41	37'559	DMA	15.59	46.1	0.41	58'460	0	37.8
WDN-7	**29.73**	**64.9**	**0.56**	**87'819**	**DMA+PC**	**24.65**	**60.5**	**0.56**	**204'879**	**0**	**44.4**
WDN-8	11.71	50.5	0.23	17'301	DMA+PC	10.59	47.9	0.23	27'345	0	46.1
WDN-9	21.13	68.1	0.85	39'135	DMA+PC	18.76	65.5	0.81	59'776	0	23.2
WDN-10	**15.07**	**47.6**	**0.51**	**93'641**	**DMA+PC**	**11.95**	**41.9**	**0.47**	**317'251**	**0**	**25.7**
WDN-11	**19.26**	62.4	**0.70**	**118'698**	**DMA+PC+PR 16%**	**12.30**	**51.5**	**0.40**	**586'094**	**36.9**	**30.5**
WDN-12	9.09	40.8	0.27	16'337	DMA	8.50	39.2	0.28	21'780	0	30.9

* Pressure control (PC) - Districtualization (DMA) - Pipe replacement (PR)

From water saving perspective, Table 1 shows that the sum of annual water volume recovered in WDN 7-10 is about the same as got replacing 37 km pipes in WDN 11. Therefore, in water scarcity scenarios, when it is urgently needed to save water, the AMSI approach allows the regulator and water utility to address investments towards WDNs where pressure control actions can provide a significant reduction in water losses volume in a short time. Conversely, greater investments on pipe replacement, requiring a longer time to be implemented, will provide a reduction in water losses in a longer horizon. Since water regulation should push towards sustainable use of water resources, especially under water scarcity conditions due to climate changes, such analysis based on AMSI provides a useful support to efficiently allocate public funds among diffent water utilities. This can help in benchmarking best practices, so that water companies can be supported in designing efficient water loss reduction plans across the different networks under their control.

References

Alegre H, Baptista JM, Cabrera et al. (2016) Performance Indicators for Water Supply Services: Third Edition. Water Intelligence Online, 15(0). https://doi.org/10.2166/9781780406336

ARERA - Autorità di Regolazione per Energia Reti e Ambiente (2017) Delibera 917/2017/R/IDR (in Italian)

Berardi L, Ripani S, Laucelli D, Piazza S, Freni G (2025) Using water loss performance indicators to support regulation and planning in real water distribution systems. Digital Water (in press)

Farley M, Trow S (2015) Losses in Water Distribution Networks: A Practitioners' Guide to Assessment, Monitoring and Control (Vol. 4). https://doi.org/10.2166/9781780402642.

Giustolisi O, Mazzolani G, Berardi L, Laucelli D (2024) From advanced hydraulic modelling to performance indicator for the efficiency of investments in leakage management of pressurized water systems. Water Research, 258, 121765. https://doi.org/10.1016/j.watres.2024.121765.

Kleiner Y, Rajani B (2001) Comprehensive review of structural deterioration of water mains: Statistical models. Urban Water, 3(3). https://doi.org/10.1016/S1462-0758(01)00033-4.

OFWAT (2013) Key performance indicators - guidance. Available at: https://www.ofwat.gov.uk/publication/key-performance-indicators-guidance.

Prospects for PFAS removal from wastewater using nitrogen-containing mesoporous silica

O. Dudarko[1,2*], P. Agback[1], T. Agback[1], G. Seisenbaeva[1]
[1] Department of Molecular Sciences, Swedish University of Agricultural Sciences, Box 7015 SE-75007 Uppsala, Sweden
[2] Chuiko Institute of Surface Chemistry of NAS of Ukraine, 17 General Naumov Str., 03164 Kyiv, Ukraine
*e-mail: oksana.dudarko@slu.se

Introduction

Perfluorooctanoic acid (PFOA), also known as C8 and perfluorooctanoate, is a synthetic, stable fluorosurfactant used in various applications, including as a surfactant for the emulsion polymerization of fluoropolymers such as Teflon and Gore-Tex. PFOA has been produced in industrial quantities since the 1940s. It is also formed by the degradation of precursors such as some fluorotelomers. PFOA is a known toxicant and carcinogen in animals (Wang et al., 2021). PFOA has been detected in the blood of more than 98% of the U.S. population at low levels, typically not exceeding parts per billion, with higher levels found in chemical plant workers. Exposure is associated with increased cholesterol and uric acid levels. Exposure has been associated with increased cholesterol and uric acid levels. Additionally, recent studies have linked higher serum levels of PFOA to an increased risk of chronic kidney disease (Choi et al., 2022). This association was independent of factors such as age, sex, race/ethnicity, body mass index, diabetes, hypertension, and serum cholesterol levels (Guidance on PFAS Exposure, Testing, and Clinical Follow-Up, 2022).

The present study was focused on the development and application of special mesoporous silica sorbents (SBA-15) functionalized with amino groups (SBA-NH, SBA-DA and SBA-TA) for the effective removal of PFOA from aqueous media. The adsorbents were synthesized using a templated process involving the condensation of alkylaminosilanes, resulting in materials with high adsorption capacities (up to 649 mg/g for SBA-TA). This work highlights the synergistic role of surface morphology and functionalization in enhancing PFAS adsorption and lays the foundation for scalable, cost-effective solutions to PFAS contamination in water systems.

Materials and methods

All chemicals used in this study, including sodium metasilicate (SS, $NaSiO_3 \cdot 5H_2O$), (3-aminopropyl)triethoxysilane (APTES, Pluronic 123 (P123), N^1-(3-trimethoxysilylpropyl)diethylenetriamine (TPETA, $(CH_3O)_3Si(CH_2)_3NHCH_2CH_2NHCH_2CH_2NH_2$, techn. grade), N-[3-(trimethoxysilyl)propyl]ethylenediamine (TPEDA, $(CH_3O)_3Si(CH_2)_3NHCH_2CH_2NH_2$, 97%), hydrochloric acid (HCl) (37%, w/w), ethanol, were purchased from Merck (Darmstadt, Germany) and Sigma-Aldrich (St. Louise, Missori, USA). PFOA (purity of >90%) was obtained from Fluka Chemical (Switzerland).

Several techniques, including SEM, TEM, IR, XRD, and NMR spectroscopy, were used to confirm the structural and chemical properties of obtained adsorbents. Adsorption studies demonstrated fast kinetics and high efficiency. Electrostatic interactions between protonated amino groups and anionic PFOA molecules were identified as key mechanisms in the adsorption process.

Results and concluding remarks

Details of the characterization methods and the resulting physicochemical properties of synthesized adsorbents have been previously reported. (Dudarko et al., 2024)

^{19}F NMR was used to characterize unbound PFOA and its interaction with the different surface types. The spectra of adsorbed PFOA exhibited distinct characteristics (Fig. 1). It was observed that as the concentration of $–NH_3^+$ groups increased from SBA-DA to SBA-TA, the amount of monomeric PFOA with

narrower linewidths decreased, while the aggregated state increased, as indicated by the broadening of ^{19}F NMR resonances.

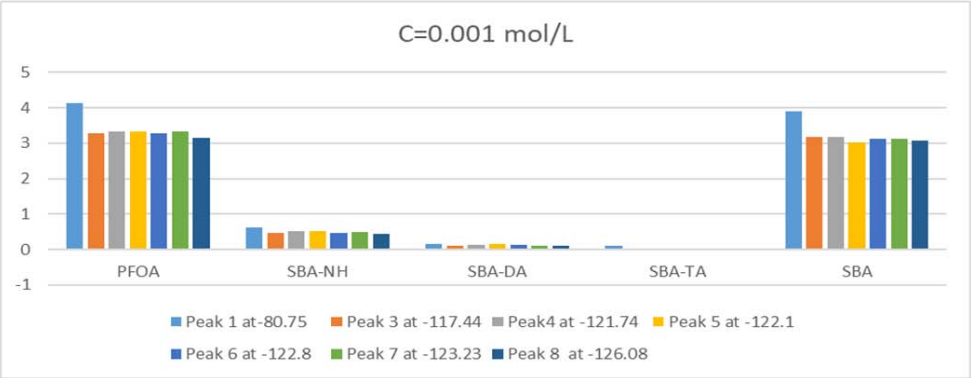


Figure 1. The dependence of the intensities of ^{19}F resonances corresponding to PFOA left in solution (H_2O) after adsorption on the synthesized samples. Intensities were calibrated against a synthetic eretic signal placed at -90 ppm, corresponding to the same concentration in all experiments.

The solid-state NMR spectrum of unbound PFOA (SBA) displayed well-resolved ^{19}F signals with slightly different chemical shifts compared to the solution-state NMR spectra of PFOA (Fig. 1). This phenomenon suggests that PFOA does not interact with NH groups. The adsorption efficiency trend observed via ^{19}F NMR spectroscopy (TA > DA > NH > SBA) aligns well with the results obtained from HPLC analysis (Table 1).

Table 1. Comparison of adsorption capacities of the functionalized SBA-15 materials

Sample	Sorption capacity, mg/g	c_{sorb}, mmol/g	c_{fg}, mmol/g	Ratio c_{sorb}/ c_{fg}
SBA	125.0	0.3	-	-
SBA-NH	294.3	0.7	2.0	0.36
SBA-DA	569.5	1.3	1.25	1.03
SBA-TA	649.1	1.6	1.3	1.20

As a result of this study, several highly effective polyfunctional hybrid organo-inorganic materials were developed as adsorbents for PFAS removal. These materials were synthesized using templated methods and demonstrated high functional group content, well-defined surface area and structure, and uniform pore-size distribution. The amino groups on the adsorbent were protonated, enhancing their ability to interact with PFOA. These protonated amino groups facilitated PFOA adsorption through electrostatic attraction, hydrogen bonding, and Van der Waals forces.

Acknowledgments: Authors are grateful to the project “Multifunctional hybrid adsorbents for water purification" supported by the Swedish Research Council (Vetenskapsrådet) Swedish Research Program, Dnr. 2018-2021, and MCAS4Ukraine 2024-2026.

References

Choi, J., Kim, J.-Y., Lee, H.-J., 2022. Human Evidence of Perfluorooctanoic Acid (PFOA) Exposure on Hepatic Disease: A Systematic Review and Meta-Analysis. International Journal of Environmental Research and Public Health 19, 11318. https://doi.org/10.3390/ijerph191811318

Dudarko, O., Budnyak, T., Tkachenko, O., Agback, T., Agback, P., Bonnet, B., Ahrens, L., Daniel, G., Seisenbaeva, G., 2024. Removal of Poly- and Perfluoroalkyl Substances from Natural and Wastewater by Tailored Silica-Based Adsorbents. ACS EST Water 4, 1303–1314. https://doi.org/10.1021/acsestwater.3c00408

Guidance on PFAS Exposure, Testing, and Clinical Follow-Up, 2022. National Academies Press, Washington, D.C. https://doi.org/10.17226/26156

Wang, Zhongyuan, Zhang, T., Wu, J., Wei, X., Xu, A., Wang, S., Wang, Zengjun, 2021. Male reproductive toxicity of perfluorooctanoate (PFOA): Rodent studies. Chemosphere 270, 128608. https://doi.org/10.1016/j.chemosphere.2020.128608

A new perspective on head loss estimation in water systems: Refining the Hazen-Williams equation

N. Samarinas*, C. Arapakis, C. Evangelides, A. Loukas
Laboratory of Hydraulic Works and Environmental Management, Department of Rural and Surveying Engineering, Aristotle University of Thessaloniki, 54124, Thessaloniki, Greece
** e-mail: smnikiforos@topo.auth.gr*

Introduction

Over the years, numerous equations have been developed for calculating head losses in pressurized pipes. Two of the most widely known and utilized formulas are the Darcy–Weisbach (D–W) (Rouse, 1943) and the Hazen–Williams (H–W) equations. The D–W equation is renowned for its reliability and versatility, as it can be applied to various types of fluids (Amartian et al., 2021; Abdulameer et al, 2022). However, despite its widespread use, it poses challenges due to the difficulty of determining the dimensionless friction factor (f).

In contrast, the H–W equation offers a more user-friendly approach, as it does not require the friction factor for its application. Instead, it relies on a constant coefficient C, which is independent of the Reynolds number and unaffected by factors such as temperature or water viscosity—unlike the friction factor in the D–W equation. Additionally, C depends on the pipe material and its age but does not account for flow type, whereas the D–W equation's friction factor does. Despite this advantage, previous studies (Ormsbee, L. and Walski, T, 2016) have shown that the original H–W equation is less accurate than the D–W equation.

Given these considerations, this work thoroughly examines the original H–W equation with the objective of improving and modifying it to be more efficient for water network design. Through a series of calculations and tests, head losses per unit length of the pipeline were analyzed across various combinations of discharge rates, pipe diameters, and roughness coefficients. Adhering to all necessary constraints and regulations governing pressurized pipes—such as acceptable flow velocities and pipeline continuity—efforts were made to align the results of the H–W equation with those of the D–W equation, using the latter as a reference. The ultimate goal was to develop a modified H–W equation applicable across different ranges of roughness coefficients for pipe of PVC (Polyvinyl Chloride) material.

Materials and methods

Both D–W (Equation 1) and H–W (Equation 2) equations are empirical relations that demands the knowledge of several initial parameters.

$$H_f = f \cdot \frac{L \cdot V^2}{D \cdot 2 \cdot g} \tag{1}$$

$$H_L = L \cdot \frac{10.67 \cdot Q^{1.852}}{C^{1.852} \cdot D^{4.8704}} \tag{2}$$

In the above equations the H_f and H_L are the head losses per meter for D–W and H–W equations, respectively. Furthermore, f is the friction factor of D–W equation, L is the length of the pipe, V is the velocity inside the pipes, D is the pipe diameter, g is the gravitational acceleration, Q is the discharge in the pipe and C is the constant coefficient of H–W equation. The primary data used in the numerical experimental procedure are those illustrated in the Table 1.

Table 1. Primary data used in the numerical experimental procedure

Pipe Length (L) (m)	Roughness Coeff. (K) (mm)	Kin. Viscosity (ν) (m^2/s)	Discharge (Q) (l/s)	Internal Diam. (D) (mm)	Coeff. C for PVC
1	0.003	$1.31 \cdot 10^{-6}$	20 to 500	97 to 552.8	150

Results and concluding remarks

After calculating head losses using both equations and the data in Table 1, the Relative Mean Square Error (RMSE) was minimized using the Generalized Reduced Gradient nonlinear optimization method, assuming constant values of C=150 and K=0.003mm. This led to a modified H–W equation. However, applying the modified equation to a real pressurized water network in Greece (Limnochori irrigation network) (Samarinas et al., 2024) with varying K values (≠0.003 mm) revealed significant deviation s from the D–W reference equation. This necessitated further refinement to improve accuracy.

The new testing procedure used representative roughness values for PVC pipes (approx. 0.0015-0.007mm) rather than arbitrary selections, because these materials have smooth inner surfaces and low resistance to flow. Using representative PVC roughness values enhances modelling accuracy, aiding flow prediction, design optimization, and efficiency. To define the roughness coefficient range for further tests, the widely accepted Moody diagram was consulted, which showed that absolute roughness coefficient, K, varies from 10^{-6} mm to $5 \cdot 10^{-2}$ mm. Higher roughness values were also considered, as pipe roughness increases with age. The individual five sections and the corresponding developed modified formulas are presented in Table 2 supported also by the RMSE results against the D–W equation.

Table 2. Proposed H-W formulas based on the roughness coefficient value ranges supported by the RMSE against the D-W equation

Roughness Coefficient (K) range	Hazen–Williams formula	RMSE
10^{-6} to 10^{-4}	$H_L = L \cdot \frac{10.67 \cdot Q^{1.8150}}{C^{1.8619} \cdot D^{4.8151}}$	0.0036
10^{-4} to 10^{-3}	$H_L = L \cdot \frac{10.67 \cdot Q^{1.8164}}{C^{1.8617} \cdot D^{4.8177}}$	0.0034
10^{-3} to $5 \cdot 10^{-3}$	$H_L = L \cdot \frac{10.67 \cdot Q^{1.8225}}{C^{1.8607} \cdot D^{4.8317}}$	0.0035
$5 \cdot 10^{-3}$ to $2 \cdot 10^{-2}$	$H_L = L \cdot \frac{10.67 \cdot Q^{1.8425}}{C^{1.8570} \cdot D^{4.8779}}$	0.0047
$2 \cdot 10^{-2}$ to $5 \cdot 10^{-2}$	$H_L = L \cdot \frac{10.67 \cdot Q^{1.8748}}{C^{1.8494} \cdot D^{4.9533}}$	0.0073

The application of the proposed modified H–W equations to the real pressurized water network of Limnochori irrigation network showed that the results are in great agreement with the corresponding results of the D–W equation. Small deviations appeared in some branches of the network which presented extremely small flow rates and pipe lengths. In conclusion, the proposed methodology provides engineers and researchers with a simpler, more efficient way to calculate head losses in pressurized pipelines and networks. By selecting one of the five modified equations based on the roughness coefficient rather than the friction factor, engineers can achieve accuracy comparable to the D–W equation.

References

Abdulameer L.S., Dzhumagulova N., Zhuravleva L., Alshammari M.H. (2022) Comparison Between Hazen – Williams and Darcy – Weisbach Equations to Calculate Head Loss Through Conveyancing Treated Wastewater in Kerbala City, Iraq, Eastern-European journal of Enterspire Technologies,115(1): 36-43. https://doi.org/10.15587/1729-4061.2022.251385.

Amatriain A., Rubio G., Parra I., Valero E., Andreu D., (2021) Mathematical modeling of nitrogen-pressurized Halon flow in fire extinguishing systems, Fire Safety Journal, 122. https://doi.org/10.1016/j.firesaf.2021.103356.

Ormsbee, L., Walski, T. (2016) Darcy-Weisbach versus Hazen-Williams: No Calm in West Palm. World Environmental and Water Resources Congress. doi:10.1061/9780784479865.048.

Rouse, H. (1942) Elementary Mechanics of Fluids, John Wiley & Sons, Inc., London

Samarinas N, Gravani A, Evangelides C, A Loukas (2024) A Smart Pipe Length Splitting Method for Cost Minimization of a Pressurized Irrigation Network. Water Resources Management. https://doi.org/10.1007/s11269-024-03978-7

Residential water consumption data: integrating parametric and non-parametric approaches to select suitable probability models

A. Cozzolino*, R. Padulano, G. Del Giudice
Department of Civil, Architectural and Environmental Engineering, Università degli Studi di Napoli Federico II, Naples, Italy
** e-mail: alfonso.cozzolino@unina.it*

Introduction

User-level water demands can significantly influence pressure and flow patterns in distribution networks. To fully understand their impact, it is necessary to incorporate in the models the water volumes requested at each node, representing one or more users, while accounting for the associated temporal and spatial variability. In the recent years, advanced monitoring systems have been introduced in water distribution networks, allowing the exact amount of water requested by each user to be recorded at specific time intervals over an extended measurement period. This knowledge can be used to calibrate a procedure for generating synthetic demand patterns at the user or node scale, which are probabilistically consistent with the observational database.

This contribution shows how the integration of non-parametric and parametric approaches can help in reproducing the variability of probabilistic features of water consumption during the day. This is the first step required to realistically reproduce the behaviour of users while properly accounting for different sources of uncertainty.

Materials and methods

The consumption database used refers to a set of 1838 smart meters located in the Soccavo district of Naples. Data refers to year 2016, and a subset of this database has already been processed under different perspectives in multiple scientific works (Padulano and Del Giudice 2018, 2019, 2020; Del Giudice et al., 2020; Evangelista et al., 2023). To ensure homogeneity, only hourly data from weekdays (Mon-Fri, excluding holidays) from all months of the year except August were considered valid for this analysis, totalling 225 measured days and thus 225×24 data points for each of the 1838 meters.

Below are the key points of the approach used:

- For each hour of the day and each individual user (which actually corresponds to a household), hourly consumption can be considered a random variable. In this contribution, only nonzero consumption is considered, and only samples with at least 10 data are processed (this particularly affects samples representing night consumption).
- For each random variable the main moments can be computed, including skewness and kurtosis. Each moment shows a distribution with its own moments.
- High-order moments are used to drive the selection of appropriate probability distributions. Suitability of distributions is investigated by means of the L-moments ratio diagram. Parsimoniously, the "best" distribution is the one that fits well all the investigated samples (each hour, each household).

Results and concluding remarks

Results show a significant variability in the skewness parameter, which ranges between -2 and 8, thus spanning from negative to positive values. This makes typical distributions considered by many authors (such as the Gamma distribution) not suitable, leaving to test only probability models that can exhibit both positive and negative skewness coefficients. Figure 1 shows the distribution of the skewness coefficient for three hours of the day (hour of minimum consumption, peak hour, hour of intermediate consumption). For

all the figures, only a subset of 100 households among the 1838 available is used, for better visualization. However, for numerical assessments all the records are used.

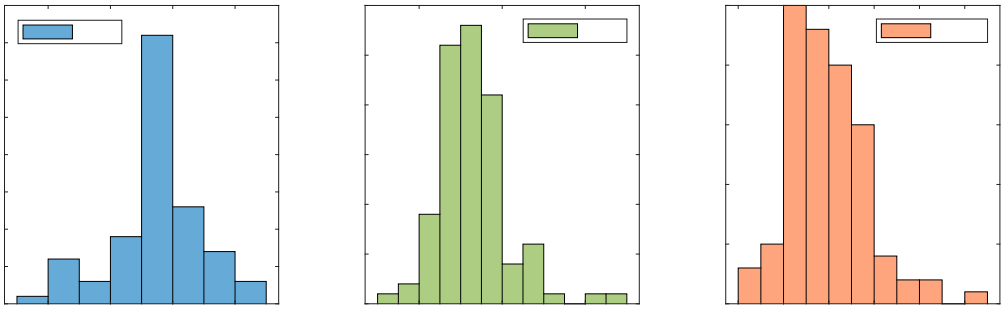


Figure 1. Histogram of skewness coefficient for three hours referring to consumption data of 100 households.

Figure 2 shows the L-moments ratio diagram for all the data, sampled according to the previous section. This means that each point in the figure represents a sample corresponding to a specific household, and the colour represents the hour of the day. It can be noted that the larger negative skewness is exhibited by hours of low consumption. Also, Figure 2 shows that the distributions that seem to best fit the ensemble of data are Weibull and Pearson Type III, although a large variability can be observed. The performance of candidate distributions will be demonstrated by appropriate metrics such as q-q plots, RMSE, MAE, PBIAS.

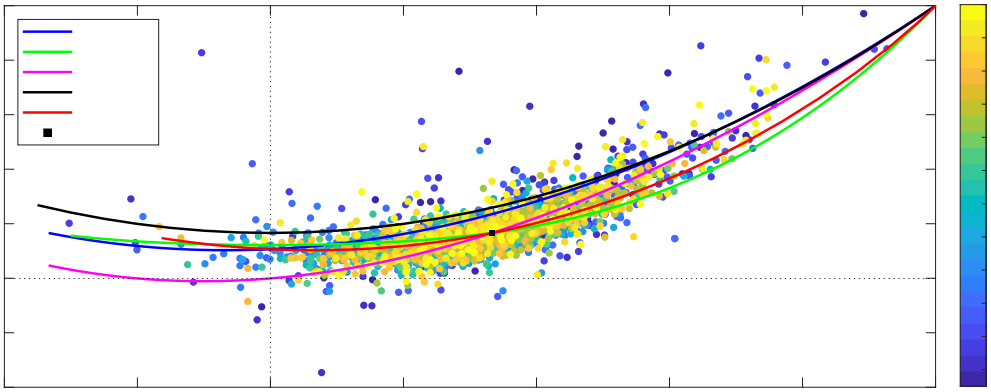


Figure 2. L-moments ratio diagram for water consumption data of 100 households for each hour of the day.

References

Del Giudice, G., Di Cristo, C., and Padulano, R. (2020) Spatial aggregation effect on water demand peak factor. Water, 12(7), 2019.

Evangelista, S., Nardi, M., Padulano, R., Di Cristo, C., & Del Giudice, G. (2023) Analysis of the effects of COVID-19 restriction policies on drinking water consumption by smart water network data filtering. Water Supply, 23(9), 3746-3760.

Padulano, R., and Del Giudice, G. (2018) A mixed strategy based on self-organizing map for water demand pattern profiling of large-size smart water grid data. Water Resources Management, 32, 3671-3685.

Padulano, R., and Del Giudice, G. (2019) Pattern detection and scaling laws of daily water demand by SOM: an application to the WDN of Naples, Italy. Water Resources Management, 33, 739-755.

Padulano, R., and Del Giudice, G. (2020) A nonparametric framework for water consumption data cleansing: an application to a smart water network in Naples (Italy). Journal of Hydroinformatics, 22(4), 666-680.

Resilience and performance indices for water supply systems: The case study of Valle Umbra

M. Ferrante[1*], G. Piccirillo[2], F. Provvisiero[2], F. Rossi[1], S. Schiaroli[2]
[1] Department of Civil and Environmental Engineering, University of Perugia, Perugia, Italy, EU
[2] Valle Umbra Servizi s.p.a., Spoleto, Italy, EU
* e-mail: marco.ferrante@unipg.it

Introduction

Resilience indices have been introduced to evaluate two different characteristics of water infrastructure systems, i.e., the ability to bounce back and recover from failures (Hashimoto et al. 1982) and the available surplus of energy to be dissipated in case of failure (Todini, 2000). The latter has been widely used in the multi-objective design of water distribution systems, for which the redundancy of the topology is one of the main characteristics. Only a few attempts have been made to analyse the performances of water supply dendritic systems by similar indices (Beygi et al, 2019). In this case, the failure of a pipe cannot be bypassed by the natural ability of the system to redistribute the water flows among concurrent pipes, and the water distribution cannot be ensured downstream from the failed pipe.

Besides failures, resilience can also be measured by considering all other accidents affecting water supply and distribution systems, such as water shortages due to droughts and abnormal and unpredicted demands. The availability of alternative water sources and the change in the energy balance, increasing input and reducing output, can increase the ability of some systems to respond to crises better than others. In this sense, single system improvements, such as the change in diameters, pipe doubling, and change in the pumping system, can increase the resilience of each system, as system interconnections can lead to an increase in the overall resilience.

Valle Umbra Servizi s.p.a. (VUS) manages the water supply and distribution systems of the Valle Umbra in the Umbria region of Italy, comprising the cities of Foligno and Spoleto. In the activities related to defining a new master plan, VUS funded a research project with the Department of Civil and Environmental Engineering of the University of Perugia, Italy. The main aim of the master plan was to define different resource and demand scenarios in the next decade and, consequently, investigate the possible improvements and interconnections of the existing water supply and distribution system to increase global resilience to demand peaks and water scarcity.

Materials and methods

Concerning the system improvement strategies, different possible solutions were considered to satisfy the changing demands, assuming a spatial and temporal variation of the available resources. To help compare quantitatively different possible strategies of system interconnection and to investigate how they can also allow further developments in the forthcoming decades, resilience and other indices have been evaluated for water supply systems before and after the interconnections.

The two main systems manged by VUS, Valle Umbra and Argentina, have been modelled assuming different configuration and interconnection hypotheses. The functioning scenarios have been defined considering two demand conditions, normal and stress, and two resource availability conditions, normal and scarcity. The normal and stress demand conditions were evaluated by analysing the measured discharge outflows, considering the mean and the maximum daily demands. The normal and scarcity resource availability were evaluated by the analysis of the measured discharge time series at springs and wells, considering the mean and the minimum flow for a return period of 20 y.

In addition to the already available, two new indices have been introduced and tested to evaluate the resilience as the difference between the available energy and discharge in normal and extreme conditions.

Results and concluding remarks

The possible improvements and interconnections of the Argentina and Valle Umbra supply systems were compared. The hydraulic models of the systems were used to simulate the different demand and feeding conditions. The resilience index was only evaluated for the possible scenarios, excluding the simulations resulting in inconsistent water and energy balances and pressure distributions. This allowed the evaluation of the energy and water surplus with reference only to feasible and actual stress conditions, excluding from the evaluation the energy and mass surplus that could be considered in principle but not involved in practice.

The original contributions are both in the extensive application of performance indices to water supply systems and in the case study results.

Acknowledgments: This work was supported by the Valle Umbra Servizi S.p.A. grant *Scientific and technical support for the Integrated Water Service infrastructure plan, consistently with AURI documents and guidelines.*

References

Beygi, S., Tabesh, M., and Liu, S. (2019). Multi-Objective Optimization Model for Design and Operation of Water Transmission Systems Using a Power Resilience Index for Assessing Hydraulic Reliability. Water Resources Management, 33(10):3433–3447.

Hashimoto, T., Stedinger, J. R., and Loucks, D. P. (1982). Reliability, resiliency, and vulnerability criteria for water resource system performance evaluation. Water Resources Research, 18(1):14–20.

Todini, E. (2000). Looped water distribution networks design using a resilience index based heuristic approach. Urban Water, 2(2):115–122.

LIFE SAFE_T_WATER: Validation of a new natural organic polymer for drinking water treatment

M. Añó[1*], P. Almenar[1], J.F. Cabeza[2]
[1] Empresa Mixta Valenciana de Agua, S.A.(EMIVASA) - Grupo Global Omnium, València, Spain
[2] Serviecología y Tratamientos de Aguas S.L (SERVYECO), Castelló, Spain
*e-mail: miaso@globalomnium.com

Introduction

The drinking water treatment process aims to produce a high-quality effluent suitable for human consumption. This process begins with a pre-oxidation stage, where organic and inorganic matter is treated with substances such as chlorine, chlorine dioxide, ozone, and potassium permanganate to break down harmful compounds.

Next, during the coagulation stage, colloidal substances and microorganisms responsible for turbidity are removed by adding inorganic salts such as aluminium sulphate or ferric chloride, forming flocs that facilitate the separation of impurities. Subsequently, coagulant polymers are introduced to enhance flocculation and the aggregation of suspended particles. After settling and filtration, the water undergoes disinfection using chlorine, chlorine dioxide, ozone, and chloramines to eliminate pathogens. These disinfectants remain in the treated water, ensuring its quality.

However, these processes generate by-products with a significant environmental impact. To address this issue, the LIFE SAFE_T_WATER project (LIFE19 ENV/ES000049) has validated a sustainable technology that employs a natural organic polymer to replace synthetic substances in key stages such as coagulation, flocculation, and pH adjustment, thereby reducing environmental impact and improving overall efficiency.

Materials and methods

Raw water contains solids of various types, including clays, plant materials, algae, and other organic and inorganic substances of different sizes. Larger particles settle easily, whereas smaller ones remain in a colloidal suspension due to their negative electric charge, which causes mutual repulsion and prevents aggregation. To facilitate their separation, aluminium sulphate is commonly used as a coagulant, neutralizing the charge. However, this process introduces aluminium ions into both the treated water and the sludge generated.

The concentration of these ions in treated water is regulated and limited. In Spain, 99.37% of water supplies comply with the standards established by national regulations (Ministry of Health, 2019).

Although these chemical reagents pose no risk to human health through water consumption, their accumulation in sludge—subsequently disposed of in landfills—can lead to environmental contamination of the air and soil.

The technology was tested at two Drinking Water Treatment Plants (DWTPs), one located in Madrid and the other in the city of València. For the latter, the validation was carried out using a pilot-scale installation at the La Presa DWTP (Figure 1). This pilot plant included a coagulation, flocculation, and lamellar settling stage, with a nominal flow rate ranging from 1 to 6 m^3/h.

Raw water was transferred from the intake to a homogenization tank, from which it was pumped into the coagulation basin, where the natural coagulant was added under rapid mixing conditions. The next stage involved slow mixing in the flocculation basin, followed by passage through a lamellar settler. The process was then completed with chlorination, pH adjustment, and final sand filtration.



Figure 1. Pilot plant.

The comparison between the natural polymer and polyaluminum chloride shows that, at influent turbidities of 13 NTU and flow rates of 2-5 m^3/h, the natural coagulant achieves 20-30% higher turbidity removal. This performance improves in the absence of pre-oxidation, also allowing for a reduction in the dosage of the natural coagulant.



Figure 2. Flocs using polyaluminum chloride and natural coagulant.

The formation of flocs exhibits a larger size when using the natural coagulant, achieving a higher flocculation density with lower dosages (Figure 2). Additionally, the floc adheres more effectively to the surface of the lamella compared to the floc formed by the aluminum salt.

Results and concluding remarks

The LIFE SAFE_T_WATER project has demonstrated that it is possible to implement a more sustainable drinking water treatment process by using natural coagulants as a replacement for traditional chemical products. This approach not only enhances treatment efficiency, achieving higher turbidity removal and the formation of denser and more stable flocs, but also reduces the associated environmental impact.

The sludge generated, being free of metals and rich in organic matter with a high active surface area, presents significant potential for reuse in agricultural applications or as a substrate in constructed wetlands, thereby contributing to a more eco-friendly and circular approach to water treatment.

Acknowledgments: LIFE SAFE_T_WATER is a project co-financed by the European Commission (LIFE19 ENV/ES000049) through the Environmental and Climate Action financial instrument (LIFE).

References

Ministerio de Sanidad (2019) Informe de la Calidad del agua de consumo humano en España. Ministerio de Sanidad, Madrid.

Combining SCADA and smart meter data to improve anomaly detection at the DMA-level

C. Cincotta[1*], L. Pedroni[2], M. Lombardi[2], G. Nicoli[3], L.C. Zingali[1], C. Bragalli[1]
[1] Dept. of Civil, Chemical, Environmental and Materials Engineering – DICAM, University of Bologna, Bologna, Italy
[2] Dept. of Computer Science and Engineering – DISI, University of Bologna, Bologna, Italy
[3] Hera S.p.A., Modena, Italy
* e-mail: chiara.cincotta@unibo.it

Introduction

In the past decade, increasing adoption of smart sensors in addition to SCADA (Supervisory Control and Data Acquisition) systems has motivated the development of novel data analytics to improve the quality and efficiency of drinking water services (Wu et al. 2022). A vast amount of data, commonly referred to as big data, is collected by this advanced metering infrastructure. A critical issue in utilizing this data for water system management and operation is the prompt detection of anomaly events, which may result from sensor malfunctions, communication failures, new pipe breaks and unauthorized water uses.

The datasets used in this study are provided by Hera S.p.A, one of the main utility companies responsible for water supply and distribution in Emilia-Romagna, IT. For water distribution management, the network is divided into district metered areas (DMAs), where flow is measured at the inlet and outlet points at regular time-intervals. This study focuses on a specific DMA ("w-CO"), which is mainly residential and where smart water metering has been applied for more than 3 years at around 35% of the users. Furthermore, w-CO includes an industrial user with high water demand which is monitored by multiple smart meters. For w-CO, the net flow data (in l/s) is available at 15-minute intervals from January 2022 to July 2024, as well as the repair logs during that period, with corresponding indication of urgency (deferrable/non-deferrable) and repair dates (intervention assignment, start and end of the work). The tree-based unsupervised machine learning algorithm known as Isolation Forest (Liu et al. 2008) is used to identify anomalies in the dataset, which are cross-referenced with repair records (McMillan et al. 2023, 2024), mainly indicating the occurrence of leakage or damage to pipes and connections.

The main novelty of this study lies in the effort to leverage all available field data to enhance anomaly detection at the DMA-level and this is achieved by integrating SCADA system data with that obtained from remote meter reading. By comparing w-CO net flow data with consumption data of the large industrial user present in the DMA, the significant impact of the latter on the former is highlighted, thus justifying the attempt to apply the Isolation Forest (IF) algorithm to net flow time series cleansed of industrial water consumption.

Materials and methods

Abnormal flow rates are identified using the IF algorithm (Liu et al. 2008), which is based on the concept that outliers are typically easier to isolate using separating hyperplanes than normal data points. In terms of decision trees, this places outliers closer to the root node than expected data points. A hyperparameter called Contamination Fraction (CF) sets the outliers/non-outliers classification threshold. In this study, a range of CFs varying from 0.001 to 0.05 is tested. First, raw sensor flow data is pre-processed to smooth spikes caused by system usage (filter backwash) in w-CO, thus increasing the efficiency of the anomaly detection algorithm with equal CFs. It is assumed that each repair assignment date corresponds to the date when the anomaly occurred, which marks the start of a corresponding time window, terminating with the completion date of the work. We restrict our analysis to windows with a duration of six days or less, assuming they correlate with more significant events. These windows are then labelled as deferrable or non-deferrable and cross-referenced with anomalies identified in the flow dataset. Non-deferrable interventions are supposed to be associated with major (and readily detectable) leakage events. In this

study, anomaly detection is carried out on the following w-CO's flow datasets: (1) 15-minute interval flow rates, (2) daily minimum flow rates, (3) 1-hour interval flow rates obtained from (1), (4) 1-hour interval flow rates calculated as (3) minus hourly consumption values of the industrial user. The most common methods for identifying leaks utilize the concept of minimum night flow (MNF), which recognizes that water usage during night-time hours is less variable compared to the daytime (García Vicente et al. 2012). In this study, the concept of MNF is extended to daily minimum flow (DMF) and anomaly detection is applied to the corresponding dataset (2). Hence, the DMFs can be used as a baseline for comparison with new minimum flow data, with a significant increasing indicating a leakage. It is expected that an automated analysis of DMFs could simplify what is currently a periodic analysis carried out by employees of the water utility.

The idea behind applying IF to dataset (4) is to identify anomalies potentially harmful to the system, discarding those attributable to actual authorized consumption within the DMA. Given the presence of an industrial user with highly variable water demand (l/h), it is decided to subtract its contribution from the net inflow into the district, which is aligned with the large user's dataset, resulting in dataset (3).

For each dataset and CF, anomalies identified through IF are counted and marked with a cross. In this way, it is possible to assess the performance of the algorithm in terms of both the nature of detected anomalies (e.g., a cross within a repair window is assumed to correspond to a leakage event) and the efficiency in identifying all and only the actual anomalies in the datasets.

Results and concluding remarks

It is observed that the algorithm performs well in identifying both extreme outliers and extended periods of unusual flow rates. Sensor failures and data transmission errors are indeed easily detected as they commonly result in unrealistic plateaus (occasionally with null values) or erratic and spiky trends. A striking example of extreme anomalies that affected w-CO and were effectively detected by the IF algorithm, even for the simplest flow series (1) and for very low CFs (e.g., CF = 0.001), is the two floods occurred in the W-CO area in May 2023 due to the breach of a riverbank. As far as burst/leakage events are concerned, some of the unusual flow data points flagged by the algorithm correlate well with repair interventions, while some repair dates are observed to be away from the outlier data even for high values of contamination, probably due to the limited magnitude of the burst/leakage event. The IF algorithm tends to capture increases in the DMFs, identifying them as anomalies that frequently fall within the repair time windows. The gradual increase in flow is almost never detected in (1), (3) and (4), whereas sudden changes are effectively identified. It can therefore be concluded that the anomaly detection of flows at 15-minute or hourly intervals and DMFs are somehow complementary. Moreover, with the aim of detecting leaks, it seems promising to consider DMFs derived from (4), as they are not influenced by the industry.

The proposed approach is compatible with the current set-up of water distribution systems managed by most water utilities. It may facilitate a time- and cost-efficient identification of anomalies at the DMA-level and better protect it from disruptions and major water losses, which is an important step towards smart and sustainable urban water management.

References

García Vicente J, Cabrera E, Cabrera Jr E (2012) A significant and interesting scientific report. Journal of Scientific Reports 205(4): 83-97. https://doi.org/10.1061/40941(247)35

Liu FT, Ting KM, Zhou Z-H (2008) Isolation Forest. In: 2008 Eighth IEEE International Conference on Data Mining, pp 413-422. https://doi.org/10.1109/ICDM.2008.17

McMillan L, Fayaz J, Varga L (2023) Flow forecasting for leakage burst prediction in water distribution systems using long short-term memory neural networks and Kalman filtering. Sustainable Cities and Society 99: 104934. https://doi.org/10.1016/j.scs.2023.104934

McMillan L, Fayaz J, Varga L (2024) Domain-informed variational neural networks and support vector machines based leakage detection framework to augment self-healing in water distribution networks. Water Research 249: 120983. https://doi.org/10.1016/j.watres.2023.120983

Wu ZY, Chew A, Meng X, Cai J, Pok J, Kalfarisi R, Lai KC, Hew SF, Wong JJ (2022) Data-driven and model-based framework for smart water grid anomaly detection and localization. AQUA - Water Infrastructure, Ecosystems and Society 71(1): 31–41. https://doi.org/10.2166/aqua.2021.091

13th World Congress on Water Resources and Environment (EWRA 2025)
"New challenges in understanding and managing water-related risks in a changing environment"
Palermo, Italy, 24 - 28 June 2025

Liquid and solid phase effects of elevated bioreactor dissolved oxygen

G. Posadas[1], K. Davis[2], S. Miller[1*]
[1] *Department of Civil Engineering, Boise State University, Boise, Idaho, U.S.A.*
[2] *EnviroTech Catalyst, LLC, Boise, ID 83702, U.S.A.*
** e-mail: sondramiller1@boisestate.edu*

Introduction

The concentration of dissolved oxygen (DO) in biological wastewater treatment systems plays a crucial role in both liquid- and solid-phase treatment dynamics, influencing microbial activity, nutrient removal, and biosolids production. This study examines the effects of elevated DO concentrations in an oxidation ditch induced by a high concentration DO infusion system retrofitted into a wastewater treatment plant (WWTP) in Greenleaf, Idaho, evaluating its impacts on both nutrient reduction and biosolids generation. Multi-correlation analyses indicate that elevated DO concentrations enhance nitrogen and phosphorus removal and contribute to increased sludge volume index (SVI), suggesting shifts in microbial community structure and sludge settling quality. Machine learning models reveal a statistically significant, albeit weak, negative correlation between elevated DO and biosolids generation. These findings underscore the dual impacts of increased DO, improving liquid-phase treatment efficiency while altering solid-phase biosolids generation, offering insight into optimizing bioreactor operation for enhanced sustainability.

Materials and methods

This study was conducted at the Greenleaf WWTP in Idaho, a 0.24 MGD facility retrofitted in January 2024 with a high concentration DO infusion system. The system pre-dissolves oxygen into return activated sludge (RAS) before reintroduction into the oxidation ditch.

Wastewater samples were collected over a one-year period (January 2024 to December 2024) from the raw influent, oxidation ditch effluent, RAS before and after DO infusion, and final effluent. The following parameters were monitored: DO, 5-day biochemical oxygen demand (BOD_5), chemical oxygen demand (COD), total nitrogen, total phosphorus, total suspended solids (TSS), volatile solids, sludge volume index (SVI), and adenosine triphosphate (ATP) fractions. On-site measurements for DO, pH, temperature, and ATP, were conducted using a Hach HQ4200 multi-meter and a LuminUltra QG21W test kit. Laboratory analyses followed Standard Methods for the Examination of Water and Wastewater (APHA 2017) and Hach Test 'N Tube (TNT) reagent kit procedures. Biosolids generation data was collected through conveyor runtimes and time-standardized weight monitoring, which was limited by reliance on intermittent operator records and variability in dewatering operations, leading to inconsistencies in measurement availability.

A multi-correlation analysis was performed to assess the impact of elevated DO concentrations on liquid-phase treatment processes using combined Pearson, Spearman, and Kendall coefficients. These analyses evaluated relationships between DO concentrations at the RAS return point and nutrient removal efficiencies, including changes in total nitrogen and total phosphorus. Sludge settleability trends were also analyzed, with a focus on the sludge volume index (SVI) and cellular ATP (cATP) as indicators of microbial activity.

A machine learning-based predictive modeling approach was used to interpolate the limited biosolids generation data. A Random Forest regression model was applied to identify key predictors influencing biosolids generation, while multiple imputation methods addressed missing data in conveyor runtimes. A secondary XGBoost regression model was implemented to refine biosolids generation estimates. Feature selection techniques were used to prioritize the most influential parameters, allowing for a data-driven assessment of the relationship between elevated DO levels and biosolids reduction.

Results and concluding remarks

The high-concentration DO infusion system significantly impacted both liquid-phase treatment and biosolids generation at the Greenleaf WWTP. Correlation analyses showed that increasing DO concentrations at the RAS return point (Figure 1) enhanced nitrogen and phosphorus removal efficiencies. Nitrate concentrations in the oxidation ditch effluent decreased with the increasing DO concentrations in the RAS return point (r = -0.47) which subsequently led to a decrease of total nitrogen in the final effluent. Similarly, phosphorus concentrations in the final effluent declined following system implementation (r = -0.59). A notable operational trade-off was observed in the sludge volume index (SVI), which increased with rising DO levels (r = 0.55), potentially due to microbial shifts negatively affecting sludge settleability.

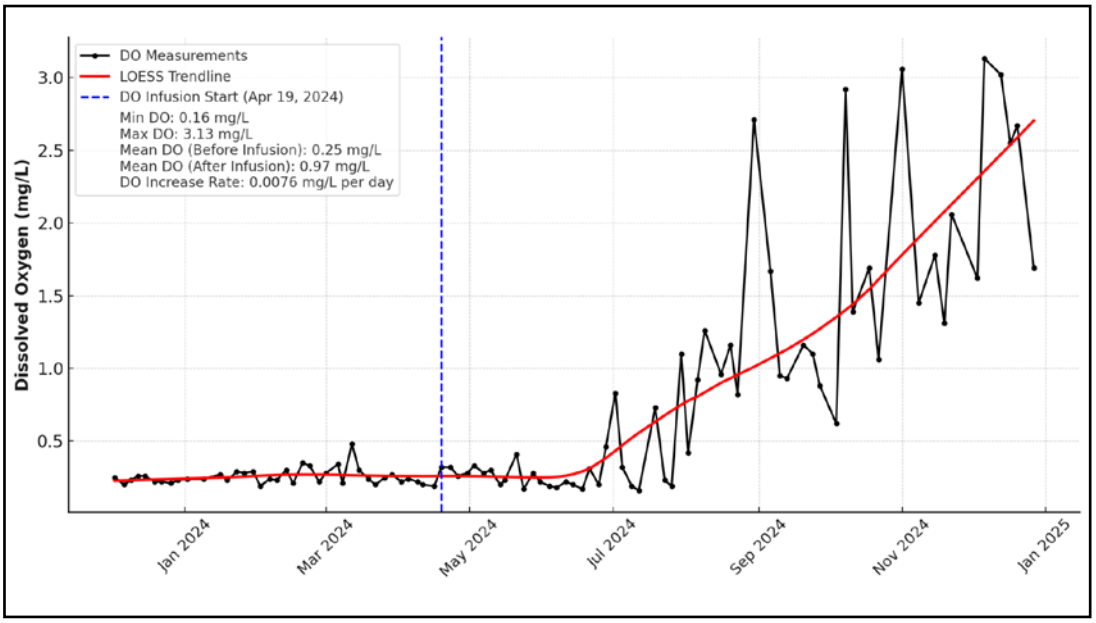


Figure 1. DO increase at RAS return point in oxidation ditch.

Machine learning imputed biosolids generation data revealed a weak statistically significant negative correlation (r = -0.26) between elevated DO and biosolids production. This suggests that higher DO concentration may contribute to reduced biosolids generation, likely by enhancing organic matter degradation before sludge separation. Feature selection methods further highlighted influent BOD_5 (r = 0.76), RAS return point pH (r = -0.72), and oxidation ditch effluent 30-minute sludge volume (r = -0.71) as the strongest predictors of biosolids generation, underscoring the complexity of solids-phase responses to DO enrichment.

These findings demonstrate the dual-phase impacts of high-DO infusion in wastewater treatment. While enhanced oxygenation supports improved nutrient removal, it also introduces operational challenges such as increased SVI. Future research should focus on optimizing DO delivery strategies to balance nutrient removal efficiency with sludge settleability while integrating real-time monitoring systems for better control of liquid-phase and solid-phase treatment dynamics.

Acknowledgments: This research was funded by a grant from BioSolution Holdings Co., Ltd., a company with an interest in the development of high concentration DO delivery systems. The authors also wish to thank research assistants Brandon Osborne, Roy Henson, and Zuly Lapa for their invaluable support and contributions to this project.

References

APHA (2017) Standard Methods for the Examination of Water and Wastewater, 23rd ed. American Public Health Association, Washington, D.C.

Water meter management in water distribution systems: An experimental analysis

A.N. Rizvanoglu[1], F.B. Guneysu[1], I.E. Karadirek[1*]
[1] Department of Environmental Engineering, Akdeniz University, Antalya, Turkey
[2] Antalya Water and Wastewater Administration (ASAT), Antalya, Turkey
* e-mail: ethemkaradirek@akdeniz.edu.tr

Introduction

The sustainable management of water resources has gained growing importance. Minimizing water losses in distribution systems is a key aspect of sustainable water management, as these losses result in resource depletion, elevated water demand, and increased energy and treatment needs for supply (Karadirek and Aydin, 2022). Water losses are defined as the difference between the amount of water supplied to the system and the authorized consumption. These losses are categorized into real and apparent losses. Real losses result from leaks in distribution pipelines, service connections, and reservoir overflows. In contrast, apparent losses stem from unauthorized consumption and metering inaccuracies, where water is provided to consumers without yielding revenue for water utilities (Alegre et al. 2016). In well-managed water distribution systems, metering inaccuracies represent the primary source of apparent losses (Arregui et al., 2018). Precise water metering is crucial for promoting socially equitable pricing (Kanakoudis and Tsitsifli, 2016), while detecting metering inaccuracies is vital for achieving a proper water balance to manage water losses effectively (Lambert and Hirner, 2000). Minimizing apparent losses not only improves the accuracy of water consumption measurements but also generates short-term revenue increases for utilities, thereby contributing to the enhancement of long-term water services for consumers.

This study aims to evaluate the impact of water meter age on measurement errors in large-scale water distribution systems. To achieve this, a series of experimental analyses was conducted to assess the accuracy of customer water meters under realistic operating conditions. The study specifically examines metering errors at different flow rates, which were determined based on actual water consumption profiles of consumers. The findings provide valuable insights into the relationship between meter aging and accuracy, contributing to the development of effective water loss management strategies.

Materials and methods

The metering errors of water meters were determined using the gravimetric method specified in the ISO4064-2 (2014) standard. A test bench, illustrated in Figure 1, was used to evaluate metering errors under varying flow rates. Each individual water meter of varying ages (multijet water meter, R160) was tested, and the measurement errors were calculated using the weighing method, as defined in Equation (1):

$$\varepsilon = \frac{V_m - V_a}{V_a} * 100 \quad (1)$$

where ε represents the error (%), V_m denotes the volume of water recorded by meter, and V_a refers to the actual volume of water.

Results and concluding remarks

The measurement errors of multijet water meters (R160) across varying flow rates and meter ages are presented in Figure 2. The results indicate that measurement errors are significantly higher at low flow rates, with older meters (10–12 years) displaying the largest deviations, often exceeding the maximum permissible errors (MPEs) defined by the ISO4064-1 (2014). At higher flow rates (above 450 L/h), the measurement errors of all meters tend to converge and remain within or near the MPE limits, suggesting that flow rate has a diminishing impact on error as it increases. The results highlight the aging effect on water meter performance, with older meters demonstrating reduced accuracy across all flow rates,

particularly at low flow rates. This decline in accuracy, exacerbated by aging, contributes to apparent water losses due to under-registration of water consumption.

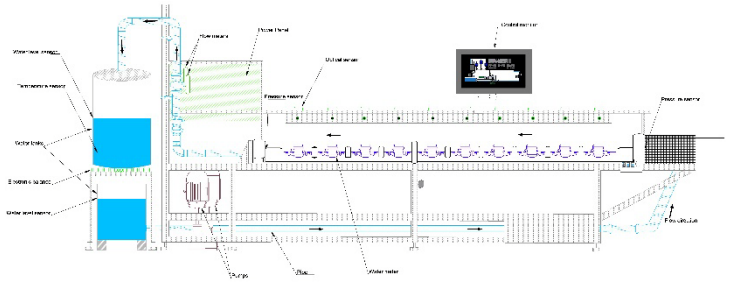


Figure 1. Experimental test setup for analysis of water meter inaccuracies

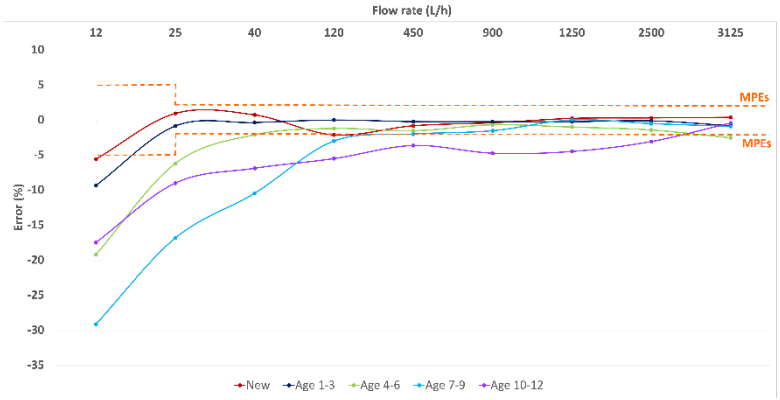


Figure 2. Error curves of tested multi-jet water meter of varying ages

The observed decline in measurement accuracy has critical implications for water resource management. Water utilities face financial losses due to the under-registration of consumption, making periodic meter replacement a cost-effective strategy. The results suggest the need for regulations mandating periodic calibration and replacement of water meters to ensure accurate billing and efficient resource management. Implementing predictive maintenance programs based on error trends can further optimize meter replacement cycles, reducing both apparent losses and operational costs. To mitigate the adverse effects of aging meters, utilities should implement proactive meter replacement programs, consider alternative metering technologies, and enhance regulatory frameworks to ensure sustained metering accuracy. By adopting these strategies, water utilities can improve revenue recovery, enhance water distribution efficiency, and support long-term sustainability in water resource management.

Acknowledgments: This study was funded by The Scientific and Technological Research Council of Turkey (TUBITAK) (Grant No 122Y390) and The Scientific Research Projects Coordination Unit of Akdeniz University (FBA-2023-6444). Authors would like to thank Antalya Water and Wastewater Administration (ASAT) and Emre Akdemir for his support during meter collection.

References

Alegre H, Baptista JM, Cabrera E, Cubillo F, Duarte P, Hirner W, Merkel W, Parena R (2016) Performance Indicators for Water Supply Services: Third Edition. IWA Publishing, London.

Arregui FJ, Gavara FJ, Soriano J, Pastor-Jabaloyes L (2018) Performance Analysis of Ageing Single-Jet Water Meters for Measuring Residential Water Consumption. Water 10(5):18. https://doi.org/10.3390/w10050612

ISO4064-1. (2014). Water meters for cold potable water and hot water – Part 1: metrological and technical requirements.

ISO4064-2 (2014) Water meters for cold potable water and hot water - Part 2: Test Methods. Geneva: International Organization for Standardization

Kanakoudis V, Tsitsifli S (2016) Socially fair domestic water pricing: who is going to pay for the non-revenue water? Desalination and Water Treatment 57(25):11599-11609. https://doi.org/10.1080/19443994.2015.1067169

Karadirek IE, Aydin M.E. (2022) Water Losses Management in Urban Water Distribution Systems. In: Bahadir M, Haarstrick A (eds) Water and Wastewater Management: Global Problems and Measures, 1st ed, Springer International Publishing, Cham, pp 53-65

Lambert A, Hirner W (2000) Losses from water supply systems: Standard terminology and recommended performance measures. IWA's Blue Pages:1-13

Short-term water demand forecast using machine learning models in northern Italy across different time resolutions

M. Niazkar[1,2,3*], A. Menapace[3], F. Peretti[3], M. Righetti[3]
[1] Risk Assessment and Adaptation Strategy division, Euro-Mediterranean Center of Climate Change, Venice, Italy
[2] Ca' Foscari University of Venice, Venice, Italy
[3] Faculty of Engineering, Free University of Bozen-Bolzano, Piazza Domenicani 3, 39100, Bolzano, Italy
* e-mail: majid.niazkar@cmcc.it

Introduction

Water resources management plays a vital role in everyday of human lives. Due to the inevitable growth of population in cities around the globe, the need for drinking water put available water distribution networks under excessive pressure of water demands, particularly during the peak of water use (Antunes et al. 2018). To this end, many studies have been done on applying artificial intelligence techniques to develop estimation models to forecast short-term water demand in water distribution systems (Guo et al. 2018). This study aims to investigate performances of four Machine Learning (ML) models for short-term water demand forecasting.

Materials and methods

In this study, the discharge values were recorded in the water supply systems of two cities, named Aldeno and Cadine, in northern Italy from 2013 to 2022. The data indicated the water demand of each city because the water demand is the summation of water consumption and water leakage in a pipe network. The data can be used to analyze how much water each city needs during the 10-year period of data. The discharge values supplied by water utilities were measured at arbitrary time intervals. Furthermore, the dataset has missing data. The arbitrary time intervals and missing data were addressed to have a consistent one-hour time-step for the whole period of discharge measurements and also aggregated in 3-, 6-, 12-, and 24-hour resolutions. Finally, the water demand at the time t+1 is the target, while discharges at t, t-1, and t-2 were utilized as input.

The four Machine Learning (ML) models used in this study are Linear Regression (LR), Decision Tree Regression (DTR), Support Vector Regression (SVR), and eXtreme Gradient Boosting (XGBoost). The hyperparameters of DTR (max_depth and min_samples_split), SVR (C), and XGBoost (n_estimators, reg_alpha, reg_lambda, learning_rate, and max_depth) were optimized using a grid search technique (Niazkar et al. 2024).

Results and concluding remarks

Figure 1 compares performances of different ML models for predicting water demand in Aldeno and Cadine over various time resolutions. As shown, the results indicate that XGBoost outperformed other ML models over different time scales in terms of four metrics (root mean square errors (RMSE), mean absolute errors, Nash–Sutcliffe efficiency, and determination coefficient). Furthermore, LR and SVR overall yielded less accurate estimations of water demand in comparison with DT and XGBoost. To be more specific, XGBoost reduced the RMSE values achieved by DTR and SVR for forecasting water demands in Aldeno by 2.5% and 30.2% (hourly), by 4.0% and 22.0% (3-hour), by 5.8% and 22.0% (6-hour), by 3.5% and 19.4% (12-hour), and by 7.1% and 20.8% (daily), respectively. Furthermore, XGBoost yielded final solutions within less time in comparison to DTR and SVR. Thus, the comparative analysis not only provides a perspective on the water demand in two cases of northern Italy but also explores the performances of several ML models including XGBoost for water demand forecast. Finally, further investigations are suggested for examining XGBoost potentials for developing versatile water-demand estimators.

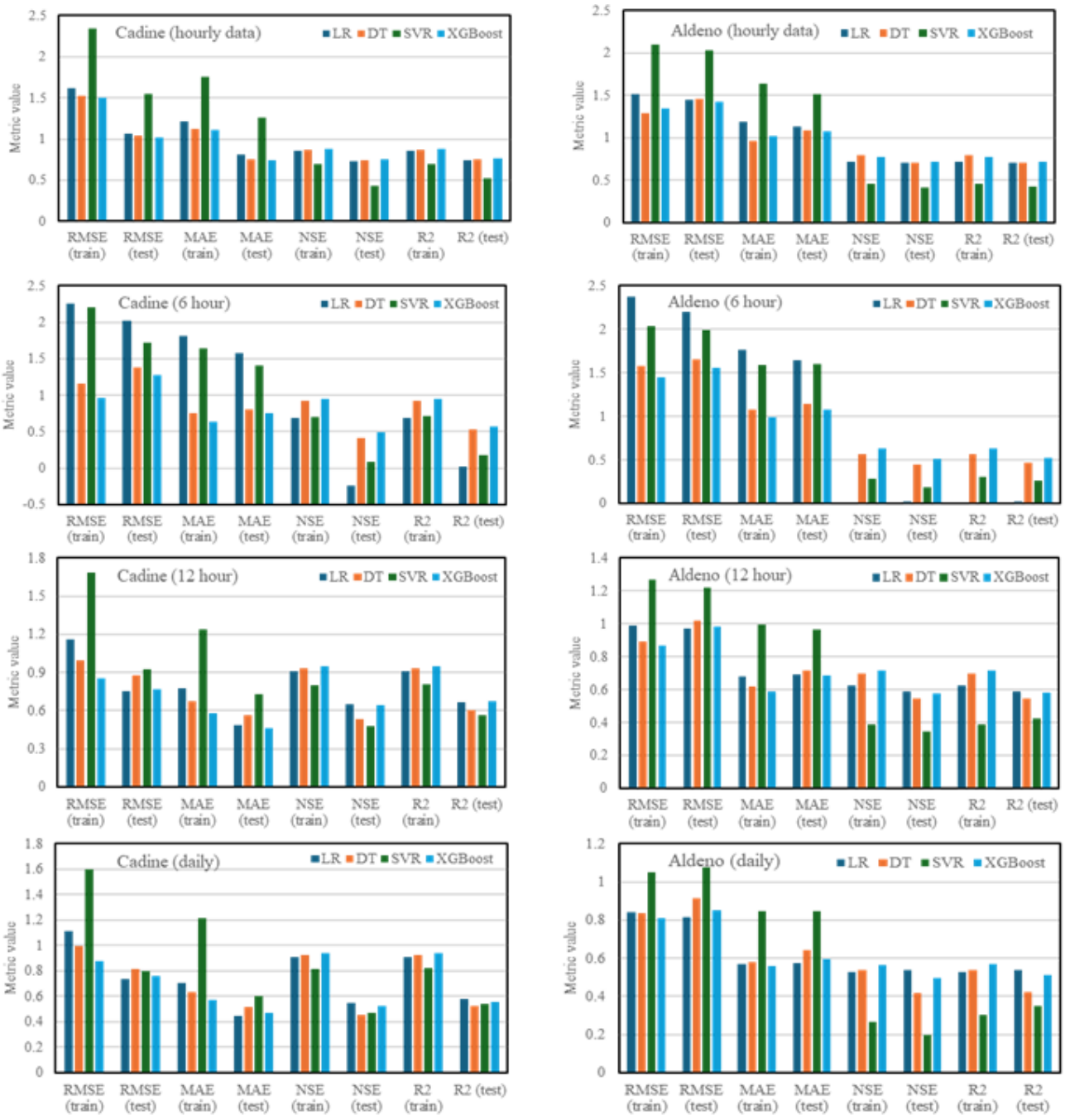


Figure 1. Performances of different ML models for predicting water demand in Aldeno and Cadine over various time resolutions

Acknowledgments: This study has been partially funded by the project "Data driven anomaly detection for sustainable water and energy smart grids management" (DIADEM) of the Free University of Bozen-Bolzano, Italy.

References

Antunes A, Andrade-Campos A, Sardinha-Lourenço A, Oliveira MS (2018) Short-term water demand forecasting using machine learning techniques. Journal of Hydroinformatics 20: 1343-1366. https://doi.org/10.2166/hydro.2018.163

Guo G, Liu S, Wu Y, Li J, Zhou R, Zhu X (2018) Short-term water demand forecast based on deep learning method. Journal of Water Resources Planning and Management 144(12): 04018076. https://doi.org/10.1061/(ASCE)WR.1943-5452.000099

Niazkar M, Menapace A, Brentan B, Piraei R, Jimenez D, Dhawan P, Righetti M (2024) Applications of XGBoost in water resources engineering: A systematic literature review (Dec 2018–May 2023). Environmental Modelling & Software 174: 105971. https://doi.org/10.1016/j.envsoft.2024.105971

Surplus volumes in the Hornád river basin in eastern Slovakia

P. Nagy*, M. Zeleňáková, R. Fijko, P Purcz
Department of Environmental Engineering, Faculty of Civil Engineering, Technical University of Košice, 04200 Košice, Slovakia
**e-mail: patrik.nagy@tuke.sk*

Introduction

River flow is an important element characterizing the size of water resources. The assessment of low flows and high flows is important in hydrology. Low and high flows depend on climatic conditions and are an integral part of the hydrological regime of many rivers. Climate change is increasing the intensity and frequency of dry periods. During long periods, the flow of water from small rivers disappears. Increasing air temperature and increasing variability of precipitation will increase the rate of evapotranspiration. Such changes increase the risk of extremely high flows, which are critical for water management. High flow in studies ranges between the 70th and 95th percentiles. The analysis of low flow is important for research, but also for practical purposes and as an example for water resources planning and management (Tallaksen et al., 1997, Tomaszewski et al., 2021).

Materials and methods

The Hornád Basin is located in the eastern part of Slovakia. It is formed by the Hornád, Torysa and Hnilec rivers [7]. In the current study, 20 hydrological stations were used to assess the discharge in the Hornád

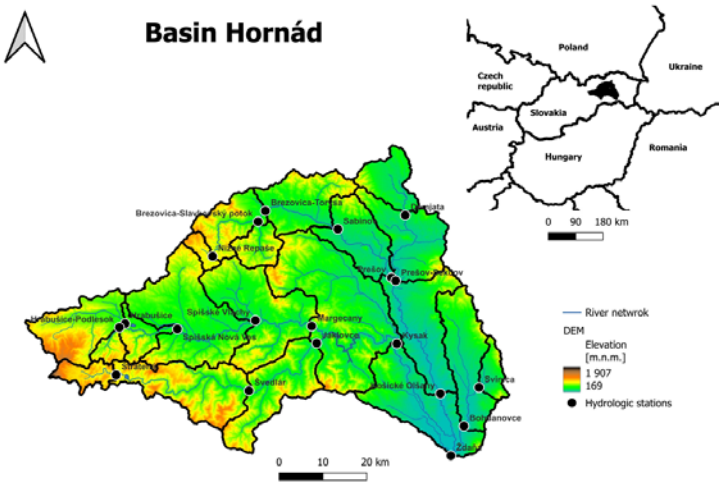


Figure 1. Basin Hornád.

The data were provided by the Slovak Hydrometeorological Institute and covered the research period 1961-2020. For the purposes of this study, a threshold of 90% was adopted to define periods of high discharge. The research period 1961-2020 was divided into 20-year periods. The use of 20-year periods is an appropriate sample size for this study (Hope and Barta, 2012). Excess volumes are volumes that are larger than the Q90 flows. First, the maximum value of surface runoff was chosen - the Q90 quantile. First, it was necessary to calculate the quantile value for all hydrological stations in the Hornád basin. The average daily surface runoff for the period 1961-2020 was used to calculate the quantile, and subsequently the quantiles were calculated for each 20-year period. Subsequently, the Q90 quantile value was subtracted from the daily average surface runoff. Subsequently, all values that represented excess daily flow were selected. If the number of days was more than one, the surface flows were summed, so we know when the high daily flows occurred, how large they were, when they started and when they ended (Tomaszewski and Kubiak-Wójcicka, 2021).

Results and concluding remarks

The results show that there is enough water in the Hornád basin. For the period 1961-2020, the average number of days per year when the flow rates are higher than Q90 is an average of 75-90 days. From the entire basin for the period 1961-2020, an average of 236 million m^3 of water above Q90 will flow out annually. On average, over a period of 60 years, 909.29 million m^3 of water will flow out of the Hornád basin at the Ždaňa hydrological station. In Slovakia, 236 million m^3 of this is above Q90.

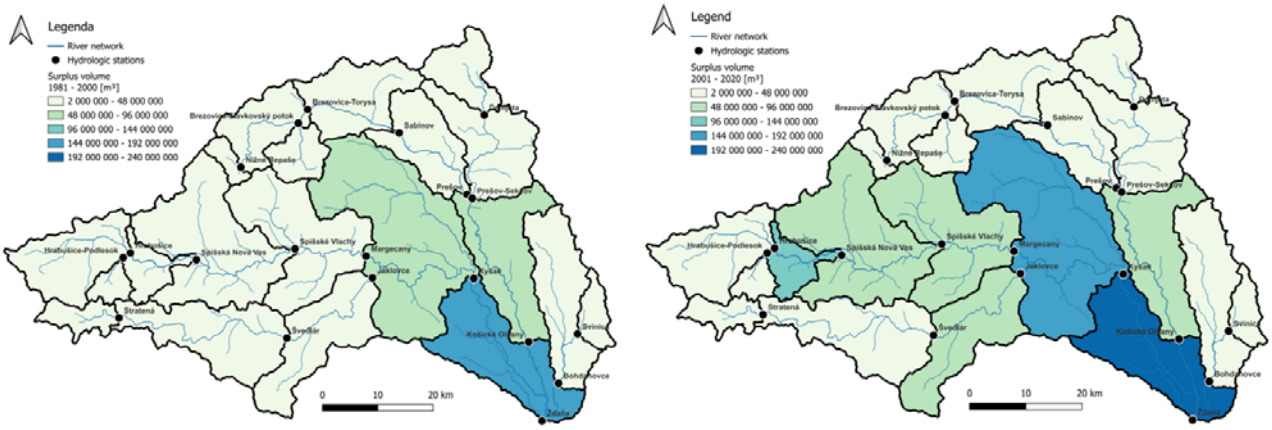


Figure 2. Basin Hornád Surplus volume

The results show that there is enough water in the basin and if we only retained part of the water in the basin, we could cover the periods when the flows were low. In the Spišská Nová Ves sub-basin, if there were periods when the flows were low, there was a lack of water, but on the other hand, if the flows were high, the water from this area only drained away and subsequently local floods occurred in the Spišské Vlachy basin, which is located below the Spišská Nová Ves basin. The results showed us that in the Košické Oľšany sub-basin, in the period 1981-2000 there was a deficit of precipitation, but the maximum surface runoff increased in that period, which could have caused the hydromelioration adjustments made in the 1970s and 1980s, which were aimed at the outflow of water from the area. In the future, it would be necessary to reassess the given adjustments and improve them so that the longitudinal slopes that slowed down the surface runoff are changed.

Acknowledgments: This work was supported by the Slovak Research and Development Agency under the Contract no. APVV-20-0281.

References

Fidlerová, D., & Hlúbiková, D. (2016). Relationships between benthic diatom assemblages' structure and selected environmental parameters in Slovak water reservoirs (Slovakia, Europe). Knowl. Manag. Aquat. Ecosyst. 417, 27 DOI: https://doi.org/10.1051/kmae/2016014

Tallaksen, L. M., Madsen, H., & Clausen, B. (1997). On the definition and modelling of streamflow drought duration and deficit volume. Hydrological Sciences Journal, 42(1), 15-33.

Tomaszewski E., Kubiak-Wójcicka K., (2021), Low-Flows in Polish Rivers, in book Management in Water Resources in Poland, Springer, Cham, Elvetia, DOI: https://doi.org/10.1007/978-3-030-61965-7_11.

An innovative management strategy for WDN under water scarcity conditions

L. Bozzelli[1*], D.B. Laucelli[1], D. Laforgia[2]
[1] Technical University of Bari, Dept. of Civil, Environmental, Land, Building Engineering and Chemistry, Bari, Italy
[2] Acquedotto Pugliese S.p.A., Bari, Italy
*e-mail: l.bozzelli@phd.poliba.it

Introduction

Climate change poses new challenges to managers of urban water distribution networks (WDNs). In particular, long periods of drought, increasingly frequent, put the management of water resources in crisis, having to consider not only the residential user's needs, but also irrigation and industrial users. This situation could potentially create conflicts between stakeholders. Therefore, new management strategies are needed to help water managers to be prepared for water scarcity scenarios. The ongoing digital transition, thus the greater availability of data and digital strategies to transform them in information for decision, provides the opportunity to improve management efficiency for water utilities.

This work will start studying a novel digital strategy to mitigate climate change impacts on urban WDNs. It is based on the novel concept of phenomenological digital twin integrating advanced hydraulic modelling into a Digital Water Services based strategy (Laucelli et al., 2023). The aim is to study operational, tactical and strategic approaches to be prepared to water scarcity scenarios, increasing the system reliability. These strategies are particularly useful for multi-source water networks that, under standard conditions, supply water to certain subsystems, while in water scarcity scenarios need to be reorganized, having to supply other parts of the network differently.

To this purpose the phenomenological digital twin of private tanks (with or without pumping system) is mandatory together with the analysis and modification of District Metering Areas (DMAs) normal configuration. In fact, the goal is preventing from adopting harmful management strategies, such as intermittent flow, which is often adopted under water scarcity conditions (Vairavamoorthy et al. 2008), increasing the leakage rate and generating water quality problems.

Materials and methods

The strategy will be developed starting from the advanced hydraulic model, capable of realistically representing the functioning of real WDNs, considering, among others, georeferenced users and corresponding flow meters (which are therefore not represented collectively in model nodes, but where they are) and background leakages, representative of the WDN deterioration. The model will be calibrated on a certain number of operational cycles representative of the WDN functioning (e.g., weekends, working days, holidays), assuming that the water sources are fully available.

It will be assumed that WDN are fed by more than one type of supply source (e.g., wells, reservoirs, springs, wastewater treatment plants, desalination plants, etc.). This condition is quite common with reference to the most traditional sources, for example in hilly-mountainous areas characterized by the presence of spring emergencies, or in flat areas often characterized by very large aquifers, drawn through well fields; moreover, dealing with climate change consequences (e.g., long periods of drought, reduction of water volumes stored by dams, etc.), leads water companies to make their networks increasingly redundant, also using new sources such as treated wastewater or desalinated water. Another very common condition will be considered, namely the subdivision of the WDN into subnetworks (hydraulically independent) or real DMAs, often used to manage water losses due to network deterioration. The strategy will also consider the use of private storage tanks, usual in latitudes where historically the conditions of limited water availability are frequent, to fully consider the capacity of the WDN in facing water shortages (Fontanazza et al., 2007; Giustolisi et al. 2014).

The assumed supply schemes (with or without pumping capacity) at the single user level are in Figure 1.

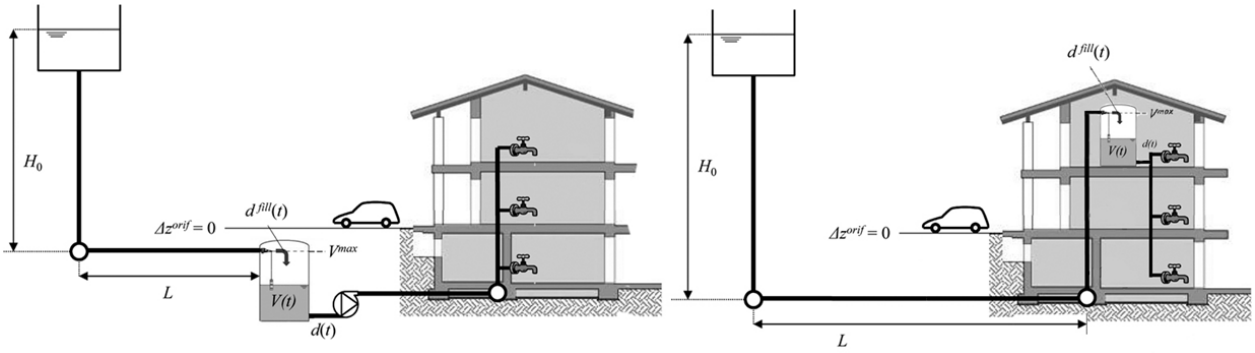


Figure 1. Functional schemes of private storage tanks adopted in the hydraulic modelling of the network (with pumping – left; without pumping right).

The proposed approach will analyse the resilience of a WDN to possible interruptions of one or more supply sources, for example, wells unavailable due to its depletion/contamination of the aquifer. The methodology will expose the users affected by deficit, allowing to simulate the impact of possible technical choices by the water manager, based on the use of the WDN phenomenological twin. Possible actions considered could be (but are not limited to):

- the connection with alternative supply schemes, where existing.
- the increase of WDN hydraulic capacity, e.g., by increasing the diameter of some important supply pipes, or by opening some sectioning valves.
- the determination of new pressure control valves settings, where present, if necessary.

The innovative procedure will be accomplished through the implementation of the achieved innovation as additional features within Digital Water Services, for example to explicitly display the deficit users, the aggregated performances as a reliability indicator (e.g., M2 in Italy) for the entire WDN, and possible criticalities in terms of abnormal functioning of pumps and tanks.

Results and concluding remarks

This paper presents the embryonic phase of a methodology that we will develop in a doctoral thesis at the Polytechnic University of Bari and applied to real Italian networks, as those managed by Acquedotto Pugliese. The methodology aims at exploiting tools and paradigm of the digital transition to improve the efficiency of WDN management in water scarcity conditions, at operational, tactical and strategic term. Additionally, the capacity of the adopted tools (digital/phenomenological twin) will allow to exploit the increasing presence of smart meters at users, which will allow to analyse the real consumptions at shorter time intervals than the current ones (e.g., daily, weekly). This will enhance the support to technical choices for managing water emergencies, as could happen for example, in touristic cities that have completely different consumption and distribution of users from summer to winter. Finally, a further challenging development could be analysing the influence on water quality (e.g., on dynamics of chlorine decay/formation of trihalomethanes) determined by flow paths modifications due to facing water scarcity conditions (and the consequent technical actions undertaken).

References

Fontanazza CM, Freni G, La Loggia G (2007). Analysis of intermittent supply systems in water scarcity conditions and evaluation of the resource distribution equity indices, Water Resources Management IV, WIT Transactions on Ecology and the Environment, doi:10.2495/WRM070591.

Giustolisi O, Berardi L, Laucelli D (2014) Modeling local water storages delivering customer demands in WDN models. Journal of Hydraulic Engineering 140(1). doi: 10.1061/(ASCE)HY.1943-7900.0000812

Laucelli D, Enriquez L, Ariza A, Ciliberti F, Berardi L, Giustolisi O (2023) A digital water strategy based on the digital water service concept to support asset management in a real system. J. Hydroinformatics, IWA, 25(5), doi: 10.2166/hydro.2023.313

Vairavamoorthy K, Gorantiwar SD, Pathirana A (2008) Managing Urban Water Supplies in Developing Countries – Climate Change and Water Scarcity Scenarios. Physics and Chemistry of the Earth 33: 330-339. doi: 10.1016/j.pce.2008.02.008

Emerging contaminants occurrence and treatment with Natural Based Solutions: A pilot setup

M. Perdikaki[1*], E. Chrysanthopoulos[1], K. Markantonis[1], P. Kofakis[1], E. Efstathiou[2], S. Samios[2], I. Dafnos[2], G. Fragkogiannis[3], A. Kallioras[1]
[1] School of Mining and Metallurgical Engineering, National Technical University of Athens, Athens, Greece
[2] Athens water supply and sewerage company (E.YD.A.P.)
[3] PFMEP Rethnink Energy - Electromechanical Consultang and Installation Company
*e-mail: mpredikaki@metal.ntua.gr

Introduction

Emerging contaminants (ECs), such as pharmaceuticals, everyday care products and Per- and Polyfluoroalkyl Substances (PFAS) have been widely discussed throughout the last years due to their strong environmental footprint and their impact on human health (e.g., Li et al. 2024, Gebbink and van Leeuwen 2020). Amongst other sources, wastewater treatment plants (WWTPs) are considered a major point-medium of contamination on surface water, groundwater and the aquatic environment (Jiang et al. 2024). Since ECs treatment technologies are still in process, monitoring and treatment standards have not yet been regulated in the EU legislation on urban wastewater (Directive EU 2024/3019). Yet, the need for ECs and PFAS treatment technologies has emerged to minimize the environmental impact and to comply with EU guidelines and limits in the future.

Nature Bases Solutions (NBS) have been used successfully in the sector of water management and environmental remediation (Alves et al. 2024). NBS technologies seem to be very promising to address ECs and provide environmental remediation on surface water and groundwater bodies (Savvidou et al. 2024). NBS have to offer several benefits against traditional water treatment methods, regarding sustainability, financial and environmental cost (Vineyard et al., 2015). In this research, an innovative NBS pilot system is presented, as a solution to emerging contaminants removal on WWTP effluent. The NBS system was constructed near a WWTP unit in Athens, Greece. The proposed setup includes several compartments with different treatment stages. The main goal of this study is to specify NBS efficiency on targeted contaminants of emerging concern.

Materials and methods

Wastewater Treatment Plant of Metamorphosis (WWTPM) of Athens Water Supply and Sewerage Company -EYDAP- is located at the northern part of Athens Metropolitan area. WWTPM is a receiving and co-treatment facility of domestic wastewater (both septic sewage and municipal wastewater) with an average wastewater inflow of 24,000 m^3/day. WWTPM produces effluent of advanced secondary treatment.

A NBS pilot facility was constructed at the disposal area of the WWTP, designed to improve the treated wastewater, targeting mainly PFAS and ECs in general. The treatment process takes place in three different treatment stages. For this purpose, three cement tanks of 1 m^3 each were constructed and placed at the location of effluent disposal. Different NBS systems are used for every treatment stage. The NBS units involve the following sequence of treatment technologies (Figure 1):

- A phytoremediation unit that provides sufficient removal of nutrients through a floating root constructed wetland (Cyperus papyrus root mat),
- A biochar unit that treats specific pollutants removal. Biochar can remove effectively several PFAS from water
- A Soil-Aquifer-System (SAT), that provides a Managed Aquifer Recharge (MAR) component for improving the advanced secondary treated urban wastewater through contaminants sorption in the solid phase.

The NBS system is energy self-sufficient using solar power (2 x 415W P-TYPE JA solar panel) coupled with a hydro-electrical generator (12V 200W Hydraulic generator inverter generator water turbine). The hydraulic operation is fully automated and controlled remotely. Furthermore, the NBS pilot setup is constantly monitored- in terms of hydrologic and hydraulic variables- through LoRaWAN (Long Range Wide Area Network). communication technologies. The specific technology operates under minimal energy consumption and zero-cost in terms of data transfer capabilities. Frequent sampling campaigns of the NBS effluent will take place at the pre- and post-treatment stages. Advanced analytical techniques for the determination of ECs and PFAS will be utilised. The performance of each technology will be assessed based on the removal of the ECs load that will be succeeded on each treatment stage. Furthermore, the NBS system will be modeled and calibrated with chemical analysis data.

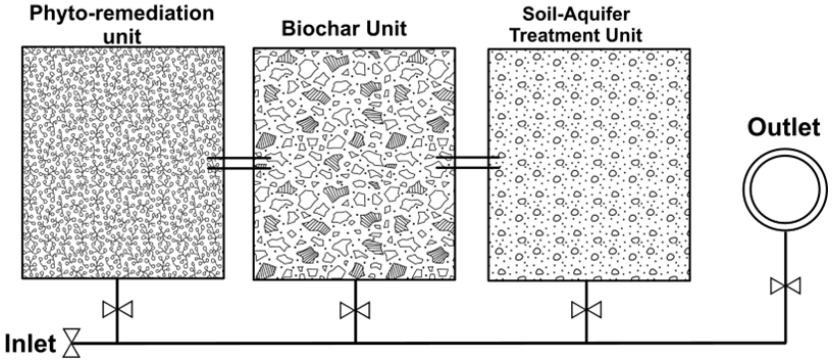


Figure 1. Plan of three stages treatment NBS unit

Results and concluding remarks

Domestic wastewater is considered to be a major source of environmental pollution for contaminants of emerging concern. The newly developed energy self-sufficient pilot setup is equipped with cutting edge technologies in terms of automation and monitoring. The NBS system is expected to isolate and remove ECs from treated wastewater. The performance of the NBS will be monitored and modelled separately at different stages. Useful conclusions on the best NBS technique for ECs removal will arise. Furthermore, this research will provide further insights on emerging contaminants kinetics on the subsurface.

Acknowledgments: This research is part of the project UPWATER (Understanding groundwater Pollution to protect and enhance WATERquality) that has received funding from the European Union under grant agreement No 101081807.

References

Alves, R. A., Rudke, A. P., Martins, L. D., de Melo Souza, S. T., Bovo, A. B., Goroski Rambalducci, M. J., & Martins, J. A. (2024). Urban stormwater management from the perspective of nature-based solutions: A bibliometric review. Journal of Ecohydraulics, 9(2), 218–238. https://doi.org/10.1080/24705357.2023.2284392

Gebbink, W. A., & van Leeuwen, S. P. J. (2020). Environmental contamination and human exposure to PFASs near a fluorochemical production plant: Review of historic and current PFOA and GenX contamination in the Netherlands. Environment International, 137, 105583. https://doi.org/10.1016/j.envint.2020.105583

Jiang, T., Wu, W., Ma, M., Hu, Y., & Li, R. (2024). Occurrence and distribution of emerging contaminants in wastewater treatment plants: A globally review over the past two decades. Science of The Total Environment, 951, 175664. https://doi.org/10.1016/j.scitotenv.2024.175664

Li, X., Shen, X., Jiang, W., Xi, Y., & Li, S. (2024). Comprehensive review of emerging contaminants: Detection technologies, environmental impact, and management strategies. Ecotoxicology and Environmental Safety, 278, 116420. https://doi.org/10.1016/j.ecoenv.2024.116420

Savvidou, P., Dotro, G., Campo, P., Coulon, F., & Lyu, T. (2024). Constructed wetlands as nature-based solutions in managing per-and poly-fluoroalkyl substances (PFAS): Evidence, mechanisms, and modelling. Science of The Total Environment, 934, 173237. https://doi.org/10.1016/j.scitotenv.2024.173237

Vineyard, D., Ingwersen, W. W., Hawkins, T. R., Xue, X., Demeke, B., & Shuster, W. (2015). Comparing Green and Grey Infrastructure Using Life Cycle Cost and Environmental Impact: A Rain Garden Case Study in Cincinnati, OH. JAWRA Journal of the American Water Resources Association, 51(5), 1342–1360. https://doi.org/10.1111/1752

Deep learning approaches for water distribution networks: A comparative study on pressure estimation

G. Restuccia[1,3*], F. Giuliano[1,3], A. Pagano[1,3], D. Croce[1,3], D. Garlisi[2,3], I. Tinnirello[1,3]
[1] Department of Engineering, University of Palermo, Palermo, Italy
[2] Department of Mathematics and Computer Science, University of Palermo, Palermo, Italy
[3] CNIT, Parma, Italy
*e-mail: gabriele.restuccia@unipa.it

Introduction

Water Distribution Networks (WDNs) are dynamic systems that play a critical role in contemporary society by providing a consistent water supply for everyday needs. However, their efficient management faces significant obstacles due to growing urbanization, fluctuating water demands, limited resources, and substantial water losses, estimated at 32 billion cubic meters annually in developing countries (González-Vidal et al. 2019). These challenges are exacerbated by insufficient financial resources and the constraints of conventional measurement and management technologies. To overcome these issues, Smart Water Distribution Networks (SWDNs) have been introduced as innovative solutions. By integrating Internet of Things (IoT) devices with artificial intelligence (AI) methodologies, these systems facilitate real-time monitoring, leakage detection, and pressure regulation through data-driven insights (Kashid et. Al 2014). Building on advancements in SWDNs, Digital Twins have emerged as transformative tools for WDNs. A Digital Twin connects the physical system to its digital counterpart through a continuous data flow. Through AI integration, they simulate network behavior, optimize operations, and derive actionable insights from sensor data, addressing key management challenges and improving efficiency (Ramos et al. 2023). This work introduces a novel strategy to enhance SWDNs. Specifically, it outlines a deep learning approach for pressure prediction, designed for integration into a Digital Twin (DT) to enable predictive analytics, detect anomalies, and support real-time control. Using deep neural networks, the method achieves highly accurate hydraulic predictions with minimal input data, showcasing its potential to transform WDNs and promote their sustainability in addressing contemporary challenges.

Materials and methods

We generate a custom dataset for three benchmark WDNs, Hanoi, Net3, and C-Town, by systematically varying water demand across junction nodes (Shirajuddin et al. 2023). Each network differs in size and complexity, ensuring a broad evaluation framework for Machine Learning (ML) models. For each network, we create 20,000 unique demand scenarios by applying distinct demand multipliers at fixed simulation intervals. These multipliers are generated using Latin Hypercube Sampling (LHS) to ensure diverse and well-distributed demand patterns. The sampled values are rescaled in the range [0.1,2.0], covering demand variations from 10% to 200% of the expected base demand. These multipliers are integrated into hydraulic simulations using the WNTR/EPANET framework with the Pressure-Dependent Analysis (PDA) mode, executing 20,000 independent simulations per network. This dataset ensures ML models learn and generalize WDN behavior under a wide range of operating conditions.

Results and concluding remarks

To validate the predictive capabilities in SWDNs, various types of Neural Networks (NN) are used, such as Multilayer Perceptron (MLP), Convolutional Neural Networks (CNN), and Graph Neural Networks (GNN). All these models take as input an estimate of the predicted demand at each node of the network, obtained by combining baseline values with specific multipliers. For GNNs, additional edge features, such as pipe length and diameter, are included to represent structural relationships between nodes. Each model is designed to predict pressure for all nodes simultaneously, treating the task as a multilabel regression

problem.

The data is then split into 70% for training, 15% for validation, and 15% for testing, with features normalized using a standard scaler. Models are trained over 100 epochs with a learning rate of 0.001, using Mean Squared Error (MSE) as the loss function. The best model is selected based on the lowest validation loss recorded.

Table 1. Performance comparison of DNNs on different SWDN

WDN	DNN	Loss	MSE	MAE	R^2
Hanoi	MLP	0.0001	0.0003	0.0133	0.9999
	CNN	0.0019	0.0064	0.0603	0.9980
	GNN	0.5055	3.2712	1.3719	0.4998
Net3	MLP	0.0001	0.0003	0.0133	0.9999
	CNN	0.0019	0.0064	0.0603	0.9980
	GNN	0.5055	3.2712	1.3719	0.4998
Ctown	MLP	0.0062	0.0233	0.0488	0.9874
	CNN	0.0922	0.2497	0.1844	0.8662
	GNN	0.1456	43.587	2.3886	0.8545

To provide an overview of the results, Table I displays the evaluation metrics for the test set, including Mean Squared Error (MSE), Mean Absolute Error (MAE), and R^2, which assess the accuracy of pressure predictions for the WDNs discussed earlier. The outcomes show an R^2 value of up to 0.9999, highlighting the excellent accuracy and reliability of the models in predicting pressure. Fig. 1 compares the runtime of a one-month simulation using WNTR with the prediction of the same period using NN models. The results demonstrate that, once trained, NNs achieve significantly faster computations.

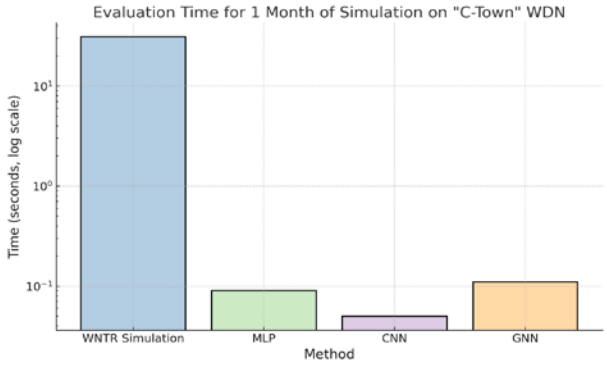


Figure 1. Running time comparison between WNTR and NNs.

In conclusion, the trained ML models can be integrated into the DTs for SWDNs, enhancing efficiency in sustainable water management. The integration of DNNs with DTs is currently under development, with future work focusing on planning the IoT infrastructure and anomaly detection, including leak management.

Acknowledgments: This work was supported by the project “TiSento” (Azione 1.1.5. - POC Sicilia Asse 1 - PO FESR 2014/2020 - CUP G18I18001710007).

References

González-Vidal, A., Cuenca-Jara, J., & Skarmeta, A. F. (2019, April). IoT for water management: Towards intelligent anomaly detection. In 2019 IEEE 5th World Forum on Internet of Things (WF-IoT) (pp. 858-863). IEEE.

Kashid, S. G., & Pardeshi, S. A. (2014, August). A survey of water distribution system and new approach to intelligent water distribution system. In 2014 First International Conference on Networks & Soft Computing (ICNSC2014).

Ramos, H. M., Kuriqi, A., Besharat, M., Creaco, et al. Smart water grids and digital twin for the management of system efficiency in water distribution networks. Water, 15(6), 1129.

Shirajuddin, T. M., Muhammad, N. S., & Abdullah, J. (2023). Optimization problems in water distribution systems using Non-dominated Sorting Genetic Algorithm II: An overview. Ain Shams Engineering Journal, 14(4), 101932

A novel methodological approach to handle high-turbidity events of drinking water treatment plant

F. De Marines*, A. Cosenza, M. Capodici, M Torregrossa, G. Viviani, S.F. Corsino
Department of Engineering, University of Palermo, Palermo, Italy
**e-mail: federica.demarines@unipa.it*

Introduction

Climate change is increasingly impacting the operation of drinking water treatment plants (DWTPs) by degrading surface water quality due to extreme weather events like heavy rainfall and flooding (Verlicchi et al., 2024). This leads to higher levels of turbidity, soluble metals, natural organic matter, and algal blooms, potentially compromising the ability of DWTPs to provide safe drinking water (Yadava et al., 2023). To mitigate these risks, stricter regulations have been introduced, such as the EU Directive 2020/2184, which sets a turbidity threshold of 0.30 NTU for 95% of measurements to prevent microbial contamination and ensure water safety. Additionally, the new EU Directive for the first time incorporated the concept of robustness into a regulatory framework compliance. Traditionally, DWTP performance has been assessed by monitoring the removal efficiency of specific contaminants like iron, E. coli, and turbidity from inlet to outlet (Bwapwa et al., 2024). However, this reactive approach fails to detect early signs of operational issues, only identifying problems after they have already impacted the system. A more proactive method is needed to provide early warnings and ensure process stability under varying raw water conditions. Robustness, defined as a plant's ability to maintain high performance despite operational challenges, has been proposed as a key metric for evaluating DWTPs (Nemani et al., 2023). A recent study (De Marines et al., 2025) has introduced a Turbidity Robustness Index (TRI) to quantify plant stability over time. This index has shown greater sensitivity and specificity in identifying process failures than existing ones.

This study proposes a new TRI-based methodology, named ALERT (hAndLe high-turbidity Events in drinking water tReatment planTs) to assess DWTP performance under fluctuating water quality conditions, identifying vulnerable treatment stages and critical thresholds above which a noticeable robustness loss is observable. The findings could have direct applications in defining management strategies to handle critical operational scenarios and achieve DWTP adaptation to climate change.

Materials and methods

ALERT method is a step-wise procedure. The first step involves collecting long-term influent and effluent water data using online acquisition systems. Key parameters include flow rates and turbidity, aggregated over fixed time intervals. Statistical measures such as the 95th percentile, median, and maximum turbidity are calculated for specific periods. Additionally, the average flow rate and a critical turbidity threshold (TD) are determined based on plant operations. During the second step all the statistics and calculation of the previous method's step are used to calculate the TRI_{95B} according to De Marines et al. (2025). The third step aims at quantifying the Turbidity Load Index (TLI), representing the total contribution of turbidity and thus, indirectly, suspended solids entering with the raw water per unit of time. TLI is aimed to predict the expected TRI_{95B} at global and process scales, based on the quality characteristics of raw water entering the plant. The fourth step aims at identifying the "turbidity event", which refers to a considerable increase in the influent turbidity, exceeding a predefined threshold compared to a baseline value, which persisted for a defined duration. Once the n-turbidity events are identified, the method establishes to assign a score to each event. On the basis of the results and the evidence raised from the previous ALERT method steps the plant's operators identify critical operational thresholds referred to both the TLI and turbidity event score above which the plant, or a specific process or even unit, losses in robustness. ALERT method has been applied to a full-scale DWTP by using a 3-years long dataset.

Results and concluding remarks

Results showed that ALERT method allows identifying TLI thresholds above which the case study DWTP exhibited a lower robustness and frequent deviations from the regulation turbidity goal. In more detail, ALERT method allowed to identify the individual process steps and the specific units that resulted most vulnerable to variations in the influent turbidity. Precisely, while the overall plant demonstrated robustness, the study identified process-specific vulnerabilities. The robustness of the clariflocculation process varied among its three reactors (CH1, CH2, CH3); in fact, while CH2 and CH3 could withstand increasing turbidity loads, CH1 required closer monitoring and potential operational adjustments to maintain stable performance. Similarly, the robustness of the filtration process varied among its three units (FS1, FS2 and FS3). Unlike FS1 and FS2, which consistently performed well even under higher turbidity loads, FS3 exhibited frequent robustness losses. The study also found that filtration played a crucial role in mitigating the instability of the upstream clariflocculation process. Although variations in the latter did not significantly affect overall plant robustness, filtration failures directly contributed to process instability. Therefore, maintaining the robustness of FS3 is essential for ensuring compliance with regulations.

The ALERT method also allows identifying extreme operational conditions to ensure high-standard water quality under high turbidity load. Over a three-year period, ten turbidity events were observed; these events varied in duration and had widely differing scores, reflecting their varying intensities. For events with scores exceeding 100, the filtration unit exhibited a faster decline in robustness compared to clariflocculation. This was primarily attributed to the FS3 filter, which had previously been identified as highly sensitive to high turbidity loads. The study also found that the TRI_{95B} trend for the entire plant closely mirrored that of the filtration unit, highlighting filtration as the key determinant of overall plant stability. While filtration plays a crucial role in mitigating process instability, its effectiveness depends on proper upstream turbidity reduction, emphasizing the importance of clariflocculation performance.

The application of the TRI_{95B} and the comparative analysis with other process indicators allowed to highlight the system's vulnerabilities and to define operational thresholds that if exceeded could cause a noticeable decrease in process performance and robustness loss. The identification of high-turbidity events, a phenomenon increasingly common in the context of climate change, and understanding how the DWTP withstands such stressors, could allow for reducing the process failures. Indeed, identification of the treatment units that are most sensitive to these overloads could enable to adapt their operation to ensure adequate process robustness.

The proposed method provides a valuable tool for early detection of performance degradation, enabling operators to implement proactive corrective measures to maintain high water quality and safeguard the integrity of the treatment processes.

References

Bwapwa, J.K., Mkhize, N., Seyam, M., 2024. Evaluation of operational efficiency and performance for a water treatment plant. South African J. Chem. Eng. 49, 11–34. https://doi.org/10.1016/j.sajce.2024.04.003

De Marines, F., Corsino, S.F., Cosenza, A., Capodici, M., Torregrossa, M., Viviani, G., 2025. A modified robustness index for assessing operational performance of drinking water treatment plants: A comparative study within a new regulatory framework. Water Res. 268, 122668. https://doi.org/10.1016/j.watres.2024.122668

Nemani, K.S., Peldszus, S., Huck, P.M., 2023. Practical Framework for Evaluation and Improvement of Drinking Water Treatment Robustness in Preparation for Extreme-Weather-Related Adverse Water Quality Events. ACS ES T Water 3, 1305–1313. https://doi.org/10.1021/acsestwater.2c00627

Verlicchi, P., Grillini, V., Maffini, F., Benini, A., Mari, M., Casoni, R., 2024. A proposed methodology to evaluate the influence of climate change on drinking water treatments and costs. J. Environ. Manage. 366, 121726. https://doi.org/10.1016/j.jenvman.2024.12172

Yadava, P.K., Kumar, H., Singh, A., Kumar, V., Verma, S., 2023. Impact of climate change on water quality and its assessment, in: Visualization Techniques for Climate Change with Machine Learning and Artificial Intelligence. Elsevier B.V, pp. 39–54. https://doi.org/10.1016/b978-0-323-99714-0.00002-9

Water loss estimation and pipe deformation in water distribution network: Laboratory and numerical experiments

M. De Marchis[1*], F. Bruno[2], D. Saccone[2], G. Freni[2], E. Napoli[1]
[1] Department of Engineering, University of Palermo, Palermo, Italy
[2] Department of Engineering and Architecture, University of Enna Kore, Enna, Italy
* e-mail: mauro.demarchis@unipa.it

Introduction

The management of Water Distribution Systems (WDSs) has become more and more critical due to various factors such as population growth, urbanization, climate change, and aging infrastructure. The issue of leakage detection and control is particularly significant because water loss through leaks not only wastes a valuable resource but also adds unnecessary costs for water utilities and can lead to infrastructure damage and service disruptions.

Several technologies and strategies have been developed to address the challenge of leak detection and control in water distribution systems. Among the most used strategies, those based on pressure monitoring through advanced sensors are the most applied. Sensors can, in fact, provide real-time data on the condition of the pipes and all the collected data can be used by water utilities to predict potential leak locations based on factors such as pressure levels, flow rates, and historical data. This proactive approach enables targeted interventions to prevent leaks before they occur. Automated control systems can also be employed to isolate sections of the network in the event of a leak, minimizing water loss and damage. Another possibility to reduce water losses is to perform regular inspection, maintenance, and rehabilitation of water distribution infrastructure. A comprehensive asset management programs is unfortunately quite expensive in term of resources and money, so it is difficult to apply.

By integrating these technologies and strategies into their operations, water utilities can improve the efficiency and reliability of their distribution systems while minimizing water loss due to leaks. It has been widely demonstrated (De Marchis et al., 2016; 2019) how water losses are affected by two main features: network pressure and leak geometry. For this reason, a lot of study analysed the relationship between leak outflow, pressure and geometry. Various researchers focused the attention on leaks estimation and it is nearly impossible to cite the entire literature findings on this issue. All of these studies have been performed through experimental campaign in hydraulic laboratory or in real WDNs. These studies aimed at finding a definition or a relation able to estimate water outflow once the pressure and leak geometries are known.

All previous mentioned studies have been mainly performed using laboratory experiments; very few studies have been recently performed using numerical tecniques. One of the first contribution in this field was given by Barbosa et al. (2012), who numerically studied three-phase flow (heavy oil, water and gas) in vertical pipeline using ANSYS-CFX. The results showed that the effect of small leak on the velocity and temperature distribution along the pipe can be negligible. Later, Zeng and Luo (2019) numerically investigated the water flow phenomena in a short pipe with leakage. The results showed that the relationship between the pressure change at the upstream and downstream of the leak location and leak mass flow rate is approximately linear, with dominant effect of the inlet mass flow rate and negligible effect of the pipe length.

In order to further investigate on leakage through CFD techniques, the main objective of the proposed research is to investigate on the most conventional head-leakage law, through fully 3D numerical simulations. Specifically, to investigate on the head-area leakages and on the head-discharge relationships, some laboratory experiments were reproduced numerically by means of a commercial software Ansys, able to simulate both the fluid dynamics and the structural analysis.

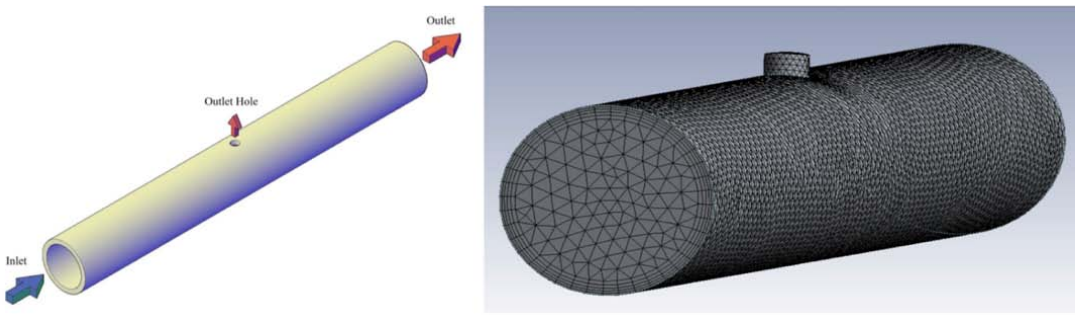


Figure 1. Domain layout and computational grid.

Materials and Methods

The experiments were conducted at the Environmental Hydraulic Laboratory of the University of Enna Kore (Italy), where a small water distribution network is located. The WDN is composed of three main loops (M=3) of high-density polyethylene (HDPE 100 PN16) pipes (nine internal nodes, N=9, one external node, S=1, and thirteen pipes, L=13) having nominal diameter (DN) of 63 mm. Each pipe is about 45 m long. For a detailed description of the facility see De Marchis et al. (2016). To investigate at a local scale the relationship between the leak outflow, Q_L, and the pressure, H, inside the pressurised pipe, several tests were conducted considering rectangular transversal and circular cracks of different sizes. The presence of cracks has been considered replacing a small portion of the pipe with a leak trunk, approximately 70 cm. The leak discharges into a free surface tank and thanks to a recirculation system, discharges are pumped to supply water tanks. To investigate on the head-area leakages and on the head-discharge relationships, the laboratory experiments were reproduced numerically by means of a commercial software Ansys, able to simulate both the fluid dynamics and the structural analysis. Basically, the flow field inside the pipe was simulated using the Fluent software module, whereas the deformation analysis was studied using the toolbox of Ansys known as Mechanical. To investigate the relationship between leak outflow and water head, as a function of the crack shape, several experiments were conducted considering cracks of different shape and size. Specifically, two sets of cracks were investigated: circular and rectangular transversal cracks, artificially generated. The two sets of experiments were designed with the aim to have different geometries maintaining almost the same leak area. For each experimental test the head at the inlet node of the network was modified by means of the pump station from 1.0 to 5.0 bar, with a step of 0.2 bar, in order to have a detailed variation of the leak outflow as a function of the water head upstream.

Results and concluding remarks

Based on the pressure distribution within the pipe, especially close to the holes, a structural analysis was performed aiming to investigate on the deformation of the leak hole. Substantially, the achieved results are coherent with the experimental observation, where longitudinal and circular cracks were analysed.

The stresses analysis versus the pressure shows that the rectangular cracks are generally characterized by highest values of deformation than circular holes. Moreover, in circular shapes the stress concentrations increase in a roughly linear fashion with increasing hole size and pressure; on the other hands in rectangular leak shapes the linear trend is not observed and the stresses is affected by a spreading of the data. Further analyses are required to confirm the achieved results.

Acknowledgments: TiSento - Sensorialized Composite Pipe for Hydraulic Applications, Italy, n. 084221000550 CUP G18I18001710007. Funded under measure 1.1.5 of the PO FESR SICILY 2014–2020

References

De Marchis M., Fontanazza C.M., Freni G., Notaro V., Puleo V. (2016) Experimental Evidence of Leaks in Elastic Pipes, Water Resources Management, 30(6), pp. 2005–2019

De Marchis M., B. Milici, (2019) Leakage Estimation in Water Distribution Network: Effect of the Shape and Size Cracks. In Water Resour. Manag., 33, 1167–1183. Int. Jnl. of Multiphysics 8(3), 2014.

Zeng Y., Luo R. (2019) Numerical Analysis on Pipeline Leakage Characteristics for Incompressible Flow. Journal of Applied Fluid Mechanics, 12(2): 485-494.

Lab experiments on an innovative smart pipe for potable water supply

F. Bruno[1*], G. Freni[1], C. Giaconia[2], M. De Marchis[2]
[1] Department of Engineering and Architecture, University of Enna "Kore", Enna, Italy
[2] Department of Engineering, University of Palermo, Palermo, Italy
* e-mail: federica.bruno@unikore.it

Introduction

Hydraulic networks are essential components in various industrial and urban systems, crucial for power transmission, water distribution, and energy generation. Their complexity and importance have increased focus on monitoring and maintenance to ensure optimal performance and prevent failures. Hydraulic systems are widely used for power transmission and control in industrial settings. As these systems become more complex and transfer more power, they are prone to unexpected operating accidents (Gu & Shi, 2019).

Researchers have proposed novel approaches for monitoring hydraulic systems, employing indirect measurement systems or embedded sensors. In water distribution networks, digitalisation of hydraulic systems has become critical in urban development. This transition towards digital services presents opportunities to address changing public needs and workforce shortages. However, small cities often face challenges implementing these solutions due to limited budgets and resources. To overcome these obstacles, researchers have proposed methodologies allowing water utilities with limited budgets to initiate digitalisation and construct hydraulic models of their networks (Bonilla et al., 2023). These approaches typically involve low-cost monitoring, digital twin development, and machine learning integration to predict system states. Machine learning techniques have shown promise in enhancing condition monitoring of hydraulic systems. Random forest classifiers have been successfully applied to hydraulic system condition monitoring, achieving classification rates exceeding 99% for various system components (Alenany et al., 2021). Despite these advancements, several challenges remain in the field of hydraulic network monitoring. These include the need for more robust and reliable sensors, improved data analysis techniques, and the development of cost-effective solutions for smaller utilities and cities. Additionally, there is a growing emphasis on incorporating equity considerations into evaluating hydraulic system improvements, as highlighted by the emerging field of distributional cost-effectiveness analysis (Selvakumar et al., 2017).

Smart water pipe systems represent a significant advancement in water distribution infrastructure, offering numerous benefits for water utilities and consumers. These systems integrate advanced technologies, sensors, and data analytics to monitor, manage, and optimize water flow, pressure, and quality in real time (Altowayti et al., 2021). By incorporating intelligent features, innovative water pipe systems address critical challenges such as leakage detection, water quality maintenance, and efficient supply management. One primary advantage is their ability to detect and prevent leaks, a major source of water loss in distribution networks. Through pressure management strategies and advanced monitoring techniques, these systems significantly reduce water losses and improve overall system efficiency (Mathye et al., 2022). Smart water pipe systems also enable utilities to better understand and predict water flow patterns, losses, and performance through mathematical modeling and data analysis (Altowayti et al., 2021).

In the present research, we present the lab experiments run at the University of Enna "Kore" to characterise the pipe from a hydraulic point of view and test its sensing abilities in a controlled laboratory environment. The tests were carried out using a novel large diameter hydraulic test bench, solving much of the scaling issues connected with lab-scale hydraulic physical models.

Materials and methods

The lab advanced hydraulic test bench addresses this challenge by integrating two powerful inverter-driven pumps capable of generating up to 16 bar of pressure and delivering flow rates exceeding 150 cubic

meters per hour. Central to its design is a dual-circuit arrangement: a dedicated test circuit for replicating real operating conditions and a bypass circuit that stabilises flow through continuous regulation. Automated valves precisely fine-tune pressure and flow, allowing seamless adjustments even under demanding conditions. The bench's outstanding measurement accuracy, with flow readings accurate to within 0.2% (both upstream and downstream) and pressure readings to within 0.5%, assures precise, reproducible performance data. This robust system is ideally suited for testing various components, including valves, fittings, and pipe segments, ensuring meticulous quality control and confident compliance with industry standards. Its modular design enables flexible setup, minimising downtime and supporting varied testing requirements. By combining consistent flow control, high-pressure capabilities, and superior measurement precision, this innovative hydraulic test bench represents an indispensable resource for manufacturers, researchers, and quality assurance professionals seeking reliable, verifiable results for their large-scale fluid transport systems. It redefines reliable testing.

The test bench was used to characterise the innovative smart pipe developed in the project, providing its hydraulic characterisation and certifying its suitability to be used in potable water distribution networks.



Figure 1. The large diameter pipes experimental test bench at the University of Enna "Kore".

Acknowledgments: TiSento - Sensorialized Composite Pipe for Hydraulic Applications, Italy, n. 084221000550 CUP G18I18001710007. Funded under measure 1.1.5 of the PO FESR SICILY 2014–2020.

References

Alenany, A., Nasef, B. M., & Helmi, A. M. (2021). Comprehensive Analysis for Sensor-Based Hydraulic System Condition Monitoring. International Journal of Advanced Computer Science and Applications, 12(6). https://doi.org/10.14569/ijacsa.2021.0120615

Altowayti, W. A. H., Al-Gheethi, A., Tajarudin, H. A., Othman, N., Al-Dhaqm, A., Al-Towayti, F. A. H., Alshalif, A. F., Asharuddin, S. M., Salem, A. A., Din, M. F. M., & Fitriani, N. (2021). Evaluating the Pressure and Loss Behavior in Water Pipes Using Smart Mathematical Modelling. Water, 13(24), 3500. https://doi.org/10.3390/w13243500

Bonilla, C., Montalvo, I., Brentan, B., Ayala-Cabrera, D., & Izquierdo, J. (2023). Digitalization of Water Distribution Systems in Small Cities, a Tool for Verification and Hydraulic Analysis: A Case Study of Pamplona, Colombia. Water, 15(21), 3824. https://doi.org/10.3390/w15213824

Gu, L., & Shi, Y. (2019). Online Monitoring Technique of Power Condition for Inverter-Fed Motor Driven Hydraulic System. Mathematical Problems in Engineering, 2019, 1–16. https://doi.org/10.1155/2019/4908942

Mathye, R. P., Nyende-Byakika, S., & Scholz, M. (2022). Optimal Pressure Management in Water Distribution Systems: Efficiency Indexes for Volumetric Cost Performance, Consumption and Linear Leakage Measurements. Water, 14(5), 805. https://doi.org/10.3390/w14050805

Selvakumar, A., & Matthews, J. C. (2017). Demonstration and Evaluation of Innovative Rehabilitation Technologies for Water Infrastructure Systems. Journal of Pipeline Systems Engineering and Practice, 8(4). https://doi.org/10.1061/(asce)ps.1949-1204.0000268

Investigating transient flow phenomena and measurement accuracy in revenue water meters

F. Traina[1], A. Vella[2], F. Lo Valvo[2], S. Sapienza[2], C. Giaconia[2], M. De Marchis[2*]
[1] Department of Engineering and Architecture, University of Enna Kore, Enna, Italy
[2] Department of Engineering, University of Palermo, Palermo, Italy
* e-mail: mauro.demarchis@unipa.it

Introduction

The study of transient phenomena in water distribution networks presents a new challenge for the scientific community, particularly in the context of understanding and mitigating apparent losses. These losses, which result from inaccuracies in water metering and unauthorized consumption, have become a growing concern for international water task forces aiming to improve water management efficiency.

During the first decade of the 2000s, most scientific contributions primarily focused on real losses, which refer to physical water loss through leaks in the distribution system (De Marchis et al., 2016). However, recent studies have shifted toward apparent losses, recognizing their significant role in non-revenue water estimation and overall system performance (*Al-washali et All, 2016)*.

These transient phenomena involve rapid pressure and velocity variations caused by sudden changes in system operation, such as valve closures, pump startups, or intermittent water supply. Such rapid fluctuations can significantly impact system stability and lead to measurement inaccuracies, affecting both operational efficiency and data reliability (Ferrante et al., 2022).

Additionally, some of these effects are driven by climate change, which contributes to water scarcity and extreme weather events that exacerbate supply fluctuations. As a result, the study of transient phenomena has gained increasing attention, with researchers focusing on experimental and numerical approaches to enhance the resilience and accuracy of hydraulic measurement systems.

One critical issue is the effect of transient conditions on the accuracy of measuring instruments, particularly volumetric water meters, which may not register flow variations correctly under dynamic conditions. Understanding these impacts is essential for ensuring reliable water distribution monitoring and management.

This work aims to propose a new approach for studying the accuracy of water meters during transient conditions within a full-scale 1:1 (Figure 1) laboratory water distribution network. Laboratory experiments were conducted to simulate real-world conditions and compare experimental results with numerical models.



Figure 1. Layout of the WDN experimental facility

These tests analysed both a complete water distribution network and a simplified pipeline system, allowing for an evaluation of discrepancies between experimental observations and model predictions. Additionally, volumetric meters were tested under both transient and steady-state conditions to assess their performance and validate existing measurement standards.

Materials and Methods

The experiments were conducted in a controlled laboratory environment, utilizing polyethylene pipelines with a diameter of 64 mm and multilayer pipelines with a diameter of 16 mm. The multilayer connection was designed to replicate a single-user connection in a WDN. Along this section, four different revenue water meters were installed in series to analyse their performance under transient conditions.

A series of pressure transducers and volumetric meters were installed along the pipeline to capture variations in pressure and flow rate during the filling process. The pressurization unit was activated to gradually fill the pipeline, allowing water to flow through and be collected in a recirculating tank. To ensure the accuracy of the water volume measurements the recirculating tank was positioned on a balance scale to precisely measure the amount of water used in each test. The measurements were performed thanks to an in-house efficient system, named hydroscope. Experimental data were then compared with numerical model predictions to assess wave propagation and transient effects. In the experiments, volumetric meters were tested under both transient and steady-state conditions. The steady-state tests followed the UNI EN ISO 4064-5:2023 standard, which defines characteristic flow rates—minimum flow rate (Q1), transitional flow rate (Q2), permanent flow rate (Q3), and overload flow rate (Q4)—to evaluate measurement accuracy. The analysis of the experimental results provided a detailed comparison between measured and expected flow rates, showcasing the variations in meter accuracy under different conditions. For steady-state conditions, the error curves demonstrate the consistency of volumetric meters when operating at predefined flow rates. The transient flow experiments, on the other hand, reveal fluctuations in measurement accuracy due to rapid changes in flow and pressure, as well as the presence of air in the water-air mixture. The graphical representation highlights the impact of transient conditions on meter performance, showing deviations from standard measurement accuracy, which are crucial for understanding the limitations of current metering technologies. By analysing these trends, the study aims to enhance the accuracy and reliability of revenue water meters under real-world operating conditions.

Results and concluding remarks

The results demonstrated how water meters measurements are affected by the presence of entrapped air in the pipe. Air is, in fact, entrapped within the pipes during the filling process occurring in intermittent water supply conditions, and it is released by the user connections.

The volumetric meters exhibited slight deviations from the prescribed UNI standard error limits, influenced by factors such as meter age and the absence of ideal test bench conditions. Transient flow conditions were found to impact measurement accuracy, highlighting the need for further investigations to refine numerical models and improve water meter reliability in dynamic network environments. These findings contribute to a better understanding of transient phenomena and their effects on hydraulic measurement systems.

Acknowledgments: TiSento - Sensorialized Composite Pipe for Hydraulic Applications, Italy, n. 084221000550 CUP G18I18001710007. Funded under measure 1.1.5 of the PO FESR SICILY 2014–2020

References

Al-Washali, T., Sharma, S., Kennedy, M (2016) Methods of assessment of water losses in water supply systems: a review. Water Resources Management 30 (2016): 4985-5001.

De Marchis, M., Fontanazza, C.M.,Freni, G.,Notaro, V.,Puleo, V. (2016) Experimental Evidence of Leaks in Elastic Pipes, Water Resources Management, 30(6): 2005–2019

Ferrante, M., et al. (2022) Impact of intermittent supply on water meter accuracy. AQUA—Water Infrastructure, Ecosystems and Society 71(11): 1241-1250.

Distributed vibration monitoring system for AI leakage detection

F. Lo Valvo[1], A. Vella[1], S. Sapienza[1], F. Di Puma[2], K. Ladjeri[2], G.C. Giaconia[1*]
[1] Department of Engineering, University of Palermo, 90128 Palermo, Italy
[2] EKSO srl, Contrada Tabuna, 97100 Ragusa, Italy
* e-mail: costantino.giaconia@unipa.it

Introduction

Aging public water infrastructure, particularly pipes, is leading to significant water loss due to leakages. Decades of service have caused wear and tear, resulting in critical failures. In some European regions, drinkable water loss exceeds 40%, reaching as high as 70% in certain areas. The underground and extensive nature of these pipe networks makes traditional leakage detection methods, like visual inspection and listening devices, ineffective and impractical for continuous, large-scale monitoring.

To address this, new approaches and methods revolving around data and models are emerging (Nimiri et al. 2023). In this work, a new vibration-based sensing method is proposed to detect unique vibration patterns caused by water leaks. These sensors, installed along the pipes, enable continuous monitoring of the water distribution network. However, the vast amount of data generated necessitates the use of Machine Learning (ML) models. ML enhances both efficiency and accuracy by automating the analysis, overcoming the limitations of human operators who are prone to fatigue. This allows for round-the-clock monitoring and rapid detection of leaks.

Materials and methods

The system developed in this study is based on the principle that water flow and leaks generate distinct vibration patterns that can be captured using vibration sensors. This approach has proven to be promising in (Martini et al. 2013), (Mistretta et al. 2018), (Restuccia et al. 2023) and (Lo Valvo et al. 2023). The research process was structured into several key phases: an initial experimental setup using a controlled, simulated leakage environment, followed by the application of machine learning algorithms to interpret and analyse the collected vibration data.

In the experimental phase, the research team simulated leakages using a fire hydrant to mimic real-world conditions with predefined timing. This setup facilitated the collection of a dataset that represented potential leakage scenarios. The core of the detection system comprises 10 sensors (numbered 2 to 11), organized into two chains, attached to a newly laid underground water polyethylene pipe with a 135 Ø mm diameter in an urban setting. These sensors are placed at distances of about 10 meters to ensure comprehensive coverage and effective data capture. Their topology is depicted in Figure 1.

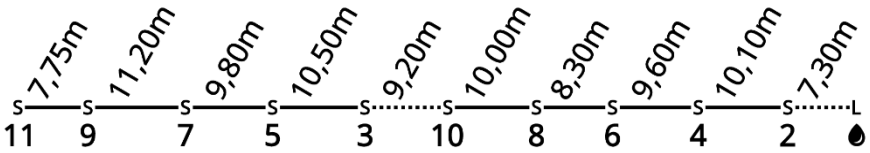


Figure 1. Sensors disposition on the pipes.

The hardware infrastructure is designed around MEMS accelerometers, specifically the IIS3DWB by STMicroelectronics, chosen for its frequency range and high output data rate. These sensors are capable of operating at a scale of ±2 g and feature a high sensitivity and a low noise level. Data acquisition and partial processing are handled by STM32L476RG microcontrollers, which then transmit the data to a Raspberry Pi for further analysis, compression, and cloud delivery.

For the analysis of the collected data, different machine learning approaches have been tested out, comparing training models on data coming from the sensor nearest to the leak, the sensor furthest from

the leak and all 10 sensors at the same time. The models employed in this research are RIPPER (Cohen 1995), Support Vector Machines (Vapnik 1995) and a one hidden layer Artificial Neural Network (Goodfellow et al. 2016), each performing differently on the training dataset. A big improvement in leak detection has been carried out by considering the last 10 seconds of recording as a single training data chunk.

Results and concluding remarks

All models have shown improvements when all sensors are used in training and when using 10 seconds data chunks in the training phase, as shown in Table 1.

Table 1. ML models accuracy on leakage detection.

Trained on	RIPPER	SVM	ANN
Sensor 2	57,24%	55,88%	55,27%
Sensor 2 (10s chunk)	98,22%	96,33%	96,43%
Sensor 11	59,60%	55,88%	54,60%
Sensor 11 (10s chunk)	97,96%	55,88%	56,06%
All Sensors	77,64%	58,66%	75,00%
All Sensors (10s chunk)	99,88%	96,74%	98,28%

The system uses a network of sensors to monitor pipe vibrations, with data processed through machine learning models to identify and locate leaks. The results showed high accuracy in detecting leaks, particularly when using data from sensors closest to the leak and when incorporating memory values (i.e., largest value read in an immediate previous short time interval) in the analysis.

The study successfully demonstrated the potential of using modern sensor technology and machine learning for effective water leakage detection in urban infrastructure.

Future work should focus on expanding the sensor network to cover larger areas and different pipe diameters and integrating the system with a local area map. Additionally, there is a need for more research into improving the resilience and reliability of the system, possibly through a denser sensor distribution.

Acknowledgments: This study was funded by the Project “TiSento” (Azione 1.1.5. - POC Sicilia 2014/2020 Asse 1 - PO FESR 2014/2020).

References

Cohen WW (1995) Fast Effective Rule Induction. Machine Learning Proceedings 1995,115-123. https://doi.org/10.1016 /B978-1-55860-377-6.50023-2

Goodfellow I, Bengio Y, Courville A (2016) Deep learning. MIT press.

Lo Valvo F, Baiamonte G, Giaconia C, (2023) Microcontroller Based Edge Computing for Pipe Leakage Detection. ApplePies 2022 4.pp. 16-22. https://doi.org/10.1007/978-3-031-30333-3_3

Martini A, Troncossi M, Rivola A, (2013) Vibration Monitoring as a Tool for Leak Detection in Water Distribution Networks.

Mistretta L, Giaconia C, Valenza A, Napoli E, Gianguzzi C, Presti M, Di Puma F. (2018) Embedding Monitoring Systems for Cured-In-Place Pipes. ApplePies 2016: 12-17. http://doi.org/10.1007/978-3-319-55071-8_2

Nimiri W, et al. (2023) Data-driven approaches and model-based methods for detecting and locating leaks in water distribution systems: a literature review. Neural Computing and Applications, 06 04, Volume 35: 1-13. http://doi.org/10.1007

Restuccia G, Tinnirello I, Lo Valvo F, Baiamonte G, Garlisi D, Giaconia C, (2022) A distributed analysis of vibration signals for leakage detection in Water Distribution Networks, AIMETA2022 Materials Research Proceedings Vol. 26: 543-548, http://doi.org/10.21741/9781644902431-88

Vapnik VN (1995) The nature of statistical learning theory. Springer-Verlag, New York

Impulsive force acquisition system for drop test stress analysis on composite materials

S. Sapienza, A. Vella, F. Lo Valvo, R. Miranda, M. Luciano, V. Fiore, A. Valenza, C.G. Giaconia*
Dipartimento di Ingegneria, Università degli Studi di Palermo.
**e-mail: costantino.giaconia@unipa.it*

Introduction

In the last few decades composite material has become the main competitor of traditional alloys in aerospace and aviation fields, but also for pipe and vessel construction, due to their excellent characteristics of mechanical strength and stiffness.

In order to perform a mechanical characterization of these materials, different kind of tests must be carried out: tensile, bending and torsion test but also delamination and impact studies.

The kind of defects generated from an impact depends on the energy of the collision, in particular low velocity impacts are the most critical due to the low evidence of superficial damage (*BVID Barely Visible Impact Damage*) .

This type of damage spreads deeply causing delamination of the materials below the impact point.

Low speed impacts are often characterized by means of Drop Test, where a sample of materials is hit by a free falling impactor. The degrees of freedom of this test are height of release and impactor's weight.

The aim of this work is to develop an electronic system able to perform data acquisition of impact force in order to add some extra information for drop test stress analysis on composite materials.

Materials and methods

The discussed embedded system (see Figure 1) was developed with the aim to retrofit an existing drop test machine situated in "Laboratorio di materiali compositi naturali ed ibridi", dipartimento di Ingegneria, Unipa.

For the sake of reducing the overall design time, the system consists in a custom daughter board and a commercial microcontroller evaluation board.

The daughter board is essentially an analog front end for the signal coming from the four piezo-resistive sensors, when the sensor is compressed increase its conductivity linearly with the load.

It is equipped with four channels for each of which a dedicated amplifier stage has been provided, in order to make a single precision adjustment of the gain for each sensor. This amplifier stages drives the four 16 Bits Analog to Digital converters at a sampling frequency of 70 kSps, on the microcontroller board NUCLEO-H743ZI-II, that makes the data acquisition of the measure and sends it to a User's PC via an USB port.

For the sake of simplify the acquisition process, a custom Graphic User Interface for Windows PC was developed. With this software a user can send START and STOP measure commands to the system, and when the measure is complete, user can visualize data and save or delete it.

For each sensor a calibration curve was retrieved by a static calibration method that consist in a modified suspension for a drill press on top of which was loaded multiple Bumper Plates weights, see Figure 2.

With the presented system four different energy drop test was carried out (2.5 J , 5 J, 7.5 J ,10 J), on four different composite materials: Glass Fiber Matrix, Carbon Fiber Matrix, Basalt Matrix and Juta Matrix.

Results and concluding remarks

For the aforementioned scenario, the developed embedded system is capable of measure with a suitable amplitude and time resolution the impact forces due to the impact with different material sample.

A measurement campaign is underway with the aim of validate experimental measurement with FEM simulations.

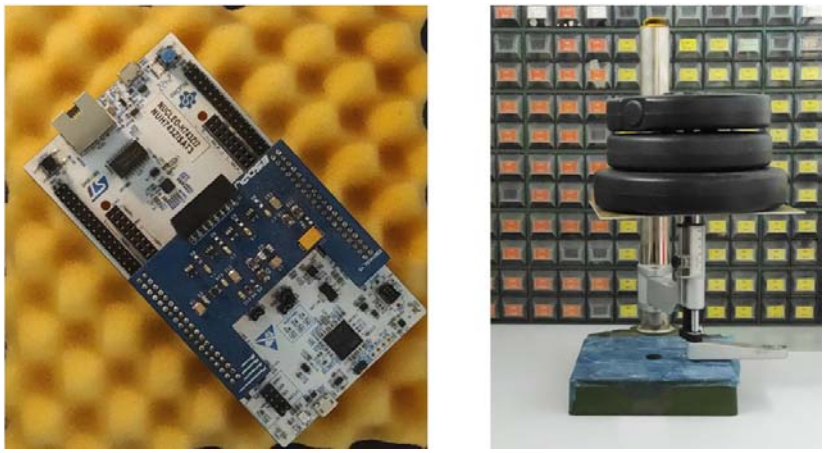


Figure 1 (Left) Presented Embedded System; (Right) Static Calibration Apparatus.

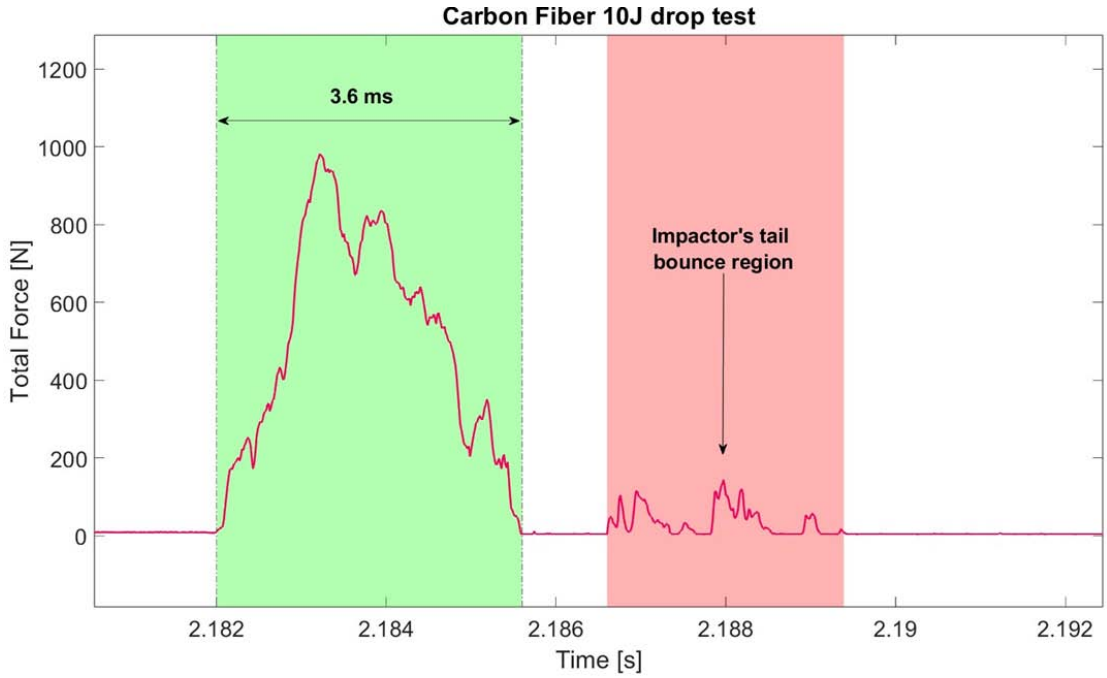


Figure 2. Time-Force curve obtained with the presented embedded system.

Acknowledgments: This study was funded by the Project "TiSento" (Azione 1.1.5. - POC Sicilia 2014/2020 Asse 1 - PO FESR 2014/2020).

References

ASTM International (2013) Standard test method for measuring the damage resistance of a fiber reinforced polymer matrix composite to a drop weight impact event.

Olsson R. (2000), Mass criterion for wave controlled impact response of composite plates,. Composite Part A: Applied Science and Manufacturing, 31: 879-887. https://doi.org/10.1016/S1359-835X(00)00020-8

PCB Piezotronics (2021) Impact and drop testing with ICP Force Sensors. Amphenol company

Richardson, M. O. W., & Wisheart, M. J. (1996) Review of low velocity impact properties of composite materials. Composite Part A: Applied Science and Manufacturing, 27(12): 1123-1131. https://doi.org/10.1016/1359-835X(96)00074-7

Synchronous data aggregation system for flow and pressure measurements in water distribution networks

A. Vella[1], S. Sapienza[1], F. Lo Valvo[1], F. Traina[2], M. De Marchis[1], G.C. Giaconia[1*]
[1] Department of Engineering, University of Palermo, 90128 Palermo, Italy
[2] Faculty of Engineering and Architecture, University of Enna "Kore", 94100 Enna, Italy
*e-mail:costantino.giaconia@unipa.it

Introduction

Monitoring pressure and flow dynamics in hydraulic systems is crucial for understanding system performance, identifying potential issues, and optimizing operational efficiency. Traditional monitoring methods often rely on manual data collection or standalone data loggers (Bruno et al. 2021). Such kind of measurement equipment is usually characterized by low sampling frequencies and by the absence of data synchronization.

In order to overcome those limitations and to monitor the temporal evolution of pressures and flows within the hydraulic system under investigation, an embedded system has been designed. This system, acquires measurements from flow and pressure sensors strategically positioned along the hydraulic line, enabling real-time visualization and data logging. The system acquires all the signals synchronously with a sampling frequency of 100 samples per second, allowing for simultaneous acquisition of up to 22 signals provided by distinct sensors. Acquisition, visualization, and storage are managed through a custom-designed Graphic User Interface (GUI). Furthermore, the system incorporates a feature for server-based data storage, complementing local storage capabilities.

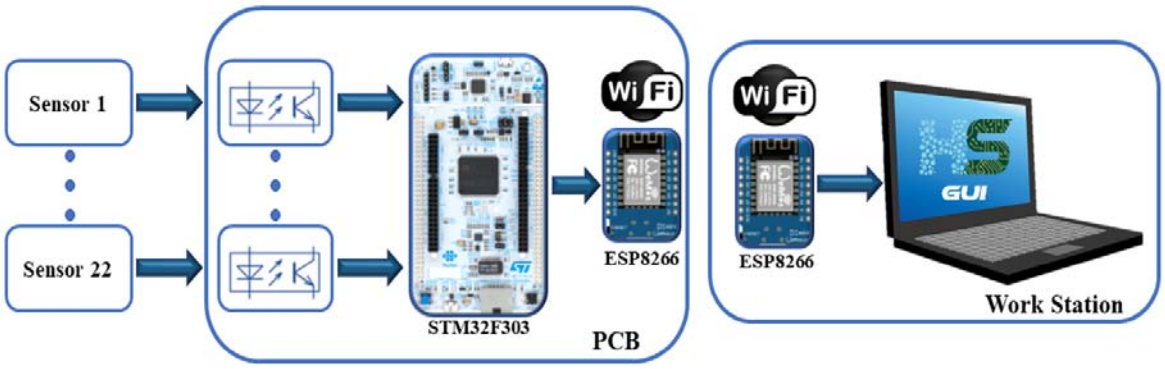


Figure 1. System architecture block diagram.

Materials and methods

As depicted in the block diagram in Figure 1, the system comprises a signal conditioning stage for each sensor input, a central microcontroller unit (STM32F303) responsible for timing, sampling, and initial transmission of acquired signals, and a second microcontroller unit (ESP8266) dedicated to Wi-Fi transmission of samples. Data are received by a second ESP8266 unit, connected via USB to a host computer, which delivers the received data to the GUI for visualization and storage. Each of the 22 available inputs can be connected interchangeably to a flow or pressure sensor, using the 4-20mA industrial communication standard.

The signal conditioning circuit, which is identical for each input channel, receives an input current ranging from 4mA to 20mA from the sensors and replicates this current at the output of a phototransistor. The output current is converted into a voltage signal by a sensing resistor placed between the transistor's emitter and ground, and this voltage signal is then sampled by the main microcontroller. The optical

coupling assures that the input signals are also electrically isolated from the rest of the PCB to decouple the different power supplies required for various sensor types.

The samples acquired by the 12 bits Analog-to-Digital converters of the STM32F303 are transmitted via the UART interface to the ESP8266 microcontroller, that acts as a client in the UDP communication between the system board and the ESP8266, acting as a server, connected to the workstation. All the data are visualized using the custom GUI. This interface enables users to selectively acquire data streams from specified sensors and to independently adjust calibration parameters for each sensor, thereby facilitating precise and tailored data acquisition. Furthermore, it offers the possibility to locally save the acquired measurements in multiple data formats and to store the data on an SFTP (Secure File Transfer Protocol) hosting server.

Results and concluding remarks

The designed system is installed in the Kore Water Lab of the "Kore" University in Enna. Figure 2 shows a measurement involving five pressure sensors and three flow meters. The experimental procedure consists of a water pipe filling test (Ferrante et al. 2022), as demonstrated by the trend of flows and pressures along the line.

As can be seen from the graphs, the pressure progressively rises until it reaches a steady state across the entire line. The flow sensors instead show how, as the water line fills, the flow decreases to zero and the various sensors sequentially detect the waterfront.

The outcomes of the measurement process validate the accuracy and quality of the acquired data, providing a comprehensive understanding of the phenomena observed within the studied water network.

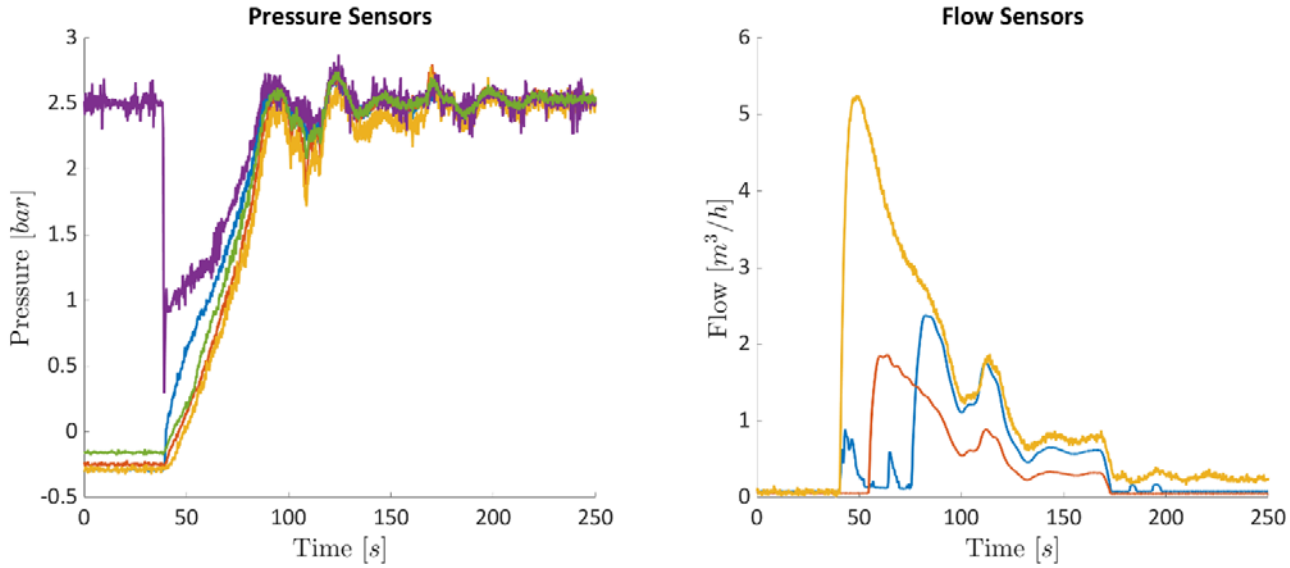


Figure 2. Measured data.

Acknowledgments: This study was funded by the Project "TiSento" (Azione 1.1.5. - POC Sicilia 2014/2020 Asse 1 - PO FESR 2014/2020).

References

Bruno F, De Marchis M, Milici B, Saccone D, Traina F (2017) A pressure monitoring system for water distribution networks based on arduino microcontroller. Water, 13(17), 2321. https://doi.org/10.3390/w13172321

Ferrante M, Rogers D, Mugabi J, Casinini F (2022) Impact of intermittent supply on water meter accuracy. AQUA - Water Infrastructure, Ecosystems and Society (2022) 71 (11): 1241–1250. https://doi.org/10.2166/aqua.2022.091

XII. Groundwater Hydrology and Contamination

Managed aquifer recharge as an effective climate change adaptation strategy: a case study in Friuli Venezia Giulia region, Italy

M. Sufyan[1*], G. Martelli[1], P. Teatini[2], D. Goi[1]
[1] Polytechnic Department of Engineering and Architecture (DPIA), University of Udine, Udine, Italy
[2] Department of Civil, Environmental, and Architectural Engineering, University of Padova, Padova, Italy
*e-mail: sufyan.muhammad@spes.uniud.it

Introduction

The Friuli Venezia Giulia (FVG) region in northeastern Italy has experienced an imbalance in the hydrogeological system over the years, resulting in the lowering of groundwater levels. Reduced and erratic precipitation patterns, rising temperatures, and increased abstraction have all contributed to the decline in piezometric levels in the Friuli Plain's phreatic aquifers (Teatini et al. 2015). These changes in the hydrogeological system have resulted in a decrease in direct infiltration, and an increase in the surface run-off and evapotranspiration rate, thus affecting both the surface and groundwater resources in the region. The groundwater of the region is also polluted by nitrate content, whose concentrations in some parts of the region exceed the threshold value (50 mg/l as per Italian legislation) for potable use (Teatini et al. 2020). To address declining water resources and improve underground storage of high-quality surface waters, three recharge sites (Carpeneto, Mereto di Tomba, and Sammardenchia), located to the east of Tagliamento River in the upper Friuli Plain have been suggested for managed aquifer recharge (MAR) practice. MAR potential in this pre-Alpine region is characterized by the availability of high-quality surface waters (primarily from rivers), a highly permeable thick aquifer system, and numerous existing structures such as pits and large-diameter wells (Martelli and Granati 2007). The present study aims to investigate the effect of MAR on groundwater resources at the Sammardenchia site.

Materials and methods

Figure 1 shows the study area (45°58'43.8"N 13°13'20.1" E), located in the upper plain of the FVG region, which is characterized by an unconfined aquifer system. The subsurface geology obtained from boreholes drilled within the study area revealed the presence of a top-thick gravel unit, with underlying cemented gravel and a thin clay unit. The regional groundwater flow pattern was estimated using the historical piezometric data (1976-2022) from 8 monitoring wells located within the 10 km^2 area, which helped establish the groundwater model's boundary conditions. The water table in the natural conditions, which was derived from the regional piezometric network served as the initial condition for the groundwater model. The modelling was performed using the MODFLOW package. To evaluate the effect of MAR on the aquifer, the recharge from an existing infiltration pond (45×10×6.5 m) was simulated. The nearby Ledra channel, currently used for irrigation purposes, is assumed to provide the water for the MAR scheme, as shown in Figure 1.

Results and concluding remarks

The groundwater flow simulation, performed using the MODFLOW-6, assessed the impact of MAR through the infiltration pond on the water table at the Sammardenchia site. Figure 2 presents the hydraulic heads in normal conditions, before recharge by the pond.

The simulations were performed for a period of 12 months. Considering the water availability for recharge from the Ledra channel for nine months, with the channel dedicated to irrigation for the remaining three months (summer period) each year, the simulations were divided into two stress periods. The first stress period (wet period) continued for 270 days, during which water is available for recharge. This was followed by a second stress period (dry period) when the pond was dry, which continued up to

365 days. A constant water level of 3 m above the pond bottom was assumed during the recharge period.

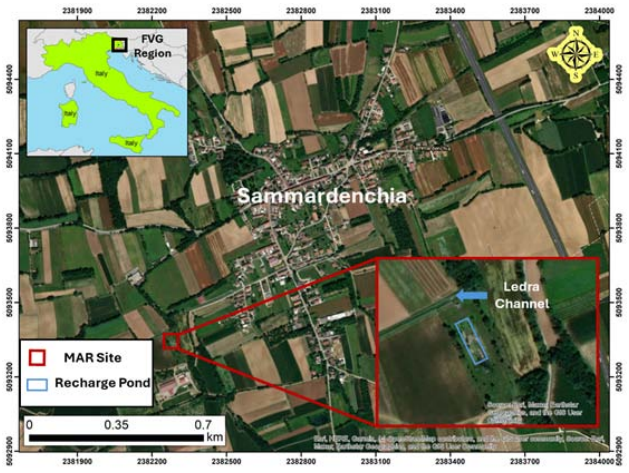


Figure 1. Location of study area.

The simulation results were analyzed at different time steps, as presented in Figure 3. The results revealed a significant increase in the water level just under the pond and in the vicinity of the pond. At the end of the dry period, a maximum rise in the water table of around 0.27 m was observed just beneath the pond, with a minimum rise of 0.1 m at a distance of 500 m from the pond (Figure 3c).

The study outcomes highlight the potential of MAR in the study area and encourage the extension of MAR practice in the upper Friuli plain, supported by the presence of several gravel pits and a dense network of artificial channels, to replenish the declining groundwater resources in the region.

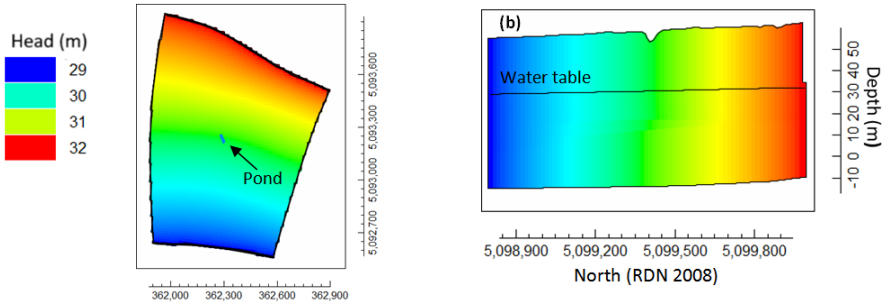


Figure 2. Hydraulic heads under normal conditions prior to recharge, represented in (a) plan view and (b) cross-sectional view.

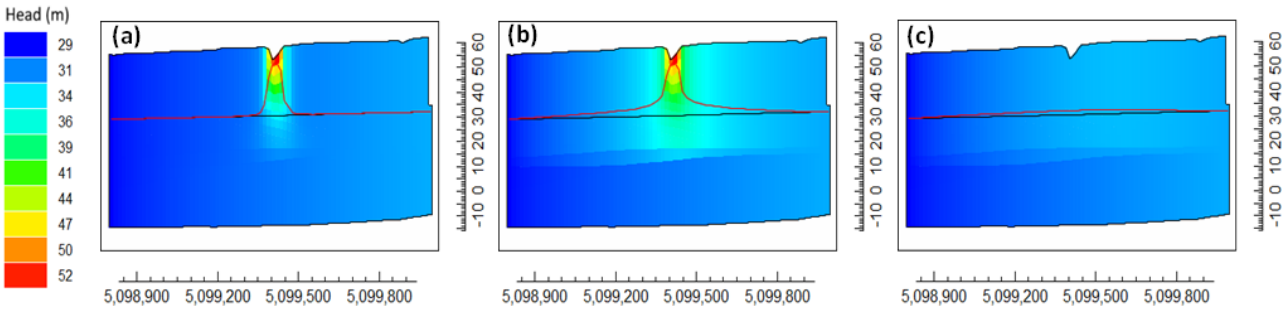


Figure 3. Model outcomes during the wet and dry periods (a) after 7 days of recharge, (b) at 270 days, the end of wet period, and (c) at 365 days, the end of dry period.

References

Martelli G, Granati C (2007) Valutazione della ricarica del sistema acquifero della bassa pianura friulana. Giornale di Geologia Applicata 5: 89–114. https://doi.org/10.1474/GGA.2007-05.0-07.0169

Teatini P, Comerlati A, Carvalho T, Gütz AZ, Affatato A, Baradello L, Accaino F, Nieto D, Martelli G, Granati G, Paiero G (2015) Artificial recharge of the phreatic aquifer in the upper Friuli plain, Italy, by a large infiltration basin. Environmental Earth Sciences 73: 2579-2593.

Teatini P, Martelli G, Comerlati A, Paiero G, Zoccarato C (2020) Managed versus natural recharge to pre phreatic aquifers. Water Resources Research 56(9): e2020WR027848.

Groundwater index development for mapping suitable borehole sites: A case study of the Dakhla aquifer, southwestern Morocco

Y. Ez-zaouy[1,2*], L. Bouchaou[2,3], A. Saad[4], A. Afquir[4,5], G. Busico[1], M. Mastrocicco[1], M. Bordbar[1], F. Raibi[2], S.M. El Kanti[5], M. Hssaisoune[2,6], Y. Ait Brahim[2]

[1] *Di.S.T.A.Bi.F/University of Campania "Luigi Vanvitelli"/Via A. Vivaldi 43, 81100 Caserta, Italy*
[2] *International Water Research Institute/ Mohammed VI Polytechnic University (UM6P)/43150 BenGuerir, Morocco*
[3] *Laboratory of Applied Geology and Geo-environment/Ibn Zohr University/80000 Agadir, Morocco*
[4] *Laboratory of Geo-Bio-Environment Enginnering and Innovation (2GBEI)/Ibn Zohr University/83000 Taroudant,Morocco*
[5] *Hydraulic Agency of Sakia El Hamra Oued Eddahab Basin/70000 Laayoune, Morocco*
[6] *Faculty of Applied Sciences, Ibn Zohr University, B.O. 6146 Azrou District, 86153, Ait Melloul, Morocco*
** e-mail: yassin.zawi@gmail.com*

Introduction

Morocco's Sahara has the country largest aquifer (Edoulati et al. 2013). The aquifer in the Dakhla region, located in the southwest of Moroccan Sahara, stands out as particularly significant. Over recent decades, the region has experienced notable growth across various sectors, including population increase, tourism expansion, industrial development, and the extension of agricultural lands, highlighting the need for a sound management of groundwater resources (El Kanti et al. 2018). The deep aquifer in the region is under significant pressure due to limited recharge, excessive pumping and high-water demand driven by various uses (Edoulati et al. 2013). Moreover, the aquifer is affected by salinization processes from both natural and anthropogenic sources, rendering the groundwater unsuitable for drinking and domestic use (Ez-zaouy et al., 2022; Mizeb et al. 2022). This situation poses a significant threat to the sustainability of groundwater resources, increasing their vulnerability. Consequently, identifying suitable sites for drilling new boreholes is crucial to support decision makers and sustainable groundwater management in the region. In this study, we present an approach that integrates chemistry and machine learning to map potential sites for implanting new boreholes in the Dakhla region.

Materials and methods

To identify suitable sites of low salinity for drilling new boreholes, an approach integrating machine learning (ML) was used. The methodology employed the Random Forest (RF) algorithm to prioritize chemical factors influencing groundwater quality. Sodium Adsorption Ratio (SAR) is one of the indices used to evaluate the suitability of groundwater for irrigation purposes. This index considers only Na^+, Mg^{2+}, and Ca^{2+} concentrations. However, there are other elements which could influence the quality of groundwater. Hence, a new index was created based on HCO_3^-, Cl^-, Br^-, SO_4^{2-}, Na^+, K^+, Mg^{2+}, and Ca^{2+}, which have been assigned weights on the basis of their contribution to the mineralization process. In this regard, the RF algorithm was applied to determine the ranking of parameters (Pourghasemi et al. 2022; Bordbar et al. 2023). This method combines multiple classification and regression trees (CART) using bagging and randomization methods to create a composite model with higher diversity. The two main measures were the average decrease in accuracy (MDA) and the average decrease in Gini (MDG) (Wang et al. 2015; Bordbar et al. 2023). In this study, MDA was employed to assign weight and prioritize chemical factors influencing aquifer salinity, offering a superior solution for prioritizing factors, particularly in scenarios where there are relationships between parameters.

Results and concluding remarks

The final map produced (Figure 1a) shows four classes for drilling new boreholes in the study site: the highly recommended sites are highlighted in dark green, the suitable sites in green, the not recommended

sites in yellow, and the unsuitable sites in red. Results indicate that the study area presents 6.6%, 62.1%, 23.0%, and 8.3% of highly recommended, suitable, not recommended, and unsuitable sites, respectively. The comparison of the final map (Figure 1a) with electrical conductivity of groundwater samples (Figure 1a), illustrates that 74% of samples with electrical conductivity less than 2700 µS/cm (according to the Moroccan standard) are in suitable to high recommended sites. Moreover, the final map shows similar distribution of classes compared to SAR index (Figure 1b). The areas with low and medium SAR have almost the same location as highly recommended and suitable sites. Areas with high and very high SAR show classes of not recommended and unsuitable sites for drilling new boreholes in the study site. The best locations are in the north and northeast part, whereas the middle, extreme south, middle of peninsula, and southeast of the study area are not suitable.

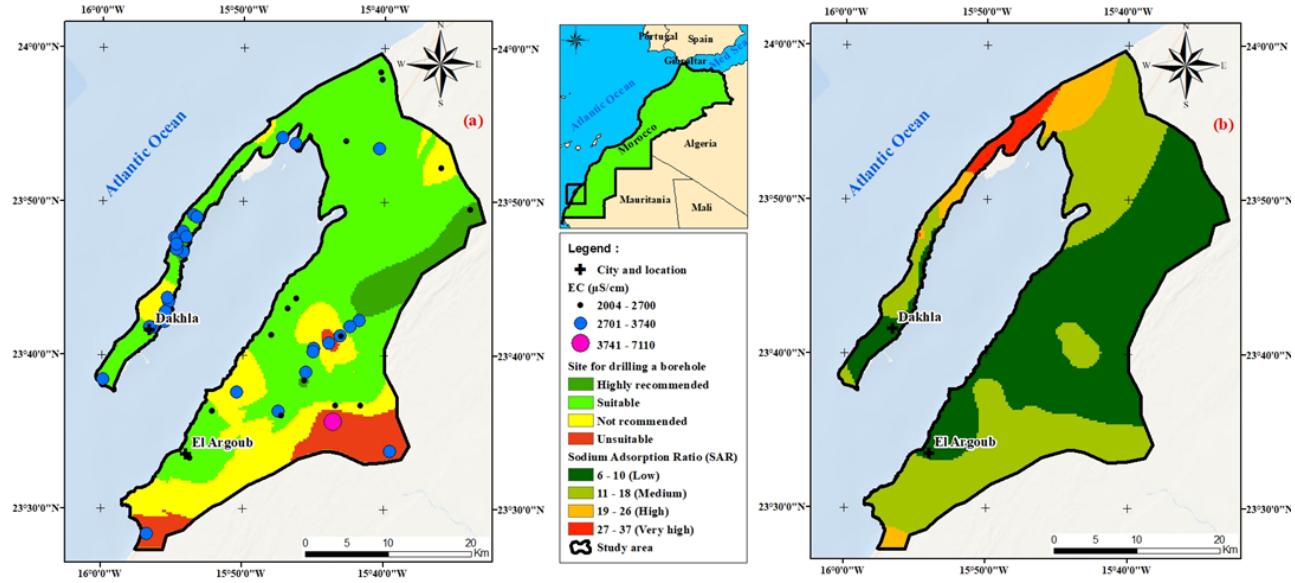


Figure 1. Suitability map for drilling boreholes and Electrical conductivity values according to the Moroccan standard limit (2700 µS/cm) (a); Sodium adsorption index (SAR) (b).

References

Bordbar M, Nikoo MR, Sana A, Nematollahi B, Al-Rawas G, Gandomi AH (2023). Assessment of the vulnerability of hybrid coastal aquifers: application of multi-attribute decision-making and optimization models. Hydrological Sciences Journal, 68(8), 1095-1108. https://doi.org/10.1080/02626667.2023.2203825

Edoulati N, Boutaleb S, Bettar I, Ouchbani A (2013) Contributions of Chemical and Isotopic Tools for Understanding the Groundwater Modes Recharge and Flow in the Lower Cretaceous Aquifer in the Moroccan Sahara. Journal of Water Resource and Protection. 2013 (5), 183–199. https://doi.org/10.4236/jwarp.2013.52020

Ez-zaouy Y, Bouchaou L, Saad A, Hssaisoune M, Brouziyne Y, Dhiba D, Chehbouni A (2022). Morocco's coastal aquifers: Recent observations, evolution, and perspectives towards sustainability. Environmental Pollution, (293), 118498. https://doi.org/10.1016/j.envpol.2021.118498

El Kanti S, El Mansouri B, Arjdal Y (2018). Management of the Laayoune-Dakhla Deep Aquifer System (South Sahara, Morocco). In: Kallel, A et al. (eds) Recent Advances in Environmental Science from the Euro-Mediterranean and Surrounding Regions. EMCEI 2017. Advances in Science, Technology & Innovation. Springer, Sousse. pp 603-605

Mizeb K, Doubi M, Ghalit M, El Kanti M, Hachi T, Abba EH, Erramli H (2022). Quality assessment of groundwater in the region of Laayoune-Dakhla (southern Sahara Morocco) for drinking and irrigation purposes. Moroccan Journal of Chemistry, 10(3): 464-475. https://doi.org/10.48317/IMIST.PRSM/morjchem-v10i3.33070

Pourghasemi HR, Pouyan S, Bordbar M, Clague JJ (2022). Environmental multi-hazard assessment and its importance role in land use planning and hazard management. Natural Hazards: 1-28 https://doi.org/10.21203/rs.3.rs-2022191/v1

Wang H, Wang C, Lv B, Pan X (2015). Improved variable importance measure of random forest via combining of proximity measure and support vector machine for stable feature selection. Journal of Information & Computational Science, 12(8), 3241-3252. https://doi.org/10.12733/jics20105854

Multi-dimensional assessment of groundwater sustainability in South Korea using groundwater sustainability management indicators

Y. Hyun*, A. Jeong
Division of Integrated Water Management, Korea Environment Institute, Sejong, South Korea
** e-mail: yjhyun@kei.re.kr*

Introduction

Groundwater is a critical water resource, especially in regions with limited surface water availability. However, over-extraction and contamination have led to severe challenges such as groundwater depletion, land subsidence, and water quality degradation, with significant socioeconomic impacts. With increasing concern of groundwater depletion and degradation, South Korea establish and operate legislative measures for sustainable groundwater management. However, there lacks a systematic system to assess groundwater sustainability. This study aims to develop a robust framework of groundwater sustainability management indicators (GSMIs) to evaluate groundwater sustainability including the status of groundwater resources as well as the degree of implementation of groundwater policy. Then, this study aims to propose indices to assess multi-dimensional aspects of groundwater sustainability using GSMIs.

Materials and methods

The study employed the Drivers-Pressure-State-Impact-Response (DPSIR) framework to construct GSMIs. It categorized GSMIs into two main groups: status (groundwater quantity and quality) and policy (management foundation and policy implementation). GSMIs were standardized and aggregated to develop several indices associated with groundwater sustainability. These indices assess multi-dimensional aspects of groundwater sustainability and facilitate spatial comparisons. Indices were developed through three phases. In the first phase, standardized GSMIs were aggregated into four integrated indices including quantitative adequacy, water quality safety, implementation base robustness, and policy execution efficiency. In the next (second) phase, standardized GSMIs were aggregated into two integrated indices including status index and policy index. In the third phase, standardized status and policy indices were aggregated into a Groundwater Sustainability Management Index (GSM Index) (Figure 1).

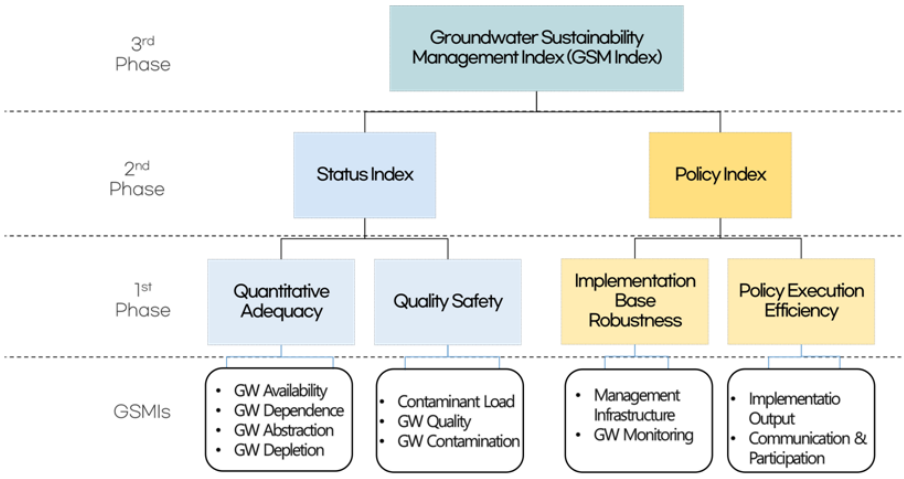


Figure 1. Multi-dimensional Indices of Groundwater Sustainability Management Indicators (GSMIs).

Results and concluding remarks

South Korea has 16 provincial governors, each responsible for managing groundwater in their respective

provinces. This study assessed the sustainability of groundwater in the 16 provinces using GSMIs. Key findings include that Gangwon scored the highest in terms of quantitative adequacy due to its abundant groundwater recharge, driven by favorable climatic and hydrological conditions. Conversely, Chungnam exhibited lower scores, largely attributed to over-extraction for agricultural and industrial purposes. The nationwide average for quantitative adequacy was calculated at 0.43, with significant disparities highlighting regional differences in groundwater recharge and use patterns. As to water quality safety, Jeju and Gwangju excelled, achieving above-average scores due to stringent water quality management and naturally favorable conditions. In contrast, Gyeonggi and Incheon faced challenges, with multiple monitoring points indicating contamination risks. The nationwide average for water quality safety was 0.61, emphasizing the need for targeted water quality improvement measures in specific regions. Jeju also received the highest evaluation for implementation base stability, supported by robust institutional frameworks and consistent monitoring systems. On the other hand, Gyeongbuk recorded relatively low scores, indicating insufficient infrastructure and limited personnel training for effective groundwater management. The nationwide average for this category was 0.49. For Policy Execution Efficiency, Jeju, Seoul, and Chungnam demonstrated strong policy execution efficiency, attributed to proactive governance and community engagement. However, Sejong and Gyeonggi lagged behind, with lower levels of stakeholder participation and inadequate policy enforcement. The nationwide average for policy execution efficiency stood at 0.47. Overall multi-dimensional Indices revealed significant regional variations in groundwater sustainability across South Korea (Figure 2). These findings underscore the importance of localized management strategies tailored to regional characteristics.

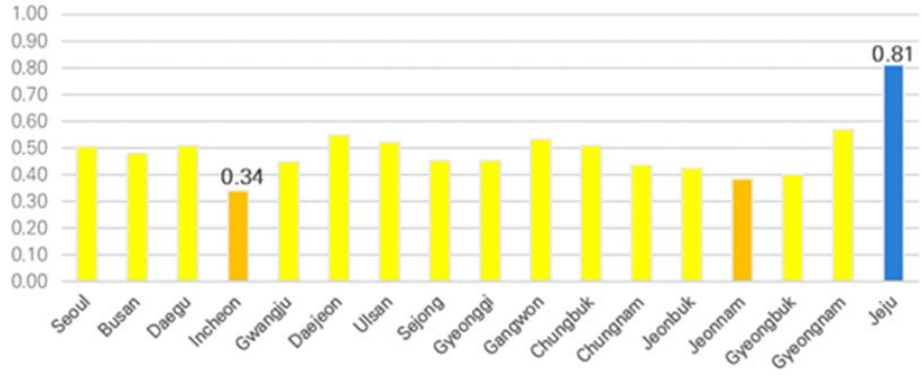


Figure 2. Groundwater Sustainability Management Index Values Evaluated for 16 Provinces of South Korea

In conclusion, the development of GSMIs provides a meaningful tool for evaluating and managing groundwater sustainability in South Korea. These indicators offer actionable insights for policymakers and local governments, supporting tailored strategies to address regional challenges. Future efforts should focus on refining evaluation systems, integrating spatial data, and institutionalizing the GSMI framework to enhance policy effectiveness. This approach can contribute to sustainable groundwater management of South Korea, ensuring water security and resilience against climate change.

Acknowledgments: This paper was written following the research work “RE2024-10” and “GP2025-08”, funded by the Korea Environment Institute (KEI)

References

Hosseini, S. M. et al. (2019) Assessment of Sustainable Groundwater Resources Management Using Integrated Environmental Index: Case Studies across Iran, Science of the Total Environment 676: 792-810. https://doi.org/10.1016/j.scitotenv.2019.04.257

Hyun Y, Jeong A, Cha E, Lee G, Park W, Kim O (2023) Development and Application of Groundwater Management Indicators for Groundwater Sustainability (I), Korea Environment Institute, Seoul

UNESCO, IAEA, IAH Groundwater Indicators Working Group (2007) Groundwater Resources Sustainability Indicators, IHP-VI Series on Groundwater No. 14, UNESCO, Paris

Modelling scenarios of contaminant transport in an equivalent porous medium

A. Campobasso
DICATECh, Polytechnic University of Bari, Bari, Italy
e-mail: alessandra.campobasso@poliba.it

Introduction

The expansion of urban areas, industrial activities, and increasing water demand due to climate change have led to greater urban runoff from impervious surfaces, negatively affecting groundwater quality and quantity. One proposed solution is the reuse of urban runoff for groundwater recharge through soil infiltration. Managed Aquifer Recharge (MAR) techniques allow for controlled aquifer replenishment, aiding in water recovery and preventing seawater intrusion (Dillon et al., 2018). In the U.S.A., injection wells are commonly used to convey runoff into urban aquifers, especially in semi-arid regions, though residual contaminants in the injected stream pose potential health risks This research aims to address hydrogeological challenges by using a case study in Avetrana (Apulia Region, South of Italy) as a reference. In this context, the study focuses on developing a model that accurately represents the groundwater system, providing a valuable tool for managing water resources and preventing pollution in karst aquifers. A channel was designed in Avetrana to collect and divert stormwater, protecting the built-up area. The region experiences significant hydraulic disturbances, requiring an evaluation of the karst aquifer's vulnerability, given its low natural filtration capacity and fragility. Karst aquifers are highly susceptible to contamination due to their interconnected void network, allowing rapid pollutant transfer to springs. Restoring these aquifers after contamination is extremely difficult, if not impossible, emphasizing their vulnerability (Parise et al., 2007).

Materials and methods

To model pollutant behaviour in soil and develop effective remediation strategies, selecting an appropriate groundwater flow model is essential. In karst aquifers, the identification and spatial distribution of conduits pose challenges, affecting the accuracy of numerical models (Chen et al., 2014). To address this, the Equivalent Porous Medium approach was adopted, approximating fractured rock as a continuous medium by considering rock matrix properties over a statistically representative volume. This method helped determine aquifer properties that are difficult to detect through tectonic and geophysical studies. Geological analysis identified two hydrogeological environments: an upper calcarenite layer with low absorption capacity and a lower limestone layer with primary and secondary discontinuities, hosting the deep-water table. Hydrological parameters were obtained from in-situ sounding tests, treating both geological units as isotropic media. The Equivalent Porous Medium approach facilitated the simulation of groundwater flow and pollutant transport. For numerical modelling, FEFLOW software (https://www.dhigroup.com/technologies/mikepoweredbydhi/feflow), based on the finite element method, was used to develop a three-dimensional groundwater model. The objective was to simulate groundwater flow and pollutant transport in the unsaturated zone, assessing soil infiltration capacity and potential deep aquifer contamination. FEFLOW is an advanced tool for modelling flow and transport in porous media under both saturated and unsaturated conditions. Its graphical interface enables detailed simulations of subsurface flow dynamics and contaminant transport in complex aquifer systems.

Results and concluding remarks

The modelling process involved multiple phases, including steady-state and transient simulations of flow and pollutant transport, both with and without an injection well. Steady-state models represented system

conditions under fixed parameters, while transient simulations tracked pollutant movement over a defined period. Groundwater flow patterns were determined using data from hydrogeologic reports, field tests, and literature. Three scenarios were analysed, varying the limestone layer's equivalent porosity at 50%, 70%, and 90%, as direct in-situ measurements were unavailable, and estimates were based on observed fractures. Pollutant transport simulations assessed concentration levels and particle movement trends. The spread of contamination varied depending on the infiltration method, whether through direct ground entry or an injection well. In both cases, pollutant plumes expanded with increasing porosity. Injection wells exhibited a dilution effect due to changes in initial transport conditions. Maximum concentration values were studied across three depth slices, showing containment at shallow levels but wider dispersion at greater depths. Velocity comparisons highlighted that diffusion was faster through injection wells, with transport speeds increasing as porosity rose. Under transient conditions, higher porosity led to greater pollutant diffusion (Figure 1), but movement slowed when transitioning from calcarenite to limestone. The results suggest that lithological characteristics influence pollutant movement, with geological structures potentially acting as natural barriers under specific conditions. The methodology used in this study enabled the development of a conceptual hydrogeological model of the karst aquifer, supporting mass transport simulations under different conditions. This approach provided a reliable representation of groundwater dynamics, aiding in pollution prevention for karst aquifers, which are highly sensitive due to their inherent variability. Numerical modelling proved to be an effective tool for systematically analysing complex hydrogeological systems, identifying areas vulnerable to contamination, such as pollutant plumes and inverse conoids. The findings offer valuable insights for regulatory decisions regarding pollutant release management, with potential applications in similar karst aquifer settings. Given the widespread presence of karst systems, this study presents a practical framework for managing contamination risks, contributing to water resource protection and sustainable environmental management.

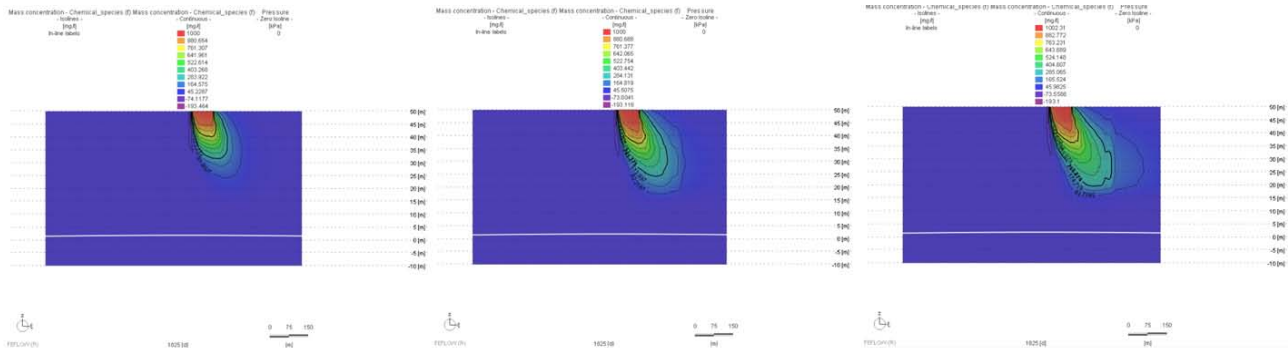


Figure 1. Simulation of the transport in transient state. Scenarios of plume trend (50% - 70% - 90% limestone porosity)

References

Castiglioni S, Valsecchi S, Polesello S, Rusconi M, Melisa M, Palmiotta M, Manenti A, Davoli E, Zuccato E (2015) Sources and fate of perfluorinated compounds in the aqueous environment and in drinking water of a highly urbanized and industrialized area in Italy. https://doi.org/10.1016/j.jhazmat.2014.06.007

Chen Z, Goldscheider N (2014) Modeling spatially and temporally varied hydraulic behavior of a folded karst system with dominant conduit drainage at catchment scale. Journal of Hydrology 514(6): 41-52. https://doi.org/10.1016/j.jhydrol.2014.04.005

Dillon P, Stuyfzand P.J, Grischek T, Liuria M (2018) Sixty years of global progress in managed aquifer recharge. Hydrogeology Journal. https://doi.org/10.1007/s10040-018-1841-z

Lazarova V, Levine B, Sack J, Cirelli G, Jeffrey P, Muntau H (2001) Role of water reuse for enhancing integrated water management in Europe and Mediterranean countries. Water Sci. Technol 43: 25–33. https://doi.org/10.2166/wst.2001.0571

Li F, Fang X, Zhou Z, Liao X, Zou J, Yuan B, Sun W (2019) Adsorption of perfluorinated acid onto soils: Kinetics, isotherms, and influences of soil properties. https://doi.org/10.1016/j.scitotenv.2018.08.209

Parise M, Gunn J (2007) Natural and anthropogenic hazards in karst areas: an introduction. Geological Society, London 279(1): 1-3. https://doi.org/10.1144/sp279.1

Van Genuchten M, Leij F, Skaggs T, Toride N, Bradford S, Pontedeiro E (2013) Exact analytical solutions for contaminant transport in rivers Journal of Hydrology and Hydromechanics 61(3):250-259. https://doi.org/10.2478/johh-2013-0032

Hydrological modelling of a fractured volcanic aquifer: Interactions between anthropogenic usage and the natural system

M. Silipigni[1,2*], C. Di Salvo[3], E. Preziosi[4], I. Borzì[5], B. Bonaccorso[2]
[1] *School for Advanced Studies IUSS, Pavia, Italy*
[2] *Department of Engineering, University of Messina, Messina, Italy*
[3] *Institute of Environmental Geology and Geoengineering, CNR, Rome Research Area 1, Monterotondo (Rome), Italy*
[4] *Water Research Institute, CNR, Rome Research Area 1, Monterotondo (Rome), Italy*
[5] *Department of Mathematical and Computer Sciences, Physical Sciences, Earth Sciences, University of Messina, Italy*
** e-mail: marco.silipigni@iusspavia.it*

Introduction

The Alcantara River basin, located in Sicily (Italy), covers an area of 606 km², including the northern slopes of Mount Etna, Europe's highest active volcano (3357 m a.s.l.). The river stretches for 55 km, originating from the Nebrodi Mountains at 1400 m a.s.l. and discharging into the Ionian Sea approximately 5.5 km south of Taormina (Messina). Groundwater significantly sustains the river's flow. On average, irrigation and drinking water wells extract 0.23 m³/s, while a drainage gallery collects water from three springs, supplying the Alcantara aqueduct with an average flow rate of 0.48 m³/s, as measured from January 2009 to December 2022.

The purpose of this study is to enhance the understanding of the aquifer-river interactions and assess the impacts of groundwater extractions on the natural system. Given the challenges associated with the lack of systematic monitoring data (e.g., hydraulic head, discharge rate, aquifer thickness), we integrated available information from multiple sources. These include historical climate and discharge records, measured inflows to the conveyance system, hydraulic head data from previous surveys, and aquifer thickness derived by previous studies and the stratigraphic profile of a geologically analogous section of the Mount Etna. This dataset was used to calibrate and validate MODFLOW 6. The calibrated model was then applied to simulate system behaviour under different water management scenarios. Furthermore, climate change scenarios were introduced to evaluate the system's resilience under altered recharge and extraction conditions.

Materials and methods

The aquifer system was modelled using MODFLOW 6 (Langevin et al. 2017), a finite-difference numerical code developed by the U.S. Geological Survey (USGS). The study covered 14 years (2009–2022), utilizing monthly groundwater withdrawal records provided by the aqueduct operator. Hydraulic conductivity was calibrated using PEST (Doherty 2016), a software tool for parameter estimation and uncertainty analysis.

Two scenarios were considered: (1) *the current condition*, including all known groundwater extractions, and (2) a *hypothetical scenario without extractions*.

Recharge was applied directly to the water table, bypassing the delay/dampening processes typically associated with the unsaturated zone. Specifically, net precipitation was calculated using total precipitation data (including both liquid and solid forms), actual evapotranspiration, and average temperature data from the ISPRA BIGBANG 1km x 1km gridded dataset (Braca et al. 2021).

The geological sequence was schematized into two formations: the uppermost Ancient Volcanic Rocks and the Ancient Mongibello Volcanic-Pyroclastic Complex, and the lowermost Sedimentary Complex. The bottom of the Ancient Volcanic Rocks and the Ancient Mongibello Volcanic-Pyroclastic Complex, which is coincident with the top of the sedimentary substratum, was reconstructed by referencing the study by Branca and Ferrara (2001). Hydraulic head data date back to surveys conducted for the realization of the Hydrogeological Map of the volcanic massif of Etna (Ferrara et al. 2008). Additional data were extracted from the National Underground Investigations Archive (Law 464/1984) of the Department for Geological

Survey of Italy – ISPRA. These data were interpolated using the Ordinary Kriging method to generate an initial hydraulic head distribution for steady-state simulations. Model validation was performed by comparing observed and simulated discharge trends from the drainage gallery.

Results and concluding remarks

Simulation results indicate that groundwater extractions reduce natural spring discharge to the river by an average of 22%. This reduction exhibits significant seasonal variability, with the most pronounced impacts in spring and less severe effects in winter. Interestingly, despite this reduction, the midstream section of the river did not experience zero discharge, even during the driest periods (e.g., the summers of 2020 and 2021). This discrepancy suggests the influence of additional unaccounted factors, such as unauthorized or unrecorded water withdrawals, or potential hydrogeological changes induced by seismic activity.

Ongoing research aims to integrate climate change scenarios into the modelling framework. Specifically, building on previous studies by Peres et al. (2020, 2023), an optimized weighted ensemble average (OWEA) of selected Euro-CORDEX climate models will be used, considering RCP4.5 and RCP8.5 scenarios over two projection periods (2021–2050 and 2041–2070). Simulations under these climate scenarios will provide insights into climate change impacts on groundwater levels, spring discharges feeding the Alcantara River, and flow captured by the drainage gallery. This will enable a comprehensive assessment of the system's response to future climatic conditions. Preliminary results suggest increased stress on the aquifer system, with reduced recharge exacerbating the effects of existing extractions.

These findings underscore the importance of adapting groundwater management strategies to account for both anthropogenic pressures and climatic variability. Furthermore, enhanced monitoring of groundwater and surface water resources is crucial for reducing model uncertainty and identifying sustainable extraction limits under future scenarios.

References

Braca G, Bussettini M, Lastoria B, Mariani S, Piva F (2021) Il Bilancio Idrologico Gis BAsed a scala Nazionale su Griglia regolare – BIGBANG: metodologia e stime. Istituto Superiore per la Protezione e la Ricerca Ambientale, Rapporti 339/21, Roma, Italy

Branca S, Ferrara V (2001) An example of river pattern evolution produced during the lateral growth of a central polygenic volcano: the case of the Alcantara river system, Mt Etna, Italy. Catena 45(2): 85–102. https://doi.org/10.1016/S0341-8162(01)00144-8

Doherty J (2016) PEST: Model-independent parameter estimation. Watermark Numerical Computing, Melbourne, Australia

Ferrara V, Pappalardo G (2008) La carta idrogeologica del massiccio vulcanico dell'Etna come utile strumento per la gestione razionale delle risorse idriche sotterranee. Italian Journal of Engineering Geology and Environment, Special Issue 1

Langevin C.D, Hughes J.D, Prudic D.E (2017) MODFLOW 6: The U.S. Geological Survey modular groundwater model. U.S. Geological Survey, Reston, Virginia

Peres D.J, Bonaccorso B, Palazzolo N, Cancelliere A, Mendicino G, Senatore A (2023) A dynamic approach for assessing climate change impacts on drought: an analysis in Southern Italy. Hydrological Sciences Journal 68(9): 1213-1228. https://doi.org/10.1080/02626667.2023.2217332

Peres D.J, Senatore A, Nanni P, Cancelliere A, Mendicino G, Bonaccorso B (2020) Evaluation of EURO-CORDEX (Coordinated Regional Climate Downscaling Experiment for the Euro-Mediterranean area) historical simulations by high-quality observational datasets in southern Italy: insights on drought assessment. Natural Hazards and Earth System Sciences 20: 3057–3082

Assessment of groundwater nitrate pollution in agricultural catchments at the southwestern Thessaly plain, Greece

V. Sapountzis[1], G. Tziatzios[2], A. Lyra[2], P. Sidiropoulos[1*], A. Loukas[1]
[1] Laboratory of Hydraulic Works and Environmental Management, School of Rural and Surveying Engineering, Aristotle University of Thessaloniki, 54124 Thessaloniki, Greece
[2] Laboratory of Hydrology and Aquatic Systems Analysis, Department of Civil Engineering, School of Engineering, University of Thessaly, 38334 Volos, Greece
* e-mail: pasidirop@topo.auth.gr

Introduction

Thessaly is an agricultural region in Greece, significantly contributing to the country's food supply. Elevated nitrate ion/salts in the region's groundwater systems have been of great concern in recent years, mainly due to intensive agriculture and the increased use of nitrogen fertilizers (Sidiropoulos et al. 2019). This study presents the results of the application of an agronomic-hydrological modeling framework aiming at assessing factors and practices that influence nitrate pollution, on the groundwater system of the Southwestern Thessaly plain. The study area has an extent of 1,262 km^2 and it is covered with a wide variety of cultivations, namely cotton, winter wheat, maize and alfalfa.

Materials and methods

The study uses two advanced models. The APEX (Agricultural Policy/Environmental eXtender) (Williams and Izaurralde 2006) model which is a powerful simulation tool for assessing the impact of agronomic practices and land use on multiple environmental and agronomic parameters and the UTHBAL (Loukas et al. 2007) model which is a conceptual hydrological model that aims to simulate the monthly surface water balance. The main purpose of the simulation system is to evaluate the factors contributing to nitrate pollution and simulate hydrological and agricultural processes providing detailed insights into nutrient cycling, water balance, and pollutant transport in agroecosystems.

Daily meteorological data of precipitation, maximum and minimum temperature, relative humidity and wind speed were collected and processed from local meteorological stations strategically distributed across the study area. The spatial distribution of precipitation was determined using the Thiessen polygon method, ensuring accurate representation of rainfall variability within the study area. Evapotranspiration was estimated using the Thornthwaite method, which calculates potential evapotranspiration (PET) based on temperature records. Furthermore, geomorphological and soil data of the study area such as soil texture, bulk density and organic carbon as well as soil hydrodynamic parameters, Wilting Point and Field Capacity, were also used as input data. Crop management data such as seeding, tillage, fertilization, irrigation and crop residue management are also necessary.

The UTHBAL model was applied, to simulate the surface water balance and estimate the surface runoff and groundwater recharge, using as inputs monthly timeseries of precipitation, temperature and potential evapotranspiration. The model was calibrated using observed runoff data for the Enipeas river basin, allowing for the estimation of water flow and storage within the study area.

The APEX model and the ArcAPEX interface were employed to simulate processes at the sub-basin scale, focusing on water movement, nutrient cycling, and nitrate leaching. The ArcAPEX was used for the delineation of subareas, channels and connectivity between them taking into account flow direction and flow accumulation. The calibration of the model consists of two parts. The initial calibration was based on the potential evapotranspiration derived by the Thornthwaite method and the final calibration of the model was based on crop yields. This calibration ensured the model accurately reflected the region's agricultural and environmental conditions, enabling reliable simulations of nitrate dynamics.

Nitrate leaching, a primary focus of the study, was estimated by integrating the outputs of the two

models. The combined modeling framework provides a comprehensive understanding of nitrate pollution, linking agricultural activities with hydrological processes to evaluate its spatial and temporal variability. The methodology is presented in Figure 1.

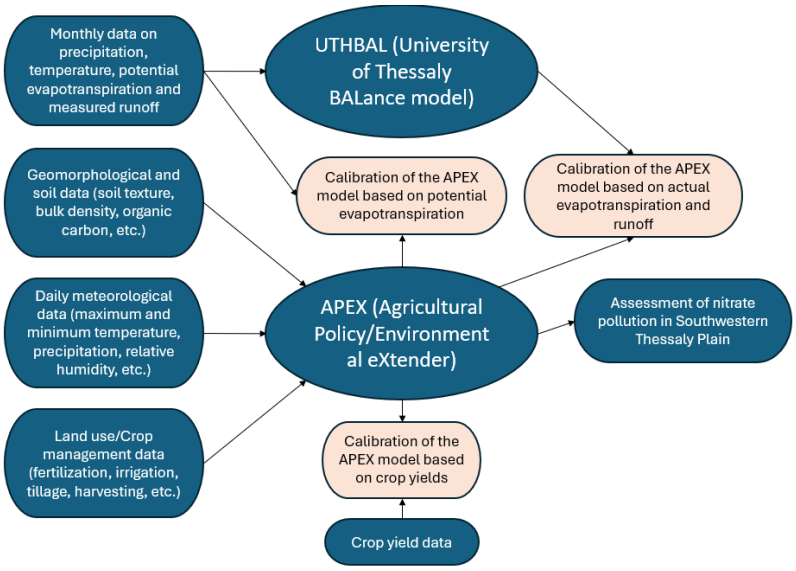


Figure 1. Flow chart of the methodological approach.

Results and concluding remarks

The simulation period was defined as the period from January 1980 to December 2022 and the averaged values of yield for cotton, maize and wheat, the annual estimated potential evapotranspiration (PET), actual evapotranspiration (AET), surface runoff and the nitrate leached towards groundwater are presented in Table 1.

Table 1. Simulation Statistics of the application of UTHBAL and APEX models in Southwestern Thessaly.

Variable	Annual Mean	Eff (Calibration)	Eff (Validation)	R^2 (Calibration)	R^2 (Validation)	Calibration Period	Validation Period
Cotton Yield	3.3 kg/ha	0.52	0.27	0.68	0.89	2000-2015	2016-2021
Wheat Yield	2.5 kg/ha	-0.66	0.29	0.69	0.84	2000-2015	2016-2021
Maize Yield	9.3 kg/ha	0.71	0.46	0.75	0.96	2000-2015	2016-2021
PET (APEX Hargreaves /Thornthwaite)	996/900 mm	0.89	0.87	0.93	0.93	1980-2010	2011-2022
Runoff (UTHBAL)	170 mm	0.70	0.52	0.70	0.68	1980-1988	1989-1993
AET (UTHBAL)	226 mm	-	-	-	-	-	-
Nitrate Leaching (APEX)	62 kg/ha	-	-	-	-	-	-

Hydrological components such as PET and AET, as well as surface runoff, achieved commendable results. The simulated crop yields closely match observed annual averages, highlighting the models' ability to effectively reproduce agricultural output with accuracy. These results emphasize the robustness of the modeling framework in supporting both hydrological and agricultural assessments, satisfactory estimating the nitrate leaching.

References

Loukas A, Mylopoulos N, Vasiliades L (2007) A modelling system for the evaluation of water resources management strategies in Thessaly, Greece. Water resources management 21(10): 1673-1702. http://doi.org/10.1007/s11269-006-9120-5

Sidiropoulos P, Tziatzios G, Vasiliades L, Mylopoulos N, Loukas A (2019) Groundwater Nitrate Contamination Integrated Modeling for Climate and Water Resources Scenarios: The Case of Lake Karla Over-Exploited Aquifer. Water 11(6), 1201. https://doi.org/10.3390/w11061201

Williams JR, Izaurralde RC (2006) The APEX Model. In: Singh VP and Frevert DK (eds.), Watershed Models. CRC Press, Boca Raton, pp 437-482

13th World Congress on Water Resources and Environment (EWRA 2025)
"New challenges in understanding and managing water-related risks in a changing environment"
Palermo, Italy, 24 - 28 June 2025

Integrated modelling of diffuse and point-source pollutants fate and transport in surface water and groundwater using SWAT+gwflow

L. Estrada[1*], R.T. Bailey[2], V. Acuña[1]
[1] Catalan Institute for Water Research (ICRA – CERCA), Girona, Spain
[2] Department of Civil and Environmental Engineering, Colorado State University, Fort Collins, USA
* e-mail: lestrada@icra.cat

Introduction

The chemical pollution of surface waters and groundwater has become a growing concern due to the threat it presents to both ecosystems and public health, and many countries have instated laws and regulations to address this worldwide issue (Arman et al. 2021; Islam et al. 2022). Despite these efforts, water quality frequently does not improve or experiences further deterioration, mostly due to the influence of factors such as climate change, urbanization growth, and demographic shifts. Some of the most concerning compounds are pesticides and pharmaceuticals, which enter the freshwater system either through diffuse or direct sources. Understanding the processes and pollutant dynamics driving water quality is imperative to support efficient, sustainable, and resilient decision-making in the water management sector, and numerical modelling is a powerful tool in order to achieve this. Water quality modelling can easily characterize and assess the impact of pollutants in surface waters and groundwater under current or future conditions, and thus promote best management practices.

During the last decades, many modelling frameworks have been developed to characterize and assess pollutant fate and transport in freshwater systems (Datta et al. 2018; Addis et al. 2023), but their application are mostly limited due to these frameworks not being pollutant-independent and/or relying on coarse (geo)hydrological estimates. Rafiei and Nejadhashemi (2023) addressed the latter by developing an integrated hydrogeochemical model to assess PFAS fate and transport using SWAT-MODFLOW-RT3D. Following a similar approach, we aim to further improve upon it by developing a pollutant-independent modelling framework to assess pollutant fate and transport in surface waters and groundwater using SWAT+gwflow (Bailey et al. 2020), and successfully apply it to several watersheds from the Catalan River Basin District (CRBD), in northeastern Spain (western Mediterranean).

Materials and methods

The structure of the modelling framework is illustrated in Figure 1. It comprises a domestic pollution generation model to simulate pollutant loads after wastewater treatment. Subsequently, these loads as well as industrial discharges and diffuse pollution are inputted into SWAT+gwflow, where the fate and transport module simulate pollutant attenuation and transport in the stream network, reservoirs, and aquifers. The original SWAT+ model only accounts for diffuse pollutant dynamics in surface waters, so we added routines for diffuse pollutant dynamics in groundwater and point-source pollutant dynamics in both surface waters and groundwater. Lastly, the coupling of the generation model and SWAT+gwflow as well as the simultaneous calibration of both models is handled by the custom Python library pySWATPlus.

In previous research, we successfully applied the modelling framework without including the gwflow module and pollutant dynamics in groundwater to assess ciprofloxacin and venlafaxine concentrations in three small to medium-sized Mediterranean basins of the CRBD: Llobregat, Besòs and Tordera basins. The newer modelling framework including groundwater dynamics will also be applied to these basins. We will perform multi-objective model calibration of streamflow, groundwater head, river water quality, and groundwater water quality using the pySWATPlus library, and we will compare results from the surface waters-only framework and the integrated surface waters-groundwater framework.

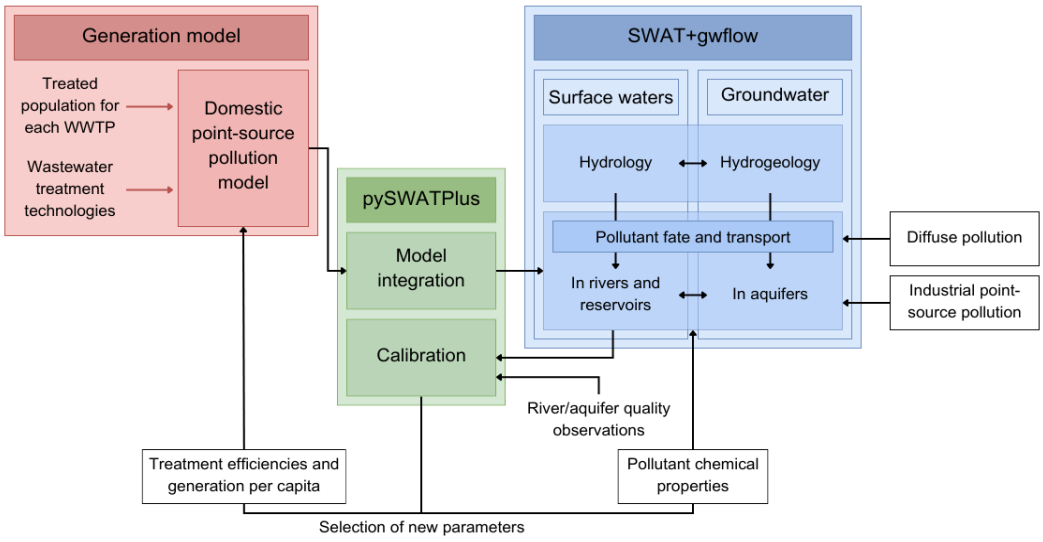


Figure 1. Overview of the modelling framework including the domestic pollution generation model, the surface and subsurface pollutant fate and transport modules within SWAT+gwflow, and the pySWATPlus library.

Results and concluding remarks

Not including the gwflow module and pollutant dynamics in groundwater, the calibrated modelling framework demonstrates good model performance (R^2 > 0.6, PBIAS < -10.3%) for ciprofloxacin and venlafaxine concentrations in the Llobregat and Besòs-Tordera basins of the CRBD, respectively (Saló-Grau et al. 2025). These results provide a comprehensive spatio-temporal assessment of pollutant concentrations, leading to the identification of dynamics and patterns that could not be captured with the available scarce observations, such as attenuation along the stream network and seasonal variability.

The incorporation of groundwater processes using the gwflow module for SWAT+ is expected to further improve the modelling framework, resulting in a better representation of real system and pollutant dynamics. This process-based modelling approach will deepen our understanding of how diffuse and point-source pollution impact both surface waters and groundwater, including different climatic and/or management scenarios, and thus supporting better-informed, sustainable decision-making.

Acknowledgments: This research was funded by the European Union's Horizon 2020 research and innovation programme under grant agreement No 101036337 (project MERLIN).

References

Addis TZ, Adu JT, Kumarasamy M, Demlie M (2023) Assessment of Existing Fate and Transport Models for Predicting Antibiotic Degradation and Transport in the Aquatic Environment: A Review. Water 15:1511. https://doi.org/10.3390/W15081511

Arman NZ, Salmiati S, Aris A, et al (2021) A Review on Emerging Pollutants in the Water Environment: Existences, Health Effects and Treatment Processes. Water 13:3258. https://doi.org/10.3390/w13223258

Bailey RT, Bieger K, Arnold JG, Bosch DD (2020) A New Physically-Based Spatially-Distributed Groundwater Flow Module for SWAT+. Hydrology 7:75. https://doi.org/10.3390/HYDROLOGY7040075

Datta AR, Kang Q, Chen B, Ye X (2018) Fate and Transport Modelling of Emerging Pollutants from Watersheds to Oceans: A Review. In: Chen B, Zhang B, Zhu Z, Lee K (eds) Emerging Pollutants and Their Effects on Marine Ecosystems. Academic Press, pp 97–128

Islam MA, Amin SMN, Rahman MA, et al (2022) Chronic effects of organic pesticides on the aquatic environment and human health: A review. Environmental Nanotechnology, Monitoring & Management 18:100740. https://doi.org/10.1016/j.enmm.2022.100740

Rafiei V, Nejadhashemi AP (2023) Watershed scale PFAS fate and transport model for source identification and management implications. Water Research 240:120073. https://doi.org/10.1016/j.watres.2023.120073

Saló-Grau J, Estrada L, Llorente O, et al (2025) Integrated modeling of the generation, attenuation, and transport of point-source pollutants at the watershed-scale using SWAT+. Environmental Modelling & Software [manuscript submitted for publication]

Determination of baseline values in evaporitic aquifers: A case study from southern Sicily (Montallegro-Siculiana area)

E. Rotigliano[1], F. Lo Medico[1*], P. Rizzo[2], C. Cappadonia[1], F. Celico[2]
[1] Department of Earth and Marine Sciences, University of Palermo, Palermo, Italy
[2] Department of Chemistry, Life Sciences and Environmental Sustainability, University of Parma, Parma, Italy
*e-mail: federica.lomedico@unipa.it

Introduction

In Italy, groundwater quality is regulated by predefined values, known as Threshold Concentration Limits ("Concentrazione Soglia di Contaminazione": CSC), are established by the Legislative Decree 152/2006 (Annex 5, Part IV, Table 2 – Groundwater Contamination Threshold Concentrations). However, these values cannot be considered universally applicable across the entire national territory, necessitating a highly site-specific approach for an accurate assessment of real baseline levels, coherent to the hydrogeochemical characteristics of groundwater systems. Natural baseline values for an evaporitic aquifer in the Montallegro-Siculiana (Southern Sicily) area were investigated. In facts, in this area a wide folded sector of Miocene (Serravallian to Messinian) formation rocks results in a very specific hydrogeological setting, with the superimposition of highly permeable fissured gypsum sequences on a very low permeable clayey substratum (Feo et al., 2023; Rizzo et al., 2020). Along the valleys of the drainage network alluvial and colluvial permeable deposits are also found. In light of their limited interest for domestic or agriculture uses, few data are available for characterizing these groundwater systems. At the same time, any land use planning issues (e.g., crops, landfill, mines) always requires comparing monitoring data to a reference baseline, dependent on the local geological, hydrogeological, and environmental context. This study was conducted in accordance with the methodology outlined by ISPRA (Italian Institute for Environmental Protection and Research) guidelines (SNPA, 2018) and adopts an integrated approach that combines environmental monitoring data with advanced geochemical characterization of the local context. Several studies (Bulut et al., 2020; Zanotti et al., 2022) have emphasized the need to define baseline values, which are essential for distinguishing natural from potential anthropogenic contaminated conditions, thereby enabling a more precise evaluation of groundwater quality.

Materials and methods

The methodology adopted in this study was developed through several phases of data acquisition, analysis, and evaluation. The initial phase focused on the collection and preliminary analysis of available information, which was crucial for constructing a conceptual model of the study area and for defining an effective monitoring network. Exploiting a very refined piezometric network (39 piezometers and six springs, for a less than 10 km^2 area), two years (2021–2023) piezometric monthly survey, allowed us to reconstruct the piezometric surface and its primary groundwater flow directions. In light of this hydrogeological framework, a subset of 13 piezometers located upstream of areas identified as potential any sources of anthropogenic pollution were extracted. At these sampling points, physicochemical parameters were measured, and detailed analyses of cations, anions, metals were conducted quarterly over a two-year period. A total of more than one-hundred analysis was processed and accepted into the final database). The collected data underwent in-depth multivariate statistical analysis to determine baseline values. The statistical methods included normality tests (Anderson-Darling Test), outlier detection tests (boxplot and Huber test), temporal trend analysis (Mann-Kendall and Theil-Sen tests), and principal component analysis (PCA). Leaching tests were also available for soil/rock samples in all the piezometers to assess species mobility across different environmental compartments. The application of rigorous hydrogeological criteria enabled the identification of key factors influencing groundwater chemistry, facilitating a more accurate interpretation of baseline processes and potential contamination sources.

Results and concluding remarks

The data analysis revealed exceedances of the Threshold Concentration Limits (CSC) for B, F^-, Fe, Mn, Ni, NO_2^-, and SO_4^{2-} which are defined at Legislative Decree 152/2006 in all the piezometers. Leaching tests confirmed the natural presence of high levels of these elements, attributable to the geological composition of the area, which is characterized by Messinian evaporitic deposits and basal clays (Lo Medico et al., 2025). In particular, exceedances are observed in the leaching tests for B, Fe, Ni, predominantly in clayey lithologies, and for SO_4^{2-} in all the lithologies outcropping in the area. The calculated distribution coefficients (Kd) indicate a natural tendency of the elements to pass into the liquid phase (Kd≤ 1). In cases where the Kd values are greater than 1, the physicochemical conditions of the water, monitored during the monitoring campaigns, determine situations where the analyzed elements are in the liquid phase (e.g., Ni). Furthermore, the analysis of hydrochemical facies highlighted a clear correlation between groundwater chemistry and subsurface lithology, identifying three main geochemical facies (basal clays, gypsum, alluvial deposits). The collected evidence suggests that the observed exceedances result from natural processes of dissolution and mobilization of elements rather than anthropogenic contamination. Based on the obtained data, new baseline value has been proposed, ensuring a more accurate representation of local natural conditions and providing a more appropriate reference for groundwater protection. The baseline values, calculated for hydrochemical facies, are significantly higher than the thresholds proposed by the CSC. In the case of B, SO_4^{2-}, Fe, Mn, and $NO_2^-$the values exceed the thresholds by 1-2 orders of magnitude, while for Ni and F^-, the values remain similar, but still higher. This new scenario is very different from the one pictured by Legislative Decree 152/2006, which is obviously not referred to such an extreme hydro-geochemical context. Therefore, the assessed baselines serve as a valuable tool for the sustainable management of water resources and the protection of the environment in areas subject to anthropogenic pressures.

Acknowledgments: We warmly acknowledge Fabio Catanzaro, Giuseppe Panebianco, Salvatore Accardo, and Rosario Varsalona (Catanzaro Costruzioni S.r.l. Unipersonale) for their useful discussions.

References

Bulut O, Duru B, Çakmak Ö, Günhan Ö, Dile, F B, Yetis U (2020) Determination of groundwater threshold values: A methodological approach. Journal of Cleaner Production, 253, 120001, https://doi.org/10.1016 /j.jclepro.2020.120001

Feo, A, Lo Medico, F, Rizzo, P, Morticelli, M.G, Pinardi, R, Rotigliano, E, Celico, F. (2023) How to Predict the Efficacy of Free-Product DNAPL Pool Extraction Using 3D High-Precision Numerical Simulations: An Interdisciplinary Test Study in South-Western Sicily (Italy). Hydrology, 10, 143. https://doi.org/10.3390/hydrology10070143

Legislative Decree 152/2006 (2006) Norme in Materia Ambientale. Allegato 5, Parte IV, Tabella 1. Gazzetta Ufficiale n. 88 del 14 Aprile 2006, Supplemento Ordinario n. 96. Available online: (accessed on 20 January 2025).https://www.gazzettaufficiale.it/dettaglio/codici/materiaAmbientale

Lo Medico F, Rizzo P, Rotigliano E, Celico F (2025) Groundwater Contamination: Study on the Distribution and Mobility of Metals and Metalloids in Soil and Rocks. Int. J. Environ. Res. Public Health 22, 182, https://doi.org/10.3390/ijerph22020182

Rizzo, P, Cappadonia, C, Rotigliano, E, Iacumin, P, Sanangelantoni, A.M, Zerbini, G, Celico, F. (2020) Hydrogeological behaviour and geochemical features of waters in evaporite-bearing low-permeability successions: A case study in Southern Italy. Appl. Sci., 10, 8177. https://doi.org/10.3390/app10228177

SNPA – Sistema nazionale per la protezione ambientale (2018). Linea guida per la determinazione valori di fondo per i suoli e per le acque sotterranee. (accessed 30 January 2025). https://www.isprambiente.gov.it /files2018/pubblicazioni/manuali-linee-guida/MLG_174_18.pdf

Zanotti C, Caschetto M, Bonomi T, Parini M, Cipriano G, Fumagalli L, Rotiroti M. (2022). Linking local natural background levels in groundwater to their generating hydrogeochemical processes in Quaternary alluvial aquifers. Sci Total Environ. 805: 150259. https://doi.org/10.1016/j.scitotenv.2021.150259

Assessment of the NPI index in Algerian bottled water

N. Bougherira[1*], D. Nechem[2], H. Bouguerra[1], L. Djabri[1], H. Chaffai[1], A. Hani[1], S. Ouled Meriem[1]
[1] *Laboratory Water Resources and Sustainble Development (REDD),Department of Geology, Faculty of EarthSciences, University Badji Mokhtar-Annaba, Algeria.*
[2] *Laboratory of Geology,Department of Geology, Faculty of EarthSciences, University Badji Mokhtar-Annaba, Algeria.*
** e-mail: nabil.bougherira@univ-annaba.dz*

Introduction

In Algeria, the total flow of underground reservoirs (mineral water and spring water) revealed by the Ministry of Water Resources is 699 L/s, or 60394 m^3/d. This flow covers 71 source water concessions and 26 mineral water and is equivalent to approximately 40 million bottles. The annual consumption of mineral water according to the Association of Algerian Beverage Producers, estimated at 2.7 billion litres, or 63 L/Hab.

The aim of this work is to examine a considerable number of bottled water samples (41 brand) to cover the entire range of physic chemical concentrations, given the high demand for bottled water for consumption; the high concentrations could seriously jeopardize the safety of human health due to the nitrates collected during the labelling of bottled waters.

Once we examined their physic chemical characteristics, we compared them to Algerian standards for mineral and spring waters, as well as international standards. (W.H.O). subsequently, we analyzed and classified these waters using both hydrochemical methods such as the Piper, Sholler Berkaloff and Gibbs diagrams.

Based on their nitrate content, bottled water was, classified according to the nitrate pollution index (NPI) method. This method plays an essential role in the detection of pollution, which allows us to choose our water properly.

Materials and methods

A fairly wide number of sampling points were studied in this work to cover the entire temporal and spatial range. A total of 41 bottled water samples were collected in February 2024 from different hydrogeological units (Fig. 1 (a)), and various physical and chemical parameters were collected from bottled water labels, given the brand. They included the assessment of electrical conductivity (EC), pH, Laboratory analysis involved determining major concentrations (cations and anions) and total dissolved solids (TDS).

Thus, the main objectives of this study are to:

- Analyse the water quality and spatiotemporal variation characteristics of bottled water;
- Evaluate the possible sources and transformation processes for NO3-, especially by using the nitrate pollution index
- Estimate the risks of contamination related to various sources of NO3-, under physicochemical changes on human health.
- Nitrate contamination is a form of water pollution that can be quantified using the Nitrate Contamination Index (NPI).

$$NPI = (Cs-HAV)/HAV \quad (1)$$

Results and concluding remarks

Gibbs (1970) proposed a scatter diagram illustrating three significant natural mechanisms governing the chemistry of major ions in groundwater, water-rock interaction, evaporation, and atmospheric precipitation (Fig. 1 (b)).

The Piper diagram (Fig. 1 (c)) gives a general view of the type of spring waters encountered. Reporting the results on this type of diagram shows for most of the samples analyzed that the cations are located in

the triangle of —non-dominance— of the cations and that the anions tend to approach the bicarbonate pole. we distinguish three families:

- Chloride and sulfate waters, calcium and magnesium (20%)
- Chloride sodium and potassium or sulfate sodium waters (0%)
- Bicarbonate calcium and magnesium waters (80%)

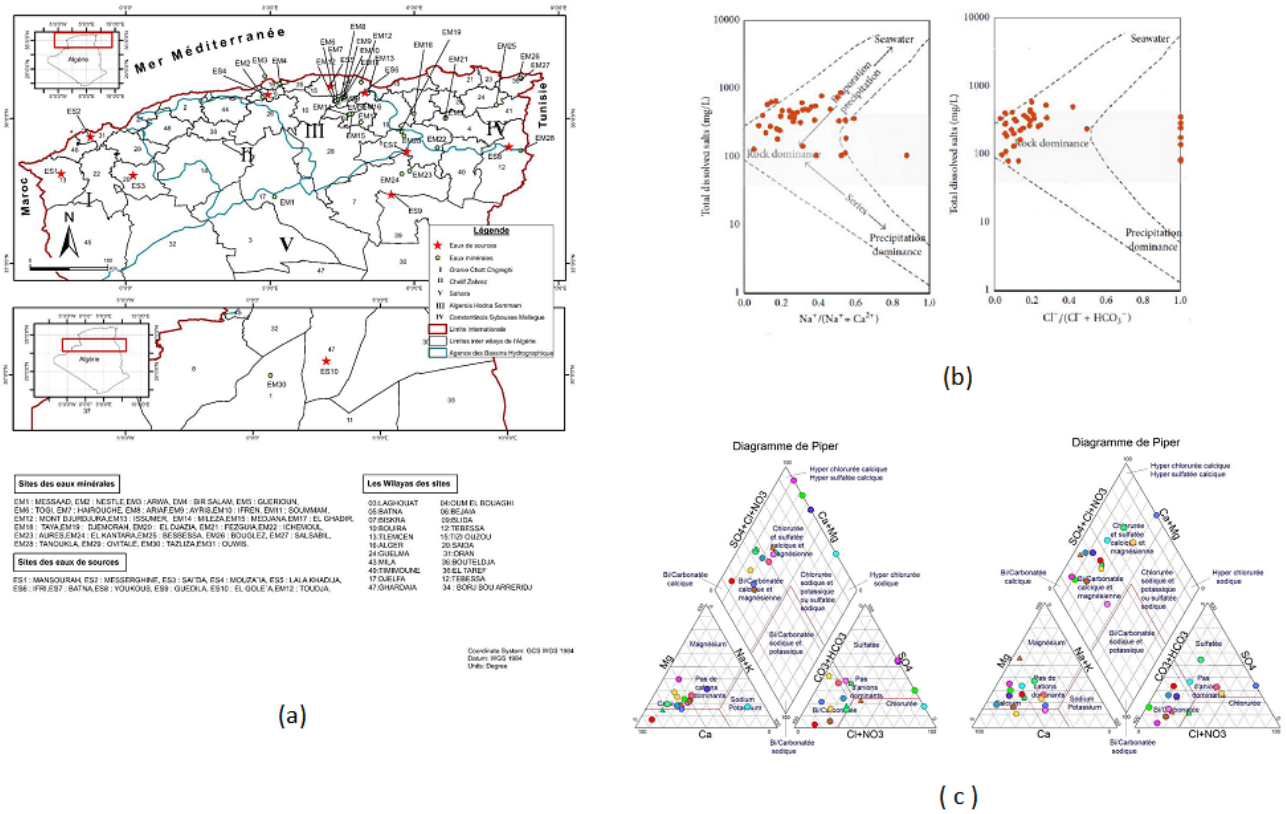


Figure 1. (a) Distribution of mineral water and spring water sites in Algeria. (b) Gibbs diagram. (c) Piper diagram

We note that the majority of bottled waters are classified as clean (Fig. 2), unpolluted waters. The presence of low pollution in 07 waters studied (Mont Djurdjura, El Ghadir, Guerioune, Hairouch, Djemourah, El Djazia, Tanoukla)

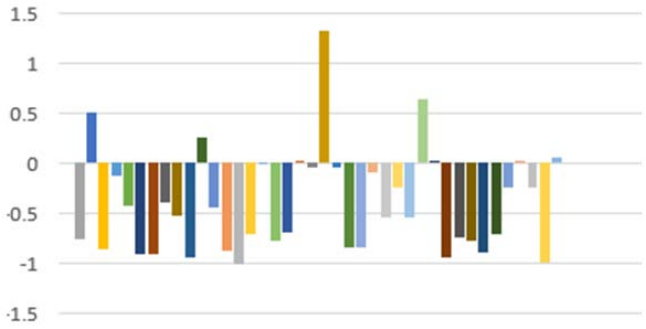


Figure 2. The N.P. Index of bottled waters

References

Abdelkrim H, (2011) Eaux minérales naturelles et eaux de sources en Algérie. Elsevier C. R. Geoscience 343 (2011)20-

Djabri L. et al. (2023) Les eaux embouteillées et leurs incidences sur la santé humaine : cas des eaux Algériennes. https://www.researchgate.net/publication/376883598_Les_eaux_embouteillees_et_leurs_incidences_sur_la_sante_humaine_cas_des_eaux_Algeriennes [accessed Jun 01 2024]

Sabra D, Houcem M, Kalthoum H (2023) Evaluation of groundwater quality in the takelsa basin (northeastern tunisia) for irrigation and drinking suitability using water quality index.DOI: https://doi.org/10.21203/rs.3.rs-3192878/v1

Control of seawater intrusion in semi-arid Mediterranean islands through brackish groundwater desalination and artificial recharge

V. Christelis[1*], G. Kopsiaftis[2], K. Mazi[3], A.D. Koussis[3]
[1] British Geological Survey, Keyworth, United Kingdom
[2] Laboratory of Reclamation Works and Water Resources Management, School of Rural, Surveying and Geoinformatics Engineering, NTUA, Greece
[3] Institute for Environmental Research & Sustainable Development, National Observatory of Athens
* e-mail: vc@bgs.ac.uk

Introduction

Worldwide, coastal groundwater is a valuable freshwater resource, which, particularly in arid and semi-arid areas, is threatened by seawater intrusion (SWI) due to anthropogenic activities such as uncontrolled abstractions and land use changes, or natural causes such as the decrease in groundwater recharge due to climate variability (Werner et al., 2013, Jiao and Post 2019). Often, to meet the increased freshwater demands in coastal areas, the technological approach of desalination is selected through which seawater or brackish groundwater is desalted to acceptable salinity levels for human, industrial, or agricultural uses (Georgopoulou et al. 2001; Zheng et al., 2022). However, the operation of desalination plants in coastal areas remains a timely research topic as it involves several economic and environmental challenges regarding the near-shore practices for the source of feed water and the discharge of brine (Abbas et al. 2023).

The use of variable-density flow and solute transport numerical models has been an indispensable computational tool for studying the complex interplay of SWI process with the hydrogeological properties of the coastal aquifer system, the pumping and injection regimes for desalination and the complementary artificial recharge strategies which support aquifer's hydraulic status (Abd-Elhamid and Javadi 2011; Stein et al. 2019). In this study, we investigate the SWI dynamics during the operation of desalination plants and the implementation of artificial recharge schemes for coastal aquifer typologies that are representative of small Mediterranean islands. These coastal areas typically encounter increased stresses on freshwater demands, while natural groundwater recharge is usually affected by long rainfall deficits. Our focus is set on aspects that have received less attention in similar numerical studies, such as the role of seasonal variations in recharge and transient pumping/injection schemes, as well as that of preferential flow paths due to the spatial heterogeneity of the aquifer's hydraulic conductivity.

Materials and methods

Numerical models are developed using MODFLOW 6 through the FloPy Python library for simulating SWI. Due to the exploratory nature of this work, the study is initially conducted on an idealized modelling domain that resembles the size of a real Mediterranean island aquifer of the Aegean Sea. The SWI extent is simulated subject to fresh groundwater (FGW) pumping from a gallery of production wells while saline groundwater (SGW) is pumped for desalination purposes. In addition, we investigate SWI mitigation by simultaneously replenishing the aquifer with treated waste water (TW) through a set of injection wells. Further, we examine transient flow conditions by incorporating seasonal variations in groundwater recharge and freshwater demands, reflecting typical patterns observed in eastern Mediterranean islands. Using geostatistical software we also investigate the impact of spatial heterogeneity in aquifer's hydraulic conductivity on the SWI dynamics during the operation timeline of desalination plants.

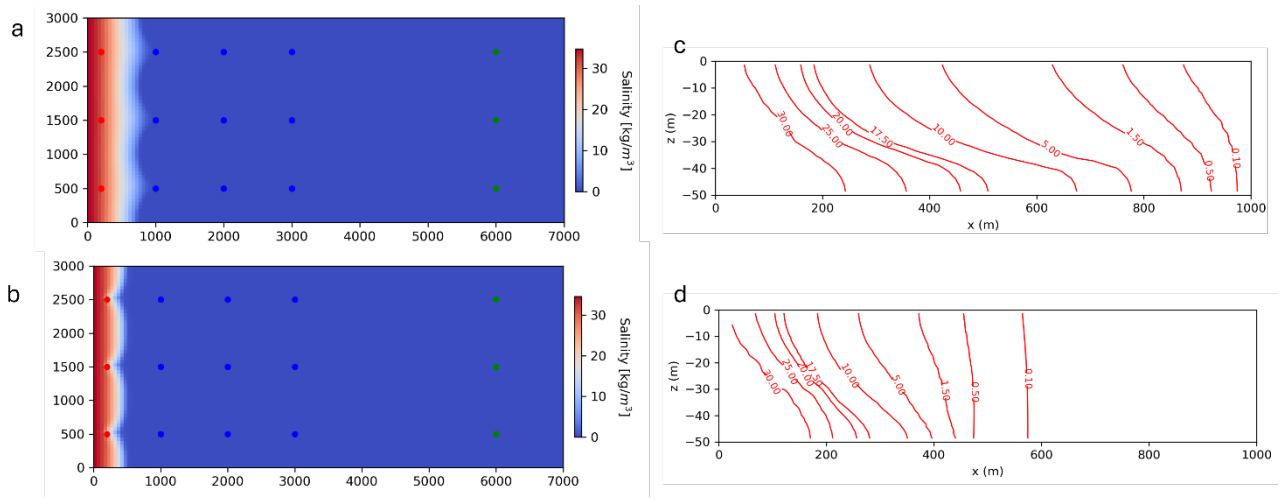


Figure 1. Left panels: Plan view of dispersion zone under FGW pumping only (a) and effect of distributing demand to SGW (b). Right panels: Corresponding vertical cross-sections of iso-salinities contours.

Results and concluding remarks

Preliminary results show that the combined approach of SGW pumping and TW injection effectively controls the SWI extent (Figure 1) for cases where FGW pumping is up to 80% of total recharge. The consideration of low to moderate heterogeneity in aquifer's hydraulic conductivity has a weaker contribution compared to scenarios of reduced recharge due to rainfall deficits. The impact of transient conditions is particularly significant, as periods of low recharge coincide with increased water demands in Mediterranean islands, further stressing the aquifer system.

Acknowledgments: K. Mazi and A.D. Koussis have been partially funded by the projects CLIMPACT (MIS 5201588, Co-funded by The National Development Program 2021-2025, Ministry of Development and the General Secretariat for Research and Innovation) and NHSOS (TAEDR-0537029, Co-funded by The National Recovery and Resilience Plan 'Greece 2.0' and Next Generation EU).

References

Abbas F, Al-Naemi S, Farooque AA, Phillips M, Rose D A (2023) Understanding the phenomenon of saltwater intrusion sourced from desalination plants at coastal aquifers. Environmental Science and Pollution Research, 30(50), 109181-109197.

Abd-Elhamid HF, Javadi AA (2011). A cost-effective method to control seawater intrusion in coastal aquifers. Water resources management, 25, 2755-2780.

Georgopoulou E, Kotronarou A, Koussis A, Restrepo PJ, Gómez-Gotor A, Jimenez JJR (2001) A methodology to investigate brackish groundwater desalination coupled with aquifer recharge by treated wastewater as an alternative strategy for water supply in Mediterranean areas. Desalination, 136(1-3), 307-315.

Jiao J, Post V (2019) Coastal hydrogeology. Cambridge University Press.

Stein S, Yechieli Y, Shalev E, Kasher R, Sivan O (2019). The effect of pumping saline groundwater for desalination on the fresh–saline water interface dynamics. Water research, 156, 46-57.

Werner AD, Bakker M, Post VE, Vandenbohede A, Lu C, Ataie-Ashtiani B, Simmons CT, Barry DA (2013) Seawater intrusion processes, investigation and management: Recent advances and future challenges. Advances in water resources, 51, pp.3-26.

Zheng T, Gao M, Chang Q, Zheng X, Walther M (2022) Dynamic desalination of intruding seawater after construction of cut-off walls in a coastal unconfined aquifer. Frontiers in Marine Science, 9, 857807.

Simulation and optimization of the Agia aquifer in Crete

G.P. Karatzas[1*], N.A Diangelakis[1,2]
[1] School of Chemical and Environmental Engineering, Technical University of Crete, Polytexneioupolis, Chania, Greece
[2] Institute of GeoEnergy, Foundation for Research and Technology-Hellas, Chania, Greec
* e-mail: gkaratzas@tuc.gr

Introduction

The area of Lake Agia and its aquifers is the primary source of drinking water for the city of Chania and is crossed by the Keritis River, which carries water from the White Mountains at an altitude of about 1900m. It is in the centre of the prefecture, has an area of about 210 km2 with an average altitude 734 meters and lies 12 km southwest of the city of Chania. The main concern in the study area is an optimal groundwater management plan. To this end, a numerical simulation model has been developed to describe groundwater flow and the effects of pumping on the underground system. The numerical simulation model will be used to construct an optimization model for groundwater management to determine the best well locations for pumping and their pumping rates.

In the present study the Princeton Transport Code (PTC) (Babu and Pinder, 1984) was employed as the numerical simulator that solves a system of partial differential equations to represent the subsurface flow, the velocities and the contaminant mass transport in the simulated aquifer. PTC employs a unique splitting algorithm for solving the fully three-dimensional equations, which significantly reduces the computational burden. The algorithm discretizes the domain into approximately parallel horizontal layers and within each layer a finite element discretization is used allowing for the accurate representation of irregular domains. The layers are connected vertically by a finite difference discretization. The model considers all the springs and the pumping wells that exist in the area of study.

The groundwater management problem is focused on maximizing the pumping quantity of groundwater system of Agia and minimizing the total pumping cost subject to a set of constraints.

The decision variables are the pumping rates at each well. The objective of the management model is the maximization of the total extracted groundwater volume from n pre-selected pumping locations (production wells). The constraints are imposed at J pre-selected observation points. Constraints for all the n production wells regarding the maximum allowable extracting rate were also set. An additional constraint is the total pumping at each management period to be greater or equal to the water needs. Two management periods: dry and wet period are considered.

Materials and methods

The aquifer was divided in two layers to model the groundwater discharges from spring and pumping wells from different depths. The calibration of the model was based on real data (hydraulic heads) observed in the period 2017-2021. The parameters that were used to calibrate the PTC model were: boundary conditions, hydraulic conductivity and porosity. The simulation period was divided into two stress periods (summer and winter) with different sets of data imposed at each one regarding the water demand, the precipitation rate and the natural inflow from the southern boundary.

The groundwater management problem is focused on maximizing the pumping quantity of groundwater system of Agia and minimizing the total pumping cost subject to a set of constraints.

The mathematical formulation of the problem is summarized as follows:

$$max \sum_{i=1}^{n} q_i + min \sum_{i=1}^{n} q_i \, C_o (H_i - h_i) T_{sp} \quad (1)$$

The objective function will be transformed into the following expression:

$$max \, \alpha \sum_{i=1}^{n} q_i - (1-\alpha) \sum_{i=1}^{n} q_i \, C_o (H_i - h_i) T_{sp} \quad (2)$$

where: α is a parameter within [0,1] and will be determined either manually or as a result of the Paretto front, q_i: the pumping rates at each well (decision variables), C_o : pumping cost / depth, H_i : the surface elevation of the well location i, h_i: the hydraulic head at the location i at the end of the stress period, T_{sp}: the time length of the stress period. The constraints of the optimization problem are:

$$h_j \geq H_{j_{ref}} j = 1, \ldots, J \tag{3}$$

$$\sum_{i=1}^{n} q_i \geq Q_{needs} \qquad 0 \leq q_i \leq Q_i^*$$

For the solution of the groundwater management problem the Gurobi Optimization software is used. Gurobi (Gurobi Optimization, LLC, 2024) is used to solve linear programming, quadratic programming, quadratically constrained programming, mixed-integer linear programming, mixed-integer quadratic programming and mixed-integer quadratically constrained programming. Gurobi is a special type of software called a "solver". The Gurobi interface for MATLAB allows users to create an optimization model, pass the model to Gurobi, and obtain the optimization result - all within the MATLAB environment.

Results and concluding remarks

Figure 1 shows the calibration results of the groundwater model for the period 2017-2021. The calibration of the model shows a good agreement between the numerical results and the field measurements. The water demand is 5 million m^3 higher than the existing situation for the dry period. The optimization model needs to identify the best locations for new pumping wells to meet the water demand in the dry season.

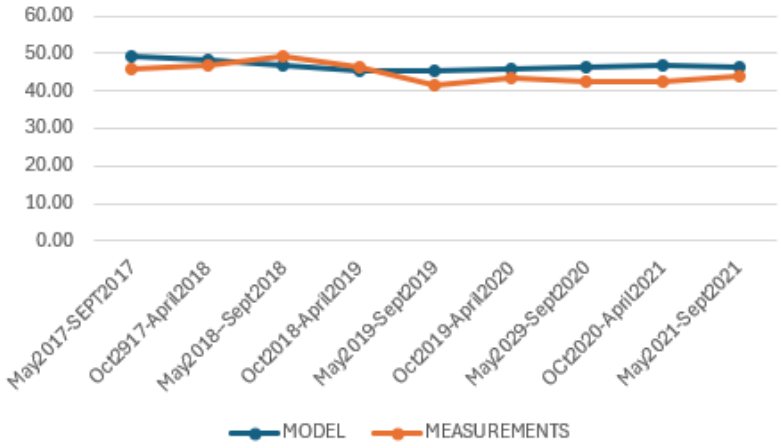


Figure 1. Calibration results of the groundwater model

Acknowledgment: This work was supported by the OurMED PRIMA Program project funded by the European Union's Horizon 2020 Research and Innovation programme under grant agreement No. 2222.

References

Babu DK, Pinder GF, 1984. A Finite Element – Finite Difference Alternating Direction Algorithm for 3-Dimensional Groundwater Transport. Advances in Water Resources 7(3): 116-119

Gurobi Optimization, LLC, 2024. Gurobi Optimizer Reference Manual, https://www.gurobi.com

XIII. Non-Conventional Water Resources, Wastewater Reuse, and Desalinization

Use of nanofiltration and reverse osmosis filtration for treatment the rainwater runoff from expressway

I.A. Tałałaj*, P. Biedka
Faculty of Civil Engineering and Environmental Science, Bialystok University of Technology, Bialystok, Poland
** e-mail: i.talalaj@pb.edu.pl*

Introduction

Rainwater stands out as an alternative natural resources that ca be easily collected to address limited water resources problem. Studies on harvesting and reuse of rainwater for potable or non-potable water production focus mainly on rainwater collected from various roofs coverings (Alim et al., 2020; Köse-Mutlu, 2020; Liu et al., 2021; Ortiz et al., 2022). However, another important dimension attracting little attention is the possibility of rainwater gathering from hardened/sealed surfaces, i.e. parking lots, traveler's service places, expressways. As a required part of the drainage system for these areas, retention basins are located next to most roads to collect surface runoff from the sealed surface. So far, these reservoirs have not been widely analysed in the context of the possibility of recovering rainwater.

A review of the literature indicates that rainwater from sealed areas is characterized by a high content of inorganic pollutants and low biodegradability (Köse-Mutlu, 2020; Liu et al., 2021; Marszałek & Dudziak, 2021). Hence, their treatment by membrane methods can give good results. Therefore, the study aims to evaluates the efficiency and performance of nanofiltration (NF), reverse osmosis (RO) for the purification of rainwater runoffs collected from expressways areas. In this contest, the novelty of the paper is assessment of the possibility of reusing rainwater as an alternative water source as well as comparison of effectiveness for their purification selected membrane methods.

Materials and methods

The rainwater runoff used in this study was taken from the reservoir of stormwater drainage system for National Road No. 8. The drainage system collects rainwater from the main road, shoulders, and access roads. The rainwater runoff flows gravitationally through a collector into a retention reservoir, from which samples were taken for analysis.

The rainwater purification process was carried out using the RO20NS.1 laboratory membrane system, which was designed and constructed to reflect the real operating parameters of membrane systems on a technical scale. The process was carried out in a cross-flow system with concentrate recirculation to the feed tank supplying the rainwater to the NF/RO system. During filtration processes following parameters were monitored: permeate flux, removal rate of salts, concentration factor, degree of rainwater recovery and removal efficiency. After membrane processes, membrane was physically washed using distilled water. Next, chemical cleaning procedure has been carried out. After both physical and chemical cleaning, its effectiveness was assessed by measuring the value of permeate flux. A flux reduction ratio associated with fouling was calculated as a ratio of water flux through clean membrane before filtration process and water flux after physically cleaning. Collected rainwater from reservoir and after filtration processes were analysed for general pollutants (pH, EC, Total Dissolved Solids, Polycyclic Aromatic Hydrocarbons, Total Organic Carbon, Turbidity), anions and cations (F^-, Cl^-, SO_4^{2-}, Na^+, K^+, Mg^{2+}, Ca^{2+}) and metals (Cr, Co, Cu, Zn, As, Cd, Pb, Al, Mn, Fe) to determine its quality and efficiency of membrane separation.

Results and concluding remarks

In assessing the permeate flux characteristics, the ratio J/J_0 was used, where J_0 is the water flux through the clean membrane before the filtration process and J is the flux during rainwater filtration. The results of filtration process are presented in the Table 1.

Table 1. Characteristics of reverse osmosis and nanofiltration process performance.

	Reverse osmosis	Nanofiltration
average J/J_0	48%	73%
minimal J/J_0	40%	68%
EC concentration factor	2.26	1.65
EC removal rate	99.6%	40.2%
recovery rate	70%	70%

J_0 – clean water flux

The nanofiltration process was characterized by better flux flow and higher efficiency compared to reverse osmosis. However, higher removal rates were achieved during the RO filtration. Efficiency for analyzed anions and cations removal was over 38% for NF and over 98% for RO process. Metals were removed with sufficiency of over 27% for NF and over 87% for RO. In the case of NF, the problem was the effective removal of chlorides and sodium from the rainwater, which were present in large quantities in the expressway runoff. Their source is the use of road and street maintenance products. The high content of non-organic substances in the analyzed express runoff was also the cause of the dominant inorganic fouling (Figure 1). The total (inorganic and organic) fouling process resulted in a reduction in flow of 50% and 20% for RO and NF, respectively.

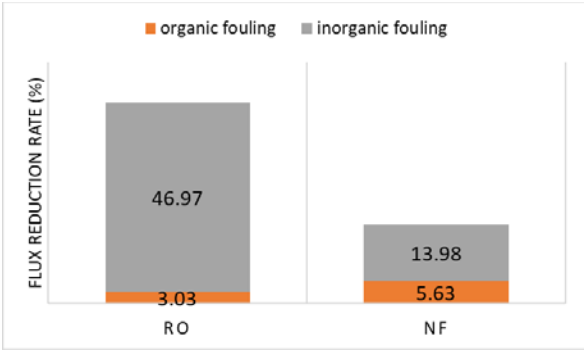


Figure 1. Flux reduction rate during membrane filtration.

The analyses carried out showed that the quality of the permeate obtained after RO processes allows it to be used for economic purposes, such as flushing toilets, washing floors, and watering green areas. In order to use the permeate as a source of drinking water, it would be necessary to expand the scope of analyses and control it from a microbiological point of view. Due to high heavy metal content in permeate, the NF process should be preceded by a pre-treatment to remove or minimize them in inlet.

Acknowledgments: The research was carried out as part of research work MEiN/2022/DPI/2577 at the Bialystok University of Technology and financed from a grant subsidy provided by the Ministry of Education and Science.

References

Alim M A, Rahman A, Tao Z, Samali B, Khan M M, Shirin S. (2020). Suitability of roof harvested rainwater for potential potable water production: A scoping review. Journal of Cleaner Production 248, 119226. https://doi.org/10.1016/j.jclepro.2019.119226

Köse-Mutlu B. (2020). Natural organic matter and sulphate elimination from rainwater with nanofiltration technology and process optimisation using response surface methodology. Water Science and Technology 83. https://doi.org/10.2166/wst.2020.591

Liu X, Ren Z, Ngo H H, He X, Desmond P, Ding A. (2021). Membrane technology for rainwater treatment and reuse: A mini review. Water Cycle, 2, 51–63. https://doi.org/10.1016/j.watcyc.2021.08.001

Marszałek A, Dudziak M. (2021). Application of the Ultrafiltration and Photooxidation Process for the Treatment of Rainwater. Water, Air, & Soil Pollution, 232(12), 504. https://doi.org/10.1007/s11270-021-05465-w

Ortiz S, de Barros Barreto P, Castier M. (2022). Rainwater harvesting for domestic applications: The case of Asunción, Paraguay. Results in Engineering 16, 100638. https://doi.org/10.1016/j.rineng.2022.100638

Development of a proxy for optimally treated wastewater chemical composition focused on fertigation purposes

A. Osorio[1*], A. Panico[2], G. Busico[1], M. Mastrocicco[1]
[1] Di.S.T.A.Bi.F., University of Campania "Luigi Vanvitelli", Via A. Vivaldi 43, 81100 Caserta, Italy
[2] Department of Engineering, University of Campania "Luigi Vanvitelli", Via Roma 29, 81031, Aversa, Italy
*e-mail: aahilynbelen.osorioinostroza@unicampania.it

Introduction

The sustainability of agricultural operations will present significant concerns by 2030 as the projected worldwide freshwater demand exceeds 160% of the planet's natural resources (Ricart and Rico, 2019). Since treated wastewaters could preserve freshwater resources and supply nutrients to crops, treated wastewater has become a recognized sustainable alternative to freshwater as well as chemical fertilizers. Fertigation, a technique that combines fertilization with irrigation, increases the efficiency of resource usage by supplying nutrients straight to the root zone of the plant (Mainardis et al., 2022). Despite its potential, the application of treated wastewater in fertigation raises several concerns. These include risks to public health and soil salinization, the challenge of adhering to regulatory standards, and the environmental implications of emerging contaminants such as pharmaceuticals and industrial residues, which may persist in soils and enter the food chain (Chojnacka et al., 2020; Radini et al., 2023). To mitigate these risks, recommendation and regulatory frameworks like the FAO water quality standards and the EU Regulation 2020/741 provide essential guidance. These standards aim to ensure that treated wastewater used in fertigation contains safe nutrient levels, safeguarding groundwater, public and livestock health as well as the environment in general (EU Regulation 2020/741) and both soil integrity and crop health (FAO, 1992; EU Regulation 2020/741). However, the heterogeneous nature of wastewater sources and variations in crop tolerance to nutrient availability and salinity stress necessitate tailored fertigation strategies. To address this, the focus of this research lies in identifying the optimal concentration ranges of key organic and inorganic constituents in treated wastewater for fertigation purposes, relying on the outcomes derived from a comprehensive systematic review analyzing a wide range of existing studies. The goal of this paper is to create, through a proxy of representative concentrations of dissolved solids in treated wastewaters, robust scientific a basis that can support for the publication of guidelines and promulgation or modification of regulations as well as the setting of controlled laboratory trials that simulate fertigation conditions. This method aims to maximize agricultural wastewater reuse techniques, ensuring crop yield, public health and environmental sustainability.

Materials and methods

This study followed the PRISMA framework to ensure a thorough and unbiased analysis. Scopus and Web of Science databases were searched extensively, targeting studies published between 2005 and 2024. The search strategy was designed with a precise search string incorporating keywords such as "wastewater reuse", "fertigation", "nutrient composition," and "crop productivity," allowing for the precise identification of relevant literature to develop an indicator of wastewater composition in fertigation. Inclusion criteria focused on studies that examined the application of treated wastewater or effluent in fertigation systems, specifically reporting quantitative data on the concentrations of key organic and inorganic species. Studies were included if they provided detailed assessments of these concentrations in relation to crop yield, soil types, and growing conditions (field or greenhouse). The data mining process systematically recorded concentrations of nutrients and other relevant chemical species, along with information on crop types, soil characteristics, and fertigation outcomes. Particular attention was paid to identifying ranges of nutrient concentrations that optimize crop productivity while maintaining soil health. This analysis aimed to generate a comprehensive indicator of nutrient concentrations suitable for

laboratory simulations of fertigation scenarios, supporting the development of sustainable wastewater reuse strategies tailored to diverse agricultural environments.

Results and concluding remarks

The results revealed significant differences in the nutrient and contaminant concentrations among domestic wastewater, leachates, and reclaimed water, which directly influence crop yield, and the risks associated with their use in fertigation. The chemical composition of the analysed wastewater sources exhibited notable variability that must be considered to optimize their agricultural application (Table 1).

Domestic wastewater showed moderate levels of key nutrients, such as nitrates (NO_3^-=16.6 mg/L) and phosphates (PO_4^{3-}=13.3 mg/L), achieving the highest crop yield (33.57 ton/ha) compared to the other water sources. This indicates a balanced composition that could stimulate crop growth under certain conditions. In contrast, leachates displayed extremely high concentrations of total nitrogen (N= 900.0 mg/L) and sodium (Na^+= 345.0 mg/L), which may lead to significant risks of soil salinization and nutrient leaching, thus resulting in minimal crop yields (5.66 ton/ha). Reclaimed water from urban wastewaters presented a more balanced composition, with elevated levels of phosphates (PO_4^{3-}: 123.7 mg/L) and magnesium (Mg^{2+}= 76.2 mg/L). However, it also exhibited moderate sodium (Na^+= 138.4 mg/L) and chloride (Cl^-: 358.7 mg/L) concentrations, which could contribute to soil salinity accumulation over time. Crop yield with reclaimed water reached an average of 9.49 ton/ha, showing greater stability compared to leachates. These results highlight the need to adapt fertigation strategies to the specific chemical composition of the water being used. The identified optimal concentration ranges for key nutrients, such as nitrates (16–120 mg/L), phosphates (10–130 mg/L), potassium (30–120 mg/L), and magnesium (20–80 mg/L) were determined based on their ability to optimize crop yield as reported in the literature. These ranges represent nutrient levels that have consistently demonstrated improved plant growth and productivity across various studies. Therefore, they can serve as a reference for future experimental applications under controlled conditions and for being included in guidelines and legislations.

Table 1. Proxy ranges and median concentrations of some key inorganic compounds in water used for fertigation.

Parameter	Possible Range (mg/L)	Domestic Wastewater (mg/L)	Leachate (mg/L)	Reclaimed Water (mg/L)
Nitrates (NO_3^-)	16–120	16.6	328.6	236.0
Phosphates (PO_4^{3-})	10–130	13.3	31.7	123.7
Potassium (K^+)	30–120	29.8	136.8	113.1
Sodium (Na^+)	<150	135.7	345.0	138.4
Chloride (Cl^-)	<300	257.5	443.2	358.7
Sulphates (SO_4^{2-})	150–350	165.1	307.2	348.6
Copper (Cu)	<0.1	0.05	0.02	2.38
Zinc (Zn)	0.1–4.0	0.29	0.02	4.12
Magnesium (Mg^{2+})	20–80	24.3	6.46	76.2

References

Chojnacka, K., Witek-Krowiak, A., Moustakas, K., Skrzypczak, D., Mikula, K., & Loizidou, M. (2020). A transition from conventional irrigation to fertigation with reclaimed wastewater: Prospects and challenges. Renewable and Sustainable Energy Reviews, 130, 109959. https://doi.org/10.1016/j.rser.2020.109959

Food and Agriculture Organization of the United Nations (FAO). (1992). Wastewater treatment and use in agriculture. FAO Irrigation and Drainage Paper 47. Available at: https://www.fao.org/3/t0551e/t0551e.pdf

Mainardis, M., Cecconet, D., Moretti, A., Callegari, A., Goi, D., Freguia, S., & Capodaglio, A. G. (2022). Wastewater fertigation in agriculture: Issues and opportunities for improved water management and circular economy. Environmental Pollution (Barking, Essex: 1987), 296, 118755. https://doi.org/10.1016/j.envpol.2021.118755

Radini, S., González-Camejo, J., Andreola, C., Eusebi, A. L., & Fatone, F. (2023). Risk management and digitalisation to overcome barriers for safe reuse of urban wastewater for irrigation – A review based on European practice. Journal of Water Process Engineering, 53, 103690. https://doi.org/10.1016/j.jwpe.2023.103690

Ricart, S., & Rico, A. M. (2019). Assessing technical and social driving factors of water reuse in agriculture: A review on risks, regulation and the yuck factor. Agricultural Water Management, 217, 426–439. https://doi.org/10.1016/j.agwat.2019.03.017

Assessing environmental impacts in rice production with treated domestic wastewater: a life cycle perspective

Y. Ahi[1*], H.T. Gültaş[2], Ç. Coşkun Dilcan[1], U. Çebi[3], M.A. Gürbüz[3], S. Özer[3], G. Yıldız Töre[4], Ü. Geçgel[5]
[1] Water Management Institute, Ankara University, Ankara, Turkey
[2] Department of Biosystems Engineering, Faculty of Agricultural and Natural Science, University of Bilecik Şeyh Edebali, Bilecik, Turkey
[3] Atatürk Soil Water and Agricultural Meteorology Research Institute, Kırklareli, Turkey
[4] Department of Environmental Engineering, Faculty of Engineering, University of Tekirdağ Namık Kemal, Tekirdağ, Turkey
[5] Department of Food Engineering, Faculty of Agriculture, University of Tekirdağ Namık Kemal, Tekirdağ, Turkey
* e-mail: ysmahi@ankara.edu.tr

Introduction

Ensuring the sustainability of food along with natural resources within the ecosystem has become a priority across all sectors. Evaluating the environmental impacts of water and energy consumption, which are fundamental to production, is essential for sustainability. In the agricultural sector, where water is used most extensively, strong indicators are needed for controlled and efficient water management. In this context, life cycle assessment (LCA) is increasingly used to comprehensively account for the environmental impacts of water use from a life cycle perspective and to evaluate the trade-offs and synergies between water and other agricultural practices in crop production, and also serves as a strong decision support tool in many studies (Jirapornvaree et al. 2021; Canaj and Mehmeti 2022; Garcia Gonzalez and Björnsson 2022; Mehmeti et al. 2024). This study utilizes an LCA model to measure the impact of irrigation on the product life cycle in rice crops irrigated with treated domestic wastewater.

Life Cycle Assessment (LCA) evaluates all stages of a product's life cycle to compare alternatives and identify high-impact stages, using environmental profiles that consider factors like climate change, water, and land use (Huijbregts et al. 2017). Life Cycle Impact Assessment (LCIA) models convert emissions and resource consumption into environmental impact scores using characterization factors at midpoint and endpoint levels. The midpoint approach is more directly related to environmental flows and has lower uncertainty, whereas the endpoint approach corresponds to three areas of protection—human health, ecosystem quality, and resource scarcity—offering a clearer representation of environmental significance but with higher uncertainty (Hauschild and Huijbregts 2015). The ReCiPe2008 method, which integrates these two approaches, was developed by Goedkoop et al. (2009) through various academic and institutional collaborations and was later updated as ReCiPe2016. In this study, the ReCiPe2016 model was used, and the results were discussed in terms of resource sufficiency.

Materials and methods

The study analyses the life cycle of rice cultivation irrigated with effluent from a Domestic Wastewater Treatment Plant in Turkey's Meriç-Ergene basin. The treatment plant effluent was reclaimed by removing pollutants and reused for irrigation, with control plots using clean water for comparison. The research was conducted in a split-block strip plot experimental design with three replications. Drip irrigation was selected as the irrigation method, and additional elements required by the treatment system (carbon and UV filters) were incorporated. The yield obtained from field trials, along with data on fertilization, pesticide application, irrigation, mechanization, electricity, diesel consumption, and water-energy usage collected from the treatment plant, were used in the life cycle analysis (LCA) to assess the environmental impacts of water quality and the drip irrigation method.

The study fundamentally followed the four phases on which LCA is based, namely 1) goal and scope definition, 2) inventory analysis, 3) impact assessment, and 4) interpretation. In this study, the ReCiPe2016 method (Huijbregts et al. 2017) was used, integrating midpoint and endpoint approaches to assess the

environmental footprint of rice cultivation with treated wastewater irrigation. While midpoint indicators addressed specific environmental issues such as water use, climate change, toxicity, acidification, and eutrophication, the endpoint level focused on categories like human health, ecosystem quality, and resource scarcity (Mehmeti et al. 2024). The study also employed the Single Score approach (weighted impact), which converts endpoint results into a single numerical value to simplify impact information and facilitate comparisons between different scenarios (Goedkoop et al. 2009).

Direct and indirect input materials used during the cultivation process—such as chemical fertilizers, crop protection chemicals, fuel, machinery, irrigation water, irrigation infrastructure, and electricity—were considered as materials. To improve characterization factors for pollutants like ammonia, nitrogen oxides, phosphorus, phosphates, and water use, Turkey-specific factors derived by Huijbregts et al. (2017) were included in the study. For data provision, the Ecoinvent v3.1 database (Ecoinvent Database 2014) was used, while the modeling of product systems and calculation of environmental impacts were carried out using the OpenLCA v.1.10.3 software (GreenDelta 2022).

Results and concluding remarks

The cradle-to-grave environmental footprint of rice per ton and per hectare was analyzed using the ReCiPe2016 method, which integrates midpoint and endpoint approaches, and was made more comprehensible through the single score approach. In rice production carried out using drip irrigation and treated domestic wastewater, the total environmental impacts per ton of product was found to be 317 p/ton. The LCA results show that irrigation has the highest environmental impact in rice production (200 p/ton). This highlights the importance of efficient water management and the sustainability level of using reclaimed wastewater. Besides water use, fertilization (50.3 p/ton), mechanization (44.9 p/ton), and pesticide use (17.8 p/ton) also significantly impact the environment. Adopting practices like optimized fertilization, Integrated Pest Management, and energy-efficient technologies can reduce these impacts and promote more sustainable agriculture.

The findings support policy development by promoting circular water use and sustainable agriculture through data-driven insights. Integrating LCA results into regulations can encourage wastewater reuse, low-impact irrigation, and climate-smart farming practices. Future research and implementation should analyze the long-term agronomic effects of treated wastewater irrigation on soil and crop health, the economic feasibility of alternative irrigation systems at different scales, and the scalability of sustainable farming practices in diverse climatic and hydrological conditions. By integrating LCA insights into agricultural water management, stakeholders can ensure resilient food production systems that balance productivity with ecological responsibility in the face of a changing climate.

Acknowledgement: The authors would like to thank the Turkish Scientific and Technical Research Council (TUBITAK) for its financial support to the project of 221O254.

References

Canaj K, Mehmeti A (2022) Analyzing the water-energy-environment nexus of irrigated wheat and maize production in Albania. Energy Nexus, 7, 100100.

Ecoinvent Database 3.1. (2014) Ecoinvent Database 3.1. Ecoinvent Centre. https://doi.org/10.4018/978-1-59140-342-5.ch003

Goedkoop M, Heijungs R, Huijbregts M, De Schryver A, Struijs J, Van Zelm R (2009) ReCiPe 2008. A life cycle impact assessment method which comprises harmonised category indicators at the midpoint and the endpoint level, 1, 1-126.

Gonzalez MNG, Björnsson L (2022) Life cycle assessment of the production of beet sugar and its by-products. Journal of Cleaner Production, 346, 131211.

GreenDelta (2022) OpenLCA 1.10.3. Retrieved from https://www.openlca.org/download/

Huijbregts MAJ, Steinmann ZJN, Elshout PMF, Stam G, Verones F, Vieira M, van Zelm R (2017) ReCiPe2016: A harmonized life cycle impact assessment method at midpoint and endpoint level. The International Journal of Life Cycle Assessment, 22(2), 138–147. https://doi.org/10.1007/s11367-016-1246-y

Jirapornvaree I, Suppadit T, Kumar V (2021) Assessing the economic and environmental impact of jasmine rice production: Life cycle assessment and Life Cycle Costs analysis. Journal of Cleaner Production, 303, 127079.

Mehmeti, A., Abdelhafez, A. A. M., Ellssel, P., Todorovic, M., Calabrese, G. (2024). Performance and Sustainability of Organic and Conventional Cotton Farming Systems in Egypt: An Environmental and Energy Assessment. Sustainability (2071-1050), 16(15).

Evaluation of efficiency of MOFs/MOFCs to serve as adsorbent material to remove heavy metals from the effluent of constructed wetlands

D. Matziri[1], M P. Christodoulou[2], A. Gropali[1], E. Hadjikyprianou[2], I. Stavrakakis[1], P.K. Simeou[2], N. Remmas[1], K.N. Pantelis[2], P. Melidis[1], A. Tasiopoulos[2*], S. Ntougias[1*]

[1] *Laboratory of Wastewater Management and Treatment Technologies, Department of Environmental Engineering, Democritus University of Thrace, Vas. Sofias 12, 67132 Xanthi, Greece*

[2] *Department of Chemistry, University of Cyprus, 1678 Nicosia, Cyprus*

** e-mails: tasiopoulos.anastasios@ucy.ac.cy & sntougia@env.duth.gr*

Introduction

Although essential steps have been made by the EU member states to implement the enacted European legislation, discharges of wastewater still contribute to the lack of achieving Good Environmental Status (GES) by 11.0%, 2.5%, 19.6% and 14.7% in rivers, lakes, transitional and coastal water bodies, respectively (11th and 12th Report on the Implementation of 91/271). Moreover, conventional municipal wastewater treatment is mainly applied in cities with populations of over 2,000 inhabitants, denoting a major disparity in wastewater treatment between large cities and small, remote settlements. In parallel, agro-industries scattered in rural regions are often situated near to water bodies, further affecting water bodies' quality.

Nature-based solutions (NBS), focusing on wastewater treatment and water recovery in rural areas, can be considered as safe, decentralized, easy to operate and environmentally-friendly approaches (Marijuan et al. 2024), to meet the strict legislative EU requirements, increasing simultaneously water efficiency and sustaining water resources in the Mediterranean region.

In this context, CIRQUA, a PRIMA Horizon Section 1 Management of water IA research project, aims to upgrade existing non-conventional decentralized wastewater treatment technologies focusing on constructed wetlands (CWs) as Nature Based Solutions (NBS) via the integration of novel nanomaterials for the development of a portable nanostructured filter. In this work, new nanomaterials were tested regarding their capability of removing heavy metals to be used as adsorbent materials for the outlet of constructed wetlands.

Materials and methods

A range of metal organic framework composites (MOFCs), i.e. CaFu/Clay, CaFu/Biochar, ZrFu/Clay, ZrFu/Alginate, ZrFu/Biochar, UiO-66/Clay, UiO-66/Alginate, UiO-66/Biochar, UiO-66-NH_2/Clay, UiO-66-NH_2/Alginate, UiO-66-NH_2/Biochar (CaFu = $[Ca(Fu)(H_2O)_3]_n$, H_2Fu = fumaric acid; ZrFu = $[Zr_6O_4(OH)_4(Fu)_6]_n$; UiO-66 = $[Zr_6O_4(OH)_4(BDC)_6]_n$, H_2BDC = terephthalic acid; UiO-66-NH_2 = $[Zr_6O_4(OH)_4(NH_2\text{-}BDC)_6]_n$ (NH_2-H_2BDC = 2-aminoterephthalic acid; Clay = montmorillonite bentonite clay, Biochar = Cyprus Bamboo Biochar Alginate = Calcium Alginate), were examined regarding their capability to remove heavy metals (Table 1). Heavy metal ion solutions, containing Cd^{2+}, Cr^{6+}, Pb^{2+}, Ni^{2+} or Cu^{2+} as the sole ion, at concentrations of 10^{-4} M, $5*10^{-4}$ M, 10^{-3} M and $5*10^{-3}$ M, were mixed with the above MOFCs, one each time. The remaining metal ion concentration after a 24 h treatment period was assessed by an Inductively Coupled Plasma Optical Emission Spectrometry (ICP-OES) apparatus.

Table 1. Metal organic frameworks (MOFs) and their composites (MOFCs) examined in this study.

MOF	MOFCs
CaFu	CaFu/Clay, CaFu/Biochar
ZrFu	ZrFu/Clay, ZrFu/Alginate, ZrFu/Biochar
UiO-66	UiO-66/Clay, UiO-66/Alginate, UiO-66/Biochar
UiO-66-NH_2	UiO-66-NH_2/Clay, UiO-66-NH_2/Alginate, UiO-66-NH_2/Biochar

Results and concluding remarks

The Metal organic frameworks (MOFs) and their composites (MOFCs) examined in this study were selected on the basis that are synthesized with metals used as plant trace-elements and sustainable organic materials that enhance soil fertility and plant growth, such as clay, biochar and fumarate, serving simultaneously as adsorbent material to improve the effluent quality of CW. All metal organic framework composites (MOFCs) examined showed high absorbance capability, which exceeded 95% for all the above materials, at least in heavy metal ion concentrations of 10^{-4} M and $5*10^{-4}$ M. This indicates that these MOF composites (MOFCs) can be effectively used as absorbents for the development of innovative nanostructured filters, which can be adjusted in the effluent of CWs for recovering non-conventional water resources, i.e. wastewater and irrigation canal water, especially in the Mediterranean region, which is highly affected from extreme temperature rise, since it is warming 20% faster than the world average (Claro et al. 2024).

Acknowledgments: This work was conducted in the frame of the project, entitled “Integrated Approaches at Local Scale for Enhancing Water Reuse Efficiency and Sustainable Soil Fertilization from Wastewater’s Recovered Nutrients”, acronym ‘CIRQUA”, Grant agreement No. 2321, Call 2023 Section 1 Management of Water IA, which is part of the PRIMA programme supported by the European Union. The PRIMA programme is supported under Horizon 2020, the European Union’s Framework Programme for Research and Innovation. This content reflects only the authors’ view. The PRIMA Foundation is not responsible for any use that may be made of the information it contains.

References

Claro AM, Fonseca A, Fraga H, Santos JA (2024) Future Agricultural Water Availability in Mediterranean Countries under Climate Change: A Systematic Review. Water 16(17): 2484. https://doi.org/10.3390/w16172484

Marijuan R, Díez B, Peláez-Sánchez S, Sánchez C, Iglesias J, Şirin B, Baba A, Gündüz O, Sánchez, R. (2024). Evaluating the impact of nature-based solutions on the provision of water-related and water-dependant ecosystem services. Nature-Based Solutions 6: 100194. https://doi.org/10.1016/j.nbsj.2024.100194

XIV. Social, Political, Institutional, Legislative Aspects, and Ethics

The inviolability of water? On the trail of state violations of the norm

E. Pohnerová
Institute of Political Studies, Faculty of Social Sciences, Charles University, Prague, the Czech Republic
e-mail: eliska.pohnerova@fsv.cuni.cz

Introduction

Water weaponisation is the practice of targeting, manipulating and rendering water rare or unsafe with the objective of harm. As such, it is most often discussed in relation to non-state terrorist groups, such as ISIS, that have perfected water's violent side, which has also been reflected by the attention of academia (Daoudy, 2020; King, 2015; Von Lossow, 2016). Yet, a gap in knowledge exists in relation to states, which should stand at the front of water protection, as water inviolability is largely prohibited by international humanitarian law (IHL), both explicitly and implicitly, under the protection of civilian means of survival (Gleick, 2019). Together with a religious underpinning of water as a metaphor for God and life, the water stigma should be normative not only legally but morally, which is also captured by Grech-Madin's (2021) concept of water taboo, additionally tailored to the United States water considerations in foreign wars.

This opens up the dichotomy of water inviolability and quite tangible state water weaponisation practice. This research looks into the regularities of water campaigns to uncover the patterns that lead to water weaponisation, asking what contexts and actors require violations of water norms. This descriptive research combining qualitative and quantitative aspects brings to light not only novel expectations for future water weaponisation practice in the era of increasing water scarcity but also the limits of IL.

Materials and methods

The article draws on the Pacific Institute California's Water Conflict Chronology dataset (Pacific Institute, n.d.), which collects records of incidents in which water played a role as a weapon, trigger, victim, or a combination thereof, between 2500 BC and late 2023. The data were sorted to select only state water weaponisation after 1900, a period reflecting the evolution of water weaponisation legal prohibition between the 1899 and 1907 Hague Conventions (prohibits poison), through the 1949 Geneva Conventions (protects civilians and means of survival) and their 1977 Additional Protocols (protects dams, water and civilian infrastructure), to the modern days. The listed events were sorted for state water weaponisation only and coded for various variables of context, such as: type of conflict (inter/intra), scope of damage (low to high), necessity (yes/no), consequence (yes/no), success (yes/no), legality (legal/non-ratified/ratified), weaponisation type (poison, flood, etc.); and properties of the actor in the given year: regime type (Political Regimes of the World dataset), region, or religious supermajority (yes/no and which).

Building on the expectation that democratic states should adhere to IHL more closely, while religious states should adhere to the moral water inviolability, a set of analyses (inferential and descriptive statistics), were run to determine why, when, where, how, and by whom water weaponisation is orchestrated, thus what makes a state breach the norm. The preliminary and very concise results are presented below.

Results and concluding remarks

The analysis departs from normative expectations for moral (religious) and legal (democratic) actors in relation to water. It is not able to detect any moral constraint imposed by religion on water weaponisation practice, although it notices differences within the variable. For example, it is the Christian countries that cause the biggest water-related damage of all groups, yet it is also more probable for them to act on necessity, which complicates the evaluation of their respect for water inviolability as some contexts may appear superior (e.g., self-defence).

The same is true for democratic states, a fact that underpins the significant overlap of religion and

regime. Additionally, any such reflections must be skewed by the fact that it is the global north (heavily democratic and Christian) that controls the global regime and consequently justifies the necessity principle, especially for foreign operations. That may also explain the observation that democratic states tend to execute water weaponisation more successfully, possibly as the necessity rationale demands or allows heavier action (statistically significant correlation) such as aerial bombing.

Surprisingly, there is no statistically significant difference between democratic and undemocratic countries when it comes to the illegality of water weaponisation events. That disapproves the hypothesis justifying the water weaponisation record of supposed democratic norm defenders by the belief that the observed water-related record fits the IHL's gaps. Quite on the contrary, IHL does not seem as much of an obstruction to the states' water behaviour, given that greater damage is associated with stricter legal constraints (ratification). At the same time, there is no statistical difference between water-weaponizing parties and non-parties regarding necessity, therefore no potential moral excuse. What is more, water weaponisation by ratifiers and non-ratifiers does not face different amounts of repercussions as it ideally should in order to maintain the assumed water weaponisation stigma.

That leaves us hoping for normative constraints to be at least context-specific. That is the case for water weaponisation by poison, which is rare to see (as the chemical/biological taboo, unlike the water one, is widely respected) and restricted to autocracies. Further, given that water weaponisation is most often delivered through water infrastructure destruction or obstruction it could be perceived as unattached from water and its inviolability per se – as the perpetrator targets bricks and pipes, not water. This assumption requires further tests developed in the full-length paper.

In summary, the paper finds no relationship between water weaponisation and religion and a negative relationship between water weaponisation and law, as well as democracy. It recognizes some weaponisation-type-related stigmas that inspire further research into the specifics. It draws attention to democratic countries or ratifiers that, despite the common knowledge, threaten water more than others. These findings do not reject the notion of water taboo that may be country-specific but must lament its lack on the global scale.

References

Daoudy M (2020) Water weaponization in the Syrian conflict: Strategies of domination and cooperation. International Affairs 96(5): 1347-1366. http://doi.org/10.1093/ia/iiaa131

Gleick PH (2019) Water as a Weapon and Casualty of Conflict: Freshwater and International Humanitarian Law. Water Resources Management 33(5): 1737-1751. https://doi.org/10.1007/s11269-019-02212-z

Grech-Madin, C (2021) Water and Warfare: The Evolution and Operation of the Water Taboo. International Security 45(4): 84-125. https://doi.org/10.1162/isec_a_00404

King MD (2015) The Weaponisation of Water in Syria and Iraq. The Washington Quarterly 38(4): 153-169. https://doi.org/10.1080/0163660X.2015.1125835

Pacific Institute (n.d.) Water Conflict Chronology Timeline List [Dataset]. https://www.worldwater.org/conflict/list

Von Lossow T (2016) The Rebirth of Water as a Weapon: IS in Syria and Iraq. The International Spectator 51(3): 82-99. https://doi.org/10.1080/03932729.2016.1213063

Cascading effects of carbon neutrality: multi-tiered transition risks in floating solar, offshore wind, and hydropower

H.W. Jee[1*], S.B. Seo[2]
[1] Department of International Urban Development, University of Seoul, Seoul, South Korea
[2] International School of Urban Science, University of Seoul, Seoul, South Korea
* e-mail: heewon.jee@uos.ac.kr

Introduction

Achieving carbon neutrality has become a global imperative, prompting a broad range of studies examining the impacts of decarbonization efforts on various renewable energy technologies and systems (Thompson et al., 2024). Existing literature has reviewed recent developments in offshore photovoltaics (Wang and Lund, 2022), analyzed global research trends in offshore wind farms (Chen and Su, 2022), and discussed risk management strategies for hydropower projects (Shaktawat and Vadhera, 2021). While these studies have enhanced our understanding of environmental, technical, and social effects, they generally consider these impacts rather than differentiating between direct impacts and subsequent second- or third-order consequences.

In an increasingly interconnected world, risks rarely remain confined to their initial triggers. Instead, they propagate through multiple channels, leading to secondary and higher-order consequences that compound their overall impacts (Thompson et al., 2024). This study addresses that gap by systematically examining how carbon neutrality policies give rise to multi-tiered, cascading outcomes within the context of South Korea's energy transition. South Korea provides a compelling case, given its supportive regulatory framework and strong transition readiness (World Economic Forum, 2024), yet the broader ramifications of implementing carbon neutrality measures remain underexplored. By analyzing the interplay among floating solar power, offshore wind farms, and hydropower, this research offers a more granular perspective on how decarbonization efforts can produce layered consequences. Ultimately, these findings can guide more refined policy design and identify new research avenues that better account for the complex realities of energy transitions.

Materials and methods

This research investigates the cascading effects of carbon neutrality policies through the cases of floating solar power, offshore wind farms, and hydropower (including pumped storage). Both qualitative and quantitative aspects of domestic policies were examined to provide an initial overview of the policy landscape. To identify the pathways through which transition risks unfold, a comprehensive review of academic literature, reports, and media articles was conducted. Specific effects were extracted using keywords such as risk, impact, effect, challenge, barrier, and concern, and then categorized into five types of transition risks—technological, policy, economic, social, and environmental. Each identified effect was further classified as direct or indirect, offering a more nuanced understanding of how carbon neutrality policies can give rise to multi-layered, cascading outcomes.

Results and concluding remarks

The findings reveal several common transition risks: insufficient power system capacity, a lack of detailed implementation plans, negative public perceptions, and ecological impacts. Notably, environmental risks—such as habitat alterations and an increased likelihood of natural disasters—were the most frequently mentioned, reflecting the inherent vulnerabilities of aquatic environments where these infrastructures are deployed.

These results underscore the importance of conducting post-implementation environmental impact

assessments alongside conventional assessments to enhance environmental risk management. By addressing unforeseen hazards that may arise during or after project implementation, this approach fosters more adaptive and proactive strategies. Furthermore, effective expansion of renewable energy deployment requires detailed implementation plans that include permitting processes, research and development (R&D), and improvements to grid stability. Active governmental involvement is crucial, especially in tackling grid-related challenges, which necessitate close collaboration with local governments and communities. Co-creation methods and other participatory approaches can be leveraged to strengthen social acceptance.

Finally, balanced evaluations that consider both the positive and negative aspects of these policies are essential. In this context, quantitative research plays a key role in comprehensively assessing transition risks across environmental, social, economic, and financial dimensions. Drawing on such assessments, governments, local authorities, industries, and communities should engage in consultations and discussions to guide an equitable, safe, and sustainable transition. Such collaborative efforts are expected to pave the way for a more equitable and resilient path toward carbon neutrality.

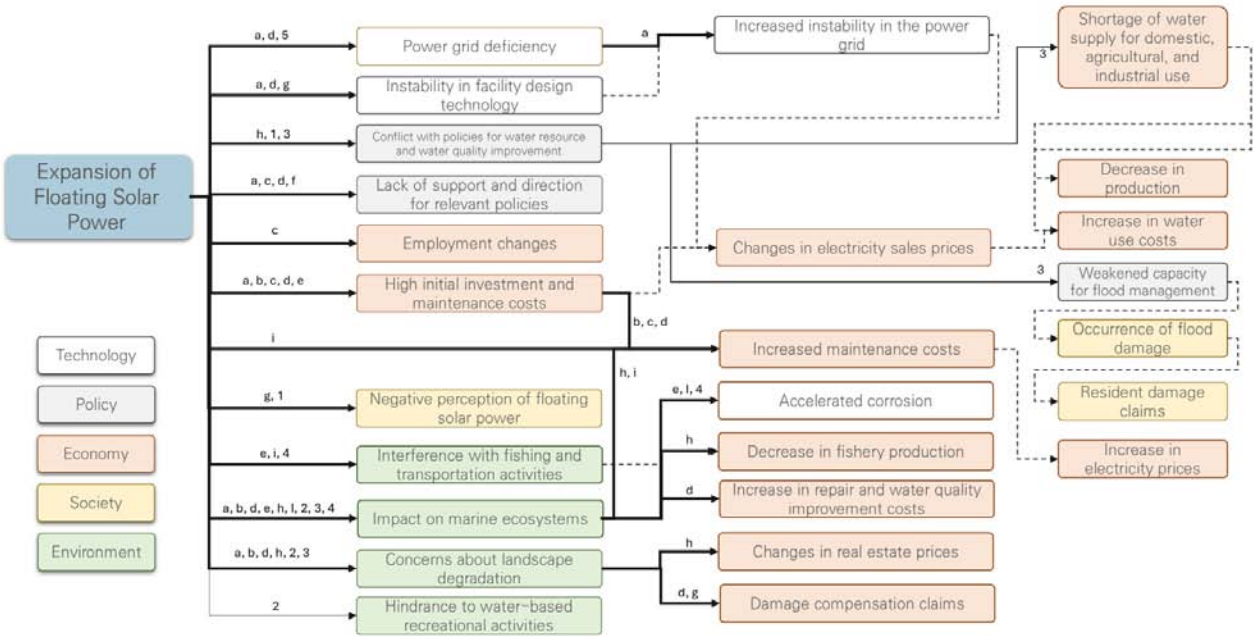


Figure 1. Example of Cascading effects (floating solar power).

Acknowledgments: This work was supported by Korea Environment Industry & Technology Institute(KEITI) through Water Management Program for Drought and the Carbon Neutrality, a specialized program of the Graduate School, funded by Korea Ministry of Environment(MOE)(RS-2022-KE002032).

References

Chen C H, Su N J (2022) Global trends and characteristics of offshore wind farm research over the past three decades: A bibliometric analysis. Journal of Marine Science and Engineering 10(10): 1339. https://doi.org/10.3390/jmse10101339

Shaktawat A, Vadhera S (2021) Risk management of hydropower projects for sustainable development: a review. Environment, Development and Sustainability 23(1): 45-76. https://doi.org/10.1007/s10668-020-00607-2

Thompson D A, Glenn D E, Trethewey L L, Blackett P, Logan T M (2022) Capturing cascading consequences is required to reflect risk from climate change and natural hazards. Climate Risk Management 44: 100613. https://doi.org/10.1016/j.crm.2024.100613

Wang J, Lund P D (2022) Review of recent offshore photovoltaics development. Energies 15(20): 7462. https://doi.org/10.3390/en15207462

World Economic Forum (2024) Fostering Effective Energy Transition. World Economic Forum, Geneva

Assessing young people's emotions and perceptions on climate crisis after experiencing a major flood hazard in a Mediterranean region

I. Tsevreni[1*], D. Tigkas[2], A.M. Kali[1], H. Vangelis[2], N. Proutsos[3]
[1] Laboratory of Science and Technology, Department of Early Childhood Education, University of Thessaly, Volos, Greece
[2] Centre for the Assessment of Natural Hazards and Proactive Planning & Lab. of Reclamation Works and Water Resources Management, School of Rural and Surveying Engineering, National Technical University of Athens, Greece
[3] Institute of Mediterranean Forest Ecosystems, Hellenic Agricultural Organization - DIMITRA, Athens, Greece
*e-mail: itsevreni@uth.gr

Introduction

Nowadays, people feel multiple ecological emotions related to climate change and climate-related hazards. Young people are included in social groups that are particularly vulnerable to the effects of climate change in many aspects of their everyday life and future, such as their health, education, work and well-being (Clayton et al., 2017; Clayton, 2020). Young people belonging to Generation Z (born between 1997-2012) are known as the climate generation since they came to the earth in the era of major consequences related to global warming (Ray, 2020).

The UN Sustainable Development Goal 3 emerges the need for ensuring environmental health at all ages, including young people's well-being. Towards this goal, it is particularly important to assess young people's climate anxiety (Pihkala, 2020). Recently, Pihkala and Kamenetz (2024) have classified climate emotions into four main categories: fear, sadness, anger and positivity. Another important aspect is the investigation of climate anxiety's effects on young people's everyday lives. Finally, it is crucial to examine young people's ideas for the future, affected by the climate crisis, as well as their trust in governments' environmental policies (Hickman et al., 2021).

The purpose of the study is to investigate and emerge young people's ecological feelings and perceptions on the climate crisis. The study focuses on young people living in the Mediterranean, which is an area particularly vulnerable to the socio-economic effects of climate change. There is also limited knowledge on young people's emotions and ideas from countries of the Mediterranean (Tsevreni et al., 2023). The recently experienced large-scale floods in the Thessaly region (Greece) are used as a paradigm to assess the effects on young people's climate anxiety.

Materials and methods

Data were collected from a broader research process aiming at investigating young people's emotions and perceptions on climate change in a period of extreme climate-related events in Greece. The participants have been chosen with two criteria: a) to belong to Generation Z, and b) to have been recently exposed to an extreme climate-related event (flood, mega-fire, drought, etc.). The current study includes data only from participants who have recently experienced extreme flood hazards caused by the Mediterranean Cyclones 'Daniel' and 'Elias' in Thessaly during September 2023. 'Daniel' has been identified as one of the worst extreme events in the Mediterranean in terms of human casualties, causing also severe damages (Argüeso et al., 2024). In Thessaly, major parts of the region were flooded, including urban and rural areas, while various public infrastructures have failed causing significant effects on vital facilities of everyday life (water supply, electricity, etc.).

In the current study, we analyse and discuss data findings that reveal the emotions on climate change that young people felt after the extensive flooding and its consequences in Thessaly and their satisfaction with the implemented policies towards handling climate change. The data were collected from November 2023 to January 2024. Sixty (60) young people, students at the University of Thessaly in the city of Volos, aged 18-26 years old who had experienced the aforementioned catastrophic flood event participated in the research. The participants completed an online questionnaire based on the measurement scales of Clayton

& Karazsia (2020) and Hickman et al. (2021). The research protocol was approved by the Pedagogical Department's Ethics Committee in 2023.

Results and concluding remarks

Most of the participants (80%) reported that they had personally been directly affected by climate change (e.g. their home, their family, their family's work, or their daily life). The participants' negative emotions about climate crisis can be classified into three main categories (Pihkala and Kamenetz 2024): a) 53.3%-91.7% of the participants felt various emotions under the major category of *sadness* (sadness, shame, guilt, hurt, melancholy, despair, grief), b) 58.3%-85% of the participants felt various emotions under the major category of *fear* (fear, helplessness, powerlessness), and c) 80%-83.3% of the participants felt various emotions under the major category of *anger* (anger, rage). Negative emotions range at high levels, clearly higher than the average emotions of young people from around the world, as assessed in the global survey of Hickman et al. (2021). The negative emotions of young people in Thessaly converge with the emotions of young people in the Global South. Only 5% of the participants reported *optimism*, while *indifference* was reported at an equally low level (5%).

Respondents reported a wide range of negative beliefs about the future. For example, 90% of the participants believe that the future is frightening and 86.7% that their family's economic, social, or physical security will be threatened. 90% of the participants were positive to the statement that people have failed to take care of the planet. Most negative thoughts have significantly higher values than the average value of the youth's opinions worldwide (Hickman et al., 2021). Regarding the role of governments in the confrontation of climate crisis, the great majority of the participants expressed their disapproval of the actions of governments on climate change. For example, 93.3% of the participants believed that governments ignore the concerns of citizens and 61.7% that they do not act in line with science to address climate change issues. The vast majority expressed untrust (95%) and betrayal (90%) on behalf of governments regarding environmental policy for the climate crisis.

This study highlights the feelings and ideas of young people from regions of the Mediterranean that are directly affected by climate-induced hazards and for which there is insufficient data. The results of the study reveal particularly negative feelings of young people about the climate crisis, pessimistic ideas about its influence on their future and dissatisfaction and disapproval of policies on the matter. The particularly negative feelings and ideas of young people in the survey compared to countries not directly affected by extreme climate-induced disasters emerge the need to take immediate measures for the health, well-being and future of new generations.

References

Argüeso, D, Marcos, M, Amores, A (2024) Storm Daniel fueled by anomalously high sea surface temperatures in the Mediterranean. NPJ Clim Atmos Sci 7: 307. https://doi.org/10.1038/s41612-024-00872-2

Clayton S (2020) Climate anxiety: Psychological responses to climate change. J. Anxiety Disord. 74: 102263

Clayton S, Karazsia B T (2020) Development and validation of a measure of climate change anxiety. Journal of Environmental Psychology, 69*:* 101434

Clayton S, Manning C, Krygsman K, Speiser M (2017) Mental Health and our Changing Climate: Impacts, Implications, and Guidance. American Psychological Association and ecoAmerica. Washington, DC, US

Hickman C, Marks E, Pihkala P, Clayton S, Lewandowski RE, Mayall EE, Wray B, Mellor C, van Susteren L. (2021) Climate anxiety in children and young people and their beliefs about government responses to climate change: a global survey. Lancet Planet Health 5(12): e863-e873, doi: 10.1016/S2542-5196(21)00278-3

Pihkala P (2020) Eco-anxiety and Environmental Education. Sustainability, 12(23): 10149. https://doi.org/10.3390/su122310149

Pihkala P, Kamenetz, A (2024) A Guide to Climate Emotions. Climate Mental Health Network

Ray S J (2020) A Field Guide to Climate Anxiety: How to Keep Your Cool on a Warming Planet; University of California Press: Oakland, CA, USA

Tsevreni I, Proutsos N, Tsevreni M, Tigkas D (2023) Generation Z worries, suffers and acts against climate crisis—The potential of sensing children's and young people's eco-anxiety: A critical analysis based on an integrative review. Climate 11(8):171, https://doi.org/10.3390/cli11080171

Trust deficit and rumours as drivers of community opposition to rural water management reforms in Ghana

E.O. Denchie[1,2*], K. Lo[1,2]
[1] Department of Geography, Hong Kong Baptist University, Hong Kong
[2] David C. Lam Institute for East-West Studies, Hong Kong Baptist University, Hong Kong
* e-mail: ernestinadenche@life.hkbu.edu.hk

Introduction

To avert potable water challenges (Dosu et al., 2022; Kotoku and Kumasi, 2022), Ghana is undertaking considerable reforms in water management in rural communities and small towns which started in 2017. A major aspect of this reform involves the transition from community-based management (CBM) of water facilities in rural communities to state or corporatized model under government control. Though this transition is intended to enhance efficiency and sustainability in water management, the reforms has been met with aggression and opposition from local actors, stakeholders and community members. To advance their interest, local actors has triggered rumours (Liu & Lo, 2022) and distrust through their social network and local social relations to influence the public to oppose the water management reforms. This paper investigated how trust deficit and rumours influenced community members opposition to water management reforms in rural Ghana and its resulting impact on the reforms.

Materials and methods

A cross-sectional survey design together with semi-structured questionnaires, in-depth interviews and participant observation of over 5 years by the first author were employed to gather primary data from 969 community members in 17 communities in the Central Region of Ghana. Multiple regression analysis was used to determine the relationship between community opposition to water management reforms, trust deficits as well as rumours. We used thematic analysis in unravelling the sources or rumours, its influence on community members' perception and local actors' reason for supporting or opposing the reforms.

Results and concluding remarks

The study found that trust for Community Water and Sanitation Agency (CWSA) (government institution in charge of direct water management in small towns and rural Ghana under the reforms) has a significant positive relationship with supporting government takeover of community-based water management. The study further revealed that information sourced from community leaders, friends and neighbours, and Local District Assembly Office have a significant negative relationship while information sourced from government Officers or through the implementing agency – CWSA official websites – have a significant positive relationship with supporting the reforms in water management.

In addition, we observed a negative relationship between rumours sourced from other means either than CWSA Officers or through CWSA official websites as influencing factor for community opposition to the water management reforms.

The findings of the study suggest that an increase in trust in CWSA will lead to an increase in support for government takeover of water facilities presently under community water management, whereas the converse holds for a decrease in trust in CWSA. This calls for policymakers who desire to do away with resistance to the ongoing water management reforms to have good insights about the channels of information diffusion and appreciate the relevance of trust from community members in fostering effective implementation of water management reforms for sustainable outcomes.

References

Dosu, B., Hanrahan, C., Johnston, T., & Spaling, H. (2022). Assessing the capacity gaps of decentralized rural water management: qualitative evidence from Ghana. *Water International*, *47*(8), 1267-1286.

Liu, J., & Lo, K. (2022). Chinese environmental activism and the environmental politics of rumors. *Political Geography*, *95*, 102593.

Kotoku, G., & Kumasi, T. C. (2022). Rethinking the sustainability of rural water delivery under the community ownership and management model. *Sustainable Water Resources Management*, *8*(5), 164.

Establishing shared governance and R&I strategies: WATERLINE

S. Duman[1*], M. Šťastná[2], M. Menšíková[2], P. Oppeltová[2], O. Ulrich[2], D. Procházka[2], J. Zloch[2], G. Onuşluel Gül[3], S.N. Yeşilyurt[3], H. Boyacıoğlu[4], F. Barbaros[3], M.C. Günaçtı[5], A. Chen[6], M. Gocic[7], A. Gül[3], R. Hassan[8], P. Leskinen[9], M. Mistretta[10], E. Zammit[11]

[1] *Department of Business Administration, Faculty of Business, Dokuz Eylül University, Izmir, Turkey*
[2] *Department of Applied and Landscape Ecology, Faculty of AgriSciences, Mendel University in Brno, Brno, Czech Republic*
[3] *Department of Civil Engineering, Faculty of Engineering, Dokuz Eylül University, Izmir, Turkey*
[4] *Department of Environmental Engineering, Faculty of Engineering, Dokuz Eylül University, Izmir, Turkey*
[5] *Department of Computer Engineering, Faculty of Engineering, Dokuz Eylül University, Izmir, Turkey*
[6] *Centre for Water Systems (CWS), University of Exeter, United Kingdom*
[7] *Faculty of Civil Engineering and Architecture, University of Nis, Nis, Serbia*
[8] *Department of Building and Environmental Technology, Norwegian University of Life Sciences, Norway*
[9] *Turku University of Applied Sciences, Turku, Finland*
[10] *Department of Information, Infrastructure and Sustainable Energy Engineering, Universita Degli Studi Mediterranea di Reggio Calabria, Italy*
[11] *Malta College of Arts Science and Technology, Paola, Malta*

Introduction

The EU Horizon WIDERA program WATERLINE project, aims to create a European Digital Water Higher Education Institution (HEI) Alliance, based on the quadruple helix model of innovation, leading to the development of the Alliance's research, educational and entrepreneurship capacities. Within this scope, the partners aimed to establish a shared governance framework and R&I capacity-building plan

Materials and methods

The WATERLINE project implemented face-to-face workshops in participating HEIs (High Education Institutions) in Malta (Malta College of Arts Science and Technology (MCAST)), Czech Republic (Mendel University in Brno (MENDELU)), Serbia (University of Nis (UNI)), Turkey (Dokuz Eylül University (DEU)), Italy (Universita Degli Studi Mediterranea di Reggio Calabria (UNIRC)), Norway (Norges Miljo-Og Biovitenskaplige Universitet (NMBU)), Finland (Turun Ammattikorkeakoulu Oy (TUAS)) and United Kingdom (University of Exeter (UNEXE)). Workshops included participants from regional stakeholder by referring to the Quadruple Helix Stakeholder Model (QHSM) which highlights the inclusion and integration of the end users (society) into the innovation development stakeholders; academia, government, and industry (Bartoloni et al., 2022). Regional Communities of Practice were established to both support the consolidation and sustainability of Digital Water Alliance and participate to the workshops. Lave and Wenger (1998) referred Community of Practice (CoP) as a group of people sharing knowledge, problems, solutions, information, and news about a specific issue, and who extend group learning through reciprocal interaction. Members of the communities were selected from academia, NGOs, industry and government in the aim of establishing a platform that enables voices from all stakeholders can be heard and collaboratively create innovation via QHSM.

The method to conduct the regional workshops was determined by MENDELU and shared with the eight HEIs. Participants engaged in brainstorming sessions to identify the top three challenges for digital water education in the region, working in groups to develop action plans. Then, the groups refined their visions into actionable points and discussed them in detail. More specifically discussions in the workshops were undertaken in the following topics: a) administrative barriers and opportunities, b) regional skill sets, c) digital water regional ecosystems, d) challenges and e) visions. The vision items addressed by the participants were subjected to content analysis via NVivo 15 qualitative research analysis software and the verbatim transcripts were analysed in terms of word frequency and coding scheme. The coding scheme aimed to identify the actionable points via QHSM. Initially the word frequency was explored, and the following results were obtained (Table 1). Then, coding was applied to the transcripts within the QHSM framework, and the findings can be seen in Figure 1. It can easily be stated that stakeholders were the mostly indicated actors by all participant partners. Participants focused on an integrated and tight-knit

collaboration among stakeholders as whole which supports the adoption of QHSM as inevitable for futureproofing digital water. Technological related developments and updates being closely monitored and adopted were also important subjects to be included in the visionary items of digital water. Lastly industry, more specifically workforce empowerment of technical skills and digital water mindset, was pointed out.

Table 1. Word frequency

Word	Length	Count	Weighted Percentage
water	5	67	6,46%
digital	7	29	2,80%
sector	6	26	2,51%
education	9	17	1,64%
public	6	12	1,16%
skills	6	12	1,16%
knowledge	9	10	0,96%
stakeholders	12	10	0,96%
experts	7	9	0,87%
data	4	8	0,77%

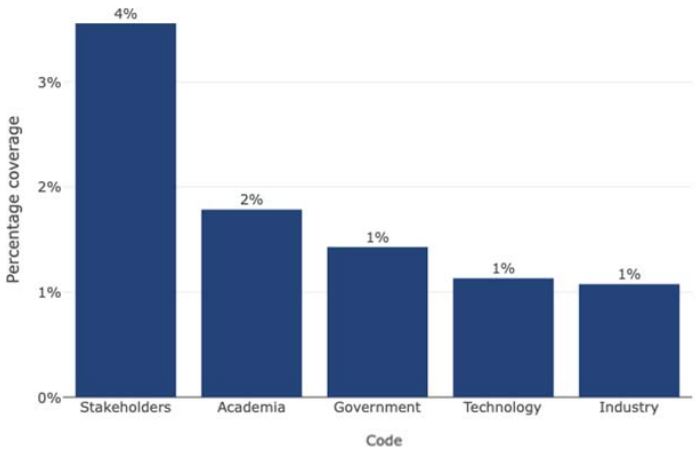


Figure 1.. Results of coding analysis

Results and concluding remarks

Results, even though were differing on certain points across different regions, can be summarized as follows: a) Majority of the institutions have institutional accreditation for master's programmes in science or engineering. b) The most frequently cited needed academic skills across states and categories are communication and networking skills, working in an international context and goal planning. Interdisciplinary teaching and learning skills needed across categories are critical thinking and problem-solving skills. Needed technical skills are data analysis, acquisition, and processing. The most needed transversal skills across different countries and sectors are reflection on strengths and shortcomings, prioritising and organising, learning to learn, and delivering quality and results, and leadership. c) Digital Water appears to be a new issue, which is not yet directly included in smart specialisation strategies in the regions. It is to be expected that more regions in all countries will follow as the technology development advances, d) The challenges outlined by the eight involved countries provide insight into the diverse range of issues facing the water sector and highlight common themes and priorities: industry needs and skills development, public awareness and education, infrastructure and technology, collaboration and stakeholder engagement, e) The qualitative analysis conducted on vision items shared by all the partners displayed a strong need for stakeholder engagement and collaboration which proves substantiation and criticality of adoption of QSHM framework in WATERLINE.

Acknowledgements: This study is presented with the support of WATERLINE project funded under the call HORIZON-WIDERA-2021-ACCESS-05, the grant agreement No. 101071306 and its project outputs.

References

Bartoloni S, Calò E, Marinelli L, Pascucci F, Dezi L, et al. (2022) Towards designing society 5.0 solutions: The new quintuple helix design thinking approach to technology. Technovation, 113, 102413, 1-14.

Lave J, Wenger E (1991) Situated Learning: Legitimate Peripheral Participation. Cambridge: Cambridge University Press

13th World Congress on Water Resources and Environment (EWRA 2025)
"New challenges in understanding and managing water-related risks in a changing environment"
Palermo, Italy, 24 - 28 June 2025

Model-assisted cost-benefit analysis for regional water supply systems: understanding the tools

C. Arena*, M. Cannarozzo, G. Gullotti
Dipartimento di Ingegneria, Università degli Studi di Palermo, Palermo, Italy
** e-mail: claudio.arena@unipa.it*

Introduction

Cost-benefit analysis (CBA) is a powerful, straightforward tool to appraise both policies and infrastructure investments and is therefore widely applied - in its full formal extent or using its principles -in several fields including water-related ones such as flood risk mitigation, water reuse etc. It uses a flow of future projected costs and benefits associated to the specific investment to be evaluated - all expressed in monetary terms - to understand if benefits generated will exceed the costs borne. The latter should encompass all negative impacts to society and hence include not only the costs associated to the inputs used to implement the investment, but also external impacts to the environment. Issues of equivalence among costs and benefits in different years are accommodated through a discount rate.

While CBA has sound roots in the theory of welfare economics (Florio, 2014), its practical use in the most diverse sectors requires suitable tools, specific to the sector of application, to simulate and quantify the investment's effects that will be then turned into monetary values. We focus here on planning in the sector of large water supply infrastructure for regional systems such as reservoirs, desalination plants, inter-basin transfers. In mature economies, the objectives of these projects are mainly associated to increased reliability of water supply, cost reduction, better quality of water resources for civil water service. As most large infrastructure, these works are now under the lens of public opinion and therefore require objective methods to be assessed, often in the framework of the complex, regional systems in which they will operate.

In the writers' opinion, a class of well-known tools, indicated as water resources models (Sulis and Sechi, 2013) is the most appropriate to simulate regional water supply systems. Unlike hydraulic models, that aim at reproducing the physics of the flow process, they simulate the *decisions* to meet a given demand with the available resources at the appropriate time scale (day, month) accounting for water resources variability, system's topology, reservoir storage and other constraints. In some of these models, these decisions are made using rules, while in some others optimization algorithms are used to solve the allocation problem. These simulation tools are all certainly capable to provide measures of change compared to a *status-quo* situation (called as Business-As-Usual -BAU in the CBA jargon) and thereby provide the basis to evaluate project's effects; yet, understanding how model architecture influences the outputs is not always straightforward; therefore in the following we will focus on some issues concerning the simulation engines and their implications on outputs relevant to the appraisal involved in CBA.

Materials and methods

As generalization is hard to achieve, given the diversity of the available models, in the following we shall focus on Aquator, a commercial platform for water resources systems simulation where the problem of water resources allocation across a network connecting demand and supply centres is solved on a daily timescale using a linear optimization model. The linear objective function used is consistent with the allocation philosophy of the model that recognizes two different resource states (RS) in which each water source may be at a certain time step: either a good or a bad one according to the value of a control parameter. For groundwater or river abstractions this control parameter is a flow value, while for reservoirs it is a water volume: thus, for example, at timestep t of simulation, a reservoir having a stored volume exceeding the control value for that time of year is in a good resource state (RS > 1) and so is a well with a withdrawal under the control flow. For groundwater, the lower the control flow the better the resources

state: the notion of control flow is related in this case to some hazard level associated to that resource so that a control flow of zero would imply that the resource may be used confidently while high values of control flow indicate that the resource should be used sparingly, possibly when no other resource is available. These concepts are in turn closely tied to those of *excess water* - the amount of water flowing from a resource when it is in a good state - and of *maximum water* – the water flowing from a resource in a bad state constrained by the maximum water withdrawable from that resource. The decision-making model underpinning the objective function (O.F.) used by the optimization algorithm is that, if demand may be met using only resources in good state, it is desirable that this be done minimizing costs, while, if other resources must be used to cover the water balance, this should rather be done maximising resources state. The O.F. is therefore the weighted sum of two components, the first being the sum of the costs of excess water over all the feasible routes connecting supply to demand centres and the second the sum of the RS of the sources multiplied by the maximum water used. Both costs and RSs are scaled, and the sign of costs is changed so that the OF is the maximization of the sum of the two components. From this general form, different decision-making styles may be simulated by e.g. ignoring RS - thereby only minimizing costs - or weighting one component more than another or even maximizing RS regardless of costs.

From the standpoint of CBA, it is relevant that the costs involved in the O.F. are only those directly depending on the flows at stake (variable costs). Quite often a relevant part of the benefits from a water supply project is associated exactly with the reduction of these variable costs, especially electricity that also has an external cost component related to the emissions of greenhouses gases, so that it is important to understand what decision-making style is appropriate for the context and subsequently what specification of the OF should drive the allocation process. In cost-driven models, minimization of energy cost (or consumption) may be considered as a primary goal, and energy may become the variable that saturates the single-objective O.F. of the model. On the other hand, the appraisal of benefits other than the reduction of energy costs may be relevant in the analysis of a water supply project, such as the improvement of water quality for municipal use. In this case, a blender, one of many in Aquator's components palette, may be used to constrain a given quality parameter (e.g. sulphates or water hardness) not to exceed a threshold, provided that a characterization of each resource's relevant quality parameters is available. While the blender may indeed represent a physical component such as tank where waters of different quality are mixed, it can also be used as a conceptual constraint to indicate what the water balance would be like if quality constraint were binding. Adding a blender into the system may result in an increase of costs, but even in water deficits, should the mix of water of suitable quality not be sufficient to meet demand in the BAU situation. In this case, methodologies to evaluate a water deficit (e.g. Arena et al, 2014) can be used.

In other instances, the convenience to leave aside a certain water resource stems from the combination of different motivations for which economic quantifications are possible but are difficult to include in the optimization model due to their multi-objective nature. In this case, a modelling strategy could be to use the resource state as a proxy to prioritise the use of resources with certain characteristics over others.

Results and concluding remarks

These ideas have been applied to a real case study located in Sicily (Italy) as a part of system's planning aimed at identifying promising infrastructure alternatives to improve municipal water service especially concerning energy outlays. The application has shown that model results vary considerably depending on the decision-making style (cost-driven, resources oriented) and that this in turn has a significant impact on the results of the economic analyses, suggesting that allocation rules used by the model should be thoroughly understood and carefully considered when using these models to support cost-benefit analysis.

References

Arena C, Cannarozzo M, Mazzola MR (2014) Screening Investments to Reduce the Risk of Hydrologic Failures in the Headwork System Supplying Apulia (Italy) - Role of Economic Evaluation and Operation Hydrology. Water Resources Management 28:1251–1275. https://doi.org/10.1007/s11269-014-0539-9

Florio M (2014) Applied Welfare Economics Cost-Benefit Analysis of Projects and Policies, Routledge, Oxfordshire, UK.

Sulis A, Sechi GM (2013) Comparison of generic simulation models for water resource systems. Environmental Modeling and Software 40:214–225. https://doi.org/10.1016/j.envsoft.2012.09.012

Local river basin water retention developments: Requirement for governance instruments

R. Ernsteins[1,2*], T. Bringulis[2], K. Konkovs[2], A. Skute[1]
[1] Institute of Life Sciences and Technology, Daugavpils University, Daugavpils, Latvia
[2] Environmental Science Department, University of Latvia, Riga, Latvia
* e-mail: raimonds.ernsteins@lu.lv

Introduction

The ongoing EU HORIZON project OPTAIN national model case studies of small river basins territories are aiming to select and optimize the spatial distribution and combination of water retention (infrastructure) measures to be planned at both local farms and catchment levels, considering their environmental and socio-economic sustainability. The case study territory in Latvia is the Dviete River basin (254 km^2), a natural and cultural-historical valley area where the 5th season of the year, locally called «Atbuda», as the regular flooding occurs for several spring months each year. Also here is established the Dviete Floodplain Meadows Natura 2000 protected area, serving as a vital habitat for diverse plant and bird species.

Significant challenges exist to manage this especially valuable territory, including the limited capacity of the responsible National Nature Conservation Agency, lacking this Natura 2000 administration and regular funding, having also limited cooperation with other stakeholders of the river basin, particularly in the conditions of still existing conflicting interest with local farmers. Local municipal authorities also face resource and capacity constraints in managing these nature-culture values rich areas. The bottom-up adaptive management approach (Graversgaard et.al., 2017) was the answer of the local communities and local NGO «Union of the Dviete Valley Municipalities» was established by that time small local municipal parishes and enthusiasts, being now the sole organization voluntarily managing river basin nature and culture protection (Van Buuren et.al., 2019).

Proposals for water retention infrastructure developments and management are set, as well as required preconditions securing – communication framework and the set of remaining governance instruments.

Materials and methods

Current studies have been planned as research-and-development framework application of complementary engineering-based infrastructure instruments studies and governance instruments studies, employing case studies research methodology, including complementary data basis and document studies, stakeholders in-depth semi-structured interviews, surveys, site visits and documentations for potential retention measures and situation monitoring. Also, various local, regional and national data basis are studied, particularly previous studies on water regimes and qualities, to secure related socio-ecological systems-based data gathering for water retention modelling at both river basin area and local agriculture farms level.

Within the framework of the OPTAIN project and in collaboration with mentioned NGO there was developed and established the multi-actor reference group (MARG) for Dviete river region – local and regional main stakeholders were involved for the implementation of this water retention governance project, subsequently, realizing socially engaged research (SER) application (Buitrago et.al., 2023). The work of the MARG was planned with regular communication exchange also using interviews and questionnaires besides the annual meetings with project research work evaluations and MARG recommendations for further research and action orientation developments throughout the 5-year project duration.

To realize this, the first task of the study was the stakeholder mapping, identifying at all administration levels the stakeholders connected to the Dviete River Basin area, initially looking for water and agriculture governance institutions and organizations, but surely expanding it further to nature and environmental

protection organizations, also nature tourism, agriculture, forest etc. businesses as well. Stakeholder mapping was planned and grouped according to the adapted (updated and enhanced) new Quintuple Helix model - based on representants of mediators (media, NGO, educators, science/academia), also from business, municipality and state, inhabitants.

The engineering study of eventual infrastructure instruments and their management study has been conducted, which includes the development of technical solutions to preserve water runoff from agricultural lands and their adaptation to local conditions. In the EU water runoff regulation measures, categorized as infrastructure measures, are divided into agrotechnical (such as green cover of the ground cover, creation of meadows and pastures, creation of buffer strips, annual change of plants (cultures) and so on) and hydrotechnical (such as creation of small ponds, restoration/creation of wetlands, restoration of floodplains, restoration of river meanders and so on) measures. To understand and adapt these solutions, modelling and further SER approaches are being employed.

Results and concluding remarks

Key proposed infrastructure-based instruments as decided by MARG meeting includes restoring the structure of riverbeds, which involves minimal farmer effort and avoids significant legislative changes, and creating buffer zones in the Dviete river basin, identified as the simplest and most effective approach. Resistance to buffer zone measures may arise from farmers seeking to maximize land cultivation. To address this, the development of improved compensation mechanisms, legislative adjustments, and cooperation-promoting instruments is essential. Current national mechanisms are insufficient to ensure farmer involvement and cooperation, highlighting the need for targeted strategies to balance agricultural interests with environmental sustainability and pro-active cooperation of both related national ministries.

Case study research done during the project realization phases have recognized, that there is obvious need for two more governance instrument groups to be complementary developed as considerably missing not only in the case region but to some extent also at the national level. First, there are *complementary set of communication instruments* (incl. information, education/training, participation and pro-environmental/water behaviour/models), which here need to be seen mostly as first generated, developed and even prioritized to deal basically, but not only, with those infrastructure instruments potential application by local farmers and communities, particularly, to understand and discuss, to consider and evaluate, and eventually pre-plan and test etc. planned interventions. And for these locally recognized needs for communication instruments design and application, could be as wide, diverse as possible, the project proposed MARG eventual instrumentation, but essentially strengthened and further developed. Here, MARG mutually beneficial strengthened partnership with the locally known, pro-active and nature-culture protection experienced NGO «Union of the Dviete Valley Municipalities» is to be highly recommended.

Finally, all the other groups of governance instruments, besides communication and not only the core infrastructure instruments for water retention development are to be not forgotten – this includes studies of *institutional and administrative instruments, political and legislative, planning, and economic-financial instruments groups* - carefully and complementary (re)developed and implemented in partnership with all main area and water retention situation stakeholders as local, regional and even some national too. Related studies have been done, and actionable recommendations are being developed.

Acknowledgments: Daugavpils University and University of Latvia supported this publication, though initially researchers were funded by EU Horizon project OPTAIN “Optimal strategies to retain and re-use water and nutrients in small agricultural catchments across different soil-climatic regions in Europe”.

References

Buitrago H., Lošťák M., Winge S., de Groot A., (2023). Deliverable 2.1. Status Quo Report on Socially Engaged Research. BETTER Life project Report

Graversgaard, M., Jacobsen, B. H., Kjeldsen, C., & Dalgaard, T. (2017). Stakeholder Engagement and Knowledge Co-Creation in Water Planning: Can Public Participation Increase Cost-Effectiveness? Water, 9(191), 1–29.

Van Buuren, A., Van Meerkerk, I., & Tortajada, C. (2019). Understanding emergent participation practices in water governance. International Journal of Water Resources Development, 35(3), 367–382.

XV. Ecohydrological Approaches for Enhancing Water Resource Sustainability

An ecohydrological waterfront management approach associated with civilian science

T. Shim[1], H.W. Jee[2], S.B. Seo[3*]
[1] Institute of Urban Sciences, University of Seoul, Seoul, 02504, South Korea
[2] Department of International Urban Development, University of Seoul, Seoul, 02504, South Korea
[3] International School of Urban Sciences, University of Seoul, Seoul, 02504, South Korea
* e-mail: sbseo7@uos.ac.kr

Introduction

The demand for ecologically healthy rivers and water-friendly spaces from citizens is increasing over time (Poff et al. 2010; Lee et al. 2022). However, alterations in the hydrological regime may cause rapid decline in biodiversity of aquatic ecosystems which can lead to reduced services of waterfronts (Bunn and Arthington 2002; Dudgeon et al. 2006). Accordingly, the importance of regional scale application has increased (Dyson et al. 2003; Arthington et al. 2006; Poff et al. 2010), requiring management or decision support systems to consider regional heterogeneity. Thus, this study proposes an ELOHA (Ecological Limitations Of Hydrological Alteration; Poff et al. 2010)-based approach for supporting the determination of release of ecological/environmental flow and timing for streams, while incorporating civilian collaboration.

Materials and methods

The study area consists of 38 stations located regulated streams in the Han River Basin, South Korea, and 3 sites of interest were selected for evaluation. This study targeted 62 freshwater fish species that occur in the Han River Basin, and the occurrence data were collected from the Water Information System (http://www.water.nier.go.kr/). In this study, period was classified by past (2011-2016) and present (2017-2023). Additionally, civilian fish monitoring data (2014-2023) was acquired from the Suwon Sustainable City Foundation. Missing data of streamflow was acquired from a simulation result that uses the Tank model driven by observed climatic data (NSE=0.233 at downstream junction of evaluation sites).

Hydrological alteration was quantified using IHA (Indicators of Hydrological Alteration) variables based on Richter et al. (1996). A total of 34 variables were derived that represents: Magnitude of monthly and annual hydrological condition (14), Magnitude and duration of annual extreme hydrological condition (10), Timing of annual extreme hydrological events (2), Frequency and duration of pulses (4), and Rate and frequency of hydrologic condition changes (4). Nine variables were selected using the variance inflation factor, while ensuring at least one IHA was chosen from each functional group. Ecological alteration was quantified using α- and β-diversity indices. α-diversity was defined as species abundance (number of occurred species), while Jaccard's similarity coefficient was used as β-diversity (Eq. 1):

$$\beta = j/(a+b-j) \quad (1)$$

where a = abundance at past, b = abundance at present, and j = number of common species.

The ecohydrological response was simulated (Orange version 3.38.1) with multiple models including LR (Logistic Regression), RF (Random Forest), NB (Naive Bayes), kNN (k-Nearest Neighbors), NN (Neural Network), SVM (Support Vector Machine). Additionally, an ensembled model was applied, that follows the majority rule (n≥3). Model performance was evaluated by comparing α- and β-diversity between observed data and simulation results using R^2 and %error.

Results and concluding remarks

The prediction results for the Han River Basin generally showed a low %error in both α- and β-diversity, particularly for RF, NN, and the ensemble model (Figure 1a, b; R^2 = 0.735–0.981). Meanwhile, the prediction results for the target site exhibited a higher %error in both α- and β-diversity indices (Figure 1c, d). The high error in β-diversity was mainly due to its sensitivity to hydrological alterations, resulting in low j values.

Despite the differences in monitoring process, the results highlight the importance of external validation. Additionally, incorporating variables including water temperature, water quality (e.g., nitrogen, phosphorous, suspended solid), and vegetation may improve model performance.

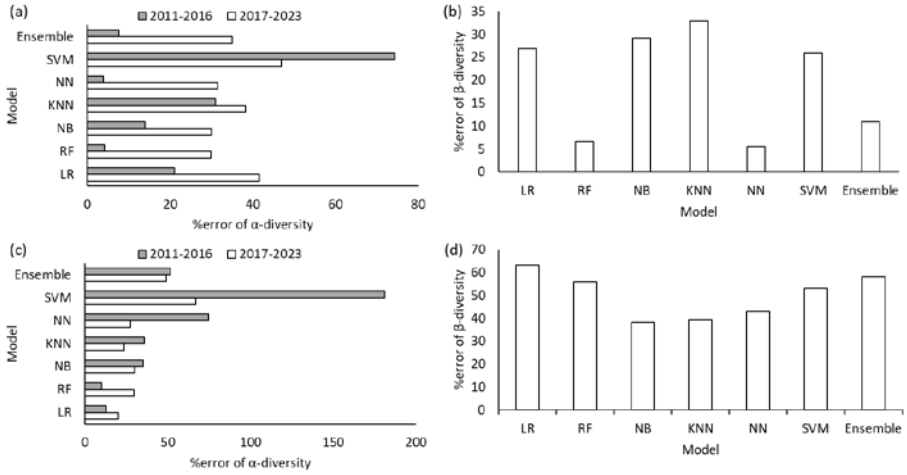


Figure 1. Comparison between predicted and observed ecological alteration: %error of (a) α-diversity in the Han River Basin; (b) β-diversity in the Han River Basin; (c) α-diversity at the target site; (d) β -diversity at the target site.

Further studies including environmental variable selection, ecohydrological response model enhancement, and enhanced citizen science collaboration will be followed (Figure 2). The framework this study proposed is anticipated to aid the management of waterfront areas and facilitate the collaboration among policy makers, scientists, and stakeholders.

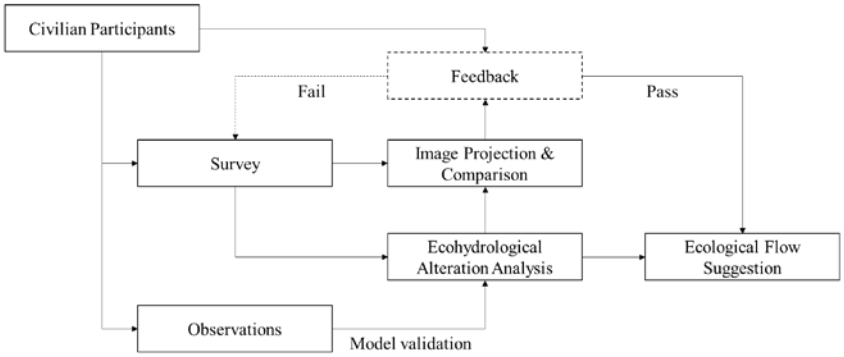


Figure 2. Detailed workflow of scientist-civilian collaboration for ecological flow determination.

Acknowledgments: This work was supported by Korea Environment Industry & Technology Institute through Climate Change R&D Project for New Climate Regime Program and Water Management Program for Drought, funded by Korea Ministry of Environment (RS-2023-00221110, RS-2022-KE002032). The authors would like to thank the Suwon Sustainable City Foundation for providing the fish monitoring data.

References

Arthington AH, Bunn SE, Poff NL, Naiman RJ (2006) The challenge of providing environmental flow rules to sustain river ecosystems. Ecological Applications 16(4): 1311-1318.

Bunn SE, Arthington AH (2002) Basic principle and ecological consequences of altered flow regimes for aquatic biodiversity. Environmental Management 30: 492-507.

Dudgeon D, Arthington AH, Gessner MO et al. (2006) Freshwater biodiversity: importance, threats, status and conservation challenges. Biological Reviews 81(2): 163-182.

Dyson M, Bergkamp M, Scanlon J (2003) Flow: The essentials of environmental flows. IUCN, Gland, Switzerland.

Lee S, Ryu M, Kim I, Choi H, Ha Y (2022) A study on river management based on the results from a survey of citizens. Journal of Korea Water Resource Association 55(2): 171-176.

Poff NL, Richter BD, Arthington AH et al. (2010) The ecological limits of hydrologic alteration (ELOHA): a new framework for developing regional environmental flow standards. Freshwater Biology 55: 147-170.

Richter BD, Baumgartner JV, Powell J, Braun DP (1996) A method for assessing hydrologic alteration within ecosystems. Conservation Biology 10(4): 1163-1174.

13th World Congress on Water Resources and Environment (EWRA 2025)
"New challenges in understanding and managing water-related risks in a changing environment"
Palermo, Italy, 24 - 28 June 2025

Estimation of wetland water balance using the WetMAT lumped model in different hydrological contexts

C. Panciera[1], I. Portoghese[2*], A. Pagano[1], R. Giordano[2]
[1] DICATECh, Politecnico di Bari, Italy
[2] Istituto di Ricerca sulle Acque del Consiglio Nazionale delle Ricerche (CNR-IRSA), Bari, Italy
* e-mail: ivan.potoghese@cnr.it

Introduction

It is nowadays evident that wetlands are subject to a progressive impoverishment and degradation that in some cases may lead to their disappearance, due to different factors including climate change and human disturbance. The increase of air temperature and reduction of precipitation are putting the conservation of wetland systems at risk. Similarly, groundwater extractions and land use changes for agricultural development poses disruptive pressure over fragile wetland environments. Given the many ecosystem services that wetlands provide such as carbon sequestration, flood prevention or climate regulation, it is necessary that wetlands are protected by guaranteeing them with the adequate amount of water they need to carry out their functions (Angeler 2021). In this regard, it is important to obtain quantitative data on the wetland hydrological regime so that effective solutions for conservation can be implemented such as monitoring, proper water management and sustainable land and water exploitation. In the frequent event of data scarcity, one solution for obtaining quantitative representation of wetland hydrological response is the use of suitable hydrological models, which can simulate water availability and environmental water requirements by incorporating key variables and processes. These kind of models may be crucial for assessing environmental inflow requirements, especially in wetlands and other water-sensitive ecosystems, providing a framework for sustainable water resource management (Lee et al. 2020).

This work presents the methodology for generalizing a lumped hydrological model named WetMAT (Panciera et al. 2024) developed for the Doñana wetland, Spain, through the parsimonious parameterization of relevant water balance and hydro-morphological processes. The model can be scaled and easily adapted to similar Mediterranean hydro-climatic contexts with different spatial extensions, thus enabling the estimation of wetland water balance signatures, especially under limited data availability.

Materials and methods

The evaluation of environmental water requirements of wetlands is a relatively underexplored topic in the literature although is recognized through the definition of the Ramsar Convention as the "adequate amount and quality of water at the right time to sustain its biodiversity and provide water-related services and benefits to people". Interannual and seasonal climate variability were adopted as main driver for the implementation of the WetMAT (Wetland MAnagement Tool) hydrological model, which allowed to describe wetland variability features such as flooding extension, depth and duration, to unable connecting the hydrological regime to water requirements needed for ecological health. The water balance model is based on daily climate data such as precipitation and evapotranspiration, and simulates natural processes contributing to flooding and drainage of plain areas. As a lumped parameters model, the flooding regimes are schematized through different and linked water balance elements such as soil profile, surface depressions, drainage network and flood surfaces. The daily time scale allows the model for a fast response when an extreme rainfall causes sudden increase of the flooded area while cascade drainage processes are represented with slow recession periods.

The WetMAT model has been developed for the Spanish case study of Doñana within the LENSES project (https://www.lenses-prima.eu/) with the aim of setting up a quantitative tool to investigate water balance fluxes and ultimately estimate the environmental water requirement of the marshland system. The Doñana wetland, one of the largest wetlands in Europe, is characterized by an extreme between-year

variability of hydrology and biodiversity due to the Mediterranean climatic regime combined with artificial drainage and levees systems. Moreover, it faces severe pressures due to agricultural activities, groundwater overexploitation, and extensive land-use changes, which led to reduced inflows to the marshland. Additionally, climate change intensified the threats to the wetland's ecological integrity, adding unpredictability to water availability and increasing habitat vulnerability (Green et al, 2016).

In a different context, a much smaller coastal wetland has been identified in which a progressive salinization is taking place due to the impoverishment of the groundwater feeding some freshwater ponds. The Torre Guaceto wetland, located along the Adriatic coast of Southern Italy, represents an extraordinary sensible ecosystem surrounded by intensive agricultural activities. The wetland inflow is sustained primarily by groundwater springs but is increasingly affected by salinization due to seawater intrusion and overextraction of groundwater for irrigation. The increasing impacts of climate change have intensified the challenge of balancing ecological preservation with human activities so that new water management strategies are under investigation that could integrate treated wastewater as a means to increase freshwater input to the wetland within the ongoing UNIVERSWATER project (https://universwater.eu/).

Results and concluding remarks

The described case studies, while sharing the common goal of estimating the environmental water requirements for coastal wetlands, appear quite different in the dominant processes that control the water balance dynamics. Starting from a detailed understanding of the climatic and physical constraints and the corresponding dynamics of flooded and ponded areas characterizing the wetland systems, the parameterization of the WetMAT model has been effectively undertaken. The scale factor is above all the distinctive feature of the a wetland system with the Doñana marshland covering approximately 300 km², whereas the Torre Guaceto marshland covers only 1.2 km². Despite this evident contrast, the soil water retention parameters are considered scale-invariant in the water balance (i.e. soil evapotranspiration and drainage), while the drainage canal network is represented though the average drainage density (km/km^2) that modulates the wetland discharge and ultimately the residence time of flowing water in the system.

Relevant differences in the hydro-geological setting required specific model adaptations as the Doñana wetland overlays an almost continuous clay layer, disconnecting the wetland from the surrounding deep aquifer, while Torre Guaceto wetland is fed by a karst brackish aquifer. This latter feature causing saline water dynamics in the wetland required a suitable representation of salt balance as a major process altering the ecological state of the entire marshland.

In both cases the WetMAT water balance modelling allowed to characterize the hydrological regimes of flooding and drainage which are particularly useful to explain the wetland response under changing climate conditions and in the case of data scarcity. The results also included robust estimates of timing and amount of wetland water requirements as quantitative information for taking active decision for environmental preservation.

Acknowledgments: The present work has been funded by the LENSES project (PRIMA Programme, GA n°2041). This paper and the content included do not represent the opinion of PRIMA Foundation, PRIMA Foundation is not responsible for any use that might be made of its content.

References

Angeler DG (2021) Conceptualizing resilience in temporary wetlands. Inland Waters 11(4): 467-475. https://doi.org/10.1080/20442041.2021.1893099

Green AJ, Bustamante J, Janss GFE, Fernández-Zamudio R, Díaz-Paniagua C (2016) Doñana Wetlands (Spain). The Wetland Book. Springer, Dordrecht. https://doi.org/10.1007/978-94-007-6173-5_139-1

Lee O, Kim HS, Kim S (2020) Hydrological simple water balance modeling for increasing geographically isolated doline wetland functions and its application to climate change. Ecological Engineering 149. https://doi.org/10.1016/j.ecoleng.2020.105812

Panciera, C., Portoghese, P, Pagano, A, Giordano, R, Nur Yesilyurt, S., Can Gunacti, M., Polat Cetinkaya, C., Onusluel Gul, S., Najar, M., Lopez, E., Bea, M. A methodological approach for supporting socio-hydrological modelling of a complex Nexus system. Proceedings of the 8th IAHR Congress, 4-7 giugno 2024, Lisbona (PT).

Key steps in the E-Flow definition under the climate change impact at the river basin scale

G. Ćosić-Flajsig[1*], B. Karleuša[2], Ivan Vučković[3], G.Volf[2]
[1] Civil Engineering Department/Zagreb University of Applied Sciences, Zagreb, Croatia
[2] Faculty of Civil Engineering/ University of Rijeka, Rijeka, Croatia
[3] Elektroprojekt Consulting Engineers Section of Ecology, Croatia
* e-mail: gcflajsig@tvz.hr

Introduction

The obligation to define the environmental flow (E-flow) in the European Water Framework Directive (EU WFD, 2000) is not explicit. The Republic of Croatia has no official methodology to define the E-flow. Integrated river basin management and good water status can be achieved if appropriate flow, sediment regimes, and related river morphology quality are guaranteed. An innovative holistic model for E-flow assessment for the present scenario was first developed and proposed in paper by Ćosić-Flajsig G. et al., 2020 (Ćosić-Flajsig G. et al., 2020) and then further developed including the impact of climate change by different scenarios (Ćosić-Flajsig G. et al., 2024), for the case study of transboundary Sutla River basin (between Slovenia and Croatia). This research aims to determine the impact of climate change on the E-flow by modelling low flows, sediment, total N, and total P under eight future climate change scenarios, using Indicators of Hydrological Alterations (IHAs) and biological indicators for the Sutla River downstream of the dam Vonarje.

Materials and methods

The proposed methodology and key steps of E-flow assessment under the climate change impacts for present scenario and future climate change impact scenarios are presented in Figure 1 for the Sutla River basin case study as the modified methodology developed by Gopal in (Gopal B., 2013). The key steps of the holistic approach E-flow assessment for future climate change impact scenarios are: (1) analyses of river basin pressures under climate change impact by SWAT model, (2) program of basic and supplementary measures, (3) hydrological analysis and abiotic factors, and (4) biological research.

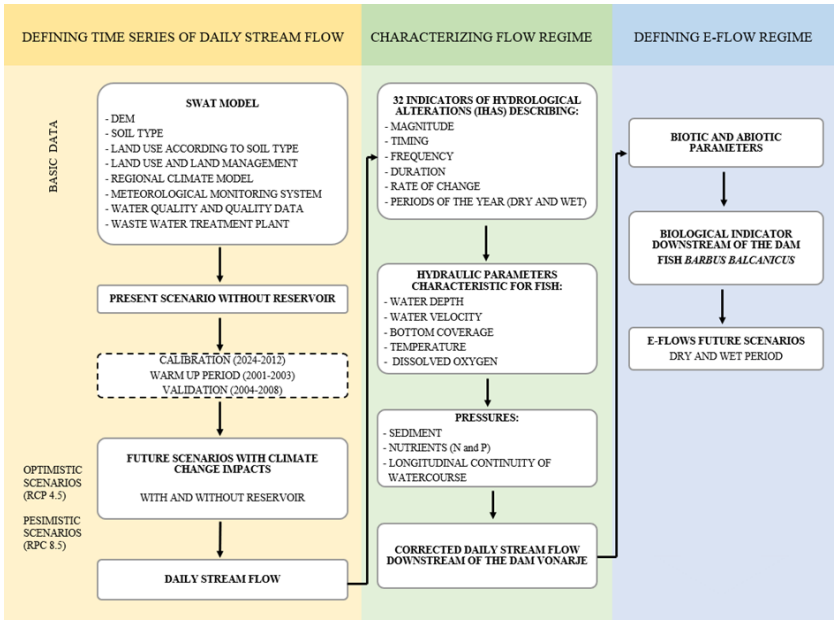
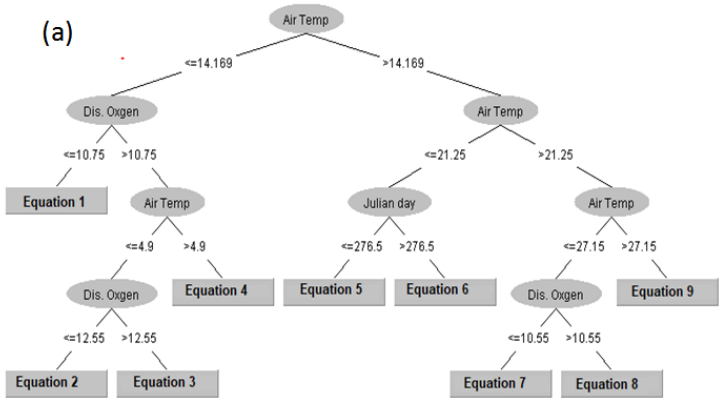


Figure 1. Methodology and key steps of a holistic approach to the assessment of E-flow for present scenario and future climate change impact scenarios (modified methodology from Gopal, 2013)

Specific average daily flow modelling results of the eight future climate change impact scenarios for the six dynamically downscaled regional climate models (RCMs), CCLM4 (drivModel: CNRM-CERFACS-CNRM-CM5), CCLM4 (drivModel: MPI-M-MPI-ESM-LR), HIRHAM5, INERIS, RACMO22E and RCA4) downstream of Vonarje dam for SUBBASIN 2 are: $Q_{av,month}$ (m^3/s); $Q_{av,month}$ (m^3/s) for dry period (April - September); $Q_{av,month}$ (m^3/s) for wet period (October - March) (Ćosić-Flajsig et al.,2024). Since water temperature is a primary abiotic factor, the water temperature model was created using the machine learning tool Weka to calculate water temperature based on air temperature, physical-chemical indicators, abiotic and biological indicators for future scenarios. The velocity forecast was based on forecasted flows, associated values of limited water levels, and the watercourse cross-section at the Zelenjak gauging station on the Sutla River in 2024. Special attention is focused on the fish bioindicators, *Barbus barbus* - barbel, species inhabiting the water course's middle part. The key abiotic factors important for the life stage spawning of the selected indicator fish species are water depth - greater than body height 20 – 45 cm, water velocity 35 – 50 cm/s, water temperature 4 - 17 (14) °C and dissolved oxygen above 6 mg/l (Mrakovčić M., 2000). The machine learning algorithm M5P for induction of model trees integrated in the Weka modelling software was used. Water temperature was set as a target (dependent) variable for building the model, whereas Julian day, air temperature, total suspended solids, total N, total P, dissolved oxygen, water level, flow and water velocity were set as independent variables (descriptors) from which the water temperature was modelled. The above parameters were mainly used because they best represent the parts of the modelled system on top of which the target variable relays.

Results and concluding remarks

Based on conducted analyses, model presented on Figure 2a was obtained. The results show that the obtained correlation coefficient (R) for the model is relatively high (0,953) and can be used for modeling purposes. Model of water temperature is composed of nine leaves, where each leave contains an equation for calculation of water temperature (Figure 2b). From the Weka model tree and equations can be concluded that water temperature mainly depends on parameters such as air temperature, dissolved oxygen and Julian day, and will be possible to define water temperature from air temperature for future scenarios under climate change impact based on this Weka model tree, which is necessary for assessing the E-flow.



(b)

Equation number	Equation
1.	Water Temp = 0.1322 * Air Temp - 0.3111 * Dis. Oxgen + 12.5546
2.	Water Temp = 0.136 * Air Temp - 0.4742 * Dis. Oxgen + 10.3094
3.	Water Temp = 0.136 * Air Temp - 0.4822 * Dis. Oxgen + 9.2411
4.	Water Temp = 0.1467 * Air Temp - 0.316 * Dis. Oxgen + 9.7317
5.	Water Temp = 0.138 * Air Temp - 0.2103 * Dis. Oxgen + 15.0872
6.	Water Temp = 0.138 * Air Temp - 0.2103 * Dis. Oxgen + 13.2791
7.	Water Temp = 0.1912 * Air Temp - 0.429 * Dis. Oxgen + 19.3492
8.	Water Temp = 0.1912 * Air Temp - 0.6061 * Dis. Oxgen + 19.5212
9.	Water Temp = 0.303 * Air Temp - 0.4584 * Dis. Oxgen + 17.9846

Figure 2. (a) Weka model tree for water temperature and (b) corresponding equations

Acknowledgements: This work has been fully supported by the University of Rijeka projects 23-67 and 23-74.

References

Ćosić-Flajsig, G., Vučković, I., Karleuša, B. (2020) An Innovative Holistic Approach to an E-flow Assessment Model, Civil Engineering Journal, 6, 11, 2188-2202, doi: 10.28991/cej-2020-03091611

Ćosić-Flajsig G., Karleuša B., Vučković I., Glavan M. (2024) E- flow Holistic Assessment in Data-limited River Basin under Climate Change Impact, Proceedings of WMHE 2024, Štrbské Pleso, High Tatras, Slovakia

European Parliament and Council (2000) EU WFD, Directive 2000/60/, European union: Maastricht, The Netherlands

Gopal B. (2013) Methodologies for the Assessment of Environmental Flows, Environmental Science, Chapter 6, Corpus ID: 30973406

Mrakovčić, M. (2000) Criteria for determining sustainable flow based on fish communities, Documentation Elektroprojekt d.d. Zagreb

A simulation-based study on the effect of bed topography on wetland performance

A. Bottacin-Busolin[1*], G. Santovito[2], A. Marion[1]
[1] Departmentof Industrial Engineering, University of Padova, Padova, Italy
[2] Department of Biology, University of Padova, Padova, Italy
* e-mail: andrea.bottacinbusolin@unipd.it

Introduction

Free water surface wetlands can be effective solutions for treatment of stormwater and agricultural runoff as well as municipal and industrial wastewaters. The removal of contaminants in these systems is controlled by natural biochemical processes, but is also fundamentally influenced by hydrodynamic processes where bed topography can play a critical role alongside vegetation.

Traditional modelling techniques like the tanks-in-series models have been widely adopted to predict wetland performance, but may not be acceptably accurate for highly heterogenous systems. Two-dimensional depth-averaged models can provide a more accurate representation of wetlands as long as bed topography and vegetation distribution are described with sufficiently high spatial resolution.

To gain a better understanding of how bed topography affects wetland performance, we performed numerical simulations of synthetic wetlands with heterogeneous bed topographies, and evaluated their hydraulic performance and contaminant removal efficiency as a function of the statistical parameters that characterize bed topography.

Materials and methods

A two-dimensional depth-averaged numerical model was used to simulate steady-state flow hydrodynamics and mass transport in a 90 m long and 40 m wide rectangular wetland, with a centrally aligned inlet-outlet configuration, and inlet-outlet widths of 5 m (Figure 1). In the simulations, we imposed a discharge Q = 3.5 L/s and set the water depth at the outlet to 0.5 m, equal to the mean water depth H, so that the mean residence time was approximately 6 days in all simulations. We considered a uniform Manning's coefficient M = 0.025 s/m$^{1/3}$ for bed friction, and a uniform vegetation density of 2000 stems/m^2. Vegetation drag is represented in the model as in the work of Sabokrouhiyeh et al. (2020).

A pseudo-random correlated field generator (Bellin and Rubin, 1996) was used to generate Gaussian random fields of bed elevation with given mean μ_b = 0 m, standard deviation σ_b, and correlation length l_c. Simulations were performed with σ_b ranging from 0 to 0.4 m, i.e., from 0 to 0.8 times the average water depth H, and l_c ranging from 0.05 to 0.20 times the longitudinal size of the wetland.

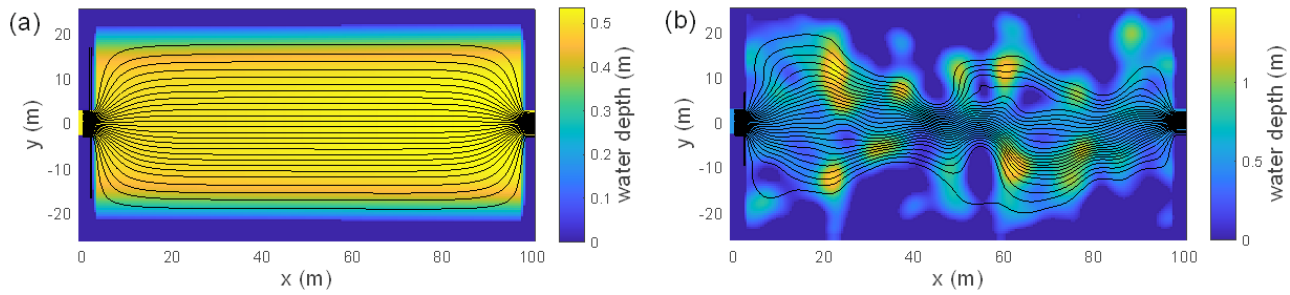


Figure 1. Bathymetric maps and simulated streamlines for (a) σ_b = 0 m and (b) σ_b = 0.4 m.

By simulating the transport of a passive tracer for a constant normalized concentration at the inlet, C/C_0 = 1, we derived the water residence time distributions in the wetlands, which were then used to evaluate the hydraulic efficiencies, λ, according to the definition of Persson et al. (1999).

Results and concluding remarks

Results show that as the variance of water depth increases, so does the variance of the residence time, resulting in a decrease of the wetland hydraulic efficiency (Figure 2). The variability of hydraulic efficiency across topographies with the same statistical parameters also increases, indicating that the hydraulic performance can vary over a broader range as bed topography becomes more heterogenous. An increase in the correlation length was found to reduce the variance of the residence time and its dispersion around the mean. This is due to the formation of more complex flow patterns for smaller correlation lengths, characterized by the presence of lateral dead zones and internal islands.

The relationship between the variability of water depth and contaminant removal efficiency was also investigated by considering a non-zero reaction rate in the mass transport model. While the mean values of removal efficiency showed relatively small variations for wetlands with non-uniform bed elevation compared to the uniform case, greater variability of removal efficiency was found for higher variances of bed elevation, with differences in excess of 20% for the more heterogeneous topographies.

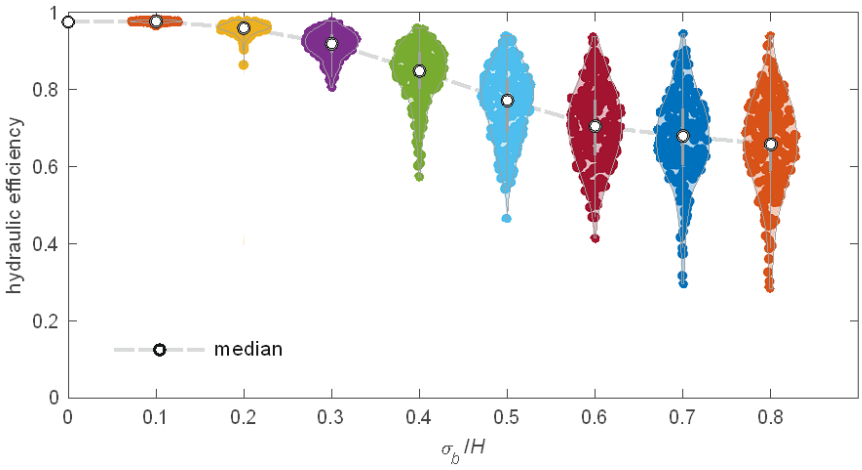


Figure 2. Hydraulic efficiency, λ, as a function of normalized standard deviation of bed elevation, σ_b/H.

The findings underscore that bed topography can considerably impact the performance of constructed wetlands, and warrant further investigation into its implications for designing effective wastewater treatment systems. By incorporating diverse bathymetric features, wetlands can be engineered to enhance residence time distribution and optimize contaminant removal efficiency, ultimately contributing to more effective and robust solutions for water treatment.

Acknowledgments: This study was carried out within the RETURN Extended Partnership and received funding from the European Union Next-GenerationEU (National Recovery and Resilience Plan – NRRP, Mission 4, Component 2, Investment 1.3 – D.D. 1243 2/8/2022, PE0000005, CUP D43C22003030002).

References

Bellin A, Rubin Y (1996) HYDRO_GEN: A Spatially Distributed Random Field Generator for Correlated Properties. Stochastic Hydrol. Hydraul. 10 (4): 253–278. https://doi.org/10.1007/BF01581869.

Persson J, Somes NLG, Wong THF (1999) Hydraulics Efficiency of Constructed Wetlands and Ponds. Water Science and Technology 40 (3): 291–300. https://doi.org/10.1016/S0273-1223(99)00448-5.

Sabokrouhiyeh N, Bottacin-Busolin A, Tregnaghi M, Nepf H, Marion A (2020) Variation in Contaminant Removal Efficiency in Free-Water Surface Wetlands with Heterogeneous Vegetation Density. Ecological Engineering 143: 105662. https://doi.org/10.1016/j.ecoleng.2019.105662.

Framing the Nature Based Solutions (NBS) in Lake Karla (Thessaly, Greece): What's the status after the storm Daniel disaster?

I. Kagalou, I. Vergos, D. Latinopoulos*
Department of Civil Engineering/School of Engineering, Democritus University of Thrace, Xanthi, Greece
** e-mail: dlatinop@civil.duth.gr*

Introduction

The twentieth century brought some notable successes in freshwater restoration (Poikane et al. 2024). According to the European Commission "*Nature-based solutions are innovations inspired and supported by nature, which are cost-effective, simultaneously provide environmental, social and economic benefits and help build resilience. They bring more, and more diverse, nature and natural features and processes into cities, landscapes and seascapes, through locally adapted, resource-efficient and systemic interventions. Nature-based solutions must benefit biodiversity and support the delivery of a range of ecosystem services*." (EC, 2023). In "water management" there is a varied concept of what actions are "NBS" such as green or blue interventions, environmental engineering projects and socio-ecological projects. Depending on their environmental intervention, NBS are classified into three types (Eggermont et al., 2015), resulting in different approaches to environmental problems and results that they can achieve also adopted by the EU.

In Greece, few such NBS measures exist, with lake Karla being considered as one such example (Panagopoulos and Dimitriou 2020). The aim of the present paper is to identify the NBS favoured over the grey solutions and to evaluate their effectiveness to address a range of challenges. Due to the high importance of the Lake Karla project per se, but also due to the catastrophic Daniel flash flood event (September 2023) that affected the basin, a secondary aim is to assess the operational works' status after the meteorological disaster.

Materials and methods

Study Area: Lake Karla is located on the lower part of the Thessaly plain. Historically, before its drying, it received surface runoff from the watershed and floodwaters of the Pinios River supplying the lake with large freshwater quantities. The structure and function of new Lake Karla is intimately linked with Pinios.

NBS analytical framework: To cope with the NBS indexing and their effectiveness in Lake Karla, a series of steps took place: a) the creation of a water-related indicator database from previous studies and research documents, b) the formation of a conceptual matrix linking challenges, objectives, operational works, solution type assessment (according to White et al. 2021 and Pistocchi 2022), limiting factors, indicators and values to see if challenges were met.

Daniel effect: To depict the devastation, Copernicus images were used to address the flood magnitude and pinpoint the operational works affected. Then two study visits (2/10/2023 and 19/11/2023) were coupled with experts' (academic, regional authority and management body) informal interviews. The damage assessment was done using a simple five scale grading (5-destroyed, 1-not affected).

Results and concluding remarks

Historical overview on major events showed hydrological related issues since 2012 and particularly, operational works (ditches, collectors, pumping stations) malfunctions or destructions appear since 2018 in almost all severe meteorological phenomena (i.e., Ianos, Daniel, Elias). The damages were estimated by the Hellenic government (Arogi.gov.gr) to be around 4 billion euros affecting more than 6,000 individuals. Proper hydraulic works (inflow or outflow) operation in such regulated lakes like Karla is of prime importance for proper system functioning and service provisioning (White et al. 2021). The challenges that were addressed are: irrigation, groundwater depletion, water storage, flood resilience, surface water

quality, habitat degradation and biodiversity preservation, cultural and leisure opportunities, sustainable food production and green growth (Figure 1). Coming to applied solution types for these challenges, of the 25 operational works identified, only 10 of them fitted with the concept of Natural solutions (the majority of them are NBS type 3; novel ecosystem creation). The rest of the solutions are hybrid or technological. All solutions were related to their limiting factors, revealing mostly biophysical and technological constraints. To see the effect of these management actions, a total number of 39 indicators formed a matrix comparing values before and after restoration (Figure 1). Of the recognized challenges, only water quality and sustainable food production systems have not responded (20%), while all the rest are partly or fully solved.

Challenges	Criterion/objective	Management action / operational work	Solution type	Limiting factor	Indicators	Before re operation	After restoration	Reference	Response
Irrigation	agricultural water abstractions	Inflow by Pinios	Hybrid	financial, technological (energy)	volume for irrigation needs	0	12 hm3	Spiliotis et al., 2022	
		Pumping stations	Technological	financial, technological (energy)	WEI	n/a	>0,73 (fresh) & 2.1 (groundwater) (data from adjacent basin)	Lyra et al., 2021	Yes
		Ditches (gravitational)	Technical	biophysical, technological	ditch capacity	0	34,4 hm3/y	masterplan	
Groundwater depletion	aquifer recharge	Re-construction of the reservoir	Natural (NBS type 2)	biophysical	depth to groundwater	heads > 50m	heads <35m	Tziatzios et al., 2021	Yes
				infiltration	Water balance	Negative (~300 hm^3)	Negative (~200hm^3)	Tziatzios et al., 2022	
Water storage	seasonal water needs	Lake	Hybrid (NBS type 3)	biophysical	level (max-ave)	n/a	(50-46,45) m	EKBY	Yes
					storage volume (max-ave)	n/a	(42,74-28,42) hm^3	Loukas et al., 2015	
Water quality	Achievement of GEP (WFD)	Riparian buffer zones (phytoremediation)	Natural (NBS type 2)	biophysical	decline from GEP	n/a	bad ecological status	Gkelis et al., 2017	
	good chemical status	Artificial wetland	Hybrid (NBS type 3)	biophysical, technological (energy)	decline from good chemical status	n/a	poor chemical status	RBMP 2nd rev	No
		Planting / forestation	Natural (NBS type 2)	biophysical	plantings	n/a	1,82 km	masterplan & Management Body	
Habitats degadation	conservation status	Re-creation of the wetland	Natural (NBS 2 & 3)	biophysical	Birds diversity (No of species)	32	200	NATIONAL INDEX OF Agricult. Species Nerco 2021	
Biodiversity preservation	protection status	Management policy	Natural (NBS type 1)	human-social	protection routine, legislation	n/a	SPA: 409km2 , SCI 237 km2	Management Body	Yes (partly)
		Fish & bird breeding sites	Hybrid (NBS type 2)	biophysical	bird islets, fish breeding sites	n/a	>1,19 km2	masterplan & Management Body	

Figure 1. Fraction of the conceptual matrix.

Depicting the current state after Daniel effect, in total, 17 damaged operational works were assessed with expert opinion. Of those, 7 were deemed as partly or totally destroyed (grade 4 and 5) and 6 were graded as temporary disabled (3) causing extra economic burden in the entire area affecting natural processes (i.e., bioremediation, filtration, erosion and biodiversity). Even though the basic concept of the Lake Karla project can be recognized as “a nature-based approach”, there are some bottlenecks limiting its characterization entirely as NBS. Despite this, there is adequate knowledge on the lake system’s most important attributes, the design and implementation of measures cannot be characterized by sustainability (several constraints) or endurance to withstand severe meteorological phenomena. Acknowledging that investment is needed for any kind of operational works and the NBS advantage in providing co-benefits, it remains to be seen which type of management solutions (grey or NBS based) will be ultimately selected in order to serve the multitude of challenges.

References

Eggermont H, Balian E, Azevedo JMN, […] Le Roux X (2015) Nature-based solutions: new influence for environmental management and research in Europe. GAIA-Ecological perspectives for science and society, 24(4), 243-248. https://doi.org/10.14512/gaia.24.4.9

European Commission: European Research Executive Agency, Nature-based solutions – EU-funded NBS research projects tackle the climate and biodiversity crisis, Publications Office of the European Union, 2024, https://data.europa.eu/doi/10.2848/8542246

Pistocchi A (2022) Nature-based solutions for agricultural water management. European Commission, Joint Research Centre (JRC). https://doi.org/10.2760/343927

Poikane S, Kell, MG, Free G, […] Irvine K (2024) A global assessment of lake restoration in practice: New insights and future perspectives. Ecological Indicators, 158, 111330. https://doi.org/10.1016/j.ecolind.2023.111330

White C, Collier MJ, Stout JC (2021) Using ecosystem services to measure the degree to which a solution is nature-based. Ecosystem Services, 50, 101330. https://doi.org/10.1016/j.ecoser.2021.101330

A novel framework to assess the hydrological connectivity of lake wetlands in plain river networks with dense hydraulic facilities

S. Yang, R. Wan*, G. Yang, B. Li
Nanjing Institute of Geography and Limnology, Chinese Academy of Sciences, Nanjing, China
** e-mail: rrwan@126.com*

Introduction

Global hydrological connectivity has undergone drastic changes in recent years because of anthropogenic interruptions, such as constructing dams or sluices to irrigate farmland, resist flooding and block the spread of pollutants. Thus, the internal hydrobiological cycle of natural river ecosystems has been disrupted (Tockner and Stanford, 2002; Duarte et al., 2021).Therefore, it is crucial to evaluate the degree of hydrological connectivity in the context of the prevalent dam and sluice construction as it significantly changed the natural flow of rivers and further changed the hydrological connectivity.

The Taihu Lake Basin, situated in the Yangtze River Delta region, hosts a dense and complex network of rivers and lake wetlands (Yang et al., 2023). The river network in the Taihu Lake Basin is profoundly disturbed by hydraulic facilities and other man-made disturbances, the setting of sluices, dams and pumping stations and their scheduling rules largely determined the extent of hydrological connectivity. Hence, the influence of sluices on the evaluation should not be neglected. However, studies considering water gates, dams and pumping stations and their scheduling regulations in the hydrological connectivity evaluation methods are still limited. In this study, we innovatively propose a new comprehensive framework based on graph theory at different spatial scales ('site scale–region scale–landscape scale') to quantitatively assess the centennial changes in hydrological connectivity of lake wetlands in a plain river network area with dense hydraulic facilities (Yang et al., 2024).

Materials and methods

We used historical maps from the 1910s and Gaofen-1 satellite images from 2019 to extract lake wetlands extent and river networks. Hydraulic facilities, such as sluices, pumping stations and levees, were acquired from the third national survey data in 2019, as they were significant factors affecting the connectivity amongst lake wetlands. The historical maps were obtained from Lake-Basin Science Data Center, Nanjing Institute of Geography and Limnology, Chinese Academy of Sciences.

By generalising lake wetlands into patches and rivers into edges, a river topological network connecting lake wetlands was constructed based on graph theory, and connectivity indices were calculated through three dimensions: individual patches - inter-patches - and study area, respectively.

The connectivity probability of a single lake wetland patch was calculated based on the number and types of hydraulic facilities surrounding it. This probability also reflects the degree to which a lake wetland patch is subject to hydraulic engineering control and can be regarded as the intrinsic attribute of the patch. We extracted the shortest river path connecting each lake wetland as the maximum hydrological connectivity probability P*ij* between them to simply the extraction process, as the river connections among lake wetland are complex and annular. Finally, we assessed the overall hydrological connectivity of the region using the Conefor tool (http://conefor.org/coneforsensinode.html) (Saura and Torne, 2009).

Results and concluding remarks

Using detailed historical topographic maps and high-resolution satellite data, this new framework, combining graph theory and connectivity indices, is applied to a river–lake wetlands district with dense sluices/pumping stations in eastern China (Figure 1). Results show that (1) Although the number of lake wetlands remained relatively stable over the past century, the average area decreased by 18.44%, and the

density of hydraulic engineering boomed to 2.2 / km2. (2) The increases in hydraulic facilities and the decrease in lake wetlands areas significantly reduced the degree of hydrological connectivity, with the overall connectivity value decreasing from 0.97 in the 1910s to 0.45 in 2019. (3) The importance of the same lake wetlands patch has progressively heightened in the last hundred years.

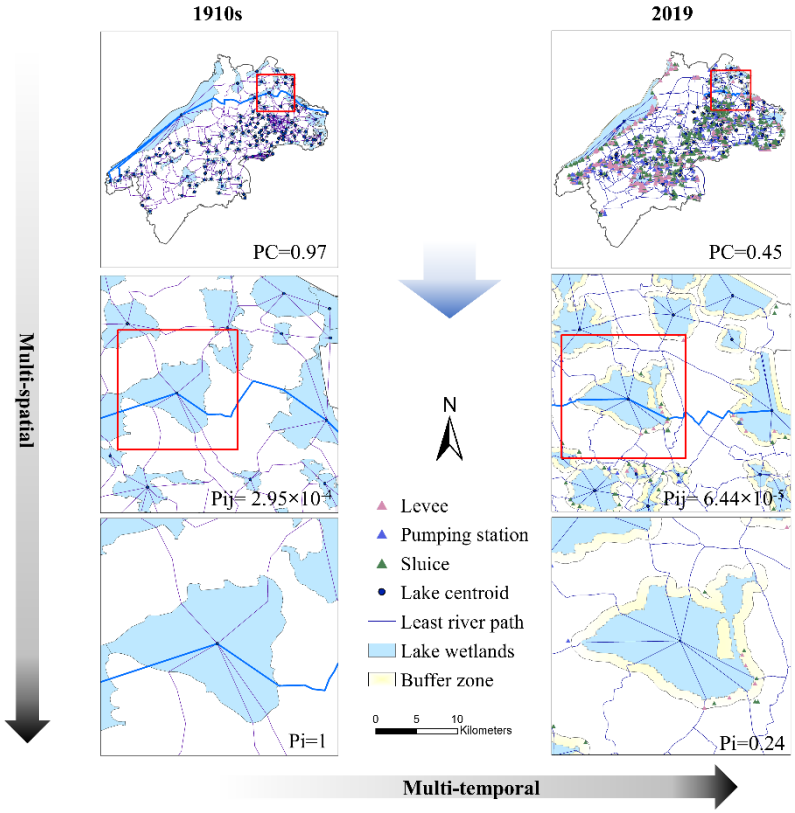


Figure 1. Changes in hydrological connectivity index at different spatial scales in the 1910s and 2019.

Our findings indicate a severe decline in hydrological connectivity (PC) in Wujiang District over the past century, from 0.97 in the 1910s to 0.45 in 2019. This widespread loss of hydrological connectivity can be attributed to a significant increase in the number of hydraulic facilities, including sluices, levees, and pumping stations, which have greatly impeded water flow in rivers among different lake wetlands, in addition to the rules and regulations that govern them.

Acknowledgments: This research received financial support from the National Key Research and Development Program of China (No.2022YFC3204100), and the National Natural Science Foundation of China (Grant No. 42071146).

References

Duarte G, Segurado P, Haidvogl G, Pont D, Ferreira M T & Branco P(2021). Damn those damn dams: Fluvial longitudinal connectivity impairment for European diadromous fish throughout the 20th century. Science of the Total Environment 761, 143293.

Saura S & Torné J (2009). Conefor Sensinode 2.2: a software package for quantifying the importance of habitat patches for landscape connectivity. Environmental Modelling & Software 24, 135-139.

Tockner K & Stanford J A(2002). Riverine flood plains: present state and future trends. Environmental Conservation 29(3), 308-330.

Yang S, Wan R, Yang G, Li B & Dong L (2023). Combining historical maps and landsat images to delineate the centennial-scale changes of lake wetlands in Taihu Lake Basin, China. Journal of Environmental Management 329, 117110.

Yang S, Wan, Yang G, Li B (2024). A novel framework to assess the hydrological connectivity of lake wetlands in plain river networks with dense hydraulic facilities: Comparing natural and disturbed states over a century. Journal of Hydrology, 630,130787.

XVI. Water Resources in Natural Ecosystems: Monitoring, Modelling, and Conserving Biodiversity

13th World Congress on Water Resources and Environment (EWRA 2025)
"New challenges in understanding and managing water-related risks in a changing environment"
Palermo, Italy, 24 - 28 June 2025

Comparing hydrologic models for improved discharge simulations in regional earth system models for the Euro-Mediterranean region

M. Hamitouche[1,2*], G. Fosser[1], A. Anav[2]
[1] University School for Advanced Studies IUSS, Pavia, Italy
[2] ENEA - Agenzia nazionale per le nuove tecnologie, l'energia e lo sviluppo economico sostenibile, Italy
* e-mail: mohamed.hamitouche@iusspavia.it

Introduction

River discharge is a critical component of the hydrological cycle, linking terrestrial water processes with ocean circulation and influencing regional climate dynamics. In the Mediterranean region, it plays a pivotal role in the water budget, affecting sea-level changes, ocean salinity, and nutrient transport. Accurate discharge estimation is essential for maintaining the salinity balance and predicting hydrodynamic behaviour, particularly as disruptions could impact ecosystems and coastal communities. Despite the advances in regional Earth System Models (ESMs) like ENEA-REG (Anav et al. 2021) and MESMAR (Storto et al. 2023), which integrate atmospheric, oceanic, and land processes, challenges persist. The Hydrological Discharge (HD) river routing model (Hagemann et al. 2020) used within ENEA-REG and other ESMs tends to underestimate freshwater input from river runoff, limiting its predictive accuracy. Enhanced models that better represent regional hydrological dynamics are then needed to address these limitations and improve discharge simulations into the Mediterranean Sea.

This study evaluates the performance of two large-scale hydrological models, CaMa-Flood (Yamazaki et al. 2013) and WRF-Hydro (Gochis et al. 2020), to simulate river discharge into the Mediterranean Sea. Besides the advantage of WRF-Hydro's possibility to be coupled in two ways to the atmospheric WRF model, it overcomes the limitations of CaMa-Flood by incorporating advanced routing dynamics, including subsurface-flow routing and spatially variable channel roughness. This study aims to assess whether these improvements lead to better discharge predictions and to evaluate the extent to which calibration enhances discharge predictions compared to non-calibrated simulations in both models.

Materials and methods

Meteorological forcing for this study was derived by downscaling ERA5 reanalysis data at a spatial resolution of 12 km over the Med-CORDEX domain using the WRF model. Runoff and meteorological variables, including incoming shortwave and longwave radiation, specific humidity, air temperature, surface pressure, near-surface wind, and precipitation rate, were generated at a 6-hourly time step. These outputs were interpolated and respectively used to force CaMa-Flood and WRF-Hydro in an uncoupled mode. Both models simulated river discharge at a spatial resolution of 3 minutes (~ 6 km) and at a daily time scale for the period 1990–2014, following a 5-year spin-up (1985–1989).

The simulated river discharge was validated against observed discharge records obtained from the Global Runoff Data Centre (GRDC) for key Mediterranean river basins, including the Rhone, Ebro, Po, Tiber, Arno, Maritsa, Ceyhan, Goeksu, and Kopru, as well as the Danube River, which drains into the Black Sea. The performances of the simulations were evaluated using a range of metrics: Kling-Gupta Efficiency (KGE), correlation coefficient (Pearson's rho: r_s), relative standard deviation (rSD), overall bias (Pbias), low-flow bias (Pbias_LF), and high-flow bias (Pbias_HF).

In addition to simulations with default parameters, WRF-Hydro was calibrated for each river basin to improve discharge simulations. A total of 16 parameters related to soil properties (bexp, smcmax, dksat, rsurfexp), runoff processes (refkdt, slope, retdeprtfac, lksatfac, ovroughrtfac), groundwater dynamics (zmax, expon, coeff), and vegetation behavior (cwpvt, vcmx25, mp, hvt) were calibrated using an iterative Dynamically Dimensioned Search (DDS) approach. The calibration involved 350 iterations of a 5-year simulation cycle, with a 1-year spin-up at each iteration, optimizing the KGE metric as the objective

function.

Finally, discharge simulation performances from CaMa-Flood and WRF-Hydro, both with default parameters, were compared against those from the calibrated WRF-Hydro.

Results and concluding remarks

The comparison between WRF-Hydro and CaMa-Flood revealed generally similar performance across most basins, with both models showing comparable non-linear correlations and relative standard deviations. WRF-Hydro demonstrated a slight improvement in terms of Kling-Gupta Efficiency (KGE), and it notably outperformed CaMa-Flood in terms of overall and high-flow bias (Table 1).

Table 1. Model performance metrics for each river basin

River basin	CaMa-Flood						WRF-Hydro (default parameters)					
	KGE	r_s	rSD	Pbias (%)	Pbias_LF (%)	Pbias_HF (%)	KGE	r_s	rSD	Pbias (%)	Pbias_LF (%)	Pbias_HF (%)
Danube	0.50	0.54	0.95	-26.1	-17.3	-14.6	0.46	0.83	1.47	-17.1	-16.7	34.8
Ebro	0.17	0.66	1.59	48.3	02.8	33.1	0.46	0.65	1.32	27.4	-01.4	12.4
Rhone	0.55	0.64	0.95	-14.8	-10.0	-24.8	0.54	0.61	0.97	-08.5	-08.9	-20.3
Po	0.43	0.68	0.76	-32.7	-18.1	-45.0	0.60	0.63	0.96	-17.7	-16.3	-21.4
Arno	0.31	0.76	0.58	-26.6	-02.6	-48.2	0.45	0.75	0.83	19.4	14.4	-23.4
Tiber	0.06	0.51	0.70	-63.0	-23.2	-42.9	0.02	0.45	0.69	-64.2	-42.0	-43.7
Maritsa	0.45	0.61	0.78	-27.5	-15.0	-34.1	0.49	0.54	1.27	-04.0	-21.6	22.8
Ceyhan	0.32	0.45	0.93	-48.3	-27.8	-34.9	0.24	0.41	1.45	-35.4	-35.6	20.1
Goeksu	0.61	0.81	1.10	-22.8	-24.0	-07.9	0.35	0.68	0.75	-48.3	-35.1	-34.0
Kopru	0.15	0.79	0.61	-69.0	-34.0	-52.0	0.06	0.80	0.52	-70.3	-44.7	-59.8

Calibration results showed that, only for 3 out of 10 basins, the default parameter values yielded better performance. However, in the remaining basins, calibration led to a substantial improvement of approximately 80% in KGE, primarily driven by reductions in flow variability. These findings highlight the importance of routing model selection for accurate discharge simulations in Mediterranean regional-scale Earth System Models (Med-CORDEX), and underscore the critical role of calibration in improving flow variability performance and overall discharge prediction accuracy.

Acknowledgments: This research was conducted as part of the Italian PhD program in Sustainable Development and Climate Change (www.phd-sdc.it) at IUSS Pavia and developed under the “Dipartimento di Eccellenza 2023–2027” project. It was financially supported by the ICSC Italian Research Center on High-Performance Computing, Big Data, and Quantum Computing, funded by the European Union's Next-GenerationEU program (NRRP, Mission 4, Component 2, Investment 1.4, CN00000013). Additional support was provided by the CIHEAM Prize for the Best MSc Thesis 2022.

References

Anav A, Carillo A, Palma M, Struglia MV, Turuncoglu UU, Sannino G (2021) The ENEA-REG system (v1.0), a multi-component regional Earth system model: sensitivity to different atmospheric components over the Med-CORDEX (Coordinated Regional Climate Downscaling Experiment) region. Geoscientific Model Development 14(7): 4159-4185. https://doi.org/10.5194/gmd-14-4159-2021

Gochis DJ, Barlage M, Cabell R, Casali M, Dugger A, FitzGerald K, McAllister M, McCreight J, RafieeiNasab A, Read L, Sampson K, Yates D, Zhang Y (2020) The WRF-Hydro® modeling system technical description, (Version 5.2.0). NCAR Technical Note. 108 pages. Available online.

Hagemann S, Stacke T, Ho-Hagemann H (2020) High resolution discharge simulations over Europe and the Baltic Sea catchment. Frontiers in Earth Science 8(12). https://doi.org/10.3389/feart.2020.00012

Storto A, Hesham Essa Y, de Toma V, Anav A, Sannino G, Santoleri R, Yang C (2023) MESMAR v1: a new regional coupled climate model for downscaling, predictability, and data assimilation studies in the Mediterranean region. Geoscientific Model Development 16: 4811–4833. https://doi.org/10.5194/gmd-16-4811-2023

Yamazaki D, de Almeida GAM, Bates PD (2013) Improving computational efficiency in global river models by implementing the local inertial flow equation and a vector-based river network map. Water Resources Research 49(11): 7221–7235. https://doi.org/10.1002/wrcr.20552

Spatio-temporal changes of littoral macrophytes along hydrological conditions in Yliki, a Greek lake

E. Mavromati*, V. Giourieva, D. Papadimos, A. Apostolakis, V. Tsiaoussi
The Goulandris Natural History Museum, Greek Biotope/Wetland Centre, 14th km Thessaloniki - Mihaniona, 57001 Thermi, Greece
** e-mail: emavromati@ekby.gr*

Introduction

Human-induced changes in hydrological conditions seem to be among the main factors affecting ecological relationships in lakes (Zhao et al., 2021). Water level fluctuation (WLF), which is often attributed to anthropogenic activities and its amplitude variations can have an impact on aquatic plant communities by altering several key environmental factors (Hill et al., 1998, Zhao et al., 2021). These fluctuations influence water depth, underwater irradiance, water quality, and dissolved oxygen levels, all of which play crucial roles in the growth and survival of macrophytes (Li et al., 2017). The interplay of these factors can significantly change the growing conditions for several macrophyte species over time. To overcome this, macrophytes have evolved to adjust gradually to periodic WLF over time, as part of their long-term evolutionary process (Zhao et al., 2021).

The aims of the study are to present the results of WLF over time in Lake Yliki, study its aquatic plant community and explore the effect of WLFs on macrophytes.

Materials and methods

Lake Yliki is a natural lake, located in the district of Viotia, Greece. It is integrated into the water supply system of Athens to address the increased water consumption demands due to the population growth in the Attica region. The Athens Water Supply and Sewerage Company (EYDAP) provided recordings of lake's Yliki water level (a.m.s.l) at a monthly time step, from 1/1/2007 to 31/12/2023.

Macrophyte samplings were conducted in 20 transects located along the lake perimeter, up to the maximum colonization depth of macrophytes during years 2014, 2017, 2020 and 2023, following the methodology described in Zervas et al. (2018). Macrophyte diversity and taxonomic metrics were calculated for each sampling campaign and depth range. The direct relationship between life forms of macrophytes and environmental data (WLF, lake size and mean depth) was explored by Redundancy analysis (RDA) using plots with type II scaling, focusing on the response variables. All statistical analyses were performed in R environment version 4.4.1 (R Core Team, 2024).

Results and concluding remarks

The inter-annual fluctuation of the lake's water level is shown in Figure 1. The fluctuating amplitude during the years of sampling (2014-2023) was 10.77m, with the maximum value recorded at 1/3/2019 (79.47m) and the minimum at 1/11/2017 (68.7m).

Macrophyte taxa richness showed a decreasing trend in median values with increasing sampling depth (Figure 2), which was confirmed by the statistically significant difference of average taxa richness across different sampling depths ($F(3) = 3.754$, $p<0.05$). A Tukey post-hoc test revealed statistically significant differences between sampling depths 0-1m and 3-4m (p-value<0.05). Lower taxa richness in the sampling depth 0-1m, seemed to coincide with years with large water level fluctuations.

In the RDA ordination analysis, among different macrophyte life forms, Helophytes and Ceratophyllids, with one representative *Ceratoplyllum demersum*, appeared to be the most sensitive to the effects of water level changes. The first two axes of the RDA explained 96.51% of the variance of macrophytes (eigenvalues $\lambda1 = 17.70$, 86.21% and $\lambda2 = 2.11$, 10.30% respectively). However, the total variance of the RDA model was 20.54.

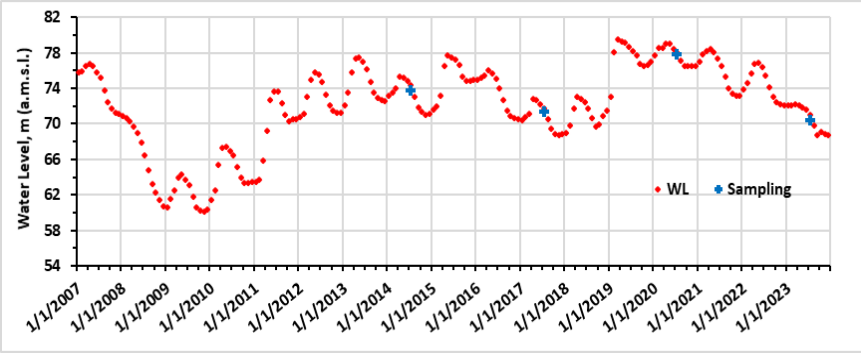


Figure 1. WLF of Lake Yliki during 1/1/2007 – 31/12/2023 with noted sampling dates of macrophytes.

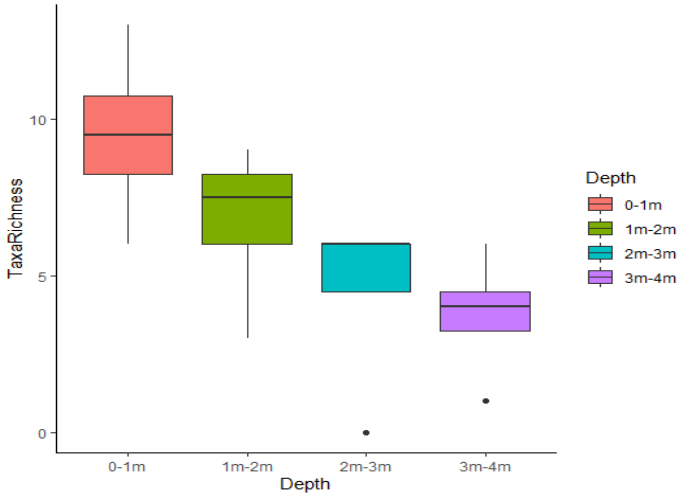


Figure 2. Box and whisker plots of taxa richness of the four different group categories of sampling depth. In the box plots, the central line represents the median; the lower and upper box limits correspond to the 25th and 75th percentiles and the upper (lower) whiskers extend to 1.5 (−1.5) times the interquartile range, respectively.

The interplay of frequency and amplitude of water level fluctuations determines the severity of their effects (Zhao et al., 2021). Although macrophytes have evolved mechanisms to cope with intermediate water-level changes, large fluctuations can lead to adverse effects on their growth and survival. The enrichment of the dataset would provide a more comprehensive view of how WLF affect macrophytes.

Acknowledgments: The present study was conducted in the frame of the Greek National Water Monitoring Network, according to the JMD 107168/1444/2021, implemented by The Goulandris Natural History Museum, Greek Biotope/Wetland Centre (EKBY). The network is supervised by the General Water Directorate of the Ministry of Environment. EYDAP provided recordings of the lake's Yliki water level (a.m.s.l), from 1/1/2007 to 31/12/2023.

References

Hill, N.M., Keddy, P.A., Wisheu, I.C. (1998) A Hydrological Model for Predicting the Effects of Dams on the Shoreline Vegetation of Lakes and Reservoirs. Environ Manage. 22(5):723-36. doi: 10.1007/s002679900142. PMID: 9680540

Li, L., Bonser, S.P., Lan, Z. et al. (2017) Water depth affects reproductive allocation and reproductive allometry in the submerged macrophyte Vallisneria natans . Sci Rep 7, 16842. https://doi.org/10.1038/s41598-017-16719-1

R Core Team (2024). R: A language and environment for statistical computing. R Foundation for Statistical Computing, Vienna, Austria. https://www.R-project.org/

Zervas, D., Tsiaoussi, V., & Tsiripidis, I. (2018) HeLM: A macrophyte-based method for monitoring and assessment of Greek lakes. Environ Monit Assess 190, 326. https:// doi. org/ 10. 1007/ s10661- 018- 6708-1

Zhao, F., Fang, X., Zhao, Z., Chai, X. (2021) Effects of Water Level Fluctuations on the Growth Characteristics and Community Succession of Submerged Macrophytes: A Case Study of Yilong Lake, China. Water, 13, 2900. https://doi.org/10.3390/w13202900

Assessment of minimum ecological water requirements in Lake Pamvotida – Greece, using an adaptation of the IFIM method

D. Papademos[1*], V. Chrysopolitou[1], H. Hadjicharalambous[1], E. Karadimou[1], D. Bousbouras[2], I. Leonardos[3], I. Kagkalou[4], K. Chiotelli[5]
[1] The Goulandris Natural History Museum-Greek Biotope Wetland Centre, Thessaloniki-Thermi,Greece
[2] Biologist – Researcher, Environmentalist. Palamidou 25 Str., GR 54633, Thessaloniki, Greece
[3] Laboratory of Zoology, Department of Biological Applications and Technology, University of Ioannina, Greece
[4] Department of Civil Engineering, School of Engineering, Democritus University of Thrace, 67100 Xanthi, Greece
[5] Natural Environment and Climate Change Agency (NECCA)/Management Unit of the Protected Areas of Epirus
* e-mail: papadimos@ekby.gr

Introduction

Human interventions and climate change in the Greek territory, so far accompanied by higher temperatures and reduced precipitations, are already exerting pressure on the water level (WL) of the lakes (Papadimos et al., 2022). The severity of the impact of the above pressures on lake ecosystems depends on the magnitude of their WL changes, the duration, the timing of their occurrence during the year and the organisms that occur in the ecosystem (Leira and Cantonati 2008). Therefore, the identification of the ecological water level requirements (EWLR) of the lakes should be considered both necessary and imperative for the conservation and protection of their ecosystems and the services they provide.

A variety of methodological approaches have been used to estimate EWLR in lakes. Among them hydraulic models, combination of historical WL data and the ecological requirements at different life stages of aquatic macrophytes, the protection requirements of specific aquatic flora and fauna species sensitive to hydrological pressures etc.

In this research, we have used an adaptation of the Instream Flow Incremental Method (IFIM, Bovee 1982), which has been mainly applied to streams and rivers, to assess the EWLR of Lake Pamvotida, on the basis of the requirements of its habitat types and species whose conservation depends directly or indirectly on water regime. In addition, justified management measures related to the water balance of the lake have been elaborated and proposed to support the EWLR.

Materials and methods

Lake Pamvotida is located at the western part of Greece, in the region of Epirus. Its basin occupies an area of 489.4 km^2 with pronounced mountainous terrain (maximum altitude 1810 m). The altitude in the plain area varies from 470 to 480 m. The lake is mainly fed with water by four torrents that drain its basin. The lake outflows above the elevation of 469.04 m a.m.s.l. to Lapsista drainage ditch through a 30m long spillway and its gate. The latter is opened for flood protection and for summer water supply to the irrigation networks of the Lapsista area. The lake's surface, mean depth and volume when it outflows are 21.9 km^2, 5.4 m and 118.6 x 10^6 m^3 respectively.

The main pressure on the lake's hydrological balance is exerted by two collective irrigation networks which cover an area of 4,600 ha and claim 9.0 - 11.5x10^6 m^3/year of water from the lake, from May to September.

The ecosystem of the lake overlaps with two Natura 2000 network sites and specifically, with the Special Area of Conservation and Special Protection Area (SAC/SPA) "GR2130005-LIMNI IOANNINON" and with the Special Protection Area (SPA) "GR2130012- EVRYTERI PERIOCHI POLIS IOANNINON".

The methodology followed for the determination of the lake EWLR belongs to the category of Habitat Suitability Simulation and is based on the Instream Flow Incremental Method (IFIM). As a first step, the inter-annual range of the lake WL and the corresponding mean monthly fluctuation were assessed. Target species of lake macrophytes (3), fish (4) and birds (9) were identified and delineated their habitats in the

lake. Furthermore, Habitat Suitability Criteria (HSC) were identified for the above species and constructed the corresponding suitability curves. The latter evaluates, using indices from 0 to 1, the suitability of a habitat for a specific species and criterion. The method (Fig.1), estimates the Usable Habitat Area (UHA), for a species and its life stages under several WLs of the lake. The WL for which UHA becomes maximum, corresponds to the minimum EWLR for the species under consideration. The final EWLR for the lake is obtained by repeating the above procedure (Fig. 1) for all the target species and their life stages and by combining the resulting EWLRs.

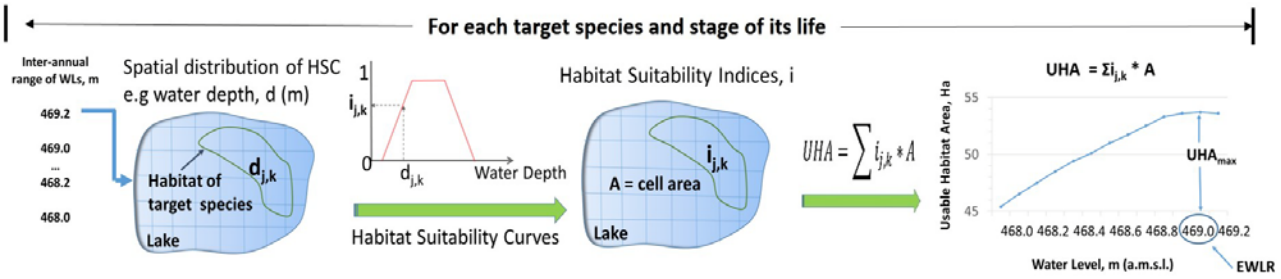


Figure 1. Process for assessing EWLR in Lake Pamvotida.

Results and concluding remarks

Three periods with different needs, in terms of WL fluctuation and its max drop of the lake have been identified, together with the maximum allowable withdrawals from the lake (Table 1).

Table 1. Proposed WL fluctuation, max drop and max withdrawal from Lake Pamvotida to meet its EWLR

Period of the Year	WL range, m	Max WL drop, m	Max withdrawal , x10^6 m^3
November – April	469.1 – 469.5		
April – June (bird nesting)	469.0 – 469.1	≤ 0.1	1.2
July – October (macrophyte growth)	468.2 – 469.1		2.4 (Jul), 2.7 (Aug), 0.7 (Sep)

The first period coincides with the rainy season in the area and therefore maintaining the WL at the proposed range is relatively easy. Care should be taken in order the WL to be kept bellow the height of 469.5 m (maximum WL for flood control). In the second period, further to the aquatic bird population, the proposed WL also preserves the reproductive habitat (macrophytes) of the fish species. Pressure on the proposed WL is mainly exerted in June due to increased evaporation rates, reduced water inflow from torrents and increased withdrawals for irrigation. The third period coincides with the maximum withdrawals (July to mid September) for irrigation purposes. In general, it is proposed the withdrawals from the lake should not exceed 8.5 x 10^6 m^3/year.

The method proved to be quite demanding in terms of scientific expertise and resources (e.g. GIS, scripting, hydrological modeling tools). Lack of “ready-to-use” habitat suitability curves for the selected criteria (water depth and rate of change of WL) and target species for the Greek territory rendered the study even more demanding. A strong advantage of the method was proven to be its ability to quantify the effect of any change in lake WL on habitat suitability, making it a strong operational management tool.

References

Bovee, K.D (1982) A guide to stream habitat analysis using the instream flow incremental methodology. Instream Flow Information Paper 12, USDI Fish and Wildlife Services, Office of Biology Services: Washington DC

Leira M, Cantonati M (2008) Effects of water-level fluctuations on lakes: an annotated bibliography. In: Wantzen et al. (eds) Ecological Effects of Water-Level Fluctuations in Lakes. Developments in Hydrobiology, vol 204, Springer, Dordrecht. https://doi.org/10.1007/978-1-4020-9192-6_16.

Papadimos D, Demertzi K, Papamichail D (2022). Assessing Lake Response to Extreme Climate Change Using the Coupled MIKE SHE/MIKE 11 Model: Case Study of Lake Zazari in Greece. Water 2022, 14(6), 921. https://doi.org/10.3390/w14060921.

Application of a 2D-hydrodynamic model to assess the impact of spring water discharge into Lake Pamvotida in Ioannina, Greece

K. Zachopoulos*, D. Papademos
The Goulandris Natural History Museum-Greek Biotope Wetland Centre, 14th km Thessaloniki - Mihaniona, 57001 Thessaloniki-Thermi, Greece
** e-mail: zachopoulosk@ekby.gr*

Introduction

According to the study conducted by the Greek Biotope Wetland Centre for the assessment of the minimum water level requirements of Lake Pamvotida, its water level (WL) should be maintained within the specified range of 469.10 - 468.20 m, a.m.s.l. However, the lake is very susceptible to larger reductions in its WL in late summer (below the proposed water level of 468.20 m) due to increased evaporation and over-pumping for irrigation purposes. This study investigates the introduction of freshwater from the Sentenikos and Kalithea Springs into Lake Pamvotida in order to mitigate the decrease in its water level (WL), during the dry season. A 2-D hydrodynamic modelling system was used to evaluate the effects of three scenarios in which the existence and location of the spring discharge inflow are differentiated. WL, temperature (T), dissolved oxygen (DO) and biochemical oxygen demand (BOD) were used for the evaluation of the effect of the scenarios on the lake's condition. The research showed a significant change on the WL fluctuation of the lake, and only minor effects locally dispersed regarding on its temperature, DO and BOD.

Materials and methods

The study area is Lake Pamvotida, which is located in the west part of Greece, in the prefecture of Ioannina. The lake's WL ranges from 468.00 to 469.5 m a.m.s.l., and is regulated by a spillway and its gate. Its mean depth is 5.4 m while its maximum 7.5-8.0 m. The lake is about 22 km^2 in size, with an estimated volume of 118.6 million m^3 of water at its overflow according to the National Lake Monitoring Network.

MIKE 21 Flow Model (FM) was used to simulate the hydrodynamic environment of Pamvotida Lake, including its hydrodynamic (HD) and the ecological (MIKE ECO Lab) modules (developed by DHI). The HD module is based on the numerical solution of the two dimensional shallow water – in depth integrated - Navier Stokes equations. The spatial discretization of the primitive equations is performed using a cell centred finite volume method (DHI, 2024a). MIKE ECO Lab module is able to simulate the spatial distribution of water quality variable concentrations in a 2D domain, based on processes such as: advective transport, biological, physical, and chemical transformation processes as well as settling, resuspension and sediment processes (DHI, 2024b).

Three different scenarios were investigated, for a period of nine years (2013-2021). The base scenario consisted of the hydrodynamic and ecological model of the lake without any spring water inflow. The horizontal discretization of the model was conducted by 3911 triangular elements with side length from 30 to 200 m. Data related to bathymetry of the lake, were acquired from Apostolakis and Papadimos (2016). Meteorological data retrieved from the open database of National Observatory of Athens (NOA). Solar radiation data were retrieved from the Copernicus Atmosphere Monitoring Service (CAMS) - Atmosphere Data Store (ADS) database. Data related to water inflow into the lake from its torrents and the corresponding outflow data from pumping stations, the spillway and its gate were acquired from the National Lake Monitoring Network. Two more scenarios (1 and 2) were investigated to assess the effect of the spring water inflow into the lake from two different locations. In Scenario 1, the water inflow is located close to Perama (700 m distance from the spillway) while in Scenario 2, the spring water inflow is located close to Amfithea, 2900 m distance from the spillway (Figure 1a). The temperature of the spring water varies from 12.5-13.5 ^oC, and the discharge ranges from 0.5 to 12.5 m^3/s.

Results and concluding remarks

The model of the Base Simulation was calibrated and validated against monthly data of WL, T, DO and BOD for the period of 2013-2021, with a time step of 5 min. The parameterization of the model after its calibration was kept the same for the models of Scenario 1 and 2. The scenarios indicated that the seasonal WL fluctuation is substantially affected by the spring water inflow. Both scenarios 1 (Sc1) and 2 (Sc2) have almost the same effect on the WL fluctuation, with an average difference of 0.17 m between them and the Base Simulation. At high WL periods, the WL in Sc1 and Sc2 is slightly elevated (+ 0.05 m) compared to the Base Simulation. Conversely, during low WL periods the WL in Sc1 and Sc2 was found to be greater (+ 0.40 m) compared to the Base Simulation (Figure 1b).

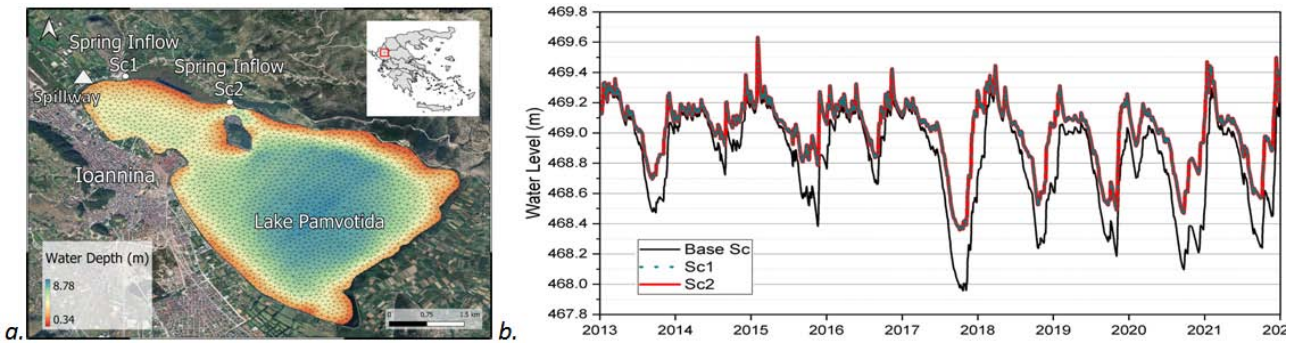


Figure 1. a. The mesh grid and lake bathymetry. White dots indicate the locations of spring water inflow scenarios; b. Water lever fluctuation for the Base Simulation (black line), Sc1 (grey dots) and Sc2 (red line).

Furthermore, the fresh spring water impact on the lake's condition (T, DO and BOD) is limited to the area close to the spring location and has no appreciable effects on the entire lake region (Figure 2). After periods of high discharge, the spring water's dispersion forms a plume that extends 0.26 km^2 in Sc1 and 0.38 km^2 in Sc2 (Figure 2). The plume area in Sc1 is substantially less since the inflow location is close to the lake's spillway and a portion of the intake water runs off.



Figure 2. Indicative results from the Base Simulation and the two scenarios simulating the temperature influence of the spring water inflow (12.5 m^3/s on January 14, 2021).

Overall, the spring water inflow into the Lake Pamvotida affected significantly the WL fluctuation, especially in low WL periods, keeping the lower WL close to the critical minimum altitude of 468.20 m. The different physiochemical consistence of the spring water did not directly affect the total area of the lake since the impact is limited to the area near to the discharge inflow point.

Acknowledgments: The present study was conducted in the frame of the Greek National Water Monitoring Network, according to the JMD 107168/1444/2021, implemented by The Goulandris Natural History Museum, Greek Biotope/Wetland Centre (EKBY).

References

Apostolakis A, Papadimos D (2016). Isobath curves of Lake Pamvotida [Geospatial Data]. Hellenic Centre for Biotopes-Wetlands (EKBY).

DHI (2024a). MIKE 21 Flow Model FM – Hydrodynamic Module User Guide. Danish Hydraulic Institute, Hørsholm, Denmark. V. 2024.

DHI (2024b). MIKE 21 ECO Lab – WQ Module User Guide. Danish Hydraulic Institute, Hørsholm, Denmark. V.2024.

Risk assessment of Ramsar areas: A multi-criteria and social choice approach to information base expansion and reduction

B. Srđević*, M. Ilić-Paunić, Z. Srđević, S. Ždero
Department of Water Management, Faculty of Agriculture, University of Novi Sad, Novi Sad, Serbia
** e-mail: bojans@polj.uns.ac.rs*

Introduction

Ramsars provide crucial ecosystem services, including water supply, flood and drought mitigation, carbon sequestration, and biodiversity. Although these functions make them vital for sustainable development, decision-makers often overlook their importance and fail to address the root causes of degradation or to properly assess their potential for conservation and sustainable use.

In Serbia, there are 10 Ramsar sites, eight of them located in Vojvodina Province. Global studies highlight the need to identify key indicators to assess the condition of wetlands in most sites, aiming to recommend effective monitoring, protection, and management measures.

The impact of changing context (multicriteria vs social choice methods) in group decision-making is simulated by determining the importance of criteria commonly employed for evaluating wetland-related risks.

Materials and methods

Srđević and Ilić (2020) established a foundation for creating a group model to evaluate criteria, using a real-life example to demonstrate the impact of grouping individual evaluation outcomes through the analytic hierarchy process (AHP) (Saaty, 1980). They further interpreted the results with reduced-information transformation in social choice theory (SCT) (D'Angelo et al., 1998) pairwise comparison rules. Seven individuals with different professions, all within the broader field of Ramsar area issues, participated independently (without consensus) in evaluating the following eight criteria: C1-Habitat Protection; C2-Biodiversity; C3-Water Regime; C4-Land Use; C5-Area Location; C6-Tourism and Education; C7-Water Quality; and C8-Cultural Heritage. AHP is implemented by calculating the weights of criteria based on individual judgments, with the consistency ratio (CR) computed for each participant. Participants used Saaty's 9-point scale for pairwise comparisons of criteria, allowing for a comparison of their evaluations with those derived from Social Choice Theory (SCT), which uses three comparison levels (weaker-equal-stronger) versus AHP's 17 levels. This enabled analysis of the impact of reducing information in ranking criteria across different environments.

Results and concluding remarks

Srđević and Ilić (2020) presented a good example of how different group decision-making contexts can lead to different results if some group members demonstrate high or low consistency while judging criteria to be used in validating Ramsars' exposure to the risks. Table 1 presents the results of criterion comparisons (weights and ranks of criteria) for the most and least consistent participants in the AHP and SCT context. Note that the CR parameter for the most consistent participant was 0.030, significantly lower than the commonly tolerated limit of 0.100 in AHP applications, and the CR for the least consistent participant was 0.394 (almost four times higher than the tolerable limit). The columns related to the AHP context show that the highest and equal weights (0.284) are assigned to criteria C3 and C7, followed by C1 and C2, which also have equal weights (0.135), more than twice as low as the weights of C3 and C7. The lowest weights are assigned to criteria C8 (0.031) and, in the last place, C4 (0.022). The weights are cardinal values opting for possible allocation of resources such as 'efforts' or 'investments' in related studies concerning Ramsar's monitoring, protection, and development.

Table 1. AHP pairwise comparisons and SCT pairings for the most and least consistent participants

Criteria	Most consistent participant				Least consistent participant			
	AHP weights	AHP ranks	SCT sums	SCT ranks	AHP weights	AHP ranks	SCT sums	SCT ranks
C1 - Habitat Protection	0.135	3-4	4.5	3-4	0.149	5	5	1-4
C2 - Biodiversity	0.135	3-4	4.5	3-4	0.208	1	5	1-4
C3 - Water Regime	0.284	1-2	6.5	1-2	0.188	2	5	1-4
C4 - Land Use	0.022	8	0	8	0.158	3	4	5
C5 - Area Location	0.044	6	2	6	0.027	8	0	8
C6 - Tourism and Education	0.065	5	3	5	0.073	6	2.5	6
C7 - Water Quality	0.284	1-2	6.5	1-2	0.153	4	5	1-4
C8 - Cultural Heritage	0.031	7	1	7	0.044	7	1.5	7

When the AHP weights obtained for the most consistent participant are interpreted in the SCT context (shadowed part of the table), the key information derived is that the rankings of the criteria are completely identical in both contexts. The 'context shift' applied is arbitrary but logical, and the point is that the obtained identical ranking of criteria is strongly supported by the fact that the consistency of evaluating criteria in the AHP manner is high (0.03 compared to the tolerant limit of 0.10).

If the same procedure is applied to the most inconsistent participant, a comparison of the 'inconsistent' rankings shows that there is a ‘smoothing’ of the rankings for criteria C1, C2, C3, and C7. In the SCT context, criterion C4 is ranked fifth, even though its weight in the AHP context is higher than the weight of C1, which is ranked among the top four criteria in the SCT context.

Considering that Saaty's scale in AHP offers 17 degrees of freedom when comparing any two criteria (1/9, 1/8, ..., 1, 2, 3, ..., 9), while SCT allows for only three levels (0, 1/2, 1), it is evident that the latter reduces the information about the individual's actual preferences during comparisons. In the SCT case, the reduced number of levels (weaker 0 – equal 1/2 – stronger 1) can alter the perception of true preferences compared to the results obtained using Saaty's scale. This result, as well as additional analyses, may easily indicate that higher consistency improves the alignment of rankings in the AHP and SCT contexts and reduces the impact of the information reduction inherent in the SCT context.

In conclusion, AHP ranks criteria based on cardinal values, while Ždero et al. (2024) and Srđević and Ilić (2020) offered a deeper analysis of individual and group evaluations. They examined a stakeholder-driven holistic approach to mitigating drought in Ramsar wetlands and the effects of expanding or narrowing the informational basis for evaluating criteria. If group members are expert and consistent, AHP can be replaced by SCT for ranking, though AHP remains essential for determining actual weights. Future research can focus on selecting group members or adjusting criteria for Ramsar area evaluations, aiming to improve climate change management and identify necessary investments.

Acknowledgments: Ministry of Science, Technological Development and Innovation of Serbia, Grant No. 451-03-47/2024-01/200117.

References

D’Angelo A, Eskandari A, Szidarovszky F (1998) Social choice procedures in water resources management. Journal of Environmental Management, 52, 203-210.

Saaty TL (1980) The Analytic Hierarchy Process, McGraw-Hill, New York.

Srđević B, Ilić M. (2020) Group model for evaluating criteria to be used in risk assessments of Ramsar protected wet areas. Vodoprivreda, 52, 273-286. (In Serbian)

Srdjevic B (2007) Linking analytic hierarchy process and social choice methods to support group decision-making in water management. Decision Support Systems, 42 (4), 2261-2273. https://doi.org/10.1016/j.dss.2006.08.001

Ždero S., Srđević B., Srđević Z. (2024) A stakeholder-driven holistic approach to mitigating drought in Ramsar wetlands: Evaluation of nature-based solutions using interval analytic hierarchy process. Water & Climate Change, 2024, 15(5) 2348-2363. https://doi.org/10.2166/wcc.2024.705

Developing a new criterion to evaluate monthly streamflow modelling in frequency domain

S. Piran, U. Panu*
Department of Civil Engineering, Lakehead University, Thunder Bay, ON, Canada
** e-mail: uspanu@lakeheadu.ca*

Introduction

The evaluation of synthesized series is challenging. To determine whether a model accurately mimics historical properties, various criteria are often employed, such as analysing the square mean error (Salas et al., 1980), comparing statistical measures (Panu & Unny, 1980), assessing autocorrelation functions (ACF) (Piran & Panu, 2023), or examining Hurst exponents (Panu & Unny, 1980). This study introduces an innovative approach to evaluate the similarity between historical and synthesized streamflow time series in the frequency domain by focusing on isolating abrupt jumps in power spectrum reported in the literature. The proposed criteria are then applied to compare synthesized streamflow generated by the Autoregressive Moving Average ARIMA(p,d,q)×(P, D, Q)$_{12}$ model and the Artificial Neural Network (ANN) across three stations in Ontario.

Materials and methods

The Fourier transform of a hydrologic time series, x(t), into its frequency domain representation, G(f), is computed as follows:

$$F(t) = \int_{-\infty}^{+\infty} x(t) e^{-2\pi i f t} dt \quad (1)$$

where t represents time, f is the frequency, and i=√(-1). If a linear relationship exists between the frequency and the power spectrum on a log-log scale, it indicates scale invariance in the temporal domain. This relationship is expressed as follows:

$$P(f) \propto 1/f^{\alpha} \quad (2)$$

where P(f) is the power spectral density (PSD) at that frequency, and α is the slope of the linear curve on a log-log plot. In this study, cross-points in the frequency domain are set to 1 year (f = 1/12 months = 0.083 month^{-1}) as utilized by (Telesca et al., 2012). Moreover, the jumps at specific months shown in Figure 1(a,b) and reported in the literature are isolated, as they indicate pattern dominance (Kim et al., 2016).

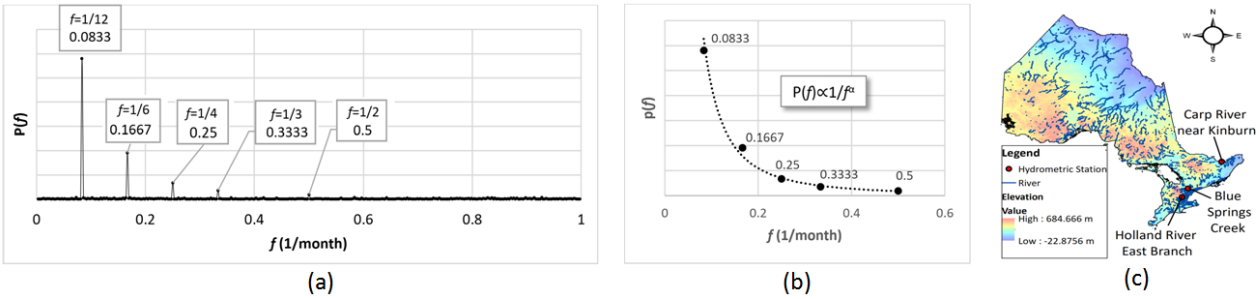


Figure 1. a) Power spectral density (PSD) plot of a hypothetical monthly streamflow; b) isolated jumps in the PSD and c) locations of hydrologic stations.

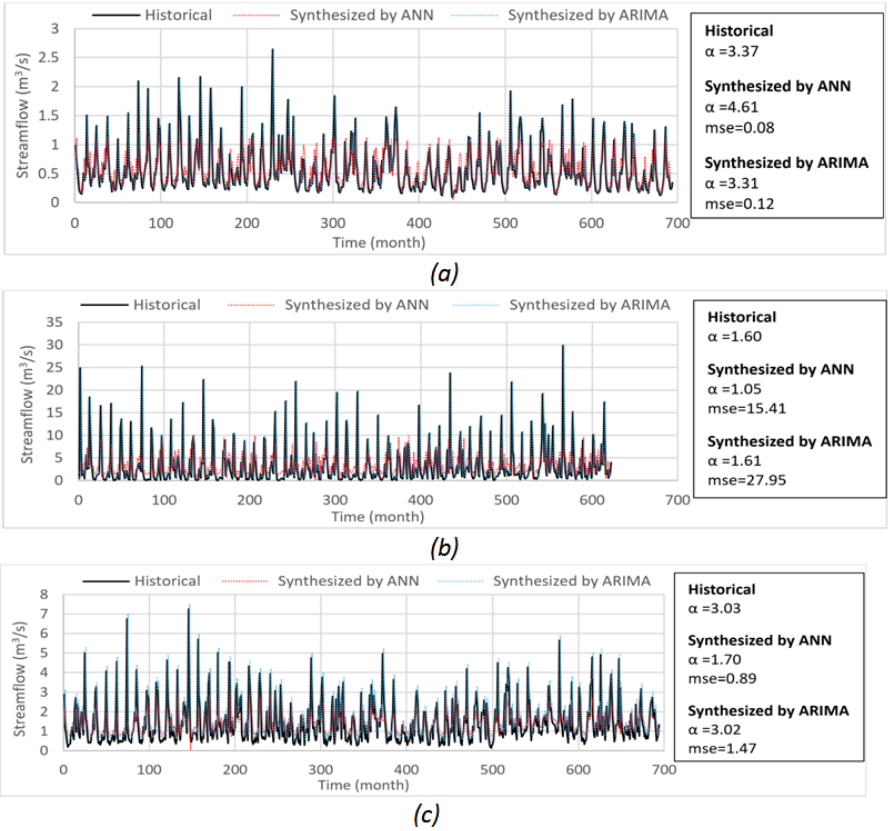
In this study, three stations are randomly selected across Ontario, with the study areas shown in Figure 1c. Additionally, the relevant information for each station is summarized in Table 1.

Table 1. Summary of information on hydrometric stations.

Station Name	Station Number	Geographical Location (Lat: & Long:)	Drainage Area (km^2)	Years of Records (Jan-Dec)
Blue Springs Creek	02GA031	43° 34' 34" N 80° 06' 32" W	41.5	1966-2023
Carp River near Kinburn	02KF011	45° 25' 03" N 76° 11' 55" W	258	1972-2023
Holland River East Branch	02EC009	44° 05' 41" N 79° 29' 22" W	176	1966-2023

Results and concluding remarks

Monthly streamflow at the stations listed in Table 1 is synthesized using both ANN and ARIMA. The *ANN model* utilizes a feedforward neural network with *five hidden neurons*, trained with the *Levenberg-Marquardt algorithm* using *one-lag and two-lag streamflow inputs*. The best ARIMA model is selected based on the minimum AIC, and the parameters are summarized in Figure 3d. Figure 3(a,b,c) shows the synthesized streamflow, and presents the values of MSE and α. As observed, although ARIMA has a higher MSE, its α value is closer to the historical data, as apparent from the time series plot in Figure 3(a,b,c).



Station	Model	Parameter
Blue Springs Creek	AR 1	$\phi_1 = -0.851$
	AR 2	$\phi_2 = -0.259$
	Seasonal AR 12	$\Phi_1 = -0.043$
	MA 1	$\theta_1 = 0.509$
	MA 2	$\Theta_2 = 0.482$
	Seasonal MA 12	$\Theta_1 = 0.912$
Carp River near Kinburn	AR 1	$\phi_1 = -1.064$
	AR 2	$\phi_2 = -0.523$
	Seasonal AR 12	$\Phi_1 = -0.092$
	Seasonal MA 12	$\Theta_1 = 0.967$
Holland River East Branch	AR 1	$\phi_1 = -0.963$
	AR 2	$\phi_2 = -0.497$
	Seasonal AR 12	$\Phi_1 = 0.026$
	Seasonal MA 12	$\Theta_1 = 0.963$

(d)

Figure 3. Historical & synthesized monthly streamflows a) Blue Springs Creek, b) Crap River near Kinburn, c) Holland River East Branch; d) ARIMA model parameters.

References

Kim, D. H., Rao, P. S. C., Kim, D., & Park, J. (2016). 1/f noise analyses of urbanization effects on streamflow characteristics. Hydrological Processes, 30(11), 1651-1664.

Panu, U. S., & Unny, T. (1980). Stochastic synthesis of hydrologic data based on concepts of pattern recognition: II. Application of natural watersheds. Journal of Hydrology, 46(3-4), 197-217.

Piran, S., & Panu, U. S. (2023). Encoded-Streamflow Synthesis using Textural Feature Recognition System. AGU Fall Meeting.

Salas, J. D., Delleur, J. W., Yevjevich, V., & Lane, W. L. (1980). Applied Modeling of Hydrologic Time Series. Water Resources Publication, Littleton, Colorado, USA.

Telesca, L., Lovallo, M., Lopez-Moreno, I., & Vicente-Serrano, S. (2012). Investigation of scaling properties in monthly streamflow and Standardized Streamflow Index (SSI) time series in the Ebro basin (Spain). Physica A: Statistical Mechanics and its Applications, 391(4), 1662-1678.

Use of a lake coupled hydrodynamic/ecological numerical model to help integrating Nature-based Solutions into environmental urban planning

C. Dresti[1*], A. Fenocchi[2], C. Cammalleri[3], G. di Chiano[3], G. Becciu[3]
[1] Water Research Institute of the National Research Council, Largo Tonolli 50, 28922, Verbania, Italy
[2] Department of Civil Engineering and Architecture, University of Pavia, Via Adolfo Ferrata 3, 27100 Pavia, Italy
[3] Department of Civil and Environmental Engineering, Politecnico di Milano, L. da Vinci 32, 20133 Milan, Italy
* e-mail: claudia.dresti@irsa.cnr.it

Introduction

Lakes are highly susceptible to both climate change and the impacts of human development. Specifically, discharges from sewer systems (such as combined sewer overflows and stormwater runoff) and bypasses from wastewater treatment plants (WWTP) are key contributors to lake pollution (Koiv-Vainik et al. 2022). Stormwater management strategies, particularly Nature-based Solutions (NBS), can effectively mitigate pollution risks to receiving water bodies. However, the design of NBS for stormwater control is often focused primarily on reducing runoff peaks and volumes, overlooking their potential for pollution control (Engström et al. 2018). The reduction of stormwater runoff and the removal of pollutant loads achieved by NBS, along with their ability to adapt to climate and urban changes, offer key advantages in developing multi-functional strategies for sustainable and resilient cities. In this context, modelling lake processes, particularly those driven by point-source pollution, is essential for an effective water resources management, especially when considering the impacts of climate change.

One-dimensional (1D) coupled hydrodynamic-ecological numerical models are effective tools for conducting long-term studies on deep lakes, with their horizontally averaged output providing valuable predictions over extended periods (Hamilton and Schladow 1997). These models can capture the interactions between the physical, chemical, and biological processes within lake basins (Hamilton and Schladow, 1997; Bruce et al. 2006), without requiring spatially distributed boundary conditions and with significantly lower computational demands compared to three-dimensional (3D) models. However, coupled hydrodynamic-ecological models are highly dependent on calibration, as biological processes are extensively parameterized (Hamilton and Schladow 1997; Trolle et al. 2012).

In this contribution, the coupled hydrodynamic/ecological General Lake Model/Aquatic EcoDynamics model (GLM/AED2; Hipsey et al. 2014), has been calibrated and validated for Lake Maggiore, which is a fluvio-glacial deep lake located at the foothills of Southern Central Alps. The final aim of this work is to use the calibrated model to evaluate the effects of NBS placed in the catchment on the chemical processes and algal blooms in the lake.

Materials and methods

The General Lake Model (GLM) v2.2.0b 1D model (Hipsey et al. 2014) was used to perform the hydrodynamic simulation of Lake Maggiore. The fixed-level enclosed-lake model configuration was calibrated in Fenocchi et al. (2017). Nutrient loads from tributaries were introduced at the lake surface, with the daily inflow concentrations derived as follows: 1) the overall mean monthly loads were linearly interpolated to a daily scale; 2) the daily concentrations were calculated by dividing the total loads by the calibrated fictitious discharges. This adjustment did not affect the accuracy of the hydrodynamic model. Assuming that input loads always enter at the surface is reasonable for smaller inflows, as their momentum and buoyancy forces are quickly dissipated. The primary tributaries, the Ticino and Toce Rivers, typically intrude at shallow depths (10-20 m) for most of the year, occasionally reaching the surface in early spring. However, they descend to much deeper depths (sometimes exceeding 200 m) during late autumn and winter (Fenocchi et al. 2017). This model representation was considered the most appropriate, given the diversity of tributaries feeding into Lake Maggiore, which include large rivers, natural and dammed

mountain streams, creeks, and outflows from smaller lakes and reservoirs, all exhibiting a wide range of discharges and temperatures (Fenocchi et al. 2017). Additionally, this approach aligns with the goal of simulating future scenarios, where changes in intrusion behavior are anticipated (Fenocchi et al. 2018). The GLM model was coupled with the Aquatic EcoDynamics (AED2) ecological model (Hipsey et al. 2013). A basic NPD (Nutrients, Phytoplankton, Detritus) structure was utilized, incorporating the cycles of oxygen, phosphorus, nitrogen, silica, carbon, organic matter, and phytoplankton.

The total time span was divided into calibration and validation periods. The calibration period covered an 8-year interval from 1 January 1999 to 31 December 2006, while the validation period spanned almost 8 years years, from 1 January 2007 to 14 October 2014. Manual trial-and-error calibration was adopted.

Results and concluding remarks

The performance of the coupled ecological-hydrodynamic model for Lake Maggiore during calibration and validation is comparable to, if not better than, that of similar studies in the literature, particularly for shallower lakes. The chemical evolution of the deep hypolimnion was successfully simulated, largely due to accurate modeling of mixing dynamics. However, a noticeable decline in model performance was observed during validation for phytoplankton dynamics and epilimnetic water chemistry, primarily due to the reliance on parameterization. The Pearson correlation coefficient R for the orthophosphate in hypolimnion is 0.61 in the calibration period and 0.7 in the validation period, for water temperature it reaches 0.81 and 0.84 and for dissolved oxygen DO it is 0.83 and 0.79, respectively. The coupled model is suitable for simulating the effects of nutrient scenarios in the lake.

Acknowledgments: The present research was funded by the project Prin Lake Pollution: Integrating Nature-Based Solutions Into Environmental Urban Planning For Risk Mitigation (ENVISION).

References

Bruce LC, Hamilton D, Imberger J, Gal G, Gophen M, Zohary T, Hambright KD (2006). A numerical simulation of the role of zooplankton in C, N and P cycling in Lake Kinneret. Israel. Ecol. Model. 193 (3-4): 412–436. https://doi.org/10.1016/j.ecolmodel.2005.09.008

Engström R, Howells M, Mörtberg U, Destouni G (2018). Multifunctionality of nature-based and other urban sustainability solutions: New York City study. Land Degradation & Development, 29(10): 3653-3662. https://doi.org/10.1002/ldr.3113

Fenocchi A, Rogora M, Sibilla S, Dresti C (2017). Relevance of inflows on the thermodynamic structure and on the modeling of a deep subalpine lake (Lake Maggiore, Northern Italy/Southern Switzerland). Limnologica 63: 42–56. https://doi.org/10.1016/j.limno.2017.01.006

Fenocchi A, Rogora M, Sibilla S, Ciampittiello M, Dresti C (2018). Forecasting the evolution in the mixing regime of a deep subalpine lake under climate change scenarios through numerical modelling (Lake Maggiore, Northern Italy/Southern Switzerland). Clim. Dynam. 51 (9-10): 3521–3536. https://doi.org/10.1007/s00382- 018-4094-6

Hamilton DP, Schladow SG (1997). Prediction of water quality in lakes and reservoirs. Part I — model description. Ecol. Model. 96 (1-3): 91–110. https://doi.org/10.1016/S0304-3800(96)00062-2

Hipsey MR, Bruce LC, Hamilton DP, (2013). Aquatic EcoDynamics (AED) model library: science manual. AED Report. The University of Western Australia, Perth, Australia.

Hipsey MR, Bruce LC, Hamilton DP (2014). GLM - General Lake Model: model overview and user information. AED Report #26. The University of Western Australia, Perth, Australia.

Koiv-Vainik M, Kill K, Espenberg M, Uuemaa E, Teemusk A, Maddison M, Kasak K (2022). Urban stormwater retention capacity of nature-based solutions at different climatic conditions. Nature-Based Solutions, 100038

Trolle D, Hamilton DP, Hipsey MR, et al. (2012). A community-based framework for aquatic ecosystem models. Hydrobiologia 683 (1): 25–34. https://doi.org/10.1007/s10750-011-0957-0.

Changes in water related ecosystem services following wildfires: The case of the Dadia-Lefkimi-Soufli Forest National Park

S. Stefanidis[1], I. Chrysafis[2], I. Kokkoris[3], I.M. Mitsopoulos[4], G. Mallinis[2]
[1] *Forest Research Institute, Hellenic Agricultural Organization "DIMITRA", Vassilika, 57006 Thessaloniki, Greece*
[2] *School of Rural and Surveying Engineering, Aristotle University of Thessaloniki, 54124 Thessaloniki, Greece*
[3] *Department of Sustainable Agriculture, University of Patras, 30131 Agrinio, Greece*
[4] *School of Forestry and Natural Environment, Aristotle University of Thessaloniki, 54124 Thessaloniki, Greece*
** e-mail: gmallin@topo.auth.gr*

Introduction

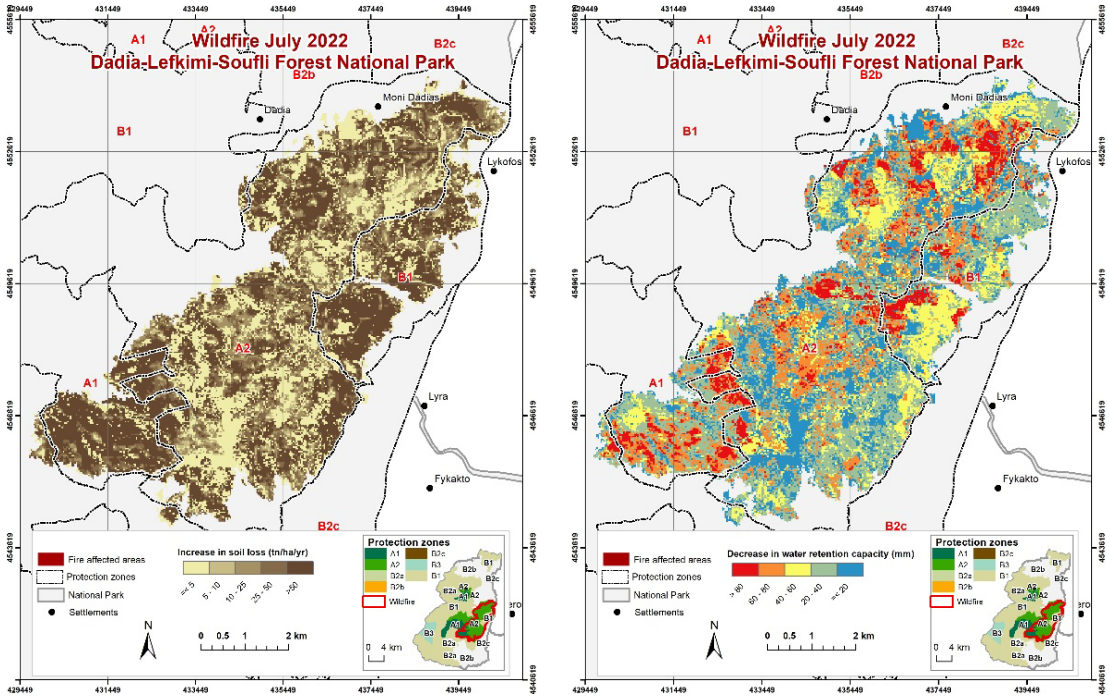
Water-related ecosystem services (WESs) over natural forest areas contribute significantly both to various ecosystem processes and human well-being. Among other, WESs are essential for water security, surface runoff control and water quality (Liu et al., 2024). Fire although an inherent process in seasonally dry areas like the Mediterranean (Pausas, and Keeley, 2009) is nowadays a major driver of land use changes and ecosystem disturbances. In forested watersheds, high severity wildfires can affect a variety of ecohydrologic processes and functions, including water storage, evapotranspiration, infiltration, and interception (Robinne et al., 2021). These processes can lead to increased surface runoff, increased erosion, and sediment delivery to streams (Robichaud et al., 2016). In such cases it can be anticipated a decline in the physical and chemical quality of the water, which could have significant and long-lasting impacts on WES. The aim of this work is to spatial explicit quantify changes in two water-related ecosystem services, following the catastrophic wildfire in Dadia-Lefkimi-Soufli Forest National Park (DLSFNP) in Greece in 2022.

Materials and methods

This study evaluates both pre-and post-fire conditions to evaluate water-related ecosystem services. To that end, very high spatial resolution imagery from the Worldview-2 και Jilin-1 satellites was used to evaluate burned severity and therefore the changes to water-related ecosystem services. The Revised Universal Soil Loss Equation (RUSLE) was employed (Renard et al., 1991) to estimate the Soil Conservation (SC) service). To evaluate maximum water retention capacity (S), a parameter that influences the water balance, groundwater rechargeand peak flows, the Soil Conservation Service-Curve Number (SCS-CN) approach was applied, based on the runoff coefficient CN (curve number). A detailed analytical description of the RUSLE and SCS-CN models, as implemented for the evaluation of Soil Conservation (SC) and Storage (S) ecosystem services, is provided in Stefanidis et al. (2024).

Results and concluding remarks

The application of the RUSLE erosion model indicated that based on the conditions prevailing in DLSFNP before the fire event, the erosion potential can be characterized as mild. More specifically, over the whole DLSFNP area, the average annual soil loss was found to be equal to 3.41 tn/ha/year, while within the park strictly protected zones (SPZs) it was found to be equal to 1.22 tn/ha/year. After the wildfire event and the destruction of the vegetation, the average annual soil loss in the whole park are was estimated at 8,56 tn/ha/year. Throughout the park the average increase in erosion rate was found to be equal to 4,75 tn/ha/year, while in the DLSFNP the average increase in erosion rate was found to be equal to 25,21 tn/ha/year (Figure 1). Subsequently, the effect of fire on the maximum water retention capacity of the soil was assessed. Before the fire, the average value of soil water retention capacity was 132.5 mm within the whole protected area and 138.4 mm in the SPZs. Following the fire event, the corresponding values were 128 and 146.1 mm.



(a) (b)

Figure 1. Changes in the soil conservation (a) and water retention (b) conservation service.

The spatially explicit results of the study highlight the magnitude of the changes induced by wildfires in WESs. The mapping layers (Figure 1) can be used to identify priority areas for developing post-fire mitigation measures.

Acknowledgments: This research was conducted as part of the project "LIFE-IP 4 NATURA-Integrated Actions for the Conservation and Management of NATURA 2000 Sites, Species, Habitats and Ecosystems in Greece" co-funded by the European Union and national funds.

References

Liu, J., Pei, X., Zhu, W., Jiao, J., 2024. Water-related ecosystem services interactions and their natural-human activity drivers: Implications for ecological protection and restoration. J. Environ. Manage. 352, 120101. https://doi.org/10.1016/j.jenvman.2024.120101

Pausas, J., Keeley, J., 2009. A Burning Story: The Role of Fire in the History of Life. BioScience 59, 593–601.

Renard, K.G., Foster, G.R., Weesies, G.A., Porter, J.P., 1991. RUSLE: revised universal soil loss equation. J. Soil Water Conserv. 46, 30–33.

Robichaud, P.R., Wagenbrenner, J.W., Pierson, F.B., Spaeth, K.E., Ashmun, L.E., Moffet, C.A., 2016. Infiltration and interrill erosion rates after a wildfire in western Montana, USA. CATENA 142, 77–88. https://doi.org/10.1016/j.catena.2016.01.027

Robinne, F.-N., Hallema, D.W., Bladon, K.D., Flannigan, M.D., Boisramé, G., Bréthaut, C.M., Doerr, S.H., Di Baldassarre, G., Gallagher, L.A., Hohner, A.K., Khan, S.J., Kinoshita, A.M., Mordecai, R., Nunes, J.P., Nyman, P., Santín, C., Sheridan, G., Stoof, C.R., Thompson, M.P., Waddington, J.M., Wei, Y., 2021. Scientists' warning on extreme wildfire risks to water supply. Hydrol. Process. 35, e14086. https://doi.org/10.1002/hyp.14086.

Stefanidis, S., Proutsos, N., Alexandridis, V., & Mallinis, G., 2024. Ecosystem services supply from Peri-Urban watersheds in Greece: soil conservation and water retention. Land, 13(6), 765.

Calliope Earth Observation Platform: the water quality monitoring service

G. Ceriola[1*], A. Zilli[2], M. Lippi[2], M. Rossi[1]
[1] Planetek Italia, Bari, Italy
[2] DTA Distretto Tecnologico Aerospaziale, Brindisi, Italy
* e-mail: ceriola@planetek.it

Introduction

CALLIOPE-EO Platform Project aims to establish a cutting-edge facility integrating research, education, and public communication in the context of the One Health paradigm. This holistic health model links human, animal, and environmental health through interdisciplinary approaches and emerging technologies, such as IoT and 5G. The project seeks to address the complex interactions between chemical, physical, and biological exposure factors to foster sustainable development.

DTA (Distretto Tecnologico Aerospaziale) has partnered with Planetek Italia, leveraging its extensive expertise in environmental monitoring to develop advanced geospatial solutions as part of the Calliope-EO Platform Project. This initiative is dedicated to enhancing the monitoring of critical environmental factors, with a particular emphasis on air quality, water quality, and urban green spaces.

Calliope-EO Platform Project is based on advanced geospatial technologies, satellite data integration, data from unmanned aerial systems (UAS) and user-oriented service platforms. Key components include:

a) Air Quality Monitoring: Rheticus® Air Quality service utilises Sentinel-5P satellite data and Copernicus Atmosphere Monitoring Service (CAMS) products for near-real-time air pollution tracking (e.g., s PM2.5, PM10, CO, CH4, NO2, and SO2).
b) Water Quality Monitoring: Rheticus® Marine service analyses satellite data (Sentinel-3 and Sentinel-2) to monitor in near-real-time chlorophyll-a concentration, water transparency, turbidity, and sea surface temperature.
c) Urban Green Monitoring: Rheticus® Urban Green service evaluates vegetation health using indices such as NDVI, SAVI, and LAI derived from Sentinel-2 data.

These services aim to improve decision-making processes for public health, urban planning, and environmental management by providing accurate, real-time, and predictive data using emerging technologies such as artificial intelligence algorithms, machine learning, and remotely piloted aerial systems.

Calliope-EO Platform Project is based on high-resolution monitoring, together with the integration of advanced data processing and visualisation tools, to ensure tailored insights for urban and environmental challenges. The Platform has a number of user-friendly dashboards, predictive capabilities, and alignment with the One Health framework to optimise health and environmental outcomes.

The following section presents the Water Quality Monitoring service.

Materials and methods

Water Quality Monitoring: Rheticus® Marine Service analyses satellite data (Sentinel-3 and Sentinel-2) to monitor chlorophyll-a concentration, water transparency, turbidity, and sea surface temperature by employing advanced EO-based algorithms (Sarelli et al., 2019; Ceriola et al., 2019).

The system consists of a series of modules that, launched sequentially by an orchestrator, implement the entire processing chain—from the acquisition of satellite data to the publication of value-added products.

The data processing workflow consists of multiple stages, beginning with the acquisition and pre-processing of satellite imagery (Sentinel-2 L1C and Sentinel-3 L2 WFR and SWT). The initial step involves the daily processing of satellite images to extract measurements at varying spatial resolutions, including 10 m

and 300 m for most parameters and 1 km for sea surface temperature. Pre-processing procedures encompass radiometric and atmospheric corrections, georeferencing, and resampling to maintain data consistency and accuracy. Additionally, rigorous quality control measures are implemented to remove cloud cover, shadows, and noise, thereby enhancing data reliability.

Following pre-processing, key water quality parameters are extracted using advanced computational techniques. For instance, chlorophyll-a concentration is estimated through an artificial intelligence-based algorithm. At the same time, total suspended matter and turbidity are determined using reflectance models specifically calibrated for the target area. Water transparency is assessed through Secchi disk depth proxies derived from satellite imagery, while sea surface temperature is obtained from thermal infrared spectral bands.

Each calculated water quality parameter is compared with reference values for different monitoring zones along the monitored coastal area. If these values are exceeded, an alert is generated for the specific zone. Depending on the extent of the exceedance, the alert can be classified as moderate, high, or critical.

For Sentinel-3 and each parameter, the system aggregates data generated over 10-day periods (considering the decades 1–10, 11–20, and 21–31) and over one month, calculating the average measurement for each pixel within the selected time frame.

Additionally, the platform provides daily and periodic reports (running since November 2024 and currently in place), aiding stakeholders in environmental policy implementation and risk management. Its cloud-based dashboard supports dynamic geo-analysis and temporal aggregation of data.

Results and concluding remarks

The implementation of the Calliope-EO Platform's Water Quality Monitoring service has demonstrated the effectiveness of integrating satellite Earth Observation (EO) data with advanced computational techniques for coastal water assessment. The system successfully processed Sentinel-2 and Sentinel-3 imagery to extract key environmental parameters such as chlorophyll-a concentration, water transparency, turbidity, and sea surface temperature.

Its near-real-time monitoring capabilities were validated through efficient data acquisition, pre-processing, and analysis workflows. Radiometric and atmospheric corrections ensured accuracy, while automated quality control reduced errors from cloud cover and noise. AI-based algorithms for chlorophyll-a estimation and reflectance models for turbidity and total suspended matter produced highly consistent results compared to in-situ data.

The platform generated high-resolution spatial data (10 m to 1 km) and aggregated information over 10-day and monthly periods, enabling trend detection and early warnings for water quality management. A threshold-based alert mechanism classifies water quality deviations into moderate, high, and critical levels, aiding environmental management and intervention.

A cloud-based dashboard provides real-time and historical data access, offering stakeholders an intuitive interface for decision-making. The Calliope-EO Platform proves to be a scalable and reliable solution for coastal water monitoring, leveraging EO technologies, AI-driven analytics, and cloud-based tools. Its adaptability supports broader environmental applications, contributing to sustainable development and climate resilience in line with the One Health paradigm.

Acknowledgements: The Lead Proponent is *Comune di Taranto*; the Financing Institutions are *Ministero delle Imprese e del Made in Italy* and *Fondo di Sviluppo e Coesione* of the Italian Government.

References

Ceriola, G., Drimaco, D., Aiello, A., Bollanos, S., 2019. From SST measurements to actionable information for public and private users: Rheticus© services. Proceedings of the GHRSST XX SCIENCE TEAM MEETING, pp. 144-148, ISSN 2049–2529

Sarelli, A., Ceriola, G., Iasillo, D., Aiello, A., 2019. Coastal Eutrophication estimation for SDG 14: innovative algorithm and novel provision approach based on the exploitation of large EO time series and a cloud-based application platform. ESA Living Planet Symposium 2019

Climate change and its impact on water quality of the Zarafshan river basin

S. Shoergashova[1,2,3], B. Karimov[3], T. Liu[4*]
[1] State Key Laboratory of Ecological Safety and Sustainable Development in Arid Lands, Xinjiang Institute of Ecology and Geography, Chinese Academy of Sciences, Urumqi, China
[2] University of Chinese Academy of Sciences, Beijing, China
[3] Department of Ecology and Water Resources Management, "Tashkent Institute of Irrigation and Agricultural Mechanization Engineers" (TIIAME) National Research University, Tashkent, Uzbekistan
[4] College of Geoinformatics, Zhejiang University of Technology, Hangzhou, China
* e-mail: liutie@zjut.edu.cn

Introduction

Climate change presents considerable challenges to global water resources, including the Zarafshan River Basin in Central Asia. Variations in temperature and precipitation impact not only the availability of water but also the concentration of pollutants and the overall condition of aquatic ecosystems. Rising temperatures can result in higher evaporation rates, diminished river flows, and increased levels of contaminants. Altered precipitation patterns, including more intense and frequent storms, can increase runoff and erosion, introducing additional pollutants into the river system. Moreover, climate change can exacerbate the effects of existing environmental stressors, such as agricultural runoff, industrial discharges, and urbanization, compounding the challenges to maintaining water quality. Changes in climate conditions affect agriculture, leading to reduced productivity in sectors dependent on water resources (Lobanova et al. 2021).

Many studies have shown a general temperature increase in the Central Asian region throughout the 20th century, with a notable acceleration starting in the 1970s (Babakholov and Hasanov 2024). Over the past 60 years, the average annual temperature has increased by 0.18 to 0.42°C per decade. Meanwhile, there have been no distinct trends observed in annual precipitation (Barros et al. 2014; Didovets et al. 2021). In this paper, the influence of climate change on the nitrogen compound content in the Zarafshan River Basin was studied. Furthermore, temperature, precipitation, and discharge trends in the basin were analyzed.

Materials and methods

The methodology of this research involved a comprehensive analysis of temperature, precipitation, discharge, and their relationships with nitrogen compounds in the Zarafshan River Basin. The Zarafshan river is a transboundary river located in Tajikistan (upper stream) and Uzbekistan (middle and downstream). The study area is the middle and downstream of the river. Data were collected from Uzbekistan Hydrometeorological Service Agency (Uzhydromet) for four meteorological stations: Samarkand (1960-2020, midstream), Kushrabod (1960-2020, midstream), Dagbit (1971-2020, midstream) and Nurabad (1966-2020 downstream). Additionally, monthly long-term data (2010-2023) for nitrogen compounds (N-NH_4, N-NO_2, N-NO_3) in Ravatkhoja gauging station, located in the border of two countries were analysed to identify dependencies.

To assess long-term trends in climate variables, the Mann-Kendall and Sen's Slope Tests were applied. The Mann-Kendall Test, a non-parametric method, was used to detect monotonic trends in time-series data, while Sen's Slope Test estimated the rate of change over time. Decadal and overall analyses of temperature and precipitation trends were also conducted to identify both short-term fluctuations and long-term patterns. Correlation analysis was performed to evaluate the relationships between key variables. Statistical tools XLSTAT 2021 were used to perform the Mann-Kendall and Sen's Slope Tests and calculate correlation coefficients.

Results and concluding remarks

We analyzed the annual precipitation and temperature data for four meteorological stations located in the Zarafshan River Basin: Samarkand (1960-2020), Kushrabod (1960-2020), Nurabad (1966-2020), and Dagbit (1971-2020). The temperature data across the meteorological stations was stable, mostly ranging from 10°C to 20°C. Furthermore, there was a noticeable variability in annual precipitation, with no consistent increasing or decreasing trend. In Samarkand precipitation data displayed considerable variability over the decades. The most noticeable peaks occurred in the 1969 (50.16 mm), 1993 (47.8 mm), and 2002 (47.1 mm). The minimum average value was observed in 2001 (13.2 mm). Similarly, in Kushrabad, the maximum average value was recorded at 55.67 mm in 1969. In Nurabad, as in Samarkand and Kushrabad, the peak in precipitation also occurred in 1969 (58.47 mm). Since the Dagbit station started operating in 1970, there is no information available for 1969. During the observed period, Dagbit recorded its maximum average precipitation in 2020 (52.27 mm).

To investigate the presence or absence of climate variables trends over time, we performed statistical analysis by using Mann-Kendall and Sen's Slope Tests. To identify long-term trends, we conducted a decadal and overall period analysis of temperature data for each meteorological station. The analysis revealed that during the 1991-2000 period, four meteorological stations exhibited an increasing temperature trend of 0.12-0.15 °C. Over the entire study period, a slight upward trend of 0.02-0.04 °C was also observed. Additionally, at the Samarkand meteorological station, an increasing trend of 0.07 °C was noted for the 2001-2010 period. Other decades did not show trend. Our analysis of precipitation and discharge trends did not indicate statistical significance, as evidenced by p-values that support the null hypothesis of no trend.

The correlation coefficients between discharge, temperature, and precipitation were conducted. Discharge and precipitation showed a moderate positive correlation ($r^2 = 0.52$), suggesting that as precipitation increases, discharge also tends to increase. The correlation between discharge and temperature is weakly positive ($r^2 = 0.07$), indicating little to no relationship. Meanwhile, the correlation between temperature and precipitation is weakly negative ($r^2 = -0.15$), implying a slight inverse relationship between these two variables. Our correlation analysis with climate variables (temperature and precipitation) and nitrogen compounds revealed some negative relationships between temperature and precipitation. However, there was no any significant relationship between nitrogen compounds and climate variables (monthly long-term data, Ravatkhoja), indicating other factors as agriculture and industrial discharges may influence nitrogen levels. Meanwhile, temperature trends show a slight upward trajectory, and precipitation and discharge patterns do not exhibit significant changes. This variability underscores the need for continuous monitoring and adaptive management recommendations to address potential impacts on water resources and quality in the region.

References

Babakholov S, Hasanov S. (2024) Perceptions towards climate change, water scarcity and adaptation strategies: Case of the Zerafshan River Basin in Uzbekistan. Italian Review of Agricultural Economics (REA) 79(2): 19-33. https://doi.org/10.36253/rea-15098

Barros VR, Field CB, Dokken DJ, Mastrandrea MD, Mach KJ (2014) IPCC chapter 24. Asia. In: Climate Change Impacts, Adaptation and Vulnerability (eds), Cambridge University Press, Cambridge, pp. 1327–1370

Didovets I, Lobanova A, Krysanova V, Menz C, Babagalieva Z, Nurbatsina A, Gavrilenko N, Khamidov V, Umirbekov A, Qodirov S, Muhyyew D, Hattermann F (2021) Central Asian rivers under climate change: Impacts assessment in eight representative catchments. Journal of Hydrology: Regional Studies 34: 100779. https://doi.org/10.1016/j.ejrh.2021.100779

Lobanova A, Didovets I, Menz C, Umirbekov A, Babagalieva Z, Hattermann F, Krysanova V (2021) Rapid assessment of climate risks for irrigated agriculture in two river basins in the Aral Sea Basin. Agricultural Water Management 243: 106381. https://doi.org/10.1016/j.agwat.2020.106381

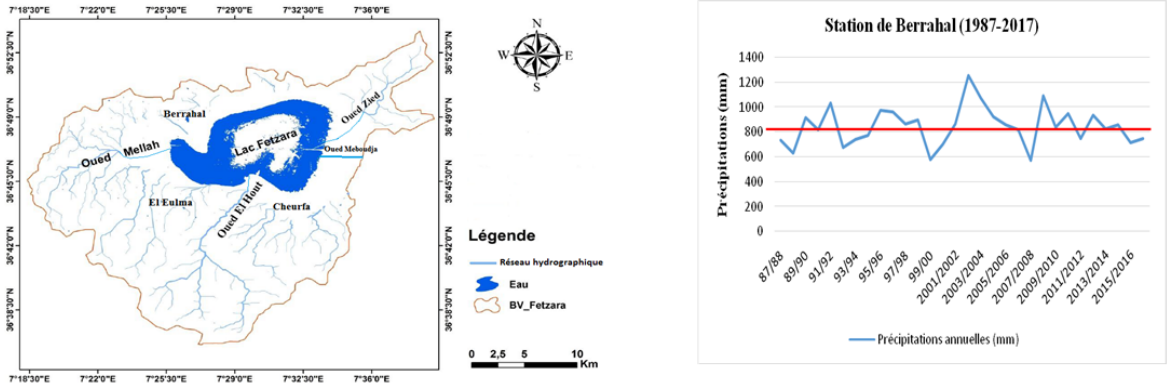
Impacts and effects of climate variations on the Lake Fetzara ecosystem (NE Algeria)

L. Djabri[1], Z. Bouhali[1], F. Halimi[2], S. Saidi[3], B. Hamza[1], S.E. Tachi[1], B. Nabil[1]
[1] Laboratory of Water Resources & Sustainable Development. Badji Mokhtar University. Annaba. Algeria
[2] Laboratory of geology. Badji Mokhtar University. Annaba. Algeria
[3] L3G Laboratory, Faculty of Sciences of Tunis, El Manar University, Tunisia
* e-mail:: Larbi.djabri@univ-annaba.dz

Introduction

Lake Fetzara is located in the extreme northeast of Algeria (Figure 1a). It lies between four municipalities of the Annaba province, bordered to the north by the municipality of Draa Erich, to the south by Ain Berda, to the west by Berrahal, and to the east by El Hadjar. This lake is considered one of the most important in the region. It has been classified as a Ramsar (the city in Iran where the international treaty concerning the protection of wetlands was signed), site since 2003, which requires its protection, especially since 17,000 migratory birds representing 15 different species pass through this ecosystem each year. Around 8,000 of these birds are Eurasian wigeons, and 800 are white-headed ducks (a small duck species with a broad, flat, blue bill).

This rich aquatic fauna and flora are now threatened by disappearance due to a lack of rainfall, leading to decreased water inflows to the lake, along with a deterioration in its water quality.



(a) (b)

Figure 1. (a) Geographical location of the lake; (b) precipitation variations in Berrahal

The interannual variations in precipitation, detected by rain gauge and pluviothermic stations surrounding the lake, indicate fluctuating water inflows from year to year, with a noticeable decline in the lake's extent even during the winter season. Figure 1b illustrates these interannual precipitation variations recorded at the Berrahal station, the closest to the lake.

To assess the impact of precipitation variations on the lake's extent between two pivotal years, we used Landsat 8 satellite imagery (path 193, row 34) for four different dates (November 2016, March 2017, November 2017, and April 2018).

Materials and methods

In order to study the spatio-temporal evolution of the wetland surface of Lake Fetzara, a single Landsat 8 image scene "p193 r34" of four different dates (November 2016; March 2017; November 2017 and April 2018) was analyzed. This scene contains 12 bands. The 6 multispectral bands (3 visible and three infrared) were used, which are: B2, B3, B4, B5, B6 and B7 at 30 m resolution. Using three applications (ArcMap, ArcCatalog and ArcToolbox) integrated into ArcGis, all GIS tasks were performed, including mapping, data

management, geographic analysis, data updating and geoprocessing.

The generated maps demonstrate a direct relationship between precipitation rates and the lake's water level. It is worth noting that the fluctuation of the water surface, driven by inflows and outflows, depends on the lake's feeding sources, which include the surrounding mountains and wadis (El Mellah, El Hout, and Zied). These inflows are crucial for the lake's sustainability.

Results and concluding remarks

The generated maps demonstrate a direct relationship between precipitation rates and the lake's water level. It is worth noting that the fluctuation of the water surface, driven by inflows and outflows, depends on the lake's feeding sources, which include the surrounding mountains and wadis (El Mellah, El Hout, and Zied). These inflows are crucial for the lake's sustainability.

What has been observed is that the lake's extent changes according to the seasons and the rainfall conditions of each year (rainy or dry). This variability makes the lake particularly vulnerable to seasonal mineralization processes.

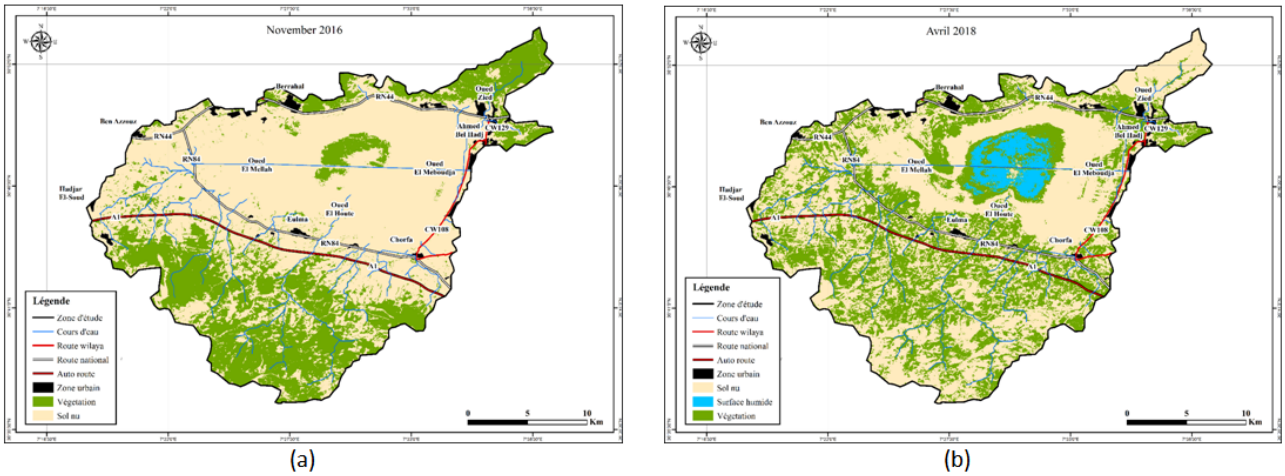


Figure 2. Hydrological Situation of Lake Fetzara in November 2016 (a) and March 2018 (b).

The observed fluctuation in the water surface between inflows and outflows is linked to contributions from the surrounding mountains and the wadis (El Mellah, El Hout, and Zied) that flow into the lake. These inflows ensure the lake's sustainability.

It is evident that the lake's extent varies depending on whether the years are rainy or dry. This seasonal variability makes the lake particularly interesting due to the renewed mineralization processes that occur each season.

References

Bouhali, Z., Djabri, L., Bouguerra, H., Trabelsi, F., Hani, A., & Chaffai, H. (2022). Use of artificial neural networks for modeling inflow, outflow, and salinity of Lake Fetzara in the Annaba region (N.E. Algeria). Journal of Food Industry and Agriculture, 107-115. Available at: www.fia.usv.ro/fiajournal

DGF (2003). Descriptive Sheet on Ramsar Wetland Sites: Lake Fetzara, Annaba Province. General Directorate of Forests (DGF).

Djamaï, R., Fadel, D., Laïfa, A., Benslama, M., Daoud, Y., & Vallès, V. (2011). The concept of residual alkalinity and the geochemical evolution of processes: Application to saline soils of Lake Fetzara (Northeastern Algeria). Synthesis Review of Science and Technology, 23: 90–98 (in French).

Saifouni, A. (2021). Wetlands in Algeria: Proposal for a New Classification, National Inventory, and Typology. Doctoral Thesis, National Higher School of Agronomy (ENSA), El-Harrach, Algiers, 282 p

Assessing water availability in the High Plain of Friuli Venezia Giulia, Italy, by integrating hydrological and hydrogeological modelling

E. Arnone[1*], L. Polese[2], M.Brandalise[1], G. Paiero[1], P. Teatini[2], G. Martelli[1]
[1] Dipartimento Politecnico di Ingegneria e Architettura, Università degli Studi di Udine, Udine, Italy
[2] Dipartimento di Ingegneria Civile, Edile e Ambientale, Università degli Studi di Padova, Padova, Italy
* e-mail: elisa.arnone@uniud.it

Introduction

In 2022 an exceptional drought hit northern Italy, including the Friuli Venezia Giulia region, located in the north-eastern part. According to the Regional Environmental Protection Agency (ARPA-FVG, 2024), the region experienced unprecedented changes in climate variables, especially in terms of maximum temperature values in spring and summer and annual cumulative precipitation. Precipitation anomalies overcome the 40% threshold in specific areas of the region (ARPA-FVG, 2024), with significant variations in the precipitation extremes detected by Arnone et al. (2024).

Drastic decreases in water availability were observed by the regional water utilities, who had to cope with an unprecedented limitation of supplies, that peaked 50% in 2022 (ARPA-FVG, 2024). The present study arises from the request of one of the local water reclamation and irrigation authorities, the *Consorzio di Bonifica della Pianura Friulana*, to identify irrigation solutions to efficiently respond to the new needs and establish new management procedures of water supply. The local stakeholders comprise 8 municipalities and 5 irrigation districts. The aim of the study is to integrate well sampling data, diversion flow rate with hydrological and hydrogeological modeling to quantify surface and subsurface water availability in the study area. The changes in the hydroclimatic conditions are assessed through statistical analyses of the meteorological variable and the model outputs.

Materials and methods

The work embraces a comprehensive and multimodeling approach to assess the surface and subsurface hydrological water balance through the following steps: 1) statistical analysis of the cumulative annual precipitation and the cumulative June-July-August (JJA) precipitation series by means of the Mann-Kendall test (Kendall, 1962); 2) hydrogeological water balance at average annual scale; 3) hydrological modeling of the surface processes at daily scale through the GEOframe-NewAge semi-distributed model (Formetta et al., 2014); 4) physics-based numerical modelling in steady-state of the phreatic aquifer system using a 3D finite-element model that solves Richards equation (Teatini et al., 2019).

The study area is the Torre-Natisone hydrographic system, which extends for more than 1100 km^2 in the eastern Friuli high plain (Figure 1a). The hydrogeology is characterized by a phreatic aquifer in the High Plain and a multi acquirer in the Low Plain (Martelli & Granati, 2007). Both the surface and subsurface basin limits are depicted in Figure 1a, which shows the administration limits of the municipalities and the hydro-meteorological gauge stations. These include 31 rain and temperature gauges, 3 hydrometer levels with corresponding discharge data (i.e. Tarcento, Zompitta and Manzano), and 74 wells. The spring line corresponds to the change from the undifferentiated aquifer to the multi-aquifer system (Figure 1a).

The hydrogeological balance, performed over an area of 500 km² (green area in Figure 1a), was defined based on the average piezometric trend between the plain/pre-Alpine foothill contact and the spring line. The groundwater partly feeds the springs and partly supports the multi-aquifer system of the low plain. Active recharge is due to effective precipitation and the leakage from the rivers. The balance parameters refer to the time interval 1993–2023. The averaged values obtained from the hydrological balance have been compared with the GEOframe-NewAge component-based model results. The Torre drainage basin (1090 km^2, blue limits in Figure 1a) has been discretized into 96 Hydrological Response Units (HRUs), in order to compute spatial variation of the water balance components at each sub-basin. The model has

been calibrated with discharge data at Tarcento outlet (upstream), with a Nash-Sutcliffe coefficient (NSE) of about 0.8, and fed with temperature and precipitation timeseries at daily scale, from 2004 to 2023. Lastly, the infiltration rate across the 96 sub-basins have been used as input to the groundwater recharge model to estimate the spatial and long term dynamics of the phreatic aquifer level.

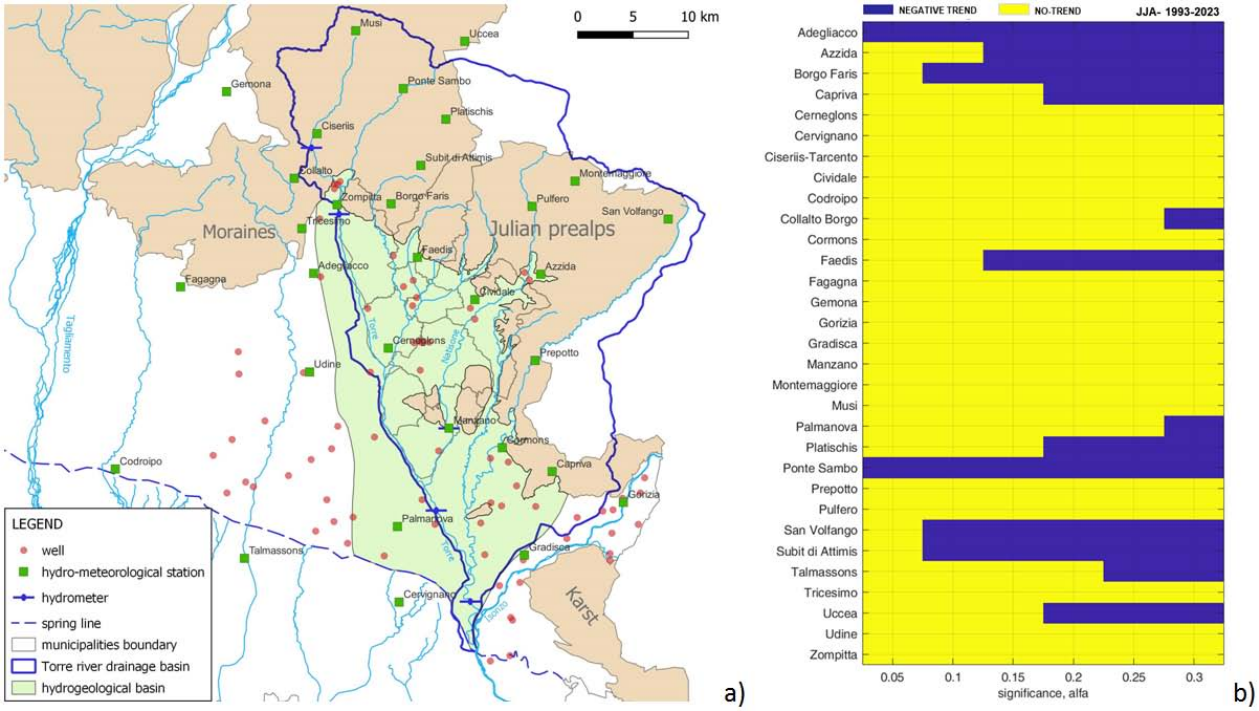


Figure 1. (a) Study area description: hydrogeological and hydrological basins limits are reported. (b) Raingauges showing negative statistical trend (blue box) of June-July-August cumulative precipitation of 1993-2023 series.

Results and concluding remarks

Figure 1b shows the MK trend results for the JJA cumulative precipitation across 31 raingauges, at varying significance level, *alfa*. If *alfa=0.3* is selected, more than 40% of the stations, mostly distributed in the upper part of the basin, exhibits a negative significant trend (blue box). Similar results were obtained for annual cumulative precipitation, proving that the area is suffering of a reduction in precipitation.

The hydrogeological balance was conducted at annual scale, and the average values over a 30-year time interval were assessed. The results indicated a total average recharge of about 27 m^3/s. The GEO-frame hydrological modelling showed a reduction in infiltration and evapotranspiration fluxes in the three consecutive years 2020,2021 and 2022, which likely led to a lowering of the water table in the phreatic aquifer system. The groundwater flow model was calibrated using the average records over the same 30-year time interval, showing how the variability of the natural recharge affects more significantly the subsurface water resources than the anthropogenic withdrawals carried out through numerous wells scattered in the study area.

References

Agenzia Regionale per la Protezione e per l'Ambiente del Friuli Venezia Giulia, ARPA-FVG. 2024. Meteo. FVG report: Segnali dal Clima, 2024.

Arnone, E., Treppiedi, D., Noto, L.V. 2024. High-resolution rain analysis in FVG, Northeastern Italy. Proceeding of XIth Scientific Assembly of IAHS (2022), Montpellier, France. IAHS2022-177, https://doi.org/10.5194/iahs2022-177.

Formetta, G., Kampf, S. K., David, O., and Rigon, R. (2014). Snow water equivalent modeling components in NewAge-JGrass. Geoscientific Model Development, 7(3), 725-736. https://doi.org/10.5194/gmd-7-725-2014

Kendall, M. G.: Rank Correlation Methods, Hafner Publishing Company, New York, 1962.

Martelli G., Granati C. (2007). Lithostratigraphical and hydrogeological characteristics of the aquifers of the low Friuli plain and sustainability of groundwater extractions. Mem. Descr. Carta Geol. d'Italia LXXVI:241 266.

Teatini P., Martelli C., Comerlati A., Paiero G. and Zoccarato C. 2020. Managed vs natural recharge of pre-Alpine phreatic aquifers, Water Resources Research, 56, doi:10.1029/2020WR027848

Investigation on the lasting effects of an extend drought on the trophic status of Lake Pusiano (Northern Italy) through numerical models

N. Pella[1,2*], D. Copetti[3], L. Valsecchi[3], P. Dezuanni[2,4], C. Dresti[2], F. Buzzi[5], A. Fenocchi[1]
[1] Department of Civil Engineering and Architecture, University of Pavia, Pavia, Italy
[2] Water Research Institute, National Research Council, Verbania Pallanza, Italy
[3] Water Research Institute, National Research Council, Brugherio, Italy
[4] Department of Electronics, Information and Bioengineering, Polytechnic University of Milan, Milan, Italy
[5] Department of Lecco, Regional Environmental Protection Agency of Lombardia, Oggiono, Italy
* e-mail:nicolo.pella01@universitadipavia.it

Introduction

The causes of eutrophication problems in lakes always lie in excess nutrient load of external and/or internal origin. Many countermeasures have been activated in the past on European basins to reduce nutrient pollution. With the introduction of the European Water Framework Directive, mandatory ecological quality standards to be reached within a deadline have been established (Bhagowati et al., 2019), whose achievement strongly depends on nutrient loading levels. Unfortunately, in recent years, some European shallow lakes displayed a water quality deterioration despite past and present countermeasures (Gonsiorczyk et al., 2024), which may be attributed both to episodic extreme hydroclimatic conditions, such as droughts, and to rising water temperatures triggered by long-term climate change.

The case study of this work is Lake Pusiano (Northern Italy). Following a protracted drought that affected Northern Italy between 2021 and 2023, the lake experienced a rapid upsurge in its trophic status, leading to enduring cyanobacterial algal blooms, lasting even during the winter. Three different models were developed to investigate on how the drought may have triggered the swift degradation of Lake Pusiano enduring to this date: 1) an eco-hydrological SWAT+ (Soil & Water Assessment Tool; Bieger et al., 2017) model, to assess the external nutrient loads entering the lake from the catchment; these loads were used as inputs to 2) a one-dimensional (1D) eco-hydrodynamic WET (Water Ecosystem Tool; Schnedler-Meyer et al., 2022) model of the lake, to determine the mixing and biogeochemical conditions of the lake from 2022 to 2024, notably including internal loading; 3) a three-dimensional (3D) hydrodynamic Delft3D (Lesser et al., 2004) model, to study the hydrodynamic conditions during dry and hot summer 2022 and understand lake circulations in Lake Pusiano under different inflowing and outflowing discharges.

Materials and methods

The SWAT+ eco-hydrological model was calibrated at monthly resolution using daily flow data from the Regional Environmental Protection Agency of Lombardy (ARPA Lombardia) and nitrogen and phosphorus concentrations from sampling activities by ARPA Lombardia and the Water Research Institute of the National Research Council (CNR-IRSA). Both datasets were available for River Lambro, the main tributary of Lake Pusiano. Streamflow was calibrasted over 2004-2013 and validated over 2014-2023, whereas nutrient concentrations were calibrated over 2014-2023 and validated over 2009-2013.

The WET 1D lake model was calibrated over 2022-2023 and validated over 2024 using detailed monthly vertical profiles of limnological data from ARPA Lombardia and CNR-IRSA. The model reproduced water temperatures, dissolved oxygen and nitrogen and phosphorus cycles, such processes being all calibrated with field observations. For the biological component, phytoplankton was implemented as a single group, being calibrated through Chlorophyll-*a* data.

The Delft3D model was tuned with turbulence model parameters obtained from Amadori et al. (2021).

Results and concluding remarks

Results from the WET model (Figure 1) suggest that phosphorus release from sediments in drought year 2022 was remarkable. The release notably extended to depths as shallow as 10 m, involving a much wider bottom surface than usual and determining an outstanding internal loading. This was triggered by extended anoxia brought about by water residence times being extended by the drought, determining oxygen depletion also in littoral areas (Gonsiorczyk et al., 2024). The rainfalls of 2023 and especially of extraordinarily wet year 2024 sustained this exceptional primary productivity through high external loads, as simulated by SWAT+, adding up to nutrient recycling. The warm 2022-23 and 2023-24 winters further made phytoplankton blooms endure through the coldest months.

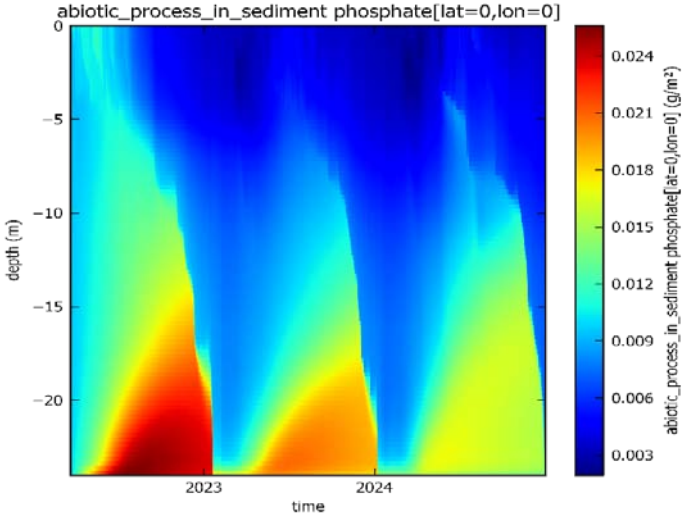


Figure 1. Simulated daily release of phosphate per unit area from the sediments of Lake Pusiano at different depths.

The results of the Delft3D model showed that, under the heavy stratification conditions of summer 2022, internal waves determined well-separated horizontal circulation cells which could transfer low-oxygen conditions and released phosphate from littoral areas towards the centre of the lake. The peculiar peripheral position of the main inlet and outlet, which are very close one another, also makes Lake Pusiano vulnerable to these events, the throughflow short-circuiting the main basin under most flow conditions.

References

Amadori M (2021) Multi scale evaluation of a 3D lake model forced by an atmospheric model against standard monitoring data. Environmental modelling & Software 139. https://doi.org/10.1016/j.envsoft.2021.105017

Bhagawati B (2019) A review on lake eutrophication dynamics and recent developments in lake modelling. Ecohydrology & Hydrobiology (19):155-166. https://doi.org/10.1016/j.ecohyd.2018.03.002

Bieger K, Arnold J.G (2017) Introduction to swat+ a completely restructured version of the soil and water assessment tool. JAWRA 53(1):115-130 https://doi.org/10.1111/1752-1688.12482

Gonsiorczyk T, Hupfer M (2024) Rapid eutrophication of a clearwater lake: Trends and potential causes inferred from phosphorus mass balance analyses. Global Change Biology 30(11). https://doi.org/10.1111/gcb.17575

Lesser G, Roelvink A (2004). Development and validation of a three-dimensional morphological model. Coastal Engineering 51(8–9): 883–915. https://doi.org/10.1016/j.coastaleng.2004.07.014

Schnedler-Meyer N.A, Andersen T.K (2022) Water Ecosystems Tool (Wet) 1.0 a new generation of flexible aquatic ecosystem model. Geoscientific Model Development 15(9): 3861–3878. https://doi.org/10.5194/gmd-15-3861-2022

ALIAS: a smart classifier for monitoring *Ailanthus altissima* expansion in hydrologically sensitive areas

F. Alongi[1,3*], D. De Caro[1], E. Badalamenti[2,3], F. Capodici[1,3], R. Silveira Bueno[2,3], D. Pumo[1,3], T. La Mantia[2,3], G. Ciraolo[1,3], L.V. Noto[1,3]
[1] *Department of Engineering, University of Palermo, Palermo, Italy*
[2] *Department of Agricultural, Food, and Forest Sciences, University of Palermo, Palermo, Italy*
[3] *NBFC, National Biodiversity Future Center, Palermo, Italy*
** e-mail: francesco.alongi01@unipa.it*

Introduction

Biodiversity loss is a growing global concern, threatening the stability of natural ecosystems. This phenomenon is driven by a combination of anthropogenic and natural factors, including urbanization, deforestation, and, most critically, climate change. Rising global temperatures and shifting precipitation patterns are altering wildfire regimes, leading to more frequent and intense fires. These disturbances create open niches and reduce competition, facilitating the establishment of invasive alien plant species. Characterized by high adaptability, rapid growth, and aggressive competition strategies, invasive plants can significantly disrupt local ecosystems. Moreover, they can profoundly impact hydrological processes by modifying evapotranspiration rates and reducing water retention capacity.

Among the most concerning invasive species, *Ailanthus altissima* (also known as tree of heaven) has rapidly spread across continents, establishing itself in both urban and natural environments (Soler & Izquierdo, 2024). Native to China, *Ailanthus* has become a widespread invader due to its remarkable adaptability and aggressive colonization strategies. Indeed, *Ailanthus* thrives in a wide range of environmental conditions, demonstrating resilience to extreme temperatures, diverse soil types, and high levels of air pollution (Iverson et al., 2019; Tarantino et al., 2019). One of the most problematic traits of *Ailanthus* is its extraordinary regenerative capacity. Even when cut or burned, the species can resprout vigorously, making eradication efforts particularly challenging (Badalamenti et al. 2015). Its seeds are primarily dispersed by wind but also spread via water, animals, and human activity, further accelerating its expansion. *Ailanthus* exhibits a strong dependence on water availability, employing deep root systems and highly efficient water uptake strategies (Petruzzellis et al., 2019). This allows it to thrive even in water-limited environments, such as Mediterranean ecosystems, where it can outcompete native vegetation for scarce water resources. By monopolizing soil moisture, *Ailanthus* alters the local ecohydrological balance, reducing groundwater recharge, increasing evapotranspiration rates, and potentially exacerbating drought conditions. Given its rapid spread and ecological impact, *Ailanthus altissima* has been the focus of multiple management strategies, but effective control remains a challenge, requiring integrated and long-term approaches to mitigate its expansion.

Materials and methods

The present work is based on high-resolution PlanetScope satellite imagery to detect and monitor the spread of *Ailanthus altissima*. PlanetScope provides multispectral data (i.e., 8 bands) at a spatial resolution of 3 meters, enabling fine-scale vegetation analysis. To automate the detection of *Ailanthus*, *ALIAS* (*Ailanthus Locator and Identification Algorithm Suite*) was developed, a machine learning-based classifier based on the *Support Vector Machine* (*SVM*) model. The model was trained using a dataset of reference points, distinguishing between *Ailanthus* and native vegetation. ALIAS was specifically calibrated to detect *Ailanthus altissima* in two key environments where the species tends to establish: (i) transportation corridors, where wind generated by vehicles facilitates seed dispersal, and (ii) hydrologically connected areas, such as riparian zones, where *Ailanthus* exploits water availability for rapid growth. Training samples were collected through a combination of field surveys and visual interpretation of high-resolution images. The model was validated in the *Vallone Piano della Corte Nature Reserve* (Sicily, Italy), a protected area sensitive to the *Ailanthus altissima* invasion. Over the past four decades, *Ailanthus altissima* has

progressively expanded, forming dense clusters on the south-facing slope, while the north-facing slope remains dominated by native forest stands (i.e., *Quercus pubescens*).

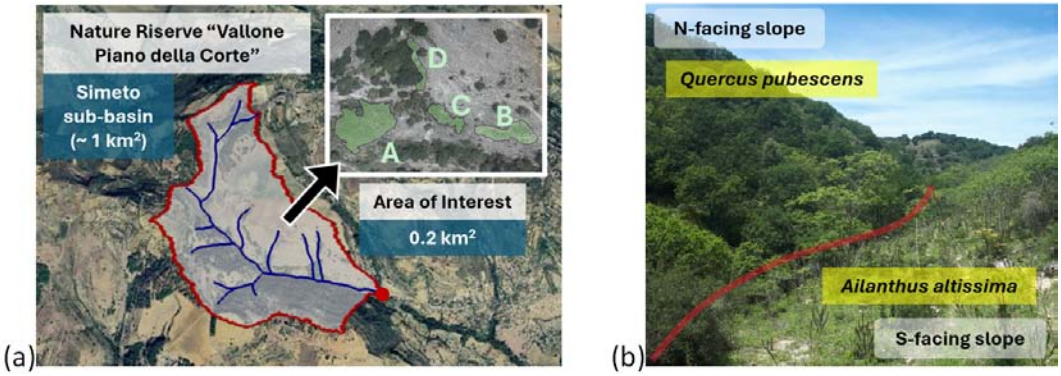


Figure 1. (a) Location of the Nature Reserve and view of the threatening Ailanthus clusters within the area of interest. (b) Aspect-dependent distribution of native species (i.e., Quercus pubescens) and Ailanthus altissima.

To further assess the reliability of ALIAS, a diachronic analysis was conducted to reconstruct the invasion history of *Ailanthus altissima* from the late 1980s to the present. Historical photogrammetric images were analysed to track the expansion of *Ailanthus* populations over time. Additionally, field surveys were carried out using drone-based imaging to obtain high-resolution ground truth data on current invasion patterns.

Results and concluding remarks

The results obtained demonstrate the potential of ALIAS as a predictive tool for identifying regions at high risk of *Ailanthus altissima* invasion, particularly in hydrologically sensitive areas. The classifier effectively detected *Ailanthus* populations in the study area, distinguishing them from native vegetation with high accuracy. By enabling efficient monitoring of *Ailanthus* in both confirmed invasion sites and potentially at-risk zones, ALIAS provides valuable insights into the ecohydrological dynamics of invasive species. The classifier, in fact, can also supports long-term ecosystem management by identifying priority areas for intervention. Furthermore, the classified images derived from ALIAS serve as a crucial dataset for validating vegetation dynamics models (e.g., CATGraSS model), which reconstructs invasion trajectories and predicts future expansion patterns under different climate change and hydrological scenarios. This integration between remote sensing, machine learning, and ecological modelling enhances our ability to anticipate invasion dynamics, assess potential ecological impacts and design effective mitigation strategies.

Acknowledgments: Project funded under the National Recovery and Mission 4 Component 2 Investment 1. Resilience Plan (NRRP), 4 - Call for tender No. 3138 of 16 December 2021, rectified by Decree n.3175 of 18 December 2021 of Italian Ministry of University and Research funded by the European Union – NextGenerationEU. Project code CN00000033, Concession Decree No. 1034 of 17 June 2022 adopted by the Italian Ministry of University and Research, CUPB73C22000790001, Project title "National Biodiversity Future Center - NBFC".

References

Badalamenti, E., Barone, E., & La Mantia, T. (2015). Seasonal effects on mortality rates and resprouting of stems treated with glyphosate in the invasive tree of heaven Ailanthus altissima (Mill.) Swingle. Arboricultural Journal, 37(3), 180-195. https://doi.org/10.1080/03071375.2015.1112163

Iverson, L. R., Rebbeck, J., Peters, M. P., Hutchinson, T., & Fox, T. (2019). Predicting Ailanthus altissima presence across a managed forest landscape in southeast Ohio. Forest Ecosystems, 6, 1-13. https://doi.org/10.1186/s40663-019-0198-7

Petruzzellis, F., Nardini, A., Savi, T., Tonet, V., Castello, M., & Bacaro, G. (2019). Less safety for more efficiency: water relations and hydraulics of the invasive tree Ailanthus altissima (Mill.) Swingle compared with native Fraxinus ornus L. Tree physiology, 39(1), 76-87. https://doi.org/10.1093/treephys/tpy076

Soler, J., & Izquierdo, J. (2024). The Invasive Ailanthus altissima: A Biology, Ecology, and Control Review. Plants, 13(7), 931. https://doi.org/10.3390/plants13070931

Tarantino, C., Casella, F., Adamo, M., Lucas, R., Beierkuhnlein, C., & Blonda, P. (2019). Ailanthus altissima mapping from multi-temporal very high resolution satellite images. ISPRS Journal of Photogrammetry and Remote Sensing, 147, 90-103. https://doi.org/10.1016/j.isprsjprs.2018.11.013

How to monitor river turbidity using camera systems: Best practice guidelines

D. Miglino[1], S. Jomaa[2], K. C. Saddi[1,4,5], A.C. Moe[1,4], M. Rode[2,3], S. Manfreda[1]
[1] Dipartimento di Ingegneria Civile, Edile e Ambientale (DICEA), Università degli Studi di Napoli Federico II, Napoli, Italy
[2] Department of Aquatic Ecosystem Analysis and Management (ASAM), Helmholtz Centre for Environmental Research – UFZ, Magdeburg, Germany
[3] Institute of Environmental Science and Geography, University of Potsdam, Potsdam-Golm, 14476, Germany
[4] University School of Advanced Studies IUSS Pavia, Pavia, Italy
[5] Department of Civil Engineering and Architecture, Ateneo de Naga University, Naga, Philippines
* e-mail: domenico.miglino@unina.it

Introduction

Monitoring river turbidity is essential for understanding sediment transport, water quality, and aquatic ecosystem health. Image-based systems offer a cost-effective, spatial and temporal distributed technique for turbidity assessment, but their accuracy depends on the right camera installation setups, and the proper image processing. This work provides recommendations, based on field experiences, for camera-based turbidity monitoring activities, ensuring reliable long term data collection.

Key considerations include selecting appropriate camera types, positioning and orientations to minimize sun glare and reflections, optimizing image processing procedures for consistent turbidity estimation, and accounting for factors such as seasonal variations in light and flow conditions.

Materials and methods

The image processing procedure of Miglino et al. (2024) was tested in different field campaigns, proving its capacity to monitor river turbidity under varying environmental and hydrological conditions. In particular, two main experiments were conducted in February and June 2023 within the Bode River, in Germany. In the first experiment, a synthetic turbidity event was recreated by adding kaolin clay into the water. In the second experiment, the synthetic turbidity event was split into three phases. The event was recreated by adding different tracers, in this order: kaolin clay, dolomite flour and lava flour. Several camera types were used during the experiments: trap camera (TC-Ceyomur CY50), multispectral camera (MSC-Tetracam ADC Snap) and an unmanned aerial vehicle (UAV-DJI Mavic 2 Enterprise Dual), fixed in different positions along the river. During both the experiments, the camera data was compared to the measurements of the turbidimeters installed underwater within the river cross-section. Figure 1 shows the trap camera results of the combined experiments. These experiments allow us to test all the factors that could affect the procedure.

Results and concluding remarks

The performance metrics, shown in Table 1, confirm the reliability of the procedure also for changing hydrological conditions. The MSC camera consistently outperforms the trap camera for all bands. The MSC NIR band provides a strong match, also better than the green band, but it is able to detect only very high turbidity concentration. Nevertheless, the trap camera also shows solid results, particularly for the red band values. Notably, the red band appears as a critical indicator for turbidity assessment, given its higher correlation in both cameras. This demonstrates the potential of the trap camera as a budget-friendly alternative for practical applications and support for water quality monitoring. The UAV showed interesting results, thanks to its zenithal point of view, but its results were excluded, due to the short battery life.

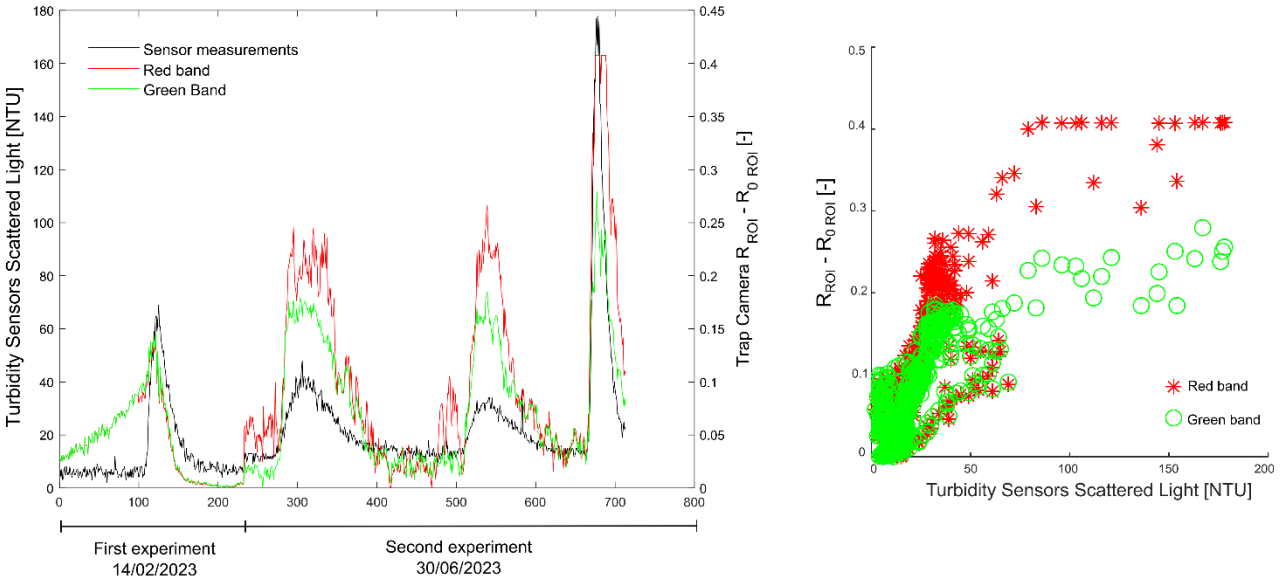


Figure 1. A) Comparison between turbidimeter measurements and trap camera red and green bands increments for all the combined synthetic turbidity events of February and June 2023; B) Scatter plot of the variables.

Table 1. Linear and quadratic correlation coefficients R^2 of multispectral camera (MSC) and trap camera (TC) bands compared to turbidity measurements, considering all the turbidity events in the combined experiments of February and June 2023.

		ALL TURBIDITY EVENTS			
		M.S. CAMERA		TRAP CAMERA	
		LIN.R^2	QUAD.R^2	LIN.R^2	QUAD.R^2
SINGLE BANDS	RED BAND	0.75	0.75	0.63	0.70
	GREEN BAND	0.62	0.67	0.54	0.65
	NIR BAND	0.72	0.73		

These experiments highlighted both the advantages and the challenges of camera systems. While initial findings clearly demonstrate the system's ability to provide insights into river system trends and dynamics, several practical issues require resolution:

- Significant variations in illumination cause notable differences in spectral signatures across days and seasons.
- Changing illumination direction and resulting tree shadows alter the scene during the day.
- Flow conditions and ripples may affect the spectral signature.
- Suspended sediment colour variations can also impact the camera signal.
- Wind, human activity, or animal presence might disrupt camera positioning or even induce vibrations.
- Shallow rivers' backgrounds can be challenging.

These critical factors should be considered to refine camera systems' effectiveness, establishing a robust workflow for high-quality measurements. This might involve optimizing camera angles, implementing effective image filtering and calibration, securing camera stability, and providing comprehensive training for floating pollutants detection (Manfreda et al., 2024).

References

Manfreda, S., Miglino, D., Saddi, K. C., Jomaa, S., Eltner, A., Perks, M., et al. (2024). Advancing river monitoring using image-based techniques: challenges and opportunities. Hydrological Sciences Journal, 69(6), 657.

Miglino, D., Saddi, K. C., Isgrò, F., Jomaa, S., Rode, M., & Manfreda, S. (2024). Image processing for continuous river turbidity monitoring–full scale tests and potential applications. EGUsphere, 2024, 1-22.

13th World Congress on Water Resources and Environment (EWRA 2025)
"New challenges in understanding and managing water-related risks in a changing environment"
Palermo, Italy, 24 - 28 June 2025

Recovery and characterization of structural extracellular biopolymers from aerobic granular sludge treating citrus industrial wastewater

M. Castiglione[1*], R. Campo[2], M. Capodici[1], S.F. Corsino[1], A. Cosenza[1], F. De Marines[1], D. Di Trapani[1], G. Di Bella[2], M. Torregrossa[1]
[1] Department of Engineering, University of Palermo, Palermo, Italy
[2] Department of Engineering and Architecture, University of Enna "Kore", Enna, Italy
* e-mail: maria.castiglione01@unipa.it

Introduction

Microbial polymer production has gained significant interest in recent years due to its potential for sustainable material recovery from renewable resources, such as wastewater, instead of using conventional petroleum-based polymers. Among these biopolymers, those extracted from aerobic granular sludge (AGS) have attracted increasing attention. AGS is an innovative wastewater treatment technology for both municipal and industrial effluents. Aerobic granules are dense, compact, and self-immobilized microbial aggregates capable of performing multiple biological treatment processes simultaneously (Campo et al., 2022). Bacteria in AGS are embedded in a complex extracellular polymeric substance (EPS) matrix, which provides structural stability and protection against external agents. Alginate-like exopolysaccharides (ALEs) are the primary components of EPS and are referred to as structural EPS (sEPS) due to their crucial role in maintaining the integrity of the granules (Felz et al., 2016). Bacterial-derived ALEs comprise a mixture of biopolymers, including polysaccharides, proteins, humic acids, and lipids. ALEs have garnered attention for their unique properties, including strong gelling ability, biocompatibility, and biodegradability, making them highly valuable for industrial applications. While the majority of literature studies on this topic focus on sEPS extracted from AGS for the treatment of municipal wastewater, limited research is available on sEPS extraction from AGS treating industrial effluents. This study aimed to evaluate the productivity and characteristics of ALEs extracted from AGS treating an industrial wastewater from a citrus industry.

Materials and methods

Structural EPS were extracted from two Granular Sequencing Batch Reactors (GSBR), named R1 and R2, which treated wastewater from a citrus processing industry. Both GSBRs were column-type acrylic reactors with an operating volume of 4 L and were inoculated with activated sludge. The reactors operated in 4-hour cycles (6 cycles/day). R1 had a 2-minute feeding phase under complete mixing conditions (0.25 L/min), followed by 58 minutes of anaerobic mixing feast, 60 minutes of aeration famine (2 L/min), 25 minutes of mixing to obtain oxygen depletion, 30 minutes of settling, and 5 minutes of effluent discharge. R2, after a rapid 2-minute of aerobic feeding phase (0.25 L/min), operated under continuous aeration (2 L/min) for 145 minutes, followed by 30 minutes of settling and 5 minutes of effluent discharge. A programmable logic controller (PLC) that managed the cycle phases automatically. The minimum settling velocity was gradually increased from 0.18 m/h to 1.8 m/h by reducing the settling time from 30 to 3 minutes, with a corresponding increase in the aeration phase duration. The influent soluble COD ranged from 1300 to 2000 mg/L during the monitoring period. The daily influent flow rate was 3 L/day per reactor, resulting in an organic loading rate (OLR) varying between 0.98 and 1.5 kgCOD/m³·d. The experiment lasted for over 90 days. The sEPS extraction was performed once mature granules were obtained in both the reactors following the method described by Feltz et al. (2016). Total solids (TS) and volatile solids (VS) of AGS and sEPS were determined according to standard methods (APHA, 2012). Total EPS (tEPS) and sEPS were characterized by colorimetric methods in terms of proteins (as bovine serum albumin equivalent) and polysaccharides (both as d-glucose and sodium alginate equivalents). Particle size distribution (PSD) was obtained by a high-speed image analyses sensor (Sympatec Qicpic). Morphologic microscopic observations

were performed by a stereomicroscope (Olympus). The percentage of granules (GR) was calculated as the cumulative particle density bigger than 200 µm. The median of the PSD (D_{50}) was assumed as reference size of the granules. Since the experiments are still in progress, further sEPS characterization will be performed including thermogravimetry, differential scanning calorimetry and Fourier Transform Infrared Spectroscopy.

Results and concluding remarks

Aerobic granular sludge was obtained in both the reactors although with different features. Granules from R1 resulted bigger in size (D_{50} = 0.9 mm), and well round-shaped, whereas granules in R2 resulted smaller (D_{50} = 0.25 mm) with irregular shape and dispersed in a flocculent sludge matrix. Complete granulation was achieved in R1 after approximately 70 days. In contrast, in R2 complete granulation was not obtained and the percentage of granules into the reactor ranged between 60-70% (Fig. 1).

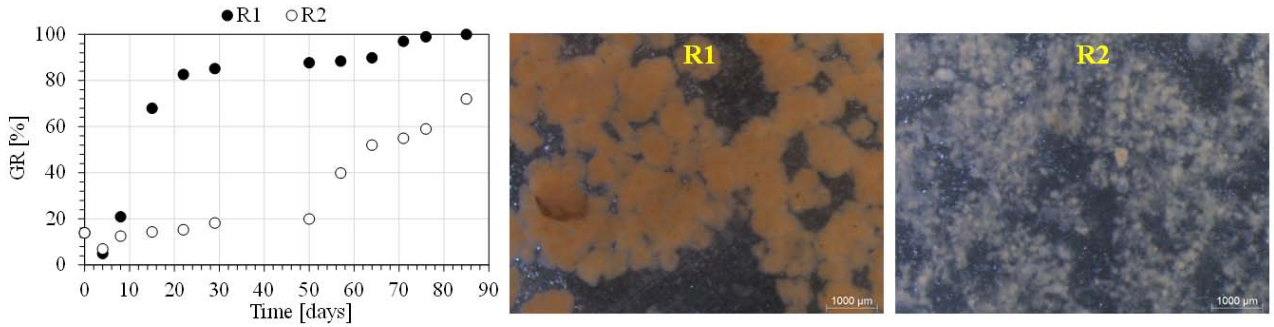


Figure 1. Trend of the granulation rate and microscopic picture of R1 and R2 granules.

EPS extraction revealed higher yields of tEPS (0.33 gTStEPS/gTSAGS vs. 0.27 gTStEPS/gTSAGS) and sEPS (0.22 gTSsEPS/gTSAGS vs. 0.15 gTSsEPS/gTSAGS) for R1 compared to R2, respectively (Fig. 2). Moreover, tEPS extracted from AGS of R1 were more enriched of sEPS than those extracted from AGS of R2 (67,74% sEPS/tEPS vs. 54,56% sEPS/tEPS). These preliminary results highlighted: 1) the more granular a mixed liquor is, the higher the tEPS; 2) AGS from anaerobic feast/aerobic famine process (as R1) produce higher sEPS due to metabolic selection of slow-growing storing microorganisms, notoriously generators of superior quality sEPS (Campo et al., 2022).

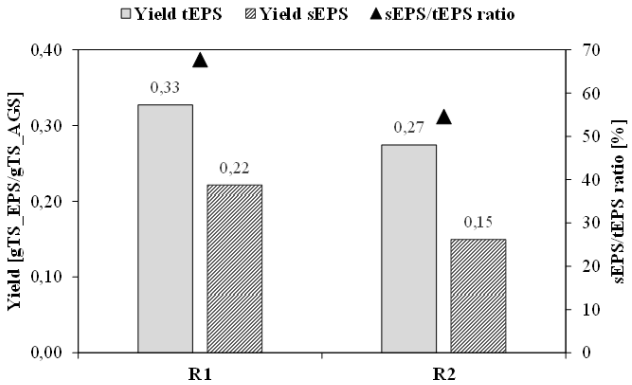


Figure 2. Yield of EPSt, sEPS and sEPS/tEPS ratio for R1 and R2.

Acknowledgments: This project was founded by SWRIPS (Sustainable Wastewater Re-use with Innovative Purification and Sensing system for the agrifood supply chain) project – PRIMA Section 2 -2022.

References

APHA, 2012. Standard Methods for the Examination of Water and Wastewater, Standard Methods.

Campo, R., Carretti, E., Lubello, C., Lotti, T., 2022. Recovery of structural extracellular polymeric substances (sEPS) from aerobic granular sludge: Insights on biopolymers characterization and hydrogel properties for potential applications. J. Environ. Manage. 324, 116247. https://doi.org/10.1016/j.jenvman.2022.116247

Felz, S., Al-Zuhairy, S., Aarstad, A.O., van Loosdrecht, M.C.M., Lin, Y.M., 2016. Extraction of structural extracellular polymeric substances from aerobic granular sludge. J Vis Exp. 2016 Sep 26:(115):54534. doi: 10.3791/54534.

ISBN: 978-618-84419-2-7

GOLD SPONSORS

ECOSEARCH
ENVIRONMENTAL MONITORING AND SAMPLING

ORION
WWW.ORION-SRL.IT

SILVER SPONSORS

AMAP S.p.A.

CAE
innovation for a safer world.

ELDES
RADAR SYSTEMS FOR METEOROLOGY AND DEFENCE

INTEA gis
INFORMATICA TERRITORIO E AMBIENTE

fisia italimpianti
webuild group

BRONZE SPONSORS

Return

Siciliacque

caltaqua
Acque di Caltanissetta S.p.A.

e.lab s.r.l.
environmental laboratory

planetek
italia

PLASSON

Sicil Condotte

SOCIETÀ DEL GRES
GRUPPO STEINZEUG-KERAMO

suez



https://ewra2025.ewra.net/